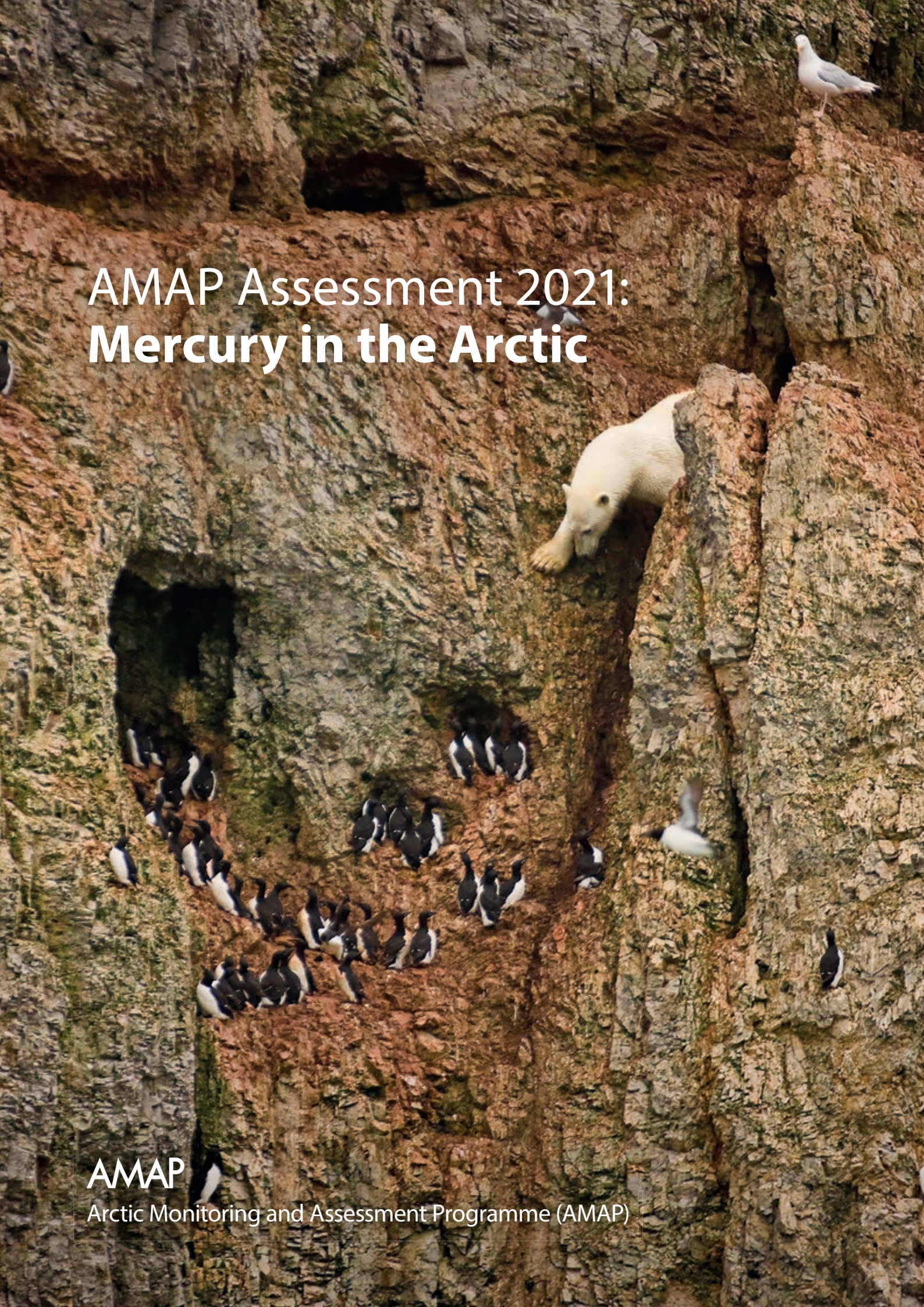

AMAP Assessment 2021: **Mercury in the Arctic**

AMAP

Arctic Monitoring and Assessment Programme (AMAP)

Educational use: This report (in part or in its entirety) and other AMAP products available from www.amap.no can be used freely as teaching materials and for other educational purposes.

The only condition of such use is acknowledgement of AMAP as the source of the material according to the recommended citation.

In case of questions regarding educational use, please contact the AMAP Secretariat (amap@amap.no).

Note: This report may contain material (e.g. photographs) for which permission for use will need to be obtained from original copyright holders.

Disclaimer: The views expressed in this peer-reviewed report are the responsibility of the authors of the report and do not necessarily reflect the views of the Arctic Council, its members or its observers.

AMAP Assessment 2021:
Mercury in the Arctic

AMAP

Arctic Monitoring and Assessment Programme (AMAP)
Tromsø, 2021

AMAP Assessment 2021: Mercury in the Arctic

ISBN – 978-82-7971-111-7

© Arctic Monitoring and Assessment Programme, 2021

Citation
AMAP, 2021. AMAP Assessment 2021: Mercury in the Arctic. Arctic Monitoring and Assessment Programme (AMAP), Tromsø, Norway. viii + 324pp

Published by
Arctic Monitoring and Assessment Programme (AMAP), Tromsø, Norway (www.amap.no)

Ordering
This report can be ordered from the AMAP Secretariat, The Fram Centre, P.O. Box 6606 Stakkevollan, N-9296 Tromsø, Norway
This report is also published as an electronic document, available from the AMAP website at www.amap.no

Production

Production management
Simon Wilson (AMAP Secretariat)

Scientific, technical and linguistic editing
Matthew Perkins (https://matthewjperkins.com) (mattjohnperkins@gmail.com)

Layout and technical production
Burnthebook, United Kingdom (www.burnthebook.co.uk)

Design and production of computer graphics
Burnthebook, United Kingdom (www.burnthebook.co.uk)

Cover photograph
'Unable to hunt seals because of sea ice loss, a polar bear climbs a cliff on Novaya Zemlya, Russian High Arctic, attempting unsuccessfully to feed on seabird eggs. Ecological impacts of Arctic climate change alter contaminant exposure pathways.' Jenny E. Ross/LifeOnThinIce.org

Printing
Narayana Press, Gylling, DK-8300 Odder, Denmark (www.narayanapress.dk)

AMAP Working Group (during period of preparation of this assessment)
Sarah Kalhok Bourque (Canada), Mikala Klint (Kingdom of Denmark), Morten S. Olsen (Kingdom of Denmark), Outi Mähönen (Vice-Chair, Finland), Sigurrós Friðriksdóttir (Iceland), Marianne Kroglund (Norway), Vladimir Bulgakov (Russia), Yuri Tsaturov† (Vice-Chair, Russia), Tove Lundeberg (Sweden), Anders Turesson (Chair, Sweden), Ben DeAngelo (United States), Eva Krümmel (ICC), Anna-Marja Persson (Saami Council), Bob van Dijken (Arctic Athabaskan Council)

AMAP Secretariat
Rolf Rødven, Simon Wilson, Janet Pawlak, Jan-René Larsen, Mario Acquarone, Heidi Sevestre, Inger Utne

Arctic Council Member States and Permanent Participants of the Council
Canada, Denmark/Greenland/Faroe Islands, Finland, Iceland, Norway, Russia, Sweden, United States, Aleut International Association (AIA), Arctic Athabaskan Council (AAC), Gwitch'in Council International (GCI), Inuit Circumpolar Council (ICC), Russian Association of Indigenous Peoples of the North (RAIPON), Saami Council

Acknowledgments

AMAP expresses its thanks to the following for their contributions to this assessment; listing is alphabetical with coordinating chapter leads (**bold**) and lead authors (***italics***) identified (see chapters for details; affiliations included at first occurence for authors only). We apologize for any unintentional omissions.

Coordinating chapter leads

Niladri Basu (McGill University, Canada; Chapter 7), John Chételat (Environment and Climate Change Canada; Chapters 1, 5 and 10), Ashu Dastoor (Environment and Climate Change Canada; Chapter 3), Rune Dietz (Aarhus University, Denmark; Chapters 1, 6 and 10), Magali Houde (Environment and Climate Change Canada; Chapter 9), Eva M. Krümmel (Inuit Circumpolar Council, Canada; Chapter 9), Robert J. Letcher (Environment and Climate Change Canada; Chapter 6), Melissa McKinney (McGill University, Canada; Chapter 5), Adam D. Morris (Northern Contaminants Program, Canada; Chapter 2), Michelle Nerentorp Mastromonaco (IVL Swedish Environmental Research Institute; Chapter 4), Sofi Jonsson (Stockholm University, Sweden; Chapter 4), Frank Rigét (Aarhus University, Denmark; Chapter 2), Amina Schartup (Scripps Institution of Oceanography, USA; Chapter 8), Noelle Selin (Massachusetts Institute of Technology, USA; Chapter 8), Feiyue Wang (University of Manitoba, Canada; Chapter 4), Pál Weihe (Department of Occupational Medicine and Public Health, Faroe Islands; Chapter 7), Simon J. Wilson (AMAP Secretariat, Norway; Chapters 1 and 2)

Authors and contributors

Jon Aars (Norway), Wenche Aas (Norway), Khaled Abass (Finland), ***Joshua T. Ackerman (U.S. Geological Survey), Bryan Adlard (Health Canada),*** Céline Albert (France), ***Marc Amyot (University of Montréal, Canada)***, Magnus Andersen (Norway), Birgitta Andreasen (Faroe Islands), Dennis Andriashek (Canada), Frédéric Angelier (France), ***Hélène Angot (École Polytechnique Fédérale de Lausanne, Switzerland),*** Aurora Aubail (France), ***Benjamin D. Barst (University of Alaska, USA), Niladri Basu (Canada),*** Claus Bech (Norway), Torunn Berg (Norway), Alicia Berthiaume (Canada), Johannes Bieser (Germany), Caty Blanchette (Canada), Pierre Blévin (Norway), David Boertmann (Denmark), Andrei Boltunov (Russia), Eva Cecilie Bonefeld-Jorgensen (Denmark), Erik W. Born (Greenland), ***Katlin Bowman (University of California Santa Cruz, USA), Jeremy Brammer (Environment and Climate Change Canada), Andrea G. Bravo (Institute of Marine Sciences, Spain), Tanya Brown (Fisheries and Oceans Canada),*** Birgit Braune (Canada), Paco Bustamante (France), ***Samantha M. Burke (Canada),*** Jan Ove Bustnes (Norway), ***Warren R.L. Cairns (CNR-Institute of Polar Sciences, Italy),*** Joao Canario (Portugal), Paloma Carvalho (Canada), Laurie Chan (Canada), ***Olivier Chastel (CNRS-Villiers-en-Bois, France), John Chételat (Canada),*** Jesper Christensen (Denmark), Tomasz M. Ciesielski (Norway), Maria Dam (Faroe Islands), Jóhannis Danielsen (Faroe Islands), Sarah Danielsen (Sweden), Krishna Das (Belgium), ***Sam Dastnai (Aarhus University, Denmark), Ashu Dastoor (Canada),*** Andrew E. Derocher (Canada), Sébastien Descamps (Norway), ***Jean-Pierre Desforges (University of Winnipeg, Canada), Theodore Dibble (State University of New York, USA), Rune Dietz (Denmark),*** Brian DiMento (USA), ***Thomas A. Douglas (U.S. Army Cold Regions Research and Engineering Laboratory, USA)***, Alexey Dudarev (Russia), ***Collin A. Eagles-Smith (U.S. Geological Survey), Kristin Eccles (National Institute of Environmental Health Sciences, Canada), Parnuna Egede Dahl (Aalborg University/Ilisimatusarfik, Greenland), Kyle Elliott (McGill University, Canada)***, Kjell Einar Erikstad (Norway), ***Igor Eulaers (Norwegian Polar Institute, Norway),*** Mark Evans (United Kingdom), ***Marlene Evans (Environment and Climate Change Canada),*** Anita Evenset (Norway), David Evers (USA), Alexey Ezhov (Russia), Suzanne Faxneld (Sweden), Steve Ferguson (Canada), ***Kim Fernie (Environment and Climate Change Canada)***, Bernard Firanski (Canada), Michelle G. Fitzsimmons (Canada), Eirik Fjeld (Norway), ***Jérôme Fort (CNRS-La Rochelle Université, France), Rob Fryer (Marine Scotland, United Kingdom),*** Eva Fuglei (Norway), Chris Furgal (Canada), Geir Wing Gabrielsen (Norway), ***Mary Gamberg (Gamberg Consulting, Canada),*** Nikolaus Gantner (Canada), Katarine Gårdfeldt (Sweden), ***Marie-Josée Gauthier (Nunavik Regional Board of Health & Social Services, Canada),*** Maria Gavrilo (Russia), Grant Gilchrist (Canada), Olivier Gilg, Sindri Gíslason, Elena Golubova (Russia), Lucy Grey (Canada), David Grémillet (France), Ingeborg G. Hallanger (Norway), Seunghee Han (Korea), Erpur Hansen (Iceland), Sophia Hansson (France), Scott Hatch (USA), ***Aviaja Lyberth Hauptmann (Institute of Nursing and Health Science, Greenland), Joel P. Heath (Arctic Eider Society, Canada),*** Mads P. Heide-Jørgensen (Greenland), ***Lars-Eric Heimbürger-Boavida (Mediterranean Institute of Oceanography, France),*** Lisa B. Helgason (Norway), ***Dominique A. Henri (Environment and Climate Change Canada),*** Paul F. Hoekstra (Canada), ***Magali Houde (Canada),*** Katrin Hoydal (Faroe Islands), ***Karista Hudelson (ETH Zurich, Switzerland),*** Nicholas Per Huffeldt (Sweden), Audrey Jæger (France), Dariusz Jakubas (Poland), Bjørn M. Jenssen (Norway), ***Martin Jiskra (University of Basel, Switzerland),*** Jon Einar Jónsson (Iceland), ***Kimmo K. Kahilainen (University of Helsinki, Finland)***, Kaare Kemp (Denmark), ***Jane Kirk (Environment and Climate Change Canada),*** Alexander Kitaysky (USA), Stephen G. Kohler (Norway), Yann Kolbeinsson (Iceland), Yuri Krasnov (Russia), ***Eva M. Krümmel (Canada),*** Aditya Kumar (USA), Katriina Kyllönen (Finland), ***Brian Laird (University of Waterloo, Canada),*** Carl Lamborg (USA), Martin M. Larsen (Denmark), Sarah Leclaire (France), Igor Lehnherr (Canada), ***Mélanie Lemire (Laval University, Canada), Ann E. Lennert (UiT Arctic University of Norway), Gretchen Lescord (Wildlife Conservation Society, Canada), Robert J. Letcher (Canada),*** Ulf Lindstrøm (Norway), Anna Lippold (Norway), ***Sarah Lord (Gwich'in Renewable Resources Board, Canada),*** Erlend Lorentzen (Norway), Manhai Long (Denmark), ***Lisa Loseto (Fisheries and Oceans, Canada),***

Nick Lunn (Canada), ***Gwyneth A. MacMillan (McGill University, Canada),*** Mark Mallory (Canada), ***Huiting Mao (State University of New York, USA), Robert Mason (University of Connecticut, USA),*** Robie McDonald (Canada), ***Melissa McKinney (Canada),*** David McLagan (Canada), Flemming Ravn Merkel (Greenland), Francoise Messier (Canada), ***Stefan Mikaelsson Saami Parliament of Sweden),*** Cecilie Miljeteig (Norway), Børge Moe (Norway), William A. Montevecchi (Canada), ***Adam D. Morris (Canada),*** Anders Mosbech (Denmark), Cuicui Mu (China), ***Derek C.G. Muir (Environment and Climate Change Canada)***, Marilena Muntean (Italy), ***Edda Mutter (Yukon River Inter-Tribal Watershed Council, USA), Tero Mustonen (Snowchange Cooperative, Finland), Jacob Nabe-Nielsen (Aarhus University, Denmark),*** Nynne H. Nielsen (Greenland), Sanna T. Nielsen (USA), ***Michelle Nerentorp Mastromonaco (Sweden),*** Karin Nordstrom (Sweden), Martyn Obbard (Canada), ***Daniel Obrist (University of Massachusetts, USA), Todd O'Hara (Texas A&M University, USA),*** Kristin Olafsdóttir (Iceland), Bergur Olsen (Faroe Islands), Rachael A. Orben (USA), ***Sonja Ostertag (University of Waterloo, Canada), Peter Outridge (Geological Survey of Canada),*** Jozef Pacyna (Poland), Allison Patterson (USA), Elizabeth Peacock (USA), Sara Pedro (Canada), ***Nicolas Pelletier (Natural Resources Canada)***, Marie Perkins (USA), Mariia Petrova (France), ***Katrine Aspmo Pfaffhuber (Norwegian Institute for Air Research), Sofi Jonsson (Sweden),*** Martin Pilote (Canada), Marianna Pinzone (Belgium/Canada), Trevor Porter (Canada), Amanda Poste (Norway), Michael Power (Canada), Isabeau Pratte (Canada), Jennifer Provencher (Canada), Mylene Ratelle (Canada), Arja Rautio (Finland), Tone Kristin Reiertsen (Norway), Helena Reinardy (United Kingdom), Heather Renner (USA), Gunn-Britt Retter (Norway), ***Frank Rigét (Denmark), Martin Robards (Wildlife Conservation Society, USA), Sarah Roberts (United Kingdom),*** Gregory J. Robertson (Canada), Nora Rojek (USA), Marc Romano (USA), Aqqalu Rosing-Asvid (Greenland), ***Heli Routti (Norwegian Polar Institute)***, ***Andrei Ryjkov (Environment and Climate Change Canada),*** Kjetil Sagerup (Norway), Filipa Samarra (Iceland), Halvor Saunes (Norway), ***Amina Schartup (USA), Noelle Selin (USA), Vyacheslav Shadrin (RAIPON, Sakha-Yakutia Chapter, Russia),*** Ursula Siebert (Germany), ***Henrik Skov (Aarhus University, Denmark)***, ***Merran Smith (Council of Yukon First Nations, Canada), Anne L. Soerensen (Swedish Museum of Natural History),*** Jens Søndergaard (Denmark), Jeroen Sonke (France), ***Christian Sonne (Aarhus University, Denmark), Kyra St. Pierre (University of British Columbia, Canada),*** Jannie Staffansson (Sweden), Frits Steenhuisen (Netherlands), ***Alexandra Steffen (Environment and Climate Change Canada),*** Garry Stenson (Canada), Gary Stern (Canada), ***Raphaela Stimmelmayr (Department of Wildlife Management, USA),*** Ian Stirling (Canada), Jakob Strand (Denmark), Hallvard Strøm (Norway), ***Geoff Stupple (Environment and Climate Change Canada), Enooyaq Sudlovenick (University of Manitoba, Canada), Heidi Swanson (University of Waterloo, Canada),*** Akinori Takahashi (Japan), Sabrina Tartu (France), Mitch Taylor (Canada), Grigori Tertitski (Russia), ***Colin Thackray (Harvard University, USA),*** Jean- Baptiste Thiebot (France), ***Philippe J. Thomas (Environment and Climate Change Canada),*** Elena Tolmacheva (Russia), Torkel Lindberg Tórarinsson (Iceland), Kenjiro Toyota (Canada), ***Oleg Travnikov (Meteorological Synthesizing Centre-East, Russia),*** Gabriel Treu (Germany), Erin Trochim (USA), Hilde Thelle Uggerud (Norway), ***Liisa Ukonmaanaho (Natural Resources Institute, Finland),*** Shannon van der Velden (Canada), Lindsay Vare (United Kingdom), Carolyn Vickers (Switzerland), Gisli A. Víkingsson (Iceland), ***Jussi Vuorenmaa (Finnish Environment Institute)***, ***Virginia Walker (Queen's University, Canada), Feiyue Wang (Canada),*** Cortney Watt (Canada), ***Pal Weihe (Faroe Islands),*** Jeffrey M. Welker (USA), Maria Wennberg (Sweden), ***Alex Whiting (Native Village of Kotzebue, AK, USA),*** Øystein Wiig (Norway), Alexis P. Will (USA), ***Simon J. Wilson (AMAP Secretariat),*** Katarzyna Wojczulanis-Jakubas (Poland), Glenn Yannic (France), ***David Yurkowski (Canada)***, ***Christian Zdanowicz (Uppsala University, Sweden), Leiming Zhang (Environment and Climate Change Canada),*** Tingjun Zhang (China), Yanxu Zhang (China)

Dedication

Robie W. Macdonald passed away on February 13, 2022. A Senior Research Scientist with Fisheries and Oceans Canada, Institute of Ocean Science and adjunct professor at the University of Manitoba's Centre for Earth Observation Science, Robie was a truly inspirational colleague, who will be greatly missed.

Robie's great intellect, multidisciplinary expertise and ability to make connections and see the 'big picture' meant that over his long career Robie conducted, spearheaded, and published ground-breaking research in areas such as marine geochemistry, oceanography, and contaminant sciences. Beyond that, it was his ability to communicate his science that made him such an inspiration to others. He was tireless in providing advice and suggestions, often with a sense of humour that was an essential part of his personality.

Over the past 30 years Robie contributed to AMAP assessments of mercury, POPs, climate change, Arctic Ocean acidification and Arctic cryosphere change. He conceived and led the first AMAP assessment addressing the impacts of Arctic climate change on contaminant pathways. This report is dedicated to his memory.

Contents

Preface

This assessment report presents the results of the 2021 AMAP Assessment of Mercury in the Arctic. The assessment updates information presented in earlier AMAP assessments delivered in 1998, 2002, 2011 and 2019.

The Arctic Monitoring and Assessment Programme (AMAP) is a Working Group of the Arctic Council. The Arctic Council Ministers have requested AMAP to:

- produce integrated assessment reports on the status and trends of Arctic ecosystems;
- identify possible causes for the changing conditions in the Arctic;
- detect emerging problems, their possible causes, and the potential risk to Arctic ecosystems including indigenous peoples and other Arctic residents;
- recommend actions required to reduce risks to Arctic ecosystems.

This report provides the accessible scientific basis and validation for any statements and recommendations made in related derivative products, including its summary for policy-makers that was delivered to the Arctic Council Ministers at their meeting in May 2021.

The present report includes extensive background data and references to scientific literature, and details the sources for graphics reproduced in summary products. Whereas the related Summary for Policy-makers contains recommendations that focus on policy-relevant actions, the conclusions and recommendations presented in this report also cover issues of a more scientific nature, such as proposals for filling gaps in knowledge, and recommendations relevant to future monitoring and research work.

This assessment of mercury in the Arctic was conducted between 2018 and 2020 by an international group of experts. The expert group members and lead authors were appointed following an open nomination process coordinated by AMAP. A similar process was used to select international experts who independently reviewed this report. Information contained in this report is fully referenced and based first and foremost on the results of research and monitoring undertaken since 2010. It incorporates some new (unpublished) information from monitoring and research conducted according to well-established and documented national and international standards as well as quality assurance/ quality control protocols. Care was taken to ensure that any critical probability statements made in this assessment were based exclusively on peer-reviewed materials. Access to reliable and up-to-date information is essential for the development of science-based decision-making regarding ongoing changes in the Arctic and their global implications.

The lead authors of this assessment have confirmed that both this report and its derivative products accurately and fully reflect their scientific assessment. All AMAP assessment reports are freely available from the AMAP Secretariat and on the AMAP website (www.amap.no), and their use for educational purposes is encouraged.

AMAP would like to express its appreciation to all experts who have contributed their time, efforts and data, in particular the lead authors who coordinated the production of this report. Thanks are also due to the reviewers who contributed to the assessment peer-review process and provided valuable comments that helped to ensure the quality of the report. A list of contributors is included in the acknowledgments at the start of this report and lead authors are identified at the start of each chapter. The acknowledgments list is not comprehensive. Specifically, it does not include the many national institutes, laboratories and organizations, and their staff that have been involved in contaminants-related monitoring and research. Apologies, and no lesser thanks are given to any individuals unintentionally omitted from the list.

The support from the Arctic and non-Arctic countries implementing research and monitoring in the Arctic is vital to the success of AMAP. AMAP work is heavily based on the ongoing activities of these countries, and the countries that provide the necessary support for the experts involved in the preparation of AMAP assessments. In particular, AMAP would like to acknowledge Canada, and the Kingdom of Denmark for their lead role in this assessment; AMAP would also like to thank Canada and Norway (Ministry of Foreign Affairs) for their financial support of this assessment work.

The AMAP Working Group is pleased to present its assessment to the Arctic Council and the international science community.

Rune Dietz (Assessment co-lead, Denmark)

John Chételat (Assessment co-lead, Canada)

Ben DeAngelo (AMAP Chair)

Rolf Rødven (AMAP Executive Secretary)

Tromsø, December 2021

1. Introduction

Authors: John Chételat, Rune Dietz, Simon Wilson

The 2021 AMAP Assessment of Mercury in the Arctic presents a comprehensive evaluation of the state of the science on mercury (Hg) in the circumpolar Arctic region. This chapter introduces the report by outlining the rationale, context and objectives of the assessment, and it provides readers with a guide to the structure and content of the report.

1.1 Why is an updated scientific assessment needed on mercury in the circumpolar Arctic?

Mercury contamination in the Arctic remains an environmental and human health issue due to the continued risk of elevated exposure in wildlife and in humans. Based on a thorough scientific assessment, a summary of the latest science-based, policy-relevant recommendations on anthropogenic and environmental drivers of Hg contamination and its effects is needed for the Arctic Council as well as to support government decision making.

Ten years have passed since the publication of the 2011 AMAP Assessment of Mercury in the Arctic (AMAP, 2011) during which time new advances have been made to address knowledge gaps in Arctic Hg science. This area of research has been highly productive; for example, a bibliometric search of journals in the Science Citation Index Expanded (SCIE) revealed 547 new articles published from 2011 to 2020 in environmental science and human health using the search terms 'Arctic' and 'mercury' (Clarivate Analytics, 2021). These studies have improved our scientific understanding of the Arctic Hg cycle, including its transport, biogeochemical processing, bioaccumulation in food webs, and the effects of Hg on wildlife and humans, which has relevant implications for policy-makers (see Figure 1.1). In addition, monitoring programs of Arctic countries have improved the time series of Hg measurements in air and biota, including humans, providing new information on recent trends in the Arctic environment.

Environmental change has continued to accelerate in the Arctic. Globally, the past decade was the warmest on record (NASA, 2020), and annual air temperatures in the Arctic between 2014 and 2018 exceeded those of any other year since the beginning of the 20th century (AMAP, 2019b). Arctic sea-ice minima for those same years were at record lows since measurements began in 1979 (AMAP, 2019b). The dramatic melting of glaciers, permafrost and icecaps, and the appearance of tundra wildfires are more symptoms of climate change in the Arctic. The 2011 AMAP Mercury Assessment concluded that climate change impacts on the Hg cycle were poorly understood (AMAP, 2011). Considerable research efforts over the last decade have now been made to address this knowledge gap, which will be summarized in the present assessment. The assessment also provides closer links between wildlife or human exposure to Hg and the related risks, as well as detailing how Indigenous Knowledge contributes to scientific work on Hg.

Since the last AMAP Hg assessment (AMAP, 2011), a new global treaty —the Minamata Convention on Mercury— has been negotiated, adopted in 2013, and entered into force in August 2017 (UNEP, 2019). This legally-binding instrument of the United Nations (UN) Environment Programme aims to protect human and environmental health from Hg pollution. The circumpolar Arctic is home to Indigenous Peoples, some of whom are among the highest Hg-exposed populations in the world (Basu et al., 2018). Biomonitoring of Hg in fish and wildlife has been conducted in the Arctic as early as the 1970s in coordination with AMAP, and the spatial and temporal trend datasets consolidated through AMAP are among the most comprehensive in the world (Evers et al., 2019); these data sets have shown the effect of the long-range transport of Hg on a presumed pristine environment. Global action is necessary to tackle this transboundary issue, and the latest advances in Arctic Hg science reported in this assessment aim to support the regulatory efforts and monitoring which have been an outcome of the Minamata Convention.

1.2 How has AMAP previously addressed the mercury pollution issue?

AMAP was established in 1991, under the Arctic Environmental Protection Strategy adopted by the eight Arctic countries (Canada, Denmark/Greenland, Finland, Iceland, Norway,

Figure 1.1 A visualization of the main fields of research investigating Hg in the Arctic based on the number of articles published in science journals from 2011 to 2020 (Clarivate Analytics, 2021). Note that multi-disciplinary journal articles may be counted in more than one field of research.

Russia, Sweden, United States of America) to monitor anthropogenic pollution in the Arctic, focusing on the levels, trends and effects of that pollution in the environment and in humans (AMAP, 1998). Over the next three decades, AMAP reported on measurements of Hg from across the circumpolar Arctic in a series of scientific assessments. The first of these, released in 1998, summarized existing information on a suite of contaminants: heavy metals (including Hg), persistent organic pollutants, and radioactive elements (AMAP, 1998). The subsequent 2002 assessment focused exclusively on metals and included greater detail on Hg pollution (AMAP, 2005). As more scientific information became available on Hg in the Arctic, an entire report was produced on the issue of Hg pollution (AMAP, 2011). Several assessments were also completed on human exposure to contaminants (including Hg), and the effects of these contaminants on Arctic populations (AMAP, 2003, 2009, 2015). In 2018, AMAP produced a scientific report on the biological effects of contaminants on Arctic fish and wildlife, which included an assessment of health risks from Hg exposure in combination with persistent organic pollutants, especially polychlorinated biphenyls (PCBs; AMAP, 2018a).

This series of AMAP scientific reports provided summaries of the most up-to-date policy-relevant science on Hg pollution in the Arctic. The assessments addressed key issues: the anthropogenic sources of Hg outside the Arctic and its transport to the Arctic; the accumulation of Hg in Arctic food webs; and the risk of effects on fish and wildlife and the humans who consume them. This work required, and continues to require, extensive international collaboration among national research and monitoring programs of the eight Arctic countries, including partnerships with Indigenous Peoples and with leading scientists. AMAP's coordination of Arctic monitoring and its network of international Hg experts has yielded strong scientific evidence to support regulatory processes on Hg pollution, particularly the UN Economic Commission for Europe's Convention on Long-Range Transboundary Air Pollution (CLRTAP; AMAP, 1998) and the UN Environment Minamata Convention on Mercury (Platjouw et al., 2018).

Since 2002, the UN Environment Programme has been producing Global Mercury Assessments (GMAs)—in 2002, 2008, 2013, and 2019—to provide science-based information in support of international efforts to reduce Hg pollution (UNEP, 2002; AMAP/UNEP, 2008, 2013; AMAP/UN Environment, 2019). Since 2005, AMAP has collaborated with the UN Environment Programme to produce the technical reports that provide the background for the GMAs. One of the outcomes of those collaborations has been the development of global inventories of Hg emissions to identify critical anthropogenic sources. The 2019 Global Mercury Assessment (AMAP/UN Environment, 2019) included an updated global inventory of Hg emissions and releases for 2015; the assessment also included information on sectors now under regulation by the Minamata Convention.

Box 1.1 The Minamata Convention, AMAP and the Arctic

The adoption of the Minamata Convention on Mercury in 2013 marked a breakthrough in the international effort to address Hg pollution. The UN treaty is the first global agreement to control emissions of Hg; it stipulates the phasing-out of the use of Hg in many products and requires parties to control, and, where feasible, to reduce Hg emissions from coal-fired power plants, coal-fired industrial boilers, non-ferrous metals production, waste incineration and cement clinker production. All Arctic Council member states apart from the Russian Federation are parties to the convention.

Under Article 22 of the convention, parties shall, beginning no later than 2023, evaluate the effectiveness of the convention. Work is underway to establish arrangements for this effectiveness evaluation that includes a provision for *"comparable monitoring data on the presence and movement of Hg and Hg compounds in the environment as well as trends in levels of Hg and Hg compounds observed in biotic media and vulnerable populations"*.

The Arctic monitoring and assessment work of AMAP, which is underpinned by national monitoring programs, has been recognized as one of the best examples of a regional Hg monitoring system that can help assess the effectiveness of the Minamata Convention. AMAP is therefore well positioned to continue to support the convention's further implementation.

1.3 How will the results of this AMAP assessment contribute to work under the UN Environment Minamata Convention on Mercury?

The 2021 AMAP Mercury Assessment is intended to contribute to future effectiveness evaluation under the Minamata Convention (see Box 1.1). The latest Arctic Hg science from the 2021 AMAP Mercury Assessment, including levels and trends, is available for use in a future evaluation of Hg contamination in the environment. Long-term temporal trend Hg datasets and broad geographic coverage of monitoring sites, compiled through AMAP's coordination of national monitoring programs of Arctic countries, provide an update on recent changes of Hg concentrations in environmental matrices and in biota. Arctic Hg databases have been generated, or updated, including DOME (ICES, 2020) and EBAS (NILU, 2020), in order to support the effectiveness evaluation. AMAP's network of Hg experts —who can provide context for and interpretation of the results— was strengthened through this assessment initiative and also through ongoing publication efforts by the scientists involved. Regionally-intensive research on Hg in the circumpolar Arctic, which is summarized in the 2021 AMAP Mercury Assessment, highlights the complexity of processes that affect the fate of global anthropogenic Hg emissions transported to the Arctic, including the role of climate change. Although environmental influences on Hg cycling likely differ in other regions of the world, Arctic Hg science provides important lessons on the interpretation of temporal and spatial trends with limited local sources of anthropogenic origin, which may be used for effectiveness evaluation of the Minamata Convention.

1.4 What are Indigenous Peoples' contributions to the study of mercury in the Arctic, and what are their perspectives on contaminant research and monitoring?

At the 2019 Arctic Council meeting in Finland, the "*important role of scientific research, together with traditional knowledge and local knowledge, in Arctic decision-making and the work of the Arctic Council*" was recognized by ministerial representatives of the eight Arctic countries (Arctic Council, 2019). As a Working Group of the Arctic Council, AMAP's strategic framework expresses this priority to work closely with Indigenous Peoples and local residents through inclusive partnerships:

> *"Arctic Indigenous Peoples are disproportionally affected by pollution and environmental change in the Arctic and have a unique understanding of how natural systems interact and change. AMAP's Guiding Principles include the respectful and comprehensive inclusion of Indigenous Peoples and their knowledge in all AMAP activities"* (AMAP, 2019a).

Active collaborations between Indigenous Peoples and scientists are critical to contaminants monitoring and research in the Arctic. Information generated from those partnerships support domestic and international initiatives to manage Hg contamination. The UN Environment Minamata Convention on Mercury, for example, includes text acknowledging findings which demonstrated "*particular vulnerabilities of Arctic ecosystems and indigenous communities because of the biomagnification of mercury and contamination of traditional foods*" (UNEP, 2019).

In the 2021 AMAP Mercury Assessment, for the first time, an entire chapter of the report is devoted to detailing the contributions of Indigenous Peoples to the study of Hg in the Arctic. Over 40 projects are reviewed to highlight the breadth of collaborations on contaminants research, including examples of bioaccumulation studies and Indigenous Knowledge which provided ecological information to interpret Hg data. Indigenous perspectives on contaminants research and monitoring are also presented with an eye to fostering further collaborations in the future and enhancing Hg programs in the Arctic.

1.5 What are the objectives of this assessment and how is it structured?

The 2021 AMAP Mercury Assessment presents a summary of recent advances in Arctic Hg science to address three overarching policy-relevant questions: (1) *What are the human and environmental drivers of Hg levels in the Arctic?* (2) *What are the effects of Hg on Arctic biota?* and (3) *What are the impacts on human health from Hg exposure in the Arctic?* The report is structured using a question-based approach where each chapter focuses on a key policy-relevant question using the latest available scientific information while also identifying uncertainties and knowledge gaps, and providing recommendations for future research and monitoring efforts. The Arctic Hg cycle is complex, with many processes occurring between the transport of Hg from anthropogenic emission sources to its bioaccumulation in biota and humans. Figure 1.2 (over page) provides a road map for the assessment, identifying where each aspect of the Hg cycle is addressed in the report.

Chapter 1: Introduction This chapter outlines the rationale, context and objectives of the assessment and provides a general overview of the report structure and content.

Chapter 2: Temporal trends of mercury in Arctic media This chapter presents a meta-analysis of available time series to evaluate changes in Hg in the Arctic over the last 20 years or longer. The datasets included measurements of Hg in air and precipitation, a new long-term time series based on analysis of tree rings, annual monitoring of Hg in marine, freshwater and terrestrial biota, and temporal studies of human exposure to Hg. Geographic patterns in trends are examined for dynamic areas of change in the circumpolar Arctic. The complex processes that influenced the temporal trends of Hg are described in subsequent chapters, particularly in chapters 3, 4, 5, 6 and 7.

Chapter 3: Changes in Arctic mercury levels: emissions sources, pathways and accumulation This chapter focuses on the sources and transport of inorganic Hg to the Arctic and its circulation within the Arctic. An updated inventory is presented of anthropogenic Hg sources contributing to contamination of the Arctic, as well as contributions of local Arctic sources of Hg. An updated Arctic Hg budget estimates how much Hg is deposited from the atmosphere and stored or transported within the Arctic in terrestrial, freshwater and marine environments.

Chapter 4: Changes in Arctic mercury levels: processes affecting mercury transformations and biotic uptake This chapter focuses on the environmental fate of methylmercury (MeHg), the more toxic organic form of Hg that biomagnifies through food webs. Environmental conditions and processes are described which result in the formation of MeHg in the environment, its entry into food webs, and its bioaccumulation in Arctic fish and wildlife. This chapter also includes a new Arctic MeHg budget which provides estimates of MeHg circulation in Arctic environments to identify key sources and transport pathways.

Chapter 5: How does climate change influence mercury in the Arctic environment and in biota? This chapter examines current evidence for the influence of climate change on Hg in the Arctic environment and in biota. The effects of climate change on physical and ecological processes are briefly summarized for Arctic marine, freshwater, and terrestrial ecosystems. Then, connections between those physical or ecological changes and the Hg cycle are assessed by examining evidence for effects on Hg transport, biogeochemical transformations of Hg, and Hg exposure to biota.

Chapter 6: What are the toxicological effects of mercury in Arctic biota? This chapter assesses the risk of toxicological effects to biota from Hg exposure. Tissue Hg concentrations are evaluated for a variety of available data on Arctic species of mammals, birds, fish, and invertebrates from terrestrial and/or marine environments. Population level effects, geographic hotspots and temporal changes in risk are examined for highly exposed wildlife.

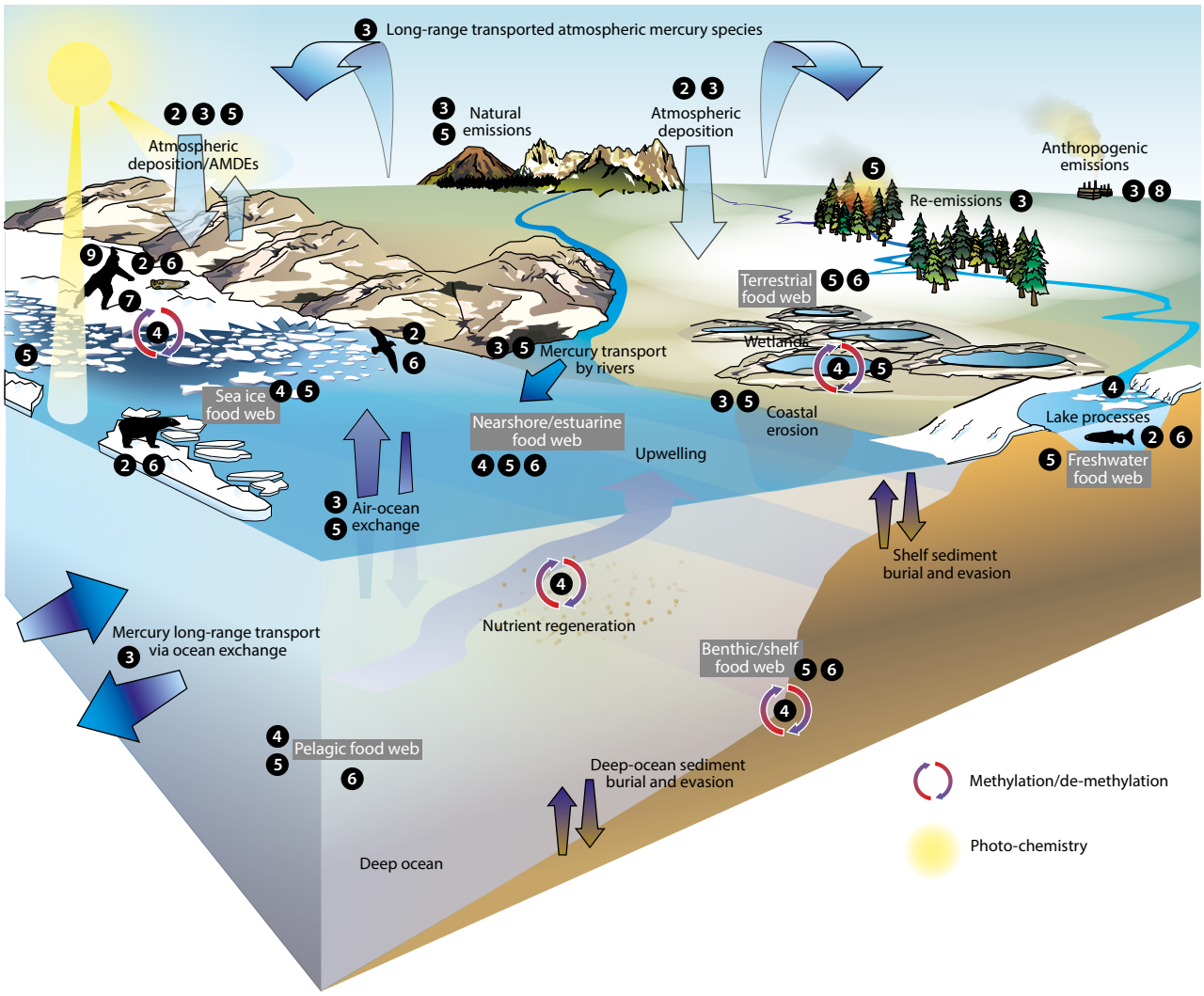

Figure 1.2 Conceptual diagram of key components of the Arctic Hg cycle. Chapter numbers (denoted by black circles) indicate where information on each component can be found in the assessment report. Note that Hg speciation is not characterized in the diagram.

Chapter 7: What is the impact of mercury contamination on human health in the Arctic? This chapter links findings from previous chapters on Hg in the environment and in biota with human exposure to Hg. Diet influences and human biomarker trends of Hg exposure are presented, as well as health effects on northern populations. Communication strategies are discussed that address the benefits of consuming traditional wild foods in balance with health risks from Hg exposure.

Chapter 8: What are the likely changes in mercury concentration in the Arctic atmosphere and ocean under future emissions scenarios? This chapter uses modeling approaches to project implications for the Arctic from different policy actions to reduce global anthropogenic emissions of Hg (i.e., no action to maximum feasible reductions). Model forecasting of changes to Hg concentrations in the atmosphere and Arctic Ocean from 2015 to 2050 show possible future effects of global reductions in anthropogenic emissions. Influences of environmental drivers related to climate change are also explored relative to anthropogenic Hg emissions.

Chapter 9: What are Indigenous Peoples' contributions to and perspectives on the study of mercury in the Arctic? This chapter highlights, for the first time, critical contributions of Indigenous Peoples to Hg research and monitoring in the Arctic, including through community-driven projects. Specific examples of recent initiatives are documented from circumpolar Arctic countries, and Indigenous contributions to policy development are also highlighted. A vision is presented for how inclusive and ethical partnerships between Indigenous Peoples and scientists should be conducted in the Arctic.

Chapter 10: Conclusions and Recommendations This chapter summarizes the main conclusions of the preceding chapters and findings in Hg science from the 2021 AMAP Mercury Assessment that address a series of policy-relevant questions concerning Hg transport, exposure and effects in the Arctic. Priorities for future research and monitoring of Arctic Hg are recommended.

2. Temporal trends of mercury in Arctic media

Coordinating Leads: Adam D. Morris, Frank Rigét, Simon Wilson

Contributing Authors: Bryan Adlard, Kristin Eccles, Rob Fryer, Karista Hudelson, Katrine Aspmo Pfaffhuber, Alexandra Steffen, Geoff Stupple, Philippe J. Thomas

Contributors: *abiotic (air, precipitation, deposition) time series data:* Wenche Aas, Torunn Berg, Kaare Kemp, Katriina Kyllönen, Katrine Aspmo Pfaffhuber, Henrik Skov, Alexandra Steffen, Geoff Stupple, Bernard Firanski. *biota time series data:* Jon Aars, Magnus Andersen, Birgitta Andreasen, Aurore Aubail, Claus Bech, Pierre Blévin, Birgit Braune, Paco Bustamante, Jan Ove Bustnes, Paloma Carvalho, Oliver Chastel, Sara Danielsson, Krishna Das, Andrew Derocher, Rune Dietz, Sandra Drewes, Igor Eulaers, Marlene Evans, Anita Evenset, Suzanne Faxneld, Steve Ferguson, Jérôme Fort, Eva Fuglei, Geir Gabrielsen, Mary Gamberg, David Gremillet, Ingeborg Hallanger, Magali Houde, Sigga Joensen, Jane Kirk, Igor Lehnherr, Robert J. Letcher, Anna Lippold, Lisa Loseto, Melissa McKinney, Børge Moe, Derek Muir, Sara Pedro, Marianna Pinzone, Trevor Porter, Amanda Poste, Frank Rigét, Heli Routti, Christian Sonne, Gary Stern, Sabrina Tartu, Philippe J. Thomas, Cortney Watt, Øystein Wiig. *human time series data:* Khaled Abass, Caty Blanchette, Alexey Dudarev, Eva Cecilie Bonefeld-Jorgensen, Brian Laird, Melanie Lemire, Manhai Long, Karin Nordstrom, Kristin Ólafsdóttir, Mylene Ratelle, Arja Rautio, Maria Wennberg. *statistical methods:* Rob Fryer

2.1 Introduction

The 2011 AMAP Mercury Report (AMAP, 2011) included a comprehensive review of the time series of mercury (Hg) in abiotic and biotic media that were available at that time. It addressed long-term datasets (i.e., those comparing modern with historical or pre-industrial Hg concentrations) to estimate the relative importance of natural and anthropogenic Hg inputs in modern biota and the environment. It also addressed short-term datasets (i.e., those covering the past one to three decades) which reflect more recent changes in Hg concentrations and used this information to project some likely trends in the near future.

Continued monitoring efforts by national programs (Denmark/Greenland: AMAP Core Program; Canada: Northern Contaminants Program; NCP; Europe: AMAP, OSPAR) have generated new time series for Hg in an array of matrices and locations in the circumpolar Arctic. Air monitoring data are available from additional stations, and several biota time series have been extended. In addition to providing information on trends at individual sites, the available data allow spatial patterns in trends to be considered.

The increasing length (and associated power) of many of the time series, especially biota time series, means that, in the current assessment, a greater emphasis has been given to trends observed over the most recent 20-year period, from 1999 to the most recent year of data available. In the case of the longer time series, the changes over the past 20 years can be compared with those over the entire period of monitoring. This can provide insight not only into trends that may be related to changing emissions but also into trends that may be due to the influence of other changes that the Arctic is undergoing, including those directly and indirectly associated with climate warming. Wildlife is exposed to Hg primarily though the diet, so environmental changes that affect Arctic food-web structure and composition are particularly relevant when assessing changes in biota over time. These aspects of Hg in the Arctic are explored in more detail in Chapters 3, 4 and 5. The temporal trends described in this current chapter are also evaluated in Chapter 6 in relation to risk thresholds for wildlife health effects.

As in the previous AMAP mercury report, the current assessment includes a chapter on the impacts associated with Hg on human health in the Arctic (see Chapter 7). This work has been coordinated with a new AMAP report on human health in the Arctic (AMAP, 2021). Only a very few time series of Hg in human populations are available and of adequate length to assess temporal trends, but they do provide some comparative international data (see Section 2.3.3). Mercury levels in human populations are more difficult to relate to global Hg emissions or environmental concentrations than to levels in other biota as they are influenced by dietary choices, including interventions such as food advisories and methods of food preparation. Monitoring of contaminants in Arctic human populations has focussed on vulnerable groups, in particular children and women of child-bearing age. Limited time series for Hg in Arctic human biomedia are therefore addressed separately from other biotic temporal trends and are referenced in Chapter 7.

The temporal trends assessment presented in this chapter focuses on recent trends (time series covering the past few decades) of Hg in air and biota, with a particular emphasis on trends since 1999. The temporal trends are evaluated using consistent, robust statistical approaches with the objective of producing results that can be compared through a meta-analysis. One objective of this chapter is to provide basic information on temporal trends and spatial patterns in the trends; this will also be considered in more detail in subsequent chapters.

This chapter is structured around a set of policy-relevant science questions as follows: 1) What are the currently available time series and statistical analysis of Hg concentrations in the Arctic for air (Section 2.2.1), for precipitation/wet deposition (Section 2.2.2), in biota (Section 2.2.3) and in humans? (Section 2.2.4); 2) Are concentrations of Hg changing over time in Arctic air and precipitation (Section 2.3.1), in Arctic biota, (Section 2.3.2) and in Arctic human populations? (Section 2.3.3); and 3) Are there spatial patterns of Hg trends in biota from the Arctic? (Section 2.4).

2.2 What time series and statistical analysis are available?

Time series for updating information on trends in recent decades were available for air and precipitation (see Appendix Table A2.1), biota (see Appendix Table A2.2) and human biomedia (see Section 2.2.4). In addition, recent development of

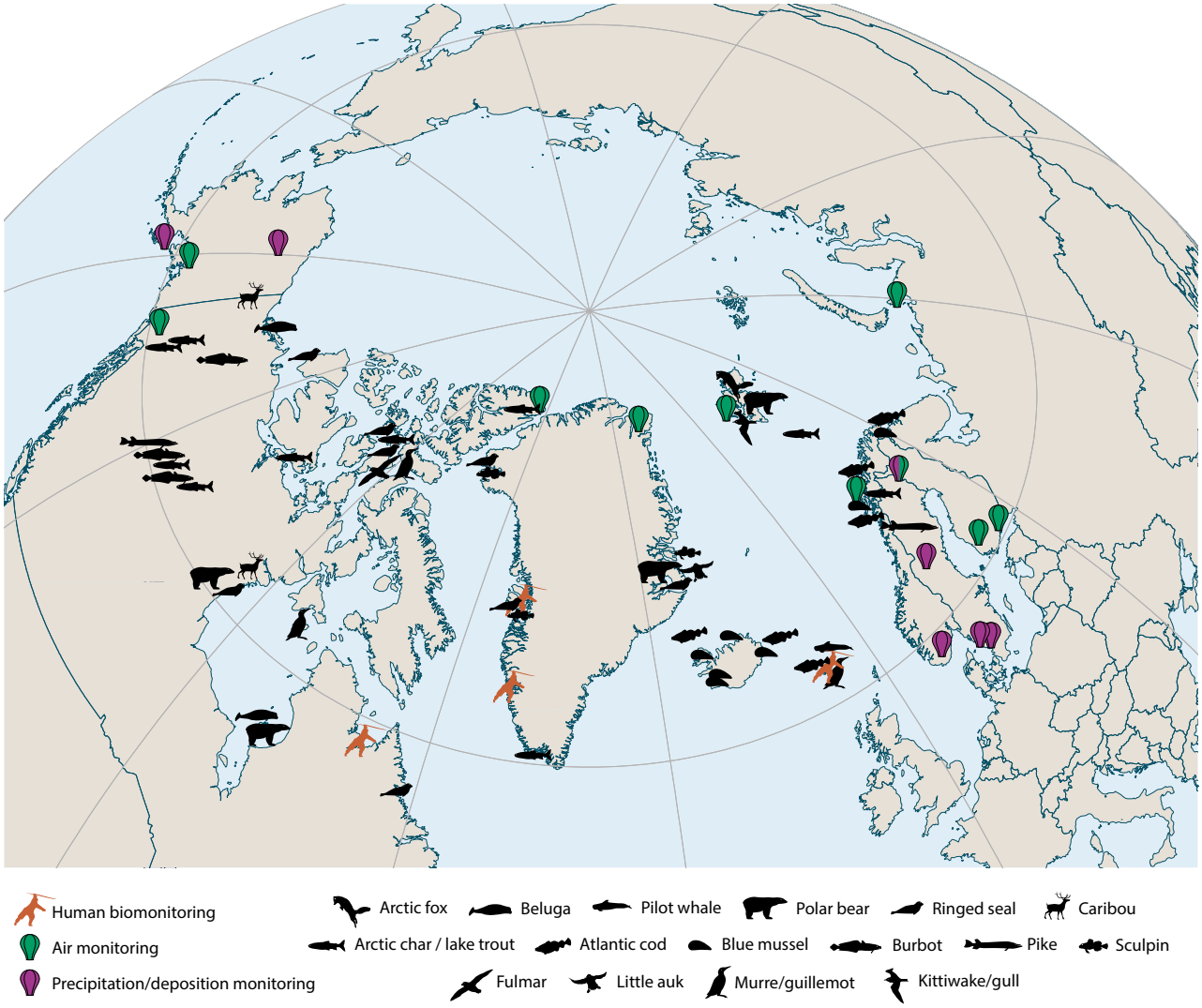

Figure 2.1 Map of sampling locations for recent Hg time series included in the current assessment. The map shows sites of air monitoring and wet deposition monitoring; human biomonitoring; and biota monitoring sites for different species.

a new environmental archive approach for measuring Hg time series in tree-rings provided new information on longer-term Hg trends from three sites in northern Canada. The locations of the time series considered in the current assessment are represented in Figure 2.1.

Time series in air and/or precipitation were available for all Arctic nations apart from Iceland, albeit with limited geographical coverage for large parts of the Arctic. Time series datasets in biota were provided by all Arctic countries except for Russia and the USA; Alaskan seabird time series datasets were reported in the 2011 AMAP Mercury Report but have not been updated with Hg data since that time. Human biomonitoring time series for Hg were available from only four locations: one in Canada (Nunavik); two in West Greenland; and one, derived from cohort studies, in the Faroe Islands.

2.2.1 Air

Time series of total gaseous mercury (TGM) in air (see Appendix Table A2.1) were available from 10 AMAP air monitoring stations spanning around half of the circumarctic region, with sites in the following locations: Alaska, USA; northern Canada; Northeast Greenland; Svalbard; Sweden; Finland; and northwestern Russia. These include three High Arctic background air monitoring stations: Alert, Canada; Villum Research Station (Station Nord), Greenland; and Zeppelin Mountain, Ny-Ålesund, Svalbard). The longest continuous record of Arctic atmospheric Hg is from Alert, Nunavut, Canada, which started monitoring in 1995 (ECCC, 2016; AMAP/UN Environment, 2019). Mercury air monitoring at Amderma, Russia has been conducted from 2001 to 2009 and between late 2015 and early 2017, but available time series data were not included in the trend analyses due to the data gap between 2009 and 2015. Similarly, data for Station Nord from 2001 and mid-2002 were excluded because of the large data gap between these earlier times and the continuous monitoring that started in 2008. The four sites (Alert, Zeppelin, Station Nord and Amderma) are considered 'coastal Arctic sites' due to their location and the propensity for the occurrence of atmospheric mercury depletion events (AMDEs). The continental North American sites (Little Fox Lake, Yukon, Canada; 2007–present and Denali National Park, Alaska, USA; 2014–present) are

considered 'Subarctic sites'. Subarctic European sites include both the coastal site Andøya, Norway (2010–present; Berg et al., 2008) and the continental site Pallas, Finland (2008–present; Angot et al., 2016). Total gaseous mercury (TGM) has also been collected through a weekly manual 24- to 48-hour integrated sampling program at Pallas since 1996. Further south in Finland, the continental site Hyytiälä (2008–2018) and the coastal site Virolahti (2008–2018) are also included in the trend analysis. Two of the coastal High Arctic sites, Alert and Zeppelin, have long-term gaseous oxidized mercury (GOM; also commonly abbreviated as RGM) and particulate bound mercury (PHg; also commonly abbreviated as PBM, HgP or PM) measurements covering the periods 2002–present and 2007–present, respectively. Air monitoring locations are shown in Figure 2.1, and daily mean TGM (ng/m^3) along with summary statistics for all available data are provided in Table A2.1.

Most of the available air monitoring data are reported as hourly-averaged data; these were aggregated to daily mean concentrations prior to statistical analysis. Data were only considered acceptable for statistical trend analysis when there was 75% daily coverage in order to avoid bias caused by diurnal variations. Samples collected with manual traps have been integrated over a 24- to 48-hour period. Sampling times for the GOM and PHg monitoring programs at Alert and Zeppelin varied (between 2- and 4-hour intervals) and there was a slight difference between the two data sets in the way GOM and PHg concentrations were calculated in the reported data. Therefore, concentrations from Alert were re-calculated from the raw data to match those from Zeppelin. Gaseous oxidized mercury and PHg daily mean concentrations were accepted for trend analyses if they met the 75% daily maximum coverage requirement (based on the sampling period of each day) to account for diurnal variability.

With temporal coverage varying from 5 years to 23 years, data analyses were performed for both entire time series and for overlapping time series from the decadal period 2008 to 2018. This dual approach permits the best understanding of trends at individual sites and allows for a direct comparison of trends over a consistent period between sites.

To calculate the trends, the seasonal Mann-Kendall test for trends and the related Theil-Sen slope calculation analysis (see Gilbert, 1987) was employed using daily mean concentration data. This method has been used to assess temporal trends with atmospheric Hg data sets such as those from the Arctic, Subarctic and temperate sites (Cole and Steffen, 2010; Berg et al., 2013; Gay et al., 2013; Cole et al., 2014; Weiss-Penzias et al., 2016). The extension of the non-parametric Mann-Kendall method is recommended for use on data that are not normally distributed and which may have data gaps; both conditions are present in the datasets considered. This method compares the same season across several years, using the Mann-Kendall test to confirm or reject the presence of a slope and the Theil-Sen regression to determine its magnitude. This methodology was applied to the atmospheric Hg data collected at the 10 Arctic and Subarctic sites discussed previously and outlined in Appendix Table A2.5.

2.2.2 Precipitation/wet deposition

Mercury wet deposition has been measured for more than 30 years within the National Atmospheric Deposition Program/Mercury Deposition Network (NADP/MDN), Environment and Climate Change Canada – Atmospheric Mercury Monitoring (ECCC-AMM, previously CAMNet) and the European Monitoring and Evaluation Program (EMEP) over varying time periods; several of the sites monitored are also part of the AMAP monitoring network. Data from the AMAP and EMEP networks are archived in the EBAS database at the AMAP atmospheric data centre at NILU, Norway.

Most precipitation monitoring sites north of 55°N are in Low Arctic or Subarctic areas, reflecting the practical difficulties associated with precipitation monitoring at High Arctic sites due to low temperatures and extreme conditions. Only four are located within the AMAP circumpolar region and classified as Subarctic sites, with only one site (Pallas, Finland) having records long enough for robust trend analysis. Therefore, long-term time series of Hg in precipitation from sites outside but close to the Arctic area have been included in this analysis (see Figure 2.1). The sites located in Scandinavia are part of the EMEP measurement network, while the sites in the USA are part of the NADP/MDN.

Samples collected weekly are averaged to monthly volume-weighted means. The months are grouped together as seasons: winter (December, January and February), spring (March, April and May), summer (June, July and August) and autumn (September, October and November).

The temporal coverage varied from 7 to 29 years, and trend analysis was performed on both all data available and on overlapping data from 2009–2018.

2.2.3 Biota

Biota time series of total mercury (THg) were constructed from data extracted from databases maintained at the AMAP Marine Thematic Data Centre at ICES[1] (mainly Icelandic and Norwegian fish and shellfish monitoring data); and additional data reported from national monitoring and research programmes in Canada (NCP),[2] the Kingdom of Denmark (Greenland and Faroe Islands), Norway and Sweden. Although time series were assessed on the basis of THg, it is worth noting that for birds and mammals considered in this trend assessment almost all Hg in tissues is present in the form of methylmercury (MeHg), with the exception of mammalian liver and kidney (AMAP, 2011).

Where appropriate, marine mammal data were sub-divided by age and sex, including some seabirds, ringed seals (*Pusa hispida/Phoca hispida*), polar bears (*Ursus maritimus*), or size, such as cetaceans. The resulting 124 biota time series were filtered to ensure they met the criteria of having at least 6 years of data and data for the post-2015 period. Time series yielding a total of 110 biota time series were appropriate for trend assessments (see Appendix Table A2.2).

[1] See: www.ices.dk

[2] See: www.science.gc.ca/NCP

The bulk of the time series concerned marine mammals (54 time series); the majority of these were freshwater fish (19), followed by seabirds (12) and marine invertebrates (mussels; 12), marine fish (11) and terrestrial mammals (2). Time series ranged from 6 to 46 years with a mean range of ~16 years. In addition to the analysis for trends, the biota the time series data were examined with respect to their adequacy to detect trends with a given statistical power (see Section 2.2.3.1).

Temporal trends of Hg in biota were analyzed using mixed models based on individual $\log_e$-transformed THg concentrations (µg/kg). The analyses used a dedicated statistical application (AMAP, 2020) coded in the R statistical environment (R Core Team, 2020). The application has evolved from a method originally developed by Fryer and Nicholson (1999) and has also been used to analyze contaminant time series in biota, sediment and water under the OSPAR and HELCOM programs. The current approach was similar to that used in previous AMAP assessments, which employed the PIA statistical application (Bignert et al., 2004; Rigét et al., 2011a). However, it modeled individual concentrations rather than annual medians and used smooth terms rather than 3-years running means to evaluate the degree of non-linearity. A full description of the methods can be found in AMAP (2020).

Two key components of the analysis were the selection of a parsimonious model that adequately described the pattern of change over time, and the construction of a summary metric that allowed patterns of change to be compared across time series. To assess the pattern of change, a model with a ($\log_e$-) linear trend was fitted:

$$\log_e \text{ THg concentration} \sim \alpha + \beta \text{ year} \quad (1)$$

This first model (1) was compared to a second model (2) with a non-linear trend, in which $\log_e$ THg concentrations varied smoothly (and non-linearly) over time:

$$\log_e \text{ THg concentration} \sim s(\text{year}) \quad (2)$$

Smoothers (s) were fitted on up to four degrees of freedom depending on the length of the time series (as described in AMAP, 2020). The selected model was that with the lowest Akaike Information Criterion corrected for small sample size (Burnham and Anderson, 2002). The significance of the fitted trend (either linear or non-linear) was assessed by a likelihood ratio test.

The metric used to summarize the pattern of change in each time series was the annual percent (%) change in concentration in the most recent 20-year period (1999–2018) which, for convenience, is referred to as the 'recent trend'. The metric was chosen because it focussed on a period covered by all the time series (only 29 of the 110 time series started after 1999) and because it allowed meaningful comparisons between time series with linear and non-linear trends. When the fitted trend was linear, the recent trend was calculated as follows:

$$\text{recent trend (\%)} = 100\,(\exp(\hat{\beta}) - 1) \quad (3)$$

In (3), $\hat{\beta}$ was the estimate of β in equation (1). The exponentiation in equation (3) back-transforms the annual absolute change in log concentration, measured by β, to the annual percentage change in concentration. When the fitted trend was non-linear, the recent trend was calculated by taking the change in concentration between the start and end of the 20 year period and converting it to the equivalent annual percentage change had the trend been linear, as follows:

$$\text{recent trend (\%)} = 100\left(\exp\left(\frac{\hat{s}(2018)-\hat{s}(1999)}{(2018-1999)}\right) - 1\right) \quad (4)$$

In (4), $\hat{s}(2018)$ and $\hat{s}(1999)$ were the fitted log concentrations in 2018 and 1999 respectively (see equation 2). Where time series began after 1999 or ended before 2018, the start and end years were adjusted accordingly. Additional details of the statistical methods are provided in Appendix 2.3 (Fryer, pers. comm., 2019).

As well as assessing the significance of the linear or non-linear trend over the whole time series (using the likelihood ratio tests mentioned above), it was also possible to assess the significance of the recent trend. For linear trends, the significance levels were identical, since they were both based on $\hat{\beta}$. For non-linear trends, the significance levels differed depending on the pattern of change. For example, it would be possible to have a significant non-linear pattern of change over the whole time series, but a non-significant recent trend if, for example, concentrations declined in the early part of the time series (before 1999) and then stabilized.

2.2.3.1 Power analysis for biota

The previous AMAP mercury assessment (AMAP, 2011) included statistical power analyses that assessed whether the biota time series available at the time were sufficient to detect statistically significant trends ($p<0.05$) with power greater than or equal to 80%. This procedure was repeated in the current assessment to re-evaluate the extent to which the AMAP monitoring program for Hg in biota is now capable of detecting trends. The power analysis is based on statistical parameters generated as part of the applied method (see Appendix 2.3 and Fryer, pers. comm., 2019; Fryer and Nicholson, 1999).

The power to detect a trend in a time series depends on the magnitude and pattern of the trend, the number of years of data and the number of samples collected each year, whether the series is sequential or contains gaps, the magnitude of the variance components in the data, the test used and the significance level of the test. The current investigation considered the power to detect a log-linear change in concentration using a two-sided F-test at the 5% significance level (α=0.05). In particular, the following metrics were calculated for each time series:

- power to detect a 5% annual increase given the current configuration of years;
- lowest annual increase detectable with power ≥80% given the current configuration of years;
- power to detect a 5% annual increase given 10 sequential years of monitoring;
- lowest annual increase detectable with power ≥80% given 10 sequential years of monitoring.

Full details of the power calculations can be found in AMAP (2020).

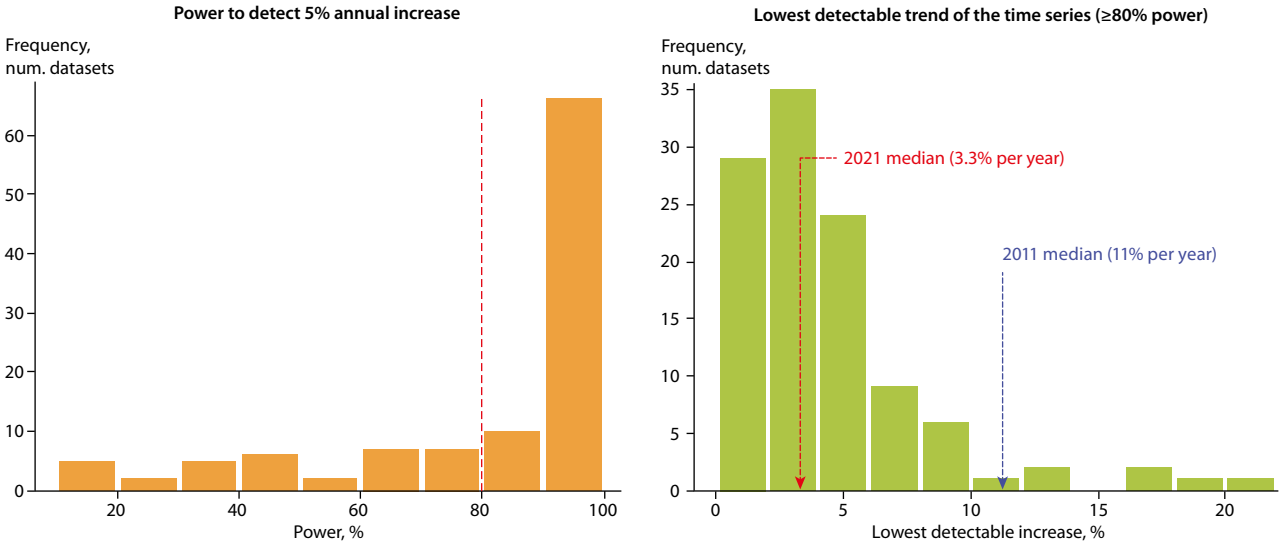

Figure 2.2 Histogram of the power to detect a 5% annual increase with ≥80% power indicated by dashed line (left panel), and the lowest annual increase detectable with ≥80% power (right panel) given the current configuration of years in the available biota time series for Hg.

In the current assessment, 77 of the 110 time series (70%) have a (statistical) power ≥80% to detect a 5% annual increase with their current configuration of years, meeting or exceeding the specified criteria for detection of trends (see Figure 2.2, left panel). This represents a major improvement over the previous assessment (AMAP, 2011), where only 16 (19%) of the 84 time series available at that time had a power ≥80% (recalculated from Rigét et al., 2011a). The improvement in power was also evident in the lowest annual increase detectable with ≥80% power, which had a median value of 3.3% in the current assessment compared to a value of 11% in the 2011 assessment (recalculated from Rigét et al., 2011a; Figure 2.2).

Overall, the ability of the AMAP monitoring programme to detect trends in time series of THg concentrations in biota with the desired level of statistical power has greatly improved since 2011. Much of the improvement in power is likely due to the additional years of monitoring, which have extended existing time series from a mean length of 11 years in the previous assessment (AMAP, 2011) to 16 years in the current assessment. The addition of new time series with high power (i.e., seabirds, mammals) has also contributed to this improvement.

Implications of the power of trend detection for AMAP monitoring

The selection of species and tissue for monitoring temporal trends in Hg concentrations in biota involves a number of considerations. These include objectives with respect to detection of trends for various purposes, as well as practical considerations including funding limitations, species availability, and the collection of samples under challenging Arctic conditions, in addition to the maintenance of monitoring efforts over a long period (decades).

Table 2.1 presents the power of the available time series for each animal group/tissue assuming 10 years of sequential annual monitoring. This makes it possible to evaluate power while ignoring the effect of different numbers of years and the influence of gaps in time series when there was no sampling. In the currently available datasets, time series based on seabird eggs have the greatest power. Seabirds are used in trend monitoring studies across the Arctic, including retrospective trend studies using archived samples. Species selection is an important consideration as some species are migratory, while others are resident and overwinter in the Arctic, and different species occupy different trophic positions. Monitoring using bird eggs generally assumes that Hg concentrations represent the uptake in the adult birds in the local (breeding) area and not areas outside the breeding season (e.g., wintering areas). However, contaminant levels are likley affected by contamination in wintering areas in (partly) capital breeders such as common eider (*Somateria molissima;* Sénéchal et al., 2011).

Table 2.1 also indicates that monitoring invertebrates (mussels) can also provide powerful time series for Hg trend evaluation; however, the spatial coverage in the current assessment is limited to Norway and Iceland. As sessile, filter-feeding organisms, mussels can provide valuable spatio-temporal information on contaminant distributions and trends. However, despite relatively high power (see Table 2.1), few significant temporal trends were detected in the current assessment. Establishing circumpolar bivalve monitoring could be a relatively practical approach to filling geographical gaps in Hg spatial trend

Table 2.1 Statistical power (mean %, and SD) and number of time series by animal group/matrix to detect a 5% annual increase in total mercury (THg) given 10 sequential years of monitoring at the 5% significance level. Only group/matrix combinations with 5 or more time series are shown.

Species group	Matrix	Power (%)	Number of series
Invertebrates (mussels)	Soft body tissue	52 (31)	12
Marine fish	Muscle	29 (16)	8
Seabirds	Eggs (homogenate)	68 (12)	5
Marine mammals	Muscle	48 (23)	15
Marine mammals	Liver	19 (13)	30
Marine mammals	Hair	28 (8)	6
Freshwater fish	Muscle	49 (24)	18

monitoring, but this may not be ideal for temporal trends. Both seabird eggs and mussels are relatively easy to sample in a standardized manner (e.g., with respect to time of sampling), though care is needed if sampling from small populations or endangered species. Powerful time series were also detected for marine mammals (muscle) and freshwater fish, the latter notably more powerful than the currently available time series for marine fish. The trends in these species' groups are also most relevant for evaluating risks to humans associated with dietary intake of traditional foods by some Arctic people, or in the case of high trophic level marine mammals, considering wildlife health concerns (see Chapter 6). As general indicators of ecosystem state, time series would ideally represent a range of ecosystem components and animal groups and take account of a number of potential confounding factors. Some of these are associated with direct and indirect influences of climate change on processes that affect exposure and uptake by biota, including changes in ecosystem structures, migration patterns, etc.; these issues are addressed in more detail in Chapters 4 and 5. These biota time series will also provide insights regarding the effectiveness of measures taken to reduce and eliminate anthropogenic Hg emissions through the Minamata Convention on Mercury.

2.2.4 Human Biomonitoring

AMAP monitoring in Nunavik (Canada), and West Greenland and the Faroe Islands (Kingdom of Denmark) produced four time series of THg levels in human blood, updating data previously reported in AMAP reports (AMAP, 2011, 2015). In the Nunavik, Disko Bay and Faroe Island time series, individual data were not available (due to ethical constraints applicable to the exchange and publication of human data); consequently, annual geometric mean concentrations were analyzed by log-linear regression analysis. Individual data were available for pregnant women from Nuuk, West Greenland and, for these data, trends were assessed using log-linear regressions of annual medians for women of 30 years or more and women of less than 30 years. Unlike the other locations, which focussed on blood concentrations in pregnant women, the Faroe Island data were collected at intervals within the same cohort of individuals over time, with 5 cohorts in total (Weihe and Joensen, 2012; AMAP, 2015; Petersen, pers. comm., 2019). Therefore, measurements in different years are not statistically independent in these time series. Differences in study design and analytical methods for humans made the results incomparable between locations. In the current assessment, the focus is on Cohort 1 as it was in this cohort that the only significant relationship was observed. Results of the human temporal trend analyses are presented in Section 2.3.3, and the factors affecting Hg in Indigenous Peoples in the Arctic are discussed in detail in Chapter 7.

2.3 Are concentrations of mercury changing over time?

Assessment of temporal trends will be an important element in the assessment of the effectiveness of international efforts aiming to reduce Hg emissions and their effects, such as the global Minamata Convention on Mercury and Heavy Metals Protocol to the UNECE Convention on Long-range Transboundary Air Pollution (CLRTAP). Understanding the underlying reasons for the direction and strength of temporal trends is equally important and requires knowledge of global, regional and local factors of influence.

The 2011 AMAP Mercury Assessment (AMAP, 2011) evaluated available time series data for Hg in air from four locations in Canada, Iceland, Sweden/Finland and Russia. It further reviewed results from an analysis of around 80 biota time series using a consistent statistical analytical methodology.

Newly available data have extended many of the time series that were evaluated in the 2011 AMAP assessment and added new time series in some areas, though some time series have been discontinued or lacked new data (see Section 2.2). Based on the statistical analyses described in Section 2.2 and Appendix 2.3, the question of whether concentrations of Hg in the Arctic are changing over time has been re-evaluated.

The increasing length (and associated power) of many of the time series, especially those in biota, means that, in this re-evaluation, a greater emphasis has been given to changes observed over the past 20 years. In the case of longer time series, the trends over the past 20 years can be compared with those over the entire period of monitoring to gain insight into changes that may be related to changing emissions or may be due to shifts in other factors of influence, such as those directly and indirectly associated with climate warming. The influence of emissions and climate change are discussed in Chapters 4 and 5, respectively.

2.3.1 Trends of total and speciated mercury in air, precipitation, and deposition

Atmospheric transport is an important input pathway of Hg to the Arctic. Long-range transport of Hg from emission sources to the Arctic is enabled by its long atmospheric residence time (AMAP/UN Environment, 2019). Deposition processes (wet or dry) in the Arctic can be enhanced by unique conditions, resulting in an input of Hg to the surface, where it may become available for methylation and subsequent bioaccumulation and biomagnification in food webs, or it may be re-emitted to the atmosphere. Therefore, understanding the transport, deposition and surface emissions of atmospheric Hg to the Arctic (see Chapter 3) is important also to understanding human and wildlife exposure to Hg.

The dominant species of Hg in the air is gaseous elemental mercury (GEM), which has an atmospheric residence time of 6 to 18 months (Steffen et al., 2014; Angot et al., 2016; Ren et al., 2020). Gaseous elemental mercury is subject to oxidation chemistry where it is converted to an ionic species in the gas phase known as gaseous oxidized mercury (GOM). Total gaseous mercury (TGM) represents the combination of GEM and GOM in the air. Frequently, GOM species associate to particles and/or aerosols and are then present as particulate mercury (PHg).

Atmospheric Hg has been measured at several sites across the Arctic for the past 25 years (Schroeder et al., 1998; Lindberg et al., 2002; Dommergue et al., 2003, 2010; Poissant and Pilote, 2003; Wängberg et al., 2003; Lu and Schroeder,

2004; Skov et al., 2004, 2020; Sprovieri et al., 2005; St. Louis et al., 2005; Brooks et al., 2006; Faïn et al., 2006; Kirk et al., 2006; Hedgecock et al., 2008; Nguyen et al., 2009; Cole and Steffen, 2010; Durnford et al., 2010; Nghiem et al., 2012; Berg et al., 2013; Steffen et al., 2013; Moore et al., 2014; Obrist et al., 2017; Kamp et al., 2018). Over varying time periods, ten sites within the AMAP circumpolar region have records of TGM that are long enough for robust trend analysis (i.e., longer than 5 continuous years). These sites have been operated and maintained by various governments and research institutes over time. TGM data have been primarily collected using an automated, continuous measurement analyzer, which captures TGM on a gold bead trap and provides subsequent *in situ* analysis. Manual sampling methods have also been used to capture TGM using various types of gold traps, which are then shipped to and analyzed in a laboratory. This latter sampling method typically results in lower frequency of data. In addition to TGM, some sites monitor GOM and PHg but, due to the complexity of this type of measurement, only data from 2 sites are currently available. GOM is operationally defined by its measurement process, which is the gaseous Hg species collected on a KCl coated annular denuder. Particulate-bound Hg is measured as Hg adhered to particles <2.5 μm. These two continuous measurements in the Arctic have been made using the Tekran 1130 and 1135 instruments, respectively. Particulate-bound Hg may also be collected on a filter surface and manually analyzed for Hg concentration in the laboratory. This method results in a lower frequency of data and is not limited to aerosol sizes below 2.5μm.

In the polar coastal boundary layer, GEM has been found to react in the springtime with halogen radicals in the atmosphere. The primary reaction species are bromine radicals (either as BrO or Br) produced through the 'bromine explosion' photochemical process (Simpson et al., 2007). In reaction to the bromine radicals, GEM is photochemically oxidized to inorganic Hg compounds in the gaseous form which results in a concurrent depletion of GEM and increase in oxidized Hg species. This leads to phenomena known as atmospheric mercury depletion events (AMDEs; Schroeder et al., 1998). The oxidized forms of GEM are thought to be some version of an Hg-Br, Hg-Cl or Hg-O species (Steffen et al., 2008, 2012). When particles are present, the produced GOM preferentially adheres to them. During AMDEs, when fewer particles are present in the air, GOM is the predominant species of Hg; when more particles are present, the predominant species of Hg is PHg (Steffen et al., 2014). This chemistry has an impact on the seasonal variation and time trends of atmospheric Hg at various Arctic locations.

Two pathways for atmospheric Hg transfer to surface environments exist, each with their own characteristic set of processes: wet and dry deposition. Wet deposition of Hg is defined as the air-to-surface flux in precipitation (occurring as rain, snow, fog or ice) which mainly scavenges GOM and PHg from the atmosphere, whereas dry deposition is air-to-surface Hg flux in the absence of precipitation and is believed to include all three Hg phases (Lindberg et al., 2007). Establishing the rate of Hg deposition as well as the surface-to-air emission of Hg is a key element in understanding the environmental cycling of Hg and its impact on aquatic and terrestrial ecosystems and on the overall Hg budget in the Arctic ecosystem. A number of researchers have estimated that direct wet deposition accounts for between 50% (Landis and Keeler, 2002) and 90% (Mason et al., 1997) of the Hg entering surface waters, whereas others find dry deposition to account for the majority of Hg deposition (Selin and Jacob, 2008; Wright et al., 2016). Since wet deposition accounts for a large component of the Hg input to the environment, monitoring Hg in precipitation is the most direct way of assessing inputs from the atmosphere to sensitive ecosystems.

2.3.1.1 Seasonality of atmospheric mercury

Total gaseous mercury (TGM) daily mean concentration data were split into four seasons: winter (December, January and February), spring (March, April and May), summer (June, July and August) and autumn (September, October and November). Mean Hg concentrations for each season were then analyzed from 1995 to 2018 (see Figure 2.3; descriptive statistics for annual and seasonal mean daily TGM concentration for all years are presented in Table A2.5).

Seasonal cycles of atmospheric Hg concentrations have been observed and reported elsewhere (Steffen et al., 2005; Cole and Steffen, 2010; Angot et al., 2016). General North American seasonal patterns have historically been observed to have low concentrations during the autumn and higher concentrations during the winter (Cole et al., 2014). In a recent investigation of Arctic coastal sites, concentrations were at a maximum in the summer, minima in the autumn and spring and slightly elevated in the winter in three of the four sites; conversely, the patterns were the opposite at the fourth site (Angot et al., 2016). At sites further inland, the seasonal variation is different from the coast and generally these sites show less intense seasonality (Steffen et al., 2015; Obrist et al., 2017). These results demonstrate that there are likely differences in atmospheric processes and anthropogenic inputs between the inland and coastal Arctic sites impacting seasonal concentrations. While this latter statement has been made before for a few locations (AMAP, 2011; Berg et al., 2013; Steffen et al., 2015), this assessment is the first time that all of the atmospheric Hg data from the circumpolar Arctic have been compared.

At High Arctic coastal sites, during the spring and summer periods when AMDEs occur, a large variability in concentrations has been reported (Berg et al., 2013; Steffen et al., 2014, 2015; Skov et al., 2020). The AMDEs are the conversion of stable GEM to rapidly depositing GOM and PHg and result in periods of low GEM air concentrations. However, periods of elevated GEM or TGM were also reported during these periods and were attributed to the rapid reduction of GOM to GEM and emission from the surface (AMAP, 2011; Steffen et al., 2013). The summer enhancement of GEM concentrations is still not fully reconciled but is thought to result from a combination of contributions from the re-emission of AMDE-deposited Hg, other emissions of Hg from surfaces (e.g., from tundra, lakes, etc.), snowmelt and evasion of Hg from the Arctic Ocean that is enhanced from large Arctic river runoff (Steffen et al., 2005; Fisher et al., 2012; Angot et al., 2016; Sonke et al., 2018).

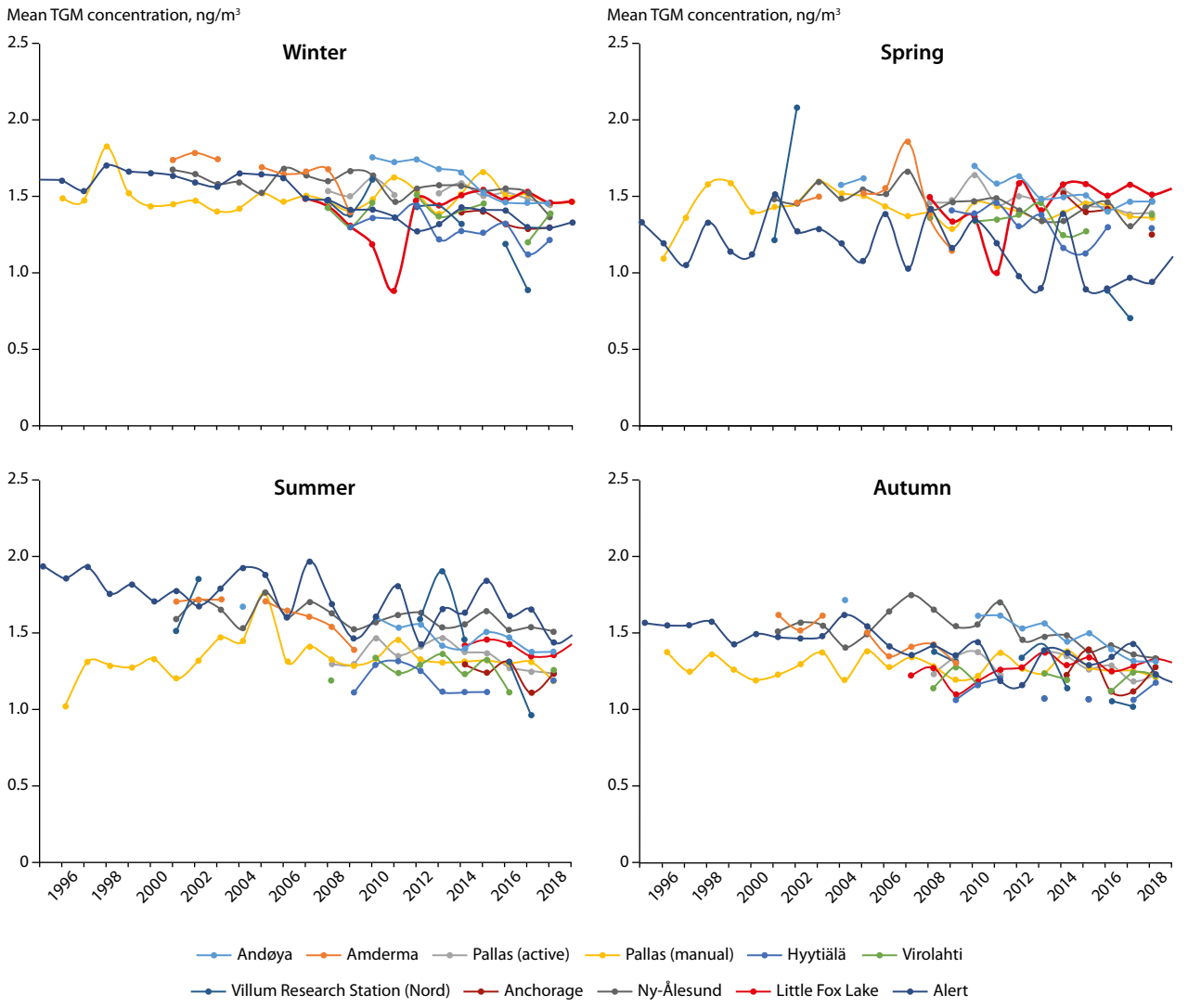

Figure 2.3 Seasonal time series of total gaseous mercury (TGM) concentrations in air (ng/m³) at 10 circumpolar locations.

Appendix Tables A2.5 and A2.6 provide descriptive statistics for annual and seasonal daily mean concentrations, which were used to help establish seasonal variability at the sites surveyed. The range and standard deviation of the mean shown in these tables may reflect seasonal, episodic, or interannual changes in concentration. This information is useful for indicating variability during the respective periods and is not a reflection of the precision of the mean. Furthermore, due to the very large sample sizes inherent in these multi-year daily datasets, the standard error is very low. It is this low standard error that provides confidence when comparing means between sites.

Annual and seasonal patterns of Hg were examined to assess both inter-site and intra-site variability. Long-term records (see Table A2.5) were used for intra-site variability, while inter-site comparisons were made for a common 10-year period (2008–2018, see Table A2.6). Broadly speaking, sites were classified as either High Arctic or Subarctic, with Subarctic sites further classified as coastal or continental sites to better understand how different deposition processes affect the seasonal patterns in the Subarctic.

High Arctic coastal sites (Alert, Amderma, Ny-Ålesund and Station Nord) showed the largest annual range and standard deviation of daily mean TGM concentrations. The high variability in TGM concentrations at these sites is also indicated by the inclusion of the lowest minimum daily mean and the highest maximum annual daily mean TGM concentrations of all ten sites (see Table A2.5). Daily mean TGM ranges for Alert, Amderma, Ny-Ålesund and Station Nord were 3.27 ng/m³, 4.21 ng/m³, 2.43 ng/m³ and 2.85 ng/m³, respectively. The large range in concentrations is driven by springtime AMDEs. In addition, the duration and magnitude of AMDEs change year-to-year due to meteorological conditions, and this impacts inter-annual variability of the seasonal concentrations as shown in Figure 2.3. Although the highest maximum daily concentrations occur in the spring, seasonal mean concentrations of TGM are highest in the summertime at Alert, Station Nord and Ny-Ålesund and Amderma. Standard deviations of the mean daily TGM concentrations for the autumn season for Alert, Amderma, Ny-Ålesund and Station Nord were 0.16 ng/m³, 0.16 ng/m³, 0.15 ng/m³ and 0.23 ng/m³, respectively, which represent the lowest seasonal variability for these High Arctic sites.

In Subarctic sites (and throughout the Northern Hemisphere) lower concentrations of TGM are typically observed during the summer (Jiskra et al., 2018). These annual atmospheric Hg patterns in the Northern Hemisphere are thought to be the result of the respiration process incorporating GEM into plant

tissue during the growing season (Obrist et al., 2017; Jiskra et al., 2018). Changes in vegetation growth patterns in the Arctic caused by climate change may influence the uptake of Hg during short growing seasons. To examine the Northern Hemispherical background Hg concentration trends, concentrations from the winter should be examined due to the influence of changing Arctic net primary production with climate change.

To examine seasonality of a particular site, all available data were used (see Table A2.5). Mean seasonal concentrations for the inland sites were observed to be the lowest during the autumn season for Hyytiälä (1.13 ng/m^3), Virolahti (1.20 ng/m^3), Denali National Park (1.20 ng/m^3), Pallas (active sampling: 1.30 ng/m^3; manual sampling: 1.28 ng/m^3) and Little Fox Lake (1.26 ng/m^3). At the coastal site Andøya, the summer mean (1.49 ng/m^3) and autumn mean (1.50 ng/m^3) were the same, while winter mean maximums were observed (1.61 ng/m^3). Winter mean maximums were also observed at Pallas (1.52 ng/m^3) and Virolahti (1.40 ng/m^3). Spring seasonal mean maximums were observed for Denali (1.44 ng/m^3), Little Fox Lake (1.47 ng/m^3) and Hyytiälä (1.31 ng/m^3).

To examine differences between sites, the period of most significant overlap should be considered (2008–2018, see Table A2.6). The coastal site Andøya is located at a similar latitude to Pallas, which is located inland approximately 350 km from the coast. Annual mean daily mean TGM concentrations were lower for the inland site, Pallas (1.40 ng/m^3), than the coastal site, Andøya (1.52 ng/m^3). A lower concentration and less variability (smaller interquartile range and lower standard deviation) at the inland site, Pallas, was also observed for each season. Similarly, the coastal site Virolahti is at a similar latitude to Hyytiälä, which is located 230 km inland. Lower annual mean daily concentrations were observed at the inland site, Hyytiälä (1.23 ng/m^3), in comparison to the similar coastal site, Virolahti (1.29 ng/m^3). In addition, the interquartile range is lower for the winter, spring, and summer at Virolahti than at Hyytiälä. Investigating the seasonality at these latitudinally paired sites shows that concentrations were primarily lower with less variability at continental sites relative to coastal sites.

At all the Arctic locations, the autumn and winter periods show less variability. All High Arctic sites in this review are coastal sites with observed AMDEs, which affect the spring concentrations of TGM. Summer periods have also been shown to have high concentrations and variability. Changes in the spring and summer concentrations may therefore indicate changes to either Hg inputs (global or regional) or localized chemistry that affects concentrations. Thus, the period with the least variability in the High Arctic was identified to be the autumn and because of this is considered the best period to examine the Northern Hemispherical background concentrations of TGM at these High Arctic coastal sites. As described above, all the Subarctic sites have a maximum seasonal mean daily concentration during the winter and/or spring period. The lower TGM concentrations observed at continental sites relative to similar coastal sites demonstrates the effect of plant uptake on seasonal concentration. The winter period removes any potential effects that climate change may play on plant growth and mercury uptake in the Subarctic, therefore the winter period may be best for examining the Northern Hemispherical background concentrations of TGM.

2.3.1.2 Recent temporal trends in total gaseous mercury

Several papers have described temporal trends of atmospheric Hg in both the Arctic and temperate regions (Boutron et al., 1998; Ebinghaus et al., 2002a; Slemr et al., 2003, 2011; Berg et al., 2004, 2013; Faïn et al., 2009; Li et al., 2009; Cole and Steffen, 2010; Cole et al., 2014; Chen et al., 2015; Lyman et al., 2020; Ren et al., 2020). Most locations have shown negative (i.e., declining) trends in the annual and seasonal data (Lyman et al., 2020). In general, declines in atmospheric Hg concentrations in the Arctic are smaller, ranging from 0.6% to 0.9% per year (Cole and Steffen, 2010; Cole et al., 2014; Chen et al., 2015), than those in more temperate regions. Some studies have concluded that the negative trends could be due to changes in Hg emissions and meteorological effects likely resulting from climate change (Cole and Steffen, 2010; AMAP, 2011; Slemr et al., 2011; AMAP/UN Environment, 2019; Lyman et al., 2020). More recently, changes in these negative trends have also been noted (Cole and Steffen, 2010; Cole et al., 2014; Chen et al., 2015; Weiss-Penzias et al., 2016; Lyman et al., 2020).

The time series of seasonal mean daily averaged TGM concentrations for each site during each season were calculated and are shown in Figure 2.4. Data coverage is variable between the sites, which complicates trend analysis interpretation. Direct comparison of trend magnitudes between sites of different temporal coverages should be avoided because of the potential for changing trends over time. To mitigate those effects, the period between 2008 and 2018 is used for comparison because this is the period during which there is more consistent data coverage (8 sites with 11 atmospheric datasets). Amderma has been excluded from this analysis because it does not meet the criteria for the seasonal Mann-Kendall analysis due to a long 6-year data gap between 2009 and 2015.

Seasonal trend analyses were performed using all data collected from each site (see Figure 2.4) and are presented as the mean change in TGM in ng/m^3 as a percentage of that site and season's mean concentration. If the 95% confidence limits of the calculated Mann-Kendall trend (as shown by the vertical line in Figure 2.4) includes the zero trend line, then the trend is not considered to be significant. Annual median concentration trends (see Table A2.7) for all available years were negative for 8 of the 11 measurements including: Alert (-0.95% per year), Station Nord (-2.8% per year), Ny-Ålesund (-0.57% per year), Denali National Park (-1.7% per year), Amderma (-2.3% per year), Pallas continuous sampling (-0.87% per year), Andøya (-1.9% per year) and Hyytiälä (-1.4% per year). Virolahti and Pallas manual sampling (1996–2018) show no significant annual trend, while Little Fox Lake shows a positive (increasing) annual trend of 0.94% per year. Seasonally, the trends were negative at all sites except at Little Fox Lake (all seasons, significant), Hyytiälä (autumn, but not significant), Virolahti (summer and autumn) and Denali National Park (autumn, but not significant). Manual sampling at Pallas shows little trend and a higher amount of error associated with the calculated trend, which is likely a

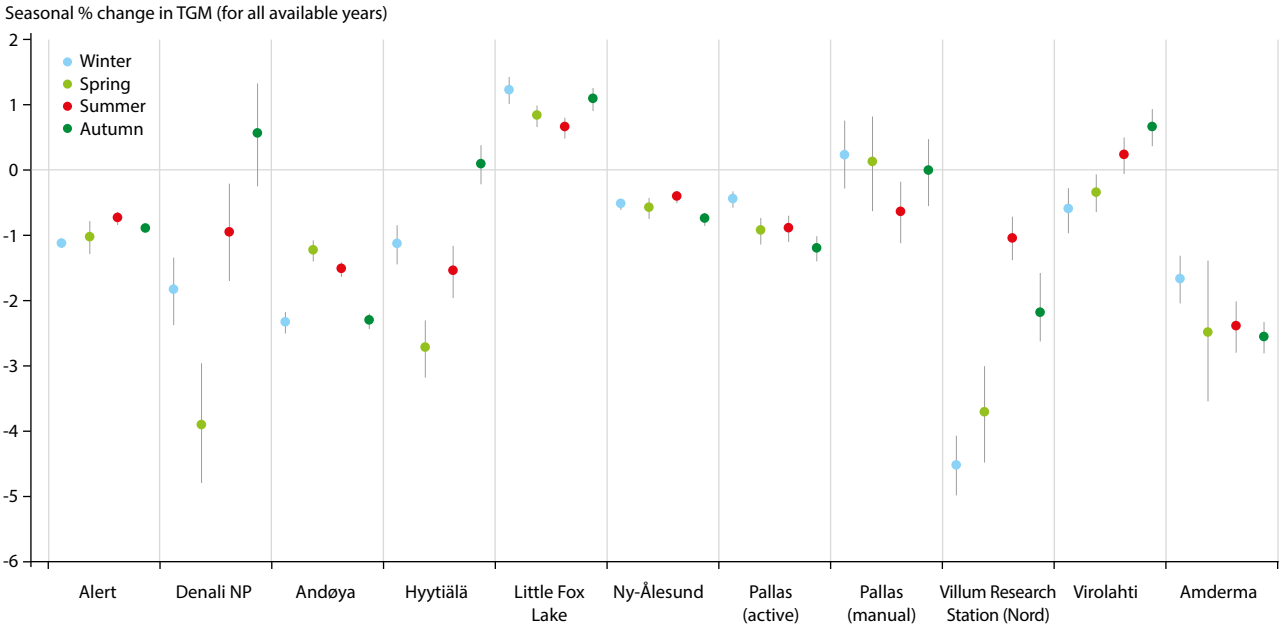

Figure 2.4 Seasonal change (winter, spring, summer and autumn, respectively by site) in total gaseous mercury (TGM) based on daily mean concentrations for all years of available data. If the dot is below the grey zero line, it indicates a decreasing trend, and if it is above the zero line, it indicates an increasing trend. The error bars show minimum and maximum trends. If the zero line on the y-axis falls within the bars, no significant trend is reported.

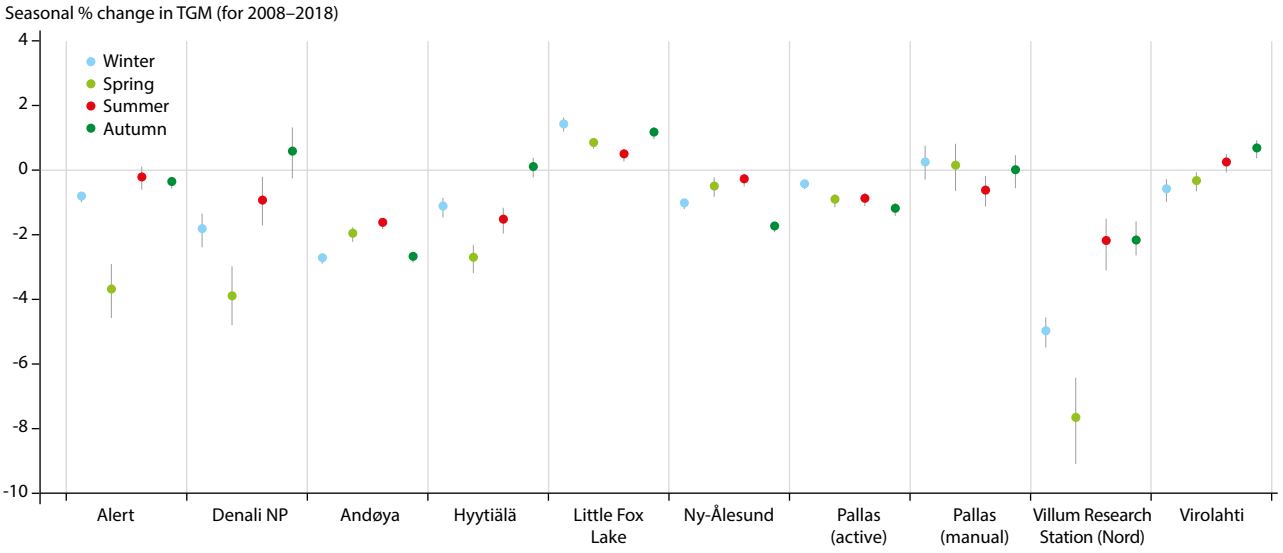

Figure 2.5 Seasonal trends (winter, spring summer and autumn, respectively by site) in total gaseous mercury (TGM) based on daily mean concentrations for the 2008–2018 period. Error bars represent 95% confidence limits.

result of lower frequency of collection (24- to 48-hour samples per week) or higher uncertainty in the measurement. Using all available data and sites we can observe that trends were negative in almost all locations throughout the Arctic.

The trends at the sites were also analyzed as a percent change in TGM in overlapping data for the years 2008 to 2018 inclusive (see Figure 2.5), allowing for the direct comparison of the magnitude of trends between sites. Note that Denali National Park only has data coverage for five of the ten years, so interpretation of these data is limited, and Amderma does not have sufficient data coverage for this period to calculate a meaningful trend for this 2008 to 2018 period. The overall trends of the overlapping 2008 to 2018 period are similar to the trends calculated for all the years of data. Changes in TGM concentrations as a percentage of the seasonal mean for the 2008 to 2018 period were calculated and are shown in Figure 2.5. Autumn concentrations were changing at a rate of -0.39% per year, -1.8% per year and -2.2% per year, for the High Arctic sites Alert, Ny-Ålesund and Station Nord, respectively. Changes in Subarctic winter concentrations were negative: -2.8% per year, -1.1% per year, -0.46% per year and -0.61% per year for Andøya, Hyytiälä, Pallas (continuous sampling) and Virolahti, respectively. The calculated trends were within the minimum and maximum for the winter period for Denali and the Pallas manual samples and thus show no significant trend. Little Fox Lake has a statistically significant positive winter seasonal trend, changing at 1.4% per year.

Examining both the full data record and the data for the 2008 to 2018 overlapping period, we can observe trends of Hg are

negative across the Arctic at most sites. Autumn concentrations in the High Arctic coastal sites show a decrease for all years of -0.91%, -0.76%, -2.2% and -2.6% per year in Alert (1995–2018), Ny-Ålesund (2001–2018), Station Nord (2008–2018) and Amderma (2001–2009), respectively. Alert and Ny-Ålesund have negative autumn seasonal trends of -0.39% per year and -1.8% per year, respectively, during the 2008 to 2018 period.

The Subarctic sites for the winter 2008 to 2018 period primarily showed a negative trend, with only Little Fox Lake (1.4% per year) having a positive trend and the Pallas manual samples having no significant trend. The other continental sites (Denali National Park, Hyytiälä, Pallas; continuous sampling) show negative trends of -1.9%, -1.2% and -0.4% per year, respectively. Both coastal Subarctic sites (Andøya and Virolahti) also show negative trends of -2.8% and -0.61% per year, respectively.

For many sites, the 2008 to 2018 period captures the entire data record (i.e., for Station Nord, Hyytiälä, continuous sampling in Pallas, Denali, Andøya and Virolahti). For sites with longer records, the trends over or during this time period may yield different results than those observed over the most recent decade. For example, the trend in the spring Alert Hg concentration was -1% per year across the entire record, compared to a decrease of -3.7% per year in the 2008 to 2018 period, which represents an increase in the rate of decline during the latter period. Similarly, the negative trend of Hg for the Ny-Ålesund autumn period increased from -0.76% per year between 2001 and 2018 to -1.8% per year between 2008 and 2018. These changes demonstrate that the trends themselves can, and do, change over time.

The annual concentration of Hg at Little Fox Lake is increasing annually by 1% per year for the 2008 to 2018 period. This increase is even more pronounced for winter concentrations, when the site is not subject to vegetative uptake; in winter at this site, an even larger positive annual trend at 1.4% per year is observed. This represents the only positive annual and winter trend in the Arctic and is thought to be due to a combination of a change in the relative frequency of air masses reaching the site from Asia and an increase in Hg emissions from this region (AMAP/UN Environment, 2019).

2.3.1.3 Recent trends in speciated mercury at Alert and Ny-Ålesund

Alert and Ny-Ålesund are the only two sites that have available long-term speciated Hg data including GOM and PHg. These locations are known to have significant seasonal variability in the data and, as a result, monthly trends were examined for these two datasets rather than the seasonal trends used for the TGM datasets. Daily mean concentrations of GOM and PHg were also calculated from data collected since 2002 and 2008 at Alert and Ny-Ålesund, respectively (see Table A2.9). In addition, weekly manual total PHg data are available from Pallas from 2001. Trends for this dataset are not presented here because of the difference in collection methodology.

Concentrations of GOM and PHg are elevated during AMDEs, typically occurring in the spring to early summer months (Steffen et al., 2014). Due to the seasonally high concentrations of GOM and PHg during the spring and summer periods caused by AMDEs, a trend of, for example, 5% during this season has a larger effect on overall concentration of the Hg species and their deposition to the surface than a similar trend during the autumn, where concentrations are significantly lower.

The PHg trends measured at Alert during the 2002 to 2018 period during the months of January, March, April, June, September and November were not significant (see Figure 2.6). The months of February, May, July, August, October and December were observed to have slight negative trends of PHg ranging from -0.13% to -7.45%. More recently, in the 2008 to 2018 period, a negative trend of a larger magnitude is observed with significant negative trends in January, February, March, May, June and July, but no significant trend in April, August, September, October, November and December. These results indicate a shift in the trends for January, March and June from no trend to a negative trend and for August, October and December from a negative trend to no trend.

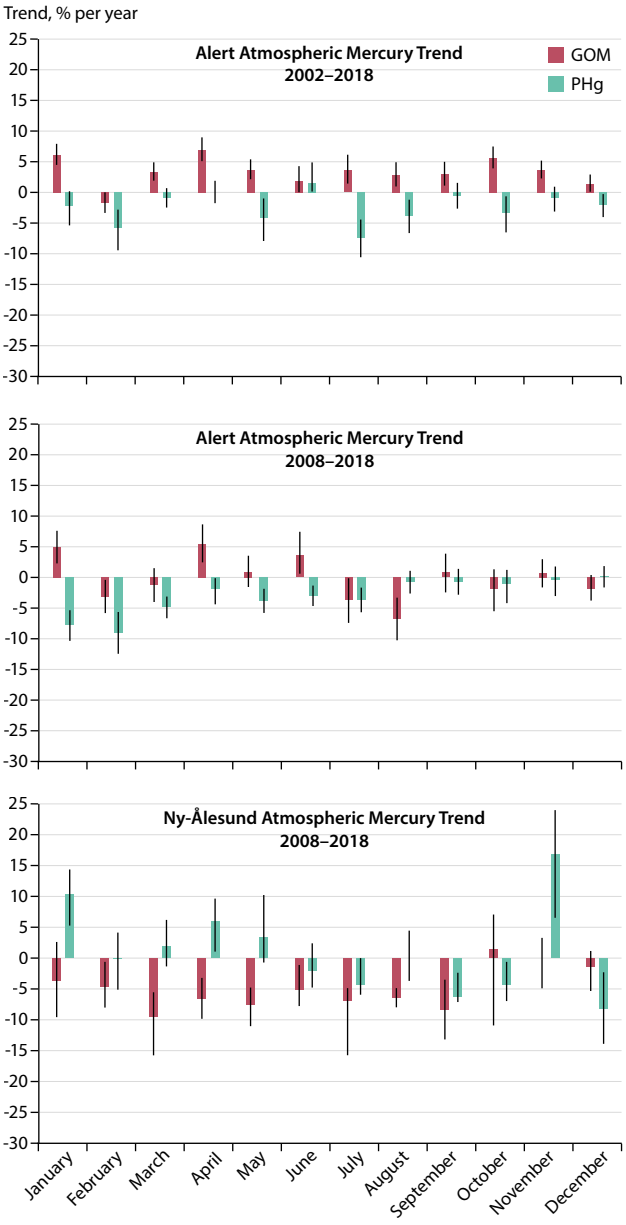

Figure 2.6 GOM (dark red) and PHg (green) trends for Alert (2002–2018 and 2008–2018) and Ny-Ålesund (2008–2018) as a change in concentration as a percentage of the monthly mean.

At Alert, GOM concentration trends are more consistent than PHg for the 2002 to 2018 period, with January, March, April, May, July, August, September, October, November and December all measuring positive. The only negative annual trend was found in February (-1.74% per year). For 2008 to 2018 there were no significant trends in the months of March, May, September, October, November and December. Negative trends are reported in February, July and August while positive trends are reported for January, April and June. By comparison to trends observed in other months during both these time periods, a negative trend in PHg is observed in February and, in the more recent years, a negative trend was also observed in March and May. In contrast to concentrations of PHg, GOM concentrations were observed to increase during April and May for both analysis periods. This represents a change from increasing PHg concentrations to increasing GOM concentrations during depletion events and may be driven by a decrease in the availability of particles during the AMDE period.

By contrast, the trends for GOM from Ny-Ålesund were negative during for the months of February through September with no significant trends for January, October, November and December. Trends in PHg were positive for the months of January, April and November and negative for September, October and December. The negative trend in GOM during the springtime may indicate a change in the conditions needed for AMDEs to occur at this site, and the positive trend of PHg in April may indicate a higher availability of particulate during this period. It is clear that the temporal trends observed at Alert and Ny-Ålesund have been impacted by different processes over time and perhaps by different anthropogenic emissions of both Hg and particulate matter.

Monthly analysis of TGM concentrations and trends from 1995 to 2007 in Alert previously showed a change in the timing of the AMDEs (Cole and Steffen, 2010). The results of the trend analysis on GOM and PHg datasets for both Alert and Ny-Ålesund suggest a change in composition of the Hg species with opposing trends for GOM and PHg; at Alert, concentrations are observed moving towards positive GOM trends, while at Ny-Ålesund, concentrations are observed moving towards positive PHg trends. Despite the differences in direction, both sites are showing changes in the process that may affect the deposition and input of Hg to the Arctic environment. The changes in the timing of Arctic haze patterns and sea-ice coverage may be driven by changes in climate but it may also result in changes to AMDEs. Although Station Nord does not have measurements of GOM and PHg, the overall negative trend TGM suggests there may also be a change in AMDEs during the spring and summer periods.

This chapter features the first comparative trend analysis of all the atmospheric Hg data available to AMAP for assessment. Total gaseous mercury (TGM) has been collected since 1995 from 11 different Arctic locations over varying time periods. Speciated atmospheric Hg data has been collected using continuous measurement methods from 2002 and 2008 at two Arctic sites, Alert and Ny-Ålesund. Global atmospheric Hg emission and concentration trends show that Canada (Cole et al., 2014; ECCC, 2016), the United States and Europe (Streets et al., 2019) have decreasing levels of Hg, while data from Asia indicates increasing or plateauing of Hg emissions (Pacyna et al., 2016; Nguyen et al., 2019). Trends during the autumn at all High Arctic sites and during the winter at all European Subarctic sites support the overall decrease in Hg emissions and concentrations (negative trends) due to a global reduction in Hg emissions. Increases (positive trend) found at one location, Little Fox Lake, may be a representation of both the increase in Hg emissions from Asia over the observed time period and the changing weather patterns that may bring air masses from these regions more frequently. While the Denali National Park site in Alaska may experience the same change in air masses and Hg levels as Little Fox Lake, for Denali National Park the data were limited to five years (2014–2018), while Little Fox Lake has been monitored since 2008, which may explain the different trend behaviour at the site.

Seasonal TGM data at coastal High Arctic sites have greater variability than Subarctic sites because of local AMDE chemistry. The four High Arctic sites included in this study are all coastal sites, and both their springtime concentrations and trends are likely influenced by AMDEs. The autumn season was found to be the most representative of background concentrations at High Arctic sites because local processes have less influence on those concentrations. Trends of TGM were observed to be decreasing at all four sites during the autumn season, similar to trends at Subarctic sites.

The magnitude of the long-term trends of TGM in Alert and Ny-Ålesund (1995–2018 and 2002–2018, respectively) differed from the more recent period (2008–2018). Similarly, differing directions of trends were observed between the 2002–2018 and 2008–2018 period of analysis used for Alert GOM and PHg. These results indicate that the trends are dynamic and that applying analyses in different time periods may yield different results and interpretations.

2.3.1.4 Regional and seasonal dependence of mercury in wet deposition

Mercury wet deposition flux is a product of the total precipitation amount and the concentration of Hg in that precipitation. Previous studies suggest that the magnitude of Hg wet deposition varies geographically and seasonally due to climatic conditions, atmospheric chemistry and human influences (VanArsdale et al., 2005; Selin and Jacob, 2008; Prestbo and Gay, 2009). Wet deposition in rural areas in North America and Europe are similar (Weiss-Penzias et al., 2016; Sprovieri et al., 2017), although in this study the sites in North America tend to have lower Hg wet deposition. There is an apparent latitude-dependent gradient in Hg concentration and wet deposition, with lower deposition rates at the Subarctic sites compared to further south in Scandinavia, in line with previous observations (Selin and Jacob, 2008; Sprovieri et al., 2017). Geographic differences in Hg wet deposition may be explained in part by the proximity to atmospheric sources, as urban industrial locations tend to have higher Hg wet deposition than remote locations, but this association can be weak because atmospheric processes, not just local emissions, are important drivers of Hg uptake by precipitation (Sprovieri et al., 2010). Many studies have noted the influence of emission sources on spatial trends in Hg wet deposition including on a global scale (Sprovieri et al., 2010, 2017).

The seasonal cycles of Hg concentrations and precipitation along with Hg wet deposition are shown in Figure 2.7. Seasonal

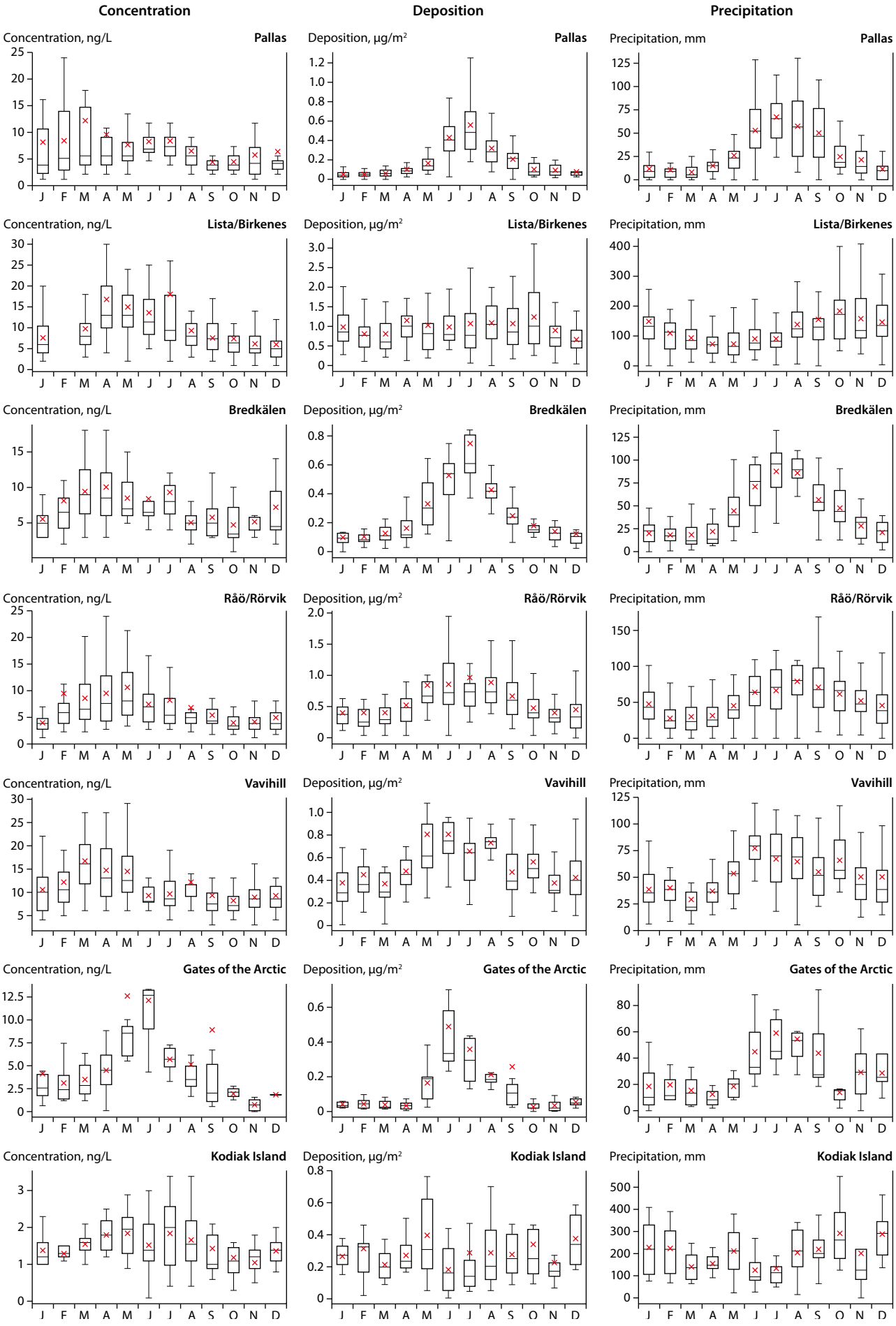

Figure 2.7 Box and whisker plots of seasonal variation in Hg concentration (ng/L), Hg wet deposition (µg/m²) and precipitation (mm).

cycles in Hg wet deposition flux are observed at all stations in this study, as has been reported elsewhere (Selin and Jacob, 2008, Prestbo and Gay, 2009; Cole et al., 2014). The amount of wet deposition is highest in summer and lowest in winter and the pattern is most pronounced at inland Subarctic sites compared to coastal sites. The seasonal patterns have been explained by the following: more precipitation in warm seasons (Sanei et al., 2010; Sprovieri et al., 2017); the fact that Hg is more effectively scavenged by rain in summer compared to snow in winter (Sorensen et al., 1994; Selin and Jacob, 2008; Gratz et al., 2009); a greater availability of soluble Hg due to convective transport in summer events (Keeler et al., 2005; Lyman et al., 2020); and an increase in Hg-containing soil-derived particles in the atmosphere in summer (Sorensen et al., 1994).

2.3.1.5 Recent temporal trends in mercury wet deposition fluxes

Several studies have examined temporal trends in Hg wet deposition fluxes over varying time periods and extent (Keeler et al., 2005; Wängberg et al., 2007; Prestbo and Gay, 2009; AMAP, 2011; Zhang and Jaeglé, 2013; Weiss-Penzias et al., 2016). These studies mainly cover North America and Europe, while Sprovieri et al. (2017) reported wet deposition trends from a global project. Many of these studies have shown declining trends in both annual and seasonal Hg concentrations and deposition, and increasing amounts of precipitation (Wängberg et al., 2007; Prestbo and Gay, 2009; Olson et al., 2020). The declines in Hg concentration and deposition have been attributed to reductions in anthropogenic emissions and changes in meteorological conditions, such as increasing precipitation. In both Europe and North America, the trends are heterogeneous and are driven by larger decreases earlier in the monitoring record (Wängberg et al., 2007; Weiss-Penzias et al., 2016; Olson et al., 2020). Weiss-Penzias et al. (2016), Zhang et al. (2016a) and a review by Obrist et al. (2018) have shown that wet deposition follows temporal trends in global and regional anthropogenic Hg emissions.

Trend calculations for Hg wet deposition were carried out using the same method as that which was used for calculating air concentration trends in this assessment and for previous calculations of Hg deposition trends (Cole et al., 2014; Olson et al., 2020). Because trends may change over time, comparison of trend magnitudes between sites with different temporal coverages and/or ranges should be avoided. Data coverage varied between sites which complicated trend analysis interpretation but was most comparable between 2009 and 2018; trend analysis in the period 2009 to 2018 was also performed for the European sites for all the available data. Percent change for precipitation parameters are summarized in Table 2.2. Trend calculations for the shorter period (2009–2018) should be treated with some caution; while indicative, they should not be considered absolute, given the relatively short time period and large annual changes. In addition, there are missing data for some sites at certain time periods. Moreover, Collaud Coen et al. (2020) clearly show that the Mann-Kendall test and the associated Theil-Sen slope test are biased when applied for shorter periods; this is due to the fact that the analysis may lead to a larger probability of false trend detection because of the low number of elements in the time series, which is particularly the case for data series with high interannual variations.

A decreasing trend in annual Hg concentration at sites in Lista/Birkenes (-2.2% per year), Råö/Rörvik (-1.6% per year) and Vavihill/Hallahus (-1.4% year), whereas a slight increasing annual trend was observed in Bredkälen (1.9% per year) and no trend was observed in Pallas for all years available (see Table 2.2). For the time period between 2009 and 2018, sites in the U.S. observed a decreasing concentration trend (-5.5% and -2.3% per year, respectively) similar to the sites in Lista/Birkenes (-3.3% per year), Råö/Rörvik (-3.2% per year) and Vavihill/Hallahus (-1.6% per year), whereas the sites in Northern Europe observed no concentration trend. An increasing trend in the amount of precipitation was observed in Pallas (3.3% per year) and Lista/Birkenes (2.9% per year), whereas all sites in Sweden observed slight declining (<1% per year) or no trend in precipitation depth for all years available. For the time period between 2009 and 2018, all sites in Europe observed increasing trends in precipitation, whereas both declining and increasing trends were observed at the sites in the USA. Similar to concentration trends, the annual deposition trend is declining in Lista/Birkenes (-1.1% per year), Råö/Rörvik (-1.6% per year) and Vavihill/Hallahus (-0.4% per year), whereas, for all years during this period, it is increasing in Pallas (3.3% per year) and Bredkälen (5.1% per year). For the 2009 to 2018 time period, the trends are similar with the only change being that in Vavihill/Hallahus the deposition trend changed direction from negative to positive. The sites in the USA show both positive and negative trends in deposition. The trend calculations for the time period between 2009 and 2018 show some extremes that may be caused by noise or gaps in the data series that have larger impacts on the shorter temporal trends, highlighting the importance of long time series when conducting robust trend analyses (see Table 2.2).

In terms of the seasonal changes, only Lista/Birkenes had a consistent trend throughout the year and seasons and for all parameters (see Figure 2.8). The Hg concentration was changing at a rate of -2.2% per year with even steeper changes in autumn and winter (see Table 2.2). Precipitation is increasing at a rate of 2.9% per year with larger increases in summer and autumn, while deposition of Hg is declining at a rate of -1.1% per year with the largest declines observed in winter. The increase in precipitation causes a dilution of Hg in precipitation (lower concentrations), and Hg deposition is declining in line with the reduction in European Hg emissions. The same general trends are observed at Råö/Rörvik and Vavihill/Hallahus, however they were not as pronounced. In Pallas and Bredkälen, the concentrations of Hg were increasing through most of the year, while precipitation is both increasing and decreasing, and the net effect is an increase in Hg deposition. These trends suggest sites close to primary local Hg emission sources (Lista/Birkenes, Råö/Rörvik and Vavihill/Hallahus) respond to reductions in Hg emissions; conversely, the observed trends in the North, far away from Hg emission sources (Pallas and Bredkälen), are likely driven by contribution of secondary emissions and changes in the global Hg pool.

This comparative trend analysis of Hg wet deposition fluxes from seven monitoring sites in North America and Europe confirms previous findings from North America and Europe. Though

Table 2.2 Annual and seasonal trends in Hg concentrations, deposition and precipitation for all years of available data (see Table A2.1 for range of years) and for the period 2009 to 2018. Trends statistically significant (p<0.5) are displayed in bold.

		All years of available data			Years 2009–2018		
		Hg concentration, % change per year	Hg wet deposition, % change per year	Precipitation, % change per year	Hg concentration, % change per year	Hg wet deposition, % change per year	Precipitation, % change per year
Pallas	Annual	**0.0**	**3.3**	**3.3**	0.0	16	12
	Spring	0.8	1.1	2.1	-8.6	8.6	6.8
	Summer	-0.6	3.6	3.4	-3.4	28	22
	Autumn	-0.7	9.6	5.4	4.1	16.2	0.7
	Winter	0.0	4.6	0.5	-4.1	**280**	**500**
Lista/Birkenes	Annual	**-2.2**	**-1.1**	**2.9**	-3.3	-3.5	1.3
	Spring	-0.9	-1.1	0.8	-6.9	-1.6	7.2
	Summer	-2.0	-1.0	3.3	-3.9	**-5.8**	-1.9
	Autumn	-2.4	-1.2	6.1	-4.2	-4.6	2.4
	Winter	-2.7	-2.0	2.6	-3.0	-2.3	1.0
Bredkälen	Annual	**0.0**	**3.3**	**3.3**	0.0	**8.0**	3.5
	Spring	0.2	14.1	11.0	-9.1	**18**	22
	Summer	5.1	2.8	-1.0	7.5	2.0	-3.1
	Autumn	3.1	0.1	-2.4	8.9	**25**	6.7
	Winter	5.7	7.2	0.9	-3.8	**37**	**61**
Råö/Rörvik	Annual	**-1.6**	**-1.6**	**-0.4**	-3.2	-0.9	4.0
	Spring	0.0	-2.0	-1.1	**-8.6**	-1.6	13
	Summer	-1.2	-1.0	0.6	-0.1	-4.2	-2.4
	Autumn	-1.9	-2.4	-0.8	-3.8	5.8	6.8
	Winter	-1.9	-2.4	-1.0	-4.5	**20**	**14**
Vavihill/Hallahus	Annual	**-1.4**	**-0.4**	**-0.7**	-1.6	3.8	1.9
	Spring	0.2	-1.6	-1.4	-7.5	4.7	8.3
	Summer	1.8	-0.6	-1.8	2.6	0.6	-2.1
	Autumn	-1.3	0.8	0.5	-0.8	3.7	-1.0
	Winter	-3.8	-1.6	2.2	**-5.9**	8.2	15
Gates of the Arctic	Annual	**-5.1**	**-9.5**	**-1.8**	-5.1	-9.5	-1.8
	Spring	5.3	-3.3	-5.3	5.3	-3.3	-5.3
	Summer	-8.3	4.9	11.3	-8.3	4.9	11
	Autumn	-10.4	-9.3	-4.4	-10	-9.3	-4.4
	Winter	32.7	1.5	-15.5	33	1.5	-16
Kodiak Island	Annual	-2.3	-2.6	-0.1	-3.0	1.6	8.5
	Spring	-2.9	-2.2	-0.6	-3.1	2.5	4.1
	Summer	-2.5	7.9	0.4	2.9	51	7.9
	Autumn	-3.0	2.0	-2.9	-5.2	-2.4	5.4
	Winter	-4.8	1.4	5.4	-3.5	1.7	6.1

wet deposition rates across rural and remote areas in North America and Europe are generally observed to be similar, in this study the sites in North America tend to have lower Hg wet deposition. A latitude-dependent gradient is apparent in the data, with lower wet deposition at sites in the far north compared to in the south. These geographic differences are explained by the sites' distance from atmospheric Hg sources; sites in the south are closer to industrial areas and emissions hotspots (e.g., metal production and coal-fired power plants). Seasonal cycles are observed in Hg concentration, amount of precipitation and Hg wet deposition, with deposition being highest in the warm season and the pattern is most pronounced at Subarctic inland sites compared to coastal sites. The seasonal pattern is due to more precipitation in summer, Hg is more effectively scavenged by rain than snow and more availability of soluble Hg in the atmosphere in summer.

Trend analysis conducted for this assessment confirms previous findings of a general decreasing trend in annual Hg concentrations and wet deposition. While precipitation amount increases for sites located further south in Subarctic sites have either increasing or no trend in Hg concentrations and wet deposition. These trends suggest sites close to primary local Hg emission sources respond to reductions in Hg emissions while the observed trends in the Arctic further away from Hg emission sources, are likely driven by contribution of secondary emissions and changes in the global Hg pool.

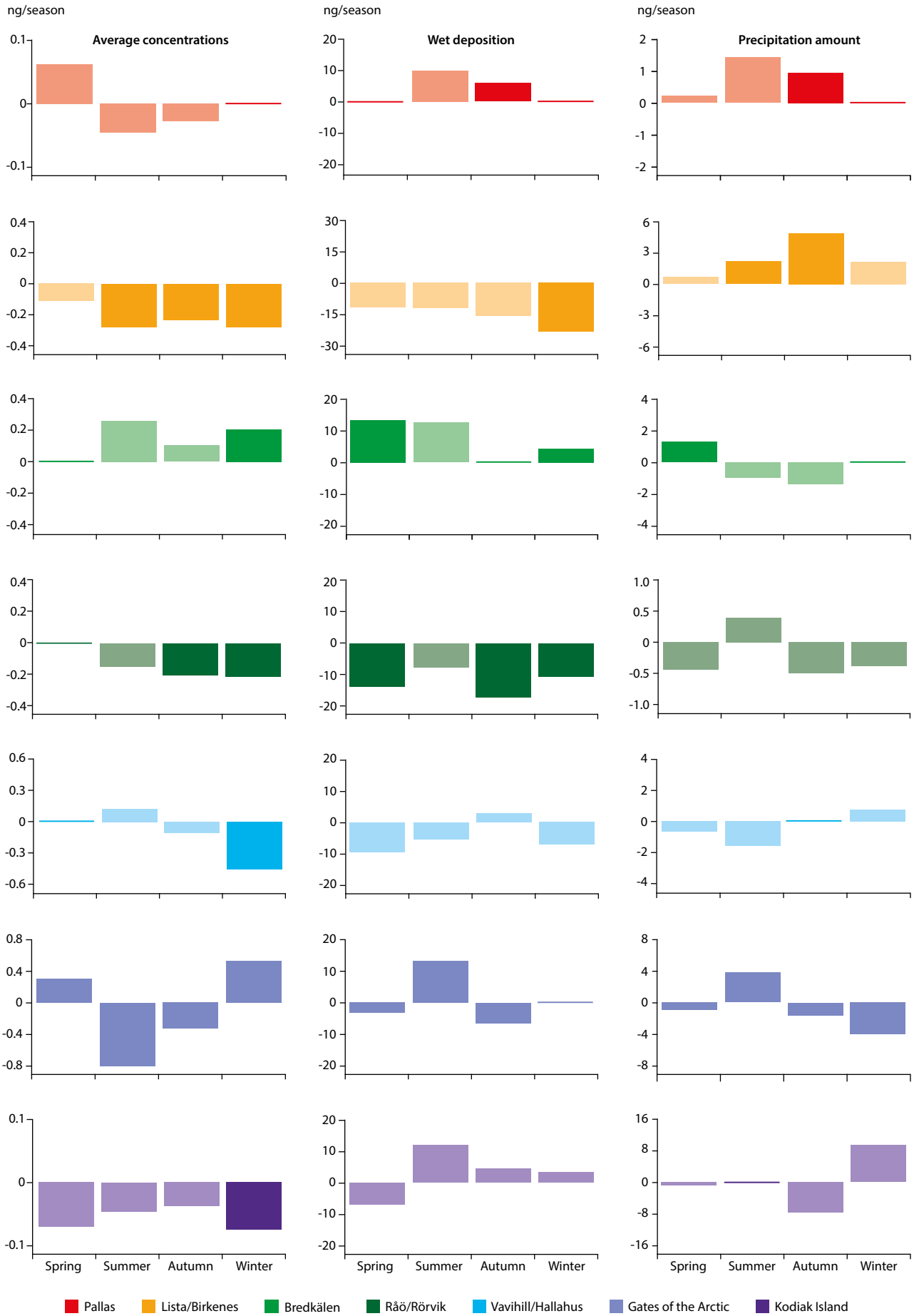

Figure 2.8 Seasonal trends in Hg concentrations (ng per season), Hg wet deposition (ng/m^2 per season) and amount of precipitation (mm per season) for all years of available data from seven Arctic air monitoring stations. Significant trends (p<0.05) are displayed in dark colors.

Table 2.3 Time series available for Hg(0) trend analysis in tree rings of white spruce trees from the Mackenzie Delta, Old Crow and Scree Hill, Canada.

Location	Species	Trees (*n*)	Interval	First year	Last year	Source
Mackenzie Delta, Canada (68.40°N, 133.80°W)	White spruce (*Picea glauca* (Moench) Voss.)	21	Mean of 5- and 25-year segments	1550	2014	Ghotra et al., 2020
Old Crow, Canada (67.5696°N, 139.8288°W)	White spruce (*Picea glauca* (Moench) Voss.)	12	5-year Segments	1698	2017	Eccles et al., 2020
Scree Hill, Canada (65.07°N, 138.157°W)	White spruce (*Picea glauca* (Moench) Voss.)	20	5-year segments	1738	2005	Clackett et al., 2018

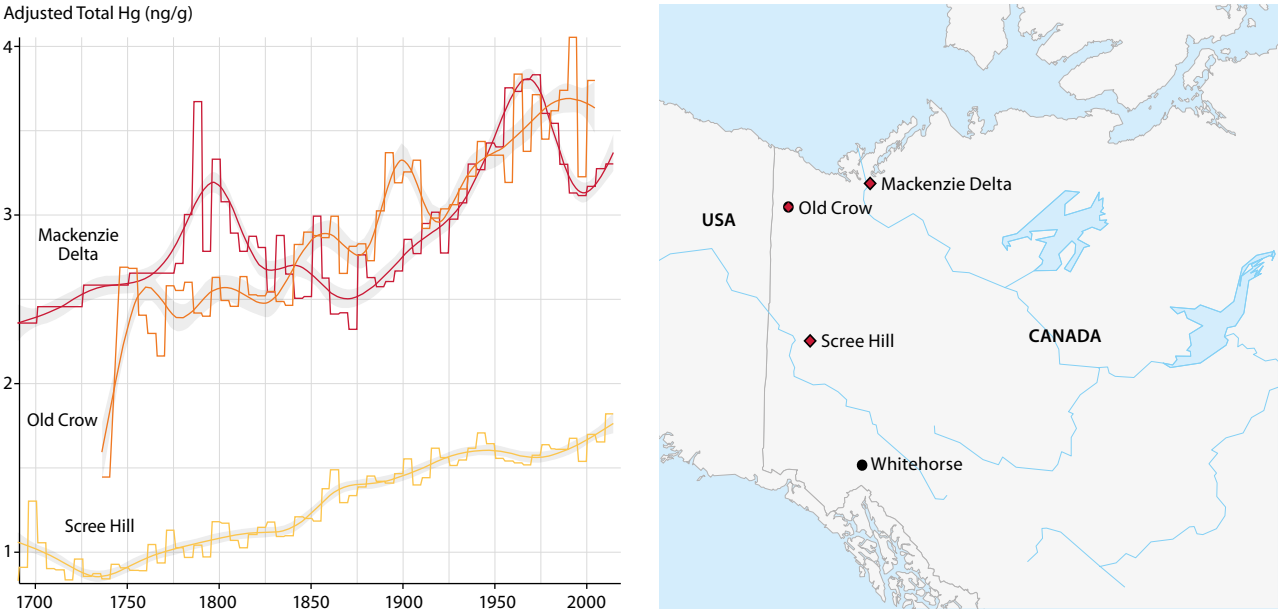

Figure 2.9 Results of temporal analysis of Hg(0) concentrations in tree rings of white spruce at three locations in Canada showing a comparison between tree-ring Hg temporal trends from Mackenzie Delta, Northwest Territories (red), Old Crow, Yukon (orange) and Scree Hill, Yukon (yellow). Site average records are represented by the ridged line, and the smooth line represents a 15-knot cubic spline with a 95% confidence interval. Site averages are only calculated for time periods that have at least three trees. The black circles are communities in the Yukon and the red diamonds represent the sample locations for the temporal Hg series. Sources: Clackett et al., 2018; Eccles et al., 2020; Ghotra et al., 2020.

2.3.1.6 Long-term trends in mercury: tree-ring studies

There are three tree-ring Hg records for white spruce (*Picea glauca* (Moench) Voss.) from northern Canada that are proxies for long-term atmospheric trends of elemental mercury (Hg(0); Clackett et al., 2018; Eccles et al., 2020; Ghotra et al., 2020; see Table 2.3). The record from the Mackenzie Delta site is the northernmost site and is situated close to the Beaufort Sea (see Figure 2.9). This record has the highest average Hg(0) concentration (for the period 1576–2015; mean: 2.98±0.43, range: 1.23–6.81 ng/g), influenced by its proximity to the Arctic Ocean. The record from Old Crow is located southwest of the Mackenzie Delta, and the Hg(0) records are similar in magnitude (for the period 1736–2005; mean: 2.96±0.45, range: 2.16–4.06 ng/g). The record from Scree Hill is the southernmost site, located just below the Arctic Circle. This continental site has the lowest measured Hg(0) concentrations (for the period 1612–2016; mean: 1.22±0.57, range: 1.68–3.66 ng/g).

While the year-to-year Hg uptake can be influenced by local factors including soil moisture (Arnold et al., 2018), long-term trends show that concentrations of Hg measured in tree rings have been steadily increasing over time, with the onset of Hg uptake coinciding with increased atmospheric Hg emissions which began during the European industrial revolution (1770–1820). This trend is more pronounced in sites closer to the Arctic Ocean. After the implementation of emission controls measures, which reduced the amount of atmospheric Hg, the Mackenzie Delta region responded the most rapidly of all sites surveyed with a pronounced decline in measured Hg concentrations. However, this decline is followed by a post-2000 rebound with increasing Hg concentrations. Old Crow was slower to respond but does show a leveling off in the 1990s. At Scree Hill, there is no decline in Hg after the implementation of emission control measures, and the Hg concentrations continue to increase for the duration of the Hg record. This is consistent with the increasing trend of total gaseous mercury (TGM) observed at Little Fox Lake in northwestern Canada, which is approximately 500 km south of Scree Hill (see Section 2.3.1.2).

2.3.2 Recent trends of mercury in biota

Results of the statistical analysis of the 110 biota time series available for the current assessment are summarized in Appendix Table A2.11. Of the biota time series analyzed, 77 met the desired criteria of having a statistical power of ≥80% to detect a 5% annual increase in THg concentrations was met by 77 time series. Of these, 38 showed a significant trend ($p<0.05$) of which 18 were non-linear and 20 were linear. In time series from over the past 20 years, 44 had a

Table 2.4 Summary of all trend results by animal group for time series with statistical power ≥80%; showing: the number of time series, the number of non-linear and linear significant trends, the number of decreasing and increasing recent trends (with significant recent trends in parentheses) and the minimum, median and maximum recent trends (% change per year).

	Time series	Significant trends		Recent trends (% change per year)				
		Non-linear	Linear	Decreasing	Increasing	Minimum	Median	Maximum
Invertebrates (mussels)	12	3	1	6 (1)	6 (2)	-2.4	~0.0	2.2
Marine fish*	8	3	1	1 (0)	6 (2)	-0.3	1.1	4.0
Freshwater fish	18	5	8	7 (6)	11 (6)	-3.3	0.80	5.3
Seabirds	9	1	5	4 (1)	5 (4)	-3.1	1.0	6.1
Marine mammals	28	6	4	13 (6)	15 (3)	-8.6	0.20	2.8
Terrestrial mammals	2	0	0	1 (0)	1 (0)	-1.0	0.80	2.6
All species	77	18	20	32 (14)	44 (18)	-8.6	0.60	6.1

* One marine fish time series trend was ~0%.

positive recent trend of which 18 were significant, and 32 had a negative recent trend of which 14 were significant (one time series had a recent trend of ~0%). Table 2.4 summarizes the results for the 77 time series with adequate power (≥80%) by animal group. All animal groups included time series with both increasing and decreasing recent trends, with median recent trends ranging from 0.0% to 1.1% per year. The most rapid decline (-8.6% per year) was in small beluga whales (*Delphinapterus leucas*) in the eastern Beaufort Sea, and the fastest increase (6.1% per year) was in Faroese guillemot (*Cepphus grylle*).

2.3.2.1 Marine bivalves

Blue mussel (*Mytilus edulis*) time series (n=12) were available from several locations in Iceland and northern Norway as part of the routine AMAP monitoring. These data (gathered jointly by AMAP and OSPAR) are reported annually to the AMAP Marine Thematic Data Centre at the International Council for the Exploration of the Sea (ICES) and were extracted from the ICES databases (ICES, 2020). One statistically significant decreasing recent trend of THg was observed in Skallneset, in northern Norway (-2.4% per year), and two significantly increasing recent trends were detected at two stations in Mjóifjörður fjord in eastern Iceland (1.5% and 2.0% per year; see Table A2.11). These results confirmed that THg continued to increase in blue mussels from eastern Icelandic stations, where the only significant trend in mussels was observed in the 2011 assessment (AMAP, 2011; Rigét et al., 2011a); it must, however, be noted that the trend observed in 2011 was from a different station in Mjóifjörður, from which no significant trend was observed in the current assessment. Two of the recent trends were part of more complex non-linear trends over the whole time series (see Table A2.11). At Skallneset, concentrations were stable and then decreased (from ~2007), and at one Mjóifjörður station, concentrations first decreased before increasing in the latter part of the time series (from ~2005). A third non-linear trend was detected at Husvågen, Norway, where concentrations decreased and then increased, with concentrations at the end of the time series similar to those at the start.

No recent temporal investigations of THg in blue mussels from these northern regions are available in the literature for comparison. Despite increasing trends of Hg in some Icelandic mussels, the concentrations in Arctic bivalves remain low and are not likely of toxicological concern to the organisms (see Chapter 6). As sessile, low trophic level filter feeders, bivalves (like other invertebrates) accumulate the toxic form of Hg, methylmercury (MeHg; Braune et al., 2015) and, since they are monitored throughout Europe, are convenient for spatial comparisons of environmental pollution. However, even with relatively long time series (15–22 years) of adequate power, THg concentrations in mussels produced few significant trends. The lack of significance, conflicting results, and narrow geographic distribution of the Arctic time series of Hg in mussels means that no general Hg trend has been observed for blue mussels.

2.3.2.2 Fish

Marine fish. Eleven time series in three species of marine fish, shorthorn sculpin (*Myoxocephalus scorpius;* n=3), Atlantic cod (*Gadus morhua;* n=7) and sea-run Arctic char (*Salvelinus alpinus;* n=1), provided information on Hg trends across the Arctic, including locations in Canada, Denmark/Greenland, the Faroe Islands, Iceland and Norway (see Table A2.11).

There were four significant recent trends in Hg in marine fish, all of which were increasing (see Table A2.11). They were in the liver of sculpin from central East and central West Greenland (2.1% and 6.1% per year), and in the muscle of Atlantic cod from the northwest Faroe Islands (of 'undefined' sizes) and northern Norway (3.9% and 7.4% per year, respectively). However, the significant Norwegian cod trend should be interpreted with caution as the time series spanned less than 10 years with only seven time points, and the power was <80% (see Table A2.11). Three time series showed significant non-linear trends over the full range of years. These were all in the muscle of Atlantic cod, two from the Faroe Islands and one from northern Norway. In all three, concentrations decreased until about 2000, increased until about 2010 and then either plateaued or decreased once more (although more time points are required to confirm the most recent decrease). The overall reduction in THg concentrations between the start and end of the time series was about 70% in the two Faroese time series (1979–2016/2017) and 50% in the Norwegian time series (1994–2017). No other time series showed a significant trend. The range of time series for marine fish in the 2011 assessment was limited (i.e., from the early 1990s to the early- or mid-2000s) with only two significant linear trends, both with decreasing levels in Atlantic cod from the Faroe Islands and Iceland (AMAP, 2011; Rigét et al., 2011a).

The Hg time series for sea-run char from Cambridge Bay (Queen Maud Gulf, Canada) did not show a significant trend in the current assessment and was not included in the 2011

assessment for comparison. In some previous models, with fork length or body condition factor included as covariates, concentrations of Hg in Cambridge Bay char were reported to be decreasing significantly between 2004 and 2013, although when assessed from 1977 an increasing trend was observed (Evans et al., 2015). Previously reported decreasing or non-significant trends of Hg in anadromous char at Pond Inlet, Nunavut (2005–2013) and Nain, Newfoundland and Labrador (1998–2010/2013; Evans et al., 2015) were not included in the current assessment as they have not been extended further. Evans et al. (2015) hypothesized that the increasing trends up to 2013 were due to slower growth dilution in less productive, higher latitude waters and greater riverine inputs that increased productivity and methylation rates in particular geographical areas. These factors were important to the spatial variation in Hg in sea-run char, though several potentially influential factors are discussed in Chapters 4 and 5.

The recent 20-year trends in marine fish were significantly increasing or non-significant. Comparisons between species are not discussed as they are complicated by differences in tissue analyzed and ecological niche, as they include benthic (sculpin), benthopelagic (Atlantic cod, char) and anadromous (char) fish. Circumpolar or national comparisons of trends among fish can be confounded by proximity to source regions (i.e., sources of Hg emissions and/or deposition), differences in the bioavailability of Hg (particularly MeHg) at the base of the marine food web, species-specific differences in bioaccumulation, as well as the type, composition, and length of the organism's food web (Kirk et al., 2012). Reports of climate-related effects and their potential influence on Hg levels are rarer for Arctic marine than for freshwater fish (see Chapter 5). Changes in productivity and related rates of methylation in marine systems as well as alterations to the structure of food webs have been identified as drivers of differences in Hg across marine locations (Wang et al., 2018; see also Chapters 4 and 5).

Broader collections of sea-run char from other circum-Arctic locations could be informative as the fish are widely distributed and are routinely fished for subsistence. Sculpin are also circumpolar (Harley et al., 2015) and could be monitored elsewhere for comparison with Greenlandic populations. However, given the relatively low concentrations of Hg and the low toxicological risk calculated for Arctic marine fish (see Chapter 6), these may be of relatively low priority for expanded monitoring. The concentrations of THg were increasing relatively rapidly in sculpin and Atlantic cod from West Greenland and Norway, respectively, from around 1999 to present, as discussed above, and should continue to be monitored with high priority, as should other locations, to generate longer and more comparable trends.

Freshwater fish. Freshwater populations of landlocked Arctic char (n=9) were available for comparison throughout northern Canada (Ellesmere and Cornwallis islands, Nunavut, Canada), Southwest Greenland, the Faroe Islands, Norway (Bjørnøya) and Sweden (see Table A2.11). There were significant decreasing recent trends in total Hg levels in char from the two most northern Canadian lakes (Amituk and Hazen, both -3.3% per year), and in the lake Abiskojaure in northern Sweden (-0.90% per year; Figure 2.10). Conversely,

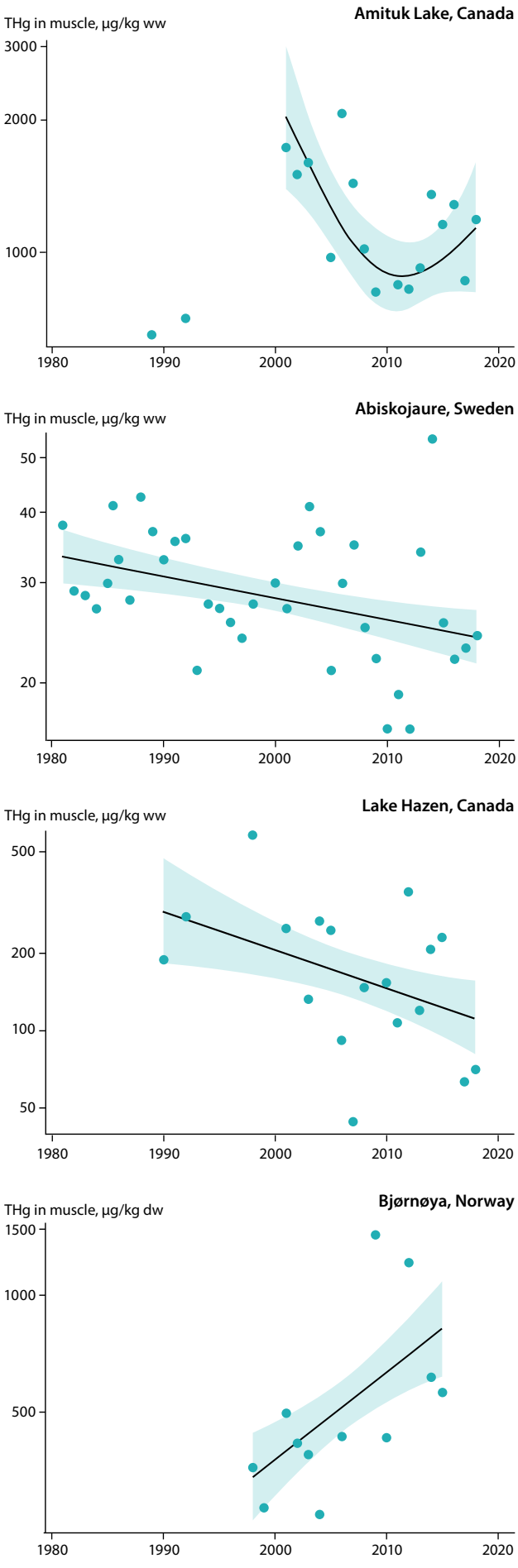

Figure 2.10 Selected trends (annual medians and 95% confidence bands) of total mercury concentrations in muscle of Arctic char.

there was a significant increasing recent trend of 5.3% per year in char from Lake Ellasjøen on Bjørnøya. The trend in Amituk Lake was non-linear and suggested that, although Hg concentrations were significantly lower at the end of the time series compared to the start (2001), concentrations have increased since 2011 (see Figure 2.10). An increase in Hg concentrations since 2013 was also suggested by the non-linear trend in char from Resolute Lake in Canada, although there, concentrations at the end of the time series were similar to those at the start (1993). In both time series, more data are required to validate the possible increases in the last few years. There were no significant trends in Greenlandic or Faroese char.

Time series available for muscle of lake trout (*Salvelinus namaycush*; n=4) showed significant, decreasing recent trends in Hg levels of -1.9% and -2.5% per year in two lakes in the Yukon (Laberge and Kusawa, respectively). Conversely, there was a significant increasing recent trend in lake trout in the west basin of Great Slave Lake (Northwest Territories, Canada), but no significant trend in lake trout from the east arm of Great Slave Lake (see Table A2.11).Time series were also available for concentrations of Hg in muscle and/or liver of burbot (*Lota lota*) from the west basin and east arm of Great Slave Lake and the Mackenzie River (Fort Good Hope, Canada; n=4) and all showed significantly increasing recent trends. Northern pike (*Esox lucius*) were not broadly monitored (n=2): there was one significant decreasing recent trend in Lake Storvindeln, Sweden (-2.1% per year) and no significant trend in pike from the west basin of Great Slave Lake. The full Hg time series for trout from Lake Laberge and pike from Sweden showed non-linear trends in which concentrations first increased, peaking in the mid-2000s or early 1990s, respectively, and then decreased (see Table A2.11), as indicated by recent trends.

Most of the time series for the freshwater fish added ~10 years to those analyzed in the previous AMAP mercury assessment (AMAP, 2011), greatly improving the statistical power of the trends (see Section 2.2.3) and providing new insights. This is the first report of decreasing Hg trends in lake trout from the Yukon (Gamberg, pers. comm., 2019; Gamberg et al., 2021) as well as the most recent assessment available for trends in Faroese, Swedish and Norwegian char, updating some of the existing time series (AMAP, 2011). The increasing concentrations in Canadian burbot and the decreasing trends in Lake Hazen char were consistent with those described in the previous Hg assessment (AMAP, 2011). However, the previously described increasing trends in char from Lake á Mýrunum (Faroe Islands) and Char Lake (Canada; AMAP, 2011) were no longer significant. These analyses previously spanned only seven to eight years, which is a short trend to interpret with confidence, and thus more credence can be given to the trends from the current assessment. Similar trends as observed in the current assessment were recently described in some of the same populations of Cornwallis Island (Canada) landlocked char, although length-normalization resulted in some different trends, which were decreasing in both Amituk and Resolute lakes (Hudelson et al., 2019). Technical reports have also described decreasing trends of Hg in Lake Hazen (Canada) and in some of the time series from lakes on Cornwallis Island (Muir et al., 2021), which is consistent with the results described here. The trends described in the current assessment were also consistent with increasing temporal trends previously described through multivariate models (including length as a covariate) for trout and burbot from Great Slave Lake (up to 2012; Evans et al., 2013). Total mercury was also increasing in more complex models in burbot from Fort Good Hope (Canada) in the most recent publication available (Carrie et al., 2010).

Regional and habit-specific differences are key drivers of variation in Hg trends in northern lake fish (Chételat et al., 2015). In Canadian High Arctic lakes with minimal inputs of terrestrial organic carbon such as those on Cornwallis and Ellesmere Islands, where the food web energetics are driven by benthic algal production (Chételat et al., 2010). Methylmercury bioaccumulation and the resulting concentrations in aquatic invertebrates (the primary food source of the char) have been shown to be inversely related to dissolved organic carbon (DOC) in lakes across a latitudinal gradient, with higher bioaccumulation observed in lakes with low DOC due to higher MeHg bioavailability (see Chapter 5; Chételat et al., 2018). In-lake water chemistry, including particulate organic carbon (POC) and/or DOC levels, was also shown to be more influential on levels of Hg in Arctic char than broader watershed variables in High Arctic lakes (Hudelson et al., 2019; see Chapter 5). Increases in algal-derived organic matter linked to higher temperatures due to climate-related warming have also been hypothesized to drive the increase of Hg in burbot at Fort Good Hope (Carrie et al., 2010).

Climate variables that significantly relate to concentrations of Hg in freshwater fish have been identified (see Chapter 5) for several time series. These include the following: for char, the duration of ice cover, precipitation levels and the phase of the North Atlantic Oscillation Index (NAO; Hudelson et al., 2019); air temperatures, and the Pacific North American Pattern (PNA) in fish from Great Slave Lake (Evans et al., 2013); and air temperatures for burbot from Fort Good Hope (Carrie et al., 2010) as well as for Arctic char from Southwest Greenland (Rigét et al., 2010). Further inclusion of relevant climate/weather, biological and ecological factors as covariates in time series analysis may improve significance of the time series and help explain variation in Hg over time and between locations (see Chapter 5), as well as give important insight into drivers of the observed trends.

The concentration levels and related toxicological risk of Hg to the fish varied considerably between freshwater fish populations; however, several have high proportions of individuals in the moderate to high risk categories (see Section 6.3.6). Further monitoring is required to determine the change in risk to fish populations over time.

2.3.2.3 Seabirds

Total Hg concentrations in circumpolar seabird populations produced 12 time series in five species for comparison across four distinct geographical regions: little auk (*Alle alle*; n=2) in Greenland, black guillemot (*Cepphus grylle*; n=6) in the Faroe Islands, northern fulmar (*Fulmarus glacialis*; n=1) and thick-billed murre (*Uria lomvia*; n=2) in Canada, and black-legged kittiwake (*Rissa tridactyla*; n=1) in Norway (see

Table A2.11). Significant increasing recent trends in THg were greatest in the Faroe Islands in the liver of black guillemot collected at Sveipur (6.1% per year) and in their eggs collected at Koltur and Skúvoy (4.6% and 5.9% per year, respectively). A more modest significant increasing recent trend was found in the eggs of northern fulmar at Prince Leopold Island in the Canadian High Arctic (1.0% per year). There was a non-linear trend in thick-billed murre eggs at Prince Leopold Island which showed concentrations increasing in the period between 1975 to 2000 and then remaining stable. Finally, there was a significant decreasing recent trend in red blood cells of black-legged kittiwake in Svalbard (-3.1% per year). All other time series in seabirds showed non-significant trends.

Trends in THg in Arctic seabirds are consistent with those published in the last AMAP mercury assessment (AMAP, 2011; Rigét et al., 2011a). Additional years of data have improved the power of the trend analysis in most of the time series, though two black guillemot datasets (for feathers and liver) from the western Faroe Islands remained well below the desired power threshold of 80% (see Table A2.11; Section 2.2.3). Though the trend for the black-legged kittiwakes at Svalbard was decreasing in the period from 2000 to 2016, a very recent publication has described a U-shaped function for the same time series with an additional 3 years of data, with the concentrations increasing between 2010 and 2019 after decreasing between 2000 and 2010 (Tartu et al., 2022). The plateaued or slightly decreasing Hg concentrations in northern fulmar and murre eggs after 1999 in the Canadian data series appear to reflect similar atmospheric trends (Braune et al., 2016). It could also be argued that changes in THg concentrations may reflect changes in diet composition and foraging habits as prey fish exposure to THg varies with depth in the water column (and between species; reviewed in Braune et al., 2016). Changing sea ice and oceanographic conditions may force seabirds to relocate their foraging grounds or adjust consumed prey items (Grémillet et al., 2015; Vihtakari et al., 2018). However, changes in prey composition may not be reflected by a change in trophic position alone and could drive various THg or MeHg exposure scenarios in the marine environment.

The THg monitoring dataset for seabird eggs from Prince Leopold Island was analyzed in the context of environmental and climate change indices in a separate study (Foster et al., 2019). For both fulmars and murres, THg was related to NAO and temperature and (for murres) snowfall, while the fulmar model also included sea ice; all variables had time lags of two to seven years. Morris et al. (2022) also described similar relationships in thick-billed murres from Coats Island (Canada), though trend direction varied with length of the time series. The climate/weather factors of influence on THg trends in seabirds are relatively consistent with those identified for mammals (see Chapter 5). Covariation of sea-ice cover and THg levels were also found for Greenland little auks and affected the body condition of adult birds and the growth rates of chicks, providing important indicators of health. However, the THg concentrations were, and largely remain, below known toxicological thresholds of concern (Amélineau et al., 2019; see Chapters 5 and 6).

2.3.2.4 Mammals

Terrestrial mammals. Only two updated THg time series were available for terrestrial mammals: from monitoring of THg in kidneys in the Porcupine and Qamanirjuaq caribou (reindeer; *Rangifer tarandus*) herds from northern Canada, neither of which show any significant temporal trends (see Table A2.11). These caribou time series had adequate power indicating that a statistically significant trend would likely be detected if present (see Table A2.11; Section 2.2.3). Temporal trends in THg were also not detected in separated male and female and/or adult and immature caribou time series (not presented here). In the previous AMAP mercury assessment, the shorter time series from the Porcupine herd (northwestern Canada/Alaska; 1994–2007) also failed to produce significant trends, though one decreasing linear and one non-linear trend were detected in the muscle and liver of reindeer from Sweden (early 1980s/mid-1990s–2005). No additional data were available for the Swedish reindeer to extend that time series in the current assessment.

Recent reports on the Porcupine and Qamanirjuaq caribou (including the data analyzed here) also concluded that temporal trends in age-normalized THg concentrations were not significant (Gamberg et al., 2020; Morris et al., 2022). Dietary differences may be less influential on Hg variation in different caribou/reindeer herds across Canada and Greenland than environmental factors, which affect the movement and deposition of Hg, with deposition to lichens being key to uptake in terrestrial herbivores (Gamberg et al., 2015). In addition to age, sex and season (Gamberg et al., 2020), recent studies have found relationships between concentrations of Hg in Hudson Bay caribou and some climate-related factors such as sea ice freeze-up (Morris et al., 2022; see Chapter 5).

Marine mammals. Marine mammals provided temporal monitoring coverage across a broader geographical range in the current assessment than that provided in the 2011 assessment (AMAP, 2011), which affected the spatial interpretation of the trends (see Section 2.4). Ringed seals provided 22 time series from adult and juvenile (<5-years-old) seals from multiple locations in Canada (n=16; muscle and liver) and in West and East Greenland (n=6; liver). The time series in cetaceans included Canadian beluga whales (*Delphinapterus leucas;* n=10; liver, muscle and epidermis), and Faroese long-finned pilot whales (*Globicephala melas;* n=5; liver and muscle). Beluga were subdivided into small/young (<380 cm) and large/adult animals (≥380 cm), while pilot whales were subdivided into adult (>495 cm), juvenile (<495 cm) male, and undefined (mixed) categories. There were 16 polar bear time series, subdivided into adult males, adult females and juveniles from Greenland (n=8; hair and liver), Svalbard (n=2; hair) and Canada (n=6; liver). Bears were classified as juveniles if less than 5 years old in Norway and Canada and less than 5 years (female) or 6 years (male) in Greenland.

In ringed seals from matched locations, the concentrations of THg in juveniles were consistently lower than those in adult animals (see Table A2.11), as previously observed for Canadian ringed seals (Brown et al., 2016; Houde et al., 2020). None of the time series for Greenlandic seals had significant trends. Seven Hg time series in Canadian seals had significant recent trends: in the eastern Beaufort Sea (western Arctic), Lancaster Sound (High

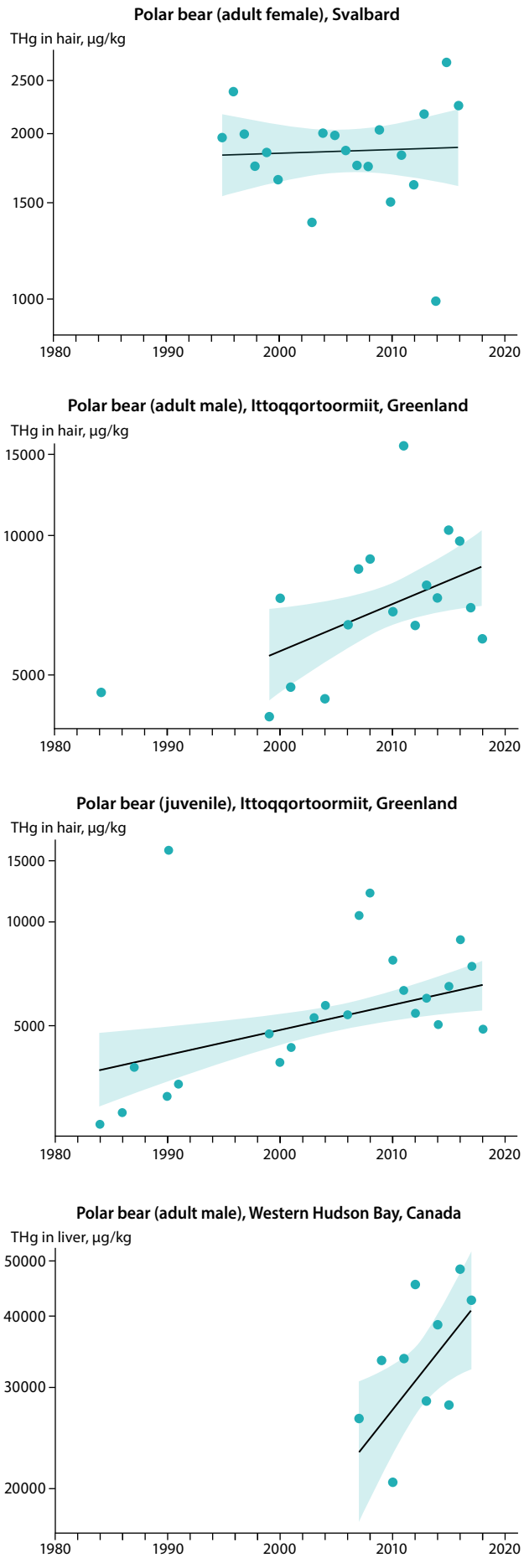

Figure 2.11 Selected trends (annual medians and 95% confidence bands) in total mercury concentrations in hair and liver of polar bears from Svalbard, Ittoqqortoormiit (Greenland), and Western Hudson Bay (Canada).

Arctic), Labrador Sea (eastern Arctic), and in western Hudson Bay. The only significant recent trend detected in liver was in liver of adult ringed seals from the Labrador Sea and showed increasing concentrations (9% per year), but caution should be taken due to the low statistical power of the trend (34%). The six significant recent trends in muscle were more robust and were all decreasing (between -2.4% and -8.0% per year) Table A2.11. Two of the significant downwards recent trends were non-linear. Muscle concentrations in adult seals from western Hudson Bay decreased in the period from 2003 to 2012 and then stabilized, whereas those in adult seals from the eastern Beaufort Sea were initially stable and then decreased from about 2009.

Three recent trends (1999–present) were significant in beluga, indicating that Hg concentrations were decreasing in the epidermis of both large and small whales and in the liver of large whales from the eastern Beaufort Sea (from -2.5% to -8.6% per year). However, the trend in the full liver time series was non-linear and showed that concentrations had increased in the period from 1981 to around 1995 and then decreased, with concentrations at the end of the time series still significantly higher than those in 1981 (Table A2.11). The trend in the epidermis of small whales was also non-linear and suggested local peaks in concentration (~1998 and 2013) with concentrations at the end of the time series significantly lower than those in 1999 but not lower than at the start of the time series in 1993. By contrast with the beluga, the only significant recent trend in long-finned pilot whales was an increasing trend in the muscle of juvenile male whales (1.7% per year). The overall trend was non-linear with a period of slow decline from 1997 to ~2005 followed by a faster increase in concentration from ~2005 to 2018.

All significant recent trends for polar bear were in hair or liver and were increasing (see Table A2.11; Figure 2.11). Mercury concentrations in hair samples from adult male bears from East Greenland (Ittoqqortoormiit) increased at 2.3% per year, while the rate of increase in hair from juvenile bears from East Greenland was slower (1.7% per year). In Norwegian female bears, the trend of 0.2% over the period 1995–2016 is lower than that in juvenile bears, 2.9% from 2008–2014. These increasing trends in Svalbard polar bear are possibly related to re-emissions of Hg from sea ice, glaciers, and permafrost due to climate change (Lippold et al., 2022). In western Hudson Bay, THg in liver of adult male polar bears increased at 5.8% per year. However, the power of most Canadian polar bear time series was below the desired level of 80% (see Table A2.11). Mercury concentrations in the liver of juveniles from East Greenland showed a significant non-linear trend with concentrations in 2018 that were significantly higher than in 1983. Concentrations were increasing from 1983 until the mid-1990s, decreasing through to about 2010 and then increasing through to 2018, a possible cyclical trend; however, more data as well as linkages to explanatory variables are required to evaluate this possibility.

In the previous AMAP mercury assessment, Hg was assessed primarily in the liver of marine mammals with few other tissues assessed and few significant temporal trends observed overall, although those trends that were significant were observed to be increasing over time (AMAP, 2011). In the current assessment, results in muscle, epidermis and hair are also reported for several species. The results in the current assessment indicate that the

trends of Hg have continued to increase in the hair of polar bears from Ittoqqortoormiit, East Greenland, as observed in the 2011 assessment (AMAP, 2011). A recent report on Hudson Bay polar bears (liver) found non-significant temporal trends of Hg in shorter (2007/2008–2015/2016) time series from the western and southern Hudson Bay subpopulations (Morris et al., 2022). Dietary changes affect Hg levels in polar bears significantly.

In the current assessment, the non-linear trend of THg in the liver of eastern Beaufort Sea beluga increases over the period from 1981 (liver) or 1993 (epidermis) to ~2002, consistent with the trend described in AMAP, 2011 and Loseto et al., 2015. The previous assessment also reported an increasing trend in beluga liver from Pangnirtung, Nunavut (Cumberland Sound beluga population); however, this time series has not been extended past 2010 and was not reanalyzed for the current assessment. In the previous assessment, Beaufort Sea beluga were divided into old and young categories for analysis of liver THg, and muscle categories were subdivided by the size of the animals (Loseto et al., 2015). However, because age and size variables were significantly correlated in both populations of beluga, size alone was used as a proxy for age for the sake of consistency in the analysis in the current assessment. Increasing concentrations of Hg in the liver of young and old and in the muscle of small and large beluga from the eastern Beaufort Sea were found in the period from 1981 to ~2002. These trends were less consistent from ~2002 to 2012, decreasing in older and large whale categories but remaining plateaued in young and small whales (Loseto et al., 2015). These previous findings are partially consistent with the decreasing, recent trends observed in liver and epidermis in eastern Beaufort Sea beluga in the current assessment.

The previously observed increasing trend in juvenile ringed seals at Avanersuaq in Northwest Greenland (1984–2008; AMAP, 2011) was no longer significant in the current assessment (p=0.06; it had previously been observed at p=0.08 in Rigét et al., 2012). In the same study, time series up to 2010 of THg in ringed seal populations were significantly decreasing in Qeqertarsuaq in central West Greenland and increasing at Ittoqqortoormiit in central East Greenland (Rigét et al., 2012). Published trends of Hg in Canadian ringed seals were generally consistent with the results described in the current assessment with no trends found in liver, while Hg in muscle was decreasing in the Labrador Sea and Hudson Bay (Houde et al., 2020). Differences in statistical approaches and years modeled, including truncation due to gaps in the time series, explain the relatively subtle differences between these observations and results in the cited publications.

Relationships between concentrations of Hg in high trophic level Arctic wildlife and atmospheric oscillation indices, sea-ice conditions, temperatures and precipitation have been described for several marine mammals in Canada and Greenland (Rigét et al., 2012; Loseto et al., 2015; Houde et al., 2020; Morris et al., 2022; see Chapter 5). These studies highlight the potential for such factors to influence Hg concentrations over time or independently. However, the role of climate/weather drivers on trends of Hg requires further investigation, as these studies are species and location specific, which limits our ability to make general conclusions. In general, these results do suggest that climate and dietary changes are highly influential factors in several wildlife models. Ecological changes in food-web composition and corresponding increases in the dietary proportions of lower trophic level prey drove decreases in Hg levels in the hair of Beaufort Sea polar bears (McKinney et al., 2017b). Furthermore, the temporal increase of Hg in polar bears from Svalbard was slightly faster when the trend was adjusted for the variation in carbon source (marine vs. terrestrial; Lippold et al., 2020), suggesting that dietary changes are a highly influential factor in several wildlife models (see Chapter 5).

Though technically terrestrial animals, Arctic foxes on Svalbard are opportunistic predators and coastal scavengers with a highly variable diet; they feed extensively on marine resources (e.g., seabirds and their eggs, seal pups and carcasses) in addition to terrestrial resources (e.g., reindeer carcasses, ptarmigans, geese; Frafjord, 1993; Eide et al., 2005; Ehrich et al., 2015; Hallanger et al., 2019). Svalbard fox time series were therefore considered together with marine mammals when investigating latitudinal and longitudinal trends, and in other metrics presented in this chapter.

Hallanger et al. (2019) reported concentrations of Hg in Svalbard foxes in the period from 1997 to 2014 increasing at ~3.5% annually, approximately the same value reported in this assessment; however the trend is not significant and had low power. The relatively poor fit to the data improved when carbon source ($\delta^{13}C$), availability of reindeer carcasses and sea-ice extent were included in the model, resulting in a more rapid increase in Hg (7.2% annually; Hallanger et al., 2019).

Most of the marine mammal species investigated, except beluga, had at least some time series with significantly increasing trends of Hg in liver over the last 20 years. Based on the toxicological assessment undertaken in Chapter 6, this could indicate ongoing and potentially increasing risk to some individual animals in these populations.

2.3.3 Recent trends in mercury in humans

The available time series demonstrated that, in the relatively few Arctic populations that have been monitored consistently over time, concentrations of THg in blood are generally decreasing (see Figure 2.12). Total Hg concentrations in blood of pregnant Inuit women from Nunavik, Canada showed an annual decrease of 3.9% (for the period 1992–2017; AMAP, 2015; Lemire and Blanchette, pers. comm., 2020). In Nuuk, West Greenland no significant trends in blood Hg levels were found for pregnant women in the ≤30 years or >30 age groups (for the period 1999–2015; p=0.58 and p=0.18, respectively). However, THg in blood from pregnant women in the Disko Bay region further north in West Greenland decreased at 6% annually from 1994 through 2013 (p=0.030; AMAP, 2015). Unlike in the other locations, blood samples were collected at several time intervals from human individuals in a Faroese cohort study; the same individuals were followed from birth, through childhood and into adulthood. Blood Hg concentrations did decrease significantly in Faroese Cohort 1 at 7% per year in samples collected from 1986/87 through the 2013 to 2016 period (p=0.05; AMAP, 2015; Petersen, pers. comm., 2019; Weihe, pers. comm., 2019).

Given the limited geographic coverage of the available human biomonitoring time trends, the circumArctic conclusions that can be drawn are limited. The available time series demonstrated that trends of Hg in humans in Nunavik, West Greenland

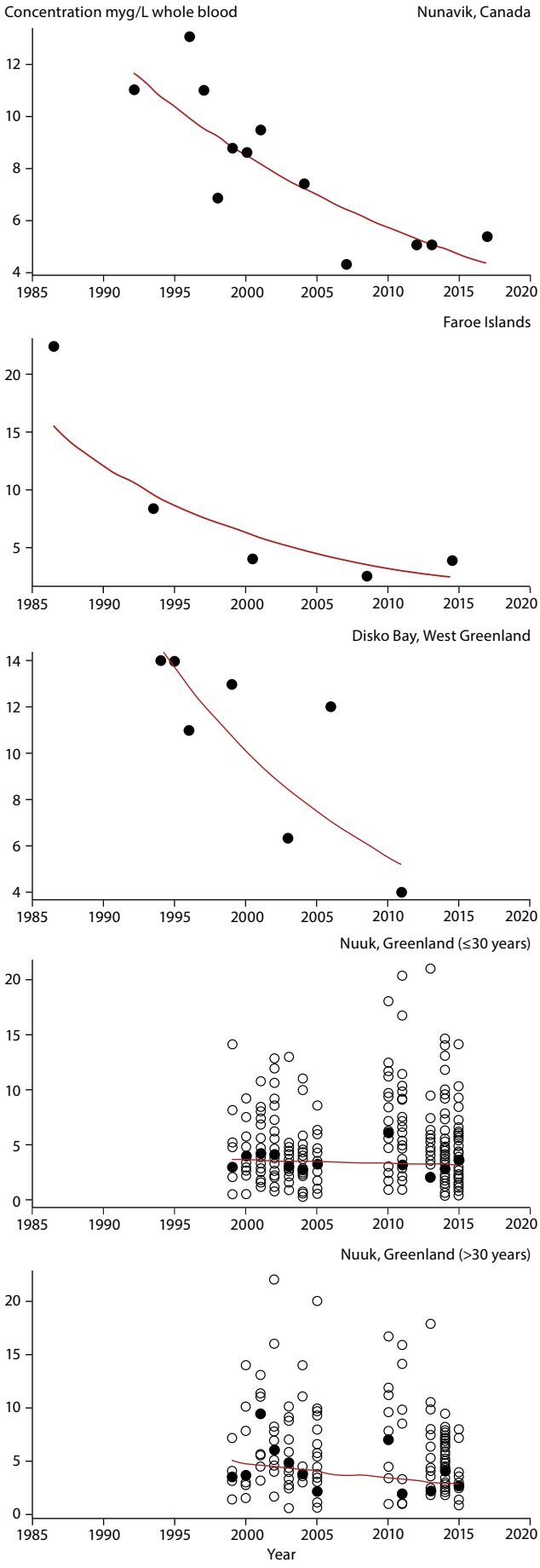

Figure 2.12 Temporal trends of THg concentrations in pregnant Inuit women from Nunavik, Canada; Faroe Islands (Cohort 1); Disko Bay, West Greenland; and Nuuk, West Greenland (women ≤30 years and >30 years).

and the Faroe Islands were decreasing over time and/or from childhood to early adulthood (Faroe Islands). Notwithstanding the limited geographical coverage, Canada and Greenland are key locations for monitoring human exposure to Hg because the traditional diets of Indigenous coastal populations include the consumption of marine mammals, generally resulting in greater dietary exposure and Hg concentrations in these areas (AMAP, 2015). A number of factors may influence Hg levels in people; however, the AMAP human health assessments have shown that the declining trends in contaminant levels in humans living in the North are strongly associated with lifestyle as well as dietary choices and advisories (AMAP, 2015). Results for Hg trends in humans can be discussed with some regionally relevant wildlife trends, but temporal trends in human blood levels and those in food items are rarely directly related, even where the sampled species may be representative of consumed foods (e.g., where market foods are used for trend analysis; AMAP, 2015). Observations comparing human trends to nearby trends in wildlife are therefore recognized as oversimplifications of the Hg exposure pathways to humans. Risk communication associated with consumption of traditional foods is complex and is described later in the current assessment (see Chapter 7). Seal liver is a more significant contributor of MeHg in Inuit in eastern Hudson Bay, Hudson Strait and Ungava Bay regions of Nunavik than muscle, but neither were the primary sources to humans from traditional foods (Lemire et al., 2015). In contrast to seal tissues, beluga meat and nikku (dried meat) were a relatively small proportion of the diet but were among the most significant sources of MeHg, especially in the Hudson Strait region (Lemire et al., 2015). The available time series of Hg in ringed seals from the Labrador Sea (the closest to eastern Nunavik) exhibited relatively rapid increases over time in adult seal liver while decreasing over the same period in juvenile muscle (see Section 2.3.2.4), a difference that could be relevant to consumption but would require further investigation. No other time series produced trends in wildlife within a reasonable range to Nunavik and given the recently reported spatial differences in THg concentrations between seals across the Ungava Peninsula and Nunatsiavut (Houde et al., 2020), this comparison between seals from Nain and Inuit from Nunavik should be treated with caution. Concentrations of Hg in liver of ringed seals sampled from Qeqertarsuaq (Disko Island, West Greenland) showed a non-significant decrease of ~1% annually, while a moderate increase was observed in sculpin from this location (see Section 2.3.2.2). These trends are considerably different from the annual decrease found in Disko Bay women. Exposure through traditional diets, particularly marine mammals and high trophic level fish do drive heavy metal levels in Greenlandic humans (Bank-Nielsen et al., 2019). However, changes in choice of food items play an important role as do a range of lifestyle factors (see Section 7.3).

In the Faroese Cohort 1, greater age, consumption of whale meat or fish, and parity (number of viable births) were the primary factors associated with higher Hg levels in blood (Grandjean et al., 1992, 2012). As discussed in Section 2.3.2.4, the concentrations of Hg were increasing in juvenile male pilot whales and appeared to be increasing in other groups of pilot whales as well, while the concentrations in Faroese people continue to decline (see Figure 2.12). The disconnect between people and whales in this region is most likely due to

increasingly strict recommendations made by the public health authorities on the consumption of pilot whale tissues from 1977 to 2008, when it was recommended that pilot whale no longer be consumed at all (Weihe and Joensen, 2012; AMAP, 2015; see Figure 7.2). Both adult and subadult pilot whales exhibited high levels of Hg and were in the top ten of marine mammal groups assessed for risk of toxicity (see Section 6.3.2). The continuation of the decreasing trend of THg in Faroese cohorts of people and decreases in cord blood of cohorts sampled later relative to those sampled in the mid-1980s are most likely due to dietary recommendations, particularly after 1998 when women were advised not to consume pilot whale. Those recommendations were to abstain from eating the following: (1) kidney or liver (applied to the entire population); (2) blubber, until after giving birth; (3) meat, within 3 months of trying to get pregnant and while pregnant or breastfeeding (Weihe and Joensen, 2012; AMAP, 2015). The decreasing trend may also be partly attributed to the growth and development of the children, who are expected to have greater blood Hg levels at a younger age due to a lesser blood volume (AMAP, 2021).

In this current assessment, Chapter 7 discusses the human health implications of Hg levels in several locations. The lack of comparable time series in people is the most obvious knowledge gap, particularly in Indigenous Peoples from Eastern Greenland, Nunavut, Nunatsiavut, and the western Canadian Arctic, where traditional foods including marine mammals are often a high proportion of the local diets. Data from Russia were available for more recent mercury health assessments (AMAP, 2009, 2015) and efforts are being made to establish national monitoring programs for contaminants (Sorokina, 2019) which would address a substantial knowledge gap in human biomonitoring and wildlife studies.

2.4 Are there spatial patterns in mercury trends in biota from the Arctic?

Mercury temporal trends at individual sites and/or in specific matrices (e.g., in air, or a certain species/tissue) will reflect a combination of both regional and local environmental contamination as well as a broad range of factors and processes that can influence Hg levels in a particular type of sample. Temporal trend monitoring protocols are often designed to minimize the influence of some of these processes and factors (e.g., by sampling biota during specific seasons or of a certain age class). However, individual temporal trend studies often require careful interpretation. In the 2011 AMAP Mercury Assessment (AMAP, 2011) a meta-analysis was conducted, combining trend results from multiple studies to see if consistent patterns of trends could be discerned at regional scales. Examining spatial patterns in Hg trends for a more integrated picture of trends may provide insight into factors and processes driving regional trends that are potentially obscured in single time series. Spatial patterns in Hg trends can be considered using different approaches. In the current assessment, this included observations based on a qualitative (visual) interpretation of the trend patterns in biota supplemented by a quantitative analysis of the magnitude and direction of the trend versus latitude and longitude.

Figure 2.13 presents trend results from selected individual biota time series for Hg for different species groups. The time series represented are those for recent trends (i.e., over the last 20 years) where trends were significant and/or time series exhibited the desired statistical power (≥80%).

Taken together, the geographical pattern of Hg trends ($p<0.05$ and/or power ≥80%) presents a complicated picture of increasing and decreasing trends that differs from the pattern presented in the 2011 assessment (AMAP, 2011), where a greater number of increasing trends were observed in the North American Arctic and West Greenland, and a greater number of decreasing trends were observed in the European sector. This may reflect the fact that, in 2011, the European sector was represented primarily by lower trophic species (i.e., fish and shellfish), whereas the North American Arctic included a larger number of time series for higher trophic level species, such as marine mammals and seabirds. In addition, the 2011 assessment reflected trends analyzed for the entire period of the available time series, which resulted in comparisons of temporally inconsistent trends. The inclusion of a greater number of marine mammal and seabird time series from European sites resulted in more uniform species and trend distribution across regions covered in this assessment (i.e., North America, Greenland and Europe).

Furthermore, in the current assessment, the focus on recent trends (i.e., trends over the most recent 20-year period) provides a more consistent basis for comparison, as many of the time series considered include relatively complete monitoring sequences for the period since 1999. In addition, the inclusion of a greater number of marine mammal and seabird time series from sites in the European sector results in a more uniform species representation across the area for which trend data are available.

Based on the information presented in Figure 2.13, several observations can be made. For the marine fish and blue mussel time series, increasing trends are observed in time series from the Faroe Islands, Iceland, and Greenland, noting that mussel series are only available from coastal sites in Iceland and northern Norway (see Figure 2.13, bottom left). Freshwater fish exhibit both increasing and decreasing trends, in some cases in the same lake systems (Figure 2.13, top left). In general, increasing trends appear to be associated with sites at lower latitudes (as well as on Bjørnøya) and decreases associated with lakes at higher latitudes. Only two terrestrial mammal time series were available (Figure 2.13, top left), both for caribou from sites in the Yukon, Canada, one with an increasing trend and the other a decreasing trend (neither significant). A reindeer time series in northern Sweden reported slow and statistically insignificant increases over the period 1983 to 2005 (AMAP, 2011) but no new data were available to extend this time series. For seabirds (Figure 2.13, top right), with some exceptions, decreasing recent trends are seen in the Canadian Arctic and Svalbard, and increasing trends in the Faroe Islands and East Greenland; no new data were available for seabird time series from Alaska reported in the 2011 assessment. Like seabirds, the majority of powerful and significant trends in marine mammals from Canada were decreasing with some exceptions (Figure 2.13, bottom right); increasing trends were observed in Faroe Islands pilot whales as well as for marine mammals from East and West Greenland and polar bears from Svalbard.

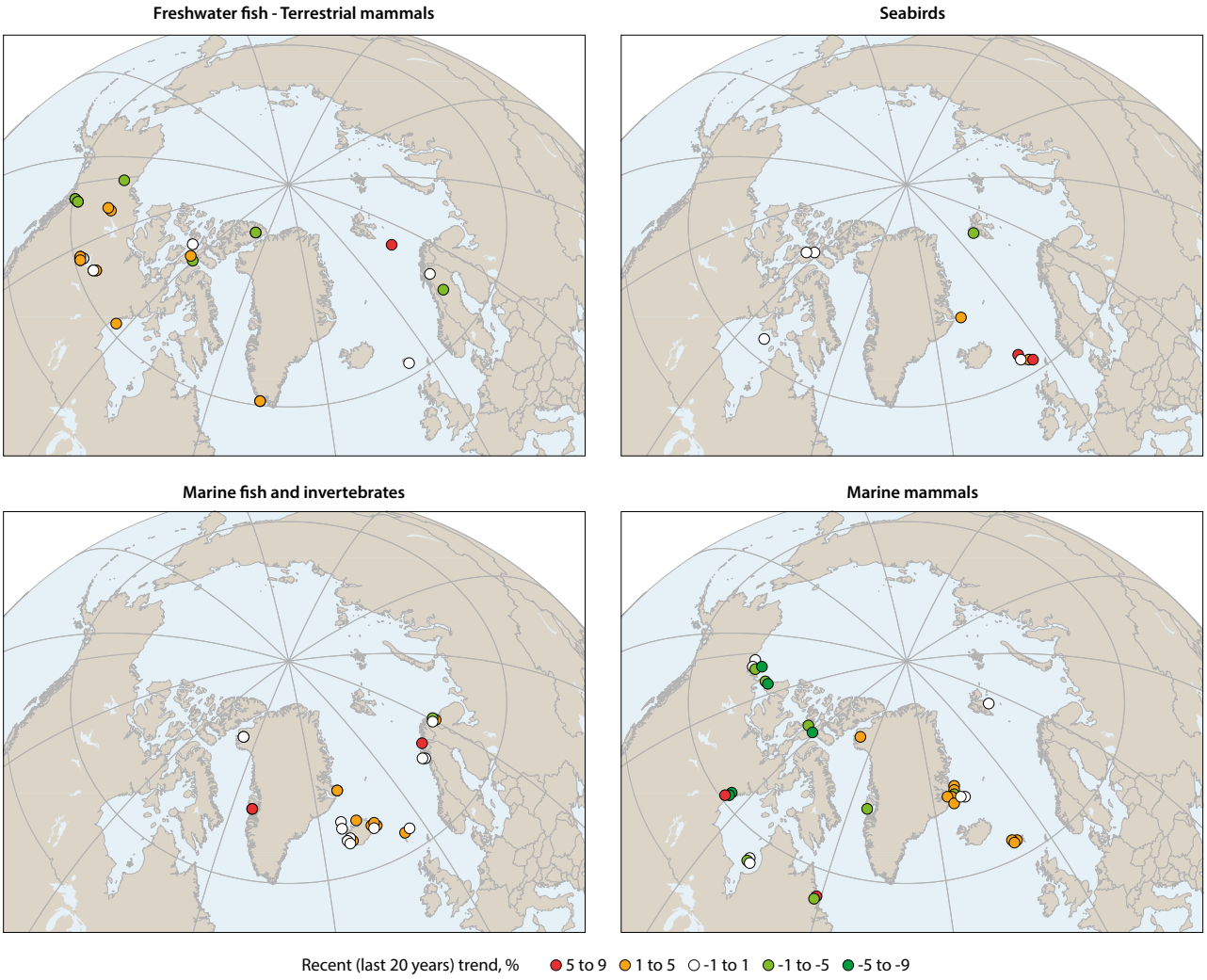

Figure 2.13 Geographical patterns in recent (last 20 years) Hg trends in biota (where trends were significant and/or time series were of a statistical power of ≥80%). The figures show freshwater fish and terrestrial mammals (top left); sea birds (top right); marine shellfish and fish (bottom left) and marine mammals (bottom right). NB: Overlapping symbols have been dispersed to make them visible, resulting in clusters of points around some monitoring locations where trends are available for multiple time series.

These patterns were further explored through statistical analyses of the relationship between observed trends, latitude and longitude. Few trends with latitude were evident when plotting all the trend data together or when the data were separated by ecological group (i.e., blue mussels, freshwater fish, marine fish, marine mammals, terrestrial mammals, and seabirds). Only seabirds exhibited a significant linear correlation with latitude (see Figure 2.13, top right) with more rapidly decreasing trends observed at higher latitudes (r^2=0.37, p=0.035). However, the time series available were primarily from lower latitudes, with few high latitude trends available, so this relationship should be interpreted with caution.

Significant relationships between trends of THg with longitude were non-linear, and unlike latitude, seabird trends had no significant longitudinal relationship. The most distinct relationship with longitude was observed in marine mammals (see Figure 2.14); THg was decreasing most rapidly in marine mammals at the most western longitudes in the Canadian Arctic (125°W) but switched from slowly decreasing to slowly increasing from west to east through Greenland before plateauing and remaining relatively consistent through the Northern European locations. As with plotting the relationship between THg trends and latitude, the data were weighted more heavily to lower longitudes, which affects the ability to infer that the observed relationships are consistent across the circumpolar Arctic.

The updated longitudinal pattern differs from that in the previous AMAP assessment, where trends of THg in marine mammals were found to be increasing in Canada and West Greenland while generally decreasing in those from Northern Europe (AMAP, 2011). In contrast, the current trends tended to be increasing at higher longitudes (i.e., towards Europe, see Figure 2.13); again, these are largely driven by strong trends in marine mammals (see Figure 2.14). The addition of two Norwegian polar bear datasets, both with increasing trends of THg, were important to these relationships. The increase in the number of years available for analysis increased the number of resulting trends that could be interpreted in the current assessment, including several time series that showed decreasing trends at western longitudes in Canada that did not meet the criteria for inclusion in the analysis in 2011 (AMAP, 2011). These additions likely affected longitudinal relationships; however, many factors likely contribute to these differences.

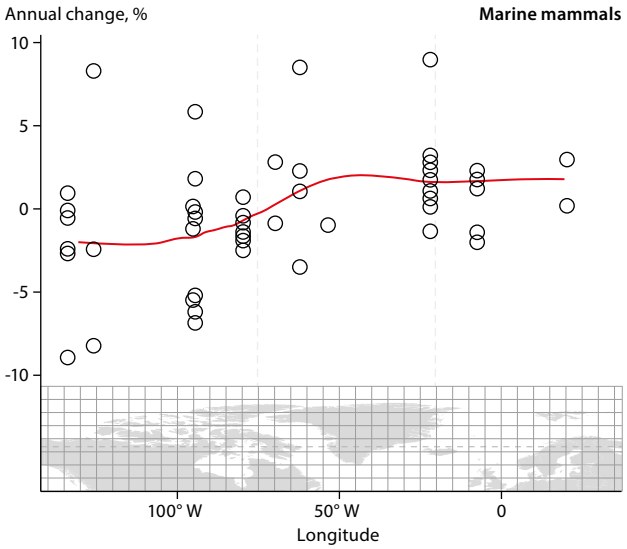

Figure 2.14 Trends of Hg over time (annual change, %) in marine mammals as a function of longitude.

2.5 Conclusions and recommendations

Conclusions (in numbered bullets) are organized under section headings (section numbers in square brackets) followed by recommendations in italics where appropriate.

What time series and statistical analysis are available? [2.2]

1. Providing an update to the time series in the previous AMAP mercury assessment (AMAP, 2011), the time series presented in this chapter encompass key Arctic environmental media and human health indicators, extend the length of the trends and collectively cover a wider geographic range. Tree ring time series, spanning back to the pre-industrial era add a new approach to investigating longer-term trends.
2. Time series of total gaseous elemental mercury (TGM) in air were available from 10 AMAP air monitoring stations from the USA, Canada, Greenland, Norway, Sweden, Finland and Russia; Russian data were not analyzed for trends due to a large gap in relatively short time series. Trends across the full time series, ranging from 1995–2018, and the recent trends from 2008–2018 were analyzed. Time series of gaseous oxidized mercury (GOM) and particle-bound mercury (PHg) were available at two sites, Alert (Canada) and Svalbard, ranging from 2002–2018 and 2007–2018, respectively.
3. Time series for wet deposition/precipitation were available at seven sites in the USA, Norway, Sweden and Finland. Trends across the full time series, ranging from 1989–2018, and the recent trends from 2009–2018 were analyzed.
4. Tree ring records of elemental mercury (Hg(0)) were available at three sites from northwestern Canada providing trends from the 16th century through the industrial revolution to the present.
5. The broadest geographic monitoring coverage for biota was for marine mammals (54), followed by freshwater fish and seabirds, with time series also available for marine fish and invertebrates and terrestrial mammals (2), though there remains substantial regional variation in coverage within all species groups. Biotic time series were available for blue mussels (12), marine (11) and freshwater (19) fish, seabirds (12), terrestrial (2) and marine mammals (54), however the coverage of the species groups varied considerably between circumarctic countries. Trends across the full time series (ranging from 1968–2018) and the recent trends from 1999 to the last year of data available were analyzed.
6. Biomonitoring to establish trends of Hg in Arctic human populations remains limited, with only four locations (one in Canada, two on Greenland and one on the Faroe Islands) providing time series appropriate for temporal trend analysis. All available time series concern levels of Hg measured in blood, with most concentrating on women of child-bearing age.
7. Connecting Hg trends in air, precipitation, biota and human populations remains challenging due to the many transformations of Hg in the environment and in monitored populations and organisms, as well as the mixture of fast and slow processes which impact these levels.

Assessing temporal trends is a key method of inquiry, which can reveal insights into relationships among key environmental and intervention drivers and should remain a priority for AMAP and its member nations.

Are concentrations of mercury changing over time? [2.3]

8. Three tree-ring records from northern Canada, from the northern Mackenzie Delta (1576–2015), Old Crow (1736–2005) and Scree Hill (1612–2016), show increasing Hg concentrations over time and that the beginning of the accumulation of Hg in the Arctic was concurrent with the European industrial revolution.
9. In air, decreasing TGM concentrations since the late-1990s across most of the 10 circumarctic stations for which time series are available are encouraging from an intervention perspective.
10. Trend analyses results confirmed previous findings of general decreasing trends in annual Hg concentrations in precipitation and wet deposition, with precipitation amount increasing at more southerly Arctic sites; sites in southern Scandinavia included for comparison had increasing or no trends in Hg concentrations and wet deposition.
11. Decreases in THg levels in blood of northern peoples are also encouraging and are partly associated with dietary changes, which are directly influenced by food advisory interventions, such as those in the Faroese populations.
12. Concentrations of Hg were found to be changing (increasing or decreasing) significantly in 37 of 77 biota time series that had sufficient statistical power (≥80%) to detect a trend, with 31 recent trends (1999–present) also meeting these criteria. There were 14 decreasing and 17 increasing recent trends in biota, thus generalizations about the direction of trends overall or within species groups are difficult to make.

The mixture of increasing and decreasing temporal trends for Hg in biota and precipitation, along with shifts in the timing of important Hg speciation processes, underscore the need for continued monitoring of Hg in Arctic environments and in a range of different media.

Are there spatial patterns of mercury trends in biota from the Arctic? [2.4]

13. Seabirds were the only species group to exhibit significant latitudinal variation in their Hg trends, with Hg levels decreasing faster at greater latitudes.
14. The addition of more high trophic level mammalian time series from Canadian and European sites changed the longitudinal pattern of trends observed in the 2011 AMAP Mercury Assessment, with more increasing trends now observed between East Greenland and Svalbard.
15. No clear spatial patterns were observed for freshwater or marine fish, or marine invertebrates (mussels).

Extending the existing Alaskan time series and adding time series in Russia would provide useful geographical coverage for future trend analyses and would facilitate more complete circumarctic comparisons.

Further conclusions and findings

Long-term historical trends in deposition

16. Historical time series are valuable for assessing the influence of anthropogenic emissions on current Hg levels, but these are completely lacking from Alaska and Russia, representing a substantial gap in knowledge at these locations.
17. Concentrations of Hg(0) in tree-rings at all three sites increased overall between the pre-industrial era and present day. However, in the last five decades, concentrations in the northern Mackenzie Delta (close to the Beaufort Sea coastline) declined rapidly, from approximately 1970–2000, possibly reflecting the implementation of emission controls. However, these appear to have rebounded and are increasing again at that location post-2000; this pattern was not observed at other inland sites.

Continued monitoring of long-term trends of Hg(0) in tree rings may be useful for tracking the effectiveness of regulatory measures implemented based on recommendations from the Minamata Convention.

Trends in air and precipitation

18. The magnitude of the long-term trends of TGM in Alert and Ny-Ålesund (for the periods 1995–2018 and 2002–2018, respectively) differed from more recent trends (2008–2018); monthly trends of GOM and PHg at Alert reversed direction and changed in magnitude when analyzed over the 2002 to 2018 period versus the 2008 to 2018 period. Seasonal TGM concentrations at the four coastal High Arctic sites had greater variability than at Subarctic sites, differences that are driven by local AMDE chemistry. Springtime concentrations and trends are likely influenced by AMDEs at those coastal sites as well. These examples indicate the importance of consistency when selecting the temporal range of data to compare time series and trends.
19. Trends of TGM in air during the autumn at all High Arctic sites and European Subarctic sites were decreasing. The autumn season is independent of processes that increase seasonal variability making it the most suitable for reflecting trends in background concentrations at High Arctic sites, in particular, at coastal sites that are influenced by AMDEs. Increasing annual and winter trends of TGM were observed at one location, Little Fox Lake in the western Canadian Subarctic. These were hypothesized to be due to increases in Asian mercury emissions and changing weather patterns delivering air masses more frequently from Asia. Continued monitoring at Denali National Park in Alaska could verify this hypothesis as its location indicates that it would likely be subjected to the same changes in air masses and mercury levels; however, the current time series of 5 years was inconclusive.
20. Analysis of GOM and PHg at Alert and Ny-Ålesund showed opposing GOM and PHg trends, with Alert moving towards increasing GOM and Ny-Ålesund moving towards increasing PHg and both sites showing changes in the process that may affect the deposition and input of Hg to the Arctic environment. Changing the timing of Arctic haze patterns and sea-ice coverage may be driven by climate and may also drive change to AMDEs. Although Station Nord does not have a measurement of GOM and PHg, the overall decreasing trend in TGM suggests there may also be a change in AMDEs during the spring and summer periods.
21. Time series for precipitation (and wet deposition) from seven sites in North America and Europe were examined for temporal trends. Latitudinal and longitudinal gradients were apparent, with lower wet deposition at sites further north and with sites in North America tending to have lower wet deposition of Hg than the sites in Europe. Deposition was highest in the warm seasons at Subarctic inland sites over coastal sites, coinciding with high precipitation levels in the summer, when Hg is most effectively scavenged from the atmosphere by rain.
22. The geographic variation in trends in Hg in precipitation in sites within and close to the Arctic seems to be influenced by proximity to Hg emission source areas and seasonal cycles in the amount of precipitation and Hg wet deposition. Precipitation Hg levels and deposition of Hg closer to primary Hg emission sources seem to respond to reductions in local Hg emissions, while those further north are likely driven by secondary emissions and changes in long-range transported mercury.

Air monitoring is a component in an eventual global Hg monitoring plan to support the effectiveness evaluation of the Minamata Convention. Analyses of Hg time series in Arctic air and precipitation illustrate a number of potential pitfalls in over-simplistic interpretation of air and precipitation data.

Analyses of Hg air and precipitation time series need to consider meteorological factors and processes that affect Hg levels at geographical (local/regional) and temporal (e.g., seasonal) scales, as well as the speciation of Hg. These factors can have an important bearing on the attribution and interpretation of trends observed in air and precipitation in relation to changes in emissions.

Biota trends

23. Continued monitoring since 2011 has resulted in a drastic improvement in the number of available biota time series and their associated statistical power. This provided the opportunity for broader circumpolar comparisons of changes in THg levels, as well as a greater ability to consider possible influences of changing processes, including climate change influences on trends.
24. Biota time series can exhibit complex, non-linear trends that may be related to changing environmental processes that require better understanding. Together with the need to improve power for specific time series, this indicates the need for continued monitoring of temporal trends in a wide range of species and media.
25. In marine mammals, there is a tendency for temporal trends in muscle tissue to be more powerful, and they may deviate in terms of magnitude and direction, from other matrices like liver, kidney or mattak/muktuk. The Hg contained in muscle is mainly MeHg; since a larger amount of muscle/meat is consumed compared to internal organs, this could be an important source of Hg and is therefore important to monitor in relation to human exposure. However further investigation (that includes human health experts) is needed as concentrations of THg in muscle of marine mammals are much lower than those in liver, and difference in dietary choices impact human exposure substantially.

The most comprehensive monitoring coverage for trends of Hg in the Arctic is observed for biota, and these monitoring efforts should be continued annually where possible. Increased attention should be given to extending temporal trend monitoring to parts of the Arctic currently lacking time series, and should include retrospective analyses of environmental archives to fill gaps while new monitoring systems are established.

Addressing concerns of Northern Peoples remains a priority, so monitoring species and tissues that are relevant for assessing both ecosystem health and human exposure through consumption are important. Therefore, time series for tissues that are most often consumed in relatively large amounts and that produce powerful trends (e.g., muscle tissue) should be considered for addition to more monitoring programs.

Statistical methods for time series analysis should be further refined to take into account additional environmental factors (in particular those associated with climate change) and existing time series should be re-evaluated as soon as possible to better understand the influence of climate-related drivers on Hg in ecosystems and food webs.

Specific findings: trends in invertebrates and fish

26. Despite substantial statistical power (≥80%) and length of time series, few significant trends were found in blue mussels and those that were found at relatively nearby locations differed, which probably reflects differences in local processes.
27. Recent trends of Hg levels were decreasing or insignificant in many of the freshwater fish populations, but were increasing in lake trout and burbot from the Mackenzie River watershed (Northwest Territories, Canada) and in landlocked char on Svalbard at a lake where local processes are known to influence levels of other contaminants.
28. Differences in watershed characteristics for Subarctic lakes, lake chemistry, and food web changes as well as impacts of changing climate and weather variables on these factors are likely sources of variation in the trends (see Chapter 5).

Establishing marine bivalve monitoring programs in additional circumarctic locations could provide cost-effective and useful information about the spatial patterns of Hg throughout the North, as well as allowing comparisons with similar programs at lower latitudes, though other species may provide more statistically powerful time series for temporal analysis.

Specific findings: trends in seabirds

29. Time series of THg in seabird eggs were particularly powerful, likely due to the consistency of the analyses under the seabird monitoring programs and the lack of confounding factors that affect the exposure of mature animals to Hg.
30. The majority of THg trends in seabird populations were increasing or were insignificant; only one seabird trend was significantly decreasing (Norwegian black-legged kittiwakes).
31. Alaskan (USA) seabird time series have not been recently extended, which along with a lack of Russian data, create a geographical gap in seabird and other biota time series.

Monitoring of seabirds for Hg throughout the North should continue, particularly for eggs which produce very powerful trends. Efforts to extend the existing Alaskan time series and produce monitoring data in seabirds from Russia would fill a substantial geographic gap in monitoring.

Specific findings: trends in mammals

32. Despite circumpolar distributions, ringed seal time series were only available from Greenland and Canada, toothed whales from the Faroe Islands and Canada, and polar bears from Greenland, Canada and Svalbard.
33. Monitoring coverage for terrestrial mammals was very limited, with caribou annually monitored at only two sites in Canada and with no other species represented in the current assessment (Arctic fox were investigated with the marine mammals in this assessment). The existing datasets are powerful, but did not produce significant trends and thus interpretation was limited.

The current marine mammal monitoring programs should continue and be expanded where possible. A broader geographic range of samples from toothed whales and ringed seals, which are particularly important subsistence animals, would make for extremely useful spatiotemporal comparisons relevant to both ecosystem health and human exposure.

Caribou, reindeer and other ungulates are also important for subsistence, have broad geographic distributions and also have different exposure pathways than marine mammals and efforts should be made to include more locations.

Specific findings: humans

34. Mercury levels in human blood continued to decrease in Nunavik (Canada), the Disko Bay area (West Greenland) and in the Faroe Islands. The time series in women from Nuuk, Greenland, did not produce significant trends. It is likely that changes in lifestyle and dietary choices of Northern Peoples help to drive the decreasing Hg exposure and concentrations in human blood; dietary advice to protect health is a contributing factor in at least the Faroese case. It should be recognized that the decreasing exposure to Hg as a result of changing diet is often associated with shifts to a less healthy diet in terms of overall nutrition; thus, advice on the relative risks and benefits associated with dietary change and Hg exposure is a topic requiring specialized expertise (see Chapter 7).
35. Establishing direct relationships between Hg levels in wildlife and concentrations in people consuming wildlife for food is not a primary objective of most current trend monitoring studies, an exception being the Faroese study of linkages between Hg level in pilot whales and Faroese people.

Human monitoring based on levels in hair is likely to be a key component in an eventual global Hg monitoring plan to support the effectiveness evaluation of the Minamata Convention. AMAP should consider introducing hair monitoring in its programme as a basis for extending the geographical coverage of temporal trend studies in humans as well as evaluating possible ways to correlate blood and hair monitoring (see Chapter 7).

Data Gaps

36. The lack of time series from Arctic Russia continues to be a significant data gap in all matrices, with Russia represented in this assessment only by a single air monitoring station (Amderma).
37. Updates to wildlife time series were not available from Alaska for the current assessment, although there are nearby marine (Beaufort Sea) and freshwater/terrestrial monitoring programs (Northwest Territories and the Yukon). Given the relatively high concentrations of THg in species from the western Canadian Arctic, data from Alaska would be valuable for comparative purposes.
38. Available air/deposition time series for Hg from Alaska were either inadequate for trend assessment (e.g., air, 4 years) or did not produce significant trends (e.g., precipitation); these should continue and be re-analyzed in the next assessment as the addition of ~10 years of data can substantially improve trend analyses.
39. Time series in low trophic level biota, including invertebrates, are rare in the Arctic, a problem also identified in the 2011 AMAP Mercury Assessment. Food web transfer and biomagnification are key processes affecting MeHg levels and trends in wildlife and cannot be assessed without information from low trophic level organisms. Including these could provide valuable insights; for example, the geographic trends in high trophic level fish and marine mammals could be due to differences lower in the food web, but cannot currently be assessed.

Countries should review their existing temporal trend monitoring activities with respect to filling the gaps identified in this assessment.

Appendix Table of Contents

Appendix 2.1 Available mercury time series and trend results

Appendix 2.1 (A2.1) contains Table A2.1, Table A2.2, Table A2.3 and Table A2.4, which together present the available mercury time series and trend results. Table A2.1 gives time series available for temporal analysis of mercury concentrations in air (A) and wet deposition/precipitation (B). Table A2.2 presents time series available for temporal analysis of Hg concentrations in biota. Table A2.3 lists time trends selected for temporal analysis of Hg concentrations in human blood (µg/L). Table A2.4 presents time series of total mercury (geometric means and range) in whole blood (µg/L) from the Faroe Islands.

Table A2.1 Time series available for temporal analysis of mercury concentrations in air (A) and wet deposition/precipitation[a] (B).

(A) Country	Location	Measurement	Years (*n*)	First year	Last year	Reference
Coastal High Arctic						
Canada	Alert	TGM	24	1995	2018	NCP/ECCC
Canada	Alert	GEM/GOM/PHg	17	2002	2018	NCP/ECCC
Northeast Greenland	Station Nord, Villum	TGM	11	2008	2018	EBAS
Norway	Ny-Ålesund (Svalbard)	TGM	18	2001	2018	EBAS
Norway	Ny-Ålesund (Svalbard)	GOM/PHg	12	2007	2018	EBAS
Russia	Amderma	TGM	9	2001	2009	EBAS
Continental Subarctic						
Canada	Little Fox Lake	TGM	12	2007	2018	NCP/ECCC
Finland	Hyytiälä	TGM	11	2008	2018	EBAS
Finland	Pallas (68.0°, 24.23°)	TGM	11	2008	2018	EBAS
Finland	Pallas (68.0°, 24.23°)	Manual TGM	23	1996	2018	EBAS
United States	Denali National Park	TGM	5	2014	2018	NADP/Pearson et al., 2019
Coastal Subarctic						
Norway	Andøya	TGM	9	2010	2018	EBAS
Finland	Virolahti	TGM	11	2008	2018	EBAS

(B) Country	Location	Station code	Latitude	Location	Years (*n*)	First year	Last year	Missing years
Finland	Pallas	FI96	67°N	Inland/Subarctic	21	1996	2018	1998, 2010
Norway	Lista/Birkenes	NO99-02	58°N	Coastal	29	1990	2018	
Sweden	Bredkälen	SE05	63°N	Inland/Subarctic	14	1998	2018	2004–2008, 2011, 2017
Sweden	Råö/Rörvik	SE02-14	57°N	Coastal	28	1989	2018	1996–1997
Sweden	Vavihill/Hallahus	SE11-20	56°N	Inland	17	1998	2018	2004–2008
United States	Gates of the Arctic National Park	AK06	67°N	Inland/Subarctic	7	2009	2015	2011
United States	Kodiak Island	AK98	57°N	Coastal/Subarctic	8	2008	2018	2010, 2016–2017

[a] The data source for Hg in precipitation was EBAS, which also holds time series for three sites in southern Finland: Valkea-Kotinen (from 1995), Virolahti (from 2009) and Hyytiälä (from 2010).

Table A2.2 Time series available for temporal analysis of Hg concentrations in biota. ICES = AMAP data reported to ICES. NCP = Northern Contaminants Program. NPI = Norwegian Polar Institute. DANCEA = Danish Cooperation for Environment in the Arctic. CEBC = Centre for Biological Studies of Chizé.

Country	Station (Lat, Long)	Species	Tissue[a]	Basis[b]	Category[c]	*n*[d]	Years[e]	Source
Marine Invertebrates (mussels)								
IS	Grímsey (66.55°, -18.02°)	*Mytilus edulis*	SB	D	--	16 (16)	1993–2013	AMAP/ICES
IS	Hvalstod Hvalfjörður (64.4°, -21.45°)	*Mytilus edulis*	SB	D	--	19 (19)	1993–2013	AMAP/ICES
IS	Hvassahraun (64.05°, -22.29°)	*Mytilus edulis*	SB	D	--	21 (21)	1993–2018	AMAP/ICES
IS	Hvítanes Hvalfjörður (64.36°, -21.5°)	*Mytilus edulis*	SB	D	--	22 (22)	1993–2018	AMAP/ICES
IS	Mjóifjörður (Dalatangi) (65.27°, -13.58°)	*Mytilus edulis*	SB	D	--	13 (13)	1997–2018	AMAP/ICES
IS	Mjóifjörður (head) (65.19°, -14.01°)	*Mytilus edulis*	SB	D	--	15 (15)	1996–2018	AMAP/ICES
IS	Mjóifjörður (Hofsá) (65.2°, -13.82°)	*Mytilus edulis*	SB	D	--	15 (15)	1995–2018	AMAP/ICES
IS	Straumur Straumsvík (64.18°, -22.24°)	*Mytilus edulis*	SB	D	--	21 (21)	1993–2018	AMAP/ICES
IS	Úlfsá Skutulsfjörður (66.06°, -23.17°)	*Mytilus edulis*	SB	D	--	17 (17)	1997–2018	AMAP/ICES
NO	Skallneset (70.14°, 30.34°)	*Mytilus edulis*	SB	D	--	22 (22)	1994–2017	AMAP/ICES
NO	Brashavn (69.9°, 29.74°)	*Mytilus edulis*	SB	D	--	19 (19)	1997–2017	AMAP/ICES
NO	Husvågen area (68.25°, 14.66°)	*Mytilus edulis*	SB	D	--	19 (19)	1997–2017	AMAP/ICES
Freshwater Fish								
CA	GSL-West Basin (60.82°, -115.79°)	*Esox lucius*	MU	W	--	23 (20)	1989*–2018	Evans et al., 2013; Evans, pers. comm., 2019; Evans and Muir, 2021b; AMAP, 2011
SE	Storvindeln (65.7°, 17.13°)	*Esox lucius*	MU	W	--	46 (46)	1968–2018	AMAP/National
CA	Fort Good Hope (66.26°, -128.63°)	*Lota lota*	LI	W	--	20 (20)	1988–2018	Carrie et al., 2010; Stern, pers. comm., 2019; Stern et al., 2021b; AMAP, 2011
CA	Fort Good Hope (66.26°, -128.63°)	*Lota lota*	MU	W	--	19 (19)	1995–2018	Carrie et al., 2010; Stern, pers. comm., 2019; Stern et al., 2021b; AMAP, 2011
CA	GSL-East Arm (62.41°, -110.74°)	*Lota lota*	MU	W	--	17 (17)	1993–2018	Evans et al, 2013; Evans, pers. comm., 2019; Evans and Muir, 2021b; AMAP, 2011
CA	GSL-West Basin (60.82°, -115.79°)	*Lota lota*	MU	W	--	26 (24)	1992–2018*	Evans et al, 2013; Evans, pers. comm., 2019; Evans and Muir, 2021b; AMAP, 2011
CA	GSL-East Arm (62.41°, -110.74°)	*Salvelinus namaycush*	MU	W	--	21 (21)	1993–2018	Evans et al, 2013; Evans, pers. comm., 2019; Evans and Muir, 2021b, AMAP, 2011
CA	GSL-West Basin (60.82°, -115.79°)	*Salvelinus namaycush*	MU	W	--	25 (25)	1979–2018	Evans et al, 2013; Evans, pers. comm., 2019; Evans and Muir, 2021b; AMAP, 2011
CA	Lake Kusawa (60.41°, -136.26°)	*Salvelinus namaycush*	MU	W	--	20 (20)	1993–2018	Gamberg et al., 2021; Gamberg, pers. comm., 2019; AMAP, 2011
CA	Lake Laberge (61.06°, -135.11°)	*Salvelinus namaycush*	MU	W	--	23 (23)	1993–2018	Gamberg et al., 2021; Gamberg, pers. comm., 2019; AMAP, 2011
CA	Amituk Lake (75.05°, -93.75°)	*Salvelinus alpinus*	MU	W	--	18 (16)	2001–2018*	Hudelson et al., 2019; Hudelson et al., pers. comm., 2019; AMAP, 2011
CA	Char Lake (74.71°, -94.9°)	*Salvelinus alpinus*	MU	W	--	13 (13)	1993–2018	Hudelson et al., 2019; Hudelson et al., pers. comm., 2019; AMAP, 2011
CA	Lake Hazen (81.8°, -71°)	*Salvelinus alpinus*	MU	W	--	18 (18)	1990–2018	Hudelson et al., pers. comm., 2019; AMAP, 2011
CA	North Lake (74.78°, -95.09°)	*Salvelinus alpinus*	MU	W	--	14 (14)	2000–2018	Hudelson et al., 2019; Hudelson et al., pers. comm., 2019; AMAP, 2011
CA	Resolute Lake (74.69°, -94.94°)	*Salvelinus alpinus*	MU	W	--	22 (22)	1993–2018	Hudelson et al., 2019; Hudelson et al., pers. comm., 2019; AMAP, 2011
GL	Isortoq (60.54°, -47.33°)	*Salvelinus alpinus*	MU	W	--	11 (11)	1994–2018	AMAP/DANCEA

Country	Station (Lat, Long)	Species	Tissue[a]	Basis[b]	Category[c]	*n*[d]	Years[e]	Source
FO	á Mýrunum (62.17°, -7.09°)	*Salvelinus alpinus*	MU	W	--	10 (10)	2000–2014	AMAP/DANCEA
NO	Bjørnøya (74.45°, 19.12°)	*Salvelinus alpinus*	MU	D	--	12 (12)	1998–2015	AMAP/Akvaplan-niva
SW	Abiskojaure (68.29°, 18.59°)	*Salvelinus alpinus*	MU	W	--	37 (37)	1981–2018	AMAP/Swedish National Monitoring Programme for Contaminants in Biota
Marine Fish								
CA	Queen Maud Gulf (69.12°, -105.06°)	*Salvelinus alpinus*	MU	W	--	17 (13)	2004–2018*	Evans et al., 2015; Evans, pers. comm., 2019; Evans and Muir, 2021a; AMAP, 2011
GL	Avanersuaq (77.28°, -69.14°)	*Myoxocephalus scorpius*	LI	W	--	9 (8)	1995–2018*	AMAP/DANCEA
GL	Ittoqqortoormiit (70.29°, -21.58°)	*Myoxocephalus scorpius*	LI	W	--	12 (11)	1995–2018*	AMAP/DANCEA
GL	Qeqertarsuaq (69.15°, -53.32°)	*Myoxocephalus scorpius*	LI	W	--	14 (14)	1994–2018	AMAP/DANCEA
FO	Mýlingsgrunnur (62.38°, -7.42°)	*Gadus morhua*	MU	W	--	27 (27)	1979–2016	AMAP/DANCEA
FO	Mýlingsgrunnur (62.38°, -7.42°)	*Gadus morhua*	MU	W	Size (Medium)	29 (29)	1979–2017	AMAP/DANCEA
IS	North-northwest off Iceland (66.92°, -22.89°)	*Gadus morhua*	MU	W	--	24 (24)	1990–2018	AMAP/ICES
IS	Northeast off Iceland (65.24°, -12.13°)	*Gadus morhua*	MU	W	--	23 (23)	1990–2018	AMAP/ICES
NO	Varangerfjorden (69.82°, 29.76°)	*Gadus morhua*	MU	W	--	21 (21)	1994–2017	AMAP/ICES
NO	Tromsø harbour (69.65°, 18.97°)	*Gadus morhua*	MU	W	--	7 (7)	2009–2017	AMAP/ICES
NO	Bjørnerøya (east) (68.19°, 14.71°)	*Gadus morhua*	MU	W	--	21 (21)	1992–2017	AMAP/ICES
Terrestrial Mammals								
CA	Old Crow (67.57°, -139.83°)	*Rangifer tarandus*	KI	D	--	26 (26)	1991–2017	Gamberg et al., 2020, AMAP, 2011
CA	Western Hudson Bay (61.11°, -94.06°)	*Rangifer tarandus*	KI	D	--	13 (13)	2006–2018	Gamberg et al., 2020, AMAP, 2011
Seabirds								
CA	Prince Leopold Island (74.04°, -90.03°)	*Fulmarus glacialis*	EH	D	--	19 (19)	1975–2017	Foster et al., 2019, AMAP, 2011
CA	Coats Island (62.47°, -83.1°)	*Uria lomvia*	EH	D	--	15 (15)	1993–2017	Morris et al., 2022, AMAP, 2011
CA	Prince Leopold Island (74.04°, -90.03°)	*Uria lomvia*	EH	D	--	19 (19)	1975–2017	Foster et al., 2019, AMAP, 2011
GL	Ittoqqortoormiit Ukaleqarteq (70.72°, -21.55°)	*Alle alle*	BL	D	--	10 (10)	2005–2015	AMAP/DANCEA
GL	Ittoqqortoormiit Ukaleqarteq (70.72°, -21.55°)	*Alle alle*	FE	D	--	10 (10)	2007–2016	Fort et al., 2016; Fort and Grémillet et al., pers. comm., 2019; ARCTOX; AMAP/DANCEA
FO	Koltur (61.99°, -6.99°)	*Cepphus grylle*	EH	W	--	11 (11)	1999–2016	AMAP/DANCEA
FO	Skúvoy (61.77°, -6.80°)	*Cepphus grylle*	EH	W	--	10 (10)	1999–2014	AMAP/DANCEA
FO	Sveipur (61.95°, -6.72°)	*Cepphus grylle*	LI	W	Juvenile	9 (9)	1995–2015	AMAP/DANCEA
FO	Sveipur (61.95°, -6.72°)	*Cepphus grylle*	FE	W	Juvenile	8 (8)	1996–2015	AMAP/DANCEA
FO	Tindhólmur (62.08°, -7.43°)	*Cepphus grylle*	FE	W	Juvenile	6 (6)	2005–2015	AMAP/DANCEA
FO	Tindhólmur (62.08°, -7.43°)	*Cepphus grylle*	LI	W	Juvenile	6 (6)	2005–2015	AMAP/DANCEA
NO	Svalbard-Kongsfjorden (79°, 11.67°)	*Rissa tridactyla*	ER	D	--	15 (15)	2000–2016	Tartu et al., 2022; AMAP/NPI, CEBC-CNRS

Table A2.2 continued

Country	Station (Lat, Long)	Species	Tissue[a]	Basis[b]	Category[c]	*n*[d]	Years[e]	Source
Marine Mammals								
CA	Eastern Beaufort Sea (69.5°, -133.58°)	*Delphinapterus leucas*	LI	W	Small	23 (23)	1981–2017	Loseto et al., 2015; Loseto et al., pers. comm., 2019; Stern et al., 2021a; AMAP, 2011
CA	Eastern Beaufort Sea (69.5°, -133.58°)	*Delphinapterus leucas*	LI	W	Large	23 (23)	1981–2017	Loseto et al., 2015; Loseto et al., pers. comm., 2019; Stern et al., 2021a; AMAP, 2011
CA	Eastern Beaufort Sea (69.5°, -133.58°)	*Delphinapterus leucas*	MU	W	Small	23 (23)	1981–2017	Loseto et al., 2015; Loseto et al., pers. comm., 2019; Stern et al., 2021a; AMAP, 2011
CA	Eastern Beaufort Sea (69.5°, -133.58°)	*Delphinapterus leucas*	MU	W	Large	22 (21)	1993–2017*	Loseto et al., 2015; Loseto et al., pers. comm., 2019; Stern et al., 2021a; AMAP, 2011
CA	Eastern Beaufort Sea (69.5°, -133.58°)	*Delphinapterus leucas*	EP	W	Small	20 (20)	1993–2017	Loseto et al., 2015; Loseto et al., pers. comm., 2019; Stern et al., 2021a; AMAP, 2011
CA	Eastern Beaufort Sea (69.5°, -133.58°)	*Delphinapterus leucas*	EP	W	Large	20 (20)	1993–2017	Loseto et al., 2015; Loseto et al., pers. comm., 2019; Stern et al., 2021a; AMAP, 2011
CA	Southern Hudson Bay (56.54°, -79.22°)	*Delphinapterus leucas*	LI	W	Small	15 (15)	1994–2016	Loseto et al., 2015; Loseto et al., pers. comm., 2019; Stern et al., 2021a; AMAP, 2011
CA	Southern Hudson Bay (56.54°, -79.22°)	*Delphinapterus leucas*	LI	W	Large	17 (17)	1994–2016	Loseto et al., 2015; Loseto et al., pers. comm., 2019; Stern et al., 2021a; AMAP, 2011
CA	Southern Hudson Bay (56.54°, -79.22°)	*Delphinapterus leucas*	MU	W	Small	15 (15)	1994–2016	Loseto et al., 2015; Loseto et al., pers. comm., 2019; Stern et al., 2021a, AMAP, 2011
CA	Southern Hudson Bay (56.54°, -79.22°)	*Delphinapterus leucas*	MU	W	Large	17 (17)	1994–2016	Loseto et al., 2015; Loseto et al., pers. comm., 2019; Stern et al., 2021a; AMAP, 2011
FO	Føroyskar Hvalvágir (62.00°, -7.00°)	*Globicephala melas*	MU	W	Undefined	20 (17)	1997–2017*	AMAP/DANCEA
FO	Føroyskar Hvalvágir (62.00°, -7.00°)	*Globicephala melas*	MU	W	Adult	15 (12)	1997–2015*	AMAP/DANCEA
FO	Føroyskar Hvalvágir (62.00°, -7.00°)	*Globicephala melas*	MU	W	Juvenile M	18 (16)	1997–2017*	AMAP/DANCEA
FO	Føroyskar Hvalvágir (62.00°, -7.00°)	*Globicephala melas*	LI	W	Adult	12 (12)	2001–2017	AMAP/DANCEA
FO	Føroyskar Hvalvágir (62.00°, -7.00°)	*Globicephala melas*	LI	W	Juvenile M	6 (6)	2001–2015	AMAP/DANCEA
CA	Eastern Beaufort Sea (71.99°, -125.25°)	*Pusa hispida*	LI	W	Adult	14 (12)	2001–2017*	Houde et al., 2020; AMAP, 2011
CA	Eastern Beaufort Sea (71.99°, -125.25°)	*Pusa hispida*	LI	W	Juvenile	13 (11)	2001–2017*	Houde et al., 2020; AMAP, 2011
CA	Eastern Beaufort Sea (71.99°, -125.25°)	*Pusa hispida*	MU	W	Adult	14 (12)	2001–2017*	Houde et al., 2020; AMAP, 2011
CA	Eastern Beaufort Sea (71.99°, -125.25°)	*Pusa hispida*	MU	W	Juvenile	14 (12)	2001–2017*	Houde et al., 2020; AMAP, 2011
CA	Resolute Passage (74.70°, -94.83°)	*Pusa hispida*	LI	W	Adult	16 (16)	1993–2017	Houde et al., 2020, AMAP, 2011
CA	Resolute Passage (74.70°, -94.83°)	*Pusa hispida*	LI	W	Juvenile	15 (15)	1993–2017	Houde et al., 2020; AMAP, 2011
CA	Resolute Passage (74.70°, -94.83°)	*Pusa hispida*	MU	W	Adult	15 (14)	2004–2017*	Houde et al., 2020, AMAP, 2011
CA	Resolute Passage (74.70°, -94.83°)	*Pusa hispida*	MU	W	Juvenile	15 (14)	2004–2017*	Houde et al., 2020; AMAP, 2011
CA	Labrador Sea (56.54°, -61.70°)	*Pusa hispida*	LI	W	Adult	9 (9)	1997–2017	Houde et al., 2020; AMAP, 2011
CA	Labrador Sea (56.54°, -61.70°)	*Pusa hispida*	LI	W	Juvenile	8 (8)	1998–2017	Houde et al., 2020; AMAP, 2011
CA	Labrador Sea (56.54°, -61.70°)	*Pusa hispida*	MU	W	Adult	10 (10)	1997–2017	Houde et al., 2020, AMAP, 2011
CA	Labrador Sea (56.54°, -61.70°)	*Pusa hispida*	MU	W	Juvenile	9 (9)	1998–2017	Houde et al., 2020; AMAP, 2011

Table A2.2 continued

Country	Station (Lat, Long)	Species	Tissue[a]	Basis[b]	Category[c]	*n*[d]	Years[e]	Source
CA	Western Hudson Bay (61.11°, -94.06°)	*Pusa hispida*	LI	W	Adult	15 (15)	1992–2017	Houde et al., 2020; AMAP, 2011
CA	Western Hudson Bay (61.11°, -94.06°)	*Pusa hispida*	LI	W	Juvenile	14 (13)	2003–2017*	Houde et al., 2020; AMAP, 2011
CA	Western Hudson Bay (61.11°, -94.06°)	*Pusa hispida*	MU	W	Adult	14 (13)	2003–2017*	Houde et al., 2020; AMAP, 2011
CA	Western Hudson Bay (61.11°, -94.06°)	*Pusa hispida*	MU	W	Juvenile	14 (13)	2003–2017*	Houde et al., 2020; AMAP, 2011
GL	Ittoqqortoormiit (70.29°, -21.58°)	*Pusa hispida*	LI	W	Undefined	6 (6)	1999–2016	AMAP/DANCEA
GL	Avanersuaq (77.28°, -69.14°)	*Pusa hispida*	LI	W	Adult	10 (10)	1994–2018	AMAP/DANCEA
GL	Avanersuaq (77.28°, -69.14°)	*Pusa hispida*	LI	W	Juvenile	12 (12)	1984–2018	AMAP/DANCEA
GL	Ittoqqortoormiit (70.29°, -21.58°)	*Pusa hispida*	LI	W	Adult	14 (14)	1986–2018	AMAP/DANCEA, Pinzone, 2021
GL	Ittoqqortoormiit (70.29°, -21.58°)	*Pusa hispida*	LI	W	Juvenile	14 (14)	1986–2018	AMAP/DANCEA, Pinzone, 2021
GL	Qeqertarsuaq (69.15°, -53.32°)	*Pusa hispida*	LI	W	Juvenile	14 (14)	1994–2018	AMAP/DANCEA
CA	Southern Hudson Bay (56.54°, -79.22°)	*Ursus maritimus*	LI	D	Adult F	10 (10)	2006–2017	Morris et al., 2022, Letcher and Dyck, 2021; Letcher, pers. comm., 2019; AMAP, 2011
CA	Southern Hudson Bay (56.54°, -79.22°)	*Ursus maritimus*	LI	D	Adult M	10 (10)	2006–2017	Morris et al., 2022, Letcher and Dyck, 2021; Letcher, pers. comm., 2019; AMAP, 2011
CA	Southern Hudson Bay (56.54°, -79.22°)	*Ursus maritimus*	LI	D	Juvenile	7 (7)	2007–2015	Morris et al., 2022, Letcher and Dyck, 2021; Letcher, pers. comm., 2019; AMAP, 2011
CA	Western Hudson Bay (61.11°, -94.06°)	*Ursus maritimus*	LI	D	Adult F	6 (6)	2007–2017	Morris et al., 2022, Letcher and Dyck, 2021; Letcher, pers. comm., 2019; AMAP, 2011
CA	Western Hudson Bay (61.11°, -94.06°)	*Ursus maritimus*	LI	D	Adult M	10 (10)	2007–2017	Morris et al., 2022, Letcher and Dyck, 2021; Letcher, pers. comm., 2019; AMAP, 2011
CA	Western Hudson Bay (61.11°, -94.06°)	*Ursus maritimus*	LI	D	Juvenile	8 (8)	2007–2015	Morris et al., 2022, Letcher and Dyck, 2021; Letcher, pers. comm., 2019; AMAP, 2011
GL	Ittoqqortoormiit (70.29°, -21.58°)	*Ursus maritimus*	LI	W	Undefined	14 (14)	1986–2018	AMAP/DANCEA
GL	Ittoqqortoormiit (70.29°, -21.58°)	*Ursus maritimus*	LI	W	Adult F	22 (22)	1984–2018	AMAP/DANCEA
GL	Ittoqqortoormiit (70.29°, -21.58°)	*Ursus maritimus*	LI	W	Adult M	24 (24)	1984–2018	AMAP/DANCEA
GL	Ittoqqortoormiit (70.29°, -21.58°)	*Ursus maritimus*	LI	W	Juvenile	28 (28)	1983–2018	AMAP/DANCEA
GL	Ittoqqortoormiit (70.29°, -21.58°)	*Ursus maritimus*	HA	D	Undefined	12 (11)	2000–2018*	AMAP/DANCEA
GL	Ittoqqortoormiit (70.29°, -21.58°)	*Ursus maritimus*	HA	D	Adult F	16 (14)	1999–2018*	AMAP/DANCEA
GL	Ittoqqortoormiit (70.29°, -21.58°)	*Ursus maritimus*	HA	D	Adult M	17 (16)	1999–2018*	AMAP/DANCEA
GL	Ittoqqortoormiit (70.29°, -21.58°)	*Ursus maritimus*	HA	D	Juvenile	21 (21)	1984–2018	AMAP/DANCEA
NO	Svalbard (77.88°, 20.98°)	*Ursus maritimus*	HA	D	Adult F	25 (25)	1990–2016	AMAP/NPI, Lippold et al., 2020, 2022
NO	Svalbard (77.88°, 20.98°)	*Ursus maritimus*	HA	D	Juvenile	10 (10)	1998–2014	AMAP/NPI, Lippold et al., 2020, 2022
NO	Svalbard (77.88°, 20.98°)	*Vulpes lagopus*	LI	W	--	11 (11)	1998–2014	AMAP/NPI, Hallanger et al., 2019; Routti et al., 2020

[a] BL = whole blood, EH = egg homogenate, EP = epidermis, ER = erythrocytes, FE = feathers, HA = hair, LI = liver, MU = muscle, SB = soft body (whole)

[b] Wet (W) or dry (D) weight concentrations

[c] Categories for marine mammals are defined under Section 2.3.2.4

[d] The total years available and the number of years used in the longest trend analyzed (in parentheses) are shown

* Indicates time series that were truncated due to gaps of more than 5 years in length

Appendix 2.2 Summary of results

Appendix 2.2 (A2.2) contains, first, a summary of results for statistics and trends in air: Tables A2.5 and A2.6 give daily mean TGM (ng/m^3) and summary statistics for all available data and for the period 2008 to 2018 exclusively, respectively; Tables A2.7 and A2.8 present median trends and 95% confidence intervals for long-term Arctic monitoring sites for all of the available data and for the period 2008 to 2018, respectively; Table A2.9 gives annual and monthly trends (% change) in GOM and PHg for Alert (2002–2018 and 2008–2018) and Ny-Ålesund (2008–2018). Next, there is a summary of results for trends in wet deposition/precipitation is presented in Table A2.10 which shows trends in precipitation/wet deposition for all years available (A2.10a) and for 2009–2018 (A2.10b). Finally, in this section, there is a summary of results for trends in biota, presented in Table A2.11.

Summary of results for summary statistics and trends in air

Table A2.5 Daily mean TGM (ng/m^3) and summary statistics for all available data.

Site	Date Range	Mean daily TGM ng/m^3	Standard deviation	Min daily mean TGM ng/m^3	Max daily mean TGM ng/m^3	Q1 daily mean TGM ng/m^3	Median daily mean TGM ng/m^3	Q3 daily mean TGM ng/m^3
Andøya	Annual	1.53	0.15	0.64	2.02	1.42	1.52	1.63
	Winter	1.61	0.14	1.28	2.02	1.50	1.62	1.71
	Spring	1.53	0.16	0.64	1.94	1.43	1.53	1.63
	Summer	1.49	0.13	1.03	1.88	1.40	1.48	1.57
	Autumn	1.50	0.15	1.14	2.01	1.37	1.50	1.59
Amderma (2001–2009)	Annual	1.54	0.31	0.17	4.38	1.40	1.57	1.72
	Winter	1.66	0.19	0.38	2.72	1.59	1.68	1.76
	Spring	1.43	0.48	0.17	4.38	1.12	1.51	1.77
	Summer	1.61	0.23	0.90	2.39	1.47	1.61	1.75
	Autumn	1.47	0.16	1.15	2.09	1.36	1.46	1.58
Pallas	Annual	1.40	0.14	0.80	1.92	1.30	1.41	1.50
	Winter	1.52	0.10	1.19	1.92	1.45	1.51	1.57
	Spring	1.45	0.14	0.80	1.85	1.37	1.46	1.56
	Summer	1.34	0.11	0.98	1.64	1.26	1.35	1.42
	Autumn	1.30	0.11	0.81	1.65	1.24	1.30	1.37
Pallas (weekly manual traps)	Annual	1.38	0.20	0.54	2.81	1.26	1.37	1.48
	Winter	1.49	0.19	1.05	2.81	1.38	1.47	1.57
	Spring	1.42	0.21	0.55	2.18	1.29	1.42	1.54
	Summer	1.33	0.18	0.73	2.14	1.25	1.33	1.41
	Autumn	1.28	0.16	0.54	2.06	1.19	1.27	1.36
Hyytiälä	Annual	1.23	0.15	0.76	1.69	1.13	1.23	1.34
	Winter	1.30	0.14	0.98	1.69	1.20	1.29	1.39
	Spring	1.31	0.14	0.77	1.69	1.21	1.32	1.41
	Summer	1.19	0.13	0.80	1.66	1.11	1.19	1.29
	Autumn	1.13	0.12	0.76	1.51	1.04	1.13	1.20
Virolahti	Annual	1.29	0.15	0.76	2.20	1.19	1.29	1.39
	Winter	1.40	0.14	1.03	2.20	1.31	1.38	1.49
	Spring	1.32	0.13	0.76	1.81	1.25	1.32	1.40
	Summer	1.28	0.13	0.93	1.67	1.19	1.28	1.36
	Autumn	1.20	0.14	0.87	1.78	1.11	1.20	1.28

Table A2.5 continued

Site	Date Range	Mean daily TGM ng/m³	Standard deviation	Min daily mean TGM ng/m³	Max daily mean TGM ng/m³	Q1 daily mean TGM ng/m³	Median daily mean TGM ng/m³	Q3 daily mean TGM ng/m³
Villum Research Station (Nord) (2008–2018)	All	1.33	0.36	0.12	2.96	1.12	1.36	1.52
	Winter	1.33	0.27	0.32	2.48	1.16	1.38	1.51
	Spring	1.24	0.56	0.12	4.47	0.87	1.26	1.49
	Summer	1.56	0.32	0.50	2.57	1.38	1.55	1.73
	Autumn	1.31	0.23	0.49	2.28	1.15	1.35	1.43
Denali National Park	Annual	1.30	0.15	0.86	1.68	1.19	1.32	1.41
	Winter	1.35	0.11	0.94	1.62	1.31	1.37	1.42
	Spring	1.44	0.10	1.06	1.68	1.37	1.44	1.51
	Summer	1.26	0.12	0.86	1.63	1.19	1.26	1.35
	Autumn	1.20	0.13	0.87	1.61	1.12	1.19	1.30
Ny-Ålesund	Annual	1.53	0.23	0.00	2.43	1.44	1.56	1.66
	Winter	1.56	0.17	0.50	2.31	1.49	1.58	1.66
	Spring	1.45	0.33	0.00	2.41	1.31	1.52	1.66
	Summer	1.61	0.19	0.34	2.43	1.52	1.61	1.71
	Autumn	1.51	0.15	0.66	1.99	1.41	1.50	1.61
Little Fox Lake	Annual	1.38	0.17	0.66	1.80	1.27	1.40	1.51
	Winter	1.40	0.20	0.66	1.80	1.33	1.45	1.51
	Spring	1.47	0.17	0.85	1.78	1.42	1.52	1.58
	Summer	1.38	0.11	1.00	1.70	1.30	1.38	1.45
	Autumn	1.26	0.12	0.71	1.64	1.19	1.27	1.34
Alert	Annual	1.44	0.38	0.00	3.27	1.30	1.47	1.65
	Winter	1.49	0.18	0.62	2.49	1.35	1.48	1.62
	Spring	1.15	0.48	0.00	3.12	0.79	1.21	1.53
	Summer	1.74	0.32	0.34	3.27	1.54	1.72	1.92
	Autumn	1.42	0.16	1.00	2.80	1.31	1.41	1.53

Table A2.6. Daily mean TGM (ng/m³) and summary statistics for the period 2008 to 2018 exclusively.

Site	Date Range	Mean Daily TGM ng/m³	Standard Deviation	Minimum daily mean TGM ng/m³	Maximum daily mean TGM, ng/m³	Q1 daily mean TGM, ng/m³	Median daily mean TGM, ng/m³	Q3 daily mean TGM, ng/m³
Andøya	All	1.52	0.15	0.64	2.02	1.41	1.51	1.62
	Winter	1.61	0.14	1.28	2.02	1.50	1.62	1.71
	Spring	1.53	0.16	0.64	1.94	1.43	1.53	1.63
	Summer	1.49	0.13	1.03	1.88	1.40	1.48	1.57
	Autumn	1.50	0.15	1.14	2.01	1.37	1.50	1.59
Pallas (Tekran)	All	1.40	0.14	0.80	1.92	1.30	1.41	1.50
	Winter	1.52	0.10	1.19	1.92	1.45	1.51	1.57
	Spring	1.45	0.14	0.80	1.85	1.37	1.46	1.56
	Summer	1.34	0.11	0.98	1.64	1.26	1.35	1.42
	Autumn	1.30	0.11	0.81	1.65	1.24	1.30	1.37
Pallas (manual traps)	All	1.37	0.20	0.54	2.81	1.25	1.36	1.47
	Winter	1.49	0.19	1.05	2.81	1.38	1.47	1.57
	Spring	1.42	0.21	0.55	2.18	1.29	1.42	1.54
	Summer	1.33	0.18	0.73	2.14	1.25	1.33	1.41
	Autumn	1.28	0.16	0.54	2.06	1.19	1.27	1.36
Hyytiälä	All	1.23	0.15	0.76	1.69	1.13	1.23	1.34
	Winter	1.30	0.14	0.98	1.69	1.20	1.29	1.39
	Spring	1.31	0.14	0.77	1.69	1.21	1.32	1.41
	Summer	1.19	0.13	0.80	1.66	1.11	1.19	1.29
	Autumn	1.13	0.12	0.76	1.51	1.04	1.13	1.20
Virolahti	All	1.29	0.15	0.76	2.20	1.19	1.29	1.39
	Winter	1.40	0.14	1.03	2.20	1.31	1.38	1.49
	Spring	1.32	0.13	0.76	1.81	1.25	1.32	1.40
	Summer	1.28	0.13	0.93	1.67	1.19	1.28	1.36
	Autumn	1.20	0.14	0.87	1.78	1.11	1.20	1.28
Villum Research Station (Nord)	All	1.33	0.36	0.12	2.96	1.12	1.36	1.52
	Winter	1.33	0.27	0.32	2.48	1.16	1.38	1.51
	Spring	1.24	0.56	0.12	4.47	0.87	1.26	1.49
	Summer	1.56	0.32	0.50	2.57	1.38	1.55	1.73
	Autumn	1.31	0.23	0.49	2.28	1.15	1.35	1.43
Denali National Park	All	1.30	0.15	0.86	1.68	1.19	1.32	1.41
	Winter	1.35	0.11	0.94	1.62	1.31	1.37	1.42
	Spring	1.44	0.10	1.06	1.68	1.37	1.44	1.51
	Summer	1.26	0.12	0.86	1.63	1.19	1.26	1.35
	Autumn	1.20	0.13	0.87	1.61	1.12	1.19	1.30
Ny-Ålesund	All	1.50	0.24	0.00	2.43	1.42	1.54	1.63
	Winter	1.56	0.17	0.50	2.31	1.49	1.58	1.66
	Spring	1.45	0.33	0.00	2.41	1.31	1.52	1.66
	Summer	1.61	0.19	0.34	2.43	1.52	1.61	1.71
	Autumn	1.51	0.15	0.66	1.99	1.41	1.50	1.61
Little Fox Lake	All	1.38	0.17	0.66	1.80	1.27	1.40	1.51
	Winter	1.40	0.20	0.66	1.80	1.33	1.45	1.51
	Spring	1.47	0.17	0.85	1.78	1.42	1.52	1.58
	Summer	1.38	0.11	1.00	1.70	1.30	1.38	1.45
	Autumn	1.26	0.12	0.71	1.64	1.19	1.27	1.34
Alert	All	1.35	0.36	0.00	3.12	1.23	1.37	1.52
	Winter	1.49	0.18	0.62	2.49	1.35	1.48	1.62
	Spring	1.15	0.48	0.00	3.12	0.79	1.21	1.53
	Summer	1.74	0.32	0.34	3.27	1.54	1.72	1.92
	Autumn	1.42	0.16	1.00	2.80	1.31	1.41	1.53

Table A2.7 Median trends and 95% confidence intervals for long-term Arctic monitoring sites for all of the available data. Amderma trends for this period could not be calculated due to insufficient data coverage.

Site	TGM trend, ng/m³/y	TGM trend, % per year	Winter trend, ng/m³/y	Winter trend, % per year
Alert	-0.014 (-0.015, -0.012)	-0.95 (-1.057, -0.842)	-0.017 (-0.018, -0.016)	-1.145 (-1.202, -1.087)
Denali National Park	-0.022 (-0.032, -0.012)	-1.665 (-2.403, -0.914)	-0.025 (-0.033, -0.018)	-1.849 (-2.386, -1.348)
Andøya	-0.029 (-0.031, -0.027)	-1.872 (-2.011, -1.732)	-0.038 (-0.041, -0.035)	-2.354 (-2.513, -2.186)
Hyytiälä	-0.017 (-0.022, -0.013)	-1.393 (-1.76, -1.037)	-0.015 (-0.019, -0.011)	-1.147 (-1.453, -0.854)
Little Fox Lake	0.013 (0.011, 0.016)	0.94 (0.761, 1.116)	0.018 (0.015, 0.021)	1.216 (1.011, 1.425)
Ny-Ålesund	-0.009 (-0.011, -0.007)	-0.574 (-0.683, -0.465)	-0.008 (-0.01, -0.007)	-0.535 (-0.616, -0.454)
Pallas	-0.012 (-0.015, -0.01)	-0.866 (-1.047, -0.686)	-0.007 (-0.009, -0.005)	-0.457 (-0.583, -0.331)
Pallas (manual traps)	-0.001 (-0.009, 0.006)	-0.076 (-0.643, 0.478)	0.003 (-0.004, 0.011)	0.217 (-0.286, 0.757)
Villum Research Station (Nord)	-0.039 (-0.046, -0.032)	-2.818 (-3.3, -2.291)	-0.063 (-0.069, -0.056)	-4.551 (-5.002, -4.085)
Virolahti	-0.001 (-0.005, 0.003)	-0.051 (-0.359, 0.244)	-0.008 (-0.013, -0.004)	-0.613 (-0.976, -0.283)
Amderma	-0.036 (-0.044, -0.027)	-2.281 (-2.79, -1.756)	-0.028 (-0.034, -0.022)	-1.689 (-2.052, -1.319)

Table A2.8 Median trends and 95% confidence intervals for long-term Arctic monitoring sites for the 2008–2018 period exclusively. Amderma trends for this period could not be calculated due to insufficient data coverage.

Site	TGM trend, ng/m³/y	TGM trend, % per year	Winter trend, ng/m³/y	Winter trend, % per year
Alert	-0.016 (-0.021, -0.011)	-1.153 (-1.52, -0.771)	-0.011 (-0.014, *f*-0.009)	-0.84 (-0.995, -0.681)
Andøya	-0.035 (-0.037, -0.032)	-2.292 (-2.462, -2.121)	-0.045 (-0.047, -0.042)	-2.75 (-2.898, -2.605)
Hyytiälä	-0.017 (-0.022, -0.013)	-1.393 (-1.76, -1.039)	-0.015 (-0.019, -0.011)	-1.147 (-1.453, -0.854)
Little Fox Lake	0.013 (0.011, 0.016)	0.955 (0.77, 1.155)	0.02 (0.017, 0.024)	1.394 (1.202, 1.636)
Ny-Ålesund	-0.014 (-0.017, -0.011)	-0.907 (-1.105, -0.704)	-0.017 (-0.019, -0.014)	-1.051 (-1.202, -0.9)
Pallas	-0.012 (-0.015, -0.01)	-0.866 (-1.047, -0.685)	-0.007 (-0.009, -0.005)	-0.457 (-0.583, -0.331)
Pallas (manual traps)	-0.001 (-0.009, 0.006)	-0.076 (-0.643, 0.476)	0.003 (-0.004, 0.011)	0.217 (-0.286, 0.757)
Villum Research Station (Nord)	-0.057 (-0.068, -0.046)	-4.145 (-4.935, -3.384)	-0.068 (-0.075, -0.062)	-5.013 (-5.492, -4.563)
Virolahti	-0.001 (-0.005, 0.003)	-0.001 (-0.306, 0.294)	-0.008 (-0.013, -0.004)	-0.613 (-0.976, -0.283)
Denali National Park	-0.022 (-0.032, -0.012)	-1.665 (-2.403, -0.914)	-0.025 (-0.033, -0.018)	-1.849 (-2.386, -1.348)

Spring trend, ng/m³/y	Spring trend, % per year	Summer trend, ng/m³/y	Summer trend, % per year	Autumn trend, ng/m³/y	Autumn trend, % per year
-0.013 (-0.016, -0.01)	-1.043 (-1.294, -0.791)	-0.013 (-0.015, -0.011)	-0.748 (-0.847, -0.647)	-0.013 (-0.014, -0.012)	-0.911 (-0.958, -0.864)
-0.057 (-0.069, -0.043)	-3.934 (-4.81, -2.971)	-0.012 (-0.022, -0.003)	-0.969 (-1.707, -0.215)	0.007 (-0.003, 0.016)	0.548 (-0.252, 1.328)
-0.019 (-0.021, -0.016)	-1.245 (-1.409, -1.082)	-0.023 (-0.024, -0.021)	-1.533 (-1.643, -1.425)	-0.035 (-0.037, -0.033)	-2.323 (-2.445, -2.209)
-0.036 (-0.042, -0.031)	-2.741 (-3.194, -2.313)	-0.019 (-0.024, -0.014)	-1.562 (-1.967, -1.167)	0.001 (-0.003, 0.004)	0.076 (-0.221, 0.378)
0.013 (0.01, 0.015)	0.823 (0.658, 0.987)	0.009 (0.007, 0.011)	0.646 (0.482, 0.8)	0.014 (0.011, 0.016)	1.083 (0.902, 1.26)
-0.009 (-0.011, -0.007)	-0.594 (-0.755, -0.433)	-0.007 (-0.008, -0.005)	-0.42 (-0.514, -0.325)	-0.011 (-0.013, -0.01)	-0.761 (-0.863, -0.661)
-0.014 (-0.017, -0.011)	-0.939 (-1.146, -0.737)	-0.012 (-0.015, -0.01)	-0.907 (-1.11, -0.705)	-0.016 (-0.018, -0.013)	-1.214 (-1.41, -1.021)
0.002 (-0.009, 0.011)	0.113 (-0.638, 0.818)	-0.009 (-0.015, -0.002)	-0.653 (-1.127, -0.181)	0 (-0.007, 0.006)	-0.019 (-0.557, 0.471)
-0.047 (-0.056, -0.038)	-3.734 (-4.497, -3.014)	-0.016 (-0.022, -0.011)	-1.062 (-1.391, -0.721)	-0.03 (-0.036, -0.021)	-2.207 (-2.638, -1.586)
-0.005 (-0.009, -0.001)	-0.358 (-0.652, -0.07)	0.003 (-0.001, 0.006)	0.22 (-0.065, 0.494)	0.008 (0.004, 0.011)	0.646 (0.364, 0.933)
-0.038 (-0.054, -0.021)	-2.511 (-3.56, -1.394)	-0.039 (-0.045, -0.032)	-2.412 (-2.81, -2.021)	-0.038 (-0.041, -0.034)	-2.579 (-2.822, -2.336)

Spring trend, ng/m³/y	Spring trend, % per year	Summer trend, ng/m³/y	Summer trend, % per year	Autumn trend, ng/m³/y	Autumn trend, % per year
-0.042 (-0.052, -0.033)	-3.729 (-4.58, -2.904)	-0.004 (-0.01, 0.002)	-0.245 (-0.609, 0.113)	-0.005 (-0.008, -0.003)	-0.394 (-0.57, -0.208)
-0.03 (-0.034, -0.027)	-1.999 (-2.222, -1.768)	-0.024 (-0.027, -0.022)	-1.663 (-1.82, -1.506)	-0.04 (-0.042, -0.038)	-2.71 (-2.863, -2.559)
-0.036 (-0.042, -0.031)	-2.741 (-3.194, -2.313)	-0.019 (-0.024, -0.014)	-1.562 (-1.967, -1.167)	0.001 (-0.003, 0.004)	0.076 (-0.221, 0.378)
0.013 (0.01, 0.015)	0.823 (0.658, 0.987)	0.006 (0.004, 0.009)	0.462 (0.266, 0.67)	0.015 (0.012, 0.017)	1.148 (0.958, 1.334)
-0.008 (-0.012, -0.003)	-0.535 (-0.83, -0.227)	-0.005 (-0.008, -0.002)	-0.311 (-0.508, -0.108)	-0.026 (-0.028, -0.024)	-1.774 (-1.926, -1.623)
-0.014 (-0.017, -0.011)	-0.939 (-1.146, -0.737)	-0.012 (-0.015, -0.01)	-0.907 (-1.11, -0.705)	-0.016 (-0.018, -0.013)	-1.214 (-1.41, -1.022)
0.002 (-0.009, 0.011)	0.113 (-0.638, 0.818)	-0.009 (-0.015, -0.002)	-0.653 (-1.127, -0.181)	0 (-0.007, 0.006)	-0.019 (-0.557, 0.471)
-0.095 (-0.112, -0.079)	-7.696 (-9.107, -6.438)	-0.034 (-0.047, -0.023)	-2.221 (-3.104, -1.506)	-0.03 (-0.036, -0.021)	-2.207 (-2.638, -1.586)
-0.005 (-0.009, -0.001)	-0.358 (-0.652, -0.07)	0.003 (-0.001, 0.006)	0.22 (-0.065, 0.493)	0.008 (0.004, 0.011)	0.646 (0.365, 0.933)
-0.057 (-0.069, -0.043)	-3.934 (-4.81, -2.971)	-0.012 (-0.022, -0.003)	-0.969 (-1.707, -0.215)	0.007 (-0.003, 0.016)	0.548 (-0.252, 1.328)

Table A2.9 Annual and monthly trends (% change) in GOM and PHg for Alert (2002–2018 and 2008–2018) and Ny-Ålesund (2008–2018).

	Alert GOM 2002–2018	Alert PHg 2002–2018	Alert GOM 2008–2018	Alert PHg 2008–2018	Ny-Ålesund GOM 2008–2018	Ny-Ålesund PHg 2008–2018
Annual trend ($pg/m^3/y$)	0.626 (0.353, 0.913)	-0.27 (-0.723, 0.174)	0.278 (-0.209, 0.797)	-0.931 (-1.532, -0.413)	-0.177 (-0.323, -0.07)	0.374 (-0.113, 0.834)
Annual trend (% per year)	3.896 (2.196, 5.682)	-1.197 (-3.211, 0.77)	1.54 (-1.158, 4.415)	-3.54 (-5.822, -1.569)	-5.478 (-10.004, -2.151)	3.854 (-1.161, 8.592)
January trend ($pg/m^3/y$)	0.146 (0.105, 0.188)	-0.278 (-0.666, 0.023)	0.134 (0.061, 0.205)	-0.987 (-1.316, -0.682)	-0.061 (-0.161, 0.044)	1.424 (0.73, 1.988)
January trend (% per year)	6.119 (4.409, 7.85)	-2.255 (-5.395, 0.189)	4.959 (2.269, 7.598)	-7.757 (-10.346, -5.359)	-3.636 (-9.614, 2.607)	10.269 (5.265, 14.337)
February trend ($pg/m^3/y$)	-0.087 (-0.171, -0.003)	-1.203 (-1.942, -0.576)	-0.156 (-0.288, -0.02)	-1.868 (-2.552, -1.156)	-0.087 (-0.152, -0.012)	-0.021 (-0.712, 0.572)
February trend (% per year)	-1.74 (-3.407, -0.057)	-5.853 (-9.45, -2.8)	-3.159 (-5.816, -0.405)	-9.114 (-12.448, -5.641)	-4.596 (-8.042, -0.626)	-0.15 (-5.126, 4.113)
March trend ($pg/m^3/y$)	0.308 (0.171, 0.449)	-0.864 (-2.374, 0.67)	-0.137 (-0.467, 0.174)	-4.986 (-6.961, -3.258)	-0.293 (-0.485, -0.171)	0.323 (-0.242, 1.083)
March trend (% per year)	3.321 (1.846, 4.838)	-0.901 (-2.476, 0.699)	-1.185 (-4.029, 1.5)	-4.785 (-6.679, -3.126)	-9.525 (-15.797, -5.555)	1.841 (-1.381, 6.177)
April trend ($pg/m^3/y$)	2.209 (1.611, 2.852)	0.015 (-1.739, 1.887)	2.119 (0.958, 3.401)	-2.085 (-4.872, 0.09)	-0.664 (-0.996, -0.327)	1.326 (0.232, 2.157)
April trend (% per year)	6.899 (5.031, 8.907)	0.015 (-1.753, 1.902)	5.384 (2.436, 8.643)	-1.883 (-4.4, 0.082)	-6.568 (-9.847, -3.233)	5.912 (1.035, 9.62)
May trend ($pg/m^3/y$)	4.198 (2.377, 6.063)	-0.241 (-0.452, -0.057)	1.154 (-1.974, 4.427)	-0.704 (-1.087, -0.351)	-0.264 (-0.389, -0.168)	0.138 (-0.029, 0.415)
May trend (% per year)	3.685 (2.086, 5.323)	-4.228 (-7.915, -0.991)	0.919 (-1.573, 3.528)	-3.764 (-5.81, -1.877)	-7.55 (-11.104, -4.808)	3.401 (-0.704, 10.201)
June trend ($pg/m^3/y$)	0.349 (-0.019, 0.77)	0.041 (0, 0.133)	0.662 (0.11, 1.374)	-0.247 (-0.382, -0.111)	-0.13 (-0.196, -0.028)	-0.079 (-0.191, 0.095)
June trend (% per year)	1.908 (-0.104, 4.215)	1.519 (0, 4.904)	3.574 (0.593, 7.42)	-3.021 (-4.674, -1.361)	-5.159 (-7.795, -1.126)	-1.974 (-4.793, 2.395)
July trend ($pg/m^3/y$)	0.188 (0.073, 0.32)	-0.129 (-0.184, -0.077)	-0.238 (-0.483, -0.01)	-0.151 (-0.232, -0.068)	-0.239 (-0.552, -0.172)	-0.148 (-0.209, 0)
July trend (% per year)	3.575 (1.378, 6.081)	-7.448 (-10.574, -4.428)	-3.661 (-7.423, -0.147)	-3.723 (-5.701, -1.677)	-6.829 (-15.781, -4.905)	-4.237 (-5.976, 0)
August trend ($pg/m^3/y$)	0.057 (0.018, 0.095)	-0.068 (-0.118, -0.021)	-0.163 (-0.25, -0.081)	-0.024 (-0.095, 0.038)	-0.225 (-0.278, -0.172)	0 (-0.13, 0.155)
August trend (% per year)	2.891 (0.905, 4.853)	-3.797 (-6.634, -1.186)	-6.694 (-10.263, -3.313)	-0.679 (-2.64, 1.063)	-6.479 (-7.995, -4.944)	0 (-3.701, 4.443)
September trend ($pg/m^3/y$)	0.028 (0.01, 0.046)	-0.022 (-0.1, 0.059)	0.008 (-0.025, 0.039)	-0.035 (-0.136, 0.066)	-0.141 (-0.223, -0.059)	-0.221 (-0.25, -0.083)
September trend (% per year)	3.034 (1.039, 4.919)	-0.586 (-2.647, 1.551)	0.804 (-2.451, 3.852)	-0.739 (-2.834, 1.367)	-8.365 (-13.225, -3.529)	-6.304 (-7.143, -2.375)
October trend ($pg/m^3/y$)	0.051 (0.035, 0.068)	-0.173 (-0.344, -0.034)	-0.021 (-0.064, 0.015)	-0.053 (-0.206, 0.06)	0.017 (-0.137, 0.088)	-0.225 (-0.365, -0.033)
October trend (% per year)	5.608 (3.854, 7.417)	-3.276 (-6.513, -0.644)	-1.816 (-5.522, 1.318)	-1.077 (-4.211, 1.215)	1.32 (-10.933, 7.013)	-4.327 (-7.019, -0.637)
November trend ($pg/m^3/y$)	0.04 (0.025, 0.057)	-0.107 (-0.345, 0.104)	0.009 (-0.021, 0.038)	-0.049 (-0.34, 0.198)	0 (-0.172, 0.114)	2.697 (1.052, 3.864)
November trend (% per year)	3.65 (2.215, 5.116)	-0.971 (-3.132, 0.942)	0.733 (-1.651, 2.961)	-0.435 (-3.045, 1.771)	0 (-4.908, 3.243)	16.737 (6.529, 23.98)
December trend ($pg/m^3/y$)	0.022 (0, 0.048)	-0.205 (-0.417, -0.028)	-0.032 (-0.067, 0.007)	0.017 (-0.2, 0.221)	-0.038 (-0.14, 0.03)	-0.726 (-1.239, -0.206)
December trend (% per year)	1.326 (0, 2.847)	-1.98 (-4.02, -0.27)	-1.789 (-3.793, 0.384)	0.142 (-1.656, 1.832)	-1.446 (-5.365, 1.138)	-8.161 (-13.934, -2.317)

Summary of results for trends in wet deposition/precipitation

Table A2.10a Trends in precipitation/wet deposition for all years available (shaded cells indicate significant trends).

Site	Name	Start year	End year	Period	Trends in volume weighted mean				
					p value	*tau*	Slope	Intercept	%/y
FI0036R	Pallas	1996	2018	Annual	0.49	-0.110	0.00	6.00	0.00
FI0036R	Pallas	1996	2018	Spring	0.58	0.095	0.07	8.07	0.81
FI0036R	Pallas	1996	2018	Summer	0.72	-0.063	-0.05	7.36	-0.64
FI0036R	Pallas	1996	2018	Autumn	0.34	-0.170	-0.03	4.11	-0.66
FI0036R	Pallas	1996	2018	Winter	1.00	0.000	0.00	4.25	0.00
NO99-01R	Lista/Birkenes	1990	2019	Annual	0.00	-0.621	-0.27	11.87	-2.25
NO99-01R	Lista/Birkenes	1990	2019	Spring	0.25	-0.153	-0.12	12.26	-0.95
NO99-01R	Lista/Birkenes	1990	2019	Summer	0.00	-0.428	-0.27	13.58	-1.99
NO99-01R	Lista/Birkenes	1990	2019	Autumn	0.00	-0.545	-0.24	9.91	-2.38
NO99-01R	Lista/Birkenes	1990	2019	Winter	0.00	-0.612	-0.28	10.45	-2.66
SE0005R	Bredkälen	1998	2018	Annual	0.23	0.242	0.10	5.35	1.87
SE0005R	Bredkälen	1998	2018	Spring	1.00	0.011	0.02	12.37	0.16
SE0005R	Bredkälen	1998	2018	Summer	0.06	0.385	0.27	5.23	5.10
SE0005R	Bredkälen	1998	2018	Autumn	0.58	0.121	0.11	3.47	3.14
SE0005R	Bredkälen	1998	2018	Winter	0.02	0.487	0.21	3.73	5.73
SE02-14R	Råö/Rörvik	1989	2018	Annual	0.01	-0.344	-0.20	12.70	-1.57
SE02-14R	Råö/Rörvik	1989	2018	Spring	1.00	-0.003	0.00	19.55	-0.01
SE02-14R	Råö/Rörvik	1989	2018	Summer	0.07	-0.267	-0.15	13.15	-1.17
SE02-14R	Råö/Rörvik	1989	2018	Autumn	0.00	-0.476	-0.20	10.68	-1.90
SE02-14R	Råö/Rörvik	1989	2018	Winter	0.00	-0.420	-0.22	11.67	-1.87
SE11-20R	Vavihill	1998	2018	Annual	0.25	-0.217	-0.14	10.07	-1.42
SE11-20R	Vavihill	1998	2018	Spring	0.89	0.033	0.03	18.34	0.18
SE11-20R	Vavihill	1998	2018	Summer	0.28	0.219	0.14	8.12	1.75
SE11-20R	Vavihill	1998	2018	Autumn	0.56	-0.117	-0.11	8.39	-1.26
SE11-20R	Vavihill	1998	2018	Winter	0.00	-0.550	-0.45	12.04	-3.77
ak06	Gates of the Arctic	2009	2015	Annual	0.55	-0.238	-0.30	5.92	-5.07
ak06	Gates of the Arctic	2009	2015	Spring	1.00	0.048	0.32	6.10	5.29
ak06	Gates of the Arctic	2009	2015	Summer	0.23	-0.429	-0.76	9.11	-8.30
ak06	Gates of the Arctic	2009	2015	Autumn	0.71	-0.200	-0.31	2.99	-10.44
ak06	Gates of the Arctic	2009	2015	Winter	0.31	0.667	0.57	1.75	32.71
ak98	Kodiak Island	2008	2018	Annual	0.17	-0.429	-0.04	1.67	-2.30
ak98	Kodiak Island	2008	2018	Spring	0.47	-0.222	-0.07	2.41	-2.90
ak98	Kodiak Island	2008	2018	Summer	0.71	-0.143	-0.04	1.77	-2.52
ak98	Kodiak Island	2008	2018	Autumn	0.54	-0.214	-0.04	1.24	-2.97
ak98	Kodiak Island	2008	2018	Winter	0.04	-0.643	-0.07	1.53	-4.81

Trends in deposition					Trends in precipitation amount				
p value	*tau*	Slope	Intercept	%/y	*p* value	*tau*	Slope	Intercept	%/y
0.16	0.229	47.11	1443.78	3.26	0.06	0.299	8.0	245.5	3.3
0.44	0.132	0.98	90.91	1.08	0.30	0.165	0.3	11.7	2.1
0.13	0.253	10.17	284.25	3.58	0.05	0.303	1.5	43.9	3.4
0.02	0.412	6.14	64.17	9.57	0.04	0.312	1.0	18.5	5.4
0.35	0.236	1.32	28.92	4.56	0.88	0.029	0.0	7.6	0.5
0.01	-0.320	-150.20	13477.90	-1.11	0.00	0.494	28.9	997.7	2.9
0.11	-0.212	-12.55	1135.29	-1.11	0.23	0.156	0.6	76.5	0.8
0.25	-0.163	-11.94	1175.17	-1.02	0.00	0.366	2.3	68.5	3.3
0.26	-0.153	-15.84	1279.13	-1.24	0.00	0.423	5.1	83.5	6.1
0.01	-0.391	-22.98	1168.38	-1.97	0.05	0.253	2.4	91.1	2.6
0.03	0.451	126.50	2487.75	5.08	1.00	0.011	1.1	508.6	0.2
0.04	0.429	13.90	98.95	14.05	0.04	0.429	1.5	13.4	11.0
0.10	0.341	12.83	460.92	2.78	0.51	-0.143	-1.0	93.8	-1.0
0.87	0.044	0.10	179.02	0.06	0.27	-0.231	-1.3	52.9	-2.4
0.04	0.436	4.73	65.93	7.18	0.62	0.110	0.2	21.5	0.9
0.00	-0.460	-128.97	8115.62	-1.59	0.43	-0.108	-2.3	656.6	-0.4
0.00	-0.410	-13.68	671.88	-2.04	0.16	-0.190	-0.5	40.8	-1.1
0.13	-0.220	-8.42	874.67	-0.96	0.30	0.140	0.4	65.2	0.6
0.01	-0.373	-17.53	715.95	-2.45	0.37	-0.122	-0.5	67.6	-0.8
0.01	-0.353	-10.98	451.69	-2.43	0.31	-0.138	-0.4	41.4	-1.0
0.56	-0.117	-24.00	6532.00	-0.37	0.86	-0.042	-4.6	696.7	-0.7
0.26	-0.217	-9.63	611.38	-1.57	0.42	-0.158	-0.6	44.7	-1.4
0.77	-0.067	-4.92	767.75	-0.64	0.24	-0.225	-1.6	91.2	-1.8
0.69	0.083	3.10	383.92	0.81	0.93	0.025	0.2	49.8	0.5
0.62	-0.100	-6.53	401.98	-1.62	0.75	0.067	0.9	39.6	2.2
0.55	-0.238	-225.00	2375.56	-9.47	0.76	-0.143	-6.3	346.4	-1.8
1.00	-0.048	-2.71	81.57	-3.32	0.76	-0.143	-0.8	15.6	-5.3
0.76	0.143	14.43	293.51	4.92	0.37	0.333	4.2	37.1	11.3
0.71	-0.200	-5.98	64.52	-9.26	1.00	-0.067	-1.5	33.0	-4.4
1.00	0.000	0.67	45.65	1.48	0.81	-0.200	-3.8	24.7	-15.5
0.71	-0.143	-93.26	3548.71	-2.63	1.00	0.000	-1.9	2077.7	-0.1
0.75	-0.111	-6.85	305.39	-2.24	1.00	0.000	-0.9	151.9	-0.6
0.90	0.071	12.32	156.68	7.86	1.00	0.000	0.6	155.4	0.4
0.90	0.071	5.09	248.85	2.05	0.71	-0.143	-7.6	267.4	-2.9
0.90	0.071	4.08	287.63	1.42	0.27	0.357	9.8	179.9	5.4

Table A2.10b Trends in precipitation/wet deposition for 2009–2018 (shaded cells indicate significant trends).

Site	Name	Start year	End year	Period	Trends in volume weighted mean				
					p value	*tau*	Slope	Intercept	%/y
FI0036R	Pallas	2009	2018	Annual	1.00	0.00	0.00	5.00	0.00
FI0036R	Pallas	2009	2018	Spring	0.18	-0.39	-2.64	30.85	-8.56
FI0036R	Pallas	2009	2018	Summer	0.75	-0.11	-0.25	7.80	-3.24
FI0036R	Pallas	2009	2018	Autumn	0.27	0.36	0.14	3.11	4.61
FI0036R	Pallas	2009	2018	Winter	0.65	-0.19	-0.30	6.71	-4.51
NO99-01R	Lista/Birkenes	2009	2019	Annual	0.14	-0.35	-0.20	6.00	-3.33
NO99-01R	Lista/Birkenes	2009	2019	Spring	0.21	-0.31	-0.99	14.37	-6.90
NO99-01R	Lista/Birkenes	2009	2019	Summer	0.28	-0.27	-0.37	9.40	-3.89
NO99-01R	Lista/Birkenes	2009	2019	Autumn	0.28	-0.27	-0.22	5.24	-4.17
NO99-01R	Lista/Birkenes	2009	2019	Winter	0.35	-0.24	-0.14	4.71	-3.02
SE0005R	Bredkälen	2009	2018	Annual	0.59	0.18	0.00	6.00	0.00
SE0005R	Bredkälen	2009	2018	Spring	0.17	-0.43	-2.01	21.93	-9.15
SE0005R	Bredkälen	2009	2018	Summer	0.27	0.36	0.41	5.51	7.49
SE0005R	Bredkälen	2009	2018	Autumn	0.54	0.21	0.30	3.42	8.88
SE0005R	Bredkälen	2009	2018	Winter	1.00	-0.05	-0.26	6.91	-3.82
SE02-14R	Råö/Rörvik	2009	2018	Annual	0.28	-0.29	-0.33	10.50	-3.17
SE02-14R	Råö/Rörvik	2009	2018	Spring	0.01	-0.69	-3.42	39.54	-8.65
SE02-14R	Råö/Rörvik	2009	2018	Summer	1.00	-0.02	-0.01	9.75	-0.06
SE02-14R	Råö/Rörvik	2009	2018	Autumn	0.47	-0.20	-0.29	7.66	-3.79
SE02-14R	Råö/Rörvik	2009	2018	Winter	0.37	-0.24	-0.42	9.22	-4.51
SE11-20R	Vavihill	2009	2018	Annual	0.65	-0.13	-0.14	9.14	-1.56
SE11-20R	Vavihill	2009	2018	Spring	0.15	-0.38	-2.11	28.19	-7.48
SE11-20R	Vavihill	2009	2018	Summer	0.18	0.39	0.20	7.86	2.59
SE11-20R	Vavihill	2009	2018	Autumn	1.00	-0.02	-0.06	7.50	-0.77
SE11-20R	Vavihill	2009	2018	Winter	0.05	-0.51	-0.54	9.18	-5.89
ak06	Gates of the Arctic	2009	2015	Annual	0.55	-0.24	-0.30	5.92	-5.07
ak06	Gates of the Arctic	2009	2015	Spring	1.00	0.05	0.32	6.10	5.29
ak06	Gates of the Arctic	2009	2015	Summer	0.23	-0.43	-0.76	9.11	-8.30
ak06	Gates of the Arctic	2009	2015	Autumn	0.71	-0.20	-0.31	2.99	-10.44
ak06	Gates of the Arctic	2009	2015	Winter	0.31	0.67	0.57	1.75	32.71
ak98	Kodiak Island	2009	2018	Annual	0.13	-0.52	-0.05	1.68	-2.95
ak98	Kodiak Island	2009	2018	Spring	0.71	-0.14	-0.07	2.38	-3.07
ak98	Kodiak Island	2009	2018	Summer	1.00	0.05	0.04	1.25	2.88
ak98	Kodiak Island	2009	2018	Autumn	0.07	-0.62	-0.08	1.48	-5.24
ak98	Kodiak Island	2009	2018	Winter	0.13	-0.52	-0.05	1.39	-3.46

Trends in deposition					Trends in precipitation amount				
p value	*tau*	Slope	Intercept	%/y	*p* value	*tau*	Slope	Intercept	%/y
0.076	0.500	28.600	236.0	12.12	0.076	0.500	206.000	1262.0	16.32
0.466	0.222	0.830	12.2	6.82	0.348	0.278	6.611	77.3	8.55
0.076	0.500	7.417	33.6	22.08	0.076	0.500	53.970	194.8	27.70
0.675	0.139	0.333	47.0	0.71	0.108	0.500	16.083	99.5	16.17
0.029	0.611	1.667	-0.3	500.00	0.016	0.810	9.333	3.3	280.00
0.436	0.200	22.000	1680.0	1.31	0.161	-0.345	-405.000	11454.0	-3.54
0.161	0.345	3.778	52.8	7.16	0.640	-0.127	-11.458	709.0	-1.62
0.640	-0.127	-2.762	149.1	-1.85	0.001	-0.782	-72.619	1245.1	-5.83
0.755	0.091	4.500	187.2	2.40	0.350	-0.236	-48.519	1058.3	-4.58
0.876	0.055	1.444	149.8	0.96	0.876	-0.055	-17.810	788.0	-2.26
0.063	0.571	15.725	443.0	3.55	0.009	0.786	206.275	2588.0	7.97
0.174	0.429	3.583	16.1	22.22	0.019	0.714	27.452	148.9	18.43
0.386	-0.286	-2.875	93.2	-3.08	0.536	0.214	10.400	524.6	1.98
0.386	0.286	2.211	33.1	6.68	0.035	0.643	22.667	91.8	24.68
0.004	0.857	3.767	6.2	61.25	0.007	0.905	15.667	42.7	36.72
0.371	0.244	21.000	520.0	4.04	0.592	-0.156	-53.833	5911.3	-0.91
0.283	0.289	2.000	16.0	12.50	0.592	-0.156	-7.429	469.8	-1.58
0.474	-0.200	-2.000	84.8	-2.36	0.074	-0.467	-38.667	917.3	-4.22
0.371	0.244	3.000	44.0	6.82	0.474	0.200	17.600	302.8	5.81
0.020	0.600	3.111	21.7	14.36	0.032	0.556	27.778	136.5	20.35
0.530	0.178	11.000	583.5	1.89	0.152	0.378	195.667	5100.5	3.84
0.210	0.333	2.222	26.7	8.33	0.592	0.156	17.133	366.6	4.67
1.000	-0.022	-1.762	84.6	-2.08	0.917	0.056	4.229	675.8	0.63
1.000	-0.022	-0.556	58.2	-0.96	0.721	0.111	13.750	372.1	3.69
0.210	0.333	4.133	27.4	15.09	0.074	0.467	19.958	243.5	8.20
0.764	-0.143	-6.330	346.4	-1.83	0.548	-0.238	-224.995	2375.6	-9.47
0.764	-0.143	-0.830	15.6	-5.31	1.000	-0.048	-2.712	81.6	-3.32
0.368	0.333	4.183	37.1	11.28	0.764	0.143	14.431	293.5	4.92
1.000	-0.067	-1.456	33.0	-4.41	0.707	-0.200	-5.977	64.5	-9.26
0.806	-0.200	-3.822	24.7	-15.50	1.000	0.000	0.674	45.6	1.48
0.548	0.238	131.317	1538.1	8.54	0.764	0.143	46.783	2893.7	1.62
0.386	0.286	5.192	128.2	4.05	0.711	0.143	6.466	253.7	2.55
0.368	0.333	8.475	107.2	7.91	0.230	0.429	29.967	59.2	50.65
1.000	0.048	10.040	185.1	5.42	0.764	-0.143	-7.971	335.5	-2.38
0.368	0.333	11.650	192.1	6.06	0.548	0.238	4.722	280.7	1.68

Summary of results for trends in biota

Table A2.11 Results from temporal trend analysis of total mercury (THg) concentrations (µg/kg wet or dry weight) in circumpolar Arctic biota using linear mixed models. Trends are presented as percent (%) change per year; 'recent trends' were analyzed from 1999 through the final year of each time series for comparative purposes. See footnotes below the table for more detailed descriptions of columns (a-o) and color coding for shaded cells.

Country	Location	Species	Tissue/ Matrix	Basis	Grouping	No. of years (*n*)	Year range (and start year)	Recent trend
						a	b	c
Iceland	Grímsey (66.55233°, -18.02333°)	*Mytilus edulis*	SB	D	--	16 (16)	1993–2013 (1993)	2.2
Iceland	Hvalstod Hvalfjörður (64.39583°, -21.445°)	*Mytilus edulis*	SB	D	--	19 (19)	1993–2013 (1993)	1.1
Iceland	Hvassahraun (64.05°, -22.2944°)	*Mytilus edulis*	SB	D	--	21 (21)	1993–2018 (1993)	0.6
Iceland	Hvítanes Hvalfjörður (64.36417°, -21.495°)	*Mytilus edulis*	SB	D	--	22 (22)	1993–2018 (1993)	0.1
Iceland	Mjóifjörður (Dalatangi) (65.2705°, -13.582°)	*Mytilus edulis*	SB	D	--	13 (13)	1997–2018 (1997)	1.5
Iceland	Mjóifjörður (head) (65.18583°, -14.0133°)	*Mytilus edulis*	SB	D	--	15 (15)	1996–2018 (1996)	2
Iceland	Mjóifjörður (Hofsá) (65.202°, -13.81667°)	*Mytilus edulis*	SB	D	--	15 (15)	1995–2018 (1995)	-0.8
Iceland	Straumur Straumsvík (64.1806°, -22.2389°)	*Mytilus edulis*	SB	D	--	21 (21)	1993–2018 (1993)	-0.3
Iceland	Úlfsá Skutulsfjörður (66.06°, -23.1661°)	*Mytilus edulis*	SB	D	--	17 (17)	1997–2018 (1997)	-0.5
Norway	10A2 Skallneset (70.13728°, 30.34175°)	*Mytilus edulis*	SB	W	--	22 (22)	1994–2017 (1994)	-2.4
Norway	11X Brashavn (69.8993°, 29.741°)	*Mytilus edulis*	SB	W	--	19 (19)	1997–2017 (1997)	-0.5
Norway	98A2 Husvågen area (68.24917, 14.6627°)	*Mytilus edulis*	SB	W	--	19 (19)	1997–2017 (1997)	-0.1
Faroe Islands	Mýlingsgrunnur (62.38333°, -7.41667°)	*Gadus morhua*	MU	W	Undefined	27 (27)	1979–2016 (1979)	4.0
Faroe Islands	Mýlingsgrunnur (62.38333°, -7.41667°)	*Gadus morhua*	MU	W	Medium	29 (29)	1979–2017 (1979)	0.9
Iceland	North-Northwest off Iceland (66.9235°, -22.89483°)	*Gadus morhua*	MU	W	--	24 (24)	1990–2018 (1990)	0
Iceland	Northeast off Iceland (65.24167°, -12.1255°)	*Gadus morhua*	MU	W	--	23 (23)	1990–2018 (1990)	1.2
Norway	10B Varangerfjorden (69.81623°, 29.7602°)	*Gadus morhua*	MU	W	--	21 (21)	1994–2017 (1994)	2
Norway	43B2 Tromsø harbour (69.653°, 18.974°)	*Gadus morhua*	MU	W	--	7 (7)	2009–2017 (2009)	7.7
Norway	98B1 Bjørnerøya (east) (68.18577°, 14.70814°)	*Gadus morhua*	MU	W	--	21 (21)	1992–2017 (1992)	-0.3
Denmark	Avanersuaq AMAP (77.28°, -69.14°)	*Myoxocephalus scorpius*	LI	W	--	8 (9)	1995–2018 (1987)	0.4
Denmark	Ittoqqortoormiit AMAP (70.29°, -21.58°)	*Myoxocephalus scorpius*	LI	W	--	11 (12)	1995–2018 (1985)	2.1
Denmark	Qeqertarsuaq AMAP (69.15°, -53.32°)	*Myoxocephalus scorpius*	LI	W	--	14 (14)	1994–2018 (1994)	6.3
Canada	Queen Maud Gulf (69.12°, -105.06°)	*Salvelinus alpinus*	MU	W	--	13 (17)	2004–2018 (1977)	-1.5
Canada	Great Slave Lake, West Basin (60.82°, -115.79°)	*Esox lucius*	MU	W	--	20 (23)	1989–2018 (1976)	-0.2
Sweden	Storvindeln (65.7°, 17.13°)	*Esox lucius*	MU	W	--	46 (46)	1968–2018 (1968)	-2.1
Canada	Fort Good Hope (66.26°, -128.63°)	*Lota lota*	LI	W	--	20 (20)	1988–2018 (1988)	3.1
Canada	Fort Good Hope (66.26°, -128.63°)	*Lota lota*	MU	W	--	19 (19)	1995–2018 (1995)	2
Canada	Great Slave Lake, East Arm (62.41°, -110.74°)	*Lota lota*	MU	W	--	17 (17)	1993–2018 (1993)	1.4

Overall trend	meanLY	clLY	p_rtrend	p_overall	p_ltrend	p_nonlinear	p_linear	dtrend_1	dtrend_3	dpower_1	dpower_3
d	e	f	g	h	i	j	k	l	m	n	o
2.2	103.4	129.9	0.0558	0.0558	0.0558	--	0.0558	3.1	9.9	99	31
1.1	49.8	63.0	0.3381	0.3381	0.3381	--	0.3381	3	9.8	100	31
0.6	47.8	60.9	0.4646	0.4646	0.4646	--	0.4646	2.2	9.4	100	34
0.1	33.9	46.7	0.9022	0.9022	0.9022	--	0.9022	2.6	11.3	100	25
0.2	106.0	125.7	0.0265	0.0004	0.7134	0.0015	0.1043	1.5	4.4	100	89
2	63.6	74.4	0.0066	0.0066	0.0066	--	0.0066	1.8	6	100	66
-0.8	43.0	56.1	0.4229	0.4229	0.4229	--	0.4229	2.7	9.1	100	35
-0.3	39.4	53.0	0.7544	0.7544	0.7544	--	0.7544	2.8	11.9	100	23
-0.5	75.4	107.9	0.7372	0.7372	0.7372	--	0.7372	4.3	12.9	90	21
-1.8	6.5	7.2	0	0	0	0.0015	0.0007	0.6	2.3	100	100
-0.5	9.1	9.8	0.0797	0.0797	0.0797	--	0.0797	0.7	2.3	100	100
-0.2	20.9	28.0	0.9045	0.0009	0.863	0.0145	0.0178	2	6.2	100	63
-3.1	38.8	58.2	0.0295	0	0.0007	0.0001	0	1.4	11.9	100	23
-3.3	27.5	39.3	0.4922	0	0.0001	0.0003	0.0001	1.3	11.7	100	24
0	31.4	42.6	0.9813	0.9813	0.9813	--	0.9813	3.1	16.2	100	15
1.2	32.3	45.8	0.2344	0.2344	0.2344	--	0.2344	2.3	11.7	100	24
-3	24.8	35.3	0.1031	0	0.0242	0	0.6751	2.5	9.4	100	33
7.7	59.2	76.7	0.0136	0.0136	0.0136	--	0.0136	8.7	6.1	38	64
-0.3	60.9	84.0	0.7717	0.7717	0.7717	--	0.7717	3.5	15.4	98	16
0.4	62.2	86.6	0.782	0.782	0.782	--	0.782	4.9	11	82	26
2.1	83.1	99.0	0.014	0.014	0.014	--	0.014	2.4	6.6	100	58
6.3	60.3	89.1	0.0016	0.0016	0.0016	--	0.0016	5	15.5	79	16
-1.5	49.7	64.5	0.4047	0.4047	0.4047	--	0.4047	5.8	10.3	68	29
-0.2	240.6	266.6	0.5982	0.5982	0.5982	--	0.5982	1.1	5.8	100	69
-0.3	215.1	247.0	0.0001	0.0001	0.1299	0.0003	0.1597	0.6	7.7	100	45
3.1	105.6	118.4	0	0	0	--	0	1.4	5.9	100	66
2	408.8	456.6	0.0013	0.0013	0.0013	--	0.0013	1.5	5.2	100	76
2.8	125.7	137.3	0.0056	0	0.0003	0.0005	0.0053	1.1	3.9	100	95

Table A2.11 continued

Country	Location	Species	Tissue/ Matrix	Basis	Grouping	No. of years (*n*)	Year range (and start year)	Recent trend
						a	b	c
Canada	Great Slave Lake, West Basin (60.82°, -115.79°)	*Lota lota*	MU	W	--	24 (26)	1992–2018 (1975)	1.2
Canada	Amituk Lake (75.05°, -93.75°)	*Salvelinus alpinus*	MU	W	--	16 (18)	2001–2018 (1989)	-3.3
Canada	Char Lake (74.71°, -94.9°)	*Salvelinus alpinus*	MU	W	--	13 (13)	1993–2018 (1993)	1.1
Canada	Lake Hazen (81.8°, -71°)	*Salvelinus alpinus*	MU	W	--	18 (18)	1990–2018 (1990)	-3.3
Canada	North Lake (74.78°, -95.09°)	*Salvelinus alpinus*	MU	W	--	14 (14)	2000–2018 (2000)	1.3
Canada	Resolute Lake (74.69°, -94.94°)	*Salvelinus alpinus*	MU	W	--	22 (22)	1993–2018 (1993)	0.9
Denmark	Isortoq (60.54°, -47.33°)	*Salvelinus alpinus*	MU	W	--	11 (11)	1994–2018 (1994)	1.3
Faroe Islands	á Mýrunum (62.16914°, -7.08579°)	*Salvelinus alpinus*	MU	W	Undefined	10 (10)	2000–2014 (2000)	0.6
Norway	Bjørnøya (74.452°, 19.115°)	*Salvelinus alpinus*	MU	D	--	12 (12)	1998–2015 (1998)	5.3
Sweden	Abiskojaure (68.287892°, 18.5857468°)	*Salvelinus alpinus*	MU	W	--	37 (37)	1981–2018 (1981)	-0.9
Canada	Great Slave Lake, East Arm (62.41°, -110.74°)	*Salvelinus namaycush*	MU	W	--	21 (21)	1993–2018 (1993)	0.5
Canada	Great Slave Lake, West Basin (60.82°, -115.79°)	*Salvelinus namaycush*	MU	W	--	25 (25)	1979–2018 (1979)	1.5
Canada	Lake Kusawa (60.41°, -136.26°)	*Salvelinus namaycush*	MU	W	--	20 (20)	1993–2018 (1993)	-2.5
Canada	Lake Laberge (61.06°, -135.11°)	*Salvelinus namaycush*	MU	W	--	23 (23)	1993–2018 (1993)	-1.9
Denmark	Ittoqqortoormiit Ukaleqarteq (70.72°, -21.55°)	*Alle alle*	BL	D	--	10 (10)	2005–2015 (2005)	1.6
Denmark	Ittoqqortoormiit Ukaleqarteq (70.72°, -21.55°)	*Alle alle*	FE	D	--	10 (10)	2007–2016 (2007)	3
Faroe Islands	Koltur (61.99447°, -6.99343°)	*Cepphus grylle*	EH	W	Undefined	11 (11)	1999–2016 (1999)	4.6
Faroe Islands	Skúvoy (61.76833°, -6.80167°)	*Cepphus grylle*	EH	W	Undefined	10 (10)	1999–2014 (1999)	5.9
Faroe Islands	Sveipur (61.95°, -6.71667°)	*Cepphus grylle*	FE	W	Juvenile	8 (8)	1996–2015 (1996)	-0.1
Faroe Islands	Tindhólmur (62.079°, -7.43217°)	*Cepphus grylle*	FE	W	Juvenile	6 (6)	2005–2015 (2005)	0.9
Faroe Islands	Sveipur (61.95°, -6.71667°)	*Cepphus grylle*	LI	W	Juvenile	9 (9)	1995–2015 (1995)	6.1
Faroe Islands	Tindhólmur (62.079°, -7.43217°)	*Cepphus grylle*	LI	W	Juvenile	6 (6)	2005–2015 (2005)	3.9
Canada	Prince Leopold Island (74.04°, -90.03°)	*Fulmarus glacialis*	EH	D	--	19 (19)	1975–2017 (1975)	1
Norway	Svalbard-Kongsfjorden area (79°, 11.6667°)	*Rissa tridactyla*	ER	D	--	15 (15)	2000–2016 (2000)	-3.1
Canada	Coats Island (62.47°, -83.1°)	*Uria lomvia*	EH	D	--	15 (15)	1993–2017 (1993)	-0.4
Canada	Prince Leopold Island (74.04°, -90.03°)	*Uria lomvia*	EH	D	--	19 (19)	1975–2017 (1975)	-0.6
Canada	Eastern Beaufort Sea (69.5°, -133.58°)	*Delphinapterus leucas*	EP	W	Large	20 (20)	1993–2017 (1993)	-2.5
Canada	Eastern Beaufort Sea (69.5°, -133.58°)	*Delphinapterus leucas*	EP	W	Small	20 (20)	1993–2017 (1993)	-8.6
Canada	Eastern Beaufort Sea (69.5°, -133.58°)	*Delphinapterus leucas*	LI	W	Small	23 (23)	1981–2017 (1981)	0.9

Overall trend	meanLY	clLY	p_rtrend	p_overall	p_ltrend	p_nonlinear	p_linear	dtrend_1	dtrend_3	dpower_1	dpower_3
d	e	f	g	h	i	j	k	l	m	n	o
1.2	167.0	190.8	0.0407	0.0407	0.0407	--	0.0407	1.6	7.6	100	46
-3.3	1142.0	1606.7	0.0351	0.0041	0.0351	0.0414	0.0434	4	10.2	94	29
1.1	397.6	622.4	0.5754	0.5754	0.5754	--	0.5754	6.3	18.2	61	13
-3.3	112.5	158.2	0.026	0.026	0.026	--	0.026	4.4	18.2	89	13
1.3	257.6	305.7	0.2612	0.2612	0.2612	--	0.2612	3.4	7.4	98	48
-0.8	169.9	196.4	0.1437	0.0004	0.2766	0.0008	0.1838	1.1	4.2	100	91
1.3	961.9	1221.5	0.1792	0.1792	0.1792	--	0.1792	2.8	8.4	100	40
0.6	251.2	306.7	0.6715	0.6715	0.6715	--	0.6715	4.4	6.8	88	55
5.3	827.1	1098.7	0.0038	0.0038	0.0038	--	0.0038	4.8	10.8	83	27
-0.9	24.1	26.9	0.0054	0.0054	0.0054	--	0.0054	0.9	7.5	100	48
0.5	156.9	186.2	0.5154	0.5154	0.5154	--	0.5154	2.3	9.3	100	34
1.5	216.1	236.6	0.0001	0.0001	0.0001	--	0.0001	0.9	5.6	100	70
-2.5	255.4	304.4	0.0077	0.0077	0.0077	--	0.0077	2.6	9.1	100	35
-0.5	302.1	373.4	0.0276	0.0086	0.4409	0.014	0.3508	1.9	7.7	100	45
1.6	944.2	1035.9	0.1027	0.1027	0.1027	--	0.1027	2.9	3.1	100	99
3	1409.2	1651.6	0.0822	0.0822	0.0822	--	0.0822	5.2	5.2	78	78
4.6	735.8	890.8	0.0004	0.0004	0.0004	--	0.0004	2.9	6.3	100	61
5.9	831.8	1041.9	0.0008	0.0008	0.0008	--	0.0008	4.1	7.2	93	51
-0.1	3191.6	3878.5	0.9036	0.9036	0.9036	--	0.9036	3.5	6.1	97	64
0.9	3504.9	4321.8	0.623	0.623	0.623	--	0.623	6.2	4.8	63	82
6.1	1400.9	1685.1	0.0001	0.0001	0.0001	--	0.0001	2.8	6.1	100	64
3.9	1589.3	2052.7	0.0943	0.0943	0.0943	--	0.0943	7.7	6	47	66
1	1330.1	1448.0	0.0009	0.0009	0.0009	--	0.0009	0.7	5.1	100	79
-3.1	817.2	946.5	0.0031	0.0031	0.0031	--	0.0031	2.7	6.3	100	61
-0.4	669.9	748.9	0.5169	0.5169	0.5169	--	0.5169	1.8	5.3	100	76
1.5	1092.1	1252.7	0.384	0	0	0.0019	0.0001	0.8	5.3	100	75
-2.5	435.1	502.1	0.0007	0.0007	0.0007		0.0007	1.9	7.6	100	47
-2	167.9	223.3	0	0	0.0599	0	0.0149	2	7.9	100	44
0.9	11122.6	14768.9	0.3389	0.3389	0.3389	--	0.3389	3.3	19.6	99	12

Table A2.11 continued

Country	Location	Species	Tissue/ Matrix	Basis	Grouping	No. of years (*n*)	Year range (and start year)	Recent trend
						a	b	c
Canada	Eastern Beaufort Sea (69.5°, -133.58°)	*Delphinapterus leucas*	LI	W	Large	23 (23)	1981–2017 (1981)	-2.7
Canada	Southern Hudson Bay (56.54°, -79.22°)	*Delphinapterus leucas*	LI	W	Small	15 (15)	1994–2016 (1994)	-2
Canada	Southern Hudson Bay (56.54°, -79.22°)	*Delphinapterus leucas*	LI	W	Large	17 (17)	1994–2016 (1994)	-2.6
Canada	Eastern Beaufort Sea (69.5°, -133.58°)	*Delphinapterus leucas*	MU	W	Small	23 (23)	1981–2017 (1981)	-0.1
Canada	Eastern Beaufort Sea (69.5°, -133.58°)	*Delphinapterus leucas*	MU	W	Large	21 (22)	1993–2017 (1981)	-0.6
Canada	Southern Hudson Bay (56.54°, -79.22°)	*Delphinapterus leucas*	MU	W	Small	15 (15)	1994–2016 (1994)	-0.5
Canada	Southern Hudson Bay (56.54°, -79.22°)	*Delphinapterus leucas*	MU	W	Large	17 (17)	1994–2016 (1994)	-1.7
Faroe Islands	Føroyskar Hvalvágir (62°, -7°)	*Globicephala melas*	LI	W	Adult	12 (12)	2001–2017 (2001)	-1.5
Faroe Islands	Føroyskar Hvalvágir (62°, -7°)	*Globicephala melas*	LI	W	Juvenile male	6 (6)	2001–2015 (2001)	-2
Faroe Islands	Føroyskar Hvalvágir (62°, -7°)	*Globicephala melas*	MU	W	Undefined	17 (20)	1997–2017 (1979)	2.3
Faroe Islands	Føroyskar Hvalvágir (62°, -7°)	*Globicephala melas*	MU	W	Adult	12 (15)	1997–2015 (1979)	1.2
Faroe Islands	Føroyskar Hvalvágir (62°, -7°)	*Globicephala melas*	MU	W	Juvenile male	16 (18)	1997–2017 (1986)	1.7
Canada	Eastern Beaufort Sea (71.99°, -125.25°)	*Pusa hispida*	LI	W	Adult	12 (14)	2001–2017 (1987)	-2.6
Canada	Eastern Beaufort Sea (71.99°, -125.25°)	*Pusa hispida*	LI	W	Juvenile	11 (13)	2001–2017 (1987)	8.7
Canada	Resolute Passage (74.7°, -94.83°)	*Pusa hispida*	LI	W	Adult	16 (16)	1993–2017 (1993)	0.1
Canada	Resolute Passage (74.7°, -94.83°)	*Pusa hispida*	LI	W	Juvenile	15 (15)	1993–2017 (1993)	0
Canada	Labrador Sea (56.54°, -61.7°)	*Pusa hispida*	LI	W	Adult	9 (9)	1997–2017 (1997)	8.9
Canada	Labrador Sea (56.54°, -61.7°)	*Pusa hispida*	LI	W	juvenile	8 (8)	1998–2017 (1998)	2.3
Canada	Western Hudson Bay (61.11°, -94.06°)	*Pusa hispida*	LI	W	Adult	15 (15)	1992–2017 (1992)	-0.6
Canada	Western Hudson Bay (61.11°, -94.06°)	*Pusa hispida*	LI	W	Juvenile	13 (14)	2003–2017 (1992)	1.8
Denmark	Avanersuaq (77.28°, -69.14°)	*Pusa hispida*	LI	W	Juvenile	12 (12)	1984–2018 (1984)	2.8
Denmark	Avanersuaq (77.28°, -69.14°)	*Pusa hispida*	LI	W	Adult	10 (10)	1994–2018 (1994)	-0.9
Denmark	Ittoqqortoormiit (70.29°, -21.58°)	*Pusa hispida*	LI	W	Adult	14 (14)	1986–2018 (1986)	0.6
Denmark	Ittoqqortoormiit (70.29°, -21.58°)	*Pusa hispida*	LI	W	Juvenile	14 (14)	1986–2018 (1986)	2.2
Denmark	Ittoqqortoormiit (70.29°, -21.58°)	*Pusa hispida*	LI	W	Undefined	6 (6)	1999–2016 (1999)	9.4
Denmark	Qeqertarsuaq (69.15°, -53.32°)	*Pusa hispida*	LI	W	Juvenile	14 (14)	1994–2018 (1994)	-1
Canada	Eastern Beaufort Sea (71.99°, -125.25°)	*Pusa hispida*	MU	W	Adult	12 (14)	2001–2017 (1987)	-2.4
Canada	Eastern Beaufort Sea (71.99°, -125.25°)	*Pusa hispida*	MU	W	Juvenile	12 (14)	2001–2017 (1987)	-8.0
Canada	Resolute Passage (74.7°, -94.83°)	*Pusa hispida*	MU	W	Adult	14 (15)	2004–2017 (1993)	-1.2

Overall trend	meanLY	clLY	p_rtrend	p_overall	p_ltrend	p_nonlinear	p_linear	dtrend_1	dtrend_3	dpower_1	dpower_3
d	e	f	g	h	i	j	k	l	m	n	o
2.8	17123.4	21513.9	0.0071	0	0.0005	0	0.8369	1.5	8.5	100	39
-2	5690.3	8147.6	0.2749	0.2749	0.2749	--	0.2749	5.8	18.2	67	13
-2.6	8357.6	12438.4	0.1206	0.1206	0.1206	--	0.1206	5.2	17.4	77	14
-0.1	775.1	904.5	0.8207	0.8207	0.8207	--	0.8207	1.7	9.6	100	32
-0.6	1210.1	1395.9	0.3283	0.3283	0.3283	--	0.3283	1.9	7.6	100	46
-0.5	672.6	801.6	0.5571	0.5571	0.5571	--	0.5571	2.8	8.5	100	39
-1.7	820.9	1010.5	0.051	0.051	0.051	--	0.051	2.7	8.9	100	37
-1.5	79267.4	113002.3	0.504	0.504	0.504	--	0.504	7.3	14.6	50	17
-2	47152.9	110540.1	0.6886	0.6886	0.6886	--	0.6886	20.4	26.1	12	9
2.3	1178.1	1569.7	0.0962	0.0962	0.0962	--	0.0962	3.7	11.5	96	25
1.2	2358.2	2964.8	0.2568	0.2568	0.2568	--	0.2568	2.9	6.4	100	60
1.2	2328.1	2612.7	0.0029	0.0004	0.0167	0.0038	0.0435	1.4	4.2	100	91
-2.6	22861.9	35409.1	0.3541	0.3541	0.3541	--	0.3541	9.6	18.5	32	13
8.7	6225.8	14817.6	0.1347	0.1347	0.1347	--	0.1347	16.1	29.2	15	8
0.1	8724.5	12379.7	0.9589	0.9589	0.9589	--	0.9589	5.4	16.1	74	15
0	2965.7	6688.7	0.9937	0.9937	0.9937	--	0.9937	7.3	21.8	49	11
8.9	13820.2	26597.5	0.012	0.012	0.012	--	0.012	9.3	23.2	34	10
2.3	1572.9	2496.0	0.4207	0.4207	0.4207	--	0.4207	9.8	18.4	32	13
-0.6	10829.7	17294.5	0.7837	0.7837	0.7837	--	0.7837	6.9	21.8	54	11
1.8	4532.1	8331.5	0.674	0.674	0.674	--	0.674	14	25.8	18	9
2.8	2686.0	4238.2	0.0614	0.0614	0.0614	--	0.0614	4.5	20.8	88	11
-0.9	5636.1	8557.9	0.5032	0.5032	0.5032	--	0.5032	5.7	15.3	69	16
0.6	8456.7	10837.0	0.499	0.499	0.499	--	0.499	2.7	10.2	100	30
2.2	4770.0	7058.0	0.1305	0.1305	0.1305	--	0.1305	4.4	17.1	89	14
9.4	11867.8	37886.2	0.0991	0.0991	0.0991	--	0.0991	20	28	12	9
-1	858.8	1180.0	0.4386	0.4386	0.4386	--	0.4386	3.9	12	94	23
-2.4	295.4	362.2	0.044	0	0.044	0.0002	0.0934	3.4	6.3	98	61
-8.0	169.1	222.4	0.001	0.001	0.001	--	0.001	5.8	10.9	69	27
-1.2	521.4	597.5	0.1979	0.1979	0.1979	--	0.1979	2.8	5	100	81

Table A2.11 continued

Country	Location	Species	Tissue/ Matrix	Basis	Grouping	No. of years (*n*)	Year range (and start year)	Recent trend
						a	b	c
Canada	Resolute Passage (74.7°, -94.83°)	*Pusa hispida*	MU	W	Juvenile	14 (15)	2004–2017 (1993)	-5.4
Canada	Labrador Sea (56.54°, -61.7°)	*Pusa hispida*	MU	W	Adult	10 (10)	1997–2017 (1997)	1
Canada	Labrador Sea (56.54°, -61.7°)	*Pusa hispida*	MU	W	Juvenile	9 (9)	1998–2017 (1998)	-3.5
Canada	Western Hudson Bay (61.11°, -94.06°)	*Pusa hispida*	MU	W	Adult	13 (14)	2003–2017 (1992)	-5.2
Canada	Western Hudson Bay (61.11°, -94.06°)	*Pusa hispida*	MU	W	Juvenile	13 (14)	2003–2017 (1992)	-6.8
Denmark	Ittoqqortoormiit (70.29°, -21.58°)	*Ursus maritimus*	HA	D	Adult female	14 (16)	1999–2018 (1984)	-1.3
Denmark	Ittoqqortoormiit (70.29°, -21.58°)	*Ursus maritimus*	HA	D	Juvenile	21 (21)	1984–2018 (1984)	1.7
Denmark	Ittoqqortoormiit (70.29°, -21.58°)	*Ursus maritimus*	HA	D	Adult male	16 (17)	1999–2018 (1984)	2.3
Denmark	Ittoqqortoormiit (70.29°, -21.58°)	*Ursus maritimus*	HA	D	Undefined	11 (12)	2000–2018 (1987)	1
Norway	Svalbard (77.875°, 20.975°)	*Ursus maritimus*	HA	D	Adult female	20 (20)	1995–2016 (1995)	0.2
Norway	Svalbard (77.875°, 20.975°)	*Ursus maritimus*	HA	D	Juvenile	10 (10)	1998–2014 (1998)	2.9
Canada	Southern Hudson Bay (56.54°, -79.22°)	*Ursus maritimus*	LI	D	Adult female	10 (10)	2006–2017 (2006)	-1.5
Canada	Southern Hudson Bay (56.54°, -79.22°)	*Ursus maritimus*	LI	D	Adult male	10 (10)	2006–2017 (2006)	0.7
Canada	Southern Hudson Bay (56.54°, -79.22°)	*Ursus maritimus*	LI	D	Juvenile	7 (7)	2007–2015 (2007)	-0.8
Canada	Western Hudson Bay (61.11°, -94.06°)	*Ursus maritimus*	LI	D	Adult female	6 (6)	2007–2017 (2007)	-6.0
Canada	Western Hudson Bay (61.11, -94.06)	*Ursus maritimus*	LI	D	Juvenile	8 (8)	2007–2015 (2007)	-0.2
Canada	Western Hudson Bay (61.11°, -94.06°)	*Ursus maritimus*	LI	D	Adult male	10 (10)	2007–2017 (2007)	6.0
Denmark	Ittoqqortoormiit (70.29°, -21.58°)	*Ursus maritimus*	LI	W	Juvenile	28 (28)	1983–2018 (1983)	2.8
Denmark	Ittoqqortoormiit (70.29°, -21.58°)	*Ursus maritimus*	LI	W	Adult female	22 (22)	1984–2018 (1984)	0.1
Denmark	Ittoqqortoormiit (70.29°, -21.58°)	*Ursus maritimus*	LI	W	Adult male	24 (24)	1984–2018 (1984)	1.8
Denmark	Ittoqqortoormiit (70.29°, -21.58°)	*Ursus maritimus*	LI	W	Undefined	14 (14)	1986–2018 (1986)	3.3
Norway	Svalbard (77.875°, 20.975°)	*Vulpes lagopus*	LI	W	--	11 (11)	1998–2014 (1998)	3.6
Canada	Old Crow (67.57°, -139.83°)	*Rangifer tarandus*	KI	D	--	26 (26)	1991–2017 (1991)	-1
Canada	Western Hudson Bay (61.11°, -94.06°)	*Rangifer tarandus*	KI	D	--	13 (13)	2006–2018 (2006)	2.6

a) Number of years in fitted time series (entire series); b) Years in fitted time series (earliest year in dataset); c) Sign and magnitude of recent trend (max 20 years; 1999–; back-transformed); d) Sign and magnitude of longest fitted trend (back-transformed); e) Mean concentrations of the last year (fitted value in the last monitoring year back-transformed from the log-scale); f) Corresponding upper one-sided 95% confidence limit; g) *p*-value for recent trend; h) *p*-value for overall trend
i) *p*-value for longest fitted trend; j) *p*-value for non-linear trend across the full time series (if present it indicates trend is significant but has non-linear characteristics); k) *p*-value for linear trend; l) % annual increase detected with 80% power (by a two-sided test of size 5%) given the current configuration of years (only when n≥5); m) % annual increase detected with 80% power given 10 sequential years of monitoring; n) Power to detect a 5% annual increase given the current configuration of years (only when n≥5); o) Power to detect a 5% annual increase given 10 sequential years of monitoring
For trends, green are decreasing and red are increasing, the darker the shade, the greater the trend.
For power, the darker the green the greater the power value.

Overall trend	meanLY	clLY	p_rtrend	p_overall	p_ltrend	p_nonlinear	p_linear	dtrend_1	dtrend_3	dpower_1	dpower_3
d	e	f	g	h	i	j	k	l	m	n	o
-5.4	244.7	333.9	0.0317	0.0317	0.0317	--	0.0317	6.5	11.5	59	24
1	210.3	317.3	0.6145	0.6145	0.6145	--	0.6145	5.9	14.9	67	17
-3.5	92.7	105.7	0.0006	0.0006	0.0006	--	0.0006	2.9	5.8	100	69
-5.2	267.6	322.8	0.0003	0	0.0003	0.0015	0.007	3.1	5.4	99	73
-6.8	173.6	218.7	0.0024	0.0024	0.0024	--	0.0024	5.5	9.8	73	32
-1.3	5501.7	7261.3	0.2935	0.2935	0.2935	--	0.2935	4	10.5	94	28
1.7	6536.7	7721.7	0.0268	0.0268	0.0268	--	0.0268	1.5	8.7	100	38
2.3	8581.1	10396.5	0.0355	0.0355	0.0355	--	0.0355	3.2	9.2	99	35
1	6666.3	9117.9	0.5023	0.5023	0.5023	--	0.5023	4.7	10.5	85	28
0.2	1887.0	2216.9	0.8425	0.8425	0.8425	--	0.8425	2.3	8.3	100	41
2.9	2344.7	3683.1	0.259	0.259	0.259	--	0.259	8.2	16.6	42	15
-1.5	19911.0	27057.6	0.5912	0.5912	0.5912	--	0.5912	8.8	11.1	37	26
0.7	21400.3	25743.5	0.6899	0.6899	0.6899	--	0.6899	5	6.3	80	61
-0.8	12832.3	17731.1	0.8258	0.8258	0.8258	--	0.8258	10.5	7.3	29	50
-6.2	21281.7	29638.9	0.1869	0.1869	0.1869	--	0.1869	12.7	10.2	22	29
-0.2	18928.1	29365.1	0.9744	0.9744	0.9744	--	0.9744	17.7	12.8	14	21
6.0	41080.2	52202.1	0.0294	0.0294	0.0294	--	0.0294	8	8.5	43	39
5.5	18815.1	32483.5	0.111	0.0004	0.0002	0.0027	0.0415	2	15.2	100	16
0.1	22565.2	37180.7	0.9622	0.9622	0.9622	--	0.9622	4.3	26.1	91	9
1.8	25769.8	39815.8	0.2305	0.2305	0.2305	--	0.2305	4.3	27.9	90	9
3.3	25020.8	43459.5	0.087	0.087	0.087	--	0.087	5.4	26.3	74	9
3.6	153.8	234.6	0.1452	0.1452	0.1452	--	0.1452	7.6	16.6	47	15
-1	1324.1	1589.0	0.1314	0.1314	0.1314	--	0.1314	1.9	9.4	100	34
2.6	5389.4	6552.4	0.1083	0.1083	0.1083	--	0.1083	4.8	7.6	83	47

Appendix 2.3 Statistical methods: details

Biota

Pre-processing of data in wildlife, fish and invertebrates

Data were supplied by individual principal investigators as individual concentrations of total mercury (THg). Data were blank corrected where necessary and were dry weight normalized when moisture data were available. The publications referenced in Table A2.2 provide the details of processing and analysis for all of the biota time series analyzed.

Pre-processing of data in humans

The publications referenced in Table A2.3 provide the details of processing and analysis for all of the human datasets analyzed.

Statistical methodology for trend assessment of contaminants in biota

Time series of contaminant concentrations in biota were assessed as changes in the log-transformed concentrations over time using linear mixed models. The type of temporal change considered was dependent on the number of years of data and differed from other forms of the models used for OSPAR and ICES assessments as datasets of less than 5 years were not considered. For the current statistical assessment, if the time series contained 5 to 6 years a log-linear trend was fit and for ≥7 years, more complex (smoothed) patterns of change were modeled over time (see Fryer and Nicholson, 1999). When a linear model was fit (i.e., when there were 5 to 6 years of data, or if there were ≥7 years of data and no evidence of nonlinearity), the statistical significance of the temporal trend was obtained from a likelihood ratio test comparing the fits of the linear model $f(year)=\mu+\beta year$ and the mean model $f(year)=\mu$. When a smooth model was fit, a plot of the model should be used to understand the patterns of change.

Modeling changes in log concentration over time

The natural log concentrations in biota were modeled by a linear mixed model with the form:

Response: log concentration of mercury

Fixed: *f*(year)

Random: Year + sample + analytical

The fixed effects model describes how log concentrations change with year, where the form of *f*(year) varies with the number of years in the time series. The random effects model components are year (random variation in log concentration between years, treated as a categorical variable), sample (random variation in log concentration between samples within years; when there is only one sample each year, this term is omitted and implicitly subsumed into the between-year variation) and analytical (random variation inherent in the chemical measurement process; this is assumed known and derived from the 'uncertainties' reported with the data). If u_i, $i=1...n$, were the uncertainties associated with concentrations c_i (expressed as the standard deviations of the concentration measurements), then the standard deviations of the log concentration measurements $log\ c_i$ were taken to be u_i/c_i. Measurements with $u_i>c_i$ (i.e., an analytical coefficient of variation of more than 100%) were omitted from the time series.

The model is fitted by maximum likelihood assuming each of the random effects were independent and concentrations were log-normally distributed. The form of *f*(year) depends on the number of years of data:

5–6 years: linear model $f(year) = \mu + \beta year$

These models assume log concentrations vary linearly with time; the fitted models were used to assess temporal change.

≥7 years: smooth model $f(year) = s(year)$

These models assume that log concentrations vary smoothly with time; the fitted models were used to assess temporal change, but the form of the smoother varied with the length of the time series.

7–9 years: linear models and smoothers on 2 degrees of freedom (*df*) were fit.

10–14 years: linear models and smoothers on 2 and 3 *df* were fit.

15+ years: linear models and smoothers on 2, 3 and 4 *df* were fit.

For these longer trends (≥7 years), the model chosen to make inferences about status and temporal trends was based on the lowest Akaike's Information Criterion corrected for small sample size (*AICc*).

Refinements to the analysis were required to prevent over-fitting if there were many less-than values (values below detection or quantitation limits) or if they were unevenly distributed across the dataset. None of the time series analyzed in the current assessment had extensive less-than values. If uncertainties were not supplied with the concentration measurements, uncertainties were estimated using fixed and relative standard deviations derived from the uncertainties in the ICES database.

For more information see https://ocean.ices.dk/OHAT/trDocuments/2019/help_methods_less_thans.html and https://ocean.ices.dk/OHAT/trDocuments/2019/help_methods_missing_uncertainties.html.

Assessing environmental status

AMAP assessments do not currently apply environmental assessment criteria as part of their (temporal) trend assessment process. Wildlife effects for some species were, however, evaluated in relation to risk thresholds. For further information, see the recent AMAP assessment of Biological Effects of Contaminants on Arctic Wildlife and Fish (AMAP, 2018a) and Chapter 6 of this report.

Metadata column headers for Analysis

Country: country that reported the data.

StationName: station name. If blank station is used. (Station_LongName in ICES station dictionary.)

Latitude: nominal latitude of station.

Longitude: nominal longitude of station.

Species: species latin name.

Matrix: tissue the mercury concentration is measured in (e.g., muscle, soft body, hair, egg.)

Basis: basis of measurement (i.e., wet or dry).

Group: grouping of data. Mostly used for mercury data (from a single station, species or matrix) that are split up into several time series corresponding to different ages (sizes) and/or sex combinations; for example, into juveniles, adult males and adult females. The class 'not grouped' is used in two ways:

* for data that are not split up and are modelled as a single time series;

* for the data that remain after specific age (size) and/or sex combinations have been removed; they might remain because they weren't the target population (e.g., fish outside a target length range) or because a key variable (e.g., age) wasn't recorded.

Nyall: number of years with mercury concentration data.

Nyfit: number of years included in the statistical analysis. Some early years might be excluded because they are separated from the bulk of the data by large gaps in time.

firstYearAll: first year with mercury concentration data.

firstYearFit: first year included in the statistical analysis. See ***nyfit*** for explanation.

Last year: last year of data. Time series are only included if there is at least one year of data in the period 2013 through 2018.

p_nonlinear: the significance of the nonlinear component of the trend. This assesses whether log concentrations changed nonlinearly over the monitoring period. It is based on a likelihood ratio test comparing the smooth model with a linear model and is only given if a smooth model is selected by AICc.

p_linear: the significance of the linear component of the trend. This test only has a simple interpretation when the trend is linear (rather than smooth) in which case it assesses whether concentrations changed (log-linearly) over the monitoring period. It is based on a likelihood ratio test comparing the linear model with the null model (in which only an intercept if fitted). For smooth models, the terms pltrend and prtrend are more relevant.

p_overall: the overall signficance of the trend. This assesses whether mean concentrations changed over the monitoring period. It is based on a likelihood ratio test comparing the fitted model (smooth or linear) with the null model. This will be identical to p_linear if the fitted model is linear.

ltrend: an estimate of the change in mean concentration between the start and end of the monitoring period. Specifically,

ltrend=100 y^N−y^1tN−t1

where y^1 and y^N are the fitted mean log concentrations in firstYearFit and lastyear and t1 and tN are firstYearFit and lastyear respectively. Loosely, ltrend can be interpreted as the percentage annual change in concentration between firstYearFit and lastyear assuming the trend in concentration is log-linear. More formally, ltrend corresponds to a percentage annual change of

Annual Change (%) = 100(exp(rtrend/100)−1))

rtrend: an estimate of the change in mean concentration in the last 20 years. Specifically,

rtrend=100y^N−y^*tN−t*

where y^* is the fitted mean log concentration in 1999 (or firstYearFit whichver is later) and t* is 1999 (or firstYearFit). Loosely, rtrend can be interpreted as the percentage annual change in concentration in the last 20 years assuming the trend in concentration is log-linear. More formally, rtrend corresponds to a percentage annual change of

100(exp(rtrend/100)−1))

meanly: the fitted mean concentration in last year.

clLY: the upper one-sided 95% confidence limit on the fitted mean concentration in lastyear.

dtrend_1: the percentage annual increase in concentration that would be detected by the monitoring programme with ≥80% power using a test at the 5% significance level.

dtrend_3: the percentage annual increase in concentration that would be detected with 90% power based on a test at the 5% significance given 10 years of annual monitoring and variability typical of the time series.

dpower_1: the power of the monitoring programme to detect an annual 5% increase in concentration using a test at the 5% significance level.

dpower_3: the power to detect an annual 5% increase in concentration using a test at the 5% significance level given 10 years of annual monitoring and variability typical of the time series.

3. Changes in Arctic mercury levels: emissions sources, pathways and accumulation

Coordinating lead author: Ashu Dastoor

***Lead Authors**/contributors*: *Section 3.1:* **Ashu Dastoor** *Section 3.2:* **Simon Wilson**, Johannes Bieser, Marilena Muntean, David McLagan, Frits Steenhuisen, Ashu Dastoor *Section 3.3:* **Hélène Angot, Ashu Dastoor, Theodore Dibble**, **Huiting Mao**, **Robert Mason, Daniel Obrist, Andrei Ryjkov, Colin Thackray, Oleg Travnikov, Leiming Zhang,** Jesper Christensen, Brian DiMento, Thomas A. Douglas, Martin Jiskra, Jane Kirk, Derek C.G. Muir, Sarah Roberts, Henrik Skov, Anne Soerensen, Kenjiro Toyota, Yanxu Zhang *Section 3.4:* **Thomas A. Douglas, Martin Jiskra**, **Daniel Obrist**, **Peter Outridge, Kyra St. Pierre**, **Christian Zdanowicz,** Ashu Dastoor, Cuicui Mu, Jeroen Sonke, Erin Trochim, Tingjun Zhang *Section 3.5:* **Robert Mason**, **Peter Outridge, Michelle Nerentorp Mastromonaco,** Brian DiMento, Lars-Eric Heimbürger-Boavida, Mariia Petrova, Jane Kirk, Carl Lamborg, Anne Soerensen, Yanxu Zhang, Amina Schartup and Ashu Dastoor *Section 3.6:* **Ashu Dastoor**, Oleg Travnikov, Hélène Angot, Jesper Christensen, Andrei Ryjkov, Simon Wilson and Frits Steenhuisen *Section 3.7:* **Ashu Dastoor**, Oleg Travnikov, Hélène Angot, Jesper Christensen, Andrei Ryjkov *Section 3.8:* **Ashu Dastoor,** Oleg Travnikov, Hélène Angot, Jesper Christensen, Andrei Ryjkov *Section 3.9:* **Ashu Dastoor**

Additional contributors: Katarine Gårdfeldt, Sofi Jonsson, Aditya Kumar, Katriina Kyllönen

3.1 Where does mercury in the Arctic environment come from, and how does it get there?

This chapter addresses the policy question: where does mercury in the Arctic environment come from, and how does it get there? Evidence of a notable increase in present-day mercury (Hg) concentrations in Arctic environments compared to pre-industrial levels has led to substantial scientific investigation in the past few decades concluding the majority of Hg in the region originates from sources outside the Arctic (AMAP, 2011). Mercury is released into the air from both anthropogenic and natural sources in inorganic form, which then circulates and accumulates in global environments through a series of complex physicochemical processes involving advection, diffusion, chemical and phase transformations as well as flux exchanges between air, land and water. Mercury enters the Arctic environment via the atmosphere, ocean currents and river runoff. The Arctic being a large and remote region, there is still a paucity of Hg observations in Arctic environments. However, since the last AMAP mercury assessment (AMAP, 2011), major ongoing measurements efforts (e.g., the GEOTRACES program; DiMento et al., 2019; Petrova et al., 2020) and new analytical techniques such as mercury stable isotopic signatures (Blum et al., 2014; Obrist et al., 2018) are elucidating Hg pathways with greater clarity. Strides have also been made in the understanding of Hg chemistry and the development of models, reducing uncertainties in estimates of Hg deposition and source attribution in the Arctic (Angot et al., 2016; Dibble et al., 2020). The aim of this chapter is to assess the impact of global sources of Hg emission on contemporary Hg levels in Arctic ecosystems based on scientific progress made in the past decade. The chapter provides a quantitative synthesis of recent advances in the understanding of the global sources of Hg emissions, transport pathways, the spatial distributions of Hg fluxes as well as of Hg budgets in abiotic atmospheric, terrestrial and marine environments in the Arctic.

The main species of Hg emitted to the atmosphere, gaseous elemental mercury (Hg(0)), has a long lifetime in air (0.5–1 year; Horowitz et al., 2017); its long life means that Hg is transported and deposited on a global scale. In terrestrial ecosystems, direct uptake of ambient Hg(0) by vegetation is a major pathway for Hg removal from the atmosphere. Hg(0) reacts with strong oxidants in air, such as halogens, to form oxidized mercury species (Hg(II)). Hg(II) species are readily deposited to global ecosystems by direct uptake and precipitation scavenging on a shorter timescale (up to two weeks). In coastal and marine Arctic environments, Hg oxidation and deposition processes intensify during springtime, facilitated by increased photochemical production of bromine (Br) species from snowpacks over sea ice (Moore et al., 2014; Toyota et al., 2014a; Wang et al., 2019a). Due to its volatile nature, a fraction of historically deposited Hg re-enters the atmosphere from earth's surfaces, significantly amplifying environmental Hg circulation. Burial in long-term storage archives such as lake sediments, ocean sediments, subsurface soils, and glacial ice ultimately immobilizes Hg from its circulation in global environments.

This chapter begins by describing the global sources of emissions that contribute to Hg contamination in the Arctic (Section 3.2). Sections 3.3, 3.4 and 3.5 respond to the question: how does Hg enter Arctic environments? These sections present an up-to-date understanding of Hg transport pathways, inter-compartmental fluxes, and levels in abiotic Arctic environments. This chapter also discusses potential contributions of melting permafrost, ice sheets, ice caps and glaciers to Hg levels in downstream Arctic environments (Sections 3.4.2 and 3.4.3). Source apportionment of atmospheric Hg deposition in the Arctic with respect to global and local emissions is presented in Sections 3.6 and 3.7. Section 3.8 provides a comprehensive picture of how much Hg is circulating in Arctic environments. Key results and recommendations are summarized in Section 3.9. Processes leading to or affecting Hg uptake by biota are described in Chapter 4.

3.2 What are the sources of mercury emissions to air contributing to mercury in Arctic environments, and how much mercury is being emitted?

3.2.1 Global estimates of natural and anthropogenic mercury emissions to air

The Global Mercury Assessment 2018 (AMAP/UN Environment, 2019) presents an updated global Hg budget that estimates present day, total global emissions of Hg to air at approximately 8000 t/y (4600 t/y and 3400 t/y from terrestrial and marine sources, respectively). These emissions originate from the following sources: ~500 t/y from natural (geogenic) sources; ~1600 t/y from re-emissions from soil, vegetation and open biomass burning; ~3400 t/y from evasion from surface ocean waters; and ~2500 t/y from anthropogenic sources. The atmosphere is estimated to hold ~4400 t of Hg, representing a percentage increase due to human activities of ~450% since around the mid-15th century (see Figure 3.1).

Current annual emissions to air from anthropogenic sources (contributing ~30% of total Hg emissions) and natural sources (contributing <10%) are substantially lower than re-emissions/evasion from soils/vegetation and surface ocean waters, which together contribute ~60% of total Hg emissions; however, it should be recognized that the re-emissions—essentially a result of natural processes—are themselves largely a consequence of the build-up of Hg in the environment following historical anthropogenic emissions and releases. In the context of the budget, emissions from Hg released or disposed of to land (e.g., landfill, mine tailings and waste rock, etc.) are also treated as re-emission sources. Action to reduce present day anthropogenic Hg emissions and releases (through, for example, the global Minamata Convention on Mercury) is therefore the key to reducing further accumulation of Hg in environmental media and future re-emissions of Hg.

The global budget also includes an estimate of ~600 t of Hg released to aquatic environments in 2015 from anthropogenic sources; this amount does not include releases associated with artisanal and small-scale gold mining (ASGM) activities, which are estimated to contribute ~1200 t of Hg in combined releases to land and water in 2015 (AMAP/UN Environment, 2019). These releases are additional to the significant contribution that ASGM makes to emissions of Hg to air. The following sections provide estimates of anthropogenic, geogenic and secondary emissions of Hg relevant to Arctic Hg contamination. The emissions described here were used to develop present-day budgets and geospatial distributions of Hg levels in the Arctic air and deposition (see Sections 3.3 and 3.8), and to assess the source apportionment of Hg deposition (see Sections 3.6 and 3.7) in the Arctic using multiple models.

3.2.2 Anthropogenic emissions

3.2.2.1 Global anthropogenic emissions in 2015

As part of the work to produce the Global Mercury Assessment 2018 (UN Environment, 2019), a joint AMAP/UN Environment expert group was established to prepare a global inventory of Hg emissions to air from anthropogenic sources in 2015. This work built on earlier AMAP global anthropogenic emissions

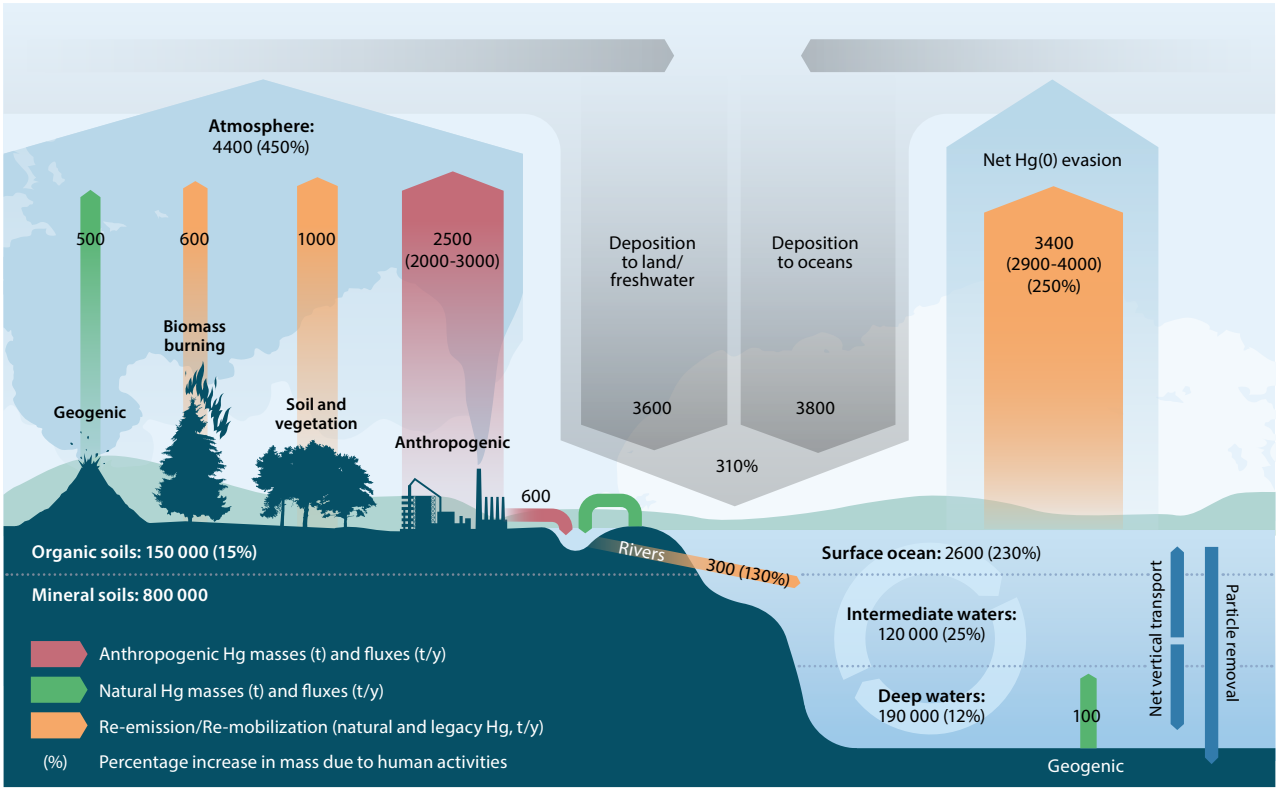

Figure 3.1. Global Hg budget showing best estimate values and (in parentheses) associated ranges; percentage values represent the estimated increase in mass or flux due to human activities since the pre-anthropogenic period (i.e., since ~1450 AD; AMAP/UN Environment, 2019). The budget balances within the stated ranges only, reflecting the considerable uncertainty associated with several of the budget terms represented.

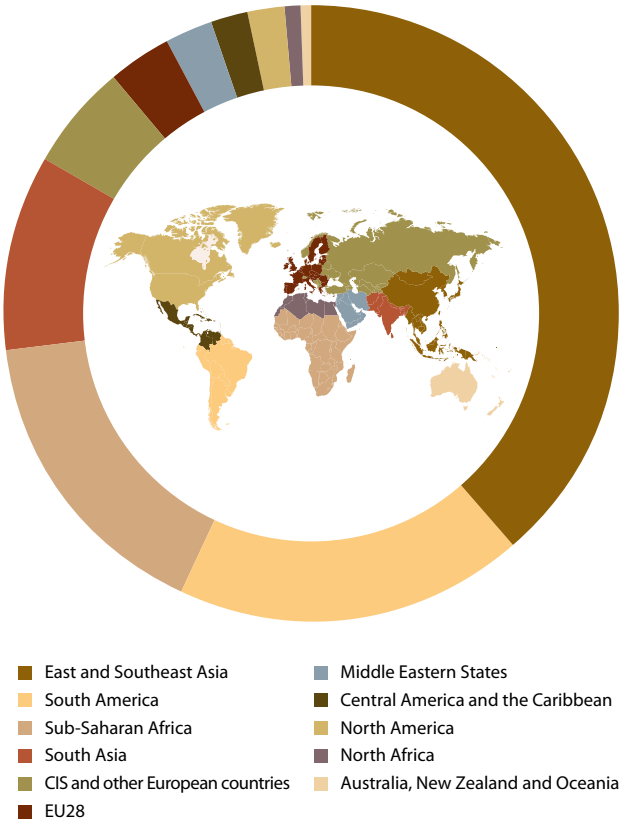

Figure 3.2. Contributions from various regions to the estimated global inventory of anthropogenic Hg emissions to air in 2015 (AMAP/UN Environment, 2019).

inventory work reported in AMAP mercury assessments as well as assessments of other heavy metals (AMAP, 1998, 2005, 2011) and applied a revised methodological approach that was introduced in preparing the global inventory of Hg emissions for 2010 (AMAP/UNEP, 2013).

Results of this 2015 anthropogenic emissions inventory are presented in detail in the Technical Background Report to the Global Mercury Assessment 2018 (AMAP/UN Environment, 2019). The inventory estimates national emissions for ~220 countries in 11 subcontinental regions for each of the 17 main emission sectors. Figure 3.2 and Tables 3.1 and 3.2 summarize, by region and source sector, the resulting 2015 emission estimates, which total ~2220 t of Hg (2000–2820 t).

The 2015 inventory estimates (AMAP/UN Environment, 2019) identify sources in Asia as responsible for about 50% of global Hg emissions in 2015, with East and Southeast Asia contributing ~40% and South Asia contributing ~10% (see Figure 3.2). This reflects the growth in industrial development in these regions in recent decades and, in particular, the use of coal as a primary source of energy. Stationary combustion of fossil fuels and biomass burning is responsible for some 24% of estimated global Hg emissions (21% from coal burning). Industrial activities involving high temperature processes, such as metal smelting and cement production, are responsible for a further 28% of global Hg emissions.

The other main sources of Hg emissions are associated with the intentional use of Hg. These include use in mercury-added products, such as lamps, batteries, and instruments (e.g., medical instruments, such as thermometers, sphygmomanometers and measuring devices, such as barometers) as well as in dental amalgam, all of which generate wastes that are sources of emissions, especially where these wastes are subject to uncontrolled burning. The intentional use of Hg also includes its use in industrial processes, such as the manufacture of vinyl chloride and the production of chlor-alkali using the mercury-cell process. However, by far the largest source of Hg emissions from intentional Hg use is that associated with ASGM, which globally is estimated to contribute ~38% of the total anthropogenic emissions inventory. ASGM contributes ~70% of emissions in South America and up to 80% of emissions in Sub-Saharan Africa as well as contributing a significant part of the emissions in East and Southeast Asia. As a result, South America and Sub-Saharan Africa are responsible for ~18% and ~16% of global emissions of Hg, respectively. However, if ASGM emissions are excluded, the pattern of regional contributions changes and regions such as South Asia and CIS (Commonwealth of Independent States) and other European

Table 3.1. Contributions from various regions to the estimated global inventory of anthropogenic Hg emissions to air in 2015 for four main groups of emissions sectors (AMAP/UN Environment, 2019). Sectors comprising the respective groups are indicated in Table 3.2.

	Sector group (emissions, t)				Regional total (range), t	% of global total
	Fuel combustion	Industry sectors	Intentional-use (including product waste)	Artisanal and small-scale gold mining		
Australia, New Zealand and Oceania	3.57	4.07	1.15	0.0	8.79 (6.93–13.7)	0.4
Central America and the Caribbean	5.69	19.1	6.71	14.3	45.8 (37.2–61.4)	2.1
CIS and other European countries	26.4	64.7	20.7	12.7	124 (105–170)	5.6
East and Southeast Asia	229	307	109	214	859 (685–1430)	38.6
EU28	46.5	22.0	8.64	0.0	77.2 (67.2–107)	3.5
Middle Eastern States	11.4	29.0	12.1	0.225	52.8 (40.7–93.8)	2.4
North Africa	1.36	12.6	6.89	0.0	20.9 (13.5–45.8)	0.9
North America	27.0	7.63	5.77	0.0	40.4 (33.8–59.6)	1.8
South America	8.25	47.3	13.5	340	409 (308–522)	18.4
South Asia	125	59.1	37.2	4.50	225 (190-296)	10.1
Sub-Saharan Africa	48.9	41.9	17.1	252	360 (276–445)	16.2
Global inventory	533	614	239	838	2220 (2000–2820)	100.0

Table 3.2. Contributions from various source sectors to the estimated global inventory of anthropogenic Hg emissions to air in 2015 (AMAP/UN Environment, 2019).

Sector	Sector group	Mercury emission (range), t	Sector % of total
Artisanal and small-scale gold mining (ASGM)	ASGM	838 (675–1000)	37.7
Biomass burning (domestic, industrial and power plant) *	Fuel combustion	51.9 (44.3–62.1)	2.33
Cement production (raw materials and fuel, excluding coal)	Industry	233 (117–782)	10.5
Cremation emissions	Intentional-use	3.77 (3.51–4.02)	0.17
Chlor-alkali production (mercury-cell process)	Intentional-use	15.1 (12.2–18.3)	0.68
Non-ferrous metal production (primary Al, Cu, Pb and Zn)	Industry	228 (154–338)	10.3
Large-scale gold production	Industry	84.5 (72.3–97.4)	3.8
Mercury production	Industry	13.8 (7.9–19.7)	0.62
Oil refining	Industry	14.4 (11.5–17.2)	0.65
Pig iron and steel production (primary)	Industry	29.8 (19.1–76.0)	1.34
Stationary combustion of coal (domestic/residential, transportation)	Fuel combustion	55.8 (36.7–69.4)	2.51
Stationary combustion of gas (domestic/residential, transportation)	Fuel combustion	0.165 (0.13–0.22)	0.01
Stationary combustion of oil (domestic/residential, transportation)	Fuel combustion	2.70 (2.33–3.21)	0.12
Stationary combustion of coal (industrial)	Fuel combustion	126 (106–146)	5.67
Stationary combustion of gas (industrial)	Fuel combustion	0.123 (0.10–0.15)	0.01
Stationary combustion of oil (industrial)	Fuel combustion	1.40 (1.18–1.69)	0.06
Stationary combustion of coal (power plants)	Fuel combustion	292 (255–346)	13.1
Stationary combustion of gas (power plants)	Fuel combustion	0.349 (0.285–0.435)	0.02
Stationary combustion of oil (power plants)	Fuel combustion	2.45 (2.17–2.84)	0.11
Secondary steel production *	Industry	10.1 (7.65–18.1)	0.46
Vinyl-chloride monomer (mercury catalyst) *	Intentional-use	58.2 (28.0–88.8)	2.6
Waste (other waste)	Intentional-use	147 (120–223)	6.6
Waste incineration (controlled burning)	Intentional-use	15.0 (8.9–32.3)	0.67
Total		2220 (2000–2820)	100

countries appear higher in the ranking. Overall, the patterns of both regional and sectoral contributions to global emissions in 2015 were similar to those in 2010.

The inventory methodology also recognizes that there may be additional emissions from sectors that it is not possible to quantify using the current methodology and available data; these could contribute between an additional few tens to several hundreds of tonnes (t) of Hg emissions per year. These include anthropogenic emissions associated with incineration of industrial and sewage sludge and some hazardous wastes, oil and gas extraction (upstream of refineries) and agricultural burning. Some of these sources may be significant in a local and/or Arctic context.

Estimates of emissions from agricultural burning, totaling ~90 t in 2012, are included in global Hg emissions inventories prepared by the Emissions Database for Global Atmospheric Research (EDGAR; see Section 3.2.2.3). The EDGARv4.tox2 (Muntean et al., 2018) dataset includes estimates of Hg emissions from field burning of agricultural residues for individual countries. Between 1970 and 2012, the EDGAR agricultural emissions estimates show a consistent increasing trend, almost doubling since 1970. In 2012, their share in the total global Hg emissions estimated by EDGAR was about 5%, with the greatest contributions to agricultural emissions from Brazil (17%), India (15%) and Indonesia (11%).

Comparing the 2015 global inventory results (AMAP/UN Environment, 2019) with other national and regional emissions estimates is not straight-forward. No comparable global inventories exist for 2015. However, Muntean et al. (2018) have compared global emissions estimates of Hg from the Emission Database for Global Atmospheric Research (EDGAR) in 2010 (totaling ~1770 t) with the 2010 GMA inventory estimates reported in AMAP/UNEP, 2013 (which after being updated in 2018 totaled ~1810 t).

Comparisons of the 2015 GMA inventory estimates with preliminary national estimates prepared as Minamata Convention Initial Assessments (MIAs; UNDP, 2020) for a number of mainly developing countries, which lack routine emissions reporting mechanisms, revealed inconsistencies (AMAP/UN Environment, 2019). In some cases, these could be explained by the fact that MIA estimates applied activity data for recent years rather than a specific target year. Together with emissions factors, activity data—data on production of industrial materials and Hg-added products, and consumption of raw materials including fossil fuels—form the basis for most national/regional emissions estimates. Both emissions factors and activity data have associated uncertainties that were considered in the inventory work. Measurement-based emissions data are still only available for a relatively few, generally large, point sources of emissions; these data have

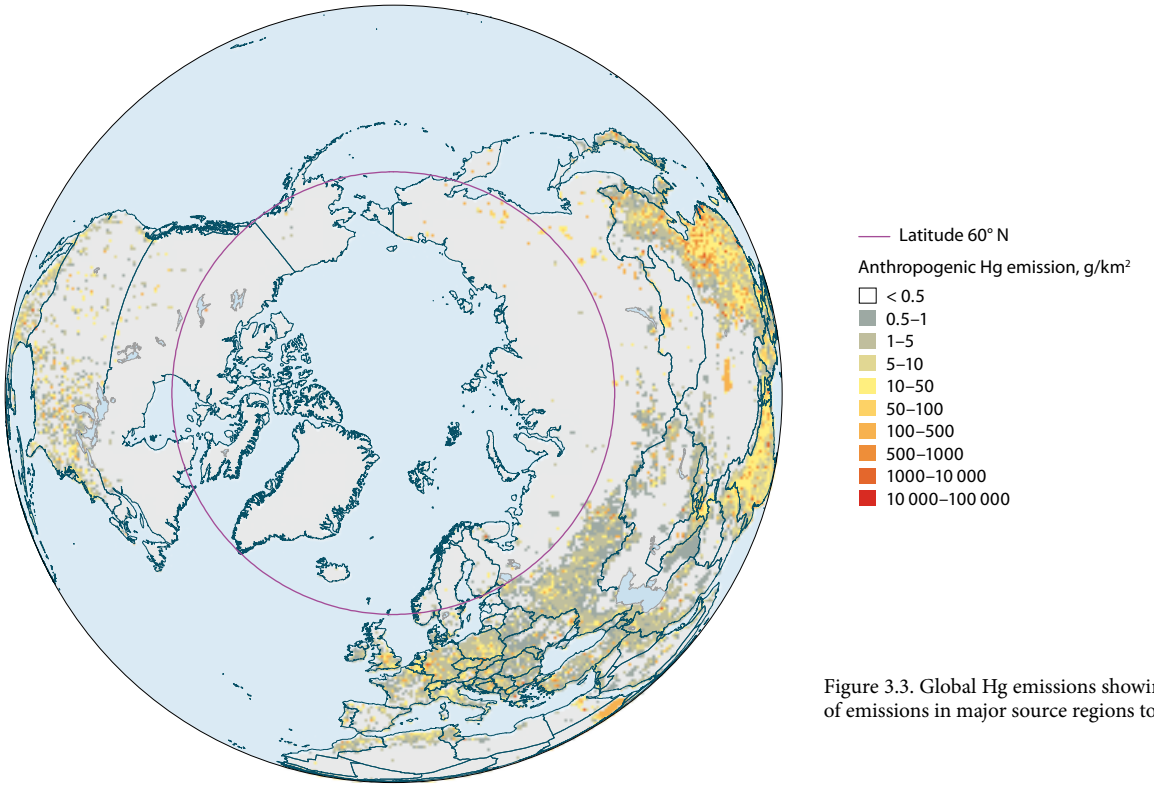

Figure 3.3. Global Hg emissions showing proximity of emissions in major source regions to the Arctic.

other associated uncertainties that must be considered when they are used to calculate annual emissions totals.

Comparisons between the 2015 GMA inventory estimates and other national estimates from countries that maintain emissions inventory systems and with regional estimates for 2015 reported under the United Nations Economic Commission for Europe (UNECE) Convention on Long-Range Transboundary Air Pollution (CLRTAP) indicated a generally reasonable level of consistency with respect to estimates for national total emissions, considering the associated uncertainties (AMAP/UN Environment, 2019). However, estimates for particular emissions sectors were more variable, reflecting to a large degree differences in the way emissions are classified or categorized under different Hg emissions reporting systems, many of which have been adapted from systems developed for reporting emissions of other pollutants. These major considerations would need to be addressed in any regulatory emissions reporting context.

3.2.2.2 Geospatial distribution

An important additional component of the work on the 2015 inventory was its geospatial distribution used to generate datasets that could then be used by modelers investigating, for example, long-range atmospheric transport of Hg (see Sections 3.3 and 3.6). This work comprised of allocating national Hg emissions totals to specific point sources or their area-wide distribution (within 0.25° grid cells), based on expected emissions distributions for the sectors concerned. The methods applied and the results of this work are detailed in Steenhuisen and Wilson (2019); Figure 3.3 presents the geospatially distributed inventory for total mercury emissions (THg) viewed from an Arctic perspective; for further information on how emissions specifically impact Arctic environments see Section 3.2.2.5.

3.2.2.3 Trends in anthropogenic emissions

Mercury emissions to air have changed over time. Historically, gold and silver mining have been major sources of mercury emissions and releases. Following the industrial revolution and the subsequent rise of fossil fuel economies (i.e., from the 1850s onwards), Hg emissions increased (AMAP, 2011; AMAP/UN Environment, 2019). Emissions during the first part of the 21st century are estimated globally at around 2000 to 2500 t/y with emissions increasing in some geographical regions and decreasing in others.

Comparisons between global anthropogenic emission inventories produced at different times since the 1990s (AMAP, 1998, 2005, 2011; Pacyna and Pacyna, 2002; Pacyna et al., 2006, 2010) is complicated by the fact that, over time, additional sectors have been added to the inventories, as well as by changes in the methods applied for calculating emissions.

In the GMA 2018 work (AMAP/UN Environment, 2019) it was only considered appropriate to compare the 2015 inventory results with results from the 2010 inventory (AMAP/UNEP, 2013), which was prepared using a similar methodology, and then only after the latter had been updated to introduce new sectors which were considered in 2015 (e.g., biomass burning in power generation, industry and domestic sources), newly available 2010 activity data, and some changes in methods for calculating emissions from ASGM and the disposal of Hg-added product wastes). The results (Figure 3.4) indicate that estimated global anthropogenic emissions of Hg to the atmosphere for 2015 were approximately 20% higher than in 2010. Within this trend, modest decreases in emissions in North America and the European Union associated with continuing action to reduce emissions and shifts in fuels used for energy (i.e., away from coal) are more than offset by increased emissions in other regions, in Asia in particular. The overall trend appears

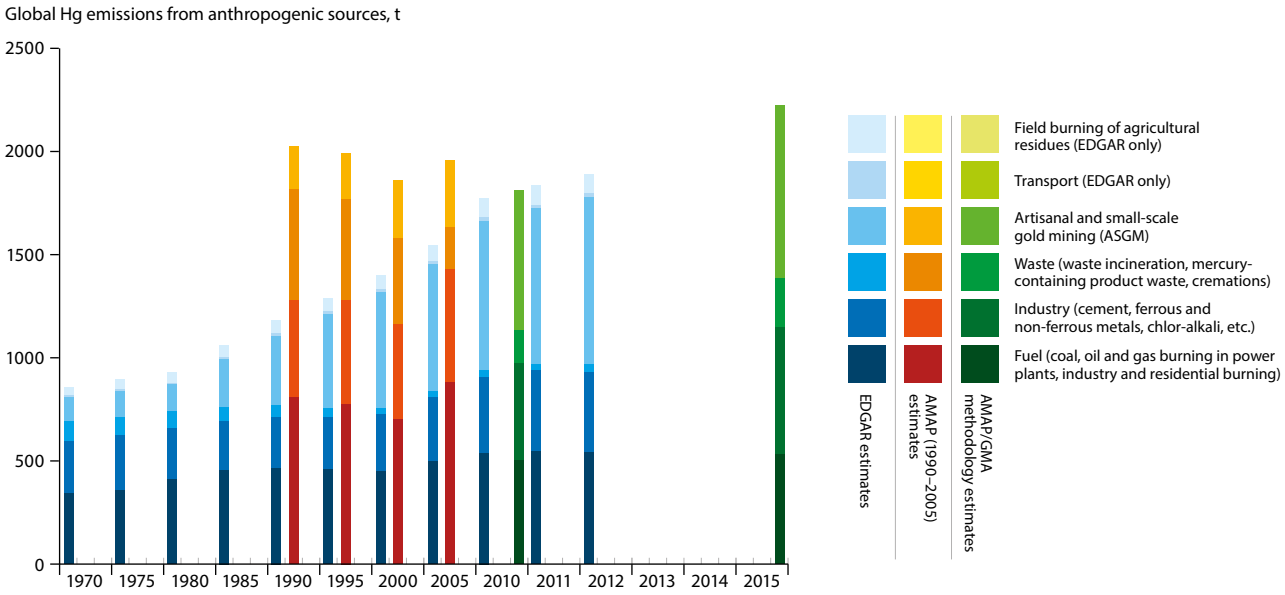

Figure 3.4. Trends in global emissions of Hg to the atmosphere as produced by three emission inventory approaches. Note: these three approaches are not directly comparable as they use different methodologies and do not necessarily include the same set of source sectors. AMAP/GMA estimates are reported in AMAP/UN Environment, 2019; AMAP 1900–2005 estimates are from AMAP, 2010; EDGAR estimates are from Muntean et al., 2014, 2018.

to reflect a continuation of an upturn in global Hg emissions following decreasing emissions during the last decades of the 20th century as described in the previous AMAP mercury assessment (AMAP, 2011).

This contrasts somewhat with results of global Hg emissions estimates from EDGAR (Muntean et al., 2014, 2018) which show an increasing rather than a decreasing trend in global emissions in the last decades of the 20th century. Muntean et al. (2018) report global anthropogenic Hg emission trends over the period 1970 to 2012 based on an analysis of data from EDGAR (see Figure 3.4). The EDGAR dataset applies a consistent methodology across all years, showing global emissions (excluding ASGM) increasing by 45% between 1970 and 2012).

Analysis of the magnitude of changes in estimated Hg emissions between 2010 and 2015 by region and sector in the GMA work (AMAP/UN Environment, 2019) reveals that emissions in North America and the European Union (EU28) decreased across most sectors, resulting in modest decreases (~11 t) in total estimated emissions in each of these two regions (see Table 3.5). In all other regions, total regional Hg emissions increased between 2010 and 2015. In some regions, notably South America, increased ASGM activity contributed significantly to the increase in emissions both in percentage and absolute terms; in other regions, such as East and Southeast Asia, increased emissions are associated with industrial development and therefore are reflected in the figures for industry and energy sectors, in particular in non-ferrous metal production (NFMP). On a relative basis, the greatest increase was associated with Hg production in Central America and the Caribbean where Hg emissions grew by a factor of almost 20 due to new Hg production from mines in Mexico; industrial coal combustion also increased considerably in the same region (440%); however, in absolute terms this corresponds to only a few tonnes (t) of emitted Hg. In absolute terms, the sectors showing the largest increases in estimated emissions of Hg were ASGM (159 t), NFMP (79 t), cement production (47 t), Hg-product waste disposal (32 t) and coal combustion in power plants (24 t), contributing to a total increase for all sectors of 413 t. Sectors with decreasing estimated emissions included (mercury-cell process) chlor-alkali production, which is being phased-out globally, and oil combustion in industry; however, the associated reductions were relatively small in absolute terms (6 t and 2 t, respectively). In general, apart from ASGM-related emissions, Hg emissions are strongly related to a growth in industrial activity that in most regions reflects a growth in the consumption of fuels and raw materials to produce energy, cement, and ferrous and non-ferrous metals, among other activities. Increased industrial activity in many regions more than offsets emissions reductions achieved through, for example, more widespread application of air pollution control devices.

In addition to the challenges in comparing national/sector estimates over time, there are similar challenges with respect to comparing geospatially-distributed Hg emissions for different years/periods; here, there is the added complexity of documenting changes in the locations of emissions, particularly in the case of major point sources. Information concerning new power plants and industrial facilities, the closure of plants and changes in fuels and technology applied at energy production and industrial facilities (e.g., to control emissions) is generally lacking or is not available in the public domain. This is a particular problem in areas with rapidly developing economies and in countries lacking consistent long-term tracking of Hg emissions.

The increasing trends in anthropogenic emissions in recent years are not generally reflected in Hg air concentrations observed at Arctic background air monitoring sites, most of which show decreasing trends (see Section 2.3.1). This inconsistency between emissions estimates and air concentration trends may be related to the proximity of monitoring sites to regions where Hg emissions have declined significantly in recent decades (North America and Europe), to the effects of changes in

Table 3.5. Change in estimated anthropogenic emissions of Hg between 2010 and 2015 measured in kg and in percentage change across different regions for four main emissions sector groups (see Table 3.2 for specification of the sectors concerned; AMAP/UN Environment, 2019).

Absolute change by sector group (t)	Fuel	Industry	Waste	ASGM	All sectors
Australia, New Zealand and Oceania	-0.36	0.06	0.31	0	0.02
Central America and the Caribbean	-0.07	4.13	0.86	2.22	7.17
CIS and other European countries	-2.20	8.42	4.59	0.68	11.5
East and Southeast Asia	16.3	114	62.3	-30.2	163
EU28	-1.82	-2.59	-6.6	0	-11 0
Middle Eastern States	-0.51	3.63	3.36	0.26	6.69
North Africa	0.29	0.34	2.22	0	2.85
North America	-7.12	0.86	-4.97	0	-11.2
South America	1.41	0.95	0.076	163	165
South Asia	25.6	10 3	9.99	3.38	49.2
Sub-Saharan Africa	-2.1	1.62	10.6	19.9	29.9
Global change	29.4	142	82.8	159	413
Percentage change by sector group	**Fuel**	**Industry**	**Waste**	**ASGM**	**All sectors**
Australia, New Zealand and Oceania	-9.0	-9.0	-9.0	-9.0	-9.0
Central America and the Caribbean	-1.1	27.6	15.2	18.4	18.6
CIS and other European countries	-7.7	15.0	28.4	5.6	10.2
East and Southeast Asia	7.6	59.5	132.5	-12.4	23.4
EU28	-3.8	-10.5	-43.3	--	-12.5
Middle Eastern States	-4.3	14.3	38.5	--	14.5
North Africa	27.1	2.8	47.5	--	15.8
North America	-20.9	12.7	-46.2	--	-21.8
South America	20.6	2.0	0.6	91.6	67.6
South Asia	25.9	21.0	36.8	300	28.0
Sub-Saharan Africa	-4.1	4.0	161.0	8.6	9.1
Global percentage change	5.8	30.1	52.9	23.4	22.8

speciation of emitted Hg (see Section 3.2.2.4) or to the influence of remobilization, natural sources, deposition rates and the impacts of meteorology (as discussed in Sections 3.2.1, 3.2.3, 3.3.1.3 and 3.3.2); however, this is a subject requiring further investigation as it is highly relevant for the use of air monitoring results as an indicator of changes in emissions, for example under the Minamata Convention.

3.2.2.4 Mercury emissions speciation

An acknowledged deficiency in the GMA inventory work and its associated geospatial distribution concerns the approach currently employed to define the Hg species that are emitted to the atmosphere. The GMA work applied an outdated and simplistic generic speciation scheme to classify total mercury (THg) emissions between gaseous elemental mercury (GEM, Hg(0)), gaseous oxidized mercury (GOM) and particulate mercury (HgP) according to the source sector concerned. Mercury species emitted depend on a number of factors, including the air pollution control devices (APCDs) that are applied at emission point sources. Application of APCDs has changed considerably over recent decades, with developments taking place in different countries at different times. The applied GMA inventory methodology attempts to reflect this in terms of quantifying emission totals, but this has not been reflected in GMA inventory geospatial distribution work to date—although the most recent inventory tools allow for this to be done, it has been outside the scope of the work.

A large number of recent publications have documented speciation aspects of emissions, generally at large point sources such as power plants, smelters and other industrial facilities, in particular in Asia (e.g., Wu et al., 2012; Zhang et al., 2015). This represents a considerable body of new information available to improve speciation schemes.

Muntean et al. (2018) performed a comprehensive literature review on Hg speciation for different sectors and developed three retrospective emissions scenarios (S1, S2 and S3) based on different hypotheses related to the proportion of Hg species in the THg emissions. The reference scenario S1 uses the split factors provided in AMAP/UNEP (2008). This scheme has been applied to all global anthropogenic Hg emissions inventories reported in AMAP and UN Environment GMA work (inventories for the years 1990–2015) as well as in EDGARv4.tox2. The other two scenarios apply split factors derived primarily from field measurements: S2, from the

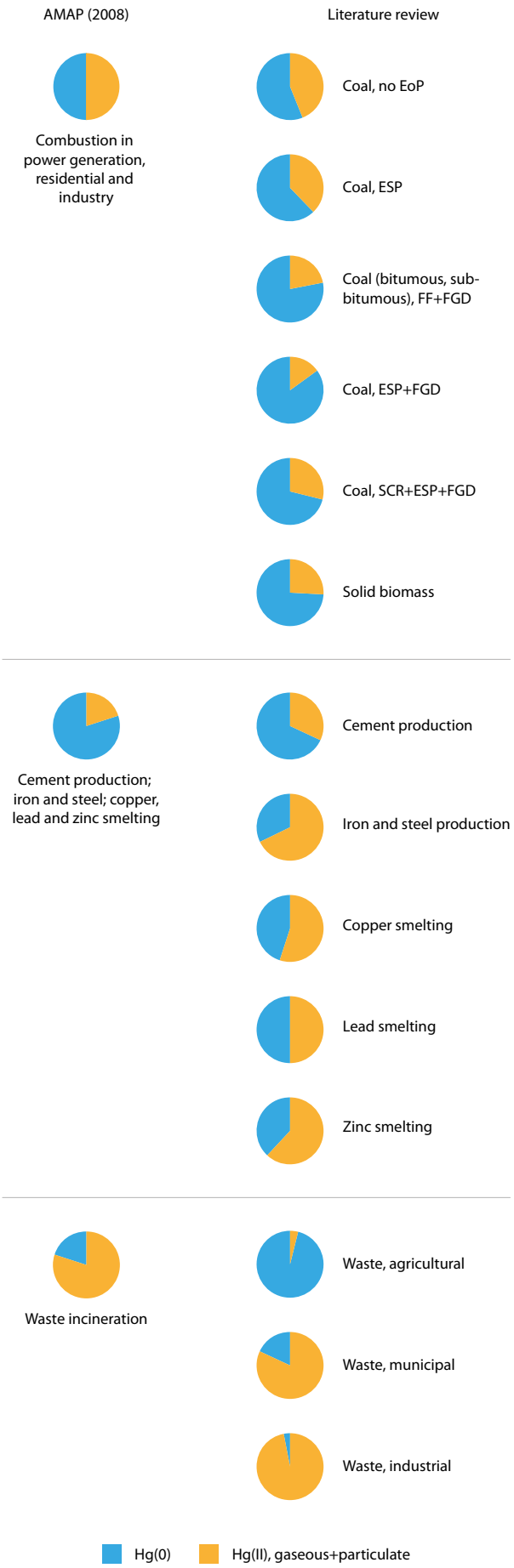

Figure 3.5. Proportions of elemental mercury (Hg(0)) and reactive mercury (HgP and Hg(II)) in the speciation scheme applied to the AMAP/GMA inventories for different sectors compared with information presented in recent literature. Modified from Muntean et al., 2018 and references therein.

United States Environmental Protection Agency's (EPA's) Information Collection Request (ICR; Bullock and Johnson, 2011); and S3 from recent scientific literature (Friedli et al., 2001, 2003a, 2003b; Park et al., 2008; Wu et al., 2012; Chen et al., 2013; UNEP, 2014; Giang et al., 2015; Zhang et al., 2015). Figure 3.5 presents the variation between the proportion of Hg(0) and reactive mercury (HgP and gaseous Hg(II)) in the scenarios corresponding to the speciation scheme applied to the AMAP/GMA inventories (S1) and the scheme based on recent scientific literature (S3) for different sectors. The share of the THg emissions that comprise of Hg(II) species (gaseous and particulate) emissions was 25.3% for the reference scenario (S1) and 22.9% and 21.4% for the other two emissions scenarios (S2 and S3, respectively). However, regional Hg speciation footprints may differ considerably depending on the characteristics of Hg-emitting sources located in different regions (see details in Muntean et al., 2018). Much of the recent literature on emissions speciation at industrial facilities concerns plants in East Asia (China, Japan and the Republic of Korea), with speciation often dependent on the air pollution control technologies employed at the different plants. An evaluation of the three scenarios using the GEOS-Chem global 3-D Hg model showed a variation in deposition estimates of approximately ±10%. A comparison with measurements within a nested grid in sensitivity simulations for the United States indicated that speciated emissions estimated based on field measurements can improve wet deposition estimates near sources.

Changes in speciation from GEM/Hg(0) to HgP or Hg(II) would imply that Hg may be captured or deposited closer to its source regions and therefore have less potential for transport to the Arctic.

Appropriate speciation of (geospatially distributed) Hg emissions datasets is important to modeling atmospheric transport from source to receptor regions including the Arctic (see Sections 3.3.3 and 3.7). Newly available information on the speciation of emissions at major point sources presents the possibility for better addressing this aspect in future work; however, a significant gap in knowledge still concerns the fate of Hg emitted from ASGM activities. Mercury used to amalgamate or concentrate gold is evaporated to recover the gold and is therefore by definition emitted as GEM/Hg(0). ASGM emissions occur close to the ground and thus the emitted Hg may be subject to chemical transformations through interaction with surfaces that alter speciation more rapidly than might be the case for GEM emitted, for example, from power plant stacks.

3.2.2.5 Anthropogenic emissions and releases in an Arctic context

This report includes an updated Hg budget for the Arctic Ocean (see Section 3.8), and the Arctic region is also evaluated in atmospheric transport source-receptor modeling work (see Section 3.7).

Sources within the Arctic region contribute only a small part of global anthropogenic Hg emissions, ~14 t (<1%) of the total estimated inventory of 2220 t in 2015. The respective contributions from different countries in Arctic areas (areas north of 60°N) are shown in Table 3.6.

Table 3.6. Mercury emissions in the Arctic region (north of 60°N) sources; values calculated from the spatially distributed inventory of anthropogenic emissions to air in 2015 (see Section 3.2.2.2).

Country	Estimated anthropogenic Hg emissions in the Arctic (north of 60°N in 2015; kg)
Canada	355
Kingdom of Denmark (Faroe Islands)	1.34
Kingdom of Denmark (Greenland)	2.66
Finland	1011
Iceland	30.5
Norway (mainland)	261
Norway (Svalbard, Jan Mayen)	6.1
Russia	12 400
Sweden	307
United Kingdom (Shetland Islands)	0.62
United States (Alaska)	132
Total	14 470

The majority of the anthropogenic Hg emissions in the Arctic region occur in Russia and are associated with relatively few point sources, including the non-ferrous metal smelters at Norilsk and on the Kola Peninsula (see Figure 3.6). The Arctic also hosts coal-fired power plants along with other industrial facilities (including cement and ferrous metals production, mining and oil refining operations) in or in close proximity to the Arctic. In North America, small point source emissions are associated with diesel generators and waste dumps in a number of communities; similar emission occurs in other parts of the Arctic, but locations of these sources are not defined in the available datasets.

Although the anthropogenic Hg emissions within the Arctic region are small, it should be recognized that the Arctic Council countries contribute significantly to global Hg emissions, and together with Arctic Council observer countries, were responsible for ~44% of estimated global anthropogenic Hg emissions in 2015 (see Table 3.7).

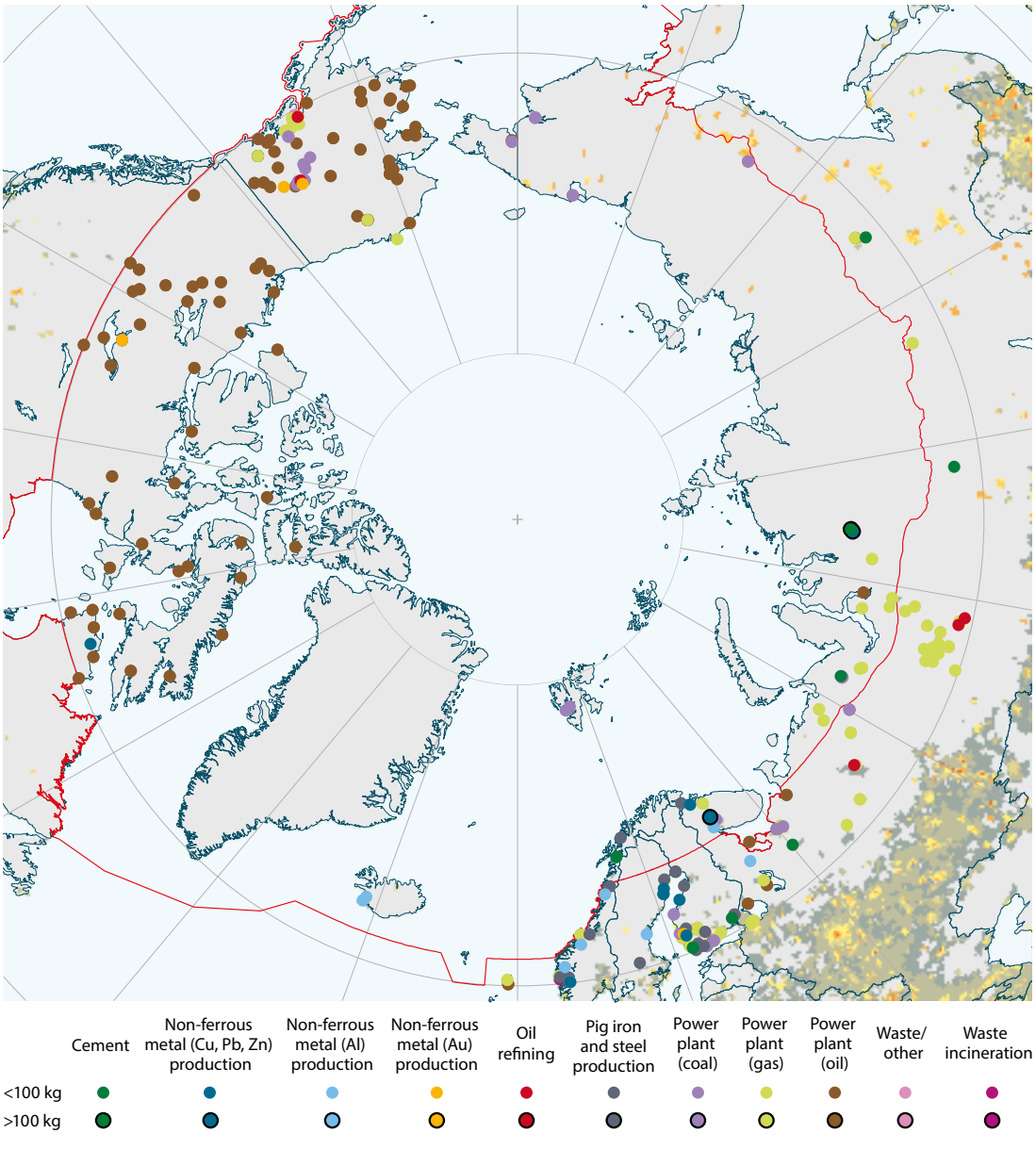

Figure 3.6. Locations of point source Hg emissions in or close to the Arctic.

Table 3.7. Contributions of Arctic Council members, observers and the rest of the EU to global Hg emissions in 2015, in tonnes (t), and percentage changes in estimated emissions between 2010 and 2015.

Country	Total estimated Hg emissions in 2015, in t (AMAP/UN Environment, 2019)*	% Global total	Percentage change in estimated Hg emissions between 2010 and 2015
Canada	4.02	--	-14.3
Denmark	0.43	--	-35.9
Faroe Islands	0.00	--	42.7
Greenland	0.00	--	-43.5
Finland	1.21	--	-13.7
Iceland	0.03	--	-11.9
Norway	0.55	--	15.2
Russia	60.95	--	13.1
Sweden	0.86	--	-13.6
United States	36.33	--	-22.5
Arctic Council Members	116.1	5.2	-3.3
China	563.78	--	12.6
China, Hong Kong	1.46	--	12.5
France	3.79	--	-25.7
Germany	16.28	--	-1.4
India	205.86	--	28.1
Italy	4.09	--	-26.4
Japan	15.01	--	16.1
Republic of Korea	6.95	--	0.8
Netherlands	1.55	--	8.9
Poland	11.38	--	-8.4
Singapore	1.62	--	3.0
Spain	3.99	--	-29.0
Switzerland	0.58	--	20.0
United Kingdom	4.27	--	-18.4
Arctic Council Observers	840.6	37.8	14.2
Other EU countries	17.6	0.8	-20.8
Arctic Council members, observers and rest of EU	974.4	43.8	10.9

*Differences between GMA estimates (AMAP/UN Environment, 2019) and national estimates reported under CLRTAP, along with possible reasons for these differences, are discussed in Section 3.3.3 of the AMAP/UN Environment 2019 report.

3.2.3 Primary geogenic and secondary emissions as a result of natural processes in the Arctic

Anthropogenic and legacy Hg emissions in global regions are important sources of Hg input into the Arctic, transported there via the atmosphere or ocean currents. In addition, due to the sparse population and limited human activities in the Arctic, natural emissions within the Arctic, including geogenic (primary), legacy (previously deposited) emissions, and wildfire emissions, also play an important role in the region. A large fraction of Hg from atmospheric long-range transport is deposited to ecosystems in the Arctic and thus is subject to natural processes that can lead to storage and rerelease of both geogenic and anthropogenic legacy pollution within the region. Observation-based estimates of geogenic and legacy Hg emissions in the Arctic are currently not available. Atmospheric Hg models parameterize primary and secondary emissions from terrestrial surfaces as a function of environmental conditions and soil Hg content (Selin et al., 2008; Durnford et al., 2012). Geogenic Hg emission is distributed according to the locations of Hg deposits, and the revolatilization of legacy Hg from soils and vegetation is distributed based on patterns of historic Hg deposition fluxes. Modeling estimates of combined geogenic and legacy Hg emissions from soils and vegetation are in the range of 6.5 to 59.1 Mg/y (median of 24 Mg/y) north of 60°N in the Arctic (based on the four Hg models used in this report; see Box 3.1). Another important source of Hg in the Arctic is the release of Hg from biomass burning as a result of wildfires, which is described in the next section (Section 3.2.3.1). Increased melting of permafrost, glaciers and ice sheets in the Arctic over the last 30 to 40 years is suggested to be releasing Hg into the Arctic environment (Milner et al., 2017; Schuster et al., 2018). Estimates of Hg emission into the air from these sources are currently lacking (Schaefer et al., 2020). However, releases of Hg from recent melting of permafrost, glaciers and ice sheets to downstream environments in the Arctic have been reported (Søndergaard et al., 2015; Vermilyea et al., 2017; St. Pierre et al., 2018, 2019; Zdanowicz et al., 2018). The current understanding of the releases of Hg from the melting of long-term cryospheric reservoirs to downstream Arctic environments is discussed in Sections 3.4.2 and 3.4.3.

3.2.3.1 Biomass burning

The term 'biomass burning' can refer to a range of different processes both anthropogenic and natural. Anthropogenic biomass burning typically means the intentional combustion of plant material in agriculture as a means of waste incineration. More broadly, it can also include energy production from biomass combustion. In this chapter, by the term 'biomass burning' we are referring solely to natural emissions, which are usually distinguished from anthropogenic emissions by using the term 'wildfires'. Wildfires include forest fires, which make up the majority of global Hg emissions from this sector. However, they include a range of other sources such as grassland fires and smoldering natural fires (e.g., peat, bog, or subsurface coal-bed fires). Especially in the Arctic region, in recent years, smoldering fires have been observed ever more frequently (Mack et al., 2011). Due to satellite observations, today it is possible to detect even small fires with remote sensing techniques capable of detecting temperature anomalies (Giglio et al., 2006). Mercury released from wildfires is not a primary emission source as it is typically introduced into biota and soils by atmospheric deposition. The two sources for Hg released by fires are from the Hg stored in biomass and soils. There are three primary pathways of Hg uptake by plants: stomatal uptake of GEM from the atmosphere, foliar adsorption of oxidized mercury, and roots uptake of ionic Hg from soils (Obrist et al., 2017; Jiskra et al., 2018). As the boreal forests consist of evergreen trees, there is no significant release of Hg through litterfall. Arctic soils have been found to be a long-term storage for a large amount of Hg (Schuster et al., 2018), and Hg releases from soils can be significant under large-scale fire events.

The average global mercury emissions by wildfires has been estimated in the range of 400 to 675 Mg/y (Friedli et al., 2009; De Simone et al., 2017; Kumar et al., 2018). Kumar et al. (2018) estimated that around 95% of Hg wildfire emissions in the Arctic are from boreal forests and 5% are from other vegetation types. The wildfires in the Arctic typically show a pronounced seasonal cycle with more than 90% of Hg emissions occurring during July and August in some years, although the fire season, and resultant Hg emissions, can start as early as June (van der Werf et al., 2017). Emissions estimates from all boreal forest fires are even more variable, ranging from ~20 Mg/y (Friedli et al., 2003a; McLagan et al., 2021) up to 200 Mg/y (Kumar et al., 2018).

Uncertainties of these estimates are high and are predominantly associated with variability in the annual burned area (particularly for boreal forests), non-biome specific emissions ratios or factors, and the limited near-source atmospheric Hg measurements in wildfire plumes (Friedli et al., 2009; De Simone et al., 2017; McLagan et al., 2021). Moreover, these emissions estimates typically incorporate mean measured atmospheric Hg to carbon monoxide (CO) emissions ratios from the literature, many of which have been taken at receptor sites distant from fire sources (Friedli et al., 2009; De Simone et al., 2017; Kumar et al., 2018). Mercury to CO emissions ratios measured at large distances tend to be high, which McLagan et al. (2021) relate to the lower lifetime of CO compared with Hg (particularly over continental landmasses in the summer) and the variability in CO emissions from fires based on biome and fire intensity. Another factor in the uncertainty of these estimates is that speciated wildfire Hg emission inventories are not available. The proportion of Hg released as GEM in wildfires varies between 50% and 95% based on aircraft measurements (Friedli et al., 2003a), satellite measurements (Finley et al., 2009) and laboratory experiments (Obrist et al., 2008; Kohlenberg et al., 2018).

Following the empirical emission factor based method from McLagan et al. (2021), an improved estimate of atmospheric Hg emitted from Arctic fires (fires which occur north of 60°N) is 8.8±6.4 Mg/y for the period 2001 to 2019 based on two boreal forest aircraft studies (Friedli et al., 2003a; McLagan et al., 2021). This estimation uses the mean burned area based on three separate algorithms (Giglio et al., 2013, 2016; Lizundia-Loiola et al., 2020), the mean fuel load of Canadian Arctic biomes (Taiga Plains, Taiga Shield East and West, Taiga Cordillera, Hudson Plains, and Southern Arctic; 2.31±0.81 kg/m^2) from Amiro et al. (2001), and a generally accepted total release of Hg from biomass during burning (100±5%). Atmospheric Hg is assumed to consist of 96.2% Hg(0) and 3.8% HgP according to the measured ratio in Friedli et al. (2003b).

Peatlands are an important sink for organic matter and Hg in the circumboreal regions, and the burning of peat-rich soils likely leads to a significantly greater release of Hg than is currently estimated (Turetsky et al., 2006; Fraser et al., 2018). A better estimation of the proportion of GEM to HgP and the propensity of different biomes (such as boreal peatlands) to release Hg during wildfires are needed to reduce uncertainties in modeling estimates (De Simone et al., 2017; Fraser et al., 2018; Kumar et al., 2018). The observed warming of the atmosphere has been especially pronounced in the Arctic. It is critical that wildfire emissions estimates are improved and constrained, particularly for the boreal forests and the Arctic, within which fire frequency, intensity and length of burning season are expected to increase in the future under warming conditions (Mack et al., 2011; Veira et al., 2016; Walker et al., 2019). Forest fires outside the Arctic are also expected to increase, which will lead to additional long-range transport of Hg to the Arctic from this source.

3.3 How much mercury does atmospheric circulation transport to Arctic environments?

3.3.1 How does atmospheric mercury enter Arctic environments?

3.3.1.1 Atmospheric circulation

In-situ measurements and modeling provide evidence for year-round transport of pollution from southern latitudes to the Arctic troposphere; this pollution is dominated by northern Eurasian sources in winter and by mid-latitude Asian and North American sources in spring (Sharma et al., 2013; Law et al., 2014; Monks et al., 2015; Willis et al., 2019). Fuelberg et al. (2010) noted that, during spring, mid-latitude cyclones were more frequent (and followed a northerly course) over eastern Asia and the North Pacific and were less common over the

North Atlantic. Evidence for springtime long-range transport events of atmospheric Hg from Asian sources to western North America and the Arctic is well documented (Jaffe et al., 2005; Weiss-Penzias et al., 2007; Obrist et al., 2008; Durnford et al., 2010; Moran et al., 2014). Durnford et al. (2010) analyzed Hg transport pathways to the Arctic and confirmed that Eurasian transport dominated in winter, while Asian and North American transport dominated in spring. The study estimated that the majority of long-range transport events in the Arctic originated in Asia (~55%) followed by events from Eurasian (~29%) and North American (~16%) sources.

The thermal stratification of the lower atmosphere at high latitudes, especially during the winter months, causes an isolation of the High Arctic lower troposphere from lower latitudes creating a transport barrier referred to as the polar dome (coincident with the Arctic front; Klonecki, 2003). The polar dome exhibits a strong influence on the transport of air masses from mid-latitudes, enhancing transport during winter and inhibiting it during summer. The spatial extent of the polar dome strongly varies seasonally, from about 40°N polewards in the winter, when it envelopes snow-covered North America and, especially, Eurasia, to roughly north of the 70°N in the summer (Klonecki, 2003; Jiao and Flanner, 2016). Synoptic-scale weather systems frequently disturb this transport barrier and foster exchange between mid-latitude and Arctic air masses.

Atmospheric transport into the Arctic lower troposphere requires a diabatic cooling of air masses to facilitate penetration into the polar dome either from above, or sideways (Stohl, 2006). Using a modeling study, Stohl (2006) identified three major pollution transport mechanisms to the Arctic lower troposphere from major anthropogenic emission regions, recently confirmed by the POLARCAT-IPY and NETCARE measurement campaigns (Law et al., 2014; Bozem et al., 2019). These three transport mechanisms are: (1) wintertime low-level transport over snow-covered regions at timescales of 10 to 15 days, primarily from northern Eurasia; (2) fast low-level transport (taking four days or less) from mid-latitude regions located within the polar front (mainly in Europe) followed by uplift at the Arctic front and slow descent; and (3) convective lifting in southern mid-latitudes followed by upper tropospheric transport in warm conveyor belts associated with frontal systems and slow descent due to radiative cooling at timescales of roughly two weeks. Only the third pathway is frequently a means of pollution transport from North America and Asia. In contrast to the low-level transport, oxidation and wet scavenging can remove significant amount of Hg outside the Arctic in high-level transport. The lower troposphere in the Arctic is highly stably stratified during the winter months, with surface inversions persisting for several days; these conditions result in reduced dry deposition of pollutants during the transport process. Furthermore, the lower troposphere is extremely dry in winter, which prevents scavenging by precipitation. The lifetime of air masses near the surface in the High Arctic is about one week in winter and two weeks in summer; this rapidly decreases with altitude to about three days in the upper troposphere (Stohl, 2006). In addition to the pathways above, studies have reported transport of smoke plumes from boreal wildfires into the Arctic (Paris et al., 2009); Hg emitted during strong boreal wildfire events can be lofted by pyroconvection and entrained into the polar environment (Peterson et al., 2018a).

Lower tropospheric transport in and around the Arctic is marked by a pronounced continental flow in wintertime and a zonal transport to the marine environment in summer. In winter, synoptic-scale atmospheric transport into the Arctic is primarily driven by three major semi-permanent pressure systems: a low-pressure system located in the sub-polar North Pacific Ocean, just south of the Bering Sea area (the Aleutian Low); a low-pressure system southeast of Greenland, near Iceland (the Icelandic Low); and a high-pressure system situated over eastern Siberia (the Siberian High; Bottenheim et al., 2004). Less intense high-pressure systems are located over western North America and the mid North Atlantic Ocean (the Subtropical High). Atmospheric circulation around the Icelandic Low in combination with the Siberian High transports pollution from source regions in northern Europe and Siberia into the Arctic. Also, North American pollutants flow along the southern portion of the Icelandic Low to northern Europe. The Aleutian Low induces the eastward transport of air from East Asia to North America along its southern portion over mid- to subtropical latitudes, and then along western Canada and Alaska into the western Arctic. The same circulation also transports chemical species from western North America into the Arctic. The weakening of the low-pressure centers and the replacement of continental highs by low-pressure systems in summertime caused by the changing land-sea contrast in surface heating leads to seasonal changes in transport patterns.

Mid-latitude atmospheric blocking events, which can last up to 15 days, are quasi-stationary features characterized by high-pressure centers around 60°N and a low-pressure center to the south of the feature; these blocking events are known to significantly increase the transport of air pollution to the Arctic (Davini et al., 2012). More frequent in winter and spring, blocking events are predominantly observed in the northeastern Atlantic Ocean and to a lesser extent in northeastern Pacific Ocean. Two major low-frequency atmospheric circulation patterns influence atmospheric transport to the Arctic on monthly to decadal timescales: the North Atlantic Oscillation (NAO) and the Pacific-North America pattern (PNA; Feldstein, 2002; Eckhardt et al., 2003). During the positive phase of the NAO, associated with strengthening of Icelandic Low, transport mainly from Europe but also from North America and Asia into the Arctic is enhanced, resulting in higher pollution levels, particularly in winter and spring (Eckhardt et al., 2003). Conversely, during the negative phase of the NAO (or the positive phase of the PNA), the weaker Icelandic Low leads to reduced air transport from Europe and Siberia and increased transport from North America to the Arctic.

The above atmospheric pathways can directly transport Hg-rich air masses from global anthropogenic Hg source regions to the Arctic. Since the atmospheric lifetime of Hg(0), the most dominant Hg species in air, is over several months, global-scale transport and mixing of Hg(0) results in a well-mixed tropospheric background of Hg. Atmospheric transport of background Hg accounts for the majority of Hg found in the Arctic environment. In addition, Hg transport to the Arctic is amplified via a global distillation phenomenon: emitted Hg is successively deposited to surfaces from where it is re-emitted back into the air and continues to move through the environment in the direction of the prevailing winds favoring accumulation in the colder regions, such as the Arctic.

In recent decades, nearly twice the rate of rise in surface and lower tropospheric temperatures in the Arctic compared to rises in temperature at lower latitudes (Arctic amplification) is causing changes in the mid-latitude circulation patterns (Dobricic et al., 2016; Pithan et al., 2018). Warmer sea-surface temperatures and lower sea-ice concentrations in the Arctic are linked to atmospheric circulation anomalies in winter (Lee et al., 2015; Francis et al., 2017). These atmospheric circulation changes are shown to impact pollution transport in the Arctic (Pozzoli et al., 2017; see Chapter 5).

3.3.1.2 Atmospheric chemistry and phase transformations

The oxidation of GEM to Hg(II) strongly influences the residence time of Hg in the atmosphere. This influence arises from the high deposition velocities of oxidized Hg, relative to GEM, for both gaseous oxidized mercury (GOM) and particulate-bound mercury (PBM). Faster oxidation of GEM leads to a shorter residence time for Hg in the atmosphere. Conversely, the reduction of Hg(II) to GEM extends the lifetime of Hg in air. Both oxidation and reduction can occur homogeneously and heterogeneously, but the uncertainties in these processes are still significant. Laboratory experiments and investigations using theoretical chemistry have suggested rate constants for many homogeneous processes. Theoretical work carried out in the last several years has reported rate constants for many gas-phase reactions in the Br- and OH-initiated oxidation of GEM, but rate constants derived from theory have larger uncertainties than that can be obtained from laboratory experiments under favorable conditions (Subir et al., 2012).

Gas-phase oxidation of Hg occurs in two steps (Goodsite et al., 2004; Dibble et al., 2012, 2020)

$$X + Hg + M \leftrightarrows XHg\bullet + M \ (X = OH, Cl, Br) \quad (1, -1)$$

$$XHg\bullet + \bullet Y + M \rightarrow XHgY + M \quad (2)$$

Where M is any gas-phase molecule and •Y = NO_2, HOO, ROO•, and halogen oxides (but not NO). Decomposition of XHg• (reaction -1) competes with reaction (2) to a modest extent for X=Br, but severely limits the effectiveness of oxidation by OH. Table 3.8 lists recommended rate constants for use in modeling GEM oxidation initiated by Br, Cl, and OH. Recently, Saiz-Lopez et al. (2019) suggested that photolysis of BrHg• would be non-negligibly fast in the atmosphere. Almost all our chemical and kinetic knowledge relies on computational chemistry, and experimental data are needed to reduce uncertainties. Table 3.8 includes estimates of uncertainties in rate constants.

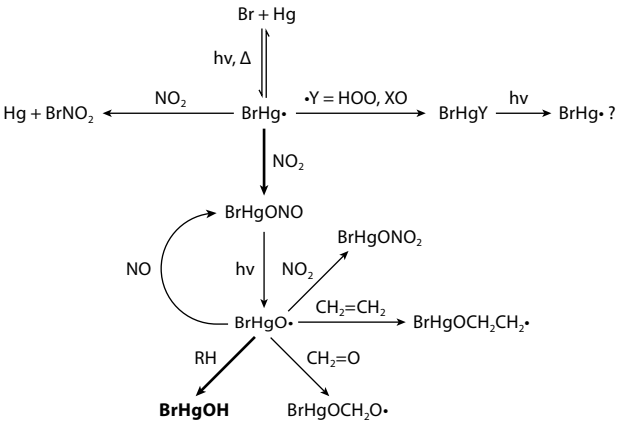

Scheme 3.1. The chemistry of BrHgO•. Source: Lam et al., 2019a, 2019b.

Computations further indicate that most BrHgY compounds and BrHgOH will readily undergo photoreduction to BrHg•+•Y or even GEM (Saiz-Lopez et al., 2018; Francés-Monerris et al., 2020). By contrast, BrHgONO photolysis generates mostly BrHgO•+NO (Lam et al., 2019a; Francés-Monerris et al., 2020). Lam et al. (2019a, 2019b) mapped out the chemistry of BrHgO•, finding that it largely abstracted hydrogen atoms to make BrHgOH, as shown in Scheme 3.1.

While the mechanism of Br-initiated oxidation of GEM is more advanced than for initiation by other radicals, there exists huge uncertainty in the concentration field of Br. Recent advances in instrumentation may change this situation (Wang et al., 2019a).

Most models of the oxidation of Hg use OH and ozone as the primary oxidants. The reaction of OH with Hg(0) proceeds via:

$$OH + Hg\ (+M) \leftrightarrows HOHg\bullet\ (+M) \quad (1c, -1c)$$

The reversibility of this reaction was highlighted by Calvert and Lindberg (2005) and conclusively demonstrated by Dibble et al. (2020). It has also been suggested that HOHg• would react with O_2 to make Hg(II):

$$HOHg\bullet + O_2 \leftrightarrows HgO + HOO \quad (3)$$

Table 3.8. Recommended rate constants (k) and uncertainties (f) for GEM oxidation initiated by X = Br, Cl, and OH derived from Horowitz et al., 2017 and Dibble et al., 2020. An estimate of 1 SD can be obtained by considering the range of rate constant from k/f to $k \times f$.

Reaction	Rate Constant[a, b]	f[c]
Br + Hg + M→BrHg• + M	$k_{1a}(T)=1.4\times10^{-32}\ (T/298)^{-1.9}$	1.5
BrHg• + M→Br + Hg + M	$k_{-1a}(T)=1.6\times10^{-9}\ (T/298)^{-1.9}\ e^{-7800/T}$	2
Cl + Hg + M→ClHg• + M	$k_{1b}(T)=2.2\times10^{-32}\ e^{(680(1/T-1/298))}$	1.5
OH + Hg + M→HOHg• + M	$k_{1c}(T)=3.34\times10^{-33}\ e^{+43/T}$	1.2
HOHg• + M→OH + Hg + M	$k_{-1c}(T)=1.22\times10^{-9}\ e^{-5720/T}$	1.15[d]
XHg• + NO_2 + M → *syn*-XHgONO	$k_0(T)=7.1\times10^{-29}\ (T/300)^{-4.5}$ $k_\infty(T)=1.2\times10^{-10}\ (T/300)^{-1.9}$	3
XHg• + •Y→XHgY •Y = (HOO, ROO, ClO, BrO, IO)	$k_0(T)=2.3\times10^{-29}\ (T/300)^{-4.4}$ $k_\infty(T)=6.9\times10^{-11}\ (T/300)^{-2.4}$	3

(a) Values of k_1 and k_0 possess units of cm^6/molecule/s; values of k_{-1} and k_∞ are in cm^3/molecule/s; (b) $k_0(T)$ and $k_\infty(T)$ are used to get $k([M],T)$; (c) estimated values at 298 K; (d) uncertainty estimate at 1 atm at 298 K.

However, reaction (3) is endothermic due to the instability of gaseous HgO (Shepler and Peterson, 2003; Peterson et al., 2007; Cremer et al., 2008). This makes reaction (3) irrelevant in the atmosphere. Dibble et al. (2020) concluded that OH only contributes significantly to initiating GEM oxidation in very polluted areas of the continental boundary layer; however, it should be pointed out that the reaction of HOHg• with O_3 has yet to be considered. This is especially intriguing since models broadly suggest that, in the continental boundary layer, initiation of oxidation by OH and/or by O_3 better match observations than does oxidation by Br (Travnikov et al., 2017). A more recent study by Gabay et al. (2020) indicated the important role of smog oxidants in the polluted continental boundary layer whereas Br was highlighted as a predominant oxidant in the marine boundary layer.

The reaction of Hg(0) with ozone has been studied several times (Pal and Ariya, 2004; Spicer et al., 2005; Rutter et al., 2012). The rate constant is very low, and the propensity of Hg(0) to be oxidized at surfaces is very high (Hynes et al., 2009) making it difficult to interpret the experiments. The reaction had initially been proposed to proceed via:

$$Hg + O_3 \rightarrow HgO + O_2 \quad (4)$$

However, gaseous HgO is highly unstable and would immediately fall apart to regenerate GEM, which is inconsistent with the observed loss of GEM in experiments.

Sommar et al. (1997) reported the reaction $Hg+NO_3$ to possess a rate constant of 4×10^{-15} cm^3/molecule/second but with enormous uncertainty. One computational study suggested that the Hg-NO_3 bond energy in •$HgNO_3$ was only 5 kcal/molecule, which would render •$HgNO_3$ so unstable that it would fall apart before it could react with another radical to make GOM in the experiment, let alone in the atmosphere (Dibble et al., 2012).

GEM oxidation has been proposed to be initiated by Cl_2, Br_2, HOOH, BrO, and ClO (Subir et al., 2012). Rate constants for these reactions have been measured in environmental chambers. These reactions are proposed to occur by the insertion of the Hg atom into the middle of the oxidant to produce, for example, $HgBr_2$ or $Hg(OH)_2$. GEM is rather unreactive so it seems unlikely that these reactions would proceed without very high activation energies. In fact, high-level calculations (Balabanov and Peterson, 2003) find rate constants below 10^{-30} cm^3/molecule/second for Hg + Br_2 and Hg + BrO.

Lin and Pehkonen (1999) provided solid thermodynamic reasons why the uptake of GOM onto aqueous aerosols will typically convert Hg(II) compounds to $HgCl_2$. At high Cl^-, such as in sea salt aerosols, this may result in partitioning a significant fraction of GOM to the aqueous phase as $HgCl_4^{2-}$ (Hedgecock and Pirrone, 2001). At lower [Cl^-], this will result in emission of $HgCl_2$ to the gas phase. The partitioning of GOM to solid surfaces has been the subject of limited experimentation (Rutter and Schauer, 2007a, 2007b; Malcolm et al., 2009); these experiments have been used to guide some models (Holmes et al., 2010; Amos et al., 2012; Toyota et al., 2014b). Gas-particle partitioning in the fine mode (<2.5 μm) was treated with a gas-aqueous phase equilibrium assumption in a regional chemical transport model, the Community Multiscale Air Quality modeling system (CMAQ; Bullock and Brehme, 2002; Foley et al., 2010).

Numerous investigators reported on the oxidation and reduction of aqueous mercury compounds in the dark and under illumination (Fitzgerald et al., 2007). Major oxidants include OH, O_3 and HOCl. Reduction of Hg(II) by HOO and O_2^- has been proposed but appears to be sufficiently endothermic that it can be ignored (Gårdfeldt and Jonsson, 2003). Photoreduction of Hg species in the aqueous phase may be occurring by interaction of Hg compounds with organic matter and/or metals. Recently, Saiz-Lopez et al. (2018) reported photoreduction rate constants from rainwater samples for use in modeling dissolved organic matter effects on Hg(II) photoreduction. Curiously, they noted that in almost half their experiments, Hg(II) concentrations initially increased or stayed constant before decreasing. Above studies suggest that our understanding of Hg photoreduction is far from complete.

Regional and global chemical transport models (CTMs) are applied to simulate spatiotemporal distributions of atmospheric Hg concentrations with the ultimate goal of accurately quantifying atmospheric Hg deposition, which is essential to developing Hg emission reduction policies and assessing the efficacy of the Minamata Convention. To accurately simulate Hg deposition, it is of foremost importance for models to reproduce the observed atmospheric concentrations of GEM, GOM and PBM. Currently, annual mean GEM concentrations can be simulated reasonably well with models, but modeled oxidized mercury (GOM and PBM) concentrations show large overprediction compared with observations (Seigneur et al., 2004; Ryaboshapko et al., 2007; Selin et al., 2007; Baker and Bash, 2012; Bieser et al., 2014; Ye et al., 2018). This overprediction stems from at least three sources: (1) under biased GOM concentrations in measurements (Gustin et al., 2015); (2) overestimated gas-phase GEM oxidation kinetics in models (Zhang et al., 2012a; Bieser et al., 2014); and (3) neglect of gas-phase reduction (e.g., Kos et al., 2013; Saiz-Lopez et al., 2018). Despite great uncertainties in simulated GOM and PBM, modeled Hg wet deposition has shown good agreement with measurements (e.g., 21% fractional bias; Holloway et al., 2012). Since GOM and PBM dominate Hg wet deposition, this reasonable agreement suggests underestimation of Hg(II) in observations (Kos et al., 2013; Bieser et al., 2014).

As reviewed above, major progress has been made in understanding complex GEM oxidation mechanisms using computational approaches in recent years. Incorporating the new findings in a few models has led to significant improvement in the simulation of Hg wet deposition. By including the second stage oxidation of HgBr by HO_2, NO_2 and BrO as well as new kinetics for HgBr dissociation in the global CTM GEOS-Chem, Horowitz et al. (2017) reduced the overestimation of Hg wet deposition to 0–30% globally compared to previous studies. Ye et al. (2018) implemented detailed Hg and Br chemical mechanisms, including new kinetic data from Dibble et al. (2012), in CMAQ-Hg and captured observed spatiotemporal variations in GOM concentrations and Hg wet deposition with a few percentages of fractional bias and normalized mean bias over the northeastern United States.

The springtime photochemical release of gaseous Br to air from snow on sea ice and coastal land surfaces in the polar

region and the rapid oxidation of ambient Hg(0) to Hg(II) via Br chemistry and subsequent deposition of Hg(II) to the surfaces lead to atmospheric mercury depletion events (AMDEs; Steffen et al., 2008). During these events, the gaseous Br concentrations increase to excessive levels not observed in other seasons of the polar atmosphere or in other domains of the global atmosphere (Abbatt et al., 2012; Simpson et al., 2015). Oxidized Hg can either remain in the gas phase (GOM), adsorb to the surface of aerosol particles or be absorbed to aerosol bulk volumes (PBM; Lyman et al., 2020). Both forms of Hg (GOM and PBM) can either dry deposit directly to surfaces or be taken up by episodic precipitation and wet deposit in snowfall (Skov et al., 2006; Steffen et al., 2014). Atmospheric Hg chemistry is a key factor when it comes to accurately simulating Hg deposition during Arctic AMDEs. The deposition of Hg to surface snow is anomalously elevated during AMDEs, resulting in Hg concentrations in snow of up to 1500 ng/L (Wang et al., 2017a). About 75% of the deposited Hg(II) is reduced to Hg(0) and evaded back to the atmosphere (Durnford et al., 2012). Hg(II) is primarily reduced to Hg(0) within snow due to photolytic induced reactions (in the presence of reductants such as H_2O_2, HO_3*, oxalic acid, humic acids and sulphite based compounds). However, dark and biological reduction mechanisms in snow have been reported (Douglas et al., 2012). Oxidants such as H_2O_2, bromine radicals, Br_2, ozone and OH can also oxidize Hg(0) in snow.

In conclusion, understanding of the mechanisms of gas-phase mercury redox chemistry has been worked out to a large degree, but major gaps remain. These mechanisms are mostly known from computational studies, so the associated rate constants are highly uncertain. There is a clear need for laboratory experiments to determine reaction kinetics. This may be particularly difficult for OH-initiated oxidation, as the gaseous HOHg• radical has never been detected in the laboratory. Moreover, the lack of measurement data on atmospheric concentrations of atomic Br creates large uncertainties in model predictions of the extent of Br-initiated oxidation. Because the oxidation of GEM is so slow compared to the transport of Hg (except during AMDEs), it is difficult for regional and global measurements of GEM/GOM/PBM to diagnose specific problems in chemical mechanisms. This problem is exacerbated by the uncertainties in measurements of PBM and GOM. AMDEs provide the most fruitful cases to test ambient and snow Hg chemistry because the rapid concentration changes during these events are largely controlled by chemical processes rather than transport; therefore, model-measurement intercomparison studies specifically targeted to simulating AMDEs are recommended. Another factor is that springtime Br concentrations in the Arctic are much higher than in the rest of the atmosphere, making it feasible to carry out point measurements of the concentrations of Br and other radicals that drive the chemistry (Wang et al., 2019a). Last but not least, the ability to determine the molecular composition of GOM in the field would enable more specific diagnoses of the limitations of our current mechanisms and rate constants.

3.3.1.3 Mercury exchange between air and Arctic surfaces

High-latitude locations, particularly in the northern Arctic, experience two markedly different seasons, each with their own unique Hg deposition mechanisms. As in lower latitudes, Hg species can be deposited directly to vegetation surfaces (Demers et al., 2013; Jiskra et al., 2017; Obrist et al., 2017; Douglas and Blum, 2019), organic matter (Bartels-Rausch et al., 2011) and water during the summer and to snow/ice surfaces in winter by precipitation and dry deposition (Skov et al., 2006). In earth's high latitudes, where winter lasts for up to nine months, wintertime deposition of Hg to snow and ice surfaces can be significant. In the springtime, GOM produced during AMDEs is persistently scavenged from the air by snow and ice crystals as well as dry deposited to snowpacks leading to anomalously elevated Hg deposition to snow and ice surfaces along the coast and over Arctic Ocean (Brooks et al., 2006; Douglas et al., 2008; Douglas et al., 2012; Douglas and Blum, 2019). Once deposited to the snowpack, an average of 75% of Hg in the High Arctic snowpack is re-emitted to the atmosphere by photoreduction prior to snowmelt (Ferrari et al., 2005; St. Louis et al., 2005; Johnson et al., 2008; Durnford et al., 2012). However, in coastal and oceanic regions, a high percentage of snowpack Hg is believed to be retained and available as a component in snowmelt (Douglas et al., 2012; Durnford et al., 2012; Dastoor and Durnford, 2014; Douglas and Blum, 2019). The rates of dry and wet deposition control the overall lifetime of Hg in the atmosphere.

a. Uptake by precipitation

Clouds provide a medium for aqueous or heterogeneous reactions via gas-particle partitioning, adsorption, photoredox and methylation (Seigneur et al., 1998; Gårdfeldt et al., 2003; Siciliano et al., 2005; Bergquist and Blum, 2007; Hammerschmidt et al., 2007; Andersson et al., 2008; Gu et al., 2011; Subir et al., 2012; Amirbahman et al., 2013; Ariya et al., 2015; Wang et al., 2015; Li et al., 2018), and precipitation clouds as well as precipitation in general removes reactive mercury (GOM and PBM) from the atmosphere; when reactive Hg is removed from the atmosphere by precipitation it is referred to as wet deposition. Wet deposition has been suggested to contribute between 50% and 90% of THg deposition to surface waters, especially in precipitation-abundant regions (Sorensen et al., 1990; Lamborg et al., 1995; Mason and Sullivan, 1997; Scherbatskoy et al., 1998; Landis and Keeler, 2002). In the Arctic, a smaller Hg wet deposition flux has been observed and estimated than in lower latitudes due to a lower amount of rain and shorter seasons favoring GEM oxidation (Sanei et al., 2010; Obrist et al., 2017).

A measurement-based Hg wet deposition flux is determined from Hg concentrations in precipitation and rates of precipitation. GOM and PBM comprise the majority of Hg wet deposition due to their high solubility (Schroeder and Munthe, 1998; Guentzel et al., 2001; Sakata and Asakura, 2007). In addition to anthropogenic emissions, reactive Hg is produced from the photochemical oxidation of GEM, and hence emissions and meteorological factors affect Hg wet deposition and Hg concentrations in precipitation. Over the past decades, anthropogenic emissions of Hg have been decreasing over North America and Europe while increasing in East Asia (UNEP, 2013). However, studies have

not shown a strong consistent relationship between changes in anthropogenic Hg emissions and wet Hg deposition (Risch and Fowler, 2008; Prestbo and Gay, 2009; Weiss-Penzias et al., 2016), indicating complex mechanisms driving large variabilities in Hg wet deposition over different regions and time periods.

Wet deposition fluxes of Hg in three-dimensional chemical transport models are estimated using the precipitation rate and in some models the cloud water (ice) concentration (Byun and Ching, 1999) while in others in- and below-cloud scavenging ratios were used (Berge and Jakobsen, 1998; Jacob et al., 2000;). The transfer of gas-phase compounds to the surface of an ice particle is not well represented or not represented at all. For example, it was not accounted for in CMAQ, and in GEOS-Chem the ratio of sticking coefficients of trace gases on the ice surface was assumed (Jacob et al., 2000). All approaches ultimately depend, in large part, on simulated precipitation rates and vertical distributions of atmospheric reactive Hg concentrations, and yet the latter is limited by significant uncertainty in our current understanding of the atmospheric chemistry of Hg as reviewed in Section 3.3.1.3b.

Arctic warming can potentially influence Hg wet deposition, at least to some extent, by increasing reactive Hg through increasing GEM emissions from permafrost thaw (Rowland et al., 2010) and altering kinetics of Hg oxidation reactions (Goodsite et al., 2004; Dibble et al., 2012). Therefore, accurate estimates of Hg wet deposition in the Arctic are becoming increasingly critical to Arctic Hg budgets and developing Hg pollution mitigation strategies to protect human and ecosystem health.

b. Surface uptake

Any gaseous or particulate pollutants in the atmosphere can be transported to Earth's surfaces where they are adsorbed and removed from the atmosphere. This process is referred to as dry deposition and is quantified as flux ($\mu g/m^2/y$) representing pollutant mass removed from the atmosphere by per unit surface area in unit time. On the other hand, the Earth's surfaces can also be a source of certain chemical species when it releases them into the atmosphere, a process that is referred to as emission. For such chemical species, dry deposition and emission happen simultaneously and constantly, resulting in bi-directional air-surface flux exchange. One process can dominate over the other, resulting in net dry deposition or emission flux, depending on the chemical species' physical and chemical properties as well as meteorological and biological conditions. In the case of speciated atmospheric Hg, the dry deposition process dominates for GOM (Skov et al., 2006) followed by PBM (Brooks et al., 2006) over nearly any natural surface (Wright and Zhang, 2015); additionally, bi-directional flux exchange has been frequently observed for GEM (Zhang et al., 2009, Wright and Zhang, 2015, Kamp et al., 2018).

Most existing measurement methods for quantifying dry deposition and air-surface exchange fluxes of speciated atmospheric Hg can be grouped into three major categories, including micrometeorological approaches, dynamic gas flux chambers and surrogate surface approaches (Wright et al., 2016; Zhu et al., 2016). Flux measurements using any of these approaches are subject to large uncertainties. For example, micrometeorological methods combine measured concentrations at different heights, but measuring small differences of Hg at very low concentrations is very challenging due to the technological limitations of the available instruments (Jaffe et al., 2014). Alternatively, fluxes can be measured by eddy covariance (EC) but this method needs a fast detector (i.e., >5 Hz) not currently available for atmospheric Hg species. As a compromise, relaxed eddy accumulation (REA) can be used (Businger and Oncley, 1990; Brooks et al., 2006; Skov et al., 2006; Kamp et al., 2018). In the REA technique, in contrast to the EC technique, slower-responding sensors can be used. The separation of updrafts (C_{up}) and downdrafts (C_{down}) is obtained by the sonic anemometer and fast shifting valves, which separates the airstream according to the direction of fluctuations in the vertical wind velocity. The introduction of a dead band ensures that C_{up} and C_{down} are very different, minimizing the uncertainty of the entity (C_{up} - C_{down}) which is proportional with flux. The measured flux is a function of the average flux over the footprint area.

Dynamic gas flux chambers can be deployed over soil, water, low canopy, or tree branches; however, the measured fluxes may not be representative of an entire area due to heterogeneity in land-use cover. In addition, different designs inside the dynamic gas flux chambers can cause the measured fluxes to differ by up to one order of magnitude (Eckley et al., 2010). Surrogate surfaces may not perform the same way as natural surfaces in collecting Hg, and uncertainties in the measured GOM and PBM dry deposition are larger than a factor of two depending on the selected surrogate surfaces and instrument setup (as detailed in Wright et al., 2016). A new surrogate surface sampler was recently developed utilizing a three-dimensional deposition surface, which is expected to mimic the physical structure of many natural surfaces more closely than the traditional flat surrogate surface designs (Hall et al., 2017). Collocated measurements using different techniques should be performed to constrain the measurements' uncertainties (Zhu et al., 2015; Osterwalder et al., 2018). Standardized protocols should be developed for commonly used measurement techniques.

Measurements of Hg in litterfall and throughfall can also provide some knowledge of Hg deposition over forest canopies. Mercury in litterfall is considered to be mostly from atmospheric dry deposition of GEM and can be used as a rough and conservative estimation of atmospheric Hg dry deposition (the portion that is retained in leaves). Mercury in throughfall also includes a portion of previously dry-deposited Hg (the portion that is washed off from the canopy). Concurrent measurements of litterfall, throughfall and open space wet deposition can be used to estimate dry deposition on seasonal or longer timescales, whereby dry deposition is approximated as litterfall plus throughfall minus open space wet deposition (Wright et al., 2016). Yet woody tissue deposition (including tree blowdown) can also be important and can add considerably to dry depositon (Obrist et al., 2018).

Modeling methods for estimating Hg dry deposition either use the inferential approach, which calculates flux as a product of surface air concentration and the modeled dry deposition velocity of speciated mercury, or use the bidirectional air-surface exchange model, which simulates emission from and deposition to land surfaces simultaneously (see a detailed review in Wright et al., 2016). Briefly, early modeling studies mostly only considered dry deposition of GOM and PBM using the inferential approach, while later studies have also

Box 3.1 Models for simulating Hg levels in Arctic environments

Four global atmospheric Hg models have been applied to study Hg cycling in polar regions: GLEMOS (Travnikov and Ilyin, 2009), GEOS-Chem (Holmes et al., 2010; Fisher et al., 2012), GEM-MACH-Hg (Dastoor et al., 2008; Durnford et al., 2012; Kos et al., 2013; Dastoor and Durnford, 2014; Fraser et al., 2018) and DEHM (Christensen et al., 2004; Skov et al., 2020). These atmospheric models simulate gaseous elemental mercury (Hg(0); GEM) and gaseous and particle bound oxidized mercury (Hg(II), GOM and PBM) concentrations and deposition resulting from redox chemistry based on oxidant concentrations and reaction rates, and physics and transport based on meteorological variables. The largest differences among models in the polar regions are related to the representation of the Hg(0)-Br oxidation mechanism and its reaction rates (see Section 3.3.1), concentrations of Br species, photoreduction and re-emission parameterization of Hg from snowpack and Hg evasion fluxes from the Arctic Ocean (Angot et al., 2016). Durnford et al. (2012) developed and implemented a dynamic multi-layer snowpack-meltwater parameterization in GEM-MACH-Hg. Fisher et al. (2012) and Durnford et al. (2012) introduced the evasion of Hg from the Arctic Ocean during summer to explain the observed summertime maximum in Hg(0) concentrations (Steffen et al., 2005; Berg et al., 2013). Toyota et al. (2014b) developed a detailed one-dimensional air-snowpack model for interactions of Br, ozone and Hg in the springtime Arctic that provided a physicochemical mechanism for AMDEs and concurrently occurring ozone depletion events (ODEs). The authors also developed a temperature dependent GOM-PBM partitioning mechanism explaining its observed seasonal transition (Steffen et al., 2014).

Several ocean models have been developed for ocean Hg cycles including MITgcm (Zhang et al., 2014, 2019; Wu et al., 2020), NEMO (Semeniuk and Dastoor, 2017), HAMOCC (Archer and Blum, 2018) and FATE-Hg (Kawai et al., 2020). These models simulate the photochemical/abiotic and biological transformations between Hg(0) and inorganic Hg(II) and methylmercury (MeHg, both monomethylmercury; MMHg and dimethylmercury; DMHg); the models also simulate the partitioning of Hg(II) and MMHg onto particulate organic carbon (POC) to form particle-bound HgP and MMHgP, and the sinking of HgP and MMHgP to deeper waters. This POC pool includes both detritus and living plankton. These models also simulate the exchange of Hg(0) and DMHg with the atmosphere and are forced by atmospheric Hg(II) deposition and Hg(0) concentrations in the marine boundary layer using an atmospheric Hg model

The uptake of seawater MeHg by plankton and its transfer to higher trophic levels is included in some studies (e.g., Schartup et al., 2018; Zhang et al., 2020b). The uptake of MeHg by phytoplankton is modeled as an instantaneous equilibrium process with the ratio of MeHg concentration in phytoplankton over the seawater concentration as a function of the cell diameter and dissolved organic carbon (DOC) concentrations. Trophic transfer of MeHg from phytoplankton to zooplankton is calculated after phytoplankton uptake based on the biomass of phytoplankton grazed by zooplankton, the biomass concentration of phytoplankton and the assimilation efficiency of zooplankton. Unassimilated MeHg grazed by zooplankton returns to the seawater in the form of MMHgP. Losses from plankton reflect MMHg elimination through fecal excretion and mortality. Isotope fractions are also included in Archer and Blum (2018) by slightly perturbing the rates of chemical transformations between the isotopes. Reaction rates for the transformation between species in the ocean are based on experimentally measured values but are sometimes adjusted to match available observations or scaled based on environmental parameters (e.g., organic carbon reaction rate, solar radiation intensity, and temperature).

Calculation of a balanced Arctic Ocean Hg budget has been performed using a multi-compartment box model (Soerensen et al., 2016a). Mercury species (Hg(0), Hg(II) and MeHg) in the polar mixed layer, subsurface ocean, deep ocean, shelf sediments and Central Basin sediments were modeled using boundary inputs dictated by coastal erosion, river inputs, atmospheric deposition, snow and ice melt and advective transport, with removal controlled by evasion, diffusion, particle settling and advective transport. These calculations show that high THg in Arctic seawater relative to other basins reflects large freshwater inputs and sea-ice cover which inhibits losses through evasion. Sources of uncertainty include the magnitude of the benthic sediment resuspension for coastal regions, the magnitude of terrestrial influence on river discharges to the Arctic, and how these and internal rates vary over time. To compensate for its lack of spatial resolution, it is worth noting that this type of model can be applied over longer timescales (e.g., between 1850 and 2010) than spatially resolved models (Soerensen et al., 2016a).

included GEM in the dry deposition budget using either the inferential approach (dry deposition only; De Simone et al., 2014; Dastoor et al., 2015; Song et al., 2015) or the bidirectional air-surface exchange approach (Bash et al., 2014; Wang et al., 2014). Note that flux uncertainties from using these modeling approaches are expected to be on a similar order of magnitude to those of field flux measurements because models were initially developed and validated using limited flux measurements.

While wet deposition processes are episodic, dry deposition process happens all the time, even during precipitation, and over any surface. On regional to global scales, dry and wet deposition are equally important for the majority of atmospheric pollutants, including Hg (Wright et al., 2016; Zhang et al., 2016a). Dry deposition velocity varies by up to two orders of magnitude between GOM, PBM and GEM or between different surface types (Zhang et al., 2009). The lifetime in air due to dry deposition removal is best estimated to be hours to days for GOM, days to weeks for PBM and months to years for GEM, depending on surface type among other conditions. For example, GEM can be effectively removed by canopies with large leaf area if soil emission is limited (resulting in its lifetime of a few months), while its dry removal can be very limited over bare soil and water surfaces (resulting in its lifetime of years; Cohen et al., 2016).

Despite significant advances in model representations of Hg cycling in the Arctic atmosphere and the Arctic Ocean, important gaps remain. Two major uncertainties for atmospheric models are reduction processes and oxidant concentrations. Atmospheric reduction of Hg(II) has been represented as a heterogeneous process in models, but recent work has shown that photoreduction of oxidized mercury species could be significant in the gas phase (Saiz-Lopez et al., 2018, 2019; see Section 3.3.1.2). This process is inadequately represented in existing Arctic studies and challenges elements of the current model of atmospheric redox.

Reduction in the atmosphere acts in opposition to oxidation, which also carries significant uncertainty in the models. While recent advances in computational chemistry studies have narrowed down some of the major gaps in the kinetics and mechanisms of gas-phase Hg oxidation, leading to increased confidence in the primary role of Br-initiated oxidation in the global troposphere (see Section 3.3.1.3b), concentrations of Br are uncertain. Along with their role in oxidizing Hg(0), Br radicals also participate in other photochemistry (e.g., the catalytic destruction of O_3). The modeling of Br chemistry is challenging in general and is especially complicated in polar environments. The photochemical production of gaseous inorganic bromine occurs when salt-containing substrates (i.e., from saline surface snowpack on sea ice, wind-blown snow particles and sea-salt aerosol) mix with acid compounds ubiquitous in the atmosphere, are exposed to gaseous oxidants or are illuminated by sunlight (Abbatt et al., 2012; Pratt et al., 2013; Wren et al., 2013; Custard et al., 2017). Knowledge gaps exist in the quantification of all of the processes controlling Br chemistry, and model studies have simulated springtime Br chemistry in the polar boundary layer with various levels of complexity.

For simulating the Br-initiated Hg oxidation in atmospheric models, concentrations from other models of tropospheric chemistry and transport are used for Br radical and other reactive chemical compounds such as NO_2, HO_2, BrO and OH (reacting with HgBr to form Hg(II) products; e.g., Horowitz et al., 2017). However, given the currently limited capabilities of models to compute Br chemistry in the polar boundary layer over sea ice, atmospheric Hg models employ indirect approaches to derive Br radical concentrations (e.g., assuming BrO concentrations are in the boundary layer over sunlit sea ice; Holmes et al., 2010; Fisher et al., 2012; Angot et al., 2016) or using the monthly satellite climatology of BrO over sea ice (Dastoor et al., 2008). Toyota et al. (2014b) proposed that multiphase Br chemistry could also play a role in partitioning between gaseous Hg(II) and PBM. This model simulated the formation of PBM occurring as Hg(II)-bromide complexes after ozone depletion, when the concentrations of particulate bromine (Br^-) are relatively high. The model also predicted the formation of PBM to occur more favorably at lower temperatures, in accordance with observed seasonal trends of the Hg(II)-PBM partitioning at Alert in the Canadian Arctic (Cobbett et al., 2007; Steffen et al., 2014). This partitioning is a factor in determining the atmospheric lifetime of Hg against dry and wet depositions (Amos et al., 2012; Steffen et al., 2014) and highlights the deep connection between the dually uncertain Hg and Br cycles.

Terrestrial inputs of Hg to the Arctic Ocean via rivers have been shown to contribute to the seasonality and magnitude of atmospheric and ocean concentrations (Fisher et al., 2012; Soerensen et al., 2016a; Sonke et al., 2018). The Arctic terrestrial loading of Hg is connected to the atmosphere through deposition and evasion and to the Arctic Ocean via river outflow. Changes in atmospheric Hg deposition to, and retention in, Arctic soils, permafrost and watersheds through time make this a dynamic contributor to the fate of Arctic Hg. Currently, models of terrestrial Hg loading, transformation and export are not used in conjunction with models of the coupled atmosphere-ocean system to build a consistent estimate of these connected fluxes. A future coupling of terrestrial models with existing atmosphere and ocean simulations would fill an important gap in simulating the Arctic Hg cycle.

3.3.2 How much mercury is present in Arctic surface air?

For this AMAP assessment, Hg concentrations in Arctic surface air were investigated by an ensemble of chemical transport models using the 2015 inventory of Hg anthropogenic emissions developed for the latest Global Mercury Assessment (AMAP/UN Environment, 2019). Four global-scale Hg chemical transport models were applied in the study: GLEMOS (Travnikov and Ilyin, 2009), GEOS-Chem (Holmes et al., 2010; Fisher et al., 2012), GEM-MACH-Hg (Dastoor et al., 2008; Durnford et al., 2012; Kos et al., 2013; Dastoor and Durnford, 2014; Fraser et al., 2018); and DEHM (Christensen et al., 2004; Skov et al., 2020). The median distribution of Hg(0) concentrations in Arctic surface air in 2015 as simulated by the model ensemble is shown in Figure 3.7 (left panel). The annual mean Hg(0) concentration at Arctic monitoring stations, based on observations, is 1.38±0.11 ng/m^3 and 1.42±0.04 ng/m^3 with the model ensemble. With a relative bias (RBIAS)[1] of 2.8%, the model ensemble slightly overestimates Hg(0) concentrations. When a 10% uncertainty for observations is considered, the model results are within the range of expected values. The GEM-MACH-Hg estimated annual average burden of THg in the Arctic atmosphere north of 60°N is 330 Mg, (seasonal variation, 290-360 Mg).

Dastoor and Durnford (2014) conducted a comprehensive evaluation of GEM-MACH-Hg simulated concentrations of Hg(0) and Hg(II) in the air with measurements at Alert (Canada), Ny-Ålesund (Norway), Amderma (Russia), and Utqiaġvik (Barrow; USA) from 2005 to 2009 while Angot et al., (2016) evaluated GEM-MACH-Hg, GEOS-Chem and GLEMOS using atmospheric monitoring data of Hg concentrations for 2011 to 2015 at four Arctic sites: Alert, Station Nord (Greenland), Ny-Ålesund and Andøya. The model median concentrations of Hg(0) were found within the range of observed medians at all locations. DiMento et al. (2019) reported Hg(0) concentrations over the western Arctic Ocean during the 2015 U.S. Arctic GEOTRACES cruise (August–October; from Dutch Harbor, Alaska to the North Pole and back). Observed Hg(0) concentrations, averaging 1.2±0.1 ng/m^3, are in the range of values simulated by the model ensemble in the autumn of 2015 (Figure 3.8d) when the 10% uncertainty for observations is taken into account.

[1] $RBIAS = \frac{\overline{M} - \overline{O}}{\overline{O}} 100\%$

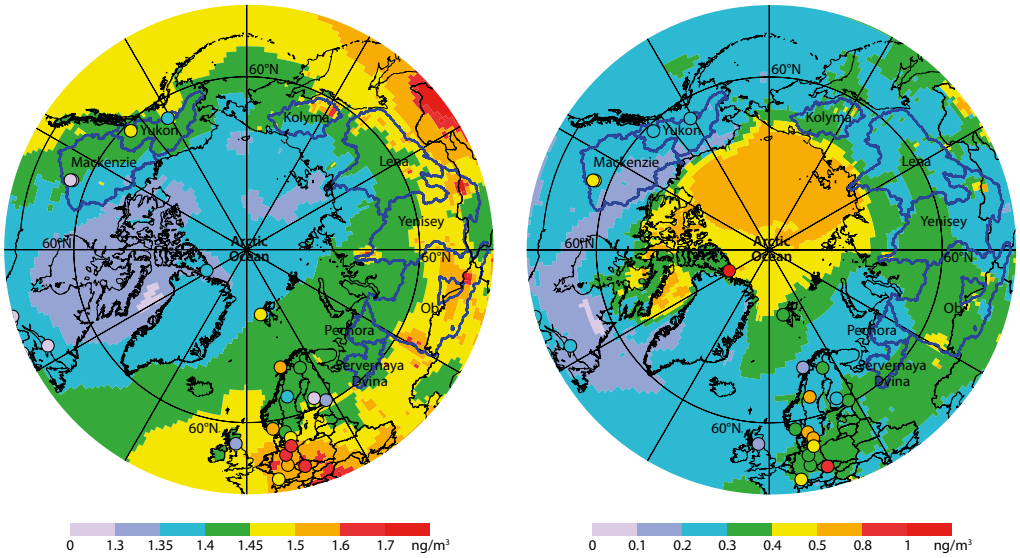

Figure 3.7. Model ensemble median Hg(0) concentration in Arctic surface air (in ng/m³) in 2015 (left) and seasonal amplitude of Hg(0) concentration (i.e., the difference between the highest and lowest monthly values) in 2015 (right). Circles show observations in the same color scale.

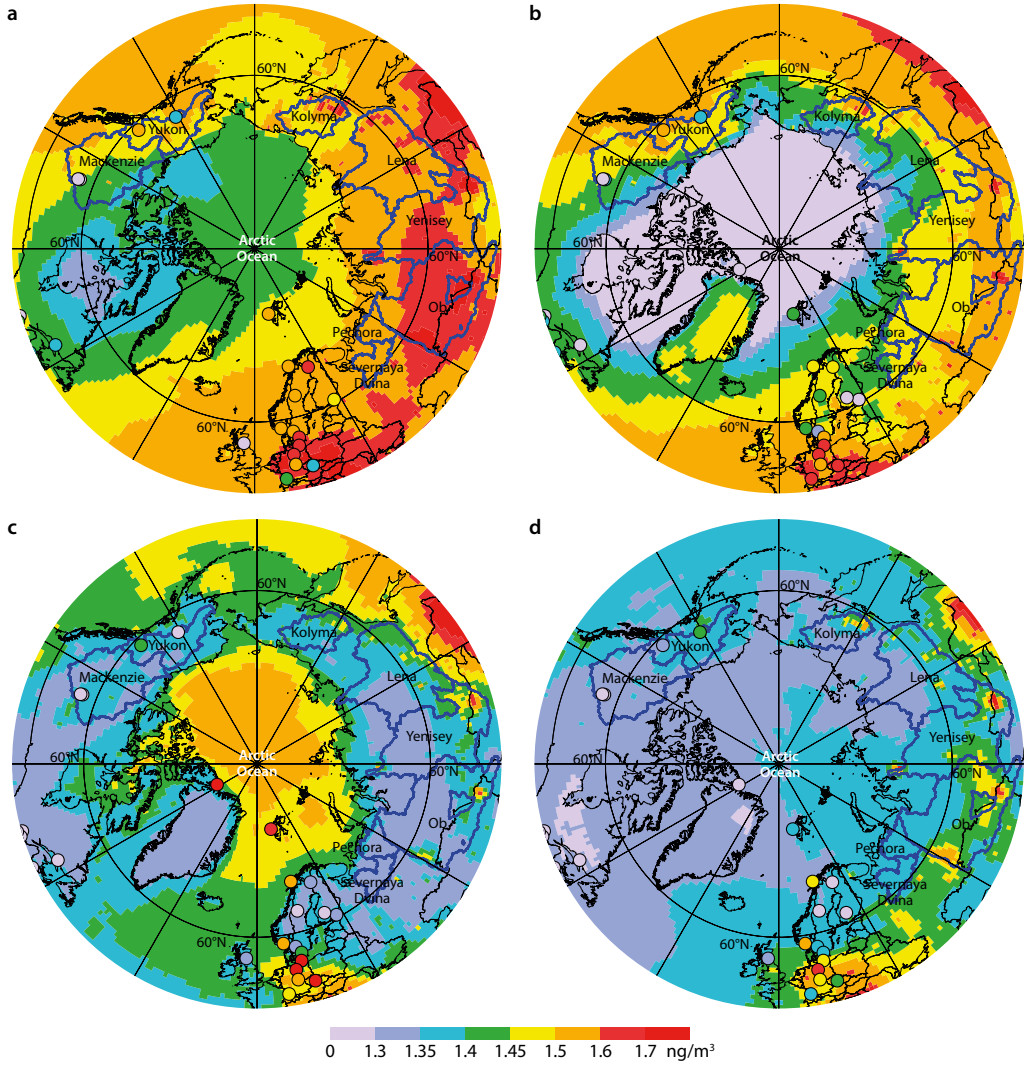

Figure 3.8. Model ensemble median Hg(0) concentration in surface air (in ng/m³) in 2015 in (a) winter (December–February), (b) spring (March–May), (c) summer (June–August) and (d) autumn (September–November). Circles show observations in the same color scale.

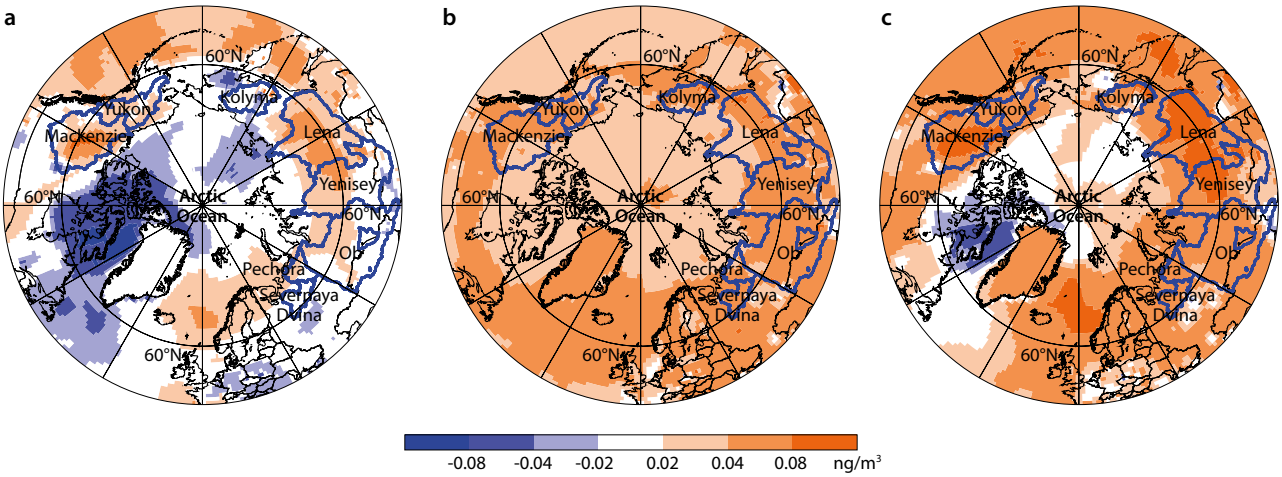

Figure 3.9. Simulated (model ensemble median) changes in Hg(0) concentration in surface air (in ng/m^3) between 2010 and 2015 due to (a) changes in meteorology only, (b) changes in global anthropogenic emissions only and (c) cumulative changes.

Kalinchuk et al. (2021) performed continuous measurements of Hg(0) concentrations in the marine boundary layer of eastern Arctic seas during a cruise from September to October 2018 and reported median Hg(0) concentration of 1.45±0.11 ng/m^3 from the Chukchi Sea to the eastern Arctic Ocean. In comparison, the model ensemble autumn median Hg(0) concentrations are 1.3 to 1.35 ng/m^3 along the transact. However, a more thorough evaluation of model outputs is hampered by the limited number of ground-based monitoring sites and by the absence of year-round measurements over the Arctic Ocean. Measurements carried out onboard the RV Polarstern under the umbrella of the Multidisciplinary drifting Observatory for the Study of Arctic Climate (MOSAiC) expedition from October 2019 to September 2020 will partly fill this gap.[2]

According to Figure 3.7 (left panel), the distribution of Hg(0) concentrations is characterized by a clear latitudinal gradient suggesting the transport of anthropogenic Hg from lower latitudes to the Arctic. Concentrations above 1.4 ng/m^3 are found in most of the terrestrial Arctic, while they are minimal (below 1.4 ng/m^3) in Nunavut (Canada), Greenland and above the Arctic Ocean. This can partly be attributed to the seasonal amplitude of Hg(0) concentrations (Figure 3.7, right panel). The model ensemble reproduces the characteristic seasonality in the western Arctic, with minimal Hg(0) concentrations in spring driven by AMDEs (Figure 3.8b) and maximal Hg(0) concentrations in summer attributed to oceanic re-emission of Hg (Figure 3.8c). The more pronounced seasonal cycle (in comparison to other Arctic sites) observed at Alert is also well captured by the model ensemble. The temporal correlation between the model ensemble results and observations at Arctic sites is 0.75.[3]However, it should be noted that the model ensemble underestimates the seasonal amplitude at Alert due to the underestimation of the amplitude of both the spring minimum and summer maximum Hg(0) concentrations (Figure 3.8). As noted by Angot et al. (2016), the models correctly reproduce enhanced total oxidized mercury concentrations (i.e., oxidized gaseous and particulate mercury) at Alert and Ny-Ålesund during the AMDEs season but underestimate the values compared to measurements. Angot et al. (2016) evaluated modeled interannual variability in Hg(0) concentrations using GEOS-Chem and GEM-MACH-Hg simulations from 2011 to 2014. Interannual variability in the frequency of AMDEs was fairly well reproduced by GEM-MACH-Hg but real-time modeling of the distribution of Br concentrations and sea-ice dynamics is needed to improve the models (Moore et al., 2014).

Changes in Arctic surface air Hg(0) concentrations between 2010 and 2015 were investigated using three models (DEHM, GEOS-Chem and GEM-MACH-Hg). The simulations were conducted in the following order: 2010 anthropogenic emissions (AMAP/UNEP, 2013) with 2010 meteorology; 2010 anthropogenic emissions with 2015 meteorology; and 2015 anthropogenic emissions (AMAP/UN Environment, 2019) with 2015 meteorology. These simulations show cumulative change from 2010 to 2015 as a result of changes in meteorology and anthropogenic emissions (i.e., expected changes from 2010–2015 are due to changes in meteorology only, and additional change is due to changes in anthropogenic emissions). Changes in meteorology only (Figure 3.9a) enhance the transport (and the impact) of both global anthropogenic and legacy Hg emissions in different regions of the Arctic but significantly decrease Hg(0) concentrations in the Canadian Arctic Archipelago (CAA). As discussed in Section 3.3.1.1, pollution transport to the Arctic from southern latitudes is influenced by three major semi-permanent pressure systems (i.e., the Aleutian Low, the Icelandic Low, and the Siberian High) and two major low-frequency variability modes (i.e., the PNA and the NAO). The negative phase of the NAO (NOAA, 2020) might have increased the transport of Hg from North America to the western Arctic in 2010 explaining the simulated decrease in Hg(0) concentration between 2010 and 2015 in the CAA.

[2] For more information, visit the expedition website https://mosaic-expedition.org

[3] Temporal correlation coefficient of monthly mean values averaged over the measurement sites.

Changes in anthropogenic emissions only (Figure 3.9b) lead to an overall increase in Hg(0) concentration in the Arctic between 2010 and 2015, driven by the 20% increase in global anthropogenic emissions to the atmosphere from 2010 to 2015 (see Section 3.2.2.3). The simulations suggest a 0.04–0.10 ng/m^3 increase in Hg(0) concentrations from 2010 to 2015 due to cumulative (meteorology plus emission) changes in most of the Arctic and a 0.02–0.08 ng/m^3 decrease in the CAA. These cumulative changes are relatively small (1% to 7%), in good agreement with observations in the High Arctic (see Chapter 2). The main message from this modeling experiment is that the general pattern of change suggested by the models is in-line with observations and is helpful in explaining observed trends (e.g., the increasing trend at Little Fox Lake, Canada, and the decreasing trend at Station Nord, Greenland). Using measurements and DEHM simulation, Skov et al. (2020) found that the contribution of contemporary anthropogenic emissions to Villum Research Station (or Station Nord) in the High Arctic accounted for only 14% to 17% of the total GEM concentrations.

3.3.3 How much mercury is exchanged between the atmosphere and Arctic surfaces?

3.3.3.1 Mercury uptake by precipitation

The median distribution of Hg wet deposition fluxes in 2015 as simulated by the model ensemble is shown in Figure 3.10. According to the simulations, the Arctic is characterized by relatively low wet deposition fluxes (0–5 μg/m^2/y), especially in arid areas of Greenland, northern Canada, and Siberia. To put these fluxes in perspective, global measurement data have shown annual wet deposition fluxes varying from a couple of μg/m^2 to ~30 μg/m^2 (Qin et al., 2016; Mao et al., 2017; Sprovieri et al., 2017; Zhou et al., 2018). In good agreement with the simulated fluxes, smaller Hg wet deposition fluxes have been observed in the Arctic due to less rain amounts, shorter seasons favoring GEM oxidation and less anthropogenic influence. Obrist et al. (2017) estimated that 71% of THg deposition in the Arctic resulted from dry deposition of GEM and the remaining from the deposition of reactive Hg, indicative of a small contribution from wet deposition.

Sanei et al. (2010) reported wet deposition fluxes of 0.5 to 2.0 μg/m^2/y at two Canadian Subarctic sites. A multi-year (2008–2015) wet deposition record from an Arctic tundra site reported by Pearson et al. (2019) at Gates of the Arctic National Park in Alaska showed a mean annual wet deposition flux of 2.1±0.7 μg/m^2/y, with an interannual range of 1.2 to 3.0 μg/m^2/year. Annual Hg wet deposition at this site was the lowest annual flux measured across any of the National Atmospheric Deposition Program (NADP) network stations in the U.S. and Canada, accounting only for about 20% of mean Hg wet deposition measured across 99 lower-latitude stations (a mean of 9.7±3.9 g/km^2/y). A comparison to four other Alaskan Subarctic and boreal sites showed consistently low Hg wet deposition across all northern stations (annual fluxes of 2.3 μg/m^2/y at Nome; 3.0 μg/m^2/y at Glacier Bay; 4.8 μg/m^2/y in Kodiak and 4.5 μg/m^2/y at Dutch Harbor). These low Hg wet deposition fluxes were attributed to a combination of low annual precipitation (363 mm/y on average at Gates of the Arctic) and low Hg concentrations in precipitation (a median of 3.6 ng/L) and are consistent with low snow Hg concentrations (0.5–1.7 ng/L; Douglas and Sturm, 2004; Agnan et al., 2018). The model ensemble satisfactorily reproduces these low fluxes, with simulated median fluxes ranging from 2 to 4 μg/m^2/y over Alaska (Figure 3.10). However, available measurement data cover limited regions of the Arctic and cannot provide complete evaluation of the regional spatial pattern.

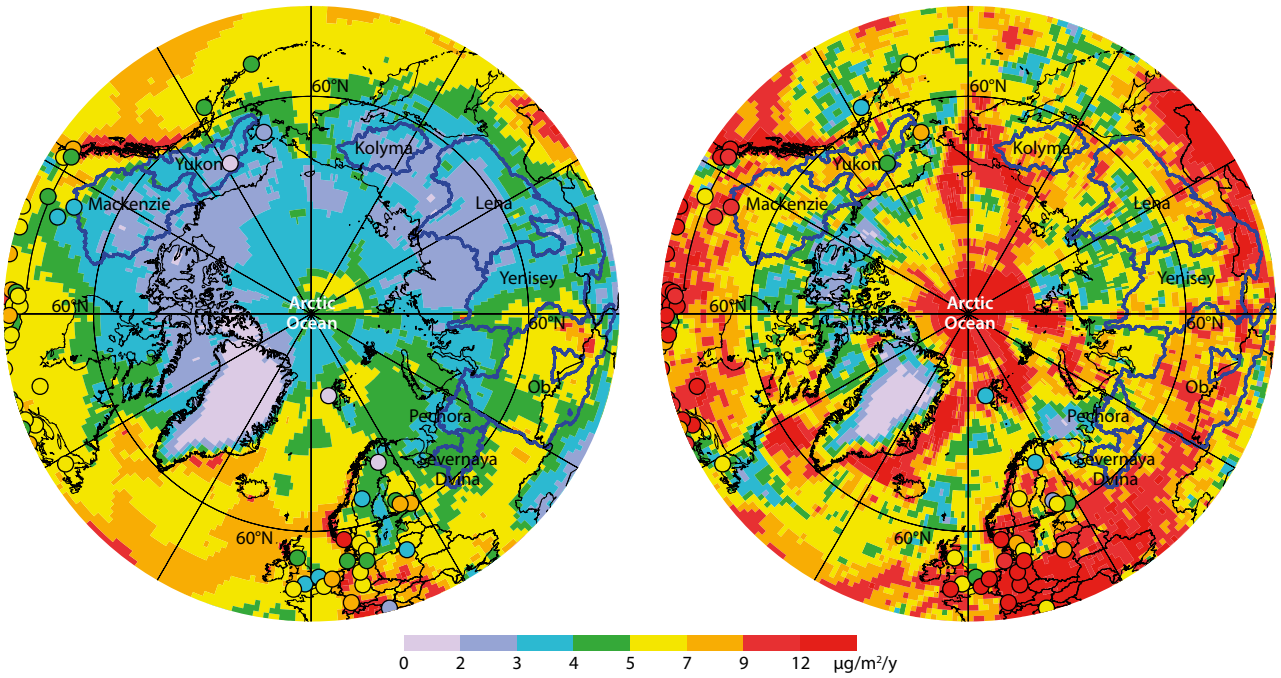

Figure 3.10. Model ensemble median Hg wet deposition flux (left) and seasonal variation of monthly Hg wet deposition (right) in 2015; model simulated values are shown by background contour, and observed values are presented in circles.

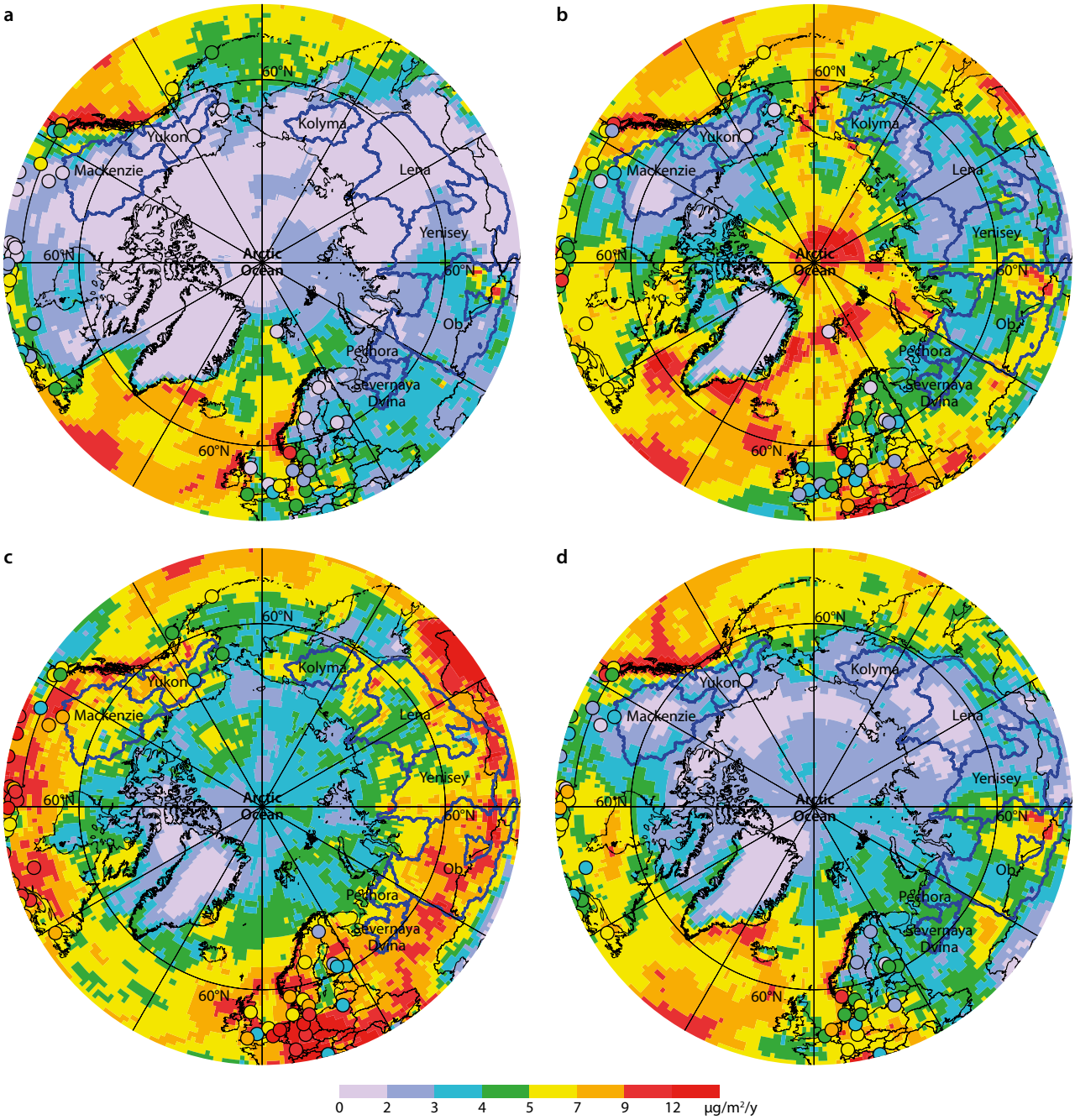

Figure 3.11. 2015 model ensemble median Hg wet deposition in (a) winter (December–February), (b) spring (March–May), (c) summer (June–August) and (d) autumn (September–November). Circles show observations in the same color scale.

An evaluation of the performance of the model ensemble at reproducing the observed seasonal cycle at selected Arctic sites is given by Figure 3.11. Overall, the model ensemble accurately reproduces the seasonal pattern—with higher wet deposition of Hg in summertime—but overestimates annual fluxes by a factor of two on average at the eight sites above 60°N (2.4±0.9 vs. 4.8±1.7 µg/m²/y). The models also overestimated precipitation amount by a factor of two to five at these sites, which can explain the discrepancy between modeled and measured wet deposition fluxes. A comprehensive evaluation of three of the participating models (GEM-MACH-Hg, GEOS-Chem and GLEMOS) against measurements in the Arctic taken between 2011 and 2014 was recently performed by Angot et al. (2016) The authors suggested that the known difficulty with collection efficiency of precipitation in polar regions due to frequent strong winds and blowing snow condition leads to significant underestimation of measured precipitation amounts, which implies underestimation of measured wet deposition Hg fluxes (Liljedahl et al., 2017).

Changes in annual Hg wet deposition between 2010 and 2015 in the Arctic were investigated using the set of simulations described in Section 3.3.2 (Figure 3.12). With an estimated ~20% increase in global anthropogenic emissions from 2010 to 2015 (see Section 3.2.2.3), the annual average Hg deposition flux in the Subarctic is estimated to be slightly higher in 2015 than in 2010 by 0.27 µg/m²/y (0.12 µg/m²/y due to emission and 0.15 µg/m²/y due to meteorology); on the other hand, the changes simulated

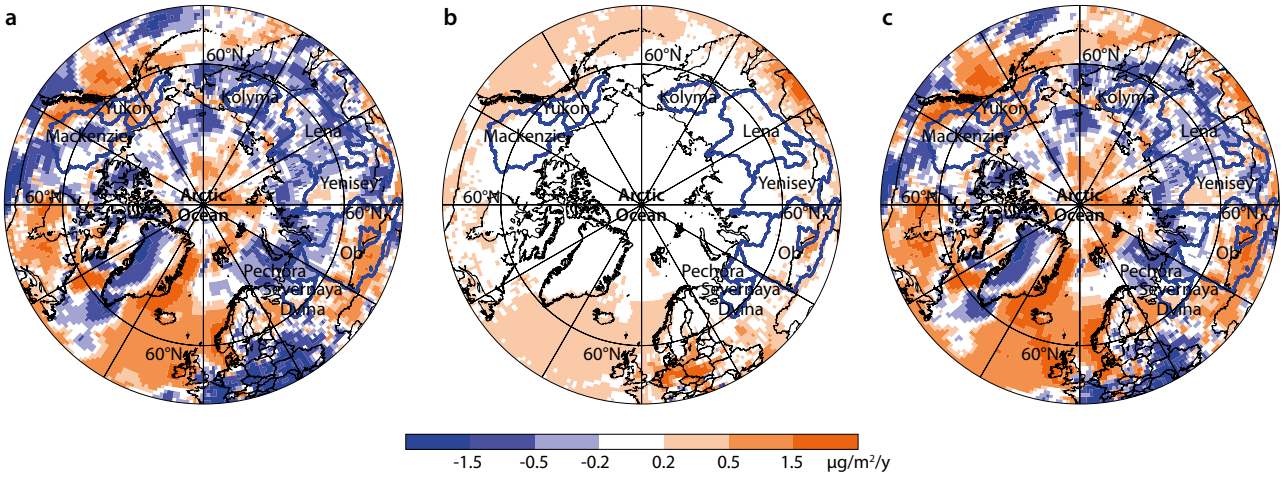

Figure 3.12. Simulated (model ensemble median) changes in Hg annual wet deposition between 2010 and 2015 due to (a) changes in meteorology only, (b) changes in global anthropogenic emissions only and (c) cumulative changes.

in the High Arctic are negligible. These results suggest an overall increasing trend in present-day wet deposition partially driven by increasing precipitation amounts, which is in good agreement with the literature (Sprovieri et al., 2017).

3.3.3.2 Interfacial exchange of mercury between air and terrestrial surfaces

Lower-latitude studies show that atmospheric Hg deposition to terrestrial environments is dominated by plant uptake of gaseous atmospheric Hg(0) via stomatal and cuticular uptake pathways (between 50% and 90% of THg deposition), which is transferred to soils when plants die off or shed leaves (litterfall) or when Hg on plant surfaces is washed off by rain (throughfall). Plant-driven deposition dominates over wet deposition in all land regions of the world (Fu et al., 2016; Wang et al., 2016; Wright et al., 2016; Zhang, et al., 2016c). Stable Hg isotopes analyses confirm that plant-derived gaseous Hg(0) deposition is the dominant source in most upland soils accounting for 54% to 94% of Hg (Demers et al., 2013; Jiskra et al., 2015; Enrico et al., 2016; Zheng et al., 2016; Obrist et al., 2017; Wang et al., 2017b).

Plant-driven Hg deposition is likely to be the dominant source of Hg in the tundra as well. A recent mass balance deposition study in the tundra at Toolik Field Station, Alaska, measured dry deposition of gaseous elemental Hg(0) by a micrometeorology flux-gradient approach (Obrist et al., 2017) (Figure 3.13). The study reported that gaseous Hg(0) dry deposition, 6.5±0.7 µg/m²/y, accounted for 71% of total atmospheric Hg deposition, dominating annual total net Hg deposition. In addition, atmospheric Hg(II) accounted for average dry deposition of 2.5 µg/m²/y (with a range of 0.8–2.8 µg/m²/y). Much of the Hg(0) deposition occurred via plant Hg uptake and the subsequent transfer of Hg to tundra soils (Olson et al., 2018; Jiskra et al., 2019). Due to annual plant turnover, much of this biomass is conveyed to soils via plant senescence and litterfall each year. In addition to summertime Hg(0) deposition via plants, Hg(0) deposition is also observed during winter under the snowpack which may be attributable to sorption to soils, litter or lichen under the snowpack (Obrist et al., 2017; Agnan et al., 2018; Jiskra at al., 2019), although the importance of this process for deposition loads is unknown. In barren tundra areas of the Arctic that lack significant vegetation cover (e.g., the CAA, northern Greenland, Svalbard etc.), wet and dry deposition processes directly to snow and soil surfaces probably dominate because the plant-uptake pathway is unavailable.

Skov et al. (2006) found in a study at a High Arctic site (Barrow, Alaska) that the deposition velocity of GOM is very fast over snow with surface resistance close to zero. From the deposition measurements of GOM and re-emission estimates based on meteorology and measured GEM concentrations, 1.7 µg/m² of GOM deposition was measured for a period of 14 days. The flux of PBM was assumed to be insignificant and GEM re-emission of 1.0 µg/m² was measured, leading to a net accumulation of 0.7 µg/m² for the 14 days. In a recent air-snow Hg flux study at Villum Research Station (Station Nord, North Greenland) from the 23rd of April to the 12th of May during spring 2016, the average emission of GEM from snow was 8.9 ng/m²/min (up to 179.2 ng/m²/min during short events) and a GEM deposition flux of 8.1 ng/m²/min was also measured (Skov et al., 2020).

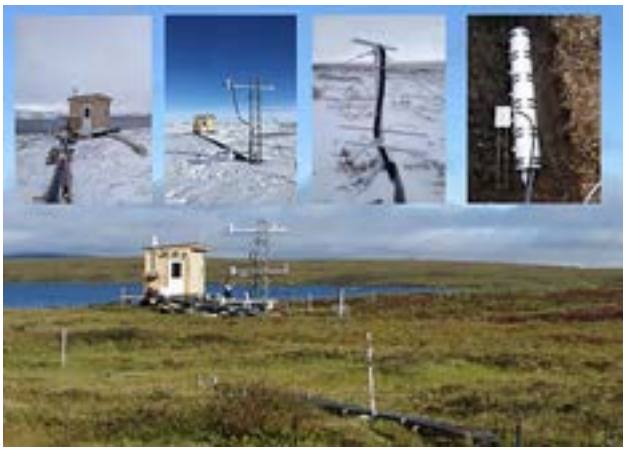

Figure 3.13. Mass balance deposition study in the tundra of northern Alaska (Toolik Field Station). Instrumentation to measure gaseous Hg(0) deposition includes a tower system to measure ecosystem-level atmosphere-surface Hg(0) exchanges. Figure from Obrist et al., 2017.

3.3.3.3 Interfacial exchange of mercury between air and marine surfaces

Inputs of Hg by precipitation (see Section 3.3.3.1) and dry deposition to the surface waters of the Arctic from the atmosphere and evasion fluxes to the air have been estimated from measurements made at coastal locations, studies in the CAA, and from limited measurements from vessels in the Arctic (Angot et al., 2016; Soerensen et al., 2016a; DiMento et al., 2019; Kalinchuk et al., 2021; Table 3.9). Estimates of wet and dry deposition of inorganic Hg from U.S. GEOTRACES cruise data (DiMento et al., 2019), which are from the fall, are lower than those likely found during polar sunrise where AMDEs and Hg deposition are heightened in spring and in summer when the precipitation rate peaks (Fisher et al., 2013; Angot et al., 2016). Based on the measurements in aerosols and an estimated dry deposition velocity of 0.5 cm/s (Holmes et al., 2009), given that there appeared to be mainly fine particulate aerosols over the open Arctic, 0.05 Mg of Hg were deposited per month via dry aerosol deposition in autumn 2015 (DiMento et al., 2019). Similarly, GOM was deposited at a rate of 0.3/Mg/month, based on the measured ionic Hg concentrations over open water, which were all near the method detection limit for the Tekran instrument. Overall, the total measured dry deposition flux (0.35 Mg/month) by DiMento et al. (2019) is much lower than other measurements in the Arctic region (see Table 3.9), which are mostly measured at coastal land locations or in the CAA (Steffen et al., 2015; Angot et al., 2016; Sorensen et al., 2016). Concentrations of GOM and HgP measured from coastal sites can be above 500 pg/m^3 during MDEs and during the polar spring but are mostly <20 pg/m^3 during autumn and winter (e.g., Steffen et al., 2015) but still higher than over the open ocean.

The DiMento et al. (2019) atmospheric input estimates of Hg to the Arctic Ocean are also lower than modeled estimates of Soerensen et al. (2016a), whose estimate covers the entire year, of 2.5 Mg/month of Hg on average (30 Mg/y; see Table 3.9). The recent estimates (Soerensen et al., 2016a; Sonke et al., 2018) are lower than other estimates for atmospheric input (Outridge et al., 2008; Dastoor and Dunford, 2014), which all appear high compared with the actual measurements over the offshore waters of the Arctic (DiMento et al., 2019; see Table 3.9).

In terms of evasion to the atmosphere, while various studies have measured water column Hg(0) concentrations and estimated evasion fluxes within the CAA (see Table 3.9), there are only two studies that have made high resolution measurements of Hg(0) within the central Arctic Ocean (Andersson et al., 2008; DiMento et al., 2019; Kalinchuk et al., 2021; Figure 3.14). These studies found different concentrations in Arctic open waters with higher concentrations found in the summer (July–September; Andersson et al., 2008) compared to the late summer to autumn (August–October) measurements (DiMento et al., 2019). However, both studies showed the build-up of Hg(0) in the surface waters under the ice, suggesting the potential for a substantial release of Hg(0) from the underlying water during ice melt in spring/summer, in agreement with atmospheric observations and modeling (Durnford et al., 2012; Fisher et al., 2013). Significantly, this suggests that the seasonal gas exchange dynamics of Hg(0) could change substantially with the rapidly decreasing ice cover of the warming Arctic Ocean.

Table 3.9 Dissolved elemental Hg ($Hg(0)_{diss}$) (fM) in the Arctic Ocean mixed layer, and estimated deposition and evasion fluxes (Mg/month). Data from the literature as noted.

Study/location	$Hg(0)_{diss}$ (fM)	Evasion flux (Mg/month)	Deposition flux (Mg/month)
GEOTRACES 2015 open water	32±30[a]	1.4	0.55
GEOTRACES 2015 continuous ice	101±98	<0.2	
Kirk et al., 2008, CAA	130±50[b]	--	--
Andersson et al., 2008	220±110[c]	19	--
Fisher et al., 2013, model average	210[d]	7.5	3.8
Dastoor and Durnford, 2014, model[e]	--	2.8	9.0
Soerensen et al., 2016a, model average	180	8.3	6.3
Zhang et al., 2020b, model average	37	8.2	--

[a]autumn; [b]summer/autumn; [c]summer; [d]maximum summer value; [e]estimate for Arctic Ocean north of 66.50°N.

Overall, the model estimates for Arctic Ocean Hg(0) evasion from 2015 in Table 3.9 are contrasted with the results of earlier studies in the CAA (Kirk et al., 2008; Soerensen et al., 2016a) and the Andersson et al. (2008) work. These studies reported higher Hg concentrations in surface waters of the Arctic Ocean overall than those measured by DiMento et al. (2019) during the 2015 Arctic GEOTRACES cruise and result in much higher evasion estimates than would be predicted based on the cruise data (see Table 3.9) and require there to have been substantial inputs of Hg from the terrestrial environment (e.g., rivers, ice melt, glacial inputs, etc.; Fisher et al., 2013). Kalinchuk et al. (2021) measured a low evasion flux of Hg (a mean of 0.70±0.26 ng/m^2/h) in the eastern Arctic Ocean in autumn 2018 similar to the mean evasion flux of 0.4±2.8 ng/m^2/h measured in the open waters of the Bering Sea and the Arctic Ocean in autumn 2015 by DiMento et al. (2019). Zhang et al. (2015) modeled Arctic Ocean Hg concentrations (Figure 3.14c) considering both atmospheric deposition and riverine inputs; they also suggested a higher evasion flux, as reported in Soerensen et al. (2016a). The lower values for Hg(0) evasion measured on the 2015 cruise during autumn is consistent with modeled estimates of Dastoor and Dunford (2014) and riverine Hg input estimates to the Arctic Ocean from terrestrial sources (Outridge et al., 2008; Sonke et al., 2018). However, the cruise data cannot explain the modeled higher inputs and evasion in spring/summer (Fisher et al., 2013; Soerensen et al., 2016a). Observations representing annual variations are currently lacking.

Higher Hg(0) concentrations under ice (as opposed to open water) during the 2015 GEOTRACES cruise and the 2008 cruise (Andersson et al., 2008; DiMento et al., 2019; Figure 3.15) and with Antarctic studies (Nerentorp Mastromonaco, 2016; Nerentorp Mastromonaco et al., 2016, 2017a, 2017b) were measured. The timescale for surface water Hg(0) concentrations to return to open water values after ice removal, assuming the only sink to be gas evasion and no additional formation, is in the order of several weeks (DiMento et al., 2019). The radon data collected by Rutgers van der Loeff et al. (2014) in the Arctic concur with this estimate for the rate of change in concentration for an unreactive gaseous tracer. However, net formation of Hg(0) would impact this rate of change in the Arctic mixed

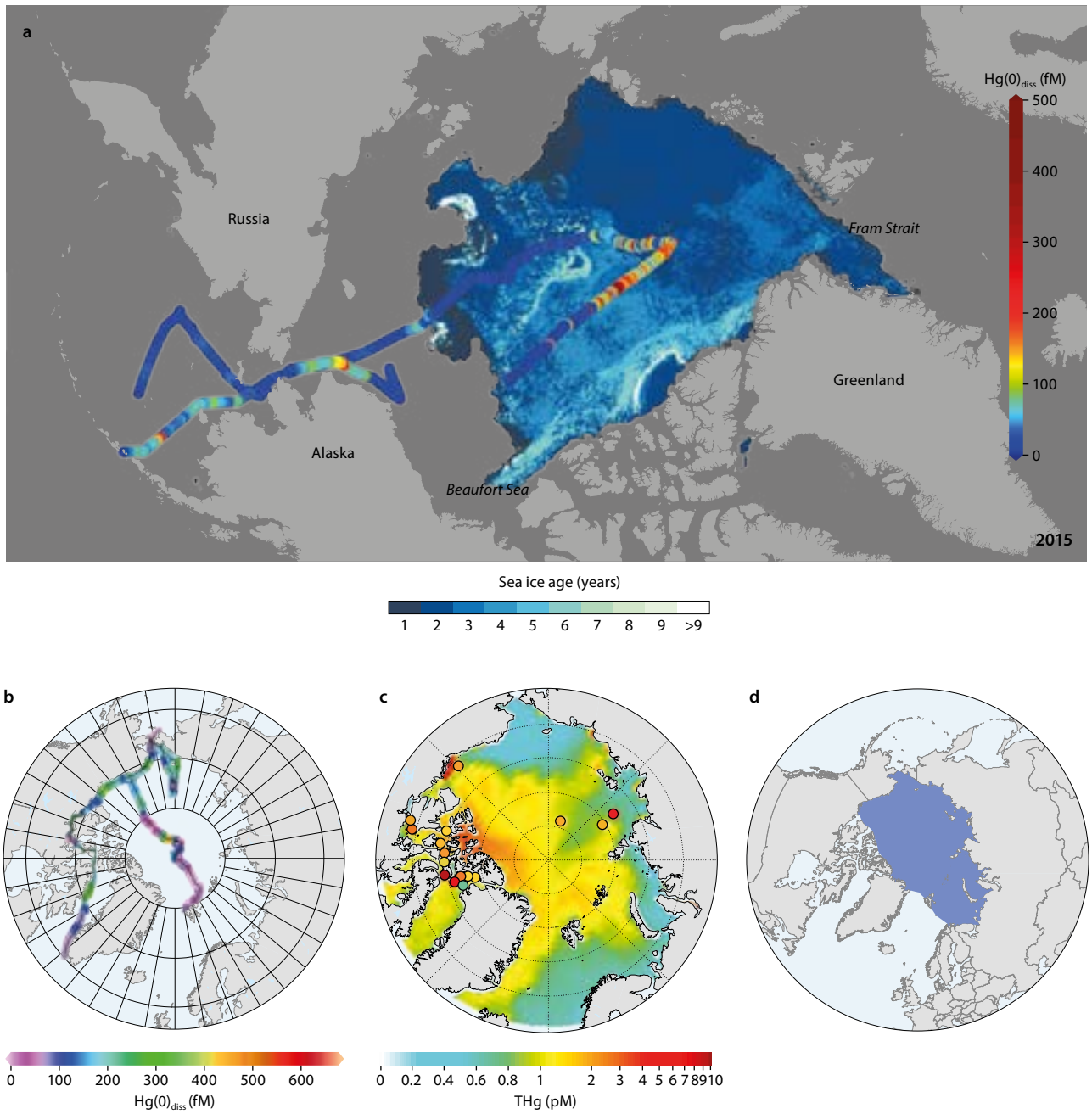

Figure 3.14 Dissolved elemental Hg ($Hg(0)_{diss}$) in Arctic Ocean surface waters in (a) early summer to autumn 2015 from DiMento et al., 2019 (b) summer 2008 from Andersson et al., 2008, and (c) modeled annual mean total Hg concentrations (pM) compared to observations from 2002–2011 (ship cruises, colored dots) from Zhang et al., 2015; (d) the blue area (~9.45 million km^2) defines the AMAP Arctic Ocean boundary used in this report.

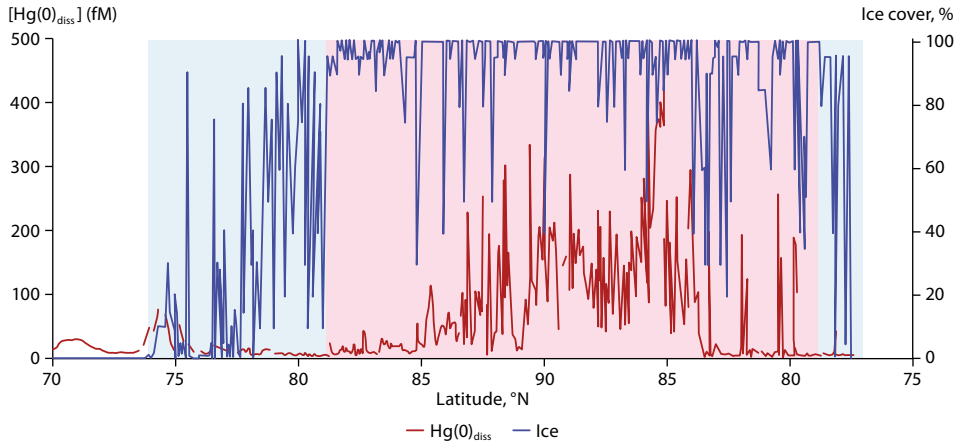

Figure 3.15 The dissolved Hg(0) ($Hg(0)_{diss}$) concentration; fM; red line) and the ice cover (%, dark blue line) along the 2015 U.S. Arctic GEOTRACES cruise track within the marginal ice zones (light blue shading; 73.5–81°N, 79–77.5°N) and contiguous ice zones (light red shading; 81–90–79°N). Data from Dimento et al., 2019.

layer as it could influence the overall concentration and degree of saturation. Both photochemical oxidation and reduction will occur, and the redox reactions are enhanced by UV radiation (Whalin and Mason, 2006; O'Driscoll et al., 2007; Jeremiason et al., 2015; Ci et al., 2016), which does not penetrate through the ice to any significant degree (Perovich, 2006). The rates of these reactions (10^{-4}–10^{-6}/s depending on light levels and light penetration) indicate that the mixed layer open waters should come to steady state in terms of photochemical transformations within days (Whalin et al., 2007).

With the decrease in ice cover, there should be a relative rapid decline in Hg(0) concentration. Under the opposite scenario, the build-up of Hg(0) under ice after its formation is likely a slower, biologically-mediated process. Biotic reduction rates have been related to primary productivity and range from 10^{-2}/d (~10^{-7}/s), with dark (non-photochemical) oxidation rates of the same order (Whalin et al., 2007; Soerensen et al., 2010; Hu et al., 2013; Kim et al., 2016; Wang et al., 2016). Overall, the characteristic time it would take to reach a steady state would be several months, if no other losses occurred.

For gas exchange of Hg in the AMAP defined Arctic Ocean area (see Figure 3.14d), applying an average Hg(0) flux for ice-free waters (28 ng/m^2/d) based on cruise data (Andersson et al., 2008; DiMento et al., 2019) to the average area of open water (ranging from 10% in winter to 65% in summer), we estimate an evasion from open waters of 24.9 Mg/y. Additionally, the loss of Hg(0) from its build-up under ice upon ice melt can be estimated based on the changes in ice amount and the measured concentration of Hg(0) under ice. This is estimated at an additional 2.9 Mg/y, resulting in a total evasional flux of 27.8 Mg/y, with an uncertainty range of 20 to 36 Mg/y. The loss of any Hg residing in surface snow and ice by reduction and evasion during ice melt is not included in this estimate. Modeling estimates of Hg evasion from the AMAP defined Arctic Ocean are 45 Mg and 23.3 Mg in 2015 for GEOS-Chem and GEM-MACH-Hg, respectively, using simulations performed for this report. Averaging measurement-based and two modeling estimates (27.8, 45 and 23.3 Mg/y), the best estimate for AMAP Arctic Ocean Hg evasion is 32 Mg/y (with a range of 23–45 Mg/y). This flux estimate is ~3 times lower than the annual flux reported by Soerensen et al. (2016a), which was based on earlier modeling estimate.

3.3.3.4 Total deposition of mercury to Arctic surfaces

This section presents the spatially distributed annual accumulation of Hg (i.e., wet plus dry deposition) in the Arctic terrestrial and marine environments in 2015 simulated by the ensemble of four models (DEHM, GEM-MACH-Hg, GEOS-Chem and GLEMOS) as a consequence of Hg transport into the Arctic from worldwide contemporary and legacy anthropogenic and geogenic Hg emission sources (see Sections 3.2.1 and 3.2.2). The significance of annual Hg deposition to the pan-Arctic watershed and river Hg runoff and the impacts of recent changes in emissions and meteorological conditions on Hg deposition are also discussed.

Model ensemble annual average deposition flux north of 60°N is 7.1±1.2 μg/m^2/y, seasonally distributed approximately as 0.9, 2.6, 2.3 and 1.3 μg/m^2/y in winter, spring, summer and fall, respectively (see Table 3.10). Compared to fluxes on land, average ocean deposition fluxes are larger in winter and spring, and lower in summer. These seasonal variations are driven by the dominance of summertime vegetation Hg uptake over land and larger wintertime precipitation and springtime AMDE-related deposition over ocean compared to over land. While annual deposition modeling uncertainty in the Arctic is low (±17%, 1σ inter-model variation), large modeling uncertainties in Hg deposition estimates are found over marine surfaces in springtime and over terrestrial surfaces in summertime

Table 3.10 Model ensemble average Hg deposition flux (μg/m^2/y) to terrestrial and aquatic areas of the Arctic (north of 60°N and 66.5°N). The range indicates a ±1σ variation interval among the models.

Region	Annual	Winter	Spring	Summer	Fall
Arctic (N of 60°N)	7.1±1.2	3.5±2.1	10.5±5.0	9.1±2.7	5.1±1.6
Land (N of 60°N)	6.8±1.2	2.3±1.9	6.7±4.2	12.8±5.5	5.4±1.9
Ocean (N of 60°N)	7.4±1.6	4.8±3.1	14.4±7.6	5.3±2.1	4.9±1.7
Arctic (N of 66.5°N)	6.3±1.5	3.0±2.7	11.4±6.3	6.6±2.1	4.1±1.4
Land (N of 66.5°N)	5.2±1.2	1.7±2.0	5.5±4.3	9.4±4.8	4.0±1.8
Ocean (N of 66.5°N)	6.9±1.9	3.7±3.9	14.9±8.9	4.9±3.1	4.1±1.6

Table 3.11 Total Hg deposition to terrestrial and aquatic areas (t/y and t/season) in the Arctic (north of 60°N and 66.5°N). The range indicates a ±1σ variation interval among the models.

Region	Annual	Winter	Spring	Summer	Fall
Arctic (N of 60°N)	243±41	30±18	90±43	78±23	44±14
Land (N of 60°N)	118±20	10±8	29±18	55±24	23±8
Ocean (N of 60°N)	125±27	20±13	61±32	23±9	21±7
Arctic (N of 66.5°N)	133±31	16±15	60±33	35±11	22±8
Land (N of 66.5°N)	41±9	3±4	11±8	19±10	8±3
Ocean (N of 66.5°N)	92±25	12±13	49±29	16±10	14±5

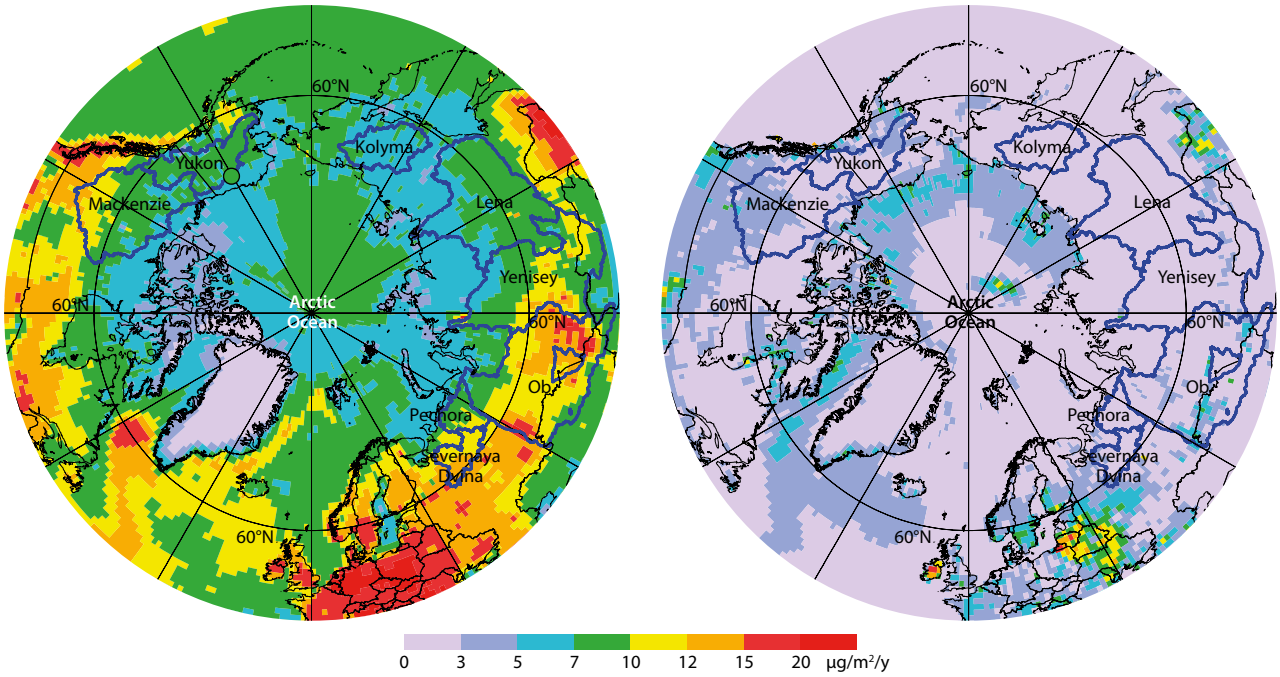

Figure 3.16 Model ensemble median annual Hg deposition in the Arctic (left) and inter-model variability of Hg deposition (1σ) (right) in 2015.

(see Table 3.10). Total annual deposition in the Arctic within 60°N is estimated at 243±41 Mg/y (118±20 Mg/y over land and 125±27 Mg/y over ocean) with seasonal contributions of 30 Mg in winter, 90 Mg in spring, 78 Mg in summer and 44 Mg in autumn (see Table 3.11). Annual Hg deposition north of 66.5°N is 133±31 Mg/y (41±9 Mg/y, land; 92±25 Mg/y, ocean) and the annual Hg deposition to the Arctic Ocean area considered in this study is 64.5±19.8 Mg/y. By upscaling yearly deposition measurement at an Arctic tundra site (Obrist et al., 2017), Sonke et al. (2018) suggested a total deposition of 210 Mg/y to the Arctic permafrost region. In comparison, the model ensemble deposition estimate of Hg to terrestrial surfaces north of 60°N is 118±20 Mg/y, and the estimate to pan-Arctic watershed is 180 Mg/y. Durnford et al. (2012) estimated Hg loading in seasonal snowpacks to be 39 Mg/y using a snowpack/meltwater Hg model.

There are notable spatial variations in Hg deposition fluxes in the Arctic, ranging from ~1 μg/m²/y (Ellesmere Island, Canada, and Greenland Plateau) to 20 μg/m²/y (Davis Strait and northern Europe; see Figure 3.16). Over land, there is a declining gradient in the Hg deposition rate south to north in the Arctic and west to east in Eurasia and North America. Regionally averaged Hg deposition fluxes in the Arctic ranged from 7.6 to 10.7 μg/m²/y in Subarctic regions (10.7, 9.5, 8.6, 7.6, 10.4 and 8.6 μg/m²/y in 1L, 2L, 3L, 4L, 5L and 6L, respectively) and 3.6 to 8.9 μg/m²/y in High Arctic regions (8.1, 7.7, 8.9, 6.3, 3.6 and 5.9 μg/m²/y in 1H, 2H, 3H, 4H, 5H and 6H, respectively; see definition of regions in Figure 3.27a). Higher Hg deposition fluxes are estimated in the regions which are more impacted by local (mainly in Eurasia) and long-range transport (western North America) of emissions as well as by the regions that receive higher precipitation (the ocean around southern Greenland, Greenland Sea, Norwegian Sea, and western coastal Europe and North America) and in regions where there is high vegetation uptake of Hg (western North America and Europe). The lowest deposition fluxes are found in arid regions of the High Arctic (North America) and in Eastern Siberia.

Direct measurements of annual THg deposition are scarce in the Arctic. A mass balance deposition study at a tundra site in the Arctic (Toolik Field Station, Alaska) measured an annual THg deposition of 9.2 μg/m²/y (average for 2014–2016; Obrist et al., 2017). Model ensemble median annual Hg deposition in the Toolik region is 7.2±2.2 μg/m²/y, with summertime (June–September) deposition accounting for 77% of the annual deposition in 2015. Although local biogeochemical features and climate change have been shown to impact the lake sediment fluxes, on a broader scale, the sediment Hg record represents reasonable estimates of catchment-scale deposition fluxes and trends. An earlier mass balance study in northern Alaska based on sediment records estimated an Hg deposition flux between 4.2 and 8.9 μg/m²/y (Fitzgerald et al., 2005). Sediment-inferred average deposition fluxes of 3.5 μg/m²/y in the Canadian High Arctic (11 cores from 65–82°N; Kirk et al., 2011; Lehnherr et al., 2018), 7.5 μg/m²/y in the Canadian Subarctic (Muir et al., 2009) and 10.0 μg/m²/y in the Northwest Territories, Canada (4 cores from 60–62°N; Kirk et al., 2011; Korosi et al., 2015) have been reported. These lake sediment deposition fluxes are in excellent agreement with model ensemble average deposition fluxes in the Canadian High Arctic, where the average is ~3.6 μg/m²/y (with a range from 0.5–5 μg/m²/y), and the Subarctic, where the average is ~7.65 μg/m²/y (with a range from 5–10 μg/m²/y).

Using continuous flux measurements, Obrist et al. (2017) reported that atmospheric Hg(0) contributes to 71% of the annual deposition in the Arctic tundra, mainly by vegetation uptake. Hg(0) deposition during the snow-cover period from October to mid-May (except in March and April when net emission of Hg(0) to the atmosphere was observed after AMDEs) accounted for 37% of total annual Hg(0) deposition. Douglas and Blum (2019) suggested that the majority of Hg

present in Arctic meltwater is derived from Hg(0) uptake in snowpack during the entire snow-cover period, particularly in coastal snow. It is worth noting that terrestrial Hg(0) deposition to vegetation and snow in the Arctic is currently underestimated in models, which need improving in this regard.

a. Mercury deposition to major pan-Arctic watersheds

The eight largest Arctic rivers in Eurasia (the Yenisey, Lena, Ob, Pechora, Kolyma and Severnaya Dvina rivers) and North America (the Yukon and Mackenzie rivers) drain about 70% of the pan-Arctic watershed extending up to 45°N. In Eurasia, the Ob River encompasses the largest fraction of drainage area south of 60°N followed by the Yenisey and Lena rivers; whereas the Severnaya Dvina, Pechora, and Kolyma rivers mostly drain the Arctic landmass north of 60°N. In North America, the Mackenzie Basin extends south of 60°N, while the drainage of the Yukon River is largely within 60°N. The model results exhibit declining Hg deposition fluxes from west to east in Eurasian watersheds, with the highest average Hg deposition flux simulated for the Severnaya Dvina River (11.7 μg/m^2/y, annually; 6.3 μg/m^2/y, September–May) and the lowest for Kolyma (6.5 μg/m^2/y, annual; 3.0 μg/m^2/y, September–May; see Figure 3.16). Ensemble model deposition flux estimates are comparable for the Mackenzie and Yukon watersheds north of 60°N (7.8 and 7.5 μg/m^2/y annually and 3.5 and 3.4 μg/m^2/y from September–May in Yukon and Mackenzie, respectively; see Figure 3.16). Mercury deposition fluxes south of 60°N are largest in the Ob and Mackenzie catchments, 12.3 and 10.3 μg/m^2/y (annually), respectively.

Model ensemble median Hg depositions to the major Arctic river basins (entire basins and their portions north of 60°N) annually and during the snow-cover period (assumed from September–May here) along with observed annual river Hg exports to the Arctic Ocean are reported in Table 3.12. Approximately half of the annual Arctic watershed Hg deposition occurs in summer (predominantly via vegetation and soil uptake), and roughly the other half occurs from autumn to spring (mainly to snowpack via precipitation and dry deposition). With an exception of the Ob River, the general gradient of simulated THg deposition to the pan-Arctic watershed is in line with the measurement-based river Hg exports. The Ob watershed receives the highest Hg deposition of all Arctic river watersheds, but the majority of Hg deposition to the Ob watershed occurs south of 60°N (83%), owing to higher deposition fluxes and a greater percentage of watershed area being south of 60°N. It is likely that much of the deposited Hg south of 60°N is bound to organic soils and sediments during the river transport. Zolkos et al. (2020) and Sonke et al. (2018) reported the lowest Hg yields (river Hg flux normalized to the watershed area) for the rivers that have the higher watershed proportions south of 60°N (i.e., 1–2 μg/m^2/y for the Ob, Yenisey and Mackenzie rivers and ~3 μg/m^2/y for the Lena River), despite high Hg deposition fluxes in these watersheds south of 60°N. In contrast, higher Hg yields were measured for the smaller watersheds that mainly drain Arctic landmasses north of 60°N (~3-5 μg/m^2/y for the Kolyma, Yukon and Severnaya Dvina rivers). Model simulated average Hg deposition fluxes in the Yukon, Kolyma, and Severnaya Dvina watersheds from autumn to spring (3.0–6.3 μg/m^2) are in excellent agreement with their measured river Hg yields. A previous modeling study estimated annual average transfer of THg from the snowpack to meltwater in the range of ~1 to 3 μg/m^2/y (with higher concentrations in coastal regions) in pan-Arctic watersheds (Dastoor and Durnford, 2014).

The annual spring freshet following snowmelt and river ice break-up provides up to 60% of the total annual water flow volume to the Arctic Ocean, peaking in late May to early June (Lammers et al., 2001). Measurement studies have reported the largest fluxes of dissolved and particulate Hg (approximately half in each form) during the spring flood followed by a smaller Hg pulse during the autumn flood (Leitch et al., 2007; Sonke et al. 2018; Zolkos et al., 2020). Zolkos et al. (2020) estimated that over 90% of river Hg export to the Arctic Ocean occurred during spring and summer. Measured Hg export from the eight major Arctic rivers (21.1–22.4 Mg/y; Sonke et al., 2018; Zolkos et al., 2020) is about half of their watershed annual Hg deposition north of 60°N (47.6 Mg) and comparable to the summer and snow cover period watershed Hg depositions of 25.2 Mg and 22.4 Mg north of 60°N, respectively (see Table 3.12). Considering that majority of annual river discharge occurs during spring freshet when the ground is still frozen, it is likely that Hg runoff from melting snowpacks and mobilization from surface soils comprise the majority of river Hg export to the Arctic Ocean. A two to three

Table 3.12 Model ensemble median annual and cryospheric (September–May) Hg depositions to the major Arctic river watersheds (entire watersheds and watershed portions north of 60°N) and measurement-based river Hg exports to the Arctic Ocean from Sonke et al., 2018 and Zolkos et al., 2020; blue shaded rows indicate watershed drainages mostly located north of 60°N.

River basin	Modeled deposition (±1σ) Annual (Mg)		Modeled deposition (±1σ) September to May (Mg)		Measurement-based annual river export* (Mg)
	Entire basin	Basin >60°N	Entire basin	Basin >60°N	
Yenisey	23.09±3.24	7.53±1.03	12.1±2.65	3.78±1.49	5.8 and 3.6
Lena	18.85±2.29	9.15±1.88	8.59±2.49	3.93±1.57	4.8 and 6.6
Ob	34.32±5.38	6.58±1.42	19.27±1.95	3.26±0.55	2.5 and 2.4
Mackenzie	15.74±5.00	7.34±2.30	7.79±2.18	3.38±0.91	2.2 and 2.6
Yukon	6.49±1.97	6.30±1.91	2.84±0.82	2.74±0.78	2.0 and 3.3
Pechora	2.88±0.57	2.88±0.57	1.43±0.69	1.43±0.69	1.7
Severnaya Dvina	4.13±0.67	3.60±0.57	2.23±0.19	1.94±0.19	1.2
Kolyma	4.23±0.58	4.23±0.58	1.95±1.11	1.95±1.11	0.93 and 1.1
Total	109.7	47.6	56.2	22.4	21.1

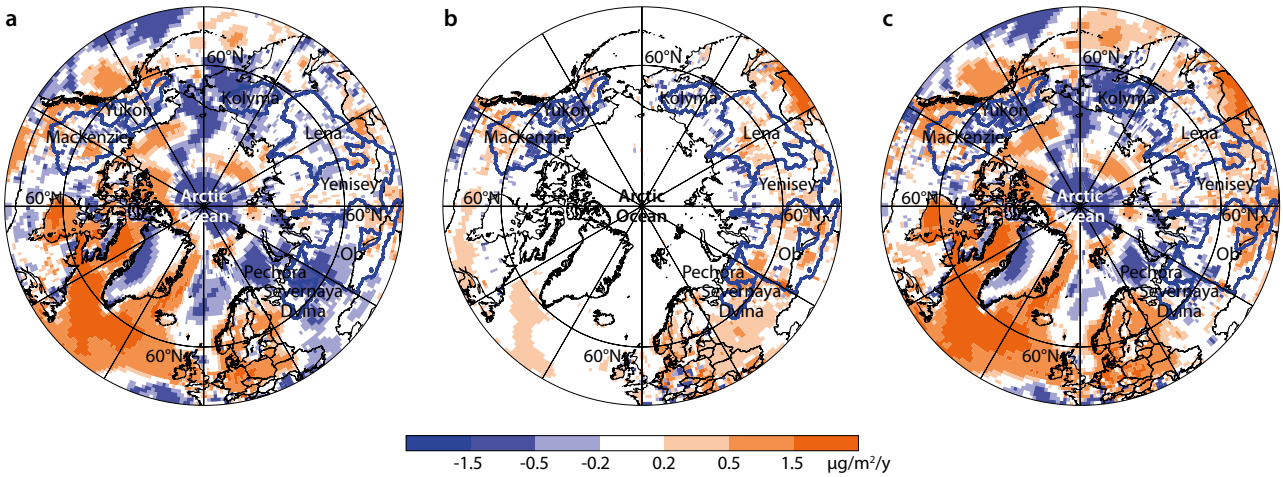

Figure 3.17 Simulated (model ensemble median) changes in annual THg deposition between 2010 and 2015 due to changes in (a) meteorology, (b) emissions and (c) cumulative changes.

times higher Hg:C ratio was observed in spring waters from Western Siberian rivers compared to other seasons, indicating Hg runoff from melting seasonal snowpacks (Lim et al., 2020). Douglas et al. (2017) measured 40% to 80% Hg runoff from melting snowpacks. Applying the snowpack Hg export rate measured by Douglas et al. (2017) to the pan-Arctic snowpack Hg loading north of 60°N (39 Mg/y) suggests that seasonally accumulated snowpack Hg and active layer surface soils each supply roughly half of the pan-Arctic river Hg export. This is in line with observations of roughly equal amounts of dissolved and particle-bound Hg in river runoff to the ocean (Sonke et al., 2018). Summertime permafrost thawing-led percolation of precipitation through soil profiles likely contributes to the minor river Hg flux in the autumn flood (Lim et al. 2019).

Soil Hg concentrations (largely driven by atmospheric deposition) decline by ~14% from the surface organic soils to the deeper mineral soil layer, and geogenic Hg contribution ranges from 0% in organic soil horizons to around 40% in mineral soil horizons in the Arctic tundra (see Section 3.4.1.2; Obrist et al., 2017; Olson et al., 2018). The dominance of snowpack and surface soil Hg in the spring river runoff suggests that present-day Hg deposition currently contributes more Hg to river Hg exports than geogenic Hg in soils. Declining Hg levels in river runoff and burbot (*Lota lota*) tissues in recent decades in major Russian rivers are thought to reflect more recent local declines in Hg emissions (Castello et al., 2014; Pelletier et al., 2017). However, intensifying hydrological cycle, permafrost thaw, and increasing river discharges due to Arctic warming are likely modifying the sources of river Hg runoff. Atmospheric Hg models integrated with terrestrial Hg models incorporating hydrology and Hg biochemistry are required to mechanistically link Hg deposition to river Hg fluxes and estimate the sources of present-day and future river Hg exports to the Arctic Ocean.

b. Recent changes in mercury deposition

Global anthropogenic Hg emissions have risen between 2010 and 2015 by about 20%, primarily due to the rise in emissions from increased industrial activity in South East Asia and ASGM (see Section 3.3). Cumulative change in Arctic Hg deposition in the period from 2010 to 2015 in response to changing emissions and meteorological conditions was investigated using three models (i.e., DEHM, GEOS-Chem and GEM-MACH-Hg) as explained in Section 3.3.2 (see Figure 3.17).

The model ensemble estimates annual average Hg deposition flux in the Subarctic to be higher in 2015 than in 2010, by ~0.5 µg/m²/y (with wet and dry deposition contributing equally). Changes in meteorology and emissions accounted for increases of 0.3 and 0.2 µg/m²/y, respectively. In the High Arctic, an increase in emissions in 2015 enhances deposition (+0.11 µg/m²/y) but no impact of meteorology variations is simulated. Models likely underestimate the impacts of meteorology on Hg deposition owing to the lack of mechanistic or interactive representation of Br sources and sea-ice dynamics, both of which are especially important in the High Arctic. Model results suggest an overall increasing Hg deposition trend in the Subarctic, driven by increasing precipitation (most notably in the northeast Pacific Ocean, the Davis Strait and the North Atlantic), changing air circulation patterns, and anthropogenic emissions. The model ensemble results suggest that changes in meteorology can exacerbate the impact of global anthropogenic emissions on Hg deposition in the Arctic regions susceptible to increasing transport and precipitation. It should be noted that there are uncertainties in estimated changes in global anthropogenic emissions (see Section 3.2).

The models applied here to temporal changes in deposition considered the changes in air circulation, temperature and precipitation. However, the models did not account for the impacts of changes occurring in the terrestrial biosphere (such as the extent of vegetation cover and the length of growing season, frequency of wildfires, the volume of legacy Hg emissions, and the re-emission of Hg from thawing permafrost) and marine environment (such as sea-ice extent and thickness or whether it was multi-year sea ice or first-year sea ice) on the Hg redox and exchange processes across the air-surface interface (Zhang et al., 2016b; Wang et al., 2020a). Climate change is expected to have a larger impact on the Hg surface exchange processes (see Chapter 5). The biogeochemical changes in the terrestrial ecosystem are likely altering the legacy Hg fluxes. The development of fully interactive atmosphere-land-ocean biogeochemical models is needed to simulate the impacts of concurrent changes in biogeochemistry in the Arctic and global Hg emissions on Hg levels and explain Hg trends in the Arctic.

3.4 How much mercury do terrestrial systems transport to downstream environments in the Arctic?

3.4.1 How much mercury is present in Arctic terrestrial environments?

The isotopic fingerprint of tundra soil Hg (see Box 3.2), characterized by terrestrial ecosystem Hg(0) uptake, has been identified in the Arctic Ocean, providing evidence of the importance of tundra soils and river runoff as an important Hg pathway. For Hg stable isotopes measured in coastal seawater, a river source was suggested to be responsible for between 50% and 80% of terrestrial Hg (Štrok et al., 2015). In a paleo-reconstruction of Hg sources to deep Arctic Ocean sediments, Gleason et al. (2017) concluded that tundra soil Hg represented the major source of Hg to ocean sediments. Mercury stable isotope signatures have been reported for a number of different marine biota in the Arctic Ocean, namely murre eggs (Point et al., 2011; Day et al., 2012), ringed seals (Masbou et al., 2015, 2018), polar bears and beluga whales (Masbou et al., 2018) and pilot whales (Li et al., 2014). Masbou et al. (2018) reviewed Hg stable isotope values in marine biota and concluded that terrestrial Hg represents the dominant source based on Δ^{200}Hg values, which are not affected by post-deposition processes. Masbou et al. (2018) further suggested that terrestrial Hg is exported from the Arctic Ocean to the North Atlantic where it represents a significant source of Hg in the food web.

3.4.1.1 Vegetation

Olson et al. (2019) summarized vegetation Hg concentration across multiple studies with a total of 150 Arctic vegetation samples and showed substantial variability among different functional groups. Mercury concentrations averaged 64±6 µg/kg in lichen (46 samples; 23–186 µg/kg); 59±6 µg/kg in mosses (n=40; 19–195 µg/kg), and 9±1 and 11±2 µg/kg in vascular plants (grasses and herbaceous plants). Pronounced concentration differences between vascular plants and lichen and mosses have been reported before across temperate sites as well as in the Arctic, including by Wojtuń et al. (2013) in Greenland (lichen: 30–100 µg/k; mosses: 20–100 µg/kg; vascular plants: 10–30 µg/kg). Mercury concentrations from Arctic vascular plants are generally below concentrations from temperate plants; for example, Wang et al. (2016) summarized vegetation Hg concentrations across 168 lower-latitude sites globally and estimated mean vegetation Hg concentrations of 54±22 µg/kg. On the other hand, bulk vegetation Hg concentrations in the Arctic can be high due to a high representation of non-vascular vegetation (i.e., mosses and lichen; Olson et al., 2018) which has implications for plant-derived Hg deposition as discussed in Section 3.3.3. Overall, these studies suggest that tundra ecosystems contain above-ground Hg biomass pools of up to 28.8 µg/m^2 (Obrist et al., 2017; Olson et al., 2019) which is similar in magnitude as foliar Hg biomass residing in forests (15 to 45 µg/m^2). For a boreal forest site (Pallas, Finland), a foliar Hg pool size of 20.7 µg/m^2 was estimated (Wohlgemuth et al., 2020).

St. Pierre et al. (2018) provide a detailed analysis of Hg concentrations in Arctic lichen, which are critically important forage substrates for caribou, showing median total Hg concentrations on Bathurst and Devon islands in northern Canada of 66.8 µg/kg (with a range from 36–361 µg/kg). Lichen Hg concentrations were two orders of magnitude higher than in underlying soils suggesting atmospheric deposition as a dominant source of Hg, with sources likely including Hg(0) uptake, dust, and wet Hg deposition. Total Hg and MeHg enrichment in lichen were greater at coastal sites than at inland sites; this suggests proximity to polynyas leads to enhanced Hg deposition, possibly via AMDEs, halogens, ocean evasion and/or boundary layer mixing. Summarizing Hg levels in lichen from other Arctic studies, St. Pierre et al. (2018) show substantial variability in lichen Hg concentrations (10–270 µg/kg). Lichen concentrations were 48±5 to 107±123 µg/kg (Gamberg, 2009) and 43 to 255 µg/kg (Chiarenzelli et al., 2001) in the Northwest Territories, Canada; 10 to 270 µg/kg in northern Quebec, Canada (Crête et al., 1992); 43 to 56 µg/kg (Landers et al., 1995) and 32 to 47 µg/kg (Lokken et al., 2009) in Alaska; and 13 to 98 µg/kg in the White Sea, Russia (Shevchenko et al., 2013). Earlier studies also reported moss Hg data, including 55 µg/kg in feather moss (*Ptilium crista-castrensis*) across northern Alaska (Landers et al., 1995) and 113 µg/kg in fringe mosses and lichen from Svalbard (Drbal et al., 1992). A general south-north declining gradient in Hg concentrations in moss was observed in Sweden in a 2015 report by the Swedish Environmental Research Institute (IVL, 2015); the concentration of Hg was lower in samples from the inland and mountain area in northern Sweden compared to the coastal area in northern Sweden as well as to other parts of the country.

The potential use of lichen and mosses as monitors for atmospheric Hg exposure and/or deposition in the Arctic has shown limited success. Nickel et al. (2015) correlated concentrations of heavy metals in atmospheric deposition with Hg accumulation in moss and soils across large south-to-north gradients in Norway, including Arctic locations, and showed that correlations were weak for Hg. Harmens et al. (2010, 2015) previously showed a lack of correlations between modeled atmospheric Hg deposition and moss concentrations across a large network of sites in Europe and reported that moss collected in Norway showed no distinct north-to-south patterns in spite of expected gradients in atmospheric Hg pollution.

3.4.1.2 Soils

a. Mercury concentrations and Hg:C ratios in active layer and permafrost soils

Substantial progress has been made to understand Hg levels in Arctic soils and in the Arctic and boreal permafrost zone. We summarized data from five publications with available Arctic soil data with a total sample size of 1294 data points (Leitch, 2006; Outridge and Sanei, 2010; Olson et al., 2018; Schuster et al., 2018; Lim et al., 2020) to provide the following summary statistics of Arctic soil Hg concentrations.

Schuster et al. (2018) measured Hg concentrations across 13 northern permafrost cores (taken from a depth of 0–300 cm) along a ~500 km transect in northern Alaska. They reported THg concentrations in permafrost ranging from 17 to 207 µg/kg (with a mean of 64 µg/kg) and across all soil samples (including active layer samples) they reported median Hg

Box 3.2 Mercury stable isotopes: identification of mercury sources in Arctic terrestrial ecosystems

Mercury has seven stable isotopes that can undergo both mass-dependent fractionation (MDF, reported as δ^{202}Hg) and mass-independent fractionation of odd mass number (odd-MIF, reported as Δ^{199}Hg and Δ^{201}Hg) and even mass number (even-MIF, reported as Δ^{200}Hg and Δ^{204}Hg) isotopes (Blum et al., 2014; Obrist et al., 2018). Sources of atmospheric Hg in Arctic tundra ecosystems and subsequent processes are associated with characteristic MDF and MIF (see Figure 3.18).

Uptake of atmospheric Hg(0) by vegetation is associated with mass-dependent fractionation (MDF; δ^{202}Hg) and discriminates heavy isotopes, resulting in an enrichment of lighter Hg in vegetation (negative δ^{202}Hg values, see arrow 1 in Figure 3.18) and consequently a depletion of light isotopes in atmospheric Hg(0) (positive δ^{202}Hg values; Obrist et al., 2017; Olson et al., 2019; Jiskra et al., 2019). The absence of mass-independent fractionation (the MIF; Δ^{199}Hg and Δ^{200}Hg) has been observed during the foliar uptake of Hg(0) in temperate regions (Yuan et al., 2019) and is not expected to occur in the Arctic either. Using a chamber experiment, Sherman et al. (2010) showed that following Hg(II) deposition during AMDEs there was a strong re-emission of Hg(0) driven by photo-induced reduction processes. The photoreduction of Hg(II) in snow was associated with a strong fractionation of odd-mass Hg stable isotopes (see arrow 2 in Figure 3.18) and Δ^{199}Hg values of -5.5‰ were observed, some of the most negative Δ^{199}Hg values reported globally (Sherman et al., 2010). The two characteristic Hg stable isotope fractionation processes, uptake of Hg(0) by vegetation and snow and photoreduction of AMDE-derived Hg(II) in snow, make Hg stable isotopes a potent tracer for sources of atmospheric Hg and processes in the Arctic.

Obrist et al. (2017) measured the Hg stable isotope signature of atmospheric Hg deposition (Hg(0), Hg(II)) in snow and different ecosystem sinks (bulk vegetation, organic and mineral soils) at Toolik Field Station, on the Arctic Coastal Plain in northern Alaska, 200 km from the Arctic Ocean. Using a multi-isotope mixing model, they concluded that the uptake of Hg(0) by vegetation was the dominant source of atmospheric Hg deposition, representing 90% of the THg in vegetation (interquartile range; IQR: 86% to 94%), 71% in organic soils (IQR: 56% to 81%) and between 25% and 54% in mineral soils. The absence of large negative Δ^{199}Hg values in ecosystem sinks suggests a large part of Hg deposited during AMDEs is emitted back to the atmosphere. For Utqiaġvik on the coast of the Arctic Ocean, a re-emission between 76% to 91% was estimated based on Hg stable isotopes (Douglas and Blum, 2019). Other studies focused on identifying the fraction of AMDE-derived Hg that remains in the snowpack and reported that roughly 75% of the AMDE Hg is re-emitted (Douglas et al., 2012, 2017; Durnford et al., 2012). At inland sites, such as the Toolik Field Station, a re-emission of >95% has been estimated (Obrist et al., 2017). As a consequence, AMDE-derived Hg(II) deposition appears to have only a minor contribution to total Hg in Arctic ecosystems.

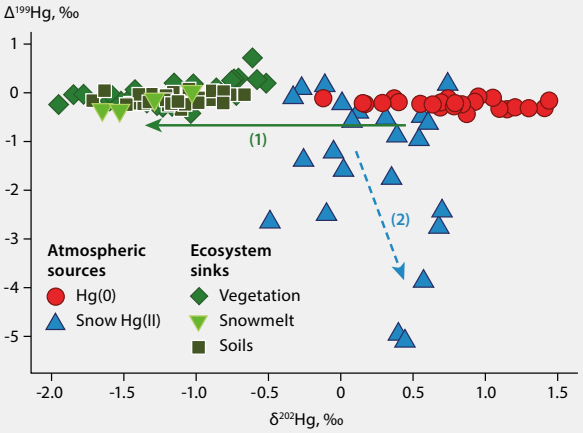

Figure 3.18 Synthesis of Hg stable isotope fingerprints in terrestrial Arctic Hg cycling. Mass independent (Δ^{199}Hg) versus mass dependent (δ^{202}Hg) of atmospheric sources (Hg(0) and Hg(II) in snow (Sherman et al., 2010; Obrist et al., 2017; Jiskra et al., 2019) and ecosystem sinks (vegetation, snowmelt and soils; Biswas et al., 2008; Obrist et al., 2017; Olson et al., 2019; Douglas and Blum, 2019). Two processes drive Hg stable isotope fractionation in the terrestrial Arctic: (1) the uptake of atmospheric Hg(0) by vegetation and snow (Demers et al., 2013; Jiskra et al., 2019; Douglas and Blum, 2019) and (2) photochemical reduction of Hg(II) in snow (Sherman et al., 2010).

Douglas and Blum (2019) observed that Hg(0) dry deposition to the snowpack represented a significant contribution of the total deposition of Hg to snow close to the Arctic coast. They suggested high concentrations of reactive halogens promoted the oxidation of atmospheric Hg(0) within the snowpack and contributed significantly to Hg(0) dry deposition to the ecosystem. A similar process has been observed in frost flowers (ice crystals forming over sea ice containing high halogen concentrations) which were characterized by positive Δ^{199}Hg (max=0.9‰) resulting from re-emission of Hg(0) after AMDEs (Sherman et al., 2012). On the Arctic Coastal Plain, 200 km from the coast and where halogen concentrations in snow are substantially lower, no significant deposition of Hg(0) to the snowpack was observed, and net Hg(0) deposition fluxes during winter were consistent with the uptake of Hg(0) by surface vegetation including lichen (Jiskra et al., 2019). Olson et al. (2019) measured Hg stable isotope signatures in different plant species and suggested that the uptake of atmospheric Hg(0) was the major source of Hg in all plant species. Different Δ^{199}Hg values in plant species, however, suggested a different extent of photoreductive Hg loss inducing Δ^{199}Hg anomalies, with lichen showing significant Hg loss through photoreduction whereas no indication for photoreductive loss was observed for vascular plants.

concentrations of 43±30 µg/kg and Hg-to-carbon ratios (Hg:C) of 1600±900 µg Hg/kg C. Olson previously summarized Hg concentrations of Arctic soils (478 data points) of 40 µg/kg in both organic and mineral soils with and Hg:C ratios (295 sample points) of 174 µg/kg C in upper organic soils (0–30 cm, organic) and 621 µg/kg C in deeper mineral soils (30–100 cm). Lim et al. (2020) reported Hg concentrations and Hg:C ratio for six peat cores along a latitudinal transect (56°N–67°N) in the Western Siberian lowlands, an area for which few Hg observations exist, despite the fact that Eurasian permafrost contains 54% of the C inventory in northern soils. Mercury concentrations in peat cores ranged from 7 to 284 µg/kg with a

Table 3.13 Concentrations of Hg in active layer soils and permafrost layers reported from the Arctic. All concentrations are reported in µg/kg. Parentheses are Hg:C concentration ratios in µg Hg/kg C.

Soil type	Mean	Median	IQR	Min	Max	Data points
Soil samples, all	68 (1740)	55 (813)	37–95 (196–1855)	3	303	1294
Active layer, all	81 (582)	65 (270)	45–103 (86–487)	4	303	380
Active layer, surface (top 30 cm + peat + organic soils)	87 (191)	70 (148)	45–121 (61–318)	7	303	277
Active layer, below-surface (>30 cm and mineral soils)	66 (1510)	60 (927)	45–87 (548–2058)	4	149	103
Permafrost, all	63 (2042)	48 (1225)	36–91 (261–2087)	3	284	912

median (±IQR) of 67±57 µg/kg. The Hg:C ratio ranged from 50 to 2000 µg Hg/kg C with a median of 133 µg Hg/kg C. Mercury soil pool (0–100 cm) increased with latitude from 0.8 mg Hg/m^2 at 56°N to 13.7 mg Hg/m^2 at 67°N.

Several studies have evaluated depth distributions in active layer soils. Olson et al., 2018 reported the highest Hg concentrations in organic surface layers at Toolik Field Station (151±7 µg/kg), followed by A-horizons (108±10 µg/kg), B-horizons (with a mean of 87± 5µg/kg), and lowest in the frozen horizon at the bottom of the pits (i.e., in the transient permafrost layer; 56±2 µg/kg). Although soil Hg concentrations declined with depth as observed previously in temperate soil studies (e.g., Obrist et al., 2011), Olson et al. (2018) suggested that this trend was not as pronounced in Arctic soils compared to temperate studies possibly due to enhanced soil mixing via cryoturbation processes. The data summary on Arctic soil Hg concentrations in Table 3.13 shows a 14% decline in Hg concentrations between the surface organic soils and the deeper mineral soil layer. Similar depth distributions were observed across other Alaskan sites such as in Halbach et al. (2017), who also reported higher ranges, medians and means in organic surface soils compared to minerals soils in Svalbard.

Other recent Arctic soil Hg studies include the following: Hao et al. (2013), who reported a baseline of 270 µg/kg and a range of 210 to 380 µg/kg in surface soils at Ny Ålesund; Loseto et al. (2004a), who reported a range of 10 to 250 µg/kg in the humus layer of wetland soils; St. Pierre et al. (2015), who reported a range of <1 to 86 µg/kg in surface soils from the High Canadian Arctic; Rigét et al. (2000), who reported geometric means of <10 to 30 µg/kg in mineral and 20 to 117 µg/kg in organic soils from Greenland; the previous AMAP assessment (2011) which reported a range of 40 to 150 µg/kg in soils from the Russian Arctic; St. Pierre et al. (2015), who reported a range of 0.98 to 86.4 µg/kg in soils from Bathurst and Devon islands in the CAA; and Douglas and Blum (2019), who reported Hg concentrations of 320 µg/kg in surface organic soils, 63 to 80 µg/kg in active layer soils, and 66 to 83 µg/kg in permafrost soils from northern Alaska. Peat deposits from drained thaw lake basins near Utqiaġvik, Alaska, have yielded elevated THg concentrations in surface layers (<100 years old; Biswas et al., 2008), and peat core cross sections showed elevated Hg concentrations in surface vegetation and the upper soil horizon compared to lower (older and more decomposed) permafrost peats (Douglas and Blum, 2019).

It is now widely understood that sources of Hg in active layer soils are largely driven by atmospheric Hg deposition. Source attribution based on elemental ratios and Hg stable isotopes showed that for Toolik Field Station in Alaska about 70% (IQR: 56% to 81%) of Hg in surface O-horizons were derived from atmospheric Hg(0); 54% (IQR:43% to 62%) in A-(mineral) horizons and 24% (IQR: 14% to 34%) in B-horizons (Obrist et al., 2017), with the rest originating from oxidized Hg deposition and geogenic background (i.e., Earth crustal) sources. Based on limited samples, geogenic bedrock concentrations along the Dalton Highway in Alaska, where most Arctic samples were taken (Olson et al., 2018; Schuster et al., 2018), were estimated at 32 µg/kg (Obrist et al., 2017; Olson et al., 2018). Geogenic fractions in mineral soils of Alaska were estimated between 20% in A-horizons to 40% in B-horizons (Obrist et al., 2017; Olson et al., 2018), with the rest originating from external sources such as atmospheric deposition. Halbach et al. (2017) similarly reported that surface soil Hg in Svalbard was not associated with typical geogenic elements (e.g., Al, As, Cr, Cu, Fe, Ni) indicating soil Hg to be largely derived from atmospheric deposition accumulating in organic-rich surface soils.

b. Mass estimates of soil Mercury in Arctic active layer and permafrost soil

Schuster et al. (2018) estimated Hg pools contained in Northern Hemisphere permafrost regions, and, extrapolating, measured Hg:C ratios along the Alaska transect using soil carbon maps from the Northern Circumpolar Soil Carbon Database (NCSCD; Hugelius et al., 2013, 2014). They estimate that permafrost soils (0–3 m) contain 1656±962 Gg Hg of which 793±461 Gg Hg is frozen in permafrost layers and 863±501 Gg Hg are stored in the active layer. With regards to spatial distribution, they predicted that soils with high C content and high sedimentation show the highest Hg mass, for example in soils across the North Slope of Alaska and the Mackenzie River Basin in Canada. Using a similar scaling approach, Olson et al. (2018) summarized Hg:C ratios derived from 15 published studies on Arctic soils reporting a median Hg:C ratio of 274 µg/kg (with a range of 25–833 µg/kg) for organic soils and 621 µg/kg (with a range of 450–911 µg/kg) for mineral soils. Using the same soil C inventory as Hugelius et al. (2014), they estimated a lower median Arctic tundra active layer soil Hg pool in the upper 0–30 cm of 26 Gg with a range of 21 to 42 Gg. For a depth of 30–100 cm, they estimated a Hg mass of 158 Gg (with a range of 115–232 Gg) for a total active layer soil Hg pool size

in the Arctic in the upper 100 cm estimated at 184 Gg (with a range of 136–274 Gg). Lim et al. (2020) reviewed pan-Arctic Hg/C ratios including new data from Western Siberia and estimated Hg:C ratios of 190 µg/kg (IQR: 90–240 µg/kg) for organic soils and 770 µg/kg (IQR: 320–800 µg/kg) in mineral soils. Using the pan-Arctic C budget of Hugelius et al. (2014), they estimated a Hg pool of 72 Gg (IQR: 39–91 Gg) for a depth of 0 to 30 cm, 240 Gg (IQR:110–336 Gg) for 0 to 100 cm, and 597 Gg (IQR: 384–750 Gg) for 0 to 300 cm. In summary, both Olson et al. (2018) and Lim et al. (2020) suggest about three to four times lower soil Hg pools compared to Schuster et al. (2018). For example, they estimate 184 Gg (Olson et al., 2018) and 240 Gg (Lim et al., 2020) of Hg to reside in the top 1 m of soils (largely in the active layer), compared to Schuster et al.'s estimate of 863 Gg in the active layer. Similarly, Lim et al. estimated 597 Gg of Hg in the top 3 m of permafrost compared to 1656 Gg estimated by Schuster et al. (2018). These lower estimates are in part due to new data from Western Siberia in Lim et al. (2020), who reported lower Hg:C ratios and possibly lower geogenic Hg concentrations in Siberian soils compared to northern Alaskan soils. Another likely reason is that Hg:C ratios in Schuster et al. (2018) are based exclusively on permafrost data, leading to a bias towards higher Hg:C ratios. Our data summary in Table 3.13 shows that Hg:C ratios in surface soils and active layer soils to be much lower compared to permafrost soils, which is driven by higher C contents of upper soils due to high rates of C input by vegetation from the surface. It has been proposed that Arctic active layer and permafrost soils contain massive amounts of Hg and form the largest Hg pool size of Hg globally storing nearly twice as much Hg as in all other soils, the ocean and the atmosphere combined (Schuster et al., 2018). A caveat to this statement, however, is that the Arctic pool sizes by Schuster et al. were estimated to a depth of 300 cm while global soil pool estimates are generally limited to surface soils only (i.e., the upper 30 cm) as illustrated by the following estimates: ~240 Gg (Smith-Downey et al., 2010); ~300 Gg (Hararuk et al., 2013); 250 to 1000 Gg with a best estimate of 500 Gg (Amos et al., 2015); 1078 Gg (IQR: 842–1254 Gg; Lim et al., 2020). When comparing the same soil depths, Lim et al. (2020) estimate Arctic soil pools of the upper 30 cm to account for about 7% of the global soil pool.

3.4.1.3 Snowpack and snowmelt

Studies from coastal Utqiaġvik (formerly Barrow, Alaska) indicate Arctic inland and coastal deposition pathways may differ substantially and this is likely due to the presence of halogen-rich snow and ice at coastal locations (Poulain et al., 2007a; Krnavek et al., 2012). It has recently been reported that the presence of halogens in snow decreases the photoreductive loss of Hg (Mann et al., 2015, 2018). At coastal sites, snowmelt is a critical source of Hg to soils and watersheds (Dommergue et al., 2003; Douglas et al., 2017). One of the most unique aspects of the Arctic terrestrial system is the spring freshet: during spring melt, which can occur in as little as 10 days (see Figure 3.19), up to 70% of the yearly surface water discharge runs from the land to the sea (McNamara et al., 1998). Riverine DOC concentrations peak during melt, and roughly 60% of the annual DOC export from major Arctic rivers occurs during breakup (Guo et al., 2012). Ultimately, Hg in the snowpack meets one of three fates during spring snowmelt: (1) it is re-emitted during snow metamorphism and melt, (2) it ends up in the freshwater or marine system from runoff, or (3) it is taken up by tundra and taiga ecosystems. The early pulse of meltwater from this snow includes an ionic pulse of major elements and Hg; however, the majority of the Hg deposited during the winter season is re-emitted prior to the movement of meltwater across the landscape (Dommergue et al., 2003; Douglas et al., 2017).

Numerous studies have focused on the fate of snowpack Hg upon melt. There are some discrepancies in the overall assessment of the snowpack as a source of Hg via meltwater. For example, St. Louis et al. (2005, 2007) and Dommergue et al. (2010) report that spring meltwater was not a major source of THg or MeHg to Arctic seawater at coastal locations. However, other studies have identified elevated THg and MeHg in snow meltwater (Berg et al., 2003; Dommergue et al., 2003; Loseto et al., 2004b).

On the basis of the overall snowpack depth measurements in a small coastal watershed (Alaska), Douglas et al. (2017) calculated the net end of winter snowpack Hg prior to the melt as ~1.8 to 2 µg/m^2 in 2008 and 2009. They further reported a strong ionic pulse of major ions and Hg in the watershed during spring snowmelt, reporting measurements of dissolved Hg meltwater runoff of 8 and 14 ng/L for 2008 and 2009, respectively, up to seven times greater than runoff reported from non-coastal Arctic locations (Douglas et al., 2017). Douglas and Blum (2019) subsequently measured even higher snow Hg concentrations (69–416 ng/L), which was more than 30 times greater than the highest concentration reported from inland snow (e.g., Agnan et al., 2018). Based on stable Hg isotope signatures, they attribute atmospheric gaseous elemental mercury to comprise the majority of Hg in snow while AMDE-related Hg(II) comprised less (9% to 24% of total snow Hg). The suggested mechanism that dominates Hg

Figure 3.19 Repeat images during spring melt in Utqiaġvik (formerly Barrow), Alaska, during a typical spring melt. In a matter of a few weeks, the tundra surface transforms from being completely snow-covered to a wet vegetation and soil surface exposed to continuous sunlight.

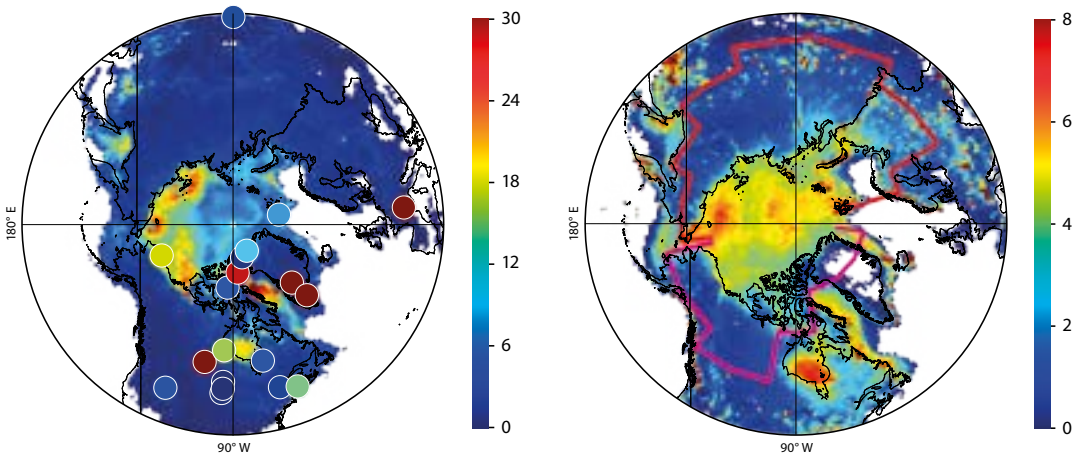

Figure 3.20 Modeled 5-year average (2005–2009) concentration (ng/L) of THg in snowpack along with sample-size weighted measured (mainly springtime) mean concentrations from multiple years, compiled from literature in Durnford and Dastoor, 2011 (left); and average meltwater Hg yield (μg/m^2/y) in an Arctic watersheds simulation using GEM-MACH-Hg (right). The areas in North America and Russia that drain into the Arctic Ocean are outlined in magenta and red, respectively (Durnford et al., 2012; Dastoor and Durnford, 2014). Sources: (a) adapted from Durnford et al., 2012 (Figure 2b); (b) adapted from Dastoor and Durnford, 2014 (Figure 3).

deposition at the coastal site is Hg(0) deposition and oxidation of Hg(0) within the snowpack mediated by halogens which are enriched in coastal snowpack.

In a modeling study, Durnford et al. (2012) simulated average springtime concentrations of THg exceeding 10 ng/L in snowpacks over land and sea ice in coastal regions of the Canadian Arctic Archipelago, between Canada and Greenland, and in Hudson Bay (see Figure 3.20). Simulated and observed average inland snowpack concentrations of THg are generally well below 10 ng/L. Dastoor and Durnford (2014) simulated transfer of snowpack deposited Hg to meltwater in the range of ~1 to 3 μg/m^2/y (with highest concentrations in coastal regions) with total atmospheric contributions to meltwater of 8.0, 31.2 and 39 Mg/y in North America, Russia and circumpolar Arctic watersheds, respectively.

3.4.2 How much mercury does permafrost contribute to downstream environments in the Arctic?

Estimates of THg stores in permafrost within Arctic soils range between 793±461 Gg Hg (Schuster et al., 2018) and 332 Gg Hg (Lim et al., 2020). These estimates are equivalent to 48% or 60% of the total Arctic soil Hg pool (1656±962 Gg or 557 Gg; 371–699 Gg) according to Schuster et al. (2018) and Lim et al. (2020), respectively (see Section 3.4.1.2b). As permafrost thaw is already widespread across the Arctic, these stores are thus a potentially important source of Hg to downstream environments. Although THg stores in permafrost across the Arctic are now somewhat constrained—a key development since the previous AMAP Hg assessment in 2011—the contribution of permafrost thaw to THg mobilization to downstream ecosystems is more difficult to quantify. Ultimately, this contribution depends on local conditions affecting Hg storage and permafrost properties (e.g., ice and C content, glacial history, vegetation cover; Vonk et al., 2015a; Tank et al., 2020).

In regions underlain by ice-rich permafrost, other landscape and climatic characteristics (e.g., topography and precipitation regimes) determine landscape susceptibility to different modes of thermokarst formation (Olefeldt et al., 2016). St. Pierre et al. (2018) estimate that ~5% of the THg in Arctic soils (based on Schuster et al., 2018; 88 Gg) of the circumarctic may occur in regions susceptible to the development of hillslope thermokarst features, such as retrogressive thaw slumps. These large features (up to 40 ha) can quickly mobilize vast amounts of previously stored, mostly particulate-bound Hg directly into streams, rivers or lakes and through to downstream ecosystems. On the Peel Plateau in the western Canadian Arctic, concentrations of THg in streams were up to two orders of magnitude higher downstream of slumps than upstream, reaching concentrations of up to 1270 ng/L (mean: 448±87 ng/L), some of the highest Hg concentrations ever recorded. While concentrations were only measured up to 2 km downstream of the slumps in St. Pierre et al. (2018), Emmerton et al. (2013) reported THg concentrations in the mainstem Peel River (18 ng/L) higher than elsewhere in the Canadian Arctic (Northern Contaminants Program, 2012), suggesting that these elevated concentrations could be at least partially attributed to permafrost thaw across the watershed. Permafrost thaw has also been invoked to explain longer term increases in THg exports in the Yukon River (Schuster et al., 2011). Conversely, Hg mobilized by thaw slumps along lake shorelines is rapidly deposited to the bottom of the lakes. Deison et al. (2012) reported no difference in THg deposition rates between slump-affected (26.61±6.92 μg/m^2/y) and reference lakes (25.35±3.01 μg/m^2/y) of the Mackenzie uplands, an observation driven by lower THg concentrations, but higher sedimentation rates in the slump-affected lakes. The impact of slumps on lake shorelines may, however, differ depending on the lake and region.

With sampling sites spanning a 1700 km transect in the Western Siberian Arctic, Lim et al. (2019) quantified particulate Hg yields from sites across a permafrost gradient: from where permafrost was absent (0.189±0.048 g/km^2/6-months), through to the isolated (0.205±0.056 g/km^2/6-months), sporadic (0.379±0.096 g/km^2/6-months), discontinuous (0.350±0.225 g/km^2/6-months), and continuous (0.170±0.042 g/km^2/6-months) permafrost zones. Maximal

particulate Hg yields from areas underlain by sporadic and discontinuous permafrost zones suggest that these zones may be hotspots of Hg fluxes to the Arctic Ocean.

Much of the cited work, though, is biased to regions underlain by ice-rich permafrost, which favours the dramatic landscape destabilization and rapid (years to decades) pulses of materials to downstream ecosystems (termed 'pulse disturbances'; Vonk et al., 2015a). So called 'press disturbances' from thawing permafrost (i.e., active layer deepening) occur more widely across northern landscapes, but are much more subtle, and, therefore, the consequences are more difficult to detect without longer term monitoring (across multiple decades). Given the spatial and temporal variability in thaw processes, it is difficult (if not impossible) at present to quantify how much permafrost thaw contributes to THg exports from Arctic watersheds. Permafrost thaw is highly irregular across the landscape and may result in vastly different trends in Hg mobilization and accumulation rates, even within a single geographic region (Burke et al., 2018). However, the well-documented relationships (e.g., Schuster et al., 2018; Sonke et al., 2018) between permafrost organic carbon (OC) and Hg exports can be exploited to constrain the permafrost Hg contribution to downstream ecosystems.

3.4.3 How much mercury do ice sheets, ice caps and glaciers contribute to downstream environments in the Arctic?

Continuous spaceborne gravimetric observations since 2002 confirm that all glaciated areas of the Arctic and Subarctic are presently shrinking due to climate warming, and the overall ice-mass loss rate is accelerating at a rate of 50±20 Gt/y per decade (Forsberg et al., 2017; Ciracì et al., 2020). Melting glaciers can export both inorganic and organic Hg to freshwater networks and the Arctic Ocean. The Hg is transported in meltwater streams produced by both seasonal thaw and long-term mass wastage (i.e., sustained negative mass balance), and the latter contribution is forecasted to increase in most glaciated areas of the Arctic and Subarctic as high latitudes continue to warm in the 21st century (Milner et al., 2017). The Hg exported from glaciated basins comes from both anthropogenic and geogenic sources. Some of it is atmospheric Hg which was deposited to snow (primarily as Hg(0) and Hg(II) but also as MeHg) in the accumulation zone of glaciers and was subsequently buried in firn and glacier ice, to be later released by melt. This includes Hg that was emitted from anthropogenic sources in the past two centuries. Accumulation of atmospheric deposition over millennia has also led to the build-up of a large pool of Hg in Arctic soils (see Section 3.4.1.2), some of which may enter glacier-fed rivers. An additional geogenic Hg fraction is derived from bedrock by glacial erosion. The Hg derived from soils and bedrock is bound or absorbed to suspended clay and silt mineral particles in turbid, glacier-fed streams.

While the release of Hg from melting glaciers may be of concern, the rate at which it occurs now, or might proceed in the future, is highly uncertain. This is in part because the size of the anthropogenic pool of Hg stored in glaciers is poorly quantified. Data from high-latitude (>50°N) glacier ice cores in Greenland, North America and central Asia show that some firn and ice strata that formed between the mid 19th and late 20th centuries are enriched in THg by factors of ~2 up to 15 relative to older, pre-industrial ice, the largest enrichments being reported in mountain ice caps of central Asia and the Yukon (Zheng, 2015; Zdanowicz et al., 2016; Eyrikh et al., 2017, and references therein). However, to quantify the mass and release rate of legacy anthropogenic Hg in glaciers requires site-specific knowledge of their internal age structure, which is largely missing outside of Greenland, and of their mass turnover rates, which are likely to change in a warming climate.

Meltwater issued from recent (20th–21st century) firn and ice strata might contain higher THg levels than older ice, but the largest increases in surface ablation on glaciers and ice caps occur at their margins, where older ice strata usually outcrop, which are likely to contain less Hg. Hence, as Arctic and Subarctic glacier recession accelerates, the relatively Hg-enriched water issued from melt-out of recent (industrial-age) layers will be increasingly diluted by larger volumes of old ice meltwater with lower Hg content, such that the concentration of Hg in mixed glacial meltwater might not change greatly, although the total mass released will. A compilation of worldwide hypsometric data shows that outside Greenland ~75% of northern high-latitude (>50°N) glaciers and ice caps have net accumulation zones that cover less than half of their total area, and frequently less than a third of it (Mernild et al., 2013). Many of these glaciers may therefore only store a limited mass of legacy anthropogenic Hg deposited in past centuries. In addition, some mountain glaciers with fast turnover rates (e.g., in Alaska) and stagnant or nearly-stagnant Arctic ice caps (with little or no net accumulation) have had sustained negative mass balances for many decades, or even longer (e.g., Sneed et al., 2008; Malcomb and Wiles, 2013; Serreze et al., 2017) and might therefore have already released most or all of the legacy anthropogenic Hg that was stored in firn and ice.

The largest potential glacial reservoir of anthropogenic Hg in the Northern Hemisphere, the Greenland Ice Sheet, is experiencing accelerating wastage, but only ~35% of mass losses in the past half-century occurred through surface melt, the remainder being due to dynamic discharge of tidewater glaciers, which drain both old and young ice from marginal sectors of the ice sheet (Mouginot et al., 2019). Furthermore, an unquantified, and possibly large, fraction of meltwater produced at the surface of Greenland is not immediately discharged but accumulates instead within the firn, either by refreezing or in liquid form within 'firn aquifers', the extent, volume and water quality of which are largely unknown (e.g., Christianson et al., 2015). Similar aquifers may exist on other Arctic ice caps (e.g., Svalbard). The mixing of meltwater issued from different parts of glaciers (or groundwater) within their drainage system further complicates matters, making accurate forecasts of Hg releases presently difficult.

Estimates of the total mass of atmospherically-derived Hg (from anthropogenic and natural sources) presently stored in Arctic glaciers can be made using THg measurements from snow and ice cores and current glacier ice volume assessments. Decadal mean THg concentrations in Greenland snow, firn and ice cores spanning the period between approximately 1748 and 2010 have increased over time from 1.0 pg/g in 1748–1850, to 1.6 pg/g in 1851–1970, and 2.2 and 3.4 pg/g in the 1970s and

Table 3.14 Estimates of Hg storage in large Arctic glacial reservoirs (>10^3 km^3) and of annual Hg releases to Arctic marine waters from glacier ice melt.

	Ice volume* (10^3 km^3) mean±SD	Hg storage (tonnes; t) mean±SD	Ice loss rate* (10^9 t/y) mean±SD	Hg release rate (kg/y) mean±SD
Greenland	2866±716	2348±22	265±25	241.5±6.3
Canada	37±10	29.8±0.5	73±9	66.5±1.7
Alaska	19±5	15.6±0.3	73±8	68.2±1.7
Russia	15±4	12.3±0.1	20±6	13.4±0.5
Svalbard	7±2	5.6±0.1	12±3	6.2±0.3
Iceland	4±1	3.3±0.1	16±4	3.6±0.1
Rounded totals:		2415±22		400±7

*Ice volume estimates from the Geological Survey of Denmark and Greenland, and from Farinotti et al., 2019, assuming uncertainties of ±25%.
** Ice loss rates from Forsberg et al., 2017 (Greenland) and Ciracì et al., 2020 (other areas). Mercury release estimates do not include Hg from terrestrial subglacial sources. The Greenland figures include the ice sheet and peripheral ice caps.

1990s, respectively (Boutron et al., 1998; Brooks et al., 2011; Zheng, 2015). The THg concentrations in pre-20th century firn and ice strata are mostly ≤1.5 pg/g of ice, comparable to levels in pre-industrial, Holocene ice layers (~0.7–1.4 pg/g; unpublished data, GISP2 core) and also in Holocene layers from Canadian Arctic ice caps (≤1 pg/g; Zdanowicz et al., 2016). Since glacial ice layers of different ages contain different Hg levels that mix upon melt, the Hg concentration in meltwater is likely to vary in space and time. Furthermore, because the probability distribution of THg in snow and ice is positively skewed, mean concentrations overestimate the central tendency in these data. For example, decadal mean THg concentrations in cores from Greenland and some Canadian Arctic ice caps are up to 50% to 60% greater than median concentrations (Zheng, 2015; Zdanowicz et al., 2016). Based on available data from these cores (n=1027), a realistic estimate of the median THg concentration that can be expected in mixed-source Arctic glacial meltwater is 0.8 ng/L, with an interquartile range of 0.5 to 1.2 ng/L. The size of the Arctic glacial Hg reservoir can be assessed by scaling up these figures using current estimates of glacier ice volumes from Farinotti et al. (2019). This was done though a Monte Carlo simulation (n=1000 iterations) in which a log-normal distribution was assumed for THg concentrations in ice and a normal distribution for uncertainties on glacier volumes. Based on this probabilistic approach, the mean size of the Arctic glacial Hg reservoir is estimated to be 2415±22 t, ~97% of which is in Greenland (see Table 3.14).

The annual rate at which Hg is being released from thawing glacier ice into Arctic marine waters can also be estimated using spaceborne gravimetric measurements of glacier mass shrinkage, which include losses from melt as well as tidewater calving (Forsberg et al., 2017; Ciracì et al., 2020). Such an estimate does not, however, include Hg from subglacial geogenic (organic or inorganic) sources. Assuming, as before, a median THg concentration in glacial meltwater of 0.8 ng/L and using glacier mass loss rates in the past ~15 to 17 years from Forsberg et al. (2017; Greenland) and Ciracì et al. (2020; other areas) yields a figure of 400±7 kg for the average mass of Hg released annually from melting Arctic glacier ice, with Greenland contributing ~60%; see Table 3.14).

Presently, data on Hg in glacier-fed streams of the Arctic and Subarctic are available from northern Greenland (Rigét et al., 2011b; Søndergaard et al., 2015), Svalbard (Dommergue et al., 2010), the CAA (Baffin and Ellesmere islands; St. Louis et al., 2005; Zdanowicz et al., 2013; St. Pierre et al., 2019), the Yukon (Halm and Dornblaser, 2007; Zdanowicz et al., 2018) and Southeast Alaska (Nagorski et al., 2014; Vermilyea et al., 2017; see Table 3.15). Most of these data come from measurements made in late spring or summer months (May–August). Together, they show that THg concentrations in glacier meltwater filtered to 45 mm (filtered total mercury; FTHg) are very low, typically <1 ng/L (cf. Section 3.4.3). The FTHg concentrations in glacier-fed rivers are also within the range of values found in the pre-industrial sections of Arctic glacier ice cores (Zdanowicz et al., 2016), so there is presently no compelling evidence of anthropogenic Hg enrichment in meltwater issued from Subarctic or Arctic glaciers. If such Hg is being released, it is too diluted to be distinguished from that naturally present in glacier ice. Mercury concentrations in unfiltered waters (UTHg) of turbid subglacial or proglacial streams are commonly much higher than those of FTHg, up to 73.73 ng/L, indicating that the bulk of Hg in these streams is particle-bound (PHg). Estimates of the PHg fraction in glacier-fed streams range from between 34% and 98%, and are typically >50%.

The reported data above make it clear that most riverine Hg export from glaciers is in particulate form and is likely from deposited Hg in soils and from bedrock erosion. The Hg content in stream sediments of upslope basins that are unimpacted by pollution point sources (e.g., mines) reflects that of Hg deposition and bedrock lithologies (e.g., Nasr et al., 2011; Nasr and Arp, 2017), and the same should be expected in suspended sediments of glacier-fed streams. Reported dry-weight concentrations of sediment-bound Hg (SHg) in these streams range between 5 and 259 ng/g, and are typically in the tens of ng/g (see Table 3.15). This is consistent with published data on SHg in streambed sediments of glacier-fed tributaries of the Yukon River (~6–80 ng/g; Friske et al., 1994; Halm and Dornblaser, 2007) or seafloor sediments of inner fjords in Svalbard that are fed by glacial rivers (~1–90 ng/g; Bełdowski et al., 2015; Liu et al., 2015). Episodic, yet locally significant exports of riverine Hg can also occur during extreme flow outbursts accompanying Icelandic subglacial eruptions (jokülhlaups). In the 1996 jokülhlaup from Vatnajökull, a riverine THg concentration of 68 ng/L was recorded (Kristmannsdóttir et al., 1999).

Published estimates of riverine Hg exports to Subarctic or Arctic marine waters mostly concern the large rivers of Siberia and North America (cf. Section 3.4.4). The Lena, Yukon, and Mackenzie rivers are partially fed by meltwater from limited glacier-covered mountain areas (<6% of the total catchment area), but the magnitude of Hg contributions from glacial meltwater in these rivers is unknown. Melting glaciers could also account for a substantial part of the Hg-enriched upper waters of the Labrador Current issued from the eastern Canadian Arctic (Cossa et al., 2018), but just how large this contribution may be is not known at present. Estimates of Hg fluxes based on direct or indirect measurements in glacier-fed streams of the Arctic

Table 3.15 Published data on Hg content in glacier-fed streams in the Arctic and Subarctic.

River basin/glacier	Basin area km^2	Glacier cover %	Sampling period		Hg in glacial streams				Data sources
			Month(s)	Year(s)	UTHg (ng/L)	PHg (ng/L)	FHg (ng/L)	SHg (ng/g)	
Greenland									
Zackenberg River	514	21	July–Aug	2009–13	4.5–7.5	4.1–7.2	0.25–0.53	s25–42	1
Svalbard									
A. Lovénbreen Glacier (supra)*	--	--	May–June	2007	0.6–7.2	--	--	--	2
A. Lovénbreen Glacier (sub)*	--	--	May–June	2007	1.9–5.9	--	--	--	2
Bayelva River	32	55	June	2007	7.3	--	--	--	2
Kongsvegen Glacier (supra)*	--	--	May	2007	<0.2	--	--	--	2
Alaska									
Lemon Creek	32	55	May–Sept	2010	0.4–8.2	1–13	--	37–259	3
Stonefly Creek	13	31	July	2007	1.44	0.97	0.47	33	4
Gull Creek	6	2	July	2007	0.59	0.20	0.39	130	4
Nunatak Creek	38	2	July	2007	0.27	0.19	0.08	--	4
Reid Creek	17	5	July	2007	4.62	3.73	0.89	90	4
Taiya Creek	466	33	July	2007	0.88	0.53	0.35	15	4
Skagway Creek	376	17	July	2007	--	--	0.37	--	4
Yukon									
Kusawa River	4200	5	June	2013	--	--	--	6–28	5
Atlin River	6812	--	June, Aug	2004	0.43–2.13	0.06–0.08	0.37–2.05	--	6
Takhini River	7050	2	June, Aug	2004	1.55–3.31	1.02–2.77	0.53–0.54	--	6
White River	6230	30	June, Sept	2004	22.7–28.24	22.0–26.3	0.70–1.94	80	6
Canadian Low Arctic									
Penny Ice Cap (sub)*	--	--	June–July	2008-10	0.74–5.93	--	--	--	7
Penny Ice Cap (supra)*	--	--	June–July	2008-10	0.28–3.91	--	--	--	7
Weasel River	--	--	June	2008	1.52–2.04	--	--	--	7
Owl River	--	--	July	2008	1.13–1.53	--	--	--	7
Canadian High Arctic									
J. Evans Glacier (sub)*	--	--	June–July	2001–02	1.52–4.06	1.22–3.68	0.17–0.57	--	8
J. Evans Glacier (supra)*	--	--	June–July	2001–02	0.17–0.93	0.03–0.53	0.14–0.60	--	8
Blister Creek	--	--	July–Aug	2015–16	0.41–73.73	--	0.24–0.64	14	9
Snowgoose River	222	39	July–Aug	2015–16	0.57–26.00	--	0.20–0.62	26	9
Abbé River	390	52	July–Aug	2015-16	4.36–5.72	--	0.27–0.38	--	9
Gilman River	992	71	July–Aug	2015–16	2.53–5.58	--	0.26–0.44	--	9
Henrietta Nesmith River	1274	82	July–Aug	2015-16	2.93–21.31	--	0.27–0.53	--	9
Turnabout River	678	38	July–Aug	2015–16	3.19–5.11	--	0.28–0.68	5	9
Very River	1035	26	July–Aug	2015–16	11.82–23.90	--	0.40–0.59	100	9
Ruggles River**	7516	41	July–Aug	2015–16	0.17–1.20	0.31	0.26–0.32	--	9

UTHg: Total Hg in unfiltered water, UTHg=FHg+PHg; FHg: Total Hg in filtered water (0.45 μm), operationally equivalent to dissolved Hg (DHg); PHg: Total particulate-bound Hg retained after filtration (0.45 μm); SHg: Hg mass concentration (dry weight) in suspended or riverbed sediments. *sub=subglacial or proglacial stream flow; supra=supraglacial stream flow. **Underlined figure is an average value. Data sources: 1=Rigét et al., 2011b and Søndergaard et al., 2012; 2=Dommergue et al., 2010; 3=Vermilyea et al., 2017; 4=Nagorski et al., 2014; 5=Friske et al., 1994 and Zdanowicz et al., 2018; 6=Chesnokova et al., 2020 and Halm and Dornblaser, 2007; 7=Zdanowicz et al., 2013; 8=St. Louis et al., 2005; 9=St. Pierre et al., 2019.

Table 3.16 Published estimates of riverine Hg fluxes in glaciated basins of the Arctic and Subarctic.

River basin/glacier	Basin area km^2	Glacier cover %	Averaging period	Estimated annual Hg mass fluxes and yield UTHg (kg/y)	PHg (kg/y)	FHg (kg/y)	THg (g/km^2/y)	Data sources
Greenland								
Zackenberg River	514	21	2009–13	0.90–2.646	0.67–2.6	0.036–0.140	1.4–5.4	1
Svalbard								
Kongsfjorden*	3074	77	2007	1.5–2.6	--	--	0.5–0.8	
Alaska								
Lemon Creek**	32	55	2009	--	--	--	*19.9*	3
Yukon								
Kusawa River***	4200	5	2001–11	0.20–0.28	--	--	0.05–0.07	4
Canadian High Arctic								
Blister Creek			2015–16	0.01–0.03	--	--	0.61–1.96	
Snowgoose River	222	39	2015–16	0.14–0.44	--	--	0.61–2.63	9
Abbé River	390	52	2015–16	0.24–1.03	--	--	0.72–3.30	9
Gilman River	992	71	2015–16	0.72–3.27	--	--	0.98–3.88	9
Henrietta Nesmith River	1274	82	2015–16	1.25–4.95	--	--	0.57–2.04	9
Turnabout River	678	38	2015–16	0.39–1.38	--	--	1.32–2.91	9
Very River	1035	26	2015–16	1.37–3.01	--	--	0.61–1.96	9
Ruggles River	7516	41	2015–16	0.26–0.65	--	0.12–0.32	0.03–0.09	9
		Overall range of values:		0.01–4.95	0.67–2.6	0.036–0.32	*0.05–19.9*	
		Excluding Lemon Creek:					0.05–3.88	

*Total THg runoff input to fjord from tundra snowpack and glaciers. **THg from glacier meltwater contribution only, not including subglacial flow. ***THg fluxes and basin yield estimated from fluorescent dissolved organic matter. The basin yield (italicized) is a possible outlier compared to all other reported values. Data sources are as listed in Table 3.15.

and Subarctic range between 0.01 and 4.95 kg/y for THg (see Table 3.16). When the fluxes are normalized by catchment area, they translate to annual yields ranging from 0.03 to 3.88 g/km^2/y for THg in basins with 21% to 82% glacier coverage. A published figure of 19.9 g THg km^2/y from the Lemon Creek Basin, Alaska (32 km^2; 55% glacier cover), which was estimated from fluorescing organic matter measurements, presently stands out as an outlier (Vermilyea et al., 2017).

The majority of glaciated Arctic river basins have too limited ice coverage to strongly control their mean annual sediment yield (Overeem and Syvitski, 2008), although years of high summer melt rates may disproportionally impact sediment export in mountain catchments (Wada et al., 2011). The data in Tables 3.15 and 3.16 suggest that the same holds true of THg yields from glaciated basins, which likely depend on additional factors such as climate, relief, stream length and drainage pattern. In the relatively near term (i.e., in the coming years to decades), the continued recession of mountain glaciers and small ice caps is expected to enhance sediment discharge into streams and lakes, followed by a longer-term decrease of the sediment flux as glaciers continue to shrink and thin becoming less dynamic (Milner et al., 2017). This has, in fact, been observed in the Alps (Delaney et al., 2018). In Greenland, sustained, larger sediment fluxes to surrounding marine waters are expected, particularly from fast-flowing tidewater glaciers, and a current estimate of the total suspended sediment output in meltwater is 1.294 Gt/y (Overeem et al., 2017). Using a median SHg concentration of ~31 ng/g (after Søndergaard et al., 2015), this translates to a sediment-bound export of ~40 t THg/y, which is an order of magnitude greater than an estimate of 4.6 t THg/y previously made by Rigét et al. (2011) from simple upscaling of data from the Zackenberg River. Because the concentration of suspended sediments in glacial rivers is highly variable in both space (between glacier catchments) and time (through the melt season), and as the Hg content in these sediments can also vary from ~1 to 80 ng/g according to catchment geology, it is presently very difficult to properly quantify the total sediment-bound Hg flux from Arctic glaciers to the Arctic Ocean. However, the simple estimate from Greenland above clearly shows that this flux is far larger than that of Hg released from melting ice alone (see Table 3.14).

3.4.4 How much mercury do rivers transport to the Arctic Ocean?

Rivers are an important transport pathway between the atmospheric Hg deposited in terrestrial watersheds, natural Hg eroding from catchment geology and thawing from permafrost, and the Arctic Ocean. There have been no recent studies on groundwater transport of Hg into the Arctic Ocean, and so this potential source will not be considered further in detail. Early work on coastal groundwater flows directly into the Arctic Ocean suggested that the total volume is <10% of the river flows (Stein and Macdonald, 2004). Groundwater is an

important and increasing component of total river discharge in at least some Arctic rivers (e.g., the Yukon River; Walvoord and Striegl, 2007). It is also noteworthy that in other parts of the world, subsurface groundwater discharge may contribute as much Hg to coastal marine environments as direct atmospheric deposition (Outridge et al., 2018).

Earlier sections of this chapter (Sections 3.3.3 and 3.4.1, 3.4.2 and 3.4.3) summarized the current state of knowledge of present-day rates of atmospheric Hg wet and dry deposition onto Arctic catchment areas, uptake of Hg by Arctic vegetation, soil and snow meltwater Hg concentrations, and the role of permafrost and glaciers in mobilizing Hg into Arctic streams and rivers. Permafrost is a unique feature of the Arctic and underlies much of the Arctic Ocean river catchment areas. Permafrost accumulated a large mass of Hg through the 10 millenia of the Holocene and previous inter-glacial stages; approximately 184–755x10^3 tonnes resides in the upper 1 m of tundra soils including permafrost, with the highest Hg concentrations in surface soils (Olson et al., 2018; Schuster et al., 2018). Consideration of the Hg sources feeding into Arctic rivers must therefore encompass soil and snowmelt, as well as permafrost.

Arctic catchment soils act as a buffer between atmospherically-sourced Hg and the Hg in river and lake waters. The soil buffer acts to temporally and quantitatively 'dislocate' deposited Hg from riverine Hg by slowing the transfer of atmospheric Hg into freshwater environments. This dislocation accounts for the finding that much of the Hg in tundra soil active layers was deposited prior to the industrial period (Olson et al., 2018), the implication being that it has been stored in soils for millennia. Many environmental factors that vary between Arctic river catchments, including precipitation, river discharge rates, topography, land use, proportion of permafrost area, active layer thickness, vegetation cover and hydrogeological features, also influence river Hg flux (Domagalski et al., 2016; Sonke et al., 2018; Lim et al., 2019; Mu et al., 2019). Catchment differences and soil retention of Hg partly explain the lack of a clear relationship between the rates of current atmospheric Hg deposition and river Hg fluxes in the Arctic and elsewhere (Brigham et al., 2009; Domagalski et al., 2016).

There is a distinct seasonality in the dominant sources of Hg (and water) flowing through rivers to the ocean. There remains much uncertainty about the hydrological and geomorphological processes responsible for mobilizing soil, permafrost and snowpack Hg and transporting it downslope to freshwater environments. However, since snowmelt occurs at the end of winter when the ground is still frozen, percolation through the soil column is not likely a major Hg source in spring freshet. Thus, the melting of snowpacks and glaciers, as well as the overland transport of surface soil particles and vegetation detritus, are probably the main springtime sources of river water Hg to the Arctic Ocean (Douglas et al., 2017). The spring freshet also exhibits the highest Hg concentrations and fluxes over the entire annual hydrological cycle (Schuster et al., 2011; Emmerton et al., 2013; Sonke et al., 2018; Lim et al., 2019; Zolkos et al., 2020). Dastoor and Durnford (2014) estimated (using the GEM-MACH-Hg model) the annual transfer of THg from snowpack to meltwater of 8.0, 31.2 and 39.2 t/y in North American, Russian, and all pan-Arctic watersheds, respectively. The areal yields of total dissolved Hg in Arctic coastal meltwater are reported to be the highest in the world, markedly greater than in meltwater from temperate watersheds and up to seven times greater yields (with a range of 8–14 ng Hg/ha) than non-coastal Arctic locations (Douglas et al., 2017). Summer precipitation and active layer percolation and permafrost thaw lead to a second peak in riverine water and Hg export in autumn (Lim et al., 2019; Zolkos et al., 2020). Seasonal freshwater discharge from snowmelt and permafrost thaw also releases large amounts of sediment as well as dissolved organic carbon (DOC), particulate organic carbon (POC) and total organic carbon (TOC) to Arctic rivers (Stein and Macdonald, 2004).

Permafrost, soil and landscape properties strongly influence the spatial distribution of riverine Hg fluxes. Lim et al. (2019) found that maximum particulate Hg concentrations and fluxes in Western Siberian rivers occurred in areas of sporadic/discontinuous permafrost, and were mainly sourced from thawing discontinuous permafrost. Rivers draining southern permafrost-free and northern continuous permafrost regions exhibited lower Hg concentrations and fluxes than the intermediate regions of discontinuous permafrost. Small catchments with large areas of organic matter-rich permafrost were especially important sources of suspended Hg load. At the thawing permafrost boundary, where the active layer was deepest, deep and intermediate peat horizons were dominant contributors to the riverine Hg loading rather than soil mineral layers, surface peat and plant litter (Lim et al., 2019). St. Pierre et al. (2018) estimated that ~5% of the Hg in Arctic permafrost soils may occur in regions susceptible to the development of hillslope thermokarst features, such as retrogressive thaw slumps, that can quickly mobilize vast amounts of stored, particulate-bound Hg directly into downstream environments. Most riverine export of Hg in glacier-fed streams is in particulate form, with total Hg fluxes ranging between 0.14 and 16.4 kg/y in the Arctic and Subarctic (see Section 3.4.3).

The proportion of natural and anthropogenic Hg present in Arctic river water is another area of uncertainty. Arctic lake sediments record a three to five times increase in atmospheric deposition loads since the Industrial Revolution (Fitzgerald et al., 2005; Muir et al., 2009), similar to those in temperate zones (Schuster et al., 2002; Drevnick et al., 2016). This Hg is likely accumulated in surface soil layers. Obrist et al. (2017) reported geogenic Hg contributions in the range of 0% in organic soil horizons to around 40% in mineral soil horizons in Arctic tundra. However, most of the Hg accumulated in deeper layers, including all of the large mass in permafrost, was accumulated during pre-industrial times and is therefore of natural origin (Olson et al., 2018). Since the Hg in the springtime freshet reflects recent atmospheric deposition, while summer permafrost thaw liberates ancient Hg, it is likely that both pre- and post-industrial (natural and anthropogenic) Hg sources contribute to annual riverine export of Hg to the Arctic Ocean. However, based on the observations of higher Hg concentration and water discharge rate during spring flood (over 60% of the annual discharge) and evidence of recent Hg in lake sediments, a more significant contribution of post-industrial Hg in river export is likely. Lim et al. (2019) suggested that a two to three times higher Hg:C ratio in spring waters of

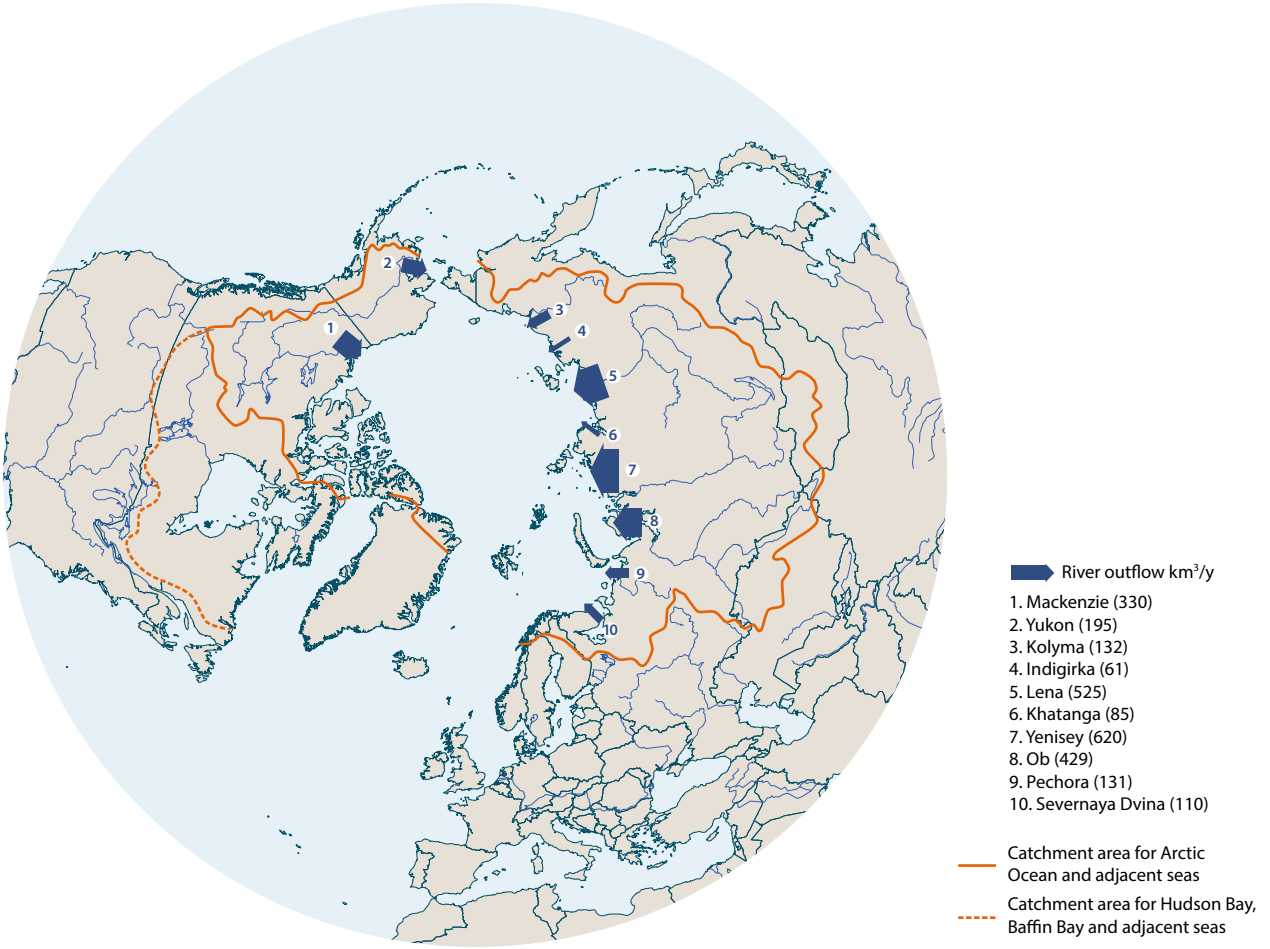

Figure 3.21 Map of Arctic river catchments as employed by AMAP (2011), showing annual freshwater discharges into the Arctic Ocean (km³/y). Note that the rivers draining into Hudson Bay, Hudson Strait and Baffin Bay are not included in this definition but are encompassed by some of the river Hg mass balance studies discussed here. Source: Outridge et al., 2008.

Western Siberian rivers compared to other seasons reflects the runoff of Hg accumulated in seasonal snowpacks. However, the proportion of recent versus legacy Hg deposition annually mobilized in river waters likely varies between watersheds. Better understanding of processes that mobilize the Hg from different sources in tundra soils to aquatic environments will be critical to assessing how future levels of Hg in Arctic aquatic systems may change in response to actions taken under the Minamata Convention (i.e., emission reductions), and to climate change.

The river catchments that drain into the Arctic Ocean (as defined by AMAP, 2011; see Figure 3.21) yield an annual freshwater runoff of about 3300 km³, with the Russian rivers, the Yenisey (620 km³), Lena (523 km³) and Ob (404 km³) rivers, and the Mackenzie River (330 km³) in Canada contributing the highest flows and the Mackenzie the largest sediment load (Stein and Macdonald, 2004). The earliest oceanic Hg mass balance (Outridge et al., 2008; see also AMAP, 2011) estimated a total riverine Hg outflow to the ocean of about 13 t/y THg based on sparse riverwater Hg concentration data from the Mackenzie River (Leitch, 2006; Leitch et al., 2007) and three Siberian rivers (Coquery et al., 1995). Since then, expanded sampling campaigns and the use of different upscaling or modeling approaches have yielded total pan-Arctic river THg estimates of between 16 and 108 t/y (Durnford et al., 2012; Fisher et al., 2012; Kirk et al., 2012; Amos et al., 2014; Dastoor and Durnford, 2014; Zhang et al., 2015; Soerensen et al., 2016a; Sonke et al., 2018; Mu et al., 2019; Zolkos et al., 2020).

The latter three studies are notable additions to the Arctic river Hg estimates because they are based on measurements of river water Hg concentrations in seven of the largest rivers, including, for the first time, seasonal data from the Russian sector of the Arctic. Based on data for the period 2012 to 2015 from the Arctic Great Rivers Observatory (GRO; Holmes et al., 2018), Mu et al. (2019) calculated the export of THg from the six largest rivers (the Yenisey, Lena, Ob, Mackenzie, Yukon and Kolyma rivers) to be 20.1 t/y (IQR: 14.8–28.8 t/y). Similarly, Zolkos et al. (2020), also using the GRO database but for 2012 to 2017, calculated a Hg export of 19.7 t/y for these rivers. Approximately 53% of Hg exports occurred during spring, 43% in summer and 5% in winter (Mu et al., 2019), a pattern also observed in small Siberian rivers (Lim et al., 2019).

Sonke et al. (2018) made multi-year observations at a relatively high temporal resolution of dissolved and particulate Hg and DOC in the Severnaya Dvina, Yenisey and Great Whale rivers, confirming a strong Hg export during the spring freshet in May to June, but also during the autumn wet season. They supplemented these measurements with THg:DOC data and riverine DOC fluxes from earlier studies to estimate the pan-

Arctic Hg flux. Two contrasting methodologies were used, which produced similar pan-Arctic results: total Hg:DOC relationships for rivers upscaled to the whole Arctic using riverine DOC flux data; and total Hg yield:runoff relationships for multiple Arctic watersheds upscaled to include all Arctic rivers. Annual total Hg outflows calculated by these methods were 43 t/y, and 44±4 (SD=1) t/y, respectively, consisting of equal parts dissolved (22 t/y) and HgP (22 t/y). These estimates include the relatively small rivers draining into Hudson Bay and Baffin Bay; with those excluded, the Arctic Ocean riverine flux was 41±4 t/y. The THg estimates by both methods are similar to the most recent modeling-based values of 46 to 50 t/y (Dastoor and Durnford, 2014; Zhang et al., 2015) and to a pan-Arctic flux of 37±2 t/y calculated from GRO data for the period 2012 to 2017 (Zolkos et al., 2020). For the oceanic mass balance presented later in this chapter (see Section 3.8), the best estimate for the riverine Hg flux to the Arctic Ocean (as defined in Section 3.8) is taken to be 41±4 t/y from Sonke et al. (2018). This is of similar magnitude, within uncertainty, to the coastal erosion Hg flux of 39 t/y derived in Section 3.4.5. An increase over recent decades in the discharge of major Arctic rivers is well established (e.g., Serreze et al., 2006; Box et al., 2019), and rivers may become more important Arctic Ocean Hg sources in future (see Chapter 5).

The importance of terrestrial Hg sources in the Arctic Ocean Hg cycle is supported by stable Hg isotope data on Arctic marine sediments and biota. Paleo-sediment Hg isotope patterns clearly indicate terrestrial soil Hg sources were dominant prior to the industrial period (Gleason et al., 2017). A recent re-evaluation of published marine biota Hg isotope data also suggests that soil-derived Hg dominates the MeHg present in many top predators in the Arctic Ocean today (Masbou et al., 2018). The isotope data cannot at present distinguish between riverine and erosion Hg sources, since both represent a terrestrial soil isotope signal. Nonetheless, the importance of riverine and coastal erosion sources of Hg to the pelagic areas of the Arctic Ocean contrasts with other world oceans in which direct atmospheric Hg deposition generally dominates (Soerensen et al., 2016a; Outridge et al., 2018). The finding of Hg- and organic carbon-enrichment in Labrador Current waters exiting from the Canadian Arctic Archipelago also suggests a significant terrestrial contribution to the overall Arctic Ocean Hg budget (Cossa et al., 2019).

3.4.5 How much mercury does coastal erosion contribute to the Arctic Ocean?

Coastal erosion rates along some parts of the Arctic Ocean coastline are among the highest in the world owing to the occurrence of long reaches of unlithified glacial till sediments occurring in elevated bluffs, comparatively rapid changes in relative sea level, and the widespread presence of exposed ground ice that is susceptible to the eroding action of wind and water (Overduin et al., 2014; Gibbs et al., 2015). The overall long-term erosion rates in different sectors of the Arctic coastline, expressed in spatial terms, are typically between 0.5 and 1.5 m/y, with high local and regional variability (Lantuit et al., 2012; Overduin et al., 2014; Couture et al., 2018). Susceptible sections of the Laptev, East Siberian and Beaufort sea coasts commonly exhibit losses of between 3 and 10 m/y with localized sites exceeding 20 m/y (Jones et al., 2009; Lantuit et al., 2012; Günther et al., 2013). Furthermore, there is substantial evidence that average erosion rates are significantly increasing across many Arctic regions and are now higher than at any time since observations began 50 to 60 years ago (Overduin et al., 2014; Irrgang et al., 2018). For example, erosion rates in rapidly eroding sections of the Laptev and Beaufort seas have doubled over the past 50 years (Jones et al., 2009; Günther et al., 2013). Possible contributing factors for this increase are discussed in Chapter 5.

Previous estimates of the Hg mass input to the Arctic Ocean from coastal erosion vary within a factor of three, between 15 and 47 t/y, and were based on either scaled-up local measurements or inferences from atmospheric-ocean models (Outridge et al., 2008; Fisher et al., 2012; Zhang et al., 2015; Soerensen et al., 2016a). All of these studies suggested that erosion contributed a significant fraction of the total inputs to the oceanic Hg mass balance. However, the paucity of data on permafrost and tundra soil Hg concentrations, and uncertainties around the erosion mass flux were acknowledged weaknesses. Based on soil/permafrost cores from eroding coastal bluffs along the Beaufort Sea coast (Leitch, 2006), Outridge et al. (2008; see also AMAP, 2011) used a median soil Hg value of 110 ng/g dw to develop an oceanic erosion Hg mass estimate, whereas Soerensen et al. (2016a) used a value of 81 ng/g dw.

Recently, Olson et al. (2018), Schuster et al. (2018) and Lim et al. (2020) provided new permafrost and tundra soil Hg concentration data for different areas of the Arctic. Olson et al. (2018) synthesized most of the available Arctic tundra soil Hg data (see Olson et al., 2018 for references), to which we have added data from Leitch (2006; n=262) and Lim et al. (2020; n=207, excluding data from a non-permafrost site in Central Russia). Schuster et al.'s (2018) data were omitted from this calculation because their data excluded active layer soils, which would be eroded into the ocean along with permafrost. The exclusion of active layer soil could have significantly biased the results lower, because the active layer often contains higher Hg concentrations than the underlying permafrost (e.g., Leitch, 2006; Outridge and Sanei, 2010; Olson et al., 2018). The combined data summary (n=985) indicates a mean (±SD) Hg concentration of 66.1±52.3 ng/g dw (median of 54.8 ng/g dw). The 25% and 75% confidence intervals (CIs) were 30.0 and 88.8 ng/g, respectively. These concentrations are used below to derive a new coastal erosion Hg flux estimate with uncertainties.

Published estimates of soil erosion mass loss into the Arctic Ocean as a whole remain rare since Rachold et al.'s (2004) calculation of 430 Mt/y. However, based on the Arctic Coastal Dynamics Database (ACD), Lantuit et al. (2012) estimated mean volumetric erosion losses for different sectors of the Arctic Ocean coastline, which were used here to calculate a soil erosion mass for the ocean (see Table 3.17). There are two key assumptions in the calculation of eroded mass from eroded volume. The first is the use of a common bulk density of 1.2 g/cm^3 for the eroding material, which was derived from a significant inverse relationship between bulk density and soil organic carbon content in Canadian Arctic and Subarctic soils (Hossain et al., 2015). The second assumption is that the average soil organic carbon content in eroding coastal bluffs in the Yukon (4.5% TOC; Couture et al., 2018) is applicable to

Table 3.17 Calculation of coastal erosion total Hg flux into the Arctic Ocean.

Sector name[a]	Length (km)[b]	Percent total length (%)	Mean cliff height (m a.s.l.)	Mean erosion rate (m/y)	Mean vol. ground ice (vol. %)	Total vol. eroded (km^3/y)	Vol. corrected for ice (km^3/y)	Soil mass eroded (Mt/y)[c]	Hg flux (t/y)[d]
Russian Chuckchi Sea	2736	2.7	14.5	0.27	13.9	0.011	0.009	11.1	0.7
American Chuckchi Sea	4662	4.6	5.0	0.49	24.0	0.011	0.009	10.4	0.7
American Beaufort Sea	3376	3.3	1.5	1.15	26.9	0.006	0.004	5.2	0.3
Canadian Beaufort Sea	5672	5.6	6.7	1.12	29.4	0.043	0.030	36.3	2.4
Greenland Sea/ Canadian Arctic Archipelago	4656	4.6	No data	0.01	14.2	--	--	--	--
Svalbard	8782	8.7	14.0	0	0.0	0.000	--	--	--
Barents Sea	17965	17.7	10.5	0.42	16.2	0.079	0.067	79.8	5.3
Kara Sea	25959	25.6	14.0	0.68	23.7	0.248	0.189	227	15.0
Laptev Sea	16927	16.7	11.9	0.73	17.1	0.147	0.122	146	9.7
East Siberian Sea	8942	8.8	8.8	0.87	19.6	0.068	0.055	66.0	4.4
Total or Mean	**101 447**	**100.0**	**9.7**	**0.57**	**18.5**	**0.614**	**0.485**	**582**	**38.5**

a) Arctic Ocean boundaries and areas conform to AMAP definitions.
b) Data on coastal geomorphology and erosion rates from the Arctic Coastal Dynamics Database (Lantuit et al., 2012). Erosion data are weighted with the length of the coastline in each sector to accurately represent the input of each sector in the whole ocean calculation.
c) Eroded volume corrected for ground ice volume, and converted to mass assuming a mean bulk density of 1.2 g/cm^3 derived from a significant inverse relationship between bulk density and soil organic carbon (SOC) in Arctic soils (Hossain et al., 2015) and the mean SOC of eroding Yukon coastal soils of 4.5% (Couture et al., 2018).
d) Hg flux calculated from soil mass eroded assuming a mean Hg concentration of 66.1 ng/g dw in Arctic tundra and coastal soils (n=985; see text).

the whole Arctic coastline. Couture et al. (2018) represents the most comprehensive survey published to date of OC in eroding Arctic coastal soils, although it is restricted to the Beaufort Sea coast of the Yukon.

By combining the resulting total coastal erosion rate (582 Mt/y) with the mean and 25% to 75% CI soil Hg concentration values described above, erosion is estimated to contribute 38.5 t/y THg to the ocean, with a 25% to 75% CI of 17.5 to 51.5 t/y (see Table 3.17). This value falls within the range of previous estimates (see above). Using the median soil Hg value of 54.8 ng/g gives an erosion flux of 32 t/y. The Eurasian Arctic coastline, where erosion rates are highest, contribute the overwhelming majority (89%) of the total Hg influx; the Greenland Sea, the sea around Svalbard, and Canadian Arctic Archipelago sectors contribute negligible amounts because their average erosion rates are very low (≤0.01 m/y). This Hg flux calculation assumes that tundra soil Hg concentrations in the Eurasian sector of the Arctic, from which there are relatively few data (see Schuster et al., 2018 and Lim et al., 2020), are similar to the Alaskan and Canadian sectors.

The majority of the Hg contained in eroding coastal soils is likely to be natural in origin, deposited from the atmosphere during millennia of peat growth and soil formation after the end of the last global glaciation and before the industrial era. Olson et al. (2018) estimated that ~90% of the Hg in tundra soil profiles is natural, but pointed out that this estimate is affected by uncertainties such as the degree of thermokarst mixing of surface and mineral soils in active layers, and the timing and size of the anthropogenic atmospheric influx during the 20th century.

The speciation and fate of the eroded Hg once in the ocean has not been studied. Like Hg in other soils worldwide (O'Connor et al., 2019), Hg in the eroding material may be predominantly in particulate form bound to organic matter and minerals, with a minor fraction dissolved and bound to dissolved organic matter (DOM) in soil porewater. Initially, eroded material was thought to predominantly settle out in coastal sediments (Hill et al., 1991), suggesting that this may also be the fate of much of the associated Hg. However, Couture et al. (2018) calculated that only a minor fraction (~13%) of the eroded soil organic carbon was actually present in near-shore sediments, indicating that most of the C was either rapidly metabolized in the near-shore environment or was exported off the continental shelf by waves or sea ice. Because of the often-strong association of Hg and organic matter in tundra soils and permafrost (e.g., Schuster et al., 2018; Lim et al., 2020), Couture et al.'s findings suggest the possibility that the Hg from coastal erosion may also be remobilized during organic matter mineralization and transported from coastal sediments to elsewhere in the oceanic environment. The finding, based on stable Hg isotopes, that top marine predators in the Arctic Ocean contain a predominance of Hg from terrestrial sources (Masbou et al., 2018) supports this suggestion, although Hg isotope analysis cannot distinguish between riverine and coastal erosion sources of terrestrial Hg in the ocean.

3.5 How much mercury enters the Arctic Ocean, and how does ocean circulation transport mercury to the Arctic Ocean?

3.5.1 How much marine mercury enters the Arctic Ocean?

The four main gateways for seawater Hg exchange between the Arctic Ocean and the Pacific and North Atlantic oceans are the Bering Strait, the Canadian Arctic Archipelago and the Davis Strait, the Fram Strait, and the Barents Sea Opening (BSO; see Figure 3.22), with the BSO and Davis Strait exhibiting the largest flow volumes. Seawater exchanges with the Pacific and Atlantic oceans were estimated by Tsubouchi et al. (2018) to be: a northward inflow through the Bering Strait of 22.1±22.1x10^3 km^3/y; a northward net inflow through the BSO of 72.5±37.8x10^3 km^3/y; a southward net water outflow through the Fram Strait of 34.7±37.8x10^3 km^3/y; and a southward net outflow of 66.2±22.1x10^3 km^3/y through the Davis Strait. There is a net volume outflow from the Arctic Ocean of 6.3x10^3 km^3/y, with the inflow-outflow difference made up by river inflows and direct precipitation onto the ocean surface (Haine et al., 2015).

Water from the North Pacific Ocean flows unidirectionally into the Arctic Ocean through the Bering Strait which has a broad, shallow (~50 m depth) sill that effectively restricts water inflow (Carmack et al., 2016). From the Atlantic Ocean, surface, mid-depth and deep ocean waters enter the Arctic Ocean via the Fram Strait and the Barents Sea; Arctic waters, representing a mixture of Pacific Ocean and internally-modified Atlantic Ocean waters, exit into the North Atlantic via the Fram and Davis straits (Haine et al., 2015). The Fram Strait is the only deep-water connection between the Arctic Ocean and the North Atlantic Ocean via the Nordic Seas. Relatively warm and saline North Atlantic water enters the Arctic Ocean here as the West Spitsbergen Current, while cold and less saline Arctic water masses exit the Arctic Ocean as the East Greenland Current. Because the salinity of Pacific water is less than that of the Atlantic water, Pacific waters overlie the Atlantic Layer over much of the western half of the Arctic Ocean (Carmack et al.,

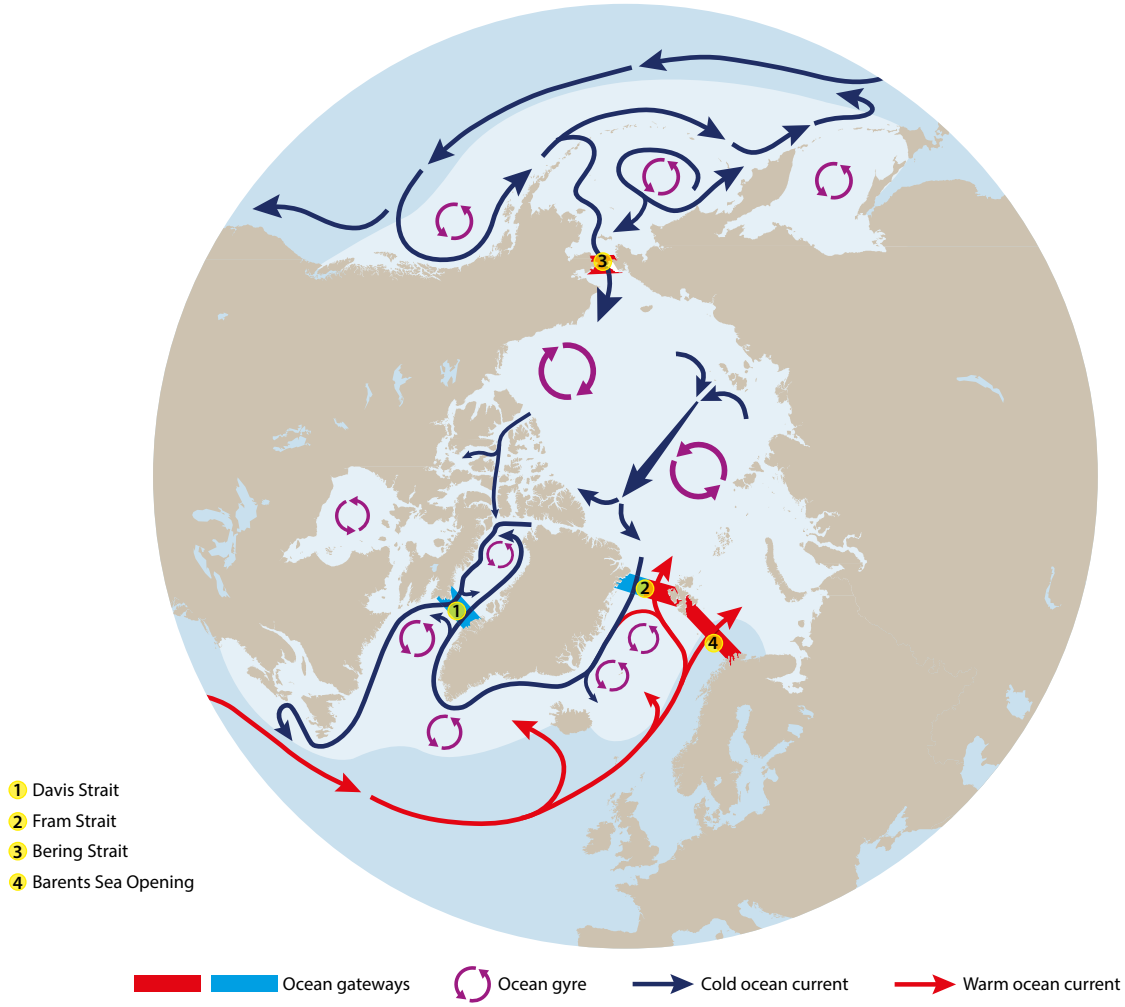

Figure 3.22 The Arctic Ocean and its seawater exchanges with the rest of the world's oceans. The major ocean currents (long arrows), the four Arctic Ocean gateways in the Fram Strait, the Barents Sea Opening, the Davis Strait, and the Bering Strait, and the gyral circulation patterns (purple arrows) are shown. Relatively warm, salty Atlantic waters (red arrows) enter the Arctic Ocean through the Fram Strait and the Barents Sea Opening, and are distributed within the Arctic Ocean in subsurface, topographically constrained boundary currents along the continental margin and undersea ridge system. Cooler and fresher Pacific-origin waters (blue arrows) enter the Arctic Ocean through the Bering Strait and, together with internally modified Atlantic-origin waters, exit through the Canadian Arctic Archipelago, the Davis Strait, and the Fram Strait along eastern Greenland. The salt-stratified ocean domains are shown in light blue. Source: Carmack et al., 2016.

2016). The northward penetration and vertical mixing of Atlantic water with Pacific water is enhanced during periods of positive Arctic Oscillation Index, which results in generally stronger southerly winds over the Barents and Greenland seas. There is a net west-to-east movement of water, gases, and other constituents via the Transpolar Drift from the Pacific to the Atlantic side, which is driven by the pressure gradient created in part by salinity and temperature differences between the two oceans (Carmack et al., 2016).

Two earlier studies estimated ocean current THg inputs to the Arctic Ocean based on current volumes and published THg concentrations in Pacific and Atlantic seawater, and reported similar results: 48 t/y THg (Outridge et al., 2008; see also AMAP, 2011) and 53 t/y (with a range of 40–62 t/y; Soerensen et al., 2016a). Most of this Hg comes from the North Atlantic (47 t/y; Soerensen et al., 2016a), particularly from deep and mid-depth waters, and is driven by the much greater Atlantic inflow volume and the similar range of THg concentrations for Atlantic and Pacific waters. Support for the low Hg estimate in the Bering Strait of 6 t/y comes from seawater Hg measurements in the Bering Sea and Strait, conducted during a GEOTRACES 2015 cruise, which calculated a Hg inflow range of 1 to 14 t/y (Agather et al., 2019). Recent estimates based on the 2015 GEOTRACES TransArc II and the 2016 GEOTRACES GRIFF cruises suggest an influx of 49 t/y of THg into the Arctic Ocean via the Fram Strait and Barents Sea Opening (Petrova et al., 2020).

The Hg flux calculations referred to above are based on average current volumes measured in the 1990s or 2000s. Evidence from a series of permanent *in situ* moorings indicates that the seawater volume flowing through the Bering Strait has increased significantly over the last two decades at an average rate of 1.8% per year (Østerhus et al., 2019). There is considerable interannual variability to the northward Bering flow, but the difference between the minimum in 2001 and maximum in 2014 represented an overall 70% increase (Woodgate, 2018). The most likely explanation for this trend is lower water pressure in the East Siberian Sea caused by increasing westerly winds over the past two decades; the winds drive surface water from the shelf into the deeper ocean basin thereby creating a pressure differential between the Bering Sea and Arctic Ocean (Peralta-Ferriz and Woodgate, 2017). Inflow volumes from the North Atlantic side have remained relatively stable between the mid-1990s and mid-2010s, although there is a slight, non-significant, increasing trend (Østerhus et al., 2019). Because the Pacific Ocean supplies only about 10% of the total seawater inflow to the Arctic Ocean (Woodgate, 2018; Østerhus et al., 2019), the impact on Hg delivery to the Arctic Ocean as a whole from increasing Pacific inflows is likely to be minor. However, the Hg delivered could affect Hg budgets in the East Siberian, Chukchi and Beaufort seas, where the effects of Pacific waters are noticeable on regional water chemistry, nutrient and heat budgets (Woodgate et al., 2010; Torres-Valdéz et al., 2013; Haine et al., 2015).

The Hg losses from the Arctic Ocean are due to outflowing ocean currents, evasion, and sedimentation on the continental shelves and deep ocean basins. Evasion processes and flux estimates were reviewed in Section 3.3.3d. To provide perspective for the ocean losses discussion, it should be reiterated that Hg evasion from ocean surface waters accounts for 12 to 99 t/y (Outridge et al., 2008; Soerensen et al., 2016a; see Section 3.3.3d). Losses in sedimentation is covered in the following Section (Section 3.5.2). Previous estimates of the overall Hg loss rate in ocean outflows (excluding Hg entrained in sea ice and snow) are reasonably similar to each other: 68 t/y (Outridge et al., 2008); 83 t/y (with a range of 49–123 t/y; Soerensen et al., 2016a), and 73 t/y (Petrova et al., 2020). For the purposes of the ocean mass balance budget (Section 3.8), the latter best estimate by Petrova et al. will be used. Compared to the surface waters of all other oceans, Arctic Ocean surface waters are enriched in Hg (Wang et al., 2012a; Heimbürger et al., 2015; Agather et al., 2019) so that outflowing Arctic water entering the North Atlantic Ocean has a higher average THg concentration than Atlantic waters flowing into the Arctic (Cossa et al., 2018, 2019; Petrova et al., 2020). Riverine Hg inputs together with sea ice restricting dissolved gaseous mercury (DGM) evasion have been cited as the explanation for higher seawater Hg concentrations in Arctic surface water (Wang et al., 2012; Soerensen et al., 2016a), although coastal erosion likely also plays an important role (see Section 3.4.5).

3.5.2 How much mercury exchanges between water and sediments in the Arctic Ocean?

Marine sediments exchange Hg with overlying seawater in two ways: sedimentation/resuspension of particulate Hg, and bidirectional diffusion of dissolved and gaseous species. Only few studies have estimated some of these parameters on an Arctic-wide scale (Outridge et al., 2008; Soerensen et al., 2016a; Tesán Onrubia et al., 2020). While their accuracy is limited by sparse sediment Hg concentration and speciation data, the sedimentation rates prevailing on the continental shelves and deep basin are relatively well constrained (Rachold et al., 2004). Rivers (especially the Yukon and Mackenzie rivers) and coastal erosion provide most of the organic and inorganic material accumulating in Arctic marine sediments, with the remainder from within-ocean primary production and wind-blown dust (Holmes et al., 2002; Rachold et al., 2004; Gamboa et al., 2017). Based on a balanced solids budget for the ocean developed largely from Rachold et al. (2004), sedimentation rates of solids on shelves and the deep basin amount to 490 Mt/y and 134 Mt/y, respectively (Soerensen et al., 2016a).

Estimation of an average THg concentration in ocean sediments is difficult because of the continuing paucity of measurements, especially in the deep basin. Outridge et al. (2008; used in AMAP, 2011) relied on an early estimate of an average THg concentration of 210 ng/g in shelf sediments (Macdonald and Thomas, 1991) to develop their shelf sedimentation Hg flux. Canário et al. (2013) and Fox et al. (2014) calculated the average shelf THg concentration to be in the 20 to 55 ng/g range based on additional sampling. Gobeil et al. (1999) reported much higher THg in basin surface sediments (up to 116 ng/g) but attributed that to the diagenetic redistribution of Hg within the sediment profile. Soerensen et al. (2016a) chose 45 ng/g as the best estimate THg value for both shelf and basin sediments in their Arctic Ocean mass budget study. Suspended sediment analyses from continental shelf waters show THg concentrations to be in

the 30 to 70 ng/g range (Graydon et al., 2009a; Pućko et al., 2014). Similarly, the most recent available study suggests THg concentrations of 36 to 145 ng/g in the deep basin and 38 to 98 ng/g in the shelf sediments of the Barents Sea (Tesán Onrubia et al., 2020).

Soerensen et al. (2016a) combined the best estimates of THg with the solids budget and arrived at a sedimentation load of 30 and 8 t/y of THg to the shelf and deep basin, respectively. Resuspension was not estimated due to an absence of data on solids resuspension. As no estimates on the partitioning of Hg(II) between the dissolved and solid phases are available from Arctic sediments, dissolved phases of Hg were calculated with data from North Atlantic estuarine and shelf regions (log K_d:Hg=4.0, Sunderland et al., 2006; Hollweg et al., 2010; Schartup et al., 2015a). The dissolved concentrations were used to calculate upper and lower bounds for the diffusion of Hg species at the sediment-water interface. Diffusion to the overlaying water column was estimated at 5 t/y of THg from both shelf and deep basin sediments (from a figure of 10 t/y for the entire ocean; Soerensen et al., 2016a).

Based on Hg and Th-234 radionuclide tracer measurements, Tesan-Onrubia et al. (2020) estimated high settling fluxes of THg from the surface ocean waters (100 meters depth) of 122±55 Mg/y in the shelf (7.2±17 Mg/y, deep basin); these fluxes are adjusted for the Arctic Ocean area considered in this report. Tesan-Onrubia et al. (2020) estimated net burial of Hg in deep and outer shelf ocean sediments of 16 t/y and in total Arctic Ocean sediments of 28 t/y (24 and 4 t/y of THg to the shelf and deep basin, respectively) are in agreement with Soerensen et al. (2016a). A recent Th-230 radionuclide tracer-based study constrained the deep basin Hg burial flux to 3.9±0.7 Mg/y (Hayes et al., 2021). Surface waters THg settling flux measured by Tesan-Onrubia et al. (2020) suggests shelf sediments Hg burial flux to be higher than current estimates. Shelf Hg burial flux is likely underestimated due to a lack of measurements in the inner shelf. New measurements on the Siberian shelf suggest Hg burial rates of up to 75 Mg/y (Aksentov et al., 2021) and that earlier estimates are biased low because of underestimated sediment density. Using all available data (Tesan-Onrubia et al., 2020; Aksentov et al., 2021; Hayes et al., 2021), revised shelf Hg burial flux of 42±31 Mg/y (n=114) is estimated for this report.

3.5.3 How much mercury is present in Arctic sea ice?

The sea-ice environment takes up and transports Hg and other contaminants between the air-sea-ocean interface and the Siberian Shelf, and significant amounts of Hg is reported to reside within snow and sea ice in the Arctic (Chaulk et al., 2011; Beattie et al., 2014; Schartup et al., 2020) and the Antarctic (Cossa et al., 2011; Nerentorp Mastromonaco et al., 2016).

Deposited Hg on sea ice can be transported further down the snow column and reach the ice (Chaulk et al., 2011; Durnford and Dastoor, 2011). The vertical profile of one-year-old ice shows great variations in structure, having first a layer of snow on top, followed by an infiltrated layer of snow and ice. Shortly after the skim ice is the transition zone where the crystal orientation changes from being relatively ordered to being more disordered. The ice below (the columnar zone) has a fairly uniform structure. Arctic first-year sea ice consists mostly of columnar ice. The bottom of the ice consists of a mushy region (the skeleton layer) where the brine entrapment originates in the root area. Brine and gas can become trapped in between platelets or cells, and the ice becomes denser with growth; the brine reduces in volume due to the expulsion and drainage processes. The remaining brine inclusions become brine pockets that connect and form brine channels, similar to drainage tubes. As sea ice ages, it gets denser and less salty due to brine loss (Løset et al., 2006). Brine is enriched in Hg and brine expulsion is possibly an effective transport mechanism of Hg from the bulk ice to the underlying seawater and to the ice surface, forming frost flowers (Cossa et al., 2011; Schartup et al., 2020).

How Hg adsorbs and diffuses into sea ice depends largely on the charge of the Hg atom; i.e., depending on whether it is Hg(0), Hg(I) or Hg(II). A stronger charge and smaller atom makes diffusion easier into the bulk ice due to a lower diffusion barrier (Asaduzzaman et al., 2012). It is believed that Hg can enter sea ice either from above, from net-deposited atmospheric Hg onto surface snow, or from below via 'the underlying seawater or shelf-sediments' and travel through brine channels. Snow and frost flowers are great scavengers of atmospheric contaminants due to their large surface area (Douglas et al., 2005; Sherman et al., 2012). Gaseous elemental mercury can adsorb to snowflakes and frost crystals. Wet and dry net-deposited Hg onto those surfaces could transport Hg further down into the ice.

When sea ice is formed, Hg and other contaminants can become incorporated within the ice during processes like freeze rejection and particle entrapment (Chaulk et al., 2011; Wang et al., 2017a). Freeze rejection is a process where halogen ions (like Br and chlorine; Cl) and contaminants dissolved in the water are rejected from the ice structure during sea-ice formation, due to their size and/or charge. The rejected ions or contaminants are either pushed back into the underlying water or collected in shallow brine channels. Due to this process, the vertical profile of contaminant concentrations in the ice often follows the salinity profile.

Sea ice formed around coastal areas can entrain sediment from rivers and form so-called dirty ice (Klunder et al., 2012), which can reach the central Arctic Ocean via the Transpolar Drift (Charette et al., 2020). Another process of how Hg and other contaminants can enter sea ice is through particle entrapment. Small aquatic particles play a role in the process when ice crystals are formed around a nucleus. Contaminants, such as Hg, that have a high affinity to particles during this process become incorporated within the ice during sea-ice formation. These particles can originate from sediments in shallow shelf waters due to scavenging from turbulent waters. Particle-bound contaminants are less prone to move into brine and reside within the ice structure. As ice ages, dissolved contaminants leak out of the ice during ice melt, which makes particle-bound contaminants more pronounced in multi-year ice (Beattie et al., 2014). The Transpolar Drift is an important vector for shelf sourced sea ice, water and contaminants across the Arctic Ocean (Charette et al., 2020).

Reported THg concentrations vary between 0.5 and 20 pM in first-year Arctic sea ice and between 0.5 and 60 pM in multi-

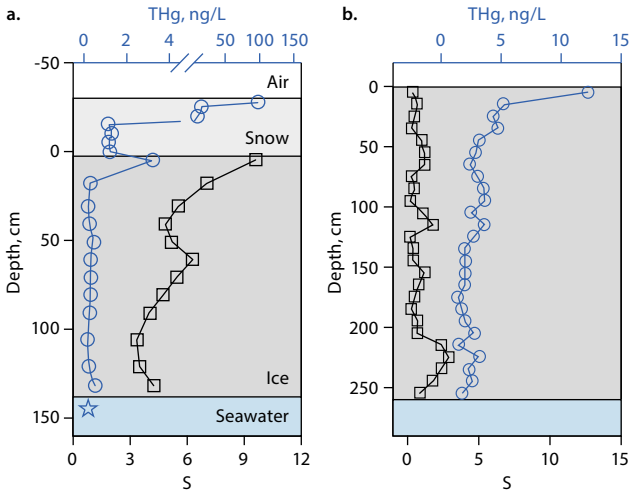

Figure 3.23 Profiles of THg in air, snow, seawater and first-year sea ice (left) and multi-year sea ice (right) along with salinity (S). This figure is adapted from Wang et al., 2017a.

year ice (Figure 3.23; Wang et al., 2017a). Recent studies in the central Arctic Ocean find no difference between first-year sea ice, 3.0±2.6 pM, and multi-year ice, 2.6±2.2 pM (see Table 3.18; DiMento et al., 2019; Schartup et al., 2020). Mercury concentrations in the sea ice cores are similar or slightly higher compared to those in the sea water directly underlying the sea ice (5.22±2.61 pM) and in the polar mixed layer (~1.5 pM). An accumulation of Hg in the ice might be due to Hg being highly particle-reactive and attaching to particles within the ice (Chaulk et al., 2011; Beattie et al., 2014). Using Schartup et al.'s (2020) average sea-ice Hg concentration (3.0 pM) and the yearly mean sea-ice volume for 2015 (1.54 x 10^4 km^3), the Arctic Ocean sea-ice Hg reservoir is estimated to be 9.2 Mg (ranging from 3.5 to 14.6 Mg), depending on that year's sea-ice volume. Assuming that approximately 2400±640 km^3 of sea ice are exported yearly out of the Arctic Ocean, 1.4±0.4 Mg of sea-ice Hg are exported yearly through the Fram Strait (these figures are used as best estimates in Section 3.8).

3.5.4 How much mercury is present in the Arctic Ocean?

There were few published data showing the vertical distributions of Hg in the open waters of the Arctic Ocean before the pan-Arctic GEOTRACES cruises (Heimbürger et al., 2015), with more data measured in coastal waters and within the Canadian Arctic Archipelago (St. Louis et al., 2007; Kirk et al., 2008; Lehnherr et al., 2011; Wang et al., 2012a) with the earlier data summarized in Sorensen et al. (2016). Some recent studies have included the Labrador Sea (Cossa et al., 2018; Wang et al., 2018). The 2015 to 2016 German, Canadian and US GEOTRACES cruises have largely expanded the Arctic Ocean Hg database (Wang et al., 2018; Agather et al., 2019; Charette et al. 2020; Petrova et al., 2020; Tesán Onrubia et al., 2020). The overall dataset suggests that river discharge and other surface and sediment inputs are important sources of Hg to the coastal zone of the Arctic, and that much of this Hg is strongly removed in the shelf regions. Atmospheric inputs to the central basin are low given the low precipitation, except for periods when substantial AMDEs are occurring (Soerensen et al., 2016a).

Table 3.18 Total Hg concentrations in brine, under-ice water, melt ponds, frost flowers and snow (average±standard deviation). This table is adapted from Schartup et al., 2020 (Supporting Information Table S2).

Sample type	Station*	Number of samples	Salinity	Total Hg (pM)
Brine	46	1	--	17.3
Under-ice water	All	7	--	5.22±2.61
	46	2	30.9	7.27, 5.12
	54	1	14.0	2.38
	81	1	--	9.96
	69	1	--	3.23
	96	1	--	3.86
	117	1	--	4.73
Melt pond water	All	5	--	9.90±5.42
	46	1	--	7.54
	81	3	0.8	13.73, 5.66, 3.12
	69	1	0.110	11.74
	96	1	13.0	17.60
Melt pond ice	All	2	--	3.83
	81	1	--	2.17
	96	1	--	5.48
Frost flowers	104	1	--	3.24
Snow	All	3	--	2.63±0.38
	81	1	--	1.01
	69	1	0.05	2.92
	96	1	0	2.77

* Schauer, 2016

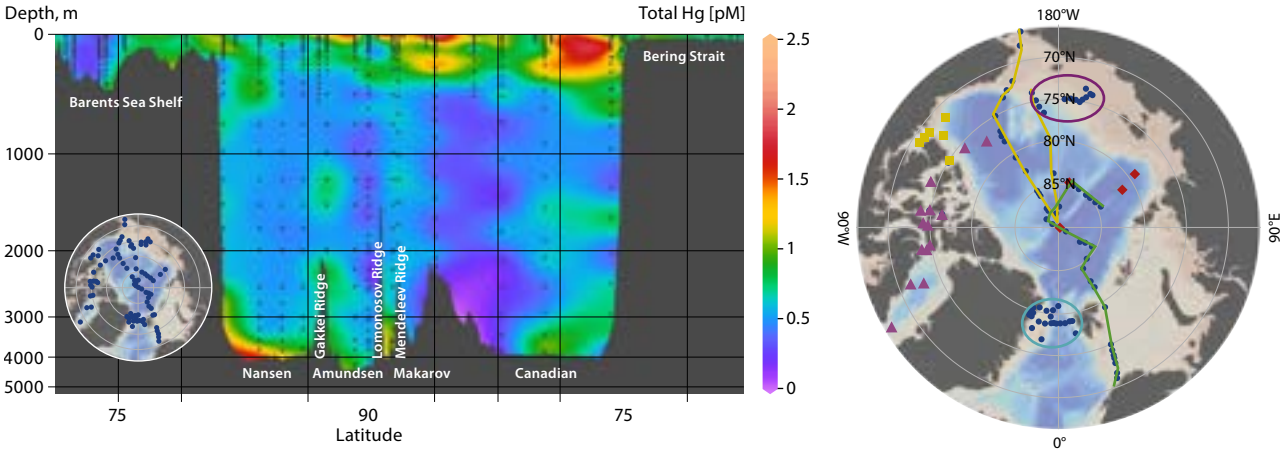

Figure 3.24 Transect of total Hg across the Arctic Ocean compiled from Heimbürger et al., 2015; Agather et al., 2019; Charette et al., 2020; Petrova et al., 2020 (left), and compilation of all recent Arctic Hg data (right): yellow squares represent Wang et al., 2012a; red diamonds represent Heimbürger et al., 2015; pink triangles represent Wang et al., 2018; yellow transect represents Agather et al., 2019; light green transect represents Charette et al., 2020; violet area represents Kim et al., 2020b; and the light blue area represents Petrova et al., 2020.

The recent observations make the Arctic Ocean one of the best covered ocean basins (n=1911; see Figure 3.24). All studies suggest higher Hg concentrations in surface waters (0–20 m, Hg=1.21±0.60 pM, n=159), which is contrary to all other ocean basins (Bowman et al., 2020a). The surface Hg enrichment suggests inputs from melting sea ice, atmospheric deposition, erosion and rivers (Heimbürger et al., 2015; Charette et al., 2020). The halocline waters contain slightly lower Hg concentrations (20–200 m, Hg=0.94±0.46 pM, n=465). The North Atlantic-sourced waters contain lower Hg concentrations (200–500 m, Hg=0.76±0.36 pM, n=164) reflecting also their origin. The Arctic deep waters below 500 m are also low (Hg=0.67±0.30 pM, n=369). Higher coastal values were observed in the CAA (1.82±1.06 pM; Wang et al., 2018; Lehnherr et al., 2011) and on the North-Eastern Greenland Shelf (1.58±0.53 pM; Petrova et al., 2020), but not on the Barents Sea Opening (0.43±0.14 pM; Petrova et al., 2020). Concentrations in the Bering Sea and Chukchi shelf (<200 m) averaged 1.06±0.6 pM (n=78, Agather et al., 2019). Kim et al., 2020b also found lower values of 1.0±0.3 pM over the East Siberian Shelf. The Hg concentrations in the central Arctic Ocean are somewhat higher than those measured on recent cruises in the far North Atlantic Ocean (Cossa et al., 2018) and the global ocean (Bowman et al., 2020a) but lower than those measured in the CAA (Wang et al., 2018) and the North-Eastern Greenland Shelf (Petrova et al., 2020). The distinct characteristics of the Arctic and Atlantic water masses are present at Fram Strait in the outflowing East Greenland Current and inflowing West Spitzbergen Current, respectively (Petrova et al., 2020).

An estimate of the amount of Hg in the Arctic water column can be made based on all the available Hg observations (Wang et al., 2012a, 2018; Heimbürger et al., 2015; Agather et al., 2019; Charette et al., 2020; Kim et al., 2020b; Petrova et al., 2020; Tesán Onrubia et al., 2020). The overall Arctic dataset suggests that there is ~1871 Mg of Hg in the Arctic Ocean, distributed with depth, as follows: 44 (0–20 m), 228 (20–200 m), 224 (200–500 m) and 1375 (500–bottom) Mg. This estimate is comparable with the value of 1900 Mg found by Petrova et al. (2020), which was based only on the German GEOTRACES central Arctic data. The new value using all available Arctic Hg data is however lower value than 2870 Mg of Hg found by Soerensen et al. (2016a) and substantially lower than the early estimate of 7920 Mg by Outridge et al. (2008).

The measured values from these Arctic cruises are lower than the modeled values for surface water THg, such as those of Fisher et al. (2012), who predicted a autumn sea-water concentration near 2 pM. The observations suggest that such estimates are too high, and this likely reflects the fact that such modeling was relying on the data from coastal waters and the CAA, which are higher than found in the open waters of the Arctic Ocean, as noted above. Overall, the deep waters of the Arctic Ocean have a long residence time, between 50 and 100 years based on the Soerensen et al. (2016a) model and the more recent data, and therefore suggest that the deep Arctic Ocean concentration will be changing slowly in response to anthropogenic emissions and climate change. There is no difference in Hg concentrations between the Nansen, Amundsen, Makarov and Canadian basins.

3.6 What are the relative contributions of primary geogenic and anthropogenic, and re-emission sources of mercury to Arctic environments?

Since the AMAP 2011 report, Dastoor et al. (2015; Hg emissions for 2005), GMA Update 2015 (Hg emissions for 2010) and GMA 2018 (Hg emissions for 2015) have reported model-based anthropogenic deposition contributions to annual THg deposition in the Arctic from East Asia, Europe and North America of 9.3% to 12%, 2.3% to 2.5% and 0.7% to 2.2%, respectively. The GMA 2018 study was performed using four models: ECHMERIT, GEM-MACH-Hg, GEOS-Chem, and GLEMOS, to analyze global Hg source apportionments. ECHMERIT currently lacks some of the Arctic specific Hg oxidation processes, especially important to springtime deposition. Therefore, the GMA 2018 model simulations conducted by the three models (GEM-MACH-Hg, GEOS-Chem and GLEMOS) using AMAP anthropogenic emissions of 2224 t/y in 2015 (see Section 3.2) were re-analyzed to develop detailed model ensemble source apportionment estimates of

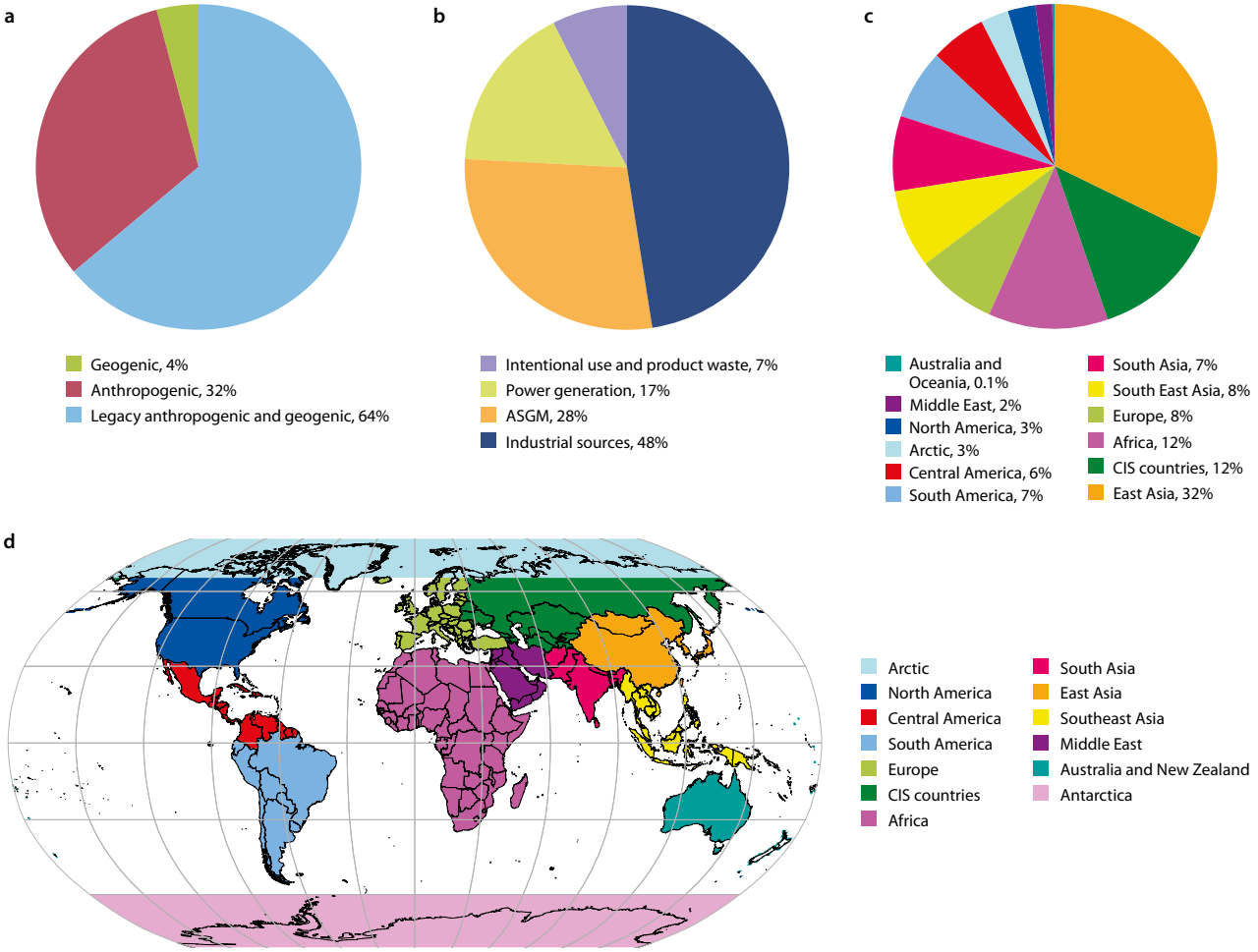

Figure 3.25 (a) Relative contributions of global anthropogenic, legacy (re-emission of historic anthropogenic and geogenic deposition) and geogenic emissions to annual total Hg deposition, (b) relative contributions of annual anthropogenic Hg deposition originating from different anthropogenic emission sectors, (c) relative annual anthropogenic deposition contributions originating from each source region, and (d) definitions of global anthropogenic source regions in the Arctic in 2015.

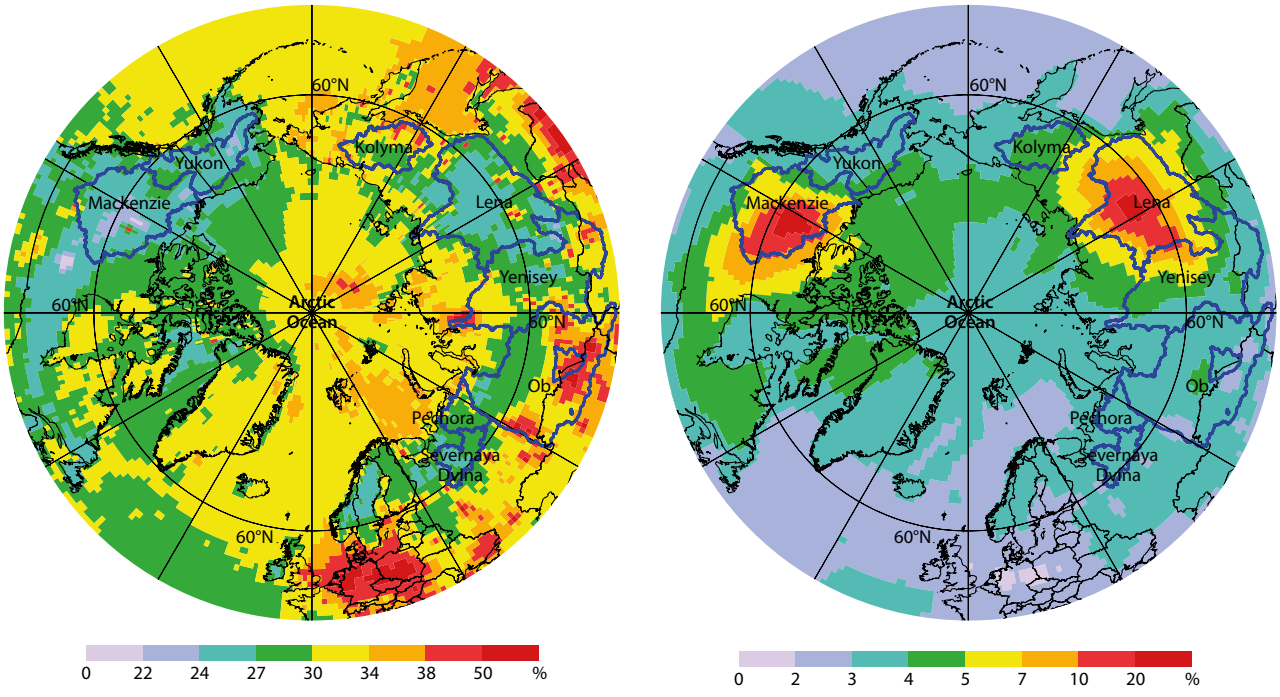

Figure 3.26 Relative contributions of annual Hg deposition originating from global anthropogenic and biomass burning. Emission sources in 2015 simulated by the (a) model ensemble and (b) GEOS-Chem.

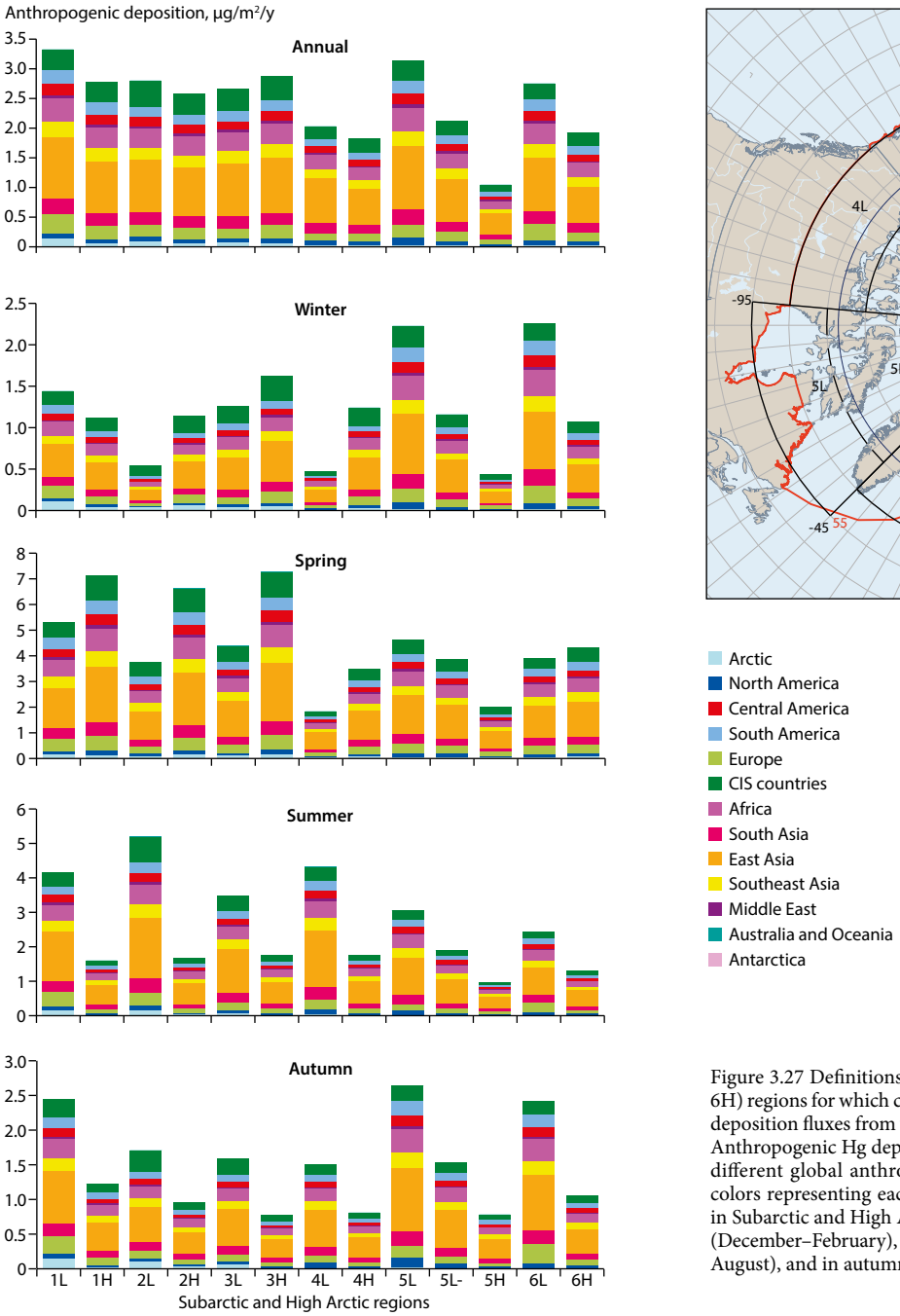

Figure 3.27 Definitions of Subarctic (1–6L) and High Arctic (1–6H) regions for which contributions of average anthropogenic Hg deposition fluxes from worldwide source regions were estimated. Anthropogenic Hg deposition flux contributions (μg/m²/y) from different global anthropogenic source regions (see legend for colors representing each source region) to total Hg depositions in Subarctic and High Arctic regions in 2015, annually, in winter (December–February), in spring (March–May), in summer (June–August), and in autumn (September–November).

Hg deposition in various regions of the Arctic for this report, discussed in this section (see Figures 3.25. 3.26 and 3.27).

Model ensemble median annual Hg deposition (i.e., originating from contemporary global anthropogenic and geogenic emissions, and re-emission of legacy deposition) estimates within 60°N and 66.5°N in the Arctic in 2015 are 243±41 and 133±31 Mg/y, respectively. In the Arctic, contemporary global anthropogenic Hg emissions are responsible for 32% of annual Hg deposition, and seasonally for 35% in spring, 30% in winter, 28% in autumn and 26% in summer (see Figure 3.25a). Re-emissions of legacy deposition (of anthropogenic and geogenic origin) from soils and oceans and primary geogenic emissions contribute to 64% and 4% of the annual Hg deposition in the Arctic, respectively (see Figure 3.25a). It should be noted that accumulated anthropogenic deposition in global ecosystems since the inception of industrial activities contribute to a larger portion of legacy re-emissions, which is expected to grow in future in the absence of (or delayed) anthropogenic emission reduction efforts (Kwon and Selin, 2016). Seasonal contributions to annual anthropogenic Hg deposition in the Arctic (i.e., the portion of Hg deposition of anthropogenic origin) are estimated to be largest in spring (50%) followed by summer (25%), autumn (13%) and winter (12%). The proportions of annual anthropogenic Hg deposition from emissions in various global source regions to the Arctic are in the following order: East Asia (32%), CIS countries (12%), Africa (12%), Europe (8%), Southeast Asia (8%), South Asia (7%), South America (7%), Central America (6%), Arctic (3%), North America (3%), Middle East (2%), and Australia and New Zealand (0.1%; see Figure 3.25d). However, some seasonal differences marked by distinct atmospheric circulations and deposition processes also exist. For example: the anthropogenic contributions from East Asia are 1.2, 1.5, 2.0 and 1.8 times higher than that of combined

CIS and European contributions in winter, spring, summer and fall, respectively; and anthropogenic contribution from Africa dominates CIS countries contribution while South Asian contribution dominates European contribution in summer and fall, and the converse is the case in winter and spring.

The models were also applied to estimate the relative contributions of anthropogenic emissions of Hg from different sectors to the total annual anthropogenic Hg deposition in the Arctic (see Figure 3.25b). Total anthropogenic emissions of Hg were aggregated into four general groups: (i) power generation, 347 t/y (15.6%); (ii) industrial sources, 874 t/y (39.3%); (iii) intentional use and product waste, 166 t/y (7.5%); and (iv) ASGM, 838 t/y (37.6%; see Section 3.2). Chemical speciation of Hg emissions differs considerably between different sectors. Emissions from power generation consist of approximately equal contributions of elemental and oxidized forms of Hg. The proportion of oxidized Hg is much smaller in emissions from industrial sources (20%). One fourth of the total Hg emissions from intentional use and product waste are emitted in the oxidized Hg forms, whereas all Hg emitted from ASGM is in elemental gaseous form. It should be noted that available estimates of Hg speciation from emission sources are associated with significant uncertainties (see Section 3.2). Due to the large proportion of oxidized Hg emissions from the power generation sector, a significant portion of Hg from this sector is deposited locally in the regions of major stationary combustion sources located in East and South Asia, Europe, North America, and South Africa. The power generation sector accounts for 17% of the total anthropogenic deposition of Hg in the Arctic. Mercury emissions from the industrial sector are more widely distributed over the world and contain a substantial fraction of GEM (80%), resulting in approximately half (48%) of the anthropogenic deposition of Hg in the Arctic. The majority of ASGM emission sources are located in the low latitudes of both hemispheres; however, Hg emission from this sector, being in the elemental form, is transported globally and makes up 28% of the total anthropogenic deposition of Hg in the Arctic. The contribution from intentional use and product waste comes to 7%, which is consistent with the proportion of its share in total Hg emissions.

Measurements and modeling confirms that Hg deposition to vegetation, and thus summertime deposition, dominates other terrestrial deposition pathways and is a major source of Hg to boreal forests and tundra soils (Giesler et al., 2017; see Section 3.4.1), making the Arctic susceptible to the impact of northern wildfires (Friedli et al., 2001 Obrist et al., 2017; Fraser et al., 2018). Legacy Hg deposition accumulated in vegetation and active soils is released back to the atmosphere during wildfires. Present-day global and Arctic (north of 60°N) wildfire emissions are estimated at 400–675 Mg/y and ~20–200 Mg, respectively (Friedli et al., 2003a and 2009; De Simone et al, 2017; Kumar et al., 2018; McLagan et al., 2021; see Section 3.2.3.1). Dominant source regions of wildfire emissions are Africa (43.8% of global emissions), Eurasia (31%) and South America (16.6%), and global wildfire Hg emissions are estimated to increase by 14% in 2050 due to climate change (Kumar and Wu, 2019; see Section 5.4). Models estimate that global wildfire emissions are responsible for 12–17 Mg/y of Hg deposition in the Arctic, representing 6% to 10% of annual Hg deposition in the Arctic (Kumar and Wu, 2019; GEOS-Chem and GEM-MACH-Hg, and spatial distribution in Figure 3.26b). Using GEOS-Chem, Kumar and Wu (2019) estimated wildfire contributions to the annual Hg deposition from Eurasia, Africa, and North America of 5.3%, 2.5% and 1% in the Arctic spread across all seasons, but more than 50% of wildfire-induced Hg deposition originated from Eurasia and North America boreal forest fires in summer and fall. Fraser et al.'s (2018) modeling study reported the western Canadian Arctic (the Northwest Territories and Yukon) to be consistently more impacted by wildfires and found the Great Slave Lake region, in the Northwest Territories, to be a wildfire Hg deposition 'hotspot'. Recent measurements from lake sediment collected north of Great Slave Lake reported that charcoal deposition from wildfires since the late 1800s co-occurred with excess deposition of Hg to the lakes (Pelletier et al., 2020). Figure 3.26b shows highly variable spatial distribution of the impact of wildfire emissions in 2015 simulated by GEOS-Chem with wildfire contributions of over 20% in the Subarctic regions of western Canada and Eastern Siberia.

The proportion of Hg released as gaseous elemental Hg in wildfires varies between 50% and 95% based on aircraft measurements (Friedli et al., 2003b), satellite measurements (Finley et al., 2009) and laboratory experiments (Obrist et al., 2008; Kohlenberg et al., 2018), but models currently assume wildfire Hg emissions mostly in GEM form due to a lack of speciated wildfire emission inventories. Peatlands are an important sink for organic matter and Hg in the circumboreal regions, and the burning of peat-rich soils likely leads to a significantly greater release of Hg than currently estimated (Turetsky et al., 2006; Fraser et al., 2018). A better estimation of the proportion of gaseous Hg to particulate Hg and the propensity of different biomes (such as boreal peatlands) to release Hg during wildfires are needed to reduce uncertainties in modeling estimates (De Simone et al., 2015; Fraser et al., 2018; Kumar et al., 2018).

Spatial distribution of the relative contribution of anthropogenic Hg deposition to the total annual Hg deposition simulated by the model ensemble in the Arctic is presented in Figure 3.26a. The central and eastern Arctic Ocean are estimated to receive a relatively higher proportion of annual Hg deposition from anthropogenic sources (30% to over 50%) than in the western Arctic Ocean including the Canadian Arctic Archipelago (≤30%). Anthropogenic deposition contributions of Hg are lower to terrestrial surfaces (below 30%) than they are to the ocean with an exception of watersheds of the Yenisey and Kolyma rivers in Eurasia. The lowest anthropogenic contributions are estimated for the Mackenzie, Yukon and Lena river basins, but these watersheds accumulate a relatively higher percentage of Hg deposition from wildfires (see Figure 3.26b). Measurements and model ensemble both suggest Hg runoff from Yenisey and Lena rivers to the Arctic Ocean to be the largest (see Sections 3.3.3.4 and 3.4.4).

In order to further analyze the spatiotemporal variations of global anthropogenic Hg emission contributions within the Arctic, seasonally distributed median anthropogenic Hg deposition contributions were estimated in six Subarctic regions (defined as 1–6L) and six High Arctic regions (defined as 1–6H) using the model ensemble simulations (see Figure 3.27).

Subarctic regions mostly encompass terrestrial regions and High Arctic regions cover oceanic surfaces, with the exception of the regions defined as 5L and 5H (eastern Canada to western Greenland). Generally, differences in relative anthropogenic deposition contributions from emissions in various worldwide geographic regions to different Arctic regions (1–6L and 1–6H) are found to be small, reflecting a long lifetime of Hg in the atmosphere giving rise to a well-mixed distribution. The largest total anthropogenic contributions are simulated in 1L (3.33 μg/m²/y) and 5L (3.13 μg/m²/y), primarily reflecting their proximity to mid-latitude anthropogenic sources and higher precipitation rates in these regions. Although total anthropogenic deposition contributions are comparable in 1L and 5L, the European contribution is two times the North American contribution in 1L, and the converse is the case in 5L. In the High Arctic, eastern regions (1–3H) receive larger total anthropogenic deposition contributions (2.6–2.9 μg/m²/y) than the western regions (1.05–1.9 μg/m²/y in 4–6H). The western High Arctic regions are characterized by both lower precipitation and the import of emissions to the Arctic.

Seasonally, there are notable spatial variations in total anthropogenic Hg deposition contributions, mainly arising from inter-seasonal shifts in atmospheric circulation, precipitation and vegetation regimes. In autumn and winter, there is no clear distinction in contributions between Subarctic and High Arctic regions; the highest anthropogenic depositions in the Subarctic occur in 5L and 6L. Springtime anthropogenic contributions are exacerbated by AMDEs over sea ice, meaning that deposition is highest in High Arctic regions, especially in 1–3H. In summer, the northward retreat of the polar front limits the pollution transport to the High Arctic (see Section 3.3.3.1); additionally, efficient vegetation Hg uptake in temperate and Subarctic regions enhances anthropogenic Hg deposition in the Subarctic regions and lessens in the High Arctic regions (see Section 3.3.3.2). Overall, relative contributions of anthropogenic Hg to the total Hg deposition are found to be slightly higher in the High Arctic regions compared to the Subarctic regions, and anthropogenic contributions are estimated to be highest in winter and spring (31% to 38%) and lowest in summer (25% to 28%).

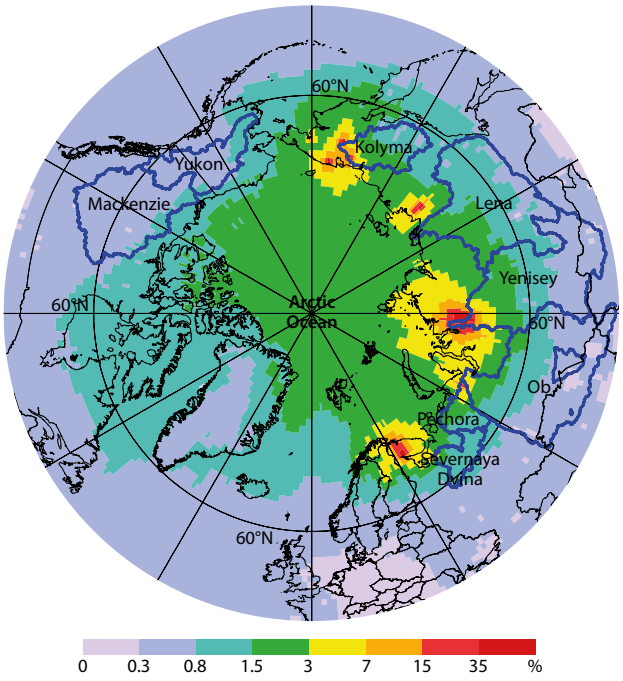

Figure 3.28 Relative contribution of local anthropogenic Hg emission sources (located north of 66°N) to annual anthropogenic Hg deposition in 2015.

3.7 What is the relative contribution of local anthropogenic sources of mercury to Arctic environments?

Three global models (GEOS-Chem, GEM-MACH-Hg and GLEMOS) were applied to estimate the relative contribution of Arctic region emissions (emissions located north of 66°N) from human activities to total anthropogenic Hg deposition in the Arctic. Sources within the Arctic region contribute <1% (~14 Mg/y) of the total estimated anthropogenic emissions of 2220 Mg/y in 2015, the majority of which are located in Russia (see Section 3.2.2.5). As reported in the section above (Section 3.6), the model ensemble estimates an average contribution of 3% from Arctic region anthropogenic emissions to the annual total anthropogenic Hg deposition in the Arctic (see Figure 3.25d), which is comparable to the contribution from North American anthropogenic sources. This section explores the spatial distribution of the impact of Arctic region anthropogenic emissions on anthropogenically deposited Hg within the Arctic. Model ensemble results suggest that the relative contribution of Arctic region anthropogenic emissions to annual anthropogenic Hg deposition varies between 2% and 7% over the Arctic Ocean (see Figure 3.28). On land, local anthropogenic sources account for up to 35% of anthropogenic Hg deposition in Eurasia annually. Anthropogenic emissions include a fraction of Hg emission as oxidized Hg, which contributes to high deposition to local landscapes owing to its short lifetime. Model results show that local anthropogenic sources influence the Hg deposition in Eurasian river watersheds (e.g., the Yenisey and Kolyma watersheds), thus also contributing to river Hg runoff to the Arctic Ocean. It should be noted that there are additional anthropogenic Hg sources between 60 and 66°N that are not considered here.

Figure 3.29 presents the seasonal differences in anthropogenic emission contributions to Hg deposition in the Arctic from Arctic regions (north of 66°N). Notable seasonal differences in Hg deposition contributions from local anthropogenic origin are simulated by the model ensemble, driven by distinct seasonal atmospheric transport and deposition pathways (see Section 3.3.3). In winter and fall, efficient low-level Hg transport of north Eurasian emissions over frozen surfaces combined with inefficient removal processes lead to relative local anthropogenic contributions of 3% to 15% and over 15% to the eastern Arctic Ocean and High Arctic terrestrial regions, respectively. Conversely, in summer and spring, both weak transport into the Arctic polar dome and efficient wet and dry removal of Hg result in more deposition in the vicinity of sources on land and generally <3% contribution of local anthropogenic sources to the ocean.

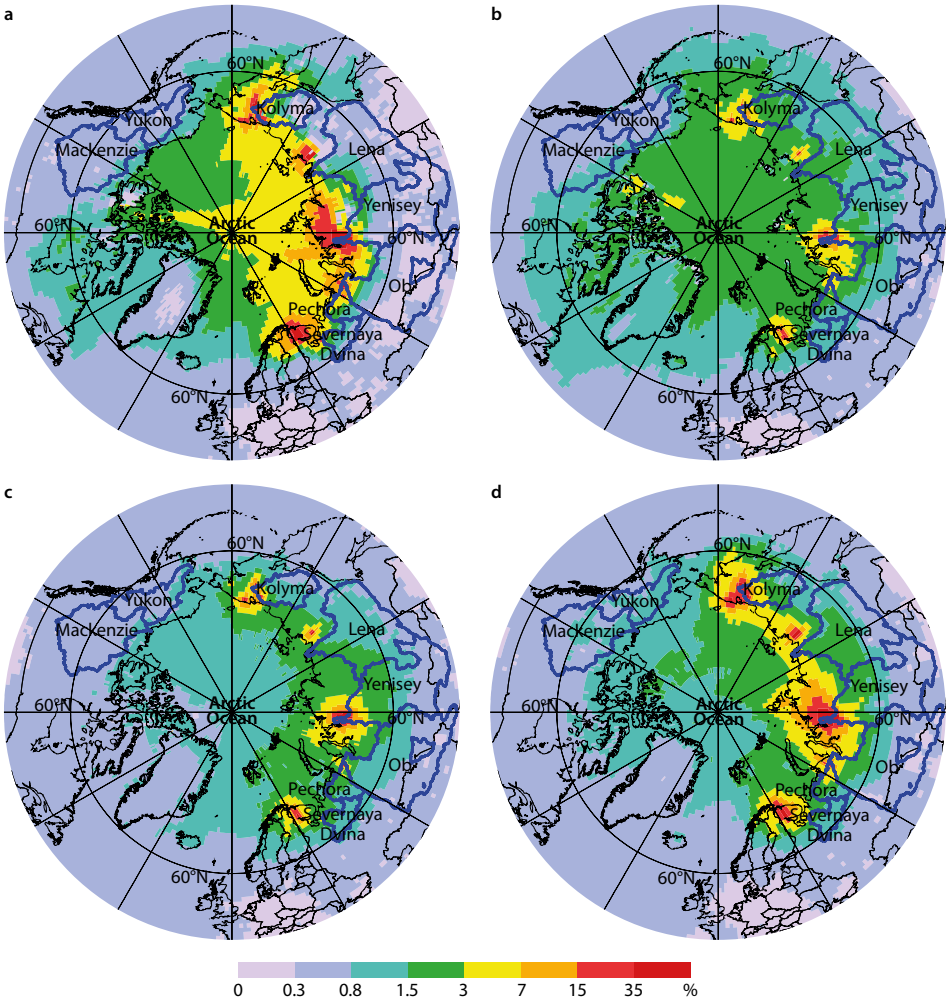

Figure 3.29 Relative contributions of local anthropogenic sources (emissions north of 66°N) to anthropogenic Hg depositions in winter (a), spring (b), summer (c) and autumn (d) of 2015.

3.8 How much mercury is circulating in Arctic environments?

Mercury accumulation in different parts of the Arctic (land, air and waters) is interlinked, and reflects the sources, transport pathways and lifetime of Hg in environmental media inside and outside the Arctic. Development of inter-compartmental fluxes and mass budgets of Hg in the Arctic is important to assessing the status of Arctic Hg and establishing a benchmark for evaluating future changes of Hg in support of the effectiveness evaluation objective of the Minamata Convention. In addition, this exercise allows identification of uncertainties and gaps in the current understanding of Arctic Hg cycling. In the last decade (i.e., since the last AMAP report in 2011), several studies have published the Arctic Ocean Hg mass budget based on observations and modeling, reflecting the progress that has been made (Fisher et al., 2012; Dastoor and Durnford, 2014; Soerensen et al., 2016a; Sonke et al., 2018; Tesan-Onrubia et al., 2020; Petrova et al., 2020). This report provides a revised Arctic Ocean and, for the first time, a terrestrial system Hg mass balance assessment in the Arctic (Figure 3.30; Table 3.19).

Fisher et al. (2012) estimated a net deposition flux of atmospheric Hg to land of 10 Mg/y, oceanic deposition of 45 Mg/y (25 Mg/y, ice-free ocean; 20 Mg/y, meltwater on sea ice) and oceanic evasion of 90 Mg/y north of 70°N, and inferred terrestrial input of Hg to the Arctic Ocean of 95 Mg/y (80 Mg/y, rivers; 15 Mg/y, coastal erosion). Durnford et al. (2012) and Dastoor and Durnford (2014) estimated a net Hg deposition of 42 Mg/y to terrestrial surfaces and 75 Mg/y to marine surfaces (deposition of 58 Mg/y to the open ocean and 50 Mg/y via meltwater; evasion of 33 Mg/y) north of 66.5°N, and 50 Mg/y of riverine Hg input to the Arctic Ocean. Soerensen et al. (2016a) estimated atmosphere-ocean Hg fluxes by combining modeled direct deposition to ice-free ocean from Fisher et al. (2012), an average meltwater contribution from Fisher et al. (2012) and Dastoor and Durnford (2014), and evasion from Zhang et al. (2015). Combining modeling and observed estimates, Soerensen et al. (2016a) presented a complete mass budget of THg in the Arctic Ocean (76 Mg/y, deposition; 99 Mg/y, evasion; 50 Mg/y, river input; 32 Mg/y, coastal erosion; 53 Mg/y, ocean inflow; 79 Mg/y, ocean outflow; and 28 Mg/y, sediment burial). Sonke et al. (2018), Petrova et al. (2020), Tesan-Onrubia et al. (2020) and Zolkos et al. (2020) have further refined the Soerensen et al. (2016a) Arctic Ocean Hg mass balance by constraining pan-Arctic riverine input (44±4 Mg/y), oceanic sediment burial (28±13 Mg/y), and inflow (55±7 Mg/y) and outflow (73±8 Mg/y) fluxes of Hg based on recent observations.

Table 3.19 Total Hg fluxes and levels in Arctic abiotic environments; fluxes and levels for land are for the area north of 60°N, and for the ocean are for the AMAP defined oceanic region (see Figure 3.30).

Compartment	Best estimate	Reference to the corresponding section in this chapter
Mercury exchange flux (Mg/y)		
Anthropogenic emission	14	3.2.2.5
Geogenic/legacy soils/vegetation emission	24 (6.5–59.1)	3.2.3
Biomass burning emission	8.8±6.4 (SD)	3.2.3.1
Atmospheric deposition to land	118±20 (SD)	3.3.3.4
Atmospheric deposition to the Arctic Ocean	64.5±19.8 (SD)	3.3.3.4
Arctic Ocean evasion to atmosphere	32 (23–45)	3.3.3.3
Riverine input to the Arctic Ocean	41±4	3.4.4
Coastal erosion input to the Arctic Ocean	39 (18-52; 25% to 75% quartiles)	3.4.5
Ocean current inflow to the Arctic Ocean	55±7 (SD)	3.5.1
Ocean current outflow from the Arctic Ocean	73±8 (SD)	3.5.1
Burial flux in shelf sediments	42±31 (SD)	3.5.2
Burial flux in deep sediments	3.9±0.7 (SD)	3.5.2
Benthic flux from shelf sediments	5	3.5.2
Sea-ice outflux from Arctic Ocean	1.4±0.4 (SD)	3.5.3
Mercury mass (Mg)		
Atmosphere	330 (290–360, seasonal variation)	3.3.2
Surface soils (0–0.3 m)	49 000 (26 000–72 000)	3.4.1.2
Active layer soils (0–1 m)	212 000 (184 000–240 000)	3.4.1.2
Permafrost soils (0–3 m)	597 000 (upper limit: 1 656 000)	3.4.1.2
Terrestrial snowpack	39 (35–42)	3.4.1.3
Glaciers	2 415±22 (SD)	3.4.3
Sea ice	9.2 (3.5–14.6)	3.5.3
Arctic Ocean surface layer (0–20 m depth)	44±22 (SD)	3.5.4
Arctic Ocean subsurface layer (20–200 m depth)	228±112 (SD)	3.5.4
Arctic Ocean intermediate layer (200–500 m depth)	224±106 (SD)	3.5.4
Arctic Ocean deep layer (500–base)	**1375±616 (SD)**	**3.5.4**

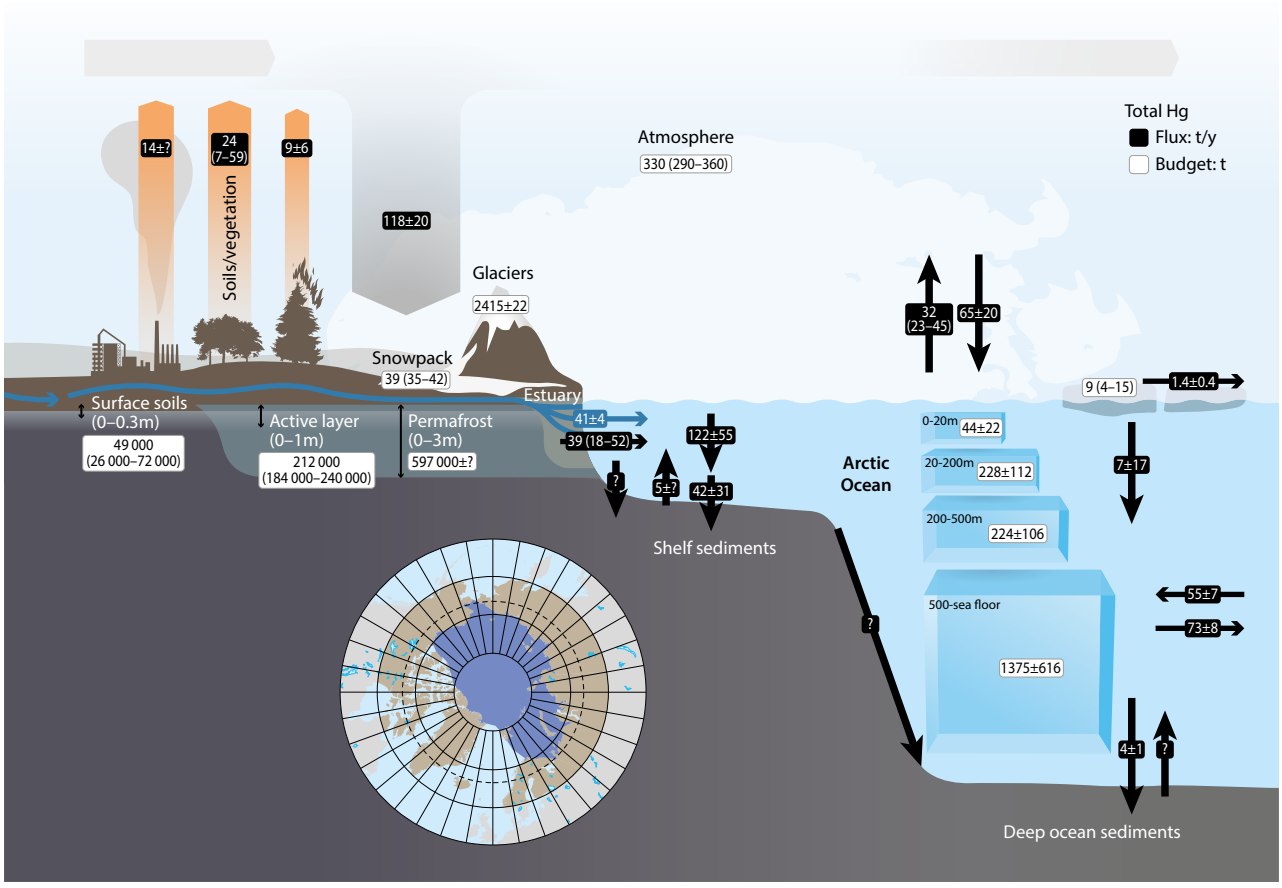

Figure 3.30 Annual Hg fluxes and mass budgets in the Arctic. A more restricted definition of the Arctic Ocean consisting of the almost landlocked ocean including the oceanic deep Arctic Ocean Basin; the broad continental shelves of the Barents, Kara, Laptev, East Siberian, Chukchi and Beaufort seas; the White Sea; and the narrow continental shelf off both the Canadian Arctic Archipelago and northern Greenland is used in the Hg mass balance estimates presented in this chapter.

Based on a synthesis of literature published since the last AMAP report (AMAP, 2011) and new multi-model ensemble simulations, a comprehensive understanding of the present-day total Hg exchange fluxes and mass budgets in the Arctic is developed in this report as described in previous sections (see corresponding section numbers in Table 3.19). Definitions of what constitutes 'the Arctic Ocean' vary in the literature. The studies reviewed above, in most cases, defined the Arctic Ocean as the area north of 66.5 or 70°N, whereas the region of the Arctic Ocean considered in this assessment is the same as that which was used for the AMAP 2011 assessment so that they can be directly compared. This area was based on Jakobsson (2002, 2004) and represents a restricted definition of the Arctic Ocean that excludes the Greenland, Iceland and Norwegian seas, Baffin Bay and the Davis Strait, and the interior waters of the Canadian Arctic Archipelago (see Figure 3.30). Given the importance of Hg fluxes and budgets in terrestrial environments to the circumpolar riverine Hg export to the Arctic Ocean, the terrestrial region north of 60°N, encompassing the majority of pan-Arctic watersheds, is represented here. Best estimates of total Hg fluxes and masses in Arctic abiotic environments have been developed using a combination of the following four approaches: (1) measurement-based literature estimates; (2) new estimates derived based on recent measurements; (3) average of measurement-based and model ensemble estimates; and (4) model ensemble estimates. Mercury emissions and model results represent the year 2015, and the majority of the measurements used were obtained within few years of 2015 in the Hg fluxes and budget estimates presented here. Model-based estimates were constrained using the multi-model ensemble simulations (DEHM, GEM-MACH-Hg, GEOS-Chem and GLEMOS).

In the atmosphere, ~330 Mg of Hg burden is estimated north of 60°N. The best estimates of total Hg in Arctic terrestrial environments are: ~597 000 Mg (0–3 m depth) in permafrost soils; ~39 Mg in seasonal snowpack; and ~2415 Mg in glaciers. Air-terrestrial Hg exchange fluxes north of 60°N are: ~14 Mg/y of anthropogenic emissions; ~24 Mg/y of soils/vegetation evasion; ~9 Mg/y of wildfire emissions; and ~118 Mg/y of deposition. Mercury export fluxes from terrestrial systems to the Arctic Ocean are ~41 Mg/y from rivers and ~39 Mg/y from coastal erosion. The terrestrial Hg mass balance developed in this report suggests that present-day annual atmospheric Hg deposition of ~118 Mg/y to the Arctic terrestrial system is in balance with Hg re-emissions from soils and vegetation (including wildfires) and riverine and erosional exports totaling ~113 Mg/y. It should be noted that several major Arctic rivers (i.e., the Yenisey, Lena, Ob and Mackenzie rivers) also import a portion of Hg deposited to their watershed portions south of 60°N (~62 Mg/y) into the Arctic (north of 60°N) since their drainage basins extend up to 45°N. Riverine Hg import to the Arctic was not determined here, which is currently a knowledge gap. Significant uncertainties remain in the determination of air-terrestrial Hg exchange fluxes. Observations suggest that Hg(0) uptake by vegetation and soils is a dominant pathway for terrestrial Hg deposition (Obrist et al., 2017; Agnan et al., 2018; Douglas and Blum, 2019), which is currently underestimated in models. Mercury emissions (and its speciation) from biomass burning from tundra and boreal wildfires are highly uncertain (Fraser et al., 2018; Kumar et al., 2018). Biomass Hg constitutes a significant Hg reservoir in the Arctic, and is responsible for transferring Hg to soils, and partially rereleasing Hg to the air by evasion and wildfires (Štrok et al., 2015; Giesler et al., 2017; Obrist et al., 2017). Above-ground biomass Hg levels of up to 28.8 μg/m^2 for a tundra site (Toolik Field Station, Alaska, USA) and 20.7 μg/m^2 (foliar Hg) for a boreal forest site (Pallas, Finland) have been estimated (Obrist et al., 2017; Olson et al., 2019; Wohlgemuth et al., 2020). The above-ground vegetation Hg budget could not be determined here, since representative data for the entire Arctic is still lacking.

The best estimates of total Hg amounts in the Arctic Ocean are ~9 Mg in sea ice and ~1870 Mg in the Arctic Ocean waters. Arctic Ocean Hg fluxes are constrained as follows: ~64 Mg/y, deposition; ~32 Mg/y, evasion; ~41 Mg/y, river input; ~39 Mg/y, coastal erosion; ~55 Mg/y, ocean inflow; ~73 Mg/y, ocean outflow; ~46 Mg/y, sediment burial; and ~1 Mg/y, sea-ice export. In comparison to the previous Arctic Ocean mass budget studies reviewed above, the revised modeled (ensemble median) oceanic deposition and evasion fluxes north of 66.5°N are 92 Mg/y and 63 Mg/y, respectively. The revised Arctic Ocean THg inputs (~204 Mg/y) exceed outputs (~152 Mg/y) by ~52 Mg/y and indicate that Hg removal from the Arctic Ocean waters is currently underestimated. The Arctic Ocean Hg exchange fluxes of riverine input, and oceanic inflow and outflow are relatively well-constrained (see Table 3.19). Recent observations on the Siberian Shelf suggest that Hg burial rates of up to 75 Mg/y are possible, and that earlier estimates are biased low because of underestimated sediment density (Aksentov et al., 2021). Observation-based shelf Hg settling of 122±55 Mg/y from surface waters estimated by Tesán Onrubia et al. (2020) also indicates that the estimated shelf burial flux of ~42 Mg/y might be underestimated by up to 80±63 Mg/y. Mercury exports from rivers and coastal erosion to the Arctic Ocean are highly seasonal, primarily occurring during spring freshet and summer months. The fate of terrestrial Hg input in the Arctic Ocean is currently uncertain and likely varies between watersheds due to differences in the reactivity of particulate organic carbon-bound Hg (Bianchi, 2011; Rontani et al., 2014; Zhang et al., 2015). Furthermore, external Hg inputs due to global anthropogenic activity and possibly increasing terrestrial Hg export due to Arctic warming in recent decades suggest a slow ongoing increase in deep ocean Hg concentrations.

Atmosphere-ocean Hg exchange fluxes have been largely determined by modeling studies. Models suggest that Hg deposition flux to the Arctic Ocean is highest in springtime due to AMDEs. Field studies have reported high Hg deposition rates in coastal marine snow during spring (Steffen et al., 2013), but observed estimates of the role of marine snowpack Hg to the central ocean are still lacking. In order to constrain the oceanic Hg evasion fluxes, the models have thus far primarily relied on the observed concentrations of Hg(0) in surface air at the High Arctic land-based sites, which are elevated in late spring to early summer (Cole and Steffen, 2010; Durnford et al., 2012; Fisher at al., 2012; Zhang et al., 2015). Enhanced air Hg(0) concentrations in late spring and early summer are believed to result from increased Hg evasion from melting snowpacks (Dastoor and Durnford, 2014), influx of riverine Hg in the ocean (Durnford et al., 2012; Fisher et al., 2012; Kirk et al.,

2012), and surface ocean waters following the break-up of sea ice (Andersson et al., 2008; DiMento et al., 2019). Based on ocean modeling, Zhang et al. (2015) suggested that the majority (80%) of riverine Hg in the Arctic Ocean is subject to evasion in the estuarine and shelf regions. Mechanistic knowledge of the springtime release of reactive bromine species (leading to Hg oxidation and deposition), sea-ice/snowpack dynamics and air-sea Hg exchange processes based on observations in all seasons is needed for improving model implementation of these processes (Moore et al., 2014; Toyota et al., 2014a, 2014b; Wang et al., 2019a).

While a direct quantitative link between terrestrial Hg deposition and river Hg export is not yet possible, observation-based Hg runoffs from the eight major pan-Arctic rivers are strongly positively correlated (r=0.87) with modeled (ensemble) Hg deposition fluxes to their watershed components north of 60°N. These results suggest that majority of Hg deposited to the pan-Arctic watershed at latitudes south of 60°N is subject to re-emission and/or sedimentation. The observation-based total Hg runoff from the eight largest Arctic rivers (23.6 Mg/y; Sonke et al., 2018; Zolkos et al., 2020) is about half of the modeled annual Hg deposition (47.6 Mg/y) and comparable to summertime (25.2 Mg/y) or snow-cover period (22.4 Mg/y) Hg deposition to their watershed components north of 60°N (see Table 3.12). Douglas et al. (2017) measured 40% to 80% Hg runoff from melting snowpacks. Applying Douglas et al.'s (2017) measured snowpack Hg export rate to the pan-Arctic snow-cover period modeled Hg deposition suggests that seasonal snowpacks and active layer surface soils each supply roughly half of the pan-Arctic river Hg export. This is in line with observations of roughly equal amounts of dissolved and particle-bound Hg in river runoff to the Arctic Ocean (Sonke et al., 2018) and a 2 to 3 times higher Hg:C ratio observed in spring waters from Western Siberian rivers compared to summer and autumn (Lim et al., 2019).

Permafrost thaw is an important source of THg to downstream ecosystems. However, its impact varies significantly over time and space, and current observations are insufficient to estimate its overall impact on Hg cycling in the Arctic (see Section 3.4.2). Melting glaciers can export Hg to freshwater networks and the Arctic Ocean (see Section 3.4.3). However, the rate at which the release of Hg from melting glaciers occurs now, or might occur in the future, is highly uncertain. The estimated size of the Arctic glacial Hg reservoir is ~2415 Mg, approximately 97% of which is in Greenland. Approximately ~400 kg Hg is estimated to be released annually from melting Arctic glacier ice (Greenland contributing ~60%). However, the total sediment-bound Hg output from Greenland meltwater is estimated to be ~40 Mg/y, which is far in excess of Hg releases from melting ice and is likely derived from bedrock and soil erosion in glacial-fed streams.

There has been significant progress in constraining Arctic Hg fluxes and budgets in the past decade, yet important uncertainties remain. This assessment further constrains previously reported fluxes and budgets, and reports fluxes and budgets in additional compartments to close the Hg mass balance in the Arctic. The following processes and model development efforts are recommended to further improve the understanding of Hg cycling in the Arctic (see details in respective sections). The sources, mobilization pathways and fate of river Hg export to the Arctic Ocean should be investigated using observations, and integrated terrestrial biogeochemical and hydrological models. Measurement and modeling studies should investigate the importance of the Transpolar Drift, known to carry Eurasian river-sourced Hg across the Arctic Ocean (Charette et al., 2020). We must also reach a full mechanistic understanding of the role of the rapidly changing Arctic cryosphere (i.e., in snowpacks, permafrost, glaciers and sea ice) in mercury cycling. While recent studies have improved estimates of Hg burial fluxes in deep and outer shelf sediments (Tesan-Onrubia et al. 2020; Hayes et al., 2021), improved estimates of Hg burial fluxes in inner shelf sediments are needed. Finally, year-round observations of Hg concentrations and exchange fluxes in terrestrial and marine environments, and the development of dynamically coupled atmosphere-terrestrial-ocean Hg models are needed to assess the concurrent impacts of emission reduction efforts and climate change on Hg cycling in the Arctic.

3.9 Conclusions and recommendations

Conclusions (in numbered bullets) are organized under section headings (section numbers in square brackets) followed by recommendations in italics where appropriate.

What are the sources of mercury emissions to air contributing to mercury in Arctic environments, and how much mercury is being emitted? [3.2]

1. Mercury models indicate anthropogenic and legacy Hg emissions in global regions are important sources of Hg to the Arctic, which is transported there via the atmosphere and ocean currents.
2. Estimated global anthropogenic emissions of Hg to the atmosphere for 2015 were 2220 t (range: 2000–2820 t), approximately 20% higher than a revised estimate for emissions to air in 2010. Most anthropogenic emissions of Hg occurred outside the Arctic, with only an estimated 14 t (0.63%) emitted north of 60°N.
3. The increasing trend in global anthropogenic emissions in recent years was not generally reflected in observed Hg air concentrations at Arctic background air monitoring stations, most of which showed decreasing trends.
4. Wildfires around the globe are an important re-emission pathway of legacy Hg to the atmosphere, including fires in the boreal forest in the Arctic (north of 60°N).

In addition to developing emissions/release estimates at the national (or sub-national) level for key emissions sectors, additional data are needed to support and improve the process of assigning these emissions/releases to point sources or distributed sources. Geospatially distributed emissions and release inventories are needed to support (global) modeling that provides information on source-receptor relationships and Hg transport to and fate within the Arctic.

Further work is needed to better define the speciation of geospatially distributed Hg emissions, where there is currently a gap in our knowledge that requires urgent attention.

Further understanding of the fate of Hg emitted as GEM from ASGM activities is needed; in particular, further research is needed into whether these emissions are subject to long-range transport or are transformed and contribute primarily to local contamination.

There is a need to better understand the reasons for inconsistency between trends of increasing (global) Hg emissions estimates and decreasing air Hg concentration observed at Arctic air monitoring sites.

How much mercury does atmospheric circulation transport to Arctic environments? [3.3]

5. Knowledge about the mechanisms of gaseous Hg transport and oxidation/reduction chemistry in the atmosphere has significantly improved modeling capacity since the last AMAP assessment (2011). Annual mean Hg(0) concentrations of 1.42±0.04 ng/m^3 estimated with the four model ensemble used in this assessment (DEHM, GEM-MACH-HG, GEOS-Chem and GLEMOS) were comparable to observations at Arctic monitoring stations of 1.38±0.11 ng/m^3.
6. The distribution of Hg(0) concentrations is characterized by a clear latitudinal gradient suggesting transport of anthropogenic Hg from lower latitudes.
7. The model ensemble reproduces the characteristic seasonality of atmospheric Hg in the Arctic, with minimum Hg(0) concentrations in spring driven by depletion events and maximum concentrations in summer attributed to snowmelt/sea-ice and oceanic re-emissions, but significant inter-model differences remain, mainly reflecting uncertainties in Hg uptake by vegetation, and cryosphere and redox processes.
8. Model simulations suggest a small (1% to 7%) increase of air Hg(0) concentrations in most of the Arctic and a decrease in the Canadian Arctic Archipelago and northern Greenland from 2010 to 2015. The modeled general increase in Arctic air Hg(0) is inconsistent with observations; this increase is mainly driven by increase in global anthropogenic emissions reflected in the emissions inventories. The decline in air Hg(0) at High Arctic sites is consistent with the observed trend at these sites, and results from changes in meteorological conditions.
9. The Arctic is characterized by relatively low wet deposition fluxes (0–5 μg/m^2/y) compared to lower latitudes. Low Hg wet deposition fluxes in the Arctic are attributed to a combination of lower annual precipitation and lower Hg concentrations in precipitation.
10. Modeling results suggest that changes in annual Hg wet deposition between 2010 and 2015 are mostly driven by changes in meteorology (e.g., precipitation amount) rather than by changes in global anthropogenic emissions.
11. The model ensemble estimated an annual total deposition of Hg in the Arctic within 60°N of 243±41 Mg with higher seasonal contributions in spring and summer relative to autumn and winter.
12. The model ensemble estimated an average Hg deposition flux of 6.8±1.2 μg/m^2/y over land and 7.4±1.6 μg/m^2/y over the Arctic Ocean (north of 60°N). Higher Hg deposition fluxes are estimated in the regions more impacted by local emissions (mainly in Eurasia) and long-range transport (northwestern North America) of Hg, and that receive higher precipitation (the Arctic Ocean and around southern Greenland, Greenland Sea, Norwegian Sea, and western coastal Europe and North America) and vegetation (western North America and Europe) Hg uptake. The lowest deposition fluxes are found in arid regions of the High Arctic (in North America), Greenland and Eastern Siberia. Over land, there is a declining gradient in Hg deposition rate from south to north overall and west to east in Eurasia and North America in the Arctic.
13. The model simulated Hg deposition fluxes to river watersheds together with observed river runoffs suggest that Hg accumulated in active layer surface soils and seasonal snowpacks north of 60°N each supply roughly half of the annual pan-Arctic river Hg export.
14. Measurements report atmospheric Hg(0) uptake by vegetation and subsequent litterfall and plant senescence is a dominant Hg source in Arctic ecosystems (71% of total deposition), in comparison to the deposition loads by wet deposition and GOM/HgP dry deposition in vegetated Arctic ecosystems. In addition, measurements suggest that the deposition of Hg(0) throughout the snow-cover period in Arctic tundra accounts for 37% of the total annual Hg(0) deposition.
15. Model results suggest an overall increasing Hg deposition trend in the Subarctic, mainly driven by increasing precipitation (most notably in the northeast Pacific Ocean, the Davis Strait and the Greenland Sea), changing air circulation patterns, and increasing anthropogenic emissions. Model ensemble results suggest that changes in meteorology can exacerbate impacts of global anthropogenic emissions on Hg deposition in those Arctic regions which are susceptible to increasing transport, and precipitation.
16. Measurements consistently point to the build-up of Hg(0) in Arctic Ocean waters under ice. These observations suggest that there is a large Hg efflux potential with ice melt, and consequently the evasion of Hg(0) will be strongly influenced by the changing ice cover as a result of climate change.
17. Atmospheric Hg deposition to and gas evasion fluxes from the Arctic Ocean are seasonally highly variable. However, measured estimates of atmosphere-ocean Hg fluxes are only available for fall; year-round observations are needed to confirm modeled atmosphere-ocean Hg exchange fluxes.

Additional kinetic and mechanistic studies are needed to improve Hg transport modeling by filling gaps in our understanding of oxidation and reduction reactions of Hg in the gas phase, including the rate of Br-initiated oxidation of Hg(0), as well as in our understanding of the chemistry of Hg at environmental surfaces and in illuminated aqueous environments.

The Hg(0) deposition pathway to Arctic terrestrial ecosystems is likely to be underestimated in current models, and needs improvement.

Model evaluation is hampered by the limited number of air concentration and wet deposition monitoring sites in the Arctic. Measurements of wet deposition fluxes are difficult to perform in polar regions due to frequent strong winds and blowing snow condition. An alternative is to improve the spatial resolution of measurements of THg in snow samples.

The model ensemble underestimates the amplitude of both the spring minimum and the summer maximum of surface air Hg(0) concentrations at Arctic measurement sites. Real-time modeling of the distribution of bromine concentrations and sea-ice dynamics is needed to improve the models.

Additional cruise studies in open waters are needed (especially in Siberia and over the Arctic Ocean) at different times of the year to further constrain atmospheric inputs and gas evasion.

Studies of atmospheric Hg speciation over open water are needed during the Arctic spring/early summer for comparison with data collected at coastal sites, to further constrain dry deposition fluxes to the open Arctic Ocean.

Climate change-related Arctic warming, the intensifying hydrological cycle, permafrost thaw, and increasing river discharges are likely modifying the sources of river Hg runoff. Atmospheric Hg models integrated with terrestrial Hg models incorporating hydrology and Hg biochemistry are required to mechanistically link Hg deposition to river Hg fluxes and to estimate the sources of present-day and future river Hg exports to the Arctic Ocean.

Models currently do not adequately account for the impacts of changes occurring in the terrestrial biosphere (such as vegetation cover and growing season, wildfires, and legacy Hg emissions and re-emission from thawing permafrost) and in the marine environment (such as sea-ice extent, thickness, multi-year vs. first-year sea ice) on Hg exchange and redox processes across the air-surface interface. The development of fully interactive atmosphere-land-ocean biogeochemical models is needed to simulate the impacts of concurrent changes in biogeochemistry in the Arctic and global Hg emissions on Hg levels and to explain Hg trends in the Arctic.

How much mercury do terrestrial systems transport to downstream environments in the Arctic? [3.4]

How much mercury is present in Arctic terrestrial environments? [3.4.1]

18. Lichen and mosses, which take up atmospheric Hg, show higher concentrations of Hg than other plants and are a potential Hg source to foraging herbivores.
19. Mercury concentrations in vascular plants are lower in the Arctic than in temperate and tropical regions, yet plant assimilation of Hg (largely of atmospheric GEM) constitutes a significant Hg pool and impacts Arctic Hg deposition and cycling.
20. Remote Arctic soils show substantial Hg concentrations, equivalent and often exceeding soil concentrations in temperate sites closer to emission sources.
21. Spatial and depth patterns of Hg in active layer and permafrost soils show the highest Hg concentrations in organic top soils, while concentrations in permafrost soils are about two-thirds of those in surface soils. Spatial patterns of soil Hg are currently unclear, and research is in process to address this.
22. Across the Arctic, very large pools of Hg are sequestered in active layer and permafrost soils (597 000 t, 0–3 m depth) due to their depth extent and are linked to the accumulation of organic carbon therein. These soil pools are formed by a long-term legacy of Hg deposition from natural and anthropogenic sources.
23. The estimated size of the Arctic glacial Hg reservoir is ~2415 t, ~97% of which is in Greenland. In addition, seasonal snowpacks accumulate ~39 t/y of Hg in the Arctic.

Further research is recommended to better constrain the processes and extent of Hg uptake and sequestration in Arctic terrestrial environments, including accumulation pathways by different plant communities, fate of plant-derived Hg deposition, and soil and permafrost Hg distribution patterns across larger spatial scales.

There are significant uncertainties in our understanding of the mechanisms of Hg exchange fluxes between the air and the cryosphere. A measurement-based budget of Hg accumulation in snow and the fraction transferred to meltwater in the Arctic is not yet available. Given the importance of meltwater Hg runoff to lakes and the Arctic Ocean during spring freshet when riverine Hg concentrations and water discharge rates are highest, Hg cycling in the cryosphere needs to be understood across the Arctic.

How much mercury does permafrost contribute to downstream environments in the Arctic? [3.4.2]

24. Permafrost thaw may be an important source of THg to downstream ecosystems. However, its impact varies significantly over time and space. As such, the contribution of permafrost thaw to downstream ecosystems is impossible to estimate at this time.

Future quantification of the permafrost contribution of Hg to downstream ecosystems will require concerted sampling efforts across the Arctic to better represent the diversity of permafrost landscapes and conditions across the circumarctic. There is potential to exploit the well-documented relationships between organic carbon and Hg to constrain the permafrost THg contribution to rivers and lakes. In particular, unique permafrost thaw signatures have been identified for dissolved organic carbon in parts of the Arctic that could potentially be linked to Hg.

How much mercury do ice sheets, ice caps and glaciers contribute to downstream environments in the Arctic? [3.4.3]

25. Dissolved Hg concentrations in glacier meltwater are typically <1 ng/L, and the estimated median concentration in mixed meltwater from pre-industrial and modern ice is 0.8 ng/L.

26. Total Hg concentrations (THg) in turbid subglacial or proglacial streams are commonly much higher, ranging up to ~74 ng/L, indicating that the bulk of Hg in these streams is particle-bound (HgP) and typically accounts for >50% of THg.

27. Reported Hg fluxes in individual glacier-fed streams range from <1 to 5 kg/y, and translate to annual yields of <1 to 4 μg/m^2/y from Subarctic and Arctic basins with 21% to 82% glacier coverage, which is within the range of pan-Arctic watershed Hg yields.

28. Approximately 400±7 kg Hg are released annually from melting Arctic glacier ice, with Greenland contributing ~60% of this amount. The total sediment-bound Hg output from Greenland meltwater is estimated to be ~40 t/y.

In situ optical measurements of fluorescent dissolved organic matter and turbidity in streams may be useful proxies for quantifying riverine Hg and MeHg fluxes from glaciers, but these methodologies need to be tested, calibrated and validated in various proglacial streams (e.g., alpine, open tundra) to verify their reliability and usefulness.

In Arctic streams issuing from glacier-covered catchments, Hg stable isotope ratios may help quantify the respective contributions of atmospherically-derived Hg released from melting ice and of Hg derived from terrestrial sources (anthropogenic and geogenic).

How much mercury do rivers transport to the Arctic Ocean? [3.4.4]

29. There have been significant improvements over the past decade in our understanding of the sources of Hg in Arctic river water, and the climatic, hydrological and geomorphological processes that control river Hg flux. Estimates by multiple recent studies of the pan-Arctic river flux into the Arctic Ocean have coalesced around a common range, with a best estimate of 41 t/y.

30. Multi-year observations at a relatively high temporal resolution of dissolved and particulate Hg and DOC in major pan-Arctic rivers confirm that the highest Hg concentrations and export fluxes occur during the spring freshet in May to June, and during a smaller peak during the autumn wet season. Dissolved and particulate Hg forms each constitute about half of the total river load.

31. Since snowmelt occurs at the end of winter when the ground is still frozen, percolation through the soil column is not likely a major Hg source in spring freshet. Thus, the melting of snowpacks and glaciers as well as the overland mobilization of surface soil particles and vegetation detritus are probably the main springtime and annual sources of river water Hg to the Arctic Ocean. Observation from Western Siberia rivers report two to three times higher Hg:C ratio in spring waters compared to other seasons, suggesting runoff of Hg accumulated in seasonal snowpacks.

32. Regions of sporadic, discontinuous permafrost contribute considerably more Hg to local rivers than permafrost-free or continuous permafrost regions. Small, organic matter-rich catchments were particularly important HgP sources in rivers, with most of the Hg coming from deep and intermediate soil layers at the edges of thawing permafrost.

33. Summertime permafrost thawing and the percolation of precipitation through soil profiles both contribute to the autumn river Hg flux. Given that permafrost and other Arctic soil profiles contain mostly natural Hg accumulated over many millennia in pre-industrial times, natural Hg is likely to be a significant yet poorly constrained fraction of the total riverine Hg flux as a consequence of climate change.

The proportion of anthropogenic and natural Hg present in Arctic river water is an uncertainty requiring further study. Constraining the present anthropogenic Hg component in Arctic rivers will assist in determining the future effectiveness of the Minamata Convention in reducing Arctic Ocean Hg inputs.

Stable isotope studies indicates that terrestrial sources (coastal erosion and riverine flows) contribute a large portion of the Hg found in top Arctic marine predators. However, the individual contribution of each of these sources is unknown, and they cannot be distinguished with currently available methods. A better understanding of the role of terrestrial Hg in the marine Hg cycle will require new tracing methodologies to be developed.

Additional research is needed to understand the connection between terrestrial inputs of Hg from erosion, rivers, submarine groundwater discharge, and their transfer to the inner shelf and offshore waters.

How much mercury does coastal erosion contribute to the Arctic Ocean? [3.4.5]

34. Coastal erosion rates along some stretches of Arctic Ocean coastline are among the highest in the world. Recent advances in measurements of tundra soil Hg concentrations, and of the volumetric rates of erosion, provide a best estimate of 39 t/y of Hg eroding into the Ocean, with an uncertainty range of 18–52 t/y. The Eurasian Arctic, where erosion rates are highest, contributes almost 90% of the total pan-Arctic erosion Hg flux.

35. Given that entire vertical profiles of coastal tundra soils are eroding and that most of the Hg in tundra soil profiles is natural, it is likely that natural Hg dominates the erosion Hg flux.

Further studies of the Hg concentrations in Eurasian coastal soils (given the dominance of coastal erosion in the Eurasian Arctic as a source of Hg to the Arctic Ocean) are needed to improve the accuracy of the coastal erosion Hg flux.

How much mercury does ocean circulation transport to the Arctic Ocean? [3.5]

36. Compared to surface waters in all other oceans, Arctic Ocean surface waters are enriched in Hg, such that outflowing Arctic water entering the North Atlantic has a higher average THg concentration than Atlantic waters flowing into the Arctic. The significant riverine and erosion inputs coupled with the blocking effect of sea ice on dissolved gaseous Hg evasion account for the high marine Hg concentrations in the Arctic.

37. Ocean currents bring in 55±7 t/y of Hg to the Arctic Ocean, most of which (49 t/y) enters from the Atlantic Ocean while only 6 t/y enters from the Pacific. 73±8 t/y is exported into the Atlantic, for a net export from the Arctic Ocean of 18 t/y.

38. The central Arctic Ocean is enriched in surface Hg concentrations, which decreases strongly within the upper few hundred meters of the water column.

39. Mercury concentrations in the Arctic Ocean are higher over the CAA and the Northeast Greenland Shelf, but not over the East Siberian Shelf, Chukchi Shelf and Barents Sea Opening. This is consistent with the model ensemble-estimated distribution of Hg deposition to the Arctic Ocean.

40. The concentration of total Hg is relatively uniform for the deep ocean basins as most of the external inputs are small compared to the mass of Hg in the deeper waters and given its relatively long residence time.

41. Recent estimates suggest the removal of Hg by sediment burial is higher than previously estimated. Evidence suggests that almost 80% of THg accumulated in Arctic Ocean sediments occurs in the large areas of continental shelf.

Additional investigations need to focus on the upper water column Hg inputs and exchanges with the Atlantic and Pacific Oceans and coastal regions for the open Arctic, concentrations and distributions of Hg and its speciation in the water column of the open ocean, and seasonal variability of Hg in the Arctic Ocean.

Arctic Ocean sediments are poorly understood sinks and sources of Hg because of limited sampling and the diagenetic alteration of surface sediment Hg concentrations in the deep basin. Further studies of oceanic Hg sedimentation rates and of diffusive Hg fluxes into seawater from sediments are required to better constrain the seawater-sediment fluxes.

What are the relative contributions of geogenic, anthropogenic and re-emission sources of mercury to Arctic environments? [3.6]

42. The model ensemble estimates that contemporary global anthropogenic Hg emissions are responsible for 32% of the annual Hg deposition in the Arctic; re-emissions of legacy deposition (anthropogenic and geogenic origin) from soils and oceans are responsible for 64% and primary geogenic emissions for 4%.

43. Half of annual anthropogenic Hg deposition in the Arctic occurs in spring followed by 25% in summer, 13% in autumn and 12% in winter. Anthropogenic contributions to the total deposition of Hg in the Arctic are estimated to be highest in winter and spring (31% to 38%) and lowest in summer (25% to 28%).

44. The modeling estimates of contributions from Hg emissions in various global source regions to annual Arctic anthropogenic Hg deposition are: East Asia (32%), CIS countries (Commonwealth of Independent States; 12%), Africa (12%), Europe (8%), Southeast Asia (8%), South Asia (7%), South America (7%), Central America (6%), Arctic (3%), North America (3%), Middle East (2%), and Australia and New Zealand (0.1%).

45. The models were applied to estimate the relative contributions of global anthropogenic Hg emissions from different sectors: power generation (347 t/y; 15.6%); industrial sources (874 t/y; 39.3%); intentional use and product waste (166 t/y; 7.5%); and ASGM (838 t/y; 37.6%) to annual anthropogenic Hg deposition in the Arctic. The industrial sector contributes half (48%) of the anthropogenic deposition followed by ASGM (28%), power generation (17%) and the intentional use and product waste group (7%).

46. Models estimate that global wildfire emissions are responsible for 12–17 Mg/y of Hg deposition in the Arctic, representing 6% to 10% of annual Hg deposition in the Arctic, with wildfire contributions from Eurasia, Africa, and North America of 5.3%, 2.5% and 1%, respectively. More than 50% of wildfire-induced Hg deposition originated from Eurasian and North American boreal forest fires in summer and fall. The western Canadian Arctic and Eastern Siberia are consistently more impacted by wildfires than the other regions in the Arctic.

47. The model ensemble simulates significant geographic variation in anthropogenic Hg deposition contributions in the Arctic, primarily reflecting differences in proximity to the mid-latitude anthropogenic sources and precipitation rates in different regions. In the Arctic watershed, the Yenisey and Kolyma river basins in Eurasia receive the highest anthropogenic Hg contributions, while the Mackenzie, Yukon and Lena river basins receive higher contributions of Hg deposition from wildfires.

48. Central and eastern Arctic Ocean regions are estimated to receive relatively higher proportions of annual Hg deposition from anthropogenic sources (30% to over 50%) than in the western Arctic Ocean including the Canadian Arctic Archipelago (≤30%).

49. Generally, differences in relative anthropogenic Hg deposition contributions from emissions in various worldwide geographic regions to different Arctic regions are small, reflecting a long lifetime of Hg in the atmosphere giving rise to a well-mixed distribution.

50. There are notable variations in spatial patterns of anthropogenic Hg deposition contributions between seasons, mainly arising from inter-seasonal shift in atmospheric circulation, precipitation and vegetation regimes. In autumn and winter, there is no clear distinction in anthropogenic Hg deposition contributions between Subarctic and High Arctic regions. The springtime anthropogenic Hg deposition contribution is exacerbated by AMDEs over sea ice, meaning that deposition is highest in the High Arctic regions in spring. In summer, efficient Hg uptake by vegetation in temperate and Subarctic regions and the northward retreat of the polar front limit Hg transport and deposition in the High Arctic.

51. The proportion of Hg released as gaseous elemental Hg in wildfires varies between 50% and 95% based on aircraft measurements. Peatlands are an important sink for organic matter and Hg in the circumboreal regions, and the burning of peat-rich soils likely leads to a significantly greater release of Hg than currently estimated.

A better estimation of the proportion of gaseous Hg to particulate Hg and the propensity of different biomes (such as boreal peatlands) to release Hg during wildfires is needed to develop better wildfire Hg emission inventories and reduce uncertainties in modeling estimates.

What is the relative contribution of local anthropogenic sources of mercury to Arctic environments? [3.7]

52. The model ensemble estimates that anthropogenic emissions from the Arctic region account for 3% of the overall anthropogenic Hg deposition contribution in the Arctic. Regionally, Arctic region contributions to anthropogenic Hg deposition are 2% to 7% over the Arctic Ocean, and up to 35% over land occurring in Eurasia.

53. There are notable seasonal differences in Hg deposition contributions of local anthropogenic origin, driven by distinct atmospheric transport and deposition pathways in different seasons. In winter and fall, efficient low-level Hg transport of north Eurasian emissions over frozen surfaces combined with inefficient removal processes lead to higher local anthropogenic contributions of 3% to 15% to the eastern Arctic Ocean region and over 15% to the High Arctic terrestrial region. In summer and spring, both weak transport into the Arctic polar dome and efficient wet and dry removal of Hg result in <3% contributions of local anthropogenic sources to the Arctic Ocean.

How much mercury is circulating in Arctic environments? [3.8]

54. Mercury deposition to the terrestrial system north of 60°N (~118 Mg/y) appears to be in balance with Hg removal from Arctic soils (~113 Mg/y) by rivers (~41 Mg/y), coastal erosion (~39 Mg/y) and re-emissions from soils/vegetation (~24 Mg/y) and wildfires (~9 Mg/y), but large uncertainties remain in constraining air-terrestrial Hg exchange fluxes.

55. Estimated Arctic Ocean Hg inputs (~204 Mg/y) from atmospheric deposition (~64 Mg/y), river runoff (~41 Mg/y), coastal erosion (~39 Mg/y), ocean current inflow (~55 Mg/y) and benthic flux from sediments (~5 Mg/y) exceed outputs (~152 Mg/y) via oceanic evasion (~32 Mg/y), ocean current outflow (~73 Mg/y), sediment burial (~46 Mg/y) and sea-ice export (~1 Mg/y) by ~52 Mg/y. These revised estimates suggest that Hg removal from the ocean waters to shelf sediments is currently underestimated, likely due to poorly-constrained burial rates on the inner shelf.

56. The best estimates of THg amounts in the Arctic abiotic environments are ~330 Mg in atmosphere, ~597 Gg (0–3 m depth) in permafrost soils, ~39 Mg in seasonal snowpack, ~2415 Mg in glaciers, ~9 Mg in sea ice and ~1870 Mg in the Arctic Ocean.

To further constrain Hg fluxes and budgets in Arctic environments, process-focused studies and model developments (as detailed in previous sections) are needed to close the budget gaps and to assess the concurrent impacts of emission reduction efforts and climate change on Hg cycling in the Arctic.

4. Changes in Arctic mercury levels: processes affecting mercury transformations and biotic uptake

Coordinating authors: Michelle Nerentorp Mastromonaco, Sofi Jonsson, Feiyue Wang

Co-authors: Andrea G. Bravo, Warren R.L. Cairns, John Chételat, Thomas A. Douglas, Lars-Eric Heimbürger-Boavida, Gretchen Lescord, Daniel Obrist, Peter Outridge, Kyra A. St. Pierre, Liisa Ukonmaanaho, Christian Zdanowicz

4.1 Introduction

The majority of mercury (Hg) in the Arctic environment exists in inorganic forms. A fraction is converted to methylmercury (MeHg) in waters, sediments and soils. After uptake of MeHg at the base of aquatic food webs, MeHg can biomagnify up the food webs to reach concentrations of concern. The potential risk Hg pollution poses to Arctic ecosystems is thus not only controlled by the amounts of inorganic Hg transported into the system and cycling within the Arctic environment but also by the extent the pool of Hg is methylated and accumulated in aquatic food webs. The 2011 AMAP Assessment of Mercury in the Arctic included an extensive discussion of the processes leading to environmental exposure (AMAP, 2011). This chapter provides new or updated information about these transformation pathways as well as new observational data concerning MeHg in the Arctic environment.

Given the high complexity of the Hg biogeochemical cycle, it is not surprising that significant advances are still being made despite over 50 years of active research. This chapter begins with an update on processes controlling the pool of Hg available for bioaccumulation, with an emphasis on Hg methylation pathways (Section 4.2.1), Hg demethylation pathways (Section 4.2.2), the formation and degradation pathways of dimethylmercury (Section 4.2.3), and the role played by organic matter in controlling the amount of Hg which is methylated (Box 4.2). The chapter then provides new or updated information addressing hotspots of MeHg production in abiotic environmental compartments (Section 4.3). Section 4.4 discusses the uptake and subsequent biomagnification of MeHg in aquatic food webs, and Section 4.5 provides a summary of the MeHg pools and fluxes discussed in the chapter and includes an updated MeHg budget for the Arctic. Finally, the conclusions and recommendations of the chapter are presented in Section 4.6.

4.2 What controls the pool of mercury available for bioaccumulation?

The pool of Hg available for bioaccumulation will depend on the bioavailability as well as the size of the MeHg pool in Arctic soils, sediments and waters. While the bioavailability of MeHg is discussed later (see Section 4.4), this section focuses on the main processes controlling bulk MeHg concentrations, including formation and degradation pathways of MeHg as well as environmental factors controlling these pathways.

Box 4.1 Mercury species and their role in the global biogeochemical mercury cycle

Mercury that cycles in the Arctic environment and accumulates in Arctic biota has, at some point, been mobilized from the Earth's crust where it mainly exists as inorganic divalent mercury (Hg(II)) such as in the mineral form cinnabar (mercury sulfide; HgS). From the crust, Hg may be released through natural processes (e.g., volcanic emissions, rock and mineral weathering or wildfires) or anthropogenic activities (e.g., mining, coal combustion or manufacturing). The biogeochemical cycle, which connects these emissions to Hg in Arctic food webs, involves inorganic and organic forms of Hg that undergo a wide range of transformation processes in air and water as well as on land. Figure 4.1 shows the proportions of the three main forms of Hg present in various Arctic environmental compartments and biota: elemental mercury (Hg(0)), inorganic divalent mercury (Hg(II)) and methylated divalent mercury (MeHg). Here, we briefly describe their properties and their role in the global biogeochemical Hg cycle.

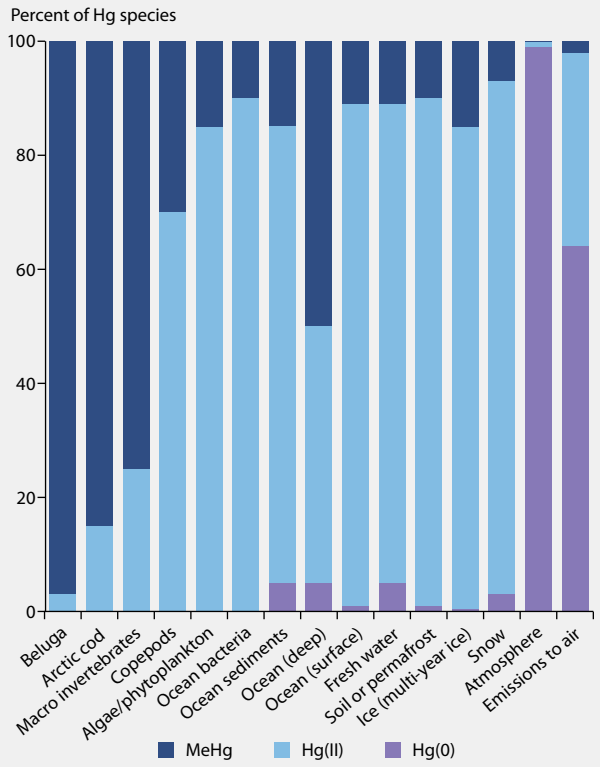

Figure 4.1 Partition of different Hg species (Hg(0), Hg(II) and MeHg) in emissions and in various Arctic environmental compartments and biota, expressed as percentages of total Hg (THg; Douglas et al., 2012; Cossa et al., 2014; Schartup et al., 2020).

Continued on next page

Box 4.1 continued…

Elemental Hg (Hg(0)) is a volatile form of Hg existing as a liquid metal at ambient temperatures (melting point: -38.83°C). Burning processes (e.g., in coal-fired power stations and other industrial processes) release both Hg(0) and Hg(II). The Hg(0) and Hg(II) which derive from anthropogenic sources are released to the atmosphere at an average ratio of about 1.8:1, although this ratio differs depending on the emission source (Zhang et al., 2016a; Streets et al., 2017). While Hg(II) is typically deposited closer to the emission source, Hg(0) has a residence time ranging from several months to over a year in the atmosphere and can be transported from the emission source to remote polar regions within a few days to weeks (AMAP, 2011). The atmospheric concentration of Hg(0) in the Arctic is about 1.4 ng/m^3 (see Chapter 3), while the concentration of Hg(II) is typically three orders of magnitude lower (~pg/m^3). A small fraction of Hg(0) dissolves in natural waters and is referred to as dissolved gaseous mercury (DGM). Currently, the majority of water surfaces are estimated to be oversaturated with Hg(0), leading to a net-evasion of Hg(0) from surface waters to the atmosphere (Andersson et al., 2008). The origin of Hg in surface water can be either natural or anthropogenic and, therefore, the evasion of Hg from water surfaces cannot be categorized as either an exclusively natural or an exclusively anthropogenic source (see Chapter 3). Instead, it is considered as re-emission of legacy natural and anthropogenic Hg that was previously deposited. On land, foliar (plant) uptake of Hg(0) drives the atmospheric deposition of Hg in the Arctic tundra (Obrist et al., 2017; Douglas and Blum, 2019). Through this process, large amounts of Hg have been accumulated from the atmosphere to northern permafrost soils over thousands of years. Today, concerns have been raised about the potential remobilization of this permafrost Hg pool as the soil temperature increases (Schaefer et al., 2020; see also Chapter 5).

Inorganic divalent Hg (Hg(II)) is the main form of Hg found in natural waters, soils and sediments. Although inorganic Hg(II) can be released to the atmosphere, it has a shorter atmospheric residence time due to its higher solubility and chemical reactivity in comparison to Hg(0). Inorganic divalent Hg in air is either in gas-phase or attached to particles as particle-bound mercury (PBM). The ratio of gas to particle-bound Hg(II) depends on aerosol abundance which is higher in colder air (Amos et al., 2012). In the atmosphere, inorganic Hg(II) is also produced from the oxidation of Hg(0), especially during springtime atmospheric mercury depletion events (AMDEs; see Section 3.3.1). These events occur in both Arctic and Antarctic regions and lead to the rapid oxidation of Hg(0) to the more easily deposited Hg(II) species. Mercury has a strong affinity towards reduced sulfur; therefore, in environments such as sediments, soils and most freshwater systems, where inorganic or organic reduced sulfur is available, Hg(II) will primarily be complexed to such ligands. Inside organisms, Hg(II) also primarily binds to organic sulfide sites (thiols) available on biomolecules as proteins (Wang et al., 2012b). In other environments, such as in the atmosphere, sea water, snow and ice (where sulfide concentrations are low and concentrations of other complexing ligands are high), Hg(II) may be primarily found as complexes with chloride, hydroxide, and organic matter. In sediments and soils, most Hg(II) is found in the solid phase due to mercury's high affinity to mineral surfaces and organic matter. After being deposited to fresh or sea water, Hg(II) can also be reduced back to Hg(0) and re-emitted to the atmosphere. Recent studies show that photoreduction of Hg(II) to Hg(0) also occurs in the atmosphere, prolonging the atmospheric lifetime of Hg (Saiz-Lopez et al., 2018, 2019; Francés Monerris et al., 2020).

Methylated mercury, or methylmercury (MeHg), is the most environmentally important of the combinations of Hg(II) with reduced carbon compounds (organomercurials). The main form of MeHg existing in natural environments is monomethylmercury (MMHg), although, in some environments, dimethylmercury (DMHg) may also be the dominant species, especially in seawater. Methylmercury is formed in water, soils and sediments from Hg(II) through both biotic and abiotic processes (see Section 4.2.1). While both MMHg and DMHg are toxic and lipophilic, only MMHg has so far been shown to biomagnify in aquatic food webs to concentrations of concern for wildlife and human health. MMHg is able to cross the blood-brain and placental barrier and poses a risk to the neurological system (see Chapter 6). Much less is known about DMHg (see Section 4.2.3).

Methylmercury can also be degraded back into Hg(II) and Hg(0) by biotic or abiotic demethylation processes (see Section 4.2.2). Since most analytical data on methylated Hg do not differentiate between MMHg and DMHg, we will use MeHg to refer to methylated Hg in general in this chapter, unless otherwise specified.

4.2.1 Mercury methylation

As discussed in the last AMAP report (AMAP, 2011), methylation of Hg is primarily thought to be a biotic process. Since then, several major new developments have been made, the most significant of which is the discovery of the gene pair involved in biological Hg methylation, the *hgcAB* genes (Parks et al., 2013). This finding opened up new possibilities to search for Hg methylators (Gilmour et al., 2013; Jones et al., 2019; Villar et al., 2020; Capo et al., 2020; Gionfriddo et al., 2020; McDaniel et al., 2020) and uncover the intracellular processes involved in Hg methylation (Smith et al., 2015). Carriers of the *hgcAB* genes that are known to methylate Hg include a wide range of sulfate-reducing bacteria, iron-reducing bacteria, methanogens and some fermentative microorganisms (Gilmour et al., 2013). Since the discovery of the *hgcAB* gene pair, genomics techniques have also lead to the discovery of the presence of *hgcA*-like genes in members of other microbial phyla that could be putative Hg methylators, including *Nitrospina* (Gionfriddo et al., 2016; Villar et al., 2020), *Spirochaetes* and the PVC superphylum (which includes seven phyla: *Planctomycetes, Verrucomicrobiae, Chlamydiae, Lentisphaera, Poribacteria, OP3* and *WWE2*; Jones et al., 2019), several strains of *Acidobacteria, Actinobacteria, Candidatus Aminicenantes, C. Firestonebacteria,* and *WOR groups* (McDaniel et al., 2020), as well as *Spirochaetes*-like and *Kiritimatiellaeota*-like bacteria (Capo et al., 2020).

However, the capacity of many of these microorganisms to methylate Hg still needs to be confirmed through laboratory studies. It is important to note that not all Hg methylating microorganisms have the same capacity to methylate Hg and that this appears to depend on individual strains rather than taxonomic ranking (Ma et al., 2019).

Traditionally, anoxic environments, such as sediments and flooded soils, were assumed to be the main site for Hg methylation. A global analysis of metagenomes was the first study to reveal the presence of *hgcAB* in the Arctic environment by identifying the genes in *Deltaproteobacteria*, *Firmicutes*, and particularly in methanogenic archaea from thawing permafrost soil (Podar et al., 2015). Fahnestock et al. (2019) also showed that concentrations of MeHg in porewater increased across a thaw gradient along with the abundance and diversity of potential Hg methylators. Increased concentration and fraction of MeHg in thawing permafrost soils (e.g., in collapsed fen sites) compared to permafrost soil (e.g., on peat plateaus) have also been demonstrated from a set of thaw gradients in Fennoscandia (Tarbier et al., 2021).

Methylmercury accumulating in Arctic marine food webs is of concern to the Inuit and other Indigenous Peoples, and cannot be exclusively explained by the formation of MeHg in marine sediments and terrestrial MeHg inputs to the ocean (Kim et al., 2020b). In the last decade, several studies have highlighted the importance of Hg methylation in suboxic and even oxic waters for MeHg bioaccumulation and biomagnification in aquatic food webs (Sunderland et al., 2009; Mason et al., 2012; Wang et al., 2012a, 2018; Blum et al., 2013; Heimbürger et al., 2015; Gascón Díez et al., 2016, 2017; Agather et al., 2019; Petrova et al., 2020). While anaerobic biological Hg methylation is mediated by the *hgcAB* genes that are abundant in marine sediments (Podar et al., 2015), the aerobic pathway, if it exists, remains unclear. *HgcA* or *hgcAB*-like genes have recently been identified in global ocean seawater (not yet in the Arctic Ocean; Bowman et al., 2020b; Villar et al., 2020), which potentially could contribute significantly to Hg methylation in marine oxic waters, although further studies are needed to confirm their capacity for Hg methylation.

4.2.2 Methylmercury demethylation

Methylmercury demethylation can be biotically or abiotically mediated. Abiotic demethylation is mostly photochemical degradation in surface waters by different mechanisms including direct photolysis and indirect photolysis via reactions with reactive oxygen species, such as hydroxyl radicals. Research from the Arctic, Subarctic, and temperate areas has shown that photochemical demethylation from ultraviolet (UV) radiation is an important aspect of freshwater Hg budgets (Seller et al., 1996; Lehnherr et al., 2011; Poste et al., 2015; Klapstein and O'Driscoll, 2018). In the Arctic, photodemethylation rates in smaller systems are likely regulated by prolonged ice coverage (Poste et al., 2015; Klapstein and O'Driscoll 2018). Non-photochemical abiotic demethylation may also occur via reactions with selenoamino acids (Khan and Wang, 2010), but the importance of such reactions remains to be further examined outside of the laboratory.

Bacterial resistance to Hg(II) and MeHg is one of the most widely observed phenotypes in eubacteria (Barkay et al., 2003) and is mediated by the *mer* operon, which has been found in a diverse range of habitats including soils, sediment and water, both freshwater and marine systems (Barkay et al., 2003 and references therein). The *mer* operon (which usually encompasses only one copy/a maximum two copies of itself in an organism) contains three different types of genes: regulators (*merR* and *merD*), transporters (*merT, merP, merC, merG* and *merE*) and catalytics (*merA* and *merB*). Within the operon, special attention has been paid to the *merA* gene, which catalyzes the reaction transforming Hg(II) into Hg(0), and to *merB*, which codifies for the alkaline mercury lyase, a protein that demethylates MeHg into Hg(II). Little is known about the occurrence, diversity and distribution of *merA* among Arctic bacterial communities. Pioneer studies revealed the presence and expression of *merA* in the Arctic microbial mats (Poulain et al., 2007b). Later, Møller et al. (2014) performed a detailed evaluation of the taxonomic, environmental distribution and evolutionary history of the *merA* gene in High Arctic snow, freshwater and sea-ice brine. There is even less information on the abundance, diversity and expression of the *merB* gene in the Arctic region. A recent study, however, unveiled the presence of *merB* in deep waters of the Arctic Ocean (Bowman et al., 2020b).

Understanding the rates of both methylation and demethylation as well as Hg(II) reduction, which might limit the availability of this species for methylation, have implications for biotic uptake, given that MeHg is the bioaccumulative form of Hg. While photochemical processes might govern Hg chemistry at the surface of the waters, biological processes are the keystone to understand Hg cycling in deep freshwater or sea waters and in sediments.

4.2.3 Formation and degradation pathways of dimethylmercury

Dimethylmercury (DMHg) is another form of methylated Hg found in natural environments. Its role in the biogeochemical cycle of Hg and its bioaccumulative potential is not well known. Although it is mainly found in marine waters (Bowman et al., 2020a), DMHg may also be found in terrestrial environments. For example, production of DMHg has recently been shown in rice paddies (Wang et al., 2019b). However, observation of DMHg in the Arctic terrestrial environment is still missing. In marine waters, including the Arctic Ocean, concentrations of DMHg range from 0.002–0.08 ng/L and constitute a significant fraction (up to 80%) of the methylated Hg pool (the sum of MeHg and DMHg; Fitzgerald et al., 2007; Kirk et al., 2012; Agather et al., 2019; Petrova et al., 2020).

As mentioned in the previous AMAP mercury assessment (2011), formation of DMHg has been shown previously in bacterial cultures (Baldi et al., 1993; Sommar et al., 1999), and associated with polar macroalgae (Pongratz and Heumann, 1998) and marine bacteria (Pongratz and Heumann, 1999). Although these studies identify synergies between the activity of organisms and production of DMHg, there is currently no information to suggest it being a biological product. Baldi et al. (1993) suggested the formation of DMHg in bacterial cultures was the result of an abiotic reaction between dissolved sulfide

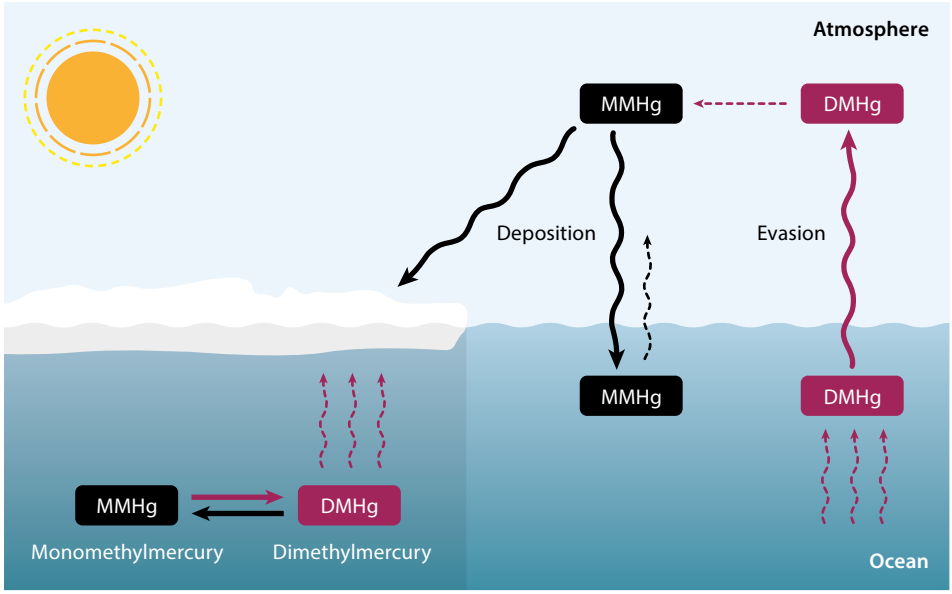

Figure 4.2 Illustration of the role of dimethylmercury in the marine biogeochemical cycle. Adapted from Baya et al., 2015.

Box 4.2. Role of organic matter in mercury methylation, demethylation, and methylmercury uptake

Organic carbon (OC) and organic matter in the Arctic. The link between the aquatic Hg and carbon cycles is well known. Many studies have also examined the relationships between abiotic or biotic Hg concentrations and dissolved organic carbon (DOC) or dissolved organic matter (DOM) in Arctic systems. Broadly speaking, and for the purpose of this chapter, DOM is defined as organic carbon-based material in origin that is smaller than a defined size fraction (generally <0.45µm). This definition includes a wide array of allochthonous and autochthonous compounds with differing molecular structures and properties (Leenheer and Croué, 2003; Hudson et al., 2007). The concentration of DOC, on the other hand, is a common measurement often used to quantify the total amount of DOM present in a given water sample. The concentration of particulate organic carbon (POC) is the fraction of organic matter larger than the defined size limit of DOC (generally >0.45µm). More generally, these parameters can all be classified as measurements of aquatic organic matter.

Hg Methylation. Organic matter has complex linkages with the Hg cycle that can both dampen or promote MeHg bioaccumulation. The complexity of these interactions is reflected in the varying relationships reported between organic matter and Hg in the literature (Lavoie et al., 2019). A recent global review found these relationships to be broadly influenced by geographic location and temporal scale, as well as by human activities (Lavoie et al., 2019). The chemical composition of DOC also plays a critical role in its effects on Hg biogeochemical cycling (Schartup et al., 2015b; Lescord et al., 2018; Jiang et al., 2020), including bioaccumulation (see Section 4.4). For example, OC of terrestrial origin is involved in the transport of MeHg to downstream freshwater and marine environments. In the Subarctic Baltic Sea, interannual variation of seawater MeHg concentrations were related to DOC inputs and composition (Soerensen et al., 2017). In Arctic fresh waters, DOC can promote or inhibit the photodegradation of MeHg depending on the amount of DOC present (Girard et al., 2016) and alter Hg(II) bioavailability to microbes (Chiasson-Gould et al., 2014) because of the multiple roles that organic matter plays in those processes. Dissolved organic carbon can play a key role in promoting MeHg bioaccumulation, although those interactions are complex, and consideration of site-specific conditions are likely important.

Hg Demethylation. Because organic matter compounds in surface waters readily absorb UV radiation, they mediate the photodemethylation of aqueous MeHg (Klapstein et al., 2017). A recent study on ponds with high DOC concentrations resulting from permafrost thaw slumps found higher rates of photodemethylation when compared to an oligotrophic lake in the polar desert with low DOC concentrations (Girard et al., 2016). Photolytically produced reactive oxygen species from organic matter have been shown to mediate MeHg demethylation in Alaskan lacustrine systems (Hammerschmidt and Fitzgerald, 2010).

MeHg uptake. Numerous studies on the effects of organic matter on Hg accumulation in Arctic biota have been conducted in lakes and rivers across the Arctic over the past ten years. For example, Hudelson et al. (2019) recently reported strong negative correlations between DOC and POC concentrations versus total Hg (THg) levels in landlocked Arctic char (*Salvelinus alpinus*) in lakes around Resolute Bay in Nunavut, Canada. In the same set of lakes, Lescord et al. (2015) reported negative correlations between DOC (in combination with total nutrient levels) and MeHg concentrations in zooplankton as well as negative correlations between DOC and the rates of Hg biomagnification in the same food webs. Similarly, MeHg concentrations in aquatic invertebrates (e.g., chironomid larvae and zooplankton) from Arctic lakes were correlated with lower DOC concentrations (Chételat et al., 2018). In High Arctic lakes, waters with very low concentrations of DOC were associated with greater bioaccumulation of MeHg at the base of the food web even when concentrations of MeHg in the water were low,

and MeHg (via the formation of bismethylmercurysulfide). Recent work has also shown abiotic formation of DMHg from MMHg when MMHg is adsorbed onto organic or inorganic surfaces containing reduced sulfur sites (Jonsson et al., 2016). Other known pathways of DMHg formation of potential relevance in natural environments include the reaction of MeHg with selenoamino acids (Khan and Wang, 2010) and methylation with methylcobalamin (Imura et al., 1971).

Volatilization of DMHg from the marine boundary layer and the subsequent demethylation of DMHg to MMHg has been suggested as a source of MeHg in surface snow (St. Louis et al., 2007; Kirk et al., 2008), marine waters (Baya et al., 2015) and coastal terrestrial environments (St. Pierre et al., 2015; Figure 4.2). Atmospheric observations of DMHg have, until recently, been missing. From work conducted in the Hudson Bay and the Canadian Arctic Archipelago, atmospheric concentrations of both MMHg (2.9±3.6 pg/m^3) and DMHg (3.8±3.1 pg/m^3) were reported (Baya et al., 2015). The authors suggested DMHg was of marine origin and that evasion of DMHg from marine waters was enough to sustain atmospheric concentrations of MMHg. Furthermore, they propose that MeHg is deposited during summer months due to wet deposition. Previous work suggests that photochemical degradation of DMHg could be mediated by OH radicals and chlorine atoms (Niki et al., 1983a, 1983b). In addition, DMHg could potentially also be degraded in marine waters. Early work suggested that enhanced demethylation occurred under light compared to dark conditions (Mason and Sullivan, 1999). Photochemical degradation in marine waters was later contradicted by incubation experiments (Black et al., 2009). It should be noted that the possibility of significant DMHg demethylation rates of environmental relevance cannot be dismissed from these experiments (Soerensen et al., 2016b). It is also possible DMHg may be degraded through other pathways which do not involve photochemical reaction pathways. Dimethylmercury has recently been shown to degrade in aqueous solutions to MeHg in the presence of reduced sulfur as dissolved sulfide or as the metastable iron sulfide mackinawite (West et al., 2020). Interestingly, recent work from the Arctic Ocean reports that DMHg was not enriched under the ice while Hg(0) was, supporting the case that the degradation of DMHg does take place in dark marine surface waters (Agather et al., 2019).

possibly due to DOC's effects on Hg bioavailability (Chételat et al., 2018). Overall, these results suggest that Arctic aquatic systems with lower DOC concentrations, in combination with other physicochemical parameters, had higher rates of Hg bioaccumulation and biomagnification in biota. However, variation in these relationships likely exists. Furthermore, climate change is rapidly altering both carbon and Hg cycling, resulting in a general increase in concentrations of organic matter in aquatic environments across the Arctic (Macdonald et al., 2005; Isles et al., 2020), though variation certainly exists.

Some research in Arctic and Subarctic systems has also suggested that the relationship between biotic Hg and organic matter concentrations may not be linear and may, in fact, be dependent on DOC concentrations. More specifically, several studies have reported a curvilinear relationship between DOC concentrations and THg or MeHg concentrations in aquatic biota, with an inflection point of ~8–11 mg/L of DOC (French et al., 2014; Braaten et al., 2018). This relationship was first suggested based on data from the Adirondack lakes and is dependent on system pH (Driscoll et al., 1994). However, given that concentrations of DOC are often strongly correlated with aqueous concentrations of both THg and MeHg, the curvilinear relationship between DOC and biotic Hg concentrations warrants further investigation with consideration of other factors such as water chemistry and trophic position (Chételat et al., 2018; Broadley et al., 2019). For example, Chételat et al. (2018) found that the ratio of aqueous MeHg concentrations to DOC concentrations was a strong and linear predictor of invertebrate MeHg concentrations across an array of Arctic lakes.

Recent studies, some related to this curvilinear Hg-DOC relationship, also consider the effect of various measures of DOM quality rather than quantity (i.e., DOC concentrations represent only the quantity of DOM) have on Hg bioaccumulation. French et al. (2014) suggest that changes in DOM compounds and bioaccessibility may account for changes in Hg bioavailability and bioaccumulation in Arctic freshwater invertebrates; at lower DOC concentrations, Hg was found to be bound with smaller fulvic acids, while at higher DOC concentrations Hg was bound with larger and less bioaccessible humic acids. More recent work in the Subarctic similarly found that biotic Hg concentrations were higher in systems with higher proportions of more bioaccessible DOM compounds and lower proportions of large and aromatic humic substances (Lescord et al., 2018). Other studies have also reported that humic lakes are associated with greater MeHg bioaccumulation in Subarctic boreal ecoregions (Braaten et al., 2018; Poste et al., 2019). Future studies on Arctic Hg and DOM interactions may benefit from incorporating simple structural measurements, such as SUVA254, which provides an estimate of DOM aromaticity (e.g., Skyllberg et al., 2009; Burns et al., 2013).

The thawing of permafrost has been found to be a considerable source of both DOM and Hg to aquatic Arctic and Subarctic environments. A recent review by Tank et al. (2020) found considerable variation in DOC concentrations and DOM quality among studies examining the impact of permafrost thawing on biogeochemical cycling across aquatic networks. Deison et al. (2012) reported higher rates of inorganic sedimentation in lakes with permafrost thaw slumps along their shorelines when compared to reference sites, resulting in lower THg, MeHg, and DOC concentrations in water. Similarly, Houben et al. (2016) report a negative correlation between levels of DOC and the percentage of catchment area affected by permafrost slumping across a series of Low Arctic lakes. The authors attribute the clearer waters in slump-affected lakes to an influx of inorganic material altering biogeochemistry and to increased sedimentation rates. To date, to the best of our knowledge, no study has examined the effects of permafrost-derived organic matter on Hg bioaccumulation in Arctic biota. This, as well as a consideration of structural measurements of DOM concentrations, may add to our understanding of the relationship between Hg and DOM concentrations as permafrost thawing increases in a changing Arctic climate.

4.3 Where are the hotspots of methylmercury in the Arctic?

Several hotspots of MeHg production in Arctic environments have been identified in the last decade, addressing an important knowledge gap in the Arctic Hg cycle. In this section, these hotspots along with recently identified methylation processes unique to the Arctic terrestrial and marine environments are discussed.

4.3.1 Terrestrial environments

4.3.1.1 Land areas

Important scientific advances have been made in characterizing Hg uptake in terrestrial primary producers. Uptake of Hg(II) into bacterial cells carrying Hg methylating genes, and of MeHg into the base of the food web (e.g., plants) are key steps linking natural and anthropogenic sources of Hg to its environmental harm. Significant advances have been made in the last 10 years with regard to the effect of organic matter on these two processes. It is generally agreed that primarily dissolved complexes of Hg(II) and MeHg are taken up by Hg-methylating bacteria at the base of aquatic food webs (Drott et al., 2007; Schaefer and Morel, 2009; Chiasson-Gould et al., 2014; Mangal et al., 2019). Adsorption of Hg(II) and MeHg to the solid phase are thus important processes limiting their biological uptake (Schartup et al., 2015a; Mazrui et al., 2016). However, as shown in previous work from other marine or brackish water systems, different dissolved and solid chemical forms of Hg differ in their bioavailability (Jonsson et al., 2012, 2014; Mazrui et al., 2016). Although recent terrestrial inputs of Hg(II) and MeHg did not contribute much to the stock of MeHg in the estuarine system, 40% to 70% of the bioaccumulated Hg pool originated from these recent terrestrial Hg inputs. In these studies, refractory pools of Hg(II) and MeHg were not fully accounted for. In the retrogressive thaw slump in the western Canadian Arctic that was recently investigated by St. Pierre et al. (2018), over 95% of the Hg was released in the particulate phase.

During summer, Hg(0) in the air is directly taken up by tundra vegetation and is the primary source of Hg in above-ground plant biomass (Obrist et al., 2017; Douglas and Blum, 2019; Olson et al., 2019). This is a phenomenon that also has been observed on the Tibetan Plateau (Wang et al., 2020a), where the succession of vegetation communities after glacier retreat is acting as an active 'pump' drawing down Hg(0) from the atmosphere and increasing the amount of Hg sequestered in areas affected by glacier retreat in a form available to plant life.

Vegetation takes up Hg(0) during the growing season via the growing foliage. Litterfall can be used to measure the dry deposition of Hg(0) and is the largest contributor to atmospheric deposition in forest areas (Bishop et al., 2020). However, in the Arctic, plant deposition (via plant turnover and senescence) from productive tundra is the dominant Hg deposition pathway (Obrist et al., 2017; Olson et al., 2018).

Mercury is a thiophile, forming strong bonds with sulfur, especially in biota (Wang et al., 2012b; Feldmann et al., 2018) and the bioaccumulation of MeHg in plants is thus driven by binding with sulfur-containing proteins via the roots. Generally, very few data are available on MeHg concentrations in Arctic vegetation. Lichens in some coastal areas of the Canadian High Arctic were more enriched in MeHg (MeHg: 1.41–17.1 ng/g) (and THg) relative to underlying soils than at inland sites. This suggests that greater uptake/deposition of MeHg may originate from the evasion of DMHg and MMHg from open marine waters in coastal areas (St. Pierre et al., 2015; see Figure 4.2). Further research is needed to identify sources and pathways of MeHg uptake in terrestrial vegetation.

Methylmercury concentrations in soil and permafrost have not been widely reported, and data from the Arctic are scarce. St. Pierre et al. (2015) reported that soil MeHg concentrations varied by two orders of magnitude (0.02–2.11 ng/g) across several sites in the Canadian Arctic Archipelago, with a median of 0.12 ng/g. Soerensen et al. (2016a) assumed a median of 0.8 ng/g (1% of THg) for their estimate of coastal erosion MeHg inputs into the Arctic Ocean. A tundra study (Olson et al., 2018) reported concentrations of MeHg between 0.5 and 3.4 ng/g in organic horizons and 0.1 to 1.0 ng/g in B horizons, with MeHg on average accounting for 1% of THg (THg with a maximum of 3% in the lower B horizon). The percentage of MeHg to THg was hence generally higher in the Arctic compared to temperate soils, where MeHg generally accounted for between 0.2% to 0.6% of THg (Grigal, 2003; Selvendiran et al., 2008; Obrist, 2012; Kronberg et al., 2016), yet further studies are needed to confirm this.

Wetlands, which include a mix of peatlands as well as rivers, lakes and shallow bays, are the main ecosystem type in the Arctic region, covering up to 60% of the total land surface area (Ramsar, 2014). Peatlands typically have high ground water levels and organic-rich soils, which create anoxic conditions, promoting Hg methylation to MeHg (Grigal, 2002). Mercury has a strong affinity to organic substances, and organic soils therefore play an important role in the mobilization and transportation of Hg from soils to water bodies. Methylation of Hg in High Arctic wetland ponds was suggested to be negatively correlated with DOC levels by decreasing Hg(II) availability to methylating microorganisms (Lehnherr et al., 2012a). Production of MeHg within Arctic wetland ponds (e.g., in Lake Hazen and northern Ellesmere Island) occurred at a rate of 1.8 to 40 ng/m^2, day. Methylmercury cycling in those systems is dominated by Hg(II) methylation as well as photodemethylation (Lehnherr et al., 2012b).

A major consequence of climate warming in the Arctic and Subarctic has been the thawing and degradation of permafrost (Jorgenson et al., 2001, 2006; Lantz and Kokelj, 2008; Walvoord et al., 2019). Given the large amounts of Hg that potentially could be released from Arctic soils in a warmer climate (Lim et al., 2020; Schaefer et al., 2020), methylation rates in the Arctic terrestrial environment have gained more attention. Thawing of permafrost can result in downward expansion of the active layer, generating wetter and more anoxic conditions that are potentially favorable for Hg methylating bacteria (Yang et al., 2016). Increased Hg methylation in wetter and more anoxic conditions has been demonstrated in temperate and tropical zones (Hsu-Kim et al., 2018), whereas few studies have covered Hg methylation in zones with thawing permafrost. In previously formed thaw ponds, Lehnherr et al. (2012a, 2012b) measured Hg methylation rates similar to rates in already identified Hg methylation hotspots. High

concentrations of dissolved MeHg, supposedly from either increased export of MeHg from peat soils, or *in situ* methylation in pond sediments, have also been found in eastern Canadian thaw ponds (MacMillan et al., 2015).

Permafrost thaw in ice-rich, low-relief regions may result in the formation of thermokarst wetlands, ponds and lakes (Vonk et al., 2015a; Olefeldt et al., 2016). These systems have been repeatedly identified as Hg methylation hotspots across the Arctic due to the concurrent mobilization of carbon and nutrients, creating conditions suitable for methylation (MacMillan et al., 2015; Gordon et al., 2016). Gordon et al. (2016) observed MeHg concentrations up to a higher order of magnitude (0.43 ng/L) in the poor fens associated with recent permafrost thaw than in hydrologically isolated bogs in the Scotty Creek catchment of the discontinuous permafrost zone.

In freshwater systems, permafrost thaw has been shown to influence microbial processes (Mackelprang et al., 2011) and biogeochemical cycling (Frey and McClelland, 2009) in downstream water bodies. Several recent studies have reported that sites with permafrost slumps (slope failures or mass-wasting features resulting from the thawing of ice-rich permafrost) are abundant with both organic matter compounds and Hg. In fact, the highest concentrations of THg and MeHg (1200 and 7 ng/L, respectively) ever recorded in natural flowing freshwater were measured downstream of a permafrost thaw slump in the Northwest Territories of Canada (St. Pierre et al., 2018). Other studies show similarly elevated levels of both THg and MeHg in water and sediments from areas influenced by permafrost degradation (MacMillan et al., 2015; Gordon et al., 2016; Houben et al., 2016).

In addition to slump age, many factors may be contributing to the reported differences in organic matter and Hg levels downstream of permafrost slumps, highlighting the need for further study of how permafrost degradation will affect interactions between organic matter and Hg across various Arctic and Subarctic landscapes. Factors such as the depth of the permafrost active layer, peatland buffering and interferences as well as ground water influences may affect organic matter-Hg dynamics downstream of thermokarst processes (Frey and McClelland, 2009; Lim et al., 2019). Furthermore, thaw slumps are likely affecting a wide range of other biogeochemical processes that will either directly or indirectly alter Hg methylation or bioaccumulation in receiving water bodies (Pokrovsky et al., 2018). Lastly, while several studies have shown changes in aqueous Hg levels in relation to permafrost degradation and changing organic matter dynamics, none (to our knowledge) have yet examined their effect on biotic Hg levels, Hg bioaccumulation potentials, or rates of biomagnification.

In the Stordalen Mire in Subarctic Sweden, MeHg concentrations increased by two orders of magnitude along the permafrost thaw gradient, from 0.01–0.05 ng/L in palsas underlain by permafrost to 1.0–2.0 ng/L in thawed fens (Fahnestock et al., 2019). The thawed fens were associated with heightened Hg accumulation, reducing conditions, higher sulfur concentrations and a greater proportional representation of putative Hg methylators within the microbial communities (from 0.5% to 7.8%), compared to the dry frozen palsas and bogs at intermediate stages of thaw (Fahnestock et al., 2019).

4.3.1.2 Freshwater systems

Arctic freshwater systems are important sources of dietary fish, especially for Indigenous northerners. Mercury enters lakes and streams primarily via terrestrial runoff and atmospheric deposition, but it can also originate from groundwater passing through unfrozen parts of permafrost below the water body (taliks). Inorganic Hg(II) entering Arctic freshwater systems can either photolytically reduce to Hg(0) and evade back to the atmosphere or be methylated to MeHg. The amount of Hg that is photoreduced by UVA (320–400 nm) and UVB (280–320 nm) radiation depends on the available Hg(II) complexes. Below the euphotic zone in the water column, biologically mediated processes for Hg reduction dominate (Douglas et al., 2012). Where exactly methylation of Hg dominates in freshwater systems has been shown to vary between different Arctic freshwater bodies (see Table 4.1; Chételat et al., 2015).

Generally, in freshwater ecosystems, the main carrier ligand for MeHg is DOC (Tsui and Finlay, 2011), which has the double role of promoting the solubility and transport of MeHg in surface waters and attenuating dissolved MeHg uptake by aquatic food webs by limiting transport across cell membranes. High Arctic lakes typically have low biological productivity, limiting Hg uptake by algae and suspended detrital organic matter. In general, many Arctic lakes have low DOC concentrations, often below the suggested threshold of 8 to 11 mg/L DOC, above which DOC is hypothesized in some studies to counteract MeHg bioaccumulation (see Box 4.2; French et al., 2014; Braaten et al., 2018). While some studies suggest that DOC concentrations may be declining in Arctic lakes (Saros et al., 2015), others show increases in DOC due to the effects of climate change, land-use practices and other water chemistry interactions (Macdonald et al., 2005; Isles et al., 2020). In streams in a forested watershed in New Hampshire, USA, dissolved THg and MeHg concentrations in the water were found to increase linearly with DOC. However, Hg concentrations in fish showed maximum bioaccumulation at intermediate DOC levels, which suggests that MeHg available for bio uptake reduces at high DOC concentrations (Broadley et al., 2019).

Mercury and MeHg dynamics in freshwater systems change with season, having low or no mobilization during freezing conditions (November–May), which increases with higher river flows and flooding during the melting season from May to June. During melting, most transported Hg is bound to particles. The largest river in the Canadian Arctic, the Mackenzie River, is estimated to export between 13 and 15 kg/y MeHg (unfiltered) into the Arctic Ocean (Emmerton et al., 2013). A total estimate of MeHg flux from all Arctic rivers was estimated by Sonke et al. (2018) to be 584 kg/y.

Methylmercury in terrestrial snow enters High Arctic lakes during snowmelt via melt streams, having higher concentrations during spring melt than during summer (Loseto et al., 2004b). Methylmercury concentrations in Canadian Arctic freshwater systems are generally low ranging from 0.04 to 0.18 ng/L in unfiltered samples in rivers, 0.02 to 0.10 ng/L in lakes and greater than 0.02 to 0.53 ng/L in ponds (see Table 4.1). Compared to deeper lakes, shallow water bodies have generally higher MeHg due to warmer temperatures and higher organic matter available for microbial metabolism and are probable

Table 4.1 Published data on methylmercury in rivers, streams, lakes and freshwater ponds in the Subarctic and Arctic Canada. Adapted from Chételat et al., 2015.

	Period	MeHg (ng/L) unfiltered	MeHg (ng/L) filtered	Reference
Rivers and streams				
Mackenzie River, NT	2003–2005	0.09±0.03	0.08±0.04	Leitch et al., 2007; Graydon et al., 2009a
Mackenzie River, NT	2007–2010	0.08±0.05	0.03±0.001	Emmerton et al., 2013
Mackenzie River tributaries, NT	2003–2005	--	0.07±0.04	Leitch et al., 2007
Peel River, NT	2007–2010	0.10±0.08	0.02±0.02	Emmerton et al., 2013
Cornwallis Island streams, NU	1994–2006	0.07±0.06	--	Loseto et al., 2004b; Semkin et al., 2005
Ellesmere Island streams, NU	2005	0.04±0.03	--	Lehnherr et al., 2012b
Devon Island river, NU	2006	0.05	--	Chételat et al., 2015
Churchill River, MB	2003–2007	0.18±0.09	0.14±0.07	Kirk and St. Louis, 2009
Nelson River, MB	2003–2007	0.05±0.03	0.04±0.02	Kirk and St. Louis, 2009
Severnaya Dvina, Russia	2012	--	0.05–0.17	Sonke et al., 2018
Lakes				
Cornwallis Island, NU	2002–2007	0.04±0.01	--	Loseto et al., 2004b; Semkin et al., 2005; Chételat et al., 2008; Gantner et al., 2010a
Devon Island, NU	2006	0.04±0.02	--	Chételat et al., 2008
Somerset Island, NU	2005–2007	0.02	--	Chételat et al., 2008; Gantner et al., 2010a
Ellesmere Island, NU	2003, 2005–2007	0.05±0.03	--	St. Louis et al., 2005; Gantner et al., 2010a; Lehnherr et al., 2012b
Mackenzie River basin, NT	1998–2002	0.07±0.04	--	Evans et al., 2005b
Mackenzie River delta, NT	2004, 2010	0.10±0.05	--	Graydon et al., 2009a; Emmerton et al., 2013
Iqaluit (surface)	2011–2014	<0.01–0.04	--	Chételat et al., 2018
Resolute Bay (surface)	2011–2014	0.02–0.05	--	Chételat et al., 2018
Ponds				
Cornwallis Island, NU	2006	<0.02	--	Chételat et al., 2015
Devon Island, NU	2006	0.08±0.05	--	Chételat et al., 2015
Ellesmere Island, NU	2003, 2005	0.53±0.68	--	St. Louis et al., 2005; Lehnherr et al., 2012b

methylation hotspots (Lehnherr et al., 2012a; Lehnherr, 2014; MacMillan et al., 2015). In Alaskan lakes, sediment methylation has been shown to be the major source of MeHg to those ecosystems (Hammerschmidt and Fitzgerald, 2006).

As mentioned before, thermokarst processes are associated with an influx of DOC and POC (as well as a suite of nutrients and inorganic constituents; Vonk et al., 2015a) which may transport Hg into Arctic freshwater environments. High concentrations of THg and MeHg, as well as DOC, have been reported in water from slump lakes around the Subarctic region of Kuujjuarapik, Quebec, Canada, and the Western Canadian Arctic (MacMillan et al., 2015; St. Pierre et al., 2018). Overall, the authors attributed the reducing conditions of the anoxic bottom waters in the stratified slump lakes to the elevated MeHg levels' high methylation potential. Furthermore, the authors suggest that the positive correlations between DOC and MeHg concentrations indicate that DOC is transporting Hg into the slump lakes from the surrounding landscape or permafrost and/or stimulating anaerobic methylation in these systems. The results of these studies, and others like them, suggest that permafrost thawing may be a significant source of both organic matter and Hg to Arctic aquatic systems, as discussed earlier.

Freshwater inputs of organic matter were observed to enhance water-column MeHg production in an Arctic estuary (Schartup et al., 2015a). Coastal sediments and oligotrophic lake sediments in a High Arctic region of the Canadian Arctic Archipelago were found to methylate Hg, though at a low rate (St. Pierre et al., 2014; Hudelson et al., 2020).

4.3.1.3 Glaciers

Methylmercury has been shown to be released in glacier-fed streams of the Canadian High Arctic (Ellesmere Island; St. Louis et al., 2005; St. Pierre et al., 2019), Yukon (Halm and Dornblaser, 2007) and Alaska (Nagorski et al., 2014; Vermilyea et al., 2017). Reported MeHg concentrations in unfiltered glacial meltwater (the sum of dissolved and particulate MeHg) vary from <0.010 to 0.26 ng/L and account for 1% to 26% of unfiltered THg in water, while concentrations of MeHg in filtered meltwater vary from <0.010 to 0.075 ng/L and account for 4% to 32% of filtered THg (see Table 4.2). Estimates of unfiltered MeHg fluxes in glacier-fed streams of Ellesmere Island are between 0.03 and 14.9 g/y, which translate to annual yields ranging from 0.49 to 11.7 mg/km^2/y in basins with 21% to 82% glacier coverage. (St. Pierre et al., 2019; see Table 4.3).

Table 4.2 Published data on MeHg concentrations in glacial-fed streams in the Arctic.

River basin/ glacier	Basin area, km^2	Glacier cover, %	Sampling period		TMeHg	PMeHg (ng/L)	FMeHg (ng/L)	SMeHg (ng/g)	Reference
			Month(s)	Year(s)					
USA: Alaska									
Lemon Creek	32	55	May–Sept	2010	--	--	--	--	Vermilyea et al., 2017
Stonefly Creek	13	31	July	2007	0.03	0.01	0.02	--	Nagorski et al., 2014
Gull Creek	6	2	July	2007	0.06	0.02	0.04	--	Nagorski et al., 2014
Nunatak Creek	38	2	July	2007	~0.010	<0.010	0.01	--	Nagorski et al., 2014
Reid Creek	17	5	July	2007	0.05	0.01	0.04	--	Nagorski et al., 2014
Taiya River	466	33	July	2007	~0.020	<0.010	0.02	--	Nagorski et al., 2014
Skagway River	376	17	July	2007	0.02	0.01	0.01	--	Nagorski et al., 2014
Canada: Yukon									
Atlin River	6812	--	June, Aug	2004	<0.040	<0.010	<0.040	--	Halm and Dornblaser, 2007; Chesnokova et al., 2020
Takhini River	7050	2	June, Aug	2004	<0.040	<0.040	<0.040	--	Halm and Dornblaser, 2007; Chesnokova et al., 2020
White River	6230	30	June, Sept	2004	<0.040	<0.060	<0.040	--	Halm and Dornblaser, 2007; Chesnokova et al., 2020
Canada: Baffin Island									
Weasel River, Baffin Island	--	>90	July	2007	<0.02–0.02	--	--	--	Zdanowicz et al., 2013
Owl River, Baffin Island	--	>90	July	2008	<0.02–0.02	--	--	--	Zdanowicz et al., 2013
Proglacial stream, Baffin Island	--	>90	July	2008	<0.02–0.03	--	--	--	Zdanowicz et al., 2013
Canada: Ellesmere Island									
J.Evans Glacier (sub)*	--	--	June–July	2001–2002	0.050–0.127	<0.010–0.067	0.035–0.060	--	St. Louis et al., 2005
J.Evans Glacier (supra)*	--	--	June–July	2001–2002	0.080–0.235	0.011–0.193	0.020–0.075	--	St. Louis et al., 2005
Blister Creek	--	--	July–Aug	2015–2016	<0.010–0.159	--	<0.010–0.020	--	St. Pierre et al., 2019
Snowgoose River	222	39	July–Aug	2015–2016	0.013–0.143	--	<0.010–0.021	0.042	St. Pierre et al., 2019
Abbé River	390	52	July–Aug	2015–2016	<0.010–0.055	--	<0.010–0.019	--	St. Pierre et al., 2019
Gliman River	992	71	July–Aug	2015–2016	0.022–0.068	--	<0.010	0.109	St. Pierre et al., 2019
Henrietta Nesmith River	1274	82	July–Aug	2015–2016	0.011–0.062	--	0.014–0.017	--	St. Pierre et al., 2019
Turnabout River	678	38	July–Aug	2015–2016	0.027–0.065	--	<0.010–0.051	--	St. Pierre et al., 2019
Very River	1035	26	July–Aug	2015–2016	0.051–0.097	--	<0.010–0.012	--	St. Pierre et al., 2019
Ruggles River	7516	41	July–Aug	2015–2016	<0.010–0.013	--	<0.010–0.013	--	St. Pierre et al., 2019

TMeHg: Total MeHg in unfiltered water, TMeHg = FMeHg + PMeHg
FMeHg: MeHg in filtered water (0.45 micrometer), operationally equivalent to dissolved MeHg
PMeHg: Total particulate-bound MeHg retained after filtration (0.45 μm)
SMeHg: MeHg mass concentration (dw) in suspended or riverbed sediments
*(sub): subglacial or proglacial stream flow; *(supra): supraglacial stream flow

Table 4.3 Estimates of riverine MeHg fluxes in glaciated basins of the Canadian High Arctic.

Creek/river	Basin area, km^2	Glacier cover, %	Averaging period	TMeHg (g/y)	MeHg mg/km^2/y
Blister Creek	--	--	2015–2016	0.03–0.11	--
Snowgoose River	222	39	2015–2016	0.51–1.51	2.28–6.78
Abbé River	390	52	2015–2016	0.87–3.38	2.23–8.68
Gilman River	992	71	2015–2016	2.45–9.99	2.47–10.1
Henrietta Nesmith River	1274	82	2015–2016	4.23–14.9	3.32–11.7
Turnabout River	678	38	2015–2016	1.37–4.48	2.02–6.61
Very River	1035	26	2015–2016	4.50–8.97	4.35–8.67
Ruggles River	7516	41	2015–2016	3.68–9.44	0.49–1.26
			Overall range of values:	0.03–14.9	0.49–11.7

All data from St. Pierre et al., 2019.

An increase in the glacial sediment Hg flux in response to enhanced glacier melt rates might lead to higher exposure risks to inorganic Hg or MeHg in downstream aquatic ecosystems in some catchments. On land, changes might occur with the development of seasonally wet areas in newly deglaciated forelands where methylation of sediment-bound Hg could take place. In southeastern Alaska, for example, watersheds with greater wetland abundance have higher Hg concentrations, in both water and aquatic fauna, than glacierized basins (Nagorski et al., 2014). An increased supply of labile and bioavailable DOM from terrestrial sources such as wetlands or newly formed organic soils (e.g., Wietrzyk-Pełka et al., 2020) might also increase the risk of riverine Hg uptake by biota in these watersheds. It could also promote Hg methylation by sulfur-reducing bacteria in catchments where subglacial oxidation of sulfides causes enhanced sulfidization of ponds, wetlands and lakes (Graham et al., 2012). Cryoconite holes (dirt-filled melt cavities on glacier surfaces) are abundant over glacier margins or stagnant ice and can accumulate atmospherically deposited impurities released by ice melt, as well as microbes (Cook et al., 2016). These micro-environments could potentially act as local hotspots of Hg methylation in glacial environments, but direct evidence supporting this is presently limited to Tibetan glaciers (Zhang et al., 2020a).

In the marine environment, meltwater plumes from tidewater glaciers carrying both dissolved and particulate Hg may be injected into zones of locally high primary productivity in coastal surface waters, where subsequent methylation and biological uptake can occur (Schartup et al., 2015b). Some glaciers of southern Alaska are sources of old (up to ~3900 ^{14}C y) and highly labile DOM, of possible subglacial bacterial origin, which is discharged into coastal waters (Hood et al., 2009, 2015). Likewise, retreating glaciers in fjords in southern Spitsbergen, Svalbard, discharge sediments containing up to 2.8% weight of OC (Kim et al., 2020a). Seafloor sediments in these fjords have THg concentrations of up to 84 ng/g. Mercury concentrations correlate closely with OC and are thought to be largely derived from glacially eroded sedimentary rocks (e.g., shales) in the glacierized basin. The discharge of Hg-bearing glacial sediments containing organic matter might promote Hg methylation and uptake by marine biota within the water column, which has not been well studied. However, as a recent and exhaustive review highlighted, the local effect of glacial runoff on coastal marine primary productivity is likely limited to a few kilometers beyond glacier termini, and whether runoff promotes or limits productivity varies between land- or marine-terminating glaciers (Hopwood et al., 2020). For example, observations in fjords in northwestern Svalbard suggest that glacial meltwater plumes could reduce the phytoplankton biomass (Piquet et al., 2014), and this might effectively limit MeHg production and uptake in the marine food chain. Furthermore, the high deposition rates of inorganic matter near tidewater glaciers, or at the mouth of proglacial channels, dilute the organic matter content in the seafloor sediments of Svalbard fjords (Liu et al., 2015), and this might limit benthic Hg methylation. On the whole, therefore, the environmental impact of Hg releases from melting glaciers and ice caps is likely to be local, rather than widespread across the Arctic.

Box 4.3 Mercury and methylmercury leaching due to deforestation in Subarctic areas

Soil disturbance such as forest harvesting may increase the mineralization of organic matter as well as mobilization and runoff fluxes of DOC (Nieminen et al., 2015) and could therefore promote the exports of Hg and MeHg to surface waters (Eklöf et al., 2016). If more intrusive harvesting practices such as whole-tree harvesting with stump lifting (WTHs) is used, the leaching of stored Hg and MeHg to recipient water bodies can potentially increase, especially in peatland forests. The impacts of intensified forest harvesting on the mobilization of Hg and MeHg were studied at eight peatland dominated forest catchments in Northern Finland (Ukonmaanaho et al., 2016). Results indicated that Hg concentrations in ditch water increased both after WTHs and conventional stem-only harvesting (SOH). However, MeHg concentrations only increased notably at the WTHs sites, indicating that stump lifting with soil disturbance increased MeHg leaching. The higher MeHg concentrations were observed typically at the end of the summer when the soil was at its warmest, which is a great concern due to predicted climate warming. Results also showed that the annual Hg and DOC concentrations correlated positively in ditch water, suggesting that Hg leaching is related to the leaching of DOC and organic matter.

The Hg and MeHg loads followed the same patterns as the concentrations, although the loads also depended on runoff and precipitation. Cumulative Hg and MeHg loads increased more at treated sites than at control sites (see Figure 4.3). However, for MeHg, there was only a slight difference in the load between control sites and SOH. These results indicated that forest harvesting increase mobilization of Hg and MeHg from soil to water bodies, which may be accelerated due to climate warming and increase in precipitation in the future (Bishop et al., 2020).

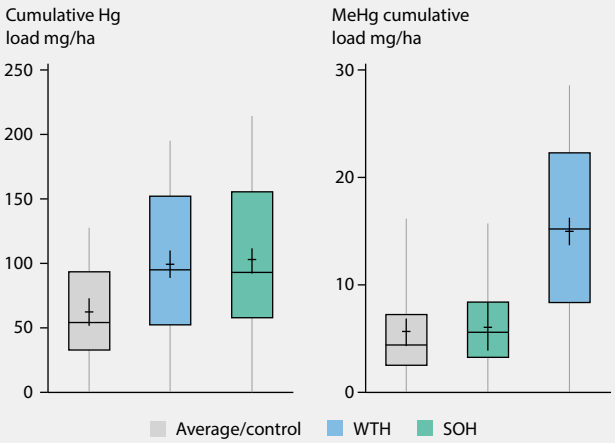

Figure 4.3 Cumulative average loads of Hg and MeHg in ditch water (2008–2012) at control sites (n=2), whole-tree harvesting + stump lifting (WTHs) sites (n=4) and stem-only harvesting (SOH) sites (n=2).

4.3.2 Marine systems

4.3.2.1 Seawater

One of the most significant discoveries since the 2011 AMAP Mercury Report is the presence of a MeHg enrichment layer at shallow depths in Arctic seawater (Wang et al., 2012a, 2018; Heimbürger et al., 2015; Agather et al., 2019; Petrova et al., 2020). This subsurface MeHg layer is clearly demonstrated in the Canadian Arctic, where the total MeHg in unfiltered seawater peaks at a depth of ~300 m up to 0.1 ng/L in the Canada Basin (see Figure 4.4; Wang et al., 2012a, 2018). From the Canada Basin eastwards to the Canadian Arctic Archipelago, the depth of the MeHg enrichment layer shoals up to ~100 m and the peak MeHg concentration slightly decreases. Further eastwards, to Baffin Bay, the MeHg concentration becomes much lower without a distinctive peak but remains higher in the mid-depths than in the surface or bottom waters. Shallow (150–200 m) peaks of total MeHg (up to 0.08 ng/L) in unfiltered seawater are also reported in the central Arctic Ocean in the marginal ice zone (Heimbürger et al., 2015).

Along a looped transect between the Chukchi Sea and North Pole, Agather et al. (2019) measured MMHg and DMHg separately in filtered seawater. A subsurface enrichment of dissolved MMHg and DMHg is also generally observed for most of the stations, although several stations also have elevated MMHg just above the ocean floor (see Figure 4.5). Enrichment of MeHg in the bottom layer of seawater is also shown in the shallow East Siberian Sea (Kim et al., 2020b).

A subsurface enrichment of MeHg in seawater has been observed in almost all major ocean basins (AMAP/UNEP, 2019), including the Atlantic Ocean (Bowman et al., 2015; Bratkič et al., 2016), Pacific Ocean (Sunderland et al., 2009; Hammerschmidt and Bowman, 2012; Munson et al., 2015; Bowman et al., 2016; Kim et al., 2017), Southern Ocean (Cossa et al., 2011; Gionfriddo et al., 2016); Mediterranean Sea (Cossa et al., 2009, 2012, 2017; Heimbürger et al., 2010), Baltic Sea (Soerensen et al., 2016a) and the Black Sea (Rosati et al., 2018) basins. However, what differentiates the Arctic Ocean basin from the others is that the MeHg enrichment occurs at a much shallower depth (100–300 m depth) where dissolved oxygen is well above 75% of the saturation value (Wang et al., 2012a, 2018; Heimbürger et al., 2015; see Figure 4.4). As this subsurface MeHg maximum lies within the habitat of zooplankton and other lower trophic level biota, it has been suggested that biological uptake of the subsurface MeHg and subsequent biomagnification explains a long-standing

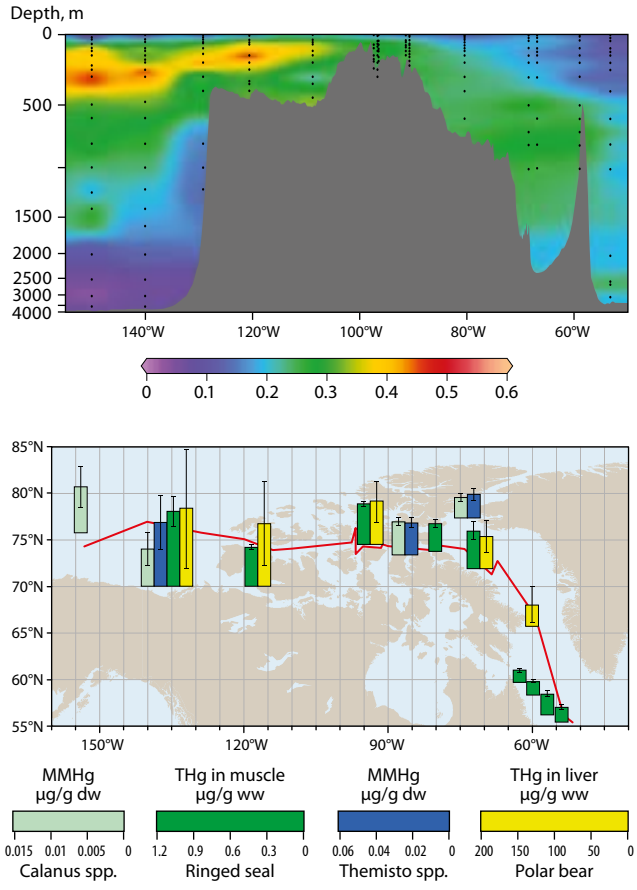

Figure 4.4 Methylmercury (MeHg) concentrations in unfiltered seawater (top panel) and the marine food web (bottom panel) along a longitudinal (west-to-east) section (the red line in the bottom panel) across the Canadian Arctic and Labrador Sea. The bar charts in the bottom panel show mean concentrations of monomethylmercury (MMHg) in *Calanus* spp. and *Themisto* spp. collected from 1998 to 2012 (±1SD), THg in muscle of adult ringed seals collected in 2007 and 2011 and THg in liver of polar bears (*Ursus maritimus*) collected from 2005 to 2008. Adapted from Wang et al., 2018.

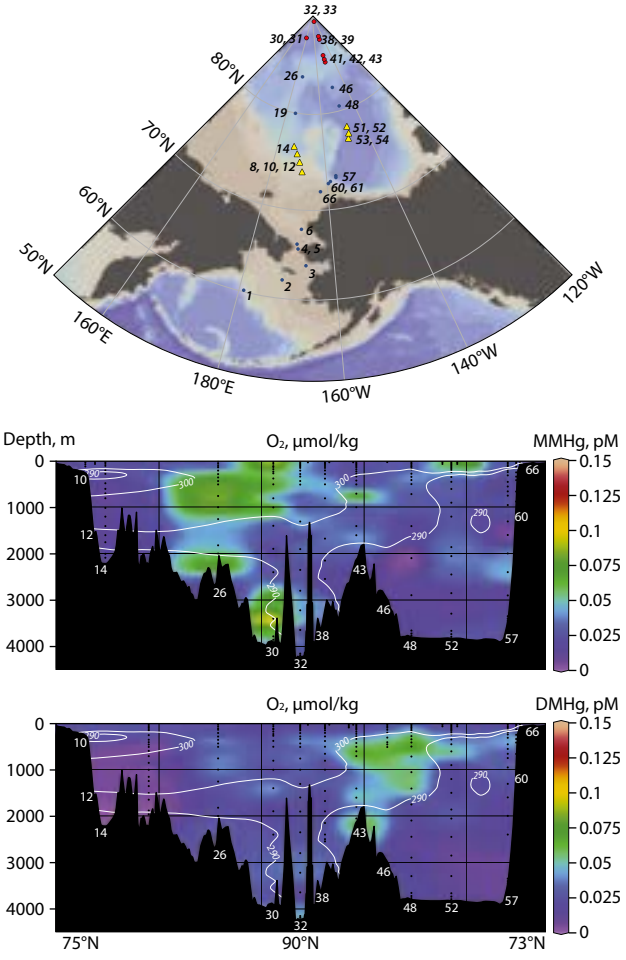

Figure 4.5 Monomethylmercury (MMHg) and dimethylmercury (DMHg) and dissolved gaseous oxygen (O_2) in filtered seawater along a looped latitudinal section (~75°N to the North Pole and then back to ~73°N) in the western Arctic Ocean. The top panel shows the sampling stations along the section. Adapted from Agather et al., 2019.

mystery in the Canadian Arctic on why marine animals in the western Arctic have higher Hg levels than those in the east (see Figure 4.4; Wang et al., 2018). The increasing amounts of bioavailable Hg in surface waters are starting to have an effect on Hg accumulation at the bottom of Arctic marine food webs (Foster et al., 2012) with THg levels of up to 242 ng/g in zooplankton.

The mechanisms of subsurface MeHg formation in the Arctic Ocean and other ocean basins in the world is debated. Most of the studies have attributed the subsurface MeHg to *in situ* Hg methylation in the water column associated with organic matter remineralization (Sunderland et al., 2009; Cossa et al., 2011; Wang et al., 2012a; Heimbürger et al., 2015), yet the biotic or abiotic processes that are responsible for the methylation remains unidentified (Bowman et al., 2020b). The recent work in the Canadian Arctic (Wang et al., 2018) shows that it is possible that the subsurface MeHg could originate from the advection of MeHg produced in shelf sediments. This is supported by three lines of evidence: (1) the spatial distribution pattern of subsurface MeHg in relationship with distinctive water masses (Wang et al., 2018); (2) the lack of known Hg methylators in the highly oxygenated subsurface water (see Section 4.2.1); and (3) the problems associated with existing Hg methylation and demethylation rates that were determined using a seawater incubation approach (Wang et al., 2020b). This calls for further studies on MeHg sources and dynamics in the Arctic and global oceans.

The total filtered MeHg in the western Arctic Ocean has been estimated at 0.011±0.010 ng/L (Agather et al., 2019). Methylmercury inflow to the Arctic Ocean totaled 9±2 Mg/y, most of which enters with deep and mid-depth waters of the Atlantic Ocean (7.5±2 Mg/y; Petrova et al., 2020). Similarly to THg, more MeHg flows out of the Arctic Ocean into the North Atlantic (16.5±3 Mg/y, 14±2 Mg/y via Fram Strait, 2.5±1 Mg/y via the Davis Strait; Petrova et al., 2020) than flows in. The MeHg outflow via Fram Strait conserves the shallow MeHg peak found throughout the Arctic Ocean, and an average DMHg:MMHg ratio of 2.5:1 (Petrova et al., 2020). *In situ* MeHg formation in the Arctic Ocean water column (Lehnherr et al., 2011; Wang et al., 2012a, 2018; Heimbürger et al., 2015; Soerensen et al., 2016a; Petrova et al., 2020) results in a net MeHg outflow of 7.5±2Mg/y (Petrova et al., 2020).

4.3.2.2 Marine sediment

Methylmercury concentration measurements in deep Arctic Ocean sediments are sparse. Based on a range of means, MeHg concentrations in Beaufort Sea and Chukchi Sea shelf sediments were estimated to range from 0.15 to 0.37 ng/g (Fox et al., 2014). A recent study in the East Siberian Sea shows that MeHg concentrations range from 0.09 to 0.17 ng/g in the shelf sediments, with much lower concentrations (~0.003 ng/g) in the slope sediments (Kim et al., 2020b). Based on estimated MeHg concentrations of 0.2 ng/g for shelf sediments and 0.05 ng/g for the deep basin, Soerensen et al. (2016a) estimated a MeHg sedimentation flux of 1.3 Mg/y and 0.1 Mg/y to the shelf and deep basin, respectively. Resuspension was not estimated due to an absence of data. Applying a distribution coefficient of 500, based on data from North Atlantic estuarine and shelf regions (Sunderland et al., 2006; Hollweg et al., 2010; Schartup et al., 2015a), MeHg diffusion to the overlying water column was estimated at 0.9 Mg/y and 0.1 Mg/y from shelf and deep basin sediments, respectively, for a total flux of 1.0 Mg/y (Soerensen et al., 2016a). However, a recent study in the East Siberian Sea suggests that the MeHg diffusion flux from sediments to the water column could be much larger, amounting to 4.6±0.2 Mg/y for the Arctic shelf system alone (Kim et al., 2020b). Clearly there is a need to better constrain this important MeHg flux.

4.3.2.3 Snow and sea ice

Snow, which covers large parts of the Arctic landscape and sea icescape, has a large interstitial surface area for air-snow exchange of Hg and plays a major role in atmospheric mercury depletion events (AMDEs; see Section 3.3.1; Douglas et al., 2012, 2017; Steffen et al., 2014). However, the bioavailable fraction of newly deposited Hg has been shown to be deposited in snowfall events in higher proportions than deposition provoked by AMDEs. Larose et al. (2011) estimate that AMDEs potentially deposit 20 Mg/y of bioavailable Hg to Arctic surfaces, whereas wet and dry deposition may provide between 135 and 225 Mg/y (Douglas et al., 2012). Douglas et al. (2012) report that the small amounts of MeHg found in snowpack before spring snowmelt does not add significantly to MeHg levels in aquatic systems.

The sea-ice environment, including first-year ice, multi-year ice and the overlying snow cover, provides a spatially and temporally dynamic interface between the ocean and the atmosphere in the Arctic Ocean where physical transport, chemical reactions, and biological uptake occur (Wang et al., 2017a). The ice is semi-permeable, which affects the transport of gases and contaminants from air to seawater. Chemical reactions occur both within sea ice and across the ocean-sea ice-atmosphere interface.

The sea-ice environment is also an important habitat and feeding ground for many organisms, including bacteria, algae, zooplankton and larger mammals such as polar bears and whales. Beattie et al. (2014) found elevated MeHg concentrations in multi-year Arctic sea ice of up to 0.5 ng/L in the lower part of the ice (see Figure 4.6). Recent work has shown concentrations of both MMHg and DMHg in sea ice, especially within first-year ice (4.4% MMHg vs. 1.5% in multi-year ice) from across the central Arctic Ocean (Schartup et al., 2020).

As the high concentrations of MeHg in the bottom layer of sea ice (Beattie et al., 2014) cannot be explained by downward transportation of MeHg from the overlying snow (Gionfriddo et al., 2016; Soerensen et al., 2016a), it has been postulated that Hg methylation could take place in sea ice. Discrete peaks in MMHg and DMHg concentrations within sea-ice cores (Schartup et al., 2020) also suggest that they may be produced biotically within the sea ice. This is supported by the fact that microbes present in snow and ice are metabolically active even under freezing temperatures (Douglas et al., 2012). Methylation of Hg has earlier been suggested to be strictly anaerobic and to occur in the anaerobic brine environment (droplets, channels or pockets of salt solution in sea ice) or in the lower part of the ice, due to the involvement of sulfate-reducing bacteria (Chaulk et al., 2011; Gilmour et al., 2013; Beattie et al., 2014). During spring melt, heterotrophic activity

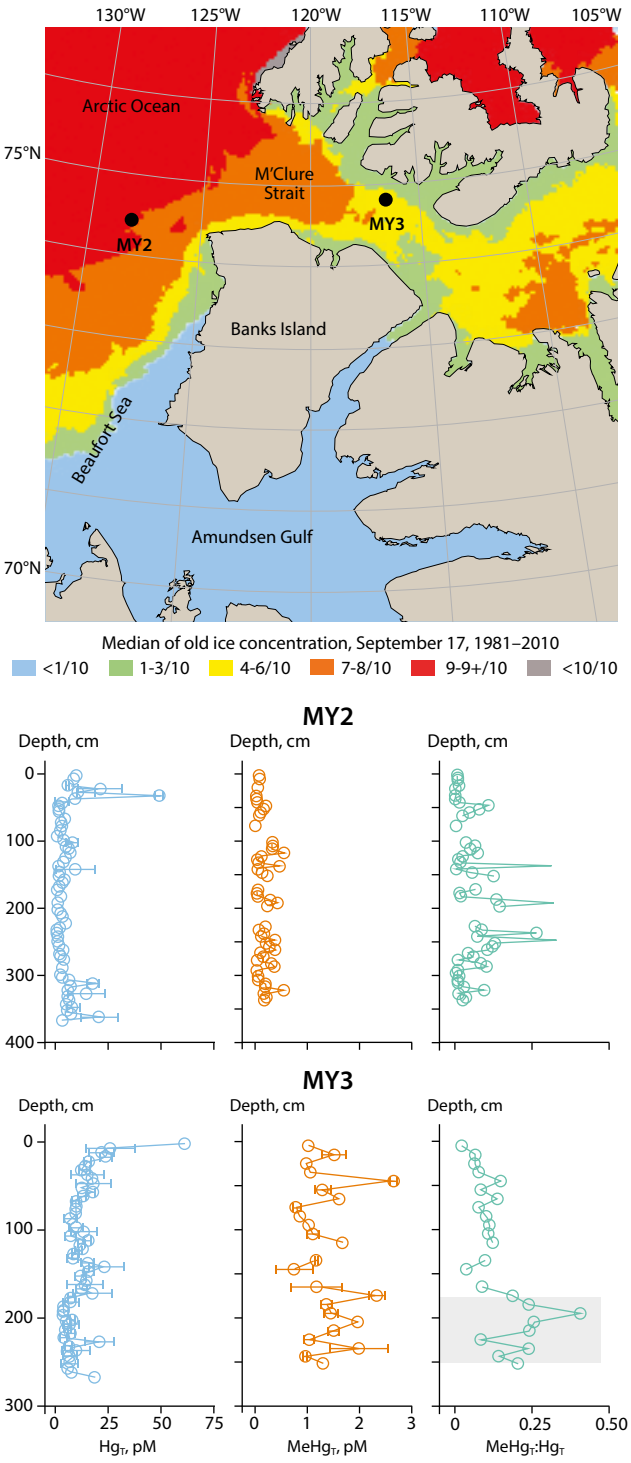

Figure 4.6 Profiles of methylmercury (MeHg) concentrations and the ratio of MeHg to THg (MeHg:THg) in multi-year sea ice sampled at two sites (MY2 and MY3) in the eastern Beaufort Sea and the M'Clure Strait. Adapted from Beattie et al., 2014.

could lead to oxygen depletion in the bottom of the ice column and denitrification processes that favor anoxic environments could then be important in the lower parts of the ice (Rysgaard and Glud, 2004). However, no known anaerobic Hg methylators have been identified in Arctic sea ice. Aerobic Hg methylation has been observed in surface seawater, and it is possible it could also occur in snow and sea ice (Heimbürger et al., 2015; Schartup et al., 2015b).

A study in the Antarctic has suggested that methylation of Hg in sea ice might be carried out by aerophilic bacteria, such as *Nitrospina*, or by sea-ice phytoplankton (Gionfriddo et al., 2016), but this has yet to be confirmed in the Arctic. Gionfriddo et al. (2016) suggest that sea-ice phytoplankton play a role in the stimulation of methylation of oxidized Hg that may occur within brine pockets and periphytic biofilms where organic matter is trapped and decaying. Due to the seasonality of primary production, MeHg formation could show seasonal variations. Chlorophyll-a (Chl-a) showed a covariation with MeHg, suggesting a microbial Hg methylation and the involvement of phytoplankton and phototrophs. Gionfriddo et al. (2016) also identify Proteobacteria, which possesses the *mer* operon, as a potentially important Hg reductive phylum.

Relationships between MeHg and Chl-a have been found both in Antarctic and Arctic ice (Cossa et al., 2011; Beattie et al., 2014). However, little is known about the processes that control the methylation and biotic uptake of Hg from sea ice in polar marine systems.

The presence of sea ice decreases photodegradation of MeHg in underlying water (Ebinghaus et al., 2002b). However, photochemical processes are still possible and depend on the thickness and structure of the sea ice and snow. Some direct photoreduction can occur, transforming Hg(II) into Hg(0) within the ice. Other photomediated processes are also important, where photolytically-produced reactive species could play a role in Hg transformation. One example is the photoproduction of halogen radicals that initiate AMDEs (see Section 3.3.1). This production is most likely occurring in the top layer of the ice or in the overlying snowpack, where the influence of solar radiation is the highest (Nerentorp Mastromonaco et al., 2016).

The uptake and transport of Hg and subsequent formation of MeHg in sea ice is determined by its thickness and permeability, which varies dramatically with temperature and season. During winter, the ice is cold and less permeable, which slows the transport of Hg species through the ice. However, exchange continues with the seawater as the bottom of the ice is warmer (greater permeability) and with the atmosphere as brine expulsion expels Hg to the overlying snowpack. In spring, the ice warms up and the brine volume increases. Contaminants such as Hg then percolate from snow to ice and could lead to their flushing into the underlying seawater. Summer sea-ice melt leads not only to dissolved Hg being released from the ice but also to particle bound Hg and MeHg being incorporated in the bulk ice (Wang et al., 2017a). The dynamic motion of sea ice also makes it possible to transport Hg and MeHg over time and space as the ice can drift over large areas in the Artic Ocean, depending on winds and underwater currents. The two main routes of sea-ice drift in the Arctic are via the Transpolar Drift that circulates from the eastern to central Arctic and the Beaufort Gyre which circulates clockwise in the western Arctic. The Transpolar Drift, which is characterized by elevated meteoric water fractions (>15%) above 84°N, contained higher THg concentrations (up to ~0.4 ng/L) and no elevated MeHg, and both Hg species had no significant correlation to meteoric water fraction (Charette et al., 2020). The export of MeHg via drifting sea ice has been calculated by Wang et al. (2017a) at less than 4% of the total Hg export from the Arctic Ocean. However,

more recently Petrova et al. (2020) estimated a net export of MeHg in sea ice of 0.4 Mg/y, which represented 10% of the total Hg export (THg estimated at 4 Mg/y). The total MeHg pool in sea ice in the Arctic Ocean was estimated by Schartup et al. (2020) to be 0.33 Mg, which is consistent with estimates of 0.3 to 2.6 Mg, based on studies performed in the M'Clure Strait and Beaufort Sea (Beattie et al., 2014; Soerensen et al., 2016a). Climate change has caused the overall thickness and summer extent of sea ice to decrease in the Arctic (Stroeve et al., 2014; Lindsay and Schweiger, 2015). More open waters and less sea-ice coverage allow direct contact between the atmosphere and the water surface of the Arctic Ocean, leading to direct atmospheric wet and dry deposition and gas exchange of Hg(0) between water and air. Climate change impacts on the Hg cycle will further be discussed in Chapter 5.

4.4 What processes are important for biological uptake of methylmercury?

Mercury speciation determines (a) how Hg is transported between different environmental compartments, (b) organismal exposure, (c) the potential toxicity of the exposure to the organism, (d) the extent to which Hg can transport between tissues within the organism, (e) the toxicity of the Hg compound (e.g., MMHg, DMHg, $HgCl_2$), (f) its ability to be taken up or excreted, and (g) its ability to bioaccumulate and biomagnify through the food web.

In its strict sense, bioavailability is *"the fraction of an administered dose that reaches the systemic circulation. Thus, by definition, the bioavailability of an intravenously injected chemical is 1 (or 100%)"* (Johanson, 2010). In the previous AMAP mercury assessment (AMAP, 2011), it was noted that bioavailability of Hg *"includes the availability of inorganic Hg forms to microbial populations responsible for Hg methylation and the availability of MeHg in prey items to predators within food webs"*. The bioavailability of Hg from the environment is controlled by many factors, such as the chemical form or speciation of the Hg ions Hg^{2+}or $MMHg^{+}$, their biochemical reactivity *in situ*, the activity of local microbial communities, and the eventual balance between the dissolved and particulate fractions of the Hg present. A recent review (Bradley et al., 2017) noted that although many risk assessor models assume a 95% to 100% bioavailability/assimilation efficiency for MMHg, studies on 25 species of fish found values that ranged from 10% to 100% for MMHg (though the majority of studies found >80% efficiency) and 2% to 51% for Hg(II). Several factors affected these results, such as the Hg source and the nutrients present. Earlier dosing studies (sometimes using radiolabeled MMHg) showed high assimilation efficiencies of dietary MMHg in mammalian species (Nielsen and Andersen, 1991; FAO/WHO, 2000a).

Monomethylmercury concentrations in fish and wildlife vary within and across geographic regions in the circumpolar Arctic, reflecting the extent of Hg loading to the ecosystem (see Chapter 3), environmental conditions that control *in situ* production of MMHg and its biological uptake at the base of the food web (see Section 4.4.1), and ecological characteristics that control trophic transfer of MMHg within the food web (see Section 4.4.2). These conditions can change over time resulting in temporal variation of MMHg concentrations in animals (see Chapter 2). The delineation of specific conditions promoting MMHg bioaccumulation is important for identifying Arctic ecosystems at greater risk of MMHg exposure (Munthe et al., 2007). Recent research has identified key environmental characteristics that enhance MMHg bioaccumulation in the Arctic.

4.4.1 Processes affecting mercury uptake at the base of the food chain

Significant advances have been made in the last 10 years with regard to the effect of organic matter on the uptake of Hg(II) by bacterial cells and of MeHg into the base of the food chain, as discussed earlier. Mercury uptake in food webs of Arctic ecosystems has been little studied, although some new information is now available since this data gap was highlighted in the previous AMAP assessment (Douglas et al., 2012). The bioconcentration of aqueous MeHg in bacteria and algae, either suspended in the water column (plankton) or growing in biofilms on surfaces such as sediment, ice and rocks, is now understood to be a critical step in the transfer of Hg to top predators in freshwater and marine environments. Aquatic food webs with greater MeHg uptake by microorganisms also have higher concentrations in subsequent trophic levels (Wu et al., 2019), and greater uptake at the base of terrestrial food webs likely has the same consequence (Tsz-Ki Tsui et al., 2019). Processes that promote the production of MeHg and its bioavailability in Arctic environments are described earlier in this chapter. In this section, the uptake of Hg at the base of Arctic aquatic and terrestrial food webs is described, with an emphasis on the biomagnified chemical form MeHg.

Despite the critical role of phytoplankton as the dominant energy source for food webs in the ocean, few measurements of MeHg have been made of Arctic phytoplankton. In the Subarctic estuary of Lake Melville, phytoplankton contained 0.03 ng/g dw of MeHg (Schartup et al., 2015a), which is low relative to concentrations in marine phytoplankton at more temperate latitudes (Schartup et al., 2018). Phytoplankton of the Chukchi Sea had MeHg concentrations below the study analytical detection limit of 1.5 ng/g dw (Fox et al., 2017). Cellular uptake of MeHg by phytoplankton may occur by passive or active transport across the cell membrane (Lee and Fisher, 2016; Skrobonja et al., 2019). Smaller phytoplankton cells have larger surface to volume ratios and, as a consequence, bioconcentrate more MeHg than larger cells (Lee and Fisher, 2016; Schartup et al., 2018). Smaller phytoplankton is known to further stimulate MeHg production (Heimbürger et al., 2010). In the Arctic Ocean, water column MeHg concentrations are often highest at subsurface depths of ~100–300 m, where phytoplankton uptake may be an important entry route into pelagic food webs (Heimbürger et al., 2015; Wang et al., 2018). Arctic estuaries may also be important zones for MeHg uptake by phytoplankton because of salinity-driven water-column stratification and the stimulation of MeHg production by inputs of terrestrial organic matter (Schartup et al., 2015b). Seasonal changes occur in Hg uptake by marine phytoplankton, such as in the Baltic Sea, where reduced sea-ice cover and eutrophication enhanced seasonal bioaccumulation (Bełdowska and Kobos, 2016; Soerensen et al., 2016b).

Sea ice is another habitat where microbial uptake of MeHg may be critical for basal uptake into food webs. As stated before, MeHg production can occur in polar sea ice (Beattie et al., 2014; Gionfriddo et al., 2016) and in marginal sea-ice waters (Heimbürger et al., 2015). Algal growth on the under-ice surface is a significant energy source for pelagic food webs in the Arctic (Kohlbach et al., 2016). Burt et al. (2013) characterized uptake of inorganic Hg by ice algae during a spring bloom associated with first-year ice and suggested that this could represent an important entry point for marine invertebrates grazing either directly on the ice or on settling particulate matter released from melting ice.

Methylmercury within the sea ice can be taken up by ice-associated biota, algae, under-ice amphipods and ice-dependent animals such as fishes, polar bears and birds and can bioaccumulate in marine food chains throughout the year. When sea ice melts, Hg and MeHg in the ice are released to the surface ocean. With greater incident light penetration into the water column, the melting period is also a period of high primary production in surface water, and the concurrent release of contaminants during this period could lead to additional uptake of contaminants within the marine food web. Mercury attached to particles is released from the ice during complete ice melt. Particle sinking makes Hg available for uptake by benthic organisms. Mercury uptake by sea-ice algae is only limited by the amount of Hg available for uptake when spring blooms commence (Burt et al., 2013). This is important since ice algae represent 10% to 60% of annual primary production in the Arctic, and they may become even more abundant under mild climate conditions. Burt et al. (2013) estimate that with the replacement of multi-year sea ice with first-year ice due to climate change, an extra 48 kg/y of particle-bound Hg could enter the Beaufort Sea in the coming years.

Benthic algae and biofilms are a dominant primary energy source for food webs in many Arctic lakes (Vadeboncoeur et al., 2003; Chételat et al., 2010; Rautio et al., 2011). In the eastern Canadian Arctic, MeHg concentrations ranged from 2 to 12 ng/g dw for rocky shoreline biofilms (Chételat et al., 2018), 0.3 to 1.3 ng/g for microbial mats (Camacho et al., 2015), and 2 to 56 ng/g for periphyton and filamentous algae (van der Velden et al., 2013a). In comparison, MeHg concentrations of water-column seston measured in some of those same lakes ranged from less than 0.4 to 30 ng/g dw, and bioconcentration factors of MeHg in biofilms and seston were higher in lakes with low aqueous DOC (Chételat et al., 2018).

Invertebrates play a key role in the trophic transfer of MeHg entering food webs via microorganisms. In the last decade, large amounts of data were compiled on MeHg concentrations in marine zooplankton from across the circumpolar Arctic (Foster et al., 2012; Pućko et al., 2014; Pomerleau et al., 2016). Zooplankton MeHg concentrations ranged from 8 to 96 ng/g dw and were highest in the southern Beaufort Sea region compared to the Chukchi Sea, Canadian Arctic Archipelago, Hudson Bay and northern Baffin Bay (Pomerleau et al., 2016; Wang et al., 2018). Larger taxa of marine zooplankton such as *Themisto* and *Paraeuchaeta* predate on smaller zooplankton, and biomagnification of MeHg was found between omnivorous and herbivorous taxa (Foster et al., 2012; Pomerleau et al., 2016). Recent measurements of MeHg concentrations in zooplankton from Arctic lakes (Lescord et al., 2015; Chételat et al., 2018) add to data from earlier studies (Chételat and Amyot, 2009; Gantner et al., 2010a), which showed that zooplankton in lakes can have higher concentrations (>100 ng/g dw) than those in the marine environment. Large-bodied grazers (Cladocera, *Daphnia*), in particular, can have elevated MeHg concentrations (Chételat and Amyot, 2009; Lehnherr et al., 2012a; MacMillan, 2018).

The developmental stage can influence the MeHg concentration of Arctic freshwater copepods, with dilution occurring as adults accumulate lipid stores (Chételat et al., 2012). A considerable number of studies of Arctic food webs have also characterized Hg concentrations in a variety of benthic invertebrate taxa in marine environments (Bidleman et al., 2013; van der Velden et al., 2013a; Fox et al., 2014; Jörundsdóttir et al., 2014; Clayden et al., 2015; McMeans et al., 2015a; Góngora et al., 2018; Pedro et al., 2019) as well as in lakes (van der Velden et al., 2013a; Chételat et al., 2015, 2018; Kahilainen et al., 2016, 2017; Keva et al., 2017; Rohonczy et al., 2020). These studies showed variation in Hg bioaccumulation among benthic invertebrate taxa, which was partly related to trophic position.

4.4.2 Processes affecting mercury bioaccumulation at higher trophic levels

Mercury concentrations in fish and wildlife reflect ecological processes that influence dietary exposure as well as animal physiology that affects internal accumulation of Hg (see Figure 4.7; Chételat et al., 2020). Trophic position shifts in diet, habitat-specific feeding, cross-ecosystem subsidies and movement or migration can be important determinants of dietary Hg consumed by fish and wildlife. Differences in the extent of assimilation and elimination of MeHg related to sex,

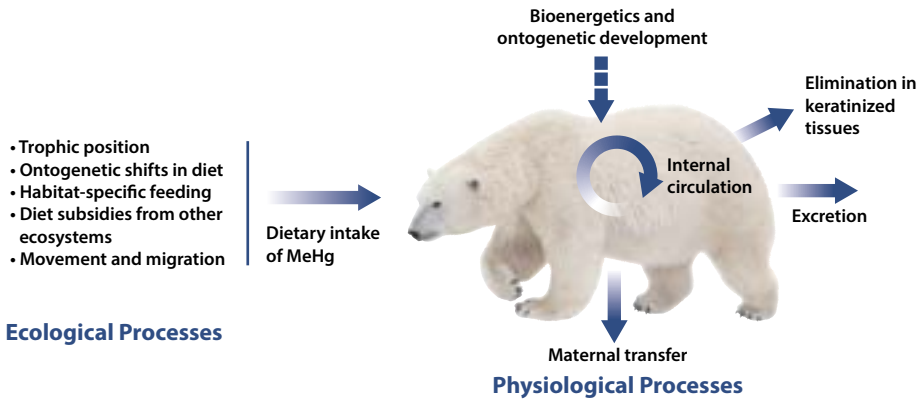

Figure 4.7 Ecological and physiological processes that influence mercury concentrations in wildlife. Source: Chételat et al., 2020.

age, body condition and species also affect animal Hg burdens. Recent advances have identified Arctic-specific processes affecting Hg bioaccumulation in fish and wildlife.

Arctic marine ecosystems have long food chains (~4–5 levels), and top predators (such as polar bear, ringed seal, beluga whale, and Greenland shark; *Somniosus microcephalus*) have elevated Hg concentrations due to feeding at a higher trophic position (St. Louis et al., 2011; McMeans et al., 2015a; Brown et al., 2016, 2018). Recent quantification of food-chain length using nitrogen stable isotopes demonstrated that regional differences in Hg concentrations of top predators, such as between western and eastern regions of the Canadian Arctic (St. Louis et al., 2011; Brown et al., 2016) is, in part, due to food-chain length. There can also be spatial variation in the carbon sources which support Arctic marine food webs, with potential consequences for food-web bioaccumulation of Hg (Cyr et al., 2019a). Similarly, considerable research effort has focused on measuring the rate that Hg biomagnifies through food webs in Arctic ecosystems. A global meta-analysis showed that biomagnification rates were higher at northern latitudes compared with the tropics (Lavoie et al., 2013). Within the Arctic, Hg biomagnification rates can vary among marine and freshwater food webs (Clayden et al., 2015; Lescord et al., 2015; McMeans et al., 2015a; Ruus et al., 2015; Fox et al., 2017), although in a study of co-located marine and lacustrine food webs of Arctic char, no difference was found in biomagnification rate (van der Velden et al., 2013b). While some evidence suggests that cold, low productivity ecosystems have higher Hg biomagnification (Lavoie et al., 2013), factors controlling the biomagnification rate of Hg through Arctic food webs remain unclear.

Marine subsidies to the diet of terrestrial carnivores and freshwater fish can strongly affect Hg bioaccumulation in the Arctic. Wolves (*Canis lupus arctos*), and Arctic foxes (*Vulpes lagopus*) that scavenged on carcasses of marine mammals had higher Hg concentrations than those that had an exclusively terrestrial diet (Bocharova et al., 2013; McGrew et al., 2014; Hallanger et al., 2019). In the case of Arctic fox at Svalbard, interannual variation in their Hg concentration was positively related to the extent of sea-ice cover, which provides a platform to access marine carcasses (Hallanger et al., 2019). Sea-run Arctic char tend to be larger and have faster growth rates than their lacustrine conspecifics, and they have lower muscle Hg concentrations (Swanson et al., 2011; van der Velden et al., 2013b). The lower Hg bioaccumulation in sea-run char was also attributed to lower Hg exposure at the base of marine food webs relative to lakes in the Arctic (van der Velden et al., 2013a). Recent research also found seasonal variation in THg concentrations of anadromous char in northern Quebec; these char had elevated concentrations in the summer months potentially due to a lower percentage of lipids and a lower body weight from winter fasting (Martyniuk et al., 2020).

Migration by wildlife such as seabirds and marine mammals can influence their dietary Hg exposure. Little auks (*Alle alle*) that breed in Greenland during summer and overwinter off the coast of eastern Canada were found to accumulate more Hg during the wintering period (Fort et al., 2014). Similarly, yellow-billed loons (*Gavia adamsii*), which breed in lakes of Arctic North America and overwinter in marine areas of eastern Asia, showed evidence of higher winter exposure (Evers et al., 2014). An evaluation of seasonal variation in Hg contamination of nine species of Arctic seabirds showed, on average, three times higher Hg concentrations in feathers grown at lower latitudes during the non-breeding period than those grown while breeding in Arctic (Albert et al., 2021). Greater Hg bioaccumulation was found for seabirds overwintering in the western Atlantic relative to the eastern Atlantic or the Pacific region (Albert et al., 2021). Thus, consideration of overwinter exposure at lower latitudes is necessary for interpreting Hg bioaccumulation in migratory Arctic seabirds. Bowhead whales (*Balaena mysticetus*) undergo long seasonal migrations within the Arctic in response to sea-ice conditions and prey availability, and examination of their baleen plates provided a record of temporal variation in Hg exposure (Pomerleau et al., 2018). Annual cycles of Hg and $\delta^{13}C$ values (an isotopic indicator of diet) in the baleen plates showed seasonal shifts in diet and Hg accumulation by bowhead whales in both the eastern and western Arctic.

Biota is also an important aspect for the mobility of contaminants in the Arctic environment (Krümmel et al., 2003; Sarica et al., 2004, 2005; Blais et al., 2007; Baker et al., 2009). For example, migrating salmonids that return to remote freshwater ecosystems to spawn act as important transport (bio) vectors of Hg from ocean to rivers and constitute a substantial portion of the total riverine MeHg budget (Blais et al., 2007). Furthermore, returning migratory fish and birds may also play an important role within local biogeochemical cycles. For instance, the carcasses contribute nutrients and organic carbon to the aquatic ecosystems, which can stimulate primary production, heterotrophic activities and secondary production and also be a source of Hg to scavengers (Cederholm et al., 1999, 2000; Sarica et al., 2005)

The body condition of fish and wildlife is sometimes correlated with their Hg concentration, although reported observations have been both positive and negative. Trudel and Rasmussen (2006) showed that Hg concentration may be either positively or negatively correlated to changes in growth and growth efficiency, depending on how fish allocate energy between activity costs and growth rates. Tissue Hg concentrations were negatively correlated with body condition in sea-run char (Evans et al., 2015), caribou (*Rangifer tarandus groenlandicus*; Gamberg et al., 2016) and little auks (Amélineau et al., 2019) positive correlations were observed for eider (Provencher et al., 2016a) and for polar bear both negative and positive correlations were found (Bechshoft et al., 2016; McKinney et al., 2017a). Those contrasting observations reflect several potential underlying physiological processes driving the effect of body condition. Fasting or lower food availability and the subsequent loss of body mass can concentrate Hg already in tissues (Seewagen et al., 2016; Peterson et al., 2018b; Martyniuk et al., 2020). The reverse has also been suggested, that poorer body condition may be a negative effect of a higher Hg burden (Provencher et al., 2016a; Amélineau et al., 2019), although this has been discounted for northern pike (*Esox lucius*; Sandheinrich and Drevnick, 2016). A positive association between body condition and Hg concentration could result from greater Hg intake associated with increased feeding (Bechshoft et al., 2016). Given these bioenergetic influences, seasonal and interannual changes in food resource availability in the Arctic can have important consequences for Hg concentrations in animals (Amélineau et al., 2019; Eckbo et al., 2019; Hallanger et al., 2019).

Long food chains in Arctic lacustrine and marine environments (van der Velden et al., 2013b; Eloranta et al., 2015; McMeans et al., 2015a; Ruus et al., 2015) result in elevated Hg concentrations in Arctic top predators due to the biomagnification of MeHg (Lavoie et al., 2013). Although the importance of biomagnification is well established, recent nitrogen stable isotope measurements specific to Arctic biota have highlighted the importance of variable trophic position in controlling MeHg concentrations among species and among populations of the same species distributed across the circumpolar Arctic such as ringed seal (*Pusa hispida*) and polar bear (St. Louis et al., 2011; Brown et al., 2016). Slow-growing, long-lived top predators in Arctic ecosystems are also prone to long-term Hg bioaccumulation with age (Masbou et al., 2018; Ewald et al., 2019). Low Hg concentrations in terrestrial wildlife have been commonly reported in the Arctic (Gamberg et al., 2015; Dietz et al., 2019a), possibly due to scarcer data from Arctic terrestrial systems compared to data from marine systems. Data could however indicate an effect of shorter food chains and low MeHg accumulation of terrestrial plants. However, recent observations have identified that marine subsidies to the diet of Arctic terrestrial mammals can promote MeHg bioaccumulation (Bocharova et al., 2013; Hallanger et al., 2019).

4.5 How much methylmercury is circulating in the Arctic environment?

Mercury uptake by biota is determined not just by the amount of Hg emissions to the Arctic, but also by biogeochemical and ecological processes occurring in the Arctic. These processes affect Hg uptake in biota by regulating the bioavailability, methylation and demethylation, uptake, bioaccumulation and biomagnification of Hg in Arctic ecosystems. Over the last decade, hotspots of MeHg production in Arctic environments, such as subsurface marine waters and in thawing permafrost, have been identified, addressing an important knowledge gap in the Arctic Hg cycle.

A summary of MeHg concentrations, fluxes and estimated MeHg pools in different environmental compartments used for this mass balance analysis (excluding biota larger than plankton) is presented in Table 4.4 and in Figure 4.8. The MeHg budget for the Arctic Ocean was first estimated by Soerensen et al. (2016a) and later revised by Petrova et al. (2020). The figures for MeHg reservoirs in Arctic waters were based on the average concentration of MeHg in seawater calculated from available data (Wang et al., 2012b, 2018; Heimbürger et al., 2015; Agather et al., 2019; Charette et al., 2020; Kim et al., 2020b; Petrova et al., 2020; Jonsson et al., 2022; Kohler et al., 2022) for the 0–20 m, 20–200 m, 200–500 m and <500 m water masses. In the current assessment, additional MeHg reservoirs were also approximated and included in the total MeHg budget estimate (see Table 3.8.1). For sea ice, the mean percent MeHg reported by DiMento et al. (2019) multiplied with the total Hg pool (see Table 3.8.1) was used, resulting in an estimated MeHg pool of 0.32 Mg. This value is close to the estimate of MeHg (0.33 Mg) previously estimated by Schartup et al. (2020). The MeHg pool in surface soils was estimated by multiplying the total Hg pool by the median percent MeHg in surface soils (St. Pierre et al., 2015: 0.82%) and wetlands (Tarbier et al., 2021: 1.7%), not impacted by recent permafrost thaw, and assuming a 25% coverage of wetlands for the Arctic region (Kåresdotter et al., 2021). Methylmercury reservoirs in snowpack and glaciers were estimated similarly using Hg pool estimates and percent MeHg measurements for snow (6.1%, range: 0.11–11%; St. Pierre et al., 2019, Varty et al., 2021 and Jonsson et al., 2022) and median percent MeHg

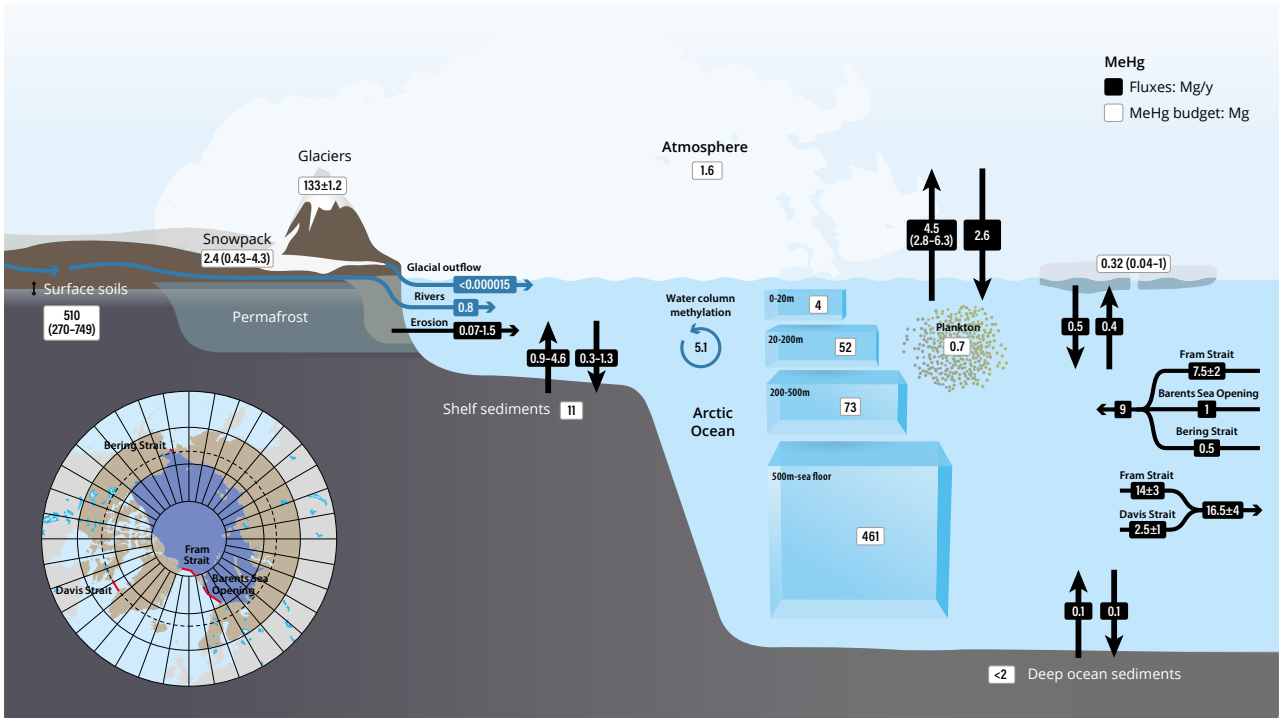

Figure 4.8 MeHg fluxes and budget in the Arctic environment. Updated from Soerensen et al., 2016a and Petrova et al., 2020, with data shown in Table 4.4.

(5.5%) reported by Zdanowicz et al. (2016) for glaciers, respectively. The atmospheric MeHg pool was estimated via the THg pool (see Table 3.8.1) and a calculated percentage of MeHg to THg using measured atmospheric concentrations of MMHg and DMHg by Baya et al. (2015). Using geochemical modeling, Soerensen et al. (2016a) estimated MeHg reservoirs in the Arctic Ocean, sediments and plankton resulting in a total of 576 Mg. In the updated MeHg budget presented by

Table 4.4 Total MeHg concentrations, fluxes and pools in the Arctic environment (excluding biota larger than plankton), as presented in Chapter 4 and relevant literature.

Environmental compartment	MeHg concentration	References
Atmosphere	2.9±3.6 pg/m^3 MMHg 3.8±3.1 pg/m^3 DMHg	Baya et al., 2015
Lichen, Canadian High Arctic coast	1.41–17.1 ng/g	St. Pierre et al., 2015
Soil	0.02–2.11 ng/g (Canada)	St. Pierre et al., 2015
	0.8 ng/g	Soerensen et al., 2016a
Tundra (organic horizon)	0.5–3.4 ng/g	Olson et al., 2018
Tundra (B-horizon)	0.1–1.0 ng/g	Olson et al., 2018
Poor fens (recent permafrost thaw)	0.43 ng/L	Gordon et al., 2016
Downstream permafrost thaw slump	7 ng/L	St. Pierre et al., 2018
Wetland permafrost thaw in palsas underlain by permafrost (Subarctic Sweden)	0.01–0.05 ng/L	Fahnestock et al., 2019
Wetland permafrost thaw in thawed fens (Subarctic Sweden)	1.0–2.0 ng/L	Fahnestock et al., 2019
Rivers	0.04–0.18 ng/L	Table 4.1
Lakes	0.02–0.10 ng/L	Table 4.1
Ponds	<0.02–0.53 ng/L	Table 4.1
Glacial meltwater (unfiltered), Canadian High Arctic, Yukon, Alaska	<0.010–0.235 ng/L	Table 4.2
Glacial meltwater (filtered)	<0.010–0.075 ng/L	Table 4.2
Western and eastern Arctic Ocean	0.011±0.01 ng/L	Wang et al., 2012a, 2018; Agather et al., 2019
Western Arctic Ocean	0.045±0.017 ng/L	Heimbürger et al., 2015
Eastern Arctic Ocean	0.034±0.022 ng/L	Heimbürger et al., 2015
Barents Sea Opening/shelf	0.013±0.004 ng/L	Petrova et al., 2020
Fram Strait	MeHg 0.049±0.03 ng/L MMHg 0.019±0.013 ng/L DMHg 0.039±0.028 ng/L	Petrova et al., 2020
Fram Strait outflow (East Greenland Current)	0.075±0.019 ng/L	Petrova et al., 2020
Beaufort Sea and Chukchi Sea shelf sediments	0.15–0.37 ng/g	Fox et al., 2014
Shelf sediment	0.002–2.4 ng/g	Fox et al., 2014; Soerensen et al., 2016a; Kim et al., 2020b; Liem-Nguyen et al., 2022
Basin sediment	0.05 ng/g	Soerensen et al., 2016a
Shelf sediments (inner plume)	0.72±0.71 ng/g	Liem-Nguyen et al., 2022
Shelf sediments (outer plume)	0.031±0.005 ng/g	Liem-Nguyen et al., 2022
Phytoplankton (Lake Melville)	0.03 ng/g	Schartup et al., 2015a
Phytoplankton (Chukchi Sea)	<1.5 ng/g	Fox et al., 2017
Shoreline rock biofilm, lakes (east Canadian Arctic)	2–12 ng/g	Chételat et al., 2018
Microbial mats, lakes (east Canadian Arctic)	0.3–1.3 ng/g	Camacho et al., 2015
Periphyton, filamentous algae, lakes (east Canadian Arctic)	2–56 ng/g	van der Velden et al., 2013a
Water column seston, lakes	<0.4–30 ng/g	Chételat et al., 2018
Phytoplankton (circumpolar Arctic)	8–96 ng/g	Foster et al., 2012; Pućko et al., 2014; Pomerleau et al., 2016
Surface snow	0.02–0.07 ng/L	Soerensen et al., 2016a
Snowpack	<0.01–0.074 ng/L	Soerensen et al., 2016a
Sea ice (multi-year)	0–0.5 ng/L	Beattie et al., 2014
Sea ice (first-year)	0.006±0.004 ng/L	Schartup et al., 2020
Sea ice (multi-year)	0.022±0.015 ng/L	Schartup et al., 2020

Petrova et al. (2020), the total pool of MeHg in the Arctic Ocean was estimated at 800 Mg MeHg. The budget for the Arctic Ocean waters in the current assessment amounts to 590 Mg MeHg.

Petrova et al. (2020) found a MeHg maxima at the depth layer (100–300 m) of the Arctic Ocean, in line with observations from Wang et al. (2012a, 2018), Heimbürger et al. (2015) and Agather et al. (2019), leading to a net export of MeHg

Environmental compartment	MeHg Fluxes	References
Atmospheric deposition	8.5 (8–10) Mg/y	Petrova et al., 2020
	2.6 Mg/y	This report
Atmospheric evasion	4.5 (2.8–6.3) Mg/y	This report
Sea-ice uptake	0.4 Mg/y	Petrova et al., 2020
Sea-ice discharge	0.5 Mg/y	Soerensen et al., 2016a
Coastal erosion	0.07–0.46 Mg/y 1.5 Mg/y	Soerensen et al., 2016a Petrova et al., 2020
Wetland ponds	1.8–40 ng/m^2/d	Lehnherr et al., 2012a
Glacial meltwater (unfiltered), Ellesmere Island	0.03–14.9 g/y 0.49–11.7 mg/km^2	St. Pierre et al., 2019
Riverine inputs	0.8 Mg/y	Sonke et al., 2018
Inflow to Arctic Ocean	3–13 Mg/y	Soerensen et al., 2016a
–of Atlantic deep and mid-depth waters	6.8 Mg/y	Soerensen et al., 2016a
Inflow to Arctic Ocean	9±1.5 Mg/y	Petrova et al., 2020
–from Fram Strait	7.5±2 Mg/y	Petrova et al., 2020
–from Barents Sea Opening	1 Mg/y	Petrova et al., 2020
–from Bering Strait	0.5 Mg/y	Petrova et al., 2020
Outflow to North Atlantic	8–27 Mg/y	Soerensen et al., 2016a
Outflow to North Atlantic	16.5±2 Mg/y	Petrova et al., 2020
–via Fram Strait	14±3 Mg/y	Petrova et al., 2020
–via Davis Strait	2.5±1 Mg/y	Petrova et al., 2020
Sedimentation load (shelf sediment)	1.3 Mg/y	Soerensen et al., 2016a
Sedimentation load (shelf sediment)	0.3 Mg/y	Petrova et al., 2020
Sedimentation load (basin sediment)	0.1 Mg/y	Soerensen et al., 2016a
Sediment diffusion to water (shelf sediment)	0.9 Mg/y	Soerensen et al., 2016a
Sediment diffusion to water (shelf sediment)	4.6±0.2 Mg/y	Kim et al., 2020b
Sediment diffusion to water (basin sediment)	0.1 Mg/y	Soerensen et al., 2016a
Environmental compartment	**MeHg Pool**	**References**
Atmosphere	1.6 (0–3.2) Mg	Baya et al., 2015; Table 3.8.1
Surface soils	510 (270–749) Mg	St. Pierre et al., 2015; Tarbier et al., 2021; Table 3.8.1
Snowpack	2.4 (0.43–4.3) Mg	St. Pierre et al., 2015; Varty et al., 2021; Jonsson et al., 2022; Table 3.8.1
Glaciers	133±1.2 Mg	Zdanowicz et al., 2016; Table 3.4.3.1, Table 4.2
Sea ice	0.32 (0.04–1.0)Mg <2 Mg	DiMento et al., 2019; Schartup et al., 2020; Soerensen et al., 2016a
Shelf sediments	11 Mg	Soerensen et al., 2016a
Deep sediments	<2 Mg	Soerensen et al., 2016a
Water column (0–20 m depth)	4±2 Mg	Wang et al., 2012a, 2018; Heimbürger et al., 2015; Agather et al., 2019; Charette et al., 2020; Kim et al., 2020b; Petrova et al., 2020; Jonsson et al., 2022; Kohler et al., 2022
Water column (20–200 m depth)	52±34 Mg	Wang et al., 2012a, 2018; Heimbürger et al., 2015; Agather et al., 2019; Charette et al., 2020; Kim et al., 2020b; Petrova et al., 2020; Jonsson et al., 2022; Kohler et al., 2022
Water column (200–500 m depth)	73±44 Mg	Wang et al., 2012a, 2018; Heimbürger et al., 2015; Agather et al., 2019; Charette et al., 2020; Kim et al., 2020b; Petrova et al., 2020; Jonsson et al., 2022; Kohler et al., 2022
Water column (500 m depth–bottom)	461±232 Mg	Wang et al., 2012a, 2018; Heimbürger et al., 2015; Agather et al., 2019; Charette et al., 2020; Kim et al., 2020b; Petrova et al., 2020; Jonsson et al., 2022; Kohler et al., 2022
Plankton	0.7 Mg	Soerensen et al., 2016a

from the Arctic Ocean to the Nordic Seas and the North Atlantic of 7.5 Mg/y. A part of the MeHg produced in the subsurface ocean layer (20–200 m; 17 Mg/y) is converted to DMHg, which diffuses up to the polar mixed layer (PML; 0–20 m), where some of it evades to the atmosphere. Here DMHg is proposed to rapidly photochemically degrade back to MeHg and deposit back to the PML. For this report, MeHg evasion was estimated at 4.5 (2.8–6.3) Mg/y using a DMHg to Hg(0) evasion ratio of 0.16 (Soerensen et al., 2016a) and the new Hg(0) evasion estimate (32 (20–45) Mg/y (see Table 3.8.1). The MeHg deposition was then calculated to be 2.6 Mg/y, assuming the evasion to deposition ratio (0.57) presented by Soerensen et al. (2016a). Riverine MeHg inputs (0.8 Mg/y) were estimated from Sonke et al. (2018), and similar inputs from coastal erosion were assumed (as for Hg, see Table 3.8.1). The benthic flux of MeHg to subsurface waters was estimated at 0.9–4.6 Mg/y (Soerensen et al., 2016a; Kim et al., 2020b). The *in situ* water-column methylation was estimated at 5.1 Mg/y (by calculating the difference between estimated inputs and outputs).

4.6 Conclusions and recommendations

Conclusions (in numbered bullets) are organized under section headings (section numbers in square brackets) followed by recommendations in italics where appropriate.

What controls the pool of mercury available for bioaccumulation? [4.2]

1. Mercury contamination in Arctic ecosystems results from several processes including the transportation of Hg to, and within, the Arctic environment, methylation and demethylation of Hg, and Hg bioaccumulation.
2. While we knew previously that methylation and demethylation were key processes controlling the pool of Hg available for bioaccumulation in Arctic food webs and that methylation of Hg in the environment was primarily a microbial process, its occurrence in the Arctic was poorly characterized; demethylation of MeHg is now understood to occur through both biotic and abiotic pathways.
3. Organic matter plays a key role in both the availability of Hg for bacterial methylation as well as the uptake of MeHg into organisms.
4. Microbial Hg methylation occurs via organisms that carry the *hgcAB* gene pair. Organisms carrying the *hgcAB* gene pair have been identified in Arctic soils and thawing permafrost, and those carrying *hgcA*- or *hgcAB*-like genes have recently been identified in global ocean seawater, though not in the Arctic Ocean. Organisms carrying genes that encode the *merA* and *merB* operons (a biotic pathway for Hg reduction and demethylation) have also been observed in the Arctic environment.
5. The potential roles of dissolved organic matter (DOM) in Hg methylation and biological uptake are important and complex.
6. Evasion of dimethylmercury (DMHg) from the marine boundary layer, and subsequent demethylation of DMHg in the atmosphere, may be a source of MeHg deposition to Arctic snow. Similarly, photochemical degradation of DMHg in surface waters may be direct source of MeHg to these waters.

Future mapping of microbial communities carrying the genes involved in methylation and demethylation of Hg should be carried out as such mapping will provide critical information on these processes across the Arctic, as well as reveal key linkages to the biogeochemical cycle of other elements such as carbon.

The thawing of permafrost represents a potential source of both DOM and Hg to Arctic and Subarctic aquatic environments; future work should examine the effects of permafrost-derived organic matter on Hg bioaccumulation in Arctic biota, which may add to our understanding of the complex Hg-DOM relationship as permafrost thawing increases in a changing climate.

Future research should also be directed towards a better understanding of the formation and environmental fate of DMHg in the Arctic, and its role in controlling the pool of Hg available for bioaccumulation in marine and coastal food webs.

Where are the hotspots of methylmercury in the Arctic? [4.3]

7. As we previously knew, the production of MeHg in natural systems is controlled by substrate availability (e.g., inorganic Hg and organic matter), the presence and abundance of microbial Hg methylators, and MeHg degradation processes. Thus, anoxic systems, such as organic-rich sediments and flooded soils, are understood to be typical hotspots for MeHg production.
8. We have now also learned that, in the terrestrial environment, foliar uptake of Hg from the atmosphere, a process that could be enhanced in recently or soon-to-be deglaciated foreland, is a key driver for sequestering inorganic Hg that may be available for methylation.
9. Permafrost thaw in low-relief regions with ice-rich soils and sediments may result in the formation of thermokarst wetlands, ponds and lakes that have been repeatedly identified as Hg methylation hotspots across the Arctic due to the concurrent mobilization of carbon and nutrients, creating conditions suitable for methylation.
10. Locally significant MeHg production may occur in newly-deglaciated forelands, especially where wetlands develop (in cryoconite holes on the margins of glaciers themselves) and also at the head of glacially-fed fjords and on the sediments within these fjords.
11. In the marine environment, MeHg is found to be enriched in subsurface, oxic seawater at shallow depths (100–300 m) in many regions of the Arctic Ocean.

Future work is needed to better identify sources and pathways of MeHg production and storage in the Arctic terrestrial environment and how melting glaciers (and glacier sediments) and thawing permafrost would contribute to MeHg loading of downstream environments.

The processes that are responsible for the enrichment of MeHg in Arctic subsurface seawater remain unidentified. Methylation and demethylation rates of Hg in Arctic seawater need to be better quantified.

Future work should also aim to confirm the occurrence, or lack thereof, of Hg methylation in Arctic sea ice and/or snow.

What processes are important for biological uptake of methylmercury? [4.4]

12. As we understood previously, bioconcentration of aqueous MeHg in bacteria and algae is a critical step in the transfer of Hg to top predators in freshwater and marine environments. Methylmercury is biomagnified higher up in the food web. Thus, the concentration of Hg in the top of the food web depends on the amounts of MeHg taken up at the bottom of the food web, the length of the food web as well as seasonal dietary changes, migration, and body condition.
13. We have now also learned that sea-ice algae may be an important entry point for MeHg to marine ecosystems.
14. Zooplankton in Arctic lakes can have higher concentrations than those in the marine environment.
15. Recent nitrogen stable isotope measurements specific to Arctic biota have highlighted the importance of variable trophic position in controlling MeHg concentrations among species and among populations of the same species distributed across the circumpolar Arctic.

While some evidence suggests cold, low-productivity ecosystems have higher Hg biomagnification, factors controlling the biomagnification rate of Hg through Arctic food webs needs to be understood more clearly.

The large magnification at the base of the food chain and its connection to DOM is a critical process that needs further study.

How much methylmercury is circulating in the Arctic environment? [4.5]

16. While no estimates of MeHg pools in the environment reservoirs, nor fluxes, were available prior to or in the AMAP 2011 Mercury Assessment, we now have the following estimates, as presented in Table 4.4 and Figure 4.8.
17. Seawater *in situ* Hg methylation is an important feature leading to the high MeHg component (32%) and a net export of MeHg (~5–11 Mg/y) from the Arctic Ocean to the North Atlantic.
18. There is also a net evasion of MeHg to the atmosphere (via the formation and evasion of DMHg) which is higher than the atmospheric deposition of MeHg (photochemically degraded from DMHg).
19. Arctic sediments are a potential source of MeHg to the Arctic marine water column.

Estimated and modeled MeHg budgets and fluxes are based on limited in situ *measurements. Hence, more field measurements are needed to fill important knowledge gaps and complete the total Arctic MeHg budget.*

Given the biogeochemical cycling of Hg in the Arctic environment is sensitive to climate change, its effects on MeHg production and breakdown in the Arctic, including the connection between climate change and changes in DOM discharges, needs further study.

5. How does climate change influence mercury in the Arctic environment and in biota?

Leads: Melissa McKinney and John Chételat

Co-Authors: Marc Amyot, Samantha M. Burke, Ashu Dastoor, Thomas A. Douglas, Kyle Elliott, Kim Fernie, Lars-Eric Heimbürger-Boavida, Magali Houde, Jane Kirk, Kimmo K. Kahilainen, Robert J. Letcher, Adam Morris, Derek Muir, Peter Outridge, Nicolas Pelletier, Heli Routti, Henrik Skov, Kyra St. Pierre, Jussi Vuorenmaa, Feiyue Wang, David Yurkowski

5.1 Introduction

Global climate change is most pronounced in the Arctic, where surface air temperatures have risen at more than twice the rates elsewhere due to Arctic amplification (Serreze and Barry, 2011; Meredith et al., 2019). Arctic warming is also projected to continue to increase faster than the global mean under future scenarios (IPCC, 2013). Given the Arctic's particular sensitivity to global climate change, profound changes have been documented across marine, terrestrial and freshwater ecosystems. The recent Snow, Water, Ice, and Permafrost in the Arctic (SWIPA) assessment concluded that the climate in the Arctic is moving towards a new state, and that although enhanced efforts to control greenhouse gas emissions would reduce further climate-related impacts, the system will not return to earlier conditions during the course of this century (AMAP, 2017a). Physical changes to the Arctic environment are marked: reductions in sea-ice extent and thickness, dramatic loss of multi-year ice, decreased ice-season length, retreating mountain and tidewater glaciers, permafrost thaw and thermokarst development, reduced seasonal snow cover, and increased river runoff and altered nutrient availability (Perovich and Richter-Menge, 2009; Post et al., 2009; Box et al., 2019). In lockstep with these cryospheric changes, extensive ecological changes have been documented: increased marine primary production, reduced population sizes of some ice-dependent species, northward shifts in the ranges of Subarctic and temperate marine and terrestrial species, and altered trophic structuring (Post et al., 2009, 2013; Fossheim et al., 2015; Pecl et al., 2017). The strong seasonality of the Arctic is critical for Arctic ecosystem structure and function; thus, climate change-driven dampening of seasonal variation and the associated reduced ability of species to shift resource use through time are predicted to destabilize the Arctic's seasonally-structured food webs (McMeans et al., 2015b). These physical and ecological changes to Arctic ecosystems are likely to have consequences for the long-term cycling and bioaccumulation of mercury (Stern et al., 2012). Since the last mercury (Hg) assessment by the Arctic Monitoring and Assessment Programme (AMAP) released in 2011, environmental change in the Arctic has continued to accelerate, and a clearer picture is emerging of the profound shifts in the climate and the cryospheric processes (AMAP, 2019b; Box et al., 2019; Saros et al., 2019). The consequent impacts on Hg are now being investigated.

The effects of climate change on Hg cycling in the Arctic are complex and interactive because of potential alterations to multiple processes including Hg transport (St. Pierre et al., 2018; Zdanowicz et al., 2018), transformations such as methylmercury (MeHg) production (MacMillan et al., 2015; Yang et al., 2016), biological uptake of MeHg (Poste et al., 2019; Hudelson et al., 2019), and the transfer of MeHg through food webs (Braune et al., 2014b; McKinney et al., 2017b). Recent indications of climate change vary across the circumpolar Arctic, including regional differences in warming, sea-ice loss, and altered snow cover (AMAP, 2017a). Similarly, climate change is affecting ecological processes on multiple temporal scales and may be environment-specific, from lengthening of the Arctic growing season (Ernakovich et al., 2014) to continued multi-decadal declines of sea-ice and glacier extent (AMAP, 2017a). For example, the loss of multi-year sea ice in the marine environment is having profound ecological effects (Post et al., 2013), and many of those effects are not relevant to Arctic freshwater lakes. As the environmental change that is currently underway in the Arctic may differ across both spatial and temporal scales, consideration of effects specific to marine, freshwater, and terrestrial ecosystems, as well as seasonal, annual, and decadal variation and change, is warranted in an assessment of climate change impacts on Hg cycling.

This chapter presents an assessment of current evidence for climate change influences on Hg in the Arctic environment and in biota. Whereas the science on climate-Hg interactions in the Arctic was largely hypothetical in the 2011 AMAP mercury assessment, substantial new empirical, experimental and modeling evidence has emerged over the last decade. First, a brief summary is provided of what is known about climate change effects on the physical, biogeochemical, and ecological processes within Arctic marine, freshwater, and terrestrial ecosystems (Sections 5.2 and 5.3). Then, the science of connections between physical or ecological changes and the environmental and biological fate of Arctic Hg is integrated by examining effects on Hg transport, biogeochemical transformations of Hg, and Hg exposure in biota (see Figure 5.1). Some aspects of the Hg cycle (such as the fate of dissolved inorganic Hg in aquatic ecosystems, or elemental Hg fluxes between air, water and soil) are not addressed when information on climate change effects was absent. Geographic disparities are also not addressed due to limited information despite probable variation with latitude and among Arctic regions. This chapter draws on climate-related temporal trends of Hg bioaccumulation that were analyzed in Chapter 2, as well as the synthesis of processes affecting Arctic environmental Hg in Chapters 3 and 4. Finally, conclusions and recommendations for future evaluation of climate change impacts on Hg processes in the Arctic are provided.

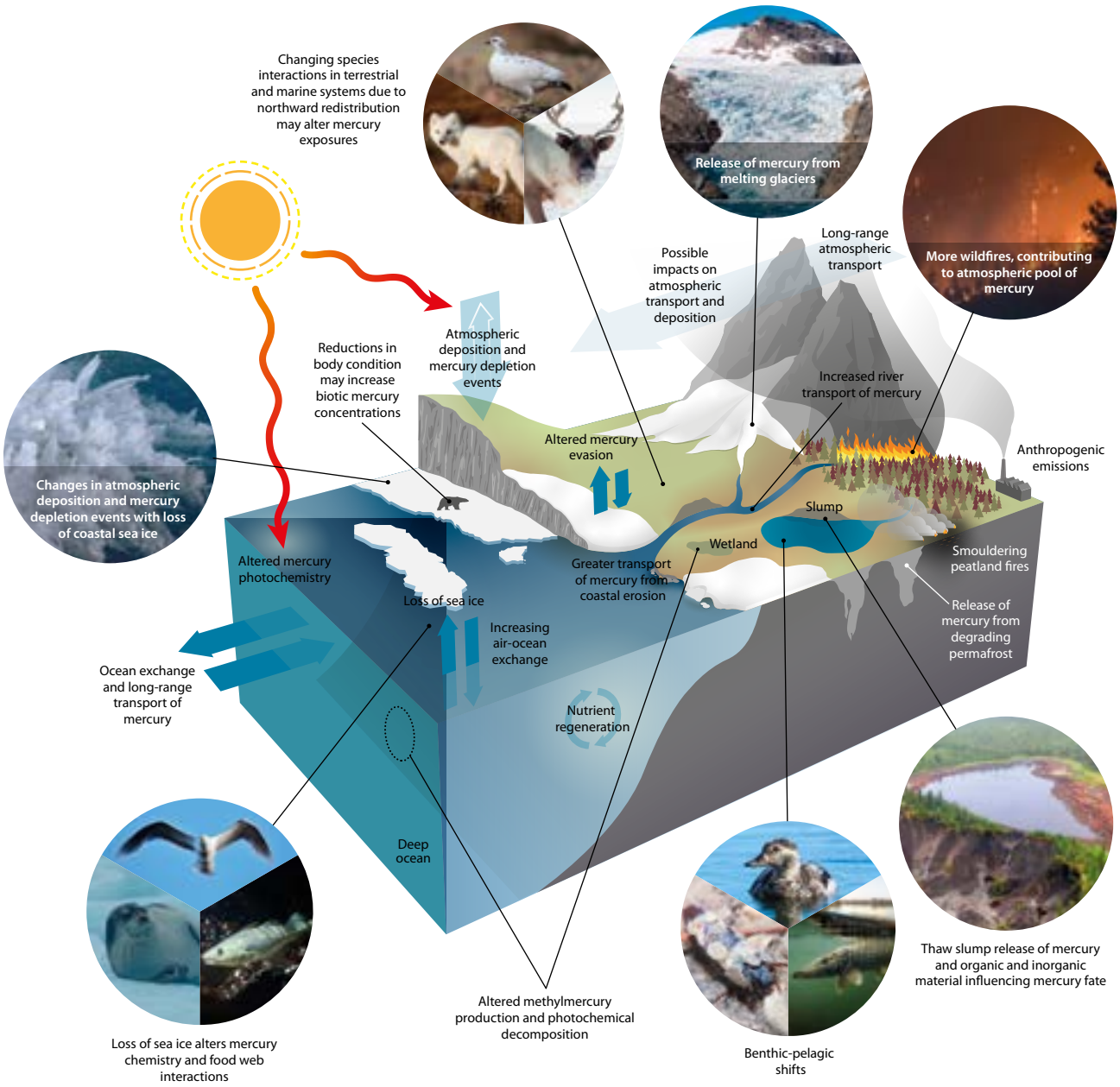

Figure 5.1 Conceptual diagram highlighting key physical and ecological changes occurring in the Arctic and links to the environmental and biological fate of Hg.

5.2 How has climate change affected the physical and biogeochemical characteristics of Arctic environments?

5.2.1 Atmosphere

Warmer air temperature is arguably the greatest agent of change for physical and biogeochemical disturbances in the Arctic. Recent climate warming is likely more than two times greater in the Arctic than at lower latitudes (Serreze and Barry, 2011; Meredith et al., 2019). The enhanced susceptibility to warming in this region is referred to as Arctic amplification, a phenomenon thought to largely be due to positive feedback with sea-ice loss (see Figure 5.2); decreased ice cover means more open water, which better absorbs solar radiation, which in turn leads to higher water temperatures and further reductions in ice cover (Screen and Simmonds, 2010; Serreze and Barry, 2011; Pistone et al., 2014). Air temperature increases are reflected in annual averages for the Arctic, seasonal temperatures (particularly in winter), and extreme warm temperatures (Meredith et al., 2019). Total annual precipitation is also increasing, such as in coastal Greenland where meteorological observations are available for the period since 1890 (Mernild et al., 2015) and more broadly across the Arctic in recent decades (Box et al., 2019). Currently, much of the Arctic's annual precipitation falls as snow, which is released from terrestrial environments during spring melt. Climate modeling projects a long-term shift towards precipitation predominantly in the form of rain instead of snow during the 21st century (Bintanja and Andry, 2017). Extreme events are occurring more frequently, such as freezing rain and rain-on-snow events due to warmer temperatures in autumn and winter (Liston and Hiemstra, 2011; Hartmann et al., 2013; IPCC, 2013; Hansen et al., 2014; AMAP, 2017a). A northward shift in storm

tracks in the North Atlantic may be occurring (Collins et al., 2013). Other changes to the Arctic atmosphere include shifts in air pressure at sea level, aerosol optical properties, and wind speeds (IPCC, 2013). Furthermore, there are regional disparities in recent atmospheric climate trends observed across the Arctic (AMAP, 2017a). These broad changes to the atmospheric environment may have implications for long-range transport of Hg to the Arctic and exchange with marine and terrestrial environments.

5.2.2 Terrestrial environments

Arctic amplification of global climate warming is leading to profound physical changes in Arctic terrestrial environments. Of particular relevance to Arctic terrestrial Hg processes are a longer summer growing season (Tagesson et al., 2012), changing precipitation patterns with an increase in summer-wet precipitation (Zhang et al., 2013; Bintanja and Andry, 2017), altered seasonality (Vihma, 2014), and increasing instability of the cryosphere, particularly permafrost thaw (AMAP, 2017a, 2019b). The major seasonal transitions (fall to winter and spring melt) have shifted two to three weeks into the winter season. This means spring melt runoff, the largest hydrologic event in many Arctic locations, is occurring earlier. In addition, there are an increasing number of days without snow cover and with soil and vegetation above freezing temperatures (growing degree days).

For soil and terrestrial environments, the largest change in the Arctic attributable to rising temperatures is an increase in permafrost thaw degradation and the melting of land ice (Liljedahl et al., 2016). Permafrost is warming around the circumpolar Arctic (Biskaborn et al., 2019), which is leading to the formation of thermokarst features on the landscape such as sinkholes and thermokarst lakes (AMAP, 2017a). For example, Lewkowicz and Way (2019) found, using satellite imagery, a 60-fold increase in retrogressive thaw slumps (large catastrophic thaw features) on Banks Island (Northwest Territories, Canada) between 1984 and 2015. The destabilization and slumping of permafrost is releasing sediment to downstream lakes and waterways as well as to the Arctic Ocean from coastal erosion (Lantuit and Pollard, 2008; Kokelj et al., 2015; Lewkowicz and Way, 2019). Thermokarst responses to climate warming are not uniform, however, and vary regionally within the circumpolar Arctic in relation to local landscape factors (AMAP, 2017a; Loranty et al., 2018).

The greatest stores of land ice (e.g., glaciers, ice sheets, ice caps, ice fields) are in Greenland, the Russian Arctic, the northern Canadian Arctic, and Alaska, and all regions are losing ice mass at an accelerating rate due to anthropogenic climate warming (AMAP, 2017a, 2019b; Box et al., 2019). Melting Arctic land ice is contributing to sea-level rise, and transporting nutrients, particulates and contaminants to downstream freshwater and marine environments (Søndergaard et al., 2015; Zdanowicz et al., 2018). Together, these large-scale changes in the terrestrial cryosphere have important implications for Hg cycling and transport in the Arctic.

Wildfire has always been a critical process in the life cycle of boreal forests while tundra ecosystems, particularly in the High Arctic, have traditionally been characterized by low wildfire occurrence because of low temperatures, short snow-free seasons, and a lack of flammable biomass (Wein, 1976; Hu et al., 2015). Wildfires within the Arctic tundra biome, though, will become increasingly common during the summer and early fall, especially within the Arctic forest tundra (French et al., 2015). Lake sediment charcoal records reveal that wildfires used to occur only in the driest and warmest regions of the tundra, such as in Western Alaska and Northeastern Siberia. Since 2007, however, some fires have begun to occur in areas where fires have been absent for the last 6500 to 35 000 years (Chipman et al., 2015). The susceptibility of tundra ecosystems to fire largely depends on the crossing of certain temperature and precipitation thresholds predicted to occur more often with climate change (Hu et al., 2015; Young et al., 2017). In Alaska, for example, by 2100, the average annual area of burned tundra is projected to double (Hu et al., 2015), the probability of fire in a 30-year window is projected to increase four-fold (Young et al., 2017), and the probability of extreme fire seasons are projected to increase by 13% to 23% relative to the period 1950 to 2009 (Hu et al., 2015). Climate change also has the potential to exacerbate the likelihood and intensity of wildfires on the tundra by impacting vegetation cover, lightning activity, fire-season length and watershed connectivity (Smith et al., 2005; Riordan et al., 2006; Hu et al., 2015; Coogan et al., 2019). A decrease in sea-ice extent and the resultant changes in precipitation patterns could also influence wildfire activity in some areas of the tundra (Hu et al., 2010, 2015). These climate-driven changes in the terrestrial environment may have complex effects on Hg cycling and transport to downstream environments.

5.2.3 Freshwater environments

Changes to the hydrological cycle in response to Arctic warming have had important implications for the number of lakes and ponds dotting Arctic tundra landscapes. While new lakes and ponds may be forming downstream of retreating glaciers (Stokes et al., 2007; Milner et al., 2017), increasing evaporation and thermokarst development have led to dramatic reductions in the number and surface area of lakes and ponds in non-glacierized regions (Carroll et al., 2011; Finger Higgens et al., 2019). Watershed geomorphology can play a role in recent shrinking and expanding of water surface area, which may be regional in nature within the Arctic (Carroll and Laboda, 2018). Water surface area has increased in parts of Alaska with warming lowland permafrost (Pastick et al., 2019), while it has decreased in lakes of the Northwest Territories that are situated on bedrock and likely isolated from groundwater (Carroll and Laboda, 2018).

In the Arctic, ice up to two meters thick can cover lakes for as much as ten months of the year and is a critical feature regulating the physics, chemistry and biology of these ecosystems. During winter, microbial metabolism can result in the build-up of gases such as methane under ice (AMAP, 2017a). With warming, lake-ice melt has been happening earlier in the summer (Surdu et al., 2016), and the onset of lake-ice formation has been delayed (Lehnherr et al., 2018), trends which are predicted to continue in the future (Brown and Duguay, 2011). These shifts in ice phenology have occurred in concert with the warming of surface waters during the summer months (O'Reilly et al., 2015). The loss of lake ice has the potential to increase the seasonal light

regime in the water column, as well as atmospheric deposition to surface waters, with implications for biological productivity, carbon processing (Cory et al., 2014) and contaminant cycling (Outridge et al., 2007).

Many Arctic lakes remain well-mixed or weakly stratified during the open-water season (Vincent et al., 2008; Priet-Mahéo et al., 2019). With rising temperatures, warmer waters and a longer ice-free period, thermal stratification patterns in lakes are expected to change by strengthening the temperature gradient in the water column and lengthening the stratification period (Prowse et al., 2006; Gebre et al., 2014). Little information is available, however, on the extent to which thermal stratification patterns are changing in Arctic lakes, likely because few long-term, high-frequency measurements are available for lake water columns. Recent studies in Greenland indicate that lake warming and the processes that affect water transparency are likely to affect lake stratification (Saros et al., 2016; Cadieux et al., 2017). These shifts in water-column mixing are important because thermal stratification has a major influence on the biogeochemistry of lakes.

Warmer temperatures and shifting precipitation patterns are contributing to altered hydrology of Arctic catchments, including streamflow, hydrological connectivity, and water storage (Bring et al., 2016). In the western Canadian Arctic, the timing of stream discharge is changing, with greater flow in winter (Déry et al., 2009; Spence et al., 2014) and this greater winter flow is affecting the water concentrations and catchment export of solutes (Spence et al., 2015). The discharge of large Arctic rivers has also been increasing in recent decades in North America and Eurasia (Box et al., 2019) due to complex processes, though ultimately from greater delivery of atmospheric moisture (Bring et al., 2016). Increasing baseflows in Arctic rivers may also be related to permafrost thaw and associated changes to groundwater storage and/or circulation (Evans et al., 2020a, 2020b). These shifts in the water cycle are significant for Hg cycling given the critical role of streams and rivers in the transport of organic matter and Hg within the Arctic.

Increased leaching of dissolved organic matter (DOM) from terrestrial catchments to rivers and lakes, often estimated by dissolved organic carbon (DOC) concentrations, has been detected from boreal to Arctic regions (Monteith et al., 2007; Garmo et al., 2014, de Wit et al., 2016; Räike et al., 2016; Wauthy et al., 2018), resulting in widespread coloring of lake and river waters with chromophoric DOM (a process termed 'browning'). A trend assessment from almost 500 lakes, rivers and streams in Norway, Sweden and Finland showed the largest trends in boreal regions. Significant long-term increases in DOC concentrations were also common in Subarctic freshwaters (de Wit et al., 2016). Browning in the 1990s and early 2000s has been attributed mainly to improved air chemistry (i.e., substantially decreased acid sulphate deposition and variations in sea-salt deposition), acting through chemically-controlled organic matter solubility in catchment soils (de Wit et al., 2007; Monteith et al., 2007; Evans et al., 2012; Oulehle et al., 2013; Valinia et al., 2015).

Recently, changes in climatic conditions, such as increased precipitation and discharge, are exerting a greater influence on varied and increasing DOC concentrations in surface waters (Räike et al., 2012; de Wit et al., 2016; Zwart et al., 2017). Increased vegetation from greening of catchments, intensive land use (e.g., forestry activity and peat mining) and elevated runoff will jointly increase DOC in Subarctic Fennoscandian watercourses (Finstad et al., 2016; Räike et al., 2016). In addition to the direct effect of changes in hydrological regimes, climate change has been observed to brown lakes in Arctic and Subarctic regions through the thawing of permafrost and deepening of the soil active layer, introducing more DOM to freshwaters (Vonk et al., 2015a; Wauthy et al., 2018) and increasing organic carbon (OC) export in large Arctic rivers (Mu et al., 2019). On the other hand, declining concentrations of DOC throughout the 2000s have been observed in Arctic lakes in Greenland, but this decline is related to drivers other than changing air temperature or discharge (Saros et al., 2015). Increasing lake-water sulfate concentrations across the area suggest that increases in soil ionic strength as a result of deposition-derived sulfate enrichment, acting through chemically-controlled organic matter solubility in catchment soils, may be linked to declining surface water DOC concentrations. Nevertheless, many studies have addressed various aspects of DOM in Arctic rivers and lakes (Cory et al., 2014; O'Donnell et al., 2016; Kaiser et al., 2017; Osburn et al., 2017; Jiang et al., 2020), reporting that DOM derived from terrestrial environments is abundant and widely distributed in Arctic surface waters, and the quality of this terrestrial DOM is highly different compared to DOM produced within the lakes. Thermokarst lakes and ponds (created by erosion and collapse of ice-rich permafrost) represent some of the most abundant freshwater lakes in the Arctic (Grosse et al., 2013; Vonk et al., 2015a). In such lakes, DOM is predominantly from old terrestrial sources. This material generally provides a lower quality resource for consumers than newer algal-derived carbon (Forsstrom et al. 2013; Wauthy et al., 2018). Climate-driven changes to carbon cycling have important implications for particulate-sorbed Hg, photochemical processes and river export.

5.2.4 Marine environments

Sea-ice loss in the marine environment, as documented by satellite records over the past four decades, has been identified as one of the most striking indications of climate change on a global basis (Meredith et al., 2019). There is much interannual variability in sea-ice extent, but an overall declining trend has been found and is projected to continue (Figure 5.2). Declines in extent are significant in all months of the year and estimated at -0.4 and -0.8 million km^2 per decade in winter (March 1979–2019) and summer (September 1979–2018), with some evidence of small recent accelerations in ice loss (Meredith et al., 2019). The declines are also found across nearly all regions but show regional variability in magnitude, with the Beaufort and Chukchi seas showing the greatest reductions (AMAP, 2017a). The Arctic Ocean is expected to become seasonally ice free in the coming decades, with some estimates suggesting as early as the next decade (2030s; Wang and Overland, 2012; AMAP, 2017a).

In addition to changes in sea-ice extent, there have also been changes in sea-ice thickness, multi-year ice, ice timing, distribution, mobility, and snow depth over the ice. Sea-ice thickness and volume over the Arctic basin have declined by

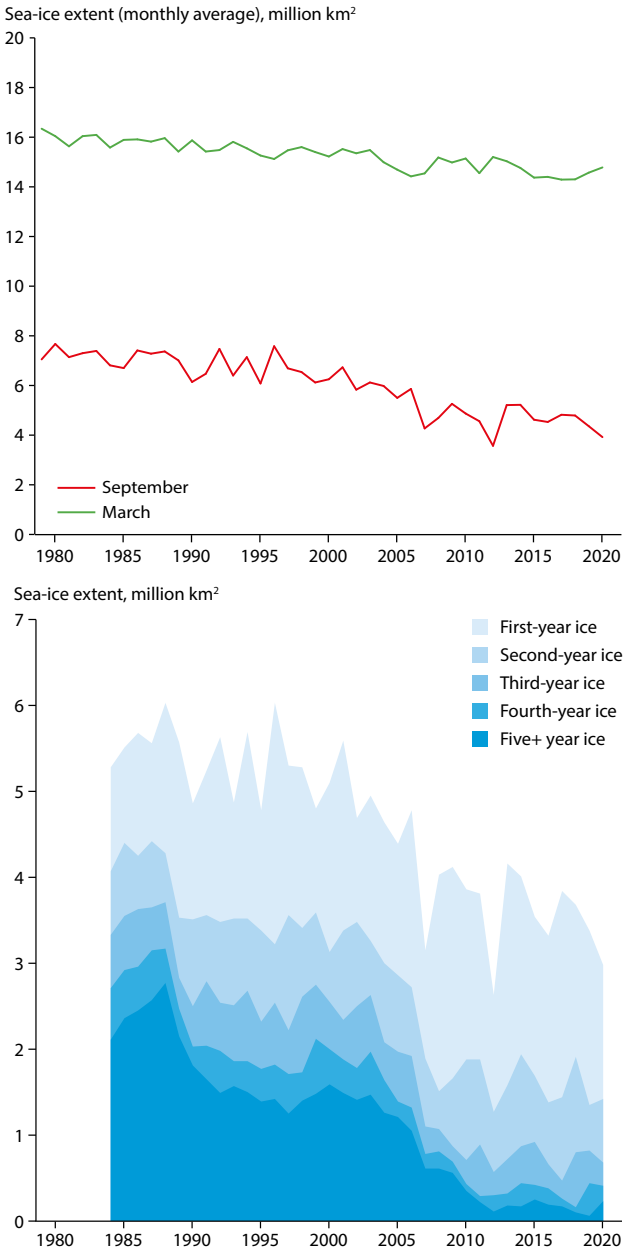

Figure 5.2 Multi-decadal decline in Arctic Ocean sea-ice extent (upper), and change in sea-ice age in period of minimum extent (lower). Source: adapted from National Snow and Ice Data Center, 2020.

two-thirds from the 1980s to the 2010s (Overland and Wang, 2013; Lindsay and Schweiger, 2015). After 2005, Arctic sea ice switched from predominantly multi-year cover to coverage dominated by annual ice (AMAP, 2017a; see Figure 5.2). The ice-covered season is now one to three months shorter than in the 1970s, with earlier melt onset and later freeze-up (Barber et al., 2015; AMAP, 2017a). The drift speed of sea ice has increased by around 10% per decade, which is related to a weaker ice pack being more susceptible to increases in wind speeds (1% to 2% per decade; Vihma et al., 2012). Likely due to later formation of sea ice in the fall, snow depth on the sea ice has shown consistent declines (Webster et al., 2014), with possible connections to rising proportions of first-year ice.

Shifts in the marine environment have been recorded related to ocean temperatures and circulation, freshwater river flux input, sea levels, and ocean acidification. Along with warming surface air temperatures in the Arctic, sea-surface temperatures have generally increased (Barents, Chukchi, Kara, East Siberian, and Laptev seas; Timmermans and Proshutinsky, 2014; Lind et al., 2018) and so have water temperatures at lower depths, due to warmer waters entering from the North Atlantic and North Pacific (AMAP, 2017a; Lind et al., 2018). Increased river discharge and melting glaciers have led to a 50% increase in freshwater flux in less than two decades off South Greenland (Bamber et al., 2012), and a related increase in icebergs recorded, for example, off the coast of Newfoundland, Canada (Bigg et al., 2014). Because salinity is an important driver of ocean currents, this increased freshwater flux has been suggested to have played a role in recently observed reductions in the Atlantic Meridional Overturning Circulation (Rahmstorf et al., 2015). Globally, sea levels have risen by 20 cm or more since 1900 (AMAP, 2017a). The Arctic is a main player in sea-level rise, with the melting of Arctic glaciers and ice caps contributing to more than one-third of the global increase in sea levels (AMAP, 2017a). As elsewhere, changing sea levels in the Arctic have led to coastal erosion and the associated destruction of sea-side homes and infrastructure in Northern communities. Nonetheless, some local sea levels have actually experienced a net decline in Arctic regions proximate to large ice-mass loss due to crustal rebound (Cazenave and Llovel, 2010). As elsewhere, due to climate change, the Arctic Ocean is taking up more carbon dioxide from the air, forming the weak acid carbonic acid and increasing hydrogen ions, thereby decreasing the pH of the Arctic Ocean. This process also consumes carbonate ions, which are needed by calciferous organisms. These processes are called ocean acidification. The Arctic Ocean is more sensitive to acidification than other oceans due to higher gas solubility at low temperatures, more freshwater inputs, Pacific Ocean contributions of low pH waters, and enhanced uptake of carbon dioxide aided by melting sea ice (AMAP, 2018b). Significant declines in pH have been reported in the Canadian Basin in the period from 1997 to 2008 and in the Nordic seas in the period from 1985 to 2009 (AMAP, 2018b).

5.3 How has climate change affected Arctic ecosystems?

5.3.1 Terrestrial ecosystems

The Arctic tundra biome comprises about 5% of the Earth's terrestrial surface, and the majority of it is located in coastal areas within 100 km of seas seasonally covered by ice (Ims et al., 2013). The longevity of sea ice may thus have a strong influence on temperature and climate and consequently on the productivity of Arctic tundra ecosystems (Bhatt et al., 2010). Terrestrial Arctic ecosystems are characterized by low primary productivity, which restricts the length and complexity of food webs and decomposer webs (Ims et al., 2013).

Ecological responses of Arctic terrestrial ecosystems to climate change show generally large variation among regions, which is related to a large spatial variation in climate change itself (Ims et al., 2013). Most research has focused on the effects of climate change on one trophic level in isolation, either plants or herbivorous mammals. The Arctic tundra vegetation is

'greening' along with increasing land surface temperature (Jenkins et al., 2020). Both monitoring and experimental studies in the circumpolar Arctic suggest that both grass and grass-like plants and shrubs have responded positively to warming and that their abundance is likely to increase over time (Elmendorf et al., 2012; Bjorkman et al., 2020). Although some studies showed earlier leaf emergence and flowering with rising temperatures, there have not been consistent responses observed in plant flowering or leaf emergence or senescence (Bjorkman et al., 2020). A warming climate in the Arctic accelerates the microbial decomposition of soil organic matter, and this process is enhanced by the increasing presence of plant roots (Schuur et al., 2015; Keuper et al., 2020). Lemmings are key herbivores of Arctic tundra ecosystems due to their important role in transferring energy from plants to mammalian and avian predators (Gilg et al., 2003). Although climate warming has been documented to negatively affect lemming populations in the Low Arctic, which co-occur with boreal voles, there is no consistent global declining trend for lemmings in the Arctic (Ehrich et al., 2020). Reindeer and caribou (*Rangifer tarandus* and its subspecies) are the most abundant large herbivores of Arctic terrestrial ecosystems. Their large range from woodlands to the High Arctic indicates they are able to cope with differing environmental conditions, which is also a possible source of resilience to climate change. Overall, studies focusing on the effects of climate change on reindeer and caribou suggest that the responses vary across their circumpolar distribution (Mallory and Boyce, 2017). Contrasting responses may also occur at local scales resulting in diverging population trends (Hansen et al., 2019b). Warm spells and rain-on-snow events that entirely encapsulate short-growing vegetation across large areas of High Arctic tundra are occurring more frequently in the High Arctic (Bintanja and Andry, 2017; Peeters et al., 2019). These events have been shown to negatively affect reproduction and survival of High Arctic tundra herbivores and to have further consequences on the abundance of Arctic carnivores (Hansen et al., 2013). However, the effects of higher summer temperatures are also variable to different populations of reindeer. Net effects of climate change were negative for a coastal population of Svalbard reindeeer (*Rangifer tarandus platyrhynchus*), but positive for a continental reindeer population (Hansen et al., 2019b). Also, behavioral changes and use of alternative landscapes and food resources may provide a buffer for the effects of environmental change (Loe et al., 2016; Hansen et al., 2019a). For example, the proportion of Svalbard reindeer feeding along the shoreline, partly on kelp, has increased during icier winters (Hansen et al., 2019a). Relatively large changes have been observed in tundra bird populations. Opposing trends have been observed for waders and waterfowl across the circumpolar Arctic: over half of wader taxa are declining and almost half of all waterfowl are increasing (Smith et al., 2020). Peregrine falcon (*Falco peregrinus*) and gyrfalcon (*Falco rusticolus*) populations are generally stable (Franke et al., 2020) whereas ptarmigan (*Lagopus muta and Lagopus lagopus*) population trends vary regionally (Fuglei et al., 2020).

Several studies have shown boreal species are increasingly present in the Arctic tundra. Range expansion of moose (*Alces alces*) and several boreal and Subarctic birds in the Arctic tundra has been related to longer growing seasons and increasing shrub habitat (Sokolov et al., 2012; Tape et al., 2016), whereas both climate-related changes in tundra stream habitat and population recovery after overhunting may have led to beaver (*Castor canadensis*) colonization of the Arctic tundra (Tape et al., 2018). Increased abundance of red foxes (*Vulpes vulpes*) and hooded crows (*Corvus cornix*) was related to high mortality of domestic reindeer following icing of the snow layer in Yamal, Russia (Sokolov et al., 2016), but red fox expansion into the Canadian Arctic has been explained by increased human activity (Gallant et al., 2020).

Climate change has also been documented to affect the structure and functioning of Arctic terrestrial food webs. A study on seven Arctic terrestrial food webs indicated that these food webs are more complex and diverse and have stronger predation of small herbivores in warmer locations compared to colder locations (Legagneux et al., 2014). A study from the Canadian High Arctic (Juhasz et al., 2020) showed that reproduction of snow geese (*Anser caerulescens*) increased with increasing precipitation and temperature, whereas lemmings were not affected by local or regional climate. Arctic fox (*Vulpes lagopus*) breeding success was also positively related to reproduction of snow geese. Harsher winter conditions decreased Arctic fox breeding success, likely through effects on body condition and stress. Hansen et al. (2013) demonstrated that extreme rain-on-snow events synchronized fluctuations of herbivore populations in Svalbard including Svalbard reindeer, Svalbard rock ptarmigan (*Lagopus muta hyperborea*) and sibling vole (*Microtus levis*), as well as their shared predator/scavenger, the Arctic fox.

5.3.2 Freshwater ecosystems

Some of the major impacts of climate change in Arctic regions are related to strong increases in temperature and productivity of both terrestrial catchments and aquatic ecosystems (de Wit et al., 2016; AMAP, 2017a). These increases have ubiquitous effects across ecosystems, communities, populations and individuals (e.g., Post et al., 2009; Scheffers et al., 2016; Rolls et al., 2017). Glacier melting will increase concentrations and seasonal exposure of suspended solids, with pronounced effects: reduced light penetration, lowered temperature and increased conductivity (Lento et al., 2019). At the broad level, permafrost thaw and increasing rain will bring more nutrients, carbon and catchment-stored Hg into lakes and rivers (de Wit et al., 2016; AMAP, 2017a; Schuster et al., 2018; Lento et al., 2019). In lakes and streams, an increased amount of terrestrial vegetation in catchments will elevate DOC in water with shading effects that limit benthic algal production (Forsström et al., 2013). Small and shallow lakes are reacting to changes much faster than more resilient large and deep lakes, which have thermal refuges and volumetric buffering against abrupt changes to alternative states (Scheffer and Carpenter, 2003; Hayden et al., 2019).

Climate warming will enhance the range expansion of new species adapted to warmer temperatures (Post et al., 2009; Rolls et al., 2017). Such effects can be very fast in taxa with high dispersal abilities via wind and waterbirds (e.g., plankton, benthic invertebrates, macrophytes), but dispersal of fish requires connectivity of watercourses or salt tolerance when colonizing Arctic islands (Laske et al., 2022; Lau et al., 2020). New colonizers often initially increase the links in food webs but may also have

strong competitive and predatory interactions with native fauna with potential alterations of energy and Hg flows in food webs (Thomas et al., 2016; Rolls et al., 2017; Barst et al., 2020).

5.3.3 Marine ecosystems

The Arctic Ocean and related water bodies make up about 4% of the Earth's surface. Arctic marine ecosystems are characterized by low primary productivity over much of the year when seas are covered by ice with a pulse in productivity in surface waters associated with sea-ice melt in the late spring. Many taxa in Arctic marine ecosystems are pagophilic (ice-loving) and require ice for at least part of the year (Post et al., 2013). A variety of physical changes impacting oceans worldwide, including increasing temperature, changing acidity and altered freshwater inputs, are also occurring in the Arctic (see Section 5.2.4); but, because of the importance of pagophilic species, responses to ice, unique to polar seas, often overwhelm other ecosystem changes (Post et al., 2013; Harwood et al., 2015). Shifts in Arctic marine ecosystems in response to a changing climate will ultimately be responses to changes in physical processes listed in Section 5.2.4. However, responses can be compounded by the emergent processes occurring in complex food webs (i.e., trophic cascades and food web topologies; Zarnetske et al., 2012). Thus, responses to climate change include both direct responses (thermal or acidity tolerance) and indirect responses (top-down, bottom-up and horizontal processes).

Perhaps the greatest direct impact of climate change on marine species is loss of ice. Reduced ice is increasing solar radiation and nutrient replenishment, leading to increases in primary production in the Arctic Ocean, with impacts on biogeochemical cycling as well as higher trophic position marine consumers (Tremblay et al., 2012). Pagophilic species themselves require ice to survive, and ice loss can have an impact on their population growth rates. For example, polar bears (*Ursus maritimus*) require ice to efficiently capture their preferred prey, ringed seal (*Pusa hispida*) pups. Similarly, under-ice algae require ice as a substrate to grow, and under-ice algae is at the base of many Arctic food webs (Kohlbach et al., 2016, 2017). Sea acidification can also directly impact species, especially calciferous benthic fauna (Walther et al., 2011). Finally, many cold-adapted Arctic animals may be unable to tolerate warmer waters. For example, Arctic cod (*Boreogadus saida*) do not reproduce effectively in waters above about 4°C (Drost et al., 2014; Steiner et al., 2019). Similarly, thick-billed murres (*Uria lomvia*) experience stress at temperatures that are mundane for their more southerly congeners, with many dying from overheating in warm summers (Gaston and Elliott, 2013). Thus, a warmer, more acidic, ice-free ocean may shift the range of many Arctic species northwards.

Changes in prey populations, or seasonal timing in their availability or accessibility, can lead to complex bottom-up trophic surges or temporal mismatches. For example, lack of under-ice algae, a preferred food of copepods, can lead to reduced populations of Arctic cod and consequently top predators that prefer cod (Gaston et al., 2005; Yurkowski et al., 2017, 2018). Indeed, reductions in accessible, sympagic Arctic cod are a common theme across the Arctic with reductions in Arctic cod in the diet of many marine predators; the cod may still be there but may be difficult to detect if they are not associated with readily visible ice (Gaston et al., 2005; Gaston and Elliott, 2014; Divoky et al., 2015, 2016). The match-mismatch hypothesis is a classic mechanism for bottom-up regulation associated with climate change (Thomas et al., 2004). Marine ectotherms can respond rapidly to changes in temperature and phytoplankton availability (Grémillet et al., 2015; Amélineau et al., 2019). Marine endotherms, such as seabirds and marine mammals, often respond in a more complex fashion to a hormonal pathway closely tied to photoperiod. Thus, although the timing of ice-off has advanced by over a month in Hudson Bay, the timing of the breeding of seabirds has only advanced by a few days. As a consequence, seabirds are nourishing their offspring after Arctic cod, their preferred prey, is no longer accessible, leading to smaller chicks (Gaston et al., 2005; Gaston and Elliott, 2014; Divoky et al., 2015, 2016; Figure 5.3). Presumably these changes are also happening in other taxa that are more difficult to directly monitor.

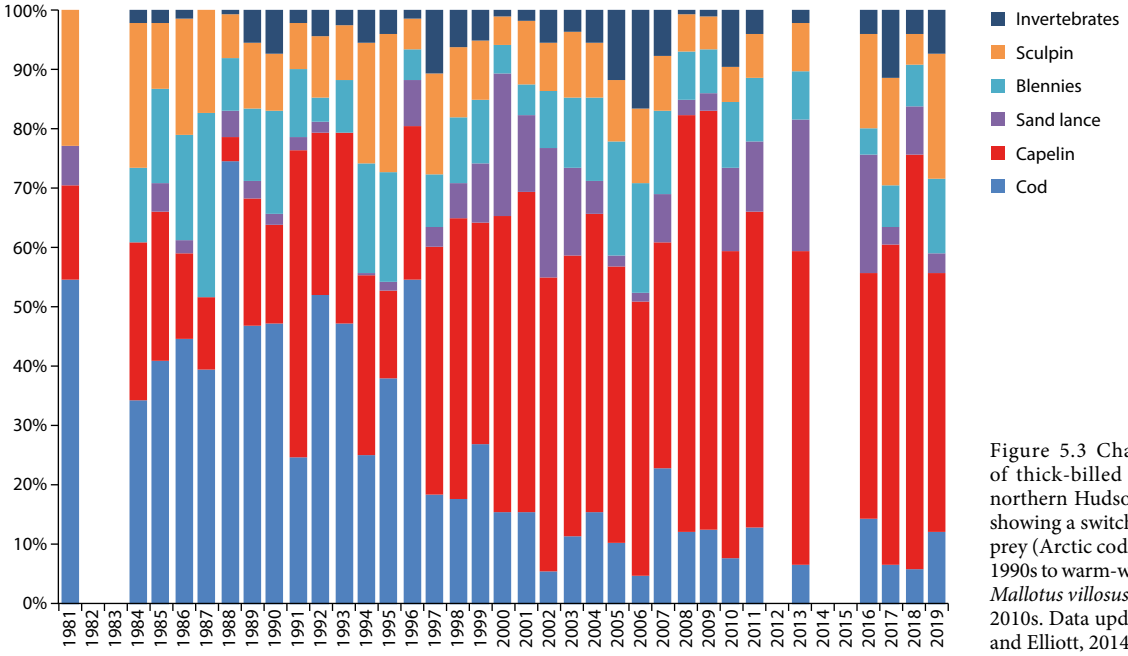

Figure 5.3 Change in the diet of thick-billed murre chicks in northern Hudson Bay since 1981 showing a switch from cold-water prey (Arctic cod) in the 1980s and 1990s to warm-water prey (capelin; *Mallotus villosus*) in the 2000s and 2010s. Data updated from Gaston and Elliott, 2014.

In contrast to bottom-up regulation, top-down regulation occurs when predators or parasites cause changes in prey populations. Examples of top-down regulation include: (1) the punctuated arrival of killer whales (*Orcinus orca*) in the Arctic during longer ice-free summers, with potential impacts on beluga (*Delphinapterus leucas*), narwhal (*Monodon monoceros*), and bowhead whale (*Balaena mysticetus*) populations (Higdon and Ferguson, 2009; Matthews et al., 2020) and (2) increased polar bear predation on terrestrial animals during the ice-free period. In the latter case, because the ice-free period now overlaps to a greater degree with seabird breeding, hungry polar bears in some regions are switching to feed on bird eggs (e.g., those of the thick-billed murre and black guillemot; *Cepphus grylle mandtii*) occasionally even eating adults (Gaston and Elliott, 2013; Divoky et al., 2015; Harwood et al., 2015). In some cases, polar bears eat tens of thousands of eggs, causing colony declines and dispersion into smaller colonies (Gaston and Elliott, 2013; Iverson et al., 2014; Prop et al., 2015). Polar bears spending an extended period of time onshore in other regions are consuming onshore remains of subsistence-harvested bowhead whales (*Balaena mysticetus*; Atwood et al., 2016; McKinney et al., 2017a), and in other regions have shown long-term shifts towards greater consumption of Subarctic seals (McKinney et al., 2013). Parasites can also cause top-down regulation, and warm summers in recent years have increased black flies and mosquitoes in some regions, leading to reproductive failure by birds (Gaston and Elliott, 2013; Franke et al., 2016). Thus, top-down effects from both predators and parasites are having strong impacts on Arctic marine ecosystems.

The various impacts have led to changes in species distributions, one of the most widely documented impacts of climate change on ecosystems (Post et al., 2009; Wassmann et al., 2011; Pecl et al., 2017). Reduced sea ice, increased water temperature and faster ocean current velocities are resulting in shifts in the northern boundary of many marine species, from phytoplankton (Oziel et al., 2020) to the oceans' top predator, the killer whale (Higdon and Ferguson, 2009; Bourque et al., 2018). Arctic species are moving northward with the retreating marginal ice zone and/or with their range-shifting prey, while boreal species are now present in the Arctic and for longer periods each year. This 'borealization' (i.e., Fossheim et al., 2015) of the Arctic marine environment in the European Arctic is referred to as Atlantification, while in the western North American Arctic it is referred to as Pacification. Sometimes such distributions include southerly invasive species moving north and outcompeting Arctic species. For example, razorbills (*Alca torda*) have moved into Hudson Bay following increased numbers of sand lance (*Ammodytes* sp.), leading to potential competition with native seabirds (Gaston and Woo, 2008). Increasingly, ecosystems are changing from benthic towards pelagic species, with energy flows becoming more pelagic (Grebmeier et al., 2006; Fossheim et al., 2015) as a longer ice-free period opens pelagic ecosystems. Ultimately, the result will be community compositions that have not previously existed (i.e., 'no-analog' communities; Williams et al., 2007; Zarnetske et al., 2012), with repercussions for biodiversity across levels of organization. Such alterations in food-web links and lengths will impact the movement of energy as well as contaminants but will likely vary among regions (Bartley et al., 2019).

5.4 What influence has climate change had on mercury transport processes?

5.4.1 Atmospheric deposition

The concentrations of gaseous elemental mercury (GEM) in the atmosphere are controlled by emission source strength (primary anthropogenic, natural emissions and re-emissions, as well as secondary legacy emissions), atmospheric relaxation time, transport and the final fate of Hg moving into terrestrial and aquatic reservoirs (Skov et al., 2020; see Sections 3.3 and 4.3.1). Atmospheric relaxation time is the net effect of all removal and formation reactions of GEM, and it represents the time needed before a change, such as to emissions, affects the atmospheric concentration of GEM. All of these processes (to a lesser extent anthropogenic emissions) have a climate component that might affect future Hg dynamics. The transport from mid-latitude regions is dependent on the position of the major weather systems, which is predicted to change with changing climate (IPCC, 2019). The relaxation time of atmospheric Hg is dependent on the oxidation rate of GEM to gaseous oxidized mercury (GOM) and particulate-bound mercury (PBM), as GOM and PBM are fast removed by either wet or dry deposition. The final fate of Hg is also dependent on the reduction of oxidized Hg (e.g., in the water column) back to elemental Hg (Skov et al., 2020). The reaction kinetics of Hg(0) in the atmosphere are temperature dependent (Goodsite et al., 2004, 2012; Donohoue et al., 2006; Jiao and Dibble, 2015), whereby oxidation decreases with increasing temperature, and thus GOM and PBM formation is expected to decrease in a future warmer climate. The deposition is dependent on the stability of the atmosphere, wind speed, and surface properties (Skov et al., 2006); thus, the Hg distribution between atmosphere and land surfaces is climate-dependent. However, the direction of this change is uncertain as reactions with bromine will be affected by the release of bromine from refreezing leads, snowpack or from marine aerosols, resulting in slower oxidation of Hg(0) in the atmosphere (Goodsite et al., 2004, 2012; Donohue et al., 2006; Dibble et al., 2012; Jiao and Dibble, 2015). However, deposition will be faster as the aerodynamic resistance is higher over vegetation and open waters than over snow and ice. Nonetheless, the concurrent impacts of changes in climate, chemical composition, land use and primary and secondary Hg emissions on Hg temporal trends make it difficult to detect the influence of changes in anthropogenic emissions in observed temporal trends. Despite increases in global anthropogenic emissions over the past several decades (Streets et al., 2011), Arctic atmospheric Hg levels have decreased or remained constant (Cole and Steffen, 2010; Berg et al., 2013; Cole et al., 2013). Implications of climate change-related factors, such as rising air temperatures (particularly in spring) and reduced sea-ice extent and thickness on Hg levels in Arctic ecosystems, are complex and multidirectional (Bekryaev et al., 2010; Cavalieri and Parkinson., 2012; Stern et al., 2012).

Fisher et al. (2013) investigated the factors controlling Hg(0) trends in the Arctic from 1979 to 2008 using the global historical anthropogenic emissions inventory of Streets et al. (2011) which used the GEOS-Chem (Goddard Earth Observing System - atmospheric chemistry) model. The model

simulated a small increasing trend in Hg(0) concentrations over 30 years mainly reflecting the growth in emissions. The model captured the springtime interannual variability in Hg(0) concentrations at Arctic sites with moderate skill and found it to be more significant compared to the temporal trend. The model reproduced the observed shift in minimum Hg(0) concentrations from May (1995–2001) to April (2002–2007) at Alert and attributed this shift to local cooling in April along with warming in May, confirming Cole and Steffen (2010). However, a shift in minimum Hg(0) concentrations at Alert was not found to be a characteristic of the Arctic as a whole. Fisher et al. (2013) concluded that high temperatures and a low sea-ice fraction in spring decrease the frequency and intensity of atmospheric mercury depletion events (AMDEs), while high solar radiation in spring enhances the photoreduction and re-emission of Hg deposited to the snowpack. During summer, the same environmental changes drive increased photoreduction of Hg(II) in the ocean and enhanced evasion of Hg(0) to the atmosphere. Thus, Fisher et al. (2013) suggested climate warming may lead to decreased fluxes of Hg from the atmosphere to the cryosphere and Arctic Ocean.

Chen et al. (2015) extended the study by Fisher et al. (2013) to quantitatively determine the contributions of changes in environmental variables (i.e., surface air temperature, sea-surface temperature, sea-ice fraction, sea-ice lead occurrence, the melting of multi-year sea ice, planetary boundary-layer depth, net shortwave radiation, surface wind speed, freshwater discharge, and net primary productivity) and anthropogenic emissions to Hg trends in the Arctic using anthropogenic emission inventories from AMAP/UNEP for the years 2000, 2005 and 2010. The model captured most of the seasonality in observed trends, especially the increasing trends in spring and fall; however, it failed to reproduce the increasing trends in July at Alert and in October at Ny-Ålesund. In addition to confirming the results of Fisher et al. (2013) in spring and summer, the study found that a decrease in Atlantic Ocean evasion of Hg at lower latitudes contributed to the decrease in Hg(0) concentrations in the Arctic from November to March.

Dastoor et al. (2015) assessed the role of changes in global anthropogenic emissions and meteorology in temporal trends of ambient Hg concentrations and deposition in the Canadian Arctic from 1990 to 2005 using GEM-MACH-Hg (Global Environmental Multi-scale, Modelling Air quality and Chemistry model, Mercury version; see Chapter 3) and AMAP anthropogenic emissions (AMAP, 2011). Interannual variability in air concentration and deposition of Hg was found to be driven by interannual variability in meteorology. Changes in meteorology and anthropogenic emissions were found to contribute equally to the decrease in surface air Hg(0) concentrations in the Canadian Arctic with an overall decline of ~12% from 1990 to 2005 in agreement with measurements at Alert (Cole and Steffen, 2010; Cole et al., 2013). In contrast, the model simulated a 15% increase due to changes in meteorology and a 5% decrease in net deposition in the High Arctic due to a decline in emissions in North America and Europe; this resulted in an overall increase of 10% in Hg deposition between 1990 and 2005 (see Chapter 3). Increasing snow-covered regions over first-year sea ice led to a decreasing trend in Hg re-emission fluxes from the snowpack, which resulted in increased net Hg deposition in the model. Halogen-enriched snowpacks over first-year sea ice suppress reduction and re-emission of Hg from snow (Durnford and Dastoor, 2011). Additionally, a decrease in snow-cover extent and a small increase in precipitation contributed to a small increase in deposition. Although the link between Hg deposition and lake sediment fluxes is not fully understood, an increase in deposition of Hg in the Arctic appears to be consistent with observed increases in Hg fluxes in some Arctic lake sediments in recent decades (Muir et al., 2009; Goodsite et al., 2013). For the marine environment, Fisher et al. (2013) and Chen et al. (2015) did not consider the impact of changing snow characteristics (i.e., halogen content in sea ice and snowpack) on the reduction and re-emission of Hg from snow, whereas Dastoor et al. (2015) neglected changes in ocean Hg evasion. Despite modeling differences, all studies suggested a dominant role of climate warming-related changes in environmental factors on Hg trends in the Arctic. Current Hg models lack a complete representation of the complexity of climate-sensitive Hg processes.

5.4.2 Catchment transport

The impacts of climate change on the transport of Hg across Arctic catchments are complex, and catchment or watershed-scale studies are becoming increasingly common (e.g., Zdanowicz et al., 2018; St. Pierre et al., 2019) in recognition that ecosystem health is dependent on biogeochemical connections and processes within the catchment (e.g., Braaten et al., 2014). In the following sections, we summarize how climate change factors, namely snowmelt and precipitation changes, permafrost degradation, forest fires, and glacial melt, have already affected and may continue to influence Hg transport across Arctic catchments.

a. Snowmelt and rainfall

Snowmelt has traditionally been considered an important vector for the transfer of Hg to both terrestrial and aquatic ecosystems across the Arctic (e.g., Obrist et al., 2018; Dommergue et al., 2010). Across non-glacierized areas, the snowmelt period may account for the largest seasonal pulse of total mercury (THg) fluxes to downstream ecosystems (Semkin et al., 2005). Douglas et al. (2017) highlight the potential enhancement of Hg deposition to, and retention in, coastal Arctic snowpacks due to the combined deposition of Hg and halogens during AMDEs. However, the re-emission of Hg from snowpacks varies with latitude (Durnford et al., 2012) such that the impact of these changes may differ spatially. In inland regions, Hg in snowpacks is often associated with mineral dusts (Agnan et al., 2018). Extreme events, including low snowpack years and large wind events (St. Pierre et al., 2019), could enhance dust deposition to snowpacks and ecosystems across the Arctic.

Summertime rainfall events, which are becoming increasingly common (Bintanja, 2018), can also mobilize significant quantities of solutes and particulate matter from landscapes at the height of thaw. Already, in more southerly regions of the Arctic like the Yukon Territory, areal rates of summertime wet deposition of Hg greatly exceed those of snowpack deposition by as much as six times (Zdanowicz et al., 2018). The impact that such shifts in precipitation patterns will have on the Hg budget

of Arctic watersheds, especially as precipitation originates from and interacts with other changes across the region (e.g., reduced sea-ice cover), largely remains to be determined.

b. Terrestrial organic matter transport

Arctic and Subarctic lakes are often characterized by clear water with low dissolved organic matter (DOM) concentrations of which dissolved organic carbon (DOC) is a major component (Henriksen et al., 1997; Pienitz et al., 1997; Lim et al., 2001; Forsström et al., 2015), but many of these systems are browning (Macdonald et al., 2005; Wauthy et al., 2018). Browning of surface waters from increasing terrestrial DOC concentrations has important environmental consequences, including for the biogeochemical cycling of Hg in Arctic and Subarctic ecosystems. DOM is the main transport vector for Hg and MeHg from catchment soils to surface waters (Grigal, 2002). DOM is known to affect the Hg cycle in aquatic environments due to its overriding influence on complexation, photochemical and microbial processes (see Sections 4.2 and 4.3). Positive correlations between Hg and DOC concentrations in water and biota are often observed; however, DOC quality and age may be important factors controlling these correlations (Forsström et al., 2015; Lescord et al., 2018; Poste et al., 2019). Browning of lakes is also known to enhance thermal stratification (Snucins and Gunn, 2000) and thereby weaken aeration of the hypolimnion, promoting anoxia (Couture et al., 2015), thus potentially enhancing in-lake methylation of inorganic Hg and accumulation of MeHg to biota in small temperate and boreal lakes (Watras et al., 1995; Eckley et al., 2005; Rask et al., 2010; Verta et al., 2010). Climate change-induced browning of lakes and oxygen-related MeHg production in the hypolimnion and its bioaccumulation may also be a concern in northern lakes. Browning of lakes will shift primary production towards secondary bacterial production, which is linked to elevated Hg levels in boreal watercourses (Forsström et al., 2013; Lescord et al., 2018). Furthermore, increasing DOC will decrease the penetration of UV-radiation into the water column and reduce demethylation processes in surface water (DiMento and Mason, 2017; Williamson et al., 2019). Thus, browning processes may further add to the existing Hg burdens in lake systems.

c. Permafrost degradation

With a loss of between 6% and 29% of high latitude permafrost projected for each 1°C of warming (Koven et al., 2013), climate change-induced permafrost thaw could mobilize a vast amount of Hg currently stored in frozen soils. Soils in the Arctic and Subarctic permafrost contain substantial reservoirs of OC (Tarnocai et al., 2009; Schuur et al., 2015) and Hg is bound to this organic matter, although the amount of stored Hg remains poorly constrained (Schuster et al., 2018; Lim et al., 2020). The turnover time for the microbial decay of frozen organic matter—with which Hg is often bound (Schuster et al., 2018; Lim et al., 2020)—is ~14 000 years, making permafrost stores of organic matter and Hg effectively stable over human time scales (Schuster et al., 2018). However, this turnover rate decreases to ~70 years with permafrost soil thaw (Koven et al., 2013; Schaefer et al., 2014). The fate of this Hg will ultimately depend on the type of permafrost deposition features created or affected (i.e., lake, wetland or hillslope thermokarst; Olefeldt et al., 2016) as well as on climatic factors controlling transport to downstream ecosystems.

Permafrost thaw across the Arctic results in the creation of small thermokarst lakes, ponds and wetlands (Gordon et al., 2016; Olefeldt et al., 2016). These highly productive systems are shallow, have high inputs of organic matter and nutrients, and are microbially active, making them excellent environments for the production of MeHg (MacMillan et al., 2015; Gordon et al., 2016). When the ponds drain following slumping, further permafrost degradation, or erosion, they become an important source of MeHg to nearby rivers (e.g., Fortier et al., 2007). Changes to thermokarst along the edges of small Subarctic lakes have led to increased Hg deposition at depth (Rydberg et al., 2010) potentially enhancing MeHg production, especially in areas with organic soils (MacMillan et al., 2015). Although MeHg photodemethylation is typically an important sink of MeHg in small pond systems (Lehnherr et al., 2012a), browning as a result of large DOM inputs with permafrost thaw may actually reduce photodemethylation and increase the net production of MeHg.

One of the most striking consequences of permafrost degradation in parts of the Arctic subject to hillslope thermokarst is the development of retrogressive thaw slumps, a form of mass wasting characteristic of hilly regions underlain by ice-rich permafrost. These features, which can be up to 40 ha in area, can release large quantities of sediments and solutes into lakes, rivers and coastal waters (Kokelj et al., 2013). Concentrations of Hg and MeHg in streams draining slumps in the western Canadian Arctic have been recorded as high as 1270 ng/L for THg and 7 ng/L for MeHg (St. Pierre et al., 2018). High sedimentation rates in slump-affected lakes have been hypothesized to dilute Hg deposition in these environments (Deison et al., 2012), but monitoring of these sites is needed to understand the long-term impact of these events. At present, Hg mobilization through the streams draining slump-affected areas is transport-limited (i.e., sediment supply exceeds water volume); however, during high-flow events, like the spring freshet, or if predictions of a wetter Arctic are realized (Bintanja and Andry, 2017), such conditions could enable the mobilization of vast quantities of Hg to downstream ecosystems. Clearly more studies need to be done to establish whether permafrost Hg hotspots exist and to identify potential pathways of the Hg cycle in high-latitude soils that could promote the transport or accumulation of Hg. From this, a better projection can be made of what permafrost Hg is most vulnerable to release from permafrost thaws.

d. Coastal erosion

There is substantial evidence that average coastal erosion rates are significantly increasing across many Arctic regions, and are now higher than at any time since observations began 50 to 60 years ago (Overduin et al., 2014; Irrgang et al., 2018). For example, erosion rates in rapidly eroding sections of the coastlines along the Laptev and Beaufort seas have doubled over the past 50 years (Jones et al., 2009; Günther et al., 2013). A number of interacting climatic, oceanographic, and on-

shore geomorphological processes have been suggested as contributing to this trend. These include: ongoing warming and destabilization of coastal ground ice, declining sea-ice extent, increasing summertime sea-surface temperatures and wind speeds, and rising sea levels. These changing oceanic conditions promote increases in storm frequency and intensity and, thus, the effects of wave action upon thawing, exposed shoreline permafrost (Jones et al., 2009; Overduin et al., 2014). Erosion of coastal soils is one of the major contributors of Hg to the Arctic Ocean (Outridge et al., 2008; Soerensen et al., 2016a; see Section 3.4.5), and this flux is likely to increase with increasing erosion rates during the 21st century.

e. Forest fires and soils

Global climate models predict both an increase in fire-season length of more than 20 days for high-latitude northern regions by 2100 (Flannigan et al., 2013) and a greater incidence of extreme or large fire seasons (Hu et al., 2015), emphasizing the future role that fire could play in the Arctic. Arctic Hg cycling will be impacted by an increase in wildfire activity caused by climate change in three ways: (1) the appearance of tundra fires, which will release terrestrial Hg to the atmosphere and streams locally; (2) the transport of wildfire-derived Hg from lower latitudes via long-range atmospheric transport, and possibly rivers that flow northwards; and (3) by causing physical and biological changes in the local environment. Understanding the impacts of fire on Hg dynamics through Arctic ecosystems, particularly on watershed connectivity and stream/river transport to downstream systems, will be critical.

Mercury dynamics across the Arctic region are affected by fires occurring both locally and further afield. Gaseous elemental mercury, typically considered the dominant species emitted by fire, can be transported long distances from source regions (Fraser et al., 2018). Conversely, PBM has a relatively short residence time in the atmosphere and is often deposited closer to the emission source (Fraser et al., 2018). Over the past 50 years, the frequency and severity of wildfires across some regions of the Northern Hemisphere have increased concomitantly with summer air temperatures and lengthening dry periods (Gillett et al., 2004; French et al., 2015).

Model estimates (GEOS-Chem) suggest ~10% of total annual Hg deposition (15 Mg/y) to the Arctic originates from forest fires, mainly from the large swaths of boreal forest in Eurasia (Kumar and Wu, 2019). Wildfires will become more frequent and severe in the mid-latitude boreal forest under a warmer climate (Coogan et al., 2019), with unknown consequences for Hg transport to the Arctic. At the same time, local wildfires are a source of Hg to Subarctic Canadian lakes (Pelletier et al., 2020) but represent less than 5% of the total Hg deposition to the Canadian High Arctic during the peak fire season (Fraser et al., 2018). The combination of increasing legacy contamination and greater fire frequency could lead to greater Hg release and deposition in the future (Biswas et al., 2007; Obrist et al., 2018). For example, the higher Hg concentrations in boreal forests could increase Hg emissions from wildfires in Eurasia by 41% between 2000 and 2050 (Kumar et al., 2018). More information is needed to better constrain estimates of Hg emissions from wildfires in boreal and Subarctic regions, including estimates of the propensity of boreal peatlands to burn and of the proportion of gaseous to particulate Hg produced by wildfires across these landscapes (Turetsky et al., 2006; Fraser et al., 2018).

Aside from the direct deposition of GEM and PBM to the landscape, local wildfires may also indirectly enhance the mobilization of Hg stored in soils through permafrost degradation, active layer deepening or warming and thermokarst feature development (Jones et al., 2015; Gibson et al., 2018). In particular, wildfires are estimated to be responsible for 2200±1500 km^2 of thermokarst bog formation over a 400 000 km^2 area of sporadic and discontinuous permafrost zones in Subarctic Canada (Gibson et al., 2018). Thermokarst development may then promote the mobilization and production of MeHg (MacMillan et al., 2015). Recent work in forested watersheds suggests that wildfires may not affect exports of dissolved Hg, though stream concentrations of particulate Hg—an important byproduct of wildfire, especially close to the source (Fraser et al., 2018; Obrist et al., 2018)—may increase substantially for up to 8 months post-fire (Jensen et al., 2017). Whether this is also true of Arctic systems remains to be seen. Furthermore, fires in permafrost zones typically result in the substantial loss of soil organic matter, increased active layer water storage and soil temperatures, leading to reductions in the permafrost, all of which can influence the biogeochemical cycling of Hg through northern ecosystems (Nossov et al., 2013).

f. Glacier melt

Within many glacierized catchments in the Arctic, glacier melt currently accounts for the largest source of both water and Hg to downstream ecosystems (Zdanowicz et al., 2018; St. Pierre et al., 2019). Glacial meltwaters integrate two principle sources of Hg: (1) legacy and modern Hg archived in glacial ice and snow; and (2) geogenic Hg transported by meltwaters as they flow across poorly consolidated proglacial landscapes (Zdanowicz et al., 2013). Mercury deposition to glaciers has varied substantially over time in response to changes in both natural (e.g., volcanic eruptions) and anthropogenic sources (Beal et al., 2015). We would therefore expect the Hg contribution from ice and snow to decline as older ice begins to melt. In many cases, however, geogenic Hg contributions to meltwaters along glacier margins or across proglacial landscapes can be as important, if not more, than those from the glacierized area (Zdanowicz et al., 2013). Large, periodic fluctuations in meltwater volume, including glacial lake outburst floods, can also mobilize substantial quantities of Hg from the surrounding landscape. In the Zackenberg River of northeast Greenland, for example, glacial lake outburst floods are responsible for between 5% and 10% of the river discharge in years when they occur, but between 15% and 31% of the Hg export (Rigét et al., 2011b; Søndergaard et al., 2015). These extreme meltwater discharge events may become increasingly common with climate change (Harrison et al., 2018; Nilsson et al., 2015), with the potential for substantial mobilization of Hg across landscapes.

Although glacial meltwaters typically contain very little MeHg (<0.1 ng/L; Zdanowicz et al., 2013; St. Pierre et al., 2019), little attention has been paid to Hg dynamics in subglacial channels or within cryoconite on glacier surfaces, both of which could support methylation. Subglacial meltwaters can

become anoxic and contain enough bioavailable carbon to support significant production of methane, similar conditions required for Hg methylation (e.g., Lamarche-Gagnon et al., 2019). Higher concentrations of MeHg (1.0 ng/g) have been detected in cryoconite of the Tibetan Plateau, suggesting either the preferential accumulation of MeHg there or active methylation (Huang et al., 2019).

Deglaciation on land also has important consequences for Hg transport and processing within downstream coastal waters. In a survey of three fjords impacted by glacial melt in Svalbard the highest THg concentrations were observed in Hornsund, which was experiencing the most dramatic glacial retreat of the three fjords at the time of sampling (Kim et al., 2020a). This Hg was strongly associated with largely terrestrial (78±17%) organic matter, suggesting that the Hg itself may have originated from the surrounding watersheds. The impact of glacial meltwaters on biological activity in nearshore marine waters remains unclear, with some studies reporting enhanced primary production (Meire et al., 2015), and thus potentially enhanced Hg uptake, and others suggesting a limit to the potential subsidy (Calleja et al., 2017; Hopwood et al., 2018).

g. Lake sediment

Lake sediments are important environmental archives that can be used to assess both climate-related changes in catchment transport and atmospheric deposition of Hg in relation to watershed ecosystem function and disturbance over time (see Figure 5.4; Goodsite et al., 2013; Drevnick et al., 2016). However, given that these two processes overlap in time, disentangling the relative contribution of each can be challenging (Korosi et al., 2018). Whereas post-industrial increases in Hg deposition, largely due to anthropogenic activities, are reported across most northern lakes, the impacts of climate change on catchments are much more variable and depend on local characteristics, such as catchment-to-lake-area ratio (Drevnick et al., 2012), the presence of glaciers, or susceptibility to different thermokarst landform types (Burke et al., 2018). Numerous studies have noted widespread increases in sedimentation rates, particularly in the more recent sediment horizons, a change attributed to increased catchment erosion (Fitzgerald et al., 2005; Muir et al., 2009; Cooke et al., 2010; Kirk et al., 2011). Geological tracers (crustal elements) or changes in sedimentation rates are thus commonly applied to Hg flux data to tease apart catchment and atmospheric Hg inputs so that these sedimentary records could be used to examine changes in atmospheric Hg deposition.

Some studies have found strong positive correlations between Hg accumulation in sediments and proxies of lake primary production, such as total organic carbon (TOC) and S2 carbon (algal-derived kerogen), and suggested that this relationship was due to algal scavenging of Hg or the absorption/adsorption of available Hg in the water column by algal biomass followed by its sinking and sedimentation (Sanei et al., 2012; Brazeau et al., 2013; Grasby et al., 2013). It has been estimated that 70% to 96% of Hg deposition recorded in sediments over the post-industrial period in Canadian and Norwegian Arctic lakes can be attributed to algal scavenging (Outridge et al., 2007; Stern et al., 2009; Rydberg et al., 2010; Jiang et al., 2011; Sanei et al., 2012; Outridge et al., 2019), which has implications for the use of sedimentary records to reconstruct Hg deposition. However, other studies have only found strong relationships between Hg and proxies of primary productivity, such as S2 carbon and chlorophyll a, in only a subset of lakes and concluded that the effect of algal scavenging on the sedimentary Hg record was not a wide-spread phenomenon across the circumpolar Arctic (Kirk et al., 2011; Cooke et al., 2012; Deison et al., 2012; Korosi et al., 2018; Lehnherr et al., 2018). Outridge et al. (2019) suggest that the absence of relationships between sediment organic matter and THg in some lakes may be due a limitation of forms of Hg and/or labile organic matter suitable for binding each other, such as complexation of Hg by humic acids (Le Faucheur et al., 2014; Schartup et al., 2015b). They suggest that the importance of algal scavenging may vary over time as the lake's climate and environmental settings change and

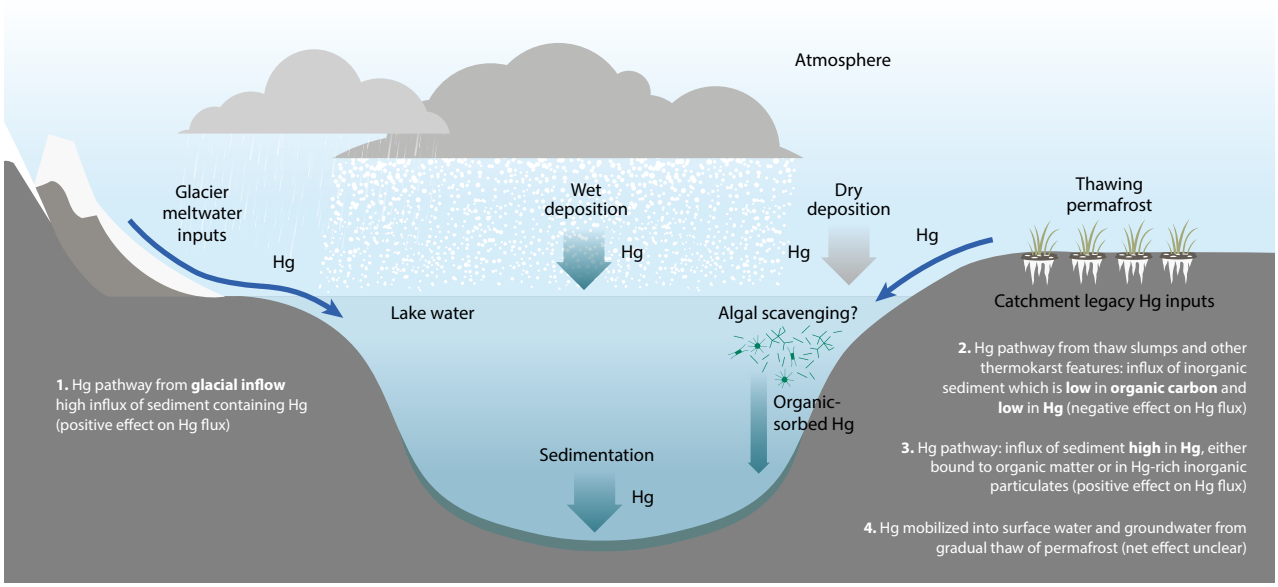

Figure 5.4 Conceptual diagram showing long-range transport of Hg from point sources outside of the Arctic and highlighting connections between climate change and catchment Hg fluxes to Arctic lake sediments.

that algal scavenging may partially explain the discrepancy between recent Hg flux increases observed in many Arctic lake sediments and decreasing or stable atmospheric Hg concentrations (Goodsite et al., 2013).

Increasingly, changes in catchment transport processes are being reflected in Hg deposition rates in lake sediment cores across the Arctic, especially in watersheds undergoing dramatic change as a result of permafrost thaw and glacial melt (St. Pierre et al., 2019) and erosion by enhanced river flows. Deison et al. (2012) analyzed dated sediment cores from 14 thermokarst-affected lakes in the Mackenzie Delta uplands (Northwest Territories, Canada) using a case-control analysis of lakes where retrogressive thaw slumps were present and absent. Focus-corrected sedimentation rates were ~two-fold higher in lakes with retrogressive thaw slump development on their shorelines (269±66 SD g/m^2/y) compared to lakes where thaw slumps were absent (120±37 g/m^2/y) due to higher influx of new material into slump-affected lakes. OC concentrations were higher in sediment profiles from reference lakes than in slump lakes, and there was a strong inverse relationship between Hg concentrations and sedimentation rate in the 14 study lakes (r^2=0.68, p<0.01), leading to the conclusion that retrogressive thaw slump development decreased concentrations of OC and Hg in the lake sediments due to dilution by rapid inorganic sedimentation in the slump-affected lakes. Korosi et al. (2015) reported that the post-1970 subsidence of permafrost-associated peatlands resulted in changes to terrestrial organic matter transport to downstream lakes but not necessarily to Hg enrichment. In a meta-analysis of lakes across Arctic Alaska, lakes with catchments susceptible to thermokarst development were more likely to have high, but variable, Hg accumulation rates (Burke et al., 2018).

Lake Hazen on Ellesmere Island (Nunavut, Canada) provides an example of dramatic climate change impacts on Hg transport recorded in its lake sediments. The Lake Hazen watershed experienced a 1°C increase in summer air temperature between 2001 and 2012 relative to the 1986 to 2000 baseline period (Lehnherr et al., 2018). This seemingly small change in temperature has translated to wholesale changes across the watershed, including the deepening of the soil active layer, large mass losses from the watershed's glaciers and a ~ten-fold increase in the delivery of glacial meltwaters to the lake, an up to 70% decrease in lake water residence time and the near certainty of summer ice-free conditions.

A number of Lake Hazen sediment cores have been analyzed for Hg, OC, carbon and nitrogen ratios (C:N), stable N and C isotopes (δ^{15}N and δ^{13}C), and algal (diatom) assemblages (Kirk et al., 2011; Lehnherr et al., 2018; St. Pierre et al., 2019). Sedimentation rates in Lake Hazen have increased eight-fold relative to the 1948 baseline, since the post-2007 acceleration of glacial melt across the watershed, translating to an increase in Hg accumulation rates from 20 to 180 µg/m^2/y. These increases have occurred concomitantly with a 1000-fold increase in OC accumulation within the sediments (Lehnherr et al., 2018) and a complete shift in the diatom community from the dominance of benthic species capable of persisting around the edges to pelagic species, which can now persist due to the reductions in lake-ice cover (Michelutti et al., 2020). Annual Hg sedimentation rates from cores collected in Lake Hazen matched well with a THg mass balance of the lake, suggesting that the sediment cores were not only a particularly good archive of interannual variability in catchment inputs (St. Pierre et al., 2019) but also of potential functional changes within the lake itself (Kirk et al., 2011; Lehnherr et al., 2018).

5.4.3 River transport

Glacier melt, permafrost thaw, and precipitation changes across the Arctic have important consequences for the transport of Hg by streams and rivers. Rivers integrate changes happening throughout their catchments, acting as conduits for previously archived Hg mobilized by increased precipitation, active-layer deepening (and other modes of permafrost thaw) and glacial melt to downstream freshwater and marine ecosystems. As rivers are one of the primary sources of Hg to the Arctic Ocean (Fisher et al., 2012), such changes have potentially important implications for the transformation and accumulation of Hg through food webs in marine ecosystems (Schartup et al., 2015a).

The dramatic transformation of Arctic landscapes in response to climate change may lead to an increase in the transport of particulate-bound Hg. The transition from sporadic to discontinuous permafrost is associated with maximal particulate-bound Hg mobilization (Lim et al., 2019). Similarly, high temporal variability in the dynamics of glacial meltwater rivers across poorly consolidated High Arctic landscapes also results in Hg fluxes dominated by the particle-bound fraction (Søndergaard et al., 2015; St. Pierre et al., 2019). The anticipated climatic effects across the regions may lead to substantial changes in landscape stability, especially in regions susceptible to hillslope thermokarst (Olefeldt et al., 2016). In these areas, we might expect to see enhanced mobilization and transport of particulate-bound Hg (St. Pierre et al., 2018). Whether this Hg is then available to organisms in downstream ecosystems remains to be determined (Gagnon and Fisher, 1997).

Model estimates and *in-situ* measurements have begun to converge on a baseline pan-Arctic riverine THg flux to Arctic marine waters (see Section 3.4.4). In particular, Zolkos et al. (2020) estimated an approximately 37 000 kg/y flux from samples collected in the six major Arctic rivers (the Kolyma, Lena, Mackenzie, Ob, Yenisey, and Yukon rivers) located across the Russian and Northern American Arctic, which is comparable to the 40 000 kg/y to 50 000 kg/y output of biogeochemical models (Zhang et al., 2015; Sonke et al., 2018). This was an important first step, against which future changes in riverine exports can be compared, though similar studies evaluating MeHg exports across the Arctic remain scarce (see Section 4.5).

The importance of rivers as a source of Hg to the Arctic Ocean may increase in the future. An increase over recent decades in the discharge of major Arctic rivers is well established (e.g., Serreze et al., 2006), with Eurasian rivers showing the greatest increase. Box et al. (2019) assessed the temporal trends in discharge for six of the largest Eurasian rivers (the Ob, Pechora, Severnaya Dvina, Yenisey, Lena, and Kolyma rivers), and for the two major North American Arctic rivers (the Mackenzie and Yukon rivers). By volume, the combined Eurasian river discharge is 1.8 times that of the two North American rivers. For the composite Eurasian river dataset, river flows increased on average by 18.7 km^3 per decade

between 1981 and 2011, whereas the two North American rivers exhibited an increase of 5.9 km^3 per decade between 1975 and 2015. These volumetric increases correspond to a 12% increase for Eurasian rivers and a 9% increase for North American rivers over approximately the past three decades.

5.4.4 Ocean currents

The largest oceanic fluxes occur at the Fram Strait, which is located between Greenland and Svalbard (Rudels, 2012), and although there is strong seasonal variability (Tsubouchi et al., 2018), these fluxes drive the largest oceanic Hg inflow and outflow (Soerensen et al., 2016a). Only little long-term change in those Hg fluxes are expected (Petrova et al., 2020). The authors used the first Hg observations at the Fram Strait to ascertain Hg species concentrations in different water masses. The largest Hg fluxes to the Arctic Ocean are associated with the West Spitzbergen Current, 43 Mg/y via the Fram Strait and 6 Mg/y via the Barents Sea Opening. The largest outflow occurs via the East Greenland Current, 54 Mg/y. Another important outflow occurs via the Davis Strait (between Greenland and Baffin Island), 19 Mg/y. Inflow volumes from the North Atlantic side have remained relatively stable between the mid-1990s and mid-2010s, although there is a slight, non-significant, increasing trend (Østerhus et al., 2019). However, the strong seasonal cycle in water mass transport (Tsubouchi et al., 2018) likely result in varying Hg fluxes throughout the year.

It is difficult to find evidence for change in seawater Hg species composition due to the lack of consistent temporal Hg observations. Wang et al. (2012a) provided the first off-shore data on the Canadian Arctic Archipelago. Heimbürger et al. (2015) provided the first four profiles of Hg in the central Arctic Ocean (with data from a 2011 cruise). Both studies reported a surface enrichment in THg and a shallow MeHg peak at the lower halocline (200 m depth compared to 1000 m in the North Atlantic), which might be responsible for the high biota Hg levels in the Arctic (see Sections 4.3.2.1 and 6.6). The GEOTRACES program organized the first pan-Arctic survey with two Canadian cruises (2015 Canadian Arctic Archipelago and Labrador Sea; Wang et al., 2018), two German cruises (2015 central Arctic Ocean, 2016 Fram Strait; Petrova et al., 2020) and one American cruise (2015 central Arctic; Agather et al., 2019; Dimento et al., 2019). The new Hg species data are comparable to the 2011 observations and now include dimethylmercury (DMHg) in addition to monomethylmercury (MMHg). It is not surprising to see no difference five years later because the expected changes are minor (Soerensen et al., 2016a) and require longer observation time series.

Evidence from a series of permanent *in situ* moorings indicates the seawater volume flowing through the Bering Strait has increased significantly over the last two decades at an average rate of 1.8% per year (Østerhus et al., 2019). There is considerable interannual variability to the northward Bering flow, but the difference between the minimum in 2001 and the maximum in 2014 represented an overall 70% increase (Woodgate, 2018). The most likely explanation for this trend is lower water pressure in the East Siberian Sea, which is caused by increasing westerly winds over the past two decades; this drives surface water from the shelf into the deeper ocean basin, thereby creating a pressure differential between the Bering Sea and the Arctic Ocean (Peralta-Ferriz and Woodgate, 2017). Because the Pacific Ocean supplies only about 10% of the total seawater inflow to the Arctic Ocean (Woodgate, 2018; Østerhus et al., 2019), the impact on Hg delivery to the Arctic Ocean as a whole from increasing Pacific inflows is likely to be minor. However, the Hg delivered could affect Hg budgets in the Chukchi and Beaufort seas, where the effects of Pacific waters are noticeable on regional water chemistry, nutrient, and heat budgets (Torres-Valdés et al., 2013; Haine et al., 2015; Woodgate et al., 2018).

5.5 What are the impacts of climate change on mercury biogeochemical processes?

The main biogeochemical processes affecting Hg cycling in the Arctic are redox reactions between divalent and elemental Hg, and methylation/demethylation reactions. These reactions can occur to different extents in a variety of matrices, including freshwater, seawater, snow, sea ice, soils and sediments. They may be biotic or abiotic in nature and are driven by environmental variables, such as temperature, exposure to solar radiation, organic matter, nutrients and chloride concentrations. All of these variables are expected to be modified by climate change. Conceptual descriptions and predictions of how these changes may occur have been presented in the previous AMAP assessment on Hg (AMAP, 2011) and in the follow-up paper by Stern et al. (2012). On a global basis, and particularly in the Arctic, it has been recently suggested that such climate-related modifications of biogeochemical processes have become prevalent drivers of trends in Hg levels in biota (Wang et al., 2019c). In this section, we focus on non-atmospheric studies providing new data that can better constrain these predictions. These data are summarized in Table 5.1.

5.5.1 Inorganic mercury redox processes

Redox processes can occur through photochemical, abiotic and microbial processes (Møller et al., 2011). These processes greatly influence interfacial fluxes because of the high volatility of Hg(0) compared to Hg(II) species. Since the last AMAP Hg assessment (AMAP, 2011), there have been few studies on redox processes in freshwater, soils and sediments in the Arctic. In contrast, recent advances have been made regarding Hg redox cycling in snow, seawater, sea ice, and the tundra, and some of these studies considered interactions with climate change.

In snow, approximately 75% of deposited Hg is revolatilized back to the atmosphere due to Hg(II) photoreduction (Wang et al., 2017a). However, precise predictions have been hampered by a lack of kinetic data (Mann et al., 2014). Recently, experiments have been conducted with High Arctic snow samples to assess photoreduction kinetics during melting as a function of chloride content and UV intensity (Mann et al., 2015, 2018). A parabolic relationship was described between reduction rate constants in frozen and melted snow with increasing UV intensity. In contrast, total photoreduced Hg (resulting from a balance between photoreduction and photooxidation)

Table 5.1 Anticipated effects of climate change on mercury biogeochemical transformations in Arctic environments, according to recent studies.

Biogeochemical transformations	Matrices	Specific process(es)	Key variables considered	Effect(s) of climate change	References
Redox transformations	Snow and sea ice	Photoreduction and oxidation	Chloride and UV	Lower photoproduction of Hg(0) Retention of Hg(II)	Steffen et al., 2013; Mann et al., 2015, 2018
	Seawater	Hg(II) reduction under ice Bacterial reduction (*merA* gene)	Sea-ice cover Temperature	Pulses of Hg(0) evasion with sea-ice loss Increased Hg(0) production	DiMento et al., 2019
	Tundra	Hg(0) uptake by plants	Vegetation cover and length of growing season	Increased accumulation of atmospheric Hg by plant uptake in the tundra	Obrist et al., 2017
Methylation and demethylation	Freshwater systems	Sediment methylation	$\delta^{201}Hg/\delta^{199}Hg$ ratios and changes in microbial communities Temperature	Lower Hg methylation during past warming events Higher net methylation in warmer sediments	Jackson, 2019; Hudelson et al., 2020
		Methylation in hypolimnia and sediments	Change in thermocline depth	Change in volume of water and sediments where methylation occurs	Perron et al., 2014
		Photodemethylation	DOC	Increased demethylation in clear lakes/decreased demethylation in high DOC systems	Girard et al., 2016
	Seawater (surface, subsurface)	Net methylation	Hg(II) Organic matter mineralization Nutrients from coastal rivers Shift in plankton communities Stratification	Increased net methylation	Wang et al., 2012a, 2018; Heimbürger et al., 2015; Schartup et al., 2015a
		Photodemethylation	UV penetration Sea-ice cover	Increased photodemethylation	Point et al., 2011; DiMento and Mason, 2017
	Snow, first-year sea ice, multi-year sea ice	Net methylation	Loss of multi-year sea ice Increased melting of sea ice and snow	Increased MeHg flux to the ocean	Beattie et al., 2014
	Marine sediments	Net methylation	Temperature	Increased net methylation	St. Pierre et al., 2014
	Arctic soils		Temperature Permafrost thaw	Increased net methylation	Yang et al., 2016

increased linearly with UV intensity. Since the snowmelt period is characterized by relatively low UV intensity, less Hg(0) should be produced and evaded at that time. These studies have also shown that chloride can enhance Hg retention in melted snow by decreasing photoreduction of Hg(0). Considering future projections for higher chloride loading in coastal snowpacks due to enhanced sea-salt deposition from thinner first-year sea ice and more open water, these experimental studies suggest that more Hg could be retained in snowpack and delivered to Arctic aquatic systems during snowmelt (Mann et al., 2018).

With respect to the Arctic marine environment, Hg(0) has been shown to significantly accumulate under contiguous ice (DiMento et al., 2019), suggesting continual under-ice net Hg reduction by yet unidentified mechanisms. Mercury evasion is therefore likely altered by ongoing and anticipated changes in the extent of sea-ice cover, with pulses of Hg evasion predicted to occur over two to three weeks when ice cover disappears (DiMento et al., 2019). One redox process occurring in the marine water column is Hg reduction by microorganisms carrying the mercuric reductase (*merA*) gene (Bowman et al., 2020a; see Section 4.2.1). Recent studies have identified *mer* genes in the Arctic basin and shown Hg(0) production in the presence of bacterioplankton possessing *merA* (Lee and Fisher, 2019). This process could be favored in a warmer ocean.

Furthermore, sea ice itself may modify fluxes through redox processes. Indeed, atmospheric Hg speciation measurements taken over sea ice and tundra have shown that Hg emissions are higher over tundra systems (Steffen et al., 2013). These trends are consistent with suppressed photoreduction in chloride-containing snow over sea ice. Climate change is also causing a decrease of multi-year ice, with saltier first-year ice being favored. This could result in more Hg being concentrated in sea ice from the underlying seawater due to freeze rejection and from the overlying snow if AMDEs are enhanced (Steffen et al., 2008; Chaulk et al., 2011; Beattie et al., 2014; Wang et al., 2017a). However, our understanding of redox and complexation processes in sea ice and sea-ice brines is too limited to make climate-related projections at this point (Wang et al., 2017a).

Ocean acidification could also influence Hg cycling in the Arctic, although no specific field study has addressed this question. The decrease in concentration of OH^- and CO_3^{2-} ions may influence the solubility, adsorption and redox processes of

metals in seawater (Millero et al., 2009). In the case of Hg(II), for which seawater speciation includes strong complexes with chloride, little change in speciation linked to acidification is anticipated, since the change in pH will not influence chloride concentrations (Millero et al., 2009). Recent laboratory studies have shown that ocean acidification could alleviate Hg toxicity in marine copepods not through change in Hg speciation, but rather through alteration of physiological processes (Li et al., 2017; Wang et al., 2017c).

For terrestrial systems, there is now evidence that Hg deposition on the Arctic tundra is controlled by the uptake of Hg(0) by plants (Obrist et al., 2017). From a mass balance analysis, it was determined that 70% of Hg in the interior tundra is derived from Hg(0), and that this Hg(0) deposition peaked during the summer. This important uptake by plants has been confirmed by Hg stable isotope analyses (Obrist et al., 2017). It follows that a climate-related increase in vegetation cover and the length of the growing season may lead to higher Hg deposition over the tundra. Also, the production and evasion of Hg(0) in this landscape (for instance in rivers, lakes and ponds) could be redeposited nearby and taken up by vegetation.

5.5.2 Methylmercury production and decomposition

Mercury methylation occurs via microbial processes. In anoxic environments (or in anoxic niches in oxic environments, such as marine particles) this methylation is controlled by the *hgcAB* gene cluster (see Section 4.2.1; Parks et al., 2013) which is present, among others, in some iron and sulfate reducing bacteria and in methanogens (Gilmour et al., 2018). However, the methylation capacity of *hgc*-like genes in the ocean environments is uncertain (Bowman et al, 2020b). Mercury demethylation can result from photochemical or microbial pathways. Microbial demethylation can occur through either an oxidative or a reductive mechanism (Lehnherr, 2014). The main recent climate-related advances on Arctic methylation and demethylation have focused on marine and freshwater systems.

In fresh waters, microbial Hg methylation and demethylation occur mostly in anoxic hypolimnia and sediments, whereas photodemethylation is confined to the upper portion of the water column (Lehnherr, 2014). Climate-related changes in thermal regimes could alter the temperature-dependent methylation and demethylation rates in sediments. A paleolimnological study of Arctic sediment cores used δ^{201}Hg:δ^{199}Hg ratios to estimate past MeHg production in lakes during the last 100 years (Jackson, 2019). According to this research, done on one core from one Arctic lake, the isotope ratio varied with climate change, decreasing during warming phases. Therefore, during warming events, net sediment methylation would be lower, presumably because of changes in the microbial community structure linked to changes in the phytoplanktonic communities providing nutrients. More research is warranted to see if such a trend holds for many freshwater systems. With respect to the direct effect of temperature on the balance between methylation and demethylation, it has been recently experimentally shown that net methylation is increased when sediment cores are warmed (Hudelson et al., 2020). Thermal shifts may also alter the depth of the thermocline of stratified systems, and therefore the volume of sediments and hypolimnetic waters where Hg methylation usually takes place. The effect of thermocline deepening has been assessed through whole-ecosystem experiments on lower latitude systems (Perron et al., 2014); such studies have shown that deeper thermoclines are associated with a smaller volume of MeHg-rich hypolimnion and an important decrease in MeHg levels along the food web.

In the water column, changes in DOC loadings have been predicted to increase epilimnetic MeHg levels by impeding photodemethylation, based on lower latitude studies (Poste et al., 2015; Klapstein et al., 2017; Klapstein and O'Driscoll, 2018). In contrast, field experiments conducted in Arctic freshwater systems with contrasting DOC levels suggest a non-linear, unimodal relationship between DOC and photodemethylation rates (Girard et al., 2016), similar to the bell-shaped relationship previously described between DOC and Hg bioaccumulation (French et al., 2014). As a result, increase in DOC inputs from thawing permafrost and other mechanisms could increase photodemethylation in clear lakes and decrease it in browner systems. Climate change is also promoting the formation of shallow thaw ponds that can become transient hotspots of MeHg production in the landscape (MacMillan et al., 2015).

In marine systems, the primary local methylation site appears to be in the water column rather than the sediments, except near littoral areas (see Section 4.3.2). Methylmercury production in Arctic seawater is thought to be tightly linked to mineralization of organic matter (Wang et al., 2012a; Heimbürger et al., 2015), although the methylation mechanism remains unknown. Hence, climate change-induced increases in primary productivity in the Arctic Ocean, which would stimulate organic matter remineralization, will likely lead to higher net MeHg production. Such an increase in MeHg production is also predicted for shallow marginal sea-ice zones because of intensified stratification and shifts in plankton dynamics (Heimbürger et al., 2015). Coastal MeHg production may also be exacerbated by increased nutrient inputs from coastal rivers (Schartup et al., 2015a). However, large uncertainties remain regarding production and loss mechanisms (e.g., changes in demethylation rates; Wang et al., 2018, 2020b). In particular, MeHg photodemethylation could be promoted by loss of sea ice and increased irradiation of surface waters (Point et al., 2011), particularly in the open ocean where UV penetration is maximal (Dimento and Mason, 2017).

In addition to the water column, MeHg can also be produced in snow, first- and multi-year sea ice, and accelerated melting of sea ice may release significant fluxes of MeHg into the Arctic Ocean (Beattie et al., 2014). Production of MeHg in coastal sediments can also be significant, and the effect of increased temperature in shallow sediments could lead to increased net methylation rates as reported for lakes (Hudelson et al., 2020), with methylation being more sensitive to these temperature changes than demethylation according to experiments with slurries of marine sediments (St. Pierre et al., 2014).

Experimental warming studies have also been conducted on homogenized Arctic soil, and they have similarly concluded that climate warming and permafrost thaw could enhance MeHg production by an order of magnitude (Yang et al., 2016).

5.6 How has climate change altered mercury exposure in Arctic biota?

Mercury trends, as measured in aquatic biota, do not always track recent atmospheric trends well; climate change has been suggested to be the leading cause of this discrepancy globally, including in the Arctic (Wang et al., 2019c). Both direct physical climate change (see Section 5.2) and indirect ecosystem change (see Section 5.3) may impact the exposure to, and accumulation of, Hg in Arctic biota. When it comes to physical changes, altered Hg transport and deposition (see Section 5.4) and biogeochemical processes (see Section 5.5) may impact Hg levels and forms within and among Arctic environments, and thus Hg exposure and uptake at the base of marine, terrestrial and freshwater food webs of the Arctic ecosystem. In addition, extensive climate-driven ecological and physiological changes, from altered ingestion and elimination rates to the introduction of northward-range-shifting Subarctic species, may alter biotic Hg exposure. In the previous AMAP Hg assessment (AMAP, 2011), the chapter dealing with how climate change influences Arctic Hg (Chapter 4) largely highlighted abiotic and biotic mechanisms by which climate change could *potentially* impact Hg levels in the Arctic and in Arctic species, although a small number of empirical studies were covered (e.g., Gaden et al., 2009; Carrie et al., 2010). Since the 2011 assessment, multiple studies have evaluated associations between physical climate variables, or climate-driven ecological variation/changes, and Hg levels in Arctic biota. Most studies have been carried out on marine organisms, with fewer studies carried out on terrestrial and freshwater biota. In this section, we focus on these new studies evaluating Hg-climate change interactions carried out on biota in marine, terrestrial, and freshwater ecosystems. Studies on the biological effects of Hg on Arctic species are discussed in Chapter 6 of this current assessment, and, along with effects of persistent organic pollutants (POPs), in a separate recent AMAP assessment (AMAP, 2018a) and the subsequent paper by Dietz et al. (2019a).

5.6.1 Terrestrial biota

There is little information available on how the exposure of terrestrial biota to Hg is affected by climate change. Mercury concentrations in Arctic terrestrial herbivores are generally low (see Section 6.3.3; Aastrup et al., 2000; Dietz et al., 2000a; Gamberg et al., 2020; Pacyna et al., 2018), but their exposure may vary according to space use and diet, which may be influenced by climate change. In the Canadian Arctic, Hg concentrations in lichen were enriched at coastal sites adjacent to polynyas compared to sites locked in by sea ice for the majority of the year (St. Pierre et al., 2015). It could be hypothesized that a decline in sea ice may lead to increased Hg exposure in terrestrial herbivores using coastal areas. For example, Svalbard reindeer have been documented to increase feeding along the shoreline during icier winters (Hansen et al., 2019a). High intake of washed-ashore kelp among reindeer feeding along the shoreline may lead to higher Hg exposure compared to animals feeding on terrestrial plants, as kelp shows higher Hg concentrations compared to terrestrial plants (Chan et al., 1995; Wojtun et al., 2013; Olson et al., 2019). Although changing vegetation as a consequence of climate change has been documented (see Section 5.3.1), the effects of changing vegetation on Hg uptake and cycling in Arctic tundra ecosystems are currently unknown.

Arctic terrestrial predators may feed on both marine and terrestrial food webs (Eide et al., 2005; Dalerum et al., 2012; Ehrich et al., 2015; McGrew et al., 2014). Terrestrial prey, such as ungulates, geese, and ptarmigans, have lower levels of Hg than marine prey species, such as seals and seabirds (Aastrup et al., 2000; Dietz et al., 2000a; Fant et al., 2001; Braune and Malone, 2006; Pedersen et al., 2006; Jæger et al., 2009; Pacyna et al., 2018). Consequently, coastal Arctic foxes which feed on marine prey items have shown three times higher levels of Hg than inland foxes which mostly feed on terrestrial food items (Bocharova et al., 2013). Coastal grey wolves (*Canis lupus*) which feed on marine prey items have shown 23 to 60 times higher levels of Hg than inland wolves (McGrew et al., 2014). Supporting this, studies using dietary tracers have indicated that Hg concentrations increased with a higher intake of high trophic level marine food items (McGrew et al., 2014; Hallanger et al., 2019). Climate-related changes in the physical environment may affect prey availability for terrestrial predators, which has been linked to their Hg exposure. Concentrations of Hg in Arctic foxes from Svalbard increased with increasing sea-ice availability and decreased with increasing reindeer mortality (Hallanger et al., 2019). Arctic foxes need sea ice to scavenge remains of seals killed by polar bears and to hunt new-born ringed seal pups (Gjertz and Lydersen, 1986), whereas rain-on-snow events that encapsulate tundra vegetation in ice (Peeters et al., 2019) are connected to reindeer mortality, and thus to the number of available reindeer carcasses for Arctic foxes (Hansen et al., 2013). Furthermore, the long-term temporal trend in Hg in Arctic foxes (1997-2014; n=109) showed that the temporal increase in liver Hg levels was slightly faster, 7.2% (95% CI: 2.3, 9.6) per year when the concentrations were adjusted for variation in diet proxies ($\delta^{13}C$ and $\delta^{15}N$) and food availability (availability of sea ice and reindeer mortality), whereas the yearly change of the measured concentrations was 3.5% (95% CI:-0.11, 7.2; Hallanger et al., 2019).

5.6.2 Freshwater biota

Methylmercury is taken up by primary producers at the base of food webs (Morel et al., 1998). In lakes, regime shifts towards pelagic-dominated energy pathways may increase Hg accumulation in food webs, as phytoplankton are more prone to absorb MeHg from the water column compared to benthic algae (Watras et al., 1998; Pickhardt and Fisher, 2007). However, subsequent bioaccumulation of Hg to consumers via pelagic and benthic food-web compartments is highly variable in different Arctic regions and no clear-cut patterns can be synthesized (e.g., Power et al., 2002; Thomas et al., 2016; Chételat et al., 2018; Burke et al., 2020; Rohonczy et al., 2020). Pelagic food webs tend to accumulate Hg more efficiently than benthic ones, potentially via longer and more chain-type food webs (Power et al., 2002; Thomas et al., 2016). Melting snow and subsequently formed melting ponds could be very important sources of MeHg draining into lakes, where this substance is quickly taken up via phytoplankton. Overall, increasing precipitation is correlated with DOC leaching from catchment into fresh waters, which transport Hg and promote bacterial

production in lakes (Forsström et al., 2013; de Wit et al., 2016; Poste et al., 2019). In lakes, increasing temperature and productivity may also lead to anoxia in deep profundal habitats and sediments, promoting within-lake methylation processes by bacteria (e.g., Morel et al., 1998). Yet, development of anoxic conditions is highly dependent on lake productivity, morphometry, regional temperature and wind exposure, where change in stratification is prone to alter Hg uptake in lake food webs (Rask et al., 2010).

Shifts in community composition and species distributions in Arctic freshwater ecosystems may have implications for Hg bioaccumulation and biomagnification. The role of filter feeding *Daphnia* in MeHg uptake and transfer from phytoplankton to fishes has been recognized and may become more pervasive in the future, as the distribution range of these cladocera is likely to increase (e.g., Chételat and Amyot, 2009; Kahilainen et al., 2016). However, such shifts in zooplankton fauna are less evident in Arctic ponds where zooplankton often lack fish predators and because pond food webs are governed by their ephemeral nature (e.g., potential desiccation in summer and complete freezing in winter; Rautio et al., 2011). Freshwater fishes in the Arctic are often generalists and cold-water adapted salmonid species (e.g., Arctic char; *Salvelinus alpinus*, whitefish; *Coregonus* spp.), which use both pelagic and benthic resources based on their seasonal abundance, influencing Hg concentrations in muscle and liver tissues (e.g., Kahilainen et al., 2016; Keva et al., 2017). Arctic Char, whitefish, and sticklebacks (*Gasterosteidae*) are all prone to diverge into sympatric morphs (or subspecies) using different prey items ranging from zooplankton, benthic macroinvertebrates or fish, differential feeding upon which leads to clear differences in Hg content that often peaks in planktivorous or piscivorous morphs (Willacker et al., 2013; Thomas et al., 2016; Kahilainen et al., 2017). Range expansions of warmer adapted species, such as percids (*Percidae*), sticklebacks and cyprinids (*Cyprinidae*), are usually related to immigration of more specialized species, and an increasing share of pelagic reliant species could elevate pelagic derived Hg (Thomas et al., 2016). Many Arctic regions contain anadromous fish species, including Arctic char, lake trout (*Salvelinus namaycush*) and Dolly Varden trout (*Salvelinus malma*), which are likely to retreat from warm southern regions or to start to form stationary freshwater populations with increasing temperatures and productivity (Finstad and Hein, 2012). These stationary freshwater populations will usually have higher levels of Hg than anadromous populations (e.g., van der Velden et al., 2013a; Tran et al., 2015; Barst et al., 2019). Decreasing winter ice and snow in Arctic freshwaters could have negative effects on native fauna via a range of abiotic and biotic processes, which will likely change year-round Hg dynamics in consumer tissues (Keva et al., 2017).

Marine and freshwater habitats are well-connected via anadromous fish, in which marine foraging is related to lower Hg exposure due to lower Hg in saltwater prey (Swanson et al., 2011; van der Velden et al., 2013b; Tran et al., 2019). In some Fennoscandian lakes, a shift from benthic invertebrate to pelagic zooplankton prey often leads to elevated Hg content in fish (Kahilainen et al., 2016, 2017; Keva et al., 2017), but there is considerable variation of patterns in different Arctic regions and different types of lakes. Another important dietary shift is related to piscivory (i.e., fish-feeding) behavior that elevates trophic level and thus the Hg content (Cabana and Rasmussen, 1994). Increasing trophic level is positively correlated with Hg concentrations within species and in food webs (Kidd et al., 2012; Clayden et al., 2013; Lescord et al., 2015; Thomas et al., 2016; Ahonen et al., 2018). The new immigrating species are prone to increase the food-chain length and may lead to elevated Hg content in top predators (Thomas et al., 2016; Braaten et al., 2019; Barst et al., 2020). However, many top predators feed on both pelagic and benthic prey fish, influencing their Hg content (e.g., Rohonczy et al., 2020). Mercury concentrations in river-resident fish and river food webs can be spatially and temporally variable (e.g., Tran et al., 2015, 2019; Pelletier et al., 2017), but usually plankton-based food chains are absent, which often results in lower Hg content in rivers than in lakes.

Arctic lakes are often known for their relatively large adult fish populations composed of few year classes and potentially growing to very old ages (>20 years old). In such highly seasonal systems, most fish are in the adult stage and use a significant part of their energy towards gonad growth (Hayden et al., 2014; McMeans et al., 2015b). In slow-growing European whitefish (*Coregonus lavaretus*) a year-round study indicated a continuum of summer growth dilution and winter condensation of Hg due to spawning and starvation during the long ice-covered period (Keva et al., 2017). In these mature, adult fish, very little somatic growth is observed and year-round Hg variation exceeds annual bioaccumulation of Hg. However, anadromous Arctic char show opposite patterns in Canada, where summer Hg content is significantly higher than in winter (Martyniuk et al., 2020), highlighting the complexity of potential outcomes.

Multi-decadal time series of Hg concentrations in Arctic fishes have been examined for influences of climate change on bioaccumulation. Based on several studies, it is clear that the effects of climate change on fish Hg concentrations are complex and difficult to predict. In the western Canadian Arctic, Hg concentrations in lake trout and burbot (*Lota lota*) of Great Slave Lake increased from the 1990s to 2018, but no change was observed for another resident species, northern pike (*Esox lucius*; see Chapter 2; Evans et al., 2013). The mean annual air temperature increased in the region during the study period and was correlated with length-adjusted Hg concentrations of lake trout and burbot (Evans et al., 2013). However, the temperature effect was negative (i.e., fish had lower mean Hg concentrations in warmer years), and it explained little of the fish Hg variation in statistical models. Other climate variables, specifically the Pacific/North American oscillation, wind speed and precipitation had little or no explanatory effect in the Hg trend models. In addition, air temperature and sediment organic matter were found not to influence Hg fluxes to sediments, based on three sediment cores from different basins of the lake. Evans et al., (2013) concluded that temperature and lake productivity were not important drivers of increasing Hg concentrations in fishes of Great Slave Lake. Interestingly, over a similar timeframe, decreasing Hg concentrations were shown in burbot in a series of Russian rivers from 1980 to 2001 (Pelletier et al., 2017) and in Fennoscandian pike (*Esox lucius*) in the Subarctic from 1965 to 2015 (Braaten et al., 2019). Hudelson et al. (2019) analyzed temporal trends of Hg concentrations in landlocked Arctic

Case Study 5.1 Diet and growth influences on mercury in lake-dwelling Arctic char in the eastern Canadian Arctic

The Arctic char is a slow-growing, long-lived salmonid species that is widely distributed in cold, unproductive lakes across the circumpolar Arctic (Power et al., 2008). Climate-change effects, such as warmer temperatures and increased aquatic productivity, are anticipated to improve growth conditions for Arctic freshwater fishes, and it has been suggested that faster growth rates may reduce Hg concentrations through somatic biodilution (Stern et al., 2012). However, recent research on Arctic char in northern Canada has demonstrated that age and dietary Hg exposure are the dominant factors controlling their Hg concentrations (van der Velden et al., 2012, 2013a, 2013b; Chételat et al., 2021). Anadromous char typically have lower Hg concentrations in their muscle than lake-dwelling char, and they are also often larger in size for a given age (van der Velden et al., 2013a; Swanson et al., 2011). A comparison of paired marine and lacustrine food webs in the eastern Canadian Arctic indicated that basal MeHg concentrations explained differences in muscle concentrations between anadromous and lake-dwelling char, rather than growth rate or trophic level (van der Velden et al., 2013a, 2013b). Among lake-dwelling char, age better explained muscle-Hg concentrations than growth rate (determined by length-at-age), and faster-growing fish did not have lower muscle-Hg concentrations (van der Velden et al., 2012; Chételat et al., 2021). This lack of a growth dilution effect can be explained by the higher trophic level of faster-growing lacustrine Arctic char (Chételat et al., 2021). Thus, while feeding at a higher trophic level may enhance growth through greater caloric intake, it can also result in a greater intake of Hg. Together, these findings suggest climate-driven environmental change that affects dietary exposure to MeHg (e.g., atmospheric deposition, MeHg production, uptake at the base of the food-web and food-web structure) may have more of an effect on Hg bioaccumulation in Arctic char than improved growth in these lake ecosystems of the eastern Canadian Arctic.

char from six lakes near Resolute Bay on Cornwallis Island in the Canadian High Arctic. The Hg trends differed among lakes, with no change in length-adjusted mean annual Hg concentration in char of three of the lakes and a decreasing trend for the other three lakes over the last two to three decades (Hudelson et al., 2019). The study lakes were in close proximity to each other, and none of the examined climate variables (wind speed, precipitation, air temperature, sea-ice duration, oscillation indices, and snow) consistently explained the length-adjusted Hg concentrations of char. However, sea-ice duration in Resolute Bay was positively correlated with char Hg for three of the lakes, which may indicate that longer lake-ice duration is influencing Hg bioaccumulation. Mean length-adjusted Hg concentrations of Arctic char varied several-fold among the study lakes and were best explained by water concentrations of dissolved and particulate organic carbon. Hudelson et al. (2019) concluded within-lake processes had a dominant influence on Hg bioaccumulation in the Arctic char populations based on the association with lake organic carbon and the occurrence of different temporal trends for lakes with the same climate. Together, these studies did not find evidence that climate change has strongly influenced Hg bioaccumulation in fishes of the Canadian Arctic since the 1990s.

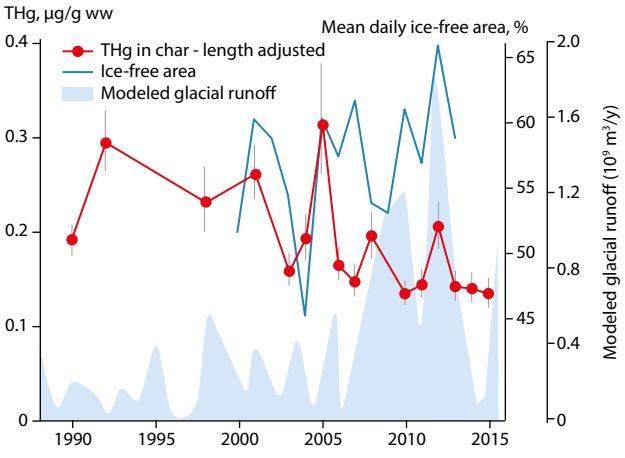

Figure 5.5 Temporal trends of length-adjusted (LS mean) THg in muscle tissue of adult Arctic char from Lake Hazen (1990–2015) along with ice-free area and modeled glacial runoff reported by Lehnherr et al., 2018.

Lake Hazen, the largest lake by volume north of the Arctic Circle, has been impacted by climate warming that has resulted in an approximately ten-fold increase in glacial meltwater inflow since the mid-2000s, increased frequency of summer ice-free conditions, and greater turbidity of inflowing and nearshore lake waters (Lehnherr et al., 2018). These dramatic changes over the past 15 years have also accelerated the delivery of Hg into the lake (St Pierre et al., 2019). Arctic char, the only fish species in the lake, are landlocked, and thus excellent sentinels of bioaccumulative contaminants in this system. In 19 collection years since 1990, adult char (>200 g) have been collected between June and July by gillnetting or angling (Gantner et al., 2009; Lehnherr et al., 2018; see Chapter 2). Over the 29-year period, no effect of the huge changes in the hydrological regime was discernible on the char body condition, growth rate, or diet. However, least square (LS) mean Hg concentrations in char muscle (length-adjusted) declined significantly from 1992 to 2019 ($p<0.001$; 3.4% per year; see Figure 5.5). The declining trend was not correlated with the increasing glacial meltwater inputs; however, a weak relationship was apparent with ice-free periods (see Figure 5.5).

The Cape Bounty Arctic Watershed Observatory on Melville Island (Nunavut, Canada) is home to two physically similar lakes located adjacent to each other (East Lake and West Lake), which have experienced significant changes in Arctic char length-adjusted Hg concentration over the past decade, albeit in opposite directions. Both lakes have experienced permafrost degradation in their catchments; however, West Lake has also undergone multiple subaqueous slumps (beginning in fall 2008), leading to a sustained increase in turbidity and resultant decrease in fish body condition (Roberts et al., 2017). There was a significant increase in length-adjusted Hg concentrations in West Lake between 2009 (after the first subaqueous slump) and 2017 (see Figure 5.6; Burke et al., 2021).

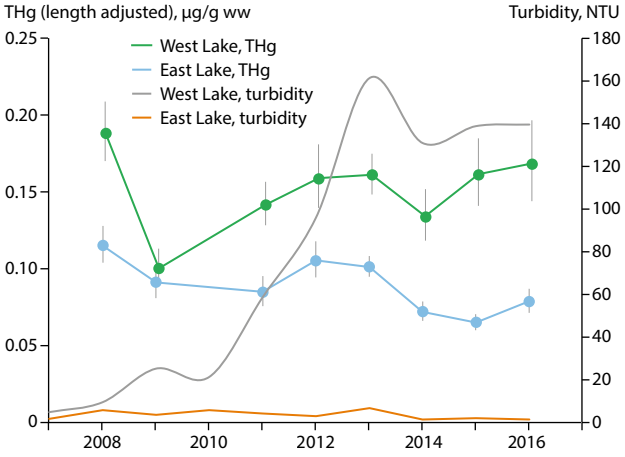

Figure 5.6 Length-adjusted (LS mean) THg (µg/g ww) for Arctic char collected between 2008 and 2016 from East Lake (blue line) and West Lake (green line) at the Cape Bounty Arctic Watershed Observatory on Melville Island (Nunavut, Canada). Lake water nephelometric turbidity units (NTU) between 2007 and 2016 in West Lake (grey line) and East Lake (orange line).

Conversely, between 2008 and 2019, there was a significant decrease in length-adjusted Hg concentrations in East Lake (see Figure 5.6; Burke et al., 2021). The best predictor of char length-adjusted Hg in East Lake was fish size-at-age (a proxy for growth), suggesting a somatic growth dilution effect (Karimi et al., 2007). The increased growth rates and resulting growth dilution were likely caused by reduced ice-cover duration resulting in increases in water temperature and/or primary production. In contrast, the best predictors of length-adjusted Hg-concentrations in West Lake were carbon and nitrogen stable isotope ratios, indicating a shift in diet likely brought on by the profound increase in lake turbidity. This paired study provides an example of how climate change can result in different proximate drivers of fish Hg concentrations in similar lakes in the same region, underscoring the difficulty of predicting trends in Arctic fish Hg under a changing climate.

5.6.3 Marine biota

In the Arctic marine environment, studies assessing how climate change-linked variation in diet or food-web composition affects THg (and persistent organic pollutant) levels in biota were reviewed earlier (McKinney et al., 2015). Reports came from marine mammals and seabirds in the Canadian Arctic, Greenland, and Svalbard, Norway. At that time, no such reports for THg in marine invertebrates or fish had been published, and no data were available from the Alaskan or Russian Arctic regions. There have since been several other reports, including in fish, and in Alaskan species, in terms of either associations between physical environmental changes or ecologically-based climate changes and biotic Hg concentrations. Below, we detail these studies, focusing first on reports in marine fish, followed by seabirds and then marine mammals.

Marine Fish. For marine fish, the concentrations of THg and other contaminants (polychlorinated biphenyls; PCBs, organochlorine pesticides and various flame retardants) were compared among native and northward redistributing non-native marine prey fishes in the eastern Canadian Arctic (Pedro et al., 2017), with particular attention to the keystone Arctic forage fish, Arctic cod, relative to its 'replacement' species, capelin (*Mallotus villosus*) and sand lance. Although not all species were collected in all regions, native benthic species, specifically sculpin spp. (*Cottoidea*) and northern shrimp (*Pandalus borealis*), showed the highest concentrations of THg (and other contaminants) of all species. Unlike for PCBs and OCs, THg concentrations were higher in Arctic cod than in capelin, and this difference was partly explained by differences in fish length. In a follow-up study, MeHg concentrations were found to be similar among Arctic cod, capelin, and sand lance (Pedro et al., 2019). For THg, another study in northern Hudson Bay also reported higher concentrations in Arctic cod than in capelin (Braune et al., 2014a). These findings together suggest that invading Subarctic capelin may be a similar or lower source of THg and MeHg relative to Arctic cod in Arctic marine food webs.

Seabirds. For Low and High Canadian Arctic seabirds, links between THg trends and diets and/or sea-ice conditions were investigated for thick-billed murres (Braune et al., 2014b). Increases in fish versus invertebrate prey have been found in the High Arctic (Provencher et al., 2012), and here, THg levels increased at a faster rate than when adjusted for diet change (using $\delta^{15}N$). Increases in lower trophic level capelin versus Arctic cod prey have been found in the Low Arctic in association with sea-ice declines, and here, THg levels did not show trends, while $\delta^{15}N$-adjusted trends increased. These findings may be partly explained by the co-occurring shift to lower trophic level prey, but it was suggested that changes in Hg cycles and bioavailability, along with other factors related to climate change, may also have played a role. In a follow-up study that focused on a suite of meteorological and climate variables, Foster et al. (2019) found that THg concentrations in both fulmar (*Fulmarus glacialis*) and thick-billed murre eggs were best explained by models that in addition to year and $\delta^{15}N$, also included time-lagged NAO, temperature, and/or sea-ice variables. This work suggests a combined effect of both physical and ecological influences of climate change on THg levels in these species. For thick-billed murres breeding in Hudson Bay, early results suggest that higher circulating concentrations of THg were related to lower circulating triiodothyronine that, in turn, was related to increased time diving under water when foraging for prey; however, these relationships were evident only when ice conditions were average (2016) or poor for the birds (2017, when the ice disappeared early) and not when there was more ice available later in the breeding season for the birds to forage from for prey (2018; Elliott et al., 2019).

A study conducted in East Greenland indicated that little auk (*Alle alle*) diet, derived from $\delta^{15}N$ and $\delta^{13}C$ values, showed only minor interannual variation over an eight-year period (Fort et al., 2016). Temporal changes in THg concentrations in little auks were not related to this minor dietary variation, but rather to contamination in their major zooplankton prey species.

For seabirds at two locations in Svalbard, two time-point comparisons of THg levels and $\delta^{15}N$ ratios (2008 and 2009) were made for black-legged kittiwake (*Rissa tridactyla*) and little auk (Øverjordet et al., 2015a). For kittiwakes, levels of THg were lower when they were feeding at a lower trophic position and with different feeding habits. The lower trophic position year had less ice and thus less access to Arctic cod, which are at a

higher trophic position than other prey. However, THg was not affected by trophic position in little auks, which exhibit more specialized feeding habits and feed mostly on invertebrates, relative to the more opportunistic feeding behavior exhibited by kittiwakes, which feed on various fish and invertebrates. A seasonal study from Svalbard indicated a decrease in THg and MeHg from May to July to October in kittiwakes and from May to July in little auks, which coincided with a decline in trophic position (Øverjordet et al., 2015b; Ruus et al., 2015). This led also to lower trophic magnification factors in October than in May and July (Ruus et al., 2015). A separate long-term temporal trend study related Hg concentrations in kittiwakes to climate-induced changes in sea-ice extent in Svalbard (Tartu et al., 2022). Mercury concentrations in chick-rearing kittiwakes captured in Kongsfjorden, Svalbard from 2000 to 2013 declined by 3% per year, after which they increased by 11% per year until 2019. Sea-ice extent and Chl-a showed a U-shape association with Hg concentrations in kittiwakes. Chlorophyll-a, but also sea-ice extent, can be used as reliable predictors of shifts in fish communities (Eisner et al., 2013; Mérillet et al., 2020). The blood Hg U-shaped trend is likely due to a shift from polar cod to Atlantic fish species in kittiwake diet, and then likely increased in the later years due to the input of MeHg from Arctic shrinking sea ice (Vihtakari et al., 2018; Schartup et al., 2020).

Marine mammals. The ringed seal has been a key biomonitoring animal for AMAP for evaluating trends of contaminants in the Arctic. Temporal trends of THg in ringed seals from different regions of the Canadian Arctic were evaluated in relation with climate variables such as air temperature, precipitation, ice coverage and climatic indices (Houde et al., 2020). More than 1500 ringed seals from regions of the Beaufort Sea, the central Arctic, eastern Baffin Island, Hudson Bay and Ungava/Nunatsiavut were collected with the help of Inuit communities between 1972 and 2017. Concentrations of THg were found to be stable through time in seal liver. However, THg levels in muscle significantly decreased over time (approximately -1% per year) in seals from Hudson Bay and Ungava/Nunatsiavut. Concentrations of THg in both liver and muscle tissues were found to significantly increase with $\delta^{15}N$ in seals. Carbon stable isotope ($\delta^{13}C$) values in the muscle of seals decreased significantly through time in several regions suggesting a shift in diet towards pelagic and/or offshore preys (Houde et al., 2020). Variation partitioning analyses across regions indicated that age (7.3% to 21.7%) was the dominant factor explaining THg accumulation in seal liver; diet (up to 9%) and climate (3.5% to 12.5%) were also variables of importance (Houde et al., 2020). Climate indices, including Arctic Oscillation (AO), North Atlantic Oscillation (NAO) and Pacific/North America pattern (PNA), mainly explain the climate variables in comparison to ice coverage and air temperature/precipitation. Correlation analyses between THg concentrations in seal liver/muscle and environmental variables indicated several significant associations which varied by regions and tissues (see Figure 5.7). For example, the total precipitation (including rain and snow) was negatively related to THg muscle concentrations

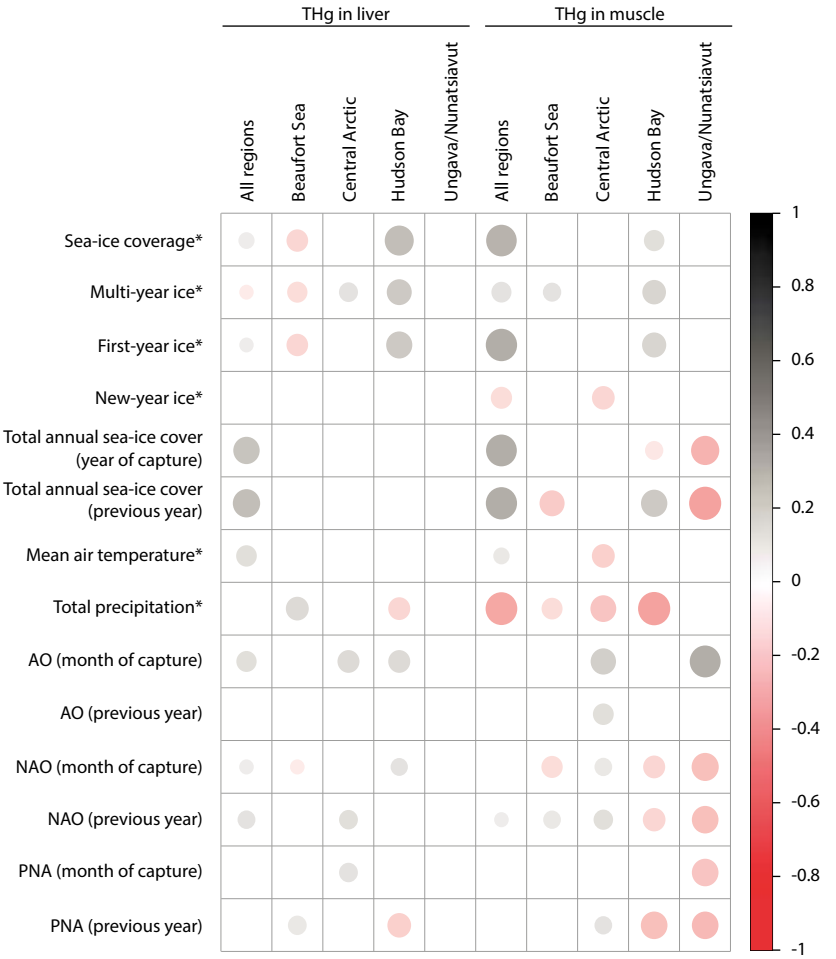

Figure 5.7 Correlations between THg in the liver and muscle of ringed seals and environmental factors for specific regions of the Canadian Arctic as well as overall. The size of the circles indicates the strength of the relationships. Black indicates positive correlations and red indicates negative associations ($p<0.05$). *Based on the available data for the month of capture. AO: Arctic Oscillation; PNA: Pacific/North American pattern; NAO: North Atlantic Oscillation. See Houde et al., 2020 for details.

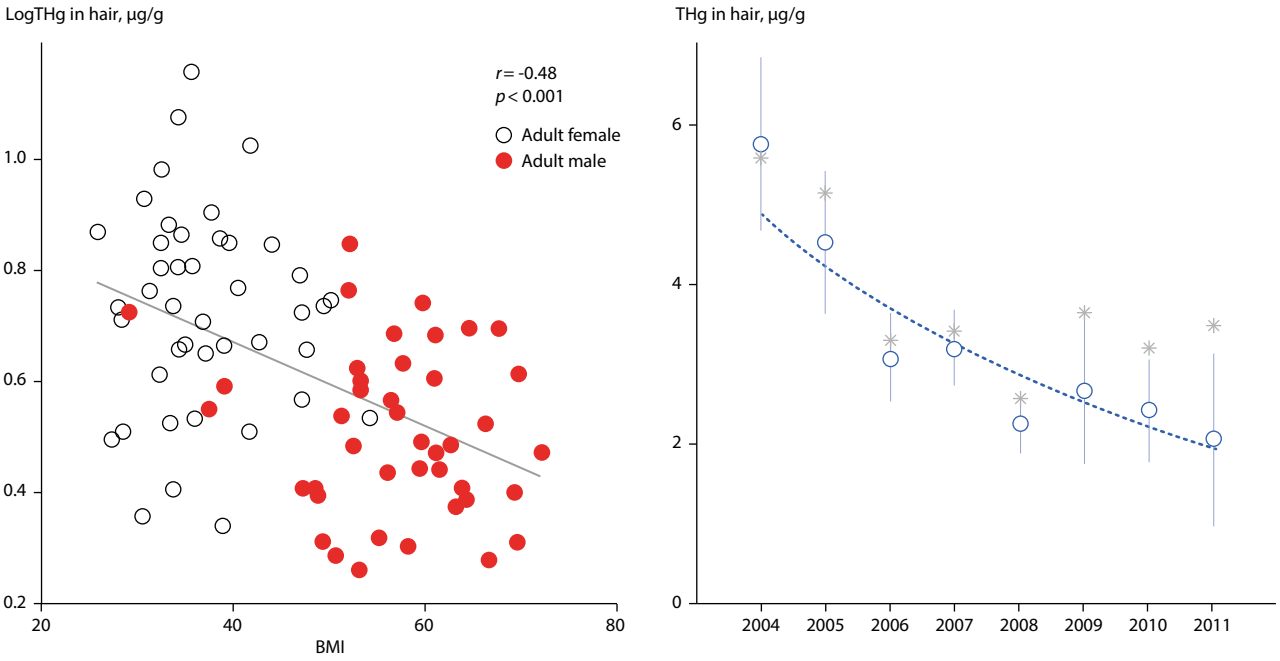

Figure 5.8 Correlation between hair log-total mercury (THg) concentrations in adult female polar bears (blue circles) and adult male polar bears (red circles) and body mass index (BMI) (left panel); time trends in median hair THg concentrations (±SE; open circles, dashed line) from adult polar bears (males and females combined) for 2004–2011 in the southern Beaufort Sea (right panel). Log-linear declining trends were significant (-13% per year, r^2=0.84, p=0.002). Annual medians adjusted to the covariate body mass index (BMI) are also shown (asterisks, no line). Log-linear trends in these adjusted means were not significant (-6.6% per year, r^2=0.41, p=0.08). Raw medians, not log-transformed values, are shown for ease of visualizing the concentration changes. Figure modified from McKinney et al., 2017b.

in seals from the Beaufort Sea, the central Arctic and Hudson Bay. Multiple site-specific relationships were also found between the total annual sea-ice coverage and THg levels in seals. Moreover, positive correlations between THg levels and the AO (recorded in the year of seal capture) were observed for several regions and both tissues. Overall, results from this study indicated that environmental factors may be influencing, in a site-specific manner, the accumulation of THg in ringed seals across the Canadian Arctic.

In central West Greenland, Northwest Greenland (Avanersuaq) and central East Greenland (Ittoqqortoormiit), THg temporal trends in ringed seal liver were assessed in relation to climate metrics, including water temperature, sea-ice coverage and Arctic Oscillation (AO) index (Rigét et al., 2012). From the early 1980s to 2010, THg levels rose by 10% and 2% per year in central East Greenland and Northwest Greenland, respectively. In addition to other factors, such as year, age and trophic position, THg levels in all three regions were explained by the winter AO index. That is, levels of THg were higher when the AO was higher (i.e., when conditions enhanced transport of air masses from North America and Europe to the region and when precipitation was higher). Rigét et al. (2012) suggested that higher THg levels may be found in ringed seal livers under climate change due to greater atmospheric and fluvial transport.

From the mid-1980s or 1990s to the 2000s in Hudson Bay and Foxe Basin, Canada, levels of THg declined in beluga whale (*Delphinapterus leucas*) but not in Atlantic walrus (*Odobenus rosmarus*) and narwhal (*Monodon monoceros*; Gaden and Stern, 2010). Values of $\delta^{13}C$ also declined in beluga, suggesting the possibility of a shift to increased consumption of prey farther offshore or pelagic-associated prey or habitat, but only weak associations of $\delta^{13}C$ with the NAO index were found. Additionally, no associations were found between $\delta^{15}N$ or THg with NAO. In another study on beluga whales in the Canadian Arctic, THg levels increased between 1981 and 2002, but then declined or stabilized between 2002 and 2012 in individuals from the Beaufort Sea (Loseto et al., 2015). Climate indices, such as the Pacific Decadal Oscillation (PDO) with an eight-year time lag, better explained variation in THg levels than did $\delta^{13}C$ or $\delta^{15}N$ ratios.

For polar bears from the southern Beaufort Sea region of Alaska, as the sea ice has declined both spatially and temporally, the proportion of the subpopulation spending an extended period of time (>21 days per year) onshore during the reduced ice season has risen (Atwood et al., 2016). While onshore, these polar bears consume the remains of subsistence-harvested bowhead whales and possibly other prey (Schliebe et al., 2008; Rogers et al., 2015; McKinney et al., 2017a; Bourque et al., 2020). Levels and trends of THg in hair were investigated in this polar bear subpopulation over a period of increasing land use from 2004 to 2011 (McKinney et al., 2017b). Levels of THg declined in spring-sampled polar bears by 13% per year, mainly driven by declines in adult males. Lower THg concentrations were associated with higher body mass index (BMI) and higher proportional consumption of lower trophic position prey. Trends in THg, adjusted for BMI, showed non-significant declines, suggesting that altered feeding and condition, not declining environmental concentrations of Hg, were responsible for these short-term declines in THg concentrations (see Figure 5.8). As longer-term studies of this polar bear population (Rode et al., 2010, 2014) and some other populations have conversely shown declines in polar bear body condition, McKinney et al. (2017b) suggested that body condition declines that occur under climate change should, in fact, drive up circulating levels of THg.

Case Study 5.2 Total mercury associations with climate variables in Hudson Bay polar bear, thick-billed murre and caribou

Total mercury concentrations (µg/g dw) did not change significantly over time in Hudson Bay wildlife, including polar bears (liver, 2007/08-2015/16), thick-billed murre (eggs, 1993–2015 normalized to the mean $\delta^{15}N$=14.2‰), or caribou from the Qamanirjuaq herd (kidney, 2006–2015, normalized to the mean age=6.2 y; Morris et al., 2022). THg concentrations in murres were normalized to the mean $\delta^{15}N$ to compensate for the significant decrease observed from 1993 to 2015, as also previously noted at both Coats Island (Akpatordjuark) and High Arctic murre colonies (Braune et al., 2014b). The $\delta^{15}N$ and $\delta^{13}C$ ratios in polar bears did vary by year, with diet previously identified as a significant factor affecting contaminant concentrations in bears from the Western Hudson Bay (WHB) subpopulation (McKinney et al., 2009, 2010); however, the extent of the data did not allow for dietary normalization in both subpopulations, which would be necessary for comparison. Regardless, these changes are important to consider as they have not been uniform over time. In polar bears from the Southern Hudson Bay (SHB) subpopulation, the mean $\delta^{13}C$ appeared to have increased by 0.037‰ per year between spring 2010 and spring 2016 while the mean $\delta^{15}N$ appeared to have decreased by -0.022‰ per year, though interpretation is limited as those regressions were not significant. Like the SHB subpopulation, the $\delta^{15}N$ signatures may have decreased in the WHB subpopulation in the period from fall 2007 to fall 2015 by -0.059‰ per year, however, only the $\delta^{13}C$ changed significantly, decreasing over that period by -0.059 ‰ per year (Morris et al., 2018, 2022), indicating changes in the opposite direction of the SHB bears and possibly a greater influence of terrestrial/inland resources and/or changes in prey species of seal as previously observed (McKinney et al., 2009).

General linear models (GLMs) tested the effects of year, climate and weather variables (time-lagged zero to three years) and their interactions with THg concentrations in these populations (see Table 5.2). First, sea ice exhibited significant relationships with THg concentrations in caribou and SHB polar bears but not in WHB bears or murres. More sea ice in the eastern Hudson Bay (later break-up dates, shorter ice-free periods, or greater fall sea-ice coverage) was consistently associated with greater concentrations of liver THg in SHB polar bears. The two strongest models for caribou found that concentrations of THg increased when the one year and two year time-lagged ordinal dates of sea-ice freeze-up were later (calculated based on 50% and 90% coverage, respectively). Compensating for the freeze-up date one year prior to sampling also produced a significant trend with year (4.4% per year) in the multivariate model with sea ice in caribou. Greater ice coverage, shorter ice-free periods and later break-up times allow polar bears to effectively hunt high trophic level prey, such as seals, for longer periods of time (Derocher et al., 2004). Macdonald et al. (2005) also hypothesized that more sea ice would limit Hg volatilization and increase bioavailability to the marine food web, both of which could increase levels of Hg as observed in Morris et al. (2022). Conversely, lower concentrations of THg in murre eggs and caribou were related to June and summer AO+ values three years prior to sampling for both species. The latitude of the Hudson Bay study sites situates them between zones of influence of the oscillation indices and directly in the latitude of the westerly winds and the jet stream, which strengthen under AO+ conditions. In murre eggs, higher annual sea-level pressures one year prior to sampling were associated with greater concentrations of THg, corroborating the June AO model, as in the AO- phase, sea-level pressure is greater at greater latitudes, and THg concentrations tended to be greater in that phase of the AO. In addition, greater precipitation levels in the summer or fall one year prior to sampling resulted in greater tissue residues of THg in WHB polar bears and caribou, which is a logical result of greater atmospheric scavenging and deposition associated with more precipitation (Macdonald et al., 2005). Greater fall and annual wind speeds (with a three year time lag) were related to lower concentrations of Hg in murre eggs, but greater winter wind speeds (with no time lag) were related to greater concentrations in WHB polar bear livers. Differences in time lags, wind direction and the status of the oscillation indices would all affect how contaminants are delivered or dispersed by greater wind speeds depending on the source region, which may explain these differences between the species. Finally, SHB bears exhibited significant positive relationships between THg and forest-fire extent (total hectares burned annually) in the Northwest Territories and Manitoba (Morris et al., 2022). These relationships could be due to emissions of Hg or, for example, from enrichment of the HB food web due to increased nutrient inputs and productivity after fires, which resulted in greater concentrations of Hg in high trophic position lake fish (Kelly et al., 2006).

Hair samples from 117 Northwest Greenland polar bears were taken between 1892 and 2008 and analyzed for total Hg. The sample, representing 28 independent years, showed yearly significant increases of 1.6% to 1.7% ($p<0.0001$) in the period from 1892 to 2008 and the two most recent median concentrations, from 2006 and 2008, were 23- to 27-fold higher respectively than the baseline level from 1300 AD in the same region, Nuullit (Dietz et al., 2011). The authors found a significant correlation ($p=0.0478$) between Hg and the $\delta^{13}C$, which together with the finding of higher Hg in ringed seals linked to shorter ice-free periods in the western Canadian Arctic (Gaden et al., 2009) and increasing trends in ringed seals in Northwest Greenland from 1984 to 2008 (Rigét et al., 2012), means that climate may have contributed to the observed increases in ringed seals and polar bears in Northwest Greenland (Dietz et al., 2011; Rigét et al., 2012).

Temporal trends of Hg in relation to variation in dietary carbon, nitrogen and sulphur were investigated in 199 hair samples from adult female polar bears sampled from Svalbard between 1995 and 2016 (Lippold et al., 2020). Temporal decline in hair $\delta^{13}C$ and $\delta^{34}S$ values indicated that the importance of terrestrial food items in polar bears' summer diet has increased over time. Alternatively, changes in $\delta^{34}S$ are hypothesized to reflect a higher sulfate reduction rate linked to higher Hg methylation in the environment (Elliott and Elliott, 2016); however, this relationship is often too confounded by dietary source to

Table 5.2 Results of general linear model[a] tests of weather and climate factors with concentrations of total mercury (THg, µg/g dw) in kidney of caribou from the Qamanirjuaq herd, eggs of thick-billed murres, and liver of southern and western Hudson Bay (SHB and WHB) polar bears. Constants (β_0) are shown with the coefficients (β_x), listed in the order in the formula given in the model (Morris et al., 2022). Models are listed in order of lowest to highest Akaike Information Criterion corrected for small sample sizes (AIC_C).

Models	n	β_0	β_1	β_2	AIC_c	MSE[b]	r^2_{ADJ}	*p* value
Caribou (Qamanirjuaq herd; kidney)[c]								
Year	10	-63	0.032	--	11.2	0.11	0.002	0.34
2-y lagged Central HB >90% freeze-up	10	-10	0.034	--	2.08	0.040	0.60	0.005
Year + 1-y lagged NW HB >50% freeze-up	10	-104	0.043	0.060	3.03	0.032	0.72	0.005
3-y lagged summer AO	10	1.4	-0.52	--	6.20	0.054	0.39	0.031
1-y lagged fall precipitation[d]	7	-0.83	0.012	--	--	--	0.58	0.029
Thick-billed murre (egg)[e]								
Year	13	-16	0.008	--	-14.54	0.013	0.11	0.139
1-y lagged annual sea-level pressure	13	-104	0.10	--	-23.97	0.006	0.57	0.002
3-y lagged fall wind speeds	13	0.20	-0.029	--	-17.51	0.010	0.29	0.032
3-y lagged June AO	13	-0.30	-0.12	--	-17.41	0.012	0.29	0.034
3-y lagged annual wind speeds	13	1	-0.072	--	-17.34	0.012	0.29	0.035
Western Hudson Bay polar bears (liver)								
Year	8	-58	0.031	--	8.59	0.060	-0.013	0.38
Winter wind speeds	8[f]	0.57	0.12	--	0.027	0.028	0.65	0.009
3-y lagged fall air temperature	8	3.4	0.12	--	3.34	0.036	0.47	0.035
1-y lagged summer precipitation	5	2.4	0.005	--	--	--	0.93	0.006
Southern Hudson Bay polar bears (liver)								
Year	7	-86	0.044	--	6.31	0.035	0.30	0.119
1-y lagged NT total ha burned (fire)	7	2.90	1.5E-07	--	0.32	0.027	0.70	0.012
Eastern HB <30% break-up date	7	1.3	0.010	--	0.39	0.027	0.70	0.012
Eastern HB ice-free days[g]	7	4.2	-0.007	--	1.01	0.026	0.67	0.015
Eastern HB summer sea-ice coverage (%)	7	2.8	0.013	--	1.05	0.029	0.67	0.015
Eastern HB fall sea-ice coverage (%)	7	2.8	0.20	--	1.42	0.031	0.65	0.018
2-y lagged MB total ha burned (fire)	7	2.9	4.2E-07	--	2.28	0.15	0.61	0.024

[a] The GLMs used a backwards stepwise procedure to find the model with the lowest AIC_C from the basic formula LN [THg µg/g dw]=$\beta_0 + \beta_1$.Year + β_2.Climate/Weather factor + β_3.(Year x Climate/Weather factor).
[b] MSE = mean squared error from leave-one-out cross-validation procedures; the MSE values indicated that the models were consistent, though the exact rankings did differ from those based on the AIC_C.
[c] Caribou THg concentrations were normalized to a mean age of 6.2 years prior to GLM modeling.
[d] AIC_C values are not shown for precipitation due to multiple missing values, which prohibits comparisons as only models with equal n values can be compared using their AIC_C.
[e] Concentrations of THg in murre eggs were normalized to a mean $\delta^{15}N$ of 14.2‰.
[f] One of the winter wind-speed values was missing and was imputed in order to facilitate comparisons using AIC_C.
[g] This ice-free period was calculated as the number of days between the date of <30% sea-ice coverage at break-up and the >10% coverage at freeze-up.

clearly quantify the importance of sulfate reduction in Hg levels in biota. THg concentrations increased with increasing $\delta^{13}C$ and $\delta^{34}S$ values, which suggested that polar bears with a more mixed diet were less exposed to Hg than those with a solely marine diet. Concentrations of THg increased between 1995 and 2016, with a steeper increase after 2000, which was possibly related to climate-change driven re-emissions from thawing sea ice, glaciers, and permafrost. When THg concentrations were adjusted for $\delta^{13}C$ or $\delta^{34}S$ variation, the increase in the later period was slightly steeper, but the trends were not significantly different. This suggests that the diet change towards more terrestrial food items exposed polar bears to lower THg concentrations; nonetheless, the temporal trend of THg in these polar bears is not yet significantly affected by dietary changes. A further study on spatial variation in THg concentrations in relation to diet in polar bears from Svalbard and the Russian Arctic indicated that spatial variation in THg concentrations was minor and not explained by variation in $\delta^{13}C$ and $\delta^{15}N$ values (Lippold et al., 2022).

The presence of sea ice likely plays a role in the exposure to Hg in polar bears. A circumpolar study on polar bears investigated how liver concentrations of Hg were related to lipid and carbon sources inferred from fatty acid composition and $\delta^{13}C$ (Routti et al., 2012). Concentrations of Hg were positively related to proportions of fatty acids abundant in sea

ice-associated copepods, suggesting that Hg levels are higher in polar bear food webs rich in sea ice associated copepods. This finding is in agreement with high MeHg concentrations below the productive surface layer in the marginal sea-ice zone, which likely enhances uptake and bioavailability of MeHg in food webs (Heimbürger et al., 2015). The polar bear study also concluded that Hg accumulates to a larger degree in polar bears feeding in areas with higher riverine inputs of terrestrial carbon versus those feeding in areas with lower freshwater inputs (Routti et al., 2012).

Polar bears and ringed seals form a strong predator-prey relationship in the Arctic and are experiencing loss of sea-ice habitat and harmful dietary exposure to THg and other pollutants. The spring sea-ice period is important for both polar bears and ringed seals, as polar bears use sea ice as a hunting platform during spring before sea-ice break-up, while ringed seals use the sea ice for pupping and their annual molt prior to feeding intensively during the open-water period. Both species are opportunistic foragers and consume a wide variety of prey items, and a recent study investigated whether both polar bears and ringed seals inhabiting the same geographic area are responding to ecosystem changes similarly by investigating temporal patterns of polar bear and ringed seal THg concentrations, niche dynamics and body fat condition (Yurkowski et al., 2020). Polar bear hair and adipose samples as well as ringed seal muscle were collected between 2003 and 2016 in southwestern Hudson Bay. Interannual changes in polar bear $\delta^{15}N$ values were strongly correlated with ringed seal $\delta^{15}N$, indicating that temporal changes in polar bear $\delta^{15}N$ values are dependent on ringed seal $\delta^{15}N$ values and suggesting that mechanisms which influence interannual variability in food chain dynamics lower in the food web may affect both polar bears and ringed seals similarly. A decline in THg concentration (by 3.8% per year) and $\delta^{13}C$ (by 1.5‰ over 13 years) occurred in ringed seals suggesting a change in feeding habits and increased use of phytoplankton carbon versus benthic or sympagic carbon over time, whereas no such changes occurred in polar bears. Additionally, three-dimensional niche size, based on $\delta^{13}C$, $\delta^{15}N$ and THg concentration, decreased in polar bears but not in ringed seals. The $\delta^{13}C$ range also decreased in polar bears, but significantly increased in ringed seals. These contrasting patterns suggest that the two species are likely responding differently to temporal changes in carbon production between pelagic, sympagic and benthic pathways as well as to interannual changes in prey availability. Finally, a ~1.5-fold increase in $\delta^{13}C$ spacing between the species niches suggested different responses to annual changes in sympagic-pelagic carbon source production. The changing foraging ecologies for both polar bears and ringed seals suggested a weakening of this predator-prey relationship; polar bears still derive most of their carbon energy from sympagic sources (~80%; Brown et al., 2018), while ringed seals are now more associated with pelagic carbon (Yurkowski et al., 2020). Indications of the polar bear-ringed seal relationship weakening with climate change is also apparent in East Greenland (McKinney et al., 2013; Dietz et al., 2018b) and Svalbard (Hamilton et al., 2017). These trends are only likely to continue with our current greenhouse gas emissions which are resulting in the continual deterioration of polar bear and ringed seal habitats (Castro de la Guardia et al., 2013).

Across Arctic regions, Arctic marine mammals go through seasonal changes in their stores of body fat. For example, polar bears generally feed extensively in spring and early summer when ringed seals are pupping and molting on sea ice. During sea-ice free periods, polar bears have reduced, if any, access to food and therefore they fast. Pregnant females spend winter in the den, so they can fast for up to eight months in a row. As discussed in their Alaskan polar bear study, McKinney et al. (2017b) suggested that hair MeHg deposition may be increased in fasting polar bears that catabolize proteins and thus mobilize MeHg into the blood circulation. This is supported by findings of a negative, although non-significant, trend between body condition and hair THg in female polar bears from Svalbard (Lippold et al., 2020). However, temporal changes in polar bear body condition did not affect temporal trends of THg in polar bears from Svalbard. Similarly to the polar bear studies, feather Hg concentrations were negatively related to body condition in little auks from East Greenland (Amélineau et al., 2019), yet an opposite relationship was found for blood Hg concentrations and body condition in common eider ducks (*Somateria mollissima*; Provencher et al., 2016a). Liver concentrations of THg in arctic foxes were not related to their body fat (Hallanger et al., 2019). Blévin et al. (2017a) hypothesized that Hg, among other pollutants, would affect metabolic rate through changes in thyroid hormone levels in kittiwakes from Svalbard. The results showed, however, that Hg was not related to metabolic rate in either males or females.

5.7 Conclusions and recommendations

Conclusions (in numbered bullets) are organized under section headings (section numbers in square brackets) followed by recommendations in italics where appropriate.

How has climate change affected the physical and biogeochemical characteristics of Arctic environments? [5.2]

1. Climate change, at local and regional scales, is profoundly affecting physical and biogeochemical characteristics that interact with the Hg cycle across all Arctic environmental compartments.
2. Atmospheric conditions are changing with warmer air temperatures in winter and summer, increasing precipitation, and a shift from snow to rain.
3. Ocean circulation and particularly Arctic sea-ice conditions are changing dramatically, including reduced extent, thickness, and snow depth over ice, altered timing, increased mobility, loss of multi-year ice and an increase in the extent of halogen-rich first-year ice.
4. In the terrestrial environment, warmer and wetter conditions are leading to permafrost thaw, glacier melt as well as changes in soil and hydrological processes; greater evaporation and drought conditions are resulting in an increase in the severity and extent of wildfires.
5. Earlier ice and snowmelt and warmer temperatures are altering lake stratification, while altered hydrology and catchment characteristics are increasing the transport of organic matter to downstream water bodies.

How has climate change affected Arctic ecosystems? [5.3]

6. Arctic marine biota are responding to climate change either directly, associated with thermal or acidity tolerance, or indirectly, in relation to other species' ranges or populations, including northward range shifting boreal species. Food web responses may be particularly important and include bottom-up effects from changing prey and top-down effects from changing predators.
7. Terrestrial monitoring and experimental studies in the circumpolar Arctic suggest that both grass and grass-like plants and shrubs respond positively to warming and their abundance is likely to increase over time.
8. Warm spells in winter and rain-on-snow events have been shown to negatively affect reproduction and survival of High Arctic tundra herbivores and have further consequences on the abundance of Arctic carnivores.
9. Warmer-adapted terrestrial and aquatic species are extending their range and abundance into the Arctic and will likely alter food web structure and function.
10. Carbon and nutrient leaching from catchments, driven by climate change, increases the overall productivity of freshwater ecosystems. Lower visibility in murky lakes from organic carbon loading (browning) promotes pelagic primary and secondary production over benthic production. Increased productivity of lakes can promote anoxic conditions, especially in winter.

What influence has climate change had on mercury transport processes? [5.4]

11. Modeling results suggest climate change may be impacting atmospheric Hg deposition in the Arctic. However, process-focused information on interactions between climate and Hg deposition is lacking, and current Hg models may not represent the complexity of those climate-sensitive processes.
12. Arguably the clearest evidence of current climate change effects on Hg cycling in the Arctic is for Hg transport from terrestrial catchments. Widespread permafrost thaw, glacier melt and coastal erosion are altering the sources and fluxes of Hg across Arctic catchments. Changes in catchment transport processes are being reflected in Hg accumulation rates in lake sediment cores, especially in watersheds undergoing dramatic change as a result of permafrost thaw and glacial melt. Greater organic matter transport, particularly dissolved organic carbon, may also be influencing the downstream transport and fate of Hg in Arctic freshwater ecosystems.
13. Recent estimates suggest that Arctic permafrost is a large global reservoir of Hg, which is vulnerable to degradation under a warming climate during the 21st century. The fate of permafrost soil Hg is not well understood.
14. Alterations to the terrestrial landscape including the development of thermokarst features, the formation and expansion of thaw lakes, and increased soil erosion will result in greater transport of particulate-bound Hg to Arctic rivers. In-stream processing and deposition processes will ultimately determine whether particulate Hg travels downstream to estuaries or is stored more locally in river and stream sediments.
15. Increasing severity and incidence of wildfires both locally within the Arctic and across boreal regions may be contributing to the atmospheric pool of Hg. Long-term implications of climate change interactions with wildfires are not well understood.
16. Limited information is available on recent climate change-driven alterations in transport of Hg by ocean currents.

Atmospheric deposition of Hg may be affected by climate change and further research to identify key climate influences on this flux is a priority. Changing winter and spring conditions and an increase in the presence of halogens in the lower atmosphere and on snow and ice surfaces are important factors to include in future modeling.

Long-term monitoring of Hg in Arctic terrestrial environments at the catchment scale would improve the detection of changes in Hg transport due to climate warming. Quantification of Hg sources and downstream fate (e.g., lake sediments) at the catchment scale should be combined with Hg transport in large rivers, which reflects processes occurring across Arctic catchments.

Improved geographic coverage for measurements and modeling of changes in Hg transport associated with thawing permafrost, melting glaciers and wildfires is a priority to better constrain implications for the Arctic Hg cycle.

Interactions between climate and Hg transport in the Arctic Ocean remains a major knowledge gap that warrants further research.

What are the impacts of climate change on mercury biogeochemical processes? [5.5]

17. Interactions with climate change remain poorly understood for many aspects of Hg biogeochemical cycling in the Arctic.
18. Redox transformations of inorganic Hg affect fluxes between the atmosphere and terrestrial or aquatic environments. Changes to the cryosphere, particularly reduced sea-ice cover and higher chloride in snow, are likely to alter the seasonal evasion or retention of inorganic Hg.
19. Mercury deposition on the Arctic tundra is controlled by uptake of Hg(0) by plants. Greater vegetation-cover and length of the growing season on the tundra may increase the accumulation of atmospheric Hg by plant uptake.
20. Experimental evidence indicates that warmer temperatures can enhance MeHg production in freshwater and marine sediments as well as in tundra soils.
21. Evidence from Hg stable isotopes in the marine environment and lake experiments suggests the

photochemical breakdown of MeHg will be enhanced in seawater due to sea-ice loss and altered in fresh waters due to changes in dissolved organic carbon loading.

Further investigation of climate change impacts on redox transformations of inorganic Hg and the production of MeHg is a priority to better constrain long-term changes in Hg bioavailability to food webs. In situ process measurements and the development of mechanistic/stochastic models that couple Hg transport and transformations with climate models would allow projections under various climate change scenarios in the Arctic.

The effects of increasing vegetation cover and length of the growing season on plant uptake of atmospheric Hg(0) are a priority for research because of the potential for enhanced Hg accumulation in the Arctic tundra.

How has climate change altered mercury exposure in Arctic biota? [5.6]

22. Climate and weather variables, including sea-level pressure oscillations and sea-ice patterns, sometimes with single- or multi-year time lags, have been linked to spatial and temporal variation in tissue Hg concentrations in some Arctic marine and terrestrial species. These findings suggest that variation and change in wind, precipitation and the cryosphere affecting the atmospheric and aquatic transport of Hg may, in turn, be impacting Hg exposures in Arctic biota.

23. Changing species interactions due to, for example, northward range shifts of Subarctic marine and terrestrial species, may alter Hg exposures in Arctic biota. At least for the keystone Arctic prey fish, Arctic cod, THg and MeHg concentrations were similar or even higher than in its Subarctic 'replacement' species, capelin, in the eastern Canadian Arctic. Consistent with this, thick-billed murres in Hudson Bay, which have switched to feeding on more capelin relative to Arctic cod, showed increases in THg levels only after adjusting for changes in trophic position. Similarly, THg concentrations in Svalbard kittiwakes, which have more Atlantic-type prey in the diet, were lower. Several studies have shown higher Hg concentrations in marine animals with low body condition, suggesting that, all else being equal, climate-related decreases in body condition may lead to higher Hg exposure in some Arctic species.

24. Climate change-related secondary emissions have likely led to increased Hg concentrations in Svalbard polar bears. Dietary changes towards food items with lower Hg concentrations have slowed down the increase slightly, but not significantly.

25. Climate-related variation in food availability (terrestrial vs. ice-associated) for Arctic foxes was associated with altered Hg concentrations in Arctic foxes but had only a minor influence on temporal trends of Hg in Arctic foxes.

26. Climate-influenced processes such as food-web exposure to MeHg, shifts in dominant energy pathways of food webs and growth dilution have been shown to affect Hg bioaccumulation in Arctic freshwater fish. The importance of climate change in affecting these processes remains unclear and likely varies due to site-specific conditions.

27. Multi-decadal time series of Hg concentrations in Arctic freshwater fishes have been examined for influences of climate change on bioaccumulation. Based on several studies and fish species, it is clear the effects of climate change on fish Hg concentrations are complex, difficult to predict, and are often lake- and region-specific.

28. Climate change may affect Hg levels in Arctic biota in myriad ways, including numerous physical changes impacting Hg transport and deposition as well as complex biological and ecological changes impacting Hg uptake and fate in organisms and trophic transfer through food webs.

Due to a limited number of populations and species examined for Hg-climate change linkages within marine, and, in particular, terrestrial and freshwater systems to date, further study of the relative importance of climate change factors and how they may vary through space and time, which would require broader geographic coverage, is needed to determine the net impact of climate change on biotic Hg concentrations in Arctic ecosystems.

Long-term pan-Arctic Hg monitoring programs on Arctic biota should consider ancillary datasets on climate and weather and develop ecological and physiological datasets (e.g., by merging traditional metrics with modern methods such as bulk and compound-specific stable isotopes, and fatty acids) to interpret spatial variation and temporal trends in Hg.

6. What are the toxicological effects of mercury in Arctic biota?

Leads: Rune Dietz and Robert J. Letcher

Co-authors: Joshua T. Ackerman, Benjamin D. Barst, Niladri Basu, Olivier Chastel, John Chételat, Sam Dastnai, Jean-Pierre Desforges, Collin A. Eagles-Smith, Igor Eulaers, Jérôme Fort, Jacob Nabe-Nielsen, Christian Sonne, Feiyue Wang and Simon Wilson

Data and Sample Contributors: Jon Aars, Magnus Andersen, Céline Albert, Birgitta Andreasen, Dennis Andriashek, Frédéric Angelier, Aurora Aubail, Claus Bech, Pierre Blevin, David Boertmann, Andrei Boltunov, Erik W. Born, Jan Ove Bustnes, Paco Bustamante, Tomasz M. Ciesielski, Jóhannis Danielsen, Sarah Danielsen, Maria Dam, Krishna Das, Andrew E. Derocher, Sébastien Descamps, Kyle Elliott, Kjell Einar Erikstad, Alexey Ezhov, Mark Evans, Anita Evenset, Steve Ferguson, Michelle G. Fitzsimmons, Eva Fuglei, Geir Wing Gabrielsen, Mary Gamberg, Nikolaus Gantner, Maria Gavrilo, Grant Gilchrist, Olivier Gilg, Sindri Gíslason, David Grémillet, Elena Golubova, Ingeborg G. Hallanger, Erpur Hansen, Scott Hatch, Mads P. Heide-Jørgensen, Lars-Eric Heimbürger-Boavida, Lisa B. Helgason, Paul F. Hoekstra, Magali Houde, Katrin Hoydal, Karista Hudelson, Nicholas Per Huffeldt, Audrey Jæger, Dariusz Jakubas, Bjørn M. Jenssen, Jon Einar Jónsson, Alexander Kitaysky, Stephen G. Kohler, Yann Kolbeinsson, Yuri Krasnov, Martin M. Larsen, Sarah Leclaire, Ulf Lindstrøm, Anna Lippold, Erlend Lorentzen, Lisa Loseto, Nick Lunn, Mark Mallory, Flemming Ravn Merkel, Francoise Messier, Cecilie Miljeteig, Børge Moe, William A. Montevecchi, Adam Morris, Anders Mosbech, Derek C.G. Muir, Nynne H. Nielsen, Sanna T. Nielsen, Martyn Obbard, Bergur Olsen, Rachael A. Orben, Allison Patterson, Elizabeth Peacock, Marie Perkins, Marianna Pinzone, Amanda Poste, Michael Power, Isabeau Pratte, Jennifer Provencher, Tone Kristin Reiertsen, Heather Renner, Frank F. Rigét, Gregory J. Robertson, Nora Rojek, Marc Romano, Aqqalu Rosing-Asvid, Heli Routti, Kjetil Sagerup, Filipa Samarra, Halvor Saunes, Ursula Siebert, Jens Søndergaard, Garry Stenson, Gary Stern, Ian Stirling, Jakob Strand, Hallvard Strøm, Heidi Swanson, Akinori Takahashi, Sabrina Tartu, Mitch Taylor, Grigori Tertitski, Jean-Baptiste Thiebot, Phil Thomas, Elena Tolmacheva, Torkel Lindberg Tórarinsson, Gabriel Treu, Gisli A. Víkingsson, van der Velden, Cortney Watt, Jeffrey M. Welker, Øystein Wiig, Alexis P. Will, Katarzyna Wojczulanis-Jakubas and Glenn Yannic.

6.1 Introduction

In order to address the question "What are the toxicological effects of mercury (Hg) in Arctic biota?", this chapter builds on the recent assessment of the risk of toxicological effects to Arctic biota from contaminant exposure (AMAP, 2018a; Dietz et al., 2019a) and previous AMAP assessments (AMAP, 1998, 2004, 2011, 2016; Letcher et al., 2010; Dietz et al., 2013). It updates the previous work by including new information on the biological effects of Hg from 20 newly published (post-2018) journal papers and new data on Hg levels in Arctic wildlife covering the period 2010 to 2020. It therefore provides the most up-to-date risk assessment of Hg effects on Arctic wildlife, covering more species, tissues (e.g., hair and feathers), regions and larger sample numbers than the previous work. It also addresses some of the knowledge gaps identified in previous AMAP assessments. This includes geographical data gaps in the Russian Arctic, where new seabird data, including a substantial amount from the ARCTOX project[1], have become available, allowing the risk analysis first carried out by Ackerman et al. (2016b) of North American birds to be extended to other parts of the circumarctic region.

Methylmercury (MeHg) biomagnifies in Arctic organisms raising concerns for the health of exposed wildlife. Most studies on the effects of contaminants, including Hg, on Arctic wildlife have focused on fish, birds, and higher tropic level marine species in the Canadian Arctic and primarily marine areas between Greenland and Svalbard. In these regions, tissue concentrations of Hg in certain species are elevated compared with other parts of the world, can reach levels of concern and lead to effects at both the individual and, in some cases, the population level.

The most recent AMAP assessment addressing the combined effects of persistent organic pollutants (POPs) and Hg (AMAP, 2018a; Dietz et al., 2019a) provided a detailed review of risks to marine and terrestrial mammals and some marine and freshwater birds as well as birds of prey. These risks were evaluated in relation to exposure risk categories defined on the basis of available information on thresholds for various biological effects. This work is extended in the current assessment to include marine and freshwater fish and invertebrates. It also draws on a comparative assessment conducted for the Baltic region for some fish, bivalve, marine mammal and bird species that also range into the Arctic (Dietz et al., 2021).

Many of the recent studies of Hg effects in fish and other Arctic wildlife, including the measurement of strategic biomarker endpoints, *in vitro* experiments for top predator species, and pathological studies on fish around Arctic mining sites, have been reported previously (see AMAP, 2018a and Dietz et al., 2019a). This information is not repeated in detail in this chapter; however, more comprehensive information is provided for birds as substantive new information concerning Hg effects on birds is now available. Information concerning the numerous natural (ecological and physiological) and anthropogenic factors, including climate change, invasive species and pathogens, changes in food-web dynamics and predator-prey interactions, that influence and confound the exposure to and effects of contaminants (e.g., Macdonald et al., 2005; UNEP/AMAP, 2011; Jenssen et al., 2015; McKinney et al., 2015) can be found in Chapter 5 of this report. Recent temporal trends of Hg in Arctic biota are considered in Chapter 2; however, this subject is also addressed in Section 6.5 in relation to species and regions where trends are approaching or exceeding thresholds associated with (severe) risks of biological effects.

Multiple health effects have been reported in field studies of Arctic species (Dietz et al., 2019a; Routti et al., 2019), although efforts to quantify population level effects of Hg exposure have proven challenging. Establishing links between contaminant exposure and health outcomes is a difficult task (Rodríguez-Estival and Mateo, 2019). Such information is, however, extremely important for managing and conserving wildlife populations. Consequently, various modeling approaches have been developed to use measurements of impacts at the individual level to estimate population-level effects. These methods take into account effects on reproduction, immune and endocrine functioning as well as energy demands (Svensson et al., 2011). This also requires a combination of *in vitro* dose-response

[1] For more information, visit: https://arctox.cnrs.fr/https://arctox.univ-lr.fr/

studies and, where available, *in vivo* studies on key species, such as those reported in the Baltic Sea and relatively pristine Arctic areas as reference populations (Desforges et al., 2016, 2017, 2018a, 2018b, 2018c).

This chapter is structured around a set of policy-relevant science questions as follows: (1) What are the combined effects of chemical stressors? (Section 6.2); (2) Does evidence exist for mercury concentrations in tissues that are harmful to Arctic biota (Section 6.3); (3) What are the population effects from mercury loads in highly exposed wildlife? (Section 6.4); (4) Do the highest exposed species have increasing mercury loads? (Section 6.5); (5) finally, for the first time in an AMAP report, the present assessment details information on combined regional hotspot patterns in the Arctic where information on MeHg in the upper 400 m of the water column is combined with information on levels in several key species (Section 6.6; see also Chapter 4).

6.2 What are the combined effects of chemical stressors?

6.2.1 Combined effects of mercury and other contaminants, and additional types of environmental stressors

Arctic animals possess physiological mechanisms and processes that impart varying degrees of tolerance to environmental stressor exposure (robustness) while maintaining a functionally normal health status. Environmental stress can be in the form of depleted or changing food resources as a consequence of habitat perturbation or loss as a result of or compounded by global warming. These environmental stressors can be combined with chemical stressors, such as Hg and organohalogen compounds (OHCs). Documented physiological perturbations that result from exposure to these stressors include the alteration of homeostatic circulating levels of thyroid hormone, corticosterone and vitamin A, and neurotransmitter function (see Chapter 5; Letcher et al., 2010; Sonne, 2010; Dietz et al., 2019a). These homeostatic perturbations can in turn influence important fitness/health parameters as has been documented for polar bears (*Ursus maritimus*) through modulations of immune functioning, reproductive success, neuroendocrine-related behavior and bone/calcium homeostasis (Letcher et al., 2010; Sonne, 2010; Routti et al., 2019; Sonne et al., 2021). At the level of the general population, for the various polar bear subpopulations, this may result in a reduction of bear numbers, changes in their circumpolar distribution pattern and possibly subpopulation extirpation (Sonne et al., 2015). Likewise, energetic stress (food depletion) and poorer body condition are known to reduce normal functioning of immune and reproductive systems (Patyk et al., 2015; Molnár et al., 2020). The use of peripheral adipose tissue to compensate for the lower energy intake will release bioaccumulated contaminants including Hg into the blood stream, increasing the risk of neuroendocrine disruption; together with a poorer body condition, this can decrease reproductive rates and increase mortality (Sonne, 2010).

Studies have suggested that global warming will induce a shift in the micropathogen composition towards higher virulence (Price et al., 2019) and the combination of this and an impaired immune and reproductive system will add further stress to Arctic top predators (Desforges et al., 2016, 2017, 2018a, 2018b). Climate change leading to increasing temperature and humidity could result in unforeseen changes in the distribution of pathogens; for example, ticks are a vector for the expansion of pathogens northward (Sonenshine and Mather, 1994; Lindgren and Gustafson, 2001; Kutz et al., 2009). In addition, it is clear that zoonoses (diseases transmitted between humans and animals) are a threat to Arctic animals and human populations, and especially because environmental contaminants such as polychlorinated biphenyls (PCBs) and Hg are immune suppressive (Desforges et al., 2016).

Global warming and climate change are also changing the food-web dynamics, exposure pathways, and leading, for example, to high Hg and PCB exposure in Arctic fish and polar bears (see Chapter 5; McKinney et al., 2013; Desforges et al., 2018c; Schartup et al., 2019). Depleted sea-ice coverage and earlier dates of ice break-up have changed and/or reduced the quality of the habitat of Arctic animals, such as polar bears, seals and toothed whales. Such ice changes affecting home range and feeding opportunities will have an impact on the metabolic and energetic profiles of these animals (Routti et al., 2016; Tartu et al., 2017; Pagano et al., 2018). In addition to this, decreased sea-ice coverage scenarios means polar bears need to spend more time on land, thereby increasing the probability of human interactions (Atwood et al., 2016). Ultimately, these factors will likely increase bear mortalities, and the regional conditions will depend on the specific ice reductions. In addition, increased oil exploration, mining and tourism activities in the Arctic will increase polar bear-human interactions, increasing the occurrence of self-defense kills and adding further stress to the affected animals (Stirling and Ross, 2011). These polar bear-human interactions are all likely to increase as a result of sea-ice decreases.

When it comes to measuring chemical exposure and ecotoxicology levels, it is not environmentally relevant to evaluate OHC and Hg exposure separately because the reality is that organisms are exposed to complex chemical mixtures of anthropogenic origin. An essential part of defining chemical mixtures and their associated cumulative effects increasingly requires a non-targeted approach to studying complex biological systems. A number of relatively recent areas of biological research growing rapidly in breadth and application have been described by Yadav (2007) under the term 'omics'. The term omics, denoting completeness, is used by Yadev to describe research approaches which incorporate many different disciplines and their discipline-specific knowledge, including analytical and environmental chemistry (e.g., exposomics), biological effect endpoints (e.g., metabolomics, proteomics and genomics), and statistical modeling and multivariate analyses (Yadav, 2007). Targeted and non-targeted omics-based studies are often used in the context of hypotheses that link exposomic and effects endpoint (biomarker) research and monitoring outcomes. In establishing such omics outcome linkages, more refined and targeted hypotheses are made possible and are then explored using semi-targeted and targeted analyses. Chemical mixtures that enter the environment include manufactured chemicals and by-products, their metabolites and abiotically-formed transformation products (AMAP, 2017b and references therein). The number of these chemicals are in the hundreds of thousands and vary as a function of location, space and time. The Arctic contains a growing number of OHCs and persistent organic

pollutants as well as metals such as Hg that are temporally and spatially monitored in Arctic abiotic and biotic media (AMAP, 2017b and references therein). Chemical mixtures are proving to contain an array of chemicals of emerging Arctic concern (CEACs) many of which remain unknown/undiscovered in various Arctic media, including in biota.

In general, the adverse health effects of exposure to chemical mixtures and the associated cumulative effects are poorly understood, including in Arctic biota (AMAP, 2018a). Further complexities to the understanding of chemical mixtures are the biochemical changes in exposed organisms as part of the toxicokinetic mechanisms and pathways and toxicodynamics. It is currently unknown how climate change and the combined effects from Hg and OHC exposure lead, for example, to oxidative stress and neuroendocrine disruption effects in Arctic animals, including polar bears (Letcher et al., 2010; Sonne, 2010; Dietz et al., 2013, 2019a). It is not yet known whether there is enough terrestrial food and whether polar bears are adaptive and robust enough to sustain themselves by relying solely on terrestrial food sources (e.g., bird eggs), which are lower in adipose tissue and thereby energy than marine food sources (e.g., seals; Pagano et al., 2018). However, polar bears have survived over the last 500 000 years, during which there have been several warm periods (Liu et al., 2014).

In Hudson Bay (Canada), an area under intense study due to climate change impacts, severe sea-ice reductions have been documented with associated effects on polar bear behavior and survival (Castro de la Guardia et al., 2013; McCall et al., 2015; Durner et al., 2017). Yurkowski et al. (2020) recently reported on the temporal patterns in Hg concentrations in western Hudson Bay polar bears (hair) and ringed seals (*Pusa hispida;* muscle), niche dynamics and body fat indices (see Chapter 5 for further details). One may view the Hudson Bay polar bears as an early warning subpopulation for the consequences of depleted sea-ice scenarios. In fact, it has been estimated that all Arctic summer sea-ice will be gone by 2040 and that this change will affect polar bear survival and reproductive rates (Molnár et al., 2011; Stroeve and Notz, 2018). A complete population collapse and possible species extinction from loss of sea-ice alone was proposed from extrapolating the sea-ice scenario into 2050 and 2100 (data from U.S. Geological Survey; Amstrup et al., 2010). However, the fact that Hudson Bay polar bears live in relatively southern habitats makes it difficult to extrapolate to other polar bear subpopulations. For example, North Greenland polar bears may benefit from the ice conditions and ringed seal breeding habitats in the Polar Basin. A similar situation is possible for the four or five High Arctic Canadian polar bear subpopulations. In general,the survival of the most southern polar bear subpopulations depends on the adaptability of the bears, such as their ability to migrate north to colder areas, or change their feeding strategies to include a diet of terrestrial mammals (high terrestrial productivity) and/or their access to new invasive marine mammals, including carcasses.

6.2.2 The role of mercury speciation in uptake and toxic effects

The uptake of organic Hg passing the intestinal mucosa occurs in the range of 10% to 100%, which is generally higher compared to inorganic Hg where 2% to 51% is absorbed (based on a review of 25 studies on fish with similar trends in humans; Bradley et al., 2017). Most Hg in muscle is in the form of organic MeHg, while Hg in liver and kidney is mostly in the form of an inorganic mercury-selenide (HgSe) complex (Dietz et al., 2000b; 2013). The organic MeHg in the blood and the muscle has the potential of crossing the blood-brain barrier (BBB), thereby resulting in higher toxicity as shown in many studies (e.g., Aschner and Aschner, 1990). The target tissues upregulate subcellular synthesis of metallothionein and Se complex binding, thereby detoxifying Hg as it becomes inert (Raymond and Ralston, 2004; Dietz et al., 2013, 2019a). Therefore, looking at the molar ratio of Hg to Se is important as it reveals whether or not Se is in surplus, and thereby capable of detoxifying Hg by forming tiemanite complexes (Dietz et al., 2013, 2019a). In the Arctic marine ecosystem, Se is in surplus, but this is not always the case in freshwater systems (Dietz et al., 2000b). Therefore, Hg exposure may pose a greater threat to terrestrial species through oxidative stress and neuroendocrine disruption. Toothed whales have a reduced ability to demethylate MeHg and lack the ability of excretion through hair, as found for polar bears and other fur bearing species, such as Arctic wolves (*Canis lupus arctos*), Arctic foxes (*Vulpes lagopus*), seals and walruses (*Odobenus rosmarus*); thus, for toothed whales, this results in higher body burdens as well as increasing risk of Hg exposure at levels that are considered toxic as compared to carnivores (Dietz et al., 2013; Sonne et al., 2018; Desforges et al., 2021). This is exemplified by a recent study of pilot whales (*Globicephala melas*) stranded off Scotland in 2012 where HgSe complexation indicated the risk of deficiencies in the bioavailable Se pool, thereby increasing the risk of toxic effects due to reduced Se-bound proteins and oxidative stress (Tinggi, 2003; Gajdosechova et al., 2016a, 2016b, 2018). Likewise, birds excrete Hg through feathers, which also helps to reduce the effects of MeHg on the central nervous system (Rutkiewicz and Basu, 2013). Selenium-containing enzymes also include deiodinase, which is important in the activation of the thyroid hormone and thereby potentially linked to endocrine disruption from Hg exposure (Hawkes and Keim, 2003). A recent study by Albert et al. (2019) provided a detailed overview of Hg contamination in the feathers and blood of Arctic seabirds and identified important interspecific variations in Hg blood concentrations according to seabird trophic status; however, all the reported Hg concentrations are below the toxicity thresholds proposed by Ackerman et al. (2016b). Hg concentrations in feathers follow similar trends.

6.3 Does evidence exist for mercury concentrations in tissues that are harmful to Arctic biota (in relation to effect thresholds)?

6.3.1 Methodology

6.3.1.1 Study design

The present assessment reviews recent literature (articles post-2000) as well as unpublished data of Hg exposure in marine mammals, seabirds, birds of prey, fish and bivalves from

Table 6.1 Estimated total mercury (THg) exposure and risk of health effects in wildlife and fish.

Species	Matrix	No risk (NRC)	Low risk (LRC)	Moderate risk (MRC)	High risk (HRC)	Severe risk (SRC)	References
Marine mammal	Liver (µg/g ww)	<16.0	16.0–64.0	64.0–83.0	83.0–123.0	≥123.0	Ronald et al., 1977
	Hair (µg/g dw)	<6.1	6.1–24.4	24.4–31.7	31.7–48.1	≥48.1	Risk intervals established from polar bear liver to hair correlation, this study
Terrestrial mammal	Liver (µg/g ww)	<4.2	4.2–7.3	7.3–22.7	22.7–30.5	≥30.5	Wobeser et al., 1976; Wren et al., 1987
Marine bird	Egg (µg/g ww)	<0.11	0.11–0.47	0.47–1.30	1.30–1.70	≥1.70	Ackerman et al., 2016b
	Liver (µg/g ww)	<1.40	1.40–7.30	7.30–22.7	22.7–30.5	≥30.5	Ackerman et al., 2016b
	Blood equivalent (µg/g ww)	<0.20	0.20–1.00	1.00–3.00	3.00–4.00	≥4.00	Ackerman et al., 2016b
	Body feather (µg/g dw)	<1.58	1.58–7.92	7.92–23.75	23.79–31.67	≥31.67	Ackerman et al., 2016b
Bird of prey	Body feather (µg/g dw)	<1.58	1.58–7.92	7.92–23.75	23.79–31.67	≥31.67	Ackerman et al., 2016b
Fish	Muscle (µg/g ww)	<0.10	0.10–0.30	0.30–0.50	0.50–2.00	≥2.00	Peterson et al., 2004; Dillon et al., 2010

the Arctic and, where possible, the raw data were extracted. In addition, Hg data were also obtained from the projects ARCTOX, BONUS BALTHEALTH, ICES and the Swedish EPA databases[2] for the following ICES ecoregions: Greenland Sea, Norwegian Sea, Barents Sea, Icelandic waters, Faroese waters, and, for comparative purposes, the Baltic Sea.

6.3.1.2 Risk analysis

The risk analysis in the present assessment for potential Hg-associated health effects was based on five risk level categories: no risk, low risk, moderate risk, high risk and severe risk (see Table 6.1). These risk thresholds reflect effects on reproduction and adverse effects on condition and behavior. For marine mammals, the hepatic Hg threshold values used were taken from Ronald et al. (1977) and Dietz et al. (2019a). For terrestrial mammals, the hepatic Hg threshold values used (as determined for mink; *Mustela vison*) were taken from Wobeser et al. (1976) and Wren et al. (1987). For birds, the assessment methodology presented earlier by Ackerman et al. (2016b) was adapted for liver, blood, egg and body feather concentrations. Similar risk categories were established for fish based on two key papers by Dillon et al. (2010) and Peterson et al. (2004). Using the latter study, whole-body Hg burdens were converted to equivalent muscle Hg concentrations.

6.3.2 Marine mammals

6.3.2.1 Liver related effects of mercury on Arctic marine mammals

The Hg risk evaluation for marine mammals is an update of a similar exercise conducted for the previous assessments (AMAP, 2018a; Dietz et al., 2019a). In the 2018 assessment, we reported on 70 species, regions and age groups with an overall number of 2371 individuals. The present assessment is based on an increase to 111 species, regions and age groups (59% increase) with a total number of 3572 individuals (51% increase). However, 15 of the species, regions and age groups in the present assessment were from regions outside the Arctic (i.e., North Atlantic Ocean, North Sea, Inner Danish Waters and Baltic Sea) with 127 individuals of ringed seals and harbour porpoises (*Phocoena phocoena*).

Overall, 29 of 112 marine mammal groups included in this assessment (divided on the basis of species, region, age and sex) had 30% of individuals within the two highest risk categories; of these, 18 groups had 19% of individuals in the SRC (>126 µg/g ww) and 11 groups had 12% of individuals in the HRC (83–126 µg/g ww; see Figure 6.1; Appendix Table 6A.1. Individuals from the 29 species, region and age groups from the two highest risk categories, however, accounted for only 200 individuals, representing only 5.8% of a total of 3445 individual marine mammals analyzed for their Hg loads. Of these 200 individuals, there were approximately 102 individuals (3.0%) in the SRC, and 98 individuals (2.8%) in the HRC (see Figure 6.1; Appendix Table 6A.1). The highest exposed animal groups (evaluated by percentage of individuals in the SRC) are in the following decreasing order: (1) adult hooded seals (*Cystophora cristata*) from the Denmark Strait (57%); (2) adult male hooded seals from Greenland Sea/Denmark Strait (45%); (3) adult polar bears from the northern Beaufort Sea (41%); (4) juvenile polar bears from Qaanaaq, Northwest Greenland (33%; see Figure 6.2, upper); (5) adult killer whales (*Orcinus orca*) from East Greenland, Iceland and the Faroe Islands (33%); (6) adult long-finned pilot whales from the Faroe Islands (27%); (7) juvenile polar bears from Lancaster/Jones Sound (20%); (8) subadult long-finned pilot whales from the Faroe Islands (20%); (9) adult female ringed seals from Sachs Harbour (12%; Figure 6.2, lower) and (10) adult male ringed seals from Sachs Harbour (7.8%).

The least exposed animal groups (based on Hg concentrations in liver, with all µg/g measurements on a wet weight basis; see Figure 6.1; Appendix Table 6A.1) in the Arctic regions (i.e., groups with 100% of individuals in the NRC) are in the following increasing order: (1) yearling harp seals (*Pagophilus groenlandicus*) from the Greenland Sea (0.17 µg/g); (2) foetus killer whales from East Greenland, Iceland and the Faroe Islands (0.18 µg/g); (3) subadult harbour porpoises from the Barents Sea (0.49 µg/g); (4) adult male harbour porpoises from the Barents Sea (0.58 µg/g); (5) subadult harbour porpoises from the Norwegian coast (0.69 µg/g); (6) subadult harp seals from the Greenland Sea/Denmark Strait (0.69 µg/g); (7) adult female harp seals from the Greenland Sea/Denmark Strait (0.76 µg/g); (8) adult harp seals from Ittoqqortoormiit (0.78 µg/g); (9) juvenile ringed seals from Qeqertarsuaq (0.92 µg/g) and (10) juvenile ringed seals from

[2] For more information, see https://dvsb.ivl.se/MetaInfo

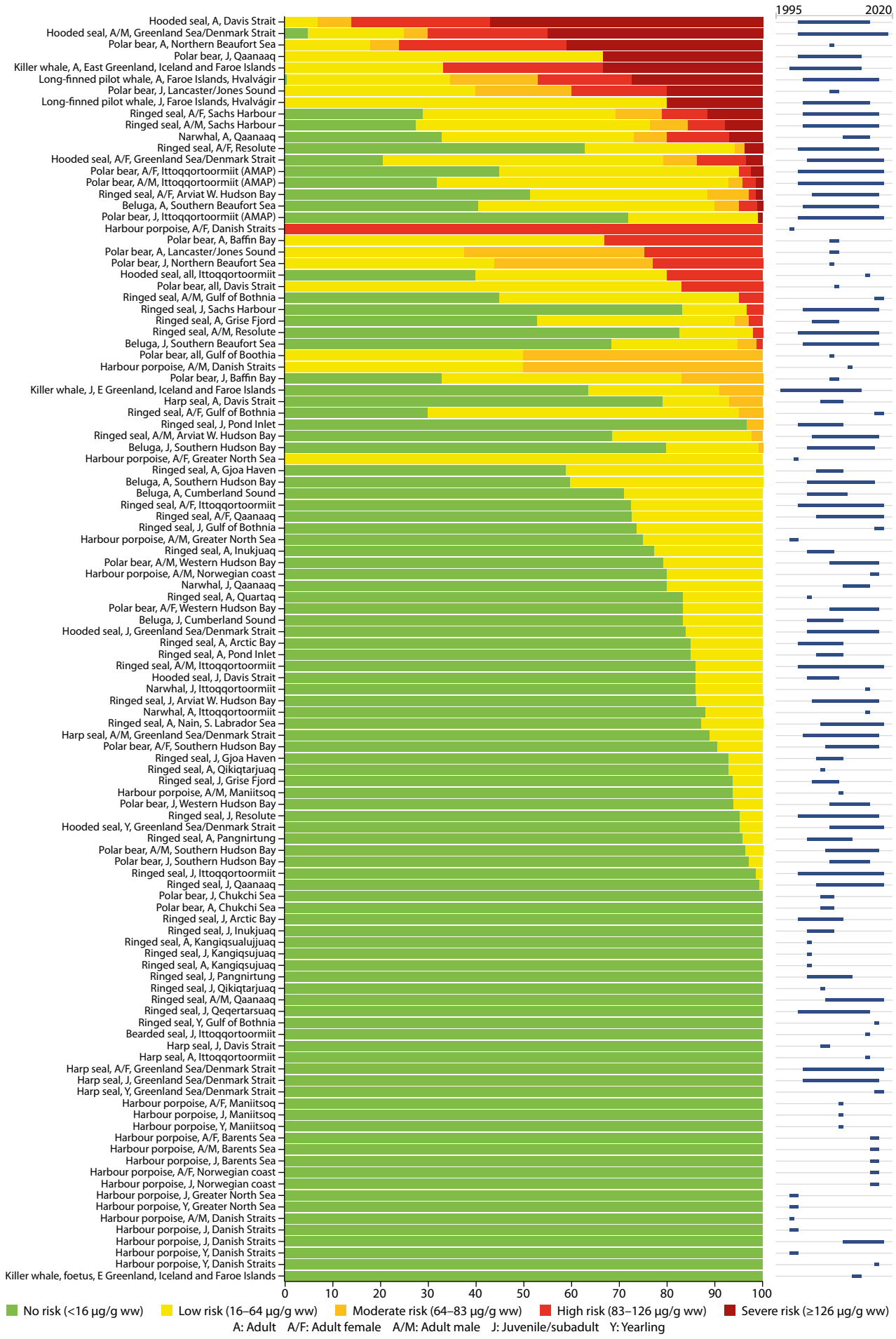

Figure 6.1 Ranked overview (from highest to lowest risk) of the proportion of marine mammal livers, per region of the Arctic, that are at risk of Hg-mediated health effects (categorized in five risk categories based upon liver Hg effect thresholds).Where possible, individuals are grouped according to maturity; where not possible 'all' indicates the general population. Appendix Table 6A.1 presents the detailed information upon which this summary graphic is based.

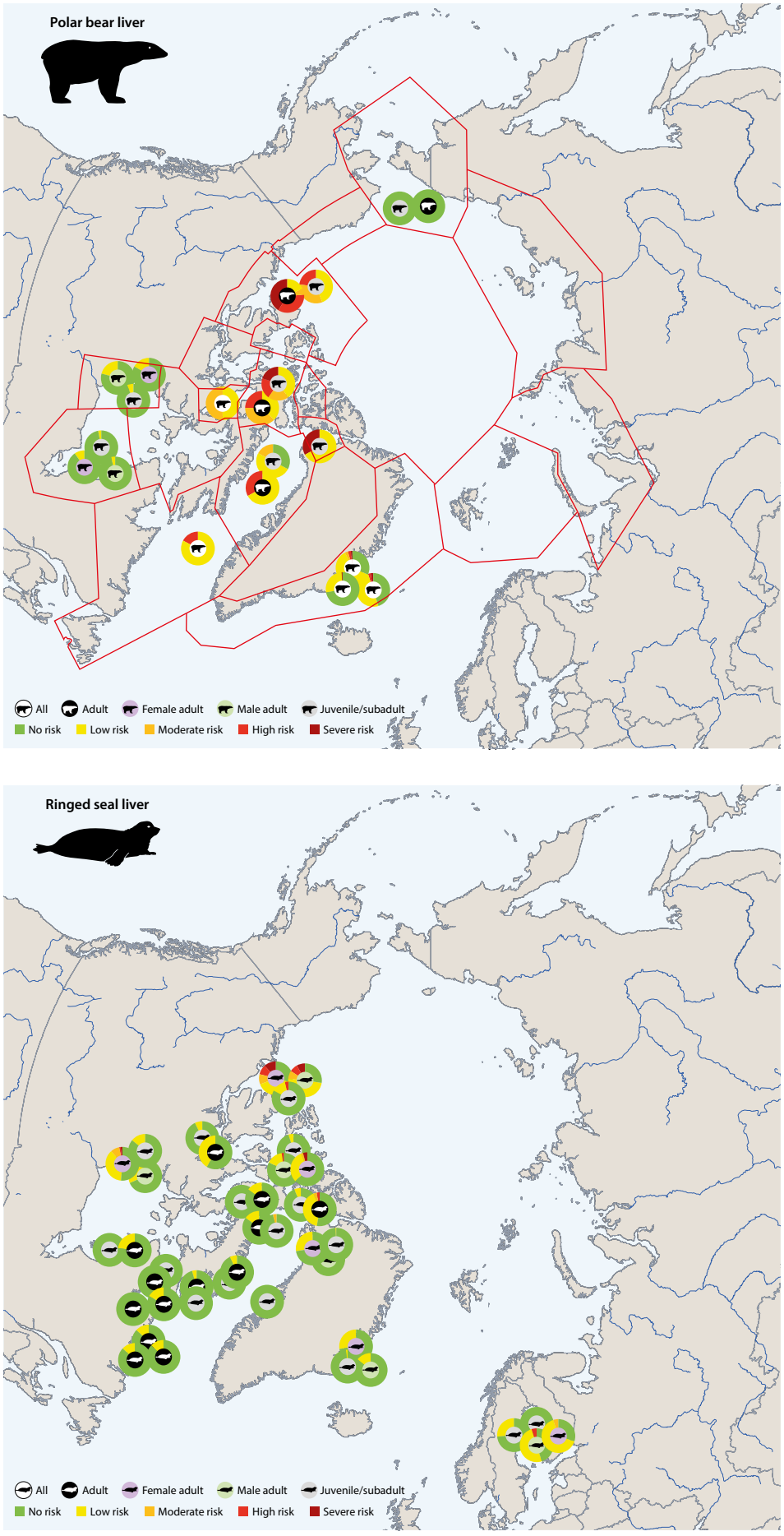

Figure 6.2 The proportion of polar bear (upper) and ringed seal liver (lower) concentrations divided on five risk categories of Hg-mediated health effects. This is based on post-2000 monitoring data, while the five risk categories are defined using thresholds observed for harp seals (Ronald et al., 1977). All metadata are found in Appendix Table 6A.1.

Kangiqsujuaq (0.92 µg/g). Appendix Table 6A.1 includes some data from regions outside the Arctic (North Atlantic, North Sea, Inner Danish Waters and Baltic) for comparative purpose for ringed seal and harbour porpoise (*Phocoena phocoena*).

There exists sufficient liver data for polar bears and ringed seals to provide an overview of the regional differences and consistencies in their Hg exposure and the related risks. Individuals in six of the 20 polar bear groups from which data are presented had concentrations in the SRC. Of these, adult polar bears from the northern Beaufort Sea were the highest exposed group, with 41% of individuals in the SRC (Figure 6.1; Figure 6.2, upper; Appendix Table 6A.1). Juvenile bears from Qaanaaq and juvenile bears from Lancaster Sound had 33% and 20% of individuals, respectively, in the SRC, although these sample sizes were small (n=6 and n=5, respectively). All three polar bear groups in Ittoqqortoormiit had between 1.0% and 2.5% percent of their populations in the SRC, based on sample sizes from 40 to 96 individuals. Four out of the six groups, as well as having individuals in the SRC also had individuals in the HRC, with between 2.5% and 35% of individuals in this category. The four groups with the highest percentage of exposed individuals in the HRC (between 17% and 33%) were adult bears from Baffin Bay, adult bears from Lancaster Sound, juvenile bears from the Northern Beaufort Sea, and a group comprising of individuals of all ages from the Davis Strait. Only two groups had individuals in the MRC, with the highest exposed groups being the overall population of bears from the Gulf of Boothia and juveniles from Baffin Bay. In the remaining eight groups, all individuals were in the two lowest risk categories; of these, 100% of individuals in the juvenile and adult groups from the Chukchi Sea were in the NRC. Information on polar bears from the Russian Arctic is lacking.

Of the 41 groups of ringed seals included in this assessment, four groups had individuals in the SRC. Adult female and male ringed seals from Sachs Harbour were the two highest exposed groups, with 11.5% and 7.8% of their individuals in the SRC, respectively (Figure 6.1; Figure 6.2, lower; Appendix Table 6A.1); the other two groups (adult female ringed seals from Resolute Bay and Arviat in western Hudson Bay) had 3.9% and 1.4% of individuals in the SRC, respectively. Three of these four groups also had individuals in the HRC and MRC, with 1.4% to 9.6% and 2.0% to 9.6%, respectively. In addition, three groups (subadult ringed seals from Sachs Harbour, adults from Grise Fjord and adult males from Resolute) had 2.1% to 3.4% of individuals in the HRC. Additionally, two groups (juvenile ringed seals from Pond Inlet and adult males from Arviat) had 3.4% and 2.3% of the individuals in the MRC, respectively, and five out of seven of the groups in the two highest risk categories also had between 2.0% and 9.6% of their individuals in the MRC. For 28 of 37 groups of Arctic ringed seals, all individuals were found in the two lowest risk categories. As was the case for polar bears, information on ringed seals from the Russian Arctic is lacking. For comparative purposes, data from Baltic ringed seals have also been included in Appendix Table 6A.1).

6.3.2.2 Comparison of marine mammal hair concentrations with effect guidelines

Hair samples are often used to evaluate human exposure to Hg and the associated risks (Petrova et al. 2020; Wang et al., 2021). Similarly, in this report we have conducted an assessment of the regional risk levels of polar bears based on Hg concentrations in polar bear hair samples collected during hunting, as well as hair sampled from polar bears routinely collected during tagging studies. This also used hair samples collected before 2000 to obtain a better spatial coverage. The analyses revealed that some bears from three populations in the central and northeastern Canadian Arctic, had concentrations in the SRC, namely bears from the Viscount Melville Sound (30%), Norwegian Bay (8.0%), and Lancaster Sound (3.6%) groups (Figure 6.3; Figure 6.4; Appendix Table 6A.2). The corresponding percentages of bears from these three populations in the HRC were 0%, 20% and 7.4%, respectively. The assessment also showed that only a low percentage (0.7%) of bears from East Greenland had individuals in the HRC. As all the Canadian populations were sampled before the year 2000, the present-day risk patterns are uncertain. Overall, the combined risk assessment based on Hg concentrations measured in hair and liver samples raises concern for polar bears in the Canadian High Arctic and Northwestern Greenland. By contrast, hair Hg concentrations in the Barents, Kara, Laptev and

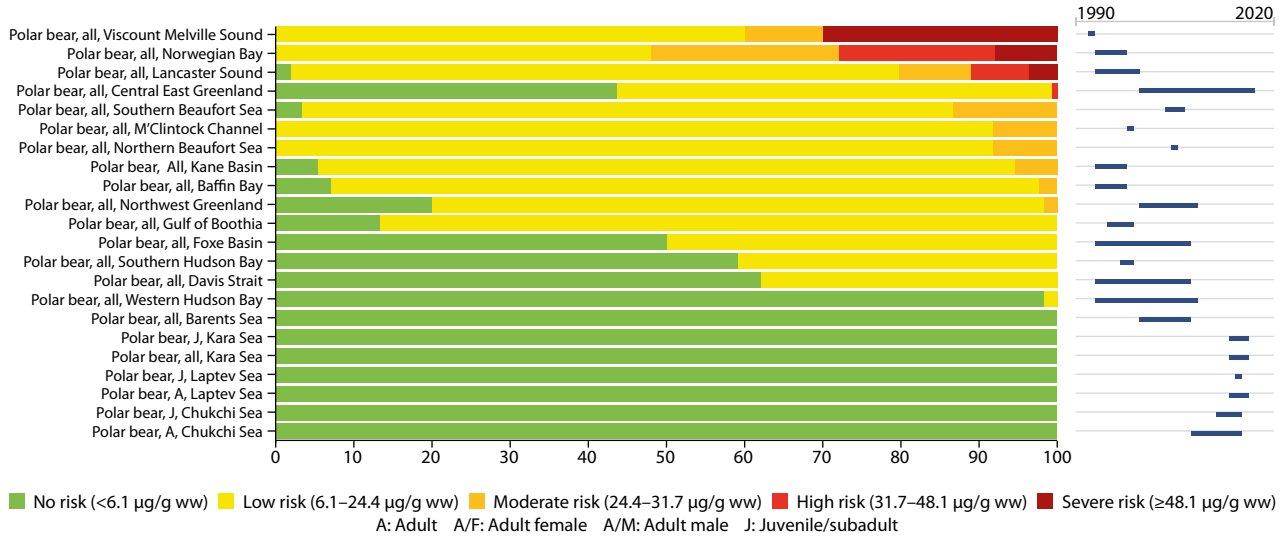

Figure 6.3 Ranked overview (from highest to lowest risk) of the proportion of polar bear hair samples, per region from the Arctic, that are at risk for Hg-mediated health effects (categorized in five risk categories based upon hair-specific Hg effect thresholds). Where possible, individuals are grouped according to maturity; where not possible 'all' indicates the general population. See Appendix Table 6A.2 for the detailed information upon which this summary graphic is based.

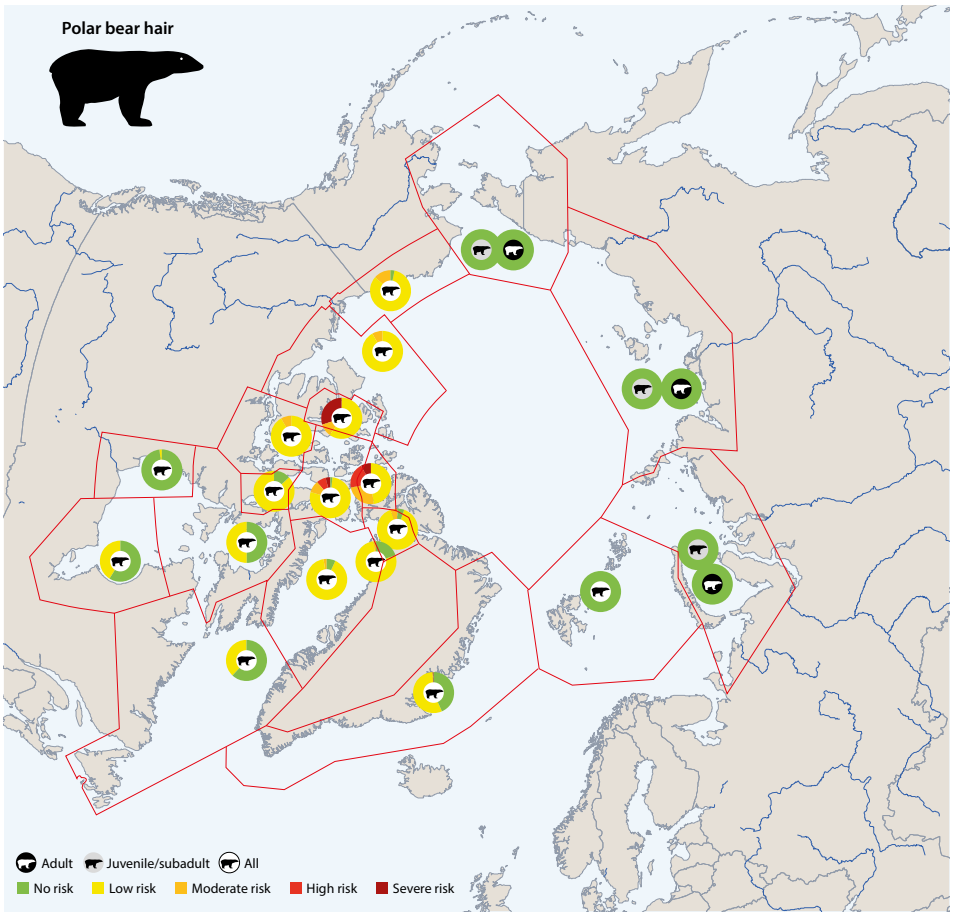

Figure 6.4 The proportion of polar bear hair concentrations divided on five risk categories of Hg-mediated health effects. This is based on post-2000 monitoring data, while the five risk categories are defined using thresholds observed for harp seals (Ronald et al., 1977) converted into hair concentrations by the East Greenland correlation between these two matrices. See Appendix Table 6A.2.

Chukchi seas all fell within the NRC; this indicates that there are no adverse implications from Hg concentrations in polar bears in the regions of Svalbard and northern Russia (Lippold et al., 2022). These data are represented in Figure 6.3 and Figure 6.4, based on data compiled in Appendix Table 6A.2.

6.3.3 Terrestrial mammals

The majority of Hg concentrations in terrestrial mammals fell within the two lowest risk categories for Hg-mediated health effects: no risk and low risk (NRC and LRC; see Figure 6.5). Icelandic Arctic fox, however, had 9% of the adult population in the severe risk category, 35% in the moderate risk category, 22% in the low risk category and 35% in the no risk category. The juvenile Arctic foxes were less exposed and the majority of the foxes (67%) in this age group fell in the no risk category, while the remaining juvenile foxes fell into the low risk (8%) and moderate risk (25%) categories. Juvenile Arctic foxes from Arviat and Svalbard had 98% and 100% in the no risk category, respectively (see Figure 6.5 and Appendix Table 6A.3); this raises the question of whether or not some local Hg sources are present in Iceland may be linked to volcanic activities. For sheep (*Ovis aries*) on the Faroe Islands, as many as 15% were found in the moderate risk category, which is higher than expected and could be attributed to agricultural fertilization by fish remains or eutrophication by bird droppings (from the extensive seabird colonies on the islands), as suggested by AMAP (2018a) and Dietz et al. (2019a). The remaining 85% of the sheep fell in the no risk category. All individuals (100%) in the seven caribou/reindeer (*Rangifer tarandus*) populations and age groups were in the no risk category with median Hg concentrations ranging from 0.12 to 1.24 µg/g ww (see Figure 6.5 and Appendix Table 6A.3).

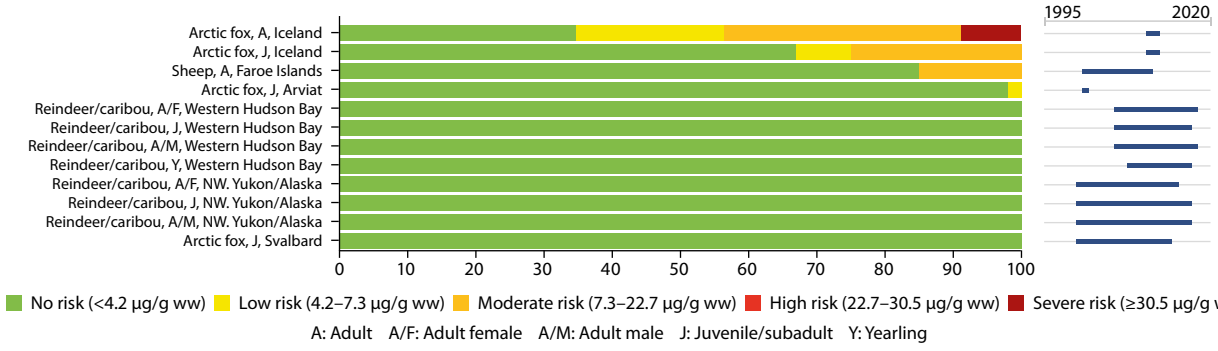

Figure 6.5 Ranked overview (from highest to lowest risk) of the proportion of individuals, where possible grouped according to maturity, of specific Arctic terrestrial mammal populations that are at risk of total Hg-mediated health effects. Following hepatic concentrations in the period 2000 to 2015, five risk categories are reported based upon effect threshold categories observed for mink (Wobeser et al., 1976; Wren et al., 1987). See Appendix Table 6A.3 for the detailed information upon which this summary graphic is based.

6.3.4 Marine and terrestrial birds

Methylmercury (MeHg) is known to have numerous detrimental effects on birds (Scheuhammer et al., 2007; Ackerman et al., 2016b). Avian reproduction is especially sensitive to MeHg toxicity, with even low levels of exposure leading to adverse effects (Wiener et al., 2003; Heinz et al., 2009). Aquatic birds typically have the highest exposures to environmental Hg contamination (Ackerman et al., 2016b), although more terrestrial birds, like riparian songbirds, are also known to bioaccumulate MeHg to potentially harmful levels (Cristol et al., 2008; Ackerman et al., 2019; Cristol and Evers, 2020). Within the Arctic, birds are primarily exposed to elevated levels of MeHg in pelagic environments (Provencher et al., 2014; Braune et al., 2015; Peck et al., 2016; Burnham et al., 2018; Albert et al., 2019, 2021), coastal shoreline and wetland foraging habitats (Hargreaves et al., 2011; McCloskey et al., 2013; Perkins et al., 2016; Sun et al., 2019).

This chapter reviews and assesses the potential for MeHg toxicity in Arctic birds using the available data (see Appendix Tables 6A.4; A-C and Figures 6.6 to 6.9). To assess risk, we used MeHg toxicity benchmarks previously established for bird blood (Ackerman et al., 2016b) and converted these values into equivalent concentrations in other bird tissues that are also commonly sampled in the Arctic, such as eggs, liver, and contour feathers. Blood-equivalent Hg concentrations <0.2 µg/g ww are below the lowest-observed effect levels, whereas birds are generally considered to be at low risk when blood Hg concentrations are 0.2–1.0 µg/g ww, moderate risk at 1.0–3.0 µg/g ww, high risk at 3.0–4.0 µg/g ww, and severe risk at >4.0 µg/g ww (Ackerman et al., 2016b). These toxicity benchmarks in bird blood were converted into equivalent concentrations in eggs, based on a review paper which established a general bird maternal transfer equation of Hg from females to their eggs (Ackerman et al., 2020). Similarly, the blood to liver Hg concentrations were converted using an intra-tissue correlation equation built for four species of birds (Eagles-Smith et al., 2008). Because many of the Arctic bird data for Hg contamination have been sampled using bird feathers (Albert et al., 2019), these toxicity benchmarks for bird blood were also converted into body feather Hg concentrations. Unlike the other equations, intra-tissue correlations for feathers and internal tissues, such as with blood or eggs, tend to be poor (Evers et al., 1998; Eagles-Smith et al., 2008; Ackerman et al., 2016a). Feather molt represents a major excretion pathway in bird during which 60% to 90% of accumulated Hg is excreted (Honda et al., 1986; Braune, 1987; Braune and Gaskin, 1987; Lewis et al., 1993; Agusa et al., 2005). Mercury in feathers becomes stable once they have grown (Appelquist et al., 1984). Since feathers have often grown months before they are collected, the existing temporal and spatial mismatch in Hg concentrations between feathers and other tissues is exacerbated. In addition, feather Hg concentrations can be difficult to interpret due to the complex timing and location of feather molt (Pyle, 2008; Pyle et al., 2018), differences among feather tracts (such as head vs. body feather; Braune and Gaskin, 1987; Ackerman et al., 2016a, Fort et al., 2016), the large-scale movements of birds, often migratory species exposed to Hg over different regions (Fleishman et al., 2019), and the extreme variability in Hg concentrations in some species both within and among individual feathers from the same individual bird (Peterson et al., 2019).

Because of these complexities, feathers of adult birds are typically not recommended for Hg biomonitoring programs if detailed information about bird-species biology is lacking (Ackerman et al., 2016b; Chételat et al., 2020), such as their precise feather molt timing or their distribution over their annual cycle (Ackerman et al., 2012; Albert et al., 2019). In these specific cases, feathers can be a useful sampling tool to represent Hg contamination, such as in remote oceanic locations where birds are difficult to sample. For example, nape feathers of red-legged kittiwakes (*Rissa brevirostris*) are thought to be grown at the end of the wintering period and were sampled on their breeding grounds, where birds can be more easily captured on their nest (Fleishman et al., 2019). This sampling strategy coupled with geolocation dataloggers demonstrated that red-legged kittiwakes wintering at more southern latitudes within the North Pacific Ocean had higher Hg concentrations than birds wintering at more northern latitudes (Fleishman et al., 2019). Similarly, head feathers of little auks (*Alle alle*), which grow on the wintering grounds were used to demonstrate that birds were 3.5 times more contaminated when outside of their Arctic breeding locations, indicating that MeHg acquired at non-Arctic wintering areas in the northwest Atlantic Ocean can be transported to Arctic breeding areas by migratory birds and has the potential to affect reproductive success (Fort et al., 2014). Therefore, feathers were useful to demonstrate that non-Arctic regions that were used by the Arctic avian community for several months per year, during which birds travel thousands of kilometers between their Arctic breeding sites and non-Arctic non-breeding grounds (e.g., Egevang et al., 2010), are of high concern due to higher Hg contamination experienced during winter (Albert et al., 2021).

Based on these toxicity benchmarks, 50% of birds were found to have tissue Hg concentrations that were above the no risk level when it came to adverse health effects (a blood-equivalent mercury concentration of 0.2 µg/g ww) and that 1% of birds were either in the high or severe risk categories (see Appendix Tables 6A4; A–C and Figures 6.6 to 6.9). In particular, northern fulmar (*Fulmarus glacialis*), ivory gull (*Pagophila eburnea*), glaucous-winged gull (*Larus glaucescens*), glaucous gull (*Larus hyperboreus*), lesser black-backed gull (*Larus fuscus*), black-legged kittiwake (*Rissa tridactyla*), red-legged kittiwake, Atlantic puffin (*Fratercula arctica*), thick-billed murre (*Uria lomvia*), black guillemot (*Cepphus grylle*), pigeon guillemot (*Cepphus columba*), rhinoceros auklet (*Cerorhinca monocerata*), double-crested cormorant (*Phalacrocorax auratus*) and ruddy turnstone (*Arenaria interpres*) had at least 5% of the individuals sampled with Hg concentrations at levels considered to be at moderate or higher risk to toxicity (see Appendix Tables 6A4; A–C and Figures 6.6 to 6.9). Mercury concentrations in birds tended to increase historically within the Arctic, but trends have flattened recently in several Arctic regions (Braune et al., 2001, 2006, 2016; Braune, 2007; Bond et al., 2015; but c.f. Fort et al., 2016 in East Greenland). As is common, bird Hg concentrations differed widely among sites in the Arctic due to differences in bioaccumulation pathways and processes (Braune et al., 2002, 2014b). Braune et al. (2014c) found that thick-billed murres breeding at two High Arctic colonies tended to have higher Hg concentrations than murres breeding at three Low Arctic locations. In contrast, birds wintering at more southern latitudes generally had higher MeHg exposure (Fort et al., 2014; Fleishman et al., 2019). In general, birds tended to have higher MeHg concentrations in the Canadian Arctic, western Canada and western Greenland than in the European Arctic and Russia (Provencher et al., 2014; Albert et al., 2021; Fort and co-workers, pers. comm., 2020). The following sections detail the recent work which has demonstrated effects of MeHg on Arctic bird health.

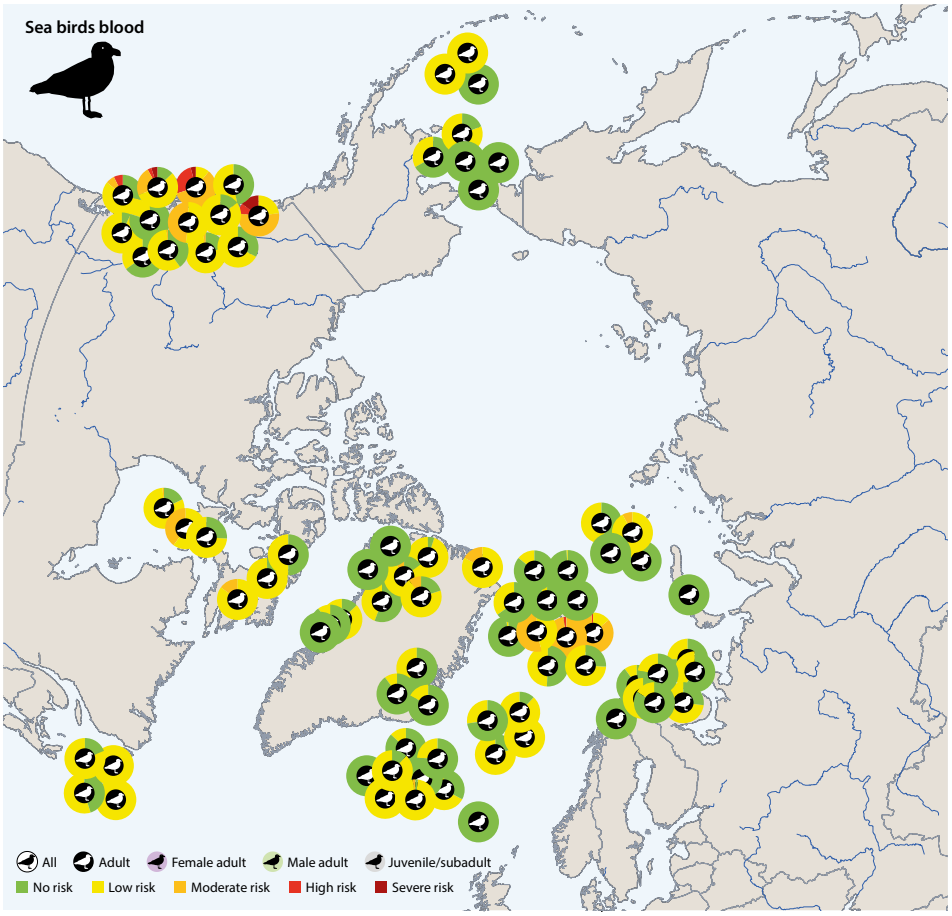

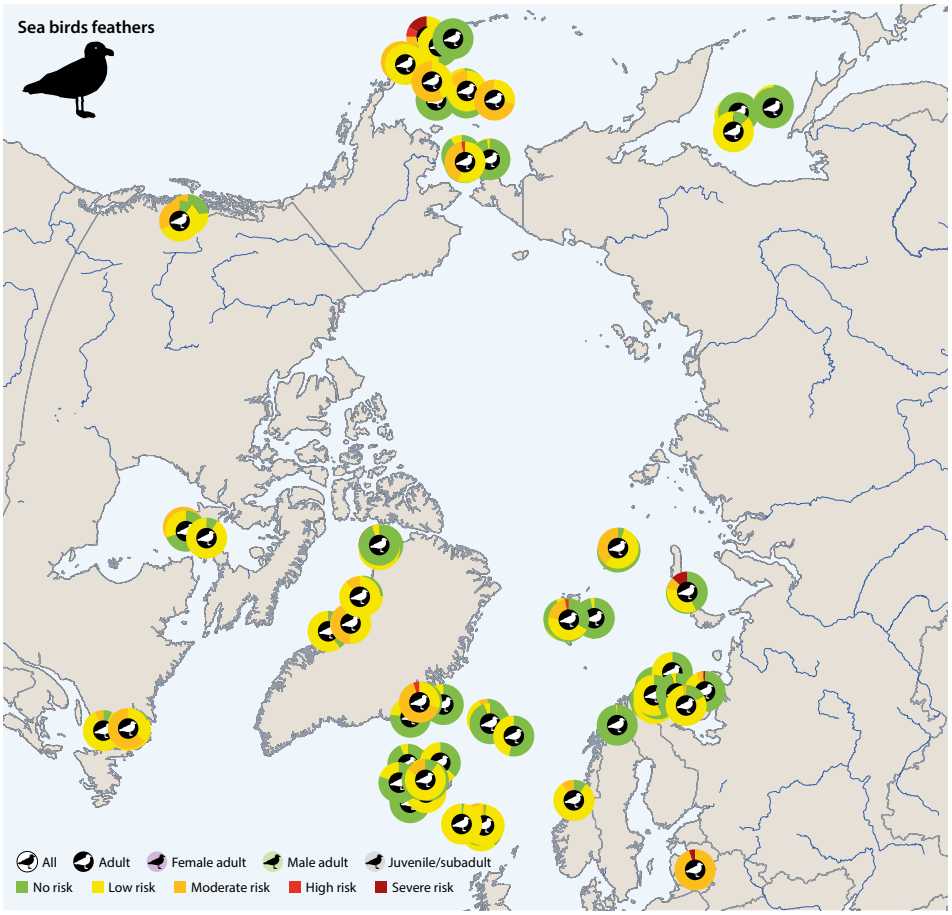

Figure 6.6 The proportion of seabirds that are at risk of Hg-mediated health effects based on data for blood (upper) and feathers (lower). For the detailed information upon which this summary graphic is based, see Appendix Table 6A.4 (A) and Appendix Table 6A.4 (B) as well as Figure 6.7 and 6.8, respectively.

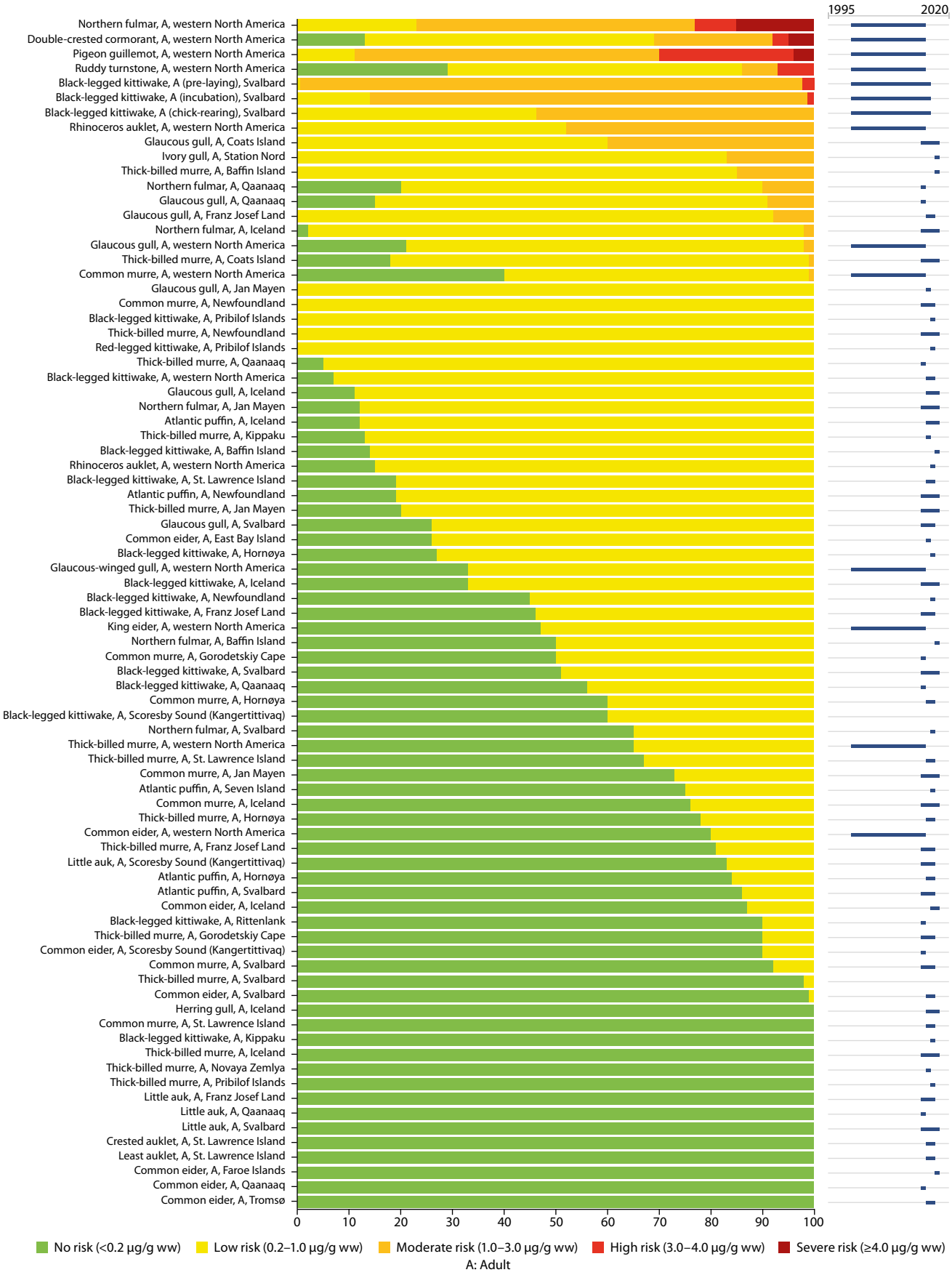

Figure 6.7 Ranked overview (from highest to lowest risk) of the proportion of seabird blood per region from the Arctic, which are at risk for Hg-mediated health effects (categorized in five risk categories based upon blood Hg effect thresholds). For the detailed information upon which this summary graphic is based, see Appendix Table 6A.4 (A).

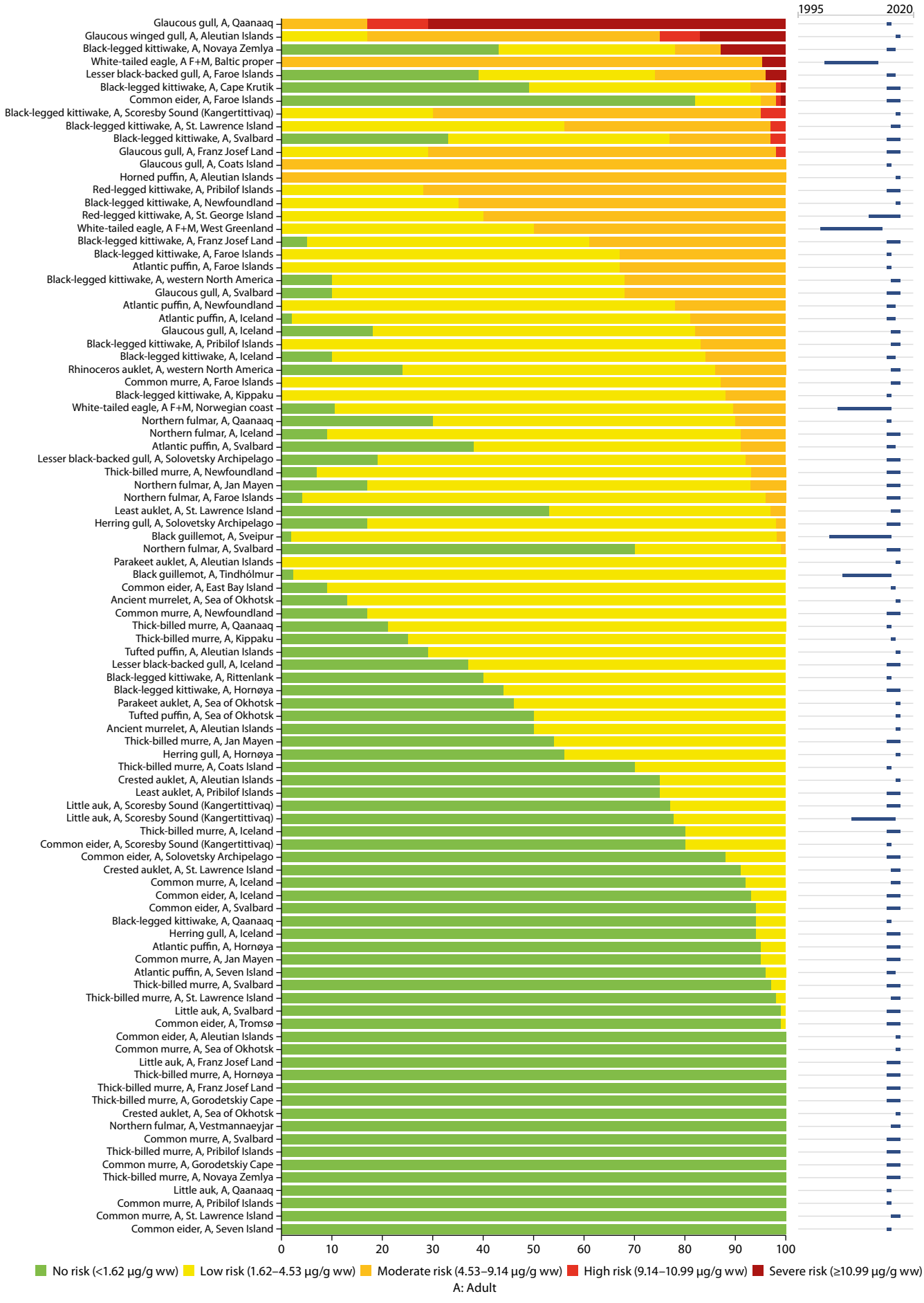

Figure 6.8 Ranked overview (from highest to lowest risk) of the proportion of seabirds and birds of prey feathers per region from the Arctic, that are at risk for Hg-mediated health effects (categorized in five risk categories based upon feather Hg effect thresholds). For the detailed information upon which this summary graphic is based, see Appendix Table 6A.4 (B).

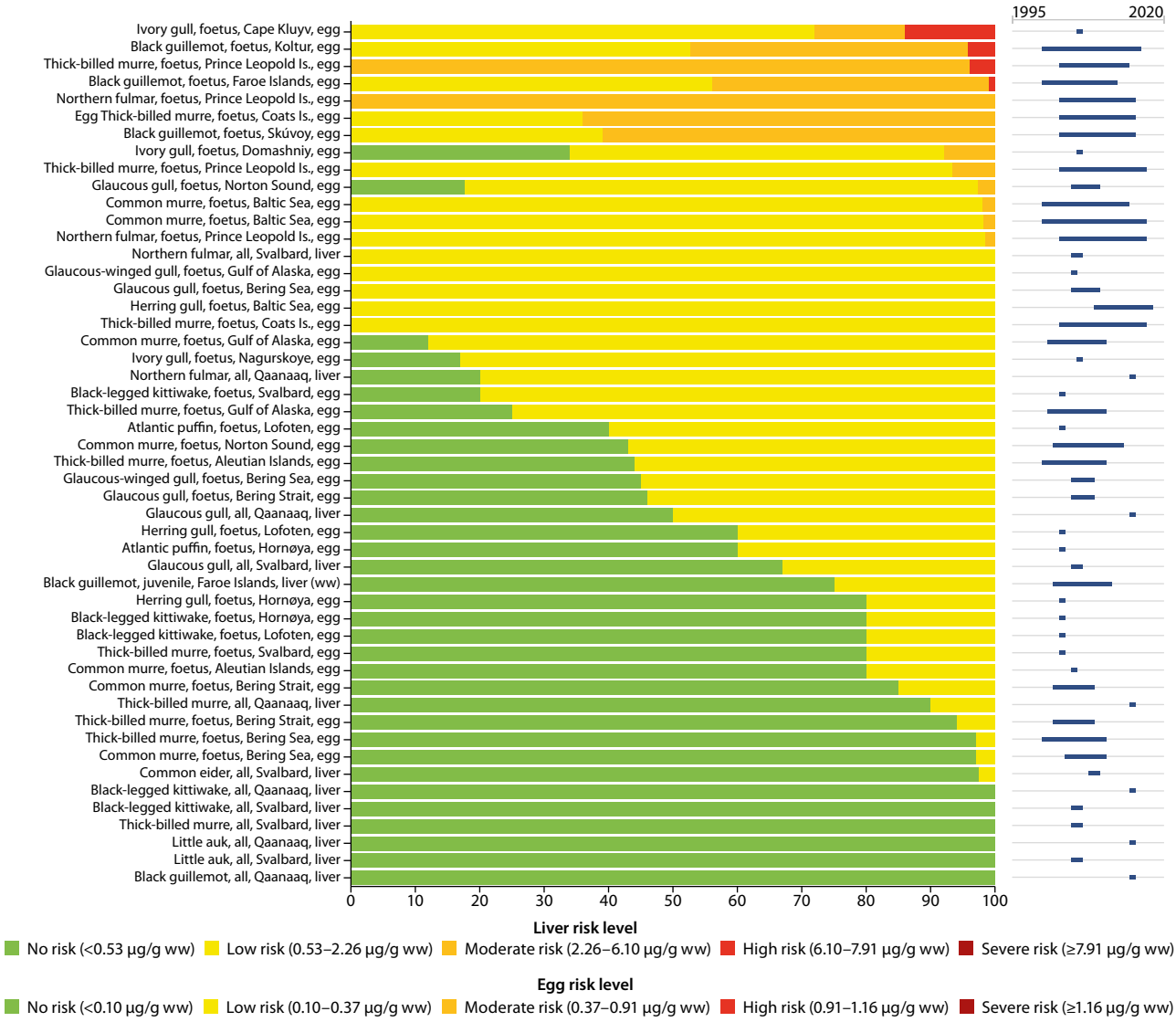

Figure 6.9 Ranked overview (from highest to lowest risk) of the proportion of seabird livers and eggs per region from the Arctic, that are at risk for Hg-mediated health effects (categorized in five risk categories based upon liver and egg Hg effect thresholds). Samples are indicated where taken from 'foetus' or 'all' indicates the sample derived from birds from the general population. See Appendix Table 6A.4 (C) for the detailed information upon which this summary graphic is based.

6.3.4.1 Reproductive performances and demographic responses in relation to mercury exposure

We report here on studies that have examined the relationships between Hg exposure and behavioral and physiological mechanisms that may explain the links between Hg exposure and Arctic seabird demography (reproduction and survival). Studies conducted on Arctic birds are put in perspective by also presenting research conducted for Antarctic and temperate fauna. This section is intended to be as exhaustive as possible, including mechanisms that have been little studied, or not significantly related to Hg exposure.

Depressed reproductive success is the most widely investigated and reported consequence of Hg exposure in wildlife (Evers et al., 2008; Scheuhammer et al., 2012; Whitney and Cristol, 2017). Chronic exposure to MeHg might compromise survival rate and long-term reproductive outputs, thus potentially leading to population declines.

Reproductive performances

Exposure to MeHg is known to alter avian sexual and mating behaviors (Frederick and Jayasena, 2011 for water birds; Spickler et al., 2020 for a domesticated songbird model species, the zebra finch; *Taenopygia guttata*). For Arctic birds, very little information is available: contrary to some legacy chlorinated POPs (Blévin et al., 2014), Hg concentrations in Svalbard kittiwakes did not appear to be associated with carotenoid-based sexual ornamentations, carotenoid concentrations in plasma, nor paring success (Blévin et al., 2018). Furthermore, the high frequency of abnormal sperm cells observed in this species in Svalbard (Humann-Guilleminot et al., 2018) was unrelated to Hg blood concentrations (Blévin et al., 2020). On the other hand, Amélineau et al. (2019) reported that adult little auks with high Hg concentrations were in reduced body condition. Non-breeding by individuals that previously bred is a common occurrence in long-lived birds (Goutte et al., 2011). Investigations conducted in Svalbard have shown that this phenomenon was associated with high Hg concentrations in pre-laying kittiwakes, whereas

laying date and clutch size were not related to Hg concentrations (Tartu et al., 2013). Similarly, it was found that Hg levels were unrelated to clutch size in common eiders (*Somateria mollissima*) and timing of breeding in Leach's storm petrel (*Oceanodroma leucorhoa*; Pollet et al., 2017; Provencher et al., 2017). In another study of Svalbard kittiwakes, Hg concentration was negatively related to breeding success (the probability of an individual raising at least one chick) in males (Tartu et al., 2016).

Impaired reproductive performance may also originate from eggshell thinning (Olivero-Verbel et al., 2013), although evidence is lacking for Arctic seabirds. Low hatching success may also be the consequence of reduced egg size: females of Greenland little auks with more feather Hg laid smaller eggs (Fort et al., 2014), whereas egg volume was not related to Hg in Leach's storm-petrels (Pollet et al., 2017). The negative effect of Hg exposure on egg hatchability was experimentally tested in thick-billed murres and Arctic terns (*Sterna paradisea*) by injecting a range of environmentally relevant concentrations (0–6.4 µg/g ww) of MeHg chloride (MeHgCl). This study by Braune et al. (2012) demonstrated the relative sensitivity of the developing embryos to MeHg in these two Arctic seabird species (Braune et al., 2012). Finally, in Greenland little auks, chicks with the highest Hg concentrations hatched with a body mass reduced by approximately 30% compared to those with the lowest concentrations, although no impact was further observed on their growth and fledging success. Nevertheless, Amélineau et al. (2019) found that the long-term increase in Hg contamination of this same population was associated with decreased chick growth rate during the last decade.

Long term demographic consequences

Our understanding of the consequences of Hg exposure on long-term fitness is still very limited in free-living Arctic birds because of the paucity of long-term data sets that would be required to address this topic. Few long-term capture-mark-recapture (CMR) studies on Antarctic seabirds (wandering albatross; *Diomedea exulans*; Goutte et al., 2014a, Subantarctic skuas; *Catharacta lonnbergi* and south polar skuas; *C. maccormicki*; Goutte et al., 2014b) and Arctic seabirds in Svalbard (Glaucous gull; Erikstad et al., 2013 and black-legged kittiwake; Goutte et al., 2015), in Greenland (Little auk; Amélineau et al., 2019) in northern Norway (Common eider; Bårdsen et al., 2018; Sebastiano et al., 2020) have estimated the impact of contaminants on long-term breeding probability, reproductive success and adult survival. These studies, based on long-term ringing programs, have mainly focused on legacy chlorinated POPs, but some of them have included blood and feather Hg concentrations in demographic models (Goutte et al., 2014a, 2014b, 2015; Pollet et al., 2017; Bårdsen et al., 2018; Amélineau et al., 2019). Regarding Arctic seabirds, a long-term study on Svalbard kittiwakes found a correlation between reduced breeding probability and higher Hg concentrations, but the overall impact of Hg on demographic parameters was modest compared to that of some legacy chlorinated POPs (Goutte et al., 2015). Importantly, all these long-term studies (reviewed in Whitney and Cristol, 2017) revealed Hg had no effect on adult survival, a key parameter for seabird population dynamics, despite a wide range in blood Hg concentrations across species (from 0.89 µg/g dw to 8.22±0.24 µg/g dw).

6.3.4.2 Behavioral and physiological mechanisms potentially involved in the reproductive and demographic consequences of mercury exposure

Parental behavior

In birds, incubation-related behaviors are influenced by hormonal regulation. In some Antarctic seabirds, Tartu et al. (2015a) showed that Hg concentrations were associated with reduced egg-incubation effort. However, relatively little is known about the effect of contaminants on incubation temperature for wild birds (Taylor et al., 2018; Hartman et al., 2019). By using loggers placed into artificial eggs, Blévin et al. (2018) investigated relationships in Svalbard black-legged kittiwakes between incubation temperature and brood patch and three groups of contaminants: organochlorines (OCs); per-/polyfluoroalkyl substances (PFAS) and Hg. This study revealed that, contrary to OCs, Hg concentrations in blood (2.0±0.59 mg/g dw in males, 1.43±0.38 mg/g dw in females) were not related to the minimum incubation temperature nor the size of the brood patch. Incubation does not solely imply the active warming of the eggs but also the active turning of eggs to facilitate albumen absorption by the embryo, reducing the likelihood of an embryo being malpositioned for hatch (Herring et al., 2010) and preventing the embryo from adhering to the inner shell membrane. Using an egg-logger, Blévin et al. (2020) found that, unlike PCBs and PFAS, blood Hg concentrations were unrelated to egg-turning behavior in Svalbard black-legged kittiwakes; this was similar to studies on egg turning in seabirds at temperate latitudes (Taylor et al., 2018).

Endocrine system

In order to maximize fitness, individuals must make behavioral decisions on their reproduction depending on environmental conditions (e.g., whether to breed or not, when to breed and what level of parental investment to make). These behavioral decisions are mediated by hormones: these include luteinizing hormone, a pituitary hormone involved in the onset of breeding (Goutte et al., 2011); stress hormones (corticosterone; Wingfield and Sapolski, 2003) and prolactin, a pituitary hormone involved in the expression of parental care (Angelier and Chastel, 2009). Because Hg is a known endocrine disruptor (Tan et al., 2009), Hg may impair breeding decisions (Hartman et al., 2019) and more generally alter the ability of Arctic seabirds to adequately respond to ongoing environmental changes (Jenssen, 2006).

Research conducted on Svalbard black-legged kittiwakes has shown that Hg (range: 0.91–3.08 µg/g dw) in the blood appears to target pituitary hormones. For example, these high Hg concentrations were related to a decreasing luteinizing hormone secretion (Tartu et al., 2013). Additionally, experimental challenges with exogenous gonadotropin-releasing hormone (GnRH) were conducted to test the ability of the pituitary to release luteinizing hormone (LH) in relation to Hg concentrations. These investigations suggested that Hg disrupted LH secretion by suppressing GnRH input to the pituitary and that elevated Hg concentrations were linked to years in which birds did not reproduce (Tartu et al., 2013). A similar pattern was observed for Antarctic seabirds

(Tartu et al., 2014). Similarly to its effect on LH, Hg seems to impact another pituitary hormone: prolactin, which is known to play a key role in the expression of avian parental care (Angelier and Chastel, 2009). In black-legged kittiwakes from Svalbard as well as in Antarctic seabirds, high Hg exposure appeared to be associated with lower plasma prolactin levels and poor incubation behavior (Tartu et al., 2015a, 2016). The effect of Hg on stress hormone secretion is less clear (see Herring et al., 2012 for temperate seabird nestlings and Provencher et al., 2016a on the common eider duck; *Somateria mollissima*). In Svalbard kittiwakes, baseline and stress-induced corticosterone levels were unrelated to Hg concentrations (range: 0.82–2.96 μg/g dw). In this population, exacerbated baseline and stress-induced corticosterone levels appeared to be triggered by organic compounds (PCBs), possibly via a stimulation of adrenocorticotropic hormone (ACTH) receptors (Tartu et al., 2015b).

Bioenergetics and thyroid hormones

Individual variations in energy metabolism may influence fitness because of the trade-off in allocating energy toward self-maintenance (survival), activity, growth and reproduction (Stearns, 1992). Basal metabolic rate (BMR), the minimal energetic cost of living in endotherms, is known to be influenced by thyroid hormones (THs), which are known to stimulate *in vitro* oxygen consumption of tissues in birds and mammals. Several environmental contaminants may act on energy expenditure through their thyroid hormone-disrupting properties. However, the effect of Hg on BMR is still poorly documented for wildlife (see Gerson et al., 2019 on lab passerine model). Blévin et al. (2017a) investigated the relationships between three groups of contaminants (OCs, PFAS and Hg) with metabolic rate and circulating total THs (thyroxine; TT4 and triiodothyronine; TT3) in adult black-legged kittiwakes from Svalbard, in the Arctic. This study indicated that, unlike in the case of some OC and PFAS (Blévin et al., 2017a; Melnes et al., 2017 for glaucous gull), metabolic rate and thyroid hormones (T3) were not associated with Hg blood levels in Svalbard kittiwakes. Further investigation on the link between Hg exposure, thyroid hormones and energy expenditure (basal and field/actual metabolic rate) are needed, especially for the most contaminated species.

Oxidative stress and telomeres

Regarding the effects of mercury on wildlife, one potential important biochemical mechanism to consider is oxidative stress because of its potential detrimental effects on key fitness traits, such as reproduction and susceptibility to disease, and thus on survival (Costantini, 2014; Sebastiano et al., 2016). Investigations of temperate or Antarctic seabirds have reported some associations between Hg and oxidative stress (Hoffman et al., 2011; Costantini et al., 2014; Gibson et al., 2014). For Arctic seabirds, Wayland et al. (2010) investigated glaucous gulls from the Canadian Arctic and found associations between some oxidative markers (i.e., thiols and lipid peroxidation) and Hg burden. In Svalbard, there was no association between blood Hg levels (1.96–4.82 μg/g dw) and several oxidative status markers for kittiwakes (Chastel et al., pers. comm., 2021). Similarly, Fenstad et al. (2016b) found no association between Hg burden and total antioxidant capacity in Baltic and Svalbard common eiders. Oxidative stress is considered to be one of the mechanisms involved in the shortening of telomeres, which are repeated sequences of non-coding DNA located at the terminal ends of chromosomes (Blackburn, 2005). Following the discoveries of telomeres and their implications for maintaining chromosome stability, health and ageing, there has been a growing interest into the study of telomere dynamics in relation to contaminant exposure (Angelier et al., 2018). Because of their association with longevity and survival in vertebrates, telomeres represent a potential physiological marker that may prove useful to estimate the toxicological consequences of contaminant exposure on wildlife (Sebastiano et al., 2020). However, to date, only a handful of studies have explored telomere-contaminant relationships in Arctic free-living birds, mainly in relation to organic pollutants (Blévin et al., 2016, 2017b; Sletten et al., 2016; Eckbo et al., 2019; Sebastiano et al., 2020). Regarding Hg, only one study has been conducted, and they found that absolute telomere length was associated, but weakly, with blood Hg levels in Svalbard kittiwakes (Angelier et al., 2018). Thus, there is a current data gap for our understanding of the relationship between Hg and telomeres.

Genotoxicity

Alterations in the genetic material may have severe consequences for the survival of individuals and ultimately on the fate of populations. Since 2010, some studies have investigated the genotoxic effects of environmental exposure to pollutants in Arctic seabirds (e.g., organohalogen contaminants; Haarr et al., 2017). Fenstad et al. (2016a) assessed the impact of blood concentrations of Hg on DNA double-strand break (DSB) frequency in blood cells of a high-exposed Baltic (0.43–1.71 nmol/g ww) and lower exposed Arctic population (in Svalbard, 0.31–0.98 nmol/g ww) of common eiders. Significant positive relationships between Hg and DNA DSB frequency were found in Baltic but not in Svalbard eiders.

Neurology

In order to understand the effects of Hg exposure on developing thick-billed murre and Arctic tern embryos, Braune et al. (2012) investigated the concentrations of receptors in the brain, a biomarker of MeHg effects in wildlife (Basu et al., 2006; Scheuhammer et al., 2015). However, no relation was found between Hg concentration and the density of specific neuroreceptors in brain tissue in either species.

Immune system

Exposure to Hg can be associated with depressed avian immune responses (Fallacara et al., 2011; Lewis et al., 2013), and this may interfere with reproduction and survival in most contaminated individuals. Furthermore, such impairment of the immune system may pose an additional threat to Arctic birds since climate change could favor the emergence of new infectious diseases or a higher prevalence of parasites in the Arctic (Eagles-Smith et al., 2018; Lee et al., 2020). For Arctic seabirds, Provencher et al. (2016a) did not find association between Hg blood levels and immunoglobulin Y (IgY) in female eider ducks from the Canadian Arctic. Similarly, in an experimental study of Svalbard barnacle geese (*Branta*

leucopsis), it was found that exposure to Hg from a historic coal mine area had little impact on four innate immune parameters (haemolysis, haemagglutination, haptoglobin-like activity, and nitric oxide) in goslings (de Jong et al., 2017). Contaminants and parasites may negatively affect wildlife health and reproduction either additively or synergistically (Marcogliese and Pietrock, 2011). To date, only one study on common eider from the Canadian Arctic indicated that Hg (breast muscle levels: 0.63±0.24 µg/g) and gastro-intestinal parasites may potentially influence each other (Provencher et al., 2016b). Because of their connection with the immune system, changes in vitamins A, D and E have been investigated as biomarkers of contaminant exposure, particularly POPs, and effects in Arctic wildlife (Helgason et al., 2010; Braune et al., 2012; Verreault et al., 2013). Since 2010, few studies addressing the relationships between Hg and vitamins in Arctic seabirds have been conducted. In the ivory gull (*Pagophila eburnea*), a year-round and significantly contaminated resident of the Arctic (Bond et al., 2015; Lucia et al., 2015) eggs from Svalbard and the Russian Arctic populations were sampled to investigate relationships between whole egg Hg content (0.06–0.30 µg/g ww), eggshell thinning, vitamin A and vitamin E (Miljeteig et al., 2012). No associations between Hg levels, eggshell thinning and the two vitamins were found in this study. More research on Hg-vitamin relationships is needed for Arctic avian species, especially in the context of thiamine (vitamin B1) deficiency observed in the Baltic Sea (Sonne et al., 2012).

6.3.5 Shorebirds

A large-scale Hg exposure assessment of Arctic-breeding shorebirds offers a unique opportunity to investigate Hg contamination and risk across an extensive geographic range. Shorebirds may represent an ideal group for Arctic Hg exposure research, as shorebirds are widespread across the Arctic during the breeding season. Most shorebirds inhabit similar nesting and foraging habitats in Arctic tundra wetlands and occupy the same foraging guild. Given that Hg research on terrestrial avian invertivores is lacking in the Arctic (Scheuhammer et al., 2015), an investigation of shorebird Hg concentrations fills an important knowledge gap in Arctic Hg exposure research. A study of the period 2012 to 2013 led by Perkins (2018), in collaboration with the Arctic Shorebird Demographics Network (ASDN) and several other partners, sampled 12 breeding shorebird species (n=1472) from five sites in Alaska located near Nome, Cape Krusenstern, Barrow, the Ikpikpuk River and the Colville River, and three sites in Canada near the Mackenzie River delta, Bylot Island and East Bay. An additional Canadian study site, Igloolik, was included with the previously sampled sites in 2013. The ASDN biologists collected blood and feather samples for Hg analysis from adult shorebirds (hatched the prior summer or earlier) captured while conducting routine fieldwork during the breeding season. In total, 1094 blood samples and 1384 feather samples were collected for THg analysis. Blood Hg concentrations in individual shorebirds ranged from 0.01 to 3.52 µg/g, with an overall mean of 0.30±0.27 µg/g. Among species, the mean blood Hg concentration for long-billed dowitchers (*Limnodromus scolopaceus*; 0.74±0.25 µg/g) was over 4.9 times greater than for American golden plovers (*Pluvialis dominica*; 0.15±0.07 µg/g). For feather, the mean THg concentration was 1.14±1.18 µg/g for all samples analyzed and ranged from 0.07 to 12.14 µg/g. Feather Hg concentrations also differed by species, with the mean feather Hg concentration for pectoral sandpipers (*Calidris melanotos*; 2.58±1.76 µg/g) over 4.3 times greater than for red phalaropes (*Phalaropus fulicarius*; 0.60±0.44 µg/g).

Hargreaves et al. (2010) studied potential effects of Hg in three biparental shorebird species nesting in Nunavut, Canada: ruddy turnstones (*Arenaria interpres*), grey plovers (*Pluvialis squatarola*), and semipalmated plovers (*Charadrius semipalmatus*). Maximum Hg concentrations in blood approached those associated with toxicological effects in other bird species and it was found that reproductive success was negatively correlated with paternal Hg concentrations.

6.3.6 Marine fish and freshwater fish

In the context of MeHg research, fish have been studied as vectors for MeHg transfer to wildlife and humans with little focus on the deleterious effects of MeHg to the fish themselves (Wiener and Spry, 1996; Scheuhammer et al., 2007; Sandheinrich and Wiener, 2011; Depew et al., 2012). Most of the early laboratory studies that investigated the health effects of MeHg exposures to fish involved aqueous exposures at high concentration rather than more realistic dietary exposures at environmentally relevant levels (Scheuhammer et al., 2007; Depew et al., 2012). Most of the relevant research into the effects of dietary MeHg exposures to fish have been conducted over the last 20 years. Clear effects on fish growth and survival occur at high tissue Hg concentrations (5–20 µg/g ww in muscle) that are generally associated with point source contamination (Sandheinrich and Wiener, 2011). Perhaps the clearest example that environmental organic Hg exposure results in toxic effects in wild fish is that of Minamata Bay, where fish tissue Hg levels reached ~10 to 20 µg/g ww and fish "rotated continuously and floated belly-up to the surface" (Harada, 1995). Locations that receive Hg through atmospheric deposition rather than through direct point source contamination typically have fish with muscle Hg concentrations well below those that result in overt toxicity (Depew et al., 2013; Eagles-Smith et al., 2016; Barst et al., 2019). Nevertheless, growing evidence provided by laboratory and field research indicates that the Hg concentrations found commonly in wild fish are sufficient to cause sublethal toxic effects (Dillon et al., 2010; Sandheinrich and Wiener, 2011; Depew et al., 2012).

The toxicity of MeHg may be linked to its ability to penetrate cellular membranes (Bridges and Zalups, 2010) and interact with sensitive subcellular sites (Barst et al., 2016). Within cells, MeHg overwhelms antioxidant defenses resulting in oxidative stress, altered gene expression, biochemical changes and tissue damage in fish exposed to MeHg naturally or in the laboratory (Sandheinrich and Wiener, 2011). Altered predator avoidance behavior has been reported for fish exposed to MeHg in the laboratory (Webber and Haines, 2003). Moreover, survival skills related to foraging and predator evasion behaviors were impaired in juvenile fish exposed to MeHg through maternal transfer (Alvarez et al., 2006). Laboratory studies demonstrate

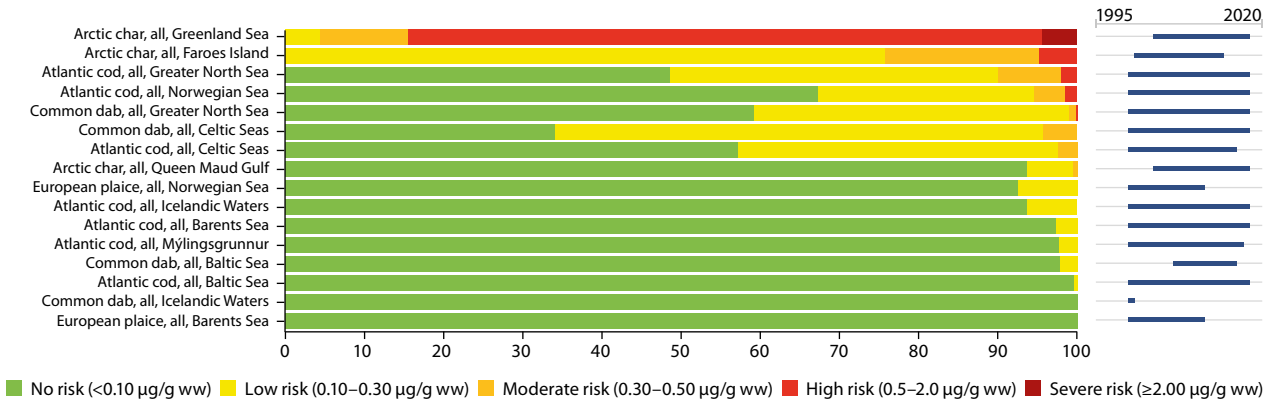

Figure 6.10 Ranked overview (from highest to lowest risk) of the proportion of marine fish, per region from the Arctic, that are at risk for Hg-mediated health effects (categorized in five risk categories based upon whole body Hg effect thresholds that were converted to muscle thresholds).

that environmentally relevant concentrations of dietary MeHg impair fish reproduction through reductions in circulating sex hormones, reduced fecundity and altered reproductive behavior (Hammerschmidt et al., 2002; Drevnick and Sandheinrich, 2003; Drevnick et al., 2006; Sandheinrich and Miller, 2006), as reviewed by Depew et al. (2012).

Effects data produced from laboratory exposures to MeHg provide the basis for understanding dietary thresholds (Depew et al., 2012) as well as for modeling MeHg residue-effects levels for fish (Beckvar et al., 2005; Dillon et al., 2010). The toxic effect level generated by Beckvar et al. (2005; 0.33 µg/g ww in edible muscle) is based on laboratory studies that assessed sublethal endpoints including behavior, development, reproduction and growth. The toxic effect level developed by Dillon et al. (2010; 0.5 µg/g ww in edible muscle) is based on laboratory studies with endpoints most relevant to ecological risk assessment, including lethal developmental abnormalities, reproductive success, mortality and survival. The residue-effect level reported by Dillon et al. (2010) is consistent with the value set by Sandheinrich and Wiener (2011), which was based on both laboratory and field studies. The dose-response model developed by Dillon et al. (2010) may be particularly useful as it is based on endpoints of interest to risk assessors and can predict percent injury across a range of tissue Hg concentrations.

Comparing Hg concentrations of wild fish to residue-effect levels is a relatively quick way to assess the potential for toxic effects in a population of interest. This approach has been used to screen large amounts of Hg data (~43 000 Hg measurements) for fish in the Great Lakes region of the United States (Sandheinrich et al., 2011). A similar approach was recently carried out to assess potential risks of MeHg for non-anadromous (i.e., restricted to lakes and rivers, landlocked or lake dwelling) Arctic char (*Salvelinus Alpinus*; Barst et al., 2019). This screening-level risk assessment included 1569 non-anadromous Arctic char that were sampled from 83 sites, which ranged from locations in the boreal forest to those from the High Arctic. Site-specific mean total Hg concentrations in muscle tissue varied from 0.01 to 1.13 µg/g ww. A comparison between site-specific mean total Hg concentrations in muscle and the lower residue-effect level (0.33 µg/g ww) suggests that 21% of the populations of non-anadromous Arctic char are at risk for MeHg toxicity. Populations of non-anadromous Arctic char that exceeded 0.33 µg/g ww were located in Greenland (7 populations) and Canada (10 populations), almost exclusively in regions of discontinuous or continuous permafrost (see Appendix Table 6A.7). The percentage of populations at risk decreased to 13% when considering the higher residue-effect level of 0.5 µg/g ww (high risk category: 0.5–2.0 µg/g ww; severe risk category: >2.0 µg/g ww). Collectively, the results of the screening-level risk assessment suggest that certain populations of non-anadromous Arctic char may be at risk of MeHg toxicity, especially those located in regions containing discontinuous or continuous permafrost soils (see Chapter 5; Barst et al., 2019).

We built upon this initial effort to assess the potential for MeHg in Arctic marine and freshwater fish by using available Hg data (see Appendix Tables 6A.6 and 6A.7, respectively) and a dose-response model that predicts injury across a range of Hg concentrations (Dillon et al., 2010). To simplify our comparisons, we converted whole-body residue effects concentrations (the basis for the dose-response model) to muscle concentrations using a conversion factor (Peterson et al., 2004). From the dose-response model we created five risk categories. Based on comparisons to the dose-response model, a lower proportion of marine fish (Figure 6.10) had Hg levels in the high and severe risk categories (above 0.5 µg/g ww) as compared with the freshwater fish (Figure 6.11). The freshwater fish dataset was biased towards a larger number of non-anadromous Arctic char populations (n=42). Of these, approximately 26 populations had individuals at high or severe risk of MeHg toxicity. Sea-run Arctic char tended to have lower concentrations of Hg and were therefore categorized as lower risk, with the exception of fish collected from Greenland, Svalbard and the Faroe Islands.

Despite the relative simplicity of screening-level assessments, there are various limitations related to the use of this approach for predicting MeHg toxicity in fish populations of interest. These limitations have been discussed elsewhere both in general terms (Dillon et al., 2010) and in the context of non-anadromous Arctic char (Barst et al., 2019). However, as studies that focus on the direct effects of MeHg exposure to Arctic fish are lacking, the screening-level approach is particularly useful.

A field study from the Canadian High Arctic aimed to assess the potential health effects of MeHg exposure to landlocked Arctic char. Arctic char (n=114) were sampled in 2011 and 2012 from four lakes (Small, 9-Mile, North and Amituk lakes) on

Figure 6.11 Ranked overview (from highest to lowest risk) of the proportion of freshwater fish, per region from the Arctic, that are at risk for Hg-mediated health effects (categorized in five risk categories based upon whole body Hg effect thresholds that were converted to muscle thresholds).

Cornwallis Island (Nunavut, Canada) that span a gradient of Hg contamination (Barst et al., 2016). Total Hg concentrations in muscle tissue were greatest in char from Amituk Lake, intermediate in char from North Lake and 9-Mile Lake, and lowest in char from Small Lake. Total Hg concentrations in livers were two to five times greater than in muscle, with a maximum of 6.5 µg/g ww for an individual from Amituk Lake. For all livers, total Hg was mainly present as MeHg (51% to 90%). A subcellular partitioning procedure based on differential centrifugation was carried out to separate liver cells from Small Lake and Amituk Lake Arctic char into six operationally defined fractions. These subcellular fractions were assigned to one of two groups, including a potentially Hg sensitive compartment (mitochondria + heat-denatured proteins; HDP including enzymes + microsomes and lysosomes) and a Hg detoxified compartment (peptides and heat-stable proteins; HSP including metallothionein + granule-like concretions). Total Hg analyses of the various fractions revealed that the sensitive compartments contributed 73% and 61% of total Hg in Small and Amituk fish livers, suggesting that Hg is not effectively detoxified in the livers of these fish. Histological investigation revealed hepatic fibrosis, predominately in the livers of Amituk Lake Arctic char. A significantly greater number of individuals from Amituk Lake (83%) exhibited this abnormality than individuals from the other study lakes. Evidence of fibrosis was also found in individuals from 9-Mile Lake (29%) and North Lake (27%). Although Hg exposure may have resulted in the observed hepatic fibrosis, the role of other factors (e.g., parasites and other contaminants) cannot be excluded (Barst et al., 2016).

Figure 6.12 presents a geographical overview of the proportion of marine fish and freshwater fish that are at risk of Hg-mediated health effects based on data compiled in Appendix Tables 6A.6 and 6A.7, respectively.

6.3.7 Aquatic Invertebrates

Few dosing studies have been conducted on aquatic invertebrates to determine critical body residues of Hg-associated toxicological effects (Gimbert et al., 2016;

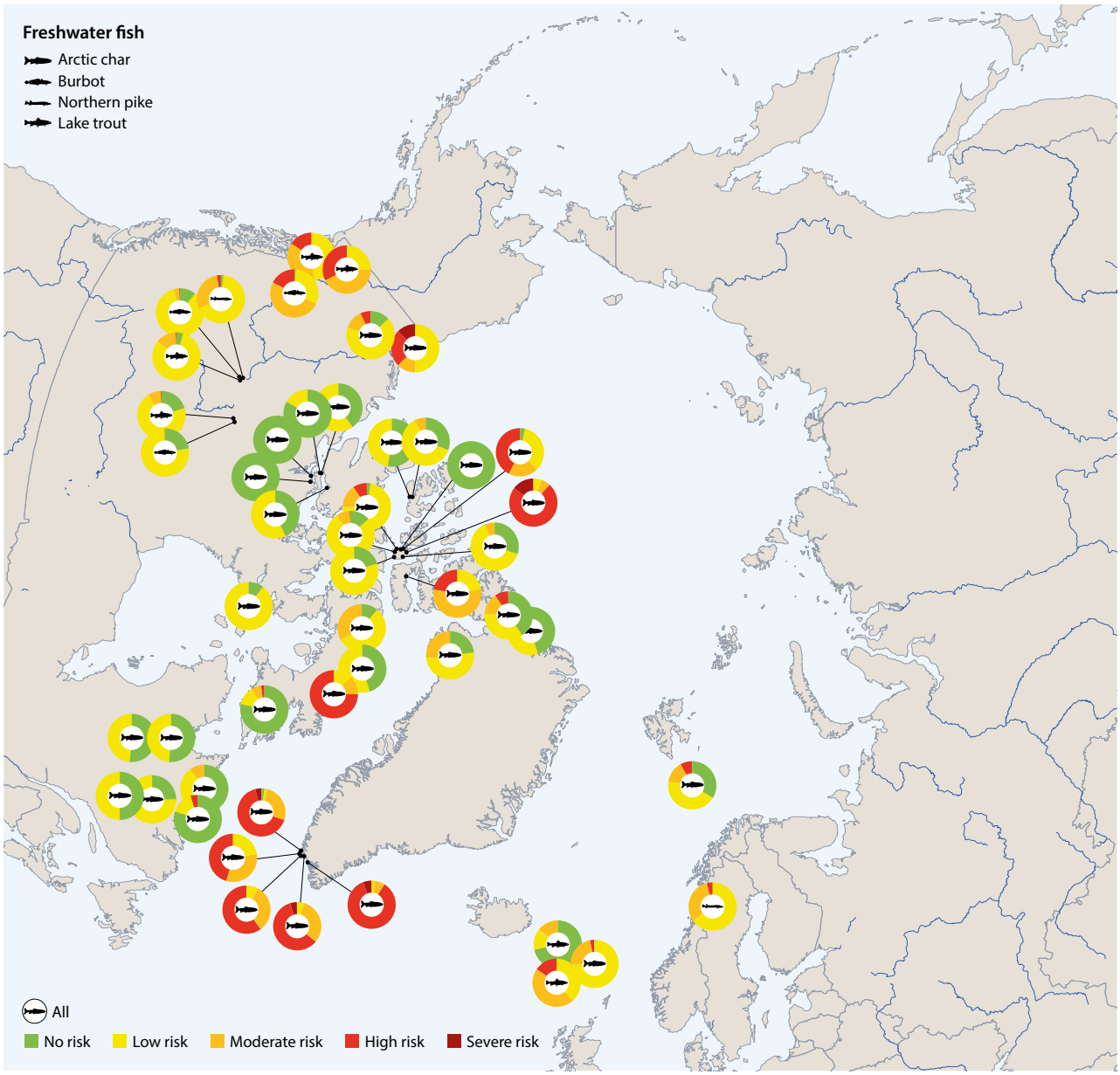

Figure 6.12 The proportion of freshwater fish that are at risk of Hg-mediated health effects. For the detailed information upon which this summary graphic is based, see Appendix Table 6A.6 and 6A.7.

Flanders et al., 2019). Furthermore, much of the toxicological information is based on short-term Hg dosing to water, even though the diet is the primary route of MeHg exposure for invertebrates (Fisher and Hook, 2002; Tsui and Wang, 2007; Williams et al., 2010). Therefore, only a preliminary risk analysis of Hg toxicity to Arctic aquatic invertebrates could presently be conducted, and invertebrates were not included in the broader risk analysis for vertebrates. Published data were compiled from 12 marine studies and 13 freshwater studies from the last two decades to characterize the ranges of Hg and MeHg concentrations in Arctic aquatic invertebrates (see Appendix Table 6A.8). Mercury concentrations varied an order of magnitude among invertebrate taxa (see Figure 6.13). Though sometimes not reported, the proportion of Hg as MeHg was also variable among invertebrates when data were available. For example, the percentage of MeHg in benthic fauna ranged from 9% to 73% in the Chukchi Sea (Fox et al., 2017). Mercury and MeHg concentrations of invertebrates were typically low with the majority of measurements less than 0.25 µg/g dw for both marine and freshwater taxa (see Figure 6.13). A recent examination of over 6000 Hg measurements of marine bivalves in the Baltic Sea found that 99% of samples had concentrations of less than 1 µg/g dw (0.1 µg/g ww; Dietz et al., 2021). The maximum Hg and MeHg concentrations reported in the published literature were 3.5 µg Hg/g for benthic invertebrates from a Fennoscandian lake (Kahilainen et al., 2017) and 0.87 µg MeHg/g for epibenthic shrimp in the Canadian High Arctic (Pedro et al., 2019).

Dosing studies have demonstrated that inorganic Hg and MeHg exposure are only lethal to aquatic invertebrates at extremely high water concentrations (Borgmann et al., 1993; Fisher and Hook, 2002; Øverjordet et al., 2014), which are well above conditions observed in Arctic environments. Similarly, published values for critical body residues of Hg or MeHg (on

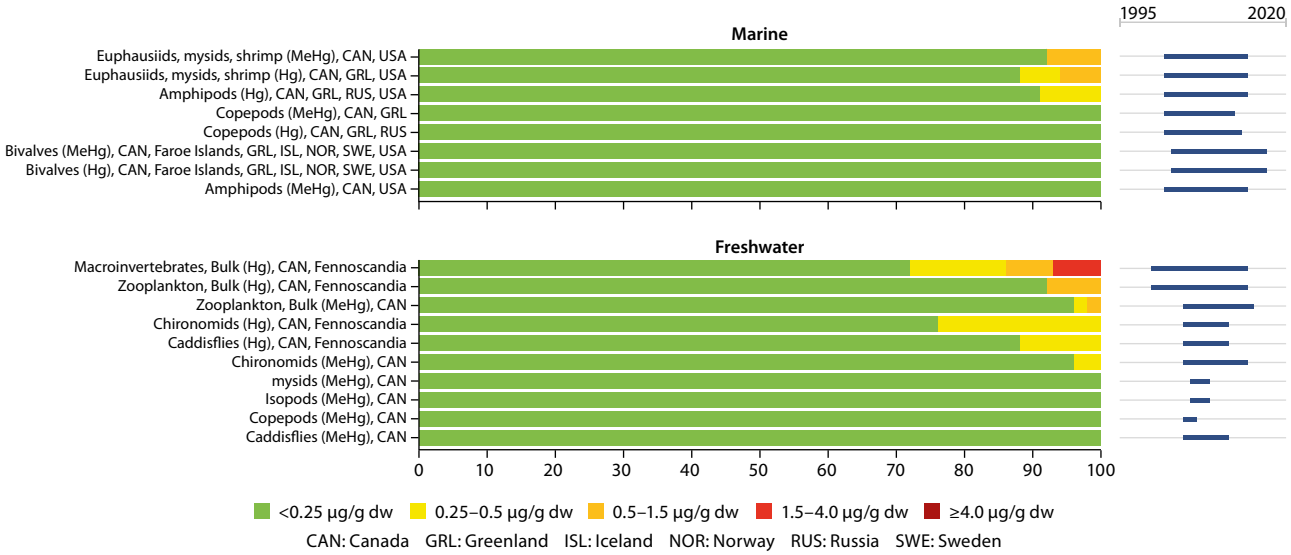

Figure 6.13 Mercury and MeHg concentrations of common marine and freshwater invertebrates, presented as proportions in five concentration categories. Data are from published studies for the circumpolar Arctic over the last two decades (see Appendix Table 6A.8). Note that the concentration categories (µg/g dw) are not associated with toxicological risk (see text above for further explanation).

a dry weight basis, assuming 75% moisture for conversion) associated with lethality are well above concentrations found in Arctic invertebrates, such as 40–104 µg Hg/g for the cladoceran *Daphnia* (Tsui and Wang, 2006), 182 µg MeHg/g for blue mussel (*Mytilus edulis*; Pelletier, 1988), 90 µg Hg/g for the freshwater amphipod *Hyalela azteca* (Borgmann et al., 1993), 15.2 µg Hg/g for the marine amphipod *Bathyporeia pilosa* (Khayrallah, 1985) and more than 10 µg Hg/g for marine copepods (*Calanus* spp.; Øverjordet et al., 2014). Those threshold values associated with lethality are at least 2 to 3 orders of magnitude higher than concentrations observed in Arctic invertebrates (see Figure 6.13). Reduced reproductive success or growth in the freshwater cladoceran *Daphnia* was associated with an elevated body burden of 16.4 µg Hg/g (Biesinger et al., 1982), while for the marine copepod *Acartia* egg production was inhibited at a much lower body Hg concentration of 0.5 µg/g (Hook and Fisher, 2002). Arctic marine copepods were found have lower Hg concentrations (0.057±0.058 µg/g, n=16; see Figure 6.13) than that threshold, although the study does suggest that sublethal effects of Hg could potentially occur in contaminated environments (Fisher and Hook, 2002). Based on the limited toxicological information available, Hg concentrations in aquatic invertebrates from Arctic environments are not likely to pose a toxicological risk to invertebrates.

6.4 What are the population effects from mercury loads in highly exposed wildlife?

Assessing the impact of Hg exposure and accumulation at the population-level is challenging for any species but especially so for species living in remote areas like the Arctic. Such assessments require long-term population monitoring to determine the link between observed tissue Hg levels and relevant long-term fitness metrics such as adult survival, reproductive success and recruitment (i.e., offspring survival to reproductive age) and ultimately population growth rates. For the Arctic, only a few studies in Arctic seabirds have been published to tackle this difficult question (see Section 6.5.3 for summary). Despite reported effects on reproductive performance linked to Hg exposure, these studies report only modest effects on demographic parameters and no effect on adult survival (Goutte et al., 2014a, 2014b, 2015, 2018; Bårdsen et al., 2018; Amélineau et al., 2019). For all other Arctic species included in this report, little to no information is available on the population impacts of Hg.

It is because of this paucity of information that we undertook the current pan-Arctic Hg risk assessment. The risk categories outlined here represent the best available information on Hg effects in a broad range of relevant species across vertebrate taxa. For species in the high and severe risk categories, there is a concern that levels of Hg may have an impact at the population-level, given the observed effects in the reference toxicity studies. The most comprehensive toxicity data are available for birds, for which dozens of studies across multiple species, life-stages and experimental designs (e.g., laboratory exposures and ecological studies) were summarized to establish the risk categories. Here, expected effects for populations in the high risk category include moderately reduced reproductive performance in the form of reduced hatching success and occasional failed reproduction as well as reduced immune-competence. Effects for populations in the severe risk category include severe reproductive impairment (low hatching success and offspring survival), oxidative stress, neurotoxicity and increased adult mortality. The available data for marine and terrestrial mammals are much less comprehensive and derived from few captive feeding studies in harp seal and mink, respectively (see Table 6.1). For harp seals, no data were reported for reproductive performance but for populations in the high risk category effects include the increased potential for organ lesions (kidney, liver), anorexia and reduced growth, while effects for populations in the severe risk category include the increased likelihood of severe impacts on organ function (i.e., kidney failure), weight loss and increased mortality. For mink, observed effects in populations in the high risk category

included reduced litter size and offspring growth rate, while effects in populations in the severe risk category included brain lesions, reduced growth, anorexia and increased adult mortality.

Given the direct consequences for reproduction and survival in populations in the the high and severe risk categories, two endpoints of key concern for potential population impacts, concern is warranted for select populations of hooded seals, killer whales and pilot whales as well as Lancaster Sound and Northern Beaufort Sea polar bears and harbour porpoises in the Danish Straits. Here, more than 20% of sampled individuals within these populations (and up to 60% to 90% in some populations) had concerning tissue Hg levels; impacts in such a large proportion of the population has the potential to meaningfully affect demographic rates and overall population fitness. For polar bears in highly exposed regions, such as Lancaster Sound and Jones Sound, the population trends are data deficient (Vongraven and York, 2014; Dietz et al., 2015). In areas like the southern Beaufort Sea and Baffin Bay the populations are declining, and the effects of climate change are likely to play a major role in these areas. Pilot whales in Faroese and Greenlandic waters are likely to be vagrants from the North Atlantic population, which numbers several hundred-thousand individuals (NAMMCO, 2018). In addition, the pilot whales with high contaminant loads are hunted in the Faroe Islands and, to an increasing extent, in Greenland where this species has become more common in recent decades due to climate change; thus, in the case of pilot whales and other toothed whale species (e.g., killer whales and narwhals) a cumulative effect has been observed on population numbers as a result of exposure to contaminants and hunting (Dietz et al., 2019b; Piniarneq, 2020). Similarly, a large portion of the Arctic fox population in Iceland is at high or severe risk for potential population relevant impacts as a result of exposure to Hg. In seabirds, 1% of birds for which Hg concentrations were measured were either in the high or severe risk category. The birds in these categories of concern include northern fulmar, double-crested cormorant and pigeon guillemot from western North America, glaucous-winged gull from the Aleutian Islands, glaucous gull from Northwest Greenland, lesser black-backed gull from the Faroe Islands and black-legged kittiwake from the Russian Arctic; for all these seabird populations, trend data are largely missing.

It is important to note, once again, that the above population assessments for marine and terrestrial mammals are based on toxicity data from only one relevant species for each group (e.g., harp seal and mink). Care must be taken to extrapolate effects across species because of potential inter-species differences in Hg toxicokinetics (e.g., uptake and distribution) and toxicodynamics (e.g., species sensitivity to effects). Because such differences are unknown at present and difficult to assess, the current risk exercise provides the best available evidence-based assessment of potential impacts across Arctic species. Furthermore, these Arctic species of concern with regard to the effects of Hg are also potentially impacted at the population level through similar effects on reproduction and adult survival due to habitat changes linked to climate warming effects (linked to POPs and other contaminants) as well as hunting (e.g., Dietz et al., 2015, 2019a; Laidre et al., 2015). Teasing out the effects of Hg from other stressors such as climate change remains a challenge for wildlife studies, although it is expected that these stressors act in concert to increase the overall stress on individuals and populations. Overall, refinement of the work on exact risk benchmark values for different species and regions are recommended as well as population effect studies in relation to Hg and other contaminant loads as conducted for killer whales by Desforges et al. (2018c).

6.5 Do the highest exposed species have increasing mercury loads?

6.5.1 Marine mammals

6.5.1.1 Polar bears

Twenty groups from 10 polar bear management areas were assessed for Hg risk based on their liver concentrations (see Figures 6.1, 6.2 and Appendix Table 6A.1). Six of these 20 groups (30%) had individuals in the severe risk category (SRC; 1% to 41%) and eight groups (40%) had individuals in the high risk category (HRC; 2.5% to 35%) representing half of the polar bear groups (10 out of 20) from six of the 10 polar bear management areas. Four polar bear management areas (Southern Hudson Bay, Western Hudson Bay, Ittoqqortoormiit and Svalbard) and four out of 13 analyzed groups showed significant increasing Hg temporal trends, but no groups showed declining Hg loads. Unfortunately, for the regions with the highest number of individuals in high or severe risk categories, namely Lancaster Sound and Jones Sound (SRC: 0% to 25%; HRG: 20% to 25%) as well as the Northern Beaufort Sea (SRG: 0 to 41%; HRG: 22% to 35%) and the Qaanaaq region (SRG: 33%), no time trend information was available (see Chapter 2). However, yearly significant Hg increases of 1.6% to 1.7% ($p<0.0001$) per year from 1892 to 2008 have previously been reported in polar bear hair from Qaanaaq, Northwest Greenland (Dietz et al., 2011; Figure 6.14). Similarly, in Western Hudson Bay a significant increasing trend of 6% per year was detected in adult male livers, whereas no trend was observed in juveniles or in adult females (see Chapter 2). Trends are of concern if, for example, in northwest Greenland, northeast Canada, Western Hudson Bay and the Beaufort Sea, Hg in polar bears is increasing in areas where loads are already at the severe and high risk levels. Despite the number of individual polar bears in risk categories of concern being lower in Ittoqqortoormiit, central East Greenland (SRC: 1% to 33%; HRC: 3%), significant increases of Hg in polar bear hair was documented for both juvenile and adult polar bears. The hair risk analyses for polar bears (see Figures 6.3 and 6.4; Appendix Table 6A.2) were quite similar to the liver risk results with Lancaster Sound, Norwegian Bay, Viscount Melville Sound, Northwest Greenland and East Greenland with animals in the severe risk and high risk categories (SRC: 4% to 33%; HRC: 1% to 20%).

6.5.1.2 Ringed seals

Thirty-seven groups from 18 Arctic regions were assessed for Hg risk based on their liver concentrations (see Figures 6.1 and 6.2; Appendix Table 6A.1). Four of these 37 groups (10.8%) from Arviat, western Hudson Bay, Resolute Bay, Sachs Harbour and the Eastern Beaufort Sea had individuals in the severe risk category (SRC; 1.4% to 12%) and six groups (16%) from the

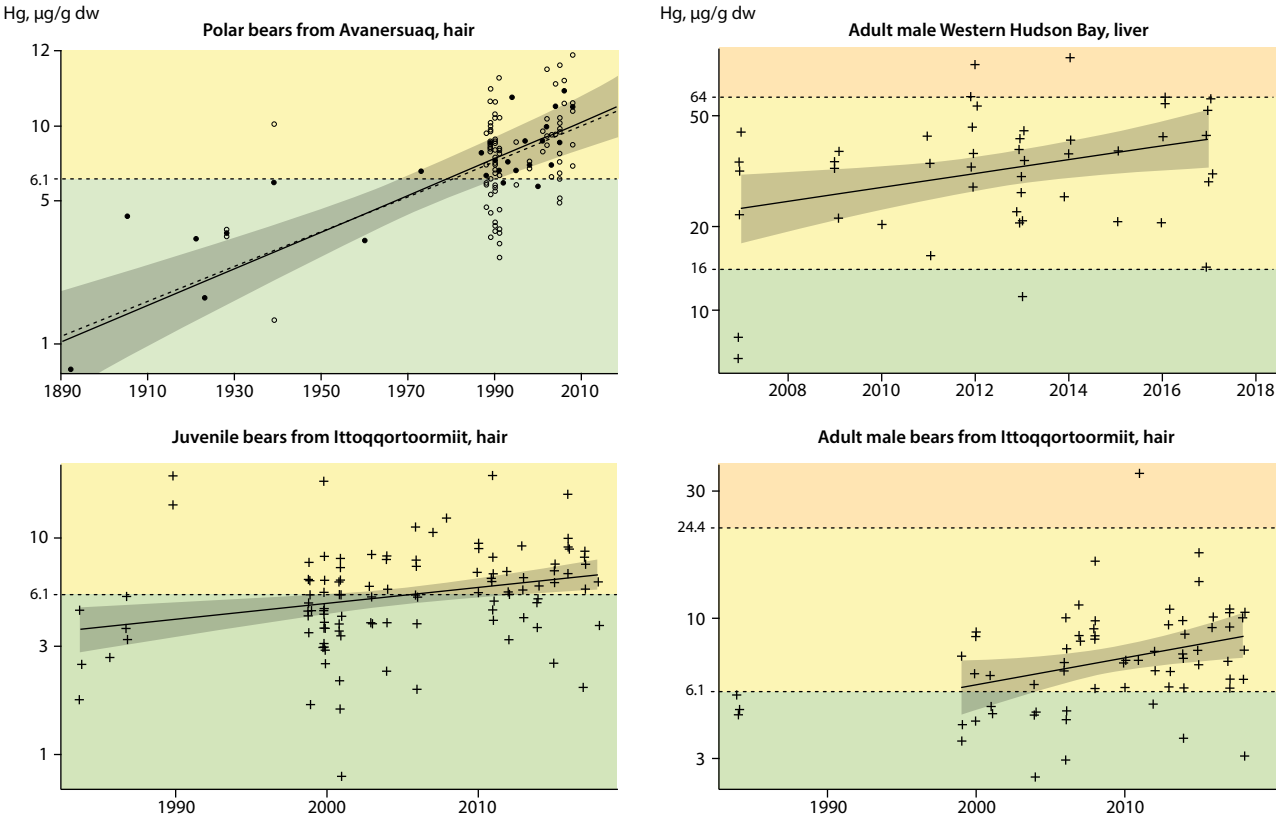

Figure 6.14 Examples of significant Hg increases in polar bear hair and liver from Canadian and Greenlandic waters plotted on top of risk intervals (no risk; green, low risk; yellow, moderate risk; orange, high risk; red and severe risk; dark red) defined in Table 6.1.

same four regions as well as Grise Fiord had individuals in the high risk category (HRC; 1.4% to 9.6%) representing a total of 19% of the ringed seal groups (7 out of 37) from five of the 18 ringed seal regions. Only one (southern Beaufort Sea) out of the seven regions where ringed seals were assessed and one out of 21 analyzed groups (4.8%) showed significant increasing Hg temporal trends. However, four (eastern Beaufort Sea, Resolute Passage, southern Labrador Sea and western Hudson Bay) out of the seven regions and six out of 21 analyzed groups (29%) showed significant declining Hg trends in ringed seals. Only adult seals (both male and female) from the southern Beaufort Sea showed significant increases of Hg in their livers. However, as this was not a hotspot for Hg risk and as 29% of individuals showed significant declines in Hg, ringed seals are not currently assessed as being at significant risk.

6.5.1.3 Beluga whales

Only one out of six groups (17%) of beluga whales from the Canadian Arctic had individuals (1.2%) in the severe risk category and two out of six groups (33%) had individuals (1.3% to 3.9%) in the high risk category based on their liver concentrations (see Figure 6.1 and Appendix Table 6A.1). Of the 10 temporal trend analyses conducted for Hg in the muscle and liver tissues of belugas from the southern Beaufort Sea and southern Hudson Bay regions in Chapter 2, three significant declines (30%) and no significant increases were detected. With the rather low percentages of belugas having individuals in the severe and high risk categories, it is encouraging that a large proportion of these whales are showing significant declines in their Hg loads with respect to the beluga health.

6.5.1.4 Pilot whales

Both groups of pilot whales assessed in the Faroe Islands had individuals in the severe risk category and one of them also had individuals in the high risk category based on liver concentrations (see Figure 6.1. and Appendix Table 6A.1). The subadult group had 20% and the adult pilot whales had 27% of individuals in the severe risk category; the adult group had 20% of individuals in the high risk category. Of the age groups and tissues assessed, one (muscle of juvenile males) out of five pilot whale groups showed significant increasing trends and none showed significant declines. Significant increasing trends were also observed in one out of three muscle groups investigated (33%). With the high percentage of pilot whales having individuals in the severe and high risk categories, it is concerning that juvenile pilot whales are showing significant increases of Hg in their meat both with respect to the pilot whales health as well as the risk related to the population consuming the whales. For human health exposure and the consumption of pilot whales in the Faroe Islands, see Chapter 7 as well as a recent AMAP (2015) report.

6.5.1.5 Other marine mammals

Of the other marine mammal species assessed, bearded seals, harp seals and harbour porpoises did not have any individuals in the two highest risk categories, as was also the case for adult hooded seals, narwhals and killer whales (see Figure 6.1; Appendix Table 6A.1). However, as no time trend analyses were available from these groups no overall evaluation can be made with respect to the temporal patterns of these risks.

6.5.2 Terrestrial mammals

Except for one group of adult Arctic fox from Iceland, none of the terrestrial mammals had individuals in the severe risk or high risk categories. Of the two caribou population time trends from Canada and the one Arctic fox population from Svalbard, no significant trends were detected. Thus, we can conclude from the concentration levels measured that terrestrial mammals are not likely to be at risk nor is risk likely to develop over time.

6.5.3 Seabirds

In each of the 16 species of seabirds studied at least some individuals were found to have Hg concentrations above the level at which there are no adverse health effects (a blood-equivalent Hg concentration of 0.2 µg/g ww). Overall, 50% of birds had total Hg concentrations that exceeded the no adverse health effects level, and 1% of birds were in the high or severe risk categories. Mercury concentrations differed widely between sites due to local MeHg bioaccumulation pathways. Long-term trends (10–19 years) in bird Hg concentrations are available for five species, with data available from one to four sites in each case; three sites have increasing trends and one site has a decreasing trend (Morris et al., 2022). Specifically, northern fulmar Hg concentrations in eggs at Prince Leopold Island have increased by 1% per year (19 years) and black guillemot Hg concentrations in eggs at Koltur (11 years) and Skúvoy (10 years) on the Faroe Islands have increased by 4.5% and 5.7%, respectively (Morris et al., 2022). By contrast, of the 12 datasets, only one decreasing trend of 3.1% per year (15 years) was detected for black-legged kittiwake at Svalbard-Kongsfjorden in Norway (Morris et al., 2022).

6.5.4 Shorebirds

Most Arctic-breeding shorebirds had blood Hg concentrations which placed individuals in no risk or low risk categories and below the level at which there are adverse effects of Hg exposure, with approximately 45% of individuals falling into the no risk category and 47% falling into the low risk category (see Figure 6.15, see Appendix). We found no individuals in the severe risk category and a low proportion of individuals with blood Hg concentrations in the moderate risk (4.5%) and high risk (2.5%) categories. The greatest proportion of individuals in the moderate risk and high risk categories were sampled at the Barrow (Alaska) study site while the Cape Krusenstern, Ikpikpuk River, Mackenzie River Delta and Bylot Island sites did not have any individual shorebirds with blood Hg concentrations falling into these risk categories. Long-billed dowitcher had the greatest proportion of individuals that fell in the moderate risk and high risk categories (approximately 22% and 17%, respectively). Pectoral sandpiper also had approximately 17% and 9% of individuals within these respective categories. While individual American golden plover, Baird's sandpiper (*Calidris bairdii*), black-bellied plover (*Pluvialis squatarola*), and black turnstone (*Arenaria melanocephala*) were found to have blood Hg concentrations only in the no effect and low risk categories. As no temporal trend data are available from shorebirds, no further information on extraction hotspot species and regions with temporal trend information can be conducted.

6.5.5 Marine fish

Seventeen groups of marine fish representing 4 different species were assessed for Hg risk based on muscle Hg concentrations. Only anadromous Arctic char from the Greenland Sea had individuals (4.4%) in the severe risk category; the majority (80%) of the Arctic char from the Greenland Sea were in the high risk category. Only six other groups had individuals in the high risk category, including anadromous Arctic char from Bjørnøya (7.9%) and the Faroe Islands (4.7%), Atlantic cod from the North Sea (2.1%) and the Norwegian Sea (1.6%), and common dab (*Limanda limanda*) from the North Sea (0.3%) and the Celtic Sea (0.1%). Time trend analyses were conducted for a subset of the marine fish included in the risk assessment. For the anadromous Arctic char from Bjørnøya, there was a significant increasing trend in muscle Hg, which is concerning given that certain individuals from this population were in the high risk category. In comparison, anadromous Arctic char from the Queen Maud Gulf showed no significant trend and none of the individuals were in either the severe or high risk categories. Atlantic cod (of undefined length) from Mýlingsgrunnur in the Faroe Islands showed an increasing recent trend in muscle Hg concentrations, although the majority of the individuals from this sample were in the no risk category. Note that medium-sized Atlantic cod from the same location showed no significant time trend.

6.5.6 Freshwater fish

Fifty-three groups of freshwater fish representing five species were assessed for risk based on Hg concentrations in muscle. Note that the dataset was heavily biased toward populations of non-anadromous Arctic char. Twenty-seven of the freshwater fish groups contained individuals in the severe or high risk categories. Arctic char from Amituk Lake (Canadian High Arctic) had the greatest proportion (15%) of individuals in the severe risk category and a large proportion (74%) in the high risk category, though time trend analysis indicates recent declines in Hg concentrations in Arctic char from this location. Minor proportions of non-anadromous Arctic char from Herbert Lake (12%; Yukon, Canada), Isortoq (5.7%; Greenland), Lake D (4.6%; Greenland) and Lake A (4.0%; Greenland) were also in the severe risk category. Of these populations, a time trend analysis was only available for non-anadromous Arctic char from Isortoq and no significant trend was detected for this population. Additional time trend analyses were available for four non-anadromous Arctic char populations that had individuals in the high risk category, including Char Lake (42.4%; Canadian High Arctic), North Lake (9.4%; Canadian High Arctic), Lake Hazen (9.2%; Canadian High Arctic), and Á Mýrunum (3.1%; Faroe Islands). Most of these groups showed no significant temporal trend with the exception of Lake Hazen, where Hg concentrations in Arctic char have recently decreased significantly.

Time trend analyses were available for four populations of lake trout (*Salvelinus namaycush*) from Canada. Lake trout from Lake Laberge and Lake Kusawa had 32% and 16% of individuals in the high risk category, respectively. Both of these populations showed significant decreasing trends in Hg concentrations.

Much lower proportions (0.5% and 0.4%) of lake trout from the West Basin and East Arm of Great Slave Lake were classified as high risk. No significant trend was detected for the East Arm group, though recent increases in Hg concentrations were noted in the West Basin group of lake trout.

Time trend analyses were available for two populations of northern pike (*Esox lucius*), both of which had minor proportions of individuals in the high risk category. Only 3.8% of the northern pike were in the high risk category from Storvindeln (Sweden) for which there is a significant decreasing trend in Hg concentrations. A similar proportion (2.6%) of northern pike sampled from the West Basin of Great Slave Lake had Hg levels consistent with the high risk category and no significant trend was found for this population.

Time trends were available for two populations of burbot *(Lota lota*) from Canada. A greater proportion of individuals from Fort Good Hope (17%) were in the high risk category than from the West Basin of Great Slave Lake (0.5%). Significant recent declines in Hg concentrations were noted for these two groups of burbot.

6.5.7 Invertebrates

As documented above, Hg and MeHg concentrations of invertebrates were typically low in the majority of measurements (<0.25 µg/g dw for both marine and freshwater taxa). In addition, very limited information is available on temporal trends in invertebrates; time series only exist for the marine bivalves blue mussels (*Mytilus edulis*). Of the 12 time series analysed in Chapter 2, increases were found in Mjóifjörður in Iceland and only one declining time series from Skallneset, Norway. Therefore, there does not seem to be any documented health related problems in regions that are Hg hotspots when it comes to particular species of invertebrate.

6.6 What are the geographical mercury hotspot areas in water and wildlife?

Previous publications have considered geographical hotspots with respect to Hg biomagnification and adverse biological effects in Arctic char, seabirds, ringed seals and polar bears (e.g., Braune et al., 1991; AMAP, 1998; Dietz et al., 1998, 2000c, 2013; Rigét et al., 2005; Routti et al., 2011, 2012; Brown et al., 2016; Albert et al., 2021). Most of these surveys have identified hotspots for Hg depletion and exposure in the Canadian Arctic Archipelago and in northwestern Greenland. Here, we go a step further by providing a comprehensive multiple species pan-Arctic Hg hotspot evaluation. A systematic way to determine hotspot areas would be to conduct the analyses exclusively on recent datasets (e.g., 2015–2020) and use same age/sex groups while correcting for dietary confounding factors (e.g., by using stable carbon and nitrogen isotope analyses). It has not been possible to conduct the analyses, data gathering and hotspot modeling in this way in the current assessment but it is recommended this be undertaken for the next AMAP Mercury Assessment.

Recent analyses of Arctic alcids suggest the eastern Canadian Arctic to have the highest biomagnified concentrations of Hg

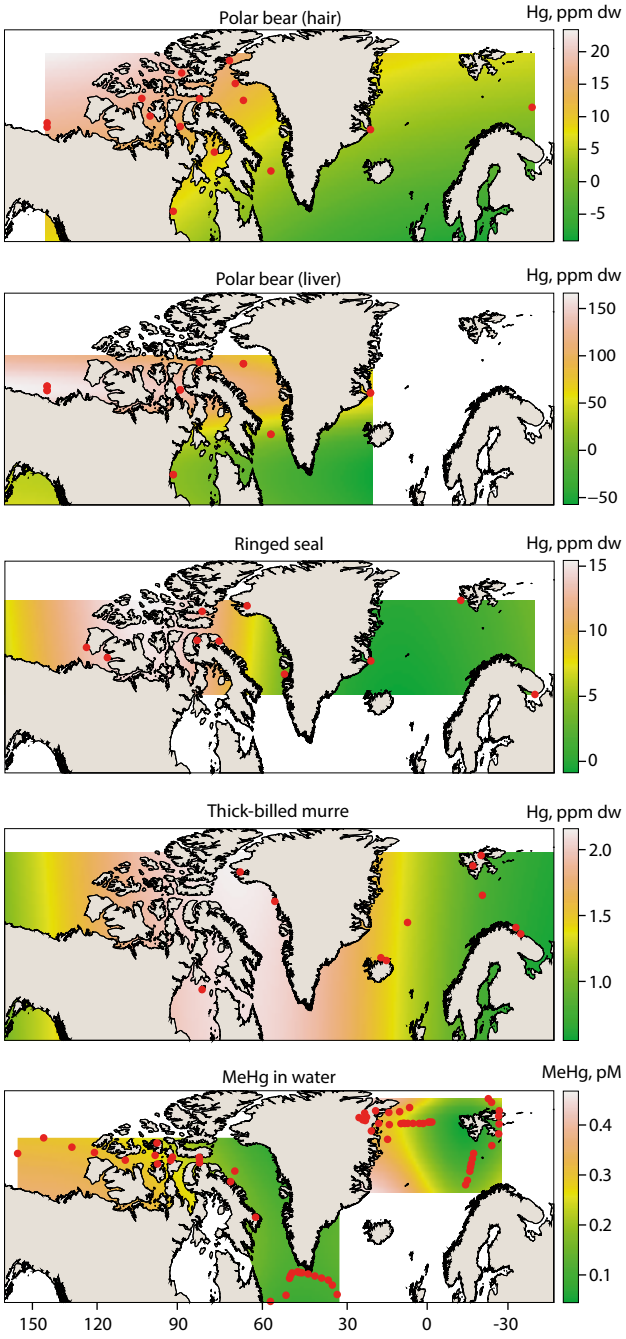

Figure 6.16 Heat maps based on a generalized additive model (GAM) of geographical patterns of Hg. From the bottom: MeHg in the upper 400 m of the ocean, Hg in belly feathers of thick-billed murre/Brünnichs guillemot, Hg in juvenile ringed seal liver, Hg in polar bear liver and polar bear hair. Sources: Rigét et al., 2005; Routti et al., 2011; Cossa et al., 2018; Wang et al., 2018; Petrova et al., 2020; Albert et al., 2021.

(Albert et al., 2021), which is supported by circumpolar studies of ringed seals (Rigét et al., 2005). Studies of polar bears adjusted for sex and age (Dietz et al., 2000c; Routti et al., 2011) based on liver analyses also points towards the Canadian Arctic as a hotspot. A later study adjusted Hg concentrations for differences in feeding ecology (through influence of carbon and lipid measurements) and found similar conclusions (Routti et al., 2012). As part of the Arctic GEOTRACES program, a ship transect was conducted in 2015 from the Labrador Sea and across Baffin Bay to the Canadian Arctic Archipelago and Canada Basin showing the highest concentrations of Hg in the Beaufort Sea. The study showed high-resolution vertical profiles of total Hg and MeHg in seawater and also suggested a link between these

measurements and animal exposure (see also Sections 3.5.4 and 4.3.2.1; Wang et al., 2018). The study also showed a distinctive subsurface maximum of MeHg in seawater in the upper 400 m of the water column, with a peak concentration of Hg decreasing from the Canada Basin eastwards (see Figure 6.16, bottom). These results were combined with recent results from the Arctic GEOTRACES programme (Cossa et al., 2018, Petrova et al., 2020) and newly collected data from 'Arven etter Nansen Seasonal Cruise Q1 2021' (Kohler et al., pers. comm., 2021) and produced a heat map from a generalized additive model (GAM) covering the upper 400 m of the water column (Petrova et al., 2020; see Figure 6.16). Similar heat maps were produced from thick-billed murre body feathers, ringed seal liver, and polar bear liver and hair indicating biota hotspot areas in the central Canadian Arctic Archipelago and, for some species, the Beaufort Sea (Rigét et al., 2005; Routti et al., 2011; Albert et al., 2021). In order to refine these heat maps, define Hg hotspots more precisely throughout the Arctic and provide a better correlation between water MeHg and wildlife exposure.

6.7 Conclusions and recommendations

Conclusions (in numbered bullets) are organized under section headings (section numbers in square brackets) followed by recommendations in italics where appropriate.

What are the combined effects of chemical stressors? [6.2]

1. Arctic biota are exposed to multiple stressors, and the impacts of Hg act in concert with both natural and other stressors (e.g., diseases, parasites, anthropogenic disturbances and climate-related environmental changes). Thus, even Hg concentrations considered as posing low or moderate risks to some mammal and bird species may cause adverse effects if they co-occur with increased levels of other stressors.
2. Our understanding of the ultimate consequences of Hg exposure for Arctic wildlife is still restricted by the limited number of available long-term demographic studies.
3. Many Arctic birds leave the Arctic after the breeding period, and some are long distance migrants, spending the winter in the Subarctic, temperate and tropical regions, and the Antarctic. Environmental stressors and Hg uptake outside the breeding season can result in sublethal to lethal effects and contribute to increased bird mortality by impacting their body condition. They can also result in non-lethal effects that may be carried over to the next breeding season and can strongly impact fitness and population dynamics.

Future investigations should be more holistic. To better assess the specific impacts of Hg on biota, information on other contaminants (e.g., chlorinated and brominated POPs, PFAS and other CEACs) as well as non-essential trace elements such as selenium should be included. Incorporating selenium, which is known to have a protective effect against the toxic effects of Hg, would be particularly relevant, especially when it comes to refining our estimates for Hg toxicity risks to Arctic species.

Does evidence exist for mercury concentrations in tissues that are harmful to Arctic biota? [6.3]

4. For most Arctic species included in this assessment whose Hg concentrations place them in increased risk categories of adverse effects, few if any studies have been conducted to verify the actual impact of Hg on their health.
5. Only a few studies in Arctic wildlife have been published that address the question of whether effects on reproductive performance can be linked to Hg exposure; most studies report only modest effects on demographic parameters and no effect on adult survival.

Further studies should be conducted on the effects of Hg exposure on specific populations, in particular focusing on species and regions where risks of effects are elevated based on the available data.

There is a need to investigate whether Hg exposure is linked to adult survival, especially in species considered at risk, including Arctic songbirds (Cristol et al., 2020). This will require substantial effort and the undertaking of capture-mark-recapture studies (CMR) of individuals that have been banded/marked and subjected to demographic monitoring over several years.

Further studies should be conducted combining miniaturized tracking systems (e.g., geolocators to document migratory movements and wintering areas) with measurements of Hg levels along with measurements of other environmental stressors and detailed demographical surveys; such studies should provide relevant information on the global impact of Hg on Arctic birds.

Further investigation on the link between Hg exposure, thyroid hormones and energy expenditure (basal and field/actual metabolic rate) is needed, especially for the most highly contaminated species, as well as further research into the link between Hg exposure and telomeres.

What are the population effects from mercury loads in highly exposed wildlife? [6.4]

6. For most Arctic species included in this report, little to no information is available on the impacts of Hg on specific populations.
7. Despite Hg exposure having been reported to affect reproductive performance in Arctic seabirds, there are only a limited number of published studies that address the difficult question of effects at the population level. The available studies generally report only modest effects on demographic parameters and do not report any effects on adult survival.
8. In those areas of the Arctic for which studies are available, most marine mammal, shorebird, seabird, fish, and invertebrate species have been found to be at low risk or not at any risk of health effects mediated by Hg exposure. Some studies, however, have raised concerns about population level effects in some marine mammals, including long-lived Arctic marine mammals, such as polar bear, pilot whale, narwhal, beluga and hooded seal, and seabirds; these concerns are also linked to possible combined effects of Hg and other contaminants and stressors.

More research efforts should be directed towards population effect studies in relation to Hg exposure for different relevant Arctic species and regions.

There is a need for more basic and applied research focusing on defining and refining risk threshold values for different relevant Arctic species and regions, along with more population effect studies in relation to Hg exposure.

Do the highest exposed species have increasing mercury loads? [6.5]

9. Mercury continues to pose a justifiable concern for some long-lived Arctic marine mammals, such as polar bear, pilot whale, narwhal, beluga and hooded seal, as well as some seabirds in hotspot areas, including the Canadian High Arctic, Northwest Greenland and the Faroe Islands, where a notable proportion of the population is at a high or severe risk of health effects as a result of Hg exposure.
10. In general, marine fish tend to have lower Hg concentrations than freshwater fish in the Arctic. Certain populations of non-anadromous Arctic char, primarily those from permafrost regions, may be at risk of Hg toxicity.
11. Several Arctic seabird populations from across the Arctic were found to have Hg concentrations that exceeded toxicity benchmarks, with 50% of birds sampled exceeding the no adverse health effect level. In particular, 5% or more individuals sampled were considered to be at moderate or higher risk of MeHg toxicity; this was the case for northern fulmar, ivory gull, glaucous-winged gull, glaucous gull, lesser black-backed gull, black-legged kittiwake, red-legged kittiwake, Atlantic puffin, thick-billed murre, black guillemot, pigeon guillemot, rhinoceros auklet, double-crested cormorant and ruddy turnstone. Toxicological effects of Hg that have been detected in Arctic birds include effects on hormone levels, changes in parental behavior and reduced reproductive performance. However, most (95%) Arctic birds were generally at lower risk (i.e., were in one of the three lowest risk categories) of toxicity from MeHg exposure.
12. Terrestrial mammals were not at risk of health effects mediated by Hg exposure based on the limited recent Hg data available, with the exception of Arctic fox in Iceland, which are at low to moderate risk.

The efficiency of current monitoring programs should be improved through pan-Arctic harmonization with regards to target species, spatial and seasonal coverage (for hotspot determination), sampling frequency, sampling methods and tissues sampled.

Future assessments of the effects of Hg should be improved through deeper research on the underlying cellular and molecular mechanisms, especially as they differ across species, sexes and life stages, including how these may be linked with adverse apical outcomes of concern (e.g., survival, growth and reproduction).

The understanding of the adverse effects of Hg on Arctic fish and wildlife must be improved, particularly in the face of a changing climate; the understanding of how such changes are altering abiotic and biotic exposure pathways and exposure-effect relationships must also be improved.

Multidisciplinary studies should be conducted to further identify cumulative and interactive effects of Hg and other environmental stressors (e.g., other chemical contaminants, climate change, food-web structure and pathogens) on Arctic biota, which should also include dialogue with human health researchers.

What are the geographical trends and mercury hotspots for wildlife, fish, invertebrates and abiotic matrices? [6.6]

13. Most of the investigations addressing geographical differences have shown possible 'hotspots' for Hg exposure in the northern Canadian Arctic and in Northwest Greenland. These hotspots may be driven by MeHg in the epipelagic layer of water masses, as well as Hg air transport and deposition as a result of Arctic mercury depletion events.

More studies are needed within these hotspot regions with respect to potential effects of Hg on species and populations; more studies are also needed into temporal trends of Hg in these regions.

For the next AMAP Mercury Assessment, a more systematic method to determine hotspot areas is recommended; the analyses should be conducted exclusively on recent datasets (e.g., 2015–2020) and the same age/sex groups should be used, while correcting for dietary confounding factors (e.g., by using stable carbon and nitrogen isotope analyses). Existing heat maps should be refined and Hg hotspots defined more precisely to provide a better correlation between water MeHg and wildlife exposure.

Further ship transects should also be conducted, building a denser sampling network of biota matrices within the same short time period to improve the likelihood of establishing potential links between ocean MeHg and Hg in biota.

Appendix Table of Contents

Appendix 6

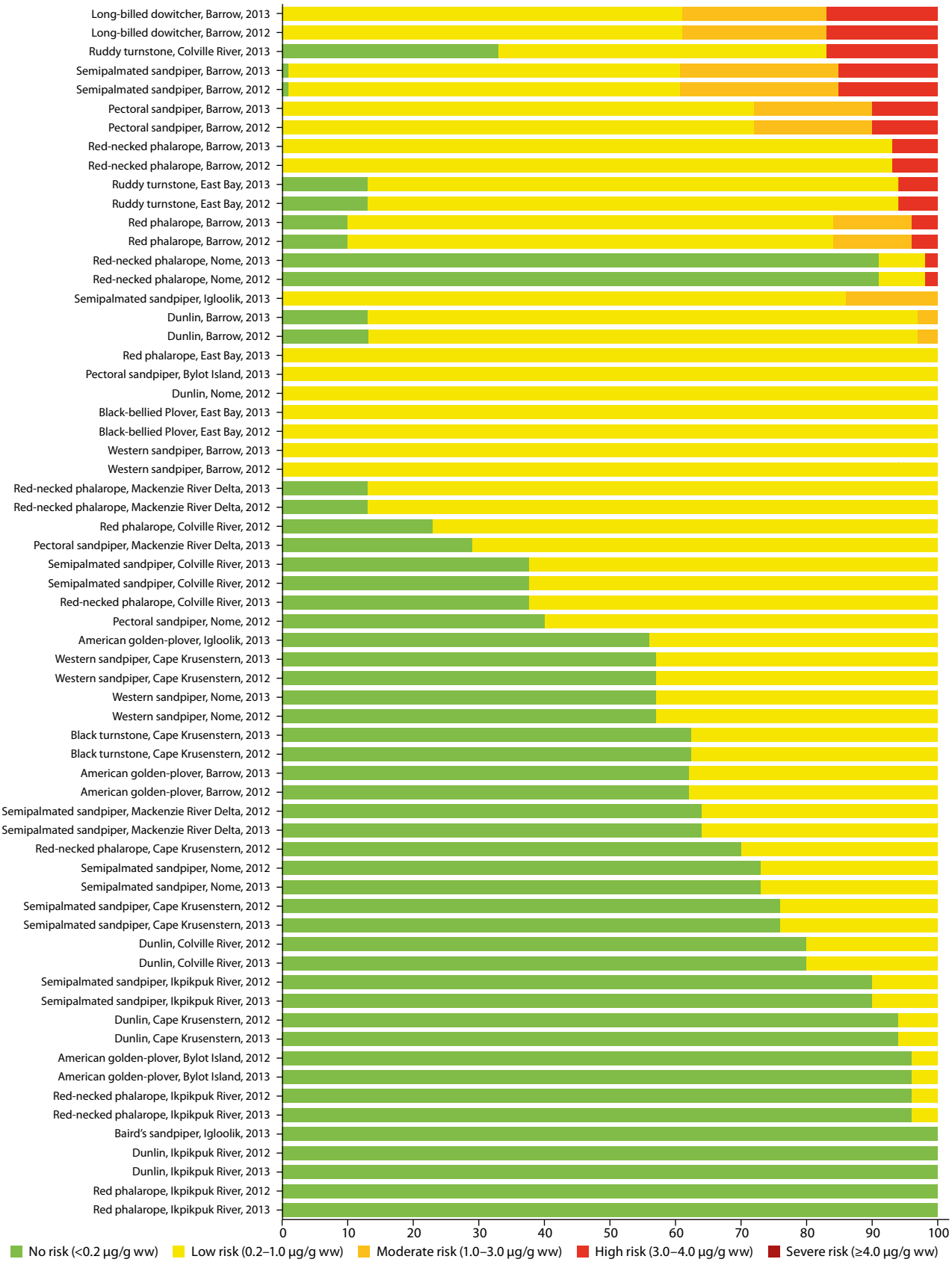

Figure 6.15 Ranked overview (from highest to lowest risk) of the proportion of shorebirds blood, per region from the Arctic, that are at risk for Hg-mediated health effects (categorized in five risk categories based upon liver Hg effect thresholds). See Appendix Table 6A.5(A) for the detailed information upon which this summary graphic is based; shorebird feather data are presented in Appendix Table 6A.5(B).

Appendix Table 6A.1 Contemporary (post-2000) Hg exposure and potential health risk for Arctic marine mammals. Individuals are categorized by study region, maturity and sex, and assigned to five risk categories based upon liver tissue-specific Hg effect thresholds. Grey shaded populations are from regions outside the Arctic.

Species	Region	Maturity	Matrix	Years	n	Hg concentration	Risk category					Refs
						Liver, µg/g	<16	16–64	64–83	83–126	≥126	
						Median (Min–Max)	No effect	Low risk	Moderate risk	High risk	Severe risk	
Polar bear *Ursus maritimus*	Baffin Bay	Juvenile	Liver, ww	2007–2008	6	46.79 (4.55–67.7)	33.0	50.0	17.0	0.0	0.0	1
		Adult	Liver, ww	2007–2008	6	52.15 (34.07–106.8)	0.0	67.0	0.0	33.0	0.0	
	Chukchi Sea	Juvenile	Liver, ww	2005–2007	5	6.09 (4.20–15.6)	100.0	0.0	0.0	0.0	0.0	
		Adult	Liver, ww	2005–2007	7	5.10 (3.93–12.7)	100.0	0.0	0.0	0.0	0.0	
	Davis Strait	All	Liver, ww	2008	6	28.85 (16.90–93.6)	0.0	83.0	0.0	17.0	0.0	
	Gulf of Boothia	All	Liver, ww	2007	6	60.77 (38.16–79.1)	0.0	50.0	50.0	0.0	0.0	
	Lancaster/Jones Sound	Juvenile	Liver, ww	2007–2008	5	67.93 (39.05–149.8)	0.0	40.0	20.0	20.0	20.0	
		Adult	Liver, ww	2007–2008	8	66.38 (24.67–95.0)	0.0	38.0	38.0	25.0	0.0	
	Northern Beaufort Sea	Juvenile	Liver, ww	2007	9	68.69 (22.08–115.1)	0.0	44.0	33.0	22.0	0.0	
		Adult	Liver, ww	2007	17	122.13 (34.96–414.3)	0.0	18.0	6.0	35.0	41.0	
	Southern Hudson Bay	Adult, F	Liver, ww	2006–2017	21	7.38 (3.46–18.57)	90.5	9.5	0.0	0.0	0.0	2
		Adult, M	Liver, ww	2006–2017	80	6.94 (3.03–17.44)	96.3	3.8	0.0	0.0	0.0	2
		Subadult	Liver, ww	2007–2015	34	5.01 (1.44–17.15)	97.1	2.9	0.0	0.0	0.0	2
	Western Hudson Bay	Adult, F	Liver, ww	2007–2017	18	8.58 (4.12–19.13)	83.3	16.7	0.0	0.0	0.0	2
		Adult, M	Liver, ww	2007–2017	48	12.12 (2.4–28.7)	79.2	20.8	0.0	0.0	0.0	2
		Subadult	Liver, ww	2007–2015	33	6.7 (1.63–22.04)	93.9	6.1	0.0	0.0	0.0	2
	Qaanaaq	Juvenile	Liver, ww	2000–2013	6	45.34 (21.32–351.2)	0.0	66.7	0.0	0.0	33.3	3
	Ittoqqortoormiit	Adult, F	Liver, ww	2000–2018	40	17.25 (2.37–127.4)	45.0	50.0	0.0	2.5	2.5	3
		Adult, M	Liver, ww	2000–2018	69	18.71 (6.54–186.84)	31.9	60.9	2.9	2.9	1.5	3
		Subadult	Liver, ww	2000–2018	96	11.91 (1.08–5962)	71.9	27.1	0.0	0.0	1.0	3
Ringed seal *Pusa hispida*	Arctic Bay	Juvenile	Liver, ww	2000–2009	18	2.03 (0.24–8.4)	100.0	0.0	0.0	0.0	0.0	4
		Adult	Liver, ww	2000–2009	41	7.16 (1.68–58.0)	85.0	15.0	0.0	0.0	0.0	
	Arviat W. Hudson Bay	Adult, F	Liver, ww	2003–2017	70	15.7 (0.16–254.86)	51.4	37.1	8.6	1.4	1.4	
		Adult, M	Liver, ww	2003–2017	89	10.4 (0.07–79.69)	68.5	29.2	2.3	0.0	0.0	
		Subadult	Liver, ww	2003–2017	86	3.84 (0.29–54.09)	86.1	14.0	0.0	0.0	0.0	
	Gjoa Haven	Juvenile	Liver, ww	2004–2009	14	0.85 (0.176–25.7)	92.9	7.1	0.0	0.0	0.0	
		Adult	Liver, ww	2004–2009	17	8.45 (0.201–40.0)	58.8	41.2	0.0	0.0	0.0	
	Grise Fjord	Juvenile	Liver, ww	2003–2008	16	0.95 (0.351–19.8)	93.8	6.3	0.0	0.0	0.0	
		Adult	Liver, ww	2003–2008	34	15.74 (0.24–87.0)	52.9	41.2	2.9	2.9	0.0	
	Inukjuaq	Juvenile	Liver, ww	2002–2007	15	1.05 (0.308–4.5)	100.0	0.0	0.0	0.0	0.0	
		Adult	Liver, ww	2002–2007	22	4.73 (0.931–60.0)	77.3	22.7	0.0	0.0	0.0	

Appendix Table 6A.1 continued

Species	Region	Maturity	Matrix	Years	n	Hg concentration	Risk category					Refs
						Liver, µg/g	<16	16–64	64–83	83–126	≥126	
						Median (Min–Max)	No effect	Low risk	Moderate risk	High risk	Severe risk	
	Kangiqsualujjuaq	Adult	Liver, ww	2002	4	4.82 (1.516–7.8)	100.0	0.0	0.0	0.0	0.0	
	Kangiqsujuaq	Juvenile	Liver, ww	2002	5	0.92 (0.367–2.0)	100.0	0.0	0.0	0.0	0.0	
		Adult	Liver, ww	2002	4	1.68 (0.616–4.1)	100.0	0.0	0.0	0.0	0.0	
	Nain, Labrador Sea	Adult	Liver, ww	2005–2016	32	4.66 (0.553–40.6)	87.1	12.9	0.0	0.0	0.0	
		Adult	Liver, ww	2005–2017	33	4.66 (0.553–40.6)	87.1	12.9	0.0	0.0	0.0	
		Adult	Liver, ww	2005–2018	34	4.66 (0.553–40.6)	87.1	12.9	0.0	0.0	0.0	
	Pangnirtung	Juvenile	Liver, ww	2002–2011	24	2.32 (0.156–15.8)	100.0	0.0	0.0	0.0	0.0	
		Adult	Liver, ww	2002–2011	24	2.41 (0.265–31.5)	95.8	4.2	0.0	0.0	0.0	
	Pond Inlet	Juvenile	Liver, ww	2000–2009	29	1.44 (0.314–69.8)	96.6	0.0	3.4	0.0	0.0	
		Adult	Liver, ww	2004–2009	20	5.36 (0.434–34.3)	85.0	15.0	0.0	0.0	0.0	
	Qikiqtarjuaq	Juvenile	Liver, ww	2005	6	3.98 (3.022–5.2)	100.0	0.0	0.0	0.0	0.0	
		Adult	Liver, ww	2005	14	8.89 (3.894–45.4)	92.9	7.1	0.0	0.0	0.0	
	Quartaq	Adult	Liver, ww	2002	6	5.35 (3.274–26.7)	83.3	16.7	0.0	0.0	0.0	
	Resolute	Adult, F	Liver, ww	2000–2017	51	11.1 (0.47–228)	62.8	31.4	2.0	0.0	3.9	
		Adult, M	Liver, ww	2000–2017	97	7.42 (0.61–96.4)	82.5	15.5	0.0	2.1	0.0	
		Subadult	Liver, ww	2000–2017	83	3.19 (0.14–23.4)	95.2	4.8	0.0	0.0	0.0	
	Sachs Harbour	Adult, F	Liver, ww	2001–2017	52	35.55 (0.62–320.31)	28.9	40.4	9.6	9.6	11.5	
	Eastern Beaufort Sea	Adult, M	Liver, ww	2001–2017	51	36.02 (0.45–145.93)	27.5	49.0	7.8	7.8	7.8	
		Subadult	Liver, ww	2001–2017	59	1.65 (0.34–117.68)	83.1	13.6	0.0	3.4	0.0	
	Ittoqqortoormiit	Adult, F	Liver, ww	2000–2018	40	10.08 (1.02–38.55)	72.5	27.5	0.0	0.0	0.0	5
		Adult, M	Liver, ww	2000–2018	57	8.51 (1.95–37.18)	86.0	14.0	0.0	0.0	0.0	
		Subadult	Liver, ww	2000–2018	139	4.54 (0.08–20.6)	98.6	1.4	0.0	0.0	0.0	
	Qaanaaq	Juvenile	Liver, ww	2004–2018	140	2.66 (0.20–23.2)	99.3	0.7	0.0	0.0	0.0	
		Adult, F	Liver, ww	2004–2018	11	7.87 (1.41–39.0)	72.7	27.2	0.0	0.0	0.0	
		Adult, M	Liver, ww	2006–2018	10	3.04 (2.07–12.5)	100.0	0.0	0.0	0.0	0.0	
	Qeqertarsuaq	Juvenile	Liver, ww	2000–2015	203	0.92 (0.18–8.19)	100	0	0	0	0	
	Gulf of Bothnia	Adult, F	Liver, ww	2017–2018	20	29.18 (3.06–82.08)	30.0	65.0	5.0	0.0	0.0	6
		Adult, M	Liver, ww	2017–2018	20	22.68 (4.51–110.21)	45.0	50.0	0.0	5.0	0.0	
		Subadult	Liver, ww	2017–2018	19	6.56 (0.51–20.62)	73.7	26.3	0.0	0.0	0.0	
		Yearling	Liver, ww	2017–2017	19	0.52 (0.14–0.95)	100.0	0.0	0.0	0.0	0.0	

Appendix Table 6A.1 continued

Species	Region	Maturity	Matrix	Years	n	Hg concentration	Risk category					Refs
						Liver, µg/g	<16	16–64	64–83	83–126	≥126	
						Median (Min–Max)	No effect	Low risk	Moderate risk	High risk	Severe risk	
Bearded seal *Erignathus barbatus*	Ittoqqortoormiit	Juvenile	Liver, ww	2015	7	1.82 (1.17–8.4)	100.0	0.0	0.0	0.0	0.0	3
Harp seal *Pagophilus groenlandicus*	Davis Strait	Juvenile	Liver, ww	2005–2006	6	1.88 (0.59–4.2)	100.0	0.0	0.0	0.0	0.0	3
		Adult	Liver, ww	2005–2009	14	11.10 (1.81–77.7)	79.0	14.0	7.0	0.0	0.0	
	Ittoqqortoormiit	Adult	Liver, ww	2015	6	0.78 (0.14–8.9)	100.0	0.0	0.0	0.0	0.0	
	Greenland Sea/ Denmark Strait	Adult, F	Liver, ww	2001–2018	16	0.76 (0.19–7.98)	100.0	0.0	0.0	0.0	0.0	7
		Adult, M	Liver, ww	2001–2017	9	0.72 (0.46–23.97)	88.9	11.1	0.0	0.0	0.0	
		Subadult	Liver, ww	2001–2017	15	0.69 (0.23–2.74)	100.0	0.0	0.0	0.0	0.0	
		Yearling	Liver, ww	2017–2018	19	0.17 (0.05–0.7)	100.0	0.0	0.0	0.0	0.0	
Hooded seal *Cystophora cristata*	Davis Strait	Juvenile	Liver, ww	2002–2008	7	3.01 (0.64–16.6)	86.0	14.0	0.0	0.0	0.0	3
		Adult	Liver, ww	2000–2015	14	154.78 (61.49–358.2)	0.0	7.0	7.0	29.0	57.0	
	Ittoqqortoormiit	All	Liver, ww	2015	5	23.06 (14.13–100.6)	40.0	40.0	0.0	20.0	0.0	
	Greenland Sea/ Denmark Strait	Adult, F	Liver, ww	2002–2018	29	30.4 (0.31–162.78)	20.7	58.6	6.9	10.3	3.5	7
		Adult, M	Liver, ww	2002–2019	20	120.76 (13.24–320.62)	5.0	20.0	5.0	25.0	45.0	
		Subadult	Liver, ww	2002–2017	31	6.11 (0.21–20.56)	83.9	16.1	0.0	0.0	0.0	
		Yearling	Liver, ww	2007–2018	21	0.44 (0.16–59.62)	95.2	4.8	0.0	0.0	0.0	
Harbour porpoise *Phocoena phocoena*	Maniitsoq	Adult, F	Liver, ww	2009	16	5.20 (1.3–15.25)	100.0	0.0	0.0	0.0	0.0	3
		Adult, M	Liver, ww	2009	14	5.65 (0.44–21.18)	93.8	6.2	0.0	0.0	0.0	
		Subadult	Liver, ww	2009	9	4.52 (0.24–9.74)	100.0	0.0	0.0	0.0	0.0	
		Yearling	Liver, ww	2009	3	4.63 (4.37–7.38)	100.0	0.0	0.0	0.0	0.0	
	Barents Sea	Adult, F	Liver, ww	2016–2017	22	2.14 (0.34–11.31)	100.0	0.0	0.0	0.0	0.0	8
		Adult, M	Liver, ww	2016–2017	28	0.58 (0.18–10.23)	100.0	0.0	0.0	0.0	0.0	
		Subadult	Liver, ww	2016–2017	27	0.49 (0.13–2.27)	100.0	0.0	0.0	0.0	0.0	
	Norwegian coast	Adult, F	Liver, ww	2016–2017	10	9.00 (1.00–17.05)	100.0	0.0	0.0	0.0	0.0	
		Adult, M	Liver, ww	2016–2017	18	6.49 (1.11–11.84)	80.0	20.0	0.0	0.0	0.0	
		Subadult	Liver, ww	2016–2017	22	0.69 (0.17–3.42)	100.0	0.0	0.0	0.0	0.0	
	Greater North Sea	Adult, F	Liver, ww	1999–1999	2	27.30 (21.80–32.80)	0.0	100.0	0.0	0.0	0.0	9
		Adult, M	Liver, ww	1998–1999	4	12.70 (3.60–23.30)	75.0	25.0	0.0	0.0	0.0	
		Subadult	Liver, ww	1998–1999	5	3.60 (0.50–7.50)	100.0	0.0	0.0	0.0	0.0	

Appendix Table 6A.1 continued

Species	Region	Maturity	Matrix	Years	n	Hg concentration	Risk category					Refs
						Liver, µg/g	<16	16–64	64–83	83–126	≥126	
						Median (Min–Max)	No effect	Low risk	Moderate risk	High risk	Severe risk	
		Yearling	Liver, ww	1998–1999	4	0.70 (0.40–0.90)	100.0	0.0	0.0	0.0	0.0	
	Danish Straits	Adult, F	Liver, ww	1998	1	92.00	0.0	0.0	0.0	100.0	0.0	9
		Adult, M	Liver, ww	1998	2	8.53 (8.12–8.94)	100.0	0.0	0.0	0.0	0.0	9
		Adult, M	Liver, ww	2011	2	68.40 (61.30–75.50)	0.0	50.0	50.0	0.0	0.0	10
		Subadult	Liver, ww	1998–1999	7	1.70 (1.00–2.30)	100.0	0.0	0.0	0.0	0.0	9
		Subadult	Liver, ww	2010–2018	11	1.12 (0.66–2.16)	100.0	0.0	0.0	0.0	0.0	10
		Yearling	Liver, ww	1998–1999	10	0.60 (0.20–2.10)	100.0	0.0	0.0	0.0	0.0	9
		Yearling	Liver, ww	2017	1	1.20	100.0	0.0	0.0	0.0	0.0	10
Beluga *Delphinapterus leucas*	Eastern Beaufort Sea	Adult	Liver, ww	2001–2017	336	19.8 (0–143.74)	40.5	49.4	5.1	3.9	1.2	11
		Subadult	Liver, ww	2001–2017	76	10.1 (0–102.63)	68.4	26.3	4.0	1.3	0.0	
	Southern Hudson Bay	Adult	Liver, ww	2002–2016	67	10.8 (0.19–53.04)	59.7	40.3	0.0	0.0	0.0	12
		Subadult	Liver, ww	2002–2016	114	7.32 (0.14–75.88)	79.8	19.3	0.9	0.0	0.0	
	Cumberland Sound	Adult	Liver, ww	2002–2010	31	12 (0.48–37.77)	71.0	29.0	0.0	0.0	0.0	13
		Subadult	Liver, ww	2002–2009	12	4.35 (0.63–23.24)	83.3	16.7	0.0	0.0	0.0	
Narwhal *Monodon monoceros*	Qaanaaq	Juvenile	Liver, ww	2010–2015	5	1.38 (0.65–20.7)	80.0	20.0	0.0	0.0	0.0	3
		Adult	Liver, ww	2010–2015	15	30.14 (0.16–132.1)	33.0	40.0	7.0	13.0	7.0	
	Ittoqqortoormiit	Juvenile	Liver, ww	2015	14	3.29 (0.62–32.5)	86.0	14.0	0.0	0.0	0.0	
		Adult	Liver, ww	2015	8	11.48 (0.42–18.1)	88.0	13.0	0.0	0.0	0.0	
Long-finned pilot whale *Globicephala melas*	Faroe Islands	Adult	Liver, ww	2001–2017	179	76.7 (3.52–574)	0.6	34.1	18.4	19.6	27.4	14
	Hvalvágir	Subadult	Liver, ww	2001–2015	10	34.8 (24.4–153)	0.0	80.0	0.0	0.0	20.0	
Killer whale *Orcinus orca*	E. Greenland, Iceland and Faroe Islands	Foetus	Liver, ww	2012–2013	3	0.18 (0.11–0.47)	100.0	0.0	0.0	0.0	0.0	3
		Juvenile	Liver, ww	1996–2013	11	2.54 (0.53–22.81)	63.6	27.3	9.1	0.0	0.0	
		Adult	Liver, ww	1998–2013	6	112.05 (26.71–199.78)	0.0	33.0	0.0	33.0	33.0	

[1] Routti et al., 2012; [2] Letcher and co-workers, pers. comm., 2020; [3] Dietz and co-workers, pers. comm., 2020 [4] Muir and Houde, pers. comm., 2020; [5] Rigét and co-workers, pers. comm., 2020; [6] Dietz et al., 2021; [7] Pinzone and co-workers, pers. comm., 2020; [8] Ciesielski and co-workers pers. comm., 2020; [9] Strand et al., 2005; [10] Present study; [11] Loseto and co-workers, pers. comm., 2020; [12] Ferguson and co-workers, pers. comm., 2020; [13] Watt and co-workers, pers. comm., 2020; [14] Andreasen and co-workers, pers. comm., 2020.

Appendix Table 6A.2 Contemporary (post-2000) Hg exposure and potential health risk for polar bear (hair samples). Individuals are categorized by study region, maturity and sex, and assigned to five risk categories based upon liver tissue-specific Hg effect thresholds.

Species	Region	Maturity	Matrix	Years	n	Hg concentration	Risk category					Refs
						Hair, µg/g	<6.1	6.1–24.4	24.4–31.7	31.7–48.1	≥48.1	
						Median (Min–Max)	No effect	Low risk	Moderate risk	High risk	Severe risk	
Polar bear *Ursus maritimus*	Kane Basin	All	Hair, dw	1993–1997	37	11.8 (5.3–36.9)	5.4	89.2	5.4	0	0	1
	Baffin Bay	All	Hair, dw	1993–1997	42	9.9 (4.6–25.3)	7.1	90.5	2.4	0.0	0.0	
	Davis Strait	All	Hair, dw	1993–2007	29	5.5 (3.7–15.2)	62.1	37.9	0.0	0.0	0.0	
	Foxe Basin	All	Hair, dw	1993–2007	10	5.8 (4.5–17.0)	50.0	50.0	0.0	0.0	0.0	
	Gulf of Boothia	All	Hair, dw	1995–1998	15	9.2 (5.1–18.5)	13.3	86.7	0.0	0.0	0.0	
	Lancaster Sound	All	Hair, dw	1993–1999	54	16.0 (3.1–72.7)	1.9	77.8	9.3	7.4	3.6	
	M'Clintock Channel	All	Hair, dw	1998	12	21.9 (8.7–18.6)	0.0	91.7	8.3	0.0	0.0	
	Northern Beaufort Sea	All	Hair, dw	2005	31	19.5 (6.4–31.0)	0.0	91.7	8.3	0.0	0.0	
	Norwegian Bay	All	Hair, dw	1993–1997	25	25.2 (13.8–90.0)	0.0	48.0	24.0	20.0	8.0	
	Southern Beaufort Sea	All	Hair, dw	2004–2006	30	12.6 5.6–28.3)	3.3	83.3	13.4	0.0	0.0	
	Southern Hudson Bay	All	Hair, dw	1997–1998	22	5.0 2.4–13.2)	59.1	40.9	0.0	0.0	0.0	
	Western Hudson Bay	All	Hair, dw	1993–2008	59	4.1 2.6–8.7)	98.3	1.7	0.0	0.0	0.0	
	Viscount Melville Sound	All	Hair, dw	1992	10	22.1 16.7–85.2)	0.0	60.0	10.0	0.0	30.0	
	Northwest Greenland	All	Hair, dw	2000–2008	55	7.9 3.2–26.4)	20.0	78.2	1.8	0.0	0.0	2
	Central East Greenland	All	Hair, dw	2000–2017	149	6.4 1.7–35.0)	43.6	55.7	0.0	0.7	0.0	1
	Barents Sea	All	Hair, dw	2000–2007	58	1.8 0.7–2.8)	100.0	0.0	0.0	0.0	0.0	3
	Kara Sea	Subadult	Hair, dw	2014–2016	9	1.12 0.04–2.48)	100.0	0.0	0.0	0.0	0.0	
		Adult	Hair, dw	2014–2016	20	1.45 0.06–3.40)	100.0	0.0	0.0	0.0	0.0	
	Laptev Sea	Subadult	Hair, dw	2015	2	1.86 0.73–2.99)	100.0	0.0	0.0	0.0	0.0	
		Adult	Hair, dw	2014–2016	4	1.84 0.93–2.00)	100.0	0.0	0.0	0.0	0.0	
	Chukchi Sea	Subadult	Hair, dw	2012–2015	5	1.85 0.96–5.33)	100.0	0.0	0.0	0.0	0.0	
		Adult	Hair, dw	2008–2015	7	1.63 0.98–2.13)	100.0	0.0	0.0	0.0	0.0	

[1] Dietz and co-workers, pers. comm., 2020; [2] Dietz et al., 2011; [3] Lippold et al., 2020

Appendix Table 6A.3 Contemporary (post-2000) Hg exposure and potential health risk for Arctic terrestrial mammals. Individuals are categorized by study region, maturity and sex, and assigned to five risk categories based upon liver tissue-specific Hg effect thresholds.

Species	Region	Maturity	Matrix	Years	n	Hg concentration	Risk category					Refs
						Liver, µg/g	<4.2	4.2–7.3	7.3–22.7	22.7–30.5	≥30.5	
							No risk	Low risk	Moderate risk	High risk	Severe risk	
Arctic fox *Vulpes lagopus*	Arviat	Juvenile	Liver, ww	2001	50	0.12 (0.03–4.7)	98.0	2.0	0.0	0.0	0.0	1
	Iceland	Juvenile	Liver, ww	2011–2012	12	2.81 (0.44–11.4)	67.0	8.0	25.0	0.0	0.0	2
		Adult	Liver, ww	2011–2012	23	5.82 (0.28–46.2)	35.0	22.0	35.0	0.0	9.0	
	Svalbard	Juvenile	Liver, ww	2000–2014	90	0.12 (0.01–1.1)	100.0	0.0	0.0	0.0	0.0	3
Reindeer/caribou *Rangifer tarandus*	NW Yukon/ Alaska	Adult, F	Liver, ww	2000–2015	52	0.46 (0.18–1.58)	100.0	0.0	0.0	0.0	0.0	4
	Porcupine	Adult, M	Liver, ww	2000–2017	238	0.19 (0.046–2.35)	100.0	0.0	0.0	0.0	0.0	
		Subadult	Liver, ww	2000–2017	19	0.34 (0.082–0.74)	100.0	0.0	0.0	0.0	0.0	
	Western Hudson Bay	Adult, F	Liver, ww	2006–2018	119	1.24 (0.29–2.82)	100.0	0.0	0.0	0.0	0.0	
	Qamanirjuaq	Adult, M	Liver, ww	2006–2018	80	0.84 (0.31–2.67)	100.0	0.0	0.0	0.0	0.0	
		Subadult	Liver, ww	2006–2017	26	0.93 (0.29–2.20)	100.0	0.0	0.0	0.0	0.0	
		Yearling	Liver, ww	2008–2017	9	0.63 (0.34–1.44)	100.0	0.0	0.0	0.0	0.0	
Sheep *Ovis aries*	Faroe Islands	Adult	Liver, ww	2001–2011	13	0.01 (0.01–29.9)	85.0	0.0	15.0	0.0	0.0	5

[1] Hoekstra et al., 2003; [2] Treu and co-workers, pers. comm., 2020; [3] Hallanger et al., 2019; [4] Gamberg, pers. comm., 2020; [5] Hoydal and Dam 2005, 2009; Nielsen et al., 2014.

Appendix Table 6A.4(A) Contemporary (post-2000) Hg exposure and potential health risk for Arctic seabirds (blood values). Individuals are categorized by study region, age group (mainly adult birds) and assigned to five risk categories based upon blood tissue-specific Hg effect thresholds.

Species	Region	Maturity	Matrix	Years	n	Hg concentration	Risk category					Refs
						Egg, µg/g fww	<0.10	0.10–0.37	0.37–0.91	0.91–1.16	≥1.16	
						Liver, µg/g ww	<0.53	0.53–2.26	2.26–6.10	6.10–7.91	≥7.91	
						Blood equivalent, µg/g ww	<0.2	0.2–1.0	1.0–3.0	3.0–4.0	≥4.0	
						Body feather, µg/g dw	<1.62	1.62–4.53	4.53–9.14	9.14–10.99	≥10.99	
						Median (Min–Max)	No effect	Low risk	Moderate risk	High risk	Severe risk	
Glaucous-winged gull *Larus glaucescens*	Western North America	Adult	Blood eq. ww	2000–2015	30	0.27 (0.14–0.95)	33.0	67.0	0.0	0.0	0.0	1
Pigeon guillemot *Cepphus columba*	Western North America	Adult	Blood eq. ww	2000–2015	27	2.08 (0.90–3.8)	0.0	11.0	59.0	26.0	4.0	1
Double-crested cormorant *Phalacrocorax auritus*	Western North America	Adult	Blood eq. ww	2000–2015	310	0.65 (0.12–3.98)	13.0	56.0	23.0	3.0	5.0	1
King eider *Somateria spectabilis*	Western North America	Adult	Blood eq. ww	2000–2015	143	0.21 (0.08–0.52)	47.0	53.0	0.0	0.0	0.0	1
Northern fulmar *Fulmarus glacialis*	Baffin Island	Adult	Blood eq. ww	2018	24	0.22 (0.07–0.56)	50.0	50.0	0.0	0.0	0.0	2
	Iceland	Adult	Blood eq. ww	2015–2018	112	0.55 (0.19–1.32)	2.0	96.0	2.0	0.0	0.0	2
	Jan Mayen	Adult	Blood eq. ww	2015–2018	84	0.30 (0.15–0.79)	12.0	88.0	0.0	0.0	0.0	2
	Qaanaaq	Adult	Blood eq. ww	2015	10	0.41 (0.07–1.72)	20.0	70.0	10.0	0.0	0.0	2
	Svalbard	Adult	Blood eq. ww	2015–2017	63	0.17 (0.07–0.41)	65.0	35.0	0.0	0.0	0.0	2
	Western North America	Adult	Blood eq. ww	2000–2015	13	2.07 (0.79–4.2)	0.0	23.0	54.0	8.0	15.0	1
Glaucous gull *Larus hyperboreus*	Coats Island	Adult	Blood eq. ww	2015–2018	10	1.01 (0.73–2.38)	0.0	60.0	40.0	0.0	0.0	2
	Franz Josef Land	Adult	Blood eq. ww	2016–2017	39	0.54 (0.25–1.94)	0.0	92.0	8.0	0.0	0.0	2
	Iceland	Adult	Blood eq. ww	2016–2018	28	0.29 (0.18–0.52)	11.0	89.0	0.0	0.0	0.0	2
	Jan Mayen	Adult	Blood eq. ww	2016	1	0.46 (0.46–0.46)	0.0	100.0	0.0	0.0	0.0	2
	Qaanaaq	Adult	Blood eq. ww	2015	33	0.42 (0.12–2.20)	15.0	76.0	9.0	0.0	0.0	2
	Svalbard	Adult	Blood eq. ww	2015–2017	53	0.26 (0.11–0.66)	26.0	74.0	0.0	0.0	0.0	2
	Western North America	Adult	Blood eq. ww	2000–2015	61	0.28 (0.13–0.53)	21.0	77.0	2.0	0.0	0.0	1
Herring gull *Larus argentatus*	Iceland	Adult	Blood eq. ww	2016–2018	13	0.11 (0.07–0.18)	100.0	0.0	0.0	0.0	0.0	2
Ivory gull *Pagophila eburnea*	Station Nord	Adult	Blood eq. ww	2018	6	0.70 (0.37–1.42)	0.0	83.0	17.0	0.0	0.0	2
Common murre *Uria aalge*	Gorodetskiy Cape	Adult	Blood eq. ww	2015	6	0.21 (0.19–0.30)	50.0	50.0	0.0	0.0	0.0	2
	Hornøya	Adult	Blood eq. ww	2016–2017	35	0.20 (0.15–0.27)	60.0	40.0	0.0	0.0	0.0	2
	Iceland	Adult	Blood eq. ww	2015–2018	85	0.17 (0.08–0.45)	76.0	24.0	0.0	0.0	0.0	2
	Jan Mayen	Adult	Blood eq. ww	2015–2018	91	0.17 (0.06–0.38)	73.0	27.0	0.0	0.0	0.0	2
	Newfoundland	Adult	Blood eq. ww	2015–2017	92	0.50 (0.27–0.84)	0.0	100.0	0.0	0.0	0.0	2
	St. Lawrence Island	Adult	Blood eq. ww	2016–2017	26	0.08 (0.04–0.17)	100.0	0.0	0.0	0.0	0.0	2
	Svalbard	Adult	Blood eq. ww	2015–2017	51	0.17 (0.10–0.26)	92.0	8.0	0.0	0.0	0.0	2
	Western North America	Adult	Blood eq. ww	2000–2015	239	0.20 (0.03–0.67)	40.0	59.0	1.0	0.0	0.0	1

Appendix Table 6A.4(A) continued

Species	Region	Maturity	Matrix	Years	n	Hg concentration	Risk category					Refs
						Egg, µg/g fww	<0.10	0.10–0.37	0.37–0.91	0.91–1.16	≥1.16	
						Liver, µg/g ww	<0.53	0.53–2.26	2.26–6.10	6.10–7.91	≥7.91	
						Blood equivalent, µg/g ww	<0.2	0.2–1.0	1.0–3.0	3.0–4.0	≥4.0	
						Body feather, µg/g dw	<1.62	1.62–4.53	4.53–9.14	9.14–10.99	≥10.99	
						Median (Min–Max)	No effect	Low risk	Moderate risk	High risk	Severe risk	
Black-legged kittiwake *Rissa tridactyla*	Baffin Island	Adult	Blood eq. ww	2018	14	0.31 (0.18–0.39)	14.0	86.0	0.0	0.0	0.0	2
	Franz Josef Land	Adult	Blood eq. ww	2015–2017	48	0.22 (0.10–0.33)	46.0	54.0	0.0	0.0	0.0	2
	Hornøya	Adult	Blood eq. ww	2017	15	0.24 (0.15–0.47)	27.0	73.0	0.0	0.0	0.0	2
	Iceland	Adult	Blood eq. ww	2015–2018	52	0.28 (0.10–0.70)	33.0	67.0	0.0	0.0	0.0	2
	Kippaku	Adult	Blood eq. ww	2017	25	0.13 (0.09–0.19)	100.0	0.0	0.0	0.0	0.0	2
	Western North America	Adult	Blood eq. ww	2016–2017	41	0.27 (0.18–0.50)	7.0	93.0	0.0	0.0	0.0	2
	Newfoundland	Adult	Blood eq. ww	2017	20	0.22 (0.12–0.36)	45.0	55.0	0.0	0.0	0.0	2
	Pribilof Islands	Adult	Blood eq. ww	2017	8	0.50 (0.31–0.66)	0.0	100.0	0.0	0.0	0.0	2
	Qaanaaq	Adult	Blood eq. ww	2015	18	0.20 (0.08–0.38)	56.0	44.0	0.0	0.0	0.0	2
	Rittenbenck	Adult	Blood eq. ww	2015	10	0.17 (0.13–0.23)	90.0	10.0	0.0	0.0	0.0	2
	St. Lawrence Island	Adult	Blood eq. ww	2016–2017	16	0.24 (0.06–0.36)	19.0	81.0	0.0	0.0	0.0	2
	Scoresby Sound	Adult	Blood eq. ww	2017	25	0.19 (0.13–0.41)	60.0	40.0	0.0	0.0	0.0	2
	Svalbard	Adult	Blood eq. ww	2015–2018	132	0.27 (0.08–0.55)	51.0	49.0	0.0	0.0	0.0	2
	Svalbard	Adult (pre-laying)	Blood eq. ww	2000–2016	211	1.91 (0.91–3.50)	0.0	0.5	97.2	2.4	0.0	3
	Svalbard	Adult (incubation)	Blood eq. ww	2000–2016	345	1.45 (0.68–3.29)	0.0	14.0	84.8	1.2	0.0	4
	Svalbard	Adult (chick-rearing)	Blood eq. ww	2000–2016	493	1.04 (0.36–2.83)	0.0	46.2	53.8	0.0	0.0	5
Thick-billed murre *Uria lomvia*	Baffin Island	Adult	Blood eq. ww	2018	20	0.84 (0.52–1.23)	0.0	85.0	15.0	0.0	0.0	2
	Coats Island	Adult	Blood eq. ww	2015–2018	72	0.27 (0.10–1.47)	18.0	81.0	1.0	0.0	0.0	2
	Franz Josef Land	Adult	Blood eq. ww	2015–2017	37	0.17 (0.08–0.27)	81.0	19.0	0.0	0.0	0.0	2
	Gorodetskiy Cape	Adult	Blood eq. ww	2015–2017	10	0.16 (0.10–0.23)	90.0	10.0	0.0	0.0	0.0	2
	Hornøya	Adult	Blood eq. ww	2016–2017	64	0.18 (0.12–0.27)	78.0	22.0	0.0	0.0	0.0	2
	Iceland	Adult	Blood eq. ww	2015–2018	65	0.10 (0.04–0.19)	100.0	0.0	0.0	0.0	0.0	2
	Jan Mayen	Adult	Blood eq. ww	2015–2018	85	0.27 (0.15–0.54)	20.0	80.0	0.0	0.0	0.0	2
	Kippaku	Adult	Blood eq. ww	2016	30	0.30 (0.15–0.65)	13.0	87.0	0.0	0.0	0.0	2
	Newfoundland	Adult	Blood eq. ww	2015–2018	41	0.45 (0.28–0.69)	0.0	100.0	0.0	0.0	0.0	2
	Novaya Zemlya	Adult	Blood eq. ww	2016	4	0.10 (0.09–0.11)	100.0	0.0	0.0	0.0	0.0	2
	Pribilof Islands	Adult	Blood eq. ww	2017	7	0.11 (0.06–0.20)	100.0	0.0	0.0	0.0	0.0	2
	Qaanaaq	Adult	Blood eq. ww	2015	19	0.46 (0.10–0.82)	5.0	95.0	0.0	0.0	0.0	2

Appendix Table 6A.4(A) continued

Species	Region	Maturity	Matrix	Years	n	Hg concentration	Risk category					Refs
						Egg, µg/g fww	<0.10	0.10–0.37	0.37–0.91	0.91–1.16	≥1.16	
						Liver, µg/g ww	<0.53	0.53–2.26	2.26–6.10	6.10–7.91	≥7.91	
						Blood equivalent, µg/g ww	<0.2	0.2–1.0	1.0–3.0	3.0–4.0	≥4.0	
						Body feather, µg/g dw	<1.62	1.62–4.53	4.53–9.14	9.14–10.99	≥10.99	
						Median (Min–Max)	No effect	Low risk	Moderate risk	High risk	Severe risk	
	St. Lawrence Island	Adult	Blood eq. ww	2016–2017	40	0.08 (0.02–0.53)	67.0	33.0	0.0	0.0	0.0	2
	Svalbard	Adult	Blood eq. ww	2015–2017	106	0.06 (0.01–0.23)	98.0	2.0	0.0	0.0	0.0	2
	Western North America	Adult	Blood eq. ww	2000–2015	141	0.12 (0.02–0.56)	65.0	35.0	0.0	0.0	0.0	1
Little auk *Alle alle*	Franz Josef Land	Adult	Blood eq. ww	2015–2017	87	0.07 (0.04–0.19)	100.0	0.0	0.0	0.0	0.0	2
	Qaanaaq	Adult	Blood eq. ww	2015	19	0.13 (0.08–0.18)	100.0	0.0	0.0	0.0	0.0	2
	Scoresby Sound	Adult	Blood eq. ww	2015–2017	88	0.17 (0.11–0.27)	83.0	17.0	0.0	0.0	0.0	2
	Svalbard	Adult	Blood eq. ww	2015–2018	172	0.08 (0.04–0.15)	100.0	0.0	0.0	0.0	0.0	2
Rhinoceros auklet *Cerorhinca monocerata*	Western North America	Adult	Blood eq. ww	2017	20	0.32 (0.19–0.46)	15.0	85.0	0.0	0.0	0.0	2
	Western North America	Adult	Blood eq. ww	2000–2015	21	0.97 (0.46–2.0)	0.0	52.0	48.0	0.0	0.0	1
Crested auklet *Aethia cristatella*	St. Lawrence Island	Adult	Blood eq. ww	2016–2017	52	0.04 (0.01–0.08)	100.0	0.0	0.0	0.0	0.0	2
Least auklet *Aethia pusilla*	St. Lawrence Island	Adult	Blood eq. ww	2016–2017	27	0.03 (0.01–0.06)	100.0	0.0	0.0	0.0	0.0	2
Red-legged kittiwake *Rissa brevirostris*	Pribilof Islands	Adult	Blood eq. ww	2017	4	0.51 (0.41–0.59)	0.0	100.0	0.0	0.0	0.0	2
Atlantic puffin *Fratercula arctica*	Hornøya	Adult	Blood eq. ww	2016–2017	56	0.17 (0.10–0.25)	84.0	16.0	0.0	0.0	0.0	2
	Iceland	Adult	Blood eq. ww	2016–2018	77	0.32 (0.17–0.63)	12.0	88.0	0.0	0.0	0.0	2
	Newfoundland	Adult	Blood eq. ww	2015–2018	98	0.27 (0.13–0.44)	19.0	81.0	0.0	0.0	0.0	2
	Seven Island	Adult	Blood eq. ww	2017	20	0.19 (0.13–0.25)	75.0	25.0	0.0	0.0	0.0	2
	Svalbard	Adult	Blood eq. ww	2015–2017	35	0.12 (0.06–0.24)	86.0	14.0	0.0	0.0	0.0	2
Common eider *Somateria mollissima*	East Bay Island	Adult	Blood eq. ww	2016	23	0.24 (0.16–0.38)	26.0	74.0	0.0	0.0	0.0	2
	Faroe Islands	Adult	Blood eq. ww	2018	11	0.08 (0.02–0.14)	100.0	0.0	0.0	0.0	0.0	2
	Iceland	Adult	Blood eq. ww	2017–2018	31	0.12 (0.07–0.56)	87.0	13.0	0.0	0.0	0.0	2
	Qaanaaq	Adult	Blood eq. ww	2015	2	0.11 (0.10–0.13)	100.0	0.0	0.0	0.0	0.0	2
	Scoresby Sound	Adult	Blood eq. ww	2015	10	0.13 (0.10–0.26)	90.0	10.0	0.0	0.0	0.0	2
	Svalbard	Adult	Blood eq. ww	2016–2017	68	0.11 (0.05–0.34)	99.0	1.0	0.0	0.0	0.0	2
	Tromsø	Adult	Blood eq. ww	2016–2017	64	0.06 (0.04–0.10)	100.0	0.0	0.0	0.0	0.0	2
	Western North America	Adult	Blood eq. ww	2000–2015	102	0.17 (0.07–0.5)	80.0	20.0	0.0	0.0	0.0	1
Ruddy turnstone *Arenaria interpres*	Western North America	Adult	Blood eq. ww	2000–2015	14	0.23 (0.15–1.9)	29.0	57.0	7.0	7.0	0.0	1

[1] Ackerman et al., 2016b; [2] Fort and co-workers, pers. comm., 2020; [3] Chastel, Bustnes, Gabrielsen and co-workers, pers. comm., 2020; Tartu et al., 2016; Goutte et al., 2015; Blévin et al., 2018, 2019; [4] Chastel, Bustnes, Gabrielsen and co-workers, pers. comm., 2020; Tartu et al., 2013, 2017; [5] Chastel, Bustnes, Gabrielsen and co-workers, pers. comm., 2020; Tartu et al., 2013, 2018.

Appendix Table 6A.4(B) Contemporary (post-2000) Hg exposure and potential health risk for Arctic seabirds and birds of prey (feather values). Individuals are categorized by study region, age group (mainly adult birds) and assigned to five risk categories based upon feather tissue-specific Hg effect thresholds.

Species	Region	Maturity	Matrix	Years	n	Hg concentration	Risk category					Refs
						Egg, µg/g fww	<0.10	0.10–0.37	0.37–0.91	0.91–1.16	≥1.16	
						Liver, µg/g ww	<0.53	0.53–2.26	2.26–6.10	6.10–7.91	≥7.91	
						Blood equivalent, µg/g ww	<0.2	0.2–1.0	1.0–3.0	3.0–4.0	≥4.0	
						Body feather, µg/g dw	<1.62	1.62–4.53	4.53–9.14	9.14–10.99	≥10.99	
						Median (Min–Max)	No effect	Low risk	Moderate risk	High risk	Severe risk	
Common murre *Uria aalge*	Faroe Islands	Adult	Body feathers, dw	2016–2017	8	1.93 (1.18–4.58)	0.0	87.0	13.0	0.0	0.0	1
	Gorodetskiy Cape	Adult	Body feathers, dw	2015–2017	47	0.64 (0.42–1.06)	100.0	0.0	0.0	0.0	0.0	1
	Iceland	Adult	Body feathers, dw	2016–2017	37	1.09 (0.59–2.69)	92.0	8.0	0.0	0.0	0.0	1
	Jan Mayen	Adult	Body feathers, dw	2015–2017	63	0.87 (0.41–1.77)	95.0	5.0	0.0	0.0	0.0	1
	Newfoundland	Adult	Body feathers, dw	2015–2017	96	2.09 (1.02–4.48)	17.0	83.0	0.0	0.0	0.0	1
	Pribilof Islands	Adult	Body feathers, dw	2015	12	0.57 (0.43–0.82)	100.0	0.0	0.0	0.0	0.0	1
	St. Lawrence Island	Adult	Body feathers, dw	2016–2017	36	0.55 (0.33–0.96)	100.0	0.0	0.0	0.0	0.0	1
	Svalbard	Adult	Body feathers, dw	2015–2017	48	0.64 (0.45–0.99)	100.0	0.0	0.0	0.0	0.0	1
	Okhotsk Sea	Adult	Body feathers, dw	2017	1	0.88 (0.88–0.88)	100.0	0.0	0.0	0.0	0.0	1
Black-legged kittiwake *Rissa tridactyla*	Cape Krutik	Adult	Body feathers, dw	2015–2017	73	1.56 (0.65–10.29)	49.0	44.0	5.0	1.0	1.0	1
	Faroe Islands	Adult	Body feathers, dw	2015	3	2.99 (2.94–5.56)	0.0	67.0	33.0	0.0	0.0	1
	Franz Josef Land	Adult	Body feathers, dw	2015–2017	80	3.58 (1.34–9.09)	5.0	56.0	39.0	0.0	0.0	1
	Hornøya	Adult	Body feathers, dw	2015–2017	73	1.93 (0.57–3.86)	44.0	56.0	0.0	0.0	0.0	1
	Iceland	Adult	Body feathers, dw	2015–2016	38	3.05 (1.25–8.63)	10.0	74.0	16.0	0.0	0.0	1
	Kippaku	Adult	Body feathers, dw	2015	26	3.29 (1.71–6.27)	0.0	88.0	12.0	0.0	0.0	1
	Western North America	Adult	Body feathers, dw	2016–2017	41	3.49 (1.23–7.11)	10.0	58.0	32.0	0.0	0.0	1
	Newfoundland	Adult	Body feathers, dw	2017	20	4.90 (3.68–7.07)	0.0	35.0	65.0	0.0	0.0	1
	Novaya Zemlya	Adult	Body feathers, dw	2015–2016	23	1.81 (0.87–12.93)	43.0	35.0	9.0	0.0	13.0	1
	Pribilof Islands	Adult	Body feathers, dw	2016–2017	41	3.36 (1.62–8.44)	0.0	83.0	17.0	0.0	0.0	1
	Qaanaaq	Adult	Body feathers, dw	2015	17	0.96 (0.39–1.82)	94.0	6.0	0.0	0.0	0.0	1
	Rittenbenck	Adult	Body feathers, dw	2015	10	1.83 (1.37–3.88)	40.0	60.0	0.0	0.0	0.0	1
	St. Lawrence Island	Adult	Body feathers, dw	2016–2017	32	4.50 (2.09–10.33)	0.0	56.0	41.0	3.0	0.0	1
	Scoresby Sound	Adult	Body feathers, dw	2017	20	6.05 (2.51–9.36)	0.0	30.0	65.0	5.0	0.0	1

Appendix Table 6A.4(B) continued

Species	Region	Maturity	Matrix	Years	n	Hg concentration	Risk category					Refs
						Egg, µg/g fww	<0.10	0.10–0.37	0.37–0.91	0.91–1.16	≥1.16	
						Liver, µg/g ww	<0.53	0.53–2.26	2.26–6.10	6.10–7.91	≥7.91	
						Blood equivalent, µg/g ww	<0.2	0.2–1.0	1.0–3.0	3.0–4.0	≥4.0	
						Body feather, µg/g dw	<1.62	1.62–4.53	4.53–9.14	9.14–10.99	≥10.99	
						Median (Min–Max)	No effect	Low risk	Moderate risk	High risk	Severe risk	
	Svalbard	Adult	Body feathers, dw	2015–2017	199	3.49 (1.08–13.06)	33.0	44.0	20.0	3.0	0.0	1
Thick-billed murre *Uria lomvia*	Coats Island	Adult	Body feathers, dw	2015	20	1.51 (1.20–2.36)	70.0	30.0	0.0	0.0	0.0	1
	Franz Josef Land	Adult	Body feathers, dw	2015–2017	61	0.73 (0.35–1.31)	100.0	0.0	0.0	0.0	0.0	1
	Gorodetskiy Cape	Adult	Body feathers, dw	2015–2017	29	0.70 (0.53–1.09)	100.0	0.0	0.0	0.0	0.0	1
	Hornøya	Adult	Body feathers, dw	2015–2017	60	0.73 (0.37–1.39)	100.0	0.0	0.0	0.0	0.0	1
	Iceland	Adult	Body feathers, dw	2015–2017	46	1.41 (0.95–1.91)	80.0	20.0	0.0	0.0	0.0	1
	Jan Mayen	Adult	Body feathers, dw	2015–2017	65	1.59 (0.91–2.34)	54.0	46.0	0.0	0.0	0.0	1
	Kippaku	Adult	Body feathers, dw	2016	20	1.71 (1.10–3.19)	25.0	75.0	0.0	0.0	0.0	1
	Newfoundland	Adult	Body feathers, dw	2015–2017	41	2.10 (1.27–5.90)	7.0	86.0	7.0	0.0	0.0	1
	Novaya Zemlya	Adult	Body feathers, dw	2015–2017	74	0.64 (0.28–1.32)	100.0	0.0	0.0	0.0	0.0	1
	Pribilof Islands	Adult	Body feathers, dw	2015–2017	42	0.64 (0.43–1.35)	100.0	0.0	0.0	0.0	0.0	1
	Qaanaaq	Adult	Body feathers, dw	2015	19	2.20 (0.46–3.91)	21.0	79.0	0.0	0.0	0.0	1
	St. Lawrence Island	Adult	Body feathers, dw	2016–2017	40	0.71 (0.32–1.92)	98.0	2.0	0.0	0.0	0.0	1
	Svalbard	Adult	Body feathers, dw	2015–2017	114	0.59 (0.29–2.11)	97.0	3.0	0.0	0.0	0.0	1
Rhinoceros auklet *Cerorhinca monocerata*	Western North America	Adult	Body feathers, dw	2016–2017	42	2.20 (0.91–6.96)	24.0	62.0	14.0	0.0	0.0	1
Crested auklet *Aethia cristatella*	Aleutian Islands	Adult	Body feathers, dw	2017	4	1.19 (0.72–2.10)	75.0	25.0	0.0	0.0	0.0	1
	Okhotsk Sea	Adult	Body feathers, dw	2017	4	0.70 (0.38–1.49)	100.0	0.0	0.0	0.0	0.0	1
	St. Lawrence Island	Adult	Body feathers, dw	2016–2017	33	0.71 (0.33–2.40)	91.0	9.0	0.0	0.0	0.0	1
Least auklet *Aethia pusilla*	Pribilof Islands	Adult	Body feathers, dw	2015–2017	65	0.95 (0.23–3.99)	75.0	25.0	0.0	0.0	0.0	1
	St. Lawrence Island	Adult	Body feathers, dw	2016–2017	34	1.31 (0.33–5.36)	53.0	44.0	3.0	0.0	0.0	1
Parakeet auklet *Aethia psittacula*	Aleutian Islands	Adult	Body feathers, dw	2017	4	2.84 (1.91–4.00)	0.0	100.0	0.0	0.0	0.0	1
	Okhotsk Sea	Adult	Body feathers, dw	2017	13	1.67 (1.00–3.80)	46.0	54.0	0.0	0.0	0.0	1

Appendix Table 6A.4(B) continued

Species	Region	Maturity	Matrix	Years	n	Hg concentration	Risk category					Refs
						Egg, µg/g fww	<0.10	0.10–0.37	0.37–0.91	0.91–1.16	≥1.16	
						Liver, µg/g ww	<0.53	0.53–2.26	2.26–6.10	6.10–7.91	≥7.91	
						Blood equivalent, µg/g ww	<0.2	0.2–1.0	1.0–3.0	3.0–4.0	≥4.0	
						Body feather, µg/g dw	<1.62	1.62–4.53	4.53–9.14	9.14–10.99	≥10.99	
						Median (Min–Max)	No effect	Low risk	Moderate risk	High risk	Severe risk	
Ancient murrelet *Synthliboramphus antiquus*	Aleutian Islands	Adult	Body feathers, dw	2017	2	1.94 (1.42–2.46)	50.0	50.0	0.0	0.0	0.0	1
	Okhotsk Sea	Adult	Body feathers, dw	2017	12	2.74 (0.94–4.75)	13.0	87.0	0.0	0.0	0.0	1
Red-legged kittiwake *Rissa brevirostris*	Pribilof Islands	Adult	Body feathers, dw	2015–2017	61	5.27 (2.35–8.05)	0.0	28.0	72.0	0.0	0.0	1
	St. George Island	Adult	Body feathers, dw	2011–2017	78	4.66 (2.84–6.46)	0.0	40.0	60.0	0.0	0.0	2
Tufted puffin *Fratercula cirrhata*	Aleutian Islands	Adult	Body feathers, dw	2017	14	2.93 (1.68–6.44)	29.0	71.0	0.0	0.0	0.0	1
	Okhotsk Sea	Adult	Body feathers, dw	2017	2	2.68 (1.99–3.37)	50.0	50.0	0.0	0.0	0.0	1
Horned puffin *Fratercula corniculata*	Aleutian Islands	Adult	Body feathers, dw	2017	1	4.61 (4.61–4.61)	0.0	0.0	100.0	0.0	0.0	1
Atlantic puffin *Fratercula arctica*	Faroe Islands	Adult	Body feathers, dw	2015	3	2.96 (2.67–4.62)	0.0	67.0	33.0	0.0	0.0	1
	Hornøya	Adult	Body feathers, dw	2015–2017	40	1.04 (0.47–2.34)	95.0	5.0	0.0	0.0	0.0	1
	Iceland	Adult	Body feathers, dw	2015–2016	47	3.58 (1.09–8.94)	2.0	79.0	19.0	0.0	0.0	1
	Newfoundland	Adult	Body feathers, dw	2015–2016	36	3.80 (1.99–9.14)	0.0	78.0	22.0	0.0	0.0	1
	Seven Island	Adult	Body feathers, dw	2015–2016	28	0.86 (0.35–2.26)	96.0	4.0	0.0	0.0	0.0	1
	Svalbard	Adult	Body feathers, dw	2015–2016	32	2.19 (0.57–5.88)	38.0	53.0	9.0	0.0	0.0	1
Common eider *Somateria mollissima*	Aleutian Islands	Adult	Body feathers, dw	2017	1	1.33 (1.33–1.33)	100.0	0.0	0.0	0.0	0.0	1
	East Bay Island	Adult	Body feathers, dw	2016	23	0.99 (0.63–3.81)	9.0	91.0	0.0	0.0	0.0	1
	Faroe Islands	Adult	Body feathers, dw	2015–2017	78	0.71 (0.21–12.30)	82.0	13.0	3.0	1.0	1.0	1
	Iceland	Adult	Body feathers, dw	2015–2017	71	0.84 (0.31–2.39)	93.0	7.0	0.0	0.0	0.0	1
	Scoresby Sound	Adult	Body feathers, dw	2015	10	0.87 (0.55–2.53)	80.0	20.0	0.0	0.0	0.0	1
	Seven Island	Adult	Body feathers, dw	2015	1	0.48 (0.48–0.48)	100.0	0.0	0.0	0.0	0.0	1
	Solovetsky Archipelago	Adult	Body feathers, dw	2015–2017	69	1.08 (0.49–3.46)	88.0	12.0	0.0	0.0	0.0	1
	Svalbard	Adult	Body feathers, dw	2015–2017	69	1.00 (0.44–2.41)	94.0	6.0	0.0	0.0	0.0	1
	Tromsø	Adult	Body feathers, dw	2015–2017	75	0.61 (0.25–4.62)	99.0	1.0	0.0	0.0	0.0	1

[1] Fort and co-workers, pers. comm., 2020; [2] Ackerman and co-workers, pers. comm., 2020.

Appendix Table 6A.4(C) Contemporary (post-2000) Hg exposure and potential health risk for Arctic seabirds (egg and liver values). Individuals are categorized by study region, age group (mainly adult birds) and assigned to five risk categories based upon egg and liver tissue-specific Hg effect thresholds.

Species	Region	Maturity	Matrix	Years	n	Hg concentration	Risk category					Refs
						Egg, µg/g fww	<0.10	0.10–0.37	0.37–0.91	0.91–1.16	≥1.16	
						Liver, µg/g fww	<0.53	0.53–2.26	2.26–6.10	6.10–7.91	≥7.91	
						Blood equivalent, µg/g fww	<0.2	0.2–1.0	1.0–3.0	3.0–4.0	≥4.0	
						Body feather, µg/g fww	<1.62	1.62–4.53	4.53–9.14	9.14–10.99	≥10.99	
						Median (Min–Max)	No effect	Low risk	Moderate risk	High risk	Severe risk	
Northern fulmar *Fulmarus glacialis*	Prince Leopold Is.	Foetus	Egg, ww	2003–2015	57	0.90 (0.54–1.3)	0.0	0.0	100.0	0.0	0.0	1, 2
	Qaanaaq	All	Liver, ww	2015	10	2.61 (0.25–5.3)	20.0	80.0	0.0	0.0	0.0	3
	Svalbard	All	Liver, ww	2005–2006	10	2.54 (1.64–3.4)	0.0	100.0	0.0	0.0	0.0	4
Glaucous-winged gull *Larus glaucescens*	Bering Sea	Foetus	Egg, ww	2005–2009	11	0.12 (0.06–0.2)	45.0	55.0	0.0	0.0	0.0	5
	Gulf of Alaska	Foetus	Egg, ww	2005	6	0.13 (0.01–0.4)	0.0	100.0	0.0	0.0	0.0	5, 6
Glaucous gull *Larus hyperboreus*	Bering Sea	Foetus	Egg, ww	2005–2009	8	0.15 (0.11–0.2)	0.0	100.0	0.0	0.0	0.0	5
	Bering Strait	Foetus	Egg, ww	2005–2008	13	0.13 (0.01–0.4)	46.0	54.0	0.0	0.0	0.0	5, 6
	Norton Sound	Foetus	Egg, ww	2005–2009	40	0.13 (0.01–0.6)	17.6	79.7	2.7	0.0	0.0	5, 7
	Qaanaaq	All	Liver, ww	2015	10	1.87 (1.06–3.0)	50.0	50.0	0.0	0.0	0.0	3
	Svalbard	All	Liver, ww	2005–2006	9	1.13 (0.40–2.0)	67.0	33.0	0.0	0.0	0.0	4
Herring gull *Larus argentatus*	Hornøya	Foetus	Egg, ww	2003	5	0.07 (0.06–0.2)	80.0	20.0	0.0	0.0	0.0	8
	Lofoten	Foetus	Egg, ww	2003	5	0.07 (0.04–0.2)	60.0	40.0	0.0	0.0	0.0	9
Ivory gull *Pagophila eburnea*	Nagurskoye	Foetus	Egg, ww	2006	6	0.24 (0.08–0.2)	17.0	83.0	0.0	0.0	0.0	10
	Cape Kluyv	Foetus	Egg, ww	2006	7	0.20 (0.16–0.5)	0.0	72.0	14.0	14.0	0.0	11
	Domashny	Foetus	Egg, ww	2006	12	0.11 (0.03–0.3)	34.0	58.0	8.0	0.0	0.0	12
Black-legged kittiwake *Rissa tridactyla*	Qaanaaq	All	Liver, ww	2015	10	0.35 (0.20–0.6)	100.0	0.0	0.0	0.0	0.0	3
	Svalbard	All	Liver, ww	2005–2006	10	0.97 (0.53–1.4)	100.0	0.0	0.0	0.0	0.0	4
	Svalbard	Foetus	Egg, ww	2003	5	0.14 (0.07–0.2)	20.0	80.0	0.0	0.0	0.0	13
	Hornøya	Foetus	Egg, ww	2003	5	0.07 (0.06–0.1)	80.0	20.0	0.0	0.0	0.0	8
	Lofoten	Foetus	Egg, ww	2003	5	0.09 (0.07–0.1)	80.0	20.0	0.0	0.0	0.0	9
Thick-billed murre *Uria lomvia*	Aleutian Islands	Foetus	Egg, ww	2000–2010	34	0.11 (0.01–0.4)	44.0	56.0	0.0	0.0	0.0	5
	Bering Sea	Foetus	Egg, ww	2000–2010	39	0.04 (0.01–0.2)	97.0	3.0	0.0	0.0	0.0	5, 6
	Bering Strait	Foetus	Egg, ww	2002–2008	32	0.13 (0.01–0.4)	94.0	6.0	0.0	0.0	0.0	5, 7

Appendix Table 6A.4(C) continued

Species	Region	Maturity	Matrix	Years	n	Hg concentration	Risk category					Refs
						Egg, µg/g fww	<0.10	0.10–0.37	0.37–0.91	0.91–1.16	≥1.16	
						Liver, µg/g fww	<0.53	0.53–2.26	2.26–6.10	6.10–7.91	≥7.91	
						Blood equivalent, µg/g fww	<0.2	0.2–1.0	1.0–3.0	3.0–4.0	≥4.0	
						Body feather, µg/g fww	<1.62	1.62–4.53	4.53–9.14	9.14–10.99	≥10.99	
						Median (Min–Max)	No effect	Low risk	Moderate risk	High risk	Severe risk	
	Gulf of Alaska	Foetus	Egg, ww	2001–2010	36	0.14 (0.02–0.6)	25.0	75.0	0.0	0.0	0.0	5, 14
	Prince Leopold Is.	Foetus	Egg, ww	2003–2017	55	0.85 (0.47–1.5)	0.0	93.3	6.7	0.0	0.0	15
	Coats Island	Foetus	Egg, ww	2003–2017	55	0.50 (0.32–0.8)	0.0	100.0	0.0	0.0	0.0	15
	Qaanaaq	All	Liver, ww	2015	10	1.06 (0.66–1.5)	90.0	10.0	0.0	0.0	0.0	3
	Svalbard	All	Liver, ww	2005–2006	10	0.34 (0.26–0.6)	100.0	0.0	0.0	0.0	0.0	4
	Svalbard	Foetus	Egg, ww	2003	5	0.03 (0.02–0.2)	80.0	20.0	0.0	0.0	0.0	13
Common murre *Uria aalge*	Aleutian Islands	Foetus	Egg, ww	2005	5	0.04 (0.02–0.1)	80.0	20.0	0.0	0.0	0.0	5
	Bering Sea	Foetus	Egg, ww	2004–2010	30	0.03 (0.01–0.2)	97.0	3.0	0.0	0.0	0.0	5, 6
	Bering Strait	Foetus	Egg, ww	2002–2008	13	0.06 (0.02–0.1)	85.0	15.0	0.0	0.0	0.0	5, 7
	Gulf of Alaska	Foetus	Egg, ww	2001–2010	85	0.13 (0.01–0.4)	12.0	88.0	0.0	0.0	0.0	5, 14
	Norton Sound	Foetus	Egg, ww	2002–2013	35	0.13 (0.05–0.6)	43.0	57.0	0.0	0.0	0.0	5, 16
Little auk *Alle alle*	Qaanaaq	All	Liver, ww	2015	10	0.25 (0.16–0.4)	100.0	0.0	0.0	0.0	0.0	3
	Svalbard	All	Liver, ww	2005–2006	11	0.22 (0.02–0.5)	100.0	0.0	0.0	0.0	0.0	4
Black guillemot *Cepphus grylle*	Faroe Islands	Foetus	Egg, ww	2000–2012	142	0.43 (0.14–1.3)	0.0	56.0	43.0	1.0	0.0	17, 18
	Faroe Islands	Juvenile	liver, ww	2002–2011	65	0.90 (0.49–2.5)	75.0	25.0	0.0	0.0	0.0	17, 18
	Qaanaaq	All	Liver, ww	2015	10	0.64 (0.43–1.3)	100.0	0.0	0.0	0.0	0.0	3
Atlantic puffin *Fratercula arctica*	Hornøya	Foetus	Egg, ww	2003	5	0.10 (0.09–0.1)	60.0	40.0	0.0	0.0	0.0	8
Atlantic puffin *Fratercula arctica*	Lofoten	Foetus	Egg, ww	2003	5	0.11 (0.08–0.1)	40.0	60.0	0.0	0.0	0.0	9
Common eider *Somateria mollissima*	Svalbard	All	Liver, ww	2008–2009	40	0.49 (0.23–1.4)	97.5	2.5	0.0	0.0	0.0	19

[1] Braune et al., 2015; [2] Braune et al., 2016; [3] Dietz and co-workers, pers. comm., 2020; [4] Jæger et al., 2009; [5] Ackerman et al., 2016b; [6] Ackerman et al., 2017; [7] Ackerman et al., 2018; [8] Helgason et al., 2008; [9] Helgason et al., 2009; [10] Miljeteig et al., 2009; [11] Miljeteig et al., 2010; [12] Miljeteig et al., 2012; [13] Helgason et al., 2011; [14] Ackerman et al., 2019; [15] Thomas and co-workers, pers. comm., 2020; [16] Ackerman et al., 2020; [17] Hoydal and Dam, 2005, 2009; [18] Nielsen et al., 2014; [19] Saunes, 2011.

Appendix Table 6A.5(A) Contemporary (post-2000) Hg exposure and potential health risk for Arctic shorebirds (blood values). Individuals (mainly adult birds) are categorized by study region and assigned to five risk categories based upon blood-specific Hg effect thresholds.

Species	Region	Matrix	Years	n	Hg concentration	Risk category					Refs
					Egg, µg/g fww	<0.10	0.10–0.37	0.37–0.91	0.91–1.16	≥1.16	
					Liver, µg/g ww	<0.53	0.53–2.26	2.26–6.10	6.10–7.91	≥7.91	
					Blood equivalent, µg/g ww	<0.2	0.2–1.0	1.0–3.0	3.0–4.0	≥4.0	
					Body feather, µg/g dw	<1.62	1.62–4.53	4.53–9.14	9.14–10.99	≥10.99	
					Median (Min–Max)	No effect	Low risk	Moderate risk	High risk	Severe risk	
American golden plover *Pluvialis dominica*	Barrow	Blood	2012	20	0.20 (0.10–0.40)	62.0	38.0	0.0	0.0	0.0	1
		Blood	2013	14	0.16 (0.09–0.35)	62.0	38.0	0.0	0.0	0.0	
	Bylot Island	Blood	2012	23	0.13 (0.06–0.30)	96.0	4.0	0.0	0.0	0.0	
		Blood	2013	24	0.11 (0.08–0.22)	96.0	4.0	0.0	0.0	0.0	
	Igloolik	Blood	2013	9	0.20 (0.10–0.32)	56.0	44.0	0.0	0.0	0.0	
Baird's sandpiper *Calidris bairdii*	Igloolik	Blood	2013	1	0.11	100.0	0.0	0.0	0.0	0.0	
Black turnstone *Arenaria melanocephala*	Cape Krusenstern	Blood	2012	15	0.20 (0.11–0.63)	63.0	38.0	0.0	0.0	0.0	
		Blood	2013	1	0.20	63.0	38.0	0.0	0.0	0.0	
Black-bellied plover *Pluvialis squatarola*	East Bay	Blood	2012	6	0.33 0.25–0.41	0.0	100.0	0.0	0.0	0.0	
		Blood	2013	2	0.40 0.36–0.44	0.0	100.0	0.0	0.0	0.0	
Dunlin *Calidris alpina*	Nome	Blood	2012	1	0.33	0.0	100.0	0.0	0.0	0.0	
	Cape Krusenstern	Blood	2012	13	0.15 0.09–0.21	94.0	6.0	0.0	0.0	0.0	
		Blood	2013	19	0.13 0.03–0.27	94.0	6.0	0.0	0.0	0.0	
	Barrow	Blood	2012	32	0.31 0.15–0.76	13.0	83.0	3.0	0.0	0.0	
		Blood	2013	57	0.33 0.09–0.70	13.0	83.0	3.0	0.0	0.0	
	Ikpikpuk River	Blood	2012	21	0.06 0.01–0.12	100.0	0.0	0.0	0.0	0.0	
		Blood	2013	11	0.11 0.07–0.19	100.0	0.0	0.0	0.0	0.0	
	Colville River	Blood	2012	12	0.17 0.13–0.24	80.0	20.0	0.0	0.0	0.0	
		Blood	2013	13	0.18 0.13–0.31	80.0	20.0	0.0	0.0	0.0	
Long-billed dowitcher *Limnodromus scolopaceus*	Barrow	Blood	2012	23	0.68 0.39–1.01	0.0	61.0	22.0	17.0	0.0	
	Barrow	Blood	2013	13	0.87 0.49–1.49	0.0	61.0	22.0	17.0	0.0	
Pectoral sandpiper *Calidris melanotos*	Nome	Blood	2012	5	0.23 0.16–0.41	40.0	60.0	0.0	0.0	0.0	
	Barrow	Blood	2012	34	0.58 0.20–2.04	0.0	72.0	18.0	10.0	0.0	
		Blood	2013	26	0.54 0.23–1.09	0.0	72.0	18.0	10.0	0.0	
	Mackenzie River Delta	Blood	2013	7	0.36 0.15–0.66	29.0	71.0	0.0	0.0	0.0	
	Bylot Island	Blood	2013	1	0.32	0.0	100.0	0.0	0.0	0.0	
Red phalarope *Phalaropus fulicarius*	Barrow	Blood	2012	36	0.42 0.12–1.12	10.0	74.0	12.0	4.0	0.0	
	Barrow	Blood	2013	32	0.54 0.20–1.60	10.0	74.0	12.0	4.0	0.0	
	Ikpikpuk River	Blood	2012	19	0.07 0.04–0.16	100.0	0.0	0.0	0.0	0.0	
		Blood	2013	13	0.14 0.09–0.19	100.0	0.0	0.0	0.0	0.0	
	Colville River	Blood	2012	13	0.26 0.11–0.38	23.0	77.0	0.0	0.0	0.0	
	East Bay	Blood	2013	10	0.52 0.28–0.66	0.0	100.0	0.0	0.0	0.0	

Appendix Table 6A.5(A) continued

Species	Region	Matrix	Years	n	Hg concentration	Risk category					Refs
					Egg, µg/g fww	<0.10	0.10–0.37	0.37–0.91	0.91–1.16	≥1.16	
					Liver, µg/g ww	<0.53	0.53–2.26	2.26–6.10	6.10–7.91	≥7.91	
					Blood equivalent, µg/g ww	<0.2	0.2–1.0	1.0–3.0	3.0–4.0	≥4.0	
					Body feather, µg/g dw	<1.62	1.62–4.53	4.53–9.14	9.14–10.99	≥10.99	
					Median (Min–Max)	No effect	Low risk	Moderate risk	High risk	Severe risk	
Red-necked phalarope *Phalaropus lobatus*	Nome	Blood	2012	16	0.11 0.07–0.18	91.0	7.0	0.0	2.0	0.0	
		Blood	2013	28	0.19 0.04–1.55	91.0	7.0	0.0	2.0	0.0	
	Cape Krusenstern	Blood	2012	10	0.17 0.07–0.30	70.0	30.0	0.0	0.0	0.0	
	Barrow	Blood	2012	10	0.48 0.26–1.43	0.0	93.0	0.0	7.0	0.0	
		Blood	2013	4	0.34 0.29–0.46	0.0	93.0	0.0	7.0	0.0	
	Ikpikpuk River	Blood	2012	15	0.07 0.03–0.17	96.0	4.0	0.0	0.0	0.0	
		Blood	2013	12	0.15 0.08–0.49	96.0	4.0	0.0	0.0	0.0	
	Colville River	Blood	2013	8	0.26 0.13–0.39	38.0	63.0	0.0	0.0	0.0	
	Mackenzie River Delta	Blood	2012	15	0.24 0.13–0.45	13.0	87.0	0.0	0.0	0.0	
		Blood	2013	23	0.37 0.21–0.64	13.0	87.0	0.0	0.0	0.0	
Ruddy turnstone *Arenaria interpres*	Colville River	Blood	2013	12	0.61 0.13–3.52	33.0	50.0	0.0	17.0	0.0	
	East Bay	Blood	2012	14	0.38 0.16–1.00	13.0	81.0	0.0	6.0	0.0	
		Blood	2013	2	0.50 0.46–0.55	13.0	81.0	0.0	6.0	0.0	
Semipalmated sandpiper *Calidris pusilla*	Nome	Blood	2012	21	0.17 0.05–0.44	73.0	27.0	0.0	0.0	0.0	
		Blood	2013	16	0.16 0.05–0.33	73.0	27.0	0.0	0.0	0.0	
	Cape Krusenstern	Blood	2012	34	0.18 0.11–0.27	76.0	24.0	0.0	0.0	0.0	
		Blood	2013	8	0.17 0.13–0.24	76.0	24.0	0.0	0.0	0.0	
	Barrow	Blood	2012	34	0.70 0.18–1.53	1.0	59.0	24.0	15.0	0.0	
		Blood	2013	40	0.61 0.25–1.56	1.0	59.0	24.0	15.0	0.0	
	Ikpikpuk River	Blood	2012	46	0.08 0.03–0.20	90.0	10.0	0.0	0.0	0.0	
		Blood	2013	31	0.16 0.10–0.32	90.0	10.0	0.0	0.0	0.0	
	Colville River	Blood	2012	14	0.25 0.17–0.41	38.0	63.0	0.0	0.0	0.0	
		Blood	2013	2	0.18 0.17–0.19	38.0	63.0	0.0	0.0	0.0	
	Mackenzie River Delta	Blood	2012	16	0.19 0.12–0.27	64.0	36.0	0.0	0.0	0.0	
		Blood	2013	20	0.19 0.11–0.28	64.0	36.0	0.0	0.0	0.0	
	Igloolik	Blood	2013	7	0.43 0.26–0.79	0.0	86.0	14.0	0.0	0.0	
Western sandpiper *Calidris mauri*	Nome	Blood	2012	15	0.26 0.16–0.48	57.0	43.0	0.0	0.0	0.0	
		Blood	2013	13	0.11 0.03–0.30	57.0	43.0	0.0	0.0	0.0	
	Cape Krusenstern	Blood	2012	28	0.21 0.11–0.35	57.0	43.0	0.0	0.0	0.0	
		Blood	2013	21	0.17 0.09–0.23	57.0	43.0	0.0	0.0	0.0	
	Barrow	Blood	2012	17	0.43 0.27–0.73	0.0	94.0	0.0	0.0	0.0	
		Blood	2013	16	0.40 0.24–0.58	0.0	94.0	0.0	0.0	0.0	

[1] Perkins et al., 2018.

Appendix Table 6A.5(B) Contemporary (post-2000) Hg exposure and potential health risk for Arctic shorebirds (feather values). Individuals (mainly adult birds) are categorized by study region and assigned to five risk categories based upon feather-specific Hg effect thresholds.

Species	Region	Matrix	Years	n	Hg concentration	Risk category					Refs
					Egg, µg/g fww	<0.10	0.10–0.37	0.37–0.91	0.91–1.16	≥1.16	
					Liver, µg/g ww	<0.53	0.53–2.26	2.26–6.10	6.10–7.91	≥7.91	
					Blood equivalent, µg/g ww	<0.2	0.2–1.0	1.0–3.0	3.0–4.0	≥4.0	
					Body feather, µg/g dw	<1.62	1.62–4.53	4.53–9.14	9.14–10.99	≥10.99	
					Median (Min–Max)	No effect	Low risk	Moderate risk	High risk	Severe risk	
American golden plover *Pluvialis dominica*	Barrow	Feather	2012	20	0.60 (0.37–1.41)	0.0	100.0	0.0	0.0	0.0	1
		Feather	2013	16	0.75 (0.23–1.71)	0.0	100.0	0.0	0.0	0.0	
	Bylot Island	Feather	2012	26	0.92 (0.31–2.27)	0.0	94.0	6.0	0.0	0.0	
		Feather	2013	25	1.27 (0.34–4.34)	0.0	94.0	6.0	0.0	0.0	
	Igloolik	Feather	2013	15	1.41 (0.35–5.83)	0.0	87.0	13.0	0.0	0.0	
Baird's sandpiper *Calidris bairdii*	Igloolik	Feather	2013	1	2.38	0.0	100.0	0.0	0.0	0.0	
Black turnstone *Arenaria melanocephala*	Cape Krusenstern	Feather	2012	14	1.69 (0.51–4.69)	0.0	84.0	16.0	0.0	0.0	
		Feather	2013	5	1.32 (0.39–4.27)	0.0	84.0	16.0	0.0	0.0	
Black-bellied plover *Pluvialis squatarola*	East Bay	Feather	2012	6	1.70 (0.29–2.61)	0.0	100.0	0.0	0.0	0.0	
		Feather	2013	6	0.86 (0.31–1.55)	0.0	100.0	0.0	0.0	0.0	
Dunlin *Calidris alpina*	Nome	Feather	2012	2	0.88 (0.59–1.17)	0.0	100.0	0.0	0.0	0.0	
	Cape Krusenstern	Feather	2012	14	1.17 (0.47–2.54)	0.0	94.0	3.0	3.0	0.0	
		Feather	2013	19	1.41 (0.49–6.38)	0.0	94.0	3.0	3.0	0.0	
	Barrow	Feather	2012	24	1.66 (0.10–5.34)	0.0	82.0	18.0	0.0	0.0	
		Feather	2013	60	1.72 (0.57–4.87)	0.0	82.0	18.0	0.0	0.0	
	Colville River	Feather	2012	12	1.36 (0.80–2.72)	0.0	83.0	17.0	0.0	0.0	
		Feather	2013	17	1.92 (0.86–4.96)	0.0	83.0	17.0	0.0	0.0	
	Ikpikpuk River	Feather	2012	21	1.02 (0.49–1.87)	0.0	100.0	0.0	0.0	0.0	
		Feather	2013	11	1.32 (0.92–1.81)	0.0	100.0	0.0	0.0	0.0	
Long-billed dowitcher *Limnodromus scolopaceus*	Barrow	Feather	2012	22	2.19 (0.31–12.14)	0.0	92.0	6.0	3.0	0.0	
		Feather	2013	14	1.07 (0.31–2.42)	0.0	92.0	6.0	3.0	0.0	
Pectoral sandpiper *Calidris melanotos*	Nome	Feather	2012	7	1.66 (0.66–3.40)	0.0	86.0	14.0	0.0	0.0	
	Barrow	Feather	2012	40	2.31 (0.56–6.67)	0.0	70.0	30.0	0.0	0.0	
		Feather	2013	33	3.21 (0.94–7.37)	0.0	70.0	30.0	0.0	0.0	
	Mackenzie River Delta	Feather	2013	8	2.23 (0.88–3.94)	0.0	88.0	13.0	0.0	0.0	
	Bylot Island	Feather	2013	1	1.91	0.0	100.0	0.0	0.0	0.0	
Red phalarope *Phalaropus fulicarius*	Barrow	Feather	2012	51	0.68 (0.14–4.00)	0.0	99.0	1.0	0.0	0.0	
		Feather	2013	40	0.50 (0.21–0.84)	0.0	99.0	1.0	0.0	0.0	
	Colville River	Feather	2012	13	0.51 (0.21–1.54)	0.0	100.0	0.0	0.0	0.0	
	Ikpikpuk River	Feather	2012	19	0.53 (0.24–1.19)	0.0	100.0	0.0	0.0	0.0	
		Feather	2013	16	0.54 (0.22–1.20)	0.0	100.0	0.0	0.0	0.0	
	East Bay	Feather	2013	15	0.77 (0.37–1.33)	0.0	100.0	0.0	0.0	0.0	

Appendix Table 6A.5(B) continued

Species	Region	Matrix	Years	n	Hg concentration	Risk category					Refs
					Egg, µg/g fww	<0.10	0.10–0.37	0.37–0.91	0.91–1.16	≥1.16	
					Liver, µg/g ww	<0.53	0.53–2.26	2.26–6.10	6.10–7.91	≥7.91	
					Blood equivalent, µg/g ww	<0.2	0.2–1.0	1.0–3.0	3.0–4.0	≥4.0	
					Body feather, µg/g dw	<1.62	1.62–4.53	4.53–9.14	9.14–10.99	≥10.99	
					Median (Min–Max)	No effect	Low risk	Moderate risk	High risk	Severe risk	
Red-necked phalarope *Phalaropus lobatus*	Nome	Feather	2012	44	1.03 (0.30–2.42)	0.0	100.0	0.0	0.0	0.0	
		Feather	2013	33	0.60 (0.24–2.17)	0.0	100.0	0.0	0.0	0.0	
	Cape Krusenstern	Feather	2012	9	0.70 (0.34–1.33)	0.0	100.0	0.0	0.0	0.0	
	Barrow	Feather	2012	12	0.46 (0.24–0.71)	0.0	100.0	0.0	0.0	0.0	
		Feather	2013	5	0.46 (0.26–0.80)	0.0	100.0	0.0	0.0	0.0	
	Colville River	Feather	2013	8	0.43 (0.27–1.02)	0.0	100.0	0.0	0.0	0.0	
	Ikpikpuk River	Feather	2012	15	0.50 (0.18–1.03)	0.0	100.0	0.0	0.0	0.0	
		Feather	2013	16	0.61 (0.24–2.30)	0.0	100.0	0.0	0.0	0.0	
	Mackenzie River Delta	Feather	2013	23	0.68 (0.21–1.78)	0.0	100.0	0.0	0.0	0.0	
Ruddy turnstone *Arenaria interpres*	Colville River	Feather	2013	14	2.25 (0.84–7.29)	0.0	71.0	29.0	0.0	0.0	
	East Bay	Feather	2012	14	1.15 (0.27–3.29)	0.0	95.0	5.0	0.0	0.0	
		Feather	2013	5	0.73 (0.49–0.93)	0.0	95.0	5.0	0.0	0.0	
Semipalmated sandpiper *Calidris pusilla*	Nome	Feather	2012	38	0.93 (0.28–3.66)	0.0	99.0	1.0	0.0	0.0	
		Feather	2013	35	0.97 (0.18–2.54)	0.0	99.0	1.0	0.0	0.0	
	Cape Krusenstern	Feather	2012	34	0.79 (0.17–2.70)	0.0	100.0	0.0	0.0	0.0	
		Feather	2013	27	0.72 (0.18–2.10)	0.0	100.0	0.0	0.0	0.0	
	Barrow	Feather	2012	55	0.96 (0.24–9.25)	0.0	99.0	1.0	1.0	0.0	
		Feather	2013	81	0.86 (0.07–2.90)	0.0	99.0	1.0	1.0	0.0	
	Colville River	Feather	2012	14	0.80 (0.34–1.83)	0.0	100.0	0.0	0.0	0.0	
		Feather	2013	2	0.83 (0.72–0.94)	0.0	100.0	0.0	0.0	0.0	
	Ikpikpuk River	Feather	2012	46	0.71 (0.18–5.18)	0.0	98.0	2.0	0.0	0.0	
		Feather	2013	36	0.85 (0.27–4.79)	0.0	98.0	2.0	0.0	0.0	
	Mackenzie River Delta	Feather	2012	17	1.04 (0.14–2.01)	0.0	100.0	0.0	0.0	0.0	
		Feather	2013	20	0.61 (0.13–1.73)	0.0	100.0	0.0	0.0	0.0	
	Igloolik	Feather	2013	11	0.59 (0.30–2.10)	0.0	100.0	0.0	0.0	0.0	
Western sandpiper *Calidris mauri*	Nome	Feather	2012	38	0.97 (0.17–2.44)	0.0	99.0	1.0	0.0	0.0	
		Feather	2013	30	1.03 (0.15–4.68)	0.0	99.0	1.0	0.0	0.0	
	Cape Krusenstern	Feather	2012	27	1.74 (0.13–10.24)	0.0	86.0	12.0	2.0	0.0	
		Feather	2013	30	1.46 (0.12–4.42)	0.0	86.0	12.0	2.0	0.0	
	Barrow	Feather	2012	19	1.64 (0.19–6.21)	0.0	81.0	17.0	2.0	0.0	
		Feather	2013	33	1.93 (0.17–10.13)	0.0	81.0	17.0	2.0	0.0	

[1] Perkins et al., 2018.

Appendix Table 6A.6 Contemporary (post-2000) Hg exposure and potential health risk for Arctic marine fish. Individuals are categorized by study region and assigned to five risk categories based upon muscle-specific Hg effect thresholds. Grey shaded populations are from regions outside the Arctic.

Species	Region	Maturity	Matrix	Years	n	Hg concentration	Risk category					Ref.
						Muscle (µg/g)	<0.10	0.10–0.30	0.30–0.50	0.5–2.0	≥2.00	
						Median (Min–Max)	No risk	Low risk	Moderate risk	High risk	Severe risk	
Atlantic cod *Gadus morhua*	Barents Sea	All, F+M	Muscle (ww)	2000–2018	866	0.03 (0.01–0.29)	97.3	2.7	0.0	0.0	0.0	1
	Norwegian Sea	All, F+M	Muscle (ww)	2000–2018	686	0.08 (0.01–1.87)	67.2	27.3	3.9	1.6	0.0	
	Icelandic Waters	All, F+M	Muscle (ww)	2000–2018	47	0.03 (0.02–0.2)	93.6	6.4	0.0	0.0	0.0	
	Mýlingsgrunnur	All, F+M	Muscle (ww)	2000–2017	266	0.03 (0.01–0.21)	97.7	2.3	0.0	0.0	0.0	2
	Baltic Sea	All, F+M	Muscle (ww)	2000–2018	223	0.03 (0–0.11)	99.6	0.5	0.0	0.0	0.0	1
	Celtic Seas	All, F+M	Muscle (ww)	2000–2016	42	0.08 (0.03–0.39)	57.1	40.5	2.4	0.0	0.0	
	Greater North Sea	All, F+M	Muscle (ww)	2000–2018	2828	0.1 (0.01–1.46)	48.5	41.5	7.9	2.1	0.0	
Common dab *Limanda limanda*	Icelandic Waters	All, F+M	Muscle (ww)	2000	1	0.07 (0.07–0.07)	100.0	0.0	0.0	0.0	0.0	1
	Baltic Sea	All, F+M	Muscle (ww)	2007–2016	90	0.03 (0–0.12)	97.8	2.2	0.0	0.0	0.0	
	Celtic Seas	All, F+M	Muscle (ww)	2000–2018	858	0.13 (0.01–0.54)	34.0	61.7	4.2	0.1	0.0	
	Greater North Sea	All, F+M	Muscle (ww)	2000–2018	2016	0.09 (0.01–1.1)	59.1	39.8	0.9	0.3	0.0	
European plaice *Pleuronectes platessa*	Barents Sea	All, F+M	Muscle (ww)	2000–2011	56	0.02 (0.01–0.08)	100.0	0.0	0.0	0.0	0.0	1
	Norwegian Sea	All, F+M	Muscle (ww)	2000–2011	53	0.03 (0.01–0.18)	92.5	7.6	0.0	0.0	0.0	
Arctic char *Salvelinus alpinus* (anadromous, sea run)	Bjørnøya	All, F+M	Muscle (ww)	2001–2015	178	0.13 (0.03–0.83)	33.7	43.8	14.6	7.9	0.0	3
	Faroe Islands	All, F+M	Muscle (ww)	2001–2014	169	0.24 (0.12–0.67)	0.0	75.7	19.5	4.7	0.0	1
	Greenland Sea	All, F+M	Muscle (ww)	2004–2018	45	0.71 (0.17–3.56)	0.0	4.4	11.1	80.0	4.4	
	Queen Maud Gulf	All, F+M	Muscle (ww)	2004–2018	155	0.06 (0.01–0.36)	93.6	5.8	0.7	0.0	0.0	4

[1] ICES Data Centre, 2020; [2] Andreasen et al., 2019; [3] Poste et al., pers. comm., 2020; [4] Evans, pers. comm., 2020.

Appendix Table 6A.7 Contemporary (post-2000) Hg exposure and potential health risk for Arctic freshwater fish. Individuals are categorized by study region and assigned to five risk categories based upon muscle-specific Hg effect thresholds.

Species	Region	Maturity	Matrix	Years	n	Hg concentration	Risk category					Refs
						Muscle (µg/g)	<0.10	0.10–0.30	0.30–0.50	0.5–2.0	≥2.00	
						Median (Min–Max)	No effect	Low risk	Moderate risk	High risk	Severe risk	
Northern pike *Esox lucius*	GSL-West Basin	All, F+M	Muscle (ww)	2000–2018	266	0.24 (0.09–0.87)	1.9	66.9	28.6	2.6	0.0	1
	Storvindeln	All, F+M	Muscle (ww)	2000–2017	160	0.27 (0.11–0.65)	0.0	65.0	31.3	3.8	0.0	2
Burbot *Lota lota*	Fort Good Hope	All, F+M	Muscle (ww)	2000–2018	671	0.36 (0–1.04)	1.0	31.2	50.4	17.4	0.0	3
	GSL-East Arm	All, F+M	Muscle (ww)	2000–2018	192	0.13 (0.04–0.36)	22.4	76.6	1.0	0.0	0.0	1
	GSL-West Basin	All, F+M	Muscle (ww)	2000–2018	223	0.16 (0.06–0.51)	10.8	85.2	3.6	0.5	0.0	1
Brown trout *Salmo trutta*	Leitisvatn	All, F+M	Muscle (ww)	2017	13	0.35 (0.15–0.71)	0.0	38.5	46.2	15.4	0.0	4
	Mjáuvøtn	All, F+M	Muscle (ww)	2017	7	0.08 (0.06–0.31)	71.4	14.3	14.3	0.0	0.0	4
Arctic char *Salvelinus alpinus*	Á Mýrunum	All, F+M	Muscle (ww)	2000–2014	197	0.23 (0.1–0.67)	0.0	74.6	22.3	3.1	0.0	5
	Amituk Lake	All, F+M	Muscle (ww)	2001–2018	144	1.14 (0.1–3.87)	0.0	5.6	6.3	73.6	14.6	6
	Char Lake	All, F+M	Muscle (ww)	2000–2018	85	0.42 (0.08–1.03)	3.5	34.1	20.0	42.4	0.0	
	Isortoq	All, F+M	Muscle (ww)	2004–2018	123	0.85 (0.17–3.56)	0.0	2.4	6.5	85.4	5.7	7
	Lake Hazen	All, F+M	Muscle (ww)	2001–2018	314	0.13 (0.02–1.63)	40.5	35.7	14.7	9.2	0.0	6
	North Lake	All, F+M	Muscle (ww)	2000–2018	181	0.21 (0.08–1.38)	2.8	72.4	15.5	9.4	0.0	
	Resolute Lake	All, F+M	Muscle (ww)	2000–2018	272	0.15 (0.06–0.53)	13.6	76.8	9.2	0.4	0.0	
	Small Lake	All, F+M	Muscle (ww)	2011–2012	30	0.09 (0.04–0.19)	100.0	0.0	0.0	0.0	0.0	8
	9-Mile Lake	All, F+M	Muscle (ww)	2011–2012	30	0.12 (0.06–0.39)	30.0	63.3	6.7	0.0	0.0	
	Boomerang Lake	All, F+M	Muscle (ww)	2012	15	0.14 (0.09–0.54)	13.3	66.7	13.3	6.7	0.0	
	East Lake	All, F+M	Muscle (ww)	2008–2009	17	0.1 (0.05–0.29)	52.9	47.1	0.0	0.0	0.0	
	West Lake	All, F+M	Muscle (ww)	2008–2009	26	0.16 (0.05–0.44)	30.8	61.5	7.7	0.0	0.0	
	Aquiatusuk Lake	All, F+M	Muscle (ww)	2008–2009	15	0.59 (0.16–1.03)	0.0	26.7	13.3	60.0	0.0	
	Saphire Lake	All, F+M	Muscle (ww)	2001	9	0.36 (0.16–1.07)	0.0	22.2	55.6	22.2	0.0	9
	Tasialuk	All, F+M	Muscle (ww)	2007	10	0.13 (0.08–0.17)	10.0	90.0	0.0	0.0	0.0	10
	Coady's Pond #1	All, F+M	Muscle (ww)	2007	10	0.1 (0.07–0.12)	50.0	50.0	0.0	0.0	0.0	
	Little Nauyuk	All, F+M	Muscle (ww)	2006	10	0.11 (0.07–0.22)	40.0	60.0	0.0	0.0	0.0	
	Radar Lake	All, F+M	Muscle (ww)	1999	8	0.91 (0.23–1.92)	0.0	12.5	12.5	75.0	0.0	
	Herbert Lake	All, F+M	Muscle (ww)	1999	8	0.35 (0.21–2.34)	0.0	50.0	12.5	25.0	12.5	
	12-Mile Lake	All, F+M	Muscle (ww)	2006	10	0.14 (0.1–0.2)	20.0	80.0	0.0	0.0	0.0	
	Coady's Pond #2	All, F+M	Muscle (ww)	2007	20	0.12 (0.06–0.21)	25.0	75.0	0.0	0.0	0.0	11

Appendix Table 6A.7 continued

Species	Region	Maturity	Matrix	Years	n	Hg concentration	Risk category					Refs
						Muscle (µg/g)	<0.10	0.10–0.30	0.30–0.50	0.5–2.0	≥2.00	
						Median (Min–Max)	No effect	Low risk	Moderate risk	High risk	Severe risk	
	Heintzelman Lake	All, F+M	Muscle (ww)	2001	119	0.11 (0.03–0.32)	45.4	52.9	1.7	0.0	0.0	12
	Tasiapik Lake	All, F+M	Muscle (ww)	2009–2010	31	0.1 (0.06–0.26)	51.6	48.4	0.0	0.0	0.0	
	Esker Lake	All, F+M	Muscle (ww)	2008	20	0.07 (0.04–0.86)	80.0	15.0	0.0	5.0	0.0	
	Upper Nakvak Lake	All, F+M	Muscle (ww)	2007	20	0.07 (0.03–0.49)	60.0	30.0	10.0	0.0	0.0	
	Tasiapik Lake	All, F+M	Muscle (ww)	2009–2010	31	0.1 (0.06–0.26)	51.6	48.4	0.0	0.0	0.0	
	Crazy Lake	All, F+M	Muscle (ww)	2010	47	0.06 (0.03–1.03)	78.7	12.8	6.4	2.1	0.0	
	Iqalugaarjuit Lake	All, F+M	Muscle (ww)	2004	20	0.11 (0.07–0.3)	45.0	55.0	0.0	0.0	0.0	
	Unnamed Lake	All, F+M	Muscle (ww)	2010	18	0.19 (0.08–0.42)	11.1	55.6	33.3	0.0	0.0	
	Lake A (Qaqortoq)	All, F+M	Muscle (ww)	1994–1995	50	0.6 (0.07–3.73)	2.0	2.0	26.0	66.0	4.0	13
	Lake B (Qaqortoq)	All, F+M	Muscle (ww)	1995	22	0.48 (0.15–1.71)	0.0	22.7	31.8	45.5	0.0	
	Lake C (Qaqortoq)	All, F+M	Muscle (ww)	1995	25	0.54 (0.22–1.32)	0.0	8.0	32.0	60.0	0.0	
	Lake D (Qaqortoq)	All, F+M	Muscle (ww)	1995	22	0.57 (0.23–2.01)	0.0	4.6	31.8	59.1	4.6	
	Avanersuaq	All, F+M	Muscle (ww)	1994–1995	26	0.21 (0.04–0.5)	23.1	50.0	26.9	0.0	0.0	
	Hovaktok Lake	All, F+M	Muscle (ww)	2006	7	0.05 (0.02–0.08)	100.0	0.0	0.0	0.0	0.0	14
	Lake 10	All, F+M	Muscle (ww)	2006	7	0.05 (0.03–0.08)	100.0	0.0	0.0	0.0	0.0	15
	Lake 32	All, F+M	Muscle (ww)	2006	12	0.08 (0.02–0.23)	75.0	0.0	25.0	0.0	0.0	
	Nauyuk Lake	All, F+M	Muscle (ww)	2006	18	0.04 (0.02–0.16)	83.3	16.7	0.0	0.0	0.0	14
	Gavia Faeces	All, F+M	Muscle (ww)	2006	8	0.08 (0.05–0.51)	75.0	0.0	12.5	12.5	0.0	16
	Keyhole Lake	All, F+M	Muscle (ww)	2006	7	0.1 (0.03–0.27)	42.9	57.1	0.0	0.0	0.0	
	Notgordie Lake	All, F+M	Muscle (ww)	2006	5	0.19 (0.15–0.34)	0.0	60.0	40.0	0.0	0.0	
	Roberts Lake	All, F+M	Muscle (ww)	2006	34	0.01 (0.01–0.04)	100.0	0.0	0.0	0.0	0.0	14
Lake trout *Salvelinus namaycush*	Lake Kusawa	All, F+M	Muscle (ww)	2001–2018	179	0.31 (0.1–1.31)	0.0	48.6	35.8	15.6	0.0	17
	Lake Laberge	All, F+M	Muscle (ww)	2000–2018	188	0.42 (0.1–1.36)	0.5	24.5	42.6	32.5	0.0	17

[1] Evans, pers. comm., 2020; [2] Danielsen and co-workers pers. comm., 2020; [3] Stern, pers. comm., 2020; [4] Andreasen and co-workers, pers. comm., 2020; [5] Andreasen et al., 2019; [6] Muir and Hudelson, pers. comm., 2020; [7] Rigét and co-workers, pers. comm., 2020; [8] Barst et al., 2016; [9] Muir et al., 2005; [10] Gantner et al., 2010a, 2010b; [11] van der Velden et al., 2013a; [12] van der Velden et al., 2012; [13] Rigét et al., 2000; [14] Swanson and Kidd, 2010; [15] Barst et al., 2019; [16] Swanson et al., 2011; [17] Gamberg, pers. comm., 2020.

Appendix Table 6A.8 Contemporary (post-2000) Hg and MeHg concentrations for Arctic aquatic invertebrates. Concentrations are categorized by invertebrate taxa in marine and freshwater environments and assigned to five concentration categories.

Taxonomic grouping	Environment	Arctic regions sampled	Years	n	Hg or MeHg concentration	Concentration category					Refs.
					µg/g dw	<0.25	0.25–0.5	0.5–1.5	1.5–4.0	≥4.0	
					Median (Min–Max)						
Amphipods (Hg)	Marine	Canada, Greenland, Russia, USA	2002–2014	35	0.053 (0.018–0.480)	91	9	0	0	0	18, 7, 19, 22, 10, 9, 20, 13, 26
Amphipods (MeHg)	Marine	Canada, USA	2002–2014	24	0.035 (0.008–0.160)	100	0	0	0	0	18, 7, 10, 20, 21, 26
Bivalves (Hg)	Marine	Canada, Faroe Islands, Greenland, Iceland, Norway, Sweden, USA	2003–2017	16	0.100 (0.060–0.200)	100	0	0	0	0	5, 10, 14, 19, 23, 26
Bivalves (MeHg)	Marine	Canada, Faroe Islands, Greenland, Iceland, Norway, Sweden, USA	2003–2017	10	0.035 (0.011–0.100)	100	0	0	0	0	5, 10, 23, 26
Copepods (Hg)	Marine	Canada, Greenland, Russia	2002–2013	16	0.038 (0.007–0.220)	100	0	0	0	0	7, 9, 18, 19, 22, 23, 26
Copepods (MeHg)	Marine	Canada, Greenland	2002–2012	10	0.010 (0.003–0.075)	100	0	0	0	0	7, 18, 22
Euphausiids, mysids, shrimp (Hg)	Marine	Canada, Greenland, USA	2002–2014	16	0.060 (0.016–0.913)	88	6	6	0	0	10, 13, 18, 19, 20, 22, 23, 26
Euphausiids, mysids, shrimp (MeHg)	Marine	Canada, USA	2002–2014	12	0.032 (0.009–0.870)	92	0	8	0	0	10, 18, 20, 21, 22, 26
Macroinvertebrates, bulk (Hg)	Freshwater	Canada, Fennoscandia	2000–2014	14	0.115 (0.023–3.498)	72	14	7	7	0	8, 15, 16
Zooplankton, bulk (Hg)	Freshwater	Canada, Fennoscandia	2000–2014	25	0.075 (0.022–0.862)	92	0	8	0	0	6, 8, 11, 17, 16, 26
Zooplankton, bulk (MeHg)	Freshwater	Canada	2005–2015	44	0.033 (0.001–0.695)	96	2	2	0	0	4, 12, 17, 24, 25, 26
Caddisflies (Hg)	Freshwater	Canada, Fennoscandia	2005–2011	8	0.087 (0.021–0.271)	88	12	0	0	0	12, 15, 26
Caddisflies (MeHg)	Freshwater	Canada	2005–2011	12	0.024 (0.011–0.133)	100	0	0	0	0	3, 12, 26
Chironomids (Hg)	Freshwater	Canada, Fennoscandia	2005–2011	17	0.216 (0.059–0.391)	76	24	0	0	0	6, 12, 15, 26
Chironomids (MeHg)	Freshwater	Canada	2005–2014	48	0.048 (0.004–0.319)	96	4	0	0	0	1, 4, 12, 25, 26
Copepods (MeHg)	Freshwater	Canada	2005–2006	9	0.027 (0.011–0.048)	100	0	0	0	0	2
Isopods (MeHg)	Freshwater	Canada	2006–2008	6	0.062 (0.030–0.082)	100	0	0	0	0	25
Mysids (MeHg)	Freshwater	Canada	2006–2008	6	0.023 (0.018–0.088)	100	0	0	0	0	25

[1] Chételat et al., 2008; [2] Chételat et al., 2012; [3] Chételat et al., 2014; [4] Chételat et al., 2018; [5] Chételat et al., pers. comm., 2021; [6] Choy et al., 2010; [7] Clayden et al., 2015; [8] Evans et al., 2005a, 2005b; [9] Fort et al., 2016; [10] Fox et al., 2017; [11] Gantner et al., 2010a; [12] Gantner et al., 2010b; [13] Gongora et al., 2018; [14] Jorunsdóttir et al., 2014; [15] Kahilainen et al., 2016; [16] Kahilainen et al., 2017; [17] Lehnherr et al., 2012a; [18] Loseto et al., 2008; [19] McMeans et al., 2015a; [20] Pedro et al., 2017; [21] Pedro et al., 2019; [22] Pomerleau et al., 2016; [23] Rigét et al., 2007; [24] Rohonczy et al., 2019; [25] Swanson et al., 2010; [26] van der Velden et al., 2013b

7. What is the impact of mercury contamination on human health in the Arctic?

Coordinating Authors: Pál Weihe, Niladri Basu

Contributing Authors: Eva M. Krümmel, Khaled Abass, Arja Rautio, Rune Dietz

7.1 Introduction

Contemporaneous concerns over mercury (Hg) pollution in the Arctic nears 50 years with past AMAP reports having examined in great detail the evidence of Hg exposure and its effects on Arctic populations (AMAP, 1998, 2003, 2009, 2011). These reports illustrate that human populations in the Arctic remain among the most exposed and impacted worldwide, and they also demonstrate that the health effects of Hg extend beyond classic toxicological effects to encompass broader issues of social and cultural well-being and food security. This chapter expands upon these works to provide an update of the scientific information since the last AMAP mercury assessment published in 2011 (AMAP, 2011). The current chapter focuses on the Arctic's Indigenous Peoples, though non-Indigenous Arctic residents may also be exposed to Hg with some groups experiencing relatively high levels of Hg exposure.

Since the last AMAP assessment, the entry into force of the Minamata Convention on Mercury in 2017 signalled the commitment by government signatories from around the world to reduce the use and environmental release of Hg in order to protect human health and the environment (Evers et al., 2016; Article 1, UNEP, 2019). As described in detail in Chapter 9 of this current assessment, information on Hg in the Arctic from AMAP and involvement from Arctic Indigenous Peoples and Arctic countries were crucial in the negotiations of the Minamata Convention on Mercury. This is particularly visible in the preamble of the Minamata Convention, which refers to "the particular vulnerabilities of Arctic ecosystems and Indigenous communities". As part of the 2018 UN Global Mercury Assessment (UN Environment, 2019), a systematic assessment of Hg exposures worldwide demonstrated that "Arctic populations who consume fish and marine mammals" were one of four priority groups of concern (Basu et al., 2018).

Arctic populations, and most notably Indigenous communities, are particularly vulnerable to Hg pollution for several reasons (Fernández-Llamazares et al., 2020). As elaborated elsewhere in this report (see Chapters 3 and 4), a range of global factors that span from socio-economic patterns to biogeochemical processes make the Arctic a major sink for Hg pollution. As a result, traditional food items (i.e., the tissues of certain marine mammals and some freshwater fish in certain regions) may have relatively high levels of Hg, raising concerns over food security as detailed below. Avoiding such food items is not an option in many cases as these traditional food items have great cultural benefit, are more affordable and far superior nutritionally compared to store-bought options and are therefore promoted by regional health officials. Furthermore, the harvesting, sharing and consuming of traditional foods supports cultural, social, and spiritual health in these communities. Finally, critical aspects of Hg pollution, food systems and northern life are interlinked; this means they are further pressured due to climate change (Nilsson et al., 2013; Berner et al., 2016).

This chapter summarizes information on the impacts of Hg on human health taken by building on information published in the last AMAP mercury assessment (AMAP, 2011) with some additional updates from recent health studies including the recent AMAP human health assessment (AMAP, 2021) as well as a greater focus on exposure assessment than prior reports. In answering the primary, policy-relevant question of this chapter—What is the impact of mercury contamination on human health in the Arctic?—the following sections illustrate links between findings presented in the rest of this current assessment and their implications for human health.

7.2 What are the global influences on mercury exposure in the North?

Other chapters in this current assessment discuss in detail temporal trends (Chapter 2), the sources of Hg and pathways to the Arctic (Chapter 3), factors that drive the movement of Hg into food webs relevant to human consumers (Chapter 4) and the influence of climate change on these processes (Chapter 5), hotspots and trends in relation to wildlife with high exposure to Hg (Chapter 6) as well as future scenarios for Hg in the Arctic (Chapter 8).

As detailed in Chapter 3, 32% of the annual Hg deposited into the Arctic, is estimated to originate from present day global anthropogenic sources, and 64% is estimated to be from re-emissions of legacy deposition (both anthropogenic and geogenic sources). The deposited Hg, largely originating from southern latitudes, is then subject to ecological processes that make it potentially bioavailable for entry into food webs (see Chapter 4), where it may ultimately build up in fish and wildlife (see Chapter 6), some of which represent key food items for Arctic Indigenous Peoples. Even though local and regional characteristics may influence Hg exposure in these species, global anthropogenic activities are ultimately driving the movement of Hg into the Arctic ecosystem, following which this contaminant may enter local food systems. Exposures are further being pushed by global drivers such as changes to hydrology or land use as well as the introduction of invasive species, which alter the structure of food webs and ecosystem energetics, ultimately having an impact on the accumulation and biomagnification of Hg (Eagles-Smith et al., 2018). The impact of climate change on Hg cycling and human exposure to Hg is thus to be regarded as multi-dimensional (Krabbenhoft and Sunderland, 2013; Sundseth et al., 2015).

Another global phenomenon influencing Hg exposures in the Arctic is the industrialization of many national economies which in turn influences international food markets and trade (Lavoie et al., 2018). As such, a nutrition transition is well underway in many Arctic communities, as elaborated upon further below, in that traditional foods are being increasingly supplemented by certain store-bought foods of low nutritional value that also tend to exemplify a western diet. This shift is also being driven by challenges associated with traditional hunting practices (e.g., changes in animal behavior, ice and snow conditions, hunting locations and seasonality), some of which may become more severe due to the effects of climate change (Pearce et al., 2015). While this may reduce human exposure to Hg (i.e., less consumption of local fish and wildlife), the shift to a western diet and away from traditional foods is also associated with a poorer, less healthy diet that largely consists of refined carbohydrates and saturated fatty acids with limited nutritional content, vitamins and unsaturated fatty acids.

7.3 What are the dietary influences on mercury exposure in the North?

Arctic Indigenous Peoples are largely exposed to Hg through their diet. In this section, we detail what is known about key foods and factors that may influence exposure, the nutrition transition underway across Arctic communities, and approaches to gauge exposures.

7.3.1 Exposure to mercury contaminated traditional foods

The amount of Hg in traditional and/or local foods can be gleaned from a review of information presented in other chapters (see Chapter 2 and 6), with levels in key food items summarized in Figure 7.1. The data presented in these chapters demonstrate that the levels of Hg can differ widely across Arctic biota (and even within a species) and that Hg levels vary greatly across space and time; moreover, the data show that Hg levels are also influenced by factors such as food-web position, sex and age. These have tremendous implications for human exposures especially since many of these biota (or their parts) represent key dietary sources. For example, Hg levels in landlocked Arctic char (*Salvelinus alpinus*) can vary 100-fold (0.01–1.13 µg/g; Barst et al., 2019) and Hg levels in ringed seal liver can vary 4500-fold based on a review of the min-max data from Chapter 6 (see Appendix Table 6A.1). Furthermore, Hg levels within an organism vary across tissues. For example, Wagemann et al. (1998) reported on Hg levels differing across the liver, muscle, skin and blubber of belugas (*Delphinapterus leucas*), ringed seals (*Pusa hispida*), and narwhals (*Monodon monocereos*); such information is important when developing dietary advisories. Finally, most monitoring and research studies tend to present data on total Hg levels, though the percent that is methylmercury (MeHg) can vary widely across species and tissues (Dietz et al., 1990; Lemes et al., 2011; Ewald et al., 2019) and is not always characterized. From a human health perspective, the MeHg component is what is most bioavailable (Bradley et al., 2017).

Mercury has been measured in thousands of fish samples from across the Arctic region. To help put some of these data into perspective, we note that the United States Environmental Protection Agency (US EPA) has a tissue-based water quality criteria of 0.3 µg/g (US EPA, 2001) which is also the screening criteria used by the Food and Agriculture Organization and World Health Organization (FAO/WHO) Codex Alimentarius Commission as a value that would present a risk of exposures exceeding the provisional tolerable weekly intake (PTWI; FAO/WHO, 2020b). Health Canada's limit for Hg in the edible portion of most retail fish is 0.5 µg/g (Health Canada, 2007) as is the value proposed by the European Commission (EEA, 2018). An analysis of Hg levels in muscle from 1569 landlocked Arctic char from across 83 sites found that Hg levels exceeded the 0.3 µg/g ww US EPA quality criteria in 21% of the sites (Barst et al., 2019). In Alaska, Jewett and Duffy (2007) measured muscle Hg in 2692 samples spanning 17 freshwater species and

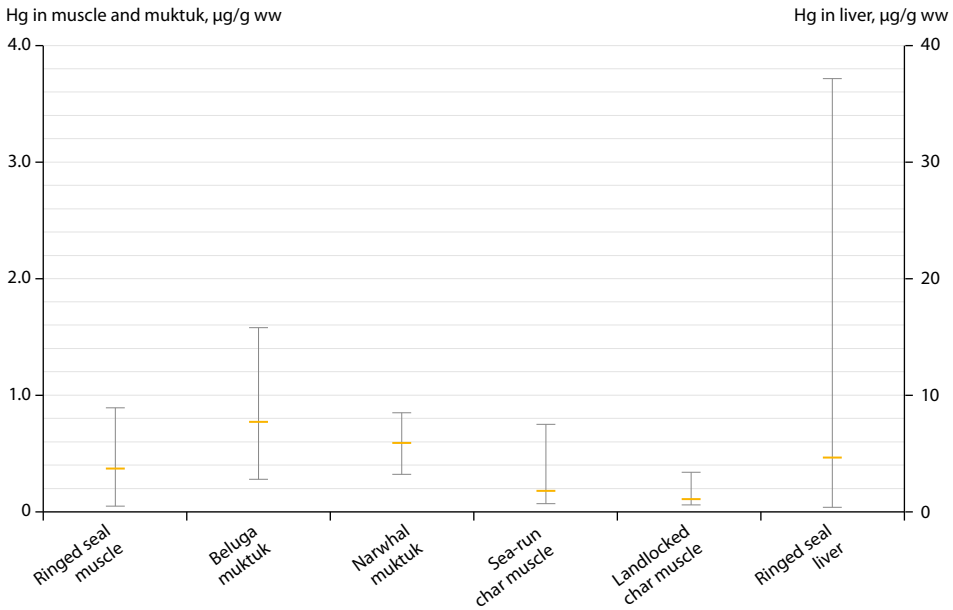

Figure 7.1 Total Hg concentrations (µg/g ww) in food items that tend to drive human exposure in Arctic communities. The Hg concentrations represent a range of central values reported from across several studies, with the minimum and maximum ranges indicated (gray lines) along with the median (orange line) (see Appendix Table A7.1). All data are from animals harvested since the year 2000, except for the two muktuk samples for which earlier data needed to be accessed given the lack of recent information.

24 anadromous and marine fish species. The highest levels, often exceeding guidelines, were found in northern pike (*Esox lucius*) and were relatively low in the most frequently consumed species including salmon, cod, halibut and herring.

The Hg levels in mammalian tissues are often much higher than in fish, and usually these exceed guideline values. For example, Hg levels in cod from the Faroe Islands (a stable food source on the islands) are about 0.02 µg/g versus 2 µg/g which may be found in the muscle of pilot whales in the same region (Nielsen et al., 2012a). The median level of liver Hg in ringed seals from across several studies was almost always above 1 µg/g (see Appendix Table A7.1), though much of this Hg is in the inorganic form sequestered to Se and likely not bioavailable.

Several dietary surveys have demonstrated that ingestion of some traditional and/or local foods, especially from certain fish and marine mammals, drives exposure to Hg. For example, in a study of children from Nunavut (Canada), the top contributors of Hg exposure were beluga muktuk (33%) followed by narwhal muktuk (26%) and ringed seal liver (15%). When coupled with fish (11%), caribou meat (6%) and ringed seal meat (5%), these food items accounted for over 95% of the total Hg intake (Tian et al., 2011). In a study of adults from the "*Qanuippitaa?* How are we?" survey of 15 communities in Nunavik in 2004 (NRBHSS, 2004; Anctil, 2008), human exposures to Hg were principally driven by beluga meat (especially nikku which is the dried form; Lemire et al., 2015). From the 2007–2008 Inuit Health Survey (of 2074 adults from 36 communities) in Canada, ringed seal liver was the largest source of Hg exposure (59%) followed by Arctic char (8.4%; Laird et al., 2013). In fact, 10 food items accounted for ~90% of the Hg intake while the remaining 72 accounted for only 10%. These ten food items include ringed seal liver, arctic char muscle, beluga muktuk (skin only), beluga muktuk (skin and fat), ringed seal meat, caribou meat, narwhal muktuk (skin and fat), dried caribou meat, narwhal muktuk (skin only) and beluga meat. A study of 2224 Inuit adults from Greenland between 2005 and 2008 studied dietary information (25 traditional and 43 imported food items) alongside whole blood Hg levels and found that seal consumption was the largest contributor of Hg exposure (Jeppesen et al., 2012). While the information contained in this paragraph exemplifies key food items that tend to drive Hg exposures, one needs to remember that these same food items afford nutritional, cultural, recreational and economic benefits, as noted elsewhere (e.g., see Section 7.6) and thus prudent and nuanced risk-benefit considerations are always called for.

The bioaccessibility and bioavailablity of Hg from a given food item into an individual may be influenced by a range of factors. A body of emerging research suggests that Hg may be less than 100% bioavailable from food items to human consumers as reviewed by Bradley et al. (2017). For example, Laird et al. (2009) used an *in vitro* system to calculate the bioaccessibility of Hg from the small intestine; the results show that the bioaccessibility of Hg may range between 1% and 93% for 16 food samples (from fish, wild game, and marine mammals) typically consumed by Inuit. While these *in vitro* results suggest that not all the ingested Hg is taken up, to our knowledge such a finding has yet to be shown in a human population study; thus, the emerging science should be viewed cautiously, though it should be followed up on.

There remains a long-standing interest in the potential protective role of selenium (Se) against Hg risk, and while experimental studies tend to suggest a protective role for Se, few population studies have provided convincing and consistent evidence. For example, consideration of Se in two waves of the Faroe Islands birth cohort studies found no evidence for a protective role for Se (Choi et al., 2008), though a study of adults from the 2007–2008 Inuit Health Survey from Canada found some cardioprotective effects of Se in relation to Hg exposure (Hu et al., 2017a; 2017b). However, more work is needed as most studies in this area focus on measuring total amounts of Se in each biological sample without characterizing specific Se molecules (e.g., selenoproteins). Recent studies have shown that selenoneine, a novel Se compound, is found in high concentrations in beluga muktuk as well as in the red blood cells of Inuit residing in Nunavik (Achouba et al., 2019; Little et al., 2019) and the significance of these observations warrants investigation.

7.3.2 Nutrition transition

The nature of Hg exposures across the Arctic is changing, and diet is playing a major role in this change. In the 2007–2008 Inuit Health Survey of 36 Canadian Arctic communities, respondents indicated that they consumed less fish, whale, seal meat and birds in the year preceding the survey, and researchers were then able to use this information to model these dietary changes with significant decreases in the intake of essential nutrients such as zinc and vitamin D (Rosol et al., 2016). Interviews with Inuit community members in Nunavut (Canada) that included elders and hunters revealed concerns about changing climate, weather patterns and species distribution (Nancarrow and Chan, 2010). From the Survey of Living Conditions in the Arctic (SLICA) that includes Greenland, Chukotka (Russia) and Alaska, more than two-thirds of the ~1000 respondents indicated having 'some' or 'great' difficulty in making ends meet with major concerns related to food security (Kruse et al., 2008). A survey of the Samoyedic ethnic group in Vaygach Island (Arctic Russia) found that the impacts of climate change are not fully understood by the community though there have been notable changes in their environment (e.g., emergence of new wildlife species, longer growing season) and economic activities which are affecting their cultural identity and traditional lifestyles (Davydov and Mikhailova, 2011).

The dietary transition has been notable in the Faroe Islands. Since the 1980s, there has been a steady decrease in the intake of fish from nearly four meals per week to less than two meals per week (Weihe, pers. comm., 2021). This has largely been driven by the Faroe Islands' increased ability to import food from other countries as well as improved household purchasing power. It is not believed that recommendations from health authorities to reduce or stop whale consumption played a vital role in this transition, although the dietary advice offered (in more recent times) likely enlightened the public about the nutritional value of marine food. As elaborated in the recent AMAP human health assessment (AMAP, 2021), messages warning against eating contaminated whale meat and blubber also included information about fish that were low in contaminants and highly nutritional

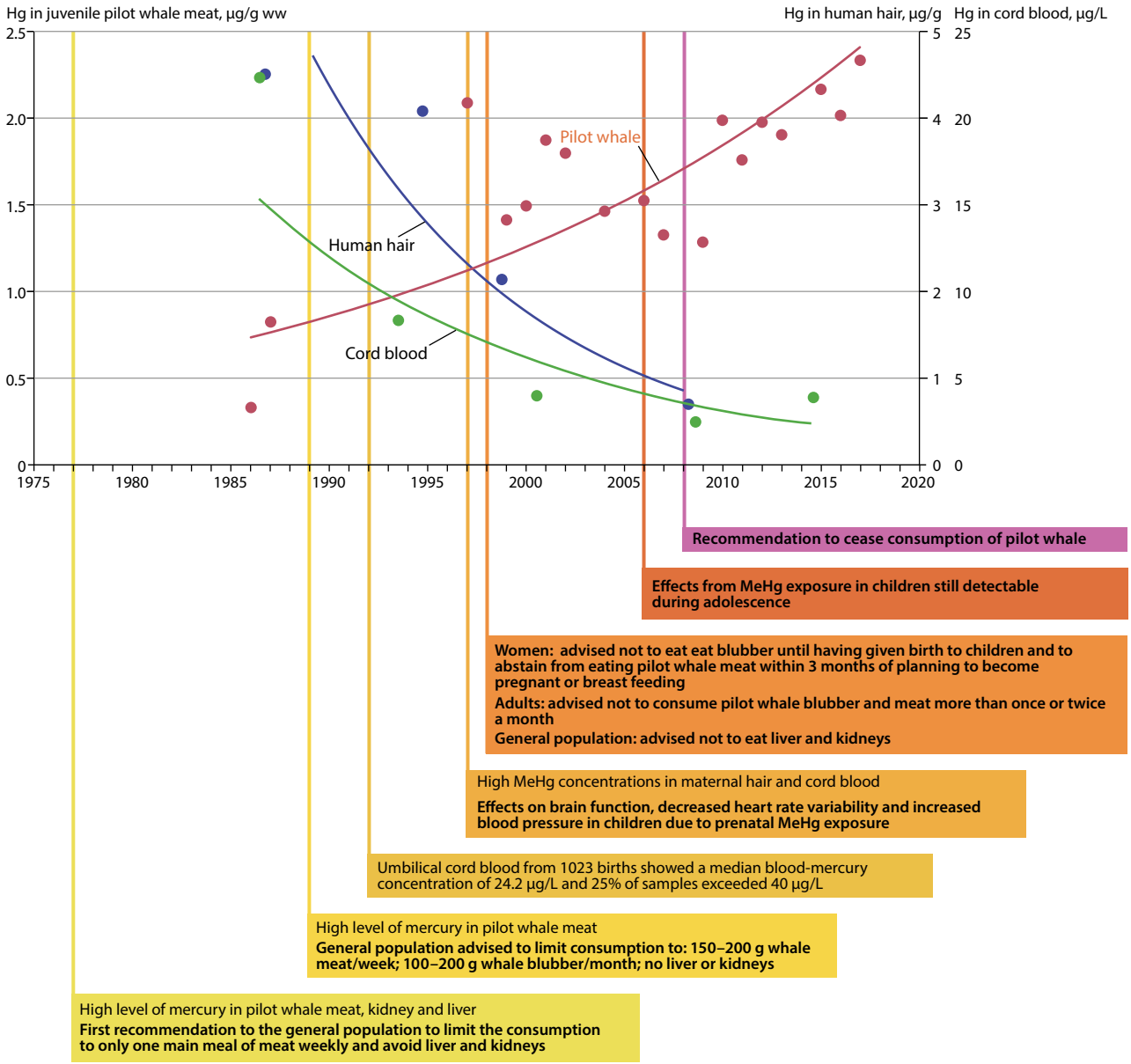

Figure 7.2 Decreasing trend of total Hg levels in hair and cord blood of Faroese study population compared with increasing trend in levels in Faroese juvenile pilot whale meat, and advisories concerning consumption of pilot whale in response to recognition of associated health risks.

(e.g., lean fish like cod and haddock as well as fatty fish like herring, mackerel and salmon; see Figure 7.2). The Faroese Board of Health (Fólkaheilsuráðið) recommends that people eat these fish without any upper limits of weekly servings. The dietary advice to pregnant women has been effective (in terms of helping reduce Hg exposures) as documented in large birth cohort studies: the Hg levels have decreased nearly five-fold from ~1987 to ~2008 (with blood Hg decreasing from 22.3 to 4.6 µg/L) in umbilical cord blood (see Section 2.3.3).

7.3.3 Food Security

Another important dimension is the high prevalence of food security concerns for Arctic Indigenous Peoples. For example, 63% of Inuit in Canada's Arctic are food insecure with 27% being classified as severely food insecure following a cross-sectional study of nearly 2000 households (Huet et al., 2012). Another survey concerning children from 16 Nunavut communities found that 70% lived in homes classified as food insecure with 25% of the homes being severely food insecure (Egeland et al., 2010). A 2013 survey on 523 randomly selected households in Iqaluit (Canada) found that 32.9% of households with children were food insecure and that this was significantly higher than the 23.3% of households without children (Huet et al., 2017). Such food insecurity estimates from the Arctic are much higher than global estimates (e.g., severe food insecurity worldwide averaged 9.2% in 2018; FAO, 2019).

Many publications have dealt with the identification of factor(s) that are important for food insecurity. For example, the Alaskan Inuit Food Security Conceptual Framework published by the Inuit Circumpolar Council in Alaska (ICC-Alaska, 2015a) stipulated that: "*Inuit food security is characterized by environmental health and is made up of six interconnecting dimensions: 1) Availability; 2) Inuit Culture; 3) Decision-Making Power and Management; 4) Health and Wellness; 5) Stability; and 6) Accessibility. This definition holds the understanding that*

without food sovereignty, food security will not exist." While the presence of Hg in certain foods is one factor contributing to food insecurity, several studies have acknowledged the high cost of food, the unavailability of healthy and affordable food choices in local markets, and challenges of hunting and fishing to be the most important factors (Mead et al., 2010; Sharma, 2010). Due to the high price of nutritional, high-quality store-bought foods in Arctic communities, commercial foods there tend to reflect a Western diet in that they consist of food items composed largely of refined carbohydrates and saturated fatty acids with limited nutritional content, vitamins and essential unsaturated fatty acids (Johnson-Down and Egeland, 2010). From an analysis of the 2007–2008 Inuit Health Survey's dietary data (i.e., 93 country foods and 1591 market foods), researchers found that country foods accounted for a majority of the participants' intake of protein, iron, niacin, and key vitamins, while three popular market foods (i.e., sweetened beverages, foods with added sugar and bread) contributed ~20% of the participants' total energy intake and little to no micronutrient intake (Kenny et al., 2018). Such a market diet coupled with a sedentary lifestyle can promote metabolic disorders, which are increasing across Arctic communities, such as diabetes and heart disease (Bjerregaard et al., 2004). This highlights the need for public health professionals to encourage healthy lifestyles, including providing food consumption guidelines that balance the health benefits of traditional diets against the increased health risks associated with the contaminants that a few country foods contain.

7.3.4 Modeling exposures

Dietary Hg exposure is most often estimated by food frequency questionnaires (FFQ) coupled with modelling (Deutch et al., 2006; Curren et al., 2015; Lemire et al., 2015). However, there are notable challenges with this approach. For example, Canuel et al. (2006) re-analyzed a 1992 dataset from Nunavik (Canada) and found that predicted hair Hg values (18.1 μg/g) in Inuit using standard calculations were nearly 5-times higher than the measured value of 3.8 μg/g of Hg in hair. In this paper they concluded that "the relation between Hg oral dose and body burden … may vary among certain ethnic groups" and "metabolic excretion rates might vary according to ethnicity". Therefore, the expected constant and linear relation between MeHg oral dose and body burden, which is used by government officials to establish guidelines on safe levels of MeHg exposure, seems to vary among ethnic groups (Canuel et al., 2006). This variation can result in MeHg levels exceeding the US EPA reference dose and can influence the derivation of a meaningful reference dose for MeHg applicable to all individuals in a population (Rand and Caito, 2019).

Such variability is not surprising. In humans, a hair to blood Hg ratio of 250 is used in risk assessment, but this value can vary widely among populations (means range from 140 to 370) and individuals (with a maximum ratio of >600; Basu et al., 2014; Liberda et al., 2014). In a study of Dene and Métis from Canada's Northwest Territories, the average hair to blood Hg ratio was 450 with a range between 260 and 1100 (AMAP, 2021). The elimination half-life of MeHg in humans is assumed to be 70 days but can vary from 20 to 128 days (Rand and Caito, 2019).

In addition, dietary exposure is routinely estimated by combining data on consumption patterns from surveys with average Hg concentration in specific food items. However, the challenges associated with FFQs are well-established (e.g., recall bias), Hg levels in a particular food item can vary tremendously and dietary habits change throughout the year. For example, seasonal variation in MeHg exposure among pregnant Inuit women (sampled 2016–2017 from Nunavik, Canada) was recently documented with mean hair Hg levels of 1.5 μg/g (range: 0.2–8.1 μg/g) found in the winter months versus 2.9 μg/g (range: 0.2–22.4 μg/g) in the summer months, and these differences aligned with seasonal variability in the consumption of country foods high in Hg (Pontual et al., 2020).

Moving ahead, coupling robust and more detailed survey instruments (to capture pertinent environmental, dietary and demographic information) with toxicokinetic modeling (to capture physiological information) may prove fruitful. The toxicokinetic approach depends on understanding the burden of Hg in different body compartments as well as the transfer coeffcient between different body compartments (Abass et al., 2018). There are several factors determining MeHg body burden. These factors include dietary exposure (e.g., frequency, quantity and MeHg content of fish eaten, seasonality), the individual's absorption, distribution, metabolism and excretion (ADME) kinetics, and the state of pregnancy and overall health.

More expansive exposure models are now being developed for Arctic Indigenous Peoples. For example, there are mechanistic models linking environmental fate and transport with human exposures to environmental contaminants, in particular persistent organic pollutants (POPs), emerging for Inuit (Czub et al., 2008; Undeman et al., 2010; Binnington et al., 2016a, 2016b). In particular for Hg (and nutrients), the ACC-Human Arctic model was developed to calculate daily dietary intake (Binnington et al., 2016a). Using this model, consumption of certain tissues from caribou (i.e., heart, liver, tongue, meat and bone marrow), ringed seal (i.e., liver, meat and blubber), beluga whale/narwhal (i.e., meat and blubber) and Canada goose (*Branta canadensis*; i.e., meat and eggs) for Hg intake was differentiated.

Estimating human Hg exposure through analysis of hunting records may represent an efficient approach for some communities. By gathering information from the Greenlandic Hunting Statistics (1993–2013) for the Avanersuaq, Ittoqqortoormiit, and Nuuk regions, the amount of Hg entering the local diet was estimated (Dietz et al., 2018a, 2018c). The meat consumption of the hunted wildlife was related to average Hg levels in these samples from which Hg intake was estimated. In this case, the provisional tolerable yearly intake (PTYI) of Hg, on average, exceeded 14-fold (range: 8–20-fold) in Avanersuaq, 5-fold (range: 3–8-fold) in the Ittoqqortoormiit region and 0.9-fold (range: 0.4–1.6-fold) in the Nuuk region.

Another approach moving forward is to consider the role that genetic variations have in explaining Hg health risks given that disease outcomes arise from a complex interaction between both genetic and environmental factors, though we tend to focus near-exclusively on the latter (Basu et al., 2014). Specifically, variants in genes that underpin Hg toxicokinetics (i.e., absorption, distribution, metabolism, and elimination of the chemical) may

influence body burdens and biomarker levels, and variants in other genes may mediate or moderate the association between Hg exposures and adverse health outcomes. To date, we are aware of only three studies from the Arctic that characterized Hg exposure in association with genetic variations. In a study of 281 Inuit from the Inuvialuit Settlement Region (Canada) there were 9 single nucleotide polymorphisms in toxicologically relevant genes (of 112 investigated) that helped explain higher or lower blood Hg levels (Parajuli et al., 2018). As an example, carriers of the minor allele version of rs1133238 (*SEPHS2* gene) had blood Hg levels that were approximately 50% higher than people carrying the more common form of the gene. In many cases, the prevalence of these genotypes in Inuit were quite distinct from other ethnic groups. In a study of 896 Inuit adults from Nunavik (Canada), genetic variants in the paraoxonase 1 (*PON1*) gene did not influence blood Hg levels, even though associations were found with plasma *PON1* enzyme activity (Ayotte et al., 2011). Another study from Nunavik involving 665 Inuit adults who participated in the 2004 "*Qanuippitaa?* How are we?" survey examined 140 single nucleotide polymorphisms against biomarker levels of Hg (along with other chemicals including cadmium, lead, DDE, PCB-153, Se and fatty acids), and found that 5 polymorphisms (i.e., rs2274976 in *MTHFR*, s174602 in *FADS2*, rs7115739 and rs74771917 in *FADS3*, and rs713041 in *GPX4*) were associated with significantly different ($p<0.005$) blood Hg levels across genotype groups (Parajuli et al., 2021). Taken together, these studies demonstrate that allelic frequencies in environmentally responsive genes differ between Inuit and other ethnic groups, and that consideration of such genetic data may help explain variations in biomarker levels of Hg (along with variations in other toxicants and nutrients) as well as exposure-biomarker associations. While there are no immediate clinical or public health implications of these findings, consideration of such gene-environment results may help improve the ability to conduct exposure (and ultimately risk) assessments of country foods.

7.4 How do mercury biomarker levels in the Arctic compare to guidelines?

Human exposure to Hg can be assessed through the measurement of Hg concentrations in a number of different biological sample types. Key approaches for Hg biomonitoring have been reviewed by the UN Environment Program and the WHO (UNEP/WHO, 2008), Basu et al. (2018), the WHO (2018), and the European Human Biomonitoring Initiative (HBM4EU, 2019). The most commonly used biomarkers for MeHg exposure are the concentrations of Hg in hair, blood, and cord blood, and their selection can depend on factors such as the potential source of exposure, the chemical form of Hg, and the exposure lifestage. Most of the Hg in hair is MeHg, and once incorporated the Hg remains in the hair. This biomarker can therefore provide an integrated measurement of Hg exposure given that hair grows at approximately 1 cm per month, and thus exposure can be tracked over time by careful sampling. Hair has the advantage that it is easy to collect, store and transport, though we note that in some communities there may be cultural objections to taking hair samples. Mercury measured in whole blood provides information about recent exposures (~1–2 months) to both MeHg and inorganic Hg.

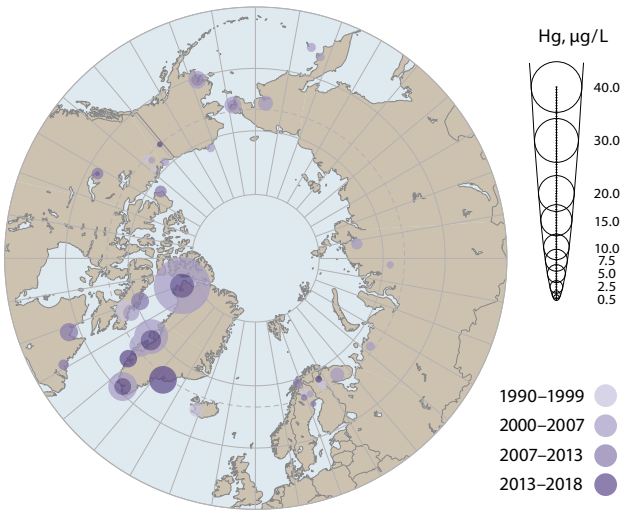

Figure 7.3 Mercury concentrations in blood of mothers, pregnant women and women of child-bearing age in Arctic communities monitored in different periods since the 1990s under the AMAP human health blood monitoring programme, showing generally decreasing levels of mercury, in particular in those communities that exhibited high levels of exposure in the 1990s.

Figure 7.3 summarises blood (total) mercury levels monitored in Arctic communities around the Arctic since the 1990s.

In most communities, the measurement of blood total Hg is an accepted biomarker for MeHg exposure as it correlates relatively well with seafood and marine mammal consumption (Sheehan et al., 2014). The use of speciation can provide an indication of potential Hg sources but requires careful sample preparation and sophisticated instrumentation. The measurement of Hg in cord blood provides information about developmental exposure. However, blood collection, storage and transport pose certain logistical and financial barriers. New approaches, such as dried blood spot sampling, may help overcome some of these challenges and should be considered in future Hg biomonitoring efforts in remote and resource-limited communities such as those in the circumpolar North (Santa-Rios et al., 2020).

As part of the 2018 UN Global Mercury Assessment, a WHO sponsored systematic search of Hg exposures worldwide was performed by reviewing 312 high quality studies (i.e., identified through strict inclusion criteria) published since the year 2000 (Basu et al., 2018). From this, 424 882 Hg biomarker measures from 336 015 individuals from 75 countries was analyzed. The effort concluded that background populations with insignificant exposures to Hg have blood Hg levels that generally fall under 5 µg/L. The analysis clearly showed that Inuit in the Arctic are exposed to some of the highest MeHg levels worldwide. Specifically, data from 15 Arctic sub-populations (7472 individuals) were studied, and the central median blood Hg concentration in these groups was 8.6 µg/L (IQR: 3.6–16.2 µg/L) with an upper bound median concentration of 70.5 µg/L. These blood Hg levels among Inuit communities are among the highest in the world alongside Indigenous Peoples from the Amazonian region or artisanal and small-scale gold miners who have median blood Hg levels of 15.4 and 10.4 µg/L, respectively.

Some of the communities reviewed in 2018 UN Global Mercury Assessment effort were previously discussed in previous AMAP human health assessments (AMAP, 2015, 2021). For example, in Canada as part of the 2007–2008 International Polar Year study of 2172 individuals, the geometric mean of blood Hg across four study regions ranged from 2.8 to 12 µg/L, with individual values ranging from 0.1 to 240 µg/L (AMAP, 2015). In another example, the Inuit Health in Transition study of 3105 participants from all geographic areas and community sizes (9 towns, 13 villages) across Greenland reported blood Hg levels to range from 0.1 to 400 µg/L (AMAP, 2015). The work from the Faroe Islands has demonstrated that cord blood Hg levels (as geometric means) have steadily decreased from 21 µg/L (1994–1995) to 12.4 µg/L (1998–2000) to 4.6 µg/L (2007–2009), although the maximum values across these three periods (102, 193, and 45 µg/L) remain high. Figure 7.4 summarizes the range of Hg levels in whole blood across Arctic communities since the year 2000 with complete details available in Appendix 7.2. These biomarker data were initially identified from the 2018 UN Global Mercury Assessment (Basu et al., 2018) and the recent AMAP Human Health Assessments (AMAP, 2015, 2021) by running the same electronic literature search strategy from the 2018 UN Global Mercury Assessment with the addition of the terms 'Arctic' OR 'Circumpolar' OR 'Inuit' and restricted to the 2018–2020 time frame to yield 59 articles of which 4 were deemed relevant for inclusion here. To help put the data into perspective, key reference or health guidance values are overlaid in Figure 7.4.

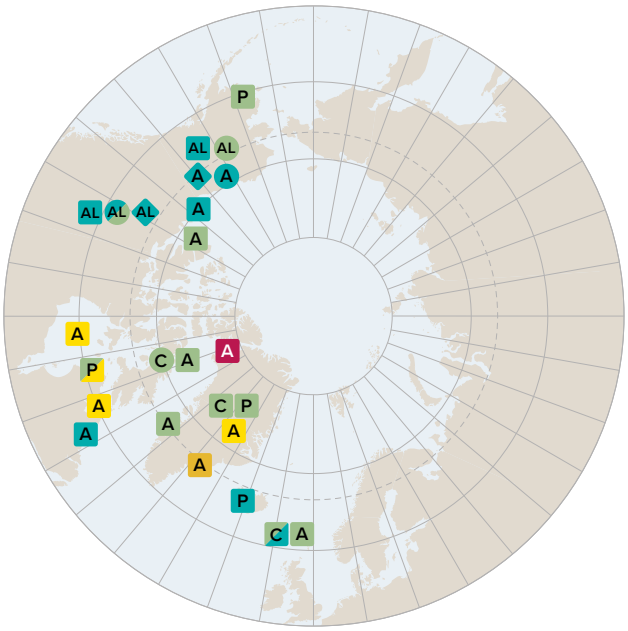

	Blood, µg/L	Hair, µg/g	Urine, µg/L
Background levels (non seafood consumers)	<2	<0.5	<1
Background levels (seafood consumers)	2–8	0.5–2	1–3
Elevated levels	8–20	2–5	3–10
Moderately high levels	20–40	5–10	10–50
High levels	>40	>10	>50

Population: **C** Child **P** Pregnant women **A** Adults **AL** All

Figure 7.4 Total Hg levels (µg/L) in blood, urine and (µg/g) in hair from adults (A), children (C), pregnant women (P) and all (AL), sampled across Arctic populations.

In addition to these data on Hg levels in whole blood, there is emerging data on hair and urine Hg levels from Arctic communities situated in northwest Canada. Measures of Hg in hair, similar to blood, largely reflect exposure to MeHg from the diet of individuals. Based on data from four studies involving 976 children and adults (Tian et al., 2011; Ratelle et al., 2020; Walker et al., 2020a; Drysdale et al., 2021), the median of the average hair Hg levels reported across the studies was 0.53 µg/g, with the median of the upper bound values (either 95th percentile or maximum value) being 2.44 µg/g. These values compare well with hair Hg levels from general background populations worldwide, in which an overall pooled central median Hg concentration was 0.7 µg/g with the upper bound median value being 4.1 µg/g (Basu et al., 2018).

Measures of Hg in urine largely reflect information about an individual's exposure to inorganic and elemental Hg. A study of 198 children and adults from nine Dene communities located in the Dehcho and Sahtú regions (Northwest Territories, Canada) reported a geometric mean of urinary Hg of 0.45 µg/L with a 95% upper value of 1.7 µg/L (Ratelle et al., 2020). A study of 44 adults from a Gwich'in community (Old Crow, Yukon, Canada) reported that 60% of the urinary Hg values fell below the analytical detection limit of 0.2 ug/L and that the 95% upper value measurement was 0.8 µg/L (Drysdale et al., 2021). These values compare well with urine Hg levels from general background populations worldwide, in which an overall pooled central median Hg concentration was 1.0 µg/L with the upper bound median value being 6.1 µg/L (Basu et al., 2018). While these results suggest relatively low exposures to inorganic Hg in the sampled communities, future studies should continue to measure Hg in urine, particularly from communities that may have relatively high inorganic Hg exposures (e.g., those consuming ringed seal liver or kidney).

7.5 What are health effects of mercury in the North?

7.5.1 General health effects

The human health impacts of Hg on Arctic populations remains of worldwide concern as exemplified by the preamble text of the Minamata Convention, which notes "the particular vulnerabilities of Arctic ecosystems and Indigenous communities" and a finding by the 2018 UN Global Mercury Assessment that human communities in the Arctic are among the most highly exposed to Hg worldwide. The health effects of Hg have been reviewed extensively in recent years by scientific experts (Ha et al., 2017; Eagles-Smith et al., 2018). While all forms of Hg have hazard potential, the most relevant form for Arctic communities is methylmercury (MeHg). Over the years, the adverse health effects associated with MeHg exposure have been documented in human populations at successively lower exposure levels, and it is now clear that real-world exposures in many populations to MeHg is sufficient to cause health impairments.

7.5.2 Neurological health effects

Epidemiological cohort studies on Arctic populations have been among the most influential worldwide in terms of demonstrating the link between early-life Hg exposure and later-life adverse health outcomes. For example, cohort studies in the Faroe Islands have demonstrated that children exposed to MeHg *in utero* exhibit decreased motor function, attention span, verbal abilities, memory and other mental functions. Follow-up studies carried out on the same children until they were 22-years-old indicates that these deficits appear to be permanent (Debes et al., 2016). Similarly, a study in Nunavik (Canada) of child development at 11 years old showed that Hg exposure was associated with poorer early processing of visual information, lower estimated IQ, poorer comprehension and perceptual reasoning, poorer memory functions, and increased risk of attention problems and behaviors associated with attention deficit hyperactivity disorder (ADHD; Boucher et al., 2009, 2010, 2011, 2012a, 2012b). While it is widely accepted that susceptibility to Hg exposure is highest during the prenatal period, there remain susceptibilities across multiple life stages. For example, neurophysiological assessments of brain function indicate that postnatal exposure to Hg up to the teenage years can cause harm (Murata et al., 2004). Thus, developing fetuses and children are at increased risk from MeHg exposure.

Some of the adverse effects of MeHg on neurodevelopment may be masked by the beneficial effects of seafood nutrients. For example, Jacobson et al. (2015) estimated the IQ in 282 school-age Inuit children in Arctic Québec from whom umbilical cord blood samples were analyzed for Hg and exposures to other environmental toxicants. They found that prenatal Hg exposure was related to poorer estimated IQ after adjustment for potential confounding variables. The entry of docosahexaenoic acid (DHA) into the model significantly strengthened the association with Hg, supporting the hypothesis that beneficial effects from DHA intake can obscure adverse effects of Hg exposure. Children with cord Hg of ≥7.5 µg/L were four times as likely to have an IQ score of less than 80, the clinical cut-off for borderline intellectual disability. Co-exposure to polychlorinated biphenyls (PCBs) did not alter the association of Hg with IQ. Studies indicate that certain genetic factors may increase vulnerability to MeHg toxicity (Julvez and Grandjean, 2013; Basu et al., 2014).

Although many studies of MeHg toxicity focus on prenatal exposure because fetal brains are developing and thus more vulnerable, the effects of adult exposures have also been documented. A key concern with exposure in adults is that it may accelerate age-related declines (Rice and Barone, 2000). Neurocognitive functions, especially fine-motor function and verbal memory, are compromised among adults who are exposed to elevated amounts of MeHg, which is consistent with the outcomes observed in children with prenatal exposures.

7.5.3 Cardiovascular health effects

An earlier report from the U.S. National Research Council concluded that MeHg accumulates in the heart and leads to blood pressure alterations and abnormal cardiac functions (NRC, 2000). Since then, expert panels, systematic reviews, and meta-analyses have documented sufficient scientific evidence linking MeHg exposures with adverse cardiovascular outcomes (Roman et al., 2011; Genchi et al., 2017; Hu et al., 2018a). Despite this body of evidence, there are some conflicting findings from the Arctic region which have been reviewed in previous AMAP human health assessments (2015, 2021). For example, prenatal Hg exposures were related to elevated blood pressure among 7-year-old Faroese children (Sorensen et al., 1999) but not children from Nunavik (Valera et al., 2012). In adults, elevated blood pressure was found to be associated with Hg exposure in the Faroe Islands among male whale hunters (Choi et al., 2009) and Inuit from Nunavik (Valera et al., 2009), but a relatively large study of Greenlandic Inuit conducted between 2005 and 2010 found no association with whole blood Hg levels and the risk of developing cardiovascular disease (Larsen et al., 2018) or blood pressure (Nielsen et al., 2012b). In a population of older men from eastern Finland, high concentrations of MeHg in blood and tissue samples have been associated with acute coronary events, coronary heart disease and cardiovascular disease (Virtanen et al., 2005).

The challenge in studying the relationship between Hg exposure and adverse cardiovascular outcomes is confounded by the benefits afforded by a traditional diet and the nutrients that this diet contains. For example, a study of 1570 adults from Nunavut who participated in the 2007–2008 Inuit Health Survey found that participants who principally consumed country foods (i.e., those with high fish consumption and low sugar intake) had a lower prevalence of coronary heart disease, myocardial infarction, stroke, and hyperlipidemia in comparison with those who consumed more store-bought food (Hu et al., 2018b). However, the consideration of Hg exposure may confound such findings. The intake of omega-3 fatty acids (EPA and DHA) was estimated to be associated with a reduced relative risk of myocardial infarction among participants in the 2007–2008 Inuit Health Survey, though these potential beneficial associations were lost when Hg exposure was considered in the models (Hu et al., 2017c). An analysis of blood biomarker data from the 2007–2008 Inuit Health Survey found that individuals with low levels of Se and high levels of Hg had a higher prevalence of hypertension, stroke and myocardial infarction, in comparison with participants who had relatively high levels of Se (with either high or low levels of Hg; Hu et al., 2017a).

7.6 What are the risk communication and risk management strategies used to address dietary mercury exposure in the Arctic?

If high contaminant levels are found in Arctic biota forming part of the traditional diet then communication of information about contaminant risks and benefits of the diet is an important and immediate means by which public health officials and clinicians can address potential exposure and help minimize adverse health effects. However, as described in past AMAP human health assessments (e.g., AMAP, 2009, 2015, 2021, and other publications referenced therein), risk communication is not an easy undertaking or a permanent solution to the issue of contaminants in country foods and can only ever be an interim

approach to protecting humans from exposure to contaminants. Risk communication in the form of, for example, public health advisories and clinical counselling also needs to be continuously updated based on the most recent scientific information and exposure data. Ultimately, to address the risks posed by Hg (and other contaminants of concern) in the Arctic appropriately, levels in the environment must be reduced.

This section summarizes the findings on risk communication that are outlined in detail in Chapter 6 of the 2021 AMAP Human Health Assessment (AMAP, 2021). This chapter provides new information on risk communication activities in several Arctic countries. Most of the risk communication information provided concerns fish or other marine biota and is based on Hg levels. In most cases, specific dietary guidelines are available on the internet as part of general nutrition advice. It should be noted that while there are many examples of risk communication with regards to Indigenous Peoples and traditional foods in Canada there is a lack of information on risk communication specifically for Indigenous Peoples in other Arctic countries (e.g., the Sámi).

Reflecting on risk communication activities draws attention to the importance of maintaining trust in the relationships between all involved; it also emphasizes the importance of taking a participatory approach to evaluating and communicating the possible risks associated with contaminants in the traditional diet alongside the benefits afforded by these foods. This is further emphasized by several authors who stress the importance of trust, who note that trust is difficult to build yet easily damaged or destroyed (Wall and Chen, 2018; Boyd et al., 2019). In terms of evaluating the effectiveness of risk communication messaging, Wall and Chen (2018) point out that "*the word 'risk' is naturally negative, and risk communication messages often relate to negative information, which may serve to increase consumers' anxiety and concern about food. […] Moving from the main focus being on 'risk communication' to a broader 'food information communication' might afford the opportunity for more positive messages to receive airtime*." However, in the report by Furgal et al. (2014) a majority of surveyed respondents in Nunavut (Canada) were aware of messages on the benefits of traditional foods, although only a minority had heard of risk messages. It therefore seems that a certain emphasis on health risks or very targeted communication is required to ensure retention of the message. Studies in the Faroe Islands (see Section 7.3.2), and other areas (U.S. and Denmark; Knobeloch et al., 2011; Kirk et al., 2017) found that targeted and personalized messaging was successful in reducing Hg exposure in pregnant women.

Overall, specific data on the effectiveness evaluation of risk communication is still limited to a few Arctic regions (AMAP, 2021). More health communication and risk perception data are important in order to compare results across regions of the circumpolar Arctic. Data from multiple regions would help to determine best practices for researchers and governments, which could then be adapted and tailored for specific geographic regions, contexts, and/or community needs. These data also help to provide the information needed to enable more culturally appropriate and relevant contaminant health messages and consumption notices. For instance, risk communication evaluation data in the Northwest Territories in Canada have provided information on two regions where there is considerable trust in doctors, elders, family and friends, university researchers and other healthcare workers. These trusted sources should be used in combination with the preferred media for disseminating health messages. Evaluating the impact of combinations of medium and messenger for various health messages would help to identify the optimal communication strategies for different communities. A priority for risk communication should be carefully planned communication strategies built in partnership with communities, which promote country food consumption while lowering contaminant exposures to maintain and improve health and wellbeing in Arctic communities. It should be highlighted that equitable partnership approaches in research activities are well suited to address many of the challenges outlined here, especially regarding capacity, resources and trust (Schott et al., 2020). Holistic projects built on a 'co-production of knowledge approach' are a good example, as these bring together different knowledge systems (such as Indigenous Knowledge and science) while building collaborative and equitable partnerships (Behe and Daniel, 2018).

Issues with confusion or fear resulting from the spread of sensationalized or alarmist messages have been found repeatedly. In some cases, this can arise due to problems with receiving audiences of a single message being both local and global (i.e., a message created for a specific target audience is being read by others). This can create misunderstandings (at a minimum), particularly if the different audiences do not share the same culture (Wendling et al., 2013; AMAP, 2015). Additionally, a message that may be perceived as contradicting cultural values is unlikely to be accepted and may be prone to counterarguments and inoculation effects, particularly if the message is delivered with weak argumentation and/or from a non-trusted source.

Social media has emerged as an important means for communicating information across the Arctic, and information that is spread without verification and/or local confirmation can result in misinformation and mistruths, which may lead to overamplification of the risks to public health and thus ultimately create confusion and undermine the confidence of the receivers of the message (Wall and Chen, 2018). Advantages for the use of social media include the unique possibility of interactive, two-way communication, the speed with which messages can be disseminated to a large or selective audience using multiple channels, and better control of the message that is originally disseminated (Wendling et al., 2013; AMAP, 2015; Regan et al., 2016; Wall and Chen, 2018).

7.7 Conclusions and recommendations

Conclusions (in numbered bullets) are organized under section headings (section numbers in square brackets) followed by recommendations in italics where appropriate.

What are the global influences on mercury exposure in the North? [7.2]

1. Mercury levels in some fish and wildlife that represent important components of the diet of northern people are

elevated and of health concern. This Hg originates from anthropogenic activities in southern regions though is transported to the Arctic, where it builds up in food chains. Climate change is expected to alter the flows and amounts of Hg with some scenarios pointing to increased exposures.

2. The Minamata Convention is now in legal force worldwide as a regulatory scheme to reduce the use and environmental release of Hg in order to protect human health and the environment in all regions, including the Arctic. Under the Convention, future reductions in global mercury emissions are expected and this should help to product human health in the Arctic. It is also important to recognize that the Convention was highly influenced by health concerns raised by northern populations as indicated in the Convention's preamble text which makes reference to "the particular vulnerabilities of Arctic ecosystems and Indigenous communities".

With the Minamata Convention now in legal force, evaluating the effectiveness of the convention (as required by Article 22) is critical to ensure that it meets its objectives. A range of short-, medium- and long-term evidence-based metrics to monitor Hg exposures (and risk) in human populations in the Arctic is needed. Once metrics are set, a database (that is easily accessible) must be developed and updated for stakeholders to monitor progress.

Continued and expanded monitoring is needed to increase understanding of key human and fish/wildlife exposure pathways to Hg, especially as the climate changes. Such monitoring is needed for the early identification of exposure situations of concern (e.g., the emergence of geographic hotspots, accelerated Hg biomagnification in food chains).

Models that link Hg fate and transport on global scales into human exposure pathways in specific Arctic communities must advance so that they are more predictive, especially as the climate changes. The models must be designed with communities and stakeholders (e.g., researchers, policy-makers) in mind, and thus be desired, valuable and credible while also being findable, accessible and usable.

What are the dietary influences on mercury exposure? [7.3]

3. The major source of Hg into northern populations is from the consumption of certain fish and marine mammals that are contaminated with Hg. The highest exposures occur among Inuit populations that routinely consume marine mammal tissues.

4. The food items that represent major sources of Hg exposure for northern populations also provide health benefits in that they represent a valuable source of essential nutrients to these populations as well as having cultural value to communities.

5. There is a transition underway in many communities to a more commercial-based diet. This transition is partly driven by the reduced access to or availability of traditional and local foods as well as issues related to food insecurity. While this dietary transition may be associated with reduced exposures to Hg, it may introduce other health problems into the region ranging from reduced intake of essential nutrients to sedentary lifestyles and western diets that promote metabolic health concerns.

6. Variability is an important dimension of gauging true exposures to Hg, and this is necessary to properly balance and assess community risk-benefits. There exists variability in Hg levels within and across food items and geographic sites. There is variability in terms of food items being consumed by community members that may be linked to the source or season. There is variability in how different people process Hg in their bodies, with new scientific information on the role that genetics, Se or bioavailability may play in a person's true exposure to Hg.

Dietary advice provided by regional health authorities needs to be built on the best available knowledge. With a dietary transition underway across Arctic communities, local health authorities need to work with Indigenous communities and stakeholders to increase understanding of the availability of such items and their nutritional value, as well as peoples' food choices and how these may vary across communities and seasons as well as age and sex.

It is established that traditional/local foods (especially those with lower levels of contaminants and high nutritional value) provide benefit to Indigenous Peoples in terms of nutrition, food security and cultural well-being, and thus programs supporting the consumption of these foods need to be evaluated and strengthened so that they can be broadly implemented.

More exposure studies are needed to link total diet surveys with human biomonitoring efforts so that better exposure estimates and dietary advice may be realized. This requires the collection of more data on both contaminants and nutrients from key food items as well as from consumers in more communities, and the publication of a database for making such data accessible to researchers. It also necessitates the development of context-specific exposure models in which variables are built around Indigenous Peoples and northern residents.

Factors that may moderate, mediate or even confound Hg exposures, such as genetic variations, bioavailability factors or Se levels, remain scientifically possible yet may over-simplify understanding (from physiological mechanisms to how such information would influence dietary guidelines). There is limited empirical evidence of these being realized in large population studies and thus more research is needed to understand the potential practical uptake of such knowledge.

How do mercury biomarker levels in the Arctic compare to guidelines? [7.4]

7. It is firmly established that Arctic populations (especially Inuit) are among the highest Hg-exposed group worldwide, with large proportions of individuals having biomarker levels that exceed health guidelines.

Biomonitoring studies of Hg exposure as well as total dietary surveys are needed to characterize exposures and trends, as well as track the effectiveness of actions (from local to international) to reduce exposures. To date, these efforts have proven important and influential though they remain prohibitively costly and inefficient, and thus new strategies and innovations are needed that harness breakthroughs in, for example, mobile phone apps to record data

or dried blood spot sampling to enable biomarker studies. The development of a more effective surveillance system is needed.

Community-based biomonitoring programs may now be realized with a focus on non-invasive biomarkers of Hg exposure (e.g., hair, urine) as well as new equipment designed for use in remote sites (e.g., field-based direct Hg analyzers). Such programs could empower locals, reduce the delay between sampling and reporting of results, and enable rapid decision making.

Guidelines are largely based on data from populations far removed from the Arctic, and thus there is a need to realize guidelines specific to Arctic communities because of differences in sociodemographic characteristics, lifestyle and dietary factors, and genetics and physiology.

What are the health effects of mercury in the North? [7.5]

8. It is established that Hg exposures at current levels among Arctic Indigenous Peoples are high enough to have adverse impacts on health, and that these are realized across life stages, from adverse neurodevelopmental outcomes in young children to cardiovascular disease in adults.

Further research on the classical health impacts of MeHg will deepen understanding with key knowledge gaps being the extent to which postnatal exposures (along the life course) contribute to neurobehavioral delays and cardiovascular disease being unclear, as well as the subtle effects associated with chronic lower-level exposures. These studies need to include detailed information on potential beneficial nutrients, fatty acids and Se, so that epidemiological models can be properly derived from such information.

The characterization of the health impacts of Hg on other physiological systems (e.g., immune function), and the potential for trans-generational effects are not well understood. Moreover, the interactions between Hg and other contaminants such POPs or non-chemical stressors (e.g., malnutrition, psychosocial stress, infectious diseases) are not fully known, even though these are common scenarios. The true burden of disease associated with Hg exposure in the Arctic is not known.

What are the risk communication and risk management strategies used to address dietary mercury exposure in the Arctic? [7.6]

9. Contaminant-related, dietary advisories in the Arctic are mainly based on the presence of Hg in key food items and largely limited to a few regions in Canada (and some other countries). Risk communication of these advisories needs to be well balanced and should take into account the nutritional as well as cultural benefits associated with consuming traditional country foods.

10. Targeted, regular, clear communication along with timely and personalized messaging is the most effective means of helping to ensure retention of messages. Sensationalized and alarmist messages that contradict cultural values of local audiences can result in confusion, fear or inoculation effects, and thus can threaten the success of future communication. Social media, when properly managed, may be a useful tool in risk communication.

11. Successful risk communication can only be developed if there is full partnership and open communication with those who are affected (i.e., between individuals, communities and/or regions), and communication efforts need to involve regional health authorities and local clinicians (e.g., nurses, physicians and Indigenous midwives). In such activities, relationships of trust among all involved parties (particularly between communicators and recipients of the messages) are crucial for the success of the communication. This trust is difficult to build and very easily damaged or destroyed.

12. Communication of contaminant risk is a complex undertaking and not a sustainable solution to ensure reduced exposures in target populations. It is thus crucial that regulations to lower contaminants in the environment are implemented effectively.

Risk messaging needs to be expanded across the Arctic as relatively few regions or communities have risk communication programs. These need to be developed with members of the affected population and ideally created by a diverse group with the necessary expertise and knowledge. Risk communication must be culturally appropriate, needs to be customized to the intended audience(s), and developed as a series of communication events using multiple channels; there is no one-size-fits-all approach. Relationships of trust between all involved are paramount.

Information needs to be provided in an open, transparent and timely manner, and it must be honest, accurate, consistent and understandable. Messages should be offered in non-scientific language, and as far as it is possible and where necessary, Indigenous languages should be used.

Specific data gathering efforts on the effectiveness evaluation of risk communication activities needs to be more broadly implemented, as, at present, data are limited to a few regions (within Canada and elsewhere) and with only Sweden providing national-level information. Focused dietary advice coupled with hair Hg analysis has been found to be successful for targeted vulnerable groups, such as pregnant women, but this practice is limited in scope. More health communication and risk perception data are necessary to compare results across settings, regions and countries, from which a deeper understanding on best practices may be realized.

Institutional capacity needs to be built to allow for sustained, regional expertise on technical and socio-cultural relevance. Ideally, this expertise would be situated in a permanent body that can store information and can readily provide advice for communities, health workers and researchers.

Appendix 7

Table A7.1 Summary table of mercury concentrations (µg/g ww) in food items that tend to drive human exposures in Arctic communities. All data are from animals harvested since the year 2000, except for the two muktuk samples in which earlier data needed to be accessed given the lack of recent information.

	Tissue	Year(s)	Sample size	Central value	Min	Max	In Ch. 6?	Reference
Ringed seal								
Arctic Bay	Liver	2000–2009	18	2.03	0.24	8.4	Y	Muir and Houde, pers. comm., 2021
Arctic Bay	Liver	2000–2009	41	7.16	1.68	58	Y	Muir and Houde, pers. comm., 2021
Arviat W. Hudson Bay	Liver	2003–2017	70	15.7	0.16	254.86	Y	Muir and Houde, pers. comm., 2021
Arviat W. Hudson Bay	Liver	2003–2017	89	10.4	0.07	79.69	Y	Muir and Houde, pers. comm., 2021
Arviat W. Hudson Bay	Liver	2003–2017	86	3.84	0.29	54.09	Y	Muir and Houde, pers. comm., 2021
Gjoa Haven	Liver	2004–2009	14	0.85	0.176	25.7	Y	Muir and Houde, pers. comm., 2021
Gjoa Haven	Liver	2004–2009	17	8.45	0.201	40	Y	Muir and Houde, pers. comm., 2021
Grise Fjord	Liver	2003–2008	16	0.95	0.351	19.8	Y	Muir and Houde, pers. comm., 2021
Grise Fjord	Liver	2003–2008	34	15.74	0.24	87	Y	Muir and Houde, pers. comm., 2021
Inukjuaq	Liver	2002–2007	15	1.05	0.308	4.5	Y	Muir and Houde, pers. comm., 2021
Inukjuaq	Liver	2002–2007	22	4.73	0.931	60	Y	Muir and Houde, pers. comm., 2021
Kangiqsualujjuaq	Liver	2002	4	4.82	1.516	7.8	Y	Muir and Houde, pers. comm., 2021
Kangiqsujuaq	Liver	2002	5	0.92	0.367	2	Y	Muir and Houde, pers. comm., 2021
Kangiqsujuaq	Liver	2002	4	1.68	0.616	4.1	Y	Muir and Houde, pers. comm., 2021
Nain, S. Labrador Sea	Liver	2005–2016	32	4.66	0.553	40.6	Y	Muir and Houde, pers. comm., 2021
Pangnirtung	Liver	2002–2011	24	2.32	0.156	15.8	Y	Muir and Houde, pers. comm., 2021
Pangnirtung	Liver	2002–2011	24	2.41	0.265	31.5	Y	Muir and Houde, pers. comm., 2021
Pond Inlet	Liver	2000–2009	29	1.44	0.314	69.8	Y	Muir and Houde, pers. comm., 2021
Pond Inlet	Liver	2004–2009	20	5.36	0.434	34.3	Y	Muir and Houde, pers. comm., 2021
Qikiqtarjuaq	Liver	2005	6	3.98	3.02	5.2	Y	Muir and Houde, pers. comm., 2021
Qikiqtarjuaq	Liver	2005	14	8.89	3.89	45.4	Y	Muir and Houde, pers. comm., 2021
Quartaq	Liver	2002	6	5.35	3.274	26.7	Y	Muir and Houde, pers. comm., 2021
Resolute	Liver	2000–2017	51	11.1	0.47	228	Y	Muir and Houde, pers. comm., 2021
Resolute	Liver	2000–2017	97	7.42	0.61	96.4	Y	Muir and Houde, pers. comm., 2021
Resolute	Liver	2000–2017	83	3.19	0.14	23.4	Y	Muir and Houde, pers. comm., 2021
Sachs Harbour	Liver	2001–2017	52	35.55	0.62	320.31	Y	Muir and Houde, pers. comm., 2021
Eastern Beaufort Sea	Liver	2001–2017	51	36.02	0.45	145.93	Y	Muir and Houde, pers. comm., 2021
Eastern Beaufort Sea	Liver	2001–2017	59	1.65	0.34	117.68	Y	Muir and Houde, pers. comm., 2021
Ittoqqortoormiit	Liver	2000–2018	40	10.08	1.02	38.55	Y	Rigét and co-workers, pers. comm., 2021
Ittoqqortoormiit	Liver	2000–2018	57	8.51	1.95	37.18	Y	Rigét and co-workers, pers. comm., 2021
Ittoqqortoormiit	Liver	2000–2018	139	4.54	0.08	20.6	Y	Rigét and co-workers, pers. comm., 2021
Qaanaaq	Liver	2004–2018	140	2.66	0.2	23.2	Y	Rigét and co-workers, pers. comm., 2021
Qaanaaq	Liver	2004–2018	11	7.87	1.41	39	Y	Rigét and co-workers, pers. comm., 2021
Qaanaaq	Liver	2006–2018	10	3.04	2.07	12.5	Y	Rigét and co-workers, pers. comm., 2021
Qeqertarsuaq	Liver	2000–2015	203	1	0	8	Y	Rigét and co-workers, pers. comm., 2021
Gulf of Bothnia	Liver	2017–2018	20	29.18	3.06	82.08	Y	Dietz et al., 2021
Gulf of Bothnia	Liver	2017–2018	20	22.68	4.51	110.21	Y	Dietz et al., 2021
Gulf of Bothnia	Liver	2017–2018	19	6.56	0.51	20.62	Y	Dietz et al., 2021
Sachs Harbour	Muscle	2001	22	0.5			N	Houde et al., 2020 (Supp. Mat. 1)[a]

	Tissue	Year(s)	Sample size	Central value	Min	Max	In Ch. 6?	Reference
Sachs Harbour	Muscle	2005	24	0.57			N	Houde et al., 2020 (Supp. Mat. 1)[a]
Sachs Harbour	Muscle	2006	19	0.89			N	Houde et al., 2020 (Supp. Mat. 1)[a]
Sachs Harbour	Muscle	2007	25	0.76			N	Houde et al., 2020 (Supp. Mat. 1)[a]
Sachs Harbour	Muscle	2010	4	0.37			N	Houde et al., 2020 (Supp. Mat. 1)[a]
Sachs Harbour	Muscle	2011	11	0.4			N	Houde et al., 2020 (Supp. Mat. 1)[a]
Sachs Harbour	Muscle	2012	25	0.56			N	Houde et al., 2020 (Supp. Mat. 1)[a]
Sachs Harbour	Muscle	2013	25	0.44			N	Houde et al., 2020 (Supp. Mat. 1)[a]
Sachs Harbour	Muscle	2014	7	0.31			N	Houde et al., 2020 (Supp. Mat. 1)[a]
Sachs Harbour	Muscle	2015	17	0.48			N	Houde et al., 2020 (Supp. Mat. 1)[a]
Sachs Harbour	Muscle	2016	22	0.32			N	Houde et al., 2020 (Supp. Mat. 1)[a]
Sachs Harbour	Muscle	2017	15	0.23			N	Houde et al., 2020 (Supp. Mat. 1)[a]
Ulukhaktok	Muscle	2002	22	0.45			N	Houde et al., 2020 (Supp. Mat. 1)[a]
Ulukhaktok	Muscle	2007	19	0.57			N	Houde et al., 2020 (Supp. Mat. 1)[a]
Ulukhaktok	Muscle	2010	20	0.52			N	Houde et al., 2020 (Supp. Mat. 1)[a]
Arviat	Muscle	2003	25	0.75			N	Houde et al., 2020 (Supp. Mat. 1)[a]
Arviat	Muscle	2005	25	0.52			N	Houde et al., 2020 (Supp. Mat. 1)[a]
Arviat	Muscle	2006	22	0.39			N	Houde et al., 2020 (Supp. Mat. 1)[a]
Arviat	Muscle	2007	20	0.24			N	Houde et al., 2020 (Supp. Mat. 1)[a]
Arviat	Muscle	2008	26	0.3			N	Houde et al., 2020 (Supp. Mat. 1)[a]
Arviat	Muscle	2009	24	0.4			N	Houde et al., 2020 (Supp. Mat. 1)[a]
Arviat	Muscle	2010	25	0.5			N	Houde et al., 2020 (Supp. Mat. 1)[a]
Arviat	Muscle	2011	28	0.23			N	Houde et al., 2020 (Supp. Mat. 1)[a]
Arviat	Muscle	2012	27	0.31			N	Houde et al., 2020 (Supp. Mat. 1)[a]
Arviat	Muscle	2014	40	0.2			N	Houde et al., 2020 (Supp. Mat. 1)[a]
Arviat	Muscle	2015	25	0.34			N	Houde et al., 2020 (Supp. Mat. 1)[a]
Arviat	Muscle	2016	14	0.37			N	Houde et al., 2020 (Supp. Mat. 1)[a]
Arviat	Muscle	2017	38	0.21			N	Houde et al., 2020 (Supp. Mat. 1)[a]
Inukjuaq	Muscle	2007	18	0.14			N	Houde et al., 2020 (Supp. Mat. 1)[a]
Arctic Bay	Muscle	2004	24	0.64			N	Houde et al., 2020 (Supp. Mat. 1)[a]
Arctic Bay	Muscle	2009	19	0.31			N	Houde et al., 2020 (Supp. Mat. 1)[a]
Grise Fjord	Muscle	2003	21	0.42			N	Houde et al., 2020 (Supp. Mat. 1)[a]
Grise Fjord	Muscle	2008	20	0.13			N	Houde et al., 2020 (Supp. Mat. 1)[a]
Pond Inlet	Muscle	2004	24	0			N	Houde et al., 2020 (Supp. Mat. 1)[a]
Pond Inlet	Muscle	2009	16	0.29			N	Houde et al., 2020 (Supp. Mat. 1)[a]
Resolute Bay	Muscle	2005	15	0.69			N	Houde et al., 2020 (Supp. Mat. 1)[a]
Resolute Bay	Muscle	2006	21	0.57			N	Houde et al., 2020 (Supp. Mat. 1)[a]
Resolute Bay	Muscle	2007	20	0.59			N	Houde et al., 2020 (Supp. Mat. 1)[a]
Resolute Bay	Muscle	2008	20	0.53			N	Houde et al., 2020 (Supp. Mat. 1)[a]
Resolute Bay	Muscle	2009	21	0.36			N	Houde et al., 2020 (Supp. Mat. 1)[a]
Resolute Bay	Muscle	2010	15	0.69			N	Houde et al., 2020 (Supp. Mat. 1)[a]
Resolute Bay	Muscle	2011	16	0.34			N	Houde et al., 2020 (Supp. Mat. 1)[a]

Table A7.1 continued

	Tissue	Year(s)	Sample size	Central value	Min	Max	In Ch. 6?	Reference
Resolute Bay	Muscle	2012	24	0.42			N	Houde et al., 2020 (Supp. Mat. 1)[a]
Resolute Bay	Muscle	2013	18	0.48			N	Houde et al., 2020 (Supp. Mat. 1)[a]
Resolute Bay	Muscle	2014	15	0.39			N	Houde et al., 2020 (Supp. Mat. 1)[a]
Resolute Bay	Muscle	2015	18	0.47			N	Houde et al., 2020 (Supp. Mat. 1)[a]
Resolute Bay	Muscle	2016	13	0.62			N	Houde et al., 2020 (Supp. Mat. 1)[a]
Resolute Bay	Muscle	2017	10	0.51			N	Houde et al., 2020 (Supp. Mat. 1)[a]
Gjoa Haven	Muscle	2004	16	0.37			N	Houde et al., 2020 (Supp. Mat. 1)[a]
Gjoa Haven	Muscle	2008	6	0.05			N	Houde et al., 2020 (Supp. Mat. 1)[a]
Gjoa Haven	Muscle	2009	15	0.31			N	Houde et al., 2020 (Supp. Mat. 1)[a]
Pangnirtung	Muscle	2002	80	0.25			N	Houde et al., 2020 (Supp. Mat. 1)[a]
Pangnirtung	Muscle	2006	25	0.25			N	Houde et al., 2020 (Supp. Mat. 1)[a]
Pangnirtung	Muscle	2008	6	0.17			N	Houde et al., 2020 (Supp. Mat. 1)[a]
Pangnirtung	Muscle	2009	6	0.2			N	Houde et al., 2020 (Supp. Mat. 1)[a]
Pangnirtung	Muscle	2010	6	0.31			N	Houde et al., 2020 (Supp. Mat. 1)[a]
Pangnirtung	Muscle	2011	14	0.25			N	Houde et al., 2020 (Supp. Mat. 1)[a]
Qikiqtarjuaq	Muscle	2005	20	0.49			N	Houde et al., 2020 (Supp. Mat. 1)[a]
Nain	Muscle	2005	25	0.19			N	Houde et al., 2020 (Supp. Mat. 1)[a]
Nain	Muscle	2006	5	0.2			N	Houde et al., 2020 (Supp. Mat. 1)[a]
Nain	Muscle	2012	14	0.22			N	Houde et al., 2020 (Supp. Mat. 1)[a]
Nain	Muscle	2013	11	0.15			N	Houde et al., 2020 (Supp. Mat. 1)[a]
Nain	Muscle	2014	5	0.17			N	Houde et al., 2020 (Supp. Mat. 1)[a]
Nain	Muscle	2015	9	0.096			N	Houde et al., 2020 (Supp. Mat. 1)[a]
Nain	Muscle	2016	15	0.1			N	Houde et al., 2020 (Supp. Mat. 1)[a]
Nain	Muscle	2017	17	0.16			N	Houde et al., 2020 (Supp. Mat. 1)[a]
Beluga								
Nunavik	Muktuk	2011	16	0.38	0.21	1.29	N	Kwan, 2011 (Table S2) in Lemire et al., 2015[b]
Mackenzie Delta	Muktuk	1996–2002	20	0.93	0.3	1.73	N	Kinghorn et al., 2008[c]
Beaufort Sea	Muktuk	1993	27	0.84	0.19	1.9	N	Wageman & Kozlowska, 2005[d]
Mackenzie Delta	Muktuk	2001	24	0.77	0.28	1.58	N	Lockhart et al., 2005[e]
Mackenzie Delta	Muktuk	2002	23	0.57	0.3	1	N	Lockhart et al., 2005[e]
Narwhal								
E. Canadian Arctic - Repulse Bay & Frobisher Bay	Muktuk	1993	20	0.59	0.32	0.85	N	Wageman & Kozlowska 2005[d]
Arctic char (non-anadromous)								
Resolute Lake	Muscle	2000–2018	272	0.15	0.06	0.53	Y	Muir and Hudelson, pers. comm., 2021
Á Mýrunum	Muscle	2000–2014	197	0.233	0.1	0.667	Y	Andreasen, pers. comm., 2021
Char Lake	Muscle	2000–2018	85	0.42	0.08	1.03	Y	Muir and Hudelson, pers. comm., 2021
North Lake	Muscle	2000–2018	181	0.21	0.08	1.38	Y	Muir and Hudelson, pers. comm., 2021
Heintzelman Lake	Muscle	2001	119	0.106	0.032	0.316	Y	van der Velden et al., 2012
Sapphire Lake	Muscle	2001	9	0.364	0.161	1.07	Y	Muir et al., 2005
Lake Hazen	Muscle	2000–2018	314	0.126	0.017	1.63	Y	Muir and Hudelson, pers. comm., 2021
Amituk Lake	Muscle	2000–2018	144	1.14	0.1	3.87	Y	Muir and Hudelson, pers. comm., 2021
Iqalugaarjuit Lake	Muscle	2004	20	0.1065	0.065	0.299	Y	van der Velden et al., 2013a, 2013b
Isortoq	Muscle	2004–2018	123	0.846	0.171	3.559	Y	Rigét and co-workers, pers. comm., 2021

	Tissue	Year(s)	Sample size	Central value	Min	Max	In Ch. 6?	Reference
Roberts Lake	Muscle	2006	34	0.0125	0.007	0.036	Y	Swanson and Kidd, 2010
Hovaktok Lake	Muscle	2006	7	0.049	0.02	0.08	Y	Swanson and Kidd, 2010
Lake 10	Muscle	2006	7	0.047	0.026	0.082	Y	Barst et al., 2019
Nauyuk Lake	Muscle	2006	18	0.0445	0.02	0.161	Y	Swanson and Kidd, 2010
12-Mile Lake	Muscle	2006	10	0.1355	0.095	0.198	Y	Gantner et al., 2010a, 2010b
Little Nauyuk	Muscle	2006	10	0.1135	0.072	0.222	Y	Gantner et al., 2010a, 2010b
Lake 32	Muscle	2006	12	0.077	0.023	0.23	Y	Barst et al., 2019
Keyhole Lake	Muscle	2006	7	0.103	0.025	0.273	Y	Swanson et al., 2011
Notgordie Lake	Muscle	2006	5	0.19	0.15	0.343	Y	Swanson et al., 2011
Gavia Faeces	Muscle	2006	8	0.079	0.045	0.507	Y	Swanson et al., 2011
Coady's Pond	Muscle	2007	10	0.1	0.07	0.12	Y	Gantner et al., 2010a, 2010b
Tasialuk (Ayr Lake)	Muscle	2007	10	0.13	0.08	0.17	Y	Gantner et al., 2010a, 2010b
Coady's Pond #2	Muscle	2007	20	0.1165	0.058	0.212	Y	van der Velden et al., 2013a, 2013b
Upper Nakvak Lake	Muscle	2007	20	0.0695	0.028	0.491	Y	van der Velden et al., 2015
East Lake	Muscle	2008	17	0.095	0.045	0.285	Y	Barst et al., 2019
West Lake	Muscle	2008	26	0.16	0.054	0.444	Y	Barst et al., 2019
Esker Lake	Muscle	2008	20	0.0655	0.039	0.864	Y	van der Velden et al., 2015
Tasiapik Lake	Muscle	2009–2010	31	0.099	0.059	0.263	Y	van der Velden et al., 2013a, 2013b
Tasiapik Lake	Muscle	2009–2010	31	0.099	0.059	0.263	Y	van der Velden et al., 2013a, 2013b
Unnamed Lake	Muscle	2010	18	0.1865	0.077	0.422	Y	van der Velden et al., 2013a, 2013b
Crazy Lake	Muscle	2010	47	0.06	0.03	1.033	Y	van der Velden et al., 2013a, 2013b
Small Lake	Muscle	2011–2012	30	0.09	0.04	0.19	Y	Barst et al., 2016
9-Mile Lake	Muscle	2011–2012	30	0.121	0.058	0.394	Y	Barst et al., 2016
Boomerang Lake	Muscle	2012	15	0.141	0.088	0.543	Y	Barst et al., 2019
Aquiatusuk Lake	Muscle	2011, 2016	15	0.593	0.156	1.031	Y	Barst et al., 2019
Bjørnøya	Muscle	2001–2015	178	0.125	0.026	0.830	Y	Poste, Evenset, Blevin, pers. comm., 2021
Faroe Islands	Muscle	2001–2014	169	0.243	0.12	0.667	Y	ICES Data Centre, 2020
Greenland Sea	Muscle	2004–2018	45	0.708	0.171	3.559	Y	ICES Data Centre, 2020
Queen Maud Gulf	Muscle	2004–2018	155	0.057	0.014	0.36	Y	Evans, pers. comm., 2021

[a] https://doi.org/10.1002/etc.4865
[b] http://dx.doi.org/10.1016/j.scitotenv.2014.07.102
[c] http://dx.doi.org/10.1016/j.scitotenv.2008.04.031
[d] doi:10.1016/j.scitotenv.2004.06.028
[e] doi:10.1016/j.scitotenv.2005.01.050

Table A7.2 Summary table of mercury human biomonitoring data from Arctic communities between the years 2000 and 2020. Central and upper measures of mercury levels in whole blood (µg/L), hair (µg/g), urine (µg/L) are provided. These biomarker data were initially identified from the 2018 UN Global Mercury Assessment report (Basu et al., 2018) and the AMAP Human Health Report (AMAP, 2015), and then updated (December 9, 2020) by running the same electronic literature search strategy from the 2018 UN Global Mercury Assessment with the addition of the terms 'Arctic' OR 'Circumpolar' OR 'Inuit' and restricted to the 2018–2020 time frame to yield 59 articles of which 4 were deemed relevant for inclusion here.

Mercury biomarker	Lifestage	Study type	Country	Study location	Year range	Sample size
Whole Blood	Adult	Birth cohort	Denmark	Faroe Islands	2008–2009	849
	Adult	Birth cohort	Denmark	Faroe Islands	2013–2016	703
	Adult	Cross-sectional	Greenland	Various areas	2005–2010	2640
	Adult	Cross-sectional	Greenland	Tasiilaq	2000–2001	92
	Adult	Cross-sectional	Greenland	Sisimiut	2002–2003	94
	Adult	Cross-sectional	Greenland	Various areas	2002–2004	194
	Adult	Cross-sectional	Greenland	Qaanaaq	2003	79
	Adult	Cross-sectional	Canada	Nunavik (Hudson Bay)	2004	497
	Adult	Cross-sectional	Canada	Nunavik (Ungava Bay)	2004	420
	Adult	Cross-sectional	Canada	Nunavut (Baffin)	2005–2007	100
	Adult	Cross-sectional	Canada	Northwest Territories (Inuvik)	2005–2006	52
	Adult	Cross-sectional	Canada	Inuvialuit Settlement Region	2007–2008	74
	Adult	Cross-sectional	Canada	Nunatsiavut	2007–2008	60
	Adult	Cross-sectional	Canada	Nunavut	2007–2008	491
	All	Cross-sectional	Canada	Yukon (Old Crow)	2019	54
	All	Cross-sectional	Canada	Northwest Territories (Dehcho and Sahtu)	2016–2018	276
	Children	Birth cohort	Denmark	Faroe Islands	2000–2001	792
	Children	Birth cohort	Denmark	Faroe Islands	2001–2002	158
	Children	Birth cohort	Denmark	Faroe Islands	2002–2005	555
	Children	Birth cohort	Denmark	Faroe Islands	2005–2007	498
	Children	Birth cohort	Denmark	Faroe Islands	2007–2009	500
	Children	Birth cohort	Denmark	Faroe Islands	2009–2011	363
	Children	Birth cohort	Denmark	Faroe Islands	2012–2014	349
	Children	Birth cohort	Denmark	Faroe Islands	2016–2018	390
	Children	Cross-sectional	Greenland	Various areas	2012–2015	333
	Pregnant women	Cross-sectional	Greenland	Various areas	2010–2015	509
	Pregnant women	Cross-sectional	Iceland	Reykjavik	2014–2015	50
	Pregnant women	Cross-sectional	Canada	Nunavik	2000	29
	Pregnant women	Cross-sectional	Canada	Nunavik	2001	19
	Pregnant women	Cross-sectional	Canada	Nunavik	2004	31
	Pregnant women	Cross-sectional	Canada	Nunavik	2007	42
	Pregnant women	Cross-sectional	Canada	Nunavik	2012	111
	Pregnant women	Cross-sectional	Canada	Nunavik	2013	95
	Pregnant women	Cross-sectional	USA	Bethel, Alaska	2004–2006	164
	Pregnant women	Cross-sectional	USA	Bethel, Alaska	2009–2012	144
Hair	Children	Cross-sectional	Canada	Nunavut	2007–2008	361
	All	Cross-sectional	Canada	Northwest Territories (Dehcho and Sahtu)	2016–2018	443
	All	Cross-sectional	Canada	NWT and Yukon	2016	101
	Adult	Cross-sectional	Canada	Yukon (Old Crow)	2019	71
Urine	All	Cross-sectional	Canada	Northwest Territories (Dehcho and Sahtu)	2016–2018	198
	Adult	Cross-sectional	Canada	Yukon (Old Crow)	2019	44

Central measure	Upper measure	Reference	URL link
2.5	45.3	AMAP, 2015	https://www.amap.no/documents/doc/1346
3.93	84.4	AMAP, 2021	https://www.amap.no/documents/doc/3593
16.4	36	Jeppesen et al., 2015	10.1016/j.envres.2015.10.013
24.8	155	Deutch et al., 2006	10.1016/j.scitotenv.2006.07.015
7.3	33	Deutch et al., 2006	10.1016/j.scitotenv.2006.07.015
9.2	386	Mocevic et al., 2013	10.1038/aja.2012.121
51.9	240	Deutch et al., 2006	10.1016/j.scitotenv.2006.07.015
11.7	240	Fontaine et al., 2008	10.1186/1476-069X-7-25
8.6	104	Fontaine et al., 2008	10.1186/1476-069X-7-25
4.1	28	Curren et al., 2015	10.1016/j.scitotenv.2015.04.079
1.1	14	Curren et al., 2015	10.1016/j.scitotenv.2015.04.079
2.1	39	AMAP, 2015	https://www.amap.no/documents/doc/1346
1.7	25	AMAP, 2015	https://www.amap.no/documents/doc/1346
5	52	AMAP, 2015	https://www.amap.no/documents/doc/1346
0.76	4.3	Drysdale et al., 2021	10.1016/j.scitotenv.2020.143339
<LOD	4.8	Ratelle et al., 2020	10.1016/j.envres.2020.110008
4.1	39.8	AMAP, 2015	https://www.amap.no/documents/doc/1346
3.2	22.1	AMAP, 2015	https://www.amap.no/documents/doc/1346
2.6	36.5	AMAP, 2015	https://www.amap.no/documents/doc/1346
2	58	AMAP, 2015	https://www.amap.no/documents/doc/1346
4.6	44.5	AMAP, 2015	https://www.amap.no/documents/doc/1346
1.4	21.3	AMAP, 2015	https://www.amap.no/documents/doc/1346
2.52	40.9	AMAP, 2021	https://www.amap.no/documents/doc/3593
1.4	41.8	AMAP, 2021	https://www.amap.no/documents/doc/3593
3.4	98.93	AMAP, 2021	https://www.amap.no/documents/doc/3593
5.7	73	AMAP, 2021	https://www.amap.no/documents/doc/3593
1.29	3.61	AMAP, 2021	https://www.amap.no/documents/doc/3593
9	38	AMAP, 2021	https://www.amap.no/documents/doc/3593
9.9	33	AMAP, 2021	https://www.amap.no/documents/doc/3593
7.6	30	AMAP, 2021	https://www.amap.no/documents/doc/3593
4	24	AMAP, 2021	https://www.amap.no/documents/doc/3593
5	40	AMAP, 2021	https://www.amap.no/documents/doc/3593
5.2	32	AMAP, 2021	https://www.amap.no/documents/doc/3593
3.41	NR	Mosites et al., 2020	https://doi.org/10.1080/22423982.2020.1726256
2.63	NR	Mosites et al., 2020	https://doi.org/10.1080/22423982.2020.1726256
0.74	5.2	Tian et al., 2011	10.1016/j.envint.2010.05.017
0.47	2.8	Ratelle et al., 2020	10.1016/j.envres.2020.110008
0.6	2.07	Walker et al., 2020a	https://bmcpublichealth.biomedcentral.com/articles/10.1186/s12889-020-09133-2
0.31	1.3	Drysdale et al., 2021	10.1016/j.scitotenv.2020.143339
0.45	1.7	Ratelle et al., 2020	10.1016/j.envres.2020.110008
<LOD (0.2)	0.76	Drysdale et al., 2021	10.1016/j.scitotenv.2020.143339

8. What are the likely changes in mercury concentration in the Arctic atmosphere and ocean under future emissions scenarios?

Leads: Noelle Selin and Amina Schartup

Contributors: Anne Soerensen, Hélène Angot, Katlin Bowman

8.1 Introduction

Future changes in mercury (Hg) concentration in the Arctic atmosphere and ocean will result from multiple, interacting societal and environmental phenomena. The amount of Hg which will be present in the Arctic in the future depends not only on how Hg emissions and releases change with time but also on emissions of other pollutants which affect atmospheric chemical interactions, and on the change in global and regional climate. Emissions of pollutants (including Hg) as well as greenhouse gases are shaped by global and regional trajectories involving economic activities, energy use, regulatory constraints and the availability and application of technologies. Assessing likely changes in Hg concentrations thus requires examining potential changes in these underlying drivers, the resulting emissions, and the environmental and climate interactions that affect Hg transport and fate in the Arctic ecosystem.

Changes in Hg concentration in the Arctic atmosphere and ocean will take place on different time scales. Short-term timescales (i.e., over the next few years) are relevant for near-term decision-making, including the first effectiveness evaluation of the Minamata Convention, which will be carried out by 2023; atmospheric models can simulate the influence of changing emissions in the present and near future. In the medium term (i.e., over the next several years to a few decades), enhancements in legacy emissions from current as well as future emissions will play a substantial role (Amos et al., 2013). The degree of climate change occurring in the medium term (i.e., over the next few decades until 2050) has largely been determined by existing greenhouse gas emission trajectories. In the longer term (i.e., beyond 2050), trajectories of future greenhouse gas emissions, in addition to anthropogenic mercury emissions, will play a substantial role in determining Arctic climate and, combined with continued anthropogenic Hg emissions, will further influence Hg concentrations.

The relative importance of primary emissions, legacy emissions, and climate change to Hg concentrations differs depending on these timescales; previous efforts have not consistently accounted for these different processes. For the atmosphere, in the short term (i.e., over an individual year), concentration changes and Hg deposition will follow changes in emissions in different regions and their relative contributions and can be calculated based on source-receptor information. Many previous modeling efforts to quantify the impacts of changes in deposition to global regions (e.g., Corbitt et al., 2011; Chen et al., 2014; Travnikov et al., 2017) have simulated these dynamics. For the ocean, the timescales of ocean circulation may result in a lag relative to changes in the atmosphere, but many of these changes will overlap. In the medium term (i.e., years to decades), enhancements in legacy emissions from current and future emissions can be accounted for using dynamical biogeochemical cycle models and coupled ocean-atmosphere models (Angot et al., 2018; Selin, 2018). For timescales of decades and longer, ecosystem changes as a result of climate change will influence the global Hg cycle (Obrist et al., 2018), and these influences will also affect the Arctic; assessing them requires quantifying future climate change trajectories and applying process-based models that account for ecosystem changes.

Mercury concentrations in the Arctic Ocean are the result of past and current emissions and processes such as atmospheric deposition, riverine inputs, biotic and abiotic degradation, and settling to the deep ocean enabled by the biological pump. When evaluating future trends in ocean Hg concentrations, it is important to not only consider trends in industrial activities and national and global policies that influence Hg emissions, and by extension depositions on the surface ocean, but also consider how concomitant climatic and environmental shifts may exacerbate or dampen seawater Hg concentrations. Biogeochemical models can be used to consider these simultaneous changes and provide integrated estimates of future trends. The ultimate forward-looking model of Hg cycling will be able to combine emission scenarios, climate change simulations and speciated Hg modeling to produce future trends. But because of a limited understanding of how Hg inputs from sources other than the atmosphere (e.g. rivers, erosion) will change, this model does not yet exist. However, currently available models can: (1) generate projections based on future anthropogenic deposition scenarios, assuming that other fluxes and processes are constant; and (2) consider the effects of some large-scale climate-related changes (e.g., increased freshwater discharge, permafrost thaw, melting of ice caps or reduction of sea ice) on Hg fluxes. These models can be used to compare the relative impact of policy decisions.

This chapter explores potential changes in Hg concentrations in the Arctic atmosphere and ocean under future Hg emissions scenarios, examining potential trajectories over the next few decades (i.e., until 2050). In doing so, it also surveys the state of the science on differentiating the impact of direct emissions and accounting for their further biogeochemical cycling in the context of other drivers, such as climate change. A key contribution of this chapter is to better quantify the importance for Arctic Hg concentrations of primary Hg emissions relative to other changes, including climate and legacy emissions changes. The chapter applies a systems approach, evaluating trajectories of Hg concentrations in the context of assumptions about emissions pathways, many of which contribute to uncertainty and variability in future projections and some of which can be determined by future decisions. In the following sections, existing Hg emissions scenarios are compared, with

particular attention to the assumptions they make about underlying socio-economic trajectories and emissions control policies, including for greenhouse gases (see Section 8.2). Next, a range of changes in future Hg concentrations in the Arctic atmosphere are projected using one set of future emissions scenarios, accounting for the direct emissions and legacy impacts that may affect the Arctic in the short and medium term until 2050; quantitative results are compared with previous literature that evaluated the impact of climatic changes on Hg emissions and concentrations in the longer term (see Section 8.3). Atmospheric deposition from these short- and medium-term scenarios are used in the next section to drive an ocean model (see Section 8.4). This chapter provides an overview of the new findings from such models that have been developed or improved since the last AMAP assessment and identify four potential drivers of changing Arctic Ocean Hg concentrations (i.e., atmospheric deposition, sea-ice extent, riverine input and net primary production); it then examines the influence of their future variability on the Arctic Ocean Hg cycle (see Section 8.5). The chapter concludes by discussing the potential for different emissions trajectories to affect Arctic concentrations in the short, medium, and long term, as well as making recommendations regarding the model development and research needed to improve the simulation of future Hg scenarios (see Section 8.6).

8.2 What are the future emissions scenarios when comparing existing literature estimates?

Several efforts have been made to project global and regional Hg emissions into the future; these differ not only on the potential trajectories of future Hg but also on their underlying assumptions, base years, and temporal and spatial extent. The processes that affect the emission of Hg globally also contribute to the emission of other pollutants, including greenhouse gases and other pollutants such as sulfur dioxide (SO_2), nitrogen oxides (NO_x) and black carbon. Anthropogenic emission scenarios for Hg thus require assumptions of underlying socio-economic activities, and some build upon scenarios that have been developed and used to understand greenhouse gas emissions and global climate change.

A number of scenarios have been developed to facilitate analysis of the pollution implications of different global socio-economic trajectories (reviewed by Hayhoe et al., 2017). Most of the emission scenarios that exist for Hg rely on the underlying socio-economic assumptions from the IPCC's Special Report on Emissions Scenarios (SRES; IPCC, 2000). The SRES scenarios are emissions-based and capture 'storylines' (A1, A2, B1, B2) which provide illustrative trajectories of socio-economic and technological change (four sets of scenarios called 'families'). The scenarios in the group denoted A1 (A1B; balanced and A1FI; fossil-fuel intensive) represent a future characterized by rapid economic growth and a convergence across regions but differ in their specifications of technological change (i.e., the A1FI scenario is more fossil fuel intensive than A1B); not explicitly discussed in this chapter are the scenarios A1T (which assumes the use of predominantly non-fossil energy sources) and A2 (which assumes more fragmented economic growth and technological development than other storylines). In the scenarios in the group denoted B, the B1 scenario includes reductions in material intensity under a globalized service-oriented economy, while the B2 scenario emphasizes local sustainability solutions. Importantly, none of the SRES scenarios includes any sort of policies or measures to limit climate change. More recent analysis of socio-economic trajectories and climate change policies have built upon the Representative Concentration Pathways (RCP) outlined in the IPCC Fifth Assessment Report (AR5; IPCC, 2014); these are radiative forcing scenarios and reflect climate policies that incorporate lower warming targets. Shared Socio-Economic Pathways (SSP) were developed and constrained to create scenarios that can be used in impact, adaptation, and vulnerability analysis (Riahi et al., 2017). However, widely-applied Hg emissions scenarios have not been built upon these more recent global-scale scenarios. This means that most future projections of anthropogenic Hg emissions are not strictly comparable to those which address other pollutants, or with associated projections of climate change. This challenges the interpretation of and comparison between the magnitudes of the concentrations changes of other pollutants projected as a result of future climate scenarios, which have been assessed in a few studies, and those in studies which project Hg concentrations. This is discussed further below.

With respect to Hg in particular, comparisons between future emissions scenarios is made more difficult because existing scenarios build from different base year inventories, make different assumptions regarding underlying activities, and specify different rates of application and varying efficiencies of air pollution and Hg-specific control technologies. These assumptions affect the total amount of Hg emitted as well as its speciation. When it comes to global emissions scenarios, there are large differences in projections, which are driven not only by differences in the scenarios but also by base case assumptions. Existing future Hg emissions scenarios from previous literature are summarized in Appendix Table A8.1; the projections of global anthropogenic Hg emissions from the different scenarios are shown in Figure 8.1.

Streets et al. (2009) used a base year of 2006 (2480 Mg) and projected Hg emissions to 2050 under four different SRES scenarios (A1B, A2, B1 and B2). Beginning with 2006, global emissions increase under the A1B, A2 and B2 scenarios (by 96%, 57% and 6%, respectively) and decrease slightly under the B1 scenario (by 4%). They found that coal combustion in developing countries is the largest driver of emission increases; they also calculated that the application of an activated carbon injection (ACI) system on all coal-fired power plants could lower the range of emissions over the different scenarios from 2386–4856 Mg to 1670–3840 Mg. Lei et al. (2014) also projected Hg emissions using IPCC SRES scenarios (A1B, B1 and A1F1); global emissions in 2050 range from 2390 to 5990 Mg, a 9% to 173% increase over a base year of 2000 (2190 Mg; from Pacyna et al., 2006). Rafaj et al. (2013) projected emissions for Hg beginning from a 2010 base year using the International Institute for Applied Systems Analysis (IIASA) Greenhouse Gas and Air Pollution Interactions and Synergies (GAINS) model under scenarios of energy consumption with no greenhouse

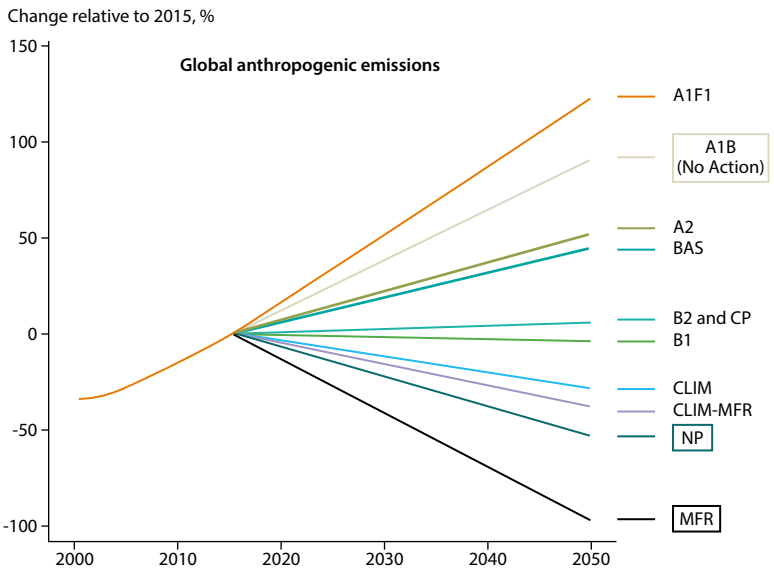

Figure 8.1 Global anthropogenic emissions projections under different scenarios. Scenarios that started before 2015 are linearly interpolated and extrapolated to 2050 (assuming constant annual growth or decrease). Emissions for 2000–2008 are from Streets et al. (2009) while emissions for 2009–2015 correspond to an A1B scenario. Current Policy (CP), New Policy (NP) and Maximum Feasible Reduction (MFR) scenarios are from Pacyna et al., 2016. A1B, A2, B1 and B2 scenarios from Streets et al., 2009. BAS, CLIM and CLIM-MFR are from Rafaj et al., 2013. A1F1 scenario is from Lei et al., 2014. The framed scenarios are used in the modeling below.

gas mitigation efforts and with climate policies which aim to limit the global temperature rise to within 2°C of pre-industrial levels. For these underlying activity scenarios, they examined two different sets of air pollution and Hg control measures: (1) current legislation to control air pollution by 2030 and no further effort between 2030 and 2050; and (2) a Maximum Feasible Reduction (MFR) scenario assuming the full adoption of the best available technologies. Under the base case scenario (BAS), emissions increase from 1554 Mg in 2010 to 2661 Mg in 2050; Hg emissions are reduced to ~850 Mg under the scenario consistent with a below 2°C temperature goal (CLIM) and to ~620 Mg if air pollution legislation and climate policies are adopted in parallel (CLIM-MFR scenario). Pacyna et al. (2016) projected future activities and emissions reduction scenarios to 2035, under Current Policy (CP), New Policy (NP) and MFR scenarios. They adopted underlying activity rates from the World Energy Outlook and based their estimates on economic projections and other trends.

Regional studies have provided additional scenarios for key source regions of importance to deposition in the Arctic and have shown that socio-economic assumptions embedded within emissions scenarios, as well as climate and energy policies, have a large impact on the overall trajectory of Hg emissions, compared with the impact of differences in application of control technologies. Giang et al. (2015) designed scenarios for the power sector in India and China based on activity use in the A1B and B1 scenarios and with a no additional control (NAC) and two different end-of-pipe (EOP) control technology scenarios consistent with Minamata Convention requirements. They found that the underlying assumptions about energy use (especially coal use) had a larger effect on emissions from the sector in question than the application of control technology. Rafaj et al. (2014) compared a baseline scenario for Europe with a scenario including the highest possible electricity generation from renewables by 2050. They found that co-control technologies used to abate air pollutants reduce Hg emissions by 35% to 45% and that the largest fraction of emissions cuts under the MFR scenario are attributed to the deployment of renewables in the power sector. Mulvaney et al. (2020) examined interactions between the Paris Agreement and Minamata Convention requirements under seven different scenarios that combined climate policies and EOP control policies to the year 2030. They found that climate policies consistent with the Paris Agreement in China can serve to mitigate Hg levels when implemented together with the Minamata Convention, with an additional 5% reduction under more ambitious climate goals simulated.

8.3 What are the predicted changes in mercury concentrations in the atmosphere?

In this chapter, a model analysis is conducted using future scenarios from Pacyna et al. (2016) to simulate a range of potential changes in Arctic concentrations under existing emissions scenarios. The scenarios described are then used to force the ocean model in Section 8.4. As summarized above, and in Table A8.1, the New Policy (NP) scenario assumes that policy commitments and plans to reduce greenhouse gases emissions are fully implemented. In this scenario, the use of Hg in products is reduced by 70%. This scenario assumes global emissions of ~1020 Mg/y. The Maximum Feasible Reduction (MFR) scenario assumes that all countries reach the highest feasible/available reduction efficiency in each emission sector (global emissions of ~300 Mg/y). It should be noted that the NP and MFR scenarios both assume a significant decrease of Chinese emissions, the main contributor to Hg deposition in the Arctic (see Chapter 3; AMAP/UN Environment, 2019).

According to the source apportionment analysis performed with the model ensemble (see Chapter 3), global natural and secondary emissions are the main contributors to Hg deposition in the Arctic (~70%). Using a global box model framework, Chen et al. (2018) showed that present-day Hg deposition over the Arctic Ocean is mainly from historical anthropogenic emissions from Asia (31%), followed by North America (18%), South America (12%), the former USSR (12%) and Europe (11%). Mercury deposition due to primary anthropogenic emissions is mostly due to emissions in East Asia (~33%; China, Korea and Japan). Europe, Southeast Asia, South Asia, Sub-Saharan/sub-Sahel Africa, South America, and Russia/Belarus/

Ukraine each contribute ~7% to ~9%. Emissions in the Arctic (north of 66°N and Greenland) currently only contribute ~2% of Hg deposition due to primary anthropogenic emissions. As a result of these source contributions, trajectories for Asia will likely be the most influential for future Arctic deposition, especially since future global emissions trajectories are greatly affected by Asia's emissions.

In this current chapter, the impact of different regulatory strategies for future Hg atmospheric concentrations and deposition to the Arctic in the short term is estimated under the NP and MFR scenarios developed by Pacyna et al. (2016). The present-day (2015) BASE simulation was performed using the AMAP/UNEP 2015 inventory developed for the latest Global Mercury Assessment (AMAP/UN Environment, 2019). The same simulation was then performed using the NP and MFR inventories (i.e., assuming global anthropogenic emissions of ~1020 for NP and 300 Mg for MFR in the year 2015).

According to the model ensemble (see Chapter 3), the annual mean atmospheric Hg(0) concentration in the Arctic (north of 60°N) is 1.4 ng/m^3 (BASE scenario). This mean Hg(0) concentration drops to 1.2 and 1.1 ng/m^3 assuming global emissions of ~1020 Mg/y (NP scenario) or ~300 Mg/y (MFR scenario), respectively. The impact of different regulatory strategies is of the same order of magnitude for both Hg(0) concentrations and atmospheric deposition. Hereafter, we focus on deposition since it is the main pathway of Hg transfer from the atmosphere to the ocean and ecosystems. The best-case estimate resulting from the emissions scenarios is a 17% or 27% reduction of Hg deposition in the Arctic compared to the BASE scenario if a NP or a MFR scenario is implemented in 2015. The best-case estimate shows the potential for short-term reductions: that is, it illustrates the maximum possible impact of the primary emissions reduction scenario without accounting for changes in legacy emissions. Under the NP case, deposition to Arctic land decreases under the base case to 5.6 μg/m^2/y from 6.8 μg/m^2/y, and to the Arctic Ocean from 7.4 μg/m^2/y to 6.1 μg/m^2/y. The MFR scenario reduces Arctic deposition further, to 5.0 μg/m^2/y and 5.4 μg/m^2/y to land and ocean, respectively.

Further simulations are conducted to investigate how delays in implementing emission reductions and the associated growing legacy Hg reservoir affect deposition fluxes to the Arctic, following the methodology of Angot et al. (2018). These simulations reflect medium-term dynamics. Because the parameterization of this effect is challenging, many global-scale chemical transport models (CTMs) hold legacy emissions constant while changing future anthropogenic Hg emission scenarios. Fully accounting for legacy emissions requires coupled atmosphere-ocean-land models that are not widely accessible and are extremely computationally intensive. To account for the effect of legacy emissions, Angot et al. (2018) developed a methodology that links CTM simulations with biogeochemical cycle modeling, which adjusts legacy deposition flux to account for future increases. To accomplish this, the impact of legacy emissions is isolated using a sensitivity simulation in the model; the resulting spatially resolved deposition flux is scaled based on the global average increase of legacy emissions calculated using the fully coupled biogeochemical cycle model. This method allows calculation of the magnitude of changes in the legacy component of deposition in a spatially resolved way but assumes that its distribution does not change from the present day. For global biogeochemical cycle modeling, in order to estimate the impacts of delay we assume that Hg emissions grow following the trajectory of a No Action scenario (+55.9 Mg/y; constructed based on the A1B scenario by Streets et al., 2009) until implementation of a NP or MFR scenario. This A1B scenario assumes rapid increases in energy use and economic growth, low population growth, continued globalization, and rapid introduction of new and more efficient technologies.

Table 8.2 Projected Hg deposition flux to land and ocean areas of the Arctic (north of 60°N; in μg/m^2/y) using future emissions scenarios and assuming a short-term or delayed implementation of global mitigation efforts.

	Land	Ocean
Base year (2015)*	6.8	7.4
NP implemented in 2015 (best-case estimate)	5.6	6.1
NP delayed by 5 years	6.1	6.6
NP delayed by 10 years	6.5	7.1
NP delayed by 15 years	6.9	7.5
NP delayed by 20 years	7.4	8.0
MFR implemented in 2015 (best-case estimate)	5.0	5.4
MFR delayed by 5 years	5.4	5.9
MFR delayed by 10 years	5.8	6.3
MFR delayed by 15 years	6.3	6.8
MFR delayed by 20 years	6.7	7.3

*Base year (2015) Hg deposition fluxes are from the model ensemble (see Chapter 3).

Table 8.2 and Figure 8.2 show deposition under 5-, 10- and 20-year delay scenarios for both NP and MFR. They show that the relative impact of NP or MFR policy on Arctic deposition decreases by ~50% or ~35%, respectively, for each 5-year delay. Under a 20-year delay, in both the NP and MFR cases, the effect of emissions added to the legacy pool during that 20-year period entirely offsets the reductions to primary emissions that occur later.

Figure 8.3 illustrates the relative change in Hg deposition over the Arctic Ocean between the year 2050 and 2015 under the three policy scenarios. It shows that the No Action scenario (A1B) results in a 51% higher Hg deposition rate by 2050. Both 'action' scenarios (NP and MFR) result in reductions in Hg deposition ranging from 7% (for NP delayed to 2035) to 30% (for MFR implemented in 2020). These deposition scenarios are used to force the ocean box model.

The atmospheric changes prompted by emissions can be compared with the magnitude of changes expected as a result of climate change, in the short, medium and long term. Lei et al. (2014) compared the influence of projected emission changes and climate change on U.S. atmospheric Hg levels in 2050. They found that anthropogenic emissions would contribute 32% to 53% of projected changes in Hg air concentration, while climate and natural emission changes would account for 47% to 68%. Although their detailed analysis focused on the U.S., they calculated changes in Hg using a global model and reported maximum future changes in the mid-latitudes, with much

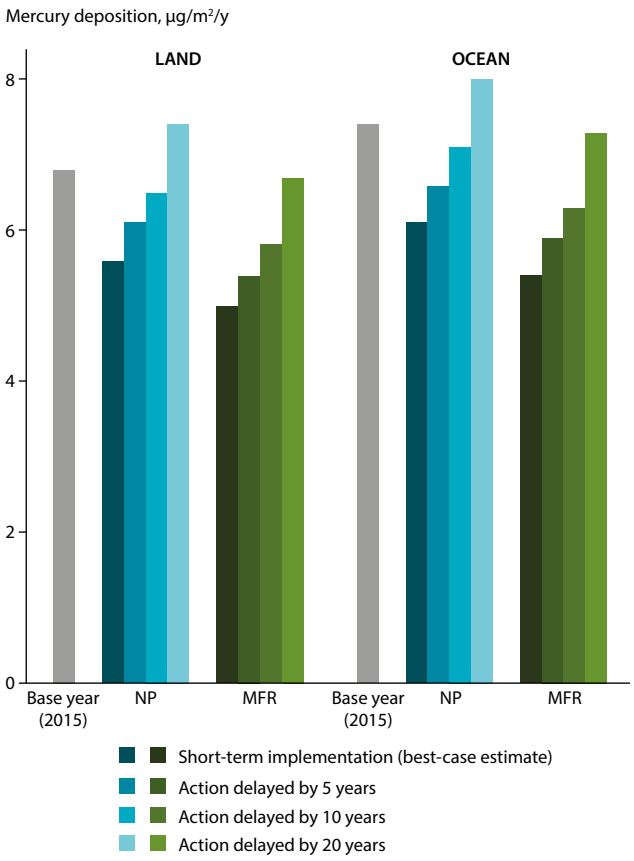

Figure 8.2 Projected Hg deposition flux to land and ocean areas of the Arctic (north of 60°N; in µg/m²/y) using future emissions scenarios and assuming a short-term or delayed implementation of global mitigation efforts. Base year (2015) Hg (gray bar) deposition fluxes are from the model ensemble (see Chapter 3). The blue bars represent Hg deposition under the New Policy (NP) scenario and green bars are deposition under the Maximum Feasible Reduction (MFR) scenario.

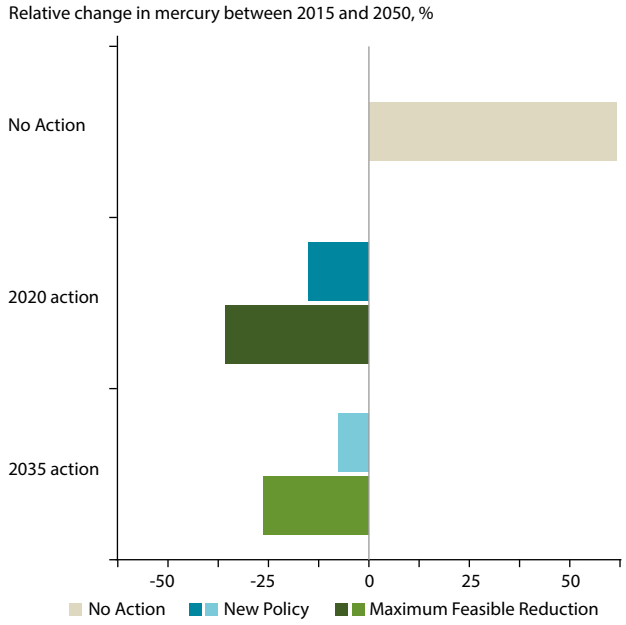

Figure 8.3 Bars represent the relative change in Hg deposition on the Arctic Ocean surface in three scenarios: the No Action (A1B) scenario (cream; Streets et al., 2009), and the New Policy (blue; Pacyna et al., 2016) and Maximum Feasible Reduction (green; Pacyna et al., 2016) scenarios implemented in 2020 and 2035.

smaller concentration changes in the high latitudes. Using a modeling approach, Dastoor et al. (2015) showed that an increase in net deposition in the Arctic under climate change is primarily driven by changes in snowpack and sea-ice conditions. Changes in sea ice extent could also affect atmospheric Hg depletion events (AMDEs), by changing the availability of reactive halogens (Douglas and Blum, 2019). It has also been suggested that air temperature changes can impact the timing of, and thus deposition fluxes (Cole and Steffen, 2010). Climate change could also increase Hg emissions from wildfires by 14% globally and by 13% in Eurasia by 2050 (Kumar et al., 2018) resulting in increased Arctic Hg deposition (as wildfires contribute ~10% of the total annual Hg deposition to the Arctic; Kumar and Wu, 2019). In addition, tundra and permafrost soils serve as reservoirs of a large legacy pool of past and present Hg emissions that have accumulated in the Arctic (Olson et al., 2018; Schuster et al., 2018; Lim et al., 2020) and climate-driven permafrost thaw could release significant amount of Hg previously locked-away (Schaefer et al., 2020). The greening of the Arctic will also likely impact air-surface exchanges (Grannas et al., 2013) and reduce the extent of re-emission of Hg from the cryosphere (Dastoor and Dunford, 2014; Dastoor et al., 2015). On the other hand, higher surface temperature may enhance the photoreduction and re-emission of Hg from the Arctic Ocean, affecting atmospheric concentrations.

8.4 What are the predicted changes of mercury concentrations in the ocean?

Significant strides have been made in Arctic Ocean Hg modeling since the last AMAP mercury report (AMAP, 2011). In the previous report, only one mass budget for total Hg (THg) was available for the Arctic Ocean (Outridge et al., 2008), and no modeling studies had been conducted. Since 2012, nine manuscripts have been published describing modeling studies of Hg in the Arctic (or global studies that include the Arctic). The models vary in resolution, spatial coverage and Hg species that are included. They also vary in design, falling into 3 categories: (1) box models; (2) slab-ocean models integrated into an atmospheric framework; and (3) global biogeochemical models of the ocean. The studies conducted using these models provide an initial quantitative assessment of important drivers of Hg concentrations and speciation in the Arctic Ocean. Table 8.3 gives an overview of these models and their major findings. Of the nine studies, only one reported projections for Hg concentrations in the Arctic Ocean (Chen et al., 2018). They did so using a global source-receptor model including a five-compartment Arctic box model based on Soerensen et al. (2016a).

Recent work has shown that the upper part of the Arctic Ocean is very responsive to changes in Hg inputs. Soerensen et al. (2016a) presented an updated mass budget for THg and the first budget for monomethylmercury (MMHg) and dimethylmercury (DMHg) in the Arctic Ocean. They used a box model to reassess the lifetime of Hg in the Arctic Ocean and reported that Hg takes 13 years to cycle out of the upper ocean (<200 m) and 45 years to cycle out of the deep Arctic Ocean (>200 m). The Arctic food web is highly dependent on planktonic activity in the upper ocean, suggesting that policy actions that reduce

Table 8.3 Existing Arctic Ocean Hg models and budgets

Model framework	Resolution	Inorganic Hg	Organic Hg	Lower food web	Coupled atmosphere	Future scenarios
Box model	Low: 5-compartment box model	Yes	Yes	Yes	No	No, but includes past emissions and climate scenarios (1850–2010)
Box model	Low: global source-receptor model including a 5-compartment Arctic box model; the Arctic box model is based on Soerensen et al. (2016a)	Yes	No	No	Yes	Yes, 4 emissions scenarios (2015–2050) but no climate change impacts
GEOS-Chem with slab-ocean module	Medium: high horizontal resolution (4x5°) but represents only the surface ocean	Yes	No	No	Yes	No
GEOS-Chem with slab-ocean module	Medium: high horizontal resolution (4x5°) but represents only the surface ocean	Yes	No	No	Yes	No, but includes past climate scenarios (1979–2008)
GEOS-Chem with slab-ocean module	Medium: high horizontal resolution (4x5°) but represents only the surface ocean	Yes	No	No	Yes	No
MITgcm	High: global biogeochemical model with nested Arctic Ocean (36x36 km, 50 vertical layers)	Yes	No	No	No	No
NEMO framework	High: global biogeochemical model—simulation not Arctic focused	Yes	Yes	No	No	No
MITgcm	High: global biogeochemical model with nested Arctic Ocean (36x36 km, 50 vertical layers)	Yes	No	No	No	No
MITgcm	High: global biogeochemical model—simulation not Arctic focused (~40x40 km)	Yes	Yes	Yes	No	No

deposition and Hg concentrations in the upper ocean can have a relative rapid impact on the food web Hg burden. The deeper central Arctic Ocean has a considerable lag in response to changing inputs to the surface ocean, which will also mean a slow response to future changes. Both changes in the external forcing and changes to the lifetime of Hg in the different parts of the water column will control the Hg concentration in the future Arctic Ocean.

The main inputs of Hg to the Arctic Ocean from outside the Arctic are to the surface layer, such as atmospheric deposition or riverine discharge (Soerensen et al., 2016a; see Chapter 3 for more information on sources of Hg to the Arctic). Atmospheric deposition currently contributes 40% to 50% of external inputs (including deposition to snow and ice released during spring/summer) and rivers and coastal erosion 50% to 55% (Kirk et al., 2014). Soerensen et al. (2016a) showed how increasing atmospheric deposition between 1850 and 2010 had an almost equal response in the increase of surface water concentrations but propagated down the water column with a long lag time to the deep Arctic water. Chen et al. (2018) ran a range of future emissions scenarios (2015–2050) with all other parameters kept constant. Under a constant emission scenario, they found that a 12% increase in atmospheric Hg resulted in a 9% increase in Arctic Ocean Hg mass, while a 'zero emissions' scenario resulted in a rapid 50% decline in Hg deposition but only a 10% Arctic Ocean Hg decline by 2050.

The importance of rivers as a source of Hg to the Arctic Ocean was demonstrated by Fisher et al. (2012). They used the GEOS-Chem model with a slab-ocean module to simulate the impact of seasonal variability of Hg fluxes with river discharge. This simulation showed the importance of seasonality in external sources in causing seasonal variability not only in the surface ocean but also in the marine boundary layer Hg concentration due to the rapid interaction between the surface ocean and atmosphere. They thus highlighted the connectedness and fast response in the Arctic surface ocean. Zhang et al. (2015) and later Sonke et al. (2018), using a global biogeochemical model (MITgcm) but with a specific focus on the Arctic Ocean processes, also found that rivers are major drivers of seasonal variability in the surface ocean. Measurements made since 2015 are consistent with these modeling results. For example, Charette et al. (2020) reported elevated Hg within the Transpolar Drift, a current that transports river-influenced Eurasian shelf waters and sea ice to the central Arctic Ocean.

Several modeling studies show that sea ice plays an important role in regulating the air-sea exchange of Hg. Fisher et al. (2012) first showed the importance of air-sea exchange as a mechanism that results in a rapid adjustment of the surface ocean Hg concentrations as the Hg influx to the surface ocean fluctuates (on seasonal scale). Zhang et al. (2015) reported that 80% of the riverine Hg input evades to the atmosphere once it reaches the Arctic Ocean. Air-sea exchange of Hg is greatly influenced by the fraction of open ocean. For example, Zhang et al. (2015) showed that the western Arctic Ocean has higher Hg concentrations than the eastern Arctic Ocean and proposed the difference is due to increased deposition because of more frequent AMDEs and greater summertime ice cover in the western Arctic Ocean. Two other modeling studies directly addressed the impact of declining ice cover and concluded that the loss will result in lower surface ocean Hg concentrations (Chen et al., 2015; Soerensen et al., 2016a). Soerensen et al.

Major drivers identified	Reference
For total Hg: erosion and rivers account for 1/3 of inputs, followed by the atmosphere, then ocean flow; declining sea ice increases the net loss of Hg to the atmosphere For MeHg: most MeHg is produced *in situ* in subsurface water	Soerensen et al., 2016a
Geogenic and North American Hg currently dominates the Arctic Ocean Hg reservoir; in future, Asian emissions will be a major driver of Hg in the Arctic Ocean	Chen et al., 2018
Rivers are a major source of Hg to the Arctic Ocean that drives the Arctic atmospheric summer peak in Hg(0) through emission from the Arctic Ocean following the spring freshet	Fisher et al., 2012
Higher temperatures and lower sea-ice area will reduce the Hg flux from the cryosphere to the ocean. High wind speed and cold springs driving frequent AMDEs increase deposition to the cryosphere; high temperature increases ice melt and thereby Hg flow to the ocean	Fisher et al., 2013
Arctic warming and declining sea ice drive an increase in net Hg evasion; melting of multi-year sea ice not a large driver	Chen et al., 2015
In continental shelf areas, heat transfer from rivers increases water turbulence and ice melt thereby increasing net evasion; the particle load and efficient degradation of the particulate organic carbon results in a labile Hg pool	Zhang et al., 2015
At depth in the Arctic water column, abiotic methylation driven by dissolved organic carbon could be important for MMHg production; once formed, MMHg remains bound to refractory dissolved organic carbon and is unavailable for demethylation and thus accumulates in the water column	Semeniuk and Dastoor, 2017
Supports previous model results from Fisher et al. (2012) and Zhang et al. (2015) on the importance of seasonal and spatial variability of Hg loads from rivers and sea-ice cover for surface ocean Hg concentrations and the evasion flux	Sonke et al., 2018
Photodemethylation in the Arctic lower than elsewhere because of weaker radiation and chlorophyll a; lower demethylation due to lower temperatures responsible for higher MeHg at the poles than elsewhere	Zhang et al., 2020b

(2016a) showed that declining sea-ice area since the 1970s resulted in an increase in the net loss of Hg to the atmosphere due to the impact of evasion (reaching a relative difference in surface ocean concentrations of ~10% in 2010).

Other processes undergoing climate-driven shifts have the potential to influence the Arctic Hg cycle, such as air and seawater temperature or Arctic sea-ice regime shifts from multi-year to first-year ice dominance (Schartup et al., 2020). For example, Zhang et al. (2020b) showed that heat transfers from rivers to estuaries increases Hg(0) evasion by accelerating snowmelt, and increasing transfer velocity of Hg(0) and turbulence. Fisher et al. (2013) used historic simulations from the GEOS-Chem global Hg model with a slab-ocean module to analyze the drivers of interannual variability in Arctic atmospheric Hg. They found that decreased fluxes of Hg from the atmosphere to the cryosphere and from the cryosphere to the ocean were associated with changes induced by climate warming: high air temperatures, low sea-ice area, strong warming in spring (Bekryaev et al., 2010) and cloudiness (Eastman and Warren, 2010).

8.4.1 Model based findings for methylmercury

In this current assessment report, Chapters 4 and 5 describe the many biogeochemical processes involved in methylmercury (MeHg) production in seawater and sediment. Until very recently, there were no high resolution MeHg concentrations profiles for the central Arctic Ocean (Heimbürger et al., 2015; see Chapters 3 and 4, and Section 6.6) and the drivers of methylation are still virtually unknown (Wang et al., 2012a). Because of these limitations, only three models include MeHg species in their simulations: the Soerensen et al. (2016a) box model and the two global biogeochemical models MITgcm and NEMO (Zhang et al., 2015; Semeniuk and Dastoor, 2017). Soerensen et al. (2016a) developed the first MeHg budget for the Arctic Ocean and concluded that most MeHg is produced *in situ* in subsurface ocean waters (20–200 m). Zhang et al. (2020b) proposed that the MeHg concentrations in the top 100 m of ocean waters are higher in the Arctic (and Antarctic) than elsewhere because of lower demethylation rather than higher methylation. Semeniuk and Dastoor (2017) suggested that abiotic methylation driven by dissolved organic carbon could be important for MeHg production at depth. Because of the limited understanding of MeHg production in the Arctic Ocean, this chapter will focus its projections on changes in THg exclusively.

8.5 What are the changes in total mercury in the future Arctic Ocean?

This section will consider the impact of anthropogenic emissions versus other drivers of changes in total mercury (THg) in the future Arctic Ocean. In this chapter, model simulations were conducted to quantify the impact of different policy scenarios (see Section 8.2) on the future Hg concentrations in the Arctic Ocean with a focus on the change during the period 2015–2050. The goal was to compare the impact of management strategies for anthropogenic Hg emissions to the influence of climate change in the Arctic ecosystem on seawater Hg concentrations. Based on the literature review of the existing model results (Table 8.3) and drivers identified in

Chapter 5, three quantifiable climate-related changes predicted to impact the Arctic Ocean Hg cycle in the coming decades were selected: sea-ice cover, river discharge and net primary production (NPP). The simulations are performed with a low spatial resolution level (box model) to capture major impacts on the total Hg cycle in the Arctic Ocean.

8.5.1 Model description

The model simulations are performed using a five-compartment box model (3 water column layers and shelf and deep ocean sediments; see Figure 8.4). This is a simplified version of the Soerensen et al. (2016a) model that only computes inorganic Hg processes (Hg(II) and Hg(0)). A full description of the model parameterizations can be found in Soerensen et al. (2016a). Briefly, the model includes external Hg inputs such as atmospheric deposition, river discharge, erosion and snowmelt as well as ocean circulation. The internal processes considered are particle settling, diffusion, evasion and chemical transformation between Hg(II) and Hg(0). Process specific rates and/or fluxes are calculated using first order differential equations deduced from the present-day Hg budget presented in Soerensen et al. (2016a). For the climate change model runs, literature-derived climate variables are used to scale rates/fluxes to evaluate their projected impact on the Hg cycle. Atmospheric Hg deposition to the surface ocean is modeled as a direct flux to the surface water or deposition on sea ice. Thus, the relative change in the fraction of open ocean to sea ice influences Hg concentrations in the water and redox transformations (see Section 8.5.2a). The extent of sea-ice coverage also impacts the release of Hg from the springtime/summertime meltwater and evasion of Hg(0).

The solids budget was adapted from Rachold et al. (2004) to include changes in net primary production and in sea ice cover (Hill et al., 2013). The settling of suspended particles is based on the fraction of solids remaining following remineralization at each depth in the water column (Moran et al., 1997; Rachold et al., 2004; Cai et al., 2010). The fraction of solids from rivers and NPP remaining after remineralization at each depth is 50% in the polar mixed layer (PML), 30% in the subsurface water and 1% in the deep ocean. Solids from erosion are assumed not to remineralize. Mercury settling is estimated based on the mass of settling particles and an average concentration of Hg in suspended solids found in the Arctic (Soerensen et al., 2016a). To estimate the impact of NPP on seawater concentrations, the model is run forced by past (1850–2015) relative changes and projected changes to 2050.

The model is run from 1850 to 2015 to create a common starting point for the scenario simulations (see Soerensen et al., 2016a). For each model run, the known variability in deposition, sea-ice area, NPP and river-water discharge is included. The individual 2015–2050 climate scenarios are run while changing only one climate variable, while the others are kept constant at the 2015 level in order to be able to quantify the impact of each driver. A final run simulates the impact of all three climate variables simultaneously with constant deposition.

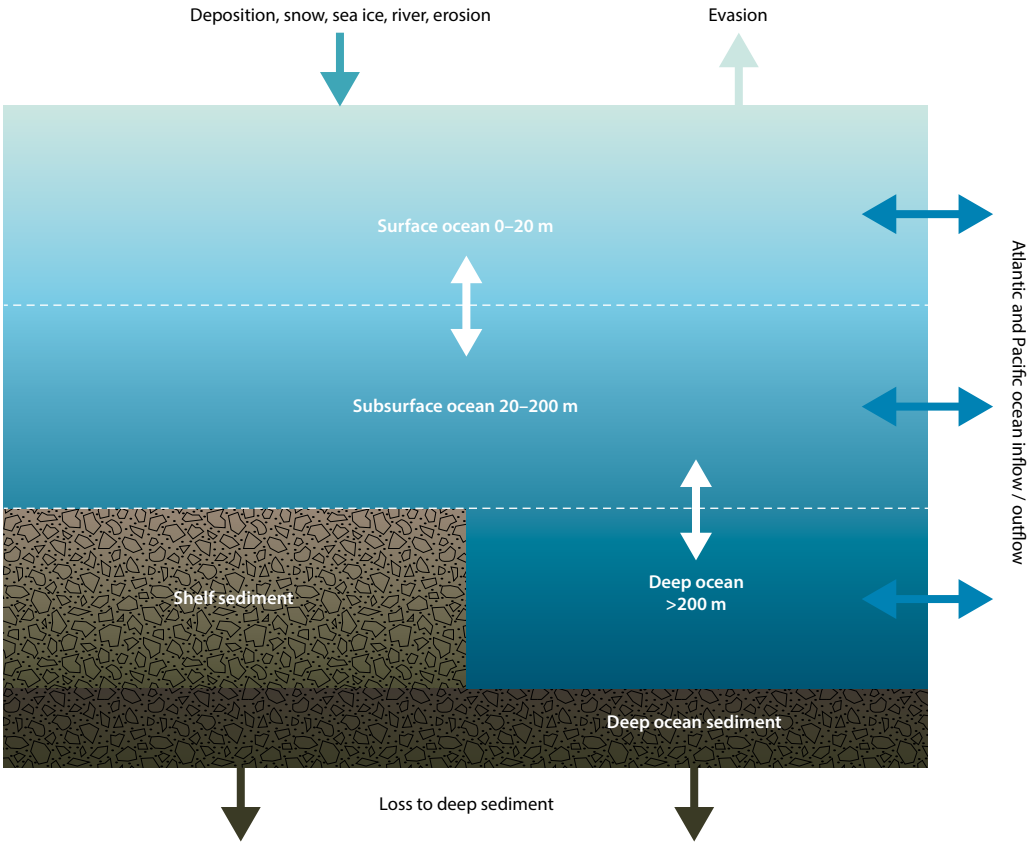

Figure 8.4 Simplified layout of the five-compartments Arctic mercury box model. Detailed parameterization of external and internal processes can be found in Soerensen et al., 2016a.

8.5.2 Mercury deposition scenarios and policy implications

This section explores the influence of changing Hg deposition under policy scenarios described in Section 8.3: the No Action scenario (A1B) emission trajectory and associated increase in deposition, the New Policy scenario (implemented in 2020 and 2035), and the Maximum Feasible Reduction scenario (implemented in 2020 and 2035). The section also explores the relative influence of sea ice, riverine input, and net primary production on Hg concentrations in the Arctic Ocean.

a. Sea ice scenario

This scenario examines the influence of changes in sea ice on the Hg ocean reservoir through simulating the relative change in the sea-ice covered area of the Arctic Ocean. The change between 1950 and the present day is based on observations (e.g., from the U.S. National Snow and Ice Data Center; NSIDC), while the future trend is based on the SIMIP community CMIP6 simulations under the SSP2-4.5 scenario, where surface air temperatures increase by ~3°C by 2100 (Notz and SIMIP, 2020). Figure 8.5 shows that according to this projection the Arctic Ocean will have lost approximately 20% of its sea-ice cover by 2050 compared to 2015. Changes in sea-ice cover impact the exchange of Hg between seawater and the atmosphere as well as the amount of Hg that can be stored or released by the sea ice in the summer. Furthermore, in the surface layer of the Arctic Ocean, about 10% to 20% of Hg is in a volatile form (Hg(0) + DMHg); thus, by capping the surface ocean, sea-ice cover regulates the air-sea exchange of these volatile species (Fisher et al., 2013; Zhang et al., 2015; Soerensen et al., 2016a; Agather et al., 2019; Dimento et al., 2019, Schartup et al., 2020). Sea ice also influences surface-water redox processes by controlling how much light penetrates the water column. The different ways in which sea ice impacts Hg cycling are discussed in more detail in Chapters 3 and 5. Thus, based on previous studies, it is expected that the observed rapid decline in sea-ice volume and extent together with the disappearance of perennial ice from the central Arctic Ocean will lead to lower seawater Hg concentrations. Reductions in sea-ice content track linear changes in global temperature and carbon dioxide emissions, although there is great uncertainty in the sensitivity of sea ice to warming (Notz and SIMIP, 2020). Sea-ice extent has been declining rapidly, at a rate of 6.6±1.2% per decade in the summer and fall, and 2.1±0.5% per decade in the winter and spring. The mean thickness of the sea ice has also decreased from an average of 3.02 m (1958–1976) to 1.43 m (2003–2007).

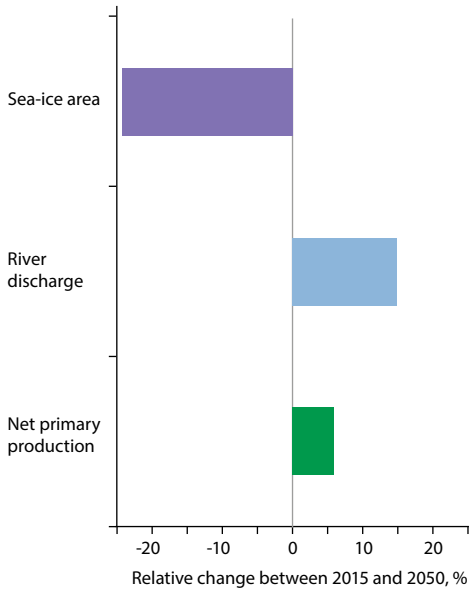

Figure 8.5 Bars represent the relative change in sea-ice area (pattern), river discharge (blue) and net primary production (green) used in future scenario simulations between 2015 and 2050.

b. Riverine input scenario

The riverine input scenario indicates the direction and proportional effect of an increase in external forcing from the terrestrial environment on Hg ocean concentrations, although it likely underestimates actual increases from terrestrial sources. Modeling studies described in Section 8.4.2 suggest that Arctic rivers contribute amounts of Hg to the Arctic Ocean that are of the same magnitude as atmospheric sources. Sonke et al. (2018) used a combination of field measurements and modeling to reduce the uncertainty on the current day riverine Hg flux into the Arctic Ocean, which they estimated to be 44±4 Mg/y. However, as discussed in Chapter 5, this riverine flux of Hg is expected to increase because river water discharge has been increasing since consistent monitoring began in 1930s (Peterson et al., 2002) and Hg laden permafrost is expected to release increasingly larger amounts of Hg (Vonk et al., 2015a; Schuster et al., 2018). To create the river scenario used in this section, river discharge data covering the period from 1936 through to 1999 was obtained from Peterson et al. (2002). Future trends were reported in Haine et al. (2015) for 1980 through to 2100 (2000–2010) reaching 5500 km^3/y by 2100. If Hg control policies are implemented, Hg deposition to the watershed should decline and decrease river Hg concentrations (with some time lag). On the other hand, thawing permafrost and increased coastal erosion are likely to release stored Hg to rivers, thus increasing Hg concentrations in river discharge (Koven et al., 2013; Schuster et al., 2018). Because the overall result of these opposing forcings is unknown, the modeling done here assumes a constant Hg concentration in river water as discharge increases given an overall increase in the Hg load from rivers. Figure 8.5 shows an approximately 12% increase in the riverine discharge scenario between 2015 and 2050. This is within the range of the increased discharge observed between 1975 and 2015 discussed in Chapter 5.

c. Net Primary Production scenario

To address the impact of changing NPP on the Hg ocean reservoir, this scenario uses the most conservative projections of NPP increase (about a 5% rise between 2015 and 2050; see Figure 8.5). Reduction in sea-ice coverage results in more light reaching the Arctic Ocean. This has been suggested to increase NPP, and most models agree that NPP will increase in the future. NPP has been shown to enhance algal scavenging in Arctic lakes (see Chapter 5) and NPP is expected to increase the removal of Hg from the upper layers of the Arctic Ocean, thus

reducing its bioavailability (Brazeau et al., 2013; Grasby et al., 2013; Soerensen et al., 2016b). However, no prior Arctic Ocean model simulations have investigated the importance of changes to the NPP scenario. Expected future trends in NPP are less well constrained than sea-ice decline or river discharge (Vancoppenolle et al., 2013). Arrigo and van Dijken (2015) show a negative correlation between NPP and sea-ice cover (i.e., increasing NPP with decreasing sea-ice volume). However, NPP in the Arctic Ocean could also decrease if the nitrate supply is not large enough to sustain the excess growth. The CMIP5 performed simulations with 11 Earth system models between 1900 and 2100 and found conflicting results (Vancoppenolle et al., 2013). Overall, the models' mean increase in NPP is smaller (+58 TgC/y) than the increases predicted from simple linear extrapolations between NPP and sea-ice observations. For example, Arrigo and van Dijken (2011) calculated a 300 TgC/y increase in NPP between 1998 and 2009, and Arrigo and van Dijken (2015) reported a 30% increase between 1998 and 2012. This model scenario does not account for the impact of higher NPP on the surface ocean chemistry.

8.5.3 Impact of anthropogenic Hg emission policies and delays in implementation

No Action, NP and MFR deposition scenarios are used to force the ocean model to predict changes in Hg concentrations for the surface, subsurface and deep Arctic Ocean in 2050 (see Figure 8.3). Figure 8.6 presents the Arctic Ocean's response as the percentage change in concentrations in 2050 compared to 2015 due to the implementation of the various policy scenarios. In this simulation, all other parameters, including climate variables, are kept constant.

The No Action scenario results in an Hg concentration increase ranging from 22% in the surface to almost 9% at depth by 2050. Under the most aggressive scenario, MFR-2020, concentrations decrease by 14%, 10% and 4% in the surface, subsurface and deep ocean, respectively, by 2050. Thus, the difference in response between the two extreme scenarios (No Action and MFR-2020) is 36% for the surface ocean and 13% for the deep ocean. These results are consistent with Chen et al. (2018) who found that the No Action scenario would result in a 9% increase in Hg mass, while a zero emissions scenario would lead to a 10% reduction in Hg mass by 2050 for the entire Arctic Ocean (surface, subsurface and deep ocean reservoirs combined). The NP scenarios also result in total Hg declines in the surface and subsurface water layers, albeit more moderate, and in the deep ocean they result in very little change (from a 1% reduction to a 3% increase). The NP and MFR simulations also show the importance of prompt action with the impact particularly visible in the surface ocean, which has a faster response time. In the surface ocean, Hg has a lifetime of about 10 years; thus, delaying implementation to 2035 results in 5% more Hg in the water by 2050 compared to policy implementation in 2020. The deep ocean, in which changes to concentration lag behind the surface ocean and where concentration has not reached a steady state, mostly continues to see increases driven by legacy Hg inputs and only the MFR-2020 scenario offers a small trend reversal by 2050 (a 4% reduction).

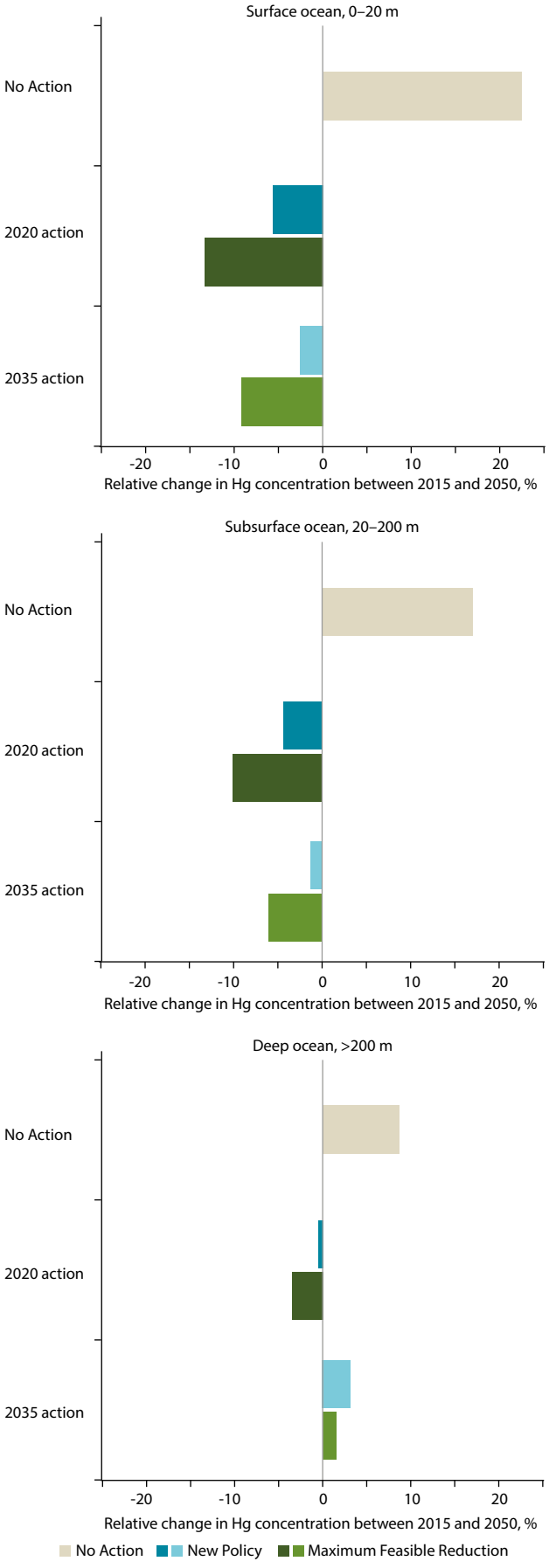

Figure 8.6 Relative change in Arctic Ocean Hg concentrations between 2015 and 2050 in the surface (0–20 m, top panel), subsurface (20–200 m, middle panel) and deep ocean (<200 m, bottom panel), under the No Action (cream), New Policy (blue) and Maximum Feasible Reduction (green) scenarios implemented in 2020 and 2035.

8.5.4 Impact of climate variables on Arctic Ocean mercury concentrations

Figure 8.7 shows the impacts of changes in sea-ice cover, river discharge and NPP individually and combined on Hg concentrations by 2050. In these simulations, the atmospheric depositions are kept constant at 2015 levels to be able to compare the influence of these drivers on Hg concentrations to the influence of policy scenarios and implementation delays shown in Figure 8.6.

The role of sea-ice extent on the Hg cycle is multi-fold. It controls the amount of atmospheric Hg that deposits directly to the surface of the water column, sunlight penetration, air-sea exchange and Hg release from melting sea ice in the spring and summer. The model considers the combined influences of these processes and projects that the continued retreat of sea ice (an additional 20% by 2050) will reduce Hg concentration in the Arctic Ocean. This is true for all depths, although the reduction is highest (-8%) in the surface ocean and smallest in the deep ocean (<1%) because of the lag time in the response. This decline in surface ocean Hg of 0.2% per year due to disappearing sea ice covered areas is in the same range as the decline calculated by Soerensen et al. (2016a) between 1975 and 2010, during which a loss of approximately 15% of sea-ice cover was observed.

The increased river discharge adds 2% to 3% to seawater Hg concentrations to all the water masses. This is because the model considers it to be a simple and uniform external input equivalent to atmospheric deposition. In reality, the impact of river discharge has a very different spatial distribution from atmospheric deposition, with a larger influence on shelves and nearshore areas. The river discharge increases by 12% by 2050 in this scenario (see Figure 8.5). The model uses the most recent estimate of riverine Hg inputs from Sonke et al. (2018) of 44±4 Mg/y. This amounts to a 5.3 Mg increase in yearly river Hg input by 2050 which corresponds to ~3.3% of external inputs to the Arctic Ocean and is reflected in the change in seawater concentration.

Sea-ice retreat increases NPP (Arrigo and van Dijken, 2015) which in turn enhances particle settling and Hg scavenging (Soerensen et al., 2016b). The model estimates that the predicted 5% increase in NPP by 2050 (Figure 8.5) will cause an increase in the removal of Hg from the surface ocean and slightly lower the concentration (<1%). Because the settling from the deep ocean to the seafloor is slow, some of this scavenged Hg accumulates in the deep ocean layer (Figure 8.7). This causes the Hg concentration in the deep ocean to increase in this scenario by 2%. Overall, the predicted NPP effect is small, but this could be due to multiple assumptions made in this modeling. As the NPP projections are very uncertain, a conservative increase was used to drive the model (Vancoppenolle et al., 2013). For example, if NPP were to double by 2050 (Arrigo and van Dijken, 2011) the model calculates a much larger (7%) decrease in surface Arctic Ocean Hg concentration. In addition, the modeling described here relies on an older solids budget; a recent study by Tesán Onrubia et al. (2020) estimated a downward flux of particulate Hg using the radionuclide pair $^{234}Th/^{238}U$ coupled to particulate Hg/^{234}Th and found a larger sinking flux that could change the aforementioned estimates and the influence of increasing NPP.

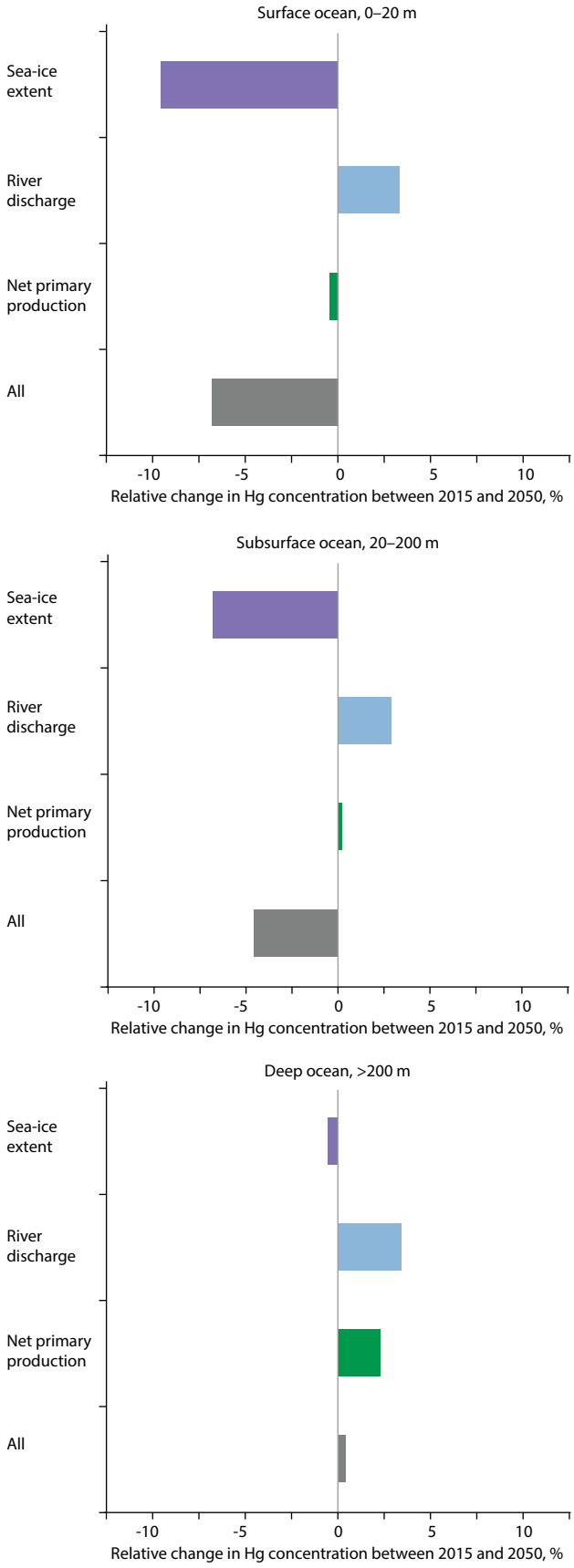

Figure 8.7 Relative change in Arctic Ocean Hg concentrations between 2015 and 2050 in the surface (0–20 m, top panel), subsurface (20–200 m, middle panel) and deep ocean (<200 m, bottom panel), under four climate scenarios: sea ice (pattern), river discharge (blue), net primary production (green) and 'all', which represents their combined impact (dark grey). For each model run, atmospheric depositions are kept constant at 2015 levels while the model is run forced by changes in one variable from 1850 to 2100. In the 'all' scenario, sea ice, river discharge and net primary production change over time while deposition is kept constant at 2015 levels.

This present study shows that, of the 3 climate variables considered, the declining sea-ice cover exerts the strongest Hg reducing forcing on all layers of the Arctic Ocean, whereas river discharge exerts the largest increase, although smaller in absolute terms than sea ice. In the final combined scenario (with atmospheric deposition still kept constant at 2015 levels), the surface and subsurface ocean layers see 5% and 4% Hg declines by 2050, respectively. The cumulative influence of these climate variables in the deep ocean is below a 1% increase. It should be noted that this model does not consider the impact of Hg that evades due to lower sea-ice cover on the atmospheric Hg levels and the potential local and global redeposition of this Hg (Chen et al., 2018). While this study does not present an exhaustive list of climate drivers, it shows their contrasting impacts on the Hg cycle in the Arctic Ocean. It also shows that the climate drivers considered here have a smaller influence on Hg concentrations than the Hg anthropogenic emission control policies.

8.6 Conclusions and recommendations

Conclusions (in numbered bullets) are organized under section headings (section numbers in square brackets) followed by recommendations in italics where appropriate.

What are the future emissions scenarios when comparing existing literature estimates? [8.2]

1. The most aggressive global emissions reductions trajectories can reduce future Arctic Hg concentrations both in the short- and medium-term.
2. Different projections of future emissions globally exhibit a large range, including both substantial increases and decreases. Thus, different trajectories of global emissions changes can have correspondingly substantial effects on Hg concentrations in the Arctic.
3. For deposition to the Arctic, the MFR scenario could lead to a 27% decrease relative to the present-day.
4. Under the No Action scenario, concentrations could increase, implying an even larger effect on Hg concentrations of emissions control policies.
5. For ocean surface concentrations, the projected decrease corresponds to a 36% difference in surface water Hg concentration between the two extreme estimates (No Action and MFR-2020).
6. The magnitude of emissions-induced future changes in Hg levels in the Arctic atmosphere and ocean are likely to be substantial in comparison with climate-induced effects, especially for the ocean.
7. For the atmosphere, climate-induced changes projected under different scenarios relative to the present are comparable in magnitude over mid-latitudes to those calculated under future emissions scenarios.
8. Sensitivity scenarios for key climate parameters and their impact on ocean Hg concentrations show that these effects are likely to be offsetting in different directions.

The changes in Hg deposition to the Arctic that are possible as a result of aggressive emissions reductions may be substantially counteracted by the growing impact of continuing emissions if emissions reductions are not implemented rapidly.

Delaying emissions reduction measures until 2030 means that emissions in the intervening years could completely counteract the impacts of less ambitious emission cuts (the NP scenario) due to the continued cycling of these pre-2030 emissions globally. This underscores the large impacts of prompt action for changing Hg concentrations in the Arctic environment.

What are the predicted changes in mercury concentrations in the atmosphere? [8.3]

9. Scenarios that project socio-economic activity associated with higher greenhouse gas emissions and thus a warmer climate would likely be associated with higher Hg emissions.
10. For the atmosphere, as a result, it is likely that the higher-end estimates of Hg cycling changes under a warming climate would be associated also with larger direct emissions contributions.
11. If climate change mitigation efforts continue and proceed together with Hg mitigation, the relative impact of Hg emissions changes compared with climate impacts for the Arctic may be even larger than that simulated here.

What are the predicted changes of mercury concentrations in the ocean? [8.4]

12. Several areas of uncertainty affect our analysis of future changes across all timescales: for the short-term, the overall magnitude of emissions is uncertain, and different models vary in their estimates of regional source contributions to Arctic deposition (see Chapter 3).
13. In the medium-term, uncertain parameters in global biogeochemical cycle models, including global ocean processes, affect the magnitude of legacy emissions.

In the longer-term, efforts to compare potential changes in Arctic Hg driven by climate and future Hg emissions in a more quantitative way should apply consistent projections of Hg emissions and future climate policy when assessing their relative magnitudes.

What are the changes in total mercury in the future Arctic Ocean? [8.5]

14. Mercury emissions projections that are fully consistent with the state-of-the-art scenarios used in climate modeling are currently not available, challenging researchers' abilities to assess and attribute potential changes in concentrations.

Further development of emissions inventories and use of consistent climate projections in coupled atmosphere-ocean-land models will be necessary to better understand the importance of future emissions changes and to monitor the effectiveness of future controls.

Future research is also necessary to better quantify the processes that influence Hg's global transport, deposition, and cycling and transformations in the Arctic environment. Also, a better understanding and integration of the influence of climate sensitive variables, such as temperature, plankton size and distribution, or erosion, on Hg inputs and speciation are needed to improve ocean Hg modeling.

Appendix 8

Table A8.1. Available literature projections of future anthropogenic Hg emissions.

Region	Base year	Policy scenarios addressed
Global	2006 Global emissions: 2480 Mg	4 IPCC SRES scenarios spanning a range of industrial growth and environmental regulation possibilities (A1B, A2, B1 and B2)
Global	2010 Global emissions: 1885 Mg	Projected (1) future activities and (2) emission factors and emission reduction technology employed in the future per country Current Policy Scenario (CPS): governmental policies and measures existing in 2010 are adopted (APCDs, climate change) New Policies Scenario (NPS): policy commitments and plans to reduce greenhouse gases emissions are fully implemented; the use of Hg in products is reduced by 70% 450 ppm scenario (Maximum Feasible Reduction; MFR): all countries reach the highest feasible/available reduction efficiency in each emission sector
Global and key source regions	2010 Africa: 159.2 Mg China: 565.4 Mg Europe: 81.9 Mg India: 162.3 Mg Latin America: 167.4 Mg North America: 108.5 Mg Russia: 35.9 Mg Rest of world: 273.8 Mg Total: 1554.4 Mg	Projections of energy consumption for: (1) no global greenhouse gas mitigation efforts (BAS); (2) 2°C climate policy scenario (CLIM) Activity projections complemented with assumptions on air pollution and Hg control measures: (1) current national legislation to control air pollution by 2030, but no further effort between 2030 and 2050 (CLE); (2) Maximum Feasible Reduction assuming full adoption of best available technologies to control Hg emissions by 2030 and beyond (MFR)
Global and key source regions	2000 Global emissions: 2189.9 Mg North America: 145.8 Mg Asia and Oceania: 1305.9 Mg Europe and Middle East: 246.8 Mg Africa: 398.4 Mg Central and South America: 92.1 Mg	3 IPCC SRES scenarios: B1, A1B and A1F1 representing the lower, middle and upper bounds of potential climate warming
Asia (India and China)	2010 India: 49 Mg China: 97 Mg (calculated for coal-fired power generation only)	3 technology scenarios: (1) no additional control (NAC); (2) Minamata Flexible (MF; technology and techniques consistent with existing domestic policy plans); (3) Minamata Strict (MS; progression in stringency of Hg control beyond those specified in MF) Two energy scenarios from IPCC SRES: (1) A1B and (2) B1
Europe	2005 Europe Emissions: 145 Mg	2 scenarios: (1) Baseline scenario (BAS), development of European energy system with no measures to control emissions of greenhouse gases and to deploy renewable energies beyond current policies; (2) Maximum Renewable Power (MAX) scenario, decarbonization of European energy system, including the highest possible electricity generation from renewables by 2050 Both scenarios assume full implementation of recent national legislation on air quality (as of mid-2012) by 2030. This includes two sets of technologies: (1) 'Conventional' APCDs reducing Hg as a side effect of their operation; (2) Hg-specific abatement measures
China	2012 China emissions: 539 Mg	7 scenarios: (1) 2030 No policy, no climate or Hg policy beyond current regulations; (2) MC-NCP, end-of-pipe control policy scenario that meets China's commitments under the Minamata Convention (MC) but no climate policy (NCP) beyond current regulations; (3,4,5) 3 climate policy scenarios of varying stringency, CINT3, CINT4 and CINT5 corresponding to carbon intensity reduced by 3% to 5% per year (CINT4 corresponds to China's commitments under the 2015 Paris Agreement); (6,7) 2 scenarios that combine Minamata and climate policies, MC-CINT4 and MC-CINT5

Projections	Underlying assumptions	Reference
2050 Global Hg emissions will likely increase (2390–4860 Mg; change of -4% to +96%); coal combustion in developing countries is the largest driver of emission increase Global emissions increase by 1670–3480 Mg if large scale deployment of advanced Hg sorbent technologies	Share of Hg(0) in total emissions declines from ~65% (base year) to between 50% and 55%; share of Hg(II) increases Sectors included: combustion, pig iron manufacture, cement manufacture, copper, lead and zinc smelting, artisanal and small-scale gold mining (ASGM), Hg mining, caustic soda production	Streets et al., 2009
2035 CPS:1960 Mg NPS: 1020 Mg MFR: 300 Mg	Countries assigned to five groupings representing different levels of technological implementation (technological profiles) of APCDs	Pacyna et al., 2016
2050 BAS scenario Africa: 253.2 Mg China: 1001.5 Mg Europe: 48.1 Mg India: 579.3 Mg Latin America: 240.0 Mg North America: 127.1 Mg Russia: 46.3 Mg Rest of world: 383.8 Mg Total: 2661.4 Mg Hg emissions under CLIM reduced by 45% in 2050 compared to 2010 If current air pollution legislation and climate policies are adopted in parallel, Hg emissions reduced by 60% in 2050 compared to 2010	Fraction of particulate Hg does not exceed 5%; particulate Hg capture efficiency up to 99.99% Hg(0) dominant form for BAS and CLIM scenarios Share of Hg(II) increases slightly over time under BAS (air pollution control measures and structural changes) while share of Hg(0) increases under CLIM (major Hg(0) emission sources remain unaffected by global climate strategies)	Rafaj et al., 2013
2050 Global emissions: 2390–5990 Mg (+9% to 173%) North America: 121.9–305.7 Mg Asia and Oceania: 1208.9–3307.1 Mg Europe and Middle East: 358.1–861.3 Mg Africa: 357.0–789.2 Mg Central and South America: 340.4–720.4 Mg	A1F1 scenario: intensive use of fossil fuel energy A1B: balances all energy sources B1: clean and ecologically friendly energy future Share of Hg(II) and Hg(0) emissions will increase and decrease, respectively (from 67% to 47%; A1B, 49%; A1F1 and 56%; B1), owing to the implementation of flue-gas desulfurization (FGD)	Lei et al., 2014 (base year emissions from Pacyna et al., 2006)
2050 India NAC/A1B: 619 Mg NAC/B1: 249 Mg MF/A1B: 468 Mg MS/A1B: 346 Mg Hg(0) emissions roughly constant between MF and MS China NAC/A1B: 247 Mg NAC/B1: 97 Mg MF/A1B: 156 Mg MS/A1B: 105 Mg	China: capture efficiency of 69%, 82% and 90% under NAC, MF and MS scenarios, respectively India: capture efficiency of 42%, 58% and 71% under NAC, MF and MS scenarios, respectively	Giang et al., 2015
2050 Co-control effects of technologies abating other air pollutants reduce Hg emissions by 35% to 45% BAS: ~145 Mg. MAX: ~100 Mg. The largest fraction of emissions cuts under MAX attributed to deployment of renewables in the power sector		Rafaj et al., 2014
2030 No Policy: 1150 Mg CINT3: 1107 Mg CINT4: 1035 Mg CINT5: 967 Mg MC-NCP: 533 Mg MC-CINT4: 493 Mg MC-CINT5: 470 Mg	Projected emissions calculated with/without changing APCDs and associated Hg speciation depending on scenarios and emission sectors	Mulvaney et al., 2020

9. What are Indigenous Peoples' contributions to and perspectives on the study of mercury in the Arctic?

Lead authors: Magali Houde and Eva M. Krümmel

Contributing authors: Jeremy Brammer, Tanya Brown, John Chételat, Parnuna Egede Dahl, Rune Dietz, Marlene Evans, Mary Gamberg, Marie-Josée Gauthier, José Gérin-Lajoie, Lucy Grey, Aviaja Lyberth Hauptmann, Joel P. Heath, Dominique A. Henri, Jane Kirk, Brian Laird, Mélanie Lemire, Ann E. Lennert, Robert J. Letcher, Sarah Lord, Lisa Loseto, Gwyneth A. MacMillan, Stefan Mikaelsson, Edda Mutter, Tero Mustonen, Todd O'Hara, Sonja Ostertag, Martin Robards, Sarah Roberts, Enooyaq Sudlovenick, Heidi Swanson, Merran Smith, Raphaela Stimmelmayr, Philippe J. Thomas, Vyacheslav Shadrin, Virginia Walker, Alex Whiting

9.1 Introduction

This chapter is devoted to detailing the contributions of Indigenous Peoples to the study of mercury (Hg) in the Arctic, a first of its kind in an AMAP mercury assessment. The overall objectives of this chapter are not to provide a systematic review of the literature, nor a scientific and/or historic analysis of Indigenous involvement in Hg research in the Arctic. Rather, the chapter aims to give a general introduction and some examples of the involvement of Arctic Indigenous Peoples in Hg research and policy development, as well as present some background of Indigenous perspectives and views on Hg contaminants research in the Arctic. Therefore, the development of the chapter relied heavily on contributions and comments from community-based projects and Indigenous representatives.

Arctic Indigenous Peoples have been research 'subjects' of interest for a long time—for example, Inuit in Canada are among the most studied Indigenous Peoples globally, particularly in relation to contaminants (ITK, 2018; Fernández-Llamazares et al., 2020). In considering Arctic Indigenous Peoples as study subjects, guides, bystanders, and other such roles, research has been associated with colonialism and closely tied to exploitation and racism (Wiseman, 2015; ITK, 2018; Moon-Riley et al., 2019). Relationships between Indigenous Peoples and researchers in academia and governments are gradually improving and, in recent years, some of these relationships have developed into partnerships, but this practice is still not a norm (ITK, 2018). A multi-decadal analysis of participatory inclusion of Indigenous Peoples in northern research revealed only a slight increase in their involvement during the period from 1965 to 2010 (Brunet et al., 2016).

A better way forward in conducting research involves recognizing the call for Indigenous self-determination (Brunet et al., 2016; ITK, 2018; Schott et al., 2020). The inclusion of this chapter in the current AMAP mercury assessment is therefore not about the necessity to 'integrate' Indigenous Knowledge (IK) into scientific work. It is about acknowledging and respecting the fact that IK should help, among other things, to direct the research, and determine what is done and how. Indigenous Knowledge should be considered as its own distinct body of knowledge owned by the knowledge holders themselves. As noted in Chapter 7, which addressed the impact of Hg contamination on human health in the Arctic, Arctic Indigenous Peoples are among the most exposed humans on Earth when it comes to Hg contamination. Mercury research in general investigates problems that are prerequisites of food security for Indigenous Peoples: the levels of Hg in the Arctic have ramifications for the safety of the traditional diet, which is part of the foundation of the life, health and culture of Arctic Indigenous Peoples. This chapter therefore provides some insight into the current involvement of Arctic Indigenous Peoples in Hg research and monitoring activities and discusses the approaches that could be used, and improved upon, when carrying out these activities in the future.

Indigenous Knowledge is acquired through year-around observations over millennia, and the holistic and wide range of perspectives that result from that knowledge, as well as the continuous evolution of information and changes that are occurring, have been highlighted in the peer-reviewed literature (e.g., Johnson et al., 2015; Lennert, 2016; Mantyka-Pringle et al., 2017). It should be noted that while many published papers refer to IK and traditional knowledge interchangeably in an Arctic context, the term 'traditional knowledge' is not limited to Indigenous Peoples and can be used for any groups with distinct cultures (Dahl and Tejsner, 2020). For this reason, and because traditional knowledge is often (mis)understood to only refer to the past, many Indigenous Peoples prefer the term 'Indigenous Knowledge', which better captures the ever-evolving aspects of Indigenous Peoples' knowledge. The term 'Indigenous Knowledge' is also preferred by five of the six Permanent Participants organizations of the Arctic Council (for a definition of IK, see Box 9.1). However, different

Box 9.1 Definition of Indigenous Knowledge

In 2015, the Permanent Participants of Arctic Council jointly created the Ottawa Traditional Knowledge Principles, updated in 2018 to the Ottawa Indigenous Knowledge Principles (Permanent Participants, 2018), to provide guidance for the use of Indigenous Peoples' Knowledge within the work of the Arctic Council.[1] The text of those principles includes the following definition:

"*Indigenous Knowledge is a systematic way of thinking and knowing that is elaborated and applied to phenomena across biological, physical, cultural and linguistic systems. Indigenous Knowledge is owned by the holders of that knowledge, often collectively, and is uniquely expressed and transmitted through Indigenous languages. It is a body of knowledge generated through cultural practices, lived experiences including extensive and multi-generational observations, lessons and skills. It has been developed and verified over millennia and is still developing in a living process, including knowledge acquired today and in the future, and it is passed on from generation to generation.*"

[1] See: https://www.arcticpeoples.com/knowledge#indigenous-knowledge

Box 9.2 Distinctions between Indigenous, local and traditional knowledge

The term 'Indigenous Knowledge' is different from the term 'local knowledge', which refers to the knowledge of the residents of a community but is not necessarily embedded within an explicit belief system or Indigenous identity, as Indigenous Knowledge often is (see Dahl and Tejsner, 2000 and references therein; Johnson et al., 2015).

The term 'Indigenous Knowledge' also implies the distinct status and collective rights of Indigenous Peoples, as seen in contrast to the terms 'traditional knowledge' or 'local knowledge' which are not limited to Indigenous Peoples.

In the Eurasian Arctic, the discussion on knowledge terminology is a diverse field. For the Sámi, Nenets, Chukchi, Evenki, Evens and other nations with the status of Indigenous Peoples, the term IK may be appropriate. By contrast, there are groups such as the Komi, Veps, Karelians, Sakha and others who are seen either as national minorities or linguistic groups even though, in other contexts, they would have been considered Indigenous Peoples. For example, although the Komi are engaged in trading and practice a culture that is very similar to Nenets reindeer herding, they are not recognized as Indigenous Peoples. In this case, the use of the terms 'local knowledge', 'traditional knowledge' or a culturally based approach to terminology, for example 'Komi knowledge', may be more appropriate.

In Greenland (part of the Kingdom of Denmark), the vast majority of the Greenlanders are Inuit and recognized as Indigenous Peoples, and yet the favoured term is 'local knowledge' (Dahl and Tejsner, 2000). Other terms, such as 'traditional knowledge', 'traditional and local knowledge', 'Indigenous Knowledge' and 'user knowledge', are used inconsistently in legislation and governmental papers relating to different sectors (Dahl and Hansen, 2019). While Greenlanders identify as 'one people' (the Government of Greenland is a territorially defined public government with equal rights for all citizens regardless of ethnicity) there is still a need to distinguish between knowledge holders living in geographically isolated settlements across a vast territory (see more under 'Greenland' in Section 9.3).

These examples show that the context of the chosen terminology varies, and the rationale for choosing a term (Indigenous Knowledge, local knowledge, or traditional knowledge) should be clear, well defined, used in a consistent manner, and not interchangeably with the other terms, to avoid confusion.

regions and peoples have different preferences and practices when referring to their knowledge, which are respected in this chapter, and some are reflected in Box 9.2.

9.2 What is the history of the contributions of Indigenous Peoples and communities to environmental monitoring in the Arctic?

Monitoring of the Arctic did not begin with the introduction of formal scientific environmental monitoring (Pfeifer, 2018). Arctic Indigenous Peoples have relied on their knowledge, which is passed down from one generation to the next (ICC-Alaska, 2015b; Johnson et al., 2015). This knowledge of environmental conditions, wildlife and vegetation has been the basis for their survival, their culture, and sense of locality (Lennert, 2016). It represents a rich repository, which can be used in symbiosis with scientific research for a better understanding of the changing environment and the interaction between components of the Arctic environment. The value of IK has been increasingly recognized by scientists and governments in the Arctic and beyond (Danielsen et al., 2014; Mantyka-Pringle et al., 2017; Arctic Council, 2018; Ban et al., 2018; Government of Canada, 2019a, 2019b), and the inclusion of IK and the involvement of Indigenous communities in decision-making processes has been found to result in more efficient and adaptative management (Danielsen et al., 2010). A good example of this is Laponia, a World Heritage site in Jokkmokk, where national parks and reserves are co-managed by Sámi reindeer herding communities, municipalities, the county administrative board and the Swedish Government.[1] There are many examples of Arctic Indigenous monitoring activities and, while an exhaustive list outlining and describing all of these activities in detail is beyond the scope of this chapter, we aim to provide a broad overview of a range of circumpolar Arctic monitoring initiatives that involve Indigenous Peoples, Hg, and mobilize IK.

Many regional and local governments in the circumpolar Arctic conduct environmental monitoring and/or research activities to support local food security and general policy and decision-making processes, and IK plays an important role in these activities. In Canada, various agreements and programs have helped to recognize the effective role of Inuit, First Nations, and Métis in wildlife and resource management, as well as in policy and program development. In Nunavik (Quebec, Canada), the Nunavik Research Centre (NRC) was established in 1978 to monitor and collect land use and ecological data in the region.[2] The NRC operates a number of ongoing wildlife monitoring programs, often working with external scientists, but under the mandate that their research responds to the needs, questions, objectives and concerns of Nunavimmiut (residents of Nunavik) and respects and utilizes Inuit values and knowledge in the process. Moreover, the Inuvialuit Settlement Region (ISR, Canada) has a community-based monitoring program (ISR-CBMP) to support Inuvialuit in protecting and preserving the Arctic wildlife, environment and biological productivity to enhance decision-making, and to achieve the principles of the Inuvialuit Final Agreement (IFA; COPE, 2005). Alongside the Gwich'in, the Inuvialuit have also been integral in the Arctic Borderlands Ecological Knowledge Society (ABEKS)'s environmental monitoring program that

[1] See: https://laponia.nu/om-oss/laponiatjuottjudus/ (Swedish Language).

[2] See: https://www.makivik.org/nunavik-research-centre/

documents and contributes local knowledge to co-management in the range of the Porcupine caribou herd (*Rangifer tarandus granti*).[3] First Nations in Northwest Canada have increasingly been stewarding their traditional territories by launching Guardian Programs that vary greatly in their scope but often engage in ecological and climate monitoring.[4] Since 2004, the Aboriginal Aquatic Resource and Oceans Management (AAROM) program has also been supporting Indigenous groups, particularly First Nations and Métis, to manage aquatic and ocean resources as well as to participate in related advisory, co-management and decision-making processes.

In other jurisdictions, Indigenous Peoples and their knowledge are not considered to be distinct entities. As Greenland is a self-governing territory where the majority of the population consists of Inuit, no specific structure for IK inclusion within the political decision-making system has been established. The internal differences in regional identities and dialects have not stood in the way of Greenlanders identifying as 'one people' while also identifying the Inuit as the Indigenous Peoples of Greenland. Through the Act on Greenland Self-Government from 2009, which constitutes an extension of powers from the Home Rule Act of 1979, the people of Greenland is a people pursuant to international law with the right to self-determination (Act on Greenland Self-Government, 2009). While the Self-Government Act does not mention Indigenous Peoples as such, Denmark has ratified ILO C169[5] and UNDRIP[6] on behalf of Greenland. The Act also established the Greenlandic language as the official language. Even though the Government of Greenland is a territorially defined public government with equal rights for all citizens regardless of ethnicity, its institutions, laws and practices have evolved on the basis of the Greenlanders' own aspirations and visions for the future and of their having *de facto* control of the democratic processes and decision-making bodies. This is reflected in legislation concerning nature conservation, fisheries and hunting, where user or exploitation rights and licenses, whether for income or recreational purposes, consistently privilege the 'permanent' residents. In the sustainable management of natural resources, including through monitoring, a strong emphasis is put on the knowledge of hunters, fishermen and the local communities. The notion of 'local knowledge' is pertinent given the vast territory and the isolated geographic settlement patterns of the country. Furthermore, the Government of Greenland is obliged through fisheries and hunting legislation to consult with the Fisheries Council and the Hunting Council on all general management issues. Hunters' and fishermens' organizations are standing members of the councils. Furthermore, the Government of Greenland is obliged through the Parliament Act on Hunting to consult with biologists and it has an obligation to also receive input from the hunters and users of marine mammal resources in decision-making processes. Additionally, the Greenland Institute of Natural Resources, whose mandate is to provide the scientific basis and advice to the Greenland Government on the sustainable utilization of living resources (such as fisheries and hunting quotas), includes local knowledge in its scientific work.

In addition to more formalized regional research and environmental monitoring activities, many Indigenous communities have established their own projects or have been, or are currently, involved in studies and/or ongoing monitoring activities led or co-led by academic, government and/or consultant scientists. In the literature, these activities are often referred to 'community-based' research (CBR) or monitoring (CBM; see Box 9.3), terms that are predominantly used in North America. It should be noted that in some regions, the terms 'community-led' or 'community-driven' monitoring are preferred, and sometimes used in this chapter, to reflect the leading nature of Indigenous communities' involvement. Monitoring and research projects carried out in partnership with Indigenous Peoples and/or Indigenous organizations that involve a co-production of knowledge approach follow similar principles of CBM/R (as outlined in Box 9.3) but do not necessarily take place in a community. A 'co-production of knowledge approach' brings together different knowledge systems (IK and science) while building collaborative and equitable partnerships (ICC, 2016).

Box 9.3 Community-Based Monitoring/Research (CBM/R)

While formal monitoring initiatives may describe themselves as 'community-based' the term is used broadly to describe a wide spectrum of different approaches to community engagement. At one end of that spectrum are approaches where government or academic researchers may recruit community members to collect data or samples for studies driven by the information needs of institutions located outside the community. Yet the problem with this kind of approach is that the community is not leading or co-leading the research; from an Indigenous perspective, community-based monitoring or research (CBM or CBR) ideally means research where a community determines the reason for the research or monitoring project, which should address a concern or issue as identified by the community based on their needs, priorities and interests (Johnson et al., 2015). At the other end of the spectrum, we find community-based approaches in which the community is indeed involved in all stages of the project (and leads or co-leads it): planning, implementation, data collection, interpretation and analysis, dissemination, communication and sharing of data, and the application of data for decision-making. In an Indigenous community, CBM/R done in full meaningful partnership with IK holders is more likely to utilize IK as deemed appropriate by the Indigenous partners.

[3] See: https://www.arcticborderlands.org/reference

[4] See: https://www.ilinationhood.ca/

[5] See: International Labour Organization (ILO). C169 - Indigenous and Tribal Peoples Convention, 1989 (No. 169). Available at: http://www.ilo.org/dyn/normlex/en/f?p=NORMLEXPUB:12100:0::NO::P12100_ILO_CODE:C169

[6] See: United Nations Declaration on the Rights of Indigenous Peoples (UNDRIP). Available at: https://www.un.org/development/desa/indigenouspeoples/declaration-on-the-rights-of-indigenous-peoples.html

To gain a better understanding of the current state of community-based monitoring in the Arctic, a multi-year initiative was launched in 2012 as part of the Sustaining Arctic Observing Networks (SAON), which yielded an in-depth report of 81 programs across the circumpolar Arctic (Johnson et al., 2016), as well as the development of a searchable online atlas, the Atlas of Community-Based Monitoring and IK in a Changing Arctic (SAON et al., 2021).[5] While the CBM atlas does not focus on contaminants, several projects listed in the atlas include work on contaminants, and some of the projects included in this chapter are featured in the CBM atlas (e.g., the project in Kotzebue, Alaska, some projects in Canada and some projects of the Snowchange Cooperative in Europe).

The present chapter reviews some of the Indigenous contributions in Hg research and monitoring activities in the Arctic. It should be noted that the described activities are not an exhaustive list but present merely a flavor of activities that have been completed or are ongoing.

9.3 What examples are there of mercury contamination research done with or by Indigenous Peoples?

A wide variety of monitoring and research programs, particularly those investigating contaminant levels in wildlife and fish, benefit from understanding the environmental and ecological contexts in which the research is being done, which IK is uniquely positioned to offer. Ongoing observations by Indigenous Peoples on sea-ice coverage and climate conditions, animal distribution, behavior, diet and body condition, the characteristics of prepared foods and so on can substantially enhance the interpretation of results related to contaminants levels, which is particularly visible in CBM/R studies. This research is crucial to support food security, health and the wellbeing of Arctic Indigenous Peoples, as well as to inform regional, national and international policy development. For example, in the case of Hg, Arctic research has been instrumental in the negotiation of the United Nations' Minamata Convention on Mercury (see details in Section 9.4).

Indigenous Peoples from several regions of the Arctic have been involved to varying degrees in Hg environmental monitoring and research (see Figure 9.1). With respect to Greenland, at least five large towns and villages have consistently participated in such work, including Qaanaaq, Qeqertarsuaq, Nuuk, Tasiilaq/Kulusuk and Ittoqqortoormiit (Glahder, 1995; Dietz et al., 2001; Sandell et al., 2001; Born et al., 2011). Community partnerships and IK are essential in East Greenland due to their input on sampling and interpretation of information from biological markers in wildlife exposed to contaminants and diseases. In Canada, numerous communities in Nunatsiavut (Labrador), Nunavik (Quebec), Nunavut, the Inuvialuit Settlement Region (ISR), the Northwest Territories, and Yukon have led or participated in wildlife and human contaminants biomonitoring and related research projects. Many of these studies have been supported for more than 25 years by the Northern Contaminants Program (NCP), as well as by local, provincial/territorial and national organizations. The consistent source of funding and the requirement of collaboration between Indigenous communities/organizations and scientists is a unique aspect to the NCP, which explains the high number of Canadian examples found in this chapter. In other Arctic countries, community-based research and monitoring efforts that focus on Hg are mainly localized efforts undertaken by communities in partnership with academic researchers and/or independent organizations, making them harder to capture.

Multiple projects are described in more detail in the following section. To include examples in this chapter, principal investigators of CBM projects in the circumpolar Arctic were contacted and asked for a description of the activities. Only those projects were included where leaders provided a response and were willing to contribute content. All are listed as contributing authors in this chapter. Additionally, it needs to be recognized that Indigenous Peoples have a holistic understanding of their environment, and while some of the CBM projects may not have a focus on Hg it may be recognized to play a role in environmental and human health and be investigated as one factor among others. Therefore, projects involving Hg research were also included in the chapter even where Hg was not the central focus. Finally, several of the described projects provided Hg data that have been included in the other chapters of this assessment (see Chapters 2, 5 and 6). Therefore, to avoid repeating material from earlier chapters, this chapter does not report Hg data. The map in Figure 9.1 and following descriptions are just an indication of the breadth of existing Hg contaminant projects by region and not a complete list of initiatives (see also Appendix Table A9.1 for detailed information). Note that the identification (ID) numbers in Figure 9.1 correspond to the superscript numbers in the project descriptions in the text of the chapter below and to the project numbers given in Appendix Table A9.1.

For Sweden, Finland and Russia, the case studies outlined are described in more detail in an electronic annex to this assessment report (see EA Case Studies 1–6); references to the annex are made, where relevant, in parentheses (see Electronic Annex).

United States of America

Alaska

In the northernmost state of the United States (Alaska), the Native Village of Kotzebue (Tribal Government) has been investigating Hg in subsistence species in Kotzebue Sound and surrounding areas using community-based and holistic perspectives.[ID1A] Earlier research in the mid-1990s directly addressed community concerns about the potential role of contaminants (e.g., radioisotopes and heavy metals) in a caribou mortality event. However, since 2004, collaborative studies, often by graduate students and published in peer-reviewed publications, have been developed between researchers and the Environmental Program at the Native Village of Kotzebue, as they work together on the Hg assessment of mostly marine biota

[5] See: www.arcticcbm.org

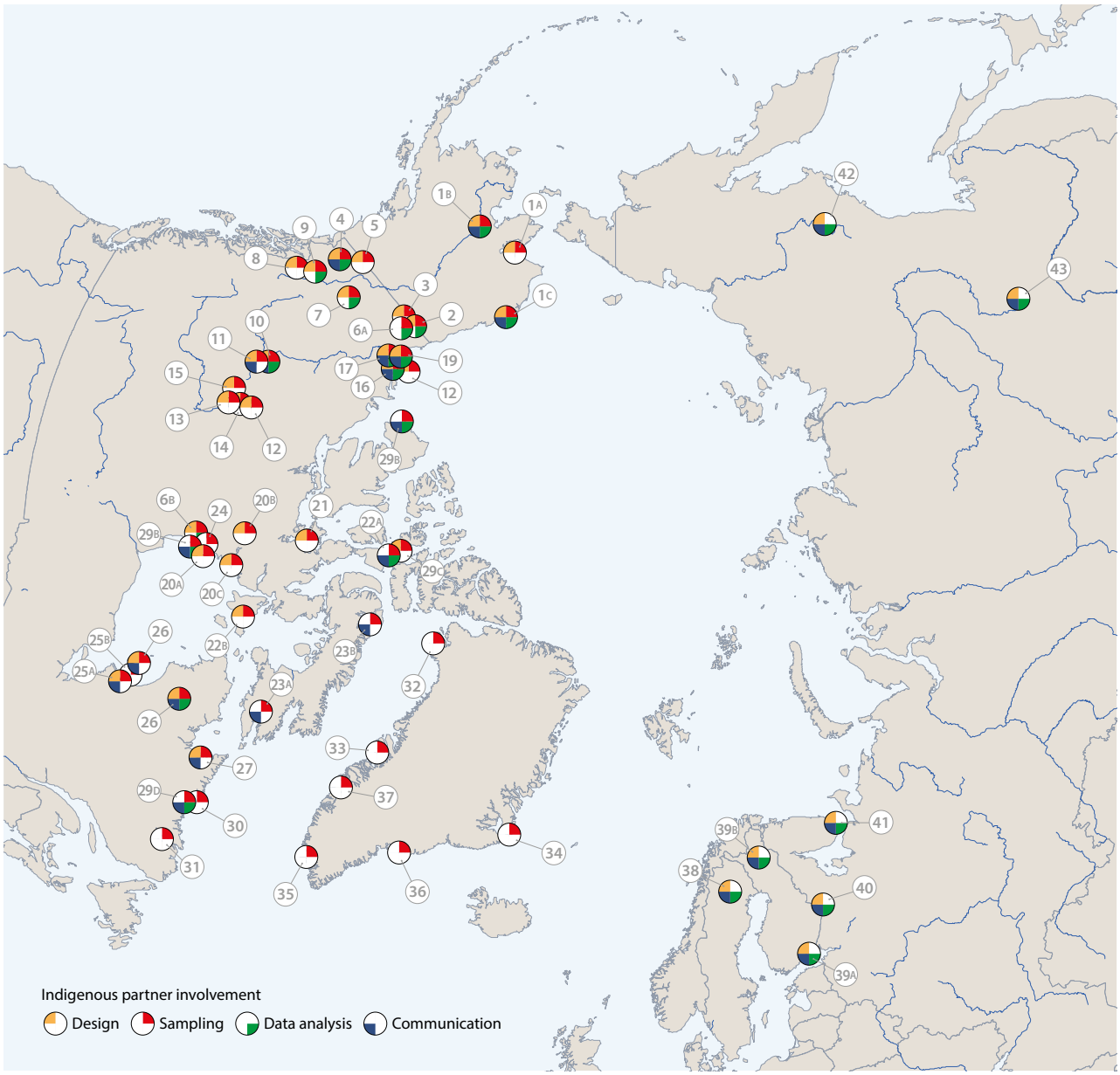

ID	Species/ matrices studied
1A	Seals, fish, caribou
1B	Water, sediment, permafrost
1C	Bowhead whales, seals, walrus, polar bears, beluga
2	Muskrats
3	Fish
4	Fish
5	Fish
6	Caribou (Qamanirjuaq and Porcupine herds)
7	Moose, fish
8	Moose, fish
9	Fish
10	Humans (hair, blood, urine)
11	Water, sediment, zooplankton, benthic invertebrates, fish
12	Invertebrates, fish
13	Fish, water, sediments
14	Fish
15	Fish

ID	Species/ matrices studied
16	Fur bearers
17	Burbot
18	Beluga
19	Husky Lakes, Canada; 2011, 2012; water, sediment, aquatic food web (zooplankton, fish)
20	Lichens, mushrooms, seaweed
21	Fish
22	Seabirds (eggs, tissues)
23	Ringed seals
24	Polar bears
25	Blue mussels, sea urchins, plankton, marine fish, common eiders, ringed seals
26	Marine, freshwater, terrestrial assessments
27	Water, sediment, lichen, fish, birds, seals
28	Humans (blood, urine, hair, blood) and country foods
29	Ringed seals
30	Ringed seals and prey
31	Water, invertebrates, fish, ringed seals

ID	Species/ matrices studied
32	Polar bears, ringed seals, black guillemots, sculpins
33	Ringed seals, black guillemots, sculpins
34	Polar bears, ringed seals, black guillemots, sculpin
35	Caribou, Arctic char
36	White-sided dolphins, pilot whales, killer whales
37	Harbor porpoises
38	Freshwater, northern pike, reindeers
39	Northern pike, burbot, sea eagles and other apex predators
40	Northern pike, perch, burbot, human health, other apex predators
41	Ponoi river
42	Kolyma fish
43	Water quality, fish, human health

Figure 9.1 Examples of community-based/led Hg monitoring and research activities involving Arctic Indigenous communities and regions described in this chapter. For further details on the projects shown in the figure, see Appendix Table A9.1.

in Northwestern Alaska. The partnership between professional researchers (primarily in academia) and the local tribal community began with outreach by the Tribe to the University of Alaska Fairbanks Wildlife Toxicology Laboratory to begin a formal relationship to identify mutual research priorities. Areas of interest and research questions were cooperatively developed between the Tribe, their IK holders (harvesters of fish and wildlife) and the researchers. The cooperative and strategic sharing of resources and the technical skills of researchers and tribal citizens were integrated into formal and informal discussions and research products. Short-term studies were then carried out in an effort to develop an understanding of baseline levels of Hg along with other nutrients and elements in subsistence species, primarily fish and ice seals (Moses et al., 2009; Cyr et al., 2019b). Indigenous Knowledge has been the motivating and organizing force behind the Kotzebue collaborative studies and has been used to elucidate the context for the local ecology (i.e., local species and their trophic level relationships) and to identify the species most of interest to local consumers. Indigenous hunting and fishing expertise and knowledge have been critical for the donation of samples with local members of the teams having played key roles within the practical and logistic aspects of the partnerships. Finally, local members have guided the development of responsible and effective ways to return information to community members; information is reported back to the community in a multimedia fashion and in detail (i.e., on specific tissues and preparation methods along with cost/benefit information related to nutrition, contaminants risks and cultural factors) such that consumers can safely and confidently make choices about their subsistence foods. These efforts were integrated with the State of Alaska Fish Biomonitoring Program to assure reliable and consistent advice to the community.

A further example of effective collaboration between IK holders and scientific researchers is the Indigenous Observation Network (ION), a community-based water quality and active layer/permafrost program, established in 2006 by Yukon River Inter-Tribal Watershed Council (YRITWC) and the U.S. Government.[ID1B] The program has been developed to assess climate change impacts to surface water in the Yukon River basin but expanded its focus to address Alaska Native Tribes' subsistence resources concerns with water sampling for Hg around landfills over the years.[6] Local community concerns have been also addressed by conducting water and sediment sampling at historical and present mining sites around Birch Creek, Tanana, Hughes and the Ruby region for Hg analysis, and support has been given to the White River First Nation and Carcross/Tagish First Nation with water quality baseline monitoring for their water governance efforts.[7] All data generated by these projects, including IK, are owned by the Alaska Native Tribes and First Nations. The scientific directives for projects are based on the resolutions adopted by the Alaska Native Tribes and First Nations signatories every two years at a summit hosted by the YRITWC. These resolutions can be related to specific regional/local concerns for water resources or larger scale concerns which affect the entire watershed. The science team identifies funding opportunities and partners, implements projects and disseminates the results/outcomes via community reports, as well as presenting project results and updates to the signatories at the next YRITWC summit. The program relies on communities' input when it comes to the development of sampling strategy, which is based on their knowledge of the area, historical information about any environmental changes over time and relies on their logistical support. The ION is also a partner on the ongoing Arctic Great Rivers Observatory (ArcticGRO) project which investigates the Hg export from major Arctic rivers (e.g., Zolkos et al., 2020).

Since the early 1980s, food safety concerns over adverse health effects of contaminants in whales and subsistence consumers on the North Slope (Alaska) led to the monitoring of contaminants, including heavy metals, in foods with a focus on the bowhead whale (*Balaena mysticetus*).[ID1C] This collaboration has been led by the North Slope Borough Department of Wildlife Management, the Alaska Eskimo Whaling Commission and the captains association of the 11 whaling communities (Braund, 2018). The bowhead whale monitoring program has resulted in one of the longest time series of contaminant information on an essential Arctic subsistence species (Bolton et al., 2020; Schultz et al., 2020). This co-production of science and the IK-based interpretation of ecological, physiological, behavioral and pathological phenomena has been expanded to include other important marine mammal subsistence resources such as ice seals, walrus (*Odobenus rosmarus*), polar bears, (*Ursus maritimus*) and belugas (*Delphinapterus leucas*).[8] The collaboration with hunters and community members is essential for this ongoing monitoring. This joint work depends greatly on IK and on the sharing of knowledge; hunters and communities provide rich and meaningful spatial-temporal scale wildlife information and data on traditional subsistence resources and the environment.

Alex Whiting (Kotzebue, Alaska):

> *"Contaminant studies are in particular an area where it is crucial that research take into consideration the potential impacts on Indigenous communities. Arctic cultures are defined by their relationship with fish and wildlife species that sustain their cultural, nutritional and spiritual needs and way of life. This means that contaminant findings should not be presented as in a vacuum, but should be contextualized along with the ameliorating effects of the nutritional, cultural, communal, psychological and physiological benefits of participating in the procurement, processing and sharing of fish and wildlife species. Researchers should always take advantage of the opportunity to develop formal relationships with communities and to develop research questions in true collaboration with Indigenous participants."*

[6] Community reports are available at https://www.yritwc.org/science and https://www.yritwc.org/library

[7] Research data produced by the YRITWC mining program for Alaska Native Tribes and First Nations is available at https://www.yritwc.org/mining and https://yritwc.maps.arcgis.com/apps/InteractiveFilter/index.html?appid=55a0f096da3345c9a0b1da0756e8a116

[8] See: http://www.north-slope.org/departments/wildlife-management

Canada

British Columbia, Yukon and Northwest Territories

The vast Arctic territories of Canada are inhabited by numerous Indigenous Peoples including Inuit, First Nations, and Métis populations. Many Hg-related initiatives have been developed by Indigenous groups in collaboration with scientists. In the Yukon, several sporadic Hg projects in fish and wildlife have been initiated, developed and carried out by First Nations. In 2007, a project on Environmental Change and Traditional Use of the Old Crow Flats, Yukon (*Yeendoo Nanh Nakhweenjit K'atr'ahanahtyaa*) was established (Wolfe et al., 2011).[ID2] This project, a collaboration between the Vuntut Gwitchin First Nation, the Government of Canada, Department of Environment (Government of Yukon), and university researchers, included the measurement of Hg concentrations in muskrat (*Ondatra zibethicus*) tissues to verify that this traditional food source remained secure. In 2014, in the same region of Old Crow, Hg was investigated in seven species of fish collected by the community to determine healthy food choices for northerners, which assisted in sample preparation for Hg analysis.[ID3] It was found that species, age, and fish length were related to Hg concentrations (Northern Contaminants Program, 2021). Mercury concentrations in burbot averaged higher than the guideline measurements for commercial sales. In 2015, Kluane First Nation, based in southwest Yukon, initiated a study on Hg in lake trout (*Salvelinus namayush*) and lake whitefish (*Coregonus clupeaformis*) in Kluane Lake that complemented an existing food security initiative.[ID4] University researchers worked in support of the First Nation; Indigenous harvesters and youth collected and processed fish, and the local council supported a youth exchange to the involved universities, where they learned how to analyze fish for Hg and age and communicated results back to the community at the First Nation annual general assembly and through radio interviews. The youth exchange was meant not only to build capacity but also to empower youth in undertaking cross-cultural stewardship initiatives, to expose them to the post-secondary environment and generate a positive experience in applying and working with science, technology, engineering and math (STEM) skills. The process and results were featured in an Indigenous-led film called 'Remembering Our Past, Nourishing our Future' (Kluane First Nation, 2016). In Yukon, fish are also currently being collected for Hg measurement by the White River First Nation in Beaver Creek.[ID5] This project was initiated, designed and carried out by the White River First Nation with some assistance by scientists.

The First Nation in Old Crow is involved in the annual Hg assessment of the Porcupine caribou herd (see Chapter 2 for temporal trend data).[ID6] Ongoing discussions between the Vuntut Gwitchin Government and the Porcupine Caribou Management Board continue to refine the project in terms of additional questions to ask and variables to consider when analyzing and interpreting Hg concentrations in caribou.

Mercury is also currently being measured in moose (*Alces alces*) and fish collected by the First Nation of Na-Cho Nyak Dun in Mayo, which have been responsible for the project from the beginning to the execution with some assistance from a scientist.[ID7] Similar projects in moose and fish were initiated in Atlin (Northern British Columbia) and Carcross (Yukon) by the Taku River Tlingit First Nation and the Carcross/Tagish First Nation, respectively.[ID8] These projects illustrate how longer-term studies evolve over time and develop into successful ongoing collaborations with Indigenous communities; interpretations of Hg concentrations in wildlife and Hg dynamics in the environment are informed by IK, new questions and variables are identified and considered. This is also the case in reference to the annual Hg monitoring conducted from trout (*Salvelinus alpinus*) in Laberge and Kusawa lakes near Whitehorse, Yukon.[ID9]

In addition to fish and wildlife, a human biomonitoring project was initiated by Gwich'in, Dene and Métis communities in collaboration with university scientists and aimed to investigate human exposures (using blood, hair and urine) to a variety of contaminants, including Hg, as well as examining biomarkers for nutrients (e.g., omega-3 polyunsaturated fatty acid and selenium).[ID10] Consultation between the university-based researchers and Indigenous communities shaped several aspects of the work plan, including the timing of the sample collections, local coordinator hiring plans, public consultation meetings, endpoint selection and participant inclusion criteria. This work, carried out over four years (2014–2018) by local coordinators in ten communities, was also linked to wildlife community-based monitoring programs. This human biomonitoring project relied on IK, firstly, in the form of community engagement, which guided the return of results and knowledge transfer. Perspectives provided by residents helped align the mission and research design with local priorities and concerns. Secondly, IK was relied upon when it came to knowledge translation. To facilitate technical communication between researchers and community members, terminology workshops were organized with local Indigenous organizations, and terms were reviewed with First Nations Elders to discuss their meaning and translations (e.g., contaminant and risk). In addition to helping better bridge Indigenous concepts and knowledge, these discussions served as catalysts to identify and develop shared values and to enable cross-cultural communication.

As well as the projects above, a multi-year study on spatial variability in Hg concentrations in food fish and freshwater lake ecosystems (e.g., water, sediment, invertebrates) is currently underway in the Dehcho Region. This multi-stakeholder, community-driven research project involves Dehcho First Nations, as well as Ka'a'gee Tu, Jean Marie River, Deh Gah Gotie, Liidlii Kue, Sambaa K'e, and Pehdzeh Ki First Nations.[ID11] Annual sampling occurs for 2 to 3 weeks each summer in wilderness camps and is conducted by a joint crew of university researchers and Indigenous Guardians (local community members employed as 'eyes on the ground' in Indigenous territories), which fosters two-way knowledge exchange. Guardians are involved with every aspect of sample collection and field processing. Indigenous Knowledge informs which lakes are fished, how/when they are fished, what types of samples should be analyzed (e.g., smoked fish, fish guts, liver) and other variables that should be considered, such as beaver (*Castor canadensis*) activity in the catchment and presence of permafrost slumps. Indigenous Knowledge has also led to a community-led spin-off project on how fish

growth rates could be stimulated by harvest. Results from projects are presented annually by scientists to individual communities in face-to-face meetings, at which time priorities for the upcoming year are re-evaluated in response to community and harvester concerns.

Other projects in the Northwest Territories have investigated metal contamination of Yellowknife Bay (Great Slave Lake) from gold mining to address concerns from the Yellowknives Dene First Nation over contamination in local fish (2013–2015). Yellowknife Bay is an important water body for subsistence fishing, including for whitefish, which were being collected for a school lunch program (Chételat et al., 2017).[ID12] The community was involved in framing the questions of this project and participated in the collection of fish.

In the region of Great Slave Lake, contaminants in fish and fish health have been monitored since the 1990s with help from the communities of Fort Resolution, Lutsel K'e, and Hay River Reserve; most of this research has been conducted under the NCP (results in Chapters 2 and 5). The earliest Hg work was with Deninu Kue First Nation at Fort Resolution, who had been concerned for many years of the impact of a decommissioned mine on metals in the lake.[ID13] A study was therefore designed with the community to investigate metals in water and sediments as well as in fish offshore of the former mining site and predatory fish commonly consumed. Community members contributed to study design and participated in the sampling. Reports were produced and meetings held in the community to discuss findings (Evans et al., 1998). Fort Resolution continued to work with researchers and has developed several successful partnerships including community-based monitoring of water quality and specialized studies, including Hg, with partners from the University of Saskatchewan (Carr et al., 2017, Baldwin et al., 2018). In the same region, the Lutsel K'e First Nation was concerned that the skinny (i.e., malnourished and thin) fish found in Stark Lake could be related to contaminants from the abandoned Stark Lake Exploration Site, an exploratory uranium mine.[ID14] Several studies were conducted in the period between 2003 and 2013 on lake trout provided by the community and fish were analyzed for contaminants and the issue of skinny fish investigated (Evans and Landels, 2015). Skinny fish have been observed elsewhere. For example, the community of Jean Marie River observed numerous skinny walleye (*Sander vitreus*) at Trout Lake and initiated the collection of skinny and normal walleye and provided them to the same researcher who investigated Stark Lake trout. This walleye study also determined that the walleyes were very old, possibly near the end of their lives, and contained relatively high Hg concentrations.[ID15]

Since 2010, the Tłı̨chǫ Aquatic Ecosystem Monitoring Program (TAEMP) in the Northwest Territories (NWT) has developed and implemented an aquatic ecosystem monitoring program of lakes important to the communities based on IK and science. The program has involved a rotating sampling through each of the four Tłı̨chǫ communities with studies designed to address questions as to whether the water is safe to drink and the fish safe to eat. A fish camp is held on the land with Elders, youth and research scientists the heart of this program. A detailed report is produced annually with results including Hg levels in fish and sediments, and data are provided to the territorial Health Department for assessment (Northern Contaminants Program, 2021; TAEMP, 2019).

In the same region, Gwich'in and Inuvialuit knowledge holders from Aklavik, Fort McPherson, Inuvik, and Tsiigehtchic had been observing, over several decades, increases in the number of beavers and river otters (*Lontra canadensis*), alongside marked declines in muskrat densities, across much of the Mackenzie Delta.[ID16] The Gwich'in Renewable Resources Board, the Gwich'in Renewable Resources Councils, and the Aklavik and Inuvik Hunters and Trappers Committees then engaged researchers to study potential drivers of change, including Hg. Project planning and reporting were conducted within the established decision-making frameworks of partner organizations (e.g., the Gwich'in Renewable Resources Board and local Renewable Resource Councils) and involved regular face-to-face meetings between scientists and IK holders (see Hovel et al., 2020). Indigenous Knowledge holders were active in the selection of sites, collection of samples, trapping of animals and recording of observations. Fieldwork was conducted with a multi-generational team of IK holders typically composed of youths, adults, and Elders; IK was recorded each day through a daily camp log. This project facilitated the sharing of both scientific and IK with the broader community through activities at local schools and college campuses, including giving talks and leading activities (e.g., animal dissections). A contaminant study was also initiated by a Gwich'in fisheries biologist in Inuvik in collaboration with federal researchers, to address concerns about the quality of loche (burbot; *Lota lota*) livers in different channels of the Mackenzie River delta. The study investigated liver appearance, contaminants and parasite load (Cott et al., 2018).[ID17] It was found that the fish with the poorest quality liver were older fish with higher parasite loads. Results also showed that traditional methods (visual examination by skilled fishers with decades of experience) effectively assessed the quality of livers by identifying the most nutritious (high in fat) and safest (low parasite load) livers. However, these methods were not effective in screening livers for anthropogenic contaminants. This highlights the importance and value of linking IK into scientific studies.

In the Inuvialuit Settlement Region (ISR), a co-management framework was put in place through the Inuvialuit Final Agreement (IFA; COPE, 1984) to conserve and manage natural resources, such as wildlife and fisheries. The Fisheries Joint Management Committee (FJMC), under the guidance of the Inuvialuit Game Council, advises and represents the collective Inuvialuit interests on policy and research. Together, the federal government and the FJMC have developed conservation management efforts including the long-term Beluga Harvest Monitoring program (1980–present) through partnerships with Inuvialuit Hunters and Trappers Committees and local hunters. This program has been providing scientists access to beluga tissues and has allowed for contaminants measurements to be taken, including Hg (results available in Chapters 2 and 5).[ID18] The program has evolved over 40 years, and is effective at responding to community questions, meeting management needs, and ensuring that scientific investigations can be carried out, bringing together a community of knowledge holders to collaborate on the study of beluga health (Loseto et al., 2018). Figure 9.2 illustrates

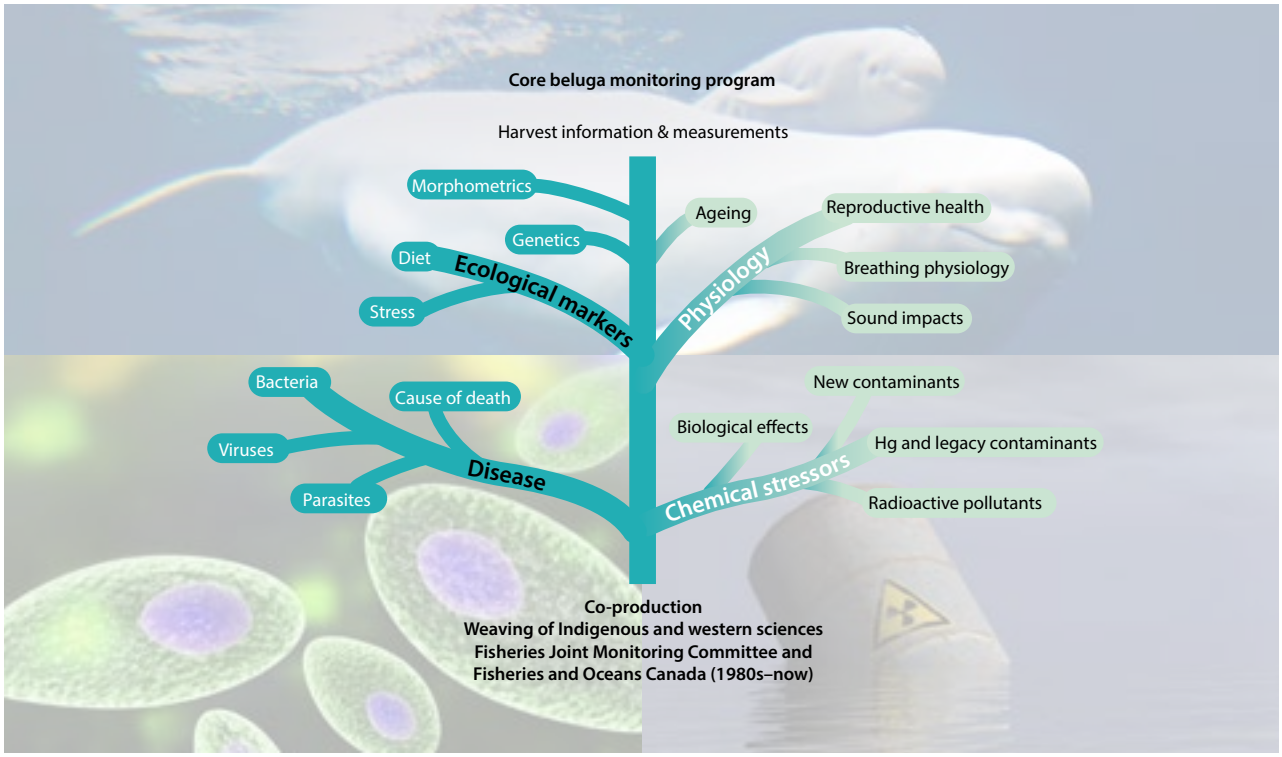

Figure 9.2 The collaborative Beluga harvest and health monitoring and research program (ISR, Canada) as an example of co-production of knowledge. The trunk of the tree is maintained by communities, their knowledge, their harvest programs and their priorities that has resulted in numerous branches of new knowledge and research focused on health, some representing short projects addressing a question and others being long term monitoring such as contaminants as part of food security and safety priorities (modified from Loseto et al., 2018).

the integrated nature of the core beluga monitoring program in the ISR, which not only covers contaminants but many other aspects that are related to beluga health. This highlights the holistic approach taken by the program, which is guided by Indigenous Knowledge, and IK holders are key to the program's investigatory aims. As the program conducted research, gained knowledge and highlighted questions with regards to beluga, the need to identify knowledge gaps and set priorities led to the first Beluga Summit, an event held in 2016 in Inuvik. Participants included members of all six ISR communities, Alaskan Iñupiat partners, as well as local, regional and national organizations and scientists (Loseto et al., 2018).

In this ongoing monitoring, Indigenous communities are part of the planning, field crew, sometimes participate in lab analyses and often are part of the dissemination of results at meetings and conferences. The documentation of IK in the beluga health program was formalized through the creation of IK indicators for long-term beluga monitoring (Ostertag et al., 2018); other projects as part of the program also document IK on hunting, on the processing of beluga, as well as on the impacts of climate change on beluga subsistence in Tuktoyaktuk (Waugh et al., 2018). Most recently, a project was developed based on outcomes from the 2016 Beluga Summit to address the decline of the beluga harvest in Aklavik, specifically to look at environmental and socio-economic changes (Worden et al., 2020). Moreover, the community of Paulatuk, which began regularly hunting beluga whales in the 1990s, initiated its own on beluga health monitoring in 2011, which has been maintained since.

Mercury was also investigated in water, food webs and fish of the Husky Lakes from the ISR region in in collaboration with the Tuktoyaktuk and Inuvik communities (2012–2013). Interaction with communities through public meetings, interviews and expert consultations helped design the study and sampling procedures. Results indicated higher Hg levels in apex species and differences in fish levels between lakes (Gantner and Gareis, 2013).[ID19]

Nunavut

Multiple Hg studies utilizing IK have taken place in Nunavut, the largest region of Inuit Nunangat (the homeland of Inuit in Canada). Hunters and trappers organizations from the Kivalliq Region helped identify potential dietary sources of Hg to caribou and supported sampling of lichen, mushrooms and seaweed around four different communities (see Section 9.4 for more information).[ID20] Another community-driven study on contaminants (including Hg) was conducted based on fish favored by residents of Gjoa Haven on King William Island.[ID21] This need was driven by the experience that in 2004, when local fishers provided several Arctic chars for a Hg study, the data from the study was not published until many years later (Chételat et al., 2015). Thus, Gjoa Haven residents wanted a variety of regularly consumed fish species to be examined and for results to be made available in a timely way. The community then initiated a contaminants project associated with a larger food security initiative and a potential sustainable commercial fishery.[9] While not all the activities were specifically undertaken

[9] See: https://www.genomecanada.ca/en/why-genomics/genomics-sector/fisheries-and-aquaculture/fish-finders

for the contaminants project, they helped to inform it. The Gjoa Haven Hunters and Trappers Association and community Elders mapped out water bodies to be fished. Structured interviews were conducted with Elders, food preparers and youth during workshops held in the community and on the land. Elder-youth field trips were also organized, and information was sought from women working in a community prenatal group and other local food programs. The IK information gathered, including favorite fishing sites and animal harvest regions, was mapped onto an online atlas (see Schott et al., 2019).[10] The contaminant aspect of the project involved the training of community youth to collect biological data on fish as well as to perform tissue dissection. In person, biannual reports on the progress of the project were presented to the Hunter and Trappers Association and at community meetings. All data has been placed in the Polar Data Catalogue where it is freely available, and posters and manuscripts for scientific audiences include the former chair of the Hunters and Trappers Association as a co-author (e.g., Walker et al., 2020b).

In another Nunavut region, a long-term Hg monitoring program of seabird eggs and bird carcasses from Resolute Bay (Prince Leopold Island) and Coral Harbour (Coats Island; Akpatordjuark) has been ongoing since 1994.[ID22] This project was initiated by the NCP based on concerns expressed by communities on high levels of contaminants in country foods (see Chapters 2 and 5). Country foods, or traditional Inuit foods, may include game meats, fish, migratory birds, eggs and other foraged foods from the land and the sea (see Chapter 7; AMAP, 2021). Annual meetings and involvement of the Sulukvaut Area Co-Management Committee and the Hunters and Trappers Association continuously inform experimental design and field collections. Some community members expressed initial concerns that field research activities might be disruptive to seabird colonies. The continued communication efforts by the research team led to a better understanding of the project and ultimately helped to secure majority community support for continued research on Prince Leopold Island. Capacity-building, field training during sampling periods and opportunities for community members to participate are routinely part of the program and have led to Inuit research assistants providing training and mentoring to other local research assistants.

As a notable example of the study of contaminants, including Hg, in land mammals from Nunavut, the Qamanirjuaq caribou herd around Arviat has been sampled and their tissues analyzed for contaminants.[ID6] The Beverly and Qamanirjuaq Caribou Management Board and Kivalliq Hunters and Trappers Organizations provide input and guidance for the evolution of this long-term monitoring study (Hg results are reported in Chapters 2 and 5).

In the marine environment, a project investigating heavy metals, including Hg, and various health parameters in ringed seals (*Pusa hispida*) from Iqaluit and Pond Inlet was conducted in the period 2017 to 2019.[ID23] Associated research was done under NCP funding and co-led by a local Inuit researcher. In Pond Inlet, narwhals (*Monodon monoceros*) were also included, and local hunters were contracted to keep a channel of communication between the researchers and community members. Surveys were also done in Iqaluit (and will be done in Pond Inlet) to investigate local concerns on ringed seal health, to define parameters of seal health to be measured by hunters, to assess trends of health over time and to explore future directions of seal research. Communication between researchers and community members has been open during the whole project, in Inuktitut and English.

Mercury has also been monitored since 1982 in polar bear tissues harvested by Inuit hunters from western and southern Hudson Bay.[ID24] Since 2007, Hg in polar bear liver has been measured on an annual basis (Northern Contaminants Program, 2021; see Chapter 2). Recently, Hg monitoring of Hudson Bay polar bears, along with bears in the Kivalliq Region, has included assessments on the trend influence of ecological and physical variables indicative to climate change (e.g., temperature and sea-ice conditions) and relationships to changes underlying food-web structure and in connection with changing contaminant levels in bears (Morris et al., 2022; see also Chapter 5). Key information provided by the hunters include behavior, foraging ecology, body condition and the breeding of bears. This collaborative sampling between communities and scientists has also allowed the investigation of the biological effects of Hg in bears from western Hudson Bay and, additionally, in bears from Baffin Bay.

As an example of a project which took a more ecosystemic approach, Indigenous organizations from five communities from Nunavut and Nunavik located around the Hudson Bay and James Bay participated in a project from 2015 to 2018 on metal accumulation in the marine food web.[ID25] Communities expressed interest in information on metal levels in marine wildlife to address concerns of contamination from hydroelectric reservoir releases into James Bay. Inuit or Cree hunters collected local marine animals in their traditional territory (e.g., blue mussel; *Mytilus edulis*, sea urchin, plankton, marine fish, common eider; *Somateria mollissima* and ringed seal) for Hg tissue analysis. The contaminants component was part of a larger community-driven research network facilitated by the Arctic Eider Society community-based initiative.

Nunavik

In the northern region of Québec, metal bioaccumulation was investigated in country food from Kuujjuaraapik (2013–2015) to assess if levels of Hg had changed 20 years after initial Hg measurements had been made for an environmental assessment of a large-scale hydroelectric project.[ID26] This study was a collaboration between a local Inuit organization (the Sakkuq Landholding Corporation), government scientists and Inuit hunters, who collected relevant marine animals, terrestrial wildlife and freshwater fish for tissue analysis within their traditional territory.

In 2016, a project named *Imalirijiit* (those who study water; Gérin-Lajoie et al., 2018) was launched by university researchers and the Inuit community of Kangiqsualujjuaq to build a community-based monitoring program in the George River Basin.[ID27] Community members chose to monitor the environmental quality of the lower George River because of mining development planned upriver from the community. This ongoing project assesses trace elements in river water,

[10] See: https://tsfn.gcrc.carleton.ca/index.html

sediment, lichen, fish, birds and seals. Indigenous Knowledge is used to select sampling stations as well as to document Inuit land use, and changes to plant and animal ecology, the river and the landscape. Each year, a community consultation is planned to co-construct the next steps of the project and to share results. At the heart of this collaborative project is a science land camp program co-organized with the Youth Committee, which involves youth, Elders, knowledge holders and researchers. Participating Elders and local guides/hunters have been interviewed with the help of interpreters. Community members, including youth participants, have been involved each year in presenting the project at scientific and regional meetings, and a short documentary was created about *Imalirijiit* to share the collaborative approach and project goals.

When it comes to studies of human health, maternal exposure to Hg and methylmercury (MeHg), as well as other contaminants and nutrients, from country food have also been monitored in Nunavik since 1992. In 2016, the biomonitoring project was given the formal title *Nutaratsaliit Qanuingisiarningit Niqituinnanut* (Pregnancy wellness with country food).[ID28] Across the fourteen communities of Nunavik, blood and hair samples from Inuit pregnant women have been analyzed and MeHg intake estimated using food frequency questionnaires as well as existing Hg/MeHg data in wildlife. Information on food security, anemia, iron deficiency and awareness of public health messages was also documented. Midwives have guided the project from the outset and an open and continuous dialogue between academic researchers, the Nunavik Regional Board of Health and Social Services (NRBHSS), the Nunavik Nutrition and Health Committee (NNHC) and communities has led to the evolution of this ongoing project. Through time, knowledge has also been shared and discussed with Nunavik caregivers, pregnant women, grandmothers and hunters to promote healthy pregnancies and better child health through country food consumption; the AMAP 2021 Human Health Assessment has more detailed information on this study, including the Hg data (AMAP, 2021).

As a further example of human health monitoring activities involving Indigenous Perspectives and IK, in 2017, a major population health survey, the *Qanuilirpitaa?* How are we now? 2017 (NRBHSS, 2017), was conducted in all Nunavik communities and involved the collection, analysis and dissemination of information on the health status of Nunavimmiut, including their exposure to several contaminants, as well as their food consumption and nutrition status. The work was guided by the *Qanuilirpitaa?* Steering Committee and coordinated by the NRBHSS, which ensured the political and administrative legitimacy of the process.[11] The general objective of this survey was to provide an up-to-date portrait of the health status of Nunavimmiut as a follow-up study on the health of participants since the last survey in 2004 (NRBHSS, 2004). A Data Management Committee was responsible for overseeing the management of the data and biological samples and to ensure that OCAP® principles (ownership, control, access and possession; FNIGC, 2007) were respected. Values and principles such as empowerment and self-determination, respect, value, relevance and usefulness, trust, transparency, engagement, scientific rigor and pragmatism were emphasized during this project (see also AMAP, 2021).

Nunatsiavut

In Nunatsiavut, ringed seals, which are an important country food in several communities, have been the subject of several studies led in collaboration between communities, the regional government and scientists. Long-term monitoring of Hg in ringed seals from Nain, and other regions from Inuit Nunangat, such as the NWT (Sachs Harbour) and Nunavut (Resolute Bay and Arviat), has been ongoing since the 1990s (see Chapters 2 and 5 for results).[ID29] This project has relied on local hunters to collect ringed seal samples over time (Houde et al., 2020). Since 2016, outreach activities in communities involved in the project have been integrated to this monitoring work (Northern Contaminants Program, 2021). This aspect of the project addressed a shared interest among Inuit and scientific researchers in enhancing communications and community capacity building related to contaminant research. Workshops conducted in northern schools across the Inuit Nunangat (i.e., Resolute and Arviat, NU; Sachs Harbour, NWT) provided opportunities for Inuit Elders to share their knowledge on seals with students and researchers. Northern college students and community-based organizations have been involved in these activities to increase capacity and training among Northerners as well as to ensure best practices for communicating contaminant research (Northern Contaminants Program, 2021).

Mercury contamination and associated health effects in ringed seals and their food web has also been investigated in the region.[ID30] This project was initiated in 2006 to address Inuit concerns about the impacts of climate change, modernization and contaminants on the health of marine ecosystems and communities in the region. Inuit have been involved in all aspects of the program, including the direction of research, design, and planning of projects, field studies and reporting of results. A goal of this research program has been to enhance capacity sharing between Inuit and researchers and integrate a training component for Inuit students (kANGIDLUASUk summer student program). The scientific study on Hg levels in ringed seals and diet and health indices has been complemented by IK, which was collected from local hunters and documented to improve our understanding of ecosystem changes that may be related to or influencing Hg and other contaminant trends in Nunatsiavut ringed seals (Northern Contaminants Program, 2012). The ringed seal health component is co-led by Inuit and all sample collections are carried out by community members. The research program has recently expanded to assess the spatiotemporal patterns of ringed seal feeding behaviour and Hg accumulation in connection with sea ice and other environmental parameters spanning a 20-year period. This research was initiated in support of priority concerns of Inuit along the coast and is supporting a marine planning initiative (*Imappivut;* Our Oceans) that is working with communities to gather knowledge about areas, uses, and activities that

[11] This health survey relied on a high degree of partnership within Nunavik (i.e., Makivik Corporation, Kativik Regional Government; KRG, Kativik Ilisarniliriniq; KI, Avataq Cultural Institute, Qarjuit Youth Council, Innulitsivik Health Center, Ungava Tulattavik Health Center, all of whom were represented on the Steering Committee) as well as between Nunavik, the Institut national de santé publique du Québec (INSPQ) and academic researchers from three Canadian universities.

have ecological, social, cultural and economic importance to Labrador Inuit. This research program aims to build capacity by providing opportunities for Inuit beneficiaries to lead or contribute to research in support of marine protection and management and to develop skills with which to conduct long-term marine monitoring in the region.

Another research project in the same region was initiated in 2012 due to concerns of communities and the Nunatsiavut Government about the levels of MeHg in Lake Melville following the hydroelectric power development on the Churchill River.[ID31] This project was co-led, designed and carried out by scientists, the Nunatsiavut Government, the Nunatsiavut Research Centre, and the communities of Happy Valley-Goose Bay, Northwest River and Rigolet. The objectives included community-led food web sample collections through fishing and hunting activities, dietary surveys across the different communities and sampling of community members for Hg in hair (Schartup et al., 2015a; Calder et al., 2016; Durkalec et al., 2016a, 2016b). Results showed that there would be increases in MeHg levels in fish, ringed seals and Indigenous Peoples if organisms originating from the hydroelectric developments were used for food. Results spurned an independent review of potential measures that could protect the health of the Indigenous and local populations from the effects of MeHg related to hydro development.[12] More vigorous monitoring is now being carried by the Government of Newfoundland and Labrador to assess potentially changing MeHg levels in Lake Melville water and biota.[13] Training is provided on all aspects of sample collection to increase scientific capacity in the region. Annual community meetings are organized to share information and obtain feedback and input from the community; these communications continued following the reservoir flooding carried out in 2019.

Finally, a long-term Hg monitoring program in the muscle tissue of Arctic char from Nain and Saglek has been ongoing since 2007 and 2014, respectively (Northern Contaminants Program, 2021). This regionally led community-based monitoring program has aimed to build capacity in the region while addressing contaminant concerns of Labrador Inuit. The project supports recommendations from the 2008 Inuit Health Survey (Egeland, 2010) and the ArcticNet IRIS 4 report (Allard and Lemay, 2012) concerning Arctic char, while supporting knowledge transmission between youth, harvesters and Nunatsiavut Government staff. To further build capacity and enhance training, knowledge exchanges between Nunatsiavut Government employees and federal scientists through training has helped towards a better understanding of the research process and enabled clear communication with community members.

Greenland

In Greenland, sampling of biota for Hg research (and other contaminants) has been conducted with the help of Inuit hunters since the 1970s.[ID32-37] The reason for initiating work on contaminants in traditional foods was, and still is, related to human health in addition to the health of Greenland's wildlife. The Ittoqqortoormiit (Scoresby Sound) polar bears project is one of the longest time series available for wildlife in the Arctic spanning from 1983 to present; these 38 years of contaminants data were made possible because of the long-term collaboration with the East Greenland Inuit population. Wildlife and fish sampling was also initiated under the Heavy Metals in the Greenland Environment program (1985–1988). Moreover, since 1995, long-term monitoring of Hg has been ongoing under the Greenland CORE program including samples from polar bears, ringed seals, black guillemots (*Cepphus grille*), sculpins (*Myoxocephalus* spp.) and Arctic char. Narwhals, beluga, killer whales (*Orcinus orca*), walrus, harp seals (*Pagophilus groenlandicus*), hooded seals (*Cystophora cristata*), bearded seals (*Erignathus barbatus*), seabirds, fish species and musk oxen (*Ovibus moschatus*) have also been collected in collaboration with the Inuit population (see Chapters 2 and 5 for Hg results). For the species with hunting quotas, only full-time hunters were allowed to collect the animals; it has been customary for scientists to conduct the sampling in close and efficient collaboration with the skilled Greenlandic Inuit hunters. Meetings have been regularly organized with Inuit hunters over the course of undertaking field work and presenting results. Moreover, the scientists involved are in year-round contact with key hunters, enabling the exchange of mutual information on relevant issues regarding the hunts and science information including contaminant exposure and health issues.

Aviaja Lyberth Hauptmann (Nuuk, Greenland):

> *"As researchers, we must not only try to understand Indigenous perspectives but at the same time become much more aware of our own imperfect perspectives as well as our motivation. We must refrain from approaching Hg research in the Arctic as an act of goodness based on our expertise, although this can be the incentive when applying for grants. Researchers must always bear in mind that we are doing research also, if not mostly, to develop our careers. The Indigenous communities we work with go into these projects with their personal lives, families, culture and emotions. To be respectful of this we need to approach our projects with an intention to not only bring our professional selves but also our personal selves, something I believe often happens naturally. Having this as an intention might help to lay the foundation for more respectful collaborations. We must also acknowledge that there are more and more scientists in local communities and we must not assume that scientific expertise is not present in Indigenous communities."*

Sweden

Very few national programs supporting the community-based monitoring of contaminants exist in Sweden. In the Eurasian North, the Snowchange Cooperative has been conducting community-based monitoring since 2000 and managing several projects, including their Hg contamination aspects.[14] Their work has included monitoring weather and ecological change, the documentation of fishing/hunting diaries, oral

[12] See: https://ieaclabrador.ca/

[13] See: https://www.gov.nl.ca/ecc/methylmercury-mrf/

[14] See: www.snowchange.org and www.landscaperewilding.org

history documentation, ecological mapping, satellite imaging and contaminant data interpretation as well as community workshops and conferences (Syrjämäki and Mustonen, 2013).

The main sources of Hg in Sweden have included construction of large-scale hydropower stations (e.g., at Luleå and Kemijoki) as well as industrial mining and forestry. These anthropogenic activities have been a cause of concern for local Indigenous communities for decades. Impact assessments of hydropower development and forestry practices on Sámi communities were conducted between 2003 and 2013 in the Jokkmokk region.[ID38] These assessments were in the form of a literature review of national Hg data alongside interviews with community members (Syrjämäki and Mustonen, 2013). Sámi leaders were also invited to assess the present questions of Hg in the area (Mikaelsson, pers. comm., 2020). Overall, Sámi knowledge holders reported considerable negative impacts due to environmental destruction and water regulation, in particular to their fisheries and reindeer grazing grounds (see EA Case Study 1). Recent reports of Hg concentrations in thawing permafrost (Schuster et al., 2018) have also been of concern to the Sámi within the Lule River basin (Mikaelsson and Mustonen, 2020).

Finland

In the Finnish Arctic, the impacts of Hg contamination in relation to hydropower development and forestry practices on Sámi communities and wildlife were investigated around the Lokka and Porttipahta reservoirs (Lapland) between 2000 and 2010.[ID39] These reservoirs, constructed in the 1960s and 1970s, significantly impacted and/or displaced Sámi and Finnish communities and altered, or in some cases even destroyed, the traditional economies and cultures of reindeer herding and hunting as well as fisheries. The potential Hg sources, impacts of contamination and concerns of the Sámi communities were identified by conducting a national literature review as well as with IK through community visits and community-based observation, by using oral histories and by conducting contemporary diary reviews (Mustonen et al., 2011; Murtomäki, pers. comm., 2020). During the establishment of the reservoirs, massive areas (spanning ~417 km^2) were clearcut and treated with Agent Orange (see EA Case Study 2). In the 1970s, public warnings about consuming fish in the Vuotso area were issued due to increased Hg levels (up to 0.99 mg/kg in northern pike; *Esox lucius*), but Sámi continued to consume the local fish. In other cases, public debate on possible Hg contamination of fish led to anecdotal storytelling about risk and risk avoidance: for instance, hanging large pike upside down in freezing temperatures was believed to transfer Hg into the fish head, which could then be cut off and, in this way, the Hg would be removed (Murtomäki, pers. comm., 2020). Such stories and narratives help provide a local perspective on how communities have responded to the rapid and often negative shifts in the state of the natural environment in the present era.

Mercury measurements in the reservoirs in the early 2000s indicated that levels in humans and fish were lower than in the 1970s (with maximum levels in certain fish at 0.99 mg/kg in 1970 to 0.34 mg/kg in 2012; see summary in Alanne et al., 2014). Similar concerns led to a community-based observation network for the Koitajoki waterway (part of the Vuoksi watershed in North Karelia, Finland and Republic of Karelia in Russia).[ID40] The network was established in 2016, with early oral history documentation starting from 2001. The work used traditional knowledge (as per definition in Box 9.2, some of the knowledge holders are not officially recognized as Indigenous Peoples and belong to minority, non-indigenous populations that possess similar knowledge) to detect and contextualize open questions regarding boreal river systems and Hg. The main data for this case study were derived from the Finnish side of Koitajoki (see EA Case Study 3). Causes of the Hg increases in the ecosystem included the increased activities of industrial plants (e.g., pulp and paper mills; Wahlström et al., 1996), peat production, forestry management and site-specific gold mining (Mustonen and Mustonen, 2018; Albrecht, 2019). Additional local concerns arose from samples that were taken by regional authorities and researchers from local people in 2016 and 2017 to investigate Hg levels but the results have not yet been reported back (Mustonen and Mustonen, 2018). Sampling of predator fish in 2014 in areas close to the hydroelectric station has also found high Hg levels in tissues (e.g., 0.74 mg/kg in young pike; Albrecht, 2019). Traditional river seining which removes organic matter and large-scale catchment restoration could help reduce Hg loading. Community-based monitoring efforts will constitute a central element of this restoration work in the near future.

Russia

As is the case in other Arctic regions, the main sources of Hg in Russia can be attributed to coal combustion, mining and the production of metals (e.g., nickel, zinc and gold). Mercury can also be released from waste management and industries. However, while Hg and other contaminants have received international attention in recent decades, Fennoscandia and the Eurasian North (i.e., the Russian Arctic) have been less studied, especially in the context of IK and local knowledge. This knowledge is of special importance in the Russian Arctic due to the role and scope of Soviet-era industrial activity (from around 1917 to 1991, with significant increases in activity in the 1930s) as well as legacy industrial releases that constitute environmental gaps in knowledge across the region.

In the Ponoi River catchment (Murmansk Region), observations of the impacts of Soviet chemical legacies on the communities of Krasnochelye, Kanevka and Ivanovka and on the Sámi and Komi communities as well as wildlife have been assessed.[ID41] During the Soviet era, the villages of Krasnochelye and the secret military installations may have been sources of Hg releases into the environment. Mercury levels were therefore investigated in the villages of Ponoi and adjacent Sosnovka between 2005 and 2020 using scientific data (Soviet and Russian observational data combined with a literature survey; Velichkin et al., 2013) and a community-based network (oral histories and community-based observation; see more in Johnson et al., 2015). Community-based observations were aimed at reconstructing pollution events, assessing convergence or divergence between scientific and historical data, and recording expertise from the local populations (see EA Case Study 4). The Ponoi example is important in yielding past environmental data for understanding the present, especially in the context of Hg monitoring and how it ultimately affects northern Indigenous communities, their health and the surrounding environment. Oral history can be useful

in identifying undeclared pollution events and directing future CBM efforts and remediation. Moreover, IK and local knowledge have often been critical in a context of (presumably) limited flow of government information that might have helped protect both community and ecological health. For example, several pollution events are reported in the CBM information; these included the dumping of chemicals, releases from mining and uranium sites, as well as diesel spills. However, data were preliminary, and further work carried out in the period 2020 to 2021 has aimed to include pike and burbot sampling to determine Hg levels in different areas of Ponoi (see EA Case Study 4).

Similar work has been done in the Kolyma River catchment to support the assessment of Hg impacts on the communities in the region as well as their environment.[ID42] Kolyma is the home of Indigenous Peoples of Eastern and Northeastern Siberia, including the Even, Chukchi, Evenki, Koryak and the Yukaghir. Kolyma basin has been affected by hydroelectric dams, artisanal and small-scale gold mining (ASGM; where Hg may be used to separate gold particles from sediment) and industrial mining operations that have sourced Hg to the river for a century; present changes include sourcing from climate change impacts including permafrost melt and floods (Eagles-Smith et al., 2018). Community voices from the region were documented between 2005 and 2020 and combined with remote sensing/satellite imagery, geographical analysis and regional governmental data to investigate the drivers of Hg contamination. A scientific study reported Hg levels of up to 1.8 mg/kg in perch (4–6 years old) in mid-Kolyma (Tiaptirgianov, 2017). Community-based observations have also reported ecosystem impacts (e.g., changes in water color and temperature, fish migration and the reduction or collapse of fish stocks), as well as direct (e.g., changes in fish smell, taste and health) and indirect (e.g. ethical and cultural) impacts of the environmental contamination by Hg on Kolyma and neighbouring streams (see EA Case Study 5; Mustonen and Shadrin, 2021).

Observations of the impact of modern-day ASGM on the communities of Evenki reindeer herders were also carried out in the Yiengra River basin (Eastern Siberia).[ID43] Sixteen years of CBM work with the Evenki has resulted in the mapping of gold mining sites and descriptions of the impacts on reindeer and wildlife health, such as the loss of fisheries and access to clean waters, alterations to waterways (depth, water color and accessibility) and the ethno-psychological impacts of alterations to the Evenki home area (see EA Case Study 6). Available chemical data supported IK in defining the poor water quality of the Yiengra River. However, the lack of information on the use and release of Hg by mines led to a large divergence between reported impacts of artisanal mining operations and impact observations made by the Evenki. This project demonstrated the use of communal mapping of problematic sites and methods of negotiating environmental issues by those who live nature-based nomadic lifestyles, particularly in relation with Hg contamination and major river contamination in an absence of state controls on pollution events. Summary results of the land use changes have been released as a part of the Evenki Atlas (ELOKA and Snowchange, 2020).[15]

9.4 What specific examples are there of Indigenous contributions to our understanding of mercury contamination in the Arctic and to policy development?

The various projects described above illustrate the important contributions that Indigenous communities and knowledge holders have made to our understanding of Hg contamination in the Arctic. Specific examples below highlight where IK has informed the interpretation of contaminants data and/or acted as a driving force through various research projects on contaminants:

- In fish research in Nunavut, scientists expected to find moderate levels of Hg in lake whitefish (*Coregonus clupeaformis*) collected around Gjoa Haven due to their freshwater habitat, but IK indicated that the whitefish migrated to the sea to feed after the ice was out. This valuable information helped explain why levels of Hg were, in fact, lower than might be expected in this species.
- Caribou research results indicated that individuals from the Qamanirjuaq herd had higher Hg concentrations than other Arctic caribou. Caribou usually get most of their Hg from lichens, but local Elders described the Qamanirjuaq caribou eating seaweed from the seashore. Since seaweed is known to accumulate metals, it was hypothesized that the caribou may be getting additional Hg from this source. Consequently, Inuit community members interviewed Elders about caribou diets; vegetation samples were collected in each of the communities and Hg was measured in lichens, mushrooms and seaweed from communities in the Kivalliq Region of Nunavut. Ultimately, Hg concentrations were found to be lower in seaweed than in mushrooms and lichens, and more research will be necessary to determine the reason for the difference.
- In the Northwest Territories, Dél̨ı̨nę fishermen have observed different types of lake trout in Great Bear Lake; fish living in different regions of the lake had different food in their stomachs and different appearances. These observations led to collaborative studies with researchers to investigate Hg concentrations in relation to feeding ecology, habitat and age of fish. While Hg concentrations differed between ecotypes, these fish also differed in their size and growth rates, all of which effect Hg concentrations. Preliminary results indicate that bottom-feeding fish seemed to have the highest Hg concentrations on average for a given length.
- Local concerns about skinny fish and low quality of burbot liver that were found in lakes and rivers in close proximity to communities have led to several studies on liver quality and contaminants including Hg in NWT and the Yukon (Chételat et al., 2015; Cott et al., 2018). Condition factors and measurements of fish 'skinniness' have been integrated in investigations of spatial and temporal variability in Hg and other contaminants in fish.

[15] See: www.evenki-atlas.org

- Research in Nunavik showed that beluga *mattaaq* (skin) had high levels of selenoneine, a compound that may be protective against negative Hg effects. Elevated levels of selenoneine were also found in the blood of Inuit from Nunavik, with mean selenoneine concentrations in women being two-fold higher compared to those in men (Little et al., 2019; see also Chapter 7). When the scientists reported the findings, Inuit experts explained to them that these differences may have to do with the fact that only Inuit women eat the tail of the beluga (Little et al., 2019). Preliminary analysis of different parts of the beluga whales then revealed that, in fact, selenoneine concentrations in the skin of the beluga tail are around twice as high compared to the skin from other areas (Little and Lemire, pers. comm., 2019).

Indigenous Knowledge can also provide invaluable ecological information that can elucidate effects of climate change, and other ecosystem changes, on contaminant levels in the Arctic environment, wildlife and peoples. For example, an extensive beluga research project in Nunavik investigated IK and included (but was not limited to) migration, body condition, foraging ecology, predation, breeding, calving and behavior of animals (Breton-Honeyman et al., 2016). This knowledge on foraging ecology provides information on diet composition, which is complementary to other dietary approaches (e.g., stomach contents, stable isotopes and fatty acids) and on the seasonality of energy intake, all of which is important in helping to understand beluga exposure to Hg and other contaminants.

Additionally, projects such as The Inuit Siku Atlas (ISIUOP, 2021)[16] as well as The Indigenous Knowledge Social Network (SIKU)[17] allow for sharing of knowledge and observations by Inuit hunters in near-real time and incorporate a variety of culturally relevant tools that allow Inuit to interpret results using their own knowledge system (Heath et al., 2015; Arctic Eider Society, 2016). In several cases, these platforms include a mobile device application for use in the field and are used as a part of community-driven programs to systematically document IK and environmental observations, such as the body condition, behavior, diet, and ecology of animals and environmental conditions. Other initiatives, such as ArctiConnexion[18] and Ikaarvik[19] are specifically engaging Inuit youth in research activities that involve studies in various natural sciences disciplines, including studies on climate change and contaminants (such as Hg).

More broadly, in the circumpolar Arctic, the utilization of IK in environmental research and monitoring and associated decision-making processes is an overarching mandate of the Arctic Council and associated Working Groups, such as AMAP, which are increasingly working towards this implementation (Arctic Council IPS, 2015; AMAP, 2019a). Within AMAP, Arctic research on contaminants and human exposure in some countries (e.g., Canada and Greenland) would not be possible without the involvement of Indigenous Peoples. Active collaboration between Indigenous Peoples and scientists are also critical to core Arctic research that supports domestic and international chemical management initiatives.

Globally, the role played by Arctic Indigenous Peoples in the negotiations of international treaties, such as the Stockholm Convention on Persistent Organic Pollutants (POPs), or the Minamata Convention on Mercury, has been highlighted (Downie and Fenge, 2003; Fernández-Llamazares et al., 2020). In these cases, the involvement of Arctic Indigenous Peoples provided the human context to the contaminants issue and ensured that negotiations were not solely based on numbers, figures and economic interests. In particular, during the negotiations of the Minamata Convention, the Inuit Circumpolar Council (ICC) used results from NCP studies and AMAP assessments, such as graphs describing the exceedances of Hg guidelines by pregnant Inuit women in the circumpolar Arctic, as well as consumption advisories based on Hg in the traditional diet of Inuit in Nunavik and Nunavut, to highlight how Inuit are affected by Hg in the Arctic. The combined efforts by Arctic Indigenous Peoples and Arctic states during the negotiations led to the inclusion of Arctic Indigenous Peoples in the preamble of the two conventions. For instance, the Minamata Convention preamble states that parties to the convention have agreed to the articles therein "*[n]oting the particular vulnerabilities of Arctic ecosystems and indigenous communities because of the biomagnification of Hg and contamination of traditional foods, and concerned about indigenous communities more generally with respect to the effects of Hg*" (UNEP, 2019). The engagement of organizations and governments in United Nations conventions continues with the involvement of Arctic Indigenous Peoples' organizations (such as ICC) who are critical to the implementation of the conventions, in particular with regards to the effectiveness evaluation of the Minamata Convention on Mercury.

9.5 What are Indigenous Peoples' perspectives on and visions for the future on contaminants research in the Arctic?

There are several documents and publications that consider the ethical conduct of research (including contaminants research) with or by Indigenous Peoples, particularly in the Arctic, and provide guidance for conducting such research. The volume of peer-reviewed articles that call for 'decolonizing science' to enable reconciliation (e.g., Jones et al., 2018; Wheeler et al., 2020; Wilson et al., 2020; Wong et al., 2020) is steadily increasing. Furthermore, some Arctic countries are recognizing the need for addressing the effects of historic colonization along with present-day biases and attitudes on research (e.g., Canada in 2019 and UN agencies, for instance within the UNESCO; Chan et al., 2020). However, this chapter is not aiming to provide an exhaustive review on the topic based on peer-reviewed literature published in international journals and is not aiming to review government

[16] See: https://sikuatlas.ca/index.html?module=module.sikuatlas.home.welcome

[17] See: https://siku.org

[18] See: https://arcticonnexion.ca/

[19] See: www.ikaarvik.org

actions. Instead, it outlines some examples on perspectives and visions for the future that Indigenous Peoples have produced themselves and which are mostly not found in the published literature. For example, some guidance documents have been published by Indigenous organizations and provide useful information for scientists on how to ensure that any given research project meets Arctic Indigenous needs; such documents truly represent an Indigenous perspective. While it is out of the scope of this chapter to produce a comprehensive review of the Indigenous guidance documents available, a few of these are briefly introduced below and where applicable, some peer-reviewed articles written by Indigenous and non-Indigenous researchers are also referenced.

In the early 1990s, the Inuit Circumpolar Conference (now Inuit Circumpolar Council) developed its Principles and Elements for a Comprehensive Arctic Policy (ICC, 1992), which included 'Principles and Elements on Northern Scientific Research' (updated in ICC's Inuit Arctic Policy; ICC, 2009). ICC continues to work on updating guidance for international research in Inuit Nunaat (the Inuit homelands across the Arctic). Together with the other Permanent Participants of the Arctic Council, they have also developed the Ottawa Indigenous Knowledge Principles on use of IK, co-production of knowledge and meaningful engagement of Indigenous Peoples in research (Permanent Participants, 2018). In 2002, the First Nations Information Governance Committee first published the principles on ownership, control, access and possession (OCAP®), which guide how information and data from Indigenous Peoples needs to be managed (FNIGC, 2007). More recently, the Canadian National Inuit organization, Inuit Tapiriit Kanatami (ITK), published the National Inuit Strategy on Research (ITK, 2018), which outlines the vision of Inuit self-determination in research in Inuit Nunangat, the context in which that vision is articulated, the objectives that must be set and the necessary actions that must be taken to achieve that vision. Additionally, the Assembly of First Nations developed a (not formally adopted) document entitled 'First Nations Ethics Guide on Research and Aboriginal Traditional Knowledge' (Assembly of First Nations, 2011) while the Dene Nation published a report entitled 'We Have Always Been Here. The Significance of Dene Knowledge' (Dene Nation, 2019), which describes in detail what Dene Knowledge (DK) is and provides recommendations for best practice when utilizing DK in decision-making. Many communities and regions in the North also have their own guidelines for research and the utilization of IK (see Dene Nation, 2019). Moreover, Ikaarvik youth recently published recommendations for science and Inuit *Qaujimajatuqangit* (Inuit Knowledge) to guide researchers in meaningful engagement with Inuit and the effective utilization of Inuit Knowledge (Pedersen et al., 2020).

While not all these reports can be listed and described in detail here, some of the overall aspects include:

History and cultural context

The historical, cultural and political contexts in which research is conducted should be understood and limitations in the understanding of Indigenous cultures and legacies of colonialism acknowledged (ITK, 2018; Schott et al., 2020). This understanding can help avoid negative consequences of research and power imbalance (Kral et al., 2011; Wiseman, 2015; Moon-Riley et al., 2019).

Knowledge forms

Indigenous Knowledge is a holistic form of knowledge that is equally valid to scientific knowledge and should be respected as such. This requires transparency, mutual trust and equitable treatment of both knowledge forms. One general problem encountered with the utilization of IK are attempts to 'incorporate' IK into 'Western' scientific studies, leading to processes of labeling or defining the knowledge in fixed ways and thereby separating it from its context or process of developing. The result risks an exploitative situation by misinterpretation and misuse (Stevenson, 1996), failure to fully capture the underlying dynamic and flexible practice, as well as losing the depth of its sociocultural content (Dahl and Hansen, 2019). Similarly, when IK is rendered and reduced to scientific terms, it strips the knowledge of its full meaning and context. Indigenous Knowledge needs to be acknowledged and valued in the context of its original form (Dene Nation, 2019).

Moreover, IK is not confined to hunting and harvesting activities; it encompasses knowledge about the whole Arctic ecosystem, Indigenous cosmologies and is imbedded in Indigenous cultures and languages (Johnson et al., 2015; ICC, 2016; Dene Nation, 2019). IK should therefore be used to inform all steps of research, and knowledge holders need to be engaged in the analysis of research results which are based on their knowledge (Schott et al., 2020). Therefore, Indigenous Peoples generally prefer a co-production of knowledge approach, where knowledge holders and scientists work together to develop research questions, sampling approaches, discuss data analysis and interpretation, and communicate and disseminate results, all which is central in undertaking effective collaborative work. Scientists should not visit Arctic Indigenous communities with the intention to bring expertise but to listen, learn and work together with Indigenous colleagues. Some authors (Schott et al., 2020) call for a knowledge co-evolution process, where information is generated by joining knowledge systems in an inclusive and iterative way to facilitate community self-determination and promote cultural resilience. One central component in this process is the fostering of progress towards improved co-management and community-led research.

Ownership of information

Indigenous partners have the right to control their intellectual property and data and should be recognized and credited for their knowledge (FNIGC, 2007; ITK, 2018).

Communication

Communication is crucial and linguistic challenges need to be recognized. Not all IK holders are comfortable speaking English, and in some Inuit regions in Canada (such as Nunavut), Inuit have the right to use their language in full equality with the other official languages (English and French). Additionally, IK is often place-based, and words and concepts from Indigenous languages are not easily transmitted in or translated into English. When this is attempted, important meanings can become lost, and the embedded, situated, collaborative and performative nature of Indigenous concepts are erased (Dene Nation, 2019).

Communication is a particularly important part of research activities and allows for good knowledge exchange and informed decision making (Schott et al., 2020). Early and regular communication between partners helps to build trust, develop/discuss research questions, learn about timelines and priorities and address changes/roadblocks. The sharing of project information and results (via plain language summaries, pamphlets, newsletters, videos, interactive games, radio broadcast, social media, community events, or food sharing) is also key to keep the community informed (Henri et al., 2020).

Finally, a very specific aspect in communication on contaminant research is related to the cultural and nutritional importance of the traditional diet, benefits and possible health risks associated with exposure to contaminants during a critical period and/or over an individual's life course. However, any human health-related messaging is the responsibility of public health officials and should not be done by the scientists. More details on this subject are discussed in Chapter 7 (see Section 7.6) and recent AMAP Human Health Assessments (AMAP, 2015, 2021).

9.6 Conclusions and recommendations

Conclusions (in numbered bullets) are organized under section headings (section numbers in square brackets) followed by recommendations in italics where appropriate.

What examples are there of mercury contamination research done with or by Indigenous Peoples? [9.2]

1. There are multiple examples of Hg research and monitoring conducted by or with Arctic Indigenous communities/regions, but a greater number of projects have been found in Canada compared to other Arctic countries. This is likely due to sustained funding programs such as the Northern Contaminants Program (NCP) in Canada, which is well connected to and represented in AMAP.

What specific examples are there of Indigenous contributions to our understanding of mercury contamination in the Arctic and to policy development? [9.4]

2. In several Arctic countries, research on contaminants and human exposure would not be possible without the involvement of Indigenous Peoples. Active collaboration between Indigenous Peoples and scientists is critical to core Arctic research that supports domestic and international chemicals management initiatives, and Arctic Indigenous Peoples have played crucial roles in the development of global agreements on contaminants (e.g., the UN Minamata Convention on Mercury).

What are Indigenous Peoples' perspectives on and visions for the future on contaminants research in the Arctic? [9.5]

3. There exist guidelines and protocols for ethical research developed by Indigenous Peoples. Important aspects include understanding the historical/cultural contexts of research in the Arctic, Indigenous self-determination in research/monitoring and processes such as co-production of knowledge, respecting IK, crediting ownership of information and an emphasis on good communication practices.

More sustained funding for community-driven monitoring and research programs in Arctic countries would be beneficial and assist in more research/monitoring capacity and the development of holistic knowledge. These activities should be well connected to circumpolar/international initiatives, such as AMAP, to ensure broader availability of the information and uptake in policy development on international scales.

Guidelines for conducting ethical research that have been developed by Indigenous regions, communities and/or organizations should be recognized and followed.

The establishment of collaborative processes and partnerships/co-production approaches with scientists and Arctic Indigenous Peoples, using good communication practices and transparency in research activities, are key to the success of long-term research and monitoring activities in the Arctic and should be fostered.

Acknowledgments

The Northwest Territories Regional Contaminants Committee, the Nunavut Environmental Contaminants Committee, Carolina Behe (ICC Alaska), the Saami Council, Kiyo Campbell (Fisheries Joint Management Committee), and anonymous peer reviewers are thanked for their review of and commenting on the chapter.

.

Appendix 9

Table A9.1 Detailed information of selected community-based/led Hg monitoring and research activities involving Arctic Indigenous communities and regions illustrated in Figure 9.1.

Project ID	Region	Year	Species/ matrices studied	Communities/ Indigenous Partners
1A	Northwestern Alaska, USA	1990s–present	Seals, fish, caribou	Alex Whiting, Native Village of Kotzebue
1B	Yukon River Basin, Alaska	2006–present	Water, sediment, permafrost	Alaska Native Tribes and First Nations
1C	North Slope, Alaska	1980s–present	Bowhead whales, ice seals, walrus, polar bears, beluga	-
2	Old Crow, Yukon, Canada	2007	Muskrats	Vuntut Gwitchin First Nation, Yukon Department of Environment
3	Old Crow, Yukon, Canada	2014	Fish	Vuntut Gwitchin First Nation
4	Kluane Lake, Yukon, Canada	2015	Fish	Kluane First Nation Arctic Institute of Community-Based Research
5	Beaver Creek, Yukon, Canada	Ongoing	Fish	White River First Nation
6	Old Crow, Yukon and Arviat, Nunavut, Canada	--	Caribou (Qamanirjuaq and Porcupine herds)	Vuntut Gwitchin Government, Porcupine Caribou Management Board, Beverly Qamanirjuaq Caribou Management Board, Hunters and Trappers Organizations
7	Mayo, Yukon, Canada	--	Moose, fish	Na-Cho Nyak Dun First Nation
8	Atlin, British Columbia and Carcross, Yukon, Canada	--	Moose, fish	Taku River Tlingit First Nation; Carcross/Tagish First Nation
9	Whitehorse, Yukon, Canada	--	Fish	Ta'an Kwach'an Council, Champagne and Aishihik First Nations, and Kwanlin Dun First Nation
10	Yukon and Northwest Territories (NWT), Canada	2014–2018	Humans (hair, blood, urine)	Vuntut Gwitchin First Nation, Sahtú communities from K'asho Got'ine, Tulit'a, and Délı̨nę, and Dehcho communities from Jean Marie River, Deh Gah Gotie, Ka'a'gee Tu, Sambaa K'e, K'atl'odeeche, and West Point First Nations
11	Dehcho Region, NWT, Canada	2013–2021	Water, sediment, zooplankton, benthic invertebrates, fish	Dehcho First Nations, Ka'a'gee Tu, Jean Marie River, Deh Gah Gotie, Liidlii Kue, Sambaa K'e, and Pehdzeh Ki First Nations
12	Yellowknife, NWT, Canada	2013–2015	Water, sediment, invertebrates, fish	Yellowknives Dene First Nation
13	Resolution Bay, Great Slave Lake, NWT, Canada	1993–present	Fish, water, sediments	Fort Resolution Deninu Kue First Nation
14	Stark Lake, NWT, Canada	1993–present	Fish	Lutsel K'e Dene First Nation
15	Trout Lake, NWT, Canada	2003–2013	Fish	Jean Marie River community
16	Mackenzie Delta, NWT, Canada	2015–present	Fur bearers	Aklavik Hunters and Trappers Committee, Gwich'in Renewable Resources Board, Ehdiitat Renewable Resources Council, Inuvialuit Hunters and Trappers Committee, Nihtat Renewable Resource Council, Gwich'in Renewable Resources Councils, Tetlit Renewable Resource Council
17	Inuvik, NWT, Canada	2007–2008	Burbot	Inuvik, Aklavik, Tsiigehtchic and Fort McPherson
18	Inuvialuit Settlement Region (ISR), NWT, Canada	1980–present	Beluga whales	Tuktoyaktuk and 6 other ISR communities, Fisheries Joint Management Committee, Hunters and Trappers Committees
19	Husky Lakes, NWT, Canada	2011–2012	Water, aquatic food web, fish	Tuktoyaktuk and Inuvik communities
20	Arviat, Baker Lake, Chesterfield Inlet, Rankin Inlet, Nunavut, Canada	2016	Lichen, mushrooms, seaweed	Hunters and Trappers Organizations from the Kivalliq Region
21	Gjoa Haven, Nunavut, Canada	2004–present	Fish	Communities of Gjoa Haven (King William Island)
22	Resolute Bay and Coral Harbour, Nunavut, Canada	1994–present	Seabirds (eggs, tissues)	Communities of Resolute Bay and Coral Harbour
23	Iqaluit and Pond Inlet, Nunavut, Canada	2017–2019	Ringed seals	Communities of Iqaluit and Pond Inlet, James Simonee
24	Western and southern Hudson Bay, Nunavut, Canada	1982–present	Polar bears	Communities of Arviat, Rankin Inlet, Whale Cove and Sanikiluaq

Name of monitoring program	Project leaders	Indigenous partner involvement in: Design (D), Sample Collection (S), Data Analysis (A), Communication (C)
--	Martin Robards, Wildlife Conservation Society; Todd O'Hara, University of Alaska Fairbanks	D, S
Indigenous Observation Network (ION)	Yukon River Inter-Tribal Watershed Council; USGS National Research Program	D, S, A, C
--	North Slope Borough Department of Wildlife Management; Alaska Eskimo Whaling Commission; captains association of 11 whaling communities	D, S, A, C
--	Jeremy Brammer, Environment and Climate Change Canada (ECCC); Universities: McGill, Carleton, Wilfrid Laurier, Northern British Columbia, Waterloo, Alberta, Victoria	D, S
Northern Contaminants Program (NCP)	Mary Gamberg, Gamberg Consulting	S, A
--	Heidi Swanson, University of Waterloo; Brian Branfireun, Western University	D, S, A, C
NCP	Mary Gamberg, Gamberg Consulting; Heidi Swanson, University of Waterloo	D, S
NCP	Mary Gamberg, Gamberg Consulting; Jeremy Brammer, ECCC	D, S, A
NCP	Mary Gamberg, Gamberg Consulting	D, S, A
NCP	Mary Gamberg, Gamberg Consulting	D, S
NCP	Mary Gamberg, Gamberg Consulting	D, S, A
NCP	Brian Laird, Kelly Sinner, Mylene Ratelle, University of Waterloo; Mary Gamberg, Gamberg Consulting	D, S, A, C
--	Heidi Swanson, University of Waterloo	D, S, C
--	John Chételat, ECCC	D, S
--	Marlene Evans, ECCC	D, S
--	Marlene Evans, ECCC	D, S
--	Marlene Evans, ECCC	D, S
--	Jeremy Brammer, ECCC	D, S, A, C
--	Amy Amos, Gwich'in Renewable Resources Board, ECCC	D, S, A, C
Beluga Harvest Monitoring Program	Lisa Loseto, Fisheries and Oceans Canada (DFO)	D, S, A, C
--	Nikolaus Gantner, U. Northern British Columbia; Jolie Gareis, Simon Fraser University	D, S
--	Mary Gamberg, Gamberg Consulting	D, S
Genome Canada, NCP	Virginia Walker, Queen's University; Stephan Schott, Carleton University	D, S, C
--	Birgit Braune, Philippe Thomas, ECCC	D, S
--	Enooyaq Sudlovenick, Pierre-Yves Daoust, University of Prince Edward Island	S, C
--	Robert Letcher, ECCC; Markus Dyck, Government of Nunavut	S

Table A9.1 continued

Project ID	Region	Year	Species/ matrices studied	Communities/ Indigenous Partners
25	Hudson Bay and James Bay, Nunavut/Nunavik/ Eeyou Marine Regions, Canada	2015–2018	Blue mussels, sea urchins, plankton, marine fish, common eiders, ringed seals	Communities of Sanikiluaq, Kuujjuaraapik, Inukjuak, Umiujaq and Chisasibi; Arctic Eider Society
26	Kuujjuaraapik, Nunavik, Canada	2013–2015	Marine, freshwater, terrestrial assessments	Community of Kuujjuaraapik; Sakkuq Landholding Corp
27	George River Basin, Nunavik, Canada	2016–present	Water, sediment, lichen, fish, birds, seals	Northern village of Kangiqsualujjuaq
28	Nunavik, Canada	1992–present	Humans (blood, urine, hair, blood) and country foods	All Nunavik communities, Nunavik Regional Board of Health and Social Services, Nunavik Nutrition and Health Committee, Makivik Corporation, Kativik Regional Government, Kativik Ilisarniliriniq, Avataq Cultural Institute, Qarjuit Youth Council, Inuulitsivik Health Centre, Ungava Tulattavik Health Centre
29	Sachs Harbour, NWT; Arviat and Resolute Bay, Nunavut; Nain, Nunatsiavut, Canada	1990s–present	Ringed seals	Hunters and trappers committees/associations and communities of Sachs Harbour, Arviat, and Resolute Bay; Nunatsiavut Government
30	Nunatsiavut, Canada	2006–present	Ringed seals and their preys	Communities and hunters of Nain, North West River and Rigolet
31	Lake Melville, Nunatsiavut, Canada	2012–present	Water, invertebrates, fish, ringed seals	Communities of Happy Valley-Goose Bay, Northwest River and Rigolet; Nunatsiavut Government; the Nunatsiavut Research Centre
32	Qaanaaq/Avanersuaq (Thule, Greenland)	1984–present	Polar bears, ringed seals, black guillemots, sculpins	Hunters of Avanarsuaq Sound
33	Qeqertarsuaq, Greenland	1996–present	Ringed seals, black guillemots, sculpins	Hunters of Qeqertarsuaq
34	Ittoqqortoormiit (Scoresby Sound), Greenland	1983–present	Polar bears, ringed seals, black guillemots, sculpin	Hunters of Scoresby Sound, Sampling coordinator: Jan Lorentzen
35	Isortoq, Greenland	1995–present	Caribou, Arctic char	Hunters from Isortoq
36	Tasiilaq, Greenland	2019–2020	White-sided dolphins, pilot whales, killer whales	Hunters from Tasiilaq
37	Maniitsoq, Greenland	2019–2020 (2009)	Harbour porpoises	Hunters from Maniitsoq
38	Jokkmokk, Sweden	2003–2013	Freshwater, northern pike, reindeer	Sámi communities of Luleå Sámi and North Sámi
39	Lokka and Porttipahta, Finland	2000–2010	Northern pike, burbot, reservoir accumulation, sea eagles and other apex predators	Sámi communities of Lokka and Porttipahta
40	Karelia, Finland and Russia (Koitajoki River catchment)	1950–2019	Northern pike, perch, burbot, other apex predators	Karelian communities of the Koitajoki catchment area: Ala-Koita, Möhkö, Koitere Lake
41	Russia (Ponoi River catchment)	2006–2018	Ponoi River	Sámi and Komi communities of Krasnochelye, Kanevka and Ivanovka
42	Russia (Kolyma River catchment)	2005–2018	Fish	Chukchi and Yukaghir communities
43	Russia (Yiengra River catchment)	2004–2018	Water, fish	Evenki reindeer herders

Name of monitoring program	Project leaders	Indigenous partner involvement in: Design (D), Sample Collection (S), Data Analysis (A), Communication (C)
NCP, AES Community-Driven Research Network	Joel Heath, Arctic Eider Society; John Chételat, ECCC	D, S, C
--	John Chételat, ECCC	S
--	Gwyneth MacMillan, Marc Amyot, Université de Montréal; José Gérin-Lajoie, Université du Québec à Trois-Rivières	D, S, C
--	Mélanie Lemire, Pierre Ayotte, Gina Muckle, Éric Dewailly (in memoriam), Université Laval; Chris Furgal, Trent University; McGill University; Institut national de santé publique du Québec	D, S, A, C
NCP	Magali Houde, Derek Muir, ECCC; Steve Ferguson, DFO	S, A, C
--	Tanya Brown, DFO	D, S, C
NCP	Jane Kirk, Sarah Roberts, ECCC	D, S
CORE Programme	Rune Dietz, Frank Rigét	S
CORE Programme	Frank Rigét	S
CORE Programme	Rune Dietz, Frank Rigét, Christian Sonne	S
CORE Programme	Frank Rigét	S
CHANGE	Rune Dietz, Christian Sonne	S
CHANGE	Rune Dietz, Mads-Peter Heide-Jørgensen, Nynne Hjort Nielsen, Christian Sonne	S
--	Tero Mustonen	D, C, A
--	Tero Mustonen	D, C, A
--	Tero Mustonen	D, C, A
--	Tero Mustonen	D, C, A
--	Tero Mustonen	D, C, A
--	Tero Mustonen	D, C, A

Chapter 9 Electronic Annex

The Electronic Annex is available at **https://www.amap.no/documents/doc/3581**

EA Case Study 1. The river Lule: a Sámi river in the heartland of the Swedish North

Primary Author: Tero Mustonen, Snowchange Cooperative

Contributing Author: Stefan Mikaelsson, Sámi Parliament

Introduction

The river Lule (Sámi: Julevädno; Swedish: Lule älv) is a major river of northern Sweden, with a total length of 460 km. The catchment area is approximately 25 000 km^2 (see Figure EA1). The river Lule has been harnessed for energy production with several hydroelectric power stations having been built along its course. These include Harsprånget, the largest in Sweden; other major stations include Porjus, Letsi, Messaure and Edefors. The first hydropower dams on the river Lule were built in 1915. There are both Lule Sámi and North Sámi communities living along the river. At the headwaters, some of the largest conservation areas in Europe constitute the Lapponian Area, an UNESCO World Heritage Site. The municipality of Jokkmokk, widely known as the 'capital' of the Swedish Sámi culture, is located within the basin.

Indigenous Knowledge regarding Hg in this area is predominantly held by those Sámi who are living and practising their livelihoods on the river Lule; the Sámi themselves consider their knowledge to be distinct and unique (Mikaelsson, 2020). They are also an important source of observations regarding Hg concentrations in the area. In this case study, Sámi views on changes to this river and associated water-quality issues are discussed.

Methods

The river Lule is a large, heavily altered river system with a lot of hydropower development. This case study on Indigenous Knowledge regarding Hg uses a literature review, community-based monitoring work mainly conducted between 2003 and 2013 (summarized in Mustonen and Syrjämäki, 2013) and additional interviews and knowledge collection conducted in the Spring of 2020 for the AMAP 2021 Mercury Report. Sámi leaders were invited to respond to current questions regarding Hg in the area by Stefan Mikaelsson, a long-time member of the Sámi Parliament Plenary Assembly, former President of the Swedish Sámi Parliament and board member of the Udtjá Forest Sámi community, who summarized their views in "Reflections on Mercury on River Lule" (Mikaelsson, 2020). Additionally, cartographic summaries are used to illustrate the Sámi communities of the area and the locations and extent of hydropower developments.

Results

The river Lule constitutes a catchment area that has been heavily altered, including the river's main channel. These alterations started in 1915 with the construction of the Porjus hydropower station in the upper part of the river basin. Subsequently, 14 other hydropower dams were constructed between 1950 and 1977, permanently altering the river (Mustonen and Syrjämäki, 2013). This development of the watershed eliminated, for the most part, the capacity of Atlantic salmon to use the river as a spawning area and thus adversely affected a key Sámi sociocultural indicator species. However, since the time the river was first altered over 100 years ago, the Sámi have continued to use the altered river and its reservoirs for subsistence fishing.

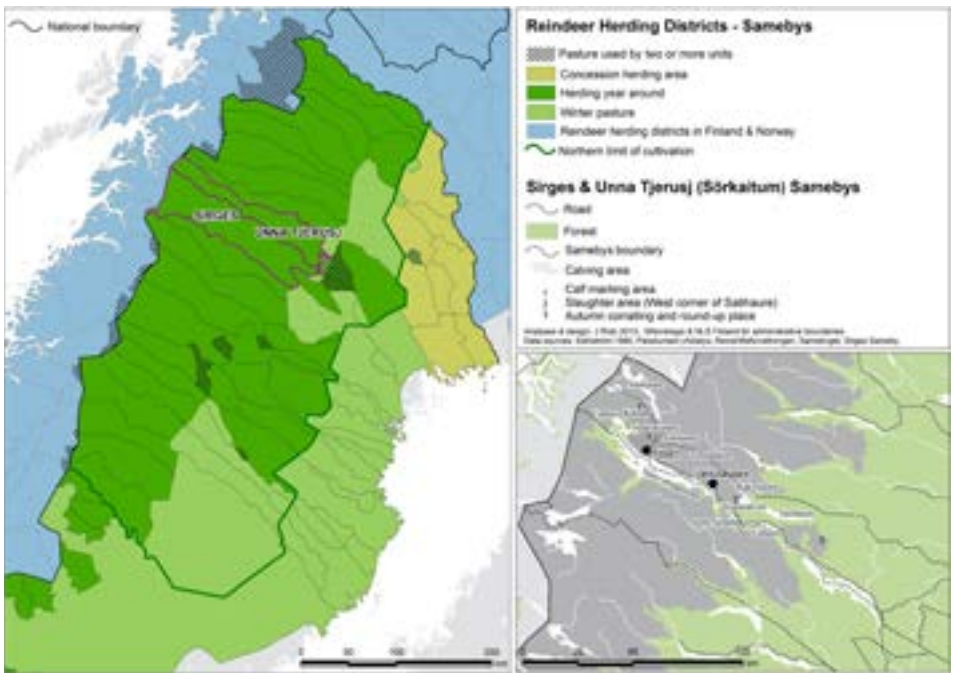

Figure EA1. Map of reindeer herding areas and Sámi communities in the upper part of the Lule River. The insert map documents historic land use and important seasonal sites from 1970s onwards. Information from the 2010s. Source: Johanna Roto/ Snowchange Cooperative, 2022, with some alterations to the map text. Used with permission.

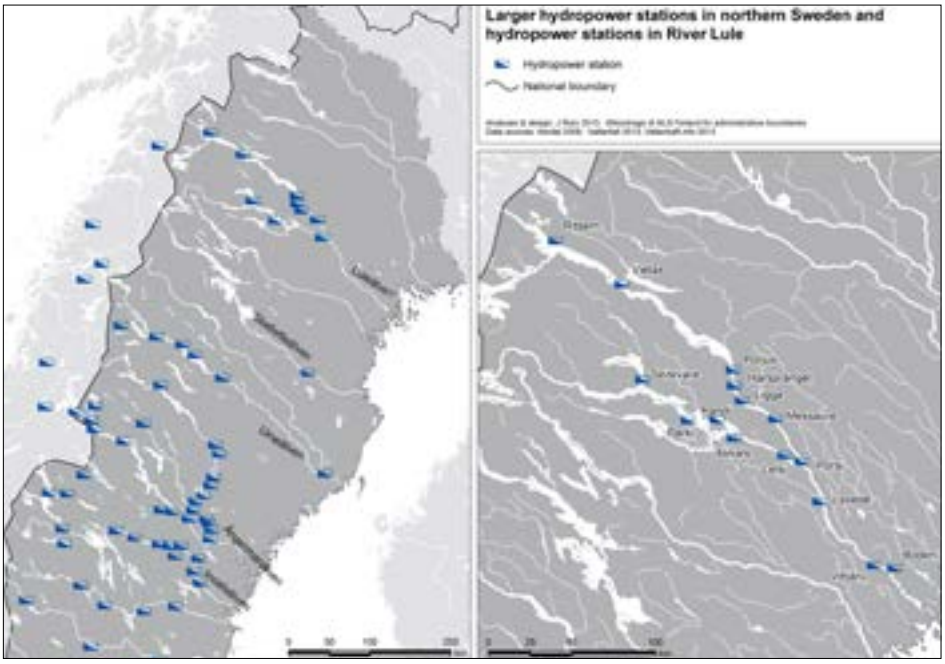

Figure EA2. Hydropower stations on River Lule. Source: Johanna Roto/Snowchange Cooperative, 2022. Used with permission.

Hsu-Kim et al. (2018) describe how releases of Hg (and subsequently of methylmercury) is characteristic of altered rivers such as the river Lule, and the associated risks. Sweden sets the threshold for safe levels of Hg contamination in fish at 0.20 mg/kg. Climate change is expected to make the accumulation of methylmercury in waters worse (Eagle-Smith et al., 2018). Skyllberg et al. (2007) in their review of national methylmercury levels, confirm its presence in the river Lule watershed at multiple locations. Åkerblom and Johansson (2008) state that, nationally, the spatial variation of Hg in lakes and streams is substantial; however, currently, in the river Lule, Hg levels can be up to five times greater than Hg concentrations under 'natural conditions'.

Given the large number of hydropower dams and reservoirs on the river Lule (see Figure EA2), we can assume that there is a large amount of sedimented Hg in all of the 15 reservoirs along its course. A national database on Swedish water bodies (VISS[1]) indicates that Hg is present in all parts of the river system (above the national safe limit of 0.20 mg/kg) and that the river is "unlikely to reach a good chemical status" in the near future (see also Nyberg et al., 2018). However, due to the size of the catchment and multiple reservoirs, the Hg levels vary greatly at different points.

The Jokkmokk area is often hailed as the hub of Indigenous Knowledge in Northern Sweden. Many Elders from the area, such as Elle-Karen Pavval, have mastered the old ways. She recalled, for example, the old weather prediction skills during the oral history work:

> *"You can forecast weather [from] reindeer behaviour. For example, winds make the reindeer run [to specific directions] here and there, [which] predicts wind. Weather was also predicted from the stars. If you wanted to predict the floods in the summer, you needed to catch a big northern pike fish, and take her liver"* (in Mustonen and Syrjämäki, 2013).

According to Mikaelsson (2020), traditional food production is valuable for Indigenous individuals themselves, who maintain better health and wellbeing by consuming traditional food than non-traditional sources of nutrition. It is important for Indigenous People to be able to control their own food and to ensure it is devoid of antibiotics and growth hormones. Water quality should also be under their control, as clean water is essential for Indigenous health and well-being.

One of the most respected knowledge holders in the river Lule Basin, Lars Pirak, discussed the connection of Sámi people to the landscape: "*[When it came to] sacred lakes that were called* saiva*, the thing was to throw some silver there, so that people would get fish*" (Mustonen and Syrjämäki, 2013). Such behaviour reveals the reciprocal relationship the Sámi had with their waters. Respect and careful mindfulness were the keys to maintaining a good relationship with the waters.

Sámi knowledge is interconnected across terrestrial, aerial and aquatic systems (see Figure EA3). Mikaelsson (2020) says that "land on which Sámi live and the natural resources on which we depend are inextricably linked to the survival of our identities, cultures, livelihoods, as well as our physical and spiritual well-being."

Large-scale alterations, such as dams, in any of these components of the Indigenous system cascade and accumulate, much like Hg itself. Sámi knowledge of Hg on the river Lule is intertwined with the experience of the human-induced changes to the basin. It cannot be separated from the history of development of the river. For this case study, a number of key oral history and written materials (Mustonen and Syrjämäki, 2013) are shared below to highlight Sámi perspectives on the situation.

From the perspective of the Sámi, the Suorva Reservoir in the upper part of the river Lule system is of key relevance when considering the history of hydroelectric development in the region. The reservoir sits 90 km upstream from Porjus (the first hydropower dam, built in 1915). The present area of the reservoir originally consisted of six smaller lakes. Water levels

[1] See: https://viss.lansstyrelsen.se/Waters.aspx?waterMSCD=WA33065308

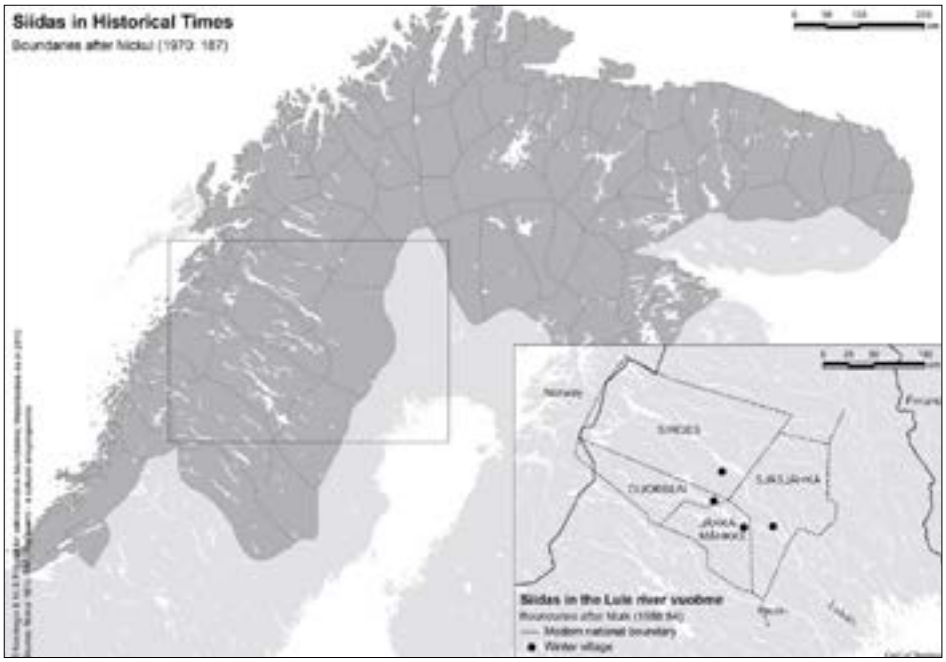

Figure EA3. Major Sámi *siidas* (i.e., historic Indigenous-governed communities of the Lule River area). Source: Johanna Roto/ Snowchange Cooperative, 2022. Used with permission

Sámi fisherman (Pittsa) fishing on Suorva Reservoir, 1970s. Photographer: Jan Håkan Dahlström, Snowchange Cooperative. Used with permission.

were raised, initially, by nine meters. At the time of construction, the county's administrative board assessed the damages caused to reindeer pastures and fisheries to be minimal, ignoring Sámi knowledge of pasture quality and seasonal rotation. Forced relocations from further north also increased the pressures on the Sámi herds in the region.

Throughout the 1900s, the Sámi voiced critical views and expressed their resistance through the media and by forming social organizations opposing the plants. For example, in 1964 Susanna Kuhmunen wrote a long letter in the *Norrbottens-Kuriren*, a regional newspaper, identifying the changes that had taken place in her lifetime (from 1925 to 1964). According to Kuhmunen, damages caused by hydroelectric development included the following:

- Changes to fish and fisheries, including amounts of fish and new damage to nets and places of importance to the Sámi (including through Hg loading)
- The destruction of several places and communal sites of importance to the Sámi, which are now underwater
- Altered conditions on lakes and lakeshores, making subsistence for Sámi much harder (including reindeer herding activity)
- Overall total impact on Sámi uses of the land, including an understanding that both economic opportunities and future land use will be greatly affected by the proposed next stage of Suorva developments in the 1960s (in Mustonen and Syrjämäki, 2013).

In the late 1950s and early 1960s, the journalist Elly Jannes and the photographer Anna Riwkin-Brick wrote about the Sámi's 'awareness' of changes as new developments were pursued, including their knowledge of flooded crossing points for reindeer, loss of spring pastures, dead fish, changes to the shorelines and the resulting impacts on transportation, fisheries and the use of lakes. Jannes and Riwkin-Brick quote Anders Pirtsi, who said at the time: "*Is it right to sell the reindeer grazing grounds of one's descendants for a few thousand crowns?*" Another Sámi person also commented at the time that: "*No matter how much I love my own life in the reindeer forest areas, I would not advise my children to inherit my work. The authorities seem to have made up their minds to destroy us, in spite of all the beautiful words they use in their reports*" (Mustonen and Syrjämäki, 2013).

Lars Pirak linked the destruction caused by the hydroelectric stations to damage to fisheries and, consequently, to income: "*[Before the time of the Vattenfall, Swedish energy company] we went and sold and exchanged our fish [for] food items*

[2] See: http://samer.se/1214

here in Jokkmokk. Now that the rivers have been harnessed and destroyed, fisheries have worsened considerably in some locations" (in Mustonen and Syrjämäki, 2013).

Despite these changes, the Lule River system remained a major commercial and Sámi fishery.[2] Infrastructure to deliver catches of fish was established with fish buyers (Mikaelsson, 2020). The buyers could buy fish from fishers by accessing fisheries by boat, airplane or helicopter and do business with the families who lived and fished on the most remote mountain lakes. Mostly, this fishing was based on catching Arctic char and whitefish, which have a higher economic value than predatory fish species; while these species do make up part of the catch in subsistence fishing, species such as perch and pike are prone to absorb Hg from their environment (as methylmercury).

Mercury loading (as observed by Browne, 2007 and Åkerblom and Johansson, 2008) in the catchment area due to industrial forestry actions has also been observed by the Sámi. Mikaelsson, who has been working as a reindeer herder for most of his life, noted that "*after cutting down a forest, it is a common practise to dig ditches in the soil, which results in faster flow of water from forest to rivers and lakes*" (in Mustonen and Syrjämäki, 2013).

Reindeer herder Per Ola Utsi has observed how the reservoirs are altered through the seasons. As the hydroelectric reservoirs fill in the autumn, waters rise. As the reservoir water levels drop through the season, ice is left 'hanging' on the beach (with water disappearing). Fluctuating water levels lead to greater levels of erosion. This is expected to further increase the loading of Hg from the banks and shoreline (Hsu-Kim et al., 2018).

Additionally, according to Utsi, the alterations to the river Lule basin (i.e., the hydropower dams and artificial lakes) contribute to the local air moisture and weather. It can now become very moist, which means that lichen close to the shores freezes when the temperatures fall. According to Utsi, while people are interested in regulating the waters of the Lule, nobody pays attention to the surrounding areas and how they are impacted by these alterations (Mustonen and Syrjämäki, 2013).

Sara Omma, a young woman at the time the oral history work was conducted, said that the century of development of the river Lule has left people at breaking point: "*This damming has taken place already four times. Four times we have had to move. Each time they have said it will never happen again. Such wrongdoings have been committed against the Sámi. Great benefits have been reaped by harnessing the lakes and now the electricity goes via Norway to southern Sweden. So that where we are living, there is no electricity, but just above our heads there are huge powerlines transferring the electricity to Norway*" (in Mustonen and Syrjämäki, 2013).

Discussion and Conclusions

The river Lule is a major Sámi watercourse, a spawning river for Atlantic salmon and many other salmonid fish as well as a migratory route of the Sámi reindeer herders. Both large-scale nature protection (Lapponia) and 15 hydropower dams have transformed the Indigenous landscapes of the river Lule into a human-controlled system.

The hydroelectric development has released Hg, which has then become methylmercury, across the Lule River system and basin; Hg levels are now consistently above 0.20 mg/kg throughout the system (Browne, 2007; Skyllberg et al., 2007; Åkerblom and Johansson, 2008; Hsu-Kim et al., 2018; Nyberg et al., 2018). Skyllberg et al. (2007) have identified Hg in Lule River sediment. Climate change may be a new driver of releases of Hg and may also affect levels of sedimented Hg (Chen and Driscoll, 2018).

According to Mikaelsson (2020), traditional Sámi food production is small-scale and requires that nature remains unchanged for a long time. The major industrial activities that have taken place have created a great deal of uncertainty in Sápmi (i.e., in Sámi land and among Sámi people; Mikaelsson, 2020). This uncertainty comes from the challenge of maintaining one of the Arctic's many Indigenous cultures, from ongoing emissions from many sources, and ultimately from how these emissions affect other areas according to two basic ecological principles: nothing disappears and everything spreads.

The Sámi had a reciprocal relationship with their waters (see Mustonen and Syrjämäki, 2013) as a part of the interconnected co-being of their home area. A century of alterations on the river Lule have destroyed this complex self-governed system. Early Sámi leaders, like Johan Turi and Elsa Laula Renberg, warned about the dangers of losing the land as a consequence of development. Mercury is one of the results of the macro-level development of the basin.

At the height of the hydropower development in 1964, Sámi women, such as Susanna Kuhmunen, identified the system-wide negative impacts, including Hg loading, that would result from the hydro dams (and from Suorva in particular). Precise monitoring of Hg levels from 1960s onwards will be left for future studies. From the 1990s onwards, forestry actions on the river Lule, included ditching and further clear-cut logging, intensified. Sámi leaders, such as Stefan Mikaelsson, have conveyed their concerns regarding these actions for decades. Browne (2007) confirms that the clear-cutting of trees may already be increasing Hg releases from soils.

Some Hg is found naturally in the environment, but much of the Hg in our environment today is transported over long distances via the atmosphere and originates in other countries (*Länsstyrelsen*/Provincial Administration, in Mikaelsson, 2020). Overall, Swedish emissions have decreased, and Hg in particular has decreased since 1990 (see VISS database). Despite this, the levels of Hg in the environment are still far too great and the levels in fish do not seem to have declined. Mercury continues to leak into lakes and streams. The problem is greatest in southern Sweden (Åkerblom and Johansson, 2008), where the precipitation of Hg is greater than in northern Sweden.

The Sámi by the river Lule have identified Hg as a concern embedded in the larger development actions. They have expressed concern via various means, from opposition and concern at the time of construction of the hydroelectric power

[3] See: https://www.youtube.com/watch?v=ZSrWPSUf8tw

plants (Susanna Kuhmunen), to the detection of loss of fisheries and fish quality (Lars Pirak, Per Ola Utsi) and concerns in connection with new forestry practices, such as ditching and increased clear-cuts. Recent assessments on the presence of Hg in the thawing permafrost areas (Schuster et al., 2018) are also concerning to the Sámi within the Lule Basin (Mikaelsson, 2020). Sámi have also expressed, throughout this time of alteration and development, their deep connections with the river (see, for example, Katarina Rimpi's yoiks).[3]

All of the changes described above are leaching Hg into the waterways. A gradient can be observed from the high mountains (where lower levels of Hg are observed) to the coast (where higher levels of Hg are observed) of the river Lule basin (Mikaelsson, 2020). Another gradient can be observed for the Norrbotten coast, with higher levels in the Piteå region (south) and lower levels towards the Kalix region (north). Earlier industrial releases and distribution of Hg from Rönnskärsverken near Skelleftea further down south is also relevant in the regional view.[4]

Another relevant source of Hg in Norrbotten is the Aitik mining site. The Aitik copper mine is located about 15 km southeast of Gällivare city center. The Aitik case has led the Sámi Parliament to demand that the mining company show in its environmental impact assessment reports how dust produced as a result of mining activity with increased levels of Hg can affect reindeer husbandry, the health of reindeer and reindeer herders, and the quality of reindeer meat (Mikaelsson, 2020; see also Sámi Parliament reply to *Mark- och miljödomstolar*; Land and Environmental Courts, Court number: M 2672-18, 5.2.2020).[5]

The Sámi have no land rights nationally in Sweden. According to Mikaelsson (2020), Sámi culture and business are mostly invisible in official statistics on the Swedish side of Sápmi (Sámi home land). In order to investigate the overall situation with regards to Hg in the river Lule, an assessment of Indigenous Knowledge and science should be conducted (Skyllberg et al., 2007). For example, Arctic char, which accumulates Hg and is a major cultural fish species for the Sámi, would be well worth investigating. Chen and Driscoll (2018) also stress the need for action following Hg research already conducted. Sweden ratified the Minamata Mercury Convention in May 2017. National implementation actions should include responses to questions of equity and Sámi rights as a part of developing a long-term solution to damages done to the river Lule.

EA Case Study 1: References

Åkerblom, S. and Johansson, K., 2008. Kvicksilver I Svensk Insjöfisk – Variationer i Tid och Rum. Rapport 2008:8, Swedish Agricultural University.

Browne, D., 2007. Freshwater Fish in Ontario's Boreal: Status, Conservation and Potential Impacts of Development. WCS Canada Conservation Report No. 2. Wildlife Conservation Society Canada (WCS), Toronto, Ontario, Canada.

Chen, C. and Driscoll, C., 2018. Integrating mercury research and policy in a changing world. Ambio, 47:111-115.

Eagle-Smith, C. et al., 2018. Modulators of mercury risk to wildlife and humans in the context of rapid climate change. Ambio, 47:170-197.

Hsu-Kim, H. et al., 2018. Challenges and opportunities for managing aquatic mercury pollution in altered landscapes. Ambio, 47:141-169.

Mikaelsson, S., 2020. Reflections on Mercury on River Lule. An unpublished manuscript available from Snowchange Cooperative.

Mustonen, T. and Syrjämäki, E., 2013. Oral Histories and Sacred Landscapes of the Jokkmokk Sámi. Snowchange Cooperative, Kontiolahti, Finland.

Nyberg, E. et al., 2018. The National Swedish Contaminant Monitoring Programme for Freshwater Biota. Swedish Environmental Protection Agency. Swedish Museum of Natural History, Stockholm, Sweden.

Schuster, P. et al., 2018. Permafrost stores a globally significant amount of mercury. Geophysical Research Letters, 45:1463-1471.

Skyllberg, U. et al., 2007. Net methylmercury production as a basis for improved risk assessment for mercury-contaminated sediments. Ambio, 36:437-442.

VISS, 2021. Luleälven Vattenförekomst, MS_CD: WA33065308. VISS EU_CD: SE729042-178707, Val av förvaltningscykel, Förvaltningscykel 3 (2017 – 2021). In: Vatteninformationssystem Sverige (VISS). Database. Available at: https://viss.lansstyrelsen.se/Waters.aspx?waterMSCD=WA33065308

[4] See: https://www.sametinget.se/klimat

[5] The Sámi Parliament's opinion regarding Boliden Minerals AB's application for change for operations at the Aitik mine with a new mine in Liikavaara, Gällivare municipality in Norrbotten County (Objective no: M 2672-18). The opinion went to the *Mark- och miljödomstolar* (Land and Environmental Courts) in Umeå and was possible thanks to a referral invitation. See more at: https://www.svt.se/nyheter/lokalt/norrbotten/kort-livslangd-for-ny-gruva-i-liikavaara-i-gallivare-kommun

EA Case Study 2. Lokka and Porttipahta reservoirs, Lapland, Finland

Author: Tero Mustonen, Snowchange Cooperative

Introduction

This case study focuses on the Lokka and Porttipahta reservoirs in Finnish Lapland that were created in the late 1960s and early 1970s. They are the largest of their kind in Europe. Lokka and Porttipahta are located in the northern part of the municipality of Sodankylä, along the tributaries of the river Kemijoki in Central Lapland. Lokka Reservoir is situated in the upper reaches of the river Luiro and Porttipahta reservoir is situated upstream of the river Kitinen.

The maximum height of water for both reservoirs is 245 meters above sea level, and the lowest permitted height of water is 240 meters for Lokka and 234 meters for Porttipahta. Due to their shallowness, the lowering of water levels diminishes the size of their basins significantly. The two reservoirs were connected in 1981 through the creation of the Vuotso Canal. The regulating dam in Lokka Reservoir is situated at the southern tip of the basin; the dam is 30 meters tall, and it has a power station capable of producing 35 MW.

Verta et al. (1989), Wahlström et al. (1996), Berglund et al. (2005), and Browne (2007) all agree that, in general, large-scale hydroelectric dams stimulate and take up a large amount of Hg from the submerged soils. Such was also the case with Lokka and Porttipahta. The creation of these reservoirs displaced a North Sámi Indigenous community and other local (Finnish) wilderness communities, and also drowned many villages. The 1950 census named 56 Sámi individuals in the Lokka area. Villages considered to be majority Sámi included Kurujärvi, Yli-Luiro, Ponku, Laiti (in Porttipahta area) and Lusma. The exact number of Sámi people impacted by the flooding remains unknown.

Vuotso is the central village of the modern Sompio area. Development along the river Kemijoki (see Figure EA4) is a central theme of this case study; the river was first harnessed for hydroelectric power production in 1948. By the late 1960s, construction work on the dams by the electricity industry had reached the headwaters of the river, an area where the Sámi and other local people were living in subsistence economies and practicing age-old traditional cultures. In the span of a few years, a whole culture was destroyed and flooded. The majority of the Sámi and other locals were resettled in Vuotso (see Figure EA5)

The nation-states of Sweden, Norway and Russia started to exercise their powers in the region more forcibly in the 18th and 19th Centuries. Sweden and Norway underwent various border disputes with Russia and between themselves. These disputes impacted the migratory lifestyle of the North Sámi, who lived on the coast of the Arctic Ocean in the summer and in the highlands of the border area between Finland, Sweden and Norway in the winter.

Aikio (1978 and in 1988) reports that families of these North Sámi moved to the Sompio (Vuotso) region in the 1870s to 1890s due to the challenges that border closures imposed on

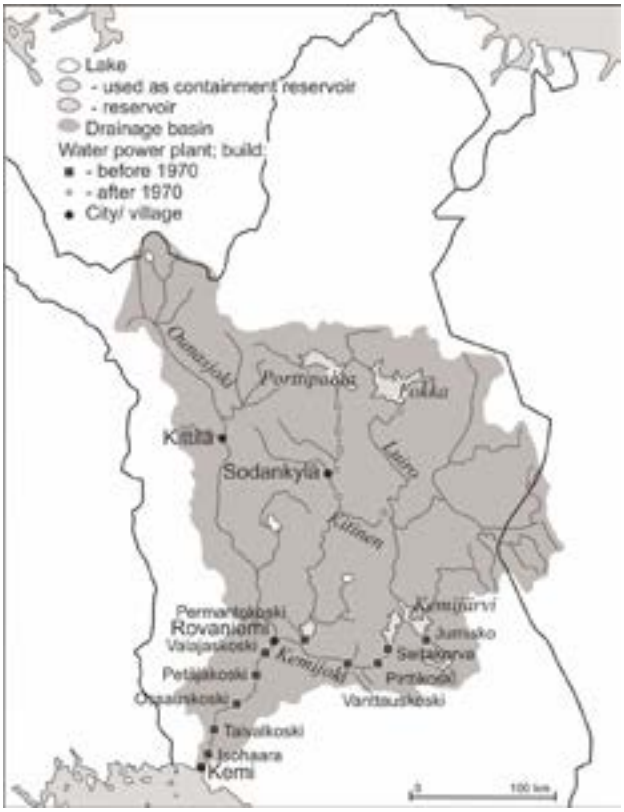

Figure EA4. Map showing the river Kemijoki and the location lakes, reservoirs and the area of the drainage basin along with power plants built before and after 1970. Source: Johanna Roto/Snowchange Cooperative, 2022. Used with permission.

their life herding reindeer and on their seasonal migrations. Rosberg (in Aikio, 1988) provides us with information that makes the case more complex; around the same time as the growing border disputes, the people in Sompio had invited some of the North Sámi to their home areas to herd and manage their reindeer during this period, which also contributed to the migration of North Sámi to the Sompio region (Rosberg, in Aikio, 1988). The hydroelectric development, border disputes between nation states and invitations from the people of Sompio all meant that the Sompio region received a totally new Sámi population at the end of the 19th century. These Sámi started to establish their own seasonal rounds in the community as they navigated the social and political challenges that arose from the land use of the descendants of the Forest Sámi of the region. Aikio (1991:92-93) also states that the North Sámi first settled around lakes Sompiojärvi and Kopsusjärvi and on the Riestovarsi, which is the location of the contemporary Vuotso community. Permanent *gammi*s (turf huts) and households were constructed there between 1883 and 1886. Even today, North Sámi, or 'reindeer Sámi' as they are known, have a clearly separate identity from other local people in the area (Aikio, 1988:65).

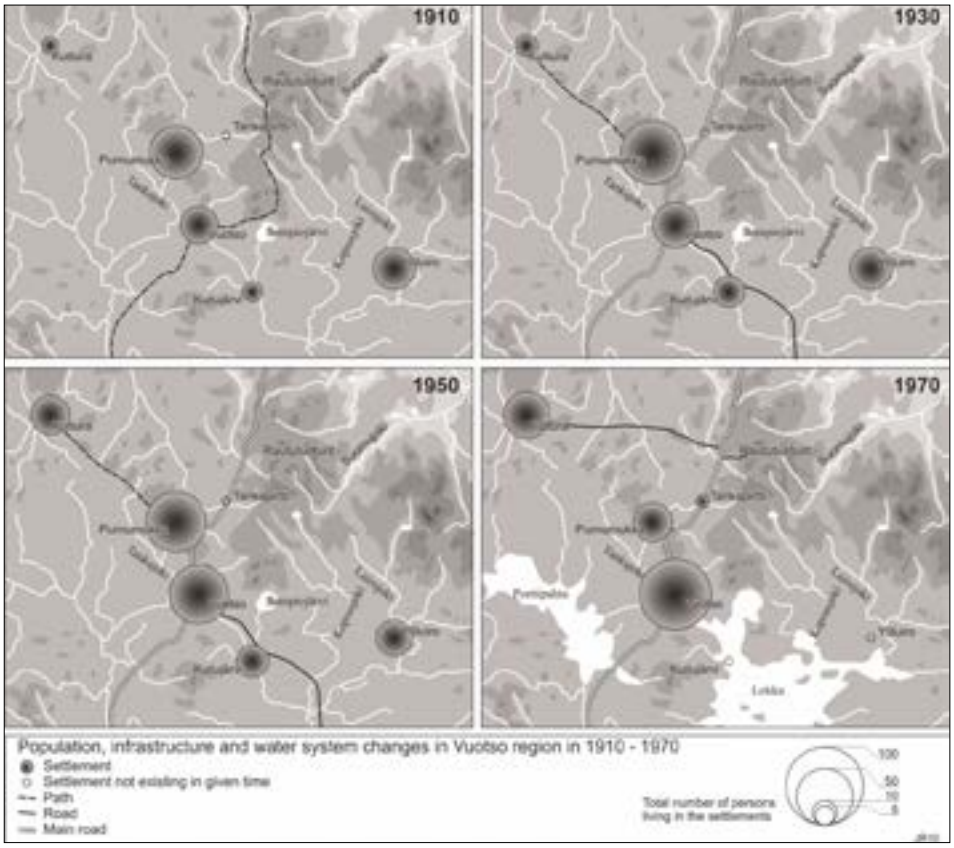

Figure EA5. Map showing changes to population, infrastructure and the water system in the Vuotso region between 1910 and 1970. Source: Johanna Roto/Snowchange Cooperative, 2022. Used with permission.

Methods

For this case study, methods have included a national literature review, community visits between 2000 and 2010, and community-based observation using oral histories and contemporary diary reviews (Aikio family, 1960–1980, summarized in Mustonen et al., 2011 and Murtomäki, 2020). Community-based monitoring (CBM) and visits have been continued after 2010 through the documentation of oral histories, especially in the communities of Purnumukka and Vuotso.

Mercury (Hg) is present in the natural boreal environment. When soils are altered — often through human disturbances such as burning, ditching, mining, and hydropower development — Hg embedded in the soil enters waterways, travels downstream, and reacts with water due to microbial actions (Browne, 2007). This results in methylmercury — a toxic substance that is ingested by wildlife and accumulates in the human body. Due to the process of biomagnification, accumulation is especially prominent among top predators, such as birds of prey and northern pike (*Esox lucius*), yellow perch (*Perca fluviatilis*), burbot (*Lota lota*) and pikeperch (*Sander lucioperca*). When the ground is churned up, and especially when it is then covered by water, Hg in the ground is released into the water system (Wahlström et al., 1996). It has been observed that this happens especially when artificial lakes have been built (Wahlström et al., 1996:159).

A full CBM study of the impacts of the reservoirs was released in 2011 (Mustonen et al., 2011). In this case study, we aim to produce a snapshot of the role of Hg in the life of Sámi and other local peoples in the post-reservoir era; for this, we have used a geographical, literature and CBM analysis. This case study includes new community materials as well as summarized findings from the CBM work from 2000 to 2011.

Results

The area of Lokka and Porttipahta, prior to the construction of reservoirs, was full of *aapa* (marsh mires) intertwined with lakes, river systems and wilderness communities. Both North Sámi and other local people used the Sompio area. The main wilderness economies were reindeer herding, hunting, fishing and small-scale farming (Mustonen et al., 2011). Murtomäki (2020) reports that the construction of the two reservoirs was preceded by large-scale clear-cut logging of an area of up to 417 km^2. The villages of Korvanen, Kurujärvi (a Sámi village) and Riesto were completely submerged; part of Mutenia was also submerged. According to Murtomäki, most of the residents of the wilderness villages were then evacuated to Vuotso.

The clear-cutting was complemented by the use of Agent Orange, a herbicide and defoliant containing toxins and hazardous chemicals. The exact amounts are unknown and have not been reported to the public. The use of Agent Orange was to speed up the removal of timber and unwanted birch trees from the future reservoir sites. Many trees were left in place and submerged underwater. For decades, the Sámi and other local people, such as Oula Aikio and Sulo Alakorva, resisted the creation of the reservoirs, but the reservoirs were eventually built in the 1960s and 1970s (Mustonen et al., 2011).

The Lokka and Porttipahta reservoirs flooded key reindeer herding pastures and hunting areas. They altered the flow of rivers and structure of lakes. Murtomäki (2020) reports that fish catches on the new reservoir (primarily northern pike, yellow perch, burbot, ide and whitefish) were plentiful at first. Murtomäki (2020) conveys an anecdote from the villages from the heyday of the mercury debate in 1970s (during the time of the construction and immediate aftermath of the competition

of the reservoirs). One of the older ladies said that by hanging large pike upside down in freezing temperatures the Hg would accumulate in the head of the fish. Then, by cutting the head off the fish, all Hg could be removed. Such stories emerged as a way of addressing and adapting to the system-wide changes created by the reservoirs, which greatly altered natural systems which were previously relied upon for subsistence living; these alterations caused fish stocks and harvesting areas to become toxic, or at least to be perceived to be toxic.

Despite this, according to Murtomäki (2020), fish, including pike, perch and burbot, continued to be consumed as traditional foods in the Vuotso area, even though warnings had been issued publicly in the 1970s about the increased levels of Hg and the related health effects. For example, the culturally significant process of the drying of northern pike for consumption continued. Murtomäki (2020) recalls there were at least two old men living in remote wilderness cabins in the new reservoir area who did not come to the Vuotso settlement at all. They subsisted only on fish and were most likely unaware of the toxins in the reservoir fish.

In the 1970s, the commercial viability of fish catches from the Lokka and Porttipahta reservoirs suffered as a result of the national discussion about the accumulation of Hg in predator fish (Valste, 2008; Murtomäki, 2020). Mustonen et al. (2011) summarized the levels of Hg in fish in the Lokka Reservoir in the early to late part of the post-dam era (see Table EA1 below). These results indicate the progression of initial high levels of Hg present in the northern pike and burbot during the so called 'erosion' phase of a reservoir (10–15 years after construction) towards an abatement of Hg levels associated with the stabilization of the reservoir (over 15 years after construction).

In the 1970s, Sulo Tanhua and other local people had a good harvest spot with their fish traps close to the now drowned river course of Riestojoki. Pike markets collapsed quickly after word spread of high levels of Hg in the pike (see above), a predatory fish that accumulates Hg.

Fish traps targeting burbot were positioned along several of the former river courses, now underwater, which fish continued to follow. Harvests of burbot were plentiful. However, the burbot could not be sold. Only the liver and roe were harvested from the fish; the rest of the fish was not taken to market to be sold as other parts of the fish are regional delicacies. The liver, for example, was consumed by the Sámi and other fishermen themselves in remote cabins. No heed was paid to the levels of Hg in the fish.

Murtomäki (2020) has also observed the emergence of a population of white-tailed sea eagles (*Haliaeetus albicilla*) on the newly constructed reservoirs. The eagles harvested burbot (of up to 78 cm long) available on the Lokka Reservoir.

Table EA1. Levels of mercury in pike and burbot in the early to late post-dam era in Lokka Reservoir. Source: National Board of Waters, Finland, 1980 and Kemijoki, 2012 summarized in Mustonen et al., 2011.

	Pike (1 kg)	Burbot (0.5 kg)
1980	0.43 mg/kg (max 0.99 mg/kg)	0.9 m/kg (max)
2012	0.34 mg/kg	0.56 mg/kg

Two fishermen on Lokka reservoir in 1970s. Photographer: Eero Murtomäki, Snowchange Cooperative.

Reservoirs thus stimulated the growth of a 'new ecosystem' which included large amounts of Hg loading (with maximum reported levels of 0.99 mg/kg in pikes, for example, in the early years) from the submerged lands and *aapa* bogs, affecting the local people and wildlife.

Discussion and Conclusions

Lokka and Porttipahta are large reservoir systems in the Finnish Arctic. They were constructed in the 1960s and 1970s. Local Sámi and Finnish communities were not consulted about the establishment of these artificial lakes which permanently altered the traditional economies and cultures of reindeer herding, hunting and fisheries (Aikio, 1991).

One of the survival strategies for these communities subsequent to the construction of the reservoirs was commercial fishing. Despite fishermen having unsuitable boats (Murtomäki, 2020) for a large lake and the wrong gear for this activity, harvests of burbot, whitefish, ide (*Leuciscus idus*) and northern pike emerged quickly. However, national public awareness of the presence of methylmercury in predator fish (e.g., pike, perch, burbot; see Table EA1 above) soon limited local fishermen's income; as a result of the toxicity levels, few fish could be sold from Lokka to markets in southern Finland.

Messages concerning the released and accumulating Hg were intertwined with and embedded within the context of the larger loss and sadness that followed from the top-down creation of these reservoirs. For the Sámi and other locals, the assumption was that all wilderness fish was 'clean' and healthy, a staple diet throughout the year, as it had been for centuries. The capacity of Sámi and other locals to fully realize that key species like pike and burbot were suddenly contaminated was limited, and the warnings related to the public health hazard represented by consuming these species, insufficient as they were, went unheeded in the early years (Murtomäki, 2020). This difficulty in accepting the threats to health from key subsistence food sources can be considered as a self-defence mechanism in the face of the large, unprecedented alterations of traditional life.

Local anecdotes have also been reported concerning 'how to remove the mercury' from possibly contaminated food sources. These anecdotes can also be seen as mechanisms of social adaptation to cope in a world turned upside-down after events including but not limited to the relocation of many

people from the wilderness villages into the Vuotso area. Those who stayed on the land in remote cabins were potentially completely unaware of the Hg pollution in the early years and were not warned of the health impacts, which amounted to a few references in public newspapers which were often not accessible in remote areas at the time.

Lokka and Porttipahta have not been discussed or debated at the national level for decades. Scientific measurements indicate that as soil humus levels have dropped, the levels of Hg in pike, perch and burbot are lower than in 1970s (peaking in the 1980s at a max level of 0.99 mg/kg and declining to 0.34 mg/kg by 2012). The reservoirs have therefore stabilized in ecological terms. For the Indigenous Sámi and other local people, however, the social and cultural cost of the construction of the reservoirs has been immense (Aikio, 1988).

Aikio (1988) also identifies that the development of the two reservoirs led to an acceleration of assimilation (of the Sámi with those already living in the Vuotso region) and, consequently, to the almost complete loss of the Sámi language in Vuotso. Integration, which in practice meant a transition from the Indigenous land-based life into the monetary economy, resulted in a major disruption to Sámi culture. Mercury loading and the presence of Hg in fish species central to Sámi cultural and economic practices, are key elements of the damage done; this damage will continue to influence the area with regards to both the Hg content in sediment (Verta et al., 1989) and in the shaping of human histories (Mustonen et al., 2011) in the long term.

EA Case Study 2: References

Aikio, P., 1978. The breakdown of a Lappish Ecosystem in Northern Finland. In: Papers of the Symposium on Unexpected Consequences of Economic Change in Circumpolar Regions at the 34th Annual Meeting of the Society for Applied Anthropology. Amsterdam, March 19-23, 1975. Boreal Institute for Northern Studies, The University of Alberta, Edmonton, Alberta, Canada. Occasional publication #14, January 1978.

Aikio, M., 1988. Saamelaiset kielenvaihdon kierteessä – Kielisosiologinen tutkimus viiden saamelaiskylän kielenvaihdosta 1910-1980. Mänttä: SKS, 1988.

Aikio, M., 1991. Mikä on Sompion Lappi? In: Aho, S., Aikio, P. and Keränen, T. (Eds). Tutkimuksen ja hallinnon vuorovaikutus ympäristörakentamisessa: Esimerkkitapauksena Lokan ja Porttipahdan tekoaltaat. Oulu: Research Institute of Northern Finland.

Berglund, M., Lind, B., Björnberg, K.A., Palm, B., Einarsson, O. and Vahter, M., 2005. Inter-individual variations of human mercury exposure biomarkers: a cross-sectional assessment. Environmental Health, 4:20.

Browne, D., 2007. Freshwater Fish in Ontario's Boreal: Status, Conservation and Potential Impacts of Development. WCS Canada Conservation Report No. 2. Wildlife Conservation Society Canada (WCS), Toronto, Ontario, Canada.

Murtomäki, E., 2020. Muistoja pohjolasta. (Memories of the North), unpublished diary entries. March 2020.

Mustonen, T. et al., 2011. Drowning Reindeer, Drowning Homes: Hydroelectricity and the Sámi in Sompio. Snowchange Cooperative, Kontiolahti, Finland.

Valste, J., 2008. Myrkkyjen leviämiseen havahduttiin. In: Telkänranta, H., 2008. Laulujoutsenen perintö: Suomalaisen ympäristöliikkeen taival. Helsinki: Suomen luonnonsuojeluliitto.

Verta M. et al., 1989. History of heavy metal pollution in Finland as recorded by lake sediments. Science of the Total Environment, 87/88:1-18.

Wahlström, E. et al., 1996. Suomen ympäristön tulevaisuus. Edita, Helsinki.

EA Case Study 3. Koitajoki: Finnish-Russian Border River

Author: Tero Mustonen, Snowchange Cooperative

Introduction

Koitajoki is a 200-kilometer-long waterway that begins in North Karelia, Finland, enters into the Republic of Karelia in Russia, and then returns to Finland. It is part of the Vuoksi watershed. The catchment area is characterized by large peat and marsh mire areas and lakes, including Koitere and Petkeljärvi.

Of importance to this case study are the endemic whitefish populations (*Coregonus lavaretus pallasi* and *Coregonus lavaretus wartmanni*). The *pallasi* species is an important species for biodiversity nationally. The lower part of Koitajoki, the Ala-Koitajoki, used to be the spawning area of the land-locked Atlantic Salmon (*Salmo salar*) of the Lake Saimaa basin. Historically, more than 30 000 fish would migrate upstream to spawn each year. The hydroelectric power plants at Kuurna, Kaltimo and Pamilo prevent these critically endangered salmon from reaching their ancestral spawning areas.

Large-scale ditching of marsh mires and peatlands for forestry and large-scale peat mining (Albrecht, 2019) have released Hg into the Koitajoki system (for example in the mid-1980s in the Koitajoki lakes, Hg levels in northern pike varied between 0.41 and 0.67 mg/kg); this Hg loading continues. Additional releases may have resulted from industrial gold mining in the catchment area (Albrecht, 2019).

The communities living along the Koitajoki are considered to have special status in Finland. The Finnish-Karelian epic *Kalevala* is based on the rune songs collected in Karelian villages, especially those along the Koitajoki (Ilomantsi, Megrijärvi, Ala-Koita and Möhkö). The population of the Koitajoki catchment on the Finnish side is predominantly comprised of Savo-Karelian (often Lutheran) and Karelian (Russian Orthodox) peoples. The local dialects of Savo-Karelia and the Karelian language are still spoken along the river. On the Russian side, there are few permanent villages left for historical reasons, but the area is used seasonally by Karelian families. Lake Vieksjärvi, part of the Koitajoki catchment, is a key location on the Russian side for traditional fishing. Of special importance is the preservation of the non-commercial river seining targeting *Coregonus lavaretus pallasi*. Seining has also been proven to cleanse the spawning areas of the endangered whitefish populations, helping to keep the spawning areas of the endangered whitefish populations free from humus and other organic matter (Mustonen and Mustonen, 2018). Regionally, plans are under way on an application for the river and its traditional culture to be included in national and international UNESCO Intangible Cultural Heritage Lists.

Residents of Koitajoki villages have been shown to possess traditional ecological knowledge of their river; yet Finland has no legislative recognition of traditional ecological knowledge (Mustonen and Mustonen, 2018). The Indigenous Sámi people in Lapland, who are linguistically related to Finns and Karelians, have secured some recognition for Sámi knowledge through national implementation of the Convention on Biological Diversity (CBD), signed by 150 government leaders at the 1992 Rio Earth Summit, specifically the implementation of Article 8j ('Traditional Knowledge, Innovations and Practices') and related legislation (CBD, 1992). In Russia, Karelians, especially the Veps, enjoy the protection of federal legislation regarding their culture, language and status. Russia considers Karelians a national minority. The Veps, a people who speak the Veps language (one of the Karelian language groups), have the status of a national Indigenous Peoples in Russia. North Karelia and Russian Karelia are today part of the Barents Euro-Arctic Region, positioning them politically as boreal northern regions, even though they reside geographically below the Arctic Circle.

Methods

For this case study, methods included a national literature review, community visits, and participant observation that led to the establishment of a community-based observation network by Snowchange Cooperative in 2016; early oral history documentation also took place between 2001 and 2015. Methods also included consulting with Traditional Knowledge holders, whose observations were geared towards the detection and contextualization of the presence of Hg in and around Koitajoki; open questions were also put to holders of Traditional Knowledge regarding boreal river systems and Hg. The main data for the case study were derived from the Finnish side of Koitajoki.

Mercury (Hg) is present in the natural boreal environment (Browne, 2007). When soils are altered — often through human disturbances such as forestry, burning, ditching, and mining — Hg embedded in the soil enters waterways, travels downstream, and reacts with water due to microbial actions (Browne, 2007). This results in methylmercury — a toxic substance that is ingested by wildlife and accumulates in the human body. Due to the process of biomagnification, accumulation is especially prominent among top predators, such as birds of prey and northern pike (*Esox lucius*), yellow perch (*Perca fluviatilis*) and pikeperch (*Sander lucioperca*).

Browne (2007:50) states that in boreal Canadian catchment areas where clear-cutting is practiced, Hg levels rose to between 2 and 9.6 times greater than normal levels, highlighting the significance of Hg contamination in boreal water systems. Systematic research on the impacts of Hg on boreal water systems began in Finland in 1966 (Valste, 2008). The issue rose to the national level in 1967 when Hg was associated with environmental impacts on the Kymijoki River. A national debate emerged between the prominent fisherman Pentti Linkola, who argued for the continued use of freshwater fish as food, and state environmental specialists, who stressed the health concerns of consuming fish (summarized in Valste, 2008). This debate lasted for over five years and resulted in more stringent public

advisory messaging around Hg levels, but left many fishermen, like Linkola, feeling that their livelihoods had been affected negatively by the state environment officials.

At that time, the drivers of Hg levels were mainly industrial plants (Wahlström et al., 1996). Between the 1960s and the mid-1990s, Hg releases from industrial plants in Finland were cut in half (Wahlström et al., 1996). However, Wahlström et al. (1996) indicate that while the discharge of Hg from the pulp and paper-mill industry, as well as other industrial sources, has been diminishing, the environmental and soil sourcing of Hg has stayed the same.

Finland officially considers fish with detected Hg levels of over 1 mg/kg to be toxic. The Food and Agriculture Organization of the United Nations (FAO) imposes a stricter limit on Hg pollution, advising against consumption of most fish with levels above 5 mg/kg (Commission Regulation (EC) No. 1881/2006; see also in Berglund et al., 2005). The impacts of Hg on humans as a result of eating fish are more dangerous when those fish are taken from waters rich in humus (i.e., marsh mire and peatland catchment areas like Koitajoki) due to the way Hg attaches to humus particles; fish taken from humus-rich waters are bound to have more Hg as a result.

Verta et al. (1989) shows that the accumulation of Hg in the sediments of boreal lakes in Finland has been very significant, especially in Southern and Eastern Finland where Koitajoki is located. Wahlström et al. (1996) also stress the role of hydroelectric reservoirs as sources of Hg in northern lakes and rivers.

In Koitajoki the drivers of Hg loading include large-scale hydroelectric development (Pamilo, the largest of Vattenfall's hydropower plants in Finland) and its erosion impacts upstream (e.g., at Lake Koitere; see Albrecht, 2019), peat production and forestry management actions (Mustonen and Mustonen, 2018; Albrecht, 2019) and site-specific potential impacts of gold mining by the company Endomines. Browne (2007) also mentions forestry itself (e.g., ponds created by the forestry tractors) as a driver of Hg loading, with groundwater and surface run-off and logging roads transporting Hg downstream.

Koitajoki Traditional Knowledge has been documented since the early 1800s (Mustonen and Mustonen, 2018). The stimulus for this was outsider interest in the wilderness cultures, economies and villages of Karelia, especially the epic songs and other 'traditional' culture. This early documentation waned during the 1940s, when researchers' interest in Karelia diminished. The years of modernity (1944–1991) altered the catchment area and its ecology. The aforementioned forestry, peat production and hydroelectric development occurred during this period. The regional Snowchange Cooperative started a new round of community-based documentation of traditions and oral histories around Koitajoki in 2001. In 2016, Snowchange was commissioned by the regional environmental authorities to document Traditional Knowledge associated with the river communities. This resulted in an on-going community-based monitoring (CBM) project in which Hg is one of the observed indicators. Mustonen and Mustonen (2018) document the first two years of the CBM work. Miller (2019) documents river seining, a local traditional practice which has cultural and environmental impacts on a national level, to monitor and maintain river health. For this case study, the main summaries of the CBM work and the science results have been included.

Results

Albrecht (2019) links a widespread increase in Hg levels in the 1970s and 1980s to the establishment of the Pamilo hydroelectric power station in 1955. The increase was particularly noticeable in Lake Koitere, where Hg levels are impacted by fluctuations in water level associated with hydropower production (i.e., the increase of Hg in pikes from 0.4 mg/kg in 1970s to 0.7 mg/kg by the 1980s; Albrecht, 2017). On Lake Koitere, water levels have sometimes fluctuated to such an extent that the shoreline has shifted up to 25 meters. Mononen et al. (1989) say that, in one section of the Koitajoki, the levels of Hg increased by a factor of five between the 1970s and the mid-1980s. Forestry has also been identified as a source of Hg in the Koitajoki system; since the 1980s, local communities have drawn associations between the use of fertilizers in forestry with increased Hg levels in the Koitajoki (Parviainen, 2014; Albrecht, 2019). The gold mining operations run by the Endomines company in the center of the catchment area may be an additional source of Hg.

From the CBM and Hg study between 2016 and 2018, Mustonen and Mustonen (2018) report that the lakes in the Koitajoki system with humus waters are a cause of concern. Mercury accumulates particularly in northern pike and burbot (*Lota lota*). For example, pike in Lake Nuorajärvi are perceived to suffer from this problem (with levels above 0.6 mg/kg reported in the mid-1980s). Pike and burbot are used extensively as a food fish in the Koitajoki system.

Markku Uusitalo, a local seine fisherman in his seventies, reports (in Mustonen and Mustonen, 2018) that his body contains twice the national average level of Hg. He feels extremely sad that increased Hg levels have ruined the northern pike fishery. He also discusses the fact that authorities did not warn about the danger of Hg accumulation in northern pike, which he ate daily in the 1970s and 1980s. Uusitalo (in Mustonen and Mustonen, 2018) shares the concerns of many fishermen on the Koitajoki in the oral history by asking: "*How can authorities even today advise eating these fish – calling [northern pike] a health food – when they contain neurotoxins?*" Uusitalo, who is a leader of local fishermen in Möhkö, reports that the fishermen associate the present loading of Hg especially with the forestry ditches that flow into the Koitajoki main stream and lakes. Mononen et al. (1989) agree with Uusitalo on the catalytic impact of ditching in releasing Hg. According to Uusitalo, regional authorities and researchers collected new samples from people living on the Koitajoki River in 2016 and 2017 to assess Hg levels in their bodies but the "*results have never been released, even though I called them and asked for them*" (Mustonen, 2019). Parviainen (2014) reports that the sampling of predator fish in the system has demonstrated high levels of Hg in the system (e.g., 0.74 mg/kg in young pikes in 2014). He says the primary impact of Hg can be most easily detected in the areas close to the Pamilo hydroelectric power station.

Discussion and Conclusions

Koitajoki is a major catchment area on the Finnish-Russian border and a centrally important part of Karelian culture (with the national epic *Kalevala* having been inspired by oral histories and epic songs collected along its course). Ecologically, it has been a very significant spawning stream for land-locked Atlantic salmon and endemic whitefish species as well as other wildlife. The catchment area consists primarily of marsh mires and peatlands (i.e., humus waters low in pH and high in Hg, embedded in the soils and part of the natural environment). Until the early 1900s, Koitajoki was in a well-preserved, close to natural state (largely undisturbed and unaltered by the subsistence fishing and agriculture carried out along its course). Between 1944 and 1991, large-scale forestry, peat mining, ditching and hydro-electric development altered the river system, activities which also led to increases in Hg levels.

Both science and community-based observations confirm the large amount of Hg currently in the system (e.g., Parviainen, 2014 has detected levels of 0.74 mg/kg in pikes; Verta et al.,1989 highlights the role of sediments, where Hg has accumulated as a future driver of concern). In the Koitajoki system, local dialects and the Karelian language have co-developed with the river; deep oral histories, customs and cultural indicators are products of this co-development, all of which local communities rely upon as part of the traditional ecological knowledge they use to assess and monitor the health of the river and the fish. Of high importance is the unbroken tradition of river seining, which is still practiced on the Koitajoki.

Community-based observations regarding Hg (e.g., fish samples delivered for scientific analysis) are in line with expert knowledge (as summarized in Parviainen, 2014). Methylmercury accumulates mainly in predator fish, especially in northern pike and burbot. Both of these culturally important species are consumed in households and are fished as part of small-scale commercial operations in the river system. Some fishermen, such as Markku Uusitalo, have expressed concern over the historic lack of effective bans on fishing for these predator fish or reliable information on the health impacts of neurotoxins.

The question of present-day Hg loading into lakes and rivers in Finland remains sensitive. While the pollution associated with plants and industrial sourcing in the 1960s was curtailed, the pollution from hydroelectricity production, forestry management, and peat mining (collectively termed 'catchment area loading') is ongoing. The specific impacts of this industrial activity, carried out by the state as well as private enterprise, have not been linked to Hg and its impacts to nature and humans clearly enough, according to the CBM data (Mustonen and Mustonen, 2018). Some fishermen even feel that their own test results have been hidden from the public. With regards to Canada's boreal zone, a similar ecosystem, Browne (2007) says that, at present, the accumulation of Hg in waterways cannot be predicted adequately due to clear-cutting. This means that the baseline of Hg loading should be urgently investigated across catchments, and thresholds of Hg for forestry operations should be put in place (Browne, 2007:11).

CBM and Traditional Knowledge holders have much to contribute to Hg monitoring efforts in the Koitajoki system. Traditional river seining is actively maintaining and renewing whitefish spawning locations, thus alleviating humus loading. Large-scale catchment restoration work has begun (e.g., the Landscape Rewilding Programme and LIFE programs, Mustonen and Mustonen, 2018; Albrecht, 2019). The promise of these actions is that they could, at least in part, lessen the impact of catchment area loading (of both organic matter and Hg) to the river and give the fish and the river time and space to recover. CBM monitoring efforts will constitute a central element of this work in the 2020s.

EA Case Study 3: References

Albrecht, E., 2019. Ilomantsin luonnonvarojen käytön historiaa Koitajoen ympäristön tilan muutosten kuvaajana. Raportteja 49. Joensuu: Pohjois-Karjalan ELY-keskus.

Berglund, M., Lind, B., Björnberg, K.A., Palm, B., Einarsson, O. and Vahter, M., 2005. Inter-individual variations of human mercury exposure biomarkers: a cross-sectional assessment. Environmental Health, 4:20.

Browne, D., 2007. Freshwater Fish in Ontario's Boreal: Status, Conservation and Potential Impacts of Development. WCS Canada Conservation Report No. 2. Wildlife Conservation Society Canada (WCS), Toronto, Ontario, Canada.

CBD, 1992. The Convention on Biological Diversity (CBD). Rio de Janeiro, 5 June 1992. United Nations, Treaty Series, vol. 1760, p.79.

Mononen, P., Antikainen, T. and Kiiski, J., 1989. Koitajoen vesistöalueen tila ja siihen vaikuttaneet tekijät v. 1977-1987. Vesi- ja ympäristöhallituksen monistesarja, Nro 244. Helsinki: Vesi- ja ympäristöhallitus, 1989.

Mustonen, T., 2019. Personal communication from M. Uusitalo to T. Mustonen, Snowchange Cooperative.

Mustonen, T. and Mustonen, K., 2018. Koitajoen erämaataloudet muuttuvassa ympäristössä. Snowchange Cooperative, Kontiolahti, Finland.

Parviainen, A., 2014. Kalojen elohopeapitoisuudet Pielisjoen, Pielisen, Höytiäisen, Koitereen ja Koitajoen vesistöalueilla. Mikkeli University of Applied Sciences. 61pp. Available at: https://www.theseus.fi/bitstream/handle/10024/73194/alojen+elohopeapitoisuudet+Pielisjoen+Pielisen+Hoytiaisen+Koitereen+ja+Koitajoen+vesistoalueilla.pdf;jsessionid=C3F91D6669C97A34C1DF26CC01326BD6?sequence=1

Valste, J., 2008. Myrkkyjen leviämiseen havahduttiin. In: Telkänranta, H., 2008. Laulujoutsenen perintö: Suomalaisen ympäristöliikkeen taival. Helsinki: Suomen luonnonsuojeluliitto.

Verta M. et al., 1989. History of heavy metal pollution in Finland as recorded by lake sediments. Science of the Total Environment, 87/88:1-18.

Wahlström, E. et al., 1996. Suomen ympäristön tulevaisuus. Edita, Helsinki.

EA Case Study 4. Linking environmental mercury data with Indigenous Knowledge

Author: Tero Mustonen, Snowchange Cooperative

Introduction

This short paper draws links between Indigenous Knowledge and observations of Hg levels in the environment and official Russian and Soviet limnological data on Hg in the Ponoi River. The 426-kilometer-long Ponoi River and its catchment area are of great ecological and cultural value in Northern Europe (Prusov et al., 2001; Feodoroff and Mustonen, 2013). The Ponoi is located in the eastern wilderness part of the Kola Peninsula in the Murmansk region of Russia. The catchment area of 15 467 km^2 is mostly in an undisturbed ecological state (Prusov et al., 2001; CAFF, 2013, Nikanorov et al., 2016).

The Ponoi, like other northern rivers, is fed by snowmelt, precipitation, groundwater, and (to a lesser extent) glacial melt (AMAP, 1998:127). As with most Arctic rivers, the peak flow of the Ponoi happens during spring melt (AMAP, 1998:19). Ecologically key fish species in rivers of the Kola Peninsula include Arctic char, brown trout (*Salmo trutta*), and Atlantic salmon (AMAP, 1998). Stocks of Atlantic salmon include genetically distinct regional populations (Tonteri et al., 2009; Ozerov et al., 2012, 2013). Salmon stocks are affected by Norwegian harvests (Thorstad et al., 2013; Ozerov et al., 2016). The Ponoi River also contains northern pike.

As well as its biodiversity, the Ponoi region is important for cultural heritage. Sámi communities speaking Eastern Ter Sámi (one of nine Sámi languages spoken across Fennoscandia) are the first historically known peoples of the Ponoi region. Prior to the 1600s, the Sámi had at least six distinct Indigenous community areas or *siidas* (Mustonen and Mustonen, 2013) in the present-day Ponoi River catchment area. Starting in the latter part of the 19th century, Komi people from the Arkhangelsk region expanded into the Murmansk region and settled many of the Ponoi villages (Konstantinov, 2009; Fryer and Lehtinen, 2013; Mankova, 2018), including the former Sámi community of Chalme-Varre, which was renamed 'Ivanovka' by the Komi (Mustonen and Mustonen, 2013; Mankova, 2018). Today, the villages of Krasnochelye, Kanevka and Sosnovka are the last roadless communities in the Murmansk region. In these villages, Sámi, Komi, Pomor and Russian cultures meet (Konstantinov, 2009; Fryer and Lehtinen, 2013; Mankova, 2018).

Methods

The detection of Hg using Arctic Indigenous Knowledge alone would be rather complex. The accumulated impact of Hg may take years to develop and often requires scientific, especially limnological, sampling to detect. For this case study, we draw links between two methods of investigation into elevated Hg levels (i.e., scientific sampling and community-based monitoring; CBM). The community-based network drawn upon for this case study has been in place since 2006.

We analyzed results of oral histories and community-based observation (CBO) from Ponoi and adjacent Sosnovka villages between 2005 and 2020 (see more in Johnson et al., 2015). These oral histories and observations have been collected and approved having secured free, prior and informed consent from participants in the following ways:

- Fieldwork trips to Krasnochelye, Chalme-Varre and Ponoi River (August, 2006)
- Oral history and land use interviews and workshops with co-researchers in Krasnochelye, Kanevka and Sosnovka (2007–2010)
- Training and data documentation by local teams in Krasnochelye, Kanevka and Sosnovka (2011–2017)
- Advanced local documentation teams, review of catch diaries and environmental data forms and collection of oral histories in Krasnochelye, Kanevka and Sosnovka, resulting in over 9000 data items (2018–2020)
- ~80 people involved in the study either as co-researchers and/or interviewees (2006–2020).

Earlier CBO results have been summarized in Mustonen and Mustonen (2013), Feodoroff and Mustonen (2013) and in yearly work reports from 2013 to 2020.

For the CBO observations we are using the analytical frame of 'river health' taken from Huntington et al. (2017), which consists of both community observation and interviews with individuals. Observations are analyzed using both Indigenous Knowledge and traditional knowledge (Ambrose et al., 2014) and available scientific information (Soviet and Russian observational data combined with a literature survey, Velichkin et al., 2013). According to AMAP (1998:51), rivers transport contaminants and also store them in ice. Pollution may have initially made its way into the river from the air, the catchment area and from sediment sourcing (AMAP, 1998). Rivers can transport contaminants away from the immediate sites of pollution events; pollution can concentrate through sedimentation in slow-flowing parts of a river system.

Results

Feodoroff and Mustonen (2013:37-38, also 2014, 2015) worked with Russian researchers to review archival data of the regional environmental monitoring stations from the late Soviet era (1975–1991) for Ponoi River. In the Russian data, high total levels of Hg were recorded (see Table EA2 below).

Other indicators of interest reviewed included phenols, heavy metals and oil substances in the Ponoi limnological data (Feodoroff and Mustonen, 2013:37-38). These Soviet-era data have recently become more accessible; at least for the time

Table EA2. Mercury levels in the Ponoi River during the late Soviet era (1975–1991) collected from regional environmental monitoring stations. Source: Feodoroff and Mustonen (2013).

	Levels of mercury (THg), in µg/L
1979–1983	High levels of mercury*
1980	300 µg/L
1983	80 µg/L
2000	High levels of mercury**

*More accurate mercury levels not available
**Exact amounts have not been made public

being, this has allowed international cooperation with academic and research organizations in Russia. Due to potentially poor scientific and data control standards and concerns with regards to censorship, the data should not be assumed to be entirely reliable. It should, however, be said that the data described above (in Table EA2) were cross-referenced by a Nordic limnologist, Tarmo Tossavainen, and found to be generally consistent.

Ponoi is a wilderness river system that, in the past, has been relatively undisturbed. However, during the Soviet era, the villages of Krasnochelye and the closed military installations in the catchment area may have released the pollutants, including Hg, found in the historical data. The Hg loading most likely dissipated downstream. Potential sedimentation may have taken place on the lake systems close to Chalme-Varre where the flow of the Ponoi slows and where the river widens into a lake. Adding to the list of unknown drivers of change in the Russian Arctic, AMAP (1998:234) identified the presence of polychlorinated biphenyls (PCBs; highly toxic industrial compounds) in sediments across northern Russian rivers, including the Ponoi. This contamination may come partly from sites outside the area via airborne pollution.

Following the discovery of a range of environmental issues in the historical data, community-based monitoring (CBM) efforts focused on documenting oral histories (see Table EA3), especially in Krasnochelye, regarding events that may have taken place in the Soviet era. Convergence or divergence between local knowledge and scientific information regarding the Hg data was sought.

The results are preliminary and will eventually be released in peer-reviewed journals. However, at this time, we can, from the CBM data, give a number of examples of events we do know to have taken place (see Table EA3).

Table EA3. Examples of events described in the CBM data. Sources: Feodoroff and Mustonen, 2013; Mustonen and Mustonen, 2013; and see also 'Methods' section above.

	Events described in CBM
1965	Uranium test sites leaked materials into Lake Yelskii
1968	Large diesel spill took place in the village of Krasnochelye
1969	Waste and hazardous materials released into the Ponoi (most likely by 'the collective farm')
1980	Mercury levels peak – "color of the river changes"
1950–1991	Fertilizers dumped into the Ponoi River (yearly)

Discussion and Conclusions

This case study has mostly focused on methods of detecting Hg and other hazardous-related observations in the Russian Arctic. We have focused on the Ponoi River in Russia's Murmansk region. Critical analysis of Soviet-era environmental data is still needed. However, where accessible, the data can provide crucial leads and identify drivers of change that may affect Hg levels, even today, in waters and sediments. Results from long-term cooperation with community-based monitoring networks in the Ponoi region, which began in 2006, have been cross-referenced with data from archives showing that high levels of Hg were detected in the river, especially in the late Soviet era between 1979 and 1983.

CBM observations were aimed at reconstructing pollution events and assessing convergence or divergence with scientific and historical data. The final conclusions are still to be made as the community work is ongoing. The CBM work, when it is reviewed for 2020–2021, will aim to include fish sampling (of pike and burbot) to determine the exact levels of Hg in different parts of Ponoi.

From looking at both the CBM and the sampling data, a range of human-induced environmental events and their impacts on a river system that was previously considered 'pristine', can be identified; these include the dumping of chemicals, the release of pollutants, including Hg, from mining and uranium sites, agriculture, diesel spills, and other events. This may also include settled sedimentation of harmful substances and toxins in lakes located along the main Ponoi channel, especially lakes close to Chalme-Varre.

Convergence between monitoring data and oral history accounts will emerge more clearly as community monitoring continues. The Ponoi model is important in making use of past environmental data to understand the present, especially in the context of Hg monitoring and how it ultimately affects northern Indigenous communities, their health and their waters. Oral history can be useful in identifying undeclared pollution events and directing future CBM efforts or scientific monitoring and remediation. Traditional, Indigenous and local knowledge has often been critical in the context of a limited flow of government information and has helped both protect community and ecological health.

EA Case Study 4: References

Community-based monitoring and oral history materials

Feodoroff, P. and Mustonen, T., 2013. Ponoi and Näätämö River Collaborative Management Plan. Snowchange Cooperative, Kontiolahti, Finland.

Mustonen, T. and Mustonen, K., 2013. Eastern Sámi Atlas. Snowchange Cooperative, Kontiolahti, Finland.

Mustonen, T. and Feodoroff, P., 2014. 2013 Work Report from Ponoi and Näätämö Rivers.

Mustonen, T. and Local Coordinators, 2015. 'Flow of Life' – Photo Essay of the Community Workshops December 2014-January 2015 devoted to the River Ponoi Traditional Knowledge Work.

Mustonen, T. and Feodoroff, P., 2015. 2014-2015 Work Report from Ponoi and Näätämö Rivers.

Mustonen, K., Mustonen, T. and Kirillov, J., 2018. Traditional Knowledge of Northern Waters. Snowchange Cooperative, Kontiolahti, Finland.

Research literature included in the literature review

Alekseev, M. and Prusov, S., 1998. Estimates of Conservation Limits for Atlantic Salmon Females for Four Russian Rivers. International Council for the Exploration of the Sea (ICES), Copenhagen, Denmark.

Alekseev, M. et al., 2019. Distribution, spawning and the possibility of fishery of the introduced pink salmon (*Oncorhynchus gorbusha Walbaum*) in rivers of Murmansk Oblast. Russian Journal of Biological Invasions, 10 (2):109-117.

Allemann, L., 2018. "I do not know if Mum knew what was going on": social reproduction in boarding schools in Soviet Lapland. Acta Borealia, 35 (2): 115-142.

Azbelov, A. et al., 1963a. Study of the seaward migration of the Pacific salmons and the perspectives of their Acclimatization in the Waters of the White Sea and the Barents Sea. International Council for the Exploration of the Sea (ICES), Copenhagen, Denmark.

Azbelov, A. et al., 1963b. Continued Study of the Seaward Migration of the Pacific Salmons and the Perspectives of their Acclimatization in the Waters of the White Sea and the Barents Sea. International Council for the Exploration of the Sea (ICES), Copenhagen, Denmark.

AMAP, 1998. AMAP Assessment Report: Arctic Pollution Issues. Arctic Monitoring and Assessment Programme (AMAP), Oslo, Norway. xii + 859pp.

AMAP, 2017. Adaptation Actions for a Changing Arctic: Perspectives from the Barents Area. Arctic Monitoring and Assessment Programme (AMAP), Oslo, Norway. xiv + 267pp.

Ambrose, W. et al., 2014. Interpreting environmental change in Coastal Alaska using traditional and scientific knowledge. Frontiers in Marine Science, 1:40.

Astakhov, V. et al., 2016. Glaciomorphological map of the Russian Federation. Quaternary International, 420:4-14.

Britskaya, T., 2019. Reindeer Under Fire in Sámi Lands. The Barents Observer, 19th February, 2019. Available at: https://thebarentsobserver.com/en/ecology/2019/02/reindeer-fire-sami-lands

CAFF, 2013. Arctic Biodiversity Assessment: Status and Trends in Arctic Biodiversity. Conservation of Arctic Flora and Fauna (CAFF), Akureyri, Iceland.

Colbourne, R. and Anderson, R., 2020. Indigenous Wellbeing and Enterprise: Self-Determination and Sustainable Economic Development. Routledge. 325pp.

Fryer, P. and Lehtinen, A., 2013. Iz'vatas and the diaspora space of humans and non-humans in the Russian north. Acta Borealia, 30 (1):21-38.

Gordeeva, N. et al., 2015. Variability of biological and population genetic indices in pink salmon, transplanted into the White Sea. Journal of Icthyology, 55 (1):69-76.

Helskog, K., 2012. Bears and meanings among hunter-fisher-gatherers in Northern Fennoscandia 9000-2500 BC. Cambridge Archaeological Journal, 22 (2):209-236.

Huntington, H.P., Begossi, A., Fox Gearheard, S., Kersey, B., Loring, P.A., Mustonen, T., Paudel, P.K., Silvano, R.A.M. and Vave, R., 2017. How small communities respond to environmental change: patterns from tropical to polar ecosystems. Ecology and Society, 22 (3):9.

Holmberg, A., 2018. Bivdit Luosa – To ask for salmon. Saami traditional knowledge on salmon and the river Deatnu: In research and decision-making. Master's thesis in Indigenous Studies. UiT – The Arctic University of Norway, Tromsø.

Carter, Jimmy, 2015. Glasnost on the Ponoi. Fly Fisherman, 46:3.

Filatov, N. et al., 2016. Water resources of the northern economic region of Russia: state and use. Water Resources, 43 (5):779-790.

ICES, 2009. Report of the Working Group on North Atlantic Salmon (WGNAS). International Council for the Exploration of the Sea (ICES), Copenhagen, Denmark. 282 pp.

ICES, 2018. Report of the Working Group on North Atlantic Salmon (WGNAS). International Council for the Exploration of the Sea (ICES), Woods Hole, MA, USA. 386 pp.

ICES, 2019. Report of the Working Group on North Atlantic Salmon (WGNAS). International Council for the Exploration of the Sea (ICES), Woods Hole, MA, USA. Available at: https://www.ices.dk/sites/pub/Publication%20Reports/Advice/2019/2019/sal.oth.nasco.pdf

Johnson, N., Alessa, L., Behe, C., Danielsen, F., Gearheard, S., Gofman-Wallingford, V., Kliskey, A., Krümmel, E., Lynch, A., Mustonen, T., Pulsifer, P. and Svoboda, M., 2015. The contributions of community-based monitoring and traditional knowledge to Arctic observing networks: reflections on the state of the field. Arctic, 68 (5; Supplement 1):28-40.

Kalinin, A. et al., 2017. New promising gold-ore objects in the Strelna Greenstone Belt, Kola Peninsula. Geology of Ore Deposits, 59 (6):453-481.

Kalinin, A. et al., 2019. Gold prospects in the western segment of the Russian Arctic: regional metallogeny and distribution of mineralization. Minerals, 9:137.

Kashulin, N., 2017. Selected aspects of the current state of freshwater resources in the Murmansk region, Russia. Journal of Environmental Science and Health, Part A, 52 (9):921-929.

Konstantinov, Y., 2009. Roadlessness and the Person: modes of travel in the reindeer herding part of the Kola Peninsula. Acta Borealia, 26 (1):27-49.

Kritzberg, E. et al., 2020. Browning of freshwaters: consequences to ecosystem services, underlying drivers and potential mitigation measures. Ambio, 49:375-390.

Lunkka, J. et al., 2018. Late Pleistocene palaeoenvironments and the last deglaciation on the Kola Peninsula. Arktos, 4:18.

Magritskii, D., 2008. Anthropogenic impact on the runoff of Russian rivers emptying into the Arctic Ocean, Water Resources, 35 (1):1-14.

Makarova, O. and Khokhlov, A., 2009. The status and management of moose in the Murmans Region, Russia. Alces, 45:13-16.

Makhrov, A. et al., 2014. Historical geography of pearl harvesting and current status of populations of freshwater pearl mussel in the western part of northern European Russia. Hydrobiologia, 735:149-159.

Mankova, P., 2018. The Komi of Kola Peninsula within ethnographic descriptions and state policies. Nationalities Papers, 46 (1):34-51.

Mustonen, T., 2014. Endemic time-spaces of Finland: aquatic regimes. Fennia - International Journal of Geography, 192 (2):120-139.

Mustonen, T. and Mustonen, K., 2016. Life in the Cyclic World – Traditional Knowledge Compendium of Eurasia. Snowchange Cooperative, Kontiolahti, Finland.

Mustonen, T. and Mustonen, K., 2019. Koitajoen erämaatalouksista (Wilderness Economies of Koitajoki River). ELY-Keskus, 2019.

Niemelä, E. et al., 2016. Pink Salmon in the Barents Region With Special Attention to the Status in the Transboundary Rivers Tana and Neiden, Rivers in Northwest Russia and in East Canada. Office of the Finnmark County Governor. Department of Environmental Affairs.

Nikanorov, A. et al., 2016. Many-year variations of water pollution and the state of river ecosystems in different latitudinal zones in European Russia. Water Resources, 43 (5):791-802.

Osherenko, G., 2001. Indigenous rights in Russia: is title to the land essential for cultural survival? Georgetown International Environmental Law Review, 13 (3):695-734.

Ozerov, M. et al., 2012. "Riverscape" genetics: river characteristics influence the genetic structure and diversity of anadromous and freshwater Atlantic salmon (*Salmo salar*) populations in northwest Russia. Canadian Journal of Fisheries and Aquatic Sciences, 69:1947-1958.

Ozerov, M. et al., 2013. Cost-effective genome-wide estimation of allele frequencies from pooled DNA in Atlantic salmon (*Salmo salar L.*). BMC Genomics, 14:12.

Ozerov, M. et al., 2016. Comprehensive microsatellite baseline for genetic stock identification of Atlantic salmon (*Salmo salar L.)* in northernmost Europe. ICES Journal of Marine Science, 74 (8):2159-2169.

Pecl. et al., 2017. Biodiversity redistribution under climate change: impacts on ecosystems and human well-being. Science, 355 (6332):eaai9214.

Polyakova, T. et al., 2016. Diatoms and aquatic palynomorphs in surface sediments of the white sea bays as indicators of sedimentation in marginal filters of rivers. Oceanology, 56 (2):289-300.

Post, E. et al., 2019. The polar regions in a 2°C warmer world. Science Advances, 5, 12.

Prusov, S. et al., 2001. Mark-recapture estimate of the stock abundance of Atlantic salmon done during catch-and-release fishing on the Ponoi River, Kola Peninsula, Russia. International Council for the Exploration of the Sea (ICES), Copenhagen, Denmark.

Rybråten, S. and Gómez-Baggethun, E., 2016. Lokal og tradisjonell økologisk kunnskap i forskning og forvaltning av laks. En forstudie (Local and traditional ecological knowledge in salmon research and management. A preliminary study). Nina Rappot 1290. Norsk institutt for naturforskning (NINA), Trondheim, Norway. 80pp.

Sandlund, O et al., 2018. Pink Salmon in Norway: the reluctant invader. Biological Invasions, 21:1033-1054.

IPCC, 2019. IPCC Special Report on the Ocean and Cryosphere in a Changing Climate. Pörtner, H.-O., et al. (Eds.). Intergovernmental Panel on Climate Change (IPCC). In press.

Simpson, L., 2017. As we have always done: Indigenous Freedom through Radical Resistance. University of Minnesota Press, Minneapolis. 320pp.

Slezkine, Y., 1996. Arctic Mirrors – Russia and the Small Peoples of the North. Cornell. 476pp.

Thorstad, E. et al., 2003. Effects of hook and release on Atlantic salmon in the River Alta, Northern Norway. Fisheries Research, 60:293-307.

Thorstad, E., 2013. Factors affecting the within-river spawning migration of Atlantic salmon with emphasis on human activities. Reviews in Fish Biology and Fisheries, 18:345-371.

Tkachenko et al., 2017. Современное состояние зараженности атлантического лосося р. Поной (Мурманская область) личинками нематоды Anisakis simplex/Current Infestation Status of Atlantic Salmon with Anisakis simplex larvae in the river Ponoi (the Murmansk Region). Вестник МГТУ. 2017. Т. 20, No 2. С. 455-462.

Tonteri, A. et al., 2009. Microsatellites reveal clear genetic boundaries among Atlantic salmon populations from the Barents and White seas, Northwest Russia. Canadian Journal of Fisheries and Aquatic Sciences, 66:717-735.

Vasiliev, A. et al., 1973. The system of Serebryansk hydroelectric plants on the Voro'ya River. Gidrotekhniches Stroitel'stvo, 10:1-5.

Velichkin, V. et al., 2013. Radioecological environment and radiogeochemical regionalisation of Northwestern Russia. Doklady Earth Sciences, 453 (1):1154-1157.

Whoriskey, F. et al., 2000. Evaluation of the effects of catch-and-release angling on the Atlantic salmon (Salmo salar) of the Ponoi River, Kola Peninsula, Russian Federation. Ecology of Freshwater Fish, 9:118-125.

Yang, X. et al., 2020. The past and future of global river ice. Nature 577 (7788):69-73.

Zozulya, D. et al., 2009. Lithosphere mantle structure and diamond prospects in the Kola Region: chemical and thermobarometric analyses of kimberlite pyrope. Doklady Earth Sciences, 427 (5):746-750.

Zubchenko, A. et al., 1996. Atlantic salmon from Russian rivers. Fisheries and state of the stocks in 1995. International Council for the Exploration of the Sea (ICES). 10pp.

Zubchenko, A. et al., 1998. Salmon rivers on the Kola Peninsula. Some Results of Acclimation of Pink Salmon. International Council for the Exploration of the Sea (ICES). 8pp. (+ table + figures).

EA Case Study 5. Kolyma: a major river in Northeastern Siberia

Lead Author: Tero Mustonen, Snowchange Cooperative

Contributing Author: Vyacheslav Shadrin

Introduction

Kolyma is a major river in northeastern Siberia. The river is 2700 kilometers long and has a catchment area of over 647 000 km^2 (see Figure EA6). It is home to Indigenous Yukaghir, Even, Chukchi, Evenki and Koryak Peoples. The Kolyma region is known for the numerous Gulags (forced labor camps) that were established by Stalin and the Soviet Union in the mid-20th century around the catchment area in Magadan, Sakha Republic and Chukotka, and the associated gold mining activities.

Community-based monitoring (CBM) and oral history work has taken place along the lower Kolyma (Mustonen and Shadrin, 2021) and the mid-Kolyma (Yukaghirs in the community of Nelimnaya). This case study draws on almost 20 years of research work on the Kolyma River, as well as existing public literature. In this study, we identify and discuss Hg pollution using a systems view that understands Indigenous communities and the lands and waters they inhabit as unified systems. Complementing this systems view are new, analytical maps of key sites and locations. It is impossible to summarize Indigenous Knowledge of several peoples and their diverse ways of knowing. Therefore, in this case study, we have focused on the main drivers affecting Indigenous health and the role Indigenous Knowledge plays in identifying and responding to these main drivers.

Methods

Applying a systems view in the context of Indigenous Peoples and Hg pollution remains challenging for large basins like the Kolyma. The specific detection of Hg impacts may be 'buried under' other drivers affecting Indigenous health. Community observations and impacts diverge from government health-related data both domestically in Russia, where Hg is rarely reported by artisanal small-scale gold mining (ASGM) operations, and internationally. This Kolyma Basin case study highlights the need to link these likely drivers of Hg levels with aquatic and biological sampling from the headwaters to the delta (see Tiaptirgianov, 2016). This study should be considered the start of longer-term monitoring work.

Methodologically, we have collected community voices from the Kolyma Basin (between 2005 and 2020), results from field surveys between 2005 and 2020, remote sensing and satellite image interpretation and geographical analysis (see Tiaptirgianov, 2016) relevant to known drivers of Hg levels in the environment and their impact on Indigenous Peoples. We have also surveyed regional governmental data reports to assess the presence or absence of Hg measurements in official data.

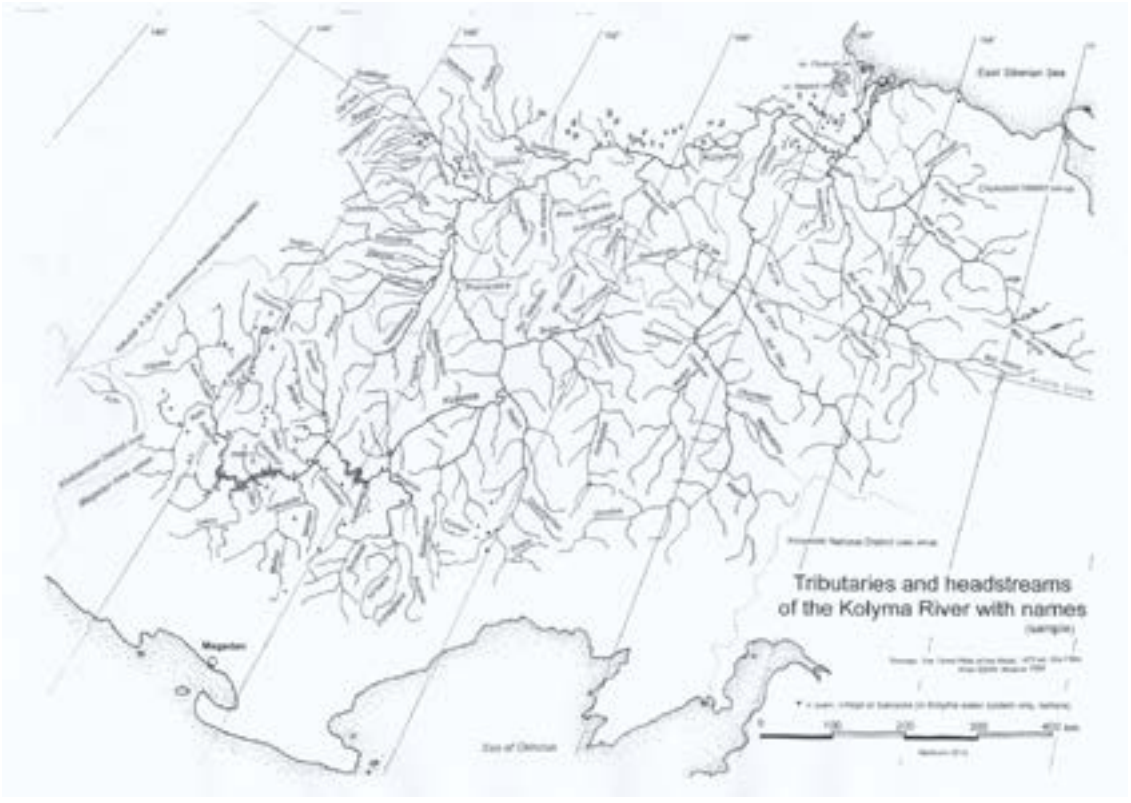

Figure EA6. A map of Kolyma River basin. Source: Jorma Mattsson, Snowchange Cooperative, 2022.

Results

Kolyma is a major Siberian river; the state of this river has consequences on an Arctic and global scale. The Kolyma Basin is home to unique Indigenous cultures, of which the Yukaghir culture and language are the most threatened. This precarious moment in time is captured in a recent oral history from Ekaterina Nikolaevna Dyachkova, a 95-year-old woman living in Nelimnaya, Kolyma, in her oral history:

> *"Almost all families are mixed.*
> *Even my grandchildren are in mixed families with Russians.*
> *You cannot even tell that they are Yukaghirs.*
> *Such is our life.*
> *We, the Yukaghirs, have our own language and our own traditions ...*
> *But we are disappearing ...*
> *We are doomed to die out.*
> *There used to be a lot of Yukaghirs.*
> *Every one of them used to have [their] own household.*
> *Ten rivers …*
> *they used to be full of people …*
> *Why are they not here now?*
> *They all had their own family …*
> *and their own yurtas.*
> *They are not here any longer. They burned out ...*
> *They burned out completely.*
> *Now I see it in my dreams …*
> *I ask, 'Where have all your friends gone?'*
> *They answer, 'They [have travelled to] other places'"*
> (Semenov, 2007).

Given the scale of Hg sourcing and the relevance of this pollution to a large number of Indigenous communities — many of which are fully dependent on the Kolyma Basin for their food security, cultural and social well-being and traditional economies — we have divided the main drivers of Hg pollution into several main categories: hydroelectric power stations and associated reservoirs; artisanal gold mining; Gulag and industrial gold mining; and permafrost loading. Each category is discussed briefly below.

In spring 2020, surveys were conducted in Kolyma Indigenous communities (with an emphasis on communities in Nelimnaya, Zyryanka and in the Lower Kolyma area). Results of these documentations included observations on the following:

- The influence of coal mining (Ugolny Razrez LLC) near the urban settlement of Zyryanka is a major source of concern. Local Indigenous residents (mostly Even) say that this coal has a high proportion of radioactivity. In the context of Hg and other pollutants, coal transportation by river remains an unknown factor (i.e., how much impact this has on Hg in the environment). Open boats transport the coal so that pollutants (in the form of coal dust) can easily enter the waters of the Kolyma.
- The use of coal in local heating stations (*kotelnaya, boilers*) is another main concern. The smoke from the burning of coal is never filtered and pollutes not only the air in urban settlements, but also enters the natural environment more widely, including rivers and lakes. Levels of Hg present in the coal itself or that enter the natural environment as a result of coal burning are unknown but remain an issue from the Indigenous viewpoint.
- Logging in the Kolyma Basin has practically been stopped because of its high cost. However, in the 1990s, the forestry industry was actively developing and many parts of the taiga were deforested. Clear-cutting has been identified as a source of Hg in boreal habitats. Indigenous Elders have said that the spirits of the forest are angry. According to Elders, timber floating has also altered parts of the Kolyma. Increased forest fires have also been identified as a source of concern with regard to Hg releases.
- Many local people in the Lower Kolyma area are concerned about the Bilibino nuclear power plant in Chukotka, the only nuclear power plant constructed on permafrost. Elders have also talked about the possible impact of nuclear weapons tests on Novaya Zemlya and underground nuclear explosions in Yakutia (for geological purposes) in the 1970s and 1980s. Additionally, the nuclear lighthouses (lighthouses powered by radioisotope thermoelectric generators and batteries; RTGs) on the tundra coasts of Chukotka have also been sources of contamination. Many herders and reindeer have suffered from exposure to radiation at these sites; because people did not know about the risk of radiation of getting too close to an RTG, they came close, examined these sites and, because reindeer graze along the coast in the summer, set up camps nearby. They are afraid these sites also release Hg.

Tiaptirgianov's assessment of Yakutian fish and freshwater bodies (Tiaptirgianov, 2016) includes Kolyma among rivers which are considered to have major issues with Hg and other pollutants (regional scale 4a – polluted). Tiaptirgianov notes that, due to a number of drivers, fish biodiversity in the Kolyma River is decreasing.

Tiaptirgianov (2016) analyzed Hg in pike and perch, which accumulate Hg through the food chain, along with a number of non-predator fish (roach; *Rutilus rutilus*, crucian carp; *Carassius carassius*, broad whitefish; *Coregonus nasus* and common dace; *Leuciscus leuciscus*). The study showed that the level of accumulated Hg is significant both in predator and non-predator fish (e.g., 1.86 mg/kg of Hg in yellow perch, 3.1 times the allowed maximum levels of 0.6 mg/kg). The accumulated Hg in each fish depends on the type of fish, the age and the season in which the fish was sampled (Tiaptirgianov, 2016). For comparison, hydroelectric power on Vilyuy River elsewhere in Yakutia has also been identified as a major source of Hg.

Kolyma has been shown to suffer from the environmental pollution, including Hg releases, that has resulted from gold mining, especially in the upper parts of the river (Tiaptirgianov, 2016:18); as a result, several species have shown to be declining , including Siberian sturgeon, Salmonidae, Coregoninae, with grayling and burbot also having suffered. Tiaptirgianov (2016) also highlights ASGM events as a source of Hg. At times, Hg levels in the waters of the Kolyma have been between 1 and 3 times the 'allowed mercury levels' (Tiaptirgianov, 2016:116). Tiaptirgianov links this elevation to a century of gold mining in Kolyma and the sediments leaching Hg downstream. Further investigation into precise regional and federal 'allowed mercury levels' is required.

Tiaptirgianov (2016:182) has also reviewed samples of small (young) perch fish from the Indigirka River, a neighboring Arctic basin to the Kolyma. According to the samples, the presence of Hg in these fish was twice as low in the summer as it was in the winter time. On the other hand, larger (adult) perch fish had higher amounts of Hg in the summer (well above the permitted threshold of 0.6 mg/kg). Tiaptirgianov (2016) associates the seasonal differences in Indigirka with the mining activities, which stop in the winter. Roach also displayed high levels of Hg content, although this is conjectured to be a 'natural' phenomenon (Tiaptirgianov, 2016).

In perch sampled from the middle reaches of the Kolyma River (fish aged 4–6 years), Hg levels in muscle were 3 times higher (up to 1.8 mg/kg) than the regional norm; elevated levels were also observed in perch liver (Tiaptirgianov, 2016:188). Again, in the winter, the levels appear to decrease. Tiaptirgianov (2016) also explains this as resulting from the cessation of ASGM activities upstream during the winter months.

Kolyma hydroelectric power stations

Literature has determined that the creation of hydroelectric power stations and associated reservoirs, particularly downstream and in the early part of their life, are major sources of Hg (e.g., Hsu-Kim et al., 2018). The first hydroelectric power station on the Kolyma was constructed in 1986 during the late Soviet period on the middle part of the river, in the Magadan region (see Figure EA7 and EA8).

It took five years for the Kolyma 1 reservoir to fill completely. The hydroelectric dam is the largest ever constructed on permafrost with a height of 134.5 meters and a length of 683 meters. The reservoir contains 15 080 million m^3 of water and measures, at its widest point, 110 km across. The station has a power generation capacity of 900 MW, with five turbines. Kolyma 1 produces over 95% of all electricity in Magadan (Mattsson, 2020).

The Kolyma 2 hydroelectric power station (see Figure EA9) is a second large hydroelectric power station that is currently being constructed on the river, 217 km downstream from Kolyma 1. When completed, it is expected to have an output of 570 MW, with four turbines. Filling the reservoir started in 2013. The reservoir is 2425 meters long with a 325 meter concrete dam structure. A part of the dam is made of earth and is 66 meters high; the other section of the dam is made of concrete and is 74 meters high. Once the reservoir is full, it is expected to have an area of 265 km^2. Kolyma 2 is constructed on permafrost that is 300 meters deep (Mattsson, 2020). The station has been operating since 2013 with the aim of reaching full capacity in 2022.

According to the plans, permafrost thaw has been addressed on the two dams through the use of piping that transports cold air into the earth, keeping the dam soils intact. Both dams are unique as no such constructions exist elsewhere on permafrost soils. Risks remain high. One potential risk associated with Kolyma 1 is that all of the stored water is used during the winter from the reservoir. This results in hydraulic pressure changes against the dam through the year. Additionally, this part of the Kolyma Basin is seismically active. This causes further dangers for dam construction and operation.

Both of these dams are probable sources of Hg downstream. Indigenous Peoples are concerned that Hg released as a result of the dam construction and operation is accumulating in predator fish, which are consumed by communities along the Kolyma (Mustonen, 2009). Mustonen and Shadrin (2020) report that some of the Indigenous Elders have observed changes in fish migration. Dams also prevent fish from travelling upstream. The Kolyma has important endemic and migratory fish (such as lenok, omul, whitefish, various species of Coregonus, muksun, and nelma). Spawning success is impacted by the fluctuation of water levels due to the irregular release of water from the dams. Before the construction of the dams, fish migration in the Kolyma River system followed natural changes in water quality and levels. Dams and their regulatory actions affect migrations and water temperatures at the 'wrong' times of the year; this results in the mislocation of fish stocks by Indigenous harvesters (Mattsson, 2020). For example, Fyodor Innokentyevich Sokorikov, former head of the fishing *sovkhoz* in Pokhodsk (at the Kolyma Delta),

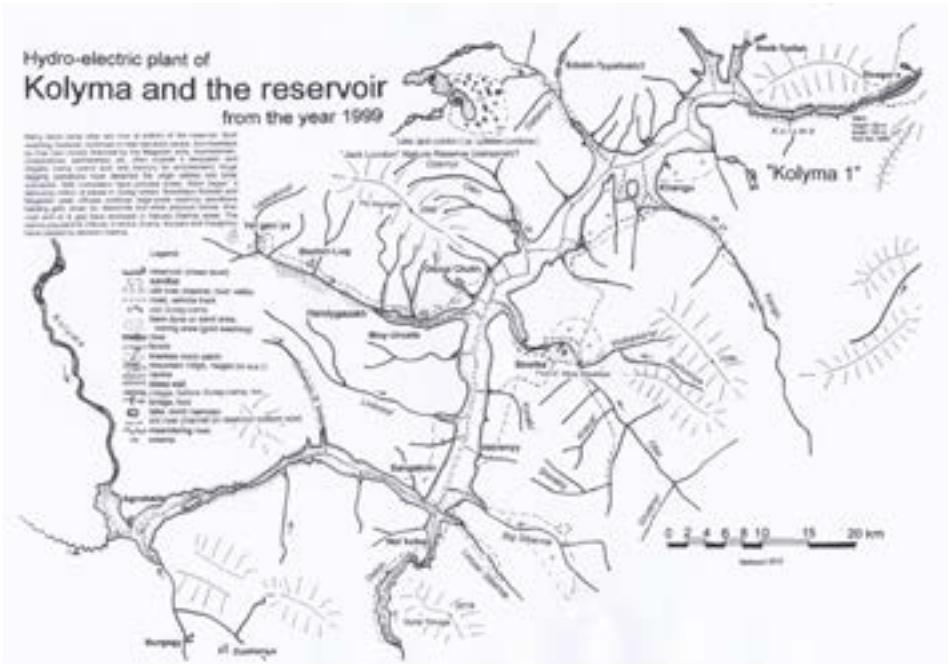

Figure EA7. Map showing the Kolyma River and the Kolyma 1 hydroelectric power station and reservoir. Source: Mattsson, 2019.

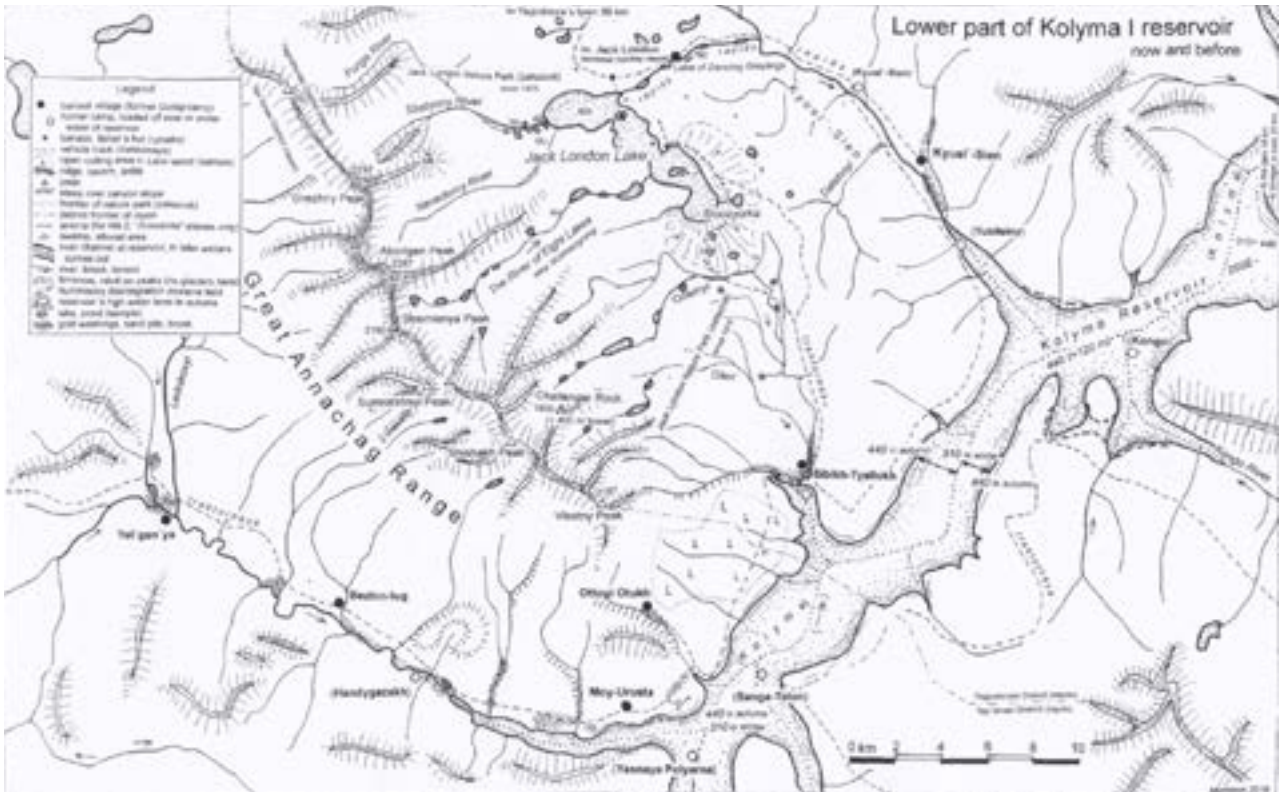

Figure EA8. Map showing the lower (southern) section of the Kolyma 1 hydroelectric power station and reservoir. Source: Jorma Mattsson, Snowchange Cooperative, 2022.

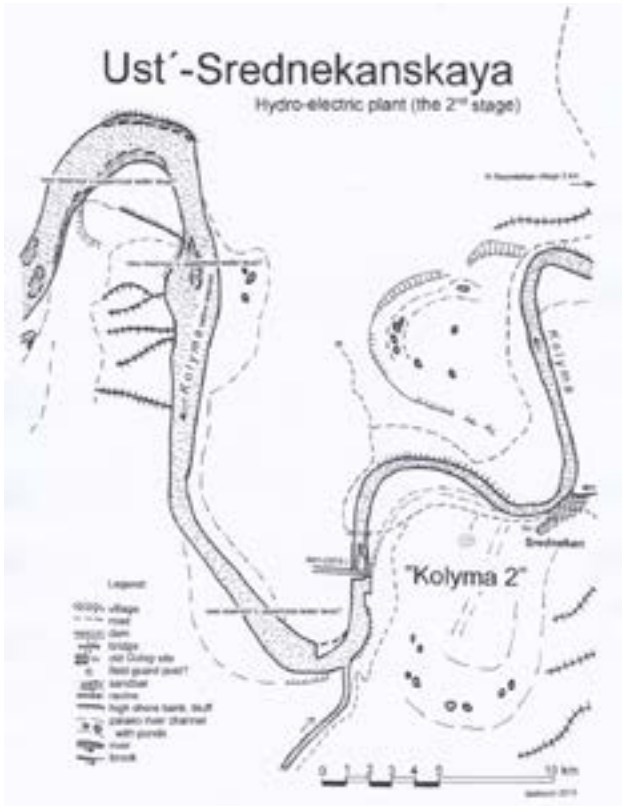

Figure EA9. Kolyma 2 hydroelectric power station and reservoir. Source: Jorma Mattsson, Snowchange Cooperative, 2022.

blames the changes brought about by the gold mining impacts in Kolyma tributaries (in Mustonen and Mustonen, 2016:115). Scientist Matvey Tyaptirgyanov also confirms significant decreases in the numbers of nelma in the Kolyma River.

Other Indigenous observations report that the Kolyma sturgeon stocks have collapsed (Mustonen and Mustonen, 2016). Observers blame the regulation of water levels by the hydroelectric power station for the population collapse; sturgeon need deep spots in the river to spawn and the hydroelectric power station has reduced the number of these spots. According to these observers, the last good year for sturgeon stocks was 1996; for the last 10 years, sturgeon have been missing almost totally from the river. Sturgeon also accumulate Hg (Tiaptirgianov, 2016).

Reservoir water level fluctuations are a driver of bank erosion. Combined with permafrost thaw, these fluctuations may lead to increased levels of Hg in the stream. Mustonen (2009) reports that some subsistence fishermen have associated 'glowing fish' with Hg and other releases from the dams.

In the Kolyma communities, reservoirs are also associated with increased flooding. Before the construction of the dams, Kolyma communities used to expect a flood every 25 to 30 years. Now, flooding occurs every other year. Elders have also observed air humidity and water regime changes adding to bank erosion, another potential driver of Hg.

Artisanal and small-scale gold mining (ASGM), industrial gold mining, and Gulag mining operations and related Indigenous health impacts

As in Southern Sakha-Yakutia, artisanal and small-scale gold mining (ASGM) is prominent in the Kolyma region. ASGM operations most likely still use Hg to process gold amalgam; they then release Hg directly into the river after processing.

Obrist et al. (2017) determine that this is the single largest sourcing of Hg globally. This practice is officially illegal, a ban on mercury-use in ASGM having come into force in 1988 (Order #124 of the USSR State Committee on Precious Metals in Tiaptirgianov, 2016), but implementation has been critically slow (Romanov et al., 2018). The release of other chemicals (including cyanide and other hazardous materials) have also impacted Kolyma River water quality, and mining operations have led to an observed darkening of the waters. This change in water color is detectable both by Indigenous harvesters close to the mining sites as well as from aerial and satellite imagery. There are also industrial-scale gold mining operations in the upper parts of the Kolyma River. Mines have released, and continue to release, both Hg and other contaminants into the river.

Historically, 'artisanal' mining in the region relied on prisoners, who used shovels and other handheld equipment to attempt to find gold, silver and tin. Since the first efforts to industrialize the region in the 1930s, hundreds of forced labor camps and mining sites have been built along the Kolyma. The separation of gold from Hg at such sites has relied on regal water (a mixture of nitric acid and hydrochloric acid), cyanide and other acids. The left-over material (tailings) and wastewaters are then released into the Kolyma. Romanov et al. (2018:42) highlight the ASGM in Magadan as a major source of Hg. According to a report on implementing federal decisions in the ASGM sector (Magadan, 2014) there is 2.5 million m^3 of mining waste in Magadan, which contains an estimated 48 tonnes of Hg from 'traditional gold mining'.

The 1988 ban on the use of Hg in ASGM, unfortunately, has not prevented the use of Hg in many sites across Siberia. As Magadan (2014) shows, the amount of Hg already present in the environment is in the tens of tonnes, even in official reporting. These older mine tailing sites will continue to leach Hg into nearby waters (including, potentially, into groundwater). Such was the case with the Karamkenski gold processing plant. In 2009, the tailing pond of this plant (now closed) burst, resulting in the release of waste containing cyanide (and also, therefore, Hg) into the Khasyn River (not in the Kolyma Basin; Magadan, 2014). This led to the government taking measures to restore the Karamkenski site in 2017; these measures were, according to official reports, 93.5% successful (Magadan, 2017). No independent survey of the site has been conducted, nor are there verifiable public records of present or historic levels of Hg at the site or in the Khasyn River.

In the 2020s, the most prominent area for ASGM is the Magadan Oblast (or region), where gold mining remains a strategic resource (Romanov et al., 2018). Service huts and operational bases are accessible using *traktornaya* (ATV trails) out into the wilderness.

Forest fires in the Kolyma Basin are frequent and increase humus loading into the river. This is affecting the accumulation of methylmercury to predators and ultimately to humans. Short summers on the Kolyma leave a lot of aquatic vegetation that rots on the river. This, in itself, causes natural chemical and water-quality changes; added methylmercury creates an overall situation which, due to its complexity, is hard to assess, but its effects include the lowering of pH in the waters of the river (Mattsson, 2020).

Figure EA10. Map of Butugychag uranium mining site showing nearby tributaries of the Kolyma River. Source: Jorma Mattsson, Snowchange Cooperative, 2022.

In the tributaries of the lower Kolyma, two industrial companies, Kinross Gold Mining Company and Polymetal, carry out industrial-scale gold mining: this occurs mainly in Omolon and in Anyui, Chukotka. Chukotka has also seen an increase since 2018 in ASGM activities, but the scale of these operations is hard to assess.

Based on regional research trips and analysis, we have determined that artisanal gold mining continues in close proximity to the Kolyma 1 hydroelectric power station (see also Romanov et al., 2018). Evidence of gold mining has also been detected on the Lednikoviy, Obo, Kango, Datshnyi and Olen rivers. All of these sites are a further source of the Hg in the Kolyma 1 reservoir, around which there are also many gold mining camps (see Figure EA10).

Of special importance in the mining history of the Kolyma Basin is the Butugychag site in the Upper Kolyma, north of the town of Magadan. Butugychag was a major source of uranium for the Soviet Union. In the 1940s and 1950s, uranium was harvested by Gulag prisoners in Butugychag without any protective gear. Prisoners and guards alike died within months of starting work on the site. While the area is today off limits, reindeer herders have reported that reindeer are losing hair from their feet close to Butugychag. Uranium mine tailings are known to contain Hg; the site should, therefore, be considered in an overall assessment of Hg loading in the Kolyma Basin.

Mercury loading from permafrost melt

Eagle-Smith et al. (2018) state that the entire Arctic area, and especially the Indigenous communities who live there, are vulnerable to Hg pollution. This is due to their dependence on fishing, not only for food security but also for cultural and social reasons. According to Eagle-Smith et al. (2018), global climate change — including permafrost thaw events — may be a major driver of releases of Hg into river systems.

Differentiation of the sources of Hg release via bank erosion and linking these releases to impacts on Indigenous health may be impossible. A solution may rest in a basin-wide survey of drivers of Hg for the Kolyma, including sedimentation, and by furthering our understanding of exactly what happens to sediments when drivers associated with hydroelectric power production and permafrost melt events increase.

Official regional reports

Positioning Indigenous-related case studies in a dialogue with regional governmental monitoring data can provide partial answers, as well as points of divergence and convergence. Tiaptirgianov (2016) has produced a monograph on Sakha-Yakutia which has been summarized above. A recent governmental monitoring report on the environmental protection in Sakha-Yakutia (Sakha, 2017) states that in waters of the Lower Kolyma near the Kolymskoe settlement, the average annual Hg amounts for 2016 and 2017 were within threshold value limits (see above regarding regional 'thresholds'). The report also states that Hg levels have been diminishing in water samples taken from the lower part of the river. In the delta area, according to the report, the loading from both the hydroelectric power stations and gold mining has lessened and Hg has, therefore, most likely sedimented. We have assessed that permafrost erosion events may be the largest single driver of Hg releases towards the delta. However, Tiaptirgianov (2016) points to the sediment leaching and continually raised Hg levels also in the lower part of Kolyma.

In the case of the Magadan region, official reports state that it is mainly the soils of urban areas that have been monitored for Hg (Magadan, 2018:41). Specific ecological restoration measures undertaken after accidents have also been identified (Magadan, 2017). It is worth noting that in the 2018 report on the ecological situation in Magadan, the section on the quality of regional water resources does not mention Hg (Magadan, 2018:24). However, in the sector specific reports (e.g., those devoted to mining) Hg is associated with older mining tailings (Magadan 2014, 2017). Remedial actions are prioritized for sites closest to human settlements.

The inconsistent way in which the presence of Hg is addressed in official reporting points to a large gap in either monitoring capacity (lack of resources), misreporting, or the ignoring of Hg for other reasons. This is especially the case for ASGM activities. Land use and industrial activities are certain to be drivers of Hg in Magadan (with impacts across a range of scales) but are mostly missing from the monitoring data. One exception is the 2014 report, where the past tailings are identified as a major source (Magadan, 2014).

Looking further afield at Hg reporting in neighboring regions beyond the Kolyma catchment, a comparative view emerges. Kamchatka (2018:91) links Hg releases to wastewater issues. Interestingly, AO Kamgold, a gold company operating on the peninsula, includes Hg as one of the monitored indicators in the discharge waters. This may be at least partly attributed to the large presence of Hg in natural soils. Additionally, Kamchatka (2018) mentions that reports from the company AO Ametistovoe also includes an analysis of Hg in the 'clean' rivers Ichigin-Unneivayam and Tklavayam, and on equally clean smaller brooks (Pryamoy, Rudnyy and Severnyy). The sources and amounts of Hg in these reports cannot be confirmed independently.

Khabarovsk (2018:209) has identified Hg pollution as an ecological problem in Khabarovsky Kray. This is especially true in the case of the area around the former Amursky cellulose-cardboard factory. The former factory is included in the federal program *Chistaya Strana* (Clean Country), which helps regions deal with pollution which has accumulated in the environment as a result of historic industrial development projects. The program has allocated federal subsidies to demolish the Amursky factory's chlorine department and to undertake remedial measures to address polluted sites.

None of the regional environmental reports from Eastern Siberia and the Russian Far East which were surveyed for this case study (i.e., from Sakha, Magadan, Kamchatka and Khabarovsk regions) had a special section on Hg. Instead, Hg was mentioned in different sections of the reports. The sections that most often mentioned Hg were sections on air, soil and water monitoring and waste handling. Mercury reporting in these reports is somewhat partial and inconsistent. Since the reports do not clearly mention all the substances they have measured and tend to report only the indicators that exceed threshold limit values, it is impossible to say based on those reports whether Hg is measured but not reported (since the concentration is not deemed to exceed threshold limit values), or if it is not measured at all.

Clearly, Hg has not been taken to be especially important in the monitoring reports of either private companies or state environmental agencies. However, all reports mentioned Hg every now and then, even though, in some reports, Hg features more prominently than in others (Tiaptirgianov, 2016). However, mercury-containing waste has started to become an important subject for all the regions mentioned in this case study. This may be due to heightened awareness of Hg waste resulting from educational campaigns about Hg in light bulbs. Romanov et al. (2018) note that ASGM is not prohibited in the Minamata Convention on Mercury and point to how this affects the way it is addressed by the regional authorities and in monitoring. On the federal level, evidence of the monitoring of Hg also remains elusive.

Tiaptirgianov (2016) has assessed the health implications of Hg levels for the Indigenous communities living on the Kolyma. The recommendation is currently that, when fish is consumed from the river, only the filet should be eaten (and this as rarely as possible) because the levels of Hg (often exceeding the maximum allowed levels of 0.6 mg/kg), lead and cadmium exceed safe levels in fish caught from the Kolyma.

Tiaptirgianov (2016) points to the backlog of Hg loading (historic Hg loading which continues to affect the environment) from a century of mining activities and how this continues to influence fish health. Indigenous observations of abnormalities have also become more common on the Kolyma (Mustonen, 2009 reports alterations in the smell, taste and coloring of the fish; see also Tiaptirgianov, 2016 for summaries of abnormalities in the river itself). However, Tiaptirgianov's recommendations are those of a single researcher; to date, none of these recommendations or observations have been implemented or had any visible effect on regional policy.

Discussion and Conclusions

Kolyma is a lifeline and home to many Indigenous Peoples of Eastern and Northeastern Siberia, including the Even, Chukchi, Evenki, Koryak and the Yukaghir. All of these Indigenous Peoples are dependent on the river for fish, which is not only consumed as food but important for cultural and spiritual well-being.

The Kolyma Basin has been affected by large-scale industrial developments that have sourced Hg to the river for a century (Tiaptirgianov, 2016). This includes the hydroelectric dams Kolyma 1 and Kolyma 2 (the latter currently under construction), artisanal and small-scale gold mining (ASGM) both past and present, and industrial mining operations, including secondary drivers of Hg levels in the environment such as the uranium mined in Butugychag. Ongoing changes to Hg levels in the basin include additional sourcing from the impacts of climate change, including permafrost thaw and flooding (Tiaptirgianov, 2016; Eagle-Smith et al., 2018).

Community-based observations undertaken along the Kolyma River have detected direct impacts of Hg (e.g., changes in fish smell, taste and health) and indirect impacts (e.g., ethical and cultural) through Indigenous Knowledge regarding Hg. Mercury is very challenging to monitor directly and exclusively using CBM methods. Individual researchers like Tiaptirgianov (2016) have begun to offer a system-wide ecological view, but much work remains, both in terms of collecting Indigenous observations and in linking these observations with systematic monitoring of the sources and impacts of Hg in the Kolyma Basin.

These same issues and research needs are also present in the neighboring Chukotka region. Chuvan Yuri Borisovich Diachkov from the village of Markovo in Chukotka has been concerned about the impact of gold mining on the river and local people (in Mustonen and Mustonen, 2016). He described how, after gold had been dredged in Chukotka, thousands of barrels of waste were left behind, leaving the rivers polluted. He added that local people have benefited very little from the industrial development in the region.

Yevgeny Remkylen (in Mustonen and Mustonen, 2016) also noted that when the mining companies dredged nearby rivers in their search for gold, they did so without consulting the local population at all. This resulted in the disappearance of fish spawning areas in the upper reaches of the rivers and the destruction of many areas previously used as important reindeer pastures.

For this case study, we have combined data from regional environmental reports, remote sensing and satellite analysis, and a limited literature review. In summary, Hg monitoring remains critically insufficient for ASGM activities. Indigenous observations, where available, have not led to action. This is in spite of the fact that some government reports do identify the backlog of mining tailings as a source of Hg (Magadan, 2014) and the fact that other reports (Magadan, 2017 and Khabarovsk, 2018) discuss Hg releases from industrial factories and sites. The Magadan government has taken remedial and restorative actions, at least officially, after the tailings pond burst at the Karamkenski site. Such events, however, have not been thoroughly followed-up on; the state of these sites, and the Hg levels at these sites, today represents a research gap that will need to be addressed in future.

A thorough, formal assessment of the impacts of Hg on Kolyma Indigenous communities is highly recommended. Tiaptirgianov (2016) is a very important starting point for baseline measurements and in mapping a system-wide ecological view. A large environmental monitoring program which includes historic events whose Hg emissions are having, most likely, an ongoing impact (such as the Karamkenski event, not in the Kolyma Basin) and an analysis of Hg loading in predator and other fish, should be the first priority.

Secondly, any future assessment program should also include a study of environmental and community health developed in consultation with local communities to ensure that free, prior and informed consent has been obtained; research into links between land/river drivers and ocean drivers of Hg, especially on the delta area, should also be undertaken; an assessment of how much Hg is being released from a range of 'natural' sources (e.g., permafrost; see Obrist et al., 2017, as well as riverbanks and soils) and human sources (hydroelectric dams, sediment loading and mining operations past and present; see Tiaptirgianov, 2016) should also be carried out. The implementation of the Minamata Convention on Mercury and the inclusion of ASGM in regional environmental monitoring, if this can be determined to have been properly sourced, is considered an important early step towards a more wide-ranging future program.

EA Case Study 5: References

British Admiralty Charts, 1948. Siberian coastal charts 1:2,830,000 by U.S.S.R. Government charts and sketch surveys to 1947 (soundings in fathoms).

Eagle-Smith, C. et al., 2018. Modulators of mercury risk to wildlife and humans in the context of rapid climate change. Ambio, 47:170-197.

Hsu-Kim H. et al., 2018. Challenges and opportunities for managing aquatic mercury pollution in altered landscapes. Ambio, 47:141-169.

Kamchatka, 2018. The Report on the Current State of Environment in Kamchatka Kray in 2018 ДОКЛАД О СОСТОЯНИИ ОКРУЖАЮЩЕЙ СРЕДЫ В КАМЧАТСКОМ КРАЕ В 2018 ГОДУ.

Khabarovsk, 2018: The State Report on the Current State and Protection of Environment of Khabarovsk Kray Государственный доклад о состоянии и об охране окружающей среды Хабаровского края в 2018.

Magadan, 2014. Passport of the State Programme "Nature Resources and Ecology of the Magadan Region", approved on 30.4.2014 by the Government of Magadan Region. Available at: https://minprirod.49gov.ru/common/download.php?file=2_366_30.04.2014_1.pdf&obj=document

Magadan, 2017. Report on the Actions of Implementing Federal Actions of Natural Resources and Ecology.Пояснительная записка о результатах реализации мероприятий государственной программы министерством природных ресурсов и экологии Магаданской области в 2017 году.

Magadan, 2018. The Report on Ecological Situation in Magadan Oblast. ДОКЛАД ОБ ЭКОЛОГИЧЕСКОЙ СИТУАЦИИ В МАГАДАНСКОЙ ОБЛАСТИ В 2018 ГОДУ.

Mattsson, J., 2020. Regional Report of Kolyma Basin 2020. An unpublished regional environmental report. Snowchange Cooperative.

Mustonen, 2009. Karhun väen ajast-aikojen avartuva avara. Joensuu: University of Joensuu.

Mustonen, T. and Mustonen, K., 2016. Life in the Cyclic World – Traditional Knowledge Compendium of Eurasia. Snowchange Cooperative, Finland.

Mustonen and Shadrin, 2021. The River Alazeya: Shifting Socio-Ecological Systems Connected to a Northeastern Siberian River. ARCTIC, 74 (1):67-86. Available at: https://doi.org/10.14430/arctic72238

Obrist, D. et al., 2017. Tundra uptake of atmospheric elemental mercury drives Arctic mercury pollution. Nature, 547 (7662):201-204.

Romanov, A., Ignatieva, Y. and Morozova, I., 2018. Mercury Pollution in Russia: Problems and Recommendations. GEF (Global Environment Facility (GEF). Available at: http://www.ecoaccord.org/pop/Rtutnoe_zagryaznenie_English_25-08.pdf

Sakha, 2017. The State Report on the Current State and Protection of Environment of the Republic of Sakha (Yakutia) Госдоклад о состоянии и охране окружающей среды РС(Я).

Semenov, V., 2007. The Yukaghirs (Film). Yakutsk.

Tiaptirgianov, M., 2016. Fish of freshwater bodies of Yakutia (systematisation, ecology, impact of anthropogenic factors), Yakutsk. 2016. ТЯПТИРГЯНОВ Матвей Матвеевич. РЫБЫ ПРЕСНОВОДНЫХ ВОДОЕМОВ ЯКУТИИ (систематика, экология, воздействие антропогенных факторов), Якутск 2016.

EA Case Study 6. Yiengra: artisanal gold mining and Evenki taiga nomadism

Author: Tero Mustonen, Snowchange Cooperative

Introduction

In this case study, Indigenous observations of health and well-being are discussed in the context of artisanal gold mining and Hg. For this case study, we focus on the community of Yiengra and its surrounding nomadic reindeer camps located in the southern Sakha-Yakutian taiga of Eastern Siberia in Russia.

The Indigenous Evenki of Yiengra have faced the pressure of displacement since the days of their first encounters with Russians in the early 17th century, and the community was forcibly resettled in the 1920s. Under the Soviet regime and during the post-Soviet years, Evenki lands and waters became the target of expansive industrial operations. Coal mining, gold digging, hydropower construction, energy pipelines and many other infrastructure projects have all made their mark on the landscape. This expansion widely and thoroughly altered the post-Ice Age landscapes of the southern Sakha-Yakutia. The Soviet Union established the village of Yiengra in the catchment area of the Yiengra River in 1926; the village is located on a point along the traditional nomadic routes of the Evenki.

The Evenki have settled over a vast geographic range in East Siberia, Russia's Far East, Northern China and Mongolia (Mertens, 2015). It is estimated that the entire Evenki community currently has approximately 36 000 members and about 7000 speak the Evenki language. Their traditional livelihoods have revolved around nomadic reindeer herding, hunting and fishing.

Neryungrinsky, the administrative area, is a southern region of the Republic of Sakha (Yakutia) in the Russian Federation. It is located close to the Chinese border. The population of the district is about 75 000, and most residents live in urban areas. Neriungri, the administrative center of the district, is also the center for coal-mining operations. The district produces 75% of the 10 million tons of coal that is produced in Sakha annually (Newell, 2004; Araseyenin, 2007).

The area is part of the continental climate zone. Coniferous trees, such as Siberian larch, as well as birch trees cover much of the taiga. Mountains and large hills dominate the landscape, with shallow rivers flowing in the valleys. For example, the Aldan River catchment area, a sub-catchment of the Lena River, is located in the district. Winters are usually very cold with small amounts of snowfall. Temperatures can plummet down to -50°C and below. Springtime is often short with snowmelt already well under way in April. Summers are continental and hot. Autumn (i.e., often September or October) brings the first frosts.

Salmonid fish, such as trout, grayling and whitefish, occupy the lakes and rivers. This is reflected in many Evenki place names around Yiengra (Lavrillier, 2006, and see the Evenki Atlas; ELOKA and Snowchange, 2020). The Evenki place significant value on local trout as a culturally important species. The Evenki have long used salmonid fish as bioindicators to assess the degradation of river health and change over time (Mustonen, 2009; ELOKA and Snowchange, 2020).

While the traditional Evenki trades of hunting, fishing and reindeer herding resemble those of other similar cultures in Eurasia (Klokov, 2016), Evenki practices are distinct. For example, reindeer are ridden and not eaten, nomadic routes are smaller in scale, traditional calendars are observed, and the taiga is ordered into 'human' and natural, remote zones.

The Yiengra River, the main catchment area addressed in this case study (see Figure EA11), is the center of Evenki seasonal

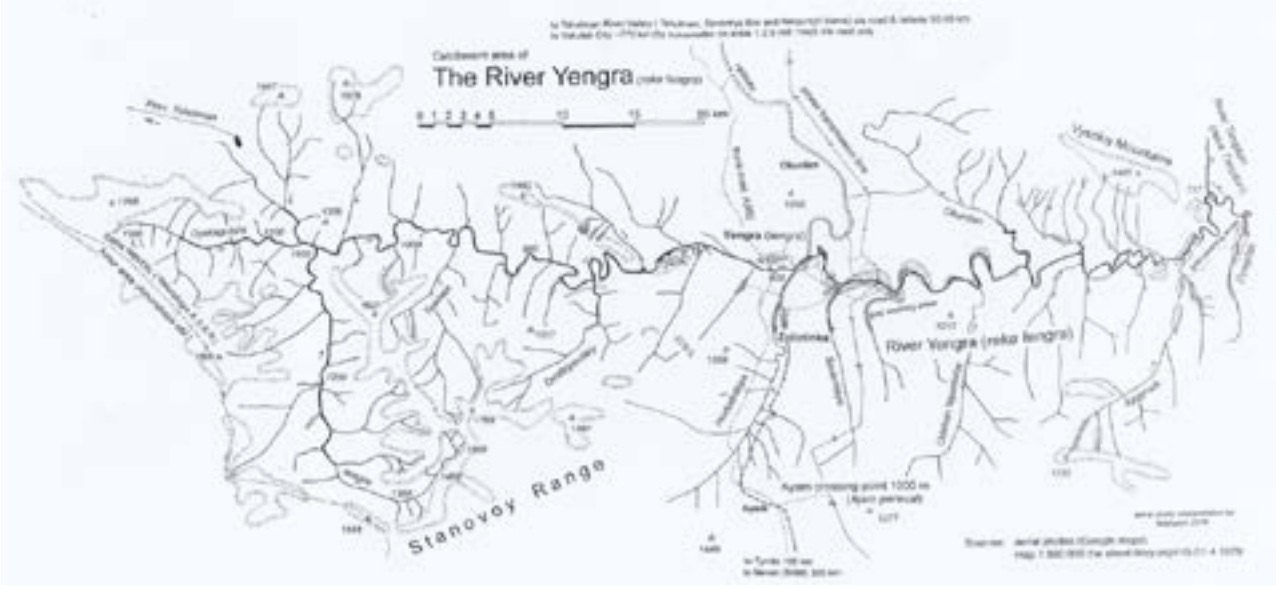

Figure EA11. Map of the Yiengra River catchment area and the village of Yiengra. Source: Jorma Mattsson, Snowchange Cooperative, 2022.

life. The Evenki are dependent on the river for drinking water (for reindeer and humans), transportation, and, in some cases, small-scale cultural fisheries.

The river catchment is also utilized by artisanal gold miners (Figure EA12). Mercury (Hg) and other chemicals, such as cyanide, are often released into waterways from small-scale gold mining operations. Mercury is used in artisanal practice to separate gold particles from sediment. The resulting amalgam is often burned to remove the Hg (Mustonen and Lehtinen, 2020), resulting in airborne pollution to nearby lands and waters. This technique is a source of Hg pollution to the Yiengra River; adjacent mining operations are also a direct source of Hg pollution. Mercury entering the waterways is transformed into methylmercury. Other chemicals also affect human and animal health along the Yiengra. Lastly, many of the riverbanks have been churned up, turned upside down, and greatly damaged as a result of the digging, affecting water quality and sedimentation patterns.

Methods

Mercury is naturally present in the boreal environment. When soils are altered — often through human disturbances such as burning, ditching, and mining — Hg embedded in the soils travels downstream and reacts with water due to microbial actions.

When it comes to Evenki observations of the impact of Hg on the Yiengra River catchment area, we are able to draw on 16 years of community-based observations, aquatic mapping and geographical analysis to identify the main artisanal mining sources of Hg. This has included working with Evenki co-researchers in reindeer camps (Mustonen, 2009; Mustonen and Lehtinen, 2020) between 2004 and 2020, field visits to river sites, and oral history documentation and mapping in the village of Yiengra.

The most significant source of Hg in the Yiengra River is artisanal and small-scale (ASGM) gold mining (Romanov et al., 2018). The actual gold mining is conducted by local and private operators, which are hard to monitor and track. Despite the national ban on unlicensed mining activities put in place in 1988 by the Soviet Union (see also Romanov et al., 2018), in practice, small-scale gold mines have been part of the landscape along the Yiengra for decades. What individual licenses and permits may allow varies and, as such, the industry is hard to control.

Additionally, we have reviewed the official monitoring reports from the government of Sakha-Yakutia to position the fieldwork alongside regional monitoring of Hg and to assess the effectiveness of this monitoring. The regional maximum allowed level of Hg in waters and fish has been set at 0.6 mg/kg by the regional authorities. Artisanal gold mining is not limited to the Yiengra; it is also present in the larger Aldan River catchment, for instance on the Timpton River.

Results

Gold mining on the Yiengra River is mostly artisanal (Romanov et al., 2018) and therefore affects smaller streams and old-growth forests of the taiga (Mustonen and Lehtinen, 2020)

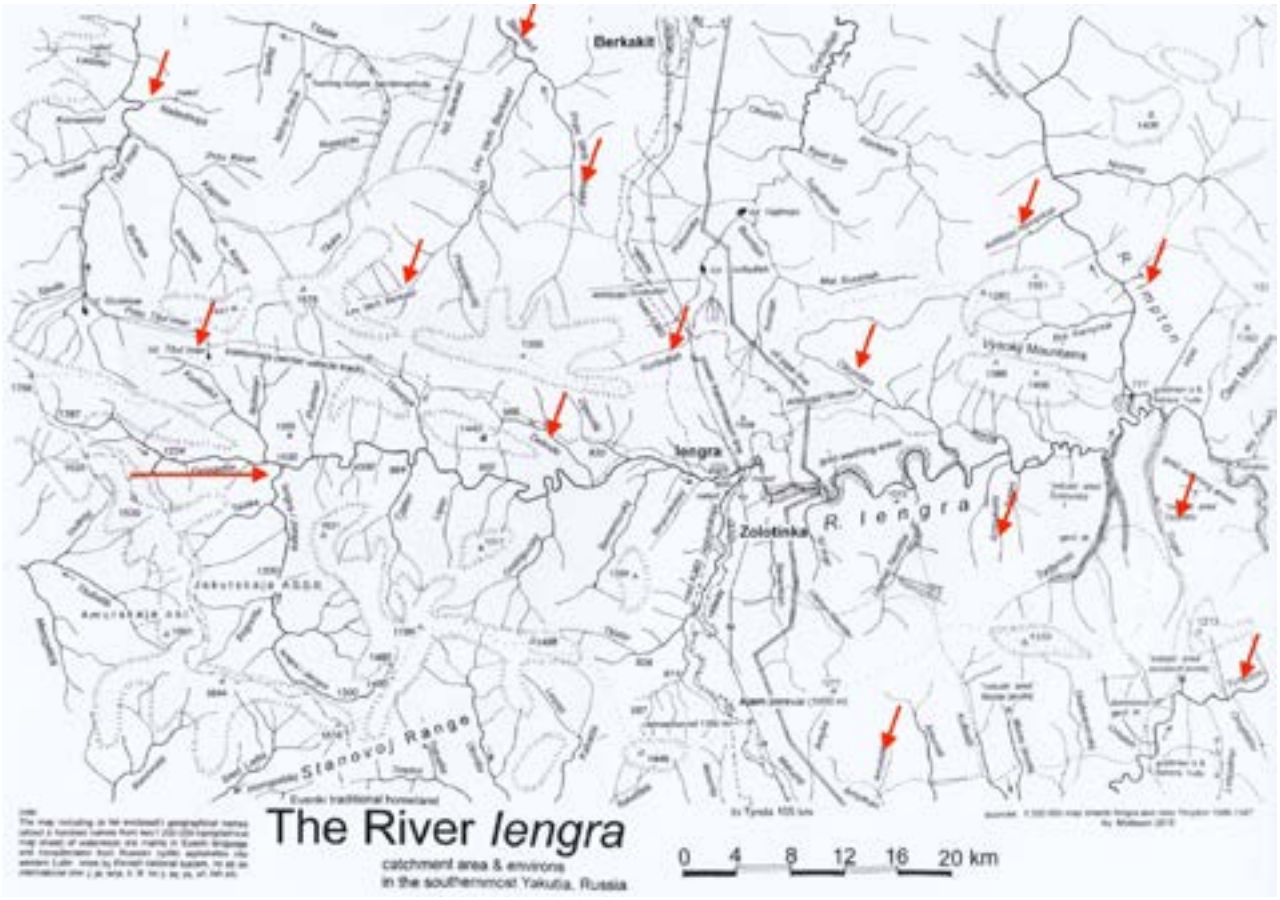

Figure EA12. Regional map of the Yiengra River and surrounding catchment areas. Gold mining areas are marked on the map (shaded areas). Red arrows point to sites of importance to the Evenki where environmental change is taking place (as of 2004–2020). Not all of this change is related to gold mining and may also be related to climate change impacts. Source: Jorma Mattsson, Snowchange 2022.

but has cumulative impacts on the main streams as well. This artisanal mining activity releases Hg, cyanide and other chemicals and hazardous materials into the rivers.

One Evenki reindeer herder in a leading position summarized the impact of gold mining on reindeer life during the oral history work (Mustonen, 2009):

> *"Reindeer do drink water, and now it is dirty. They make it dirty when they dig and wash gold. Look at Timpton river, it looks like tea with milk. Everything is poisoned there. There is not fish, nothing. So reindeer drink such water, and they get sick or even die. And [their] food [is] lichen. We have to change our route regularly, so that reindeer would get fresh food. But our territory is small, and everything around is dug up. So the reindeer are forced to graze and trample at the same spots."*

The Evenki have conducted their own observational assessment of change by reviewing historic place names, especially those related to aquatic ecosystems. In this oral history example, reindeer herder Vladimir Kolesov discusses place names and recent changes:

> *"We have two middle-sized rivers. It is enough for us. I cannot always even say why a river has the name it has. Kenerkit. Kener is a fishtrap. There are a lot of places in this river where one could place a fishtrap. A river called Kenerkit. Gonam is a long and meandering river. It was named Gonam. Or Takrekam, it is like this, twisting like a worm. It is like a lake, all shores are muddy. There are a lot of small rivers. My campsites are Kurekati-river, Kalbati, Turkit. There is Daban. Delinde refers to fishing, Nirunda. There is Davenda, from [the] word dva – artificial. These exist. Nirunda. It is a grayling river. There is Delinde. It is a river for trout. It used to be. These names are old. The names persist, but … all that is left is the name - due to the pollution from the gold mining."* (Mustonen, 2009).

Hydronyms, place names that reflect water bodies or their attributes, such as lakes and rivers, contain descriptions of the different elements and characteristics of water flow, depth, meanders, and points of safe crossing. Evenki campsites have traditionally been located at sites that provide a source of freshwater for both people and reindeer. At some of these locations, the river does not freeze in the winter due to the speed of water flow (Mustonen and Lehtinen, 2020).

At other locations, river ice compresses as a result of the deep freeze, and the river subsequently releases ice blocks as the tension breaks. These ice blocks are used as drinking water in the winter. Lavrillier (2006) points to the central role of rivers as winter highways for reindeer travel; as such, locations are often described not by using cardinal points (i.e., north, south, east and west) but rather through descriptions of riverbanks, streams and other aquatic features of travelled terrains.

Some place names are also layered; they reflect the Sakha arrivals and mixing of toponyms with the original Evenki ones. Relations and conflicts between these peoples have been encoded in these toponyms. An example of Evenki place names demonstrates the ecological connection between the Evenki language and the landscape.

According to Vladimir Kolesov, hunting and fishing grounds have been affected too:

> *"I hunt between Timpton and Gonam. In my area, [the] largest changes have taken place [at] the shoreline of large rivers. Along the shores of large rivers, the changes have been bigger than for example on mountains. Gonam is a large river, and crossing it used to be very difficult, but now it is possible [in] many places. It is becoming more shallow. In my area it is like milk. Water is the same colour as tea with milk. [The] largest changes have taken place along the big rivers. Maybe this is because of gold digging. They dig for gold. I cannot say that this would have an impact on climate, but on reindeer yes. Local environment, yes, it impacts a lot. I remember when we used to be close to lakes, we used to eat ducks for the whole summer, different kinds. Completely white and then silvery. They flew past*

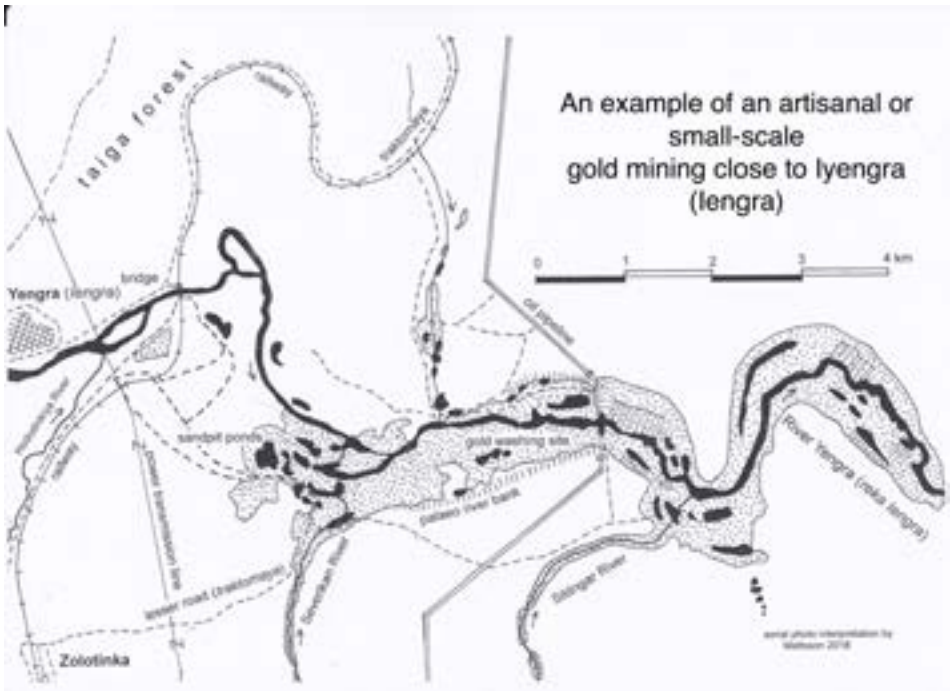

Figure EA13. Map of artisanal or small-scale gold mining sites to the west of Yiengra village. Source: Jorma Mattsson, Snowchange Cooperative.

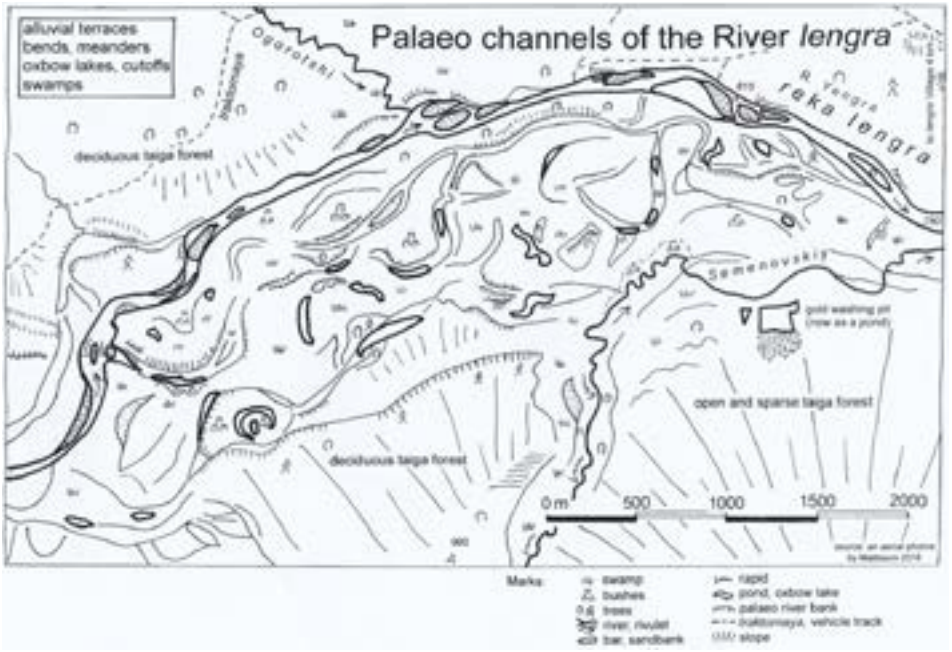

Figure EA14. Map of the western (upper) part of the Yiengra River and catchment area. Historic gold mining sites (over twenty-years-old) are now ponds, visible on the lower right-hand section of the map. Source: Jorma Mattsson, Snowchange Cooperative.

and nested here also. Incubated and geese incubated also. Now there are very few of those birds. There is no fish either, numbers have gone down also. Birds fly [to] some other places. There is no food and they change the place and the route. Well, where can you hide from civilisation? Nowhere" (Mustonen, 2009).

In this close-up map of artisanal gold digging, west of the village of Yiengra on the river (Figure EA13), we can see the scale of the mining operations and their impacts. Both the Yiengra and Sildngar rivers have been polluted. The mining sites and tailing pools are right next to the main river itself. This means that the release of Hg and other chemicals is directly affecting these waters. While point specific data are unavailable, an official environmental protection report for the state of Sakha (Sakha, 2017) records that 56% to 87% of water samples taken from the river Aldan (a major river downstream from Yiengra) had elevated levels of Hg (i.e., above maximum allowable levels). As point specific data have not been publicly released, determining the exact amounts of Hg in the water of these rivers would require sampling at the pollution sources.

Additionally, the banks of the rivers are churned up by mining operations, adding to organic loading and alterations in fish spawning locations, river depth and water quality. In certain places where the river meanders or the flow of water slows, Hg and other chemicals have most likely accumulated in the sediment. Past impacts of gold mining are visible as new 'pools' on the Western side of the Yiengra River catchment area, as in the map below (Figure EA14).

The cumulative impacts of historic land-use changes — especially those associated with the industrial megaprojects of the 2000s and 2010s — are as immense as they are difficult to assess. Artisanal gold mining and the resulting Hg loading is also hard to detect using only Indigenous Knowledge and observations. What emerges from the community-based monitoring (CBM) work and the Evenki oral histories is a distinct impact on reindeer and other animals that are using the affected waters. Understanding the specific role of Hg in these pollution events will require additional limnological and sampling studies.

We positioned the Evenki observations in a dialogue with official reporting on lakes and rivers by the Republic of Sakha (Yakutia) Ministry of Ecology, Nature Use and Forestry (Sakha, 2017). Official reporting has been compiled in the State Report on the Current State and Protection of Environment of the Republic of Sakha (Sakha, 2017). Mercury is one of the chemical elements that has been analyzed for water monitoring in the report. The presence of Hg is mentioned only for some rivers. The Aldan River basin, where Yiengra is located, has been categorized as class 3b: very polluted (using national indicators, see more in Sakha, 2017). Copper, phenol and Hg were higher than the national threshold limit value (TLV). Overall, Hg pollution resulting from surface waters of the Aldan River is said to have decreased in recent years (Sakha, 2017). However, to determine whether or not the level of Hg is now within maximum allowed levels in fish (less than 0.6 mg/kg) and in waters will require further sampling and monitoring efforts.

One of the major drivers of Hg in the region is the city of Tommot on the Aldan River, outside the area we are focusing on in this case study. In water samples taken 0.5 km upstream of Tommot, concentrations of Hg above the TLV were detected in 63% of samples (Sakha, 2017). The Yiengra, Timpton and Chulman rivers were classified as 3a or 3b (very polluted, see Sakha, 2017). The governmental report also points to the need for monitoring Hg below artisanal mining areas, but no specific data are mentioned. For example, the report states that the gold-mining company OOO Progress possesses a table of data showing the concentration of pollutants in company wastewater. While Hg is in the table, it is always marked as 'non-reported' (see Sakha, 2017:406).

Available regional data converges with Indigenous observations in defining the Yiengra, Timpton and Chulman rivers as polluted. Lack of data contributes to a large divergence between reported impacts of artisanal mining operations and observations of impacts by the Evenki. This is partly a result of understaffing at the Ministry of Ecology and the incapacity of monitoring staff to trace past and present loading on the Yiengra River.

In summary, mining, energy and infrastructure projects have thoroughly altered the Evenki land and lifescapes (i.e., emotions, health, socio-economic circumstances, cultural norms, and behaviors) in the following ways (see also Newell, 2004; Mustonen, 2009; Yakoleva, 2011; Sidortsov et al., 2016):

- Major hydrological regimes and aquatic ecosystems have been fundamentally transformed by mining operations and hydropower construction.
- Smaller streams and old-growth (naturally developed) forests have been contaminated by oil pipelines, as well as Hg releases and land churning by artisanal gold mining.
- Changes in forest cover, fish stocks, water color and quality have, in turn, thoroughly affected fishing livelihoods, household catches and reindeer herding.
- Mammals, birds and other fauna that are dependent on post-Ice Age, pristine, old-growth taiga forests have suffered and retreated elsewhere, making hunting and subsistence economies harder to maintain.
- Major transport corridors have cut across and divided up the taiga around Yiengra.
- The wastewater releases from the city of Neriungri may be an additional source of alarm, with regard to Hg in particular.

Discussion and Conclusions

The Evenki of Yiengra are one of the taiga Indigenous Peoples who continue to maintain their seasonal rounds, knowledge and land use in Eastern Siberia. This case study has focused on observations of impacts to their life from artisanal gold mining, which is known to be a major driver of Hg at the local as well as global scale (i.e., also in Africa, Asia and Latin America).

Mustonen and Lehtinen (2020) argue that Indigenous communities who are still practicing their nomadic way of life are intimately dependent on healthy terrestrial and aquatic ecosystems; the health of the environment is integral to the functioning of their socio-ecological systems. Sixteen years of CBM work with the Evenki has resulted in the mapping of gold mining sites and in the production and collection of descriptions of the following: impacts of Hg and other pollutants on reindeer and wildlife health; loss of fisheries and access to clean waters; alterations to waterways and their depth, water color, and accessibility; and the ethno-psychological impacts of alterations to the Evenki home area.

The Evenki have negotiated these impositions by recommending alternative locations for gold digging to limit the damage to their reindeer pastures, rivers and sacred places. The results of these local-scale adaptations vary. Positioning Evenki knowledge of Hg and its impacts alongside available science data (e.g., Sakha, 2017) reveals several points of convergence, including the fact that both the science and Evenki knowledge identify the Aldan Basin, in which the Yiengra River is located, as polluted. Divergence emerges with regard to the scale of the pollution described, the specificity as to how amounts of Hg are detected, and the long-term impacts of Hg on the river system. Further description and investigation into these points of divergence will have to wait for further collaborative studies.

The late reindeer herder Vladimir Kolesov recorded, in an oral history, how Evenki relations with their home area show how disturbance, loss and change are interconnected across both natural and human systems in a complex, intertwined whole:

> *"We say: Earth mother. If we go past large rivers, we hang a piece of cloth there. Close to the mountains we do that too. We hang a piece of cloth there. You are not allowed to leave pieces of firewood lying around. It is not allowed to cut more wood than what is needed. When you are someplace, for example hunting, don't leave pieces of wood crosswise. Everything needs to be in order. Don't throw bones around. I make a shelter, and all bones are put there. So that nothing is out of order. It is also because the reindeer come and bite the bones and suffocate.*
> *Clean and safe. To keep the reindeer from harm.*
> *You fish only as much as you need. If the next day you need more, you go fishing again then.*
> *If no one would buy the sable skins, it would not be hunted as much. If you need a hat, it is only then you're allowed to hunt. If there was no need, it would not be killed. This goes for all of the animals I think.*
> *And trees too. If you need wood for sleds, then you take but otherwise no. If there is no need, nothing will be cut"* (Mustonen, 2009).

Ultimately, the question of Hg loading on the Yiengra River is a debate between two human systems each of which possesses a very different kind of power — Evenki self-governance, built and continuing to build on Indigenous ways of being, and Soviet and Russian artisanal extraction of natural resources.

EA Case Study 6: References

Araseyenin, B., 2007. Jakutija – Istoriko-Kulturnii Atlas (Sakha Historical-Cultural Atlas). Yakutsk: Institute of Humanities.

ELOKA and Snowchange, 2020. Online Atlas of the Evenki of Iyengra, version 2.0. Exchange for Local Observations and Knowledge of the Arctic (ELOKA) and Snowchange Cooperative. Available at: www.evenki-atlas.org

Klokov, K., 2016. Reindeer herders' Communities of the Siberian Taiga in changing social contexts. Sibirica, 15 (1):81-101.

Lavrillier, A., 2006. S'orienter avec les rivières chez les Évenks du Sud-Est sibérien (Rivers as a spatial, social and ritual system of orientation among the Evenks of southeastern Siberia). Études mongoles et sibériennes, centrasiatiques et tibétaines, 36-37:95-138.

Mertens, K., 2015. Mobility and economy of the Evenkis in Eastern Siberia. Master of Arts in Anthropology Thesis. Boise State University. Boise State University Theses and Dissertations. 1049. Available at: https://scholarworks.boisestate.edu/td/1049

Mustonen, T., 2009. Karhun väen ajast-aikojen avartuva avara. Tutkimus kolmen euraasialaisen luontaistalousyhteisön paikallisesta tiedosta pohjoisen ilmastonmuutoksen kehyksessä (Peoples of the Bear: an inquiry into the local knowledge of three Eurasian subsistence communities in the context of northern climate change). Unpublished doctoral dissertation. University of Joensuu, Finland.

Mustonen, T. and Lehtinen, A., 2020. Lived Displacement among the Evenki of Yiengra. International Journal of Critical Indigenous Studies, 13(1):16-44.

Newell, J., 2004. Russian Far East – a reference guide for conservation and development. McKinleyville, CA: Daniel & Daniel Publishers. 466pp.

Romanov, A., Ignatieva, Y. and Morozova, I., 2018. Mercury Pollution in Russia: Problems and Recommendations. GEF (Global Environment Facility (GEF). Available at: http://www.ecoaccord.org/pop/Rtutnoe_zagryaznenie_English_25-08.pdf

Sakha, 2017. The State Report on the Current State and Protection of Environment of the Republic of Sakha (Yakutia) Госдоклад о состоянии и охране окружающей среды РС(Я). Available at: https://minpriroda.sakha.gov.ru/spravki-o-sostojanii-okruzhajuschej-sredy/spravka-o-sostojanii-okruzhajuschej-sredy-za-2017-god

Sidortsov, R., Ivanona, A. and Stammler, F., 2016. Localizing governance of systemic risks: a case study of the power of Siberia pipeline in Russia. Energy Research and Social Science, 16:54-68.

Yakovleva, N.,2011. Oil pipeline construction in Eastern Siberia: implications for Indigenous people. Geoforum, 42 (6):708-719.

10. Conclusions and Recommendations

Authors: John Chételat, Rune Dietz and Simon Wilson

10.1 Introduction

This chapter highlights key advances in mercury science from the 2021 AMAP Mercury Assessment that address policy-relevant questions on mercury (Hg) transport, exposure and effects in the Arctic. The findings are based on the latest available science generated in the last decade; recommendations for future research and monitoring efforts are identified, and uncertainties and knowledge gaps are also considered. More information, including the data and references to support the conclusions summarized below, can be found in the relevant chapters of this assessment report.

10.2 Summary of main findings

What are the temporal trends of mercury in environmental media, biota and humans?

Long-term measurements of Hg concentrations in the Arctic environment are critical for the assessment of the impacts and effectiveness of international actions on Hg pollution. The Hg time series available for the Arctic in abiotic and biotic media represent one of the most regionally comprehensive monitoring efforts in the world, and the trend analysis in this current assessment has improved coverage with longer time series (of 20 years or more) giving greater statistical power to detect temporal change when compared to previous assessments (i.e., AMAP, 2011).

In air measurements recorded at Arctic monitoring sites, gaseous Hg concentrations continued to decline over the last decade. One exception was a site in the western Canadian Subarctic, where gaseous Hg concentrations have increased since measurements began in 2008, possibly due to changing meteorology and increases in East Asian Hg emissions. Strong seasonal variability of gaseous Hg concentrations was observed across coastal sites due to the influence of environmental processes, such as atmospheric mercury depletion events (AMDEs) in spring and evasion from terrestrial surfaces and the Arctic Ocean in summer. Mercury in precipitation was also measured at Arctic sites in Europe and North America, which confirmed previous findings of general decreasing trends in annual Hg concentrations and wet deposition. Geographic differences in temporal trends of wet Hg deposition seemed to be influenced by proximity to Hg emission source areas and seasonal cycles in the amount of precipitation.

Continued monitoring since 2011 has dramatically improved the number and power of available time series for Hg concentrations in Arctic biota; as a result, there has been a greater opportunity in this assessment for broader circumpolar comparisons of changes in Hg levels, for the consideration of trends in relation to possible effects risk thresholds and for the examination of environmental processes influencing biotic Hg exposure. A total of 77 time series for Arctic biota (terrestrial and marine mammals, seabirds, freshwater and marine fish and shellfish) met the criteria for statistical analysis: 44 showed an increasing trend (often ≥1% per year), 32 showed a decreasing trend (often ≥1% per year), and 1 time series showed no change (0%). Complex temporal trends of Hg in Arctic biota reflect the influence of multiple processes and drivers, which may be site-specific.

Human biomonitoring to establish trends of Hg exposure in Arctic populations remains extremely limited, with only four studies suitable for temporal trend analysis. The time series were levels of Hg measured in blood, with most focusing on women of child-bearing age. Mercury levels in human blood continued to decrease in Nunavik (Canada), West Greenland (Disko Bay area) and the Faroe Islands. The time series of blood Hg for women from Nuuk, Greenland showed no trend. Changes in lifestyle and the dietary choices of Northerners likely affected the decreasing Hg exposure and concentrations of Hg in human blood.

Where does mercury in the Arctic environment come from, and how does it get there?

Mercury released by human activities which is deposited in the Arctic via the atmosphere primarily originates from the long-range transport of global emissions outside the region. Current estimates showed global anthropogenic emissions of Hg to the atmosphere for 2015 were approximately 20% higher than in 2010, and the main global sectors contributing to the deposition of anthropogenic Hg in the Arctic were power generation, industrial sources and artisanal and small-scale gold mining (ASGM). East Asia, CIS countries, Africa and Europe were important source regions (in order of decreasing importance) for anthropogenic Hg emissions transported to the Arctic. Anthropogenic Hg emissions within the Arctic were low relative to other regions of the world and contributed little to Hg circulating in the Arctic. Meteorology (specifically precipitation amounts) strongly influenced estimates of wet Hg deposition as did global anthropogenic Hg emissions, particularly for recent interannual differences of Hg deposition in the Arctic.

Of the total amount of Hg deposited in the Arctic from the atmosphere, modeling estimated approximately one-third originated from direct anthropogenic emission sources while two-thirds were from re-emission of previously deposited Hg from anthropogenic or geogenic sources. Legacy Hg contamination is recirculated in the Arctic via the re-emission of gaseous Hg from soils, snow and the ocean. Wildfires, which are becoming more frequent in the Arctic, are also an important re-emission pathway of legacy Hg to the atmosphere.

Air concentrations of gaseous Hg in the Arctic showed a clear latitudinal gradient consistent with the atmospheric transport of anthropogenic Hg from lower latitudes. A major new discovery since the last Hg assessment has been the importance of gaseous Hg uptake by tundra vegetation and

its dominance as a Hg source in Arctic terrestrial ecosystems, which amplifies Hg loads from other (wet and dry) deposition pathways. Arctic terrestrial catchments transport large amounts of Hg to downstream environments. Permafrost soils and glaciers are large reservoirs of Hg, which are degrading due to climate warming. Evidence from Hg stable isotopes suggests that terrestrial sources of Hg transported to the Arctic Ocean may be important for methylmercury (MeHg) bioaccumulation in marine animals.

What are the processes affecting mercury transformations and biological uptake?

Methylmercury is the more toxic, bioaccumulative form of Hg which biomagnifies in food chains, and its production in Arctic environments is thus a critical aspect of the Hg cycle. Recent scientific advances in the last decade have addressed this important knowledge gap for the Arctic.

A global analysis in the field of environmental genomics was the first to reveal the presence of specific genes linked with bacterial Hg methylation in the Arctic environment, specifically in thawing permafrost soil. Permafrost thaw in ice-rich, low relief regions may result in the formation of thermokarst wetlands, ponds and lakes, and these systems have been repeatedly identified as Hg methylation hotspots across the Arctic due to the release of carbon and nutrients, which can promote MeHg production. Anoxic environments such as sediments and flooded soils are often considered dominant sites for MeHg production. However, in the last decade, several studies have highlighted the importance of MeHg in suboxic and even well-oxygenated waters for bioaccumulation and biomagnification in marine food webs. In Arctic seawater, MeHg concentrations are often highest at subsurface depths of ~100–300 m, where phytoplankton uptake may be an important entry route into pelagic food webs. While anaerobic biological Hg methylation is mediated by the known genes which are abundant in marine sediments, the aerobic pathway for Hg methylation, if it exists, remains unclear. Possible bacterial genes, which could be involved in Hg methylation in oxic marine waters, have recently been identified although further studies are needed.

The volatilization of dimethlymercury (DMHg) from the marine boundary layer and its subsequent demethylation of MeHg has been suggested as another source of MeHg in surface snow, marine waters and coastal terrestrial environments. Atmospheric concentrations of both MeHg and DMHg were measured in Hudson Bay and the Canadian Arctic Archipelago, and the research suggested that the evasion of DMHg from marine waters was enough to sustain atmospheric concentrations of MeHg in the Arctic.

Recent, more comprehensive measurements of MeHg in the Arctic have allowed for the development of mass balance modeling to evaluate sources and transport pathways. Rivers and coastal erosion were dominant transport pathways for the delivery of MeHg to the Arctic Ocean while MeHg production in the ocean water column and sediments (coastal and deep-water) were identified as important *in situ* sources of Hg for the Arctic Ocean. Methylmercury that accumulates in Arctic food webs is produced within the Arctic.

The Hg cycle has complex linkages with the carbon cycle, and recent findings demonstrate the presence of organic matter can both dampen and promote MeHg uptake in Arctic food webs. Once MeHg enters Arctic food webs, ecological and biological processes influence the accumulation of MeHg in fish and wildlife. Regional differences in Hg concentrations in polar bear and ringed seal is, in part, due to longer food chains. Migratory wildlife that breed in the Arctic in summer and overwinter at lower latitudes, such as seabirds, may be more exposed to Hg at their southern overwintering grounds.

How does climate change influence mercury in the Arctic environment and in biota?

Climate change is profoundly affecting physical and biogeochemical characteristics that interact with the Hg cycle across all Arctic environmental compartments. Arguably, the clearest evidence of current climate change effects on Hg cycling in the Arctic is for Hg transport from terrestrial catchments. Widespread permafrost thaw, glacier melt and coastal erosion are altering the sources and fluxes of Hg from terrestrial to freshwater and marine ecosystems. Greater organic matter transport, particularly dissolved organic carbon, may also be influencing the downstream transport and fate of Hg in Arctic rivers. Interactions between climate change and the biogeochemical cycling of Hg are still largely theoretical, although changes to the cryosphere may alter the seasonal evasion or retention of inorganic Hg, and warmer temperatures may enhance MeHg production in freshwater and marine sediments, and in tundra soils.

Arctic plants and animals are responding to climate change; these responses include northward shifts in the ranges of boreal species. Climate-related changes in the diet of Arctic animals, which has been observed in seabirds and marine mammals, can affect their Hg exposure. Climate variables have been linked to spatial and temporal patterns of Hg concentrations in some Arctic marine and terrestrial species. These findings suggest that changes in wind, precipitation and the cryosphere, which affect atmospheric and aquatic transport of Hg, may in turn be affecting Hg exposures in Arctic biota. While multi-decadal monitoring of Hg concentrations in Arctic biota has identified climate change as an influence on the bioaccumulation of Hg, it is clear that the effects of climate change on biotic Hg concentrations are complex, difficult to predict and can be site-specific within a region.

What are the toxicological effects of mercury in Arctic biota?

Elevated exposure to MeHg can have adverse effects on the reproduction, body condition and behavior of fish and wildlife. Tissue burdens of Hg for diverse Arctic biota, including for marine and terrestrial mammals, seabirds, shorebirds, marine and freshwater fish, and aquatic invertebrates, were examined to assess the risk of potential health effects. In general, based on the most recently published information, most Arctic biota were at low risk or not at any risk of health effects mediated by Hg exposure. However, Hg continues to pose a justifiable concern for some long-lived Arctic marine mammals, such as polar bear, pilot whale, narwhal, beluga and hooded seal. For these keystone species, a notable proportion of the population is at a high or severe risk for health effects as a result of Hg

exposure. Some seabird species also had Hg concentrations considered a moderate or higher risk for Hg toxicity.

Spatial and temporal patterns of Hg concentrations in Arctic biota were found to influence the risk of health effects. Hotspot areas of Hg bioaccumulation were detected in the Canadian High Arctic and Northwest Greenland, with some variation dependent on the species. In a few monitored populations of Arctic wildlife, particularly polar bears (*Ursus maritimus*), recent increases of Hg concentration in the last two decades were sufficient to increase their risk of health effects. It remains unclear what environmental processes are creating the hotspots or increasing temporal trends of bioaccumulation, although MeHg in the epipelagic layer of the Arctic Ocean, summer atmospheric deposition as well as AMDEs may be contributing factors.

What is the impact of mercury contamination on human health in the Arctic?

Arctic populations (especially Inuit) are among the highest Hg-exposed people worldwide with a greater proportion of individuals having biomarker levels (in blood and hair) that exceed health guidelines. The major source of northern populations' exposure to Hg is from the consumption of certain fish, marine mammals and wildlife that are contaminated with Hg. In particular, the highest exposures occur among Inuit populations that routinely consume marine mammal tissues. Even though local and regional environmental characteristics may influence Hg accumulation in consumed country foods, it is global anthropogenic activities that are ultimately driving the dietary exposures of Arctic peoples to Hg.

Epidemiological cohort studies on Arctic populations have been among the most influential worldwide in terms of demonstrating the link between early-life Hg exposure and later-life adverse health outcomes. For example, cohort studies in the Faroe Islands have demonstrated that children exposed to MeHg *in utero* exhibit decreased motor function, attention span, verbal abilities, memory and other mental functions. Meta-analysis studies have documented sufficient scientific evidence linking MeHg exposures with adverse cardiovascular outcomes, although despite this body of evidence, there are some conflicting findings from Arctic regions.

A nutrition transition is well underway in many Arctic communities. Country foods are being increasingly supplemented by store-bought foods of low nutritional value typical of a western diet. While such a shift may reduce human exposures to Hg (i.e., due to less consumption of local fish and wildlife), the shift is also associated with a poorer and unhealthy diet that largely consists of refined carbohydrates and saturated fatty acids with limited nutrient, vitamin, and unsaturated fatty acid content. The impact of Hg contamination on human health in the Arctic must be considered in the context of the high prevalence of food security concerns for Arctic Indigenous Peoples. For example, a majority of Inuit in the Canadian Arctic are food insecure with one in four being classified as severely food insecure. Therefore, a priority for risk communication is the development of carefully planned strategies, built through engagement with communities, to promote country food consumption while lowering contaminant exposures to maintain and improve health and wellbeing in Arctic peoples.

What are the likely changes in mercury concentration in the Arctic atmosphere and ocean under future emissions scenarios?

Model forecasting was used to explore future implications for the Arctic from different policy actions to reduce global anthropogenic emissions of Hg. Potential consequences were assessed for Hg in the Arctic atmosphere and ocean by modeling trajectories over the next three decades (until 2050) under different future global emissions scenarios. The relative importance of changes to primary emissions, legacy emissions and climate change for Arctic Hg concentrations were also compared. Model estimates suggest only the most aggressive reductions in global emissions can reduce future atmospheric deposition and oceanic Hg concentrations in the Arctic both in the near term and the medium term. Model forecasting has shown that delaying significant emission reduction measures until 2030 would mean that any less ambitious emission cuts before that time would be completely counteracted by the fact that those pre-2030 emissions will continue to cycle globally in the near to medium term. Future changes in the Arctic atmosphere and ocean from reductions of anthropogenic emissions are likely to be substantial in comparison with climate-related effects, especially for the ocean. Considerable uncertainties remain, however, in forecasting future emissions scenarios and modeling the processes that influence Hg's global transport, deposition and cycling in the Arctic environment.

What are Indigenous Peoples' contributions to the study of mercury in the Arctic, and what are their perspectives on contaminant research and monitoring?

Comprehensive research on contaminants and human exposure in the Arctic would not be possible without the involvement of Indigenous Peoples. Community partnerships and Indigenous Knowledge are a critical component of wildlife and fish collections for Hg studies. A wide variety of monitoring and research programs, particularly those investigating contaminants in wildlife and fish, further profit from Indigenous understanding of environmental and ecological contexts. Ongoing observations by Indigenous Peoples on topics such as sea-ice coverage and climate, animal distribution, behavior, diet and body condition, and the characteristics of locally consumed wild foods improve the interpretation of study results. Indigenous Knowledge also plays an important role in environmental monitoring to support food security and Indigenous health and wellbeing conducted by regional governments in the circumpolar Arctic. Mercury is a food security issue for Indigenous Peoples because Hg affects the safety of their traditional diet, which is a foundational part of their health and culture. Active collaborations between Indigenous Peoples, scientists and governments are critical to core research and monitoring of Hg in the Arctic, which informs domestic and international initiatives to reduce Hg exposure. These efforts were instrumental in the negotiation of the UN Environment Minamata Convention on Mercury.

Guidelines and protocols for ethical research developed by Indigenous Peoples, exist to support further development of partnerships in the study of Arctic Hg contamination. These guidelines emphasise the importance of understanding the history and cultural context of research in the Arctic,

promoting Indigenous self-determination in research and monitoring, following established processes for the co-production of knowledge, respecting Indigenous Knowledge, crediting ownership of information and establishing good communication practices. Projects built on a shared vision of the inclusion and respectful participation of Indigenous Peoples are key to the long-term success of Hg research and monitoring in the Arctic.

10.3 Implications of the assessment findings for work under the Minamata Convention on Mercury

Multiple lines of scientific evidence, based on experimental, correlative and modeling studies, indicate Hg concentrations in fish and wildlife increase with the amount of atmospheric Hg deposition, and reductions in anthropogenic Hg emissions lower Hg exposure in the environment. The findings from this assessment, and elsewhere, also show there are complex environmental and ecological processes which influence the fate of anthropogenic Hg following its release into the atmosphere. Those processes may dampen short-term ecosystem responses to Hg emissions reductions, and time scales of recovery may differ among types of environments and under varying environmental conditions.

The temporal trend analysis for Hg in Arctic air and biota showed some incongruence between atmospheric concentrations and deposition of Hg and its bioaccumulation in food webs. In general, Hg in the Arctic atmosphere has declined in recent decades while Hg in more than half of the 77 populations of Arctic biota monitored as part of this assessment have increased over the same time period. While local environmental and ecological processes at these monitoring sites require further investigation to identify the specific drivers of greater Hg exposure, recent Arctic research has shown that climate, shifts in diet or food-web structure and animal body condition, among other factors, may be important.

Likewise, the increasing trend in global anthropogenic emissions of Hg in recent years was not generally reflected in Hg air concentrations observed at Arctic air monitoring sites. This inconsistency between anthropogenic Hg emissions estimates and air-Hg concentration trends may be related to proximity of monitoring sites to regions where emissions of Hg have declined significantly in recent decades (North America and Europe) or to the effects of changes in the speciation of the Hg emitted, but this is a subject requiring further investigation.

When it comes to Hg research, the Arctic is one of the most intensively studied regions in the world, and findings for the Arctic may provide important insights for future effectiveness evaluation of the UN Environment Minamata Convention in other regions. The complexity of the Hg cycle and fate dictates that efforts to evaluate the effectiveness of regulatory actions require a broad suite of indicators representing multiple types of matrices and environmental compartments to obtain an accurate picture of Hg contamination trends. Different environmental compartments (e.g., the atmosphere, terrestrial, freshwater and marine environments) may respond at different rates to reductions in Hg loading, and large reservoirs of legacy Hg contamination in soils and the Arctic Ocean may dampen response times.

Climate change is dramatically altering environmental conditions in the Arctic with consequences for Hg transport, cycling and fate. The climate is also changing around the world, albeit possibly at a slower pace and in different ways to the Arctic. Thus, potential implications of climate-related environmental change around the world should be taken into account in future effectiveness evaluation of the UN Environment Minamata Convention, particularly environmental change that may enhance Hg transport and exposure. Greater precipitation and more frequent and intense wildfires (from drought) are two examples of potential climate change drivers. As a consequence, efforts to enhance operational links between Hg monitoring and the monitoring of changes to local environmental conditions at those sites will benefit effectiveness evaluation activities in the long term.

10.4 Recommendations

Priorities for future research into Hg in the Arctic include the following:

- Temporal trend monitoring of Hg in Arctic biota should be continued, and program designs to identify effects of local environmental processes should be enhanced. Specifically, this should include: enhanced geographical coverage; sample matrices, including seawater and river inorganic Hg and MeHg.
- Methylmercury production in marine environments, particularly in zones which enhance the uptake of Hg in the food web, should be further investigated.
- Long-term consequences of climate change on Hg exposure in biota as the Arctic continues to warm should be evaluated.
- Multidisciplinary studies of the cumulative effects of Hg with other environmental stressors on Arctic biota should be carried out, including studies on the exposure of Arctic biota to a suite of contaminants and stresses driven by climate change and other drivers of anthropogenic origin.
- Biomonitoring should be continued and expanded to improve understanding of key human exposure pathways to Hg, including food security and safety, and tracking of the associated human health risks should be continued.
- The modeling of processes that influence Hg transport and fate in the Arctic environment to evaluate source-receptor effects should be improved.
- Partnerships between scientists and Indigenous Peoples for research and monitoring of Hg in the Arctic, using best practices for ethical research, should be further developed.

References

Personal communications

Ackerman, J. (US Geological Survey) and co-workers, 2020. Personal communication to R. Dietz.

Andreasen, B. (Environment Agency, Faroe Islands) and co-workers, 2020. Personal communication to A. Morris and R. Dietz.

Andreasen, B. (Environment Agency, Faroe Islands) and co-workers, 2021. Personal communication to R. Dietz.

Chastel, O. (La Rochelle University, France), Bustnes, J.O., Gabrielsen, G.W. and co-workers, 2020. Personal communication to R. Dietz.

Chastel, O. (La Rochelle University, France) et al., 2021. Personal communication to R. Dietz.

Chételat, J. (Environment and Climate Change Canada) et al., 2021. Personal communication to R. Dietz.

Ciesielski, T. (Norweigian University of Science and Technology, Norway) and co-workers, 2020. Personal communication to R. Dietz.

Danielsen, S. (Swedish Museum of Natural History) and co-workers, 2020. Personal communication to R. Dietz.

Dietz, R. (Aarhus University, Denmark) and co-workers, 2020. Personal communication to A. Morris.

Evans, M. (Environment and Climate Change Canada), 2019. Updated data provided (anadromous char, lake trout, burbot, Northern pike). Personal communication to A. Morris.

Evans, M., (Environment and Climate Change Canada), 2020. Personal communication to R. Dietz.

Evans, M., (Environment and Climate Change Canada), 2021. Personal communication to N. Basu.

Ferguson, S. (Fisheries and Oceans, Canada) and co-workers, 2020. Personal communication to R. Dietz.

Fort, J. (CNRS-La Rochelle Université, France) and co-workers, 2020. Personal communication to R. Dietz.

Fort, J. (CNRS-La Rochelle Université, France) and Grémillet, D. (CNRS-La Rochelle Université, France), 2019. Updated data provided (little auk). Personal communication to A. Morris (Crown-Indigenous Relations and Northern Affairs Canada).

Fryer, R. (Marine Scotland, United Kingdom), 2019. Personal communication to A. Morris.

Gamberg, M. (Gamberg Consulting, Canada), 2019. Personal communication to A. Morris.

Gamberg, M. (Gamberg Consulting, Canada), 2020. Personal communication to R. Dietz.

Hudelson, K. (ETH Zürich, Switzerland), Muir, D. (Environment and Climate Change Canada), Kirk, J. (Environment and Climate Change Canada) et al., 2019. Updated data provided (Arctic char). Personal communication to A. Morris.

Kohler, S. (Norwegian University of Science and Technology) et al., 2021. Personal communication to R. Dietz.

Lemire, M. (Laval University, Canada) and Blanchette, C. (Laval University, Canada), 2020. Personal communication to B. Adlard.

Letcher, R.J. (Environment and Climate Change Canada) and Houde, M. (Environment and Climate Change Canada), 2019. Updated data provided (polar bear). Personal communication to A. Morris.

Letcher, R.J. (Environment and Climate Change Canada) and co-workers, 2020. Personal communication to R. Dietz.

Little, M. and Lemire, M. (Laval University, Canada), 2019. Personal communication to M. Houde and E.M. Krümmel.

Loseto, L. (Fisheries and Oceans, Canada), Watt, C. (Fisheries and Oceans, Canada) and Ferguson, S. (Fisheries and Oceans, Canada), 2019. Updated data provided (beluga). Personal communication to A. Morris.

Loseto, L. (Fisheries and Oceans, Canada) and co-workers, 2020. Personal communication to R. Dietz.

Mikaelsson, S. (Sámi Parliamentary Council/Snowchange, Sweden), 2020. Personal communication to M. Houde and E.M. Krümmel.

Muir, D. (Environment and Climate Change Canada) and Houde, M. (Environment and Climate Change Canada), 2020. Personal communication to R. Dietz.

Muir, D. (Environment and Climate Change Canada) and Houde, M. (Environment and Climate Change Canada), 2021. Personal communication to P. Weihe and N. Basu.

Muir, D. (Environment and Climate Change Canada) and Hudelson, K. (Environment and Climate Change Canada), 2020. Personal communication to R. Dietz.

Muir, D. (Environment and Climate Change Canada) and Hudelson, K. (Environment and Climate Change Canada), 2021. Personal communication to P. Weihe and N. Basu.

Murtomäki, E. (Snowchange, Finland), 2020. Personal communication to to M. Houde and E.M. Krümmel.

Petersen, M.S. (Department of Occupational Medicine and Public Health, The Faroese Hospital System, Tórshavn, Faroe Islands), 2019. Personal communication to A. Morris.

Pinzone, M. (University of Winnipeg, Canada) and co-workers, 2020. Personal communication to R. Dietz.

Poste, A. (Norwegian Institute for Water Research, Norway) et al., 2020. Personal communication to R. Dietz.

Poste, A. (Norwegian Institute for Water Research, Norway) Evenset, A. (Akvaplan-niva, Norway) and Blevin, P. (Akvaplan-niva, Norway), 2021. Personal communication to P. Weihe and N. Basu.

Rigét, F. (Aarhus University, Denmark) and co-workers, 2020. Personal communication to R. Dietz.

Rigét, F. (Aarhus University, Denmark) and co-workers, 2021. Personal communication to P. Weihe and N. Basu.

Stern, G. (University of Manitoba, Canada), 2019. Updated data provided (burbot). Personal communication to A. Morris.

Stern, G. (University of Manitoba, Canada), 2020. Personal communication to R. Dietz.

Thomas, P. (Environment and Climate Change Canada) and co-workers, 2020. Personal communication to R. Dietz.

Treu, G. (Leibniz Institute for Zoo and Wildlife Research, Germany) and co-workers, 2020. Personal communication to R. Dietz.

Watt, C. (Fisheries and Oceans, Canada) and co-workers, 2020. Personal communication to R. Dietz.

Weihe, P. (Department of Occupational Medicine and Public Health, Faroe Islands), 2019. Personal communication to A. Morris.

Weihe, P. (Department of Occupational Medicine and Public Health, Faroe Islands), 2021. Personal communication to N. Basu.

General references

Aastrup, P., Rigét, F., Dietz, R. and Asmund, G., 2000. Lead, zinc, cadmium, mercury, selenium and copper in Greenland caribou and reindeer (Rangifer tarandus). Science of the Total Environment, 245 (1-3):149-159.

Abass, K., Huusko, A., Knutsen, H.K., Nieminen, P., Myllynen, P., Meltzer, H.M., Vahakangas, K. and Rautio, A., 2018. Quantitative estimation of mercury intake by toxicokinetic modelling based on total mercury levels in humans. Environment International, 114:1-11.

Abbatt, J.P.D., Thomas, J.L., Abrahamsson, K., Boxe, C., Granfors, A., Jones, A.E., King, M.D., Saiz-Lopez, A., Shepson, P.B., Sodeau, J., Toohey, D.W., Toubin, C., von Glasow, R., Wren, S. N. and Yang, X., 2012. Halogen activation via interactions with environmental ice and

snow in the polar lower troposphere and other regions, Atmospheric Chemistry and Physics, 12 (14):6237-6271.

Achouba, A., Dumas, P., Ouellet, N., Little, M., Lemire, M. and Ayotte, P., 2019. Selenoneine is a major selenium species in beluga skin and red blood cells of Inuit from Nunavik. Chemosphere, 229:549-558.

Ackerman, J.T., Overton, C.T., Casazza, M.L., Takekawa, J.Y., Eagles-Smith, C.A., Keister, R.A. and Herzog, M.P., 2012. Does mercury contamination reduce body condition of endangered California clapper rails? Environmental Pollution, 162:439-448.

Ackerman, J.T., Eagles-Smith, C.A., Herzog, M.P. and Hartman, C.A., 2016a. Maternal transfer of contaminants in birds: mercury and selenium concentrations in parents and their eggs. Environmental Pollution, 210:145-154.

Ackerman, J.T., Eagles-Smith, C.A., Herzog, M.P., Hartman, C.A., Peterson, S.H., Evers, D.C., Jackson, A.K., Elliott, J.E., Vander Pol, S.S. and Bryan, C.E., 2016b. Avian mercury exposure and toxicological risk across western North America: a synthesis. Science of the Total Environment, 568:749-769.

Ackerman, J.T., Hartman, C.A. and Herzog, M.P., 2019. Mercury contamination in resident and migrant songbirds and potential effects on body condition. Environmental Pollution, 246:797-810.

Ackerman, J.T., Herzog, M.P., Evers, D.C., Cristol, D.A., Kenow, K.P., Heinz, G.H., Lavoie, R.A., Brasso, R.L., Mallory, M.L., Provencher, J.F., Braune, B.M., Matz, A., Schmutz, J.A., Eagles-Smith, C.A., Savoy, L.J., Meyer, M.W. and Hartman, C.A., 2020. Synthesis of Maternal Transfer of Mercury in Birds: Implications for Altered Toxicity Risk. Environmental Science & Technology, 54 (5):2878-2891.

Act on Greenland Self-Government, 2009. Act no. 473, 12.06.2009.

Agather A.M., Bowman K.L., Lamborg C.H. and Hammerschmidt, C.R., 2019. Distribution of mercury species in the Western Arctic Ocean (U.S. GEOTRACES GN01). Marine Chemistry, 216:103686.

Agnan, Y., Douglas, T.A., Helmig, D., Hueber, J. and Obrist, D., 2018. Mercury in the Arctic tundra snowpack: temporal and spatial concentration patterns and trace gas exchanges. The Cryosphere, 12 (6):1939-1956.

Agusa, T., Matsumoto, T., Ikemoto, T., Anan, Y., Kubota, R., Yasunaga, G., Kunito, T., Tanabe, S., Ogi, H. and Shibata, Y., 2005. Body distribution of trace elements in black-tailed gulls from Rishiri Island, Japan: age-dependent accumulation and transfer to feathers and eggs. Environmental Toxicology and Chemistry, 24 (9):2107-2120.

Ahonen, S.A., Hayden, B., Leppänen, J.J. and Kahilainen, K.K., 2018. Climate and productivity affect total mercury concentration and bioaccumulation rate of fish along a spatial gradient of subarctic lakes. Science of the Total Environment, 637-638:1586-1596.

Aksentov, K.I., Astakhov, A.S., Ivanov, M.V., Shi, X., Hu, L., Alatortsev, A.V., Sattarova, V.V., Mariash, A.A. and Melgunov, M.S., 2021. Assessment of mercury levels in modern sediments of the East Siberian Sea. Marine Pollution Bulletin, 168:112426.

Alanne, M., Honka, A and Karjalainen, N. 2014. Lokan ja Porttipahdan tekojärvien säännöstelyn kehittäminen. Yhteenveto ja suositukset. Raportteja, 38. Lapin elinkeino-, liikenne- ja ympäristökeskus, Rovaniemi, Suomi. 69pp. (Finnish language).

Albert, C., Renedo, M., Bustamante, P. and Fort, J., 2019. Using blood and feathers to investigate large-scale Hg contamination in Arctic seabirds: a review. Environmental Research, 177:108588.

Albert, C., Helgason, H.H., Brault-Favrou, M., Robertson, G.J., Descamps, S., Amélineau, F., Danielsen, J., Dietz, R., Elliott, K., Erikstad, K.E., Eulaers, I., Ezhov, A., Fitzsimmons, M.G., Gavrilo, M., Golubova, E., Grémillet, D., Hatch, S., Huffeldt, N.P., Jakubas, D., Kitaysky, A., Kolbeinsson, Y., Krasnov, Y., Lorentsen, S.-H., Lorentzen, E., Mallory, M.L., Merkel, B., Merkel, F.R., Montevecchi, W., Mosbech, A., Olsen, B., Orben, R.A., Patterson, A., Provencher, J., Plumejeaud, C., Pratte, I., Reiertsen, T.K., Renner, H., Rojek, N., Romano, M., Strøm, H., Systad, G.H., Takahashi, A., Thiebot, J.-B., Thórarinsson, T.L., Will, A.P., Wojczulanis-Jakubas, K., Bustamante, P. and Fort, J., 2021. Seasonal variation of mercury contamination in Arctic seabirds: a pan-Arctic assessment. Science of the Total Environment, 750:142201.

Albrecht, E., 2019. Ilomantsin luonnonvarojen käytön historiaa Koitajoen ympäristön tilan muutosten kuvaajana. Raportteja, 49. Pohjois-Karjalan elinkeino-, liikenne- ja ympäristökeskus, Joensuu, Suomi. 79pp. (Finnish Language).

Allard, M. and Lemay, M., 2012. Nunavik and Nunatsiavut: From science to policy. An Integrated Regional Impact Study (IRIS) of climate change and modernization. ArcticNet Inc., Quebec City, Canada. 303pp.

Alvarez, M. del C., Murphy, C.A., Rose, K.A., McCarthy, I.D. and Fuiman, L.A., 2006. Maternal body burdens of methylmercury impair survival skills of offspring in Atlantic croaker (*Micropogonias undulatus*). Aquatic Toxicology, 80 (4):329-337.

AMAP, 1998. AMAP Assessment Report: Arctic Pollution Issues. Arctic Monitoring and Assessment Programme (AMAP), Oslo, Norway. xii + 859pp.

AMAP, 2003. AMAP Assessment 2002: Human Health in the Arctic. Arctic Monitoring and Assessment Programme (AMAP), Oslo, Norway. xiv + 137pp.

AMAP, 2004. AMAP Assessment 2002: Persistent Organic Pollutants in the Arctic. Arctic Monitoring and Assessment Programme (AMAP), Oslo, Norway. xvi + 310pp.

AMAP, 2005. AMAP Assessment 2002: Heavy Metals in the Arctic. Arctic Monitoring and Assessment Programme (AMAP), Oslo, Norway. xvi + 265pp.

AMAP, 2009. AMAP Assessment 2009: Human Health in the Arctic. Arctic Monitoring and Assessment Programme (AMAP), Oslo, Norway. xiv + 254pp.

AMAP, 2010. Updating Historical Global Inventories of Anthropogenic Mercury Emissions to Air. AMAP Technical Report No. 3. (2010). Arctic Monitoring and Assessment Programme (AMAP), Oslo, Norway. 12pp.

AMAP, 2011. AMAP Assessment 2011: Mercury in the Arctic. Arctic Monitoring and Assessment Programme (AMAP), Oslo, Norway. xiv + 193pp.

AMAP, 2015. AMAP Assessment 2015: Human Health in the Arctic. Arctic Monitoring and Assessment Programme (AMAP), Oslo, Norway. vii + 165pp.

AMAP, 2016. AMAP Assessment 2015: Temporal Trends in Persistent Organic Pollutants in the Arctic. Arctic Monitoring and Assessment Programme (AMAP), Oslo, Norway. vi + 71pp.

AMAP, 2017a. Snow, Water, Ice and Permafrost in the Arctic (SWIPA) 2017. Arctic Monitoring and Assessment Programme (AMAP), Oslo, Norway. xiv + 269pp.

AMAP, 2017b. AMAP Assessment 2016: Chemicals of Emerging Arctic Concern. AMAP, Oslo, Norway. xvi + 353pp.

AMAP, 2018a. AMAP Assessment 2018: Biological Effects of Contaminants on Arctic Wildlife and Fish. Arctic Monitoring and Assessment Programme (AMAP), Tromsø, Norway. vii + 84pp.

AMAP, 2018b. AMAP Assessment 2018: Arctic Ocean Acidification. Arctic Monitoring and Assessment Programme (AMAP), Tromsø, Norway. vi + 187pp.

AMAP, 2019a. AMAP Strategic Framework 2019+. Arctic Monitoring and Assessment Programme (AMAP), Tromsø, Norway. 7pp.

AMAP, 2019b. Arctic Climate Change Update 2019. An Update to Key Findings of Snow, Water, Ice and Permafrost in the Arctic (SWIPA) 2017. Arctic Monitoring and Assessment Programme (AMAP), Oslo, Norway. 12pp.

AMAP, 2020. AMAP Assessment Data Portal. Updated January 2020. Accessed January 2021. Available at: https://www.amap.no/ahat

AMAP, 2021. AMAP Assessment 2021: Human Health in the Arctic. Arctic Monitoring and Assessment Programme (AMAP), Tromsø, Norway. x + 240pp.

AMAP/UN Environment, 2019. Technical Background Report for the Global Mercury Assessment 2018. Arctic Monitoring and Assessment Programme (AMAP), Oslo, Norway/UN Environment Programme (UNEP), Chemicals and Health Branch, Geneva Switzerland. viii + 426pp including E-Annexes.

AMAP/UNEP, 2008. Technical Background Report to the Global Atmospheric Mercury Assessment. Arctic Monitoring and Assessment Programme (AMAP), Oslo, Norway/United Nations Environment Programme (UNEP), Chemicals Branch, Geneva, Switzerland. 159pp.

AMAP/UNEP, 2013. Technical Background Report for the Global Mercury Assessment 2013. Arctic Monitoring and Assessment Programme, Oslo, Norway/UNEP Chemicals Branch, Geneva, Switzerland. vi + 263pp.

Amélineau, F., Grémillet, D., Harding, A.M.A., Walkusz, W., Choquet, R. and Fort, J., 2019. Arctic climate change and pollution impact little auk foraging and fitness across a decade. Scientific Reports, 9 (1):1014.

Amirbahman, A., Kent, D.B., Curtis, G.P. and Marvin-DiPasquale, M.C., 2013. Kinetics of homogeneous and surface-catalyzed mercury(II)

reduction by iron(II). Environmental Science & Technology, 47 (13):7204-7213.

Amiro, B.D., Todd, J.B., Wotton, B.M., Logan, K.A., Flannigan, M.D., Stocks, B.J., Mason, J.A., Martell, D.L. and Hirsch, K.G., 2001. Direct carbon emissions from Canadian forest fires, 1959-1999. Canadian Journal of Forest Research, 31 (33):512-525.

Amos, H.M., Jacob, D.J., Holmes, C.D., Fisher, J.A., Wang, Q., Yantosca, R.M., Corbitt, E.S., Galarneau, E., Rutter, A.P., Gustin, M.S., Steffen, A., Schauer, J.J., Graydon, J.A., St. Louis, V.L., Talbot, R.W., Edgerton, E.S., Zhang, Y. and Sunderland, E.M., 2012. Gas-particle partitioning of atmospheric Hg(II) and its effect on global mercury deposition. Atmospheric Chemistry and Physics, 12 (1):591-603.

Amos, H.M., Jacob, D.J., Streets, D.G. and Sunderland, E.M., 2013. Legacy impacts of all-time anthropogenic emissions on the global mercury cycle. Global Biogeochemical Cycles, 27 (2):410-421.

Amos, H.M., Jacob, D.J., Kocman, D., Horowitz, H.M., Zhang Y., Dutkiewicz, S., Horvat, M., Corbitt, E.S., Krabbenhoft, D.P. and Sunderland, E.M., 2014. Global biogeochemical implications of mercury discharges from rivers and sediment burial. Environmental Science & Technology, 48 (16):9514-9522.

Amos, H.M., Sonke, J.E., Obrist, D., Robins, N., Hagan, N., Horowitz, H.M., Mason, R.P., Witt, M., Hedgecock, I.M., Corbitt, E.S. and Sunderland, E.M., 2015. Observational and modeling constraints on global anthropogenic enrichment of mercury. Environmental Science & Technology, 49 (7):4036-4047.

Amstrup, S.C., DeWeaver, E.T., Douglas, D.C., Marcot, B.G., Durner, G.M., Bitz, C.M. and Bailey, D.A., 2010. Greenhouse gas mitigation can reduce sea-ice loss and increase polar bear persistence. Nature, 468 (7326):955-958.

Andersson, M.E., Sommar, J., Gårdfeldt, K. and Lindqvist, O., 2008. Enhanced concentrations of dissolved gaseous mercury in the surface waters of the Arctic Ocean. Marine Chemistry, 110 (3-4):190-194.

Andreasen, B., Hoydal, K., Mortensen, R., Erenbjerg S.V. and Dam, M., 2019. AMAP Faroe Islands 2013–2016: Heavy Metals and POPs Core Programme, Umhvørvisstovan, Argir, Faroe Islands. x + 103pp.

Angelier, F. and Chastel, O., 2009. Stress, prolactin and parental investment in birds: a review. General and Comparative Endocrinology, 163 (1):142-148.

Angelier, F., Costantini, D., Blévin, P. and Chastel, O., 2018. Do glucocorticoids mediate the link between environmental conditions and telomere dynamics in wild vertebrates? A review. General and Comparative Endocrinology 256:99-111.

Angot, H., Dastoor, A., De Simone, F., Gårdfeldt, K., Gencarelli, C. N., Hedgecock, I. M., Langer, S., Magand, O., Mastromonaco, M. N., Nordstrøm, C., Pfaffhuber, K. A., Pirrone, N., Ryjkov, A., Selin, N. E., Skov, H., Song, S., Sprovieri, F., Steffen, A., Toyota, K., Travnikov, O., Yang, X. and Dommergue, A., 2016. Chemical cycling and deposition of atmospheric mercury in polar regions: review of recent measurements and comparison with models. Atmospheric Chemistry and Physics, 16 (16):10735-10763.

Angot, H., Hoffman, N., Giang, A., Thackray, C.P., Hendricks, A.N., Urban, N.R. and Selin, N.E., 2018. Global and local impacts of delayed mercury mitigation efforts. Environmental Science & Technology, 52 (22):12968-12977.

Appelquist, H., Asbirk, S. and Drabæk, I., 1984. Mercury monitoring: mercury stability in bird feathers. Marine Pollution Bulletin, 15 (1):22-24.

Archer, D.E. and Blum, J.D., 2018. A model of mercury cycling and isotopic fractionation in the ocean. Biogeosciences, 15 (20):6297-6313.

Arctic Council, 2018. Agreement on enhancing international Arctic scientific cooperation. Tromsø, Norway. 30pp. Available at: https://oaarchive.arctic-council.org/handle/11374/1916

Arctic Council, 2019. Rovaniemi Ministerial Statements. Rovaniemi, Finland. 22pp. Available at: https://oaarchive.arctic-council.org

Arctic Council IPS, 2015. Ottawa Traditional Knowledge Principles. Arctic Council Indigenous Peoples Secretariat (Arctic Council IPS), Tromsø, Norway. 2pp. Available at: https://static1.squarespace.com/static/58b6de9e414fb54d6c50134e/t/5dd4097576d4226b2a894337/1574177142813/Ottawa_TK_Principles.pdf

Arctic Eider Society, 2016. Arctic Eider Society 2015-2016 Annual Report. Arctic Eider Society, St. John's, NL, Canada. 38pp. Available at: https://legacy.arcticeider.com/annual_report/15_16_folder/Arctic%20Eider%20Society%20Annual%20Report%202015-2016.pdf

Ariya, P.A., Amyot, M., Dastoor, A., Deeds, D., Feinberg, A., Kos, G., Poulain, A., Ryjkov, A., Semeniuk, K., Subir and M., Toyota, K., 2015. Mercury physicochemical and biogeochemical transformation in the atmosphere and at atmospheric interfaces: a review and future directions. Chemical Reviews, 115 (10):3760-3802.

Arnold, J., Gustin, M.S. and Weisberg, P.J., 2018. Evidence for nonstomatal uptake of Hg by aspen and translocation of Hg from foliage to tree rings in Austrian pine. Environmental Science & Technology, 52 (3):1174-1182.

Arrigo, K. R. and van Dijken, G.L., 2011. Secular trends in Arctic Ocean net primary production. Journal of Geophysical Research: Oceans, 116 (C9):C09011.

Arrigo, K. R. and van Dijken, G.L., 2015. Continued increases in Arctic Ocean primary production. Progress in Oceanography, 136:60-70.

Asaduzzaman, A.M., Wang, F. and Schreckenbach, G., 2012. Quantum-chemical study of the diffusion of Hg(0, I, II) into the ice(Ih). The Journal of Physical Chemistry C, 116 (8):5151-5154.

Aschner, M and Aschner, J.L., 1990. Mercury neurotoxicity: mechanisms of blood-brain barrier transport. Neuroscience & Biobehavioral Reviews, 14 (2):169-176.

Assembly of First Nations, 2011. First Nations Ethics Guide on Research and Aboriginal Traditional Knowledge. Available at: https://www.afn.ca/uploads/files/fn_ethics_guide_on_research_and_atk.pdf

Atwood, T.C., Peacock, E., McKinney, M.A., Lillie, K., Wilson, R., Douglas, D.C., Miller, S. and Terletzky, P., 2016. Rapid environmental change drives increased land use by an Arctic marine predator. PLOS ONE, 11 (6):e0155932.

Ayotte, P., Carrier, A., Ouellet, N., Boiteau, V., Abdous, B., Sidi, E.A., Château-Degat, M.-L. and Dewailly, É., 2011. Relation between methylmercury exposure and plasma paraoxonase activity in Inuit adults from Nunavik. Environ Health Perspectives, 119 (8):1077-1083.

Baker, K.R. and Bash, J.O., 2012. Regional scale photochemical model evaluation of total mercury wet deposition and speciated ambient mercury. Atmospheric Environment, 49:151-162.

Baker, M.R, Schindler, D.E., Holtgrieve, G.W. and St. Louis, V.L., 2009. Bioaccumulation and transport of contaminants: migrating sockeye salmon as vectors of mercury. Environmental Science & Technology, 43 (23):8840-8846.

Balabanov, N.B. and Peterson, K.A., 2003. Mercury and reactive halogens: the thermochemistry of Hg + {Cl2, Br2, BrCl, ClO, and BrO}. The Journal of Physical Chemistry A, 197 (38):7465-7470.

Baldi, F., Pepi, M. and Filippelli, M.,1993. Methylmercury resistance in Desulfovibrio desulfuricans strains in relation to methylmercury degradation. Applied and Environmental Microbiology, 59 (8):2479-2485.

Baldwin, C., Bradford, L., Carr, M.K., Doig, L.E., Jardine, T.D., Jones, P.D., Bharadwaj, L. and Lindenschmidt, K.-E., 2018. Ecological patterns of fish distribution in the Slave River Delta region, Northwest Territories, Canada, as relayed by traditional knowledge and Western science. International Journal of Water Resources Development, 34 (2):305-324.

Bamber, J., van den Broeke, M., Ettema, J., Lenaerts, J. and Rignot, E., 2012. Recent large increases in freshwater fluxes from Greenland into the North Atlantic. Geophysical Research Letters, 39 (19):L19501.

Ban, N.C., Frid, A., Reid, M., Edgar, B., Shaw, D. and Siwallace, P., 2018. Incorporate Indigenous perspectives for impactful research and effective management. Nature Ecology & Evolution, 2 (11):1680-1683.

Bank-Nielsen, P.I., Long, M. and Bonefeld-Jørgensen, E.C., 2019. Pregnant Inuit women's exposure to metals and association with fetal growth outcomes: ACCEPT 2010–2015. International Journal of Environmental Research and Public Health, 16 (7):1171-1198.

Barber, D.G., Hop, H., Mundy, C.J., Else, B., Dmitrenko, I.A., Tremblay, J.-E., Ehn, J.K., Assmy, P., Daase, M., Candlish, L.M. and Rysgaard, S., 2015. Selected physical, biological and biogeochemical implications of a rapidly changing Arctic Marginal Ice Zone. Progress in Oceanography, 139:122-150.

Bårdsen, B, -J., Hanssen, S.A. and Bustnes, J.O., 2018. Multiple stressors: modeling the effect of pollution, climate, and predation on viability of a sub-arctic marine bird. Ecosphere, 9 (7):e02342.

Barkay, T., Miller, S.M. and Summers, A.O., 2003. Bacterial mercury resistance from atoms to ecosystems. FEMS Microbiology Reviews, 27 (2-3):355-384.

Barst, B.D., Rosabal, M., Campbell, P.G.C., Muir, D.G.C., Wang, X., Köck, G. and Drevnick, P.E., 2016. Subcellular distribution of trace elements and liver histology of landlocked Arctic char (Salvelinus alpinus) sampled along a mercury contamination gradient. Environmental Pollution, 212:574-583.

Barst, B.D., Drevnick, P.E., Muir, D.C.G., Gantner, N., Power, M., Köck, G., Chéhab, N., Swanson, H., Rigét, F. and Basu, N., 2019. Screening-level risk assessment of methylmercury for non-anadromous Arctic char (Salvelinus alpinus). Environmental Toxicology and Chemistry, 38 (3):489-502.

Barst, B.D., Hudelson, K., Lescord, G.L., Santa-Rios, A., Basu, N., Crémazy, A. and Drevnick, P.E., 2020. Effects of non-native fish on lacustrine food web structure and mercury biomagnification along a dissolved organic carbon gradient. Environmental Toxicology and Chemistry, 39 (11):2196-2207.

Bartels-Rausch, T., Krysztofiak, G., Bernhard, A., Schläppi, M., Schwikowski, M. and Ammann, M., 2011. Photoinduced reduction of divalent mercury in ice by organic matter. Chemosphere, 82 (2):199-203.

Bartley, T.J., McCann, K.S., Bieg, C., Cazelles, K., Granados, M., Guzzo, M.M., MacDougall, A.S., Tunney, T.D. and McMeans, B.C., 2019. Food web rewiring in a changing world. Nature Ecology and Evolution, 3 (3):345-354.

Bash, J.O., Carlton, A.G., Hutzell, W.T., and Bullock, O.R., Jr., 2014. Regional air quality model application of the aqueous-phase photo reduction of atmospheric oxidized mercury by dicarboxylic acids. Atmosphere, 5 (1):1-15.

Basu, N., Scheuhammer, A.M., Rouvinen-Watt, K., Grochowina, N., Klenavic, K., Evans, R.D. and Chan, H.M., 2006. Methylmercury impairs components of the cholinergic system in captive mink (Mustela vison). Toxicological Sciences, 91 (1):202-209.

Basu, N., Goodrich, J.M. and Head, J., 2014. Ecogenetics of mercury: from genetic polymorphisms and epigenetics to risk assessment and decision-making. Environmental Toxicology and Chemistry, 33 (6):1248-1258.

Basu, N., Horvat, M., Evers, D.C., Zastenskaya, I., Weihe, P. and Tempowski, J., 2018. A state-of-the-science review of mercury biomarkers in human populations worldwide between 2000 and 2018. Environmental Health Perspectives 126 (10):106001.

Baya, P.A., Gosselin, M., Lehnherr, I., St. Louis, V.L. and Hintelmann, H., 2015. Determination of monomethylmercury and dimethylmercury in the Arctic marine boundary layer. Environmental Science & Technology, 49 (1):223-232.

Beal, S.A., Osterberg, E.C., Zdanowicz, C.M. and Fisher, D.A., 2015. Ice core perspective on mercury pollution during the past 600 years. Environmental Science & Technology, 49 (13):7641-7647.

Beattie, S.A., Armstrong, D., Chaulk, A., Comte, J., Gosselin, M. and Wang, F., 2014. Total and methylated mercury in Arctic multiyear sea ice. Environmental Science & Technology, 48 (10):5575-5582.

Bechshoft, T., Derocher, A.E., Richardson, E., Lunn, N.J. and St. Louis, V.L., 2016. Hair mercury concentrations in Western Hudson Bay polar bear family groups. Environmental Science & Technology, 50 (10):5313-5319.

Beckvar, N., Dillon, T.M. and Read, L.B., 2005. Approaches for linking whole-body fish tissue residues of mercury or DDT to biological effects thresholds. Environmental Toxicology and Chemistry, 24 (8):2094-2105.

Behe, C. and Daniel R., 2018. Indigenous Knowledge and the coproduction of knowledge process: creating a holistic understanding of Arctic change (Sidebar 5.2). In: Hartfield, G., Blunden, J. and Arndt, D. (Eds.). State of the Climate in 2017, pp. S160–S161. Bulletin of the American Meteorological Society, 99 (8).

Bekryaev, R.V., Polyakov, I.V. and Alexeev, V.A., 2010. Role of polar amplification in long-term surface air temperature variations and modern Arctic warming. Journal of Climate, 23 (14):3888-3906.

Bełdowska, M. and Kobos, J., 2016. Mercury concentration in phytoplankton in response to warming of an autumn - winter season. Environmental Pollution, 215:38-47.

Bełdowski, J., Miotk, M., Zaborska, A. and Pempkowiak, J., 2015. Distribution of sedimentary mercury off Svalbard, European Arctic. Chemosphere, 122:190-198.

Berg, T., Sekkesæter, S., Steinnes, E., Valdal, A.K. and Wibetoe, G., 2003. Springtime depletion of mercury in the European Arctic as observed at Svalbard. Science of the Total Environment. 304 (1-3):43-51.

Berg, T., Kallenborn, R. and Manø S., 2004. Temporal trends in atmospheric heavy metal and organochlorine concentrations at Zeppelin, Svalbard. Arctic, Antarctic, and Alpine Research, 36 (3):284-291.

Berg, T., Aspmo, K. and Steinnes, E., 2008. Transport of Hg from Atmospheric mercury depletion events to the mainland of Norway and its possible influence on Hg deposition. Geophysical Research Letters, 35 (9):L09802.

Berg, T., Pfaffhuber, K.A., Cole, A.S., Engelsen, O. and Steffen, A., 2013. Ten-year trends in atmospheric mercury concentrations, meteorological effects and climate variables at Zeppelin, Ny-Ålesund. Atmospheric Chemistry and Physics, 13 (13):6575-6586.

Berge, E. and Jakobsen, H.A., 1998. A regional scale multilayer model for the calculation of long-term transport and deposition of air pollution in Europe. Tellus B: Chemical and Physical Meteorology, 50 (3):205-223.

Bergquist, B.A. and Blum, J.D., 2007. Mass-dependent and -independent fractionation of Hg isotopes by photoreduction in aquatic systems. Science, 318 (5849):417-420.

Berner, J., Brubaker, M., Revitch, B., Kreummel, E., Tcheripanoff, M. and, Bell, J., 2016. Adaptation in Arctic circumpolar communities: food and water security in a changing climate. Interanational Journal of Circumpolar Health, 75:33820.

Bhatt, U.S., Walker, D.A., Raynolds, M.K., Comiso, J.C., Epstein, H.E., Jia, G., Gens, R., Pinzon, J.E., Tucker, C.J., Tweedie, C.E. and Webber, P.J., 2010. Circumpolar Arctic tundra vegetation change is linked to sea ice decline. Earth Interactions, 14 (8):1-20.

Bianchi, T.S., 2011. The role of terrestrially derived organic carbon in the coastal ocean: a changing paradigm and the priming effect. Proceedings of the National Academy of Sciences of the United States of America, 108 (49):19473-19481.

Bidleman, T.F., Stern, G.A., Tomy, G.T., Hargrave, B.T., Jantunen, L.M. and MacDonald, R.W., 2013. Scavenging amphipods: sentinels for penetration of mercury and persistent organic chemicals into food webs of the deep Arctic Ocean. Environmental Science & Technology, 47 (11):5553-5561.

Bieser, J., Matthias, V., Aulinger, A., Geyer, B., Hedgecock, I., De Simone, F., Gencarelli, C. and Travnikov, O., 2014. Impact of mercury chemistry on regional concentration and deposition patterns. In: Steyn, D. and Mathur, R. (Eds.). Air Pollution Modeling and its Application XXIII, pp. 189-195. Springer, Cham.

Biesinger, K.E., Anderson, L.E. and Eaton, J.G., 1982. Chronic effects of inorganic and organic mercury on Daphnia magna: toxicity, accumulation, and loss. Archives of Environmental Contamination and Toxicology, 11:769-774.

Bigg, G.R., Wei, H.L., Wilton, D.J., Zhao, Y., Billings, S.A., Hanna E. and Kadirkamanathan, V., 2014. A century of variation in the dependence of Greenland iceberg calving on ice sheet surface mass balance and regional climate change. Proceedings of the Royal Society A: Mathematical, Physical and Engineering Sciences, 470 (2166):20130662.

Bignert, A., Rigét, F., Braune, B., Outridge, P. and Wilson, S., 2004. Recent temporal trend monitoring of mercury in Arctic biota – how powerful are the existing data sets? Journal of Environmental Monitoring, 6:351-355.

Binnington, M.J., Curren, M.S., Chan, H.M. and Wania, F., 2016a. Balancing the benefits and costs of traditional food substitution by Indigenous Arctic women of childbearing age: impacts on persistent organic pollutant, mercury, and nutrient intakes. Environment International 94:554-66.

Binnington, M.J., Curren, M.S., Quinn, C.L., Armitage, J.M., Arnot, J.A., Chan, H.M. and Wania, F., 2016b. Mechanistic polychlorinated biphenyl exposure modeling of mothers in the Canadian Arctic: the challenge of reliably establishing dietary composition. Environment International, 92-93:256-68.

Bintanja, R. and Andry, O., 2017. Towards a rain-dominated Arctic. Nature Climate Change, 7 (4):263.

Bintanja, R., 2018. The impact of Arctic warming on increased rainfall. Scientific Reports, 8 (1):16001.

Bishop, K., Shanley, J.B., Riscassi, A., de Wit, H.A., Eklöf, K., Meng, B., Mitchell, C., Osterwalder, S., Schuster, P.F., Webster, J. and Zhu, W., 2020. Recent advances in understanding and measurement of mercury in the environment: terrestrial Hg cycling. Science of the Total Environment, 721:137647.

Biskaborn, B.K., Smith, S.L., Noetzli, J., Matthes, H., Vieira, G., Streletskiy, D.A., Schoeniech, P., Romanovsky, V.E., Lewkowicz, A.G., Abramov, A., Allard, M., Boike, J., Cable, W.L., Christiansen, H.H., Delaloye, Diekmann, B., Drozdov, D., Etzelmüller, Grosse, G., Guglielmin, M., Ingeman-Nielsen, T., Isaksen, K., Ishikawa, M., Johansson, M., Johannson, H., Joo, A., Kaverin, D., Kholodov, A., Konstantinov, P., Kröger, T., Lambiel, C., Lanckman, J.-P., Luo, D., Malkova, G., Meiklejohn, I., Moskalenko, N., Oliva, M., Phillips, M., Ramos, M., Sannel, A.B.,K., Sergeev, D., Seybold, C., Skryabin, P., Vasiliev, A., Wu,

Q., Yoshikawa, K., Zheleznyak, M. and Lantuit, H., 2019. Permafrost is warming at a global scale. Nature Communications, 10 (1):264.

Biswas, A., Blum, J.D., Klaue, B. and Keeler, G.J., 2007. Release of mercury from Rocky Mountain forest fires. Global Biogeochemical Cycles, 21 (1):GB1002.

Biswas, A., Blum, J.D., Bergquist, B.A., Keeler, G.J. and Xie, Z.Q., 2008. Natural mercury isotope variation in coal deposits and organic soils. Environmental Science & Technology, 42 (22):8303-8309.

Bjerregaard, P., Young, T.K., Dewailly, É. and Ebbesson, S.O.E, 2004. Indigenous health in the Arctic: an overview of the circumpolar Inuit population. Scandinavian Journal of Public Health, 32 (5):390-395.

Bjorkman, A.D., García Criado, M., Myers-Smith, I.H., Ravolainen, V., Jónsdóttir, I.S., Westergaard, K.B., Lawler, J.P., Aronsson, M., Bennett, B., Gardfjell, H., Heiðmarsson, Stewart, L. and Normand, S., 2020. Status and trends in Arctic vegetation: evidence from experimental warming and long-term monitoring. Ambio, 49 (3): 678-692.

Black, F.J., Conaway, C.H. and Flegal, A.R., 2009. Stability of dimethyl mercury in seawater and its Conversion to monomethyl mercury. Environmental Science & Technology, 43 (11):4056-4062.

Blackburn, E.H., 2005. Telomeres and telomerase: their mechanisms of action and the effects of altering their functions. FEBS Letters, 579 (4):859-862.

Blais, J.M. and Kalff, J., 1995. The influence of lake morphometry on sediment focusing. Limnology and Oceanography, 40 (3):582-588.

Blais, J. M., Macdonald, R.W., Mackay, D., Webster, E., Harvey, C. and Smol, J. P., 2007. Biologically mediated transport of contaminants to aquatic systems. Environmental Science & Technology, 41 (4):1075-1084.

Blévin, P., Tartu, S., Angelier, F., Leclaire, S., Bustnes, J.O., Moe, B., Herzke, D., Gabrielsen, G.W. and Chastel, O., 2014. Integument colouration in relation to persistent organic pollutants and body condition in Arctic breeding black-legged kittiwakes *(Rissa tridactyla)*. Science of the Total Environment, 470–471, (1):248-254.

Blévin, P., Angelier, F., Tartu, S., Ruault, S., Bustamante, P., Herzke, D., Moe, B., Bech, C., Gabrielsen, G.W., Bustnes, J.O. and Chastel, O., 2016. Exposure to oxychlordane is associated with shorter telomeres in arctic breeding kittiwakes. Science of the Total Environment, 563-564L:125-130.

Blévin P, Tartu S, Ellis HI, Chastel O, Bustamante P, Parenteau C, Herzke D, Angelier F, Gabrielsen GW. 2017a. Contaminants and energy expenditure in an Arctic seabird: Organochlorine pesticides and perfluoroalkyl substances are associated with metabolic rate in a contrasted manner. Environmental Research 157: 118-126.

Blévin, P., Angelier, F., Tartu, S., Bustamante, P., Herzke, D., Moe, B., Bech, C., Gabrielsen, G.W., Bustnes, J.O. and Chastel O., 2017b. Perfluorinated substances and telomeres in an Arctic seabird: cross-sectional and longitudinal approaches. Environmental Pollution, 230:360-367.

Blévin, P., Shaffer, S.A., Bustamante, P., Angelier, F., Picard, B., Herzke, D., Moe, B., Gabrielsen, G.W., Bustnes, J.O. and Chastel, O., 2018. Organochlorines, perfluoroalkyl substances, mercury, and egg incubation temperature in an Arctic seabird: Insights from data loggers. Environmental Toxicology and Chemistry, 37 (11):2881-2894.

Blévin, P., Shaffer, S.A., Bustamante, P., Angelier, F., Picard, B., Herzke, D., Moe, B., Gabrielsen, G.W., Bustnes, J.O. and Chastel O., 2020. Contaminants, prolactin and parental care in an Arctic seabird: Contrasted associations of perfluoroalkyl substances and organochlorine compounds with egg-turning behavior. General and Comparative Endocrinology, 291:113420.

Blum, J.D., Popp, B.N., Drazen, J.C., Anela Choy, C. and Johnson, M.W., 2013. Methylmercury production below the mixed layer in the North Pacific Ocean. Nature Geoscience, 6 (10):879-884.

Blum, J.D., Sherman, L.S. and Johnson, M.W., 2014 Mercury isotopes in earth and environmental sciences. Annual Review of Earth and Planetary Sciences, 42 (1):249-269.

Bocharova, N., Treu, G., Czirják, G.Á., Krone, O., Stefanski, V., Wibbelt, G., Unnsteinsdóttir, E.R., Hersteinsson, P., Schares, G., Doronina, L., Goltsman, M. and Greenwood, A.D., 2013. Correlates between feeding ecology and mercury levels in historical and modern Arctic foxes (Vulpes lagopus). PLOS ONE, 8 (5):e60879.

Bolton, J.L., Ylitalo, G.M., Chittaro, P., George, J.C., Suydam, R., Person, B.T., Gates, J.B., Baugh, K.A., Sformo, T. and Stimmelmayr, R., 2020. Multi-year assessment (2006-2015) of persistent organic pollutant concentrations in blubber and muscle from Western Arctic bowhead whales (Balaena mysticetus), North Slope, Alaska. Marine Pollution Bulletin, 151:110857.

Bond, A.L., Hobson, K.A. and Branfireun, B.A., 2015. Rapidly increasing methyl mercury in endangered ivory gull (Pagophila eburnea) feathers over a 130 year record. Proceedings of the Royal Society B: Biological Sciences, 282 (1805):20150032.

Borgmann, U., Norwood, W.P. and Clarke, C., 1993. Accumulation, regulation and toxicity of copper, zinc, lead and mercury in Hyalella azteca. Hydrobiologia, 259:79-89.

Born, E.W., Heilmann, A., Kielsen Holm, L. and Laidre, K.L., 2011. Polar bears in Northwest Greenland: An interview survey about the catch and the climate. Monographs on Greenland, Vol. 351. Man & Society, 41. Museum Tusculanum Press. 232pp.

Bottenheim, J.A., Dastoor, A., Gong, S.-L., Higuchi, K. and Li, Y.-F., 2004. Long range transport of air pollution to the Arctic. In: Stohl, A. (Ed.). Intercontinental Transport of Air Pollution. The Handbook of Environmental Chemistry, Air Pollution, Volume 4G, pp. 13-39. Springer, Berlin, Heidelberg.

Boucher, O., Muckle, G., Saint-Amour, D., Dewailly, É., Ayotte, P., Jacobson, S.W., Jacobson, J.L. and Bastien, C.H., 2009. The relation of lead neurotoxicity to the event-related potential P3b component in Inuit children from Arctic Quebec. Neurotoxicology, 30 (6):1070-1077.

Boucher, O., Bastien, C.H., Saint-Amour, D., Dewailly, É., Ayotte, P., Jacobson, J.L., Jacobson, S.W. and Muckle, G., 2010. Prenatal exposure to methylmercury and PCBs affects distinct stages of information processing: an event-related potential study with Inuit children. Neurotoxicology, 31 (4):373-384.

Boucher, O., Burden, M.J., Muckle, G., Saint-Amour, D., Ayotte, P., Dewailly, É., Nelson, C.A., Jacobson, S.W. and Jacobson, J.L., 2011. Neurophysiologic and neurobehavioral evidence of beneficial effects of prenatal omega-3 fatty acid intake on memory function at school age. The American Journal of Clinical Nutrition, 93 (5):1025-1037.

Boucher, O., Burden, M.J., Muckle, G., Saint-Amour, D., Ayotte, P., Dewailly, É., Nelson, C.A., Jacobson, S.W. and Jacobson, J.L., 2012a. Response inhibition and error monitoring during a visual go/no-go task in inuit children exposed to lead, polychlorinated biphenyls, and methylmercury. Environmental Health Perspectives, 120 (4):608-615.

Boucher, O., Jacobson, S.W., Plusquellec, P., Dewailly, É., Ayotte, P., Forget-Dubois, N., Jacobson, J.L. and Muckle, G., 2012b. Prenatal methylmercury, postnatal lead exposure, and evidence of attention deficit/hyperactivity disorder among Inuit children in Arctic Quebec. Environmental Health Perspectives, 120 (10):1456-1461.

Bourque, J., Dietz, R., Sonne, C., St. Leger, J., Iverson, S., Rosing-Asvid, A., Hansen, M. and McKinney, M.A, 2018. Feeding habits of a new Arctic predator: insight from full-depth blubber fatty acid signatures of Greenland, Faroe Islands, Denmark, and managed-care killer whales Orcinus orca. Marine Ecology Progress Series, 603:1-12.

Bourque, J., Atwood, T.C., Divoky, G.J., Stewart, C. and McKinney, M.A., 2020. Fatty acid-based diet estimates suggest ringed seal remain the main prey of southern Beaufort Sea polar bears despite recent use of onshore food resources. Ecology and Evolution, 10 (4):2093-2103.

Boutron, C.F., Vandal, G.M., Fitzgerald, W.F. and Ferrari, C.P., 1998. A forty-year record of mercury in central Greenland snow. Geophysical Research Letters, 25 (17):3315-3318.

Bowman, K.L., Hammerschmidt, C.R., Lamborg, C.H. and Swarr, G., 2015. Mercury in the North Atlantic Ocean: the U.S. GEOTRACES zonal and meridional sections. Deep Sea Research Part II: Topical Studies in Oceanography, 116:251-26.

Bowman, K.L., Hammerschmidt, C.R., Lamborg, C.H., Swarr, G.J. and Agather, A.M., 2016. Distribution of mercury species across a zonal section of the eastern tropical South Pacific Ocean (U.S. GEOTRACES GP16). Marine Chemistry, 186:156-166.

Bowman, K.L., Lamborg, C.H. and Agather, A.M., 2020a. A global perspective on mercury cycling in the ocean. Science of the Total Environment, 710:136166.

Bowman, K.L., Collins, R.E., Agather, A.M., Lamborg, C.H., Hammerschmidt, C.R., Kaul, D., Dupont, C.L., Christensen, G.A. and Elias, D.A., 2020b. Distribution of mercury-cycling genes in the Arctic and equatorial Pacific Oceans and their relationship to mercury speciation. Limnology and Oceanography, 65 (S1):S310-S320.

Box, J.E., Colgan, W.T., Christensen, T.R., Schmidt, N.M., Lund, M., Parmentier, F.J.W, Brown, R., Bhatt, U.S., Euskirchen, E.S., Romanovsky, V.E., Walsh, J.E., Overland, J.E., Wang, M., Corell, R.W., Meier, W.N., Wouters, B., Mernild, S., Mård, J., Pawlak, J. and Olsen, M.S., 2019. Key indicators of Arctic climate change: 1971–2017. Environmental Research Letters, 14 (4):045010.

Boyd, A., Furgal, C.M., Mayeda, A.M., Jardine, C.G. and Driedger, S.M., 2019. Exploring the role of trust in health risk communication in Nunavik, Canada. Polar Record, 55 (4):235-240.

Bozem, H., Hoor, P., Kunkel, D., Köllner, F., Schneider, J., Herber, A., Schulz, H., Leaitch, W.R., Aliabadi, A.A., Willis, M.D., Burkart, J. and Abbatt, J.P.D., 2019. Characterization of transport regimes and the polar dome during Arctic spring and summer using in situ aircraft measurements. Atmospheric Chemistry and Physics, 19 (23):15049-15071.

Braaten, H.F.V., de Wit, H.A., Fjeld, E., Rognerud, S., Lydersen, E. and Larssen, T., 2014. Environmental factors influencing mercury speciation in subarctic and boreal lakes. Science of the Total Environment, 476-477:336-345.

Braaten, H.F.V., de Wit, H.A., Larssen, T. and Poste, A.E., 2018. Mercury in fish from Norwegian lakes: the complex influence of aqueous organic carbon. Science of the Total Environment, 627:341-348.

Braaten, H.F.V., Åkerblom, S., Kahilainen, K.K., Rask, M., Vuorenmaa, J., Mannio, J., Malinen, T., Lydersen, E., Poste, A.E., Amundsen, P.-A., Kashulin, N., Kashulina, T., Terentyev, P., Christensen, G. and de Wit, H.A., 2019. Improved environmental status: 50 years of declining fish mercury levels in boreal and Subarctic Fennoscandia. Environmental Science & Technology, 53 (4):1834-1843.

Bradley, M.A., Barst, B.D. and Basu, N., 2017. A Review of mercury bioavailability in humans and fish. International Journal of Environmental Research and Public Health, 14 (2):169.

Bratkič, A., Vahčič, M., Kotnik, J., Obu Vazner, K., Begu, E., Woodward, E.M.S. and Horvat, M., 2016. Mercury presence and speciation in the South Atlantic Ocean along the 40°S transect. Global Biogeochemical Cycles, 30 (2):105-119.

Braund, S.R. 2018. Description of Alaskan Eskimo bowhead whale subsistence sharing practices. Final report submitted to the Alaska Eskimo Whaling Commission, Utqiaġvik, Alaska. 80pp. Available at: https://static1.squarespace.com/static/5580adbbe4b020d041496999/t/5f7250717a89072b665b0287/1601327235202/AWC16_Bowhead+Sharing+Report_5-25-18.pdf

Braune, B.M., 1987. Comparison of total mercury levels in relation to diet and molt for nine species of marine birds. Archives of Environmental Contamination and Toxicology, 16:217-224.

Braune, B., Norstrom, R.J., Wong, M.P., Collins, B.T. and Lee, J., 1991. Geographical distribution of metals in livers of polar bears from the Northwest territories, Canada. Science of the Total Environment, 100:283-299.

Braune, B.M., 2007. Temporal trends of organochlorines and mercury in seabird eggs from the Canadian Arctic, 1975-2003. Environmental Pollution, 148 (2):599-613.

Braune, B.M. and Gaskin, D.E., 1987. Mercury levels in Bonaparte's gulls (Larus philadelphia) during autumn molt in the Quoddy region, New Brunswick, Canada. Archives of Environmental Contamination and Toxicology, 16:539-549.

Braune, B.M. and Malone, B.J., 2006. Organochlorines and mercury in waterfowl harvested in Canada. Environmental Monitoring Assessment, 114 (1):331-359.

Braune, B.M., Donaldson, G.M., Hobson, K.A., 2001. Contaminant residues in seabird eggs from the Canadian Arctic. Part I. Temporal trends 1975-1998. Environmental Pollution, 114 (1):39-54.

Braune, B.M., Donaldson, G.M. and Hobson, K.A., 2002. Contaminant residues in seabird eggs from the Canadian Arctic. Part II. Spatial trends and evidence from stable isotopes for intercolony differences. Environmental Pollution, 117 (1):133-145.

Braune, B.M., Mallory, M.L. and Gilchrist, H.G., 2006. Elevated mercury levels in a declining population of ivory gulls in the Canadian Arctic. Marine Pollution Bulletin, 52 (8):978-982.

Braune, B.M., Scheuhammer, A.M., Crump, D., Jones, S., Porter, E. and Bond, D., 2012. Toxicity of methylmercury injected into eggs of thick-billed murres and Arctic terns. Ecotoxicology, 21:2143-2152.

Braune, B.M., Gaston, A.J., Elliott, K.H., Provencher, J.F., Woo, K.J., Chambellant., M., Ferguson, S.H. and Letcher, R.J., 2014a. Organohalogen contaminants and total mercury in forage fish preyed upon by thick-billed murres in northern Hudson Bay. Marine Pollution Bulletin, 78 (1-2):258-266.

Braune, B.M., Gaston, A.J., Hobson, K.A., Gilchrist, H.G. and Mallory, M.L., 2014b. Changes in food web structure alter trends of mercury uptake at two seabird colonies in the Canadian Arctic. Environmental Science & Technology, 48 (22):13246-13252.

Braune, B.M., Gaston, A.J., Gilchrist, H.G., Mallory, M.L. and Provencher, J.F., 2014c. A geographical comparison of mercury in seabirds in the eastern Canadian Arctic. Environment International, 66:92-96.

Braune, B., Chételat, J., Amyot, M., Brown, T., Clayden, M., Evans, M., Fisk, A., Gaden, A., Girard, C., Hare, A., Kirk, J., Lehnherr, I., Letcher, R., Loseto, L., Macdonald, R., Mann, E., McMeans, B., Muir, D., O'Driscoll, N., Poulain, A., Reimer, K. and Stern, G., 2015. Mercury in the marine environment of the Canadian Arctic: review of recent findings. Science of the Total Environment, 509-510:67-90.

Braune, B.M., Gaston, A.J. and Mallory, M.L., 2016. Temporal trends of mercury in eggs of five sympatrically breeding seabird species in the Canadian Arctic. Environmental Pollution, 214:124-131.

Brazeau, M.L., Poulain, A.J., Paterson, A.M., Keller, W., Sanei, H. and Blais, J.M., 2013. Recent changes in mercury deposition and primary productivity inferred from sediments of lakes from the Hudson Bay Lowlands, Ontario, Canada. Environmental Pollution, 173 (3):52-60.

Breton-Honeyman, K., Hammill, M.O., Furgal, C.M. and Hickie, B., 2016. Inuit Knowledge of Beluga whale (Delphinapterus leucas) foraging ecology in Nunavik (Arctic Quebec), Canada. Canadian Journal of Zoology, 94 (10):713-726.

Bridges, C.C. and Zalups, R.K., 2010. Transport of inorganic mercury and methylmercury in target tissues and organs. Journal of Toxicology and Environmental Health, Part B, 13 (5):385-410.

Brigham, M.E., Wentz, D.A., Aiken, G.R. and Krabbenhoft, D.P., 2009. Mercury cycling in stream ecosystems. 1. Water column chemistry and transport. Environmental Science & Technology, 43 (8):2720-2725.

Bring, A., Fedorova, I., Dibike, Y., Hinzman, L., Mård, J., Mernild, S.H., Prowse, T., Semenova, O., Stuefer, S.L. and Woo, M.-K., 2016. Arctic terrestrial hydrology: a synthesis of processes, regional effects, and research challenges. Journal of Geophysical Research: Biogeosciences, 121 (3):621-649.

Broadley, H.J., Cottingham, K.L., Baer, N.A., Weathers, K.C., Ewing, H.A., Chaves-Ulloa, R., Chickering, J., Wilson, A.M., Shrestha, J. and Chen, C.Y., 2019. Factors affecting MeHg bioaccumulation in stream biota: the role of dissolved organic carbon and diet. Ecotoxicology, 28 (8):949-963.

Brooks, S.B., Saiz-Lopez, A., Skov, H., Lindberg, S.E., Plane, J.M.C. and Goodsite, M.E., 2006. The mass balance of mercury in the springtime Arctic environment. Geophysical Research Letters, 33 (13):L13812.

Brooks, S., Moore, C., Lew, D., Lefer, B., Huey, G. and Tanner, D., 2011. Temperature and sunlight controls of mercury oxidation and deposition atop the Greenland ice sheet. Atmospheric Chemistry and Physics, 11 (16):8295-8306.

Brown, L.C. and Duguay, C.R., 2011. The fate of lake ice in the North American Arctic. The Cryosphere, 5 (4):869-892.

Brown, T.M., Fisk, A.T., Wang, X., Ferguson, S.H., Young, B.G., Reimer, K.J. and Muir, D.C.G., 2016. Mercury and cadmium in ringed seals in the Canadian Arctic: influence of location and diet. Science of the Total Environment, 545-546:503-511.

Brown, T.M., Macdonald, R.W., Muir, D.C.G. and Letcher, R.J., 2018. The distribution and trends of persistent organic pollutants and mercury in marine mammals from Canada's Eastern Arctic. Science of the Total Environment, 618:500-517.

Brunet, N.D., Hickey, G.M. and Humphries, M.M., 2016. Local participation and partnership development in Canada's Arctic research: challenges and opportunities in an age of empowerment and self-determination. Polar Record, 52 (3):345-359.

Bullock, O.R. and Brehme, K.A., 2002. Atmospheric mercury simulation using the CMAQ model: formulation description and analysis of wet deposition results. Atmospheric Environment, 36 (13):2135-2146.

Bullock, D. and Johnson, S., 2011. Electric generating utility mercury speciation profiles for the clean air mercury rule (EPA-454/R-11-010). Prepared for U.S. Environmental Protection Agency (US EPA), Research Triangle Park, North Carolina, USA. 61pp.

Burke, S.M., Zimmerman, C.E., Branfireun, B.A., Koch, J.C. and Swanson, H.K., 2018. Patterns and controls of mercury accumulation in sediments from three thermokarst lakes on the Arctic Coastal Plain of Alaska. Aquatic Sciences, 80 (1).

Burke, S.M., Zimmerman, C.E., Laske, S.M., Koch, J.C., Derry, A.M., Guernon, S., Branfireun, B.A. and Swanson, H.K., 2020. Fish growth rates and lake sulphate explain variation in mercury levels in ninespine stickleback (Pungitius pungitius) on the Arctic Coastal Plain of Alaska. Science of the Total Environment, 743:140564.

Burke, S.M., Muir, D.C.G., Wang, X., Barst, B., Kirk, J., Iqaluk, D., Pope, M., Lamoureux, S.F. and Lafrenière, M.J., 2021. Climate-related drivers

cause divergent temporal trends in Arctic char mercury concentrations from paired lakes on Melville Island, Nunavut. In: Arctic Change 2020 Conference Abstracts. Arctic Science, 7 (1):ID:679.

Burnham, K.P. and Anderson, D.R., 2002. Model Selection and Inference: A Practical Information-Theoretic Approach. 2nd Edition, xxvi + 488pp. Springer-Verlag, New York.

Burnham, J.H., Burnham, K.K., Chumchal, M.M., Welker, J.M. and Johnson, J.A., 2018. Correspondence between mercury and stable isotopes in High Arctic marine and terrestrial avian species from Northwest Greenland. Polar Biology, 41 (7):1475-1491.

Burns, D.A., Aiken, G.R., Bradley, P.M., Journey, C.A. and Schelker, J., 2013. Specific ultra-violet absorbance as an indicator measurement of merucry sources in an Adirondack River basin. Biogeochemistry, 113 (1-3):451-466.

Burt, A., Wang, F., Pućko, M., Mundy, C.-J., Gosselin, M., Philippe, B., Poulin, M., Tremblay, J.-É. and Stern, G.A., 2013. Mercury uptake within an ice algal community during the spring bloom in first-year Arctic sea ice. Journal of Geophysical Research: Oceans, 118 (9):4746-4754.

Businger, J.A. and Oncley, S.P., 1990. Flux Measurement with Conditional Sampling. Journal of Atmospheric and Oceanic Technology, 7 (2):349-352.

Byun, D.W. and Ching, J.K.S. (Eds.), 1999. Science algorithms of the EPA Models-3 Community Multiscale Air Quality (CMAQ) modeling system (EPA/600/R-99/030). Prepared for U.S. Environmental Protection Agency (US EPA), Washington, D.C., USA. 22pp.

Cabana, G. and Rasmussen, J.B., 1994. Modelling food chain structure and contaminant bioaccumulation using stable nitrogen isotopes. Nature, 372 (6503):255-257.

Cadieux, S.B., White, J.R. and Pratt, L.M., 2017. Exceptional summer warming leads to contrasting outcomes for methane cycling in small Arctic lakes of Greenland. Biogeosciences, 14 (3):559-574.

Cai, P., Rutgers van der Loeff, M., Stimac, I., Nöthig, E.-M., Lepore, K. and Moran, S.B., 2010. Low export flux of particulate organic carbon in the central Arctic Ocean as revealed by 234Th:238U disequilibrium. Journal of Geophysical Research: Oceans, 115 (C10):C10037.

Calder, R.S.D., Schartup, A.T., Li, M., Valberg, A.P., Balcom, P.H. and Sunderland, E.M., 2016. Future impacts of hydroelectric power development on methylmercury exposures of Canadian Indigenous Communities. Environmental Science & Technology, 50 (23):13115-13122.

Calleja, M.L., Kerhervé, P., Bourgeois, S., Kędra, M., Leynaert, A., Devred, E., Babin, M. and Morata, N., 2017. Effects of increase glacier discharge on phytoplankton bloom dynamics and pelagic geochemistry in a High Arctic fjord. Progress in Oceanography 159:195-210.

Calvert, J.G. and Lindberg, S.E.,2005. Mechanisms of mercury removal by O3 and OH in the atmosphere. Atmospheric Environment, 39 (18):3355-3367.

Camacho, A., Rochera, C., Hennebelle, R., Ferrari, C. and Quesada, A., 2015. Total mercury and methyl-mercury contents and accumulation in polar microbial mats. Science of the Total Environment, 509-510:145-153.

Canário, J., Poissant, L. Pilote, M., Blaise, C., Constant, P., Ferard, J.-F. and Gagné, F., 2013. Toxicity survey of Canadian Arctic marine sediments. Journal of Soils and Sediments, 14 (1):196-203.

Canuel, R., de Grosbois, S.B., Atikessé, L., Lucotte, M., Arp, P., Ritchie, C., Mergler, D., Chan, H.M., Amyot, M. and Anderson, R., 2006. New evidence on variations of human body burden of methylmercury from fish consumption. Environmental Health Perspectives, 114 (2):302-306.

Capo, E., Bravo, A.G., Soerensen, A.L., Bertilsson, S., Pinhassi, J., Feng, C., Andersson, A.F., Buck, M. and Björn, E., 2020. Deltaproteobacteria and spirochaetes-like bacteria are abundant putative mercury methylators in oxygen-deficient water and marine particles in the Baltic Sea. Frontiers in Microbiology, 11:2277.

Carmack, E.C., Yamamoto-Kawai, M., Haine, T.W.N., Bacon, S., Bluhm, B.A., Lique, C., Melling, H., Polyakov, I.V., Straneo, F., Timmermans, M.-L. and Williams, W.J., 2016. Freshwater and its role in the Arctic marine system: sources, disposition, storage, export, and physical and biogeochemical consequences in the Arctic and global oceans. Journal of Geophysical Research: Biogeosciences, 121 (3):675-717.

Carr, M.K., Jardine, T.D., Doig, L.E., Jones, P.D., Bharadwaj, L., Tendler, B., Chételat, J., Cott, P. and Lindenschmidt, K.E., 2017. Stable sulfur isotopes identify habitat-specific foraging and mercury exposure in a highly mobile fish community. Science of the Total Environment, 586:338-346.

Carrie, J., Wang, F., Sanei, H., Macdonald, R.W., Outridge, P.M. and Stern, G.A., 2010. Increasing contaminant burdens in an Arctic fish, burbot (Lota lota), in a warming climate. Environmental Science & Technology, 44 (1):316-322.

Carroll, M.L. and Loboda, T.V., 2018. The sign, magnitude and potential drivers of change in surface water extent in Canadian tundra. Environmental Research Letters, 13 (4):045009.

Carroll, M.L., Townshend, J.R.G., DiMiceli, C.M., Loboda, T. and Sohlberg, R.A., 2011. Shrinking lakes of the Arctic: spatial relationships and trajectory of change. Geophysical Research Letters, 38 (20):L20406.

Castello, L., Zhulidov, A.V., Gurtovaya, T.Y., Robarts, R.D., Holmes, R.M., Zhulidov, D.A., Lysenko, V.S. and Spencer, R.G.M., 2014. Low and declining mercury in Arctic Russian rivers. Environmental Science & Technology, 48 (1):747-752.

Castro de la Guardia, L., Derocher, A.E., Myers, P.G., Terwisscha van Scheltinga, A.D. and Lunn, N.J., 2013. Future sea ice conditions in Western Hudson Bay and consequences for polar bears in the 21st century. Global Change Biology, 19 (9):2675-2687.

Cavalieri, D.J. and Parkinson, C.L., 2012. Arctic sea ice variability and trends, 1979-2010. The Cryosphere, 6 (4):881-889.

Cazenave, A. and Llovel, W., 2010. Contemporary sea level rise. Annual Review of Marine Science, 2 (1):145-173.

Cederholm, C.J., Kunze, M.D., Murota, T. and Sibatani, A., 1999. Pacific salmon carcasses: essential contributions of nutrients and energy for aquatic and terrestrial ecosystems. Fisheries, 24 (10):6-15.

Cederholm, C. J., Johnson, D.H., Bilby, R.E., Dominguez, L.G., Garrett, A.M., Graeber, W.H., Greda, E.L., Kunze, M.D., Marcot, B.G., Palmisano, J.F., Plotnikoff, R.W., Pearcy, W.G., Simenstad, C.A. and Trotter, P.C., 2000. Pacific Salmon and Wildlife - Ecological Contexts, Relationships, and Implications for Management. Special Edition Technical Report. Prepared for Johnson D.H. and O'Neil, T.A. (Managing directors), Wildlife-Habitat Relationships in Oregon and Washington (WDFW), Olympia, Washington, USA. 145pp.

Chan, H.M., Kim, C., Khoday, K., Receveur, O. and Kuhnlein, H.V., 1995. Assessment of dietary exposure to trace metals in Baffin Inuit food. Environmental Health Perspectives, 103 (7-8):740-746.

Chan, L., Hall, B., Piron, F., Tandon, R. and Williams, L., 2020. Open Science Beyond Open Access: For and with communities. A step towards the decolonization of knowledge. Prepared for the Canadian Commission for UNESCO's IdeaLab, Ottawa, Canada. 22pp. Available at: https://unescochair-cbrsr.org/wp-content/uploads/2020/07/OS_For_and_With_Communities_EN.pdf

Charette, M.A., Kipp, L.E., Jensen, L.T., Dabrowski, J.S., Whitmore, L.M., Fitzsimmons, J.N., Williford, T., Ulfsbo, A., Jones, E., Bundy, R.M., Vivancos, S.M., Pahnke, K., John, S.G., Xiang, Y., Hatta, M., Petrova, M.V., Heimbürger-Boavida, L.-E., Bauch, D., Newton, R., Pasqualini, A., Agather, A.M., Amon, R.M.W., Anderson, R.F., Andersson, P.S., Benner, R., Bowman, K.L., Edwards, R.L., Gdaniec, S., Gerringa, L.J.A., González, A.G., Granskog, M., Haley, B., Hammerschmidt, C.R., Hansell, D.A., Henderson, P.B., Kadko, D.C., Kaiser, K., Laan, P., Lam, P.J., Lamborg, C.H., Levier, M., Li, X., Margolin, A.R., Measures, C., Middag, R., Millero, F J., Moore, W S., Paffrath, R., Planquette, H., Rabe, B., Reader, H., Rember, R., Rijkenberg, M.J.A., Roy-Barman, M., Rutgers van der Loeff, M., Saito, M., Schauer, U., Schlosser, P., Sherrell, R M., Shiller, A.M., Slagter, H., Sonke, J.E., Stedmon, C., Woosley, R.J., Valk, O., van Ooijen, J. and Zhang, R., 2020. The Transpolar Drift as a source of riverine and shelf-derived trace elements to the central Arctic Ocean. Journal of Geophysical Research: Oceans, 125 (5):e2019JC015920.

Chaulk, A., Stern, G.A., Armstrong, D., Barber, D.G. and Wang, F., 2011. Mercury distribution and transport across the ocean-sea-ice-atmosphere interface in the Arctic Ocean. Environmental Science & Technology, 45 (5):1866-1872.

Chen, L., Liu, M., Fan, R., Ma, S., Xu, Z., Ren, M. and He, Q., 2013. Mercury speciation and emission from municipal solid waste incinerators in the Pearl River Delta, South China. Science of the Total Environment, 447:396-402.

Chen, L., Wang, H.H., Liu, J.F., Tong, Y.D., Ou, L.B., Zhang, W., Hu, D., Chen, C. and Wang, X.J., 2014. Intercontinental transport and deposition patterns of atmospheric mercury from anthropogenic emissions. Atmospheric Chemistry and Physics, 14 (18):10163-10176.

Chen, L., Zhang, Y., Jacob, D.J., Soerensen, A.L., Fisher, J.A., Horowitz, H.M., Corbitt, E.S. and Wang, X., 2015. A decline in Arctic Ocean mercury suggested by differences in decadal trends of atmospheric

mercury between the Arctic and northern midlatitudes. Geophysical Research Letters, 42 (14):6076-6083.

Chen, J., Hintelmann, H., Zheng, W., Feng, X., Cai, H., Wang, Z., Yuan, S. and Wang, Z., 2016. Isotopic evidence for distinct sources of mercury in lake waters and sediments. Chemical Geology, 426:33-44.

Chen, L., Zhang, W., Zhang, Y., Tong, Y., Liu, M., Wang, H., Xie, H. and Wang, X., 2018. Historical and future trends in global source-receptor relationships of mercury. Science of the Total Environment, 610-611:24-31.

Cheng, M,-D. and Schroeder, W.H., 2000. Potential atmospheric transport pathways for mercury measured in the Canadian High Arctic. Journal of Atmospheric Chemistry, 35 (1):101-107.

Chesnokova, A., Baraër, M., Laperrière-Robillard, T. and Huh, K., 2020. Linking mountain glacier retreat and hydrological changes in southwestern Yukon. Water Resources Research, 56 (1):e2019WR025706.

Chételat, J. and Amyot, M., 2009. Elevated methylmercury in High Arctic Daphnia and the role of productivity in controlling their distribution. Global Change Biology, 15 (3):706-718.

Chételat, J., Amyot, M., Cloutier, L. and Poulain, A., 2008. Metamorphosis in chironomids, more than mercury supply, controls methylmercury transfer to fish in High Arctic lakes. Environmental Science & Technology, 42 (24):9110-9115.

Chételat, J., Cloutier, L. and Amyot, M., 2010. Carbon sources for lake food webs in the Canadian High Arctic and other regions of Arctic North America. Polar Biology, 33 (8):1111–1123.

Chételat, J., Amyot, M. and Cloutier, L., 2012. Shifts in elemental composition, methylmercury content and δ15N ratio during growth of a High Arctic copepod. Freshwater Biology, 57 (6):1228-1240.

Chételat, J., Poulain, A.J., Amyot, M., Cloutier, L. and Hintelmann, H., 2014. Ecological determinants of methylmercury bioaccumulation in benthic invertebrates of polar desert lakes. Polar Biology, 37 (12):1785-1796.

Chételat, J., Amyot, M., Arp, P., Blais, J.M., Depew, D., Emmerton, C.A., Evans, M., Gamberg, M., Gantner, N., Girard, C., Graydon, J., Kirk, J., Lean, D., Lehnherr, I., Muir, D., Nasr, M., Poulain, A.J., Power, M., Roach, P., Stern, G., Swanson, H. and van der Velden, S., 2015. Mercury in freshwater ecosystems of the Canadian Arctic: recent advances on its cycling and fate. Science of the Total Environment, 509-510:41-66.

Chételat, J., Amyot, M., Muir, D., Black, J., Richardson, M., Evans, M., and Palmer, M., 2017. Arsenic, antimony, and metal concentrations in water and sediment of Yellowknife Bay. Northwest Territories Geological Survey, NWT Open File 2017-05. 40pp.

Chételat, J., Richardson, M.C., MacMillan, G.A., Amyot, M. and Poulain, A.J., 2018. Ratio of methylmercury to dissolved organic carbon in water explains methylmercury bioaccumulation across a latitudinal gradient from north-temperate to Arctic lakes. Environmental Science & Technology, 52 (1):79-88.

Chételat, J., Ackerman, J.T., Eagles-Smith, C.A. and Hebert, C.E., 2020. Methylmercury exposure in wildlife: a review of the ecological and physiological processes affecting contaminant concentrations and their interpretation. Science of the Total Environment, 711:135117.

Chételat, J., Shao, Y., Richardson, M.C., MacMillan, G.A., Amyot, M., Drevnick, P.E., Gill, H., Köck, G., Muir, D.C.G., 2021. Diet influences on growth and mercury concentrations of two salmonid species from lakes in the eastern Canadian Arctic. Environmental Pollution, 268 (Part B):115820.

Chiarenzelli, J., Aspler, L., Dunn, C., Cousens, B., Ozarko, D. and Powis, K., 2001. Multi-element and rare earth element composition of lichens, mosses, and vascular plants from the Central Barrenlands, Nunavut, Canada. Applied Geochemistry, 16 (2):245-270.

Chiasson-Gould, S.A., Blais, J.M. and Poulain, A.J., 2014. Dissolved Organic Matter Kinetically Controls Mercury Bioavailability to Bacteria. Environmental Science & Technology, 48 (6):3153-3161.

Chipman, M.L., Hudspith, V., Higuera, P.E., Duffy, P.A., Kelly, R., Oswald, W.W. and Hu, F.S., 2015. Spatiotemporal patterns of tundra fires: late-Quaternary charcoal records from Alaska. Biogeosciences, 12 (13):4017-4027.

Choi, A.L., Budtz-Jørgensen, E., Jørgensen, P.J., Steuerwald, U., Debes, F., Weihe, P. and Grandjean, P., 2008. Selenium as a potential protective factor against mercury developmental neurotoxicity. Environmental Research, 107 (1):45-52.

Choi, A.L., Weihe, P., Budtz-Jørgensen, E., Jørgensen, P.J., Salonen, J.T., Tuomainen, T.P., Murata, K., Nielsen, H.P., Petersen, M.S., Askham, J. and Grandjean, P., 2009. Methylmercury exposure and adverse cardiovascular effects in Faroese whaling men. Environmental Health Perspectives, 117 (3):367-372.

Choy, E.S., Gauthier, M., Mallory, M.L., Smol, J.P., Douglas, M.S.V., Lean, D. and Blais, J.M., 2010. An isotopic investigation of mercury accumulation in terrestrial food webs adjacent to an Arctic seabird colony. Science of the Total Environment, 408 (8):1858-1867.

Christensen, J.H., Brandt, J., Frohn, L.M. and Skov, H., 2004. Modelling of mercury in the Arctic with the Danish Eulerian Hemispheric Model. Atmospheric Chemistry and Physics, 4 (9/10):2251-2257.

Christianson, K., Kohler, J., Alley, R.B., Nuth, C. and van Pelt, W.J.J., 2015. Dynamic perennial firn aquifer on an Arctic glacier. Geophysical Research Letters, 42 (5):1418-1426.

Ci, Z., Zhang, X., Yin, Y., Chen, J. and Wang, S., 2016. Mercury redox chemistry in waters of the eastern Asian seas: from polluted coast to clean open ocean. Environmental Science & Technology, 50 (5):2371-2380.

Ciracì, E., Velicogna, I. and Swenson, S., 2020. Continuity of the mass loss of the world's glaciers and ice caps from the GRACE and GRACE follow-on missions. Geophysical Research Letters, 47 (9):e2019GL086926.

Clackett, S.P., Porter, T. J. and Lehnherr, I., 2018. 400-year record of atmospheric mercury from tree-rings in Northwestern Canada. Environmental Science & Technology, 52 (17):9625-9633.

Clarivate Analytics, 2021. Science Citation Index Expanded [database]. Document search using Web of Science and search keywords "Arctic" and "mercury" for the years 2011 to 2020. Available at: www.webofknowledge.com.

Clayden, M.G., Kidd, K.A., Wyn, B., Kirk, J.L., Muir, D.C.G. and O'Driscoll, N.J., 2013. Mercury biomagnification through food webs is affected by physical and chemical characteristics of lakes. Environmental Science & Technology, 47 (21):12047-12053.

Clayden, M.G., Arsenault, L.M., Kidd, K.A., O'Driscoll, N.J. and Mallory, M.L., 2015. Mercury bioaccumulation and biomagnification in a small Arctic polynya ecosystem. Science of the Total Environment, 509-510:206-215.

Cobbett, F.D., Steffen, A., Lawson, G. and Heyst, B.J.V., 2007. GEM fluxes and atmospheric mercury concentrations (GEM, RGM and Hgp) in the Canadian Arctic at Alert, Nunavut, Canada (February–June 2005). Atmospheric Environment, 41 (31):6527-6543.

Cohen, M.D., Draxler, R.R., Artz, R.S., Blanchard, P., Gustin, M.S., Han, Y.-J., Holsen, T.M., Jaffe, D.A., Kelley, P., Lei, H., Loughner, C.P., Luke, W.T., Lyman, S.N., Niemi, D., Pacyna, J.M., Pilote, M., Poissant, L., Ratte, D., Ren, X., Steenhuisen, F., Steffen, A., Tordon, R. and Wilson, S.J., 2016. Modeling the global atmospheric transport and deposition of mercury to the Great Lakes. Elementa: Science of the Anthropocene, 4:000118.

Cole, A.S. and Steffen, A., 2010. Trends in long-term gaseous mercury observations in the Arctic and effects of temperature and other atmospheric conditions. Atmospheric Chemistry and Physics, 10 (10):4661-4672.

Cole, A.S., Steffen, A., Pfaffhuber, K.A., Berg, T., Pilote, M., Poissant, L., Tordon, R. and Hung, H., 2013. Ten-year trends of atmospheric mercury in the High Arctic compared to Canadian Sub-Arctic and mid-latitudes sites. Atmospheric Chemistry and Physics, 13 (3):1535-1545.

Cole, A.S., Steffen, A., Eckley, C.S., Narayan, J., Pilote, M., Tordon, R., Graydon, J.A., St. Louis, V.L., Xu, X. and Branfireun, B.A., 2014. A survey of mercury in air and precipitation across Canada: patterns and trends. Atmosphere, 5 (3):635-668.

Collaud Coen, M., Andrews, E., Bigi, A., Martucci, G., Romanens, G., Vogt, F.P.A. and Vuilleumier, L., 2020. Effects of the prewhitening method, the time granularity, and the time segmentation on the Mann-Kendall trend detection and the associated Sen's slope. Atmospheric Measurement Techniques, 13 (12):6945-6964.

Collins, M., Knutti, R., Arblaster, J., Dufresne, J-L., Fichefet, T., Friedlingstein, P., Gao, X., Gutowski, W.J., Johns, T., Krinner, G., Shongwe, M., Tebaldi, C., Weaver, A.J., Wehner, M., 2013. Long-term climate change: projections, commitments and irreversibility. In: Climate change 2013: the physical science basis. Contribution of Working Group I to the Fifth Assessment Report of the Intergovernmental Panel on Climate Change. Cambridge University Press, Cambridge.

Coogan, S.C.P., Robinne, F.-N., Jain, P. and Flannigan, M.D., 2019. Scientists' warning on wildfire — a Canadian perspective. Canadian Journal of Forest Research, 49 (9):1015-1023.

Cook, J., Edwards, A., Takeuchi, N. and Irvine-Fynn, T., 2016. Cryoconite: the dark biological secret of the cryosphere. Progress in Physical Geography: Earth and Environment, 40 (1):66-111.

Cooke, C.A., Hobbs, W.O., Neal, M. and Wolfe, A.P., 2010. Reliance on ^{210}pb chronology can compromise the inference of preindustrial Hg flux to lake sediments. Environmental Science & Technology, 44 (6):1998-2003.

Cooke, C.A., Wolfe, A.P., Michelutti, N., Balcom, P.H. and Briner, J.P., 2012. A holocene perspective on algal mercury scavenging to sediments of an Arctic lake. Environmental Science & Technology, 46 (13):7135-7141.

COPE, 1984. The Inuvialuit Final Agreement (IFA). Agreement between Committee for Original Peoples' Entitlement (COPE) and the Government of Canada, Ottawa Canada. 162pp.

COPE, 2005. The Inuvialuit Final Agreement (IFA) as Amended: Consolidated version. As agreed between the Committee for Original Peoples' Entitlement (COPE) and the Minister of Indian Affairs and Northern Development. 137pp. Available at: https://irc.inuvialuit.com/sites/default/files/Inuvialuit%20Final%20Agreement%202005.pdf

Coquery, M., Cossa, D. and Martin, J.M., 1995. The distribution of dissolved and particulate mercury in three Siberian estuaries and adjacent Arctic coastal waters. Water, Air, & Soil Pollution, 80:653-664.

Corbitt, E.S., Jacob, D.J., Holmes, C.D., Streets, D.G. and Sunderland, E.M., 2011. Global source-receptor relationships for mercury deposition under present-day and 2050 emissions scenarios. Environmental Science & Technology, 45 (24):10477-10484.

Cory, R.M., Ward, C.P., Crump, B.C. and Kling, G.W., 2014. Sunlight controls water column processing of carbon in Arctic fresh waters. Science, 345 (6199):925-928.

Cossa, D., Averty, B. and Pirrone, N., 2009. The origin of methylmercury in open Mediterranean waters. Limnology and Oceanography, 54 (3):837-844.

Cossa, D., Heimbürger, L.-E., Lannuzel, D., Rintoul, S.R., Butler, E.C.V., Bowie, A.R., Averty, B., Watson, R.J. and Remenyi, T., 2011. Mercury in the Southern Ocean. Geochimica et Cosmochimica Acta, 75 (14):4037-4052.

Cossa, D., Harmelin-Vivien, M., Mellon-Duval, C., Loizeau, V., Averty, B., Crochet, S., Chou, L. and Cadiou, J.-F., 2012. Influences of bioavailability, trophic Position, and growth on methylmercury in hakes (Merluccius merluccius) from northwestern Mediterranean and northeastern Atlantic. Environmental Science & Technology, 46 (9):4885-4893.

Cossa, D., Garnier, C., Buscail, R., Elbaz-Poulichet, F., Mikac, N., Patel-Sorrentino, N., Tessier, E., Rigaud, S., Lenoble, V. and Gobeil, C., 2014. A Michaelis–Menten type equation for describing methylmercury dependence on inorganic mercury in aquatic sediments. Biogeochemistry, 119 (1):35-43.

Cossa, D., Madron, X.D. de, Schäfer, J., Lanceleur, L., Guédron, S., Buscail, R., Thomas, B., Castelle, S. and Naudin, J.-J., 2017. The open sea as the main source of methylmercury in the water column of the Gulf of Lions (Northwestern Mediterranean margin). Geochimica et Cosmochimica Acta, 199:222-237.

Cossa, D., Heimbürger, L.-E., Pérez, F.F., García-Ibáñez, M.I., Sonke, J.E., Planquette, H., Lherminier, P., Boutorh, J., Cheize, M., Menzel Barraqueta, J.-L., Shelley, R. and Sarthou, G., 2018. Mercury distribution and transport in the North Atlantic Ocean along the GEOTRACES-GA01 transect. Biogeosciences, 15 (8):2309-2323.

Cossa, D., Heimbürger, L.-E., Sonke J.E., Planquette, H., Lherminier, P., García-Ibáñez, M.I., Pérez, F.F. and Sarthou, G. 2019. Sources, cycling and transfer of mercury in the Labrador Sea (Geotraces-Geovide cruise). Marine Chemistry, 198:64-69.

Costantini, D., 2014. Oxidative Stress and Hormesis in Evolutionary Ecology and Physiology: A Marriage Between Mechanistic and Evolutionary Approaches. Springer-Verlag Berlin Heidelberg, xvii + 348pp.

Costantini, D., Meillère, A., Carravieri, A., Lecomte, V., Sorci, G., Faivre, B., Weimerskirch, H., Bustamante, P., Labadie, P., Budzinski, H. and Chastel, O., 2014. Oxidative stress in relation to reproduction, contaminants, gender and age in a long-lived seabird. Oecologia, 175 (4):1107-1116.

Cott, P.A., Amos, A.L., Guzzo, M.M., Chavarie, L., Goater, C.P., Muir, D.C.G. and Evans, M.S., 2018. Can traditional methods of selecting food accurately assess fish health? Arctic Science, 4 (2):205-222.

Couture, R.M., de Wit, H.A., Tominaga, K., Kiuru, P. and Markelov, I., 2015. Oxygen dynamics in a boreal lake responds to long-term changes in climate, ice phenology, and DOC inputs. Journal of Geophysical Research: Biogeosciences, 120 (11):2441-2456.

Couture, N.J., Irrgang, A., Pollard, W., Lantuit, H. and Fritz, M., 2018. Coastal erosion of permafrost soils along the Yukon coastal plain and fluxes of organic carbon to the Canadian Beaufort Sea. Journal of Geophysical Research: Biogeosciences, 123 (2):406-422.

Cremer, D., Kraka, E. and Filatov, M., 2008. Bonding in mercury molecules described by the normalized elimination of the small component and coupled cluster theory. ChemPhysChem, 9 (17):2510-2521.

Crête, M., Lefebvre, M.A., Zikovsky, L. and Walsh, P., 1992. Cadmium, lead, mercury and cesium-137 in fruticose lichens of Northern Quebec. Science of the Total Environment, 121:217-230.

Cristol, D.A. and Evers, D.C., 2020. The impact of mercury on North American songbirds: effects, trends, and predictive factors Ecotoxicology, 29 (8):1107-1116.

Cristol, D.A., Brasso, R.L., Condon, A.M., Fovargue, R.E., Friedman, S.L., Hallinger, K.K., Monroe, A.P. and White, A.E., 2008. The movement of aquatic mercury through terrestrial food webs. Science, 320 (5874):335-335.

Curren, M.S., Liang, C.L., Davis, K., Kandola, K., Brewster, J., Potyrala, M. and Chan, H.M., 2015. Assessing determinants of maternal blood concentrations for persistent organic pollutants and metals in the eastern and western Canadian Arctic. Science of the Total Environment, 527-528:150-158.

Custard, K.D., Raso, A.R.W., Shepson, P.B., Staebler, R.M. and Pratt, K.A., 2017. Production and release of molecular bromine and chlorine from the Arctic coastal snowpack, ACS Earth and Space Chemistry, 1 (3):142-151.

Cyr, A., López, J.A., Rea, L., Wooller, M.J., Loomis, T., Mcdermott, S. and O'Hara, T.M., 2019a. Mercury concentrations in marine species from the Aleutian Islands: spatial and biological determinants. Science of the Total Environment, 664:761-770.

Cyr, A.P., López, J.A., Wooller, M.J., Whiting, A., Gerlach, R. and O'Hara, T., 2019b. Ecological drivers of mercury concentrations in fish species in subsistence harvest from Kotzebue Sound, Alaska. Environmental Research, 177:108622.

Czub, G., Wania, F. and McLachlan, M.S., 2008. Combining long-range transport and bioaccumulation considerations to identify potential Arctic contaminants. Environmental Science & Technology, 42 (10):3704-3709.

Dahl, P.P.E. and Hansen, A.M., 2019. Does Indigenous Knowledge occur in and influence impact assessment reports? Exploring consultation remarks in three cases of mining projects in Greenland. Arctic Review on Law and Politics, 10 (165):165-189.

Dahl, P.E. and Tejsner, P., 2020. Review and mapping of Indigenous knowledge concepts in the Arctic. In: Koivurova, T., Broderstad, E.G., Cambou, D., Dorough, D. and Stammler, F. (Eds.). Routledge Handbook on Arctic Indigenous Peoples. pp. 233-248. Routledge.

Dalerum, F., Perbro, A., Magnusdottir, R., Hersteinsson, P. and Angerbjörn, A., 2012. The influence of coastal access on isotope variation in Icelandic Arctic foxes. PLOS ONE, 7 (3):e32071.

Danielsen, F., Burgess, N.D., Jensen, P.M. and Pirhofer-Walzl, K., 2010. Environmental monitoring: the scale and speed of implementation varies according to the degree of peoples involvement. Journal of Applied Ecology, 47 (6):1166-1168.

Danielsen, F., Topp-Jørgensen, E., Levermann, N., Løvstrøm, P., Schiøtz, M., Enghoff, M. and Jakobsen, P., 2014. Counting what counts: using local knowledge to improve Arctic resource management. Polar Geography, 37 (1):69-91.

Dastoor, A.P. and Larocque, Y., 2004. Global circulation of atmospheric mercury: a modelling study. Atmospheric Environment, 38 (1):147-161.

Dastoor, A.P. and Durnford, D.A., 2014. Arctic Ocean: is it a sink or a source of atmospheric mercury? Environmental Science & Technology, 48 (3):1707-1717.

Dastoor, A.P., Davignon, D., Theys, N., Van Roozendael, M., Steffen, A. and Ariya, P.A., 2008. Modeling dynamic exchange of gaseous elemental mercury at polar sunrise. Environmental Science & Technology, 42 (14):5183-5188.

Dastoor, A., Ryzhkov, A., Durnford, D., Lehnherr, I., Steffen, A. and Morrison, H., 2015. Atmospheric mercury in the Canadian Arctic. Part II: Insight from modeling. Science of the Total Environment, 509-510:16-27.

Davini, P., Cagnazzo, C., Gualdi, S. and Navarra, A., 2012. Bidimensional diagnostics, variability and trends of Northern Hemisphere blocking. Journal of Climate, 25 (19):6496-6509.

Davydov, A.N. and Mikhailova, G.V., 2011. Climate change and consequences in the Arctic: perception of climate change by the Nenets people of Vaigach Island. Global Health Action, 4:8436.

Day, R.D., Roseneau, D.G., Berail, S., Hobson, K.A., Donard, O.F.X., Vander Pol, S.S., Pugh, R. S., Moors, A.J., Long, S.E. and Becker, P.R., 2012. Mercury stable isotopes in seabird eggs reflect a gradient from terrestrial geogenic to oceanic mercury reservoirs. Environmental Science & Technology, 46 (10):5327-5335.

de Jong, M.E., Scheiber, I.B.R., van den Brink, N.W., Braun, A., Matson, K.D., Komdeur, J. and Loonen, M.J.J.E., 2017. Indices of stress and immune function in Arctic barnacle goslings (Branta leucopsis) were impacted by social isolation but not a contaminated grazing environment. Science of the Total Environment, 601-602:132-141.

De Simone, F., Gencarelli, C.N., Hedgecock, I.M. and Pirrone, N., 2014. Global atmospheric cycle of mercury: a model study on the impact of oxidation mechanisms. Environmental Science and Pollution Research (International), 21 (6):4110-4123.

De Simone, F., Cinnirella, S., Gencarelli, C.N., Yang, X., Hedgecock, I.M. and Pirrone, N., 2015. Model study of global mercury deposition from biomass burning. Environmental Science & Technology, 49 (11):6712-6721.

De Simone, F., Artaxo, P., Bencardino, M., Cinnirella, S., Carbone, F., D'Amore, F., Dommergue, A., Feng, X.B., Gencarelli, C.N., Hedgecock, I.M., Landis, M.S., Sprovieri, F., Suzuki, N., Wängberg, I. and Pirrone, N., 2017. Particulate-phase mercury emissions from biomass burning and impact on resulting deposition: a modelling assessment. Atmospheric Chemistry and Physics, 17 (3):1881-1899.

de Wit, H.A., Mulder, J., Hindar, A. and Hole, L., 2007. Long-term increase in dissolved organic carbon in streamwaters in Norway is response to reduced acid deposition. Environmental Science & Technology, 41 (22):7706-7713.

de Wit, H.A., Valinia, S., Weyhenmeyer, G.A. Futter, M.N., Kortelainen, P., Austnes, K., Hessen, D.O., Räike, A., Laudon, H. and Vuorenmaa, J., 2016. Current browning of surface waters will be further promoted by wetter climate. Environmental Science & Technology Letters, 12 (3):430-435.

Debes, F., Weihe, P. and Grandjean, P., 2016. Cognitive deficits at age 22 years associated with prenatal exposure to methylmercury. Cortex, 74:358-369.

Deison, R., Smol, J.P., Kokelj, S.V., Pisaric, M.F.J., Kimpe, L.E., Poulain, A.J., Sanei, H., Thienpont, J.R. and Blais, J.M., 2012. Spatial and temporal assessment of mercury and organic matter in thermokarst affected lakes of the Mackenzie Delta uplands, NT, Canada. Environmental Science & Technology, 46 (16):8748-8755.

Delaney, I., Bauder, A., Werder, M.A. and Farinotti, D., 2018. Regional and annual variability in subglacial sediment transport by water for two glaciers in the Swiss Alps. Frontiers in Earth Science, 6:175.

Demers, J.D., Blum, J.D. and Zak, D.R., 2013. Mercury isotopes in a forested ecosystem: implications for air-surface exchange dynamics and the global mercury cycle. Global Biogeochemical Cycles, 27 (1): 222-238. Dibble, T.S., Zelie, M.J. and Mao, H., 2012. Thermodynamics of reactions of ClHg and BrHg radicals with atmospherically abundant free radicals. Atmospheric Chemistry and Physics, 12 (21):10271-10279.

Dene Nation and Assembly of First Nations, 2019. We have always been here. The significance of Dene Knowledge. Dene National/Assembly of First Nations Office, Yellowknife, Northwest Territories, Canada. 34pp. Available on request at: https://denenation.com/

Depew, D.C., Basu, N., Burgess, N.M., Campbell, L.M., Devlin, E.W., Drevnick, P.E., Hammerschmidt, C.R., Murphy, C.A., Sandheinrich, M.B. and Wiener, J.G., 2012. Toxicity of dietary methylmercury to fish: derivation of ecologically meaningful threshold concentrations. Environmental Toxicology and Chemistry, 31 (7):1536-1547.

Depew, D.C., Burgess, N.M., Anderson, M.R., Baker, R., Bhavsar, S.P., Bodaly, R.A. (Drew), Eckley, C.S., Evans, M.S., Gantner, N., Graydon, J.A., Jacobs, K., LeBlanc, J.E., St. Louis, V.L. and Campbell, L.M., 2013. An overview of mercury concentrations in freshwater fish species: a national fish mercury dataset for Canada. Canadian Journal of Fisheries and Aquatic Sciences, 70 (3):436-451.

Derocher, A.E., Lunn, N.J. and Stirling, I., 2004. Polar bears in a warming climate. Integrative and Comparative Biology, 44 (2):163-176.

Déry, S.J., Stahl, K., Moore, R.D., Whitfield, P.H., Menounos, B. and Burford, J.E., 2009. Detection of runoff timing changes in pluvial, nival, and glacial rivers of western Canada. Water Resources Research 45 (4):W04426.

Desforges, J.-P.W., Sonne, C., Levin, M., Siebert, U., Guise, S.D. and Dietz, R., 2016. Immunotoxic effects of environmental pollutants in marine mammals. Environment International, 86:126-139.

Desforges, J.-P., Levin, M., Jasperse, L., De Guise, S., Eulaers, I., Letcher, R.J., Acquarone, M., Nordøy, E., Folkow, L.P., Hammer Jensen, T., Grøndahl, C., Bertelsen, M.F., St. Leger, J., Almunia, J., Sonne, C. and Dietz, R., 2017. Effects of polar bear and killer whale derived contaminant cocktails on marine mammal immunity. Environmental Science & Technology, 51 (19):11431-11439.

Desforges, J.-P., Bandoro, C., Shehata, L., Sonne, C., Dietz, R., Puryear, W.B. and Runstadler, J.A., 2018a. Environmental contaminant mixtures modulate *in vitro* influenza infection. Science of the Total Environment, 634:20-28.

Desforges, J.-P., Jasperse, L., Jensen, T.H., Grøndahl, C., Bertelsen, M.F., Guise, S.D., Sonne, C., Dietz, R. and Levin, M., 2018b. Immune function in Arctic mammals: natural killer (NK) cell-like activity in polar bear, muskox and reindeer. Veterinary Immunology and Immunopathology, 195:72-75.

Desforges, J.-P., Hall, A., McConnell, B., Rosing-Asvid, A., Barber, J.L., Brownlow, A., Guise, S.D., Eulaers, I., Jepson, P.D., Letcher, R.J., Levin, M., Ross, P.S., Samarra, F., Víkingson, G., Sonne, C. and Dietz, R., 2018c. Predicting global killer whale population collapse from PCB pollution. Science, 361 (6409):1373-1376.

Desforges, J.P., Mikkelsen, B., Dam, M., Rigét, F., Sveegaard, S., Sonne, C., Dietz, R. and Basu, N., 2021. Mercury and neurochemical biomarkers in multiple brain regions of five Arctic marine mammals. NeuroToxicology, 84:136-145.

Deutch, B., Dyerberg, J., Pedersen, H.S., Asmund, G., Møller, P. and Hansen, J.C., 2006. Dietary composition and contaminants in North Greenland, in the 1970s and 2004. Science of the Total Environment, 370 (2-3):372-381.

Dibble, T.S., Zelie, M.J. and Mao, H., 2012. Thermodynamics of reactions of ClHg and BrHg radicals with atmospherically abundant free radicals. Atmospheric Chemistry and Physics, 12 (21):17887-17911.

Dibble, T.S., Tetu, H.L., Jiao, Y., Thackray, C.P. and Jacob, D.J, 2020. Modeling the OH-initiated oxidation of mercury in the global atmosphere without violating physical laws. The Journal of Physical Chemistry A, 124 (2):444-453.

Dietz, R., Nielsen, C.O., Hansen, M.M. and Hansen, C.T., 1990. Organic mercury in Greenland birds and mammals. Science of the Total Environment, 95:41-51.

Dietz, R., Pacyna, J., Thomas, D.J., Asmund, G., Gordeev, V., Johansen, P., Kimstach, V., Lockhart, L., Pfirman, S.L., Riget, F.F., Shaw, G., Wagemann, R., White, W., 1998. Chapter 7: Heavy metals. In: AMAP Assessment Report: Arctic Pollution Issues, pp. 373-524. Arctic Monitoring and Assessment Programme (AMAP). Oslo, Norway.

Dietz, R., Riget, F., Cleemann, M., Aarkrog, A., Johansen, P. and Hansen, J.C., 2000a. Comparison of contaminants from different trophic levels and ecosystems. Science of the Total Environment 245 (1):221-232.

Dietz, R., Riget, F. and Born, E.W., 2000b. An assessment of selenium to mercury in Greenland marine animals. Science of the Total Environment, 245:15-24.

Dietz, R., Riget, F. and Born, E.W., 2000c. Geographical differences of zinc, cadmium, mercury and selenium in polar bears (*Ursus maritimus*) from Greenland. Science of the Total Environment, 245 (1):25-47.

Dietz, R., Sonne-Hansen, C., Born, E.W., Sandell, H.T. and Sandell, B., 2001. Forekomst af "afvigende" isbjørne i Østgrønland. Faglig rapport fra DMU, No. 359. 50pp. (Danish Language).

Dietz, R., Born, E.W., Rigét, F., Aubail, A., Sonne, C., Drimmei, R.C. and Basu, N., 2011. Temporal trends and future predictions of mercury concentrations in Northwest Greenland polar bear (*Ursus maritimus*) hair. Environmental Science & Technology, 45 (4):1458-1465.

Dietz, R., Sonne, C., Basu, N., Braune, B., O'Hara, T., Letcher, R.J., Scheuhammer, T., Andersen, M., Andreasen, C., Andriashek, D., Asmund, G., Aubail, A., Baagøe, H., Born, E.W., Chan, H.M., Derocher, A.E., Grandjean, P., Knott, K., Kirkegaard, M., Krey, A., Lunn, N., Messier, F., Obbard, M., Olsen, M.T., Ostertag, S., Peacock, E., Renzoni, A., Rigét, F.F., Skaare, J.U., Stern, G., Stirling, I., Taylor, M., Wiig, Ø., Wilson, S. and Aars, J., 2013. What are the toxicological effects of mercury in Arctic biota? Science of the Total Environment, 443:775-790.

Dietz, R., Gustavson, K., Sonne, C., Desforges, J.-P., Rigét, F.F., Pavlova, V., McKinney, M.A. and Letcher, R.J., 2015. Physiologically-based

pharmacokinetic modelling of immune, reproductive and carcinogenic effects from contaminant exposure in polar bears (*Ursus maritimus*) across the Arctic. Environmental Research, 140:45-55.

Dietz, R., Mosbech, A., Flora, J., Eulaers, I., 2018a. Interactions of climate, socio-economics and global mercury pollution in the North Water region. AMBIO, 47 (2):281-295.

Dietz, R, Desforges, J.-P., Gustavson, K., Sonne, C., Rigét, F.F., Born, E.W. and Letcher, R.J., 2018b. Immunologic, reproductive, and carcinogenic risk assessment in East Greenland polar bears (*Ursus maritimus*) during 1983-2013. Environment International 118:169-178.

Dietz, R., Eulaers, I., Søndergaard, J. and Sonne, C., 2018c. Mercury Exposure in three Greenlandic societies (MEREX-1). Report to DANCEA: 56pp.

Dietz, R., Letcher, R.J., Desforges, J.-P., Eulaers, I., Sonne, C., Wilson, S., Andersen-Ranberg, E., Basu, N., Barst, B.D., Bustnes, J.O., Bytingsvik, J., Ciesielski, T.M., Drevnick, P.E., Gabrielsen, G.W., Haarr, A., Hylland, K., Jenssen, B.M., Levin, M., McKinney, M.A., Nørregaard, R.D., Pedersen, K.E., Provencher, J., Styrishave, B., Tartu, S., Aars, J., Ackerman, J.T., Rosing-Asvid, A., Barrett, R., Bignert, A., Born, E.W., Branigan, M., Braune, B., Bryan, C.E., Dam, M., Eagles-Smith, C.A., Evans, M., Evans, T.J., Fisk, A.T., Gamberg, M., Gustavson, K., Hartman, C.A., Helander, B., Herzog, M.P., Hoekstra, P.F., Houde, M., Hoydal, K., Jackson, A.K., Kucklick, J., Lie, E., Loseto, L., Mallory, M.L., Miljeteig, C., Mosbech, A., Muir, D.C.G., Nielsen, S.T., Peacock, E., Pedro, S., Peterson, S.H., Polder, A., Rigét, F.F., Roach, P., Saunes, H., Sinding, M.-H.S., Skaare, J.U., Søndergaard, J., Stenson, G., Stern, G., Treu, G., Schuur, S.S., Víkingsson, G., 2019a. Current state of knowledge on biological effects from contaminants on arctic wildlife and fish. Science of the Total Environment, 696: 133792.

Dietz, R., Sonne, C., Desforges, J.-P., Eulaers, I., Letcher, R.J. and Jepson, P.D., 2019b. Killer whales call for further protection. Environment International, 126:443-444.

Dietz, R., Fort, J., Sonne, C., Albert, C., Bustnes, J.O., Christensen, T.K., Ciesielski, T.M., Danielsen, J., Dastnai, S., Eens, M., Erikstad, K.E., Galatius, A., Garbus, S.-E., Gilg, O., Hanssen, S.A., Helander, B., Helberg, M., Jaspers, V.L.B., Jenssen, B.M., Jónsson, J.E., Kauhala, K., Kolbeinsson, Y., Kyhn, L.A., Labansen, A.L., Larsen, M.M., Lindstøm, U., Reiertsen, T.K., Rigét, F.F., Roos, A., Strand, J., Strøm, H., Sveegaard, S., Søndergaard, J., Sun, J., Teilmann, J., Therkildsen, O.R., Thórarinsson, T.L., Tjørnløv, R.S., Wilson, S. and Eulaers, I., 2021. A risk assessment of the effects of mercury on Baltic Sea, Greater North Sea and North Atlantic wildlife, fish and bivalves. Environment International, 146:106178.

Dillon, T., Beckvar, N. and Kern, J., 2010. Residue-based mercury dose–response in fish: an analysis using lethality-equivalent test endpoints. Environmental Toxicology and Chemistry, 29 (11):2559-2565.

DiMento, B.P. and Mason, R.P., 2017. Factors controlling the photochemical degradation of methylmercury in coastal and oceanic waters. Marine Chemistry, 196:116-125.

DiMento, B.P., Mason, R.P., Brook, S. and Moore, C., 2019. The impact of sea ice on the air-sea exchange of mercury in the Arctic Ocean. Deep Sea Research Part I: Oceanographic Research Papers, 144:28-38.

Divoky, G.J., Lukacs, P.M. and Druckenmiller, M.L., 2015. Effects of recent decreases in Arctic sea ice on an ice-associated marine bird. Progress in Oceanography, 136:151-161.

Divoky, G.J., Douglas, D.C. and Stenhouse, I.J., 2016. Arctic sea ice a major determinant in Mandt's black guillemot movement and distribution during non-breeding season. Biology Letters, 12 (9):20160275.

Dobricic, S., Vignati, E. and Russo, S., 2016. Large-scale atmospheric warming in winter and the Arctic sea ice retreat. Journal of Climate, 29 (8):2869-2888.

Domagalski, J., Majewski, M.S., Alpers, C.N., Eckley, C.S., Eagles-Smith, C.A., Schenk, L. and Wherry, S., 2016. Comparison of mercury mass loading in streams to atmospheric deposition in watersheds of Western North America: evidence for non-atmospheric mercury sources. Science of the Total Environment, 568:638-650.

Dommergue, A., Ferrari, C. P., Gauchard, P.-A., Boutron, C. F., Poissant, L., Pilote, M., Jitaru, P. and Adams, F., 2003. The fate of mercury species in a sub-arctic snowpack during snowmelt. Geophysical Research Letters, 30 (12):1621.

Dommergue A., Larose, C., Faïn, X., Clarisse, O., Foucher, D., Hintelmann, H., Schneider, D. and Ferrari, C.P., 2010, Environmental Science & Technology, 44 (3):901-907.

Donohoue, D.L., Bauer, D., Cossairt, B. and Hynes, A.J., 2006. Temperature and pressure dependent rate coefficients for the reaction of Hg with Br and the reaction of Br with Br: a pulsed laser photolysis-pulsed laser induced fluorescence study. Journal of Physical Chemistry A, 110 (21):6623-6632.

Douglas, T. and Sturm, M., 2004. Arctic haze, mercury and the chemical composition of snow across northwestern Alaska. Atmospheric Environment, 38 (6):805-820.

Douglas, T.A. and Blum, J.D., 2019. Mercury isotopes reveal atmospheric gaseous mercury deposition directly to the Arctic coastal snowpack. Environmental Science & Technology Letters, 6 (4):235-242.

Douglas, T.A., Sturm, M., Simpson, W.R., Brooks, S., Lindberg, S.E. and Perovich, D.K., 2005. Elevated mercury measured in snow and frost flowers near Arctic sea ice leads. Geophysical Research Letters, 32 (4):L04502.

Douglas, T.A., Sturm, M., Simpson, W.R., Blum, J.D., Alvarez-Aviles, L., Keeler, G.J., Perovich, D.K., Biswas, A. and Johnson, K., 2008. Influence of snow and ice crystal formation and accumulation on mercury deposition to the Arctic. Environmental Science & Technology, 42 (5):1542-1551.

Douglas, T.A., Loseto, L.L., Macdonald, R.W., Outridge, P., Dommergue, A., Poulain, A., Amyot, M., Barkay, T., Berg, T., Chételat, J., Constant, P., Evans, M., Ferrari, C., Gantner, N., Johnson, M.S., Kirk, J., Kroer, N., Larose, C., Lean, D., Nielsen, T.G., Poissant, L., Rognerud, S., Skov, H., Sørensen, S., Wang, F.Y., Wilson, S. and Zdanowicz, C.M., 2012. The fate of mercury in Arctic terrestrial and aquatic ecosystems, a review. Environmental Chemistry, 9 (4):321-355.

Douglas, T.A., Sturm, M., Blum, J.D., Polashenski, C., Stuefer, S., Hiemstra, C., Steffen, A., Filhol, S. and Prevost, R., 2017. A pulse of mercury and major ions in snowmelt runoff from a small Arctic Alaska watershed. Environmental Science & Technology, 51 (19):11145-11155.

Downie, D.L. and Fenge, T. (Eds.), 2003. Northern Lights Against POPs. Published for the Inuit Circumpolar Conference (ICC) by McGill-Queens University Press. 347pp.

Drbal, K., Elster, J. and Komarek, J., 1992. Heavy metals in water, ice and biological material from Spitsbergen, Svalbard. Polar Research, 11 (2):99-101.

Drevnick, P.E. and Sandheinrich, M.B., 2003. Effects of dietary methylmercury on reproductive endocrinology of fathead minnows. Environmental Science & Technology, 37 (19):4390-4396.

Drevnick, P.E., Sandheinrich, M.B. and Oris, J.T., 2006. Increased ovarian follicular apoptosis in fathead minnows (*Pimephales promelas*) exposed to dietary methylmercury. Aquatic Toxicology, 79 (1):49-54.

Drevnick, P.E., Yang, H., Lamborg, C.H. and Rose, N.L., 2012. Net atmospheric mercury deposition to Svalbard: estimates from lacustrine sediments. Atmospheric Environment, 59:509-513.

Drevnick, P.E., Cooke, C.A., Barraza, D., Blais, J.M., Coale, K.H., Cumming, B.F., Curtis, C.J., Das, B., Donahue, W.F., Eagles-Smith, C.A., Engstrom, D.R., Fitzgerald, W.F., Furl, C.V., Gray, J.E., Hall, R.I., Jackson, T.A., Laird, K.R., Lockhart, W.L., Macdonald, R.W., Mast, M.A., Mathieu, C., Muir, D.C.G., Outridge, P.M., Reinemann, S.A., Rothenberg, S.E., Ruiz-Fernández, A.C., St. Louis, V.L., Sanders, R.D., Sanei, H., Skierszkan, E.K., Van Metre, P.C., Veverica, T.J., Wiklund, J.A. and Wolfe, B.B., 2016. Spatiotemporal patterns of mercury accumulation in lake sediments of western North America. Science of the Total Environment, 568:1157-1170.

Driscoll, C.T., Yan, C., Schofield, C.L., Munson, R. and Holsapple, J., 1994. The mercury cycle and fish in the Adirondack lakes. Environmental Science & Technology, 28 (3):136A-143A.

Drost, H.E., Carmack, E.C. and Farrell, A.P., 2014. Upper thermal limits of cardiac function for Arctic cod *Boreogadus saida*, a key food web fish species in the Arctic Ocean. Journal of Fish Biology, 84 (6):1781-1792.

Drott, A., Lambertsson, L., Björn, E. and Skyllberg, U., 2007. Importance of dissolved neutral mercury sulfides for methyl mercury production in contaminated sediments. Environmental Science & Technology, 41 (7):2270-2276.

Drysdale, M., Ratelle, M., Skinner, K., Garcia-Barrios, J., Gamberg, M., Williams, M., Majowicz, S., Bouchard, M., Stark, K., Chalil, D. and Laird, B.D., 2021. Human biomonitoring results of contaminant and nutrient biomarkers in Old Crow, Yukon, Canada. Science of the Total Environment, 760:143339.

Durkalec, A., Sheldon, T. and Bell, T. (Eds.), 2016a. Lake Melville: Avativut, Kanuittailinnivut (Our Environment, Our Health). Scientific Report. Nunatsiavut Government and Nain Research Centre, Nain, Newfoundland, Canada. 98pp.

Durkalec, A., Sheldon, T. and Bell, T. (Eds.), 2016b. Lake Melville: Avativut, Kanuittailinnivut (Our Environment, Our Health). Summary for

policymakers. Nunatsiavut Government, Nain, Newfoundland, Canada. 36pp.

Durner, G.M., Douglas, D.C., Albeke, S.E., Whiteman, J.P., Amstrup, S.C., Richardson, E., Wilson, R.R. and Ben-David, M., 2017. Increased Arctic sea ice drift alters adult female polar bear movements and energetics. Global Change Biology, 23 (9):3460-3473.

Durnford, D. and Dastoor, A., 2011. The behavior of mercury in the cryosphere: a review of what we know from observations. Journal of Geophysical Research: Atmospheres, 116 (D6):D06305.

Durnford, D., Dastoor, A., Figueras-Nieto, D. and Ryjkov, A., 2010. Long range transport of mercury to the Arctic and across Canada. Atmospheric Chemistry and Physics, 10 (13):6063-6086.

Durnford, D., Dastoor, A., Ryzhkov, A., Poissant, L., Pilote, M. and Figueras-Nieto, D., 2012. How relevant is the deposition of mercury onto snowpacks? – Part 2: A modeling study. Atmospheric Chemistry and Physics, 12 (19):9251-9274.

Eagles-Smith, C.A., Ackerman, J.T., Adelsbach, T.L., Takekawa, J.Y., Miles, A.K. and Keister, R.A., 2008. Mercury correlations among six tissues for four waterbird species breeding in San Francisco Bay, California, USA. Environmental Toxicology and Chemistry, 27 (10):2136-2153.

Eagles-Smith, C.A., Ackerman, J.T., Willacker, J.J., Tate, M.T., Lutz, M.A., Fleck, J.A., Stewart, A.R., Wiener, J.G., Evers, D.C., Lepak, J.M., Davis, J.A. and Pritz, C.F., 2016. Spatial and temporal patterns of mercury concentrations in freshwater fish across the Western United States and Canada. Science of the Total Environment, 568:1171-1184.

Eagles-Smith, C.A., Silbergeld, E.K., Basu, N., Bustamante, P., Diaz-Barriga, F., Hopkins, W.A., Kidd, K.A. and Nyland, J.F., 2018. Modulators of mercury risk to wildlife and humans in the context of rapid global change. Ambio, 47 (2):170-197.

Eastman, R. and Warren, S.G., 2010. Arctic cloud changes from surface and satellite observations. Journal of Climate, 23 (15):4233-4242.

Ebinghaus, R., Kock, H.H., Coggins, A.M., Spain, T.G., Jennings, S.G. and Temme, C., 2002a. Long-term measurements of atmospheric mercury at Mace Head, Irish west coast, between 1995 and 2001. Atmospheric Environment, 36 (34):5267-5276.

Ebinghaus, R., Kock, H.H., Temme, C., Einax, J.W., Löwe, A.G., Richter, A., Burrows, J.P. and Schroeder, W.H., 2002b. Antarctic springtime depletion of atmospheric mercury. Environmental Science & Technology, 36 (6):1238-1244.

ECCC, 2016. Canadian Mercury Science Assessment Report. Environment and Climate Change Canada (ECCC), Gatineau, Canada. 793pp. Available at: https://mspace.lib.umanitoba.ca/xmlui/handle/1993/32129

Eccles, K.M., Majeed, H., Porter, T.J. and Lehnherr, I., 2020. A continental and marine-influenced tree-ring mercury record in the Old Crow Flats, Yukon, Canada. ACS Earth and Space Chemistry, 4 (8):1281-1290.

Eckbo, N., Le Bohec, C., Planas-Bielsa, V., Warner, N.A., Schull, Q., Herzke, D., Zahn, S., Haarr, A., Gabrielsen, G.W. and Borgå, K., 2019. Individual variability in contaminants and physiological status in a resident Arctic seabird species. Environmental Pollution, 249:191-199.

Eckhardt, S., Stohl, A., Beirle, S., Spichtinger, N., James, P., Forster, C., Junker, C., Wagner, T., Platt, U. and Jennings, S.G., 2003. The North Atlantic Oscillation controls air pollution transport to the Arctic. Atmospheric Chemistry and Physics, 3 (5):1769-1778.

Eckley, C.S., Watras, C.J., Hintelmann, H., Morrison, K., Kent, A.D. and Regnell, O., 2005. Mercury methylation in the hypolimnetic waters of lakes with and without connection to wetlands in northern Wisconsin. Canadian Journal of Fisheries and Aquatic Sciences, 62 (2):400-411.

Eckley, C.S., Gustin, M., Lin, C.J., Li, X. and Miller, M.B., 2010. The influence of dynamic chamber design and operating parameters on calculated surface-to-air mercury fluxes. Atmospheric Environment, 44 (2):194-203.

EEA, 2018. Mercury in Europe's environment. A priority for European and global action (EEA Report No. 11/2018). European Environment Agency (EEA), Copenhagen, Denmark. 72pp. Available at: https://www.eea.europa.eu/publications/mercury-in-europe-s-environment/at_download/file#:~:text=The%20maximum%20safe%20mercury%20content,swordfish%20(EU%2C%202006).&text=In%20Europe%2C%20the%20highest%20concentrations,et%20al.%2C%202014)

Egeland, G.M. 2010. Inuit Health Survey 2007-2008 Nunatsiavut. International Polar Year Inuit Health Survey: Health in Transition and Resiliency. McGill University (Macdonald Campus), Quebec, Canada. 36pp. Available at: https://www.mcgill.ca/cine/files/cine/adult_report_-_nunatsiavut.pdf

Egeland, G.M., Pacey, A., Cao, Z. and Sobol, I., 2010. Food insecurity among Inuit preschoolers: Nunavut Inuit Child Health Survey, 2007-2008. Canadian Medical Association Journal, 182 (3):243-248.

Egevang, C., Stenhouse, I.J., Phillips, R.A., Petersen, A., Fox, J.W. and Silk, J.R.D., 2010. Tracking of Arctic terns Sterna paradisaea reveals longest animal migration. Proceedings of the National Academy of Sciences, 107 (5):2078-2081.

Ehrich, D., Ims, R., Yoccoz, N. G., Lecomte, N., Killengreen, S.T., Fuglei, E., Rodnikova, A.Y., Ebbinge, B.S., Menyushina, I.E., Nolet, B.A., Pokrovsky, I.G., Popov, I.Y., Schmidt, N.M., Sokolov, A.A., Sokolva, N.A. and Sokolov, V.A., 2015. What can stable isotope analysis of top predator tissues contribute to monitoring of tundra ecosystems? Ecosystems, 18 (3):404-416.

Ehrich, D., Schmidt, N.M., Gauthier, G., Alisauskas, R., Angerbjörn, A., Clark, K., Eide, N., Framstad, E., Frandsen, J., Franke, A., Gilg, O., Giroux, M.-A., Henttonen, H., Hörnfeldt, B., Ims, R.A., Kataev, G.D., Kharitonov, S.P., Killengreen, S.T., Krebs, C.J., Lanctot, R.B., Lecomte, N., Menyushina, I.E., Morris, D.W., Morrisson, G., Oksanen, L., Oksanen, T., Olofsson, L., Pokrovsky, I. J., Popov, I.Y., Reid, D., Roth, J.D., Saalfeld, S.T., Samelius, G., Sittler, B., Sleptsov, S.M., Smith, P.A., Sokolov, A.A., Sokolova, N.A., Soloviev, M.Y. and Solovyeva, D.V., 2020. Documenting lemming population change in the Arctic: can we detect trends? Ambio, 49 (3):786-800.

Eide, N.E., Eid, P.M., Prestrud, P. and Swenson, J.E., 2005. Dietary responses of Arctic foxes *Alopex lagopus* to changing prey availability across an Arctic landscape. Wildlife Biology, 11 (2):109-121.

Eisner, L., Hillgruber, N., Martinson, E. and Maselko, J., 2013. Pelagic fish and zooplankton species assemblages in relation to water mass characteristics in the northern bering and southeast Chukchi seas. Polar Biology 36, 87–113.

Eisner, L.B., Gann, J.C., Ladd, C., Cieciel, K.D. and Mordy, C.W., 2016. Late summer/early fall phytoplankton biomass (chlorophyll a) in the eastern Bering Sea: Spatial and temporal variations and factors affecting chlorophyll a concentrations. Deep Sea Research Part II: Topical Studies in Oceanography, 134:100-114.

Eklöf, K., Lidskog, R. and Bishop, K., 2016. Managing Swedish forestry's impact on mercury in fish: defining the impact and mitigation measures. Ambio, 45 (S2):163-174.

Elliott, K.H. and Elliott, J.E., 2016. Origin of sulfur in diet drives spatial and temporal mercury trends in seabird eggs from Pacific Canada 1968-2015. Environmental Science & Technology, 50 (24):13380-13386.

Elliott, K., Fernie, K.J., Braune, B., Letcher, R.J. and Head, J., 2019. Climate change, contaminants, ecotoxicology: Interactions in Arctic seabirds at their southern range limits (2016-2018). ants Program. Indigenous and Northern Affairs Canada. 15pp.

Elmendorf, S.C., Henry G.H., Hollister, R.D., Björk, R.G., Bjorkman, A.D, Callaghan, T.V., Collier, L.S., Cooper, E.J., Cornelissen, J.H.C., Day, T.A., Fosaa, A.M., Gould, W.A., Grétarsdóttir, J., Harte, J., Hermanutz, L., Hik, D.S., Hofgaard, A., Jarrad, F., Jónsdóttir, I.S., Keuper, F., Klanderud, K., Klein, J.A., Koh, S., Kudo, G., Lang, S.I., Loewen, V., May, J.L., Mercado, J., Michelsen, A., Molau, U., Myers-Smith, I.H., Oberbauer, S.F., Pieper, S., Post, E., Rixen, C., Robinson, C.H., Schmidt, N.M., Shaver, G.R., Stenström, A., Tolvanen, A., Totland, O., Troxler, T., Wahren, C.-H., Webber, P.J., Welker, J.W. and Wookey, P.A., 2012. Global assessment of experimental climate warming on tundra vegetation: heterogeneity over space and time. Ecology Letters, 15 (2):164-175.

ELOKA and Snowchange, 2020. Online Atlas of the Evenki of Iyengra, version 2.0. Exchange for Local Observations and Knowledge of the Arctic (ELOKA) and Snowchange Cooperative. Available at: www.evenki-atlas.org.

Eloranta, A.P., Kahilainen, K.K., Amundsen, P.-A., Knudsen, R., Harrod, C. and Jones, R.I., 2015. Lake size and fish diversity determine resource use and trophic position of a top predator in high-latitude lakes. Ecology and Evolution, 5 (8):1664-1675.

Emmerton, C.A., Graydon, J.A., Gareis, J.A.L., St. Louis, V.L., Lesack, L.F.W., Banack, J.K.A., Hicks, F. and Nafziger, J., 2013. Mercury export to the Arctic Ocean from the Mackenzie River, Canada. Environmental Science & Technology, 47 (14):7644-7654.

Enrico, M., Roux, G.L., Marusczak, N., Heimbürger, L.-E., Claustres, A., Fu, X., Sun, R. and Sonke, J.E., 2016. Atmospheric Mercury transfer to peat bogs dominated by gaseous elemental mercury dry deposition. Environmental Science & Technology, 50 (5):2405-2412.

ENVIRON, 2011. User's Guide, Comprehensive Air Quality Model with Extensions (CAMx), Version 5.40. Environ International Corporation, California, USA. 306pp.

Erikstad, K.E., Sandvik, H., Reiertsen, T.K., Bustnes, J.O. and Strøm H. 2013. Persistent organic pollution in a high-Arctic top predator: sex-dependent thresholds in adult survival. Proceedings of the Royal Society B, 280 (1769):20131483.

Ernakovich, J.G., Hopping, K.A., Berdanier, A.B., Simpson, R.T., Kachergis, E.J., Steltzer, H. and Wallenstein, M.D., 2014. Predicted responses of Arctic and alpine ecosystems to altered seasonality under climate change. Global Change Biology, 20 (10):3256-3269.

Evangeliou, N., Balkanski, Y., Hao, W.M., Petkov, A., Silverstein, R.P., Corley, R., Nordgren, B.L., Urbanski, S.P., Eckhardt, S., Stohl, A., Tunved, P., Crepinsek, S., Jefferson, A., Sharma, S., Nøjgaard, J.K. and Skov, H., 2016. Wildfires in northern Eurasia affect the budget of black carbon in the Arctic - a 12-year retrospective synopsis (2002-2013). Atmospheric Chemistry and Physics 16 (12):7587-7604.

Evans, M., and Landels, S., 2015. Radionuclide and metal analysis of fish muscle from Stark Lake, NWT. Phase III Environmental site assessment for uranium exploration site at Regina Bay, Stark Lake, NWT. Report submitted to Aboriginal Affairs and Northern Development Canada. 18pp.

Evans, M. and Muir, D.C.G., 2021a. Temporal trends and spatial variations of mercury in sea-run Arctic char from Cambridge Bay, Nunavut. In: Beardsall, A. and Morris, A.D. (Eds.). Synopsis of Research Conducted under the 2017-2018 Northern Contaminants Program, pp. 213-221. Crown-Indigenous Relations and Northern Affairs Canada, Gatineau, QC, Canada. Available at: https://pubs.aina.ucalgary.ca/ncp/Synopsis20172018.pdf

Evans, M., and Muir, D.C.G. 2021b. Spatial and long-term trends in persistent organic contaminants and metals in lake trout and burbot from the Northwest Territories. In: Beardsall, A., and Morris, A.D. (Eds). Synopsis of Research Conducted under the 2017-2018 Northern Contaminants Program, pp. 231-244. Crown-Indigenous Relations and Northern Affairs Canada, Gatineau, QC, Canada. Available at: https://pubs.aina.ucalgary.ca/ncp/Synopsis20172018.pdf

Evans, M.S., Klaverkamp, J.F. and Lockhart, L., 1998. Metal studies of water, sediments and fish from the Resolution Bay area of Great Slave Lake: studies related to the decommissioned Pine Point mine. Contribution Series No. 98-87. National Water Research Institute (NWRI), Environment Canada. 209pp.

Evans, M.S., Lockhart, W.L., Doetzel, L., Low, G., Muir, D., Kidd, K., Stephens, G. and Delaronde, J., 2005a. Elevated mercury concentrations in fish in lakes in the Mackenzie River Basin: The role of physical, chemical, and biological factors. Science of the Total Environment, 351-352:479-500.

Evans, M.S., Muir, D., Lockhart, W.L., Stern, G., Ryan, M. and Roach, P., 2005b. Persistent organic pollutants and metals in the freshwater biota of the Canadian Subarctic and Arctic: an overview. Science of the Total Environment, 351-352:94-147.

Evans, C.D., Jones, T.G., Burden, A., Ostle, N., Zielinski, P., Cooper, M.D.A., Peacock, M., Clark, J.M., Oulehle, F.,Cooper, D. and Freeman, F., 2012. Acidity controls on dissolved organic carbon mobility in organic soils. Global Change Biology, 18 (11):3317-3331.

Evans, M., Muir, D., Brua, R.B., Keating, J. and Wang, X., 2013. Mercury trends in predatory fish in Great Slave Lake: the Influence of temperature and other climate drivers. Environmental Science & Technology, 47 (22):12793-12801.

Evans, M.S., Muir, D.C.G., Keating, J. and Wang, X., 2015. Anadromous char as an alternate food choice to marine animals: A synthesis of Hg concentrations, population features and other influencing factors. Science of the Total Environment, 509-510:175-194.

Evans, S.G., Godsey, S.E., Rushlow, C.R. and Voss, C., 2020a. Water tracks enhance water flow above permafrost in upland Arctic Alaska hillslopes. Journal of Geophysical Research: Earth Surface, 125 (2):e2019JF005256.

Evans, S.G., Yokeley, B., Stephens, C. and Brewer, B., 2020b. Potential mechanistic causes of increased baseflow across northern Eurasia catchments underlain by permafrost. Hydrological Processes, 34 (11):2676-2690.

Evers, D.C., Kaplan, J.D., Meyer, M.W., Reaman, P.S., Braselton, W.E., Major, A., Burgess, N. and Scheuhammer, A.M., 1998. Geographic trend in mercury measured in common loon feathers and blood. Environmental Toxicology and Chemistry, 17 (2):173-183.

Evers, D.C., Savoy, L.J., DeSorbo, C.R., Yates, D.E., Hanson, W., Taylor, K.M., Siegel, L.S., Cooley, J.H., Bank, M.S., Major, A., Munney, K., Mower, B.F., Vogel, H.S., Schoch, N., Pokras, M., Goodale, M.W. and Fair, J., 2008. Adverse effects from environmental mercury loads on breeding common loons. Ecotoxicology, 17, 69-81.

Evers, D.C., Schmutz, J.A., Basu, N., DeSorbo, C.R., Fair, J., Gray, C.E.,. Paruk, J.D., Perkins, M., Regan, K., Uher-Koch, B.D. and Wright, K.G., 2014. Historic and contemporary mercury exposure and potential risk to yellow-billed loons (*Gavia adamsii*) breeding in Alaska and Canada. Waterbirds, 37 (sp1):147-159.

Evers, D.C., Keane, S.E., Basu, N. and Buck, D., 2016. Evaluating the effectiveness of the Minamata Convention on Mercury: principles and recommendations for next steps. Science of the Total Environment, 569-570:888-903.

Evers, D., Ackerman, J., Åkerblom, S., Bally, D., Basu, N., Blum, J., Bodin, N., Buck, D., Bustamante, P., Chen, C., Chetelat, J., Costa, M., Dietz, R., Drevnick, P., Eagles-Smith, C., Kim, Y., Lailson, J., Pereira, D.H.C., Rigét, F., Brianza, C.R., Sunderland, E., Takeuchi, A., Umpiérrez, E., Braaten, H.F.V., Wilson, S. and De Wit, H., 2019. Chapter 7: Mercury concentrations in biota. In: AMAP/UN Environment (Eds.). Technical Background Report for the Global Mercury Assessment 2018. Arctic Monitoring and Assessment Programme (AMAP), Oslo, Norway/UN Environment Programme, Chemicals and Health Branch, Geneva Switzerland.

Ewald, J.D., Kirk, J.L., Li, M. and Sunderland, E.M., 2016. Organ-specific differences in mercury speciation and accumulation across ringed seal (*Phoca hispida*) life stages. Science of the Total Environment, 650 (Part 2):2013-2020.

Eyrikh, S., Eichler, A., Tobler, L., Malygina, N., Papina, T. and Schwikowski, M., 2017. A 320 year ice-core record of atmospheric Hg pollution in the Altai, Central Asia. Environmental Science & Technology, 51 (20):11597-11606.

Fahnestock, M.F., Bryce, J.G., McCalley, C.K., Montesdeoca, M., Bai, S., Li, Y., Driscoll, C.T., Crill, P.M., Rich, V.I. and Varner, R.K., 2019. Mercury reallocation in thawing Subarctic peatlands. Geochemical Perspectives Letters, 11:33-38.

Faïn, X., Ferrari, C.P., Gauchard, P., Magand, O. and Boutron, C., 2006. Fast depletion of gaseous elemental mercury in the Kongsvegen Glacier snowpack in Svalbard. Geophysical Research Letters, 33 (6):L06826.

Faïn, X., Ferrari, C.P., Dommergue, A., Albert, M.R., Battle, M., Severinhaus, J., Arnaud, L., Barnola, J.-M., Cairns, W., Barbante, C. and Boutron, C., 2009. Polar firn air reveals large-scale impact of anthropogenic mercury emissions during the 1970s. Proceedings of the National Academy of Sciences of the United States of America, 106 (38):16114-16119.

Fallacara, D.M., Halbrook, R.S. and French, J.B., 2011. Toxic effects of dietary methylmercury on immune function and hematology in American kestrels (*Falco sparverius*). Environmental Toxicology and Chemistry, 30 (6):1320-1327.

Fant, M.L., Nyman, M., Helle, E. and Rudback, E., 2001. Mercury, cadmium, lead and selenium in ringed seals (*Phoca hispida*) from the Baltic Sea and from Svalbard. Environmental Pollution, 111 (3):493-501.

FAO/WHO, 2000a. Safety evaluation of certain food additives and contaminants. Prepared by the fifty-third meeting of the Joint Food Agriculture Organization of the United Nations (FAO) and World Health Organization (WHO) Expert Committee on Food Additives (JECFA). WHO Food Additives Series: 44. Geneva, Switzerland. Available at: http://www.inchem.org/documents/jecfa/jecmono/v44jec01.htm

FAO/WHO, 2020b. Discussion paper of maximum levels for methylmercury in additional fish species, (CX/CF 20/14/11). Joint Food Agriculture Organization of the United Nations and World Health Organization Food Standards programme codex committee on contaminants in foods. 20th-24th April 2020, Utrecht, The Netherlands. 37pp. Available at: http://www.fao.org/fao-who-codexalimentarius/sh-proxy/fr/?lnk=1&url=https%253A%252F%252Fworkspace.fao.org%252Fsites%252Fcodex%252FMeetings%252FCX-735-14%252FWD-2020%252Fcf14_11e.pdf

FAO, IFAD, UNICEF, WFP and WHO, 2019. The State of Food Security and Nutrition in the World 2019. Safeguarding against economic slowdowns and downturns. Food and Agriculture Organization of the United Nations (FAO), Rome, Italy. xxi + 214pp. Available at: http://www.fao.org/3/ca5162en/ca5162en.pdf

Farinotti, D., Huss, M., Fürst, J.J., Landmann, J., Machguth, H., Maussion, F. and Pandit, A., 2019. A consensus estimate for the ice thickness distribution of all glaciers on Earth. Nature Geoscience, 12:168-173.

Feldmann, J., Bluemlein, K., Krupp, E.M., Mueller, M. and Wood, B.A., 2018. Metallomics study in plants exposed to arsenic, mercury, selenium and sulphur. In: Arruda M. (Ed.). Advances in Experimental Medicine and Biology, pp. 67-100. Springer, Cham.

Feldstein, S.B., 2002. Fundamental mechanisms of the growth and decay of the PNA teleconnection pattern. Quarterly Journal of the Royal Meteorological Society, 128 (581):775-796.

Fenstad, A.A., Bustnes, J.O., Bingham, C.G., Öst, M., Jaatinen, K., Moe, B., Hanssen, S.A., Moody, A.J., Gabrielsen, K.M., Herzke, D., Lierhagen, S., Jenssen, B.M. and Krøkje, Å., 2016a. DNA double-strand breaks in incubating female common eiders (*Somateria mollissima*): comparison between a low and a high polluted area. Environmental Research, 151:297-303.

Fenstad, A.A., Moody, A.J., Öst, M., Jaatinen, K., Bustnes, J.O., Moe, B., Hanssen, S.A., Gabrielsen, K.M., Herzke, D., Lierhagen, S., Jenssen, B.M. and Krøkje, Å., 2016b. Antioxidant responses in relation to persistent organic pollutants and metals in a low- and a high-exposure population of seabirds. Environmental Science & Technology, 50 (9):4817-4825.

Fernández-Llamazares, Á., Garteizgogeascoa, M., Basu, N., Brondizio, E.S., Cabeza, M., Martínez-Alier, J., McElwee, P. and Reyes-García, V., 2020. A state-of-the-art review of Indigenous Peoples and environmental pollution. Integrated Environmental Assessment and Management, 16 (3):324-341.

Ferrari, C.P., Gauchard, P.-A., Aspmo, K., Dommergue, A., Magand, O., Bahlmann, E., Nagorski, S., Temme, C., Ebinghaus, R., Steffen, A., Banic, C., Berg, T., Planchon, F., Barbante, C., Cescon, P. and Boutron, C.F., 2005. Snow-to-air exchanges of mercury in an Arctic seasonal snowpack in Ny-Ålesund, Svalbard. Atmospheric Environment, 39 (39):7633-7645.

Finger Higgens, R.A., Chipman, J.W., Lutz, D.A., Culler, L.E., Virginia, R.A. and Ogden, L.A., 2019. Changing lake dynamics indicate a drier Arctic in Western Greenland. Journal of Geophysical Research: Biogeosciences, 124 (4):870-883.

Finley, B.D., Swartzendruber, P.C. and Jaffe, D.A.. 2009. Particulate mercury emissions in regional wildfire plumes observed at the Mount Bachelor Observatory. Atmospheric Environment, 43 (38):6074-6083.

Finstad, A.G. and Hein, C.L., 2012. Migrate of stay: terrestrial primary productivity and climate drive anadromy in Arctic char. Global Change Biology, 18 (8):2487-2497.

Finstad, A.G., Andersen, T., Larsen, S., Tominaga, K., Blumenrath, S., de Wit, H.A., Tømmervik, H. and Hesen, D.O., 2016. From greening to browning: catchment vegetation development and reduced S-deposition promote organic carbon load on decadal time scales in Nordic lakes. Scientific Reports, 6 (1):31944.

Fisher, N.S. and Hook, S.E., 2002. Toxicology tests with aquatic animals need to consider the trophic transfer of metals. Toxicology, 181-182:531-536.

Fisher, J.A., Jacob, D.J., Soerensen, A.L., Amos, H.M., Steffen, A., Sunderland, E.M., 2012. Riverine source of Arctic Ocean mercury inferred from atmospheric observations. Nature, 5 (7):499-504.

Fisher, J.A., Jacob, D.J., Soerensen, A.L., Amos, H.M., Corbitt, E.S., Streets, D.G., Wang, Q., Yantosca, R.M. and Sunderland, E.M., 2013. Factors driving mercury variability in the Arctic atmosphere and ocean over the past 30 years. Global Biogeochemical Cycles, 27 (4): 1226-1235.

Fitzgerald W.F., Engstrom, D.R., Lamborg C.H., Tseng, C.M., Balcom, P.H. and Hammerschmidt, C.R., 2005. Modern and historic atmospheric mercury fluxes in northern Alaska: Global sources and Arctic depletion. Environmental Science & Technology, 39 (2):557-568.

Fitzgerald, W.F., Lamborg, C.H. and Hammerschmidt, C.R., 2007. Marine biogeochemical cycling of mercury. Chemical Reviews, 107 (2):641-662.

Flanders, J.R., Long, G., Reese, B., Grosso, N.R., Clements, W. and Stahl, R.G., Jr., 2019. Assessment of potential mercury toxicity to native invertebrates in a high-gradient stream. Integrated Environmental Assessment and Management, 15 (3):374-384.

Flannigan, M., Cantin, A.S., de Groot, W.J., Wotton, M., Newbery, A. and Gowman, L.M., 2013. Global wildland fire season severity in the 21st century. Forest Ecology and Management, 294:54-61.

Fleishman, A.B., Orben, R.A., Kokubun, N., Will, A., Paredes, R., Ackerman, J.T., Takahashi, A., Kitaysky, A.S. and Shaffer, S.A., 2019. Wintering in the western Subarctic Pacific increases mercury contamination of red-legged kittiwakes. Environmental Science & Technology, 53 (22):13398-13407.

FNIGC, 2007. OCAP: Ownership, Control, Access and Possession. Sanctioned by the First Nations Information Governance Committee (FNIGC), Assembly of First Nations. National Aboriginal Health Organization (NAHO). Ottawa, Canada. 23pp. Available at: https://icwrn.uvic.ca/wp-content/uploads/2013/08/FNC-OCAP.pdf

Foley, K.M., Roselle, S.J., Appel, K.W., Bhave, P.V., Pleim, J.E., Otte, T.L., Mathur, R., Sarwar, G., Young, J.O., Gilliam, R.C., Nolte, C.G., Kelly, J.T., Gilliland, A.B. and Bash, J.O., 2010. Incremental testing of the Community Multiscale Air Quality (CMAQ) modeling system version 4.7. Geoscientific Model Development, 3 (1):205-226.

Fontaine, J., Dewailly, E., Benedetti, J.-L., Pereg, D., Ayotte, P. and Déry, S., 2008. Re-evaluation of blood mercury, lead and cadmium concentrations in the Inuit population of Nunavik (Québec): a cross-sectional study. Environmental Health, 7 (1):25.

Forsberg, R., Sørensen, L. and Simonsen, S., 2017. Greenland and Antarctica ice sheet mass changes and effects on global sea level. Surveys in Geophysics, 38 (1):89-104.

Forsström, L., Roiha, T. and Rautio, M., 2013. Responses of microbial food web to increased allochthonous DOM in an oligotrophic Subarctic lake. Aquatic Microbial Ecology, 68 (2):171-184.

Forstsström, L., Rautio, M., Cusson, M., Sorvari, S., Albert, R-L., Kumagai, M. and Korhola, A., 2015. Dissolved organic matter concentration, optical parameters and attenuation of solar radiation in high-latitude lakes across three vegetation zones. Ecoscience, 22 (1):17-31.

Fort, J., Robertson, G.J., Grémillet, D., Traisnel, G. and Bustamante, P., 2014. Spatial ecotoxicology: migratory Arctic seabirds are exposed to mercury contamination while overwintering in the Northwest Atlantic. Environmental Science & Technology, 48 (19):11560-11567.

Fort, J., Grémillet, D., Traisnel, G., Amélineau, F. and Bustamante, P., 2016. Does temporal variation of mercury levels in Arctic seabirds reflect changes in global environmental contamination, or a modification of Arctic marine food web functioning? Environmental Pollution, 211:382-388.

Fortier, D.., Allard, M. and Shur, Y., 2007. Observation of rapid drainage system development by thermal erosion of ice wedges on Bylot Island, Canadian Arctic Archipelago. Permafrost and Periglacial Processes, 18, (3):229-243.

Fossheim, M., Primicerio, R., Johannesen, E., Ingvaldsen, R.B., Aschan, M.M. and Dolgov, A.V., 2015. Recent warming leads to a rapid borealization of fish communities in the Arctic. Nature Climate Change, 5 (7):673-677.

Foster, K.L., Stern, G.A., Pazerniuk, M.A., Hickie, B., Walkusz, W., Wang, F. and Macdonald, R.W., 2012. Mercury biomagnification in marine zooplankton food webs in Hudson Bay. Environmental Science & Technology, 46 (23):12952-12959.

Foster, K. L., Braune, B.M., Gaston, A.J. and Mallory, M.L., 2019. Climate influence on mercury in Arctic seabirds. Science of the Total Environmental, 693:133569.

Fox, A.L., Hughes, E.A., Trocine, R.P., Trefry, J.H., Schonberg, S.V., McTigue, N.D., Lasorsa, B.K., Konar, B. and Cooper, L.W., 2014. Mercury in the northeastern Chukchi Sea: distribution patterns in seawater and sediments and biomagnification in the benthic food web. Deep Sea Research Part II: Topical Studies in Oceanography, 102:56-67.

Fox, A.L., Trefry, J.H., Trocine, R.P., Dunton, K.H., Lasorsa, B.K., Konar, B., Ashjian, C.J., Cooper, L.W., 2017. Mercury biomagnification in food webs of the northeastern Chukchi Sea, Alaskan Arctic. Deep Sea Research Part II: Topical Studies in Oceanography, 144:63-77.

Frafjord, K., 1993. Food habits of Arctic foxes (*Alopex Lagopus*) on the western coast of Svalbard. Arctic, 46:49-54.

Francés-Monerris, A., Carmona-García, J., Acuña, A.U., Dávalos, J.Z., Cuevas, C.A., Kinnison, D.E., Francisco, J.S., Saiz-Lopez, A. and Roca-Sanjuán, D., 2020. Photodissociation mechanisms of major mercury(II) species in the atmospheric chemical cycle of mercury. Angewandte Chemie International Edition, 59 (19):7605-7610.

Francis, J.A., Vavrus, S.J. and Cohen, J., 2017. Amplified Arctic warming and mid-latitude weather: new perspectives on emerging connections. Wiley Interdisciplinary Reviews Climate Change, 8 (5):e474.

Franke, A., Lamarre, V. and Hedlin, E., 2016. Rapid nestling mortality in Arctic peregrine falcons due to the biting effects of black flies. Arctic, 69 (3):281-285.

Franke, A., Falk, K., Hawkshaw, K., Ambrose, S., Anderson, D.L., Boente, B.J., Booms, T., Burnham, K.K., Ekenstedt, J., Fufachev, I., Ganusevich, S., Johansen, K., Johnson, J.A., Kharitonov, S., Koskimies, P., Kulikova, O., Lindberg, P., Kulikova, O., Lindberg, P., Lindström, B.-O., Mattox, W.G., McIntyre, C.L., Mechnikova, S., Mossop, D., Møller, S., Nielsen, Ó.K., Ollila, T., Østlyngen, A., Pokrovsky, I., Poole, K., Restani, M., Robinson, B.W., Rosenfield, R., Sokolov, A., Sokolov, V., Swem, T. and Vorkamp, K., 2020. Status and trends of circumpolar peregrine falcon and gyrfalcon populations. Ambio, 49 (3):762-783.

Fraser, A., Dastoor, A. and Ryjkov, A., 2018. How important is biomass burning in Canada to mercury contamination? Atmospheric Chemistry and Physics, 18 (10):7263-7286.

Frederick, P. and Jayasena, N., 2011. Altered pairing behaviour and reproductive success in white ibises exposed to environmentally relevant concentrations of methylmercury. Proceedings of the Royal Society B, 278 (1713):1851-1857.

French, N.H.F., Jenkins, L.K., Loboda, T.V., Flannigan, M., Jandt, R., Bourgeau-Chavez, L.L. and Whitley, M., 2015. Fire in Arctic tundra of Alaska: past fire activity, future fire potential, and significance for land management and ecology. International Journal of Wildland Fire, 24 (8):1045-1061.

French, T.D., Houben, A.J., Desforges, J.P.W., Kimpe, L.E., Kokelj, S.V., Poulain, A.J., Smol, J.P., Wang, X. and Blais, J.M., 2014. Dissolved organic carbon thresholds affect mercury bioaccumulation in Arctic lakes. Environmental Science & Technology, 48 (6):3162-3168.

Frey, K.E. and McClelland, J.W., 2009. Impacts of permafrost degradation on Arctic river biogeochemistry. Hydrological Processes, 23 (1):169-182.

Friedli, H.R., Radke, L.F. and Lu, J.Y., 2001. Mercury in smoke from biomass fires. Geophysical Research Letters, 28 (17):3223-3226.

Friedli, H.R., Radke, L.F., Lu, J.Y., Banic, C.M., Leaitch, W.R. and MacPherson, J.I., 2003a. Mercury emissions from burning of biomass from temperate North American forests: laboratory and airborne measurements. Atmospheric Environment 37 (2):253-267.

Friedli, H.R., Radke, L.F., Prescott, R., Hobbs, P.V. and Sinha, P., 2003b. Mercury emissions from the August 2001 wildfires in Washington State and an agricultural waste fire in Oregon and atmospheric mercury budget estimates. Global Biogeochemical Cycles, 17 (2):1039.

Friedli, H.R., Arellano, A., Cinnirella, S. and Pirrone, N., 2009. Initial estimates of mercury emissions to the atmosphere from global biomass burning. Environmental Science & Technology, 43 (10):3507-3513.

Friske, P.W.B., McCurdy, M.W., Day, S.J., Gross, H., Lynch, J.J., Balma, R.G. and Durham, C.C., 1994. Regional stream sediment and water geochemical reconnaissance data, southwestern Yukon (parts of NTS 115A and 115B). Geological Survey of Canada, Open File 2859. Available at: https://doi.org/10.4095/194140

Fryer, R.J. and Nicholson, M.D., 1999. Using smoothers for comprehensive assessments of contaminant time series in marine biota. ICES Journal of Marine Science, 56:779-790.

Fu, X., Yang, X., Lang, X., Zhou, J., Zhang, H., Yu, B., Yan, H., Lin, C.-J. and Feng, X., 2016. Atmospheric wet and litterfall mercury deposition at urban and rural sites in China. Atmospheric Chemistry and Physics, 16 (18):11547-11562.

Fuelberg, H.E., Harrigan, D.L. and Sessions, W., 2010. A meteorological overview of the ARCTAS 2008 mission. Atmospheric Chemistry and Physics, 10 (2):817-842.

Fuglei, E., Henden, J.-A., Callahan, C.T., Gilg, O., Hansen, J., Ims, R.A., Isaev, A., Lang, J., McIntyre, C.L, Merizon, R.A., Mineev, O.Y., Mineev, Y.N., Mossop, D., Nielsen, O.K., Nilsen, E.B., Pedersen, Å.Ø., Schmidt, N.M., Sittler, B., Willebrand, M.H. and Martin, K., 2020. Circumpolar status of Arctic ptarmigan: population dynamics and trends. Ambio, 49 (3): 749-761.

Furgal, C., Boyd, A.D. and Chan, L., 2014. Assessment of contaminant and dietary nutrient interactions in the Inuit Health Survey: Nunavut, Nunatsiavut and Inuvialuit – Part 1: Risk perception and message evaluation study, (QS-8667-010-EE-A1, 1-12). In: Synopsis of research conducted under the 2013-2014 Northern Contaminants Program, pp. 1-12. Aboriginal Affairs and Northern Development Canada, Ottawa, Ontario, Canada. Available at: http://pubs.aina.ucalgary.ca/ncp/80366.pdf

Gabay, M., Raveh-Rubin, S., Peleg, M., Fredj, E. and Tas, E., 2020. Is oxidation of atmospheric mercury controlled by different mechanisms in the polluted continental boundary layer vs. remote marine boundary layer? Environmental Research Letters, 15 (6):064026.

Gaden, A. and Stern, G.A., 2010. Temporal trends in beluga, narwhal and walrus mercury levels: links to climate change. In: Ferguson, S.H., Loseto, L.L. and Mallory, M.L. (Eds.). A Little Less Arctic: Top Predators in the World's Largest Northern Inland Sea, Hudson Bay, pp. 197-216. Springer.

Gaden, A., Ferguson, S.H., Harwood, L., Melling, H. and Stern, G.A., 2009. Mercury trends in ringed seals (*Phoca hispida*) from the western Canadian Arctic since 1973: associations with length of ice-free season. Environmental Science & Technology, 43 (10):3646-3651.

Gagnon, C. and Fisher, N.S., 1997. Bioavailability of sediment-bound methyl and inorganic mercury to a marine bivalve. Environmental Science & Technology, 31 (4):993-998.

Gajdosechova, Z., Brownlow, A., Cottin, N.T., Fernandes, M., Read, F.L., Urgast, D.S., Raab, A., Feldmann, J. and Krupp, E.M., 2016a. Possible link between Hg and Cd accumulation in the brain of long-finned pilot whales (*Globicephala melas*). Science of the Total Environment, 545-546:407-413.

Gajdosechova, Z., Lawan, M.M., Urgast, D.S., Raab, A., Scheckel, K.G., Lombi, E., Kopittke, P.M., Loeschner, K., Larsen, E.H., Woods, G., Brownlow, A., Read, F.L., Feldmann, J. and Krupp, E.M., 2016b. *In vivo* formation of natural HgSe nanoparticles in the liver and brain of pilot whales. Scientific Reports, 6 (1):34361.

Gajdosechova, Z., Mester, Z., Feldmann, J. and Krupp, E.M., 2018. The role of selenium in mercury toxicity – current analytical techniques and future trends in analysis of selenium and mercury interactions in biological matrices. Trends in Analytical Chemistry, 104:95-109.

Gallant, D., Lecomte, N. and Berteaux, D., 2020. Disentangling the relative influences of global drivers of change in biodiversity: a study of the twentieth-century red fox expansion into the Canadian Arctic. Journal of Animal Ecology, 89 (2):565-576.

Gamberg, M., Muir, D., Chan, L. and Katz, S., 2009. Mercury in Caribou Forage. In: Smith, S., Stow, J., Edwards, J. (Eds.). Synopsis of Research Conducted under the 2008-2009 Northern Contaminants Program, p.331. Public Works and Government Services Canada, Ottawa, Ontario, Canada. Available at: https://pubs.aina.ucalgary.ca//ncp/68560.pdf

Gamberg, M., Chételat, J., Poulain, A.J., Zdanowicz, C. and Zheng, J., 2015. Mercury in the Canadian Arctic terrestrial environment: an update. Science of the Total Environment, 509-510:28-40.

Gamberg, M., Cuyler, C. and Wang, X., 2016. Contaminants in two West Greenland caribou populations. Science of the Total Environment, 554-555:329-336.

Gamberg, M., Pratte, I., Brammer, J., Cuyler, C., Elkin, B., Gurney, K., Kutz, S., Larter, N.C., Muir, D., Wang, X. and Provencher, J.F., 2020. Renal trace elements in barren-ground caribou subpopulations: temporal trends and differing effects of sex, age and season. Science of the Total Environment, 724:138305.

Gamberg, M. Cooke, D., Krieger, M., Macdonald, J., Barker, O., Otto, D., and Sedlack, E., 2021. Temporal trends of contaminants in Yukon lake trout. In: Beardsall, A. and Morris, A.D. (Eds.). Synopsis of Research Conducted under the 2017-2018 Northern Contaminants Program, pp. 254-261. Crown-Indigenous Relations and Northern Affairs Canada, Gatineau, QC, Canada. Available at: https://pubs.aina.ucalgary.ca/ncp/Synopsis20172018.pdf

Gamboa, A., Montero-Serrano, J.-C., St-Onge, G., Rochon, A. and Desiage, P.-A., 2017. Mineralogical, geochemical, and magnetic signatures of surface sediments from the Canadian Beaufort Shelf and Amundsen Gulf (Canadian Arctic). Geochemistry, Geophysics, Geosystems, 18 (2):488-512.

Gantner, N. and Gareis, J., 2013. Evaluation of hydro-climatic drivers of contaminant transfer in aquatic food webs in the Husky Lakes Watershed (Inuvialuit Settlement Region, NWT). In: Synopsis of Research Conducted under the 2012-2013 Northern Contaminants Program, pp. 105-118. Aboriginal Affairs and Northern Development Canada (AANDC), Gatineau, Quebec, Canada.

Gantner, N., Power, M., Babaluk, J.A., Reist, J.D., Köck, G., Lockhart, L.W., Solomon, K.R. and Muir, D.C., 2009. Temporal trends of mercury, cesium, potassium, selenium, and thallium in arctic char (*Salvelinus alpinus*) from Lake Hazen, Nunavut, Canada: effects of trophic position, size, and age. Environmental Toxicology and Chemistry, 28 (2):254-263.

Gantner, N., Power, M., Iqaluk, D., Meili, M., Borg, H., Sundbom, M., et al., 2010a. Mercury concentrations in landlocked arctic char (*Salvelinus alpinus*) from the Canadian Arctic. Part I: Insights from trophic relationships in 18 lakes. Environmental Toxicology and Chemistry 2010; 29: 621-632.

Gantner, N., Muir, D.C., Power, M., Iqaluk, D., Reist, J.D., Babaluk, J.A., Meili, M., Borg, H., Hammar, J., Michaud, W., Dempson, B. and Solomon, K.R., 2010b. Mercury concentrations in landlocked Arctic char (*Salvelinus alpinus*) from the Canadian Arctic. Part II: Influence of lake biotic and abiotic characteristics on geographic trends in 27 populations. Environmental Toxicology and Chemistry, 29 (3):633-643.

Gårdfeldt, K. and Jonsson, M., 2003. Is bimolecular reduction of Hg(II) complexes possible in aqueous systems of environmental importance. Journal of Physical Chemistry A, 107 (22):4478-4482.

Gårdfeldt, K. Munthe, J., Strömberg, D. and Lindqvist, O., 2003. A kinetic study on the abiotic methylation of divalent mercury in the aqueous phase. Science of the Total Environment, 304 (1-3):127-136.

Garmo, Ø.A., Skjelkvåle, B.L., de Wit, H.A., Colombo, L., Curtis, C., Fölster, J., Hoffmann, A., Hruška, J., Høgåsen, T., Jeffries, D.S., Keller, W.B., Krám, P., Majer, V., Monteith, D.T., Paterson, A.M., Rogora, M., Rzychon, D., Steingruber, S., Stoddard, J.L., Vuorenmaa, J., and Worsztynowicz, A., 2014. Trends in surface water chemistry in acidified areas in Europe and North America from 1990 to 2008. Water, Air, & Soil Pollution, 225 (3):1-14.

Gascón Díez, E., Loizeau, J.-L., Cosio, C., Bouchet, S., Adatte, T., Amouroux, D. and Bravo, A.G., 2016. Role of settling particles on mercury methylation in the oxic water column of freshwater systems. Environmental Science & Technology, 50 (21):11672-11679.

Gascón Díez, E., Loizeau, J.-L., Cosio, C., Bouchet, S., Adatte, T., Amouroux, D. and Bravo, A.G., 2017. Correction to Role of settling particles on mercury methylation in the oxic water column of freshwater systems. Environmental Science & Technology, 51 (6):3594-3594.

Gaston, A.J. and Woo, K., 2008. Razorbills (*Alca torda*) follow Subarctic prey into the Canadian Arctic: colonization results from climate change? The Auk, 125 (4):939-942.

Gaston, A.J. and Elliott, K.H., 2013. Effects of climate-induced changes in parasitism, predation and predator-predator interactions on reproduction and survival of an Arctic marine bird. Arctic, 66 (1):43-51.

Gaston, A.J. and Elliott, K.H., 2014. Seabird diet changes in northern Hudson Bay, 1981-2013, reflect the availability of schooling prey. Marine Ecology Progress Series, 513:211-223.

Gaston, A.J., Gilchrist, H.G. and Hipfner, J.M., 2005. Climate change, ice conditions and reproduction in an Arctic nesting marine bird: Brunnich's guillemot (*Uria lomvia* L.). Journal of Animal Ecology, 74 (5):832-841.

Gay, D.A., Schmeltz, D., Prestbo, E., Olson, M., Sharac, T. and Tordon, R., 2013. The Atmospheric Mercury Network: measurement and initial examination of an ongoing atmospheric mercury record across North America. Atmospheric Chemistry and Physics, 13 (22):11339-11349.

Gebre, S., Boissy, T. and Alfredsen, K., 2014. Sensitivity to climate change of the thermal structure and ice cover regime of three hydropower reservoirs. Journal of Hydrology, 510:208-227.

Genchi, G., Sinicropi, M.S., Carocci, A., Lauria, G. and Catalano, A., 2017. Mercury exposure and heart diseases. International Journal of Environmental Research and Public Health, 14 (1):74.

Gérin-Lajoie, J., Herrmann, T.M, MacMillan, G.A., Hébert-Houle, É., Monfette, M., Rowell, J.A., Soucie, T.A., Snowball, H., Townley, E., Lévesque, E., Amyot, M., Franssen, J. and Dedieu, J.-P., 2018. IMALIRIJIIT: a community-based environmental monitoring program in the George River watershed, Nunavik, Canada. Écoscience, 25 (4):381-399.

Gerson, A.R., Cristol, D.A. and Seewagen, C.L., 2019. Environmentally relevant methylmercury exposure reduces the metabolic scope of a model songbird. Environmental Pollution, 246:790-796.

Ghotra, A., Lehnherr, I., Porter, T. J. and Pisaric, M. F., 2020. Tree-ring inferred atmospheric mercury concentrations in the Mackenzie Delta (NWT, Canada) peaked in the 1970s but are increasing once more. ACS Earth and Space Chemistry, 4 (3):457-466.

Giang, A., Stokes, L.C., Streets, D.G., Corbitt, E.S. and Selin, N.E., 2015. Impacts of the Minamata Convention on Mercury emissions and global deposition from coal-fired power generation in Asia. Environmental Science & Technology, 49 (9):5326-5335.

Gibbs, A.E., Ohman, K.A. and Richmond, B.M., 2015. National assessment of shoreline change: a GIS compilation of vector shorelines and associated shoreline change data for the north coast of Alaska, U.S.-Canadian border to Icy Cape (Open-File Report 2015-1030). U.S. Geological Survey. Available at: https://dx.doi.org/10.3133/ofr20151030

Gibson, L.A., Lavoie, R.A., Bissegger, S., Campbell, L.M. and Langlois, V.S., 2014. A positive correlation between mercury and oxidative stress-related gene expression (GPX3 and GSTM3) is measured in female double-crested cormorant blood. Ecotoxicology, 23:1004-1014.

Gibson, C.M., Chasmer, L.E., Thompson, D.K., Quinton, W.L., Flannigan, M.D. and Olefeldt, D., 2018. Wildfire as a major driver of recent permafrost thaw in boreal peatlands. Nature Communications, 9 (1):3041.

Giesler, R., Clemmensen, K.E., Wardle, D.A., Klaminder, J. and Bindler, R., 2017. Boreal forests sequester large amounts of mercury over millennial time scales in the absence of wildfire. Environmental Science & Technology, 51 (5):2621-2627.

Giglio, L., Csiszar, I. and Justice, C.O., 2006. Global distribution and seasonality of active fires as observed with the Terra and Aqua Moderate Resolution Imaging Spectroradiometer (MODIS) sensors. Journal of Geophysical Research: Biogeosciences, 111 (G2):G02016.

Giglio, L., Randerson, J.T. and van der Werf, G.R., 2013. Analysis of daily, monthly, and annual burned area using the fourth-generation global fire emissions database (GFED4). Journal of Geophysical Research: Biogeosciences 118, 317-328.

Giglio, L., Schroeder, W. and Justice, C.O., 2016. The collection 6 MODIS active fire detection algorithm and fire products. Remote Sensing of Environment, 178:31-41.

Gilbert, R.O., 1987. Chapter 16: Detecting and Estimating Trends and Chapter 17: Trends and Seasonality. In: Statistical Methods for Environmental Pollution Monitoring, pp. 204-240. Van Nostrand Reinhold Company, New York.

Gilg, O., Hanski, I. and Sittler, B., 2003. Cyclic dynamics in a simple vertebrate predator-prey community. Science, 302 (5646):866-868.

Gillett, N.P., 2004. Detecting the effect of climate change on Canadian forest fires. Geophysical Research Letters, 31 (18):L18211.

Gilmour, C.C., Podar, M., Bullock, A.L., Graham, A.M., Brown, S.D., Somenahally, A.C., Johs, A., Hurt, R.A., Bailey, K.L. and Elias, D.A., 2013. Mercury methylation by novel microorganisms from new environments. Environmental Science & Technology, 47 (20):11810-11820.

Gilmour, C.C., Bullock, A.L., McBurney, A., Podar, M. and Elias, D.A., 2018. Robust mercury methylation across diverse methanogenic *archae*. MBio, 9 (2):e02403-e02417.

Gimbert, F., Geffard, A., Guédron, S., Dominik, J. and Ferrari, B.J.D., 2016. Mercury tissue residue approach in *Chironomus riparius*: involvement of toxicokinetics and comparison of subcellular fractionation methods. Aquatic Toxicology, 171:1-8.

Gionfriddo, C.M., Tate, M.T., Wick, R.R., Schultz, M.B., Zemla, A., Thelen, M.P., Schofield, R., Krabbenhoft, D.P., Holt, K.E. and Moreau, J.W., 2016. Microbial mercury methylation in Antarctic sea ice. Nature Microbiology, 1 (10):16127.

Gionfriddo C.M., Stott, M.B., Power, J.F., Ogorek, J.M., Krabbenhoft, D.P., Wick, R., Holt, K., Chen, L-.,X., Thomas, B.C., Banfield, J.F., Moreau, J.W. and Cann, I., 2020. Genome-resolved metagenomics and detailed geochemical speciation analyses yield new insights into microbial mercury cycling in geothermal springs. Applied and Environmental Microbiology, 86 (15):e00176-20.

Girard, C., Leclerc, M. and Amyot M., 2016. Photodemethylation of methylmercury in Eastern Canadian Arctic thaw pond and lake ecosystems. Environmental Science & Technology, 50 (7):3511-3520.

Gjertz, I. and Lydersen, C., 1986. Polar bear predation on ringed seals in the fast-ice of Hornsund, Svalbard. Polar Research, 4 (1):65-68.

Glahder C., 1995. Hunting in Kangerlussuaq, East Greenland 1951-1991, an assessment of Local Knowledge. Meddelelser om Grønland, Man & Society, 19. The Commission for Scientific Investigations in Greenland (KVUG). 79pp.

Gleason, J.D., Blum, J.D., Moore, T.C., Polyak, L., Jakobsson, M., Meyers, P.A. and Biswas, A., 2017. Sources and cycling of mercury in the paleo Arctic Ocean from Hg stable isotope variations in Eocene and Quaternary sediments. Geochimica et Cosmochimica Acta, 197:245-262.

Gobeil, C., Macdonald, R.W. and Smith, J.N., 1999. Mercury profiles in sediments of the Arctic Ocean basins. Environmental Science & Technology, 33 (23):4194-4198.

Góngora, E., Braune, B.M. and Elliott, K.H., 2018. Nitrogen and sulfur isotopes predict variation in mercury levels in Arctic seabird prey. Marine Pollution Bulletin, 135:907-914.

Goodsite, M.E., Plane, J.M.C. and Skov, H., 2004. A theoretical study of the oxidation of Hg^0 to HgBr2 in the troposphere. Environmental Science & Technology, 38 (6):1772-1776.

Goodsite, M.E., Plane, J.M.C. and Skov, H., 2012. Correction to A theoretical study of the oxidation of Hg0 to HgBr2 in the troposphere. Environmental Science & Technology, 46 (9):5262.

Goodsite, M.E., Outridge, P.M., Christensen, J.H., Dastoor, A., Muir, D., Travnikov, O. and Wilson, S., 2013. How well do environmental archives of atmospheric mercury deposition in the Arctic reproduce rates and trends depicted by atmospheric models and measurements? Science of the Total Environment, 452-453:196-207.

Gordon, J., Quinton, W., Branfireun, B.A. and Olefeldt, D., 2016. Mercury and methylmercury biogeochemistry in a thawing permafrost wetland complex, Northwest Territories, Canada. Hydrological Processes, 30 (20):3627-3638.

Goutte, A., Kriloff, M., Weimerskirch, H. and Chastel, O., 2011. Why do some adult birds skip breeding? A hormonal investigation in a long-lived bird. Biology Letters, 7 (5):790-792.

Goutte, A., Bustamante, P., Barbraud, C., Delord, K., Weimerskirch, H. and Chastel, O., 2014a. Demographic responses to mercury exposure in two closely related Antarctic top predators. Ecology, 95 (4):1075-1086.

Goutte, A., Barbraud, C., Meillère, A., Carravieri, A., Bustamante, P., Labadie, P., Budzinski, H., Delord, K., Cherel, Y., Weimerskirch, H. and Chastel, O., 2014b. Demographic consequences of heavy metals and persistent organic pollutants in a vulnerable long-lived bird, the wandering albatross. Proceedings of the Royal Society B: Biological Sciences, 281 (1787):20133313.

Goutte, A., Barbraud, C., Herzke, D., Bustamante, P., Angelier, F., Tartu, S., Clément-Chastel, C., Moe, B., Bech, C., Gabrielsen, G.W., Bustnes, J.O. and Chastel, O., 2015. Survival rate and breeding outputs in a High Arctic seabird exposed to legacy persistent organic pollutants and mercury. Environmental Pollution, 200:1-9.

Goutte, A., Meillère, A., Barbraud, C., Budzinski, H., Labadie, P., Peluhet, L., Weimerskirch, H., Delord, K. and Chastel O., 2018. Demographic, endocrine and behavioral responses to mirex in the South polar skua. Science of the Total Environment, 631-632:317-325.

Government of Canada, 2019a. Policy on scientific and Indigenous Knowledge integrity. Crown-Indigenous Relations and Northern Affairs Canada. Ottawa, Ontario, Canada. Available at: https://www.rcaanc-cirnac.gc.ca/eng/1575567784632/1575567805298

Government of Canada. 2019b. Canada's Arctic and Northern policy framework. Crown-Indigenous Relations and Northern Affairs Canada. Ottawa, Ontario, Canada. Available at: https://www.rcaanc-cirnac.gc.ca/eng/1560523306861/1560523330587

Graham, A.M., Aiken, G.R. and Gilmour, C.C., 2012. Dissolved organic matter enhances microbial mercury methylation under sulfidic conditions. Environmental Science & Technology, 46 (5):2715-2723.

Grandjean, P., Weihe, P., Jørgensen, P.J., Clarkson, T., Cernichiari, E. and Viderø, T., 1992. Impact of maternal seafood diet on fetal exposure to mercury, selenium, and lead. Archives of Environmental Health: An International Journal, 47 (3):185-195.

Grandjean, P., Weihe, P., Nielsen, F., Heinzow, B., Debes, F. and Budtz-Jørgensen, E., 2012. Neurobehavioral deficits at age 7 years associated with prenatal exposure to toxicants from maternal seafood diet. Neurotoxicology and Teratology, 34 (4):466-472.

Grannas, A.M., Bogdal, C., Hageman, K.J., Halsall, C., Harner, T., Hung, H., Kallenborn, R., Klán, P., Klánová, J., Macdonald, R.W., Meyer, T. and Wania, F., 2013. The role of the global cryosphere in the fate of organic contaminants. Atmospheric Chemistry and Physics, 13 (6):3271-3305.

Grasby, S. E., Sanei, H., Beauchamp, B. and Chen, Z., 2013. Mercury deposition through the Permo-Triassic Biotic Crisis. Chemical Geology, 351:209-216.

Gratz, L.E., Keeler, G.J. and Miller, E.K., 2009. Long-term relationships between mercury wet deposition and meteorology. Atmospheric Environment, 43 (39):6218-6229.

Graydon, J.A., Emmerton, C.A., Lesack, L.F.W. and Kelly, E.N., 2009a. Mercury in the Mackenzie River delta and estuary: concentrations and fluxes during open-water conditions. Science of the Total Environment, 407 (8):2980-2988.

Graydon, J.A., St. Louis, V.L., Hintelmann, H., Lindberg, S.E., Sandilands, K.A., Rudd, J.W.M., Kelly, C.A., Tate, M.T., Krabbenhoft, D.P. and Lehnherr, I., 2009b. Investigation of uptake and retention of atmospheric Hg(II) by boreal forest plants using stable Hg isotopes. Environmental Science & Technology, 43 (13):4960-4966.

Grebmeier, J.M., Overland, J.E., Moore, S.E., Farley, E.V., Carmack, E.C., Cooper, L.W., Frey, K.E., Helle, J.H., McLaughlin, F.A. and McNutt, S.L., 2006. A major ecosystem shift in the northern Bering Sea. Science, 311 (5766):1461-1464.

Grémillet, D., Fort, J., Amélineau, F., Zakharova, E., Le Bot, T., Sala, E. and Gavrilo, M., 2015. Arctic warming: nonlinear impacts of sea-ice and glacier melt on seabird foraging. Global Change Biology, 21 (3):1116-1123.

Grigal, D.F., 2002. Inputs and outputs of mercury form terrestrial watersheds: a review. Environmental Reviews, 10 (1):1-39.

Grigal, D.F., 2003. Mercury sequestration in forests and peatlands. Journal of Environmental Quality, 32 (2):393-405.

Grosse, G., Jones, B.M. and Arp, C., 2013. Thermokarst lakes, drainage, and drained basins. In: Shroder, J.F., Giardino, R. and Harbor, J. (Eds.). Treatise on Geomorphology, pp. 325-353. Elsevier.

Gu, B., Bian, Y., Miller, C.L., Dong, W., Jiang, X. and Liang, L., 2011. Mercury reduction and complexation by natural organic matter in anoxic environments. Proceedings of the National Academy of Sciences of the United States of America, 108 (4):1479-1483.

Guentzel, J.L., Landing, W.M., Gill, G.A. and Pollman, C.D., 2001. Processes influencing rainfall deposition of mercury in Florida. Environmental Science & Technology, 35 (5):863-873.

Günther, F., Overduin, P.P., Sandakov, A.V., Grosse, G. and Grigoriev, M.N., 2013. Short- and long-term thermo-erosion of ice-rich permafrost coasts in the Laptev Sea region. Biogeosciences, 10 (6):4297-4318.

Guo, L., Cai, Y., Belzile, C. and Macdonald, R., 2012. Sources and fluxes of carbon and nutrient species in the seasonally ice-covered Yukon River. Biogeochemistry, 107 (1):187-208.

Gustin, M.S., Amos, H.M., Huang, J., Miller, M.B. and Heidecorn, K., 2015. Measuring and modeling mercury in the atmosphere: a critical review. Atmospheric Chemistry and Physics, 15 (10):5697-5713.

Ha, E., Basu, N., Bose-O'Reilly, S., Dórea, J.G., McSorley, E., Sakamoto, M. and Chan, H.M., 2017. Current progress on understanding the impact of mercury on human health. Environ Research, 152:419-433.

Haarr, A., Hylland, K., Eckbo, N., Gabrielsen, G.W., Herzke, D., Bustnes, J.O., Blévin, P., Chastel O., Moe, B., Hanssen, S.A., Sagerup, K. and Borgå K., 2017. DNA damage in Arctic seabirds: baseline, sensitivity to a genotoxic stressor and association to organohalogen contaminants: genotoxicity and organohalogens in Arctic avian wildlife. Environmental Toxicology and Chemistry, 37 (4):1084-1091.

Haine, T.W.N., Curry, B., Gerdes, R., Hansen, E., Karcher, M., Lee, C., Rudels, Bert., Spreen, G., de Steur, L., Stewart, K.D. and Woodgate, R., 2015. Arctic freshwater export: status, mechanisms, and prospects. Global and Planetary Change, 125:13-35.

Halbach, K., Mikkelsen, Ø., Berg, T. and Steinnes, E., 2017. The presence of mercury and other trace metals in surface soils in the Norwegian Arctic. Chemosphere, 188:567-574.

Hall, N.L., Dvonch, J.T., Marsik, F.J., Barres, J.A. and Landis, M.S., 2017. An Artificial turf-based surrogate surface collector for the direct measurement of atmospheric mercury dry deposition. International Journal of Environmental Research and Public Health, 14 (2):173.

Hallanger, I.G., Fuglei, E., Yoccoz, N.G., Pedersen, Å.Ø., König, M. and Routti, H., 2019. Temporal trend of mercury in relation to feeding habits and food availability in Arctic foxes (*Vulpes lagopus*) from Svalbard, Norway. Science of the Total Environment, 670:1125-1132.

Halm, D.R. and Dornblaser, M.M., 2007. Water and sediment quality in the Yukon River and its tributaries between Atlin, British Columbia, Canada, and Eagle, Alaska, USA, 2004 (Open-File Report 2007-1197). U.S. Geological Survey. Available at: https://doi.org/10.3133/ofr20071197

Hamilton, C.D., Kovacs, K.M., Ims, R.A., Aars, J. and Lydersen, C., 2017. An Arctic predator–prey system in flux: climate change impacts on coastal space use by polar bears and ringed seals. Journal of Animal Ecology, 86 (5):1054-1064.

Hammerschmidt, C.R. and Bowman, K.L., 2012. Vertical methylmercury distribution in the subtropical North Pacific Ocean. Marine Chemistry, 132-133:77-82.

Hammerschmidt, C.R. and Fitzgerald, W.F., 2006. Photodecomposition of methylmercury in an Arctic Alaskan Lake. Environmental Science & Technology, 40 (4):1212-1216.

Hammerschmidt, C.R. and Fitzgerald, W.F., 2010. Iron-mediated photochemical decomposition of methylmercury in an Arctic Alaskan Lake. Environmental Science & Technology, 44 (16):6138-6143.

Hammerschmidt, C.R., Sandheinrich, M.B., Wiener, J.G. and Rada, R.G., 2002. Effects of dietary methylmercury on reproduction of fathead minnows. Environmental Science & Technology, 36 (5):877-883.

Hammerschmidt, C.R., Lamborg, C.H. and Fitzgerald, W.F., 2007. Aqueous phase methylation as a potential source of methylmercury in wet deposition. Atmospheric Environment, 41 (8):1663-1668.

Hansen, B.B., Grotan, V., Aanes, R., Sæther, B.E., Stien, A., Fuglei, E., Ims, R.A., Yoccoz, N.G. and Pedersen, Å.Ø., 2013. Climate events synchronize the dynamics of a resident vertebrate community in the High Arctic. Science, 339 (6117):313-315.

Hansen, B.B., Isaksen, K., Benestad, R.E., Kohler, J., Pedersen, Å.Ø., Loe, L.E., Coulson, S.J., Larsen, J.O., Varpe, Ø., 2014. Warmer and wetter winters: Characteristics and implications of an extreme weather event in the High Arctic. Environmental Research Letters, 9 (11):114021.

Hansen, K.M., Christensen, J.H. and Brandt, J., 2015. The influence of climate change on atmospheric deposition of mercury in the Arctic—A model sensitivity study. International Journal of Environmental Research and Public Health, 12 (9):11254-11268.

Hansen, B.B., Lorentzen, J.R., Welker, J.M., Varpe, Ø., Aanes, R., Beumer, L.T. and Pedersen, Å.Ø. 2019a. Reindeer turning maritime: ice-locked tundra triggers changes in dietary niche utilization. Ecosphere, 10 (4):e02672.

Hansen, B.B., Pedersen, Å.Ø., Peeters, B., Le Moullec, M., Albon, S.D., Herfindal, I., Sæther, B.-E., Grøtan, V. and Aanes, R., 2019b. Spatial heterogeneity in climate change effects decouples the long-term dynamics of wild reindeer populations in the High Arctic. Global Change Biology, 25 (11):3656-3668.

Hao, Z.L., Wang, F. and Yang, H.Z., 2013. Baseline values for heavy metals in soils on Ny-Alesund, Spitsbergen Island, Arctic: the extent of anthropogenic pollution. Advanced Materials Research, 779-780:1260-1265.

Harada, M., 1995. Minamata disease: methylmercury poisoning in Japan caused by environmental pollution. Critical Reviews in Toxicology, 25 (1):1-24.

Hararuk, O., Obrist, D. and Luo, Y., 2013. Modelling the sensitivity of soil mercury storage to climate-induced changes in soil carbon pools. Biogeosciences, 10 (4):2393-2407.

Hargreaves, A.L., Whiteside, D.P. and Gilchrist, G., 2010. Concentrations of 17 elements, including mercury, and their relationship to fitness measures in Arctic shorebirds and their eggs. Science of the Total Environment, 408:3153-3161.

Hargreaves, A.L., Whiteside, D.P. and Gilchrist, G., 2011. Concentrations of 17 elements, including mercury, in the tissues, food and abiotic environment of Arctic shorebirds. Science of the Total Environment, 409 (19):3757-3770.

Harley, J., Lieske, C., Bhojwani, S., Castellini, J.M., López, J.A. and O'Hara, T.M., 2015. Mercury and methylmercury distribution in tissues of sculpins from the Bering Sea. Polar Biology, 38 (9):1535-1543.

Harmens, H., Norris, D., Steinnes, E., Zechmeister, H.G. et. al., 2010. Mosses as biomonitors of atmospheric heavy metal deposition: Spatial patterns and temporal trends in Europe. Environmental Pollution, 158 (10):3144-3156.

Harmens, H., Norris, D.A., Sharps, K., Mills, G., Alber, R., Aleksiayenak, Y., Blum, O., Cucu-Man, S.M., Dam, M., De Temmerman, L., Ene, A., Fernández, J.A., Martinez-Abaigar, J., Frontasyeva, M., Godzik, B., Jeran, Z., Lazo, P., Leblond, S., Liiv, S., Magnússon, S.H., Maňkovská, B., Karlsson, G.P., Piispanen, J., Poikolainen, J., Santamaria, J.M., Skudnik, M., Spiric, Z., Stafilov, T., Steinnes, E., Stihi, C., Suchara, I., Thöni, L., Todoran, R., Yurukova, L. and Zechmeister, H.G., 2015. Heavy metal and nitrogen concentrations in mosses are declining across Europe whilst some "hotspots" remain in 2010. Environmental Pollution, 200:93-104.

Harrison, S., Kargel, J.S., Huggel, C., Reynolds, J., Shugar, D.H., Betts, R.A., Emmer, A., Glasser, N., Haritashya, U.K., Klimeš, J., Reinhardt, L., Schaub, Y., Wiltshire, A., Regmi, D. and Vilímek, V., 2018. Climate change and the global pattern of moraine-dammed glacial lake outburst floods. The Cryosphere, 12 (4):1195-1209.

Hartman, C.A., Ackerman, J.T. and Herzog, M.P., 2019. Mercury exposure and altered parental nesting behavior in a wild songbird. Environmental Science & Technology, 53 (9):5396-5405.

Hartmann, D.L., Klein Tank, A.M.G., Rusticucci, M., Alexander, L.V., Brönnimann, S., Charabi, Y., Dentener, F.J., Dlugokencky, E.J., Easterling, D.R., Kaplan, A., Soden, B.J., Thorne, P.W., Wild, M. and Zhai, P.M., 2013. Observations: atmosphere and surface. In: Stocker, T.F., Qin, D., Plattner, G.-K., Tignor, M., Allen, S.K, Boschung, J., Nauels, A., Xia, Y., Bex, V. and Midgley, P.M. (Eds.). Climate Change 2013: The Physical Science Basis. Contribution of Working Group I to the Fifth Assessment Report of the Intergovernmental Panel on Climate Change, pp. 159-254. Cambridge University Press.

Harwood, L.A., Smith, T.G., George, J.C., Sandstrom, S.J., Walkusz, W. and Divoky, G.J., 2015. Change in the Beaufort Sea ecosystem: diverging trends in body condition and/or production in five marine vertebrate species. Progress in Oceanography, 136:263-273.

Hawkes, W.C. and Keim, N.L., 2003. Dietary selenium intake modulates thyroid hormone and energy metabolism in men. The Journal of Nutrition, 133 (11):3443-3448.

Hayden, B., Harrod, C. and Kahilainen, K.K., 2014. Dual-fuels: intra-annual variation in the relative importance of benthic and pelagic resources to maintenance, growth and reproduction in a generalist salmonid fish. Journal of Animal Ecology, 83 (6):1501-1512.

Hayden, B., Harrod, C., Thomas, S.M., Eloranta, A.P., Myllykangas, J.-P., Siwertsson, A., Præbel, K., Knudsen, K., Amundsen, P.-A. and Kahilainen, K.K., 2019. From clear lakes to murky waters -tracing the functional response of high-latitude lake communities to concurrent 'greening' and 'browning'. Ecology Letters, 22 (5):807-816.

Hayes, C.T., Costa, K.M., Anderson, R.F., Calvo, E., Chase, Z., Demina, L.L., Dutay, J.-C., German, C.R., Heimbürger-Boavida, L.-E., Jaccard, S.L., Jacobel, A., Kohfeld, K.E., Kravchishina, M.D., Lippold, J., Mekik, F., Missiaen, L., Pavia, F.J., Paytan, A., Pedrosa-Pamies, R., Petrova, M.V., Rahman, S., Robinson, L.F., Roy-Barman, M., Sanchez-Vidal, A., Shiller, A., Tagliabue, A., Tessin, A.C., van Hulten, M. and Zhang, J., 2021. Global ocean sediment composition and burial flux in the deep sea. Global Biogeochemical Cycles, 35 (4):e2020GB006769.

Hayhoe, K., Edmonds, J., Kopp, R.E., LeGrande, A.N., Sanderson, B.M., Wehner, M.F. and Wuebbles, D.J., 2017. Climate models, scenarios, and projections. In: Wuebbles, D.J., Fahey, D.W., Hibbard, K.A., Dokken, D.J., Stewart, B.C. and Maycock, T.K. (Eds.). Climate Science Special Report: Fourth National Climate Assessment (NCA4), Volume I, U.S. Global Change Research Program, Washington, DC, USA, pp. 133-160.

HBM4EU, 2019. Prioritised list of biomarkers, matrices and analytical methods for the 2nd prioritisation round of substances, (Deliverable report D 9.5. WP9 - Laboratory analysis and quality assurance) Human Biomonitoring for Europe (HBM4EU). Available at: https://www.hbm4eu.eu/work-packages/deliverable-9-5-prioritised-list-of-biomarkers-matrices-and-analytical-methods-for-the-2nd-prioritisation-round-of-substances/

Health Canada, 2007. Human Health Risk Assessment of Mercury in Fish and Health Benefits of Fish Consumption. Bureau of Nutritional Sciences, Food Directorate, Health Products and Food Branch, Health Canada. Ottawa, Ontario, Canada. 76pp. Available at: https://www.canada.ca/content/dam/hc-sc/migration/hc-sc/fn-an/alt_formats/hpfb-dgpsa/pdf/nutrition/merc_fish_poisson-eng.pdf

Heath, J., Ljubicic, G. and Arragutainaq, L., 2015. A social media network and interactive Knowledge mapping platform for the North: Developing the tools needed to meaningfully engage communities in research and environmental stewardship. Arctic Net Annual Scientific Meeting 7-11 December 2015 (Oral Presentation Abstracts), Vancouver, British Columbia, Canada. Available at: https://arcticnetmeetings.ca//asm2015/docs/topical-abstracts.pdf

Hedgecock, I.M. and Pirrone, N., 2001. Mercury and photochemistry in the marine boundary layer-modelling studies suggest the *in situ* production of reactive gas phase mercury. Atmospheric Environment, 35 (17):3055-3062.

Hedgecock, I.M., Pirrone, N. and Sprovieri, F., 2008. Chasing quicksilver northward: mercury chemistry in the Arctic troposphere. Environmental Chemistry, 5 (2):131-134.

Heimbürger, L.-E., Cossa, D., Marty, J.-C., Migon, C., Averty, B., Dufour, A. and Ras, J., 2010. Methyl mercury distributions in relation to the presence of nano- and picophytoplankton in an oceanic water column (Ligurian Sea, North-western Mediterranean). Geochimica et Cosmochimica Acta, 74 (19):5549-5559.

Heimbürger, L.-E., Sonke, J.E, Cossa, D., Point, D., Lagane, C., Laffont, L, Galfond, B., Nicolaus, M., Rabe, B. and Rutgers van der Loeff, M., 2015. Shallow methylmercury production in the marginal sea ice zone of the central Arctic Ocean. Scientific Report, 5 (1):10318.

Heinz, G.H., Hoffman, D.J., Klimstra, J.D., Stebbins, K.R., Kondrad, S.L. and Erwin, C.A., 2009. Species differences in the sensitivity of avian embryos to methylmercury. Archives of Environmental Contamination and Toxicology, 56:129-138.

Helgason, L.B., Barrett, R., Lie, E., Polder, A., Skaare, J.U. and Gabrielsen, G.W., 2008. Levels and temporal trends (1983–2003) of persistent organic pollutants (POPs) and mercury (Hg) in seabird eggs from Northern Norway. Environmental Pollution, 155(1):190-198.

Helgason, L.B., Polder, A., Føreid, S., Bæk, K., Lie, E., Gabrielsen, G.W., Barrett, R. and Skaare, J.U., 2009. Levels and temporal trends (1983-2003) of polybrominated diphenyl ethers and

hexabromocyclododecanes in seabird eggs from North Norway. Environmental Toxicology and Chemistry, 28 (5):1096-1103.

Helgason, L.B., Verreault, J., Braune, B.M., Borgå, K., Primicerio, R., Jenssen, B.M. and Gabrielsen, G.W., 2010. Relationship between persistent halogenated organic contaminants and TCDD toxic equivalents on EROD activity and retinoid and thyroid hormone status in northern fulmars. Science of the Total Environment, 408 (24):6117-6123.

Helgason, L.B., Sagerup, K. and Gabrielsen, G.W., 2011. Organohalogen pollutants in seabird eggs from Northern Norway and Svalbard. In: Loganathan, B.G. and Lam, P.K. (Eds.). Global Contamination Trends of Persistent Organic Chemicals, pp.547-569. CRC Press.

Henri, D.A., Brunet, N.D., Dort, H.E., Hambly Odame, H., Shirley, J. and Gilchrist, H.G., 2020. What is effective research communication? Towards cooperative inquiry with Nunavut communities. Arctic, 73 (1):81-98.

Henriksen, A., Mannio, J., Wilander, A., Moiseenko, T., Traaen, T., Skjelkvåle, B.L., Fjeld, E. and Vuorenmaa, J., 1997. Regional lake surveys in the Barents region of Finland, Norway, Sweden and Russian Kola, 1995 - Results (Acid Rain Research Report 45/97, NIVA Report SNO 3633-97). Norwegian Institute for Water Research, Oslo, Norway. 36pp.

Herring, G., Ackerman, J.T. and Eagles-Smith, C.A., 2010. Embryo malposition as a potential mechanism for mercury-induced hatching failure in bird eggs. Environmental Toxicology and Chemistry 29 (8):1788-1794.

Herring, G., Ackerman, J.T. and Herzog, M.P., 2012. Mercury exposure may suppress baseline corticosterone levels in juvenile birds. Environmental Science & Technology, 46 (11):6339-6346.

Higdon, J.W. and Ferguson, S.H., 2009. Loss of Arctic sea ice causing punctuated change in sightings of killer whales (*Orcinus orca*) over the past century. Ecological Applications, 19 (5):1365-1375.

Hill, P.R., Blasco, S.M., Harper, J.R. and Fissel, D.B., 1991. Sedimentation on the Canadian Beaufort Shelf. Continental Sea Research, 11 (8-10):821-842.

Hill, V.J., Matrai, P.A., Olson, E., Suttles, S., Steele, M., Codispoti, L.A. and Zimmerman, R.C., 2013. Synthesis of integrated primary production in the Arctic Ocean: II. *In situ* and remotely sensed estimates. Progress in Oceanography, 110:107-125.

Hoekstra, P.F., Braune, B.M., Elkin, B., Armstrong, F.A.J. and Muir, D.C.G., 2003. Concentrations of selected essential and non-essential elements in arctic fox (*Alopex lagopus*) and wolverines (*Gulo gulo*) from the Canadian Arctic. Science of the Total Environment, 309 (1–3):81-92.

Hoffman, D.J., Eagles-Smith, C.A., Ackerman, J.T., Adelsbach, T.L. and Stebbins, K.R., 2011. Oxidative stress response of Forster's terns (*Sterna forsteri*) and Caspian terns (*Hydroprogne caspia*) to mercury and selenium bioaccumulation in liver, kidney, and brain. Environmental Toxicology and Chemistry, 30 (4):920-929.

Holloway, T., Voigt, C., Morton, J., Spak, S.N., Rutter, A.P. and Schauer, J.J., 2012. An assessment of atmospheric mercury in the Community Multiscale Air Quality (CMAQ) model at an urban site and a rural site in the Great Lakes Region of North America. Atmospheric Chemistry and Physics, 12 (15):7117-7133.

Hollweg, T.A., Gilmour, C.C. and Mason, R.P., 2010. Mercury and methylmercury cycling in sediments of the mid-Atlantic continental shelf and slope. Limnology and Oceanography, 55 (6):2703-2722.

Holmes, R.M., McClelland, J.W., Peterson, B.J., Shiklomanov, I.A., Shiklomanov, A.I., Zhulidov, A.V., Gordeev, V.V. and Bobrovitskaya, N.N., 2002. A circumpolar perspective on fluvial sediment flux to the Arctic Ocean. Global Biogeochemical Cycles, 16 (4):1098.

Holmes, C.D., Jacob, D.J., Mason, R.P. and Jaffe, D.A., 2009. Sources and deposition of reactive gaseous mercury in the marine atmosphere. Atmospheric Environment, 43 (15):2278-2285.

Holmes, C.D., Jacob, D.J., Corbitt, E.S., Mao, J., Yang, X., Talbot, R. and Slemr, F., 2010. Global atmospheric model for mercury including oxidation by bromine atoms. Atmospheric Chemistry and Physics, 10 (24):12037-12057.

Holmes, R.M., McClelland, J.W., Tank, S.E., Spencer, R.G.M. and Shiklomanov, A.I., 2018. Arctic Great Rivers Observatory. Water Quality Dataset. Available at: https://www.arcticgreatrivers.org/data

Honda, K., Min, B.Y. and Tatsukawa, R., 1986. Distribution of heavy metals and their age-related changes in the eastern great white egret, *Egretta alba modesta*, in Korea. Archives of Environmental Contamination and Toxicology, 15:185-197.

Hood, E., Fellman, J., Spencer, R.G.M., Hernes, P.J., Edwards, R., D'Amore, D. and Scott, D., 2009. Glaciers as a source of ancient and labile organic matter to the marine environment. Nature, 462 (7276):1044-1047.

Hood, E., Battin, T.J., Fellman, J., O'Neel, S. and Spencer, R.G.M., 2015. Storage and release of organic carbon from glaciers and ice sheets. Nature Geoscience, 8 (2):91-96.

Hook, S.E. and Fisher, N.S., 2002. Relating the reproductive toxicity of five ingested metals in calanoid copepods with sulfur affinity. Marine Environmental Research, 53 (2):161-174.

Hopwood, M.J., Carroll, D., Browning, T.J., Meire, L., Mortensen, J., Krisch, S. and Achterberg, E.P., 2018. Non-linear response of summertime marine productivity to increased meltwater discharge around Greenland. Nature Communications, 9 (1):3256.

Hopwood, M.J., Carroll, D., Dunse, T., Hodson, A., Holding, J.M., Iriarte, J.L., Ribeiro, S., Achterberg, E.P., Cantoni, C., Carlson, D.F., Chierici, M., Clarke, J.S., Cozzi, S., Fransson, A., Juul-Pedersen, T., Winding, M.H.S. and Meire, L., 2020. How does glacier discharge affect marine biogeochemistry and primary production in the Arctic? The Cryosphere, 14 (4):1347-1383.

Horowitz, H.M., Jacob, D.J., Zhang, Y., Dibble, T.S., Slemr, F., Amos, H.M., Schmidt, J.A., Corbitt, E.S., Marais, E.A. and Sunderland, E.M., 2017. A new mechanism for atmospheric mercury redox chemistry: implications for the global mercury budget. Atmospheric Chemistry and Physics, 17 (10):6353-6371.

Hossain, M.F., Chen, W. and Zhang, Y., 2015. Bulk density of mineral and organic soils in the Canada's arctic and sub-arctic. Information Processing in Agriculture, 2 (3-4):183-190.

Houben, A.J., French, T.D., Kokelj, S. V., Wang, X., Smol, J.P. and Blais, J.M., 2016. The impacts of permafrost thaw slump events on limnological variables in upland tundra lakes, Mackenzie Delta region. Fundamental and Applied Limnology, 189:11-35.

Houde, M., Taranu, Z., Wang, X., Young, B., Gagnon, P., Ferguson, S.H. and Muir, D.C.G., 2020. Mercury in ringed seals (*Pusa hispida*) from the Canadian Arctic in relation to time and climate parameters. Environmental Toxicology and Chemistry, 39 (12):2562-2474.

Hovel, R., Brammer, J., Hodgson, E., Amos, A., Lantz, T., Turner, C., Proverbs, T. and Lord, S. 2020. The importance of continuous dialogue in community-based wildlife monitoring: case studies of dzan and łuk digaii in the Gwich'in Settlement Area. Arctic Science, 6 (3):154-172.

Hoydal, K. and Dam, M., 2005. AMAP Faroe Islands Heavy Metals and POPs Core Programme 2004 (Report no. 2005:2). Food-, Veterinary and Environmental Agency, Torshavn, Faroe Islands. 53pp.

Hoydal, K. and Dam, M., 2009. AMAP Faroe Islands Heavy Metals and POPs Core Programme 2005–2008 (Report no. US 2009:1). Environment Agency, Argir, Faroe Islands. 55pp.

Hsu-Kim, H., Eckley, C.S., Achá, D., Feng, X., Gilmour, C.C., Jonsson, S. and Mitchell, C.P.J., 2018. Challenges and opportunities for managing aquatic mercury pollution in altered landscapes. Ambio, 47 (2):141-169.

Hu, F.S., Higuera, P.E., Walsh, J.E., Chapman, W.L., Duffy, P.A., Brubaker, L.B. and Chipman, M.L., 2010. Tundra burning in Alaska: linkages to climatic change and sea ice retreat. Journal of Geophysical Research: Biogeosciences, 115 (G4):G04002.

Hu, H., Lin, H., Zheng, W., Rao, B., Feng, X., Liang, L., Elias, D.A. and Gu, B., 2013. Mercury reduction and cell-surface adsorption by *Geobacter sulfurreducens* PCA. Environmental Science & Technology, 47 (19):10922-10930.

Hu, F.S., Higuera, P.E., Duffy, P., Chipman, M.L., Rocha, A.V, Young, A.M., Kelly, R. and Dietze, M.C., 2015. Arctic tundra fires: natural variability and responses to climate change. Frontiers in Ecology and the Environment, 13 (7):369-377.

Hu, X.F., Eccles, K.M. and Chan, H.M.., 2017a. High selenium exposure lowers the odds ratios for hypertension, stroke, and myocardial infarction associated with mercury exposure among Inuit in Canada. Environment International, 102:200-206.

Hu, X.F., Sharin, T. and Chan, H.M.., 2017b. Dietary and blood selenium are inversely associated with the prevalence of stroke among Inuit in Canada. Journal of Trace Elements in Medicine and Biology, 44:322-330.

Hu, X.F., Laird, B.D. and Chan, H.M., 2017c. Mercury diminishes the cardiovascular protective effect of omega-3 polyunsaturated fatty acids in the modern diet of Inuit in Canada. Environmental Research, 152:470-477.

Hu, X.F., Singh, K. and Chan, H.M., 2018a. Mercury exposure, blood pressure, and hypertension: a systematic review and dose-response meta-analysis. Environmental Health Perspectives, 126 (7):076002.

Hu, X.F., Kenny, T.A. and Chan, H.M.. 2018b. Inuit country food diet pattern is associated with lower risk of coronary heart disease. Journal of the America Academy of Nutrition and Dietetics, 118 (7):1237-1248.

Huang, J., Kang, S., Ma, M., Guo, J., Cong, Z., Dong, Z., Yin, R., Xu, J., Tripathee, L., Ram, K. and Wang, F., 2019. Accumulation of atmospheric mercury in glacier cryoconite over Western China. Environmental Science & Technology 53 (12):6632-6639.

Hudelson, K.E., Muir, D.C.G., Drevnick, P.E., Köck, G., Iqaluk, D., Wang, X., Kirk, J.L., Barst, B.D., Grgicak-Mannion, A., Shearon, R. and Fisk, A.T., 2019. Temporal trends, lake-to-lake variation, and climate effects on Arctic char (*Salvelinus alpinus*) mercury concentrations from six High Arctic lakes in Nunavut, Canada. Science of the Total Environment, 678:801-812.

Hudelson, K.E., Drevnick, P.E., Wang, F., Armstrong, D. and Fisk, A.T., 2020. Mercury methylation and demethylation potentials in Arctic lake sediments. Chemosphere, 248:126001.

Hudson, N., Baker, A. and Reynolds, D., 2007. Fluorescence analysis of dissolved organic matter in natural, waste and polluted waters—a review. River Research and Applications, 23 (6):631-649.

Huet, C., Ford, J.D., Edge, V.L., Shirley, J., King, N., IHACC Research Team and Harper, S.L., 2017. Food insecurity and food consumption by season in households with children in an Arctic city: a cross-sectional study. BMC Public Health, 17 (1):578.

Huet, C., Rosol, R. and Egeland, G.M., 2012. The prevalence of food insecurity is high and the diet quality poor in Inuit communities. The Journal of Nutrition, 142 (3):541-547.

Hugelius, G., Tarnocai, C., Broll, G., Canadell, J.G., Kuhry, P. and Swanson, D.K., 2013. The Northern Circumpolar Soil Carbon Database: spatially distributed datasets of soil coverage and soil carbon storage in the northern permafrost regions. Earth System Science Data, 5 (1):3-13.

Hugelius, G., Strauss, J., Zubrzycki, S., Harden, J.W., Schuur, E.A.G., Ping, C.L., Schirrmeister, L., Grosse, G., Michaelson, G.J., Koven, C.D., O'Donnell, J.A., Elberling, B., Mishra, U., Camill, P., Yu, Z., Palmtag, J. and Kuhry, P., 2014. Estimated stocks of circumpolar permafrost carbon with quantified uncertainty ranges and identified data gaps. Biogeosciences, 11 (23):6573-6593.

Humann-Guilleminot, S., Blévin, P., Azou-Barré, A., Yacoumas, A., Gabrielsen, G.W., Chastel, O. and Helfenstein, F., 2018. Sperm collection in black-legged kittiwakes and characterization of sperm velocity and morphology. Avian Research, 9:24.

Hynes, A.J., Donohoue, D.L., Goodsite, M.E. and Hedgecock, I.M., 2009. Our current understanding of major chemical and physical processes affecting mercury dynamics in the atmosphere and at the air-water/terrestrial interfaces. In: Mason, R. and Pirrone, M. (Eds.). Mercury Fate and Transport in the Global Atmosphere: Emissions, Measurements and Models, pp. 427-457. Springer.

ICC, 1992. Principles and Elements for a Comprehensive Arctic Policy. Published for the Inuit Circumpolar Conference (ICC) by McGill University, Montreal, Quebec, Canada. 149pp.

ICC, 2009. Inuit Arctic Policy. Inuit Circumpolar Council (ICC), Anchorage, Alaska. 122pp. Available at: https://www.inuitcircumpolar.com/project/inuit-arctic-policy/

ICC, 2016. Application of Indigenous Knowledge in the Arctic Council. Inuit Circumpolar Council (ICC), Anchorage, Alaska. 2pp. Available at: https://iccalaska.org/wp-icc/wp-content/uploads/2016/03/Application-of-IK-in-the-Arctic-Council.pdf

ICC-Alaska, 2015a. Alaskan Inuit Food Security Conceptual Framework: How to Assess the Arctic from an Inuit Perspective: Summary Report and Recommendations Report. Inuit Circumpolar Council-Alaska (ICC-Alaska), Anchorage, Alaska. 30pp. Available at: https://iccalaska.org/wp-icc/wp-content/uploads/2016/03/Food-Security-Summary-and-Recommendations-Report.pdf

ICC-Alaska, 2015b. Alaskan Inuit Food Security Conceptual Framework: How to Assess the Arctic from an Inuit Perspective: Technical Report. Inuit Circumpolar Council-Alaska (ICC-Alaska), Anchorage, Alaska. 126pp.

ICES, 2020. DOME Marine Environment [database]. Available at: https://www.ices.dk/data/data-portals/Pages/DOME.aspx

Ims, R.A., Ehrich, D., Forbes, B.C., Huntley, B., Walker, D.A. and Wookey, P.A., 2013. Terrestrial Ecosystems (Chapter 12). In: Meltofte, H., (Ed.). Arctic Biodiversity Assessment: Status and Trends in Arctic Biodiversity, pp. 384-440. Conservation of Arctic Flora and Fauna (CAFF) Akureyri, Iceland.

Imura, N., Sukegawa, E., Pan, S.-K., Nagao, K., Kim, J.-Y., Kwan, T. and Ukita, T., 1971. Chemical methylation of inorganic mercury with methylcobalamin, a vitamin B_{12} analog. Science, 172 (3989):1248-1249.

IPCC, 2000. Special Report on Emissions Scenarios (SRES). A Special Report of Working Group III of the Intergovernmental Panel on Climate Change. Nakicenovic, N. and Swart, R. (Eds.). Intergovernmental Panel on Climate Change (IPCC), Cambridge University Press, Cambridge, UK. 570pp.

IPCC, 2013. Climate Change 2013: The Physical Science Basis. Contribution of Working Group I to the Fifth Assessment Report of the Intergovernmental Panel on Climate Change. Stocker, T.F., Qin, D., Plattner, G.-K., Tignor, M., Allen, S.K., Boschung, J., Nauels, A., Xia, Y., Bex, V. and Midgley, P.M. (Eds.). Intergovernmental Panel on Climate Change (IPCC), Cambridge University Press, Cambridge, UK and New York, NY, USA. 1535pp.

IPCC, 2014. Climate Change 2014: Synthesis Report. Contribution of Working Groups I, II and III to the Fifth Assessment Report of the Intergovernmental Panel on Climate Change. Core Writing Team, Pachauri, R.K. and Meyer, L.A. (Eds.). Intergovernmental Panel on Climate Change (IPCC), Geneva, Switzerland. 151pp.

IPCC, 2019: Summary for Policymakers. In: IPCC Special Report on the Ocean and Cryosphere in a Changing Climate, Pörtner, H.-O., Roberts, D.C., Masson-Delmotte, V., Zhai, P., Tignor, M., Poloczanska, E., Mintenbeck, K., Alegría, A., Nicolai, M., Okem, A., Petzold, J., Rama, B. and Weyer, N.M. (Eds.), pp. 3-35. Intergovernmental Panel on Climate Change (IPCC).

Irrgang, A.M., Lantuit, H., Manson, G.K., Günther, F., Grosse, G. and Overduin, P.P., 2018. Variability in rates of coastal change along the Yukon coast, 1951 to 2015. Journal of Geophysical Research: Earth Surface, 123 (4):779-800.

ISIUOP, 2021. Inuit Siku Atlas. Inuit Sea Ice Use and Occupancy Project (ISIUOP). Available at: https://sikuatlas.ca/index.html

Isles, P.D.F., Jonsson, A., Creed, I.F. and Bergström, A.-K., 2020. Does browning affect the identity of limiting nutrients in lakes? Aquatic Sciences, 82 (2):45.

ITK, 2018. National Inuit strategy on research. Inuit Tapiriit Kanatami (ITK), Ottawa, Ontario, Canada. 48pp. Available at: https://www.itk.ca/wp-content/uploads/2018/04/ITK_NISR-Report_English_low_res.pdf

Iverson, S.A., Gilchrist, H.G., Smith, P.A., Gaston, A.J. and Forbes, M.R., 2014. Longer ice-free seasons increase the risk of nest depredation by polar bears for colonial breeding birds in the Canadian Arctic. Proceedings of the Royal Society B: Biological Sciences, 281 (1779):20133128.

IVL, 2015. Metals in Mosses. Institute for Water and Air Conservation Research, Swedish Environmental Research Institute (IVL), Göteborg, Sweden. 115pp. Available at: https://www.ivl.se/download/18.76c6e08e1573302315f20e/1474381195136/C204.pdf (Swedish Language).

Jackson, T.A, 2019. Stratigraphic variations in the $\delta^{201}Hg/\delta^{199}Hg$ ratio of mercury in sediment cores as historical records of methylmercury production in lakes. Journal of Paleolimnology, 61 (4):387-401.

Jacob, D.J., Liu, H., Mari, C. and Yantosca, R.M., 2000. Harvard wet deposition scheme for GMI. Harvard University Atmospheric Chemistry Modeling Group. 6pp. Available at: https://silo.tips/download/harvard-wet-deposition-scheme-for-gmi (accessed February 2000).

Jacobson, J.L., Muckle, G., Ayotte, P., Dewailly, É. and Jacobson, S.W., 2015. Relation of prenatal methylmercury exposure from environmental sources to childhood IQ. Environmental Health Perspectives, 123 (8):827-833.

Jæger, I., Hop, H. and Gabrielsen, G.W., 2009. Biomagnification of mercury in selected species from an Arctic marine food web in Svalbard. Science of the Total Environment, 407 (16):4744-4751.

Jaffe, D., Prestbo, E., Swartzendruber, P., Weiss-Penzias, P., Kato, S., Takami, A., Hatakeyama, S. and Kajii, Y., 2005. Export of atmospheric mercury from Asia. Atmospheric Environment, 39 (17):3029-3038.

Jaffe, D.A., Lyman, S., Amos, H.M., Gustin, M.S., Huang, J., Selin, N.E., Levin, L., ter Schure, A., Mason, R.P., Talbot, R., Rutter, A., Finley, B., Jaeglé, L., Shah, V., McClure, C., Ambrose, J., Gratz, L., Lindberg, S., Weiss-Penzias, P., Sheu, G.-R., Feddersen, D., Horvat, M., Dastoor, A., Hynes, A.J., Mao, H., Sonke, J.E., Slemr, F., Fisher, J.A., Ebinghaus, R., Zhang, Y. and Edwards, G., 2014. Progress on understanding

atmospheric mercury hampered by uncertain measurements. Environmental Science & Technology, 48 (13):7204-7206.

Jakobsson, M., 2002. Hypsometry and volume of the Arctic Ocean and its constituent seas. Geochemistry, Geophysics, Geosystems, 3 (5):1-18.

Jakobsson, M., 2004. Correction to "Hypsometry and volume of the Arctic Ocean and its constituent seas." Geochemistry, Geophysics, Geosystems, 5 (2):Q02005.

Jenkins, L.K., Barry, T., Bosse, K.R., Currie, W.S., Christensen, T., Longan, S., Shuchman, R.A., Tanzer, D. and Taylor, J.J., 2020. Satellite-based decadal change assessments of pan-Arctic environments. Ambio, 49 (3):820-832.

Jensen, A.M., Scanlon, T.M. and Riscassi, A.L., 2017. Emerging investigator series: the effect of wildfire on streamwater mercury and organic carbon in a forested watershed in the southeastern United States. Environmental Science: Processes & Impacts, 19 (12):1505-1517.

Jenssen, B.M., 2006. Endocrine-disrupting chemicals and climate change: a worst-case combination for Arctic marine mammals and seabirds? Environmental Health Perspectives, 114 (Supplement 1):76-80.

Jenssen, B.M., Villanger, G.D., Gabrielsen, K.M., Bytingsvik, J., Bechshoft, T., Ciesielski, T.M., Sonne, C. and Dietz, R., 2015. Anthropogenic flank attack on polar bears: interacting consequences of climate warming and pollutant exposure. Frontiers in Ecology and Evolution, 3:16.

Jeppesen, C., Jørgensen, M.E. and Bjerregaard, P., 2012. Assessment of consumption of marine food in Greenland by a food frequency questionnaire and biomarkers. International Journal of Circumpolar Health, 71 (1):18361.

Jeppesen, C., Valera, B., Nielsen, N.O., Bjerregaard, P. and Jørgensen, M.E., 2015. Association between whole blood mercury and glucose intolerance among adult Inuit in Greenland. Environmental Research, 143 (Part A):192-197.

Jeremiason, J.D., Portner, J.C., Aiken, G.R., Hiranaka, A.J., Dvorak, M.T., Tran, K.T. and Latch, D.E., 2015. Photoreduction of Hg(II) and photodemethylation of methylmercury: the key role of thiol sites on dissolved organic matter. Environmental Sciences: Processes & Impacts, 17 (11):1892-1903.

Jewett, S.C. and Duffy, L.K., 2007. Mercury in fishes of Alaska, with emphasis on subsistence species. Science of the Total Environment, 387(1-3):3-27.

Jiang, S., Liu, X. and Chen, Q., 2011. Distribution of total mercury and methylmercury in lake sediments in Arctic Ny-Ålesund. Chemosphere, 83 (8):1108-1116.

Jiang, T., Wang, D., Meng, B., Chi, B., Laudon, H. and Liu, J., 2020. The concentrations and characteristics of dissolved organic matter in high-latitude lakes determine its ambient reducing capacity. Water Research, 169:115217.

Jiao, Y.G. and Dibble, T.S., 2015. Quality structures, vibrational frequencies, and thermochemistry of the products of reaction of BrHg• with NO_2, HO_2, ClO, BrO, and IO. Journal of Physical Chemistry A, 119 (42):10502-10510.

Jiao, C. and Flanner, M.G., 2016. Changing black carbon transport to the Arctic from present day to the end of 21st century. Journal of Geophysical Research: Atmospheres, 121 (9):4734-4750.

Jiskra, M., Wiederhold, J.G., Skyllberg, U., Kronberg, R.M., Hajdas, I. and Kretzschmar, R., 2015. Mercury deposition and re-emission pathways in boreal forest soils investigated with Hg isotope signatures. Environmental Science & Technology, 49 (12):7188-7196.

Jiskra, M., Wiederhold, J.G., Skyllberg, U., Kronberg, R.M. and Kretzschmar, R., 2017. Source tracing of natural organic matter bound mercury in boreal forest runoff with mercury stable isotopes. Environmental Science: Processes & Impacts, 19 (10):1235-1248.

Jiskra, M., Sonke, J.E., Obrist, D., Bieser, J., Ebinghaus, R., Myhre, C.L., Pfaffhuber, K.A., Wängberg, I., Kyllönen, K., Worthy, D., Martin, L.G., Labuschagne, C., Mkololo, T., Ramonet, M., Magand O. and Dommergue, A., 2018. A vegetation control on seasonal variations in global atmospheric mercury concentrations. Nature Geoscience, 11 (4):244-250.

Jiskra, M., Sonke, J.E., Agnan, Y., Helmig, D. and Obrist, D., 2019. Insights from mercury stable isotopes on terrestrial–atmosphere exchange of Hg(0) in the Arctic tundra. Biogeosciences, 16 (20):4051-4064.

Johansen, P., Muir, D., Asmund, G. and Riget, F., 2004. Human exposure to contaminants in the traditional Greenland diet. Science of the Total Environment, 331(1-3):189-206.

Johanson, G., 2010. 1.08-Modeling of Disposition. In: McQueen, C.A. (Ed.). Comprehensive Toxicology. Second edition, pp. 153-177. Elsevier, Oxford.

Johnson-Down, L. and Egeland, G.M. 2010. Adequate nutrient intakes are associated with traditional food consumption in nunavut inuit children aged 3-5 years. The Journal of Nutrition. 140 (7): 1311-1316.

Johnson, K.P., Blum, J.D., Keeler, G.J. and Douglas, T.A., 2008. Investigation of the deposition and emission of mercury in Arctic snow during an atmospheric mercury depletion event. Journal of Geophysical Research: Atmospheres, 113 (D17):D17304.

Johnson, N., Alessa, L., Behe, C., Danielsen, F., Gearheard, S., Gofman-Wallingford, V., Kliskey, A., Krümmel, E., Lynch, A., Mustonen, T., Pulsifer, P. and Svoboda, M., 2015. The contributions of community-based monitoring and traditional knowledge to Arctic observing networks: reflections on the state of the field. Arctic, 68 (5; Supplement 1):28-40.

Johnson, N., Behe, C., Danielsen, F., Krümmel, E.M., Nickels, S., and Pulsifer, 2016. Community-based monitoring and Indigenous Knowledge in a changing Arctic: A review for the sustaining Arctic observing networks. Final report to sustaining Arctic observing networks. Inuit Circumpolar Council. Ottawa, Ontario, Canada. Available at: https://www.inuitcircumpolar.com/project/community-based-monitoring-and-indigenous-knowledge-in-a-changing-arctic-a-review-for-the-sustaining-arctic-observing-networks%E2%80%8B/

Jones, B.M., Arp, C.D., Jorgenson, M.T., Hinkel, K.M., Schmutz, J.A. and Flint, P.L., 2009. Increase in the rate and uniformity of coastline erosion in Arctic Alaska. Geophysical Research Letters, 36 (3):L03503.

Jones, B.M., Grosse, G., Arp, C.D., Miller, E., Liu, L., Hayes, D.J. and Larsen, C.F., 2015. Recent Arctic tundra fire initiates widespread thermokarst development. Scientific Reports, 5 (1):15865.

Jones, J., Cunsolo, A. and Harper, S.L., 2018. Who is research serving? A systematic realist review of circumpolar environment-related Indigenous health literature. PLoS ONE, 13 (5):e0196090.

Jones, D.S., Walker, G.M., Johnson, N.W., Mitchell, C.P.J., Coleman Wasik, J.K. and Bailey, J.V., 2019. Molecular evidence for novel mercury methylating microorganisms in sulfate-impacted lakes. The ISME Journal, 13 (7):1659-1675.

Jonsson, S., Mazrui, N.M. and Mason, R.P., 2016. Dimethylmercury formation mediated by inorganic and organic reduced sulfur surfaces. Scientific Reports, 6 (1):27958.

Jonsson, S., Skyllberg, U., Nilsson, M.B., Westlund, P.-O., Shchukarev, A., Lundberg, E. and Björn, E., 2012. Mercury methylation rates for geochemically relevant HgII species in sediments. Environmental Science & Technology, 46 (21):11653-11659.

Jonsson, S., Skyllberg, U., Nilsson, M.B., Lundberg, E., Andersson, A. and Björn, E., 2014. Differentiated availability of geochemical mercury pools controls methylmercury levels in estuarine sediment and biota. Nature Communications, 5 (1):4624.

Jonsson, S., Nerentorp Mastromonaco, M.G., Gårdfeldt, K. and Mason, R.P., 2022. Distribution of total mercury and methylated mercury species in central Arctic Ocean water and ice. Marine Chemistry. 242, 104105.

Jorgenson, M.T., Racine, C.H., Walters, J.C. and Osterkamp, T.E., 2001. Permafrost degradation and ecological changes associated with a warming climate in central Alaska. Climatic Change, 48 (4):551-579.

Jorgenson, M.T., Shur, Y.L. and Pullman, E.R., 2006. Abrupt increase in permafrost degradation in Arctic Alaska. Geophysical Research Letters, 33 (2): L02503.

Jörundsdóttir, H.Ó., Jensen, S., Hylland, K., Holth, T.F., Gunnlaugsdóttir, H., Svavarsson, J., Ólafsdóttir, Á., El-Taliawy, H., Rigét, F., Strand, J., Nyberg, E., Bignert, A., Hoydal, K.S. and Halldórsson, H.P., 2014. Pristine Arctic: background mapping of PAHs, PAH metabolites and inorganic trace elements in the North-Atlantic Arctic and Sub-Arctic coastal environment. Science of the Total Environment, 493:719-728.

Juhasz, C.-C., Shipley, B., Gauthier, G., Berteaux, D. and Lecomte, N., 2020. Direct and indirect effects of regional and local climatic factors on trophic interactions in the Arctic tundra. Journal of Animal Ecology, 89 (3):704-715.

Julvez, J. and Grandjean, P., 2013. Genetic susceptibility to methylmercury developmental neurotoxicity matters. Frontiers in Genetics, 4:278.

Kahilainen, K.K., Thomas, S.M., Keva, O., Hayden, B., Knudsen, R., Eloranta, A.P., Tuohiluoto, K., Amundsen, P.-A., Malinen, T. and Järvinen, A., 2016. Seasonal dietary shift to zooplankton influences stable isotope ratios and total mercury concentrations in Arctic charr (*Salvelinus alpinus* (L.)). Hydrobiologia, 783 (1):47-63.

Kahilainen, K.K., Thomas, S.M., Nystedt, E.K.M., Keva, O., Malinen, T. and Hayden, B., 2017. Ecomorphological divergence drives differential mercury bioaccumulation of polymorphic European whitefish

(*Coregonus lavaretus*) populations of Subarctic lakes. Science of the Total Environment, 599-600:1768-1778.

Kaiser, K., Canedo-Oropeza, M., McMahon, R. and Amon, R.M.W., 2017. Origins and transformations of dissolved organic matter in large Arctic rivers. Scientific Reports, 7 (1):13064.

Kalinchuk, V.V., Lopatnikov, E.A., Astakhov, A.S., Ivanov, M.V. and Hu, L., 2021. Distribution of atmospheric gaseous elemental mercury (Hg(0)) from the Sea of Japan to the Arctic, and Hg(0) evasion fluxes in the Eastern Arctic Seas: results from a joint Russian-Chinese cruise in fall 2018. Science of the Total Environment, 753:142003.

Kamp, J., Skov, H., Jensen, B. and Sørensen, L.L., 2018. Fluxes of gaseous elemental mercury (GEM) in the High Arctic during atmospheric mercury depletion events (AMDEs). Atmospheric Chemistry and Physics, 18 (9):6923-6938.

Kåresdotter, E., Destouni, G., Ghajarnia, N., Hugelius, G. and Kalantari, Z., 2021. Mapping the vulnerability of Arctic wetlands to global warming. Earth's Future 9, e2020EF001858.

Karimi, R., Chen, C.Y., Pickhardt, P.C., Fisher, N.S. and Folt, C.L., 2007. Stoichiometric controls of mercury dilution by growth. Proceedings of the National Academy of Sciences of the United State of America, 104 (18):7477-7482.

Kawai, T., Sakurai, T. and Suzuki, N., 2020. Application of a new dynamic 3-D model to investigate human impacts on the fate of mercury in the global ocean. Environmental Modelling & Software, 124:104599.

Keeler, G.J., Gratz, L.E. and Al-Wali, K., 2005. Long-term atmospheric mercury wet deposition at Underhill, Vermont. Ecotoxicology, 14 (1-2):71-83.

Kelly, E.N., Schindler, D.W., St. Louis, V.L., Donald, D.B. and Vladicka, K.E., 2006. Forest fire increases mercury accumulation by fishes via food web restructuring and increased mercury inputs. Proceedings of the National Academy of Sciences of the United States of America, 103 (51):19380-19385.

Kenny, T.A., Hu, X.F., Kuhnlein, H.V., Wesche, S.D. and Chan, H.M., 2018. Dietary sources of energy and nutrients in the contemporary diet of Inuit adults: results from the 2007-08 Inuit Health Survey. Public Health Nutrition, 21 (7):1319-1331.

Kersten, M. and Smedes, F., 2002. Normalization procedures for sediment contaminants in spatial and temporal trend monitoring. Journal of Environmental Monitoring, 4 (1):109-115.

Keuper, F., Wild, B., Kummu, M., Beer, C., Blume-Werry, G., Fontaine, S., Gavazov, K., Gentsch, N., Guggenberger, G., Hugelius, G., Jalava, M., Koven, C., Krab, E.J., Kuhry, P., Monteux, S., Richter, A., Shahzad, T., Weedon, J.T. and Dorrepaal, E., 2020. Carbon loss from northern circumpolar permafrost soils amplified by rhizosphere priming. Nature Geoscience, 13 (8):560-565.

Keva, O., Hayden, B., Harrod, C. and Kahilainen, K.K., 2017. Total mercury concentrations in liver and muscle of European whitefish (*Coregonus lavaretus* (L.)) in a Subarctic lake - assessing the factors driving year-round variation. Environmental Pollution, 231 (Part 2):1518-1528.

Khan, M.A. and Wang, F., 2010. Chemical demethylation of methylmercury by selenoamino acids. Chemical Research in Toxicology, 23 (7):1202-1206.

Khayrallah, N.H., 1985. The tolerance of *Bathyporeia pilosa* Lindstrom (Amphipoda: Haustoriidae) to organic and inorganic salts of mercury. Marine Environmental Research, 15 (2):137-151.

Kidd, K.A., Muir, D.C.G., Evans, M.S., Wang, X., Whittle, M., Swanson, H.K., Johston, T. and Guildford, S., 2012. Biomagnification of mercury through lake trout (*Salvelinus namaycush*) food webs of lakes with different physical, chemical and biological characteristics. Science of the Total Environment, 438:135-143.

Kim, H., Rhee, T.S., Hahm, D., Hwang, C.Y., Yang, J. and Han, S., 2016. Contrasting distributions of dissolved gaseous mercury concentration and evasion in the North Pacific Subarctic Gyre and the Subarctic Front. Deep Sea Research Part I: Oceanographic Research Papers, 110:90-98.

Kim, H., Soerensen, A.L., Hur, J., Heimbürger, L.-E., Hahm, D., Rhee, T.S., Noh, S. and Han, S., 2017. Methylmercury mass budgets and distribution characteristics in the western Pacific Ocean. Environmental Science & Technology, 51 (3):1186-1194.

Kim, H., Kwon, S.Y., Lee, K., Lim, D., Han, S., Kim, T.-W., Joo, Y.J., Lim, J., Kang, M.-H. and Nam, S.-I., 2020a. Input of terrestrial organic matter linked to deglaciation increased mercury transport to the Svalbard fjords. Scientific Reports, 10 (1):3446.

Kim, J., Soerensen, A.L., Kim, M.S., Eom, S., Rhee, T.S., Jin, Y K. and Han, S., 2020b. Mass budget of methylmercury in the east Siberian Sea: the importance of sediment sources. Environmental Science & Technology, 54 (16):9949–9957.

Kinghorn, A., Humphries, M.M., Outridge, P. and Chan, H.M., 2008. Teeth as biomonitors of selenium concentrations in tissues of beluga whales (Delphinapterus leucas). Science of the Total Environment, 402:43-50.

Kirk, J.L. and St. Louis, V.L., 2009. Multiyear total and methyl mercury exports from two major Sub-Arctic rivers draining into Hudson Bay, Canada. Environmental Science & Technology, 43 (7):2254-2261.

Kirk, J. and Gleason, A., 2015. Tracking long-range atmospheric transport of contaminants in Arctic regions using lake sediments. In: Blais, J., Rosen, M., and Smol, J. (Eds.). Environmental Contaminants. Developments in Paleoenvironmental Research, Volume 18, pp. 223-262. Springer, Dordrecht.

Kirk, J.L., St Louis, V.L. and Sharp, M.J., 2006. Rapid reduction and reemission of mercury deposited into snowpacks during atmospheric mercury depletion events at Churchill, Manitoba, Canada. Environmental Science & Technology, 40 (24):7590-7596.

Kirk, J.L., St. Louis, V.L., Hintelmann, H., Lehnherr, I., Else, B. and Poissant, L., 2008. Methylated mercury species in marine waters of the Canadian High and Sub Arctic. Environmental Science & Technology, 42 (22):8367-8373.

Kirk, J.L., Muir, D.C.M., Antoniades, D., Douglas, M.S.V., Evans, M.S., Jackson, T.A., Kling, H., Lamoureux, S., Lim, D.S.S., Pienitz, R., Smol, J.P., Stewart, K., Wang, X. and Yang, F., 2011. Climate Change and mercury accumulation in Canadian High and Subarctic lakes. Environmental Science & Technology, 45 (3):964-970.

Kirk, J.L., Lehnherr, I., Andersson, M., Braune, B.M., Chan, L., Dastoor, A.P., Dunford, D., Gleason, A.L., Loseto, L.L., Steffen, A. and St. Louis, V.L., 2012. Mercury in Arctic marine ecosystems: sources, pathways and exposure. Environmental Research, 119:64-87.

Kirk, J.L., Muir, D.C.G., Gleason, A., Wang, X., Lawson, G., Frank, R.A., Lehnherr, I. and Wrona, F., 2014. Atmospheric deposition of mercury and methylmercury to landscapes and waterbodies of the Athabasca oil sands region. Environmental Science & Technology, 48 (13):7374-7383.

Kirk, L.E., Jørgensen, J.S., Nielsen, F. and Grandjean, P., 2017. Public health benefits of hair-mercury analysis and dietary advice in lowering methylmercury exposure in pregnant women. Scandinavian Journal of Public Health, 45 (4):444-451.

Klapstein, S.J. and O'Driscoll, N.J., 2018. Methylmercury biogeochemistry in freshwater ecosystems: a review focusing on DOM and photodemethylation. Bulletin of Environmental Contamination and Toxicology, 100 (1):14-25.

Klapstein, S.J., Ziegler, S.E. and O'Driscoll, N.J., 2017. Methylmercury photodemethylation is inhibited in lakes with high dissolved organic matter. Environmental Pollution, 232:392-401.

Klonecki, A., Hess, P., Emmons, L., Smith, L., Orlando, J. and Blake, D., 2003. Seasonal changes in the transport of pollutants into the Arctic troposphere-model study. Journal of Geophysical Research: Atmospheres, 108 (D4):8367.

Kluane First Nation, 2016. Remembering Our Past, Nourishing Our Future [Film]. Available at: https://www.aicbr.ca/kfn-project

Klunder, M.B., Bauch, D., Laan, P., de Baar, H.J.W., van Heuven, S. and Ober, S., 2012. Dissolved iron in the Arctic shelf seas and surface waters of the central Arctic Ocean: impact of Arctic river water and ice-melt. Journal of Geophysical Research: Oceans, 117 (C1):C01027.

Knobeloch, L., Tomasallo, C. and Anderson, H., 2011. Biomonitoring as an intervention against methylmercury exposure. Public Health Reports, 126 (4):568-574.

Kohlbach, D., Graeve, M., Lange, B.A., David, C., Peeken, I. and Flores, H., 2016. The importance of ice algae-produced carbon in the central Arctic Ocean ecosystem: food web relationships revealed by lipid and stable isotope analyses. Limnology and Oceanography, 61 (6):2027-2044.

Kohlbach, D., Schaafsma, F.L., Graeve, M., Lebreton, B., Lange, B.A., David, C. and Flores, H., 2017. Strong linkage of polar cod (*Boreogadus saida*) to sea ice algae-produced carbon: evidence from stomach content, fatty acid and stable isotope analyses. Progress in Oceanography, 152:62-74.

Kohlenberg, A.J., Turetsky, M.R., Thompson, D.K., Branfireun, B.A. and Mitchell, C.P.J., 2018. Controls on boreal peat combustion and resulting emissions of carbon and mercury. Environmental Research Letters, 13 (3):035005.

Kohler, S.G., Heimbürger-Boavida, L.E., Petrova, M.V., Digernes, M.G., Sanchez, N., Dufour, A., Simić, A., Ndungu, K. and Ardelan, M.V.,

2022. Arctic Ocean's wintertime mercury concentrations limited by seasonal loss on the shelf. Nature Geoscience, 21:621-626.

Kokelj, S.V., Lacelle, D., Lantz, T.C., Tunnicliffe, J., Malone, L., Clark, I.D. and Chin, K.S., 2013. Thawing of massive ground ice in mega slumps drives increases in stream sediment and solute flux across a range of watershed scales. Journal of Geophysical Research: Earth Surface, 118 (2):681-692.

Kokelj, S.V., Tunnicliffe, J., Lacelle, D., Lantz, T.C., Chin, K.S. and Fraser, R., 2015. Increased precipitation drives mega slump development and destabilization of ice-rich permafrost terrain, northwestern Canada. Global and Planetary Change, 129:56-68.

Korosi, J.B., McDonald, J., Coleman, K.A., Palmer, M.J., Smol, J.P., Simpson, M.J. and Blais, J.M., 2015. Long-term changes in organic matter and mercury transport to lakes in the sporadic discontinuous permafrost zone related to peat subsidence. Limnology and Oceanography, 60 (5):1550-1561.

Korosi, J.B., Griffiths, K., Smol, J.P. and Blais, J.M., 2018. Trends in historical mercury deposition inferred from lake sediment cores across a climate gradient in the Canadian High Arctic. Environmental Pollution, 241:459-467.

Kos, G., Ryzhkov, A., Dastoor, A., Narayan, J., Steffen, A., Ariya, P.A. and Zhang, L., 2013. Evaluation of discrepancy between measured and modelled oxidized mercury species. Atmospheric Chemistry and Physics, 13 (9):4839-4863.

Koven, C.D., Riley, W.J. and Stern, A., 2013. Analysis of permafrost thermal dynamics and response to climate change in the CMIP5 earth system models. Journal of Climate, 26 (6):1877-1900.

Krabbenhoft, D.P. and Sunderland, E.M., 2013. Environmental science. Global change and mercury. Science, 341 (6153):1457-1458.

Kral, M.J., Idlout, L., Minore, J.B., Dyck, R.J. and Kirmayer, L.J., 2011. Unikkaartuit: meanings of well-Being, unhappiness, health, and community change among Inuit in Nunavut, Canada. American Journal of Community Psychology, 48 (3-4):426-438.

Kristmannsdóttir, H., Björnsson, A., Pálsson, S. and Sveinbjörnsdóttir, A.E., 1999. The impact of the 1996 subglacial volcanic eruption in Vatnajökull on the river Jökulsá á Fjöllum, North Iceland. Journal of Volcanology and Geothermal Research, 92 (3-4):359-372.

Krnavek, L., Simpson, W.R., Carlson, D., Domine, F., Douglas, T.A. and Sturm, M., 2012. The chemical composition of surface snow in the Arctic: examining marine, terrestrial, and atmospheric influences. Atmospheric Environment, 50:349-359.

Kronberg, R.-M., Drott, A., Jiskra, M., Wiederhold, J.G., Björn, E. and Skyllberg, U., 2016. Forest harvest contribution to boreal freshwater methyl mercury load. Global Biogeochemical Cycles, 30 (6):825-843.

Krümmel, E. M., Macdonald, R.W., Kimpe, L.E., Gregory-Eaves, I., Demers, M.J., Smol, J.P., Finney, B. and Blais, J.M., 2003. Delivery of pollutants by spawning salmon - fish dump toxic industrial compounds in Alaskan lakes on their return from the ocean. Nature, 425 (6955):255-256.

Kruse, J., Poppel, B., Abryutina, L., Duhaime, G., Martin, S., Poppel, M., Kruse, M., Ward, E., Cochran, P. and Hanna, V., 2008. Survey of Living Conditions in the Arctic (SLiCA). In: Møller, V., Huschka, D. and Michalos, A.C. (Eds.). Barometers of Quality of Life Around the Globe. Social Indicators Research Series, vol. 33, pp. 107-134. Springer, Dordrecht.

Kumar, A. and Wu, S., 2019. Mercury pollution in the Arctic from wildfires: source attribution for the 2000s. Environmental Science & Technology, 53 (19):11269-11275.

Kumar, A., Wu, S., Huang, Y., Liao, H. and Kaplan, J. O., 2018. Mercury from wildfires: global emission inventories and sensitivity to 2000-2050 global change. Atmospheric Environment, 173:6-15.

Kutz, S.J., Jenkins, E.J., Veitch, A.M., Ducrocq, J., Polley, L., Elkin, B. and Lair, S., 2009. The Arctic as a model for anticipating, preventing, and mitigating climate change impacts on host-parasite interactions. Veterinary Parasitology, 163 (3):217-228.

Kwon, S.Y. and Selin, N.E., 2016. Uncertainties in atmospheric mercury modeling for policy Evaluation. Current Pollution Reports, 2 (2):103-114.

Laidre, K.L., Stern, H., Kovacs, K.M., Lowry, L., Moore, S.E., Regehr, E.V., Ferguson, S.H., Wiig, Ø., Boveng, P., Angliss, R.P., Born, E.W., Litovka, D., Quakenbush, L., Lydersen, C., Vongraven and D., Ugarte, F., 2015. Arctic marine mammal population status, sea ice habitat loss, and conservation recommendations for the 21st century. Conservation Biology, 29 (3):724-737.

Laird, B.D., Shade, C., Gantner, N., Chan, H.M. and Siciliano, S.D., 2009. Bioaccessibility of mercury from traditional northern country foods measured using an *in vitro* gastrointestinal model is independent of mercury concentration. Science of the Total Environment, 407 (23):6003-6008.

Laird, B.D., Goncharov, A.B., Egeland, G.M. and Chan, H.M., 2013. Dietary advice on Inuit traditional food use needs to balance benefits and risks of mercury, selenium, and n3 fatty acids. The Journal of Nutrition, 143 (6):923-930.

Lam, K.T., Wilhelmsen, C.J., Schwid, A.C., Jiao, Y. and Dibble, T.S., 2019a. Computational study on the photolysis of BrHgONO and the Reactions of $BrHgO^{\bullet}$ with CH4, C_2H_6, NO, and NO_2: implications for formation of $Hg(^{I}I)$ compounds in the atmosphere. The Journal of Physical Chemistry A, 123 (8):1637-1647.

Lam, K.T., Wilhelmsen, C.J., Dibble, T.S., 2019b. $BrHgO^{\bullet}$ + C_2H_4 and $BrHgO^{\bullet}$ + HCHO in atmospheric oxidation of mercury: determining rate constants of reactions with prereactive complexes and bifurcation. The Journal of Physical Chemistry A, 123 (28):6045-6055.

Lamarche-Gagnon, G., Wadham, J.L., Sherwood Lollar, B., Arndt, S., Fietzek, P., Beaton, A.D., Tedstone, A.J., Telling, J., Bagshaw, E.A., Hawkings, J.R., Kohler, T.J., Zarsky, J.D., Mowlem, M.C., Anesio, A.M. and Stibal, M., 2019. Greenland melt drives continuous export of methane from the ice-sheet bed. Nature, 565 (7737):73-77.

Lamborg, C.H., Fitzgerald, W.F., Vandal, G.M. and Rolfhus, K. R., 1995. Atmospheric Mercury in Northern Wisconsin: sources and species. In: Porcella, D.B., Huckabee, J.W. and Wheatley, B. (Eds.). Mercury as a Global Pollutant, pp. 189-198. Springer, Dordrecht.

Lammers, R.B., Shiklomanov, A.I., Vörösmarty, C.J., Fekete, B.M. and Peterson, B.J., 2001. Assessment of contemporary Arctic river runoff based on observational discharge records. Journal of Geophysical Research: Atmospheres, 106 (D4):3321-3334.

Landers, D.H., Ford, J., Gubala, C., Monetti, M., Lasorsa, B.K. and Martinson, J., 1995. Mercury in vegetation and lake sediments from the US Arctic. Water, Air, & Soil Pollution, 80:591-601.

Landis, M.S. and Keeler, G.J., 2002. Atmospheric mercury deposition to Lake Michigan during the Lake Michigan mass balance study. Environmental Science & Technology, 36 (21):4518-4524.

Lantuit, H. and Pollard, W.H., 2008. Fifty years of coastal erosion and retrogressive thaw slump activity on Herschel Island, southern Beaufort Sea, Yukon Territory, Canada. Geomorphology, 95 (1-2):84-102.

Lantuit, H., Overduin, P.P., Couture, N., Wetterich, S., Aré, F., Atkinson, D., Brown, J., Cherkashov, G., Drozdov, D., Forbes, D.L., Graves-Gaylord, A., Grigoriev, M., Hubberten, H.-W., Jordan, J., Jorgenson, T., Ødegård, R.S., Ogorodov, S., Pollard, W.H., Rachold, V., Sedenko, S., Solomon, S., Steenhuisen, F., Streletskaya, I. and Vasiliev, A., 2012. The Arctic coastal dynamics database: a new classification scheme and statistics on Arctic permafrost coastlines. Estuaries and Coasts, 35:383-400.

Lantz, T.C. and Kokelj, S.V., 2008. Increasing rates of retrogressive thaw slump activity in the Mackenzie Delta region, N.W.T., Canada. Geophysical Research Letters, 35 (6):L06502.

Larose, C., Dommergue, A., Marusczak, N., Coves, J., Ferrari, C.P. and Schneider, D., 2011. Bioavailable mercury cycling in polar snowpacks. Environmental Science & Technology, 45 (6):2150-2156.

Larsen, T.J., Jørgensen, M.E., Larsen, C.V.L., Dahl-Petersen, I.K., Rønn, P.F., Bjerregaard, P. and Byberg, S., 2018. Whole blood mercury and the risk of cardiovascular disease among the Greenlandic population. Environmental Research, 164:310-315.

Laske, S.M., Amundsen, P.-A., Christoffersen, K.S., Erkinaro, J., Guðbergsson, G., Hayden, B., Heino, J., Holmgren, K., Kahilainen, K.K., Lento, J., Orell, P., Östergren, J., Power, M., Rafikov, R., Romakkaniemi, A., Svenning, M.-A., Swanson, H., Whitman, M. and Zimmerman, C.E., 2022. Circumpolar patterns of Arctic freshwater fish diversity: a baseline for monitoring. Freshwater Biology, (67):176-193.

Lau, D.C.P., Goedkoop, W., Schartau, A.K., Hayden, B., Erkinaro, J., Karlsson, J., Heino, J., Ruuhijärvi, J., Holmgren, K., Kahilainen, K.K., Christoffersen, K., Forsström, L., Kahlert, M., Mjelde, M., Svenning, M., Liljaniemi, P., Karjalainen, S.M., Hellsten, S., Sandøy, S. and Vrede, T., 2020. Multitrophic biodiversity patterns and environmental descriptors of Sub-Arctic lakes in northern Europe. Freshwater Biology, 67 (1):30-48.

Lavoie, R.A., Jardine, T.D., Chumchal, M.M., Kidd, K.A. and Campbell, L.M., 2013. Biomagnification of mercury in aquatic food webs: a worldwide meta-analysis. Environmental Science & Technology, 47 (23):13385-13394.

Lavoie, R.A., Bouffard, A., Maranger, R. and Amyot, M., 2018. Mercury transport and human exposure from global marine fisheries. Science Reports, 8 (1):6705.

Lavoie, R.A., Amyot, M. and Lapierre, J.-F., 2019. Global meta-analysis on the relationship between mercury and dissolved organic carbon in freshwater environments. Journal of Geophysical Research: Biogeosciences, 124 (6):1508-1523.

Law, K.S., Stohl, A., Quinn, P.K., Brock, C.A., Burkhart, J.F., Paris, J.-D., Ancellet, G., Singh, H.B., Roiger, A., Schlager, H., Dibb, J., Jacob, D.J., Arnold, S.R., Pelon, J. and Thomas, J.L., 2014. Arctic Air Pollution: new insights from POLARCAT-IPY. Bulletin of the American Meteorological Society, 95 (12):1873-1895.

Le Faucheur, S., Campbell, P.G.C., Fortin, C. and Slaveykova, V.I., 2014. Interactions between mercury and phytoplankton: speciation, bioavailability, and internal handling. Environmental Toxicology and Chemistry, 33 (6):1211-1224.

Lee, C.-S. and Fisher, N.S., 2016. Methylmercury uptake by diverse marine phytoplankton. Limnology and Oceanography, 61 (5):1626-1639.

Lee, C.S. and Fisher, N.S., 2019. Microbial generation of elemental mercury from dissolved methylmercury in seawater. Limnology and Oceanography, 64 (2):679-693.

Lee, M.-Y., Hong, C.-C. and Hsu, H.-H., 2015. Compounding effects of warm sea surface temperature and reduced sea ice on the extreme circulation over the extratropical North Pacific and North America during the 2013-2014 boreal winter. Geophysical Research Letters, 42 (5):1612-1618.

Lee, M.M., Jaspers, V.L.B., Gabrielsen, G.W., Jenssen, B.M., Ciesielski, T.M., Mortensen, Å.-K., Lundgren, S.S. and Waugh, C.A., 2020. Evidence of avian influenza virus in seabirds breeding on a Norwegian High Arctic archipelago. BMC Veterinary Research, 16 (1):48.

Leenheer, J. and Croué, J.-P., 2003. Characterizing aquatic dissolved organic matter. Environmental Science & Technology, 37 (1):18A-26A.

Legagneux, P., Gauthier, G., Lecomte, N., Schmidt, N.M., Reid, D., Cadieux, M.-C., Berteaux, Bêty, J., Krebs, C.J., Ims, R.A., Yoccoz, N.G., Morrison, R.I.G., Leroux, S.J., Loreau, M. and Gravel, D., 2014. Arctic ecosystem structure and functioning shaped by climate and herbivore body size. Nature Climate Change, 4 (5):379-383.

Lehnherr, I., 2014. Methylmercury biogeochemistry: a review with special reference to Arctic aquatic ecosystems. Environmental Reviews, 22 (3):229-243.

Lehnherr, I., St. Louis, V.L., Hintelmann, H. and Kirk, J.L., 2011. Methylation of inorganic mercury in polar marine waters. Nature Geoscience, 4 (5):298-302.

Lehnherr, I., St. Louis, V.L., Emmerton, C.A., Barker, J.D. and Kirk, J.L., 2012a. Methylmercury cycling in High Arctic wetland ponds: sources and sinks. Environmental Science & Technology, 46 (19):10514-10522.

Lehnherr, I., St. Louis, V.L. and Kirk, J.L., 2012b. Methylmercury cycling in High Arctic wetland ponds: controls on sedimentary production. Environmental Science & Technology, 46 (19):10523-10531.

Lehnherr, I., St. Louis, V.L., Sharp, M., Gardner, A., Smol, J.P., Schiff, S.L., Muir, D.C.G., Mortimer, C.A., Michelutti, N., Tarnocai, C., St. Pierre, K.A., Emmerton, C.A., Wiklund, J.A., Köck, G., Lamoureux, S.F. and Talbot, C.H., 2018. The world's largest High Arctic lake responds rapidly to climate warming. Nature Communications, 9 (1):1290.

Lei, H., Wuebbles, D.J., Liang, X.-Z., Tao, Z., Olsen, S., Artz, R., Ren, X. and Cohen, M., 2014. Projections of atmospheric mercury levels and their effect on air quality in the United States. Atmospheric Chemistry and Physics, 14:783-795.

Leitch, D.R., 2006. Mercury distribution in water and permafrost of the lower Mackenzie Basin, their contribution to the mercury contamination in the Beaufort Sea marine ecosystem, and potential effects of climate variation. Master of Science thesis. Department of Environment and Geography, University of Manitoba, Winnipeg, Manitoba, Canada. Available at: https://mspace.lib.umanitoba.ca/xmlui/handle/1993/20852?show=full

Leitch, D.R., Carrie, J., Lean, D., Macdonald, R.W., Stern, G.A. and Wang, F., 2007. The delivery of mercury to the Beaufort Sea of the Arctic Ocean by the Mackenzie River. Science of the Total Environment, 373 (1):178-195.

Lemes, M., Wang, F., Stern, G.A., Ostertag, S.K. and Chan, H.M., 2011. Methylmercury and selenium speciation in different tissues of beluga whales (*Delphinapterus leucas*) from the western Canadian Arctic. Environmental Toxicology and Chemistry, 30 (12):2732-2738.

Lemire, M., Kwan, M., Laouan-Sidi, A.E., Muckle, G., Pirkle, C., Ayotte, P. and Dewailly, É., 2015. Local country food sources of methylmercury, selenium and omega-3 fatty acids in Nunavik, Northern Quebec. Science of the Total Environment, 509-510:248-259.

Lemire, M., Little, M., Ayotte, P. et al., 2019. The intriguing story of selenoneine in Nunavik. Taqralik Magazine, 117:37-38.

Lennert, A.E., 2016. What happens when the ice melts? Belugas, contaminants, ecosystems and human communities in the complexity of global change. Marine Pollution Bulletin, 107 (1):7-14.

Lento, J., Lento, J., Goedkoop, W., Culp, J., Christoffersen, K.S., Lárusson, K.F., Fefilova, E., Guðbergsson, G., Liljaniemi, P., Ólafsson, J.S., Sandøy, S., Zimmerman, C., Christensen, T., Chambers, P., Heino, J., Hellsten, S., Kahlert, M., Keck, F., Laske, S., Chun Pong Lau, D., Lavoie, I., Levenstein, B., Mariash, H., Rühland, K., Saulnier- Talbot, E., Schartau, A.K. and Svenning, M., 2019. Circumpolar Biodiversity Monitoring Program State of Arctic Freshwater Biodiversity Report. Conservation of Arctic Flora and Fauna (CAFF), Akureyri, Iceland. 124pp.

Lescord, G.L., Emilson, E.J.S., Johnston, T.A., Branfireun, B.A. and Gunn, J.M., 2018. Optical properties of dissolved organic matter and their relation to mercury concentration in water and biota across a remote freshwater drainage basin. Environmental Science & Technology, 52 (6):3344-3353.

Lescord, G.L., Kidd, K.A., Kirk, J.L., O'Driscoll, N.J., Wang, X. and Muir, D.C.G., 2015. Factors affecting biotic mercury concentrations and biomagnification through lake food webs in the Canadian High Arctic. Science of the Total Environment, 509-510:195-205.

Letcher, R.J. and Dyck, M., 2021. Temporal and spatial trends of legacy and emerging organic and metal/elemental contaminants in Canadian polar bears. In: Beardsall, A. and Morris, A.D. (Eds.). Synopsis of Research Conducted under the 2017-2018 Northern Contaminants Program, pp. 183-198. Crown-Indigenous Relations and Northern Affairs Canada, Gatineau, QC, Canada. Available at: https://pubs.aina.ucalgary.ca/ncp/Synopsis20172018.pdf

Letcher, R.J., Bustnes, J.O., Dietz, R., Jenssen, B.M., Jørgensen, E.H., Sonne, C., Verreault, J., Vijayan, M.M. and Gabrielsen, G.W., 2010. Exposure and effects assessment of persistent organohalogen contaminants in Arctic wildlife and fish. Science of the Total Environment, 408 (15):2995-3043.

Lewis, S.A., Becker, P.H. and Furness, R.W., 1993. Mercury levels in eggs, tissues, and feathers of herring gulls *Larus argentatus* from the German Wadden Sea coast. Environmental Pollution, 80 (3):293-299.

Lewis, C.A., Cristol, D.A., Swaddle, J.P., Varian-Ramos, C.W. and Zwollo, P., 2013. Decreased immune response in zebra finches exposed to sublethal doses of mercury. Archives of Environmental Contamination and Toxicology, 64:327-336.

Lewkowicz, A.G. and Way, R.G., 2019. Extremes of summer climate trigger thousands of thermokarst landslides in a High Arctic environment. Nature Communications, 10 (1):1329.

Li, C., Cornett, J., Willie, S. and Lam, J., 2009. Mercury in Arctic air: the long-term trend. Science of the Total Environment, 407 (8):2756-2759.

Li, M., Sherman, L.S., Blum, J.D., Grandjean, P., Mikkelsen, B., Weihe, P., Sunderland, E.M, and Shine, J.P., 2014. Assessing sources of human methylmercury exposure using stable mercury isotopes. Environmental Science & Technology, 48 (15):8800-8806.

Li, Y., Wang, W.X. and Wang, M., 2017. Alleviation of mercury toxicity to a marine copepod under multigenerational exposure by ocean acidification. Scientific Reports, 7 (1):324.

Li, T., Wang, Y., Mao, H., Wang, S., Talbot, R.W., Zhou, Y., Wang, Z., Nie, X. and Qie, G., 2018. Insights on chemistry of mercury species in clouds over eastern China: complexation and adsorption. Environmental Science & Technology, 52 (9):5125-5134.

Liberda, E.N., Tsuji, L.J., Martin, I.D., Ayotte, P., Dewailly, E. and Nieboer, E., 2014. The complexity of hair/blood mercury concentration ratios and its implications. Environmental Research, 134:286-294.

Liem-Nguyen, V., Wild, B., Gustafsson, Ö., Semiletov, I., Dudarev, O. and Jonsson, S., 2022. Spatial patterns and distributional controls of total and methylated mercury off the Lena River in the Laptev Sea sediments. Marine Chemistry, 238:104052.

Liljedahl, A.K., Boike, J., Daanen, R.P., Fedorov, A.N., Frost, G.V., Grosse, G., Hinzman, L.D., Iijma, Y., Jorgenson, J.C., Matveyeva, N. and Necsoiu, M., 2016. Pan-Arctic ice-wedge degradation in warming permafrost and its influence on tundra hydrology. Nature Geoscience, 9 (4):312-318.

Liljedahl, A.K., Hinzman, L.D., Kane, D.L., Oechel, W.C., Tweedie, C.E. and Zona, D., 2017. Tundra water budget and implications of precipitation underestimation. Water Resources Research, 53 (8):6472-6486.

Lim, D.S.S., Douglas, M.S.V., Smol, J.P. and Lean, D.R.S., 2001. Physical and chemical limnological characteristics of 38 lakes and ponds on

Bathurst Island, Nunavut, Canadian High Arctic. International Review of Hydrobiology, 86 (1):1-22.

Lim, A.G., Sonke, J.E., Krickov, I.V., Manasypov, R.M., Loiko, S.V. and Pokrovsky, O.S., 2019. Enhanced particulate Hg export at the permafrost boundary, western Siberia. Environmental Pollution, 254 (Part B):113083.

Lim, A.G., Jiskra, M., Sonke, J.E., Loiko, S.V., Kosykh, N. and Pokrovsky, O.S., 2020. A revised pan-Arctic permafrost soil Hg pool, based on Western Siberian permafrost peat Hg and carbon observations. Biogeosciences, 17 (12):3083-3097.

Lin, C.J. and Pehkonen, S.O., 1999. Aqueous phase reactions of mercury with free radicals and chlorine: implications for atmospheric mercury chemistry. Chemosphere, 38 (6):1253-1263.

Lind, S., Ingvaldsen, R.B. and Furevik, T., 2018. Arctic warming hotspot in the northern Barents Sea linked to declining sea-ice import. Nature Climate Change, 8 (7):634-639.

Lindberg, S.E., Brooks, S., Lin, C.-J., Scott, K.J., Landis, M.S., Stevens, R.K., Goodsite, M. and Richter, A., 2002. Dynamic oxidation of gaseous mercury in the Arctic troposphere at polar sunrise. Environmental Science & Technology, 36 (6):1245-1256.

Lindberg, S., Bullock, R., Ebinghaus, R., Engstrom, D., Feng, X.B., Fitzgerald, W., Pirrone, N., Prestbo, E. and Seigneur, C., 2007. A synthesis of progress and uncertainties in attributing the sources of mercury in deposition. Ambio, 36 (1):19-32.

Lindgren, E. and Gustafson, R., 2001. Tick-borne encephalitis in Sweden and climate change. Lancet, 358 (9275):16-18.

Lindsay, R. and Schweiger, A., 2015. Arctic sea ice thickness loss determined using subsurface, aircraft, and satellite observations. The Cryosphere, 9 (1):269-283.

Lippold, A., Aars, J., Andersen, M., Aubail, A., Derocher, A.E., Dietz, R., Eulaers, I., Sonne, C., Welker, J.M., Wiig, Ø. and Routti, H., 2020. Two decades of mercury concentrations in Barents Sea polar bears (*Ursus maritimus*) in relation to dietary carbon, sulfur, and nitrogen. Environmental Science & Technology, 54 (12):7388-7397.

Lippold, A., Boltunov, A., Aars, J., Andersen, M., Blanchet, M.A., Dietz, R., Eulaers, I., Morshina, T., Sevastyanov, V., Welker J.M., Routti, H. 2022. Spatial variation in mercury concentrations in polar bear (*Ursus maritimus*) hair from the Norwegian and Russian Arctic. Science of the Total Environment, 822:153572.

Liston, G.E. and Hiemstra, C.A., 2011. The changing cryosphere: pan-Arctic snow trends (1979-2009). Journal of Climate, 24:5691-5712.

Little, M., Achouba, A., Dumas, P., Ouellet, N., Ayotte, P. and Lemire, M., 2019. Determinants of selenoneine concentration in red blood cells of Inuit from Nunavik (Northern Québec, Canada). Environment International, 127:243-252.

Little, M., Achouba, A., Dumas, P., Ouellet, N., Ayotte, P. and Lemire, M. 2019. Determinants of selenoneine concentration in red blood cells of Inuit from Nunavik (Northern Québec, Canada). Environment International, 127:243-252.

Liu, S., Lorenzen, E.D., Fumagalli, M., Li, B., Harris, K., Xiong, Z., Zhou, L., Korneliussen, T.S., Somel, M., Babbitt, C., Wray, G., Li, J., He, W., Wang, Z., Fu, W., Xiang, X., Morgan, C.C., Doherty, A., O'Connell, M.J., McInerney, J.O., Born, E.W., Dalén, L., Dietz, R., Orlando, L., Sonne, C., Zhang, G., Nielsen, R., Willerslev, E. and Wang, J., 2014. Population genomics reveal recent speciation and rapid evolutionary adaptation in polar bears. Cell, 157 (4):785-794.

Liu, Y., Chai, X., Hao, Y., Gao, X., Lu, Z., Zhao, Y., Zhang, J. and Cai, M., 2015. Total mercury and methylmercury distributions in surface sediments from Kongsfjorden, Svalbard, Norwegian Arctic. Environmental Science and Pollution Research, 22 (11):8603-8610.

Lizundia-Loiola, J., Otón, G., Ramo, R. and Chuvieco, E., 2020. A spatio-temporal active-fire clustering approach for global burned area mapping at 250 m from MODIS data. Remote Sensing of Environment 236, 111493.

Lockhart, W.L., Macdonald, R.W., Outridge P.M., Wilkinson, P., DeLaronde, J.B. and Rudd, J.W.M., 2000. Tests of the fidelity of lake sediment core records of mercury deposition to known histories of mercury contamination. Science of the Total Environment, 260 (1-3):171-180.

Lockhart, W.L., Stern, G.A., Wagemann, R., Hunt, R.V., Metner, D.A., DeLaronde, J., Dunn, B., Stewart, R.E.A., Hyatt, C.K., Harwood, L. and Mount, K., 2005. Concentrations of mercury in tissues of beluga whales (Delphinapterus leucas) from several communities in the Canadian Arctic from 1981 to 2002. Science of the Total Environment, 351-352:391-412.

Loe, L.E., Hansen, B.B., Stien, A., Albon, S.D., Bischof, R., Carlsson, A., Irvine, R.J., Meland, M., Rivrud, I.M., Ropstad, E., Veilberg, V. and Mysterud, A., 2016. Behavioral buffering of extreme weather events in a High-Arctic herbivore. Ecosphere, 7 (6):e01374.

Lokken, J.A., Finstad, G.L., Dunlap, K.L. and Duffy, L.K., 2009. Mercury in lichens and reindeer hair from Alaska: 2005-2007 pilot survey. Polar Record, 45:368-374.

Loranty, M.M., Abbott, B.W., Blok, D., Douglas, T.A., Epstein, H.E., Forbes, B.C., Jones, B.M., Kholodov, A.L., Kropp, H., Malhotra, A. and Mamet, S.D.., 2018. Reviews and syntheses: changing ecosystem influences on soil thermal regimes in northern high-latitude permafrost regions. Biogeosciences 15 (17):5287-5313.

Loring, D.H., 1991. Normalization of heavy-metal data from estuarine and coastal sediments. ICES Journal of Marine Science, 48 (1):101-115.

Løset, S., Shkinek, K.N., Gudmestad, O.T., Høyland, K.V., 2006. Actions from ice on Arctic offshore and coastal structures: student's book for institutes of higher education. Lan. 272pp.

Loseto, L.L., Siciliano, S.D. and Lean, D.R.S., 2004a. Methylmercury production in high arctic wetlands. Environmental Toxicology and Chemistry, 23 (1):17-23.

Loseto, L.L., Lean, D.R. and Siciliano, S.D., 2004b. Snowmelt sources of methylmercury to High Arctic ecosystems. Environmental Science & Technology 38 (11):3004-3010.

Loseto, L.L., Stern, G.A., Deibel, D., Connelly, T.L., Prokopowicz, A., Lean, D.R.S., Fortier, L. and Ferguson, S.H., 2008. Linking mercury exposure to habitat and feeding behaviour in Beaufort Sea beluga whales. Journal of Marine Systems, 74:1012-1024.

Loseto, L.L., Stern, G.A. and Macdonald, R.W., 2015. Distant drivers or local signals: where do mercury trends in western Arctic belugas originate? Science of the Total Environment, 509-510:226-236.

Loseto, L.L., Lam, J. and Iacozza, J., 2018. Beluga summit: knowledge sharing of the eastern Beaufort Sea beluga whale. Arctic Science, 4 (3):i-iv.

Lu, J.Y. and Schroeder, W.H., 2004. Annual time-series of total filterable atmospheric mercury concentrations in the Arctic. Tellus B: Chemical and Physical Meteorology, 56 (3): 213-222.

Lucia, M., Verboven, N., Strøm, H., Miljeteig, C., Gavrilo, M.V., Braune, B.M., Boertmann, D. and Gabrielsen, G.W., 2015. Circumpolar contamination in eggs of the high-Arctic ivory gull *Pagophila eburnea*. Environmental Toxicology and Chemistry, 34 (7):1552-1561.

Lyman, S.N., Cheng, I., Gratz, L.E., Weiss-Penzias, P. and Zhang, L., 2020. An updated review of atmospheric mercury. Science of the Total Environment, 707:135575.

Ma, M., Du, H. and Wang, D., 2019. Mercury methylation by anaerobic microorganisms: a review. Critical Reviews in Environmental Science & Technology, 49 (20):1893-1936.

Macdonald, R.W. and Thomas, D.J., 1991. Chemical interactions and sediments of the western Canadian Arctic Shelf. Continental Shelf Research,11 (8-10):843-863.

Macdonald, R.W., Harner, T. and Fyfe, J., 2005. Recent climate change in the Arctic and its impact on contaminant pathways and interpretation of temporal trend data. Science of the Total Environment, 342 (1-3):5-86.

Mack, M.C., Bret-Harte, M.S., Hollingsworth, T.N., Jandt, R.R., Schuur, E.A.G., Shaver, G.R. and Verbyla, D.L., 2011. Carbon loss from an unprecedented Arctic tundra wildfire. Nature, 475 (7357):489-492.

Mackelprang, R., Waldrop, M.P., DeAngelis, K.M., David, M.M., Chavarria, K.L., Blazewicz, S.J., Rubin, E.M. and Jansson, J.K., 2011. Metagenomic analysis of a permafrost microbial community reveals a rapid response to thaw. Nature, 480 (7377):368-371.

MacMillan, G.A., 2018. Hunting for trace metals in the rapidly changing North: using limnological, ecological and collaborative approaches. Doctoral thesis, Department of Biological Sciences, University of Montreal, Quebec, Canada. Available at: https://papyrus.bib.umontreal.ca/xmlui/handle/1866/21777

MacMillan, G.A., Girard, C., Chételat, J., Laurion, I. and Amyot, M., 2015. High methylmercury in Arctic and Subarctic ponds is related to nutrient levels in the warming eastern Canadian Arctic. Environmental Science & Technology, 49 (13):7743-7753.

Malcolm, E.G., Ford, A.C., Redding, T.A., Richardson, M.C., Strain, B.M. and Tetzner, S.W., 2009. Experimental investigation of the scavenging of gaseous mercury by sea salt aerosol. Journal of Atmospheric Chemistry, 63 (3):221-234.

Malcomb, N.L. and Wiles, G.C., 2013. Tree-ring-based reconstructions of North American glacier mass balance through the Little Ice Age

– Contemporary warming transition. Quaternary Research, 79 (2):123-127.

Mallory, C.D. and Boyce, M.S., 2017. Observed and predicted effects of climate change on Arctic caribou and reindeer. Environmental Reviews, 26 (1):13-25.

Mangal, V., Stenzler, B.R., Poulain, A.J. and Guéguen, C., 2019. Aerobic and anaerobic bacterial mercury uptake is driven by algal organic matter composition and molecular weight. Environmental Science & Technology, 53 (1):157-165.

Mann, E., Meyer, T., Mitchell, C.P.J. and Wania, F., 2011. Mercury fate in ageing and melting snow: development and testing of a controlled laboratory system, Journal of Environmental Monitoring, 13 (10):2695-2702.

Mann, E., Ziegler, S., Mallory, M. and O'Driscoll, N., 2014. Mercury photochemistry in snow and implications for Arctic ecosystems. Environmental Reviews, 22 (4):331-345.

Mann, E.A., Mallory, M.L., Ziegler, S.E., Tordon, R. and O'Driscoll, N.J., 2015. Mercury in Arctic snow: quantifying the kinetics of photochemical oxidation and reduction. Science of the Total Environment, 509-510:115-132.

Mann, E.A., Ziegler, S.E., Steffen, A., and O'Driscoll, N.J., 2018. Increasing chloride concentration causes retention of mercury in melted Arctic snow due to changes in photoreduction kinetics. Journal of Environmental Sciences (China), 68:122-129.

Mantyka-Pringle, C.S., Jardine, T.D., Bradford, L., Bharadwaj, L., Kythreotis, A.P., Fresque-Baxter, J., Kelly, E., Somers, G., Doig, J.E., Jones, P.D., Lindenschmidt, K.-E. and the Slave River and Delta Partnership, 2017. Bridging science and traditional knowledge to assess. Cumulative impacts of stressors on ecosystem health, Environment International, 102:125-137.

Mao, H., Ye, Z. and Driscoll, C., 2017. Meteorological effects on Hg wet deposition in a forested site in the Adirondack region of New York during 2000–2015. Atmospheric Environment, 168:90-100.

Marcogliese, D.J. and Pietrock, M., 2011. Combined effects of parasites and contaminants on animal health: parasites do matter. Trends in Parasitology, 27 (3):123-130.

Martyniuk, M.A.C., Couture, P., Tran, L., Beaupré, L. and Power, M., 2020. Seasonal variation of total mercury and condition indices of Arctic charr (Salvelinus alpinus) in Northern Quebec, Canada. Science of the Total Environment, 738:139450.

Masbou, J., Point, D., Sonke, J.E., Frappart, F., Perrot, V., Amouroux, D., Richard, P. and Becker, P. R., 2015. Hg stable isotope time trend in ringed seals registers decreasing sea ice cover in the Alaskan Arctic. Environmental Science & Technology, 49 (15):8977-8985.

Masbou, J., Sonke, J.E., Amouroux, D., Guillou, G., Becker, P.R. and Point, D., 2018. Hg-stable isotope variations in marine top predators of the western Arctic Ocean. ACS Earth and Space Chemistry 2 (5):479-490.

Mason, R.P. and Sullivan, K.A., 1997. Mercury in Lake Michigan. Environmental Science & Technology, 31 (3):942-947.

Mason, R.P. and Sullivan, K.A., 1999. The distribution and speciation of mercury in the South and equatorial Atlantic. Deep Sea Research Part II: Topical Studies in Oceanography 46 (5):937-956.

Mason, R.P., Lawson, N.M. and Sullivan, K.A., 1997. The concentration, speciation and sources of mercury in Chesapeake Bay precipitation. Atmospheric Environment, 31 (21):3541-3550.

Mason, R.P., Choi, A.L., Fitzgerald, W.F., Hammerschmidt, C.R., Lamborg, C.H., Soerensen, A.L. and Sunderland, E.M., 2012. Mercury biogeochemical cycling in the ocean and policy implications. Environmental Research, 119:101-117.

Matthews, C.J.D., Breed, G.A., LeBlanc, B. and Ferguson, S.H., 2020. Killer whale presence drives bowhead whale selection for sea ice in Arctic seascapes of fear. Proceedings of the National Academy of Sciences of the United States of America, 117 (12):6590-6598.

Mazrui, N.M., Jonsson, S., Thota, S., Zhao, J. and Mason, R.P., 2016. Enhanced availability of mercury bound to dissolved organic matter for methylation in marine sediments. Geochimica et Cosmochimica Acta, 194:153-162.

McCall, A.G., Derocher, A.E. and Lunn, A.J., 2015. Home range distribution of polar bears in western Hudson Bay. Polar Biology, 38:343-355.

McCloskey, M., Robinson, S., Smith, P.A. and Forbes, M., 2013. Mercury concentration in the eggs of four Canadian Arctic-breeding shorebirds not predicted based on their population statuses. SpringerPlus, 2:567.

McDaniel, E.A., Peterson, B.D., Stevens, S.L.R., Tran, P.Q., Anantharaman, K., McMahon, K.D. and Kent, A.D., 2020. Expanded phylogenetic diversity and metabolic flexibility of mercury-methylating microorganisms. mSystems, 5 (4):e00299-20.

McGrew, A.K., Ballweber, L.R., Moses, S.K., Stricker, C.A., Beckmen, K.B., Salman, M.D. and O'Hara, T.M., 2014. Mercury in gray wolves (Canis lupus) in Alaska: increased exposure through consumption of marine prey. Science of the Total Environment, 468-469:609-613.

McKinney, M.A., Peacock, E. and Letcher, R.J., 2009. Sea ice-associated diet change increases the levels of chlorinated and brominated contaminants in polar bears. Environmental Science & Technology, 43 (12):4334-4339.

McKinney, M.A., Stirling, I., Lunn, N.J., Peacock, E. and Letcher, R.J., 2010. The role of diet on long-term concentration and pattern trends of brominated and chlorinated contaminants in western Hudson Bay polar bears, 1991-2007. Science of the Total Environment, 408 (24):6210-22.

McKinney, M.A., Iverson, S.J., Fisk, A.T., Sonne, C., Rigét, F.F., Letcher, R.J., Arts, M.T., Born, E.W., Rosing-Asvid, A. and Dietz, R., 2013. Global change effects on the long-term feeding ecology and contaminant exposures of East Greenland polar bears. Global Change Biology, 19 (8):2360-2372.

McKinney, M.A., Pedro, S., Dietz, R., Sonne, C., Fisk, A.T., Roy, D., Jenssen, B.M. and Letcher, R.J., 2015. A review of ecological impacts of global climate change on persistent organic pollutant and mercury pathways and exposures in Arctic marine ecosystems. Current Zoology, 61 (4):617-628.

McKinney, M.A., Atwood, T., Iverson, S.J. and Peacock, E., 2017a. Temporal complexity of southern Beaufort Sea polar bear diets during a period of increasing land use. Ecosphere, 8 (1):e01633.

McKinney, M.A., Atwood, T.C., Pedro, S. and Peacock, E., 2017b. Ecological change drives a decline in mercury concentrations in southern Beaufort Sea polar bears. Environmental Science & Technology, 51 (14):7814-7822.

McLagan, D.S., Stupple, G.W., Darlington, A., Hayden, K. and Steffen, A., 2021. Where there is smoke there is mercury: assessing boreal forest fire mercury emissions using aircraft and highlighting uncertainties associated with upscaling emissions estimates. Atmospheric Chemistry and Physics, 21 (7):5635-5653.

McMeans, B.C., Arts, M.T. and Fisk, A.T., 2015a. Impacts of food web structure and feeding behavior on mercury exposure in Greenland Sharks (*Somniosus microcephalus*). Science of the Total Environment, 509-510:216-225.

McMeans, B.C., McCann, K.S., Humpries, M., Rooney, N. and Fisk, A.T., 2015b. Food web structure in temporally-forced ecosystems. Trends in Ecology & Evolution, 30 (11):662-672.

McNamara, J.P., Kane, D.L. and Hinzman, L.D., 1998. An analysis of streamflow hydrology in the Kuparuk River basin, Arctic Alaska: a nested watershed approach. Journal of Hydrology, 206 (1-2):39-57.

Mead, E., Gittelsohn, J., Roache, C. and Sharma, S., 2010. Healthy food intentions and higher socioeconomic status are associated with healthier food choices in an Inuit population. Journal of Human Nutrition and Dietetics, 23 (S1):83-91.

Meire, L., Søgaard, D.H., Mortensen, J., Meysman, F.J.R., Soetaert, K., Arendt, K.E., Juul-Pedersen, T., Blicher, M.E. and Rysgaard, S., 2015. Glacial meltwater and primary production are drivers of strong CO_2 uptake in fjord and coastal waters adjacent to the Greenland Ice Sheet. Biogeosciences, 12 (8):2347-2363.

Melnes, M., Gabrielsen, G.W., Herzke, D., Sagerup, K. and Jenssen, B.M., 2017. Dissimilar effects of organohalogenated compounds on thyroid hormones in glaucous gulls. Environmental Research, 158:350-357.

Meredith, M., Sommerkorn, M., Cassotta, S., Derksen, C., Ekaykin, A., Hollowed, A., Kofinas, G., Mackintosh, A., Melbourne-Thomas, J., Muelbert, M.M.C., Ottersen, G., Pritchard, H. and Shuur, E.A.G, 2019. Polar Regions In: *IPCC Special Report on the Ocean and Cryosphere in a Changing Climate*. Pörtner, H.-O., Roberts, D.C., Masson-Delmotte, V., Zhai, P., Tignor, M., Poloczanska, E., Mintenbeck, K., Alegría, A., Nicolai, M., Okem, A., Petzold, J., Rama, B. and Weyer, N.M. (Eds.), pp. 203-320. Intergovernmental Panel on Climate Change (IPCC). In Press.

Mérillet, L., Kopp, D., Robert, M., Mouchet, M. and Pavoine, S., 2020. Environment outweighs the effects of fishing in regulating demersal community structure in an exploited marine ecosystem. Global Change Biology 26, 2106–2119.

Mérillet, L., Skogen, M.D., Vikebø, F. and Jørgensen, L.L., 2022. Fish assemblages of a Sub-Arctic fjord show early signals of climate change response contrary to the benthic assemblages. Frontiers in Marine Science, 9:822979.

Mernild, S.H., Lipscomb, W.H., Bahr, D.B., Radić, V. and Zemp, M., 2013. Global glacier changes: a revised assessment of committed mass losses and sampling uncertainties. The Cryosphere, 7 (5):1565-1577.

Mernild, S.H., Hanna, E., McConnell, J.R., Sigl, M., Beckerman, A.P., Yde, J.C., Cappelen, J., Malmros, J.K. and Steffen, K., 2015. Greenland precipitation trends in a long-term instrumental climate context (1890-2012): evaluation of coastal and ice core records. International Journal of Climatology, 35 (2):303-320.

Michelutti, N., Douglas, M.S.V., Antoniades, D., Lehnherr, I., St. Louis, V.L., St. Pierre, K., Muir, D.C.G., Brunskill, G. and Smol, J.P., 2020. Contrasting the ecological effects of decreasing ice cover versus accelerated glacial melt on the High Arctic's largest lake. Proceedings of the Royal Society B: Biological Sciences, 287 (1929):20201185.

Mikaelsson, S. and Mustonen, T., 2020. Hydropower reservoirs and impacts to their transmission of Sámi Knowledge in Sweden and Finland. In: Serafimova, S. (Ed.). Dimensions of Intra- and Intergenerational Justice in the Debates around Sustainability, pp. 130-149. Sofia, Avangard Prima.

Miljeteig, C., Strøm, H., Gavrilo, M.V., Volkov, A., Jenssen, B.M. and Gabrielsen, G.W., 2009. High levels of contaminants in ivory gull *Pagophila eburnea* eggs from the Russian and Norwegian Arctic. Environmental Science & Technology, 43 (14):5521-5528.

Miljeteig, C. and Gabrielsen, G.W., 2010. Contaminants in Brünnich's guillemots from Kongsfjorden and Bjørnøya in the period from 1993 to 2007. Kortrapport/Brief Report Series No.16. Norwegian Polar Institute, Tromsø, Norway. 34pp. Available at: https://brage.npolar.no/npolar-xmlui/bitstream/handle/11250/172993/Kortrapport16.pdf?sequence=1

Miljeteig, C., Gabrielsen, G.W., Strøm, H., Gavrilo, M.V., Lie, E. and Jenssen, B.M., 2012. Eggshell thinning and decreased concentrations of vitamin E are associated with contaminants in eggs of ivory gulls. Science of the Total Environment, 431:92-99.

Millero, F.J., Woolsey, R., Ditrolio, B. and Waters, J., 2009. Effect of ocean acidification on the speciation of metals in seawater. Oceanography, 22 (4):72-85.

Milner, A.M., Khamis, K., Battin, T.J., Brittain, J.E., Barrand, N.E., Füreder, L., Cauvy-Fraunié, S., Gíslason, G.M., Jacobsen, D., Hannah, D.M., Hodson, A.J., Hood, E., Lencioni, V., Ólafsson, J.S., Robinson, C.T., Tranter, M. and Brown, L.E., 2017. Glacier shrinkage driving global changes in downstream systems. Proceedings of the National Academy of Sciences, 114 (37):9770-9778.

Møller, A.K., Barkay, T., Al-Soud, W.A., Sørensen, S.J., Skov, H. and Kroer, N., 2011. Diversity and characterization of mercury-resistant bacteria in snow, freshwater and sea-ice brine from the High Arctic. FEMS Microbiology Ecology 75 (3):390-401.

Møller, A.K., Barkay, T., Hansen, M.A., Norman, A., Hansen, L.H., Sørensen, S.J., Boyd, E.S. and Kroer, N., 2014. Mercuric reductase genes (merA) and mercury resistance plasmids in High Arctic snow, freshwater and sea-ice brine. FEMS Microbiology Ecology, 87 (1):52-63.

Molnár, P.K., Derocher, A.E., Klanjscek, T. and Lewis, M.A., 2011. Predicting climate change impacts on polar bear litter size. Nature Communications, 2 (1):186.

Molnár, P.K., Bitz, C.M., Holland, M.M., Kay, J.E., Penk, S.R. and Amstrup, S.C., 2020. Fasting season length sets temporal limits for global polar bear persistence. Nature Climate Change, 10 (8):732-738.

Monks, S.A., Arnold, S.R., Emmons, L.K., Law, K.S., Turquety, S., Duncan, B.N., Flemming, J., Huijnen, V., Tilmes, S., Langner, J., Mao, J., Long, Y., Thomas, J.L., Steenrod, S.D., Raut, J.C., Wilson, C., Chipperfield, M.P., Diskin, G.S., Weinheimer, A., Schlager, H. and Ancellet, G., 2015. Multi-model study of chemical and physical controls on transport of anthropogenic and biomass burning pollution to the Arctic. Atmospheric Chemistry and Physics, 15 (6):3575-3603.

Monteith, D.T., Stoddard, J.L., Evans, C.D., de Wit, H.A., Forsius, M., Høgåsen, T., Wilander, A., Skjelkvale, B.L., Jeffries, D.S., Vuorenmaa, J., Keller, B., Kopácek, J. and Vesely, J., 2007. Dissolved organic carbon trends resulting from changes in atmospheric deposition chemistry. Nature, 450 (7169):537-540.

Moon-Riley, K.C., Copeland, J.L., Metz, G.A.S. and Currie, C.L., 2019. The biological impacts of Indigenous residential school attendance on the next generation. SSM - Population Health, 7:100343.

Moore, C.W., Obrist, D., Steffen, A., Staebler, R.M., Douglas, T.A., Richter, A. and Nghiem, S.V., 2014. Convective forcing of mercury and ozone in the Arctic boundary layer induced by leads in the sea ice. Nature, 506 (7486):81-84.

Moran, S.B., Ellis, K.M. and Smith, J.N., 1997. 234Th/238U disequilibrium in the central Arctic Ocean: implications for particulate organic carbon export. Deep Sea Research: Part II: Topical Studies in Oceanography, 44 (8):1593-1606.

Moran, M.D., Dastoor, A. and Morneau, G., 2014. Chapter 4: Long-range transport of air pollutants and regional and global air quality modelling. In: Taylor, E. and McMillan, A. (Eds.). Air Quality Management: Canadian Perspectives on a Global Issue, pp. 68-98. Springer Netherlands.

Morel, F.M.M., Kraepel, A.M.L. and Amyot, M., 1998. The chemical cycle and bioaccumulation of mercury. Annual Review of Ecology and Systematics, 29 (1):543-566.

Morris, A.D., Letcher, R.J., Dyck, M., Chandramouli, B. and Cosgrove, J., 2018. Multivariate statistical analysis of metabolomics profiles in tissues of polar bears (*Ursus maritimus*) from the Southern and Western Hudson Bay subpopulations. Polar Biology, 41 (3):433-449.

Morris, A.D., Braune, B.M., Gamberg, M., Stow, J., O'Brien, J. and Letcher, R.J., 2022. Temporal change and the influence of climate and weather factors on mercury concentrations in Hudson Bay polar bears, caribou, and seabirds. Environmental Research, 207:112169.

Moses, S.K., Whiting, A.V., Bratton, G.R., Taylor, R.J. and O'Hara, T.M. 2009. Inorganic nutrients and contaminants in subsistence species of Alaska: linking wildlife and human health. International Journal of Circumpolar Health, 68 (1):53-74.

Mosites, E., Rodriguez, E., Caudill, S.P., Hennessy, T.W. and Berner, J., 2020. A comparison of individual-level vs. hypothetically pooled mercury biomonitoring data from the Maternal Organics Monitoring Study (MOMS), Alaska, 1999-2012. International Journal of Circumpolar Health, 79:1726256.

Mouginot, J., Rignot, E., Bjørk, A.A., van den Broeke, M., Millan, R., Morlighem, M., Noël, B., Scheuchl, B. and Wood, M., 2019. Forty-six years of Greenland Ice Sheet mass balance from 1972 to 2018. Proceedings of the National Academy of Sciences, 116 (19):9239-9244.

Mu, C., Zhang, F., Chen, X., Ge, S., Mu, M., Jia, L., Wu, Q.B. and Zhang, T.J., 2019. Carbon and mercury export from the Arctic rivers and response to permafrost degradation. Water Research, 161:54-60.

Muir, D., Wang, X., Bright, D., Lockhart, L. and Köck, G., 2005. Spatial and temporal trends of mercury and other metals in landlocked char from lakes in the Canadian Arctic archipelago. Science of the Total Environment, 351-352:464-478.

Muir, D.C.G., Wang, X., Yang, F., Nguyen, N., Jackson, T.A., Evans, M.S., Douglas, M., Köck, G., Lamoureux, S., Pienitz, R., Smol, J.P., Vincent, W.F. and Dastoor, A., 2009. Spatial trends and historical deposition of mercury in eastern and northern Canada inferred from lake sediment cores. Environmental Science & Technology, 43 (13):4802-4809.

Muir, D., Köck, G., Kirk J., Iqaluk, D., Williamson, M., Barst, B., Cabreizo, A., Hudelson, K., Talbot, C., Barresi, E., Francoeur, B., Carrier, J., Mathy, M. and Hansen, E., 2021. Temporal trends of persistent organic pollutants and mercury in landlocked char in High Arctic lakes. In: Beardsall, A., and Morris, A.D. (Eds). Synopsis of Research Conducted under the 2017-2018 Northern Contaminants Program, pp. 222-230. Crown-Indigenous Relations and Northern Affairs Canada, Gatineau, QC, Canada. Available at: https://pubs.aina.ucalgary.ca/ncp/Synopsis20172018.pdf

Mulvaney, K.M., Selin, N.E., Giang, A., Muntean, M., Li, C.-T., Zhang, D., Angot, H., Thackray, C.P. and Karplus, V.J., 2020. Mercury benefits of climate policy in China: addressing the Paris Agreement and the Minamata Convention simultaneously. Environmental Science & Technology, 54 (3):1326-1335.

Munson, K.M., Lamborg, C.H., Swarr, G.J. and Saito, M.A., 2015. Mercury species concentrations and fluxes in the central tropical Pacific Ocean. Global Biogeochemical Cycles, 29 (5):656-676.

Muntean, M., Janssens-Maenhout, G., Song, S., Selin, N.E., Olivier, J.G.J., Guizzardi, D., Maas, R. and Dentener, F., 2014. Trend analysis from 1970 to 2008 and model evaluation of EDGARv4 global gridded anthropogenic mercury emissions. Science of the Total Environment, 494-495:337-350.

Muntean, M., Janssens-Maenhout, G., Song, S., Giang, A., Selin, N.E., Zhong, H., Zhao, Y., Olivier, J.G.J., Guizzardi, D., Crippa, M., Schaaf, E. and Dentener, F., 2018. Evaluating EDGARv4.tox2 speciated mercury emissions ex-post scenarios and their impacts on modelled global and regional wet deposition patterns. Atmospheric Environment, 184:56-68.

Munthe, J., Bodaly, R.A., Branfireun, B.A., Driscoll, C.T., Gilmour, C.C., Harris, R., Horvat, M., Lucotte, M. and Malm, O., 2007. Recovery of mercury-contaminated fisheries. Ambio, 36 (1):33-44.

Murata, K., Weihe, P., Budtz-Jørgensen, E., Jørgensen, P.J. and Grandjean, P., 2004. Delayed brainstem auditory evoked potential latencies in

14-year-old children exposed to methylmercury. The Journal of Pediatrics, 144 (2):177-183.

Mustonen, K. and Mustonen, T. in cooperation with Aikio, A. and Aikio, P., 2011. Drowning reindeer, drowning homes: Indigenous Sámi and hydroelectricity development in Sompio, Finland. Snowchange Cooperative, Kontiolahti, Finland. 60pp.

Mustonen, T. and Mustonen, K., 2018. Koitajoen erämaataloudet muuttuvassa ympäristössä. Snowchange Cooperative, Kontiolahti, Suomi. 85pp. (Finnish Language).

Mustonen, T., and Shadrin, V., 2021. The River Alazeya: shifting socio-ecological systems connected to a northeastern Siberian river. Arctic, 74, 1:1-112.

Nagorski, S.A., Engstrom, D.R., Hudson, J.P., Krabbenhoft, D.P., Hood, E., DeWild, J.F. and Aiken, G.R., 2014. Spatial distribution of mercury in southeastern Alaskan streams influenced by glaciers, wetlands, and salmon. Environmental Pollution, 184:62-72.

NAMMCO, 2018. NAMMCO Scientific Committee Report of the Working Group on Abundance Estimates, Copenhagen, May 22-24, 2018. North Atlantic Marine Mammal Commission. 40pp. Available at: https://nammco.no/wp-content/uploads/2019/02/12-sc-25_report_aewg_may-rev-october-2018_rev.pdf

Nancarrow, T.L. and Chan, H.M., 2010. Observations of environmental changes and potential dietary impacts in two communities in Nunavut, Canada. Rural Remote Health, 10 (2):1370.

NASA, 2020. NASA, NOAA Analyses Reveal 2019 Second Warmest Year on Record. National Aeronautics and Space Administration (NASA). Available at: https://climate.nasa.gov/news/2945/nasa-noaa-analyses-reveal-2019-second-warmest-year-on-record/

Nasr, M. and Arp, P.A., 2018. Total mercury concentrations in lake and streams sediments related to wet-area coverage and geogenic sources within upslope basins. Soil and Sediment Contamination: An International Journal, 27 (3):221-248.

Nasr, M., Ogilvie, J., Castonguay, M., Rencz, A. and Arp P.A., 2011. Total Hg concentrations in stream and lake sediments: discerning geospatial patterns and controls across Canada. Applied Geochemistry, 26 (11):1818-1831.

Nerentorp Mastromonaco, M., 2016. Mercury cycling in the global marine environment. PhD. thesis. Department of Chemistry and Chemical Engineering, Chalmers University of Technology, Göteborg, Sweden. Available at: https://research.chalmers.se/en/publication/243105

Nerentorp Mastromonaco, M.G., Gårdfeldt, K., Langer, S. and Dommergue, A., 2016. Seasonal study of mercury species in the Antarctic sea ice environment. Environmental Science & Technology 50, (23):12705-12712.

Nerentorp Mastromonaco, M.G., Gårdfeldt, K. and Langer, S. 2017a. Mercury flux over West Antarctic Seas during winter, spring and summer. Marine Chemistry, 193:44-54.

Nerentorp Mastromonaco, M.G., Gårdfeldt, K., Assmann, K.M., Langer, S., Delali, T., Shlyapnikov, Y.M., Zivkovic, I. and Horvat, M., 2017b. Speciation of mercury in the waters of the Weddell, Amundsen and Ross Seas (Southern Ocean). Marine Chemistry, 193:20-33.

Nghiem, S.V., Rigor, I.G., Richter, A., Burrows, J.P., Shepson, P.B., Bottenheim, J., Barber, D.G., Steffen, A., Latonas, J., Wang, J., Stern, G., Clemente-Coln, P., Martin, S., Hall, D.K., Kaleschke, L., Tackett, P., Neumann, G. and Asplin, M.G., 2012. Field and satellite observations of the formation and distribution of Arctic atmospheric bromine above a rejuvenated sea ice cover. Journal of Geophysical Research: Atmospheres, 117 (D17):1773-1788.

Nguyen, H.T., Kim, K., Shon, Z. and Hong, S., 2009. A review of atmospheric mercury in the polar environment. Critical Reviews in Environmental Science & Technology, 39 (7):552-584.

Nguyen, L.S.P., Sheu, G.-R., Lin, D.-W. and Lin, N.-H., 2019. Temporal changes in atmospheric mercury concentrations at a background mountain site downwind of the East Asia continent in 2006–2016. Science of the Total Environment, 686:1049-1056.

Nickel, S., Hertel, A., Pesch, R., Schröder, W., Steinnes, E. and Uggerud, H.T., 2015. Correlating concentrations of heavy metals in atmospheric deposition with respective accumulation in moss and natural surface soil for ecological land classes in Norway between 1990 and 2010. Environmental Science and Pollution Research, 22:8488-8498.

Nielsen, J.B. and Andersen, O., 1991. Methyl mercuric chloride toxicokinetics in mice. I: effects of strain, sex, route of administration and dose. Pharmacology & Toxicology, 68 (3):201-207.

Nielsen, S.T., Mortensen, R., Hoydal, K., Erenbjerg, S.V. and Dam, M., 2012a. AMAP Faroe Islands Heavy Metals and POPs Core Programme 2009-2012. Environment Agency, Faroe Islands. 64pp. Available at: http://www.us.fo/Admin/Public/DWSDownload.aspx?File=%2fFiles%2fFiler%2fUS%2futgavur%2f2014%2fAMAP+2009-2012_rapport_til_print.pdf

Nielsen, A.B.S, Davidsen, M. and Bjerregaard, P., 2012b. The association between blood pressure and whole blood methylmercury in a cross-sectional study among Inuit in Greenland. Environmental Health.11 (1):44.

Nielsen, S., Mortensen, R., Hoydal, K., Erenbjerg, S.V. and Dam, M., 2014. AMAP Faroe Islands Heavy Metals and POPs Core Programme 2009-2012 (Report no. US 12/00109-35). Environment Agency, Argir, Faroe Islands. 64pp.

Nieminen, M., Koskinen, M., Sarkkola, S., Laurén, A., Kaila, A., Kiikkilä, O., Nieminen, T.M. and Ukonmaanaho, L., 2015. Dissolved organic carbon export from harvested peatland forests with differing site characteristics. Water, Air, & Soil Pollution, 226 (6):181.

Niki, H., Maker, P.S., Savage, C.M. and Breitenbach, L.P., 1983a. A Fourier-transform infrared study of the kinetics and mechanism of the reaction of atomic chlorine with dimethylmercury. The Journal of Physical Chemistry, 87 (19):3722-3724.

Niki, H., Maker, P.D., Savage, C.M. and Breitenbach, L.P., 1983b. A long-path Fourier transform infrared study of the kinetics and mechanism for the hydroxyl radical-initiated oxidation of dimethylmercury. The Journal of Physical Chemistry, 87 (24):4978-4981.

Nilsson, L.M., Destouni, G., Berner, J., Dudarev, A.A., Mulvad, G., Odland, J.Ø., Parkinson, A., Tikhonov, C., Rautio, A. and Evengård, B., 2013. A call for urgent monitoring of food and water security based on relevant indicators for the Arctic. AMBIO, 42 (7):816-822.

Nilsson, C., Polvi, L.E. and Lind, L., 2015. Extreme events in streams and rivers in Arctic and Subarctic regions in an uncertain future. Freshwater Biology, 60 (12):2535-2546.

NILU, 2020. EBAS Atmospheric database [database]. Available at: http://ebas.nilu.no/

NOAA, 2020. Climate Variability: North Atlantic Oscillation | NOAA Climate.Gov. Available at: https://www.climate.gov/news-features/understanding-climate/climate-variability-north-atlantic-oscillation

Northern Contaminants Program, 2012. Canadian Arctic Contaminants Assessment Report III (2012): Mercury in Canada's North. Aboriginal Affairs and Northern Development Canada (AANDC), Gatineau, Quebec, Canada. xxiii + 276pp.

Northern Contaminants Program, 2021. Beardsall, A., and Morris, A.D. (Eds). Synopsis of Research Conducted under the 2017-2018 Northern Contaminants Program, pp. 231-244. Crown-Indigenous Relations and Northern Affairs Canada, Gatineau, QC, Canada. Available at: https://pubs.aina.ucalgary.ca/ncp/Synopsis20172018.pdf

Norwegian Polar Institute (NPI), 2019. Norwegian Polar Data Centre [database]. Available at: https://data.npolar.no/home/

Nossov, D.R., Torre Jorgenson, M., Kielland, K. and Kanevskiy, M.Z., 2013. Edaphic and microclimatic controls over permafrost response to fire in interior Alaska. Environmental Research Letters, 8 (3):035013.

Notz, D. and Stroeve, J., 2016. Observed Arctic sea-ice loss directly follows anthropogenic CO2 emission. Science, 354:747-750.

Notz, D. and SIMIP Community, 2020. Arctic sea ice in CMIP6. Geophysical Research Letters, 47: e2019GL086749.

NRBHSS, 2004. Nunavik Inuit Health Survey 2004, *Qanuippitaa*? How are we? Quebec: Institut national de santé publique du Québec (INSPQ) and Nunavik Regional Board of Health and Social Services (NRBHSS). Available at: https://nrbhss.ca/en/nrbhss/public-health/health-surveys/qanuippitaa-2004

NRBHSS, 2017. *Qanuilirpitaa?* How are we now? Health Survey. Nunavik Regional Board of Health and Social Services (NRBHSS). Available at: https://nrbhss.ca/en/nrbhss/public-health/health-surveys/qanuilirpitaa-2017

NRC, 2000. National Research Council (US). The Toxicological Effects of Methylmercury, National Academies Press. 364pp.

O'Connor, D., Hou, D., Ok, Y.S., Mulder, J., Duan, L., Wu, Q., Wang, S., Tack, F.M.G. and Rinklebe, J., 2019. Mercury speciation, transformation, and transportation in soils, atmospheric flux, and implications for risk management: a critical review. Environment International, 126:747-761.

O'Driscoll, N.J., Poissant, L., Canário, L., Ridal, J. and Lean, D.R.S., 2007. Continuous analysis of dissolved gaseous mercury and mercury volatilization in the upper St. Lawrence River: exploring temporal relationships and UV attenuation. Environmental Science & Technology, 41 (15):5342-5348.

O'Donnell, J.A., Aiken, G.R., Swanson, D.K., Panda, S., Butler, K.D. and Baltensperger, A.P., 2016. Dissolved organic matter composition of Arctic rivers: linking permafrost and parent material to riverine carbon. Global Biogeochemical Cycles, 30 (12):1811-1826.

O'Reilly, C., et al., 2015. Rapid and highly variable warming of lake surface waters around the globe. Geophysical Research Letters, 42 (24):10773-10781.

Obrist, D., 2012. Mercury distribution across 14 U.S. Forests. Part II: Patterns of methyl mercury concentrations and areal mass of total and methyl mercury. Environmental Science & Technology, 46 (11):5921-5930.

Obrist, D., Hallar, A.G., McCubbin, I., Stephens, B.B. and Rahn, T., 2008. Atmospheric mercury concentrations at Storm Peak Laboratory in the Rocky Mountains: evidence for long-range transport from Asia, boundary layer contributions, and plant mercury uptake. Atmospheric Environment, 42 (33):7579-7589.

Obrist, D., Johnson, D.W., Lindberg, S.W., Luo, Y., Hararuk, O., Bracho, R., Battles, J.J., Dail, D.B., Edmonds, R.L., Monson, R.K., Ollinger, S.V., Pallardy, S.G., Pregitzer, K.S. and Todd, D.E., 2011. Mercury distribution across 14 U.S. forests. Part I: Spatial patterns of concentrations in biomass, litter, and soils. Environmental Science & Technology, 45 (9):3974-3981.

Obrist, D., Agnan, Y., Jiskra, M., Olson, C.L., Colegrove, D.P., Hueber, J., Moore, C.W., Sonke, J.E. and Helmig, D., 2017. Tundra uptake of atmospheric elemental mercury drives Arctic mercury pollution. Nature, 547 (7662):201-204.

Obrist, D., Kirk, J.L., Zhang, L., Sunderland, E.M., Jiskra, M. and Selin, N.E., 2018. A review of global environmental mercury processes in response to human and natural perturbations: changes of emissions, climate, and land use. Ambio, 47 (2):116-140.

Oldfield, F. and Appleby, P.G., 1984. Empirical testing of ^{210}Pb-dating models for lake sediments. In: Haworth, E.Y. and Lund, J.W. (Eds.). Lake Sediments and Environmental History: Studies in Palaeolimnology and Palaeoecology in Honour of Winifred Tutin, pp. 93-124. Leicester University Press.

Olefeldt, D., Goswami, S., Grosse, G., Hayes, D., Hugelius, G., Kuhry, P., McGuire, A.D., Romanovsky, V.E., Sannel, A.B.K., Schuur, E.A.G. and Turetsky, M.R., 2016. Circumpolar distribution and carbon storage of thermokarst landscapes. Nature Communications, 7 (1):13043.

Olivero-Verbel, J., Agudelo-Frias, D. and Caballero-Gallardo, K., 2013. Morphometric parameters and total mercury in eggs of snowy egret *(Egretta thula)* from Cartagena Bay and Totumo Marsh, north of Colombia. Marine Pollution Bulletin, 69 (1-2):105-109.

Olson, C., Jiskra, M., Biester, H., Chow, J. and Obrist, D., 2018. Mercury in active-layer tundra soils of Alaska: concentrations, pools, origins, and spatial distribution. Global Biogeochemical Cycles, 32 (7):1058-1073.

Olson, C.L., Jiskra, M., Sonke, J.E. and Obrist, D., 2019. Mercury in tundra vegetation of Alaska: spatial and temporal dynamics and stable isotope patterns. Science of the Total Environment, 660:1502-1512.

Olson, C.I., Fakhraei, H. and Driscoll, C.T., 2020. Mercury emissions, atmospheric concentrations, and wet deposition across the conterminous United States: changes over 20 years of monitoring. Environmental Science & Technology Letters, 7 (6):376-381.

Osburn, C.L., Anderson, N.J., Stedmon, C.A., Giles, M.E., Whiteford, E.J., McGenity, T.J., Dumbrell, A.J. and Underwood, G.J.C., 2017. Shifts in the source and composition of dissolved organic matter in Southwest Greenland lakes along a regional hydroclimate gradient. Journal of Geophysical Research: Biogeosciences, 122 (12):3431-3445.

Østerhus, S., Woodgate, R., Valdimarsson, H., Turrell, B., de Steur, L., Quadfasel, D., Olsen, S.M., Moritz, M., Lee, C.M., Larsen, K.M.H., Jónsson, S., Johnson, C., Jochumsen, K., Hansen, B., Curry, B., Cunningham, S. and Berx, B., 2019. Arctic Mediterranean exchanges: a consistent volume budget and trends in transports from two decades of observations. Ocean Science, 15 (2):379-399.

Ostertag, S.K, Loseto, L.L., Snow, K., Lam, J., Hynes, K. and Gillman, D.V., 2018. "That's how we know they're healthy": the inclusion of traditional ecological knowledge in beluga health monitoring in the Inuvialuit Settlement Region. Arctic Science, 4 (3):292-320.

Osterwalder, S., Sommar, J., Åkerblom, S., Jocher, G., Fritsche, J., Nilsson, M.B., Bishop, K. and Alewell, C., 2018. Comparative study of elemental mercury flux measurement techniques over a Fennoscandian boreal peatland. Atmospheric Environment, 172:16-25.

Oulehle, F., Jones, T.G., Burden, A., Cooper, M.D.A., Lebron, I., Zieliński, P. and Evans, C.D., 2013. Soil-solution partitioning of DOC in acid organic soils: results from a UK field acidification and alkalization experiment. European Journal of Soil Science, 64 (6):787-796.

Outridge, P.M. and Sanei, H., 2010. Does organic matter degradation affect the reconstruction of pre-industrial atmospheric mercury deposition rates from peat cores? — A test of the hypothesis using a permafrost peat deposit in northern Canada. International Journal of Coal Geology, 83 (1):73-81.

Outridge, P.M., Sanei, H., Stern, G.A., Hamilton, P.B. and Goodarzi, F., 2007. Evidence for control of mercury accumulation rates in Canadian High Arctic lake sediments by variations of aquatic primary productivity. Environmental Science & Technology, 41 (15):5259-5265.

Outridge, P.M., Macdonald, R.W., Wang, F., Stern, G.A. and Dastoor, A.P., 2008. A mass balance inventory of mercury in the Arctic Ocean. Environmental Chemistry, 5 (1):89-111.

Outridge, P.M., Sanei, H., Courtney Mustaphi, C.J. and Gajewski, K., 2017. Holocene climate change influences on trace metal and organic matter geochemistry in the sediments of an Arctic lake over 7,000 years. Applied Geochemistry, 78:35-48.

Outridge, P.M., Mason, R.P., Wang, F., Guerrero, S. and Heimbürger-Boavida, L.E., 2018. Updated global and oceanic mercury budgets for the United Nations Global Mercury Assessment 2018. Environmental Science & Technology, 52 (20):11466-11477.

Outridge, P.M., Stern, G.A., Hamilton, P.B. and Sanei, H., 2019. Algal scavenging of mercury in preindustrial Arctic lakes. Limnology and Oceanography, 64 (4):1558-1571.

Overduin, P.P., Strzelecki, M.C., Grigoriev, M.N., Couture, N., Lantuit, H., St-Hilare-Gravel, D., Günther F. and Wetterrich, S., 2014. Coastal changes in the Arctic. In: Martini, I.P. and Wanless, H.R. (Eds.). Sedimentary Coastal Zones from High to Low Latitudes: Similarities and Differences. Geological Society Special Publication 388, pp. 103-130. The Geological Society.

Overeem, I. and Syvitski, J.P.M., 2008. Changing sediment supply in Arctic rivers. In: Schmidt, J., Cochrane, T., Phillips, C., Elliott, S., Davies, T. and Basher, L. (Eds.). Sediment Dynamics in Changing Environments. International Association of Hydrological Sciences Publication 325, pp. 391-397. International Association of Hydrological Sciences.

Overeem, I., Hudson, B.D., Syvitski, J.P.M., Mikkelsen, A.B., Hasholt, B., van den Broeke, M. R., Noël, B.P.Y. and Morlighem, M., 2017. Substantial export of suspended sediment to the global oceans from glacial erosion in Greenland. Nature Geoscience, 10 (11):859-863.

Øverjordet, I.B., Altin, D., Berg, T., Jenssen, B.M., Gabrielsen, G.W. and Hansen, B.H., 2014. Acute and sub-lethal response to mercury in Arctic and boreal calanoid copepods. Aquatic Toxicology, 155:160-165.

Øverjordet, I.B., Gabrielsen, G.W., Berg, T., Ruus, A., Evenset, A., Borgå, K., Christensen, G., Lierhagen, S. and Jenssen, B.M., 2015a. Effect of diet, location and sampling year on bioaccumulation of mercury, selenium and cadmium in pelagic feeding seabirds in Svalbard. Chemosphere, 122:14-22.

Øverjordet, I.B., Kongsrud, M.B., Gabrielsen, G.W., Berg, T., Ruus, A., Evenset, A., Borgå, K., Christensen, G. and Jenssen, B.M., 2015b. Toxic and essential elements changed in black-legged kittiwakes (*Rissa tridactyla*) during their stay in an Arctic breeding area. Science of the Total Environment, 502:548-556.

Overland, J. E. and Wang, M., 2013. When will the summer Arctic be nearly sea ice free? Geophysical Research Letters, 40 (10):2097-2101.

Oziel, L., Baudena, A., Ardyna, M., Massicotte, P., Randelhoff, A., Sallée, J.-B., Ingvaldsen, R.B., Devred, E. and Babin, M., 2020. Faster Atlantic currents drive poleward expansion of temperate phytoplankton in the Arctic Ocean. Nature Communications, 11 (1):1705.

Pacyna, E.G. and Pacyna, J.M., 2002. Global emission of mercury from anthropogenic sources in 1995. Water, Air, & Soil Pollution, 137 (1):149-165.

Pacyna, E.G., Pacyna, J.M., Steenhuisen, F. and Wilson, S., 2006. Global anthropogenic mercury emission inventory for 2000. Atmospheric Environment, 40 (22):4048-4063.

Pacyna, E.G., Pacyna, J.M., Sundseth, K., Munthe, J., Kindbom, K., Wilson, S., Steenhuisen, F. and Maxson, P., 2010. Global emission of mercury to the atmosphere from anthropogenic sources in 2005 and projections to 2020. Atmospheric Environment, 44 (20):2487-2499.

Pacyna, J.M., Travnikov, O., De Simone, F., Hedgecock, I. M., Sundseth, K., Pacyna, E.G., Steenhuisen, F., Pirrone, N., Munthe, J. and Kindbom, K., 2016. Current and future levels of mercury atmospheric pollution on a global scale. Atmospheric Chemistry and Physics, 16 (19):12495-12511.

Pacyna, A.D., Koziorowska, K., Chmiel, S., Mazerski, J. and Polkowska, Z., 2018. Svalbard reindeer as an indicator of ecosystem changes in the Arctic terrestrial ecosystem. Chemosphere, 203: 209-218.

Pagano, A.M., Durner, G.M., Rode, K.D., Atwood, T.C., Atkinson, S.N., Peacock, E., Costa, D.P., Owen, M.A. and Williams, T.M., 2018. High-energy, high-fat lifestyle challenges an Arctic apex predator, the polar bear. Science, 359 (6375):568-572.

Pal, B., and Ariya, P.A., 2004. Studies of ozone initiated reactions of gaseous mercury: kinetics, product studies, and atmospheric implications. Physical Chemistry Chemical Physics, 6 (3):572-578.

Parajuli, R.P., Goodrich, J.M., Chan, L.H.M., Ayotte, P., Lemire, M., Hegele, R.A. and Basu, N., 2018. Genetic polymorphisms are associated with exposure biomarkers for metals and persistent organic pollutants among Inuit from the Inuvialuit Settlement Region, Canada. Science of the Total Environment, 634:569-578.

Parajuli, R.P., Goodrich, J.M., Chan, L.H.M., Lemire, M., Ayotte, P., Hegele, R.A. and Basu, N., 2021. Variation in biomarker levels of metals, persistent organic pollutants, and omega-3 fatty acids in association with genetic polymorphisms among Inuit in Nunavik, Canada. Environmental Research, 200:111393.

Paris, J.-D., Stohl, A., Nédélec, P., Arshinov, M. Yu., Panchenko, M.V., Shmargunov, V.P., Law, K.S., Belan, B.D. and Ciais, P., 2009. Wildfire smoke in the Siberian Arctic in summer: source characterization and plume evolution from airborne measurements. Atmospheric Chemistry and Physics, 9 (23):9315-9327.

Park, K.S., Seo, Y.C., Lee, S.J. and Lee, J.H., 2008. Emission and speciation of mercury from various combustion sources. Powder Technology, 180 (1-2):151-156.

Parks, J.M., Johs, A., Podar, M., Bridou, R., Hurt, R.A., Jr., Smith, S.D., Tomanicek, S.J., Qian, Y., Brown, S.D., Brandt. C.C., Palumbo, A.V., Smith, J.C., Wall, J.D., Elias, D.A. and Liang, L., 2013. The genetic basis for bacterial mercury methylation. Science, 339 (6125):1332-1335.

Pastick, N.J., Jorgenson, M.T., Goetz, S.J., Jones, B.M., Wylie, B.K., Minsley, B.J., Genet, H., Knight, J.K., Swanson, D.K. and Jorgenson, J.C., 2019. Spatiotemporal remote sensing of ecosystem change and causation across Alaska. Global Change Biology, 25 (3):1171-1189.

Patyk, K.A., Duncan, C., Nol, P., Sonne, C., Laidre, K., Obbard, M., Wiig, Ø., Aars, J., Regehr, E., Gustafson, L.L. and Atwood, T., 2015. Establishing a definition of polar bear (*Ursus maritimus*) health: a guide to research and management activities. Science of the Total Environment, 514:371-378.

Pearce, T., Ford, J., Willox, A.C. and Smit, B., 2015. Inuit Traditional Ecological Knowledge (TEK), subsistence hunting and adaptation to climate change in the Canadian Arctic. Arctic, 68 (2):233-245.

Pearson, C., Howard, D., Moore, C. and Obrist, D., 2019. Mercury and trace metal wet deposition across five stations in Alaska: controlling factors, spatial patterns, and source regions. Atmospheric Chemistry and Physics, 19 (10):6913-6929.

Peck, L.E., Gilchrist, H.G., Mallory, C.D., Braune, B.M. and Mallory, M.L., 2016. Persistent organic pollutant and mercury concentrations in eggs of ground-nesting marine birds in the Canadian High Arctic. Science of the Total Environment, 556:80-88.

Pecl, G.T., Araújo, M.B., Bell, J.D., Blanchard, J., Bonebrake, T.C., Chen, I., Clark, T.D., Colwell, R.K., Danielsen, K., Evengård, B., Falconi, L., Ferrier, S., Frusher, S., Garcia, R.A., Griffis, R.B., Hobday, A.J., Janion-Scheepers, C., Jarzyna, M.A., Jennings, S., Lenoir, J., Linnetved, H.I., Martin, V.Y., McCormack, P.C., McDonald, J., Mitchell, N.J., Mustonen, T., Pandolfi, J.M., Pettorelli, N., Popova, E., Robinson, S.A., Scheffers, B.R., Shaw, J.D., Sorte, C.J.B., Strugnell, J.N., Sunday, J.M., Tuanmu, M.-N., Vergés, A., Villanueva, C., Wernberg, T., Wapstra, E. and Williams, S.E., 2017. Biodiversity redistribution under climate change: impacts on ecosystems and human well-being. Science, 355 (6332):1389.

Pedersen, H.C., Fossøy, F., Kålås, J.A. and Lierhagen, S., 2006. Accumulation of heavy metals in circumpolar willow ptarmigan (*Lagopus l. lagopus*) populations. Science of the Total Environment, 371 (1-3):176-189.

Pedersen, C., Otokiak, M., Koonoo, I., Milton, J., Maktar, E., Anaviapik, A., Milton, M., Porter, G., Scott, A., Newman, C., Porter, C., Aaluk, T., Tiriraniaq, B., Pedersen, A., Riffi, M., Solomon, E. and Elverum, S., 2020. ScIQ: an invitation and recommendations to combine science and Inuit Qaujimajatuqangit for meaningful engagement of Inuit communities in research. Arctic Science, 6 (3):326-339.

Pedro, S., Fisk, A.T., Tomy, G.T., Ferguson, S.H., Hussey, N.E., Kessel, S.T. and McKinney, M.A., 2017. Mercury and persistent organic pollutants in native and invading forage species of the Canadian Arctic: consequences for food web dynamics. Environmental Pollution, 229:229-240.

Pedro, S., Fisk, A.T., Ferguson, S.H., Hussey, N.E. Kessel, S.T. and McKinney, M.A., 2019. Limited effects of changing prey fish communities on food quality for aquatic predators in the eastern Canadian Arctic in terms of essential fatty acids, methylmercury and selenium. Chemosphere, 214:855-865.

Peeters, B., Pedersen, A.O., Loe, L.E., Isaksen, K., Veiberg, V., Stien, A., Kohler, J., Gallet, J.-C., Aanes, R. and Hansen, B.B., 2019. Spatiotemporal patterns of rain-on-snow and basal ice in High Arctic Svalbard: detection of a climate-cryosphere regime shift. Environmental Research Letters, 14 (1):015002.

Pelletier, E., 1988. Acute toxicity of some methylmercury complexes to *Mytilus edulis* and lack of selenium protection. Marine Pollution Bulletin, 19:213-219.

Pelletier, A.R., Castello, L., Zhulidov, A.V., Gurtovaya, T.Y., Robarts, R.D., Holmes, R.M., Zhulidov, D.A. and Spencer, R.G.M., 2017. Temporal and longitudinal mercury trends in burbot (*Lota lota*) in the Russian Arctic. Environmental Science & Technology, 51 (22):13436-13442.

Pelletier, N., Chételat, J., Blarquez, O. and Vemaire, J.C., 2020. Paleolimnological assessment of wildfire-derived atmospheric deposition of trace metal(loid)s and major ions to Subarctic lakes (Northwest Territories, Canada). Journal of Geophysical Research: Biogeosciences, 125 (8):e2020JG005720.

Peralta-Ferriz, C. and Woodgate, R.A., 2017. The dominant role of the East Siberian Sea in driving the oceanic flow through the Bering Strait — Conclusions from GRACE Ocean Mass Satellite data and *in situ* mooring observations between 2002 and 2016. Geophysical Research Letters, 44 (22):11472-11481.

Perkins, M., 2018. Exposure science to investigate factors influencing mercury concentrations in non-piscivorous birds. Doctor of Philosophy thesis, Department of Natural Resource Sciences, McGill University, Montreal, Canada. Available at: https://escholarship.mcgill.ca/concern/theses/hq37vq93w

Perkins, M., Ferguson, L., Lanctot, R.B., Stenhouse, I.J., Kendall, S., Brown, S., Gates, H.R., Hall, J.O., Regan, K., Evers, D.C., 2016. Mercury exposure and risk in breeding and staging Alaskan shorebirds. The Condor, 118 (3):571-582.

Permanent Participants, 2018. Press Release: Arctic Indigenous Peoples at the Second Arctic Science Ministerial (including the updated Ottawa Indigenous Knowledge Principles). Available at: https://iccalaska.org/wp-icc/wp-content/uploads/2018/10/ICC_PP-press-release_1026.pdf

Perovich, D.K., 2006. The interaction of ultraviolet light with Arctic sea ice during SHEBA. Annals of Glaciology, 44:47-52.

Perovich, D.K. and Richter-Menge, J.A., 2009. Loss of sea ice in the Arctic. Annual Review of Marine Science, 1 (1):417-441.

Perron, T., Chételat, J., Gunn, J., Beisner, B.E. and Amyot, M., 2014. Effects of experimental thermocline and oxycline deepening on methylmercury bioaccumulation in a Canadian Shield lake. Environmental Science & Technology, 48 (5):2626-2634.

Perry, E., Norton, S.A., Kamman, N.C., Lorey, P.M. and Driscoll, C.T., 2005. Deconstruction of historic mercury accumulation in lake sediments, northeastern United States. Ecotoxicology, 14 (1):85-99.

Peterson, B.J., Holmes, R.M., McClelland, J.W., Vörösmarty, C.J., Lammers, R.B., Shiklomanov, A.I., Shiklomanov, I.A. and Rahmstorf, S., 2002. Increasing river discharge to the Arctic Ocean. Science, 298:2171-2173.

Peterson, S.A., Van Sickle, J., Hughes, R.M., Schacher, J.A. and Echols, S.F., 2004. A biopsy procedure for determining filet and predicting whole-fish mercury concentration. Archives of Environmental Contamination and Toxicology, 48 (1):99-107.

Peterson, K.A., Shepler, B.C. and Singleton, J.M., 2007. The group 12 metal chalcogenides: an accurate multireference configuration interaction and coupled cluster study. Molecular Physics, 105 (9):1139-1155.

Peterson, D.A., Campbell, J.R., Hyer, E.J., Fromm, M.D., Kablick, G.P., III, Cossuth, J.H. and DeLand, M.T., 2018a. Wildfire-driven thunderstorms cause a volcano-like stratospheric injection of smoke. npj Climate and Atmospheric Science, 1 (1):30.

Peterson, S.H., Ackerman, J.T., Crocker, D.E. and Costa, D.P., 2018b. Foraging and fasting can influence contaminant concentrations in animals: an example with mercury contamination in a free-ranging marine mammal. Proceedings of the Royal Society B: Biological Sciences, 285 (1872):20172782.

Peterson, S.H., Ackerman, Toney, M. and Herzog, M.P., 2019. Mercury concentrations vary within and among individual bird feathers: a critical evaluation and guidelines for feather use in mercury monitoring programs. Environmental Toxicology and Chemistry, 38 (6):1164–1187.

Petrova, M.V., Krisch, S., Lodeiro, P., Valk, O., Dufour, A., Rijkenberg, M.J.A., Achterberg, E.P., Rabe, B., Rutgers van der Loeff, M., Hamelin,

B., Sonke, J.E., Garnier, C. and Heimbürger-Boavida, L.-E., 2020. Mercury species export from the Arctic to the Atlantic Ocean. Marine Chemistry, 225:103855.

Pfeifer, P., 2018. From the credibility gap to capacity building: an Inuit critique of Canadian Arctic research. Northern Public Affairs, 6 (1):29-34.

Pickhardt, P.C. and Fisher, N.S., 2007. Accumulation of inorganic and methylmercury by freshwater phytoplankton in two contrasting water bodies. Environmental Science & Technology, 41 (1):125-131.

Pienitz, R., Smol, J.P. and Lean, D.R.S., 1997. Physical and chemical limnology of 59 lakes located between the southern Yukon and the Tuktoyaktuk Peninsula, Northwest Territories (Canada). Canadian Journal of Fisheries and Aquatic Sciences, 54 (2):330-346.

Piniarneq, 2020. Jagtinformation og fangstregistrering. Available at: https://www.sullissivik.gl/-/media/Sullissivik/Blanketter-og-pdf/Jagt_fangst_og_fiskeri/Piniarneq-2020-DA.ashx?la=da-DK (Danish and Greenlandic language).

Pinzone, M., 2021. Sourcing and dynamic of mercury in Arctic true seals. PhD thesis. Université de Liège, Jandrain-Jandranouille, Belgium. vii + 245pp. Available at: http://hdl.handle.net/2268/263365

Piquet, A.M.-T., van de Poll, W.H., Visser, R.J.W., Wiencke, C., Bolhuis, H., Buma, A.G.J., 2014. Springtime phytoplankton dynamics in Arctic Krossfjorden and Kongsfjorden (Spitsbergen) as a function of glacier proximity. Biogeosciences, 11 (8):2263–2279.

Pistone, K., Eisenman, I. and Ramanathan, V., 2014. Observational determination of albedo decrease caused by vanishing Arctic sea ice. Proceedings of the National Academy of Sciences of the United States of America, 111 (9):3322-3326.

Pithan, F., Svensson, G., Caballero, R., Chechin, D., Cronin, T.W., Ekman, A.M.L., Neggers, R., Shupe, M.D., Solomon, A., Tjernström, M. and Wendisch, M., 2018. Role of air-mass transformations in exchange between the Arctic and mid-latitudes. Nature Geoscience, 11 (11):805-812.

Platjouw, F.M., Steindal, E.H. and Borch, T., 2018. From Arctic science to international law: the road towards the Minamata Convention and the role of the Arctic Council. Arctic Review, 9:226-243.

Podar, M., Gilmour, C.C., Brandt, C.C., Soren, A., Brown, S.D., Crable, B.R., Palumbo, A.V., Somenahally, A.C. and Elias, D.A., 2015. Global prevalence and distribution of genes and microorganisms involved in mercury methylation. Science Advances, 1 (9):e1500675.

Point, D., Sonke, J.E., Day, R.D., Roseneau, D.G., Hobson, K.A., Vander Pol, S.S., Moors, A.J., Pugh, R.S., Donard, O.F.X. and Becker, P.R., 2011. Methylmercury photodegradation influenced by sea-ice cover in Arctic marine ecosystems. Nature Geoscience, 4 (3):188-194.

Poissant, L. and Pilote, M., 2003. Time series analysis of atmospheric mercury in Kuujjuarapiuk/Whapmagoostui (Québec). Journal de Physique IV, 107 (2):1079-1082.

Pokrovsky, O.S., Bueno, M., Manasypov, R.M., Shirokova, L.S., Karlsson, J. and Amouroux, D., 2018. Dissolved organic matter controls seasonal and spatial selenium concentration variability in thaw lakes across a permafrost gradient. Environmental Science & Technology, 52 (18):10254-10262.

Pollet, I.L., Leonard, M.L., O'Driscoll, N.J., Burgess, N.M. and Shutler, D., 2017. Relationships between blood mercury levels, reproduction, and return rate in a small seabird. Ecotoxicology, 26 (1):97-103.

Pomerleau, C., Stern, G.A., Pućko, M., Foster, K.L., Macdonald, R.W. and Fortier, L., 2016. Pan-Arctic concentrations of mercury and stable isotope ratios of carbon ($\delta^{13}C$) and nitrogen ($\delta^{15}N$) in marine zooplankton. Science of the Total Environment, 551-552:92-100.

Pomerleau, C., Matthews, C.J.D., Gobeil, C., Stern, G.A., Ferguson, S.H. and Macdonald, R.W., 2018. Mercury and stable isotope cycles in baleen plates are consistent with year-round feeding in two bowhead whale (*Balaena mysticetus*) populations. Polar Biology, 41 (9):1881-1893.

Pongratz, R. and Heumann, K.G., 1998. Production of methylated mercury and lead by polar macroalgae — a significant natural source for atmospheric heavy metals in clean room compartments. Chemosphere, 36 (9):1935-1946.

Pongratz, R. and Heumann, K.G., 1999. Production of methylated mercury, lead and cadmium by marine bacteria as a significant natural source for atmospheric heavy metals in polar regions. Chemosphere, 39 (1):89-102.

Pontual, M.M., Ayotte, P., Little, M., Furgal, C., Boyd, A.D., Muckle, G., Avard, E., Ricard, S., Gauthier, M.-J., Sidi, E.A.-L. and Lemire, M., 2020. Seasonal variations in exposure to methylmercury and its dietary sources among pregnant Inuit women in Nunavik, Canada. Science of the Total Environment, 755 (Part 2):143196.

Post, E., Forchhammer, M.C., Bret-Harte, M.S., Callaghan, T.V., Christensen, T.R., Elberling, B., Fox, A.D., Gilg, O., Hik, D.S., Høye, T.T., Ims, R.A., Jeppesen, E., Klein, D.R., Madsen, J., McGuire, A.D., Rysgaard, S., Schindler, D.E., Stirling, I., Tamstorf, M.P., Tyler, N.J.C., van der Wal, R., Welker, J., Wookey, P.A., Schmidt, N.M. and Aastrup, P., 2009. Ecological dynamics across the Arctic associated with recent climate change. Science, 325 (5946):1355-1358.

Post, E., Bhatt, U.S., Bitz, C.M., Brodie, J.F., Fulton, T.L., Hebbelwhite, M., Kerby, J., Kutz, S.J., Stirling, I. and Walker, D.A., 2013. Ecological consequences of sea-ice decline. Science, 341 (6145):519-524.

Poste, A.E., Braaten, H.F.V., de Wit, H.A., Sørensen, K. and Larssen, T., 2015. Effects of photodemethylation on the methylmercury budget of boreal Norwegian lakes. Environmental Toxicology and Chemistry, 34 (6):1213-1223.

Poste, A.E., Hoel, C.S., Andersen, T., Arts, M.T., Frærøvig, P-J. and Borgå, K., 2019. Terrestrial organic matter increases zooplankton methylmercury accumulation in a brown-water boreal lake. Science of the Total Environment, 674:9-18.

Poulain, A.J., Garcia, E., Amyot, M., Campbell, P.G. and Ariya, P.A., 2007a. Mercury distribution, partitioning and speciation in coastal vs. inland High Arctic snow. Geochimica et Cosmochimica Acta, 71 (14):3419-3431.

Poulain, A.J., Chadhain, S.M.N., Ariya, P.A., Amyot, M., Garcia, E., Campbell, P.G.C., Zylstra, G.J. and Barkay, T., 2007b. Potential for mercury reduction by microbes in the High Arctic. Applied and Environmental Microbiology, 73 (7):2230-2238.

Power, M., Klein, G.M., Guiguer, K.R.R.A. and Kwan, M.K.H., 2002. Mercury accumulation in the fish community of a Sub-Arctic lake in relation to trophic position and carbon sources. Journal of Applied Ecology, 39 (5):819-830.

Power, M., Reist, J.D. and Dempson, J.B., 2008. Fish in high-latitude Arctic lakes. In: Vincent, W.F. and Laybourn-Parry, J. (Eds.). Polar Lakes and Rivers: Limnology of Arctic and Antarctic Aquatic Ecosystems, pp. 249-267. Oxford University Press.

Pozzoli, L., Dobricic, S., Russo, S. and Vignati, E., 2017. Impacts of large-scale atmospheric circulation changes in winter on black carbon transport and deposition to the Arctic. Atmospheric Chemistry and Physics, 17 (19):11803-11818.

Pratt, K.A., Custard, K.D., Shepson, P.B., Douglas, T.A., Pöhler, D., General, S., Zielcke, J., Simpson, W.R., Platt, U., Tanner, D.J., Huey, L.G., Carlsen, M. and Stirm, B.H., 2013. Photochemical production of molecular bromine in Arctic surface snowpacks. Nature Geoscience, 6 (5):351-356.

Prestbo, E.M. and Gay, D.A., 2009. Wet deposition of mercury in the US and Canada, 1996–2005: results and analysis of the NADP mercury deposition network (MDN). Atmospheric Environment, 43 (27):4223-4233.

Price, S.J., Leung, W.T.M., Owen, C.J., Puschendorf, R., Sergeant, C., Cunningham, A.A., Balloux, F., Garner, T.W.J. and Nichols, R.A., 2019. Effects of historic and projected climate change on the range and impacts of an emerging wildlife disease. Global Change Biology, 25:2648-2660.

Priet-Mahéo, M.C., Ramón, C.L., Rueda, F.J. and Andradóttir, H.Ó., 2019. Mixing and internal dynamics of a medium-size and deep lake near the Arctic Circle. Limnology and Oceanography, 64(1):61-80.

Prop, J., Aars, J., Bårdsen, B.-J., Hanssen, S.A., Bech, C., Bourgeon, S., de Fouw, J., Gabrielsen, G.W., Lang, J., Noreen, E., Oudman, T., Sittler, B., Stempniewicz, L., Tombre, I., Wolters, E. and Moe, B., 2015. Climate change and the increasing impact of polar bears on bird populations, Frontiers in Ecology and Evolution, 3:33.

Provencher, J.F., Gaston, A.J., O'Hara, P.D. and Gilchrist, H.G., 2012. Seabird diet indicates changing Arctic marine communities in eastern Canada. Marine Ecology Progress Series, 454:171-182.

Provencher, J.F., Mallory, M.L., Braune, B.M., Forbes, M.R. and Gilchrist, H.G., 2014. Mercury and marine birds in Arctic Canada: effects, current trends, and why we should be paying closer attention. Environmental Reviews, 22 (3):244-255.

Provencher, J.F., Forbes, M.R., Hennin, H.L., Love, O.P., Braune, B.M., Mallory, M.L. and Gilchrist, 2016a. Implications of mercury and lead concentrations on breeding physiology and phenology in an Arctic bird. Environmental Pollution, 218:1014-1022.

Provencher, J.F., Gilchrist, H.G., Mallory, M.L., Mitchell, G.W. and Forbes, M.R., 2016b. Direct and indirect causes of sex differences in mercury

concentrations and parasitic infections in a marine bird. Science of the Total Environment, 551-552:506-512.

Provencher, J.F., Forbes, M.R., Mallory, M.L., Wilson, S. and Gilchrist, H.G., 2017. Anti-parasite treatment, but not mercury burdens, influence nesting propensity dependent on arrival time or body condition in a marine bird. Science of the Total Environment, 575:849-857.

Prowse, T.D., Wrona, F.J., Reist, J.D., Gibson, J.J., Hobbie, J.E., Lévesque, L.M.J. and Vincent, W.F., 2006. Climate change effects on hydroecology of arctic freshwater ecosystems. Ambio, 35 (7):347-358.

Pućko, M., Burt, A., Walkusz, W., Wang, F., Macdonald, R.W., Rysgaard, S., Barber, D.G., Tremblay, J.-É. and Stern, G.A., 2014. Transformation of mercury at the bottom of the Arctic food web: an overlooked puzzle in the mercury exposure narrative. Environmental Science & Technology 48 (13):7280-7288.

Pyle, P. 2008. Identification Guide to North American Birds. Part II: Anatidae to Alcidae. Slate Creek Press, xi + 836pp.

Pyle, P., Saracco, J.F. and DeSante, D.F., 2018. Evidence of widespread movements from breeding to molting grounds by North American landbirds. The Auk, 135 (3):506-520.

Qin, C., Wang, Y., Peng, Y. and Wang, D., 2016. Four-year record of mercury wet deposition in one typical industrial city in southwest China. Atmospheric Environment, 142:442-451.

R Core Team, 2020. R: A language and environment for statistical computing. R Foundation for Statistical Computing, Vienna, Austria. Available at: https://www.r-project.org/

Rachold, V., Eicken, H., Gordeev, V.V., Grigoriev, H., Hubberten, H.-W., Lisitzin, A.P. and Schirrmester, L., 2004. Modern terrigenous organic carbon input to the Arctic Ocean. In: Stein, R. and Macdonald, R.W. (Eds.). The Organic Carbon Cycle in the Arctic Ocean, pp. 33-55. Springer, Berlin, Heidelberg.

Rafaj, P., Bertok, I., Cofala, J. and Schöpp, W., 2013. Scenarios of global mercury emissions from anthropogenic sources. Atmospheric Environment, 79:472-479.

Rafaj, P., Cofala, J., Kuenen, J., Wyrwa, A. and Zyśk, J., 2014. Benefits of European climate policies for mercury air pollution. Atmosphere, 5 (1), 45-59.

Rahmstorf, S., Box, J.E., Feuler, G., Mann, M.E., Robinson, A., Rutherford, S. and Schaffernicht, E.J., 2015. Exceptional twentieth-century slowdown in Atlantic Ocean overturning circulation. Nature Climate Change, 5 (5):475-480.

Räike, A., Kortelainen, P., Mattsson, T. and Thomas, D.N., 2012. 36 year trends in dissolved organic carbon export from Finnish rivers to the Baltic Sea. Science of the Total Environment, 435-436:188-201.

Räike, A., Kortelainen, P., Mattsson, T. and Thomas, D.N., 2016. Long-term trends (1975-2014) in the concentrations and export of carbon from Finnish rivers to the Baltic Sea: organic and inorganic components compared. Aquatic Sciences, 78 (3):505-523.

Ramsar, 2014. Ramsar focuses on Arctic Wetlands [press release]. The Ramsar Convention Secretariat, Gland, Switzerland. Available at: https://www.ramsar.org/news/ramsar-focuses-on-arctic-wetlands

Rand, M.D. and Caito, S.W., 2019. Variation in the biological half-life of methylmercury in humans: methods, measurements and meaning. Biochimica et Biophysica Acta (BBA) - General Subjects, 1863 (12):129301.

Rask, M., Korhonen, M., Salo, S., Forsius, M., Kiljunen, M., Jones, R.I. and Verta, M., 2010. Does thermocline change affect methyl mercury concentrations in fish? Biogeochemistry, 101 (1):311-322.

Ratelle, M., Packull-McCormick, S., Bouchard, M., Majowicz, S. and Laird, B., 2020. Human biomonitoring of metals in sub-Arctic Dene communities of the Northwest Territories, Canada. Environmental Research, 190:110008.

Rautio, M., Dufresne, F., Laurion, I., Bonilla, S., Vincent, W.F. and Christoffersen, K.S., 2011. Shallow freshwater ecosystems of the circumpolar Arctic. Écoscience, 18 (3):204-222.

Raymond, L.J. and Ralston, N.V., 2004. Mercury: selenium interactions and health implications. NeuroToxicology, 81:294-299.

Regan, Á., Raats, M., Shan, L.C., Wall, P.G. and McConnon, Á., 2016. Risk communication and social media during food safety crises: a study of stakeholders' opinions in Ireland. Journal of Risk Research, 19 (1):119-133.

Ren, X., Luke, W.T., Kelley, P., Cohen, M.D., Olson, M.L., Walker, J., Cole, R., Archer, M., Artz, R. and Stein, A.A., 2020. Long-term observations of atmospheric speciated mercury at a coastal site in the northern Gulf of Mexico during 2007–2018. Atmosphere, 11 (3):268.

Riahi, K., Vuuren, D.P. van, Kriegler, E., Edmonds, J., O'Neill, B.C., Fujimori, S., Bauer, N., Calvin, K., Dellink, R., Fricko, O., Lutz, W., Popp, A., Cuaresma, J.C., KC, S., Leimbach, M., Jiang, L., Kram, T., Rao, S., Emmerling, J., Ebi, K., Hasegawa, T., Havlik, P., Humpenöder, F., Silva, L.A.D., Smith, S., Stehfest, E., Bosetti, V., Eom, J., Gernaat, D., Masui, T., Rogelj, J., Strefler, J., Drouet, L., Krey, V., Luderer, G., Harmsen, M., Takahashi, K., Baumstark, L., Doelman, J.C., Kainuma, M., Klimont, Z., Marangoni, G., Lotze-Campen, H., Obersteiner, M., Tabeau, A. and Tavoni, M., 2017. The shared socioeconomic pathways and their energy, land use, and greenhouse gas emissions implications: an overview. Global Environmental Change, 42:153-168.

Rice, D. and Barone, S., Jr., 2000. Critical periods of vulnerability for the developing nervous system: evidence from humans and animal models. Environmental Health Perspectives, 108 (S3):511-533.

Rigét, F., Asmund, G. and Aastrup, P., 2000. The use of lichen (*Cetraria nivalis*) and moss (*Rhacomitrium lanuginosum*) as monitors for atmospheric deposition in Greenland. Science of the Total Environment, 245 (1-3):137-148.

Rigét, F., Muir, D., Kwan, M., Savinova, T., Nyman, M., Woshner V. and O'Hara, T., 2005. Circumpolar pattern of mercury and cadmium in ringed seals. Science of the Total Environment, 351-352:312-322.

Rigét, F., Møller, P., Dietz, R., Nielsen, T.G., Asmund, G., Strand, J., Larsen, M.M. and Hobson, K.A., 2007. Transfer of mercury in the marine food web of West Greenland. Journal of Environmental Monitoring, 9 (8):877-883.

Rigét, F., Vorkamp, K. and Muir, D., 2010. Temporal trends of contaminants in Arctic char (*Salvelinus alpinus*) from a small lake, southwest Greenland during a warming climate. Journal of Environmental Monitoring, 12 (12):2252-2258.

Rigét, F., Braune, B., Bignert, A., Wilson, S., Aars, J., Born, E., Dam, M., Dietz, R., Evans, M., Evans, T., Gamberg, M., Gantner, N., Green, N., Gunnlaugsdóttir, H., Kannan, K., Letcher, R., Muir, D., Roach, P., Sonne, C., Stern, G. and Wiig, Ø., 2011a. Temporal trends of Hg in Arctic biota, an update. Science of the Total Environment 409:3520-3526.

Rigét, F., Tamstorf, M.P., Larsen, M.M., Søndergaard, J., Asmund, G., Falk, J.M. and Sigsgaard, C., 2011b. Mercury (Hg) transport in a High Arctic river in Northeast Greenland. Water, Air, & Soil Pollution, 222 (1-4):233-242.

Rigét, F.F., Dietz, R. and Hobson, K.A., 2012. Temporal trends of mercury in Greenland ringed seal populations in a warming climate. Journal of Environmental Monitoring, 14 (12):3249-3256.

Rigét, F., Vorkamp, K., Eulaers, I. and Dietz, R., 2020. Influence of climate and biological variables on temporal trends of persistent organic pollutants in Arctic char and ringed seals from Greenland. Environmental Science: Processes & Impacts, 22 (4):993-1005.

Riordan, B., Verbyla, D. and McGuire, A.D., 2006. Shrinking ponds in Subarctic Alaska based on 1950-2002 remotely sensed images. Journal of Geophysical Research: Biogeosciences, 111 (G4):G04002.

Risch, M.R. and Fowler, K.K., 2008. Mercury in Precipitation in Indiana, January 2004-December 2005 (Scientific Investigations Report 2008-5148). U.S. Geological Survey. 76pp. Available at: https://pubs.usgs.gov/sir/2008/5148/pdf/sir2008-5148_web.pdf

Roberts, K.E., Lamoureux, S.F., Kyser, T.K., Muir, D.C.G., Lafrenière, M.J., Iqaluk, D., Pieńkowski, A.J. and Normandeau, A., 2017. Climate and permafrost effects on the chemistry and ecosystems of High Arctic lakes. Scientific reports, 7 (1):13292.

Roberts, S., Kirk, J.L., Wiklund, J.A., Muir, D.C.G., Yang, F., Gleason, A. and Lawson, G., 2019. Mercury and metal(loid) deposition to remote Nova Scotia lakes from both local and distant sources. Science of the Total Environment, 675:192-202.

Rode, K.D., Amstrup, S.C. and Regehr, E.V., 2010. Reduced body size and cub recruitment in polar bears associated with sea ice decline. Ecological Applications, 20 (3):768-782.

Rode, K.D., Regehr, E.V., Douglas, D.C., Durner, G., Derocher, A.E., Thiemann, G.W., Budge, S.M., 2014. Variation in the response of an Arctic top predator experiencing habitat loss: feeding and reproductive ecology of two polar bear populations. Global Change Biology, 20 (1):76-88.

Rodríguez-Estival, J. and Mateo, R., 2019. Exposure to anthropogenic chemicals in wild carnivores: a silent conservation threat demanding long-term surveillance. Current Opinion in Environmental Science & Health, 11:21-25.

Rogers, M.C., Peacock, E., Simac, K., O'Dell, M.B. and Welker, J.M., 2015. Diet of female polar bears in the southern Beaufort Sea of Alaska:

evidence for an emerging alternative foraging strategy in response to environmental change. Polar Biology, 38 (7):1035-1047.

Rohonczy, J., Cott, P.A., Benwell, A., Forbes, M.R., Robinson, S.A., Rosabal, M., Amyot, M. and Chételat, 2020. Trophic structure and mercury transfer in the Subarctic fish community of Great Slave Lake, Northwest Territories, Canada. Journal of Great Lakes Research 46 (2):402-413.

Rolls, R.J., Hayden, B. and Kahilainen, K.K., 2017. Conceptualising the interactive effects of climate change and biological invasions on Subarctic freshwater fish. Ecology and Evolution, 7 (12):4109-4128.

Roman, H.A., Walsh, T.L., Coull, B.A., Dewailly, É., Guallar, E., Hattis, D., Mariën, K., Schwartz, J., Stern, A.H., Virtanen, J.K. and Rice, G., 2011. Evaluation of the cardiovascular effects of methylmercury exposures: current evidence supports development of a dose-response function for regulatory benefits analysis. Environmental Health Perspectives, 119 (5):607-614.

Ronald, K., Tessaro, S.V., Uthe, J.F., Freeman, H.C. and Frank, R., 1977. Methylmercury poisoning in the harp seal (*Pagophilus groenlandicus*). Science of the Total Environment, 8:1-11.

Rontani, J.-F., Charrière, B., Sempéré, R., Doxaran, D., Vaultier, F., Vonk, J.E. and Volkman, J.K., 2014. Degradation of sterols and terrigenous organic matter in waters of the Mackenzie Shelf Canadian Arctic. Organic Geochemistry, 75:61-73.

Rosati, G., Heimbürger, L.E., Melaku Canu, D., Lagane, C., Laffont, L., Rijkenberg, M.J.A., Gerringa, L.J.A., Solidoro, C., Gencarelli, C.N., Hedgecock, I.M., De Baar, H.J.W. and Sonke, J.E., 2018. Mercury in the Black Sea: new insights from measurements and numerical modeling. Global Biogeochemical Cycles, 32 (4):529-550.

Rosol, R., Powell-Hellyer, S. and Chan, H.M., 2016. Impacts of decline harvest of country food on nutrient intake among Inuit in Arctic Canada: impact of climate change and possible adaptation plan. International Journal of Circumpolar Health, 75 (1):31127.

Routti, H., Letcher, R.J., Born, E.W., Branigan, M., Dietz, R., Evans, T.J., Fisk, A.T., Peacock, E. and Sonne, C., 2011. Spatio-temporal trends of selected trace elements in liver tissue from polar bears (*Ursus maritimus*) from Alaska, Canada and Greenland. Journal of Environmental Monitoring, 13 (8):2260-2267.

Routti, H., Letcher, R.J., Born, E.W., Branigan, M., Dietz, R., Evans, T.J., McKinney, M.A., Peacock, E. and Sonne, C., 2012. Influence of carbon and lipid sources on variation of mercury and other trace elements in polar bears (*Ursus maritimus*). Environmental Toxicology and Chemistry, 31 (12):2739-2747.

Routti, H., Lille-Langøy, R., Berg, M.K., Fink, T., Harju, M., Kristiansen, K., Rostkowski, P., Rusten, M., Sylte, I., Øygarden, L. and Goksøyr, A., 2016. Environmental chemicals modulate polar bear (*Ursus maritimus*) peroxisome proliferator-activated receptor gamma (PPARG) and adipogenesis *in vitro*. Environmental Science & Technology, 50 (19):10708-10720.

Routti, H., Atwood, T.C., Bechshoft, T., Boltunov, A., Ciesielski, T.M., Desforges, J.-P., Dietz, R., Gabrielsen, G.W., Jenssen, B.M., Letcher, R.J., McKinney, M.A., Morris, A.D., Rigét, F.F., Sonne, C., Styrishave, B. and Tartu, S., 2019. State of knowledge on current exposure, fate and potential health effects of contaminants in polar bears from the circumpolar Arctic. Science of the Total Environment, 664:1063-1083.

Routti, H., Fuglei, E. and Pedersen, Å.Ø., 2020. Data set for: Temporal trend of mercury in relation to feeding habits and food availability in Arctic foxes (*Vulpes lagopus*) from Svalbard, Norway [Data set]. Norwegian Polar Institute. Available at: https://doi.org/10.21334/npolar.2020.e0a55206

Rowland, J.C., Jones, C.E., Altmann, G., Bryan, R., Crosby, B.T., Geernaert, G.L., Hinzman, L.D., Kane, D.L., Lawrence, D.L., Mancino, A., Marsh, P., McNamara, J.P., Romanovsky, V.E., Toniolo, H., Travis, B.J., Trochim, E. and Wilson, C.J., 2010. Arctic landscapes in transition: responses to thawing permafrost. Eos, Transactions American Geophysical Union, 91 (26):229-230.

Rudels, B., 2012. Arctic Ocean circulation and variability - advection and external forcing encounter constraints and local processes. Ocean Science, 8 (2):261-286.

Rutgers van der Loeff, M.M., Cassar, N., Nicolaus, M., Rabe, B. and Stimac, I., 2014. The influence of sea-ice cover on air-sea gas exchange estimated with radon-222 profiles. Journal of Geophysical Research: Oceans, 119 (5):2735-2751.

Rutkiewicz, J. and Basu, N., 2013. Methylmercury egg injections: Part 1-Tissue distribution of mercury in the avian embryo and hatchling. Ecotoxicology and Environmental Safety, 93:68-76.

Rutter, A.P., Schauer, J.J., 2007a. The effect of temperature on the gas-particle partitioning of reactive mercury in atmospheric aerosols. Atmospheric Environment, 41 (38):8647-8657.

Rutter, A.P. and Schauer, J.J., 2007b. The impact of aerosol composition on the particle to gas partitioning of reactive mercury. Environmental Science & Technology, 41 (11):3934-3939.

Rutter, A.P., Shakya, K.M., Lehr, R., Schauer, J.J. and Griffin, R.J., 2012. Oxidation of gaseous elemental mercury in the presence of secondary organic aerosols. Atmospheric Environment, 59:86-92.

Ruus, A., Øverjordet, I.B., Braaten, H.F.V., Evenset, A., Christensen, G., Heimstad, E.S., Gabrielsen, G.W. and Borgå, K., 2015. Methylmercury biomagnification in an Arctic pelagic food web. Environmental Toxicology and Chemistry, 34 (11):2636-2643.

Ryaboshapko, A., Bullock, O.R., Jr., Christensen, J., Cohen, M., Dastoor, A., Ilyin, I., Petersen, G., Syrakov, D., Artz, R.S., Davignon, D., Draxler, R.R. and Munthe, J., 2007. Intercomparison study of atmospheric mercury models: 1. Comparison of models with short-term measurements. Science of the Total Environment, 376 (1-3): 228-240.

Rydberg, J., Klaminder, J., Rosén, P. and Bindler, R., 2010. Climate driven release of carbon and mercury from permafrost mires increases mercury loading to sub-Arctic lakes. Science of the Total Environment, 408 (20):4778-4783.

Rysgaard, S. and Glud, R.N., 2004. Anaerobic N_2 production in Arctic sea ice. Limnology and Oceanography, 49 (1):86-94.

Saiz-Lopez, A., Sitkiewicz, S.P., Roca-Sanjuán, D., Oliva-Enrich, J.M., Dávalos, J.Z., Notario, R., Jiskra, M., Xu, Y, Wang, F., Thackray, C.P., Sunderland, E.M., Jacob, D.J., Travnikov, O., Cuevas, C.A., Acuna, A.U., Rivero, D., Plane, J.M.C., Kinnison, D.E. and Sonke, J.E., 2018. Photoreduction of gaseous oxidized mercury changes global atmospheric mercury speciation, transport and deposition. Nature Communications, 9 (1):4796.

Saiz-Lopez, A., Ulises Acuña, A., Trabelsi, T., Carmona-García, J., Dávalos, J.Z., Rivero, D., Cuevas, C.A., Kinnison, D.E., Sitkiewicz, S.P., Roca-Sanjuan, D., Francisco, J.S., 2019. Gas-phase photolysis of Hg(I) radical species: a new atmospheric mercury reduction process. Journal of the American Chemical Society, 141 (22):8698-8702.

Sakata, M. and Asakura, K., 2007. Estimating contribution of precipitation scavenging of atmospheric particulate mercury to mercury wet deposition in Japan. Atmospheric Environment, 41 (8):1669-1680.

Sandell, H.T., Sandell, B., Born, E.W., Dietz, R. and Sonne-Hansen, C., 2001. Isbjørne i Østgrønland. En interviewundersøgelse om forekomst og fangst, 1999. Teknisk Rapport, No. 40. Grønlands Naturinstitut. 94pp. (Danish Language).

Sandheinrich M.B. and Miller, K.M., 2006. Effects of dietary methylmercury on reproductive behavior of fathead minnows (*Pimephales promelas*). Environmental Toxicology and Chemistry, 25 (11):3053-3057.

Sandheinrich, M.B. and Wiener, JG.., 2011. Methylmercury freshwater fish: recent advances in assessing toxicity and environmentally relevant exposures. In: Beyer, W.N. and Meador, J.P. (Eds.). Environmental Contaminants in Biota: Interpreting Tissue Concentrations. Second edition, pp. 169-190. CRC Press.

Sandheinrich, M.B. and Drevnick, P.E., 2016. Relationship among mercury concentration, growth rate, and condition of northern pike: A tautology resolved? Environmental Toxicology and Chemistry, 35 (12):2910-2915.

Sandheinrich, M.B., Bhavsar, S.P., Bodaly, R.A., Drevnick, P.E. and Paul, E.A., 2011. Ecological risk of methylmercury to piscivorous fish of the Great Lakes region. Ecotoxicology, 20 (7):1577-1587.

Sanei, H., Outridge, P.M., Goodarzi, F., Wang, F., Armstrong, D., Warren, K. and Fishback, L., 2010. Wet deposition mercury fluxes in the Canadian Sub-Arctic and southern Alberta, measured using an automated precipitation collector adapted to cold regions. Atmospheric Environment, 44 (13):1672–81.

Sanei, H., Outridge, P.M., Dallimore, A. and Hamilton, P.B., 2012. Mercury-organic matter relationships in pre-pollution sediments of thermokarst lakes from the Mackenzie River Delta, Canada: the role of depositional environment. Biogeochemistry, 107 (1):149-164.

Santa-Rios, A., Barst, B.D. and Basu, N., 2020. Mercury speciation in whole blood and dried blood spots from capillary and venous sources. Analytical Chemistry, 92 (5):3605-3612.

SAON et al., 2021. Atlas of Community-Based Monitoring & Traditional Knowledge in a Changing Arctic. Sustaining Arctic Observing Networks (SAON), Inuit Circumpolar Council (ICC), Brown University, Exchange for Local Observations and Knowledge of the Arctic (ELOKA) and Inuit Tapiriit Kanatami's Inuit Qaujisarvingat:

Inuit Knowledge Centre. Available at: http://www.arcticcbm.org/index.html#

Sarica, J., Amyot, M., Hare, L., Doyon, M.-R. and Stanfield, L., 2004. Salmon-derived mercury and nutrients in a Lake Ontario spawning stream. Limnology and Oceanography, 49 (4):891-899.

Sarica, J., Amyot, M., Hare, L., Blanchfield, P., Bodaly, R.A., Hintelmann, H. and Lucotte, M., 2005. Mercury transfer from fish carcasses to scavengers in boreal lakes: the use of stable isotopes of mercury. Environmental Pollution, 134 (1):13-22.

Saros, J.E., Osburn, C.L., Northington, R.M., Birkel, S.D., Auger, J.D., Stedmon, C.A. and Anderson, N.J., 2015. Recent decrease in DOC concentrations in Arctic lakes of southwest Greenland. Geophysical Research Letters, 42 (16):6703-6709.

Saros, J.E., Northington, R.M., Osburn, C.L., Burpee, B.T. and Anderson, N.J., 2016. Thermal stratification in small Arctic lakes of southwest Greenland affected by water transparency and epilimnetic temperatures. Limnology and Oceanography, 61 (4):1530-1542.

Saros, J.E., Anderson, N.J., Juggins, S., McGowan, S., Yde, J.C., Telling, J., Bullard, J.E., Yallop, M.L., Heathcote, A.J., Burpee, B.T., Fowler, R.A., Barry, C.D., Northington, R.M., Osburn, C.L., Pla-Rabes, S., Mernild, S.H., Whiteford, E.J., Andrews, M.G., Kerby, J.T. and Post, E., 2019. Arctic climate shifts drive rapid ecosystem responses across the West Greenland landscape. Environmental Research Letters, 14 (7):074027.

Saunes, H., 2011. Do mercury, selenium, cadmium and zinc cause oxidative stress in common eiders (*Somateria mollissima*) from Svalbard? Master's thesis. Norwegian University of Science and Technology, Department of Biology, Trondheim, Norway. Available at: https://ntnuopen.ntnu.no/ntnu-xmlui/bitstream/handle/11250/244727/423828_FULLTEXT01.pdf?sequence=1&isAllowed=y

Schaefer, J.K. and Morel, F.M.M., 2009. High methylation rates of mercury bound to cysteine by Geobacter sulfurreducens. Nature Geoscience, 2 (2):123-126.

Schaefer, K., Elshorbany, Y., Jafarov, E., Schuster, P.F., Striegl, R.G., Wickland, K.P. and Sunderland, E.M., 2020. Potential impacts of mercury released from thawing permafrost. Nature Communications, 11 (1):4650.

Schaefer, K., Lantuit, H., Romanovsky, V.E., Schuur, E.A.G. and Witt, R., 2014. The impact of the permafrost carbon feedback on global climate. Environmental Research Letters, 9 (8):085003.

Schartup, A.T, Balcom, P.H., Soerensen, A.L., Gosnell, K.J., Calder, R.S.D., Mason, R.P. and Sunderland, E.M., 2015a. Freshwater discharges drive high levels of methylmercury in Arctic marine biota. Proceedings of the National Academy of Sciences of the United States of America, 112 (38):11789-11794.

Schartup, A.T., Ndu, U., Balcom, P.H., Mason, R.P. and Sunderland, E.M., 2015b. Contrasting effects of marine and terrestrially derived dissolved organic matter on mercury speciation and bioavailability in seawater. Environmental Science & Technology, 49 (10):5965-5972.

Schartup, A.T., Qureshi, A., Dassuncao, C., Thackray, C.P., Harding, G. and Sunderland, E.M., 2018. A model for methylmercury uptake and trophic transfer by marine plankton. Environmental Science & Technology, 52 (2):654-662.

Schartup, A.T., Thackray, C.P., Qureshi, A., Dassuncao, C., Gillespie, K., Hanke, A. and Sunderland, E.M., 2019. Climate change and overfishing increase neurotoxicant in marine predators. Nature, 572 (7771):648-650.

Schartup, A.T., Soerensen, A.L. and Heimbürger-Boavida, L.-E., 2020. Influence of the Arctic sea-ice regime shift on sea-ice methylated mercury trends. Environmental Science & Technology Letters, 7 (10):708-713.

Schauer, U., 2016. The expedition PS94 of the research vessel POLARSTERN to the central Arctic Ocean in 2015. Reports on Polar and Marine Research, Alfred Wegener Institute for Polar and Marine Research, 703. 170pp. Available at: https://doi.org/10.2312/BzPM_0703_2016

Scheffer, M. and Carpenter, S.R., 2003. Catastrophic regime shifts in ecosystems: linking theory to observation. Trends in Ecology & Evolution, 18 (12):648-656.

Scheffers, B.R., De Meester, L., Bridge, T.C.L., Hoffmann, A.A., Pandolfi, J.M., Corlett, R.T., Butchart, S.H.M., Pearce-Kelly, P., Kovacs, K.M., Dudgeon, D., Pacifici, M., Rondinini, C., Foden, W.B., Martin, T.G., Mora, C., Bickford, D. and Watson, J.E.M., 2016. The broad footprint of climate change from genes to biomes to people. Science, 354 (6313):aaf7671.

Scherbatskoy, T., Shanley, J.B. and Keeler, G.J., 1998. Factors controlling mercury transport in an upland forested catchment. Water, Air, & Soil Pollution, 105 (1-2):427-438.

Scheuhammer, A.M., Meyer, M.W., Sandheinrich, M.B. and Murray, M.W., 2007. Effects of environmental methylmercury on the health of wild birds, mammals, and fish. Ambio, 36 (1):12-19.

Scheuhammer, A.M., Basu, N., Evers, D.C., Heinz, G.H., Sandheinrich, M. and Bank, M.S., 2012. Ecotoxicology of mercury in fish and wildlife: recent advances. In: Bank M.S. (Ed.). Mercury in the Environment: Pattern and Process, pp. 223-238. University of California Press.

Scheuhammer, A., Braune, B., Chan, H.M., Frouin, H., Krey, A., Letcher, R., Loseto, L., Noël, M., Ostertag, S., Ross, P. and Wayland, M., 2015. Recent progress on our understanding of the biological effects of mercury in fish and wildlife in the Canadian Arctic. Science of the Total Environment, 509-510:91-103.

Schliebe, S., Rode, K.D., Gleason, J.S., Wilder, J., Proffitt, K., Evans, T.J. and Miller, S., 2008. Effects of sea ice extent and food availability on spatial and temporal distribution of polar bears during the fall open-water period in the Southern Beaufort Sea. Polar Biology, 31 (8):999-1010.

Schott, S., Chapman, J., Hewitt, E., Khosraviani, P, Royle, S., Hayes, A., et al., 2019. Towards a sustainable fishery for Nunavummiut Atlas. Geomatics and Cartographic Research Centre (GCRC), 2016–2019, Ottawa, Ontario, Canada. Available at: http://tsfn.gcrc.carleton.ca

Schott, S., Qitsualik, J., Van Coeverden de Groot, P., Okpakok, S., Chapman, J.M., Lougheed, S. and Walker, V.K., 2020. Operationalizing knowledge coevolution: towards a sustainable fishery for Nunavummiut. Arctic Science, 6 (3):208-228.

Schroeder, W.H. and Munthe, J., 1998. Atmospheric mercury—An overview. Atmospheric Environment, 32 (5):809-822.

Schroeder, W., Anlauf, K., Barrie, L., Lu, J.Y., Steffen, A., Schneeberger, D.R. and Berg, T., 1998. Arctic springtime depletion of mercury. Nature, 394 (6691):331-332.

Schultz, I.R., Bolton, J.L., Stimmelmayr, R. and Ylitalo, G.M., 2020. Contaminants. In: Thewissen, J.G.M. and George, J.C. (Eds.). The Bowhead Whale: *Balaena Mysticetus*: Biology and Human Interactions, pp. 591-607. Elsevier, Academic Press.

Schuster, P.F., Krabbenhoft, D.P., Naftz, D.L., Cecil, L.D., Olson, M.L., Dewild, J.F., Susong, D.D., Green, J.R. and Abbott, M.L., 2002. Atmospheric mercury deposition during the Last 270 Years: a glacial ice core record of natural and anthropogenic sources. Environmental Science & Technology, 36 (11):2303-2310.

Schuster, P.F., Striegl, R.G., Aiken, G.R., Krabbenhoft, D.P., Dewild, J.F., Butler, K., Kamark, B. and Dornblaser, M., 2011. Mercury Export from the Yukon River basin and potential response to a changing climate. Environmental Science & Technology, 45 (21):9262-9267.

Schuster, P.F., Schaefer, K.M., Aiken, G.R.,Antweiler, R.C., Dewild, J.F., Gryziec, J.D., Gusmeroli, A., Hugelius, G., Jafarov, E., Krabbenhoft, D.P., Liu, L., Herman-Mercer, N., Mu, C., Roth, D.A., Schaefer, T., Striegl, R.G., Wickland, K.P. and Zhang, T., 2018. Permafrost stores a globally significant amount of mercury. Geophysical Research Letters, 45 (3):1463-1471.

Schuur, E.A.G., Mcguire, A.D., Schädel, C., Grosse, G., Harden, J.W., Hayes, D.J., Hugelius, G., Koven, C.D., Kuhry, P. and Lawrence, D.M., 2015. Climate change and the permafrost carbon feedback. Nature, 520 (7546):171-179.

Screen, J.A. and Simmonds, I., 2010. The central role of diminishing sea ice in recent Arctic temperature amplification. Nature, 464 (7293):1334-1337.

Sebastiano, M., Chastel, O., de Thoisy, B., Eens, M. and Costantini, D., 2016. Oxidative stress favours herpes virus infection in vertebrates: a meta-analysis. Current Zoology, 62 (4):325-332.

Sebastiano, M., Angelier, F., Blévin, P., Ribout, C., Sagerup, K., Descamps, S., Herzke, D., Moe, B., Barbraud, C., Bustnes, J.O., Gabrielsen, G.W. and Chastel, O., 2020. Exposure to PFAS is associated with telomere length dynamics and demographic responses of an Arctic top predator. Environmental Science & Technology, 54 (16):10217-10226.

Seewagen, C.L., Cristol, D.A. and Gerson, A.R., 2016. Mobilization of mercury from lean tissues during simulated migratory fasting in a model songbird. Scientific Reports, 6 (1):25762.

Seigneur, C., Abeck, H., Chia, G., Reinhard, M., Bloom, N.S., Prestbo, E. and Saxena, P., 1998. Mercury adsorption to elemental carbon (soot) particles and atmospheric particulate matter. Atmospheric Environment, 32 (14-15):2649-2657.

Seigneur, C., Vijayaraghavan, K., Lohman, K., Karamchandani, P. and Scott, C., 2004. Global source attribution for mercury deposition in the United States. Environmental Science & Technology, 38 (2):555-569.

Selin, N.E., 2018. A proposed global metric to aid mercury pollution policy. Science, 360 (6389):607-609.

Selin, N.E. and Jacob, D.J., 2008. Seasonal and spatial patterns of mercury wet deposition in the United States: constraints on the contribution from North American anthropogenic sources. Atmospheric Environment, 42 (21):5193-5204.

Selin, N.E. Jacob, D.J., Park, R.J., Yantosca, R.M., Strode, S., Jaeglé, L. and Jaffe, D., 2007. Chemical cycling and deposition of atmospheric mercury: global constraints from observations. Journal of Geophysical Research:Atmospheres, 112 (D2):D02308.

Selin, N.E., Jacob, D.J., Yantosca, R.M., Strode, S., Jaeglé, L. and Sunderland, E.M., 2008. Global 3-D land-ocean-atmosphere model for mercury: present-day versus preindustrial cycles and anthropogenic enrichment factors for deposition. Global Biogeochemical Cycles, 22 (2):GB2011.

Seller, P., Kelly, C.A., Rudd, J.W.M. and MacHutchon, A.R., 1996. Photodegradation of methylmercury in lakes. Nature, 380 (6576):694-697.

Selvendiran, P., Driscoll, C.T., Montesdeoca, M.R. and Bushey, J.T., 2008. Inputs, storage, and transport of total and methyl mercury in two temperate forest wetlands. Journal of Geophysical Research: Biogeosciences, 113 (G2):G00C01.

Semeniuk, K. and Dastoor, A., 2017. Development of a global ocean mercury model with a methylation cycle: outstanding issues. Global Biogeochemical Cycles, 31 (2):400-433.

Semkin, R.G., Mierle, G. and Neureuther, R.J., 2005. Hydrochemistry and mercury cycling in a High Arctic watershed. Science of the Total Environment, 342 (1-3):199-221.

Sénéchal, É., Bêty, J., Gilchrist, H.G., Hobson, K.A. and Jamieson, S.E., 2011. Do purely capital layers exist among flying birds? Evidence of exogenous contribution to Arctic-nesting common eider eggs. Oecologia, 165:593-604.

Serreze, M.C. and Barry, R.G., 2011. Processes and impacts of Arctic amplification: a research synthesis. Global and planetary change, 77 (1-2):85-96.

Serreze, M.C, Barrett, A.P, Slater, A.G., Woodgate, R.A., Aagaard, K., Lammers, R.B., Steele, M., Moritz, R., Meredith, M. and Lee, C.M., 2006. The large-scale freshwater cycle of the Arctic. Journal of Geophysical Research: Oceans, 111 (C11):C11010.

Serreze, M.C., Raup, B., Braun, C., Hardy, D.R. and Bradley, R.S., 2017. Rapid wastage of the Hazen Plateau ice caps, northeastern Ellesmere Island, Nunavut, Canada. The Cryosphere, 11 (1):169-177.

Sharma, S., 2010. Assessing diet and lifestyle in the Canadian Arctic Inuit and Inuvialuit to inform a nutrition and physical activity intervention programme. Journal of Human Nutrition and Dietetics, 23 (S1):5-17.

Sharma, S., Ishizawa, M., Chan, D., Lavoué, D., Andrews, E., Eleftheriadis, K. and Maksyutov, S., 2013. 16-year simulation of Arctic black carbon: transport, source contribution, and sensitivity analysis on deposition. Journal of Geophysical Research: Atmospheres, 118 (2):943-964.

Sheehan, M.C., Burke, T.A., Navas-Acien, A., Breysse, P.N., McGready, J. and Fox, M.A., 2014. Global methylmercury exposure from seafood consumption and risk of developmental neurotoxicity: a systematic review. Bulletin of the World Health Organization, 92 (4):254-269F.

Shepler, B.C. and Peterson, K.A., 2003. Mercury monoxide: a systematic investigation of its ground electronic state. The Journal of Physical Chemistry A, 107 (11):1783-1787.

Sherman, L.S., Blum, J.D., Johnson, K.P., Keeler, G.J., Barres, J.A. and Douglas, T.A., 2010. Mass-independent fractionation of mercury isotopes in Arctic snow driven by sunlight. Nature Geoscience, 3 (3):173-177.

Sherman, L.S., Blum, J.D., Douglas, T.A. and Steffen, A., 2012. Frost flowers growing in the Arctic ocean-atmosphere-sea ice-snow interface: 2. Mercury exchange between the atmosphere, snow, and frost flowers. Journal of Geophysical Research: Atmospheres, 117 (D14):D00R10.

Shevchenko, V.P., Pokrovsky, O.S., Starodymova, D.P., Vasyukova, E.V., Lisitzin, A.P., Drovnina, S.I., Zamber, N.S., Makhnovich, N.M., Savvichev, A.S. and Sonke, J., 2013. Geochemistry of terricolous lichens in the White Sea catchment area. Doklady Earth Sciences, 450:514-520.

Siciliano, S.D., O'Driscoll, N.J., Tordon, R., Hill, J., Beauchamp, S. and Lean, D.R.S., 2005. Abiotic production of methylmercury by solar radiation. Environmental Science & Technology, 39 (4):1071-1077.

Simpson, W.R., Von Glasow, R., Riedel, K., Anderson, P., Ariya, P., Bottenheim, J., Burrows, J., Carpenter, L.J., Frieß, U., Goodsite, M.E., Heard, D., Hutterli, M., Jacobi, H.-W., Kaleschke, L., Neff, B., Plane, J., Platt, U., Richter, A., Roscoe, H., Sander, R., Shepson, P., Sodeau, J., Steffen, A., Wagner, T. and Wolff, E., 2007. Halogens and their role in polar boundary-layer ozone depletion. Atmospheric Chemistry and Physics, 7 (16):4375-4418.

Simpson, W.R., Brown, S.S., Saiz-Lopez, A., Thornton, J.A. and von Glasow, R., 2015. Tropospheric halogen chemistry: sources, cycling, and impacts. Chemical Reviews, 115, (10):4035-4062.

Skov, H., Christensen, J.H., Goodsite, M.E., Heidam, N.Z., Jensen, B., Wåhlin, P. and Geernaert, G., 2004. Fate of elemental mercury in the Arctic during atmospheric mercury depletion episodes and the load of atmospheric mercury to the Arctic. Environmental Science & Technology, 38 (8):2373-2382.

Skov, H., Brooks, S.B., Goodsite, M.E., Lindberg, S.E., Meyers, T.P., Landis, M.S., Larsen, M.R., Jensen, B., McConville, G. and Christensen, J., 2006. Fluxes of reactive gaseous mercury measured with a newly developed method using relaxed eddy accumulation. Atmospheric Environment, 40 (28):5452-5463.

Skov, H., Hjorth, J., Nordstrøm, C., Jensen, B., Christoffersen, C., Bech Poulsen, M., Baldtzer Liisberg, J., Beddows, D., Dall'Osto, M. and Christensen, J H., 2020. Variability in gaseous elemental mercury at Villum Research Station, Station Nord, in North Greenland from 1999 to 2017. Atmospheric Chemistry and Physics, 20 (21):13253-13265.

Skrobonja, A., Gojkovic, Z., Soerensen, A.L., Westlund, P.-O., Funk, C. and Björn, E., 2019. Uptake kinetics of methylmercury in a freshwater alga exposed to methylmercury complexes with environmentally relevant thiols. Environmental Science & Technology, 53 (23):13757-13766.

Skyllberg, U., Westin, M.B., Meili, M. and Björn, E., 2009. Elevated concentrations of methyl mercury in streams after forest clear-cut: a consequence of mobilization from soil or new methylation? Environmental Science & Technology, 43 (22):8535-8541.

Slemr, F., Brunke, E.-G., Ebinghaus, R., Temme, C., Munthe, J., Wängberg, I., Schroeder, W., Steffen, A. and Berg, T., 2003. Worldwide trend of atmospheric mercury since 1977. Geophysical Research Letters, 30 (10):1516.

Slemr, F., Brunke, E.-G., Ebinghaus, R. and Kuss, J., 2011. Worldwide trend of atmospheric mercury since 1995. Atmospheric Chemistry and Physics, 11 (10):4779-4787.

Sletten, S., Bourgeon, S., Badsen, B.J., Herzke, D., Criscuolo, F., Massemin, S., Zahn, S., Johnsen, T.V. and Bustnes, J.O., 2016. Organohalogenated contaminants in white-tailed eagle (*Haliaeetus albicilla*) nestlings: an assessment of relationships to immunoglobulin levels, telomeres and oxidative stress. Science of the Total Environment, 539:337-349.

Smith, L.C., Sheng, Y., MacDonald, G.M. and Hinzman, L.D., 2005. Disappearing Arctic lakes. Science, 308 (5727):1429.

Smith, S.D., Bridou, R., Johs, A., Parks, J.M., Elias, D.A., Hurt, R.A., Brown, S.D., Podar, M., Wall, J.D. and Kivisaar, M., 2015. Site-directed mutagenesis of *hgcA* and *hgcB* reveals amino acid residues important for mercury methylation. Applied and Environmental Microbiology, 81 (9):3205-3217.

Smith, P.A., McKinnon, L., Meltofte, H., Lanctot, R.B., Fox, A.D., Leafloor, J.O., Soloviev, M., Franke, A., Falk, K., Golovatin, M., Sokolov, V., Sokolov, A. and Smith, A.C., 2020. Status and trends of tundra birds across the circumpolar Arctic. Ambio, 49 (3):732-748.

Smith-Downey, N.V., Sunderland, E.M. and Jacob, D.J., 2010. Anthropogenic impacts on global storage and emissions of mercury from terrestrial soils: insights from a new global model. Journal of Geophysical Research:Biogeosciences, 115 (G3):G03008.

Sneed, W.A., Hooke, R.LeB. and Hamilton, G.S., 2008. Thinning of the south dome of Barnes Ice Cap, Arctic Canada, over the past two decades. Geology, 36 (1):71-74.

Snucins, E. and Gunn, J., 2000. Interannual variation in the thermal structure of clear and colored lakes. Limnology and Oceanography, 45: 1639–1646.

Soerensen, A.L., Sunderland, E.M., Holmes, C.D., Jacob, D.J., Yantosca, R.M., Skov, H., Christensen, J.H., Strode, S.A. and Mason, R.P., 2010. An improved global model for air-sea exchange of mercury: high concentrations over the North Atlantic. Environmental Science & Technology, 44 (22):8574-8580.

Soerensen, A.L., Jacob, D.J., Schartup, A.T., Fisher, J.A., Lehnherr, I., St. Louis, V.L., Heimbürger, L.-E., Sonke, J.E., Krabbenhoft, D.P. and Sunderland, E.M., 2016a. A mass budget for mercury and methylmercury in the Arctic Ocean. Global Biogeochemical Cycles, 30 (4):560-575.

Soerensen, A.L., Schartup, A.T., Gustafsson, E., Gustafsson, B.G., Undeman, E. and Björn, E., 2016b. Eutrophication increases phytoplankton methylmercury concentrations in a coastal sea—a Baltic Sea case study. Environmental Science & Technology, 50 (21):11787-11796.

Soerensen, A.L., Schartup, A.T., Skrobonja, A. and Björn, E., 2017. Organic matter drives high interannual variability in methylmercury concentrations in a Subarctic coastal sea. Environmental Pollution, 229:531-538.

Sokolov, V., Ehrich, D., Yoccoz, N.G., Sokolov, A. and Lecomte, N., 2012. Bird communities of the Arctic shrub tundra of Yamal: habitat specialists and generalists. PLOS ONE, 7 (12):e50335.

Sokolov, A.A., Sokolova, N.A., Ims, R.A., Brucker, L. and Ehrich, D., 2016. Emergent rainy winter warm spells may promote boreal predator expansion into the Arctic. Arctic, 69 (2):121-129.

Sommar, J., Hallquist, M., Ljungström, E. and Lindqvist, O., 1997. On the gas phase reactions between volatile biogenic mercury species and the nitrate radical. Journal of Atmospheric Chemistry, 27 (3):233-247.

Sommar, J., Feng, X. and Lindqvist, O., 1999. Speciation of volatile mercury species present in digester and deposit gases. Applied Organometallic Chemistry, 13 (6):441-445.

Søndergaard, J., Riget, F., Tamstorf, M.P. and Larsen, M.M., 2012. Mercury transport in a Low-Arctic river in Kobbefjord, West Greenland (64° N). Water, Air, & Soil Pollution, 223:4333-4342.

Søndergaard, J., Tamstorf, M., Elberling, B., Larsen, M.M., Mylius, M.R., Lund, M., Abermann, J. and Riget, F., 2015. Mercury exports from a High-Arctic river basin in Northeast Greenland (74°N) largely controlled by glacial lake outburst floods. Science of the Total Environment, 514:83-91.

Sonenshine, D.E and Mather, T.N., 1994. Ecological Dynamics of Tick-Borne Zoonoses. Oxford University Press. 464pp.

Song, S., Selin, N.E., Soerensen, A.L., Angot, H., Artz, R., Brooks, S., Brunke, E.-G., Conley, G., Dommergue, A., Ebinghaus, R., Holsen, T.M., Jaffe, D.A., Kang, S., Kelley, P., Luke,W.T., Magand, O., Marumoto, K., Pfaffhuber, K.A., Ren, X., Sheu, G.-R., Slemr, F., Warneke, T., Weigelt, A., Weiss-Penzias, P., Wip, D.C. and Zhang, Q., 2015. Top-down constraints on atmospheric mercury emissions and implications for global biogeochemical cycling. Atmospheric Chemistry and Physics, 15 (12):7103-7125.

Sonke, J.E., Teisserenc, R., Heimbürger-Boavida, L-E., Petrova, M.V., Marusczak, N., Le Dantec, T., Chupakov, A.V., Li C., Thackray, C.P., Sunderland, E.M., Tananaev, N. and Pokrovsky, O.S., 2018. Eurasian river spring flood observations support net Arctic Ocean mercury export to the atmosphere and Atlantic Ocean. Proceedings of the National Academy of Sciences of the United States of America, 115 (50):E11586-E11594.

Sonne, C., 2010. Health effects from long-range transported contaminants in Arctic top predators: an integrated review based on studies of polar bears and relevant model species. Environment International, 36 (5):461-491.

Sonne, C., Alstrup, A.K.O. and Therkildsen, O.R., 2012. A review of the factors causing paralysis in wild birds: implications for the paralytic syndrome observed in the Baltic Sea. Science of the Total Environment, 416:32-39.

Sonne, C., Dyck, M., Rigét, F.F., Jensen, J.-E.B., Hyldstrup, L., Letcher, R.J., Gustavson, K., Gilbert, M.T.P. and Dietz, R., 2015. Penile density and globally used chemicals in Canadian and Greenland polar bears. Environmental Research, 137:287-291.

Sonne, C., Jepson, P.D., Desforges, J.P., Alstrup, A.K.O., Olsen, M.T., Eulaers, I., Hansen, M., Letcher, R.J., McKinney, M.A. and Dietz, R., 2018. Pollution threatens toothed whales. Science, 361 (6408):1208.

Sonne, C., Dietz, R., Jenssen, B.M., Lam, S.S. and Letcher, R.J., 2021. Emerging contaminants and biological effects in Arctic wildlife. Trends in Ecology & Evolution, 36:421-429.

Sorensen, J.A., Glass, G.E., Schmidt, K.W., Huber, J.K. and Rapp, G.R., Jr., 1990. Airborne mercury deposition and watershed characteristics in relation to mercury concentrations in water, sediments, plankton, and fish of eighty northern Minnesota lakes. Environmental Science & Technology, 24 (11):1716-1727.

Sorensen, J.A., Glass, G.E. and Schmidt, K.W., 1994. Regional Patterns of wet mercury deposition. Environmental Science & Technology, 28 (12):2025-2032.

Sørensen, N., Murata, K., Budtz-Jørgensen, E., Weihe, P. and Grandjean, P., 1999. Prenatal methylmercury exposure as a cardiovascular risk factor at seven years of age. Epidemiology, 10 (4):370-375.

Sorokina, T.Y., 2019. A national system of biological monitoring in the Russian Arctic as a tool for the implementation of the Stockholm Convention. International Environmental Agreements: Politics, Law and Economics, 19 (3):341-355.

Spence, C., Kokelj, S.A., Kokelj, S.V. and Hedstrom, N., 2014. The process of winter streamflow generation in a Subarctic Precambrian Shield catchment. Hydrological Processes, 28 (14):4179-4190.

Spence, C., Kokelj, S.V., Kokelj, S.A., McCluskie, M. and Hedstrom, N., 2015. Evidence of a change in water chemistry in Canada's Subarctic associated with enhanced winter streamflow. Journal of Geophysical Research: Biogeosciences, 120 (1):113-127.

Spicer, C.W., Sumner, A.L., Satola, J. and Mangaraj, R., 2005. Kinetics of mercury reactions in the atmosphere. Report to the Florida Department of Environmental Conservation on Florida DEP Contract No. AQ192.

Spickler, J.L., Swaddle, J.P., Gilson, R.L., Varian-Ramos, C.W. and Cristol, D.A., 2020. Sexually selected traits as bioindicators: exposure to mercury affects carotenoid-based male bill color in zebra finches. Ecotoxicology, 29 (8):1138-1147.

Sprovieri, F., Pirrone, N., Landis, M.S. and Stevens, R.K., 2005. Oxidation of Gaseous Elemental Mercury to Gaseous Divalent Mercury during 2003 Polar Sunrise at Ny-Alesund. Environmental Science and Technology 39(23):9156-65.

Sprovieri, F., Pirrone, N., Ebinghaus, R., Kock, H. and Dommergue, A., 2010. A review of worldwide atmospheric mercury measurements. Atmospheric Chemistry and Physics, 10 (17):8245-8265.

Sprovieri, F., Pirrone, N., Bencardino, M., D'Amore, F., Angot, H., Barbante, C., Brunke, E.-G., Arcega-Canbera, F., Cairns, W., Comero, S., del Carmen Diéguez, M., Dommergue, A., Ebinghaus, R., Feng, X.B., Fu, X., Garcia, P.E., Gawlik, B.M., Hageström, U., Hansson, K., Horvat, M., Kotnik, J., Labuschagne, C., Magand, O., Martin, L., Mashyanov, N., Mkololo, T., Munthe, J., Obolkin, V., Ramirez Islas, M., Sena, F., Somerset, V., Spandow, P., Vardè, M., Walters, C., Wängberg, I., Weigelt, A., Yangm X. and Zhang, H., 2017. Five-year records of mercury wet deposition flux at GMOS sites in the Northern and Southern Hemispheres. Atmospheric Chemistry and Physics, 17 (4):2689-2708.

St. Louis, V.L., Sharp, M.J., Steffen, A., May, A., Barker, J., Kirk, J.L., Kelly, D.J., Arnott, S.E., Keatley, B. and Smol, J.P., 2005. Some sources and sinks of monomethyl and inorganic mercury on Ellesmere Island in the Canadian High Arctic. Environmental Science & Technology, 39 (8):2686-2701.

St. Louis, V.L., Hintelmann, H., Graydon, J.A., Kirk, J.L., Barker, J., Dimock, B., Sharp, M.J. and Lehnherr, I., 2007. Methylated mercury species in Canadian High Arctic marine surface waters and snowpacks. Environmental Science & Technology, 41 (18):6433-6441.

St. Louis, V.L., Derocher, A.E., Stirling, I., Graydon, J.A., Lee, C., Jocksch, E., Richardson, E., Ghorpade, S., Kwan, A.K., Kirk, J.L., Lehnherr, I. and Swanson, H.K., 2011. Differences in mercury bioaccumulation between polar bears (*Ursus maritimus*) from the Canadian High- and Sub-Arctic. Environmental Science & Technology, 45 (14):5922-5928.

St. Louis, V., Graydon, J., Mitchell, C. and Oswald, C., 2016. Chapter 5: Mercury fate and methylation in terrestrial upland and wetland environments. In: ECCC Canadian Mercury Science Assessment Report, pp.233-284. Environment and Climate Change Canada (ECCC), Gatineau, Canada. Available at: https://mspace.lib.umanitoba.ca/xmlui/handle/1993/32129

St. Pierre, K.A., Chételat, J., Yumvihoze, E. and Poulain, A. J., 2014. Temperature and the sulfur cycle control monomethylmercury cycling in High Arctic coastal marine sediments from Allen Bay, Nunavut, Canada. Environmental Science & Technology, 48 (5):2680-2687.

St. Pierre, K.A., St. Louis, V.L., Kirk, J.L., Lehnherr, I., Wang, S. and La Farge, C., 2015. Importance of open marine waters to the enrichment of total mercury and monomethylmercury in lichens in the Canadian High Arctic. Environmental Science & Technology, 49 (10):5930-5938.

St. Pierre, K.A., Zolkos, S., Shakil, S., Tank, S.E., St. Louis, V.L. and Kokelj, S.V., 2018. Unprecedented increases in total and methyl mercury concentrations downstream of retrogressive thaw slumps in the western Canadian Arctic. Environmental Science & Technology, 52 (24):14099-14109.

St. Pierre, K.A., St. Louis, V.L., Lehnherr, I., Gardner, A.S., Serbu, J.A., Mortimer, C.A., Muir, D.C.G., Wiklund, J.A., Lemire, D., Szostek, L. and Talbot, C., 2019. Drivers of mercury cycling in the rapidly changing glacierized watershed of the High Arctic's largest lake by volume (Lake Hazen, Nunavut, Canada). Environmental Science & Technology, 53 (3):1175-1185.

Stearns, S.C., 1992. The Evolution of Life Histories. Oxford University Press. 262pp.

Steenhuisen, F. and Wilson, S.J., 2019. Development and application of an updated geospatial distribution model for gridding 2015 global mercury emissions. Atmospheric Environment, 211:138-150.

Steffen, A., Schroeder, W., Macdonald, R., Poissant, L. and Konoplev, A., 2005. Mercury in the Arctic atmosphere: an analysis of eight years of measurements of GEM at Alert (Canada) and a comparison with observations at Amderma (Russia) and Kuujjuarapik (Canada). Science of the Total Environment, 432 (1-3):185-198.

Steffen, A., Douglas, T., Amyot, M., Ariya, P., Aspmo, K., Berg, T., Bottenheim, J., Brooks, S., Cobbett, F., Dastoor, A., Dommergue, A., Ebinghaus, R., Ferrari, C., Gardfeldt, K., Goodsite, M. E., Lean, D., Poulain, A. J., Scherz, C., Skov, H., Sommar, J. and Temme, C., 2008. A synthesis of atmospheric mercury depletion event chemistry in the atmosphere and snow. Atmospheric Chemistry and Physics, 8 (6): 1445-1482.

Steffen, A., Scherz, T., Olson, M., Gay, D. and Blanchard, P., 2012. A comparison of data quality control protocols for atmospheric mercury speciation measurements. Journal of Environmental Monitoring, 14 (3):752-765.

Steffen, A., Bottenheim, J., Cole, A., Douglas, T.A., Ebinghaus, R., Friess, U., Netcheva, S., Nghiem, S., Sihler, H. and Staebler, R., 2013. Atmospheric mercury over sea ice during the OASIS-2009 campaign. Atmospheric Chemistry and Physics, 13 (14):7007-7021.

Steffen, A., Bottenheim, J., Cole, A., Ebinghaus, R., Lawson, G. and Leaitch, W.R., 2014. Atmospheric mercury speciation and mercury in snow over time at Alert, Canada. Atmospheric Chemistry and Physics, 14 (5):2219-2231.

Steffen, A., Lehnherr, I., Cole, A., Ariya, P., Dastoor, A., Durnford, D., Kirk, J. and Pilote, M., 2015. Atmospheric mercury in the Canadian Arctic. Part I: a review of recent field measurements. Science of the Total Environment, 509-510:3-15.

Stein, R. and Macdonald, R.W. (Eds.), 2004. The Organic Carbon Cycle in the Arctic Ocean. Springer, Berlin Heidelberg, xix + 363pp.

Steiner, N.S., Cheung, W.W.L., Cisneros-Montemayor, A.M., Drost, H., Hayashida, H., Hoover, C., Lam, J., Sou, T., Sumaila, U.R., Suprenand, P., Tai, T.C. and VanderZwaag, D.L., 2019. Impacts of the changing ocean-sea ice system on the key forage fish Arctic Cod (Boreogadus saida) and subsistence fisheries in the western Canadian Arctic-evaluating linked climate, ecosystem and economic (CEE) models. Frontiers in Marine Science, 6:179.

Stern, G.A., Sanei, H., Roach, P., DeLaronde, J. and Outridge, P.M., 2009. Historical interrelated variations of mercury and aquatic organic matter in lake sediment cores from a Subarctic lake in Yukon, Canada: further evidence toward the algal-mercury scavenging hypothesis. Environmental Science & Technology, 43 (20):7684-7690.

Stern, G.A., Macdonald, R.W., Outridge, P.M., Wilson, S., Chételat, J., Cole, A., Hintelmann, H., Loseto, L.L., Steffen, A., Wang, F. and Zdanowicz, C., 2012. How does climate change influence arctic mercury? Science of the Total Environment, 414:22-42.

Stern G., Loseto, L., Ferguson, S., Watt, C. 2021a. Temporal trends of mercury and halogenated organic compounds in Hendrickson Island, Sanikiluaq and Pangnirtung beluga. In: Beardsall, A., and Morris, A.D. (Eds.). Synopsis of Research Conducted under the 2017-2018 Northern Contaminants Program, pp. 199-204. Crown-Indigenous Relations and Northern Affairs Canada, Gatineau, QC, Canada. Available at: https://pubs.aina.ucalgary.ca/ncp/Synopsis20172018.pdf

Stern, G., Gaden, A., Burt, A., Loria, A., Jantunen, L, and Harner T., 2021b. Temporal trend studies of trace metals and halogenated organic contaminants (HOCs), including new and emerging persistent compounds, in Mackenzie River burbot, Fort Good Hope, NWT. In: Beardsall, A., and Morris, A.D. (Eds). Synopsis of Research Conducted under the 2017-2018 Northern Contaminants Program, pp. 245-253. Crown-Indigenous Relations and Northern Affairs Canada, Gatineau, QC, Canada. Available at: https://pubs.aina.ucalgary.ca/ncp/Synopsis20172018.pdf

Stevenson, M.G., 1996. Indigenous Knowledge in Environmental Assessment. Arctic, 49 (3):278-291.

Stirling, I. and Ross, J.E., 2011. Observations of cannibalism by polar bears (*Ursus maritimus*) on summer and autumn sea ice at Svalbard, Norway. Arctic, 64 (4):478-482.

Stohl, A., 2006. Characteristics of atmospheric transport into the Arctic troposphere. Journal of Geophyiscal Research: Atmospheres, 111 (D11):D11306.

Stokes, C.R., Popovnin, V., Aleynikov, A., Gurney, S.D. and Shahgedanova, M., 2007. Recent glacier retreat in the Caucasus Mountains, Russia and associated increase in supraglacial debris cover and supra-/proglacial lake development. Annals of Glaciology, 46:195-203.

Strand, J., Larsen, M.M. and Lockyer, C., 2005. Accumulation of organotin compounds and mercury in harbour porpoises (*Phocoena phocoena*) from the Danish waters and West Greenland. Science of the Total Environment, 350 (1-3):59-71.

Streets, D.G., Zhang, Q. and Wu, Y., 2009. Projections of global mercury emissions in 2050. Environmental Science & Technology, 43 (8):2983-2988.

Streets, D.G., Devane, M.K., Lu, Z.F., Bond, T.C., Sunderland, E.M. and Jacob, D.J., 2011. All-time releases of mercury to the atmosphere from human activities. Environmental Science & Technology, 45 (24):10485-10491.

Streets, D.G., Horowitz, H.M., Jacob, D.J., Lu, Z., Levin, L., ter Schure, A.F.H. and Sunderland, E.M., 2017. Total mercury released to the environment by human activities. Environmental Science & Technology, 51 (11):5969–5977.

Streets, D.G., Horowitz, H.M., Zifeng, L., Levin, L., Thackray, C.P. and Sunderland, E.M., 2019. Global and regional trends in mercury emissions and concentrations, 2010–2015. Atmospheric Environment, 201:417-427.

Stroeve, J.C., Markus, T., Boisvert, L., Miller, J. and Barrett, A., 2014. Changes in Arctic melt season and implications for sea ice loss. Geophysical Research Letters, 41 (4):1216-1225.

Štrok, M., Baya, P.A. and Hintelmann, H., 2015. The mercury isotope composition of Arctic coastal seawater. Comptes Rendus Geoscience, 347 (7-8):368-376.

Stroeve, J. and Notz, D., 2018. Changing state of Arctic sea-ice across all seasons. Environmental Research Letters, 13 (10):103001.

Subir, M., Ariya, P.A. and Dastoor, A.P., 2011. A review of uncertainties in atmospheric modeling of mercury chemistry I. Uncertainties in existing kinetic parameters - fundamental limitations and the importance of heterogeneous chemistry. Atmospheric Environment, 45 (32):5664-5676.

Subir, M., Ariya, P.A. and Dastoor, A.P., 2012. A review of the sources of uncertainties in atmospheric mercury modeling II. Mercury surface and heterogeneous chemistry – a missing link. Atmospheric Environment, 46:1-10.

Sun, J., Bustnes, J.O., Helander, B., Bårdsen, B.-J., Boertmann, D., Dietz, R., Jaspers, V.L.B., Labansen, A.L., Lepoint, G., Schulz, R., Søndergaard, J., Sonne, C., Thorup, K., Tøttrup, A.P., Zubrod, J.P., Eens, M. and Eulaers, I., 2019. Temporal trends of mercury differ across three northern white-tailed eagle (*Haliaeetus albicilla*) subpopulations. Science of the Total Environment, 687:77-86.

Sunderland, E.M., Gobas, F.A.P.C., Branfireun, B.A. and Heyes, A., 2006. Environmental controls on the speciation and distribution of mercury in coastal sediments. Marine Chemistry, 102 (1-2):111-123.

Sunderland, E.M., Krabbenhoft, D.P., Moreau, J.W., Strode, S.A. and Landing, W.M., 2009. Mercury sources, distribution, and bioavailability in the North Pacific Ocean: insights from data and models. Global Biogeochemical Cycles, 23 (2):GB2010.

Sundseth, K., Pacyna, J.M., Banel, A., Pacyna, E.G. and Rautio, A., 2015. Climate change impacts on environmental and human exposure to mercury in the Arctic. International Journal of Environmental Research and Public Health, 12 (4):3579-3599.

Surdu, C.M., Duguay, C.R. and Prieto, D.F., 2016. Evidence of recent changes in the ice regime of lakes in the Canadian High Arctic from spaceborne satellite observations. The Cryosphere, 10 (3):941-960.

Svensson, C.J., Hansson, A., Harkonen, T.J. and Harding, K.C., 2011. Detecting density dependence in growing seal populations. Ambio 40:52–59.

Swanson, H.K. and Kidd, K.A., 2010. Mercury concentrations in Arctic food fishes reflect the presence of anadromous Arctic charr (*Salvelinus alpinus*), species, and life history. Environmental Science & Technology, 44:3286-3292.

Swanson, H., Gantner, N., Kidd, K.A., Muir, D.C.G. and Reist, J.D., 2011. Comparison of mercury concentrations in landlocked, resident, and sea-run fish (*Salvelinus* spp.) from Nunavut, Canada. Environmental Toxicology and Chemistry, 30 (6):1459-1467.

Syrjämäki, E. and Mustonen, T., 2013. It is the Sámi who own this land––Sacred landscapes and oral histories of the Jokkmokk Sámi. Snowchange Cooperative, Kontiolahti, Finland. 135pp.

TAEMP, 2019. Final Report, Whatì 2018. Tłı̨chǫ Aquatic Ecosystem Monitoring Program (TAEMP). iv + 41pp. Available at: https://wrrb.ca/sites/default/files/FINAL%20Report_TAEMP_Whati_%202018_0.pdf

Tagesson, T., Mastepanov, M., Tamstorf, M.P., Eklundh, L., Schubert, P., Ekberg, A., Sigsgaard, C., Christensen, T.R. and Ström, L., 2012. High-resolution satellite data reveal an increase in peak growing season gross primary production in a High-Arctic wet tundra ecosystem 1992–2008. International Journal of Applied Earth Observation and Geoinformation, 18:407-416.

Tan, S.W., Meiller, J.C. and Mahaffey, K.R., 2009. The endocrine effects of mercury in humans and wildlife. Critical Reviews in Toxicology, 39 (3):228-269.

Tang-Péronard, J.L., Heitmann, B.L., Andersen, H.R., Steuerwald, U., Grandjean, P., Weihe, P. and Jensen, T.K., 2013. Association between prenatal polychlorinated biphenyl exposure and obesity development at ages 5 and 7 y: a prospective cohort study of 656 children from the Faroe Islands. The American Journal of Clinical Nutrition, 99 (1):5-13.

Tank, S.E., Vonk, J.E., Walvoord, M.A., McClelland, J.W., Laurion, I. and Abbott, B.W., 2020. Landscape matters: predicting the biogeochemical effects of permafrost thaw on aquatic networks with a state factor approach. Permafrost and Periglacial Processes, 31 (3):358-370.

Tape, K.D., Gustine, D.D., Ruess, R.W., Adams, L.G. and Clark, J.A., 2016. Range expansion of moose in Arctic Alaska linked to warming and increased shrub habitat. PLOS ONE 11 (4):e0152636.

Tape, K.D., Jones, B.M., Arp, C.D., Nitze, I. and Grosse, G., 2018. Tundra be dammed: beaver colonization of the Arctic. Global Change Biology, 24 (10):4478-4488.

Tarbier, B., Hugelius, G., Sannel, A.B.K., Baptista-Salazar, C. and Jonsson, S., 2021. Permafrost thaw increases methylmercury formation in Subarctic Fennoscandia. Environmental Science & Technology, 55 (10):6710-6717.

Tarnocai, C., Canadell, J.G., Schuur, E.A.G., Kuhry, P., Mazhitova, G. and Zimov, S., 2009. Soil organic carbon pools in the northern circumpolar permafrost region. Global Biogeochemical Cycles, 23 (2):GB2023.

Tartu, S., Goutte, A., Bustamante, P., Angelier, F., Moe, B., Clément-Chastel, C., Bech, C., Gabrielsen, G.W., Bustnes, J.O. and Chastel, O., 2013. To breed or not to breed: endocrine response to mercury contamination by an Arctic seabird. Biology Letters, 9 (4):20130317.

Tartu, S., Bustamante, P., Goutte, A., Cherel, Y., Weimerskirch, H., Bustnes, J.O. and Chastel, O., 2014. Age-related mercury contamination and relationship with luteinizing hormone in a long-lived Antarctic bird. PLOS ONE, 9 (7):e103642.

Tartu, S., Wingfield, J.C., Bustamante, P., Angelier, F., Budzinski, H., Labadie, P., Bustnes, J.O., Weimerskirch, H. and Chastel, O., 2015a. Corticosterone, prolactin and egg neglect behaviour in relation to mercury and legacy POPs in a long-lived Antarctic bird. Science of the Total Environment, 505:180-188.

Tartu, S., Lendvai, Á.Z., Blévin, P., Herzke, D., Bustamante, P., Moe, B., Gabrielsen, G.W., Bustnes, J.O., Chastel, O., 2015b. Increased adrenal responsiveness and delayed hatching date in relation to polychlorinated biphenyl exposure in Arctic-breeding black-legged kittiwakes (*Rissa tridactyla*). General and Comparative Endocrinology, 219:165-172.

Tartu, S., Bustamante, P., Angelier, F., Lendvai, Á.Z., Moe, B., Blévin, P., Bech, C., Gabrielsen, G.W., Bustnes, J.O. and Chastel, O., 2016. Mercury exposure, stress and prolactin secretion in an Arctic seabird: an experimental study. Functional Ecology, 30 (4):596-604.

Tartu, S., Lille-Langøy, R., Størseth, T.R., Bourgeon, S., Brunsvik, A., Aars, J., Goksøyr, A., Jenssen, B.M., Polder, A., Thiemann, G.W., Torget, V. and Routti, H., 2017. Multiple stressor effects in an apex predator: combined influence of pollutants and sea ice decline on lipid metabolism in polar bears. Scientific Reports, 7 (1):16487.

Tartu, S., Aars, J., Andersen, M., Polder, A., Bourgeon, S., Merkel, B., Lowther, A.D., Bytingsvik, J., Welker, J.M., Derocher, A.E., Jenssen, B.M. and Routti, H., 2018. Choose your poison—space-use strategy influences pollutant exposure in Barents Sea polar bears. Environmental Science and Technology, 52 (5):3211-3221.

Tartu S., Blévin P., Bustamante P., Angelier F., Bech C., Bustnes J.O., Chierici M., Fransson A., Gabrielsen G.W., Goutte A., Moe B., Sauser C., Sire J., Barbraud C. and Chastel O., 2022. A U-turn for mercury concentrations over 20 years: how do environmental conditions affect exposure in Arctic seabirds? Environmental Science and Technology. In press. DOI:10.1021/acs.est.1c07633

Taylor, G.T., Ackerman, J.T. and Shaffer, S.A., 2018. Egg turning behavior and incubation temperature in Forster's terns in relation to mercury contamination. PLOS ONE, 13(2):e0191390.

Tesán Onrubia, J.A., Petrova, M.V., Puigcorbé, V., Black, E.E., Valk, O., Dufour, A., Hamelin, B., Buesseler, K.O., Masqué, P., Le Moigne, F.A.C., Sonke, J.E., Rutgers van der Loeff, M. and Heimbürger-Boavida, L.-E., 2020. Mercury export flux in the Arctic Ocean estimated from $^{234}Th/^{238}U$ Disequilibria. ACS Earth and Space Chemistry, 4 (5):795-801.

Thomas, C.D., Cameron, A., Green, R.E., Bakkenes, M., Beaumont, L.J., Collingham, Y.C., Erasmus, B.F.N., de Siqueira, M.F., Grainger, A., Hannah, L., Hughes, L., Huntley, B., van Jaarsveld, A.S., Midgley, G.F., Miles, L., Ortega-Huerta, M.A., Peterson, A.T., Phillips, O.L. and Williams, S.E., 2004. Extinction risk from climate change. Nature 427 (6970):145-148.

Thomas, S.M., Kiljunen, M., Malinen, T., Eloranta, A.P., Amundsen, P-A., Lodenius, M. and Kahilainen, K.K., 2016. Food-web structure and mercury dynamics in a large Subarctic lake following multiple species introductions. Freshwater Biology, 61 (4):500-517.

Tian, W., Egeland, G.M., Sobol, I. and Chan, H.M., 2011. Mercury hair concentrations and dietary exposure among Inuit preschool children in Nunavut, Canada. Environmental International, 37 (1):42-48.

Tiaptirgianov, M., 2017. Fish of freshwater bodies of Yakutia (systematisation, ecology, impact of anthropogenic factors). (Russian Language). PhD thesis. Commission of the Russian Federation. Yakutsk, Russia. Available at: https://www.dissercat.com/content/ryby-presnovodnykh-vodoemov-yakutii-sistematika-ekologiya-vozdeistvie-antropogennykh-faktoro

Timmermans, M-L. and A. Proshutinsky, 2014. Arctic Ocean Sea Surface Temperature. Arctic Report Card: Update for 2014. National Oceanic and Atmospheric Administration (NOAA). Arctic Report Card 2014. Available at: http://www.arctic.noaa.gov/reportcard

Tinggi, U., 2003. Essentiality and toxicity of selenium and its status in Australia: a review. Toxicology Letters, 137 (1):103-110.

Torres-Valdés, S., Tsubouchi, T., Bacon, S., Naveira-Garabato, A.C., Sanders, R., McLaughlin, F.A., Petrie, B., Kattner, G., Azetsu-Scott, K. and Whitledge, T.E., 2013. Export of nutrients from the Arctic Ocean. Journal of Geophysical Research: Oceans, 118 (4):1625-1644.

Toyota, K., McConnell, J.C., Staebler, R.M. and Dastoor, A.P., 2014a. Air-snowpack exchange of bromine, ozone and mercury in the springtime Arctic simulated by the 1-D model PHANTAS – Part 1: In-snow bromine activation and its impact on ozone. Atmospheric Chemistry and Physics, 14 (8):4101-4133.

Toyota, K., Dastoor, A.P. and Ryzhkov, A., 2014b. Air-snowpack exchange of bromine, ozone and mercury in the springtime Arctic simulated by the 1-D model PHANTAS – Part 2: Mercury and its speciation. Atmospheric Chemistry and Physics, 14 (8):4135-4167.

Tran, L., Reist, J.D. and Power, M., 2015. Total mercury concentrations in anadromous Northern Dolly Varden from the northwestern Canadian Arctic: a historical baseline study. Science of the Total Environment, 509-510:154-164.

Tran, L., Reist, J.D., Gallagher, C.P. and Power, M., 2019. Comparing total mercury concentrations of northern Dolly Varden, *Salvelinus malma malma*, in two Canadian Arctic rivers 1986-1988 and 2011-2013. Polar Biology, 42 (5):865-876.

Travnikov, O. and Ilyin, I., 2009. The EMEP/MSC-E mercury modeling system. In: Mason, R. and Pirrone, N. (Eds.). Mercury Fate and Transport in the Global Atmosphere: Emissions, Measurements and Models, pp. 571-587. Springer.

Travnikov, O., Angot, H., Artaxo, P., Bencardino, M., Bieser, J., D'Amore, F., Dastoor, A., De Simone, F., del Carmen Diéguez, M., Dommergue, A., Ebinghaus, R., Feng, X.B., Gencarelli, C.N., Hedgecock, I.M., Magand, O., Martin, L., Matthias, V. Mashyanov, N., Pirrone, N., Ramachandran, R., Read, K.A., Ryjkov, A., Selin, N.E., Sena, F., Song, S., Sprovieri, F., Wip, D., Wängberg, I. and Yang, X., 2017. Multi-model study of mercury dispersion in the atmosphere: atmospheric processes and model evaluation. Atmospheric Chemistry and Physics, 17 (8):5271-5295.

Tremblay, J.É., Robert, D., Varela, D.E., Lovejoy, C., Darnis, G., Nelson, R.J. and Sastri, A.R., 2012. Current state and trends in Canadian Arctic marine ecosystems: I. Primary production. Climate Change, 115 (1):161-178.

Trudel, M. and Rasmussen, J.B., 2006. Bioenergetics and mercury dynamics in fish: a modelling perspective. Canadian Journal of Fisheries and Aquatic Sciences, 63 (8):1890-1902.

Tsubouchi, T., Bacon, S., Aksenov, Y., Naveira Garabato, A.C., Beszczynska-Möller, A., Hansen, E., de Steur, L., Curry, B. and Lee, C.M., 2018. The Arctic Ocean seasonal cycles of heat and freshwater fluxes: observation-

based inverse estimates. Journal of Physical Oceanography, 48 (9):2029-2055.

Tsui, M.T.K. and Wang, W.X., 2006. Acute toxicity of mercury to *Daphnia magna* under different conditions. Environmental Science & Technology, 40:4025-4030.

Tsui, M.T.K. and Wang, W.X., 2007. Biokinetics and tolerance development of toxic metals in *Daphnia magna*. Environmental Toxicology and Chemistry, 26 (5):1023-1032.

Tsui, M.T.K. and Finlay, J.C., 2011. Influence of dissolved organic carbon on methylmercury bioavailability across Minnesota stream ecosystems. Environmental Science & Technology, 45 (14):5981-5987.

Tsz-Ki Tsui, M., Liu, S., Brasso, R.L., Blum, J.D., Kwon, S.Y., Ulus, Y., Nollet, Y.H., Balogh, S.J., Eggert, S.L. and Finlay, J.C., 2019. Controls of methylmercury bioaccumulation in forest floor food webs. Environmental Science & Technology, 53 (5):2434-2440.

Turetsky, M.R., Harden, J.W., Friedli, H.R., Flannigan, M., Payne, N., Crock, J. and Radke, L., 2006. Wildfires threaten mercury stocks in northern soils. Geophysical Research Letters, 33 (16):L16403.

Ukonmaanaho, L., Starr, M., Kantola, M., Laurén, A., Piispanen, J., Pietilä, H., Perämäki, P., Merilä, P., Fritze, H., Tuomivirta, T., Heikkinen, J., Mäkinen, J. and Nieminen, T.M., 2016. Impacts of forest harvesting on mobilization of Hg and MeHg in drained peatland forests on black schist or felsic bedrock. Environmental Monitoring and Assessment, 188 (4):228.

UN Environment, 2019. Global Mercury Assessment 2018. United Nations Environment Programme (UNEP), Geneva, Switzerland. 62pp. Available at: https://www.unep.org/resources/publication/global-mercury-assessment-2018

Undeman, E., Brown, T.N., Wania, F. and McLachlan, M.S, 2010. Susceptibility of human populations to environmental exposure to organic contaminants. Environmental Science & Technology, 44 (16):6249-55.

UNDP, 2020. Minamata Initial Assessment Report, Suggested Structure and Contents: October 2020. United Nations Development Programme (UNDP), New York, NY, USA. 23pp. Available at: https://www.undp.org/content/dam/undp/library/Environment%20and%20Energy/Chemicals%20and%20Waste%20Management/2020%20MIA%20Guidance.pdf

UNEP, 2002. Global Mercury Assessment. United Nations Environment Programme (UNEP), Chemicals, Geneva, Switzerland. viii + 258pp.

UNEP, 2013. Global Mercury Assessment 2013: Sources, Emissions, Releases and Environmental Transport. UN Environment Programme (UNEP), Chemicals Branch, Geneva, Switzerland. 44pp.

UNEP, 2014. Assessment of the Mercury Content in Coal Fed to Power Plants and Study of Mercury Emissions from the Sector in India. Central Institute of Mining & Fuel Research (CIMFR), UN Environmental Programme (UNEP), Chemicals Branch, Geneva, Switzerland. Available at: https://wedocs.unep.org/handle/20.500.11822/31288

UNEP, 2019. Minamata Convention – Text and Annexes. United Nations Environment Programme (UNEP), Geneva, Switzerland. 72pp. Available at: http://mercuryconvention.org/Convention/Text/tabid/3426/language/en-US/Default.aspx

UNEP/AMAP, 2011. Climate Change and POPs: Predicting the Impacts. Report of the UNEP/AMAP Expert Group. Secretariat of the Stockholm Convention, Geneva. 62pp.

UNEP/WHO, 2008. Guidance for Identifying Populations at Risk from Mercury Exposure. United Nations Environment Programme (UNEP) and World Health Organization (WHO), Geneva, Switzerland. vi + 170pp. Available at: https://www.who.int/publications/m/item/guidance-for-identifying-populations-at-risk-from-mercury-exposure

US EPA, 2001. Water Quality Criterion for the Protection of Human Health: Methylmercury, (EPA-823-R-01-001). U.S. Environmental Protection Agency (US EPA), Washington, DC, USA. xvi + 287pp. Available at: https://www.epa.gov/sites/production/files/2020-01/documents/methylmercury-criterion-2001.pdf

Vadeboncoeur, Y., Jeppesen, E., Zanden, M.J.V., Schierup, H.-H., Christoffersen, K. and Lodge, D.M., 2003. From Greenland to green lakes: cultural eutrophication and the loss of benthic pathways in lakes. Limnology and Oceanography, 48 (4):1408-1418.

Valera, B., Dewailly, É. and Poirier, P., 2009. Environmental mercury exposure and blood pressure among Nunavik Inuit adults. Hypertension, 54 (5):981-986.

Valera, B., Muckle, G., Poirier, P., Jacobson, S.W., Jacobson, J.L. and Dewailly, É., 2012. Cardiac autonomic activity and blood pressure among Inuit children exposed to mercury. Neurotoxicology 33 (5):1067-1074.

Valinia, S., Futter, M.N., Cosby, B.J., Rosén, P. and Fölster, J., 2015. Simple models to estimate historical and recent changes of total organic carbon concentrations in lakes. Environmental Science & Technology, 49:386-394.

van der Velden, S., Reist, J.D., Babaluk, J.A. and Power, M., 2012. Biological and life-history factors affecting total mercury concentrations in Arctic charr from Heintzelman Lake, Ellesmere Island, Nunavut. Science of the Total Environment, 433:309-317.

van der Velden, S., Evans, M.S., Dempson, J.B., Muir, D.C.G. and Power, M., 2013a. Comparative analysis of total mercury concentrations in anadromous and non-anadromous Arctic charr (*Salvelinus alpinus*) from eastern Canada. Science of the Total Environment, 447:438-449.

van der Velden, S., Dempson, J.B., Evans, M.S., Muir, D.C.G. and Power, M. 2013b. Basal mercury concentrations and biomagnification rates in freshwater and marine food webs: effects on Arctic charr (*Salvelinus alpinus*) from eastern Canada. Science of the Total Environment, 444: 531-542.

van der Velden, S., Dempson, J.B. and Power, M., 2015. Comparing mercury concentrations across a thirty year time span in anadromous and non-anadromous Arctic charr from Labrador, Canada. Science of the Total Environment, 509–510:165-174.

van der Werf, G.R., Randerson, J.T., Giglio, L., van Leeuwen, T.T., Chen, Y., Rogers, B.M., Mu, M., van Marle, M.J.E., Morton, D.C., Collatz, G.J., Yokelson, R.J. and Kasibhatla, P.S., 2017. Global fire emissions estimates during 1997–2016. Earth System Science Data, 9:697–720.

VanArsdale, A., Weiss, J., Keeler, G., Miller, E., Boulet, G., Brulotte, R. and Poissant, L., 2005. Patterns of mercury deposition and concentration in northeastern North America (1996–2002). Ecotoxicology, 14 (1-2):37-52.

Vancoppenolle, M., Bopp, L., Madec, G., Dunne, J., Ilyina, T., Halloran, P.R. and Steiner, N., 2013. Future Arctic Ocean primary productivity from CMIP5 simulations: uncertain outcome, but consistent mechanisms. Global Biogeochemical Cycles, 27 (3):605-619.

Varty, S., Lehnherr, I., St. Pierre, K., Kirk, J. and Wisniewski, V., 2021. Methylmercury transport and fate shows strong seasonal and spatial variability along a High Arctic freshwater hydrologic continuum. Environmental Science and Technology, 55:331–340.

Veira, A., Lasslop, G. and Kloster, S., 2016. Wildfires in a warmer climate: emission fluxes, emission heights, and black carbon concentrations in 2090-2099. Journal of Geophysical Research: Atmospheres, 121 (7):3195-3223.

Velichkin, V.T., Vorobyova, A., Evseev, A.V. and Miroshnikov, A.Y., 2013. Radioecological environment and radiogeochemical regionalisation of Northwestern Russia. Doklady Earth Sciences, 453:1154-1157.

Vermilyea, A.W., Nagorski, S.A., Lamborg, C.H., Hood, E.W., Scott, D. and Swarr, G.J., 2017. Continuous proxy measurements reveal large mercury fluxes from glacial and forested watersheds in Alaska. Science of the Total Environment, 599-600:145-155.

Verpoorter, C., Kutser, T., Seekell, D.A. and Tranvik, L.J., 2014. A global inventory of lakes based on high-resolution satellite imagery. Geophysical Research Letters, 41 (18):6396-6402.

Verreault, J., Helgason, L.B., Gabrielsen, G.W., Dam, M. and Braune, B.M., 2013. Contrasting retinoid and thyroid hormone status in differentially-contaminated northern fulmar colonies from the Canadian Arctic, Svalbard and the Faroe Islands. Environment International, 52:29-40.

Verta, M., Salo, S., Korhonen, M. Porvari, P., Paloheimo, A. and Munthe, J., 2010. Climate induced thermocline change has an effect on the methyl mercury cycle in small boreal lakes. Science of the Total Environment, 408:3639-3647.

Vihma, T., 2014. Effects of Arctic sea ice decline on weather and climate: a review. Surveys in Geophysics, 35 (5):1175-1214.

Vihma, T., Tisler, P. and Uotila, P., 2012. Atmospheric forcing on the drift of Arctic sea ice in 1989-2009. Geophysical Research Letters, 39 (2):L02501.

Vihtakari, M., Welcker, J., Moe, B., Chastel, O., Tartu, S., Hop, H., Bech, C., Descamps, S. and Gabrielsen, G.W., 2018. Black-legged kittiwakes as messengers of Atlantification in the Arctic. Scientific Report, 8 (1):1178.

Villar, E., Cabrol, L. and Heimbürger-Boavida, L.-E., 2020. Widespread microbial mercury methylation genes in the global ocean. Environmental Microbiology Reports, 12 (3):277-287.

Vincent, W.F., MacIntyre, S., Spigel, R.H. and Laurion, I., 2008. The physical limnology of high-latitude lakes. In: Vincent, W.F. and Laybourn-Parry, J. (Eds.). Polar Lakes and Rivers: Limnology of Arctic and Antarctic Aquatic Ecosystems, pp. 65-81. Oxford University Press.

Virtanen, J.K., Voutilainen, S., Rissanen, T.H., Mursu, J., Tuomainen, T.-P., Korhonen, M.J., Valkonen, V.-P., Seppänen, K., Laukkanen, J. A. and Salonen, J.T., 2005. Mercury, fish oils, and risk of acute coronary events and cardiovascular disease, coronary heart disease, and all-cause mortality in men in eastern Finland. Arteriosclerosis, Thrombosis, and Vascular Biology, 25 (1):228-233.

Vongraven, D. and York, G., 2014. Polar Bears: Status, Trends and New Knowledge. In: Jeffries, M.O., Richter-Menge, J. and Overland, J.E. (Eds.). Arctic Report Card 2014. Available at: http://www.arctic.noaa.gov/reportcard

Vonk, J.E., Tank, S.E., Bowden, W.B., Laurion, I., Vincent, W.F., Alekseychik, P., Amyot, M., Billet, M.F., Canário, J., Cory, R.M., Deshpande, B.N., Helbig, M., Jammet, M., Karlsson, J., Larouche, J., MacMillan, G., Rautio, M., Walter Anthony, K.M. and Wickland, K.P., 2015a. Reviews and syntheses: effects of permafrost thaw on Arctic aquatic ecosystems. Biogeosciences, 12 (23):7129-7167.

Vonk, J.E., Tank, S.E., Mann, P.J., Spencer, R.G.M., Treat, C.C., Striegl, R.G., Abbott, B.W. and Wickland, K.P., 2015b. Biodegradability of dissolved organic carbon in permafrost soils and aquatic systems: a meta-analysis. Biogeosciences, 12 (23):6915-6930.

Wada, T., Chikita, K.A., Kim, Y. and Kudo, I., 2011. Glacial effects on discharge and sediment load in the Subarctic Tanana River basin, Alaska. Arctic, Antarctic, and Alpine Research, 43 (4):632-648.

Wagemann, R., and Kozlowska, H., 2005. Mercury distribution in the skin of beluga (Delphinapterus leucas) and narwhal (Monodon monoceros) from the Canadian Arctic and mercury burdens and excretion by moulting, Science of The Total Environment, 351–352: 333-343.

Wagemann, R., Trebacz, E., Boila, G. and Lockhart, W.L., 1998. Methylmercury and total mercury in tissues of Arctic marine mammals. Science of the Total Environment, 218 (1):19-31.

Wahlström, E., Hallanoro, E. and Manninen, S., 1996. Suomen ympäristön tulevaisuus. Suomen ympäristökeskus. 272pp. (Finnish Language).

Walker, X.J., Baltzer, J.L., Cumming, S.G., Day, N.J., Ebert, C., Goetz, S., Johnstone, J.F., Potter, S., Rogers, B.M., Schuur, E.A.G., Turetsky, M.R. and Mack, M.C., 2019. Increasing wildfires threaten historic carbon sink of boreal forest soils. Nature, 572 (7770):520-523.

Walker, E.V., Yuan, Y., Girgis, S. and Goodman, K.J., 2020a. Patterns of fish and whale consumption in relation to methylmercury in hair among residents of Western Canadian Arctic communities. BMC Public Health, 20 (1):1073.

Walker, V.K., Das, P., Li, P., Lougheed, S.C., Moniz, K., Schott, S., Qitsualik, J. and Koch, I., 2020b. Identification of Arctic food fish species for anthropogenic contaminant testing using geography and genetics. *Foods*, *9 (12)*:1824.

Wall, P.G. and Chen, J., 2018. Moving from risk communication to food information communication and consumer engagement. npj Science of Food, 2 (1):21.

Walther, K., Sartoris, F.-J. and Pörtner, H.-O., 2011. Impacts of temperature and acidification on larval calcium incorporation of the spider crab *Hyas araneus* from different latitudes (54° vs. 79°N). Marine Biology, 158 (9):2043-2053.

Walvoord, M.A. and Striegl, R.G., 2007. Increased groundwater to stream discharge from permafrost thawing in the Yukon River basin: potential impacts on lateral export of carbon and nitrogen. Geophysical Research Letters, 34 (12):L12402.

Walvoord, M.A., Voss, C.I., Ebel, B.A. and Minsley, B.J., 2019. Development of perennial thaw zones in boreal hillslopes enhances potential mobilization of permafrost carbon. Environmental Research Letters, 14:015003.

Wang, M. and Overland, J. E., 2012. A sea ice free summer Arctic within 30 years: an update from CMIP5 models. Geophysical Research Letters, 39 (18):L18501.

Wang, F., Macdonald, R.W., Armstrong, D.A. and Stern, G.A., 2012a. Total and methylated mercury in the Beaufort Sea: the role of local and recent organic remineralization. Environmental Science & Technology, 46 (21):11821-11828.

Wang, F., Lemes, M. and Khan, M.A.K., 2012b. Metallomics of mercury: role of thiol- and selenol-containing biomolecules. In: Cai, Y. and O'Driscoll, N. (Eds.). Environmental Chemistry and Toxicology of Mercury, pp. 517-544. John Wiley & Sons, Ltd.

Wang, X., Lin, C.-J. and Feng, X., 2014. Sensitivity analysis of an updated bidirectional air-surface exchange model for elemental mercury vapor. Atmospheric Chemistry and Physics, 14 (12):6273-6287.

Wang, Y., Li, Y., Liu, G., Wang, D., Jiang, G. and Cai, Y., 2015. Elemental mercury in natural waters: occurrence and determination of particulate Hg(0). Environmental Science & Technology, 49 (16):9742-9749.

Wang, X., Bao, Z., Lin, C.-J., Yuan, W. and Feng, X., 2016. Assessment of global mercury deposition through litterfall. Environmental Science & Technology, 50 (16):8548-8557.

Wang, F., Pućko, M. and Stern, G., 2017a. Chapter 19: Transport and transformation of contaminants in sea ice. In: Thomas, D.N. (Ed.). Sea Ice, Third Edition, pp. 472-491 John Wiley & Sons, Ltd.

Wang, X., Luo, J., Yin, R., Yuan, W., Lin, C.-J., Sommar, J., Feng, X., Wang, H. and Lin, C., 2017b. Using mercury isotopes to understand mercury accumulation in the montane forest floor of the eastern Tibetan Plateau. Environmental Science & Technology, 51 (2):801-809.

Wang, M., Lee, J.S. and Li, Y., 2017c. Global proteome profiling of a marine copepod and the mitigating effect of ocean acidification on mercury toxicity after multigenerational exposure. Environmental Science & Technology, 51 (10):5820-5831.

Wang, K., Munson, K.M., Beaupré-Laperrière, A., Mucci, A., Macdonald, R.W. and Wang, F., 2018. Subsurface seawater methylmercury maximum explains biotic mercury concentrations in the Canadian Arctic. Scientific Reports, 8 (1):14465.

Wang, S., McNamara, S.M., Moore, C.W., Obrist, D., Steffen, A., Shepson, P.B., Staebler, R.M., Raso, A.R.W. and Pratt, K.A., 2019a. Direct detection of atmospheric atomic bromine leading to mercury and ozone depletion. Proceedings of the National Academy of Sciences of the United States of America, 116 (29):14479-14484.

Wang, Z., Sun, T., Driscoll, C.T., Zhang, H. and Zhang, X., 2019b. Dimethylmercury in floodwaters of mercury contaminated rice paddies. Environmental Science & Technology, 53 (16):9453-9461.

Wang, F., Outridge, P.M., Feng, X., Meng, B., Heimbürger-Boavida, L.-E. and Mason, R.P., 2019c. How closely do mercury trends in fish and other aquatic wildlife track those in the atmosphere? – implications for evaluating the effectiveness of the Minamata Convention. Science of the Total Environment, 674:58-70.

Wang, X., Luo, J., Yuan, W., Lin, C.-J., Wang, F., Liu, C., Wang, G. and Feng, X., 2020a. Global warming accelerates uptake of atmospheric mercury in regions experiencing glacier retreat. Proceedings of the National Academy of Sciences of the United States of America, 117 (4):2049-2055.

Wang, K., Munson, K.M., Armstrong, D.A., Macdonald, R.W. and Wang, F., 2020b. Determining seawater mercury methylation and demethylation rates by the seawater incubation approach: a critique. Marine Chemistry, 219:103753.

Wang, Y., Li, L., Yao, C., Tian, X., Wu, Y., Xie, Q. and Wang, D., 2021. Mercury in human hair and its implications for health investigation. Environmental Science and Health, 22:100271.

Wängberg I., Edner H., Ferrara R., Lanzillotta E., Munthe J., Sommar J., Sjöholm M., Svanberg S. and Weibring P., 2003. Atmospheric mercury near a chlor-alkali plant in Sweden. Science of the Total Environment, 304 (1-3):29-41.

Wängberg, I., Munthe, J., Berg, T., Ebinghaus, R., Kock, H.H., Temme, C., Bieber, E., Spain, T.G. and Stolk, A., 2007. Trends in air concentration and deposition of mercury in the coastal environment of the North Sea Area. Atmospheric Environment, 41 (12):2612-2619.

Wassmann, P., Duarte, C.M., Agusti, S. and Sejr, M.K., 2011. Footprints of climate change in the Arctic marine ecosystem. Global Change Biology, 17 (2):1235-1249.

Watras, C.J., Bloom, N.S., Claas, S.A., Morrison, K.A., Gilmour, C.C. and Graig, S.R., 1995. Methylmercury production in the anoxic hypolimnion of a dimictic seepage lake. Water, Air, & Soil Pollution, 80 (1):735-45.

Watras, C.J., Back, R.C., Halvorsen, S., Hudson, R.J.M., Morrison, K.A. and Wente, S.P. 1998. Bioaccumulation of mercury in pelagic freshwater food webs. Science of the Total Environment, 219:183-208.

Waugh, D., Pearce, T., Ostertag, S., Collings, P. and Loseto, L.L., 2018. Inuvialuit Traditional Ecological Knowledge of beluga whale (*Delphinapterus leucas*) under changing climatic conditions in Tuktoyaktuk, NT. Arctic Science, 4 (3):242-258.

Wauthy, M., Rautio, M., Christoffersen, K.S., Forsström, L., Laurion, I., Mariash, H.L., Peura, S. and Vincent, W.F., 2018. Increasing dominance of terrigenous organic matter in circumpolar freshwaters due to permafrost thaw. Limnology and Oceanography Letters, 3 (3):186-198.

Wayland, M., Hoffman, D.J., Mallory, M.L., Alisauskas, R.T. and Stebbins, K.R., 2010. Evidence of weak contaminant-related oxidative stress in glaucous gulls *(Larus hyperboreus)* from the Canadian Arctic. Journal of Toxicology and Environmental Health, Part A, 73:1058-1073.

Webber, H.M. and Haines, T.A., 2003. Mercury effects on predator avoidance behavior of a forage fish, golden shiner (*Notemigonus crysoleucas*). Environmental Toxicology and Chemistry, 22 (7):1556-1561.

Webster, M.A., Rigor, I.G., Nghiem, S.V., Kurtz, N.T., Farrell, S.L., Perovich, D.K. and Sturm, M., 2014. Interdecadal changes in snow depth on Arctic sea ice. Journal of Geophysical Research: Oceans, 119 (8):5395-5406.

Weihe, P. and Joensen, H.D., 2012. Dietary recommendations regarding pilot whale meat and blubber in the Faroe Islands. International Journal of Circumpolar Health, 71 (1):18594.

Wein, R.W., 1976. Frequency and characteristics of Arctic tundra fires. Arctic, 29 (4):181-252.

Weiss-Penzias, P., Jaffe, D., Swartzendruber, P., Hafner, W. and Chand, D., 2007. Quantifying Asian and biomass burning sources of mercury using the Hg/CO ratio in pollution plumes observed at the Mount Bachelor Observatory. Atmospheric Environment, 41 (21):4366-4379.

Weiss-Penzias, P. S., Gay, D.A., Brigham, M.E., Parsons, M.T., Gustin, M.S. and ter Schure, A., 2016. Trends in mercury wet deposition and mercury air concentrations across the U.S. and Canada. Science of the Total Environment, 568:546–556.

Wendling, C., Radisch, J. and Jacobzone, S., 2013. The use of social media in risk and crisis communication. OECD Working Papers on Public Governance, No. 24. OECD Publishing, Paris, France. 41pp. Available at: https://www.oecd-ilibrary.org/the-use-of-social-media-in-risk-and-crisis-communication_5k3v01fskp9s.pdf?itemId=%2Fcontent%2Fpaper%2F5k3v01fskp9s-en&mimeType=pdf

West, J., Graham, A.M., Liem-Nguyen, V. and Jonsson, S., 2020. Dimethylmercury degradation by dissolved sulfide and mackinawite. Environmental Science & Technology, 54 (21):13731-13738.

Whalin, L.M. and Mason, R.P., 2006. A new method for the investigation of mercury redox chemistry in natural waters utilizing deflatable Teflon® bags and additions of isotopically labeled mercury. Analytica Chimica Acta, 558 (1-2):211-221.

Whalin, L., Kim, E.H. and Mason, R., 2007. Factors influencing the oxidation, reduction, methylation and demethylation of mercury species in coastal waters. Marine Chemistry, 107 (3):278-294.

Wheeler, H.C, Danielsen, F., Fidel, M., Hausner, V., Horstkotte, T., Johnson, N., Lee, O., Mukherjee, N., Amos, A., Ashthorn, H., Ballari, Ø., Behe, C., Breton-Honeyman, K.B., Retter, G.B., Buschman, V., Jakobsen, P., Johnson, F., Lyberth, B., Parrott, J.A., Pogodaev, M., Sulyandziga, R. and Vronski, N., 2020. The need for transformative changes in the use of Indigenous Knowledge along with science for environmental decision-making in the Arctic. People and Nature, 2 (3):544-556.

Whitney M.C. and Cristol, D.A., 2017. Impacts of sublethal mercury exposure on birds: a detailed review. In: de Voogt, P. (Ed.). Reviews of Environmental Contamination and Toxicology, pp. 113-163. Reviews of Environmental Contamination and Toxicology (Continuation of Residue Reviews), vol. 244. Springer, Cham.

WHO, 2018. Assessment of prenatal exposure to mercury: human biomonitoring survey. The first survey protocol. A tool for developing national protocols. World Health Organization, Regional Office for Europe (WHO). Copenhagen, Denmark. 52pp. Available at: https://apps.who.int/iris/bitstream/handle/10665/334181/WHO-EURO-2020-1069-40815-55163-eng.pdf?sequence=1&isAllowed=y

Wiener, J.G. and Spry, D.J. 1996. Toxicological significance of mercury in freshwater fish. In: Beyer, W.N., Heinz, G.H. and Redmon-Norwood, A.W. (Eds.). Environmental Contaminants in Wildlife: Interpreting Tissue Concentrations, pp. 297-339. Lewis Publishers.

Wiener, J.G., Krabbenhoft, D.P., Heinz, G.H. and Scheuhammer, A.M., 2003. Ecotoxicology of mercury. In: Hoffman, D.J., Rattner, B.A., Burton, G.A.J. and Cairns, J.J. (Eds.). Handbook of Ecotoxicology. Second edition, pp. 409-463. CRC Press.

Wietrzyk-Pełka, P., Rola, K., Szymański, W. and Węgrzyn, M.H., 2020. Organic carbon accumulation in the glacier forelands with regard to variability of environmental conditions in different ecogenesis stages of High Arctic ecosystems. Science of the Total Environment, 717:135151.

Wiklund, J.A., Kirk, J.L., Muir, D.C.G., Evans, M., Yang, F., Keating, J. and Parsons, M.T., 2017. Anthropogenic mercury deposition in Flin Flon Manitoba and the Experimental Lakes Area Ontario (Canada): a multi-lake sediment core reconstruction. Science of the Total Environment, 586:685-695.

Willacker, J.J., von Hippel, F.A., Ackerly, K.L. and O'Hara, T.M., 2013. Habitat-specific foraging and sex determine mercury concentrations in sympatric benthic and limnetic ecotypes of threespine stickleback. Environmental Toxicology and Chemistry, 32 (7):1623-1630.

Williams, J.W., Jackson, S.T. and Kutzbach, J.E., 2007. Projected distributions of novel and disappearing climates by 2100 AD. Proceedings of the National Academy of Sciences of the United States of America, 104 (14):5738-5742.

Williams, J.J., Dutton, J., Chen, C.Y. and Fisher, N.S., 2010. Metal (As, Cd, Hg, and CH3Hg) bioaccumulation from water and food by the benthic amphipod *Leptocheirus plumulosus*. Environmental Toxicology and Chemistry, 29 (8):1755-1761.

Williamson, C.E., Neale, P.J., Hylander, S., Rose, K.C., Figueroa, F.L., Robinson, S.A., Häder, D.-P., Wängberg, S.-Å. and Worrest, R.C., 2019. The interactive effects of stratospheric ozone depletion, UV radiation, and climate change on aquatic ecosystems. Photochemical & Photobiological Sciences 18 (3):717-746.

Willis, M.D., Bozem, H., Kunkel, D., Lee, A.K.Y., Schulz, H., Burkart, J., Aliabadi, A.A., Herber, A.B., Leaitch, W.R. and Abbatt, J.P.D., 2019. Aircraft-based measurements of High Arctic springtime aerosol show evidence for vertically varying sources, transport and composition. Atmospheric Chemistry and Physics, 19 (1):57-76.

Wilson, K.J., Bell, T,, Arreak, B., Koonoo, D., Angnatsiak, D. and Ljubicic, G.J., 2020. Changing the role of non-Indigenous research partners in practice to support Inuit self-determination in research. Arctic Science, 6 (3):127-153.

Wingfield, J.C. and Sapolsky, R.M., 2003. Reproduction and resistence to stress: when and how. Journal of Neuroendocrinology, 15 (8):711-724.

Wiseman, M.S., 2015. Unlocking the 'Eskimo secret': Defence science in the Cold War Canadian Arctic, 1947-1954. Journal of the Canadian Historical Association, 26 (1):191-223.

Wobeser, G., Nielsen, N.O. and Schiefer, B., 1976. Mercury and mink II. Experimental methyl mercury intoxication. Canadian Journal of Comparitive Medicine, 40 (1):34-45.

Wohlgemuth, L., Osterwalder, S., Joseph, C., Kahmen, A., Hoch, G., Alewell, C. and Jiskra, M., 2020. A bottom-up quantification of foliar mercury uptake fluxes across Europe. Biogeosciences, 17 (24):6441-6456.

Wojtuń, B., Samecka-Cymerman, A., Kolon, K., Kempers, A.J. and Skrzypek, G., 2013. Metals in some dominant vascular plants, mosses, lichens, algae, and the biological soil crust in various types of terrestrial tundra, SW Spitsbergen, Norway. Polar Biology, 36 (12):1799-1809.

Wolfe, B.B., Humphries, M.M., Pisaric, M.F.J., Balasubramaniam, A.M., Burn, C.R., Chan, K., Cooley, D., Froese, D.G., Graupe, S., Hall, R.I., Lantz, T., Porter, T.J., Roy-Leveillee, P., Turner, K.W., Wesche, S.D. and Williams, M., 2011. Environmental change and traditional use of the Old Crow Flats in northern Canada: an IPY opportunity to meet the challenges of the new northern research paradigm. Arctic, 64 (1):127-135.

Wong, C., Ballegooyen, K., Ignace, L., Johnson, M.J. and Swanson, H., 2020. Towards reconciliation: 10 calls to action to natural scientists working in Canafa. Facets, 5 (1):769-783.

Woodgate, R.A., Weingartner, T.J. and Lindsay, R.W., 2010. The 2007 Bering Strait oceanic heat flux and anomalous Arctic sea-ice retreat. Geophysical Research Letters, 37 (1):L01602.

Woodgate, R.A., 2018. Increases in the Pacific inflow to the Arctic from 1990 to 2015, and insights into seasonal trends and driving mechanisms from year-round Bering Strait mooring data. Progress in Oceanography, 160:124-154.

Worden, E., Pearce, T., Gruben, M., Ross, D., Kowana, C. and Loseto, L.L., 2020. Social-ecological changes and implications for understanding the declining beluga whale (*Delphinapterus leucas*) harvest in Aklavik, Northwest Territories. Arctic Science, 6 (3):229-246.

Wren, C.D., Hunter, D.B., Leatherland, J.F. and Stokes, P.M., 1987. The effects of polychlorinated biphenyls and methylmercury, singly and in combination, on mink. I: Uptake and toxic responses. Archives of Environmental Contamination and Toxicology, 16:441-447.

Wren, S.N., Donaldson, D.J. and Abbatt, J.P.D., 2013. Photochemical chlorine and bromine activation from artificial saline snow. Atmospheric Chemistry and Physics, 13 (19):9789-9800.

Wright, L.P. and Zhang, L., 2015. An approach estimating bidirectional air-surface exchange for gaseous elemental mercury at AMNet sites. Journal of Advances in Modeling Earth Systems. 7 (1):35-49.

Wright, L.P., Zhang, L. and Marsik, F.J., 2016. Overview of mercury dry deposition, litterfall, and throughfall studies. Atmospheric Chemistry and Physics, 16 (21):13399-13416.

Wu, Q.R., Wang, S.X., Zhang, L., Song, J.X., Yang, H. and Meng, Y., 2012. Update of mercury emissions from China's primary zinc, lead and copper smelters, 2000-2010. Atmospheric Chemistry and Physics, 12 (22):11153-11163.

Wu, P., Kainz, M.J., Bravo, A.G., Åkerblom, S., Sonesten, L. and Bishop, K., 2019. The importance of bioconcentration into the pelagic food web base for methylmercury biomagnification: a meta-analysis. Science of the Total Environment, 646:357-367.

Wu, P., Zakem, E.J., Dutkiewicz, S. and Zhang, Y., 2020. Biomagnification of methylmercury in a marine plankton ecosystem, Environmental Science & Technology, 54 (9):5446-5455.

Yadav, S.P., 2007. The Wholeness in Suffix -omics, -omes, and the Word Om. Journal of Biomolecular Techniques, 18 (5):277.

Yang, Z., Fang, W., Lu, X., Sheng, G.-P., Graham, D.E., Liang, L., Wullschleger, S.D. and Gu, B., 2016. Warming increases methylmercury production in an Arctic soil. Environmental Pollution, 214:504-509.

Ye, Z., Mao, H., Driscoll, C., Wang, Y., Zhang, Y. and Jaeglé, L., 2018. Evaluation of CMAQ coupled with a state-of-the-art mercury chemical mechanism (CMAQ-newHg-Br). Journal of Advances in Modeling Earth Systems, 10 (3):668-690.

Young, A.M., Higuera, P.E., Duffy, P.A. and Hu, F.S., 2017. Climatic thresholds shape northern high-latitude fire regimes and imply vulnerability to future climate change. Ecography, 40 (5):606-617.

Yuan, W., Sommar, J., Lin, C.-J., Wang, X., Li, K., Liu, Y., Zhang, H., Lu, Z., Wu, C. and Feng, X., 2019. Stable isotope evidence shows re-emission of elemental mercury vapor occurring after reductive loss from foliage. Environmental Science & Technology, 52 (2):651-660.

Yurkowski, D.J., Hussey, N.E., Fisk, A.T., Imrie, K.L., Tallman, R.F. and Ferguson, S.H., 2017. Temporal shifts of forage fish availability decrease intraguild predation pressure between beluga whales and Greenland halibut in a warming Arctic. Biology Letters, 13:20170433.

Yurkowski, D.J., Hussey, N.E., Ferguson, S.H. and Fisk, A.T., 2018. A temporal shift in trophic diversity among a predator assemblage in a changing Arctic. Royal Society Open Science, 5:180259.

Yurkowski, D.J., Richardson, E., Lunn, N.J., Muir, D.C.G., Johnson, A., Derocher, A.E., Ehrman, A., Houde, M., Young, B.G., Debets, C., Scuillo, L., Thiemann, G. and Ferguson, S.H., 2020. Contrasting temporal patterns of mercury, niche dynamics, and body fat indices of polar bears and ringed seals in a melting icescape. Environmental Science & Technology, 54 (5):2780-2789.

Zarnetske, P.L., Skelly, D.K. and Urban, M.C., 2012. Biotic multipliers of climate change. Science, 336 (6088):1516-1518.

Zdanowicz, C., Krümmel, E., Lean, D., Poulain, A., Yumvihoze, E., Chen, J. and Hintelmann, H., 2013. Accumulation, storage and release of mercury in a glaciated Arctic catchment, Baffin Island, Canada. Geochimica et Cosmochimica Acta, 107:316-335.

Zdanowicz, C.M., Krümmel, E M., Poulain, A.J., Yumvihoze, E., Chen, J., Štrok, M., Scheer, M. and Hintelmann, H., 2016. Historical variations of mercury stable isotope ratios in Arctic glacier firn and ice cores. Global Biogeochemical Cycles, 30 (9):1324-1347.

Zdanowicz, C., Karlsson, P., Beckholmen, I., Roach, P., Poulain, A., Yumvihoze, E., Martma, T., Ryjkov, A. and Dastoor, A., 2018. Snowmelt, glacial and atmospheric sources of mercury to a subarctic mountain lake catchment, Yukon, Canada. Geochimica et Cosmochimica Acta, 238: 374-393.

Zhang, Y. and Jaeglé, L., 2013. Decreases in mercury wet deposition over the United States during 2004–2010: roles of domestic and global background emission reductions. Atmosphere, 4 (2):113-131.

Zhang, L., Brook, J. R., and Vet, R., 2003. A revised parameterization for gaseous dry deposition in air-quality models, Atmospheric Chemistry and Physics, 3 (6):2067-2082.

Zhang, L., Wright, L.P. and Blanchard, P., 2009. A review of current knowledge concerning dry deposition of atmospheric mercury. Atmospheric Environment, 43 (37):5853-5864.

Zhang, L., Blanchard, P., Gay, D.A., Prestbo, E.M., Risch, M.R., Johnson, D., Narayan, J., Zsolway, R., Holsen, T.M., Miller, E.K., Castro, M.S., Graydon, J.A., St. Louis, V.L., and Dalziel, J., 2012a. Estimation of speciated and total mercury dry deposition at monitoring locations in eastern and central North America. Atmospheric Chemistry and Physics, 12 (9):4327-4340.

Zhang, Y., Jaeglé, L., van Donkelaar, A., Martin, R. V., Holmes, C. D., Amos, H. M., Wang, Q., Talbot, R., Artz, R., Brooks, S., Luke, W., Holsen, T. M., Felton, D., Miller, E. K., Perry, K. D., Schmeltz, D., Steffen, A., Tordon, R., Weiss-Penzias, P. and Zsolway, R., 2012b. Nested-grid simulation of mercury over North America. Atmospheric Chemistry and Physics, 12 (14):6095-6111.

Zhang, X., He, J., Zhang, J., Polyakov, I., Gerdes, R., Inoue, J. and Wu, P., 2013. Enhanced poleward moisture transport and amplified northern high-latitude wetting trend. Nature Climate Change, 3 (1):47-51.

Zhang, Y., Jaegle, L. and Thompson, L., 2014. Natural biogeochemical cycle of mercury in a global three-dimensional ocean tracer model. Global Biogeochemical Cycles, 28 (5):553-570.

Zhang Y, Jacob DJ, Dutiewicz, S., Amos, H.M., Long, M.S., and Sunderland EM., 2015. Biogeochemical drivers of the fate of riverine mercury discharged to the global and Arctic oceans. Global Biogeochemical Cycles, 29 (6):854-864.

Zhang, Y., Jacob, D.J., Horowitz, H.M., Chen, L., Amos, H.M., Krabbenhoft, D.P., Slemr, F., St. Louis, V.L. and Sunderland, E.M., 2016a. Observed decrease in atmospheric mercury explained by global decline in anthropogenic emissions. Proceedings of the National Academy of Sciences, 113 (3):526-531.

Zhang, L., Wu, Z., Cheng, I., Wright, L.P., Olson, M.L., Gay, D.A., Risch, M.R., Brooks, S., Castro, M.S., Conley, G.D., Edgerton, E.S., Holsen, T.M., Luke, W., Tordon, R. and Weiss-Penzias, P., 2016b. The estimated six-year mercury dry deposition across North America. Environmental Science & Technology, 50 (23):12864-12873.

Zhang, H., Holmes, C.D. and Wu, S., 2016c. Impacts of changes in climate, land use and land cover on atmospheric mercury. Atmospheric Environment, 141:230-244.

Zhang, Y., Horowitz, H., Wang, J., Xie, Z., Kuss, J. and Soerensen, A.L., 2019. A coupled global atmosphere-ocean model for air-sea exchange of mercury: insights into wet deposition and atmospheric redox chemistry. Environmental Science & Technology, 53 (9):5052-5061.

Zhang, B., Chen, T., Guo, J., Wu, M., Yang, R., Chen, X., Wu, X., Zhang, W., Kang, S., Liu, G. and Dyson, P., 2020a. Microbial mercury methylation profile in terminus of a high-elevation glacier on the northern boundary of the Tibetan Plateau. Science of the Total Environment, 708:135226.

Zhang, Y., Soerensen A.L., Schartup, A.T., Sunderland, E.M., 2020b. A global model for methylmercury formation and uptake at the base of marine food webs. Global Biogeochemical Cycles, 34 (2):e2019GB006348.

Zheng, J., 2015. Archives of total mercury reconstructed with ice and snow from Greenland and the Canadian High Arctic. Science of the Total Environment, 509-510:133-144.

Zheng, W., Obrist, D., Weis, D. and Bergquist, B.A., 2016. Mercury isotope compositions across North American forests. Global Biogeochemical Cycles, 30 (10):1475-1492.

Zhou, H., Zhou, C., Hopke, P.K. and Holsen, T.M., 2018. Mercury wet deposition and speciated mercury air concentrations at rural and urban sites across New York State: temporal patterns, sources and scavenging coefficients. Science of the Total Environment, 637-638:943-53.

Zhu, W., Sommar, J., Lin, C.J. and Feng, X., 2015. Mercury vapor air–surface exchange measured by collocated micrometeorological and enclosure methods - Part I: Data comparability and method characteristics. Atmospheric Chemistry and Physics, 15 (2):685-702.

Zhu, W., Lin, C.J., Wang, X., Sommar, J., Fu, X. and Feng, X., 2016. Global observations and modeling of atmosphere–surface exchange of elemental mercury: a critical review. Atmospheric Chemistry and Physics, 16 (7):4451-4480.

Zolkos, S., Krabbenhoft, D.P., Suslova, A., Tank, S.E., McClelland, J.W., Spencer, R.G.M., Shiklomanov, A., Zhulidov, A.V., Gurtovaya, T., Zimov, N., Zimov, S., Mutter, E.A., Kutny, L., Amos, E. and Holmes, R.M., 2020. Mercury export from Arctic great rivers. Environmental Science & Technology, 54 (7):4140-4148.

Zwart, J.A., Sebestyen, S.D., Solomon, C.T. and Jones, S.E., 2017. The influence of hydrologic residence time on lake carbon cycling dynamics following extreme precipitation events. Ecosystems, 20 (5):1000-1014.

Arctic Monitoring and Assessment Programme

The Arctic Monitoring and Assessment Programme (AMAP) was established in June 1991 by the eight Arctic countries (Canada, Denmark, Finland, Iceland, Norway, Russia, Sweden and the United States) to implement parts of the Arctic Environmental Protection Strategy (AEPS). AMAP is now one of six working groups of the Arctic Council, members of which include the eight Arctic countries, the six Arctic Council Permanent Participants (Indigenous Peoples' organizations), together with observing countries and organizations.

AMAP's objective is to provide 'reliable and sufficient information on the status of, and threats to, the Arctic environment, and to provide scientific advice on actions to be taken in order to support Arctic governments in their efforts to take remedial and preventive actions to reduce adverse effects of contaminants and climate change'.

AMAP produces, at regular intervals, assessment reports that address a range of Arctic pollution and climate change issues, including effects on health of Arctic human populations. These are presented to Arctic Council Ministers in 'State of the Arctic Environment' reports that form a basis for necessary steps to be taken to protect the Arctic and its inhabitants.

This report has been subject to a formal and comprehensive peer review process. The results and any views expressed in this series are the responsibility of those scientists and experts engaged in the preparation of the reports.

The AMAP Secretariat is located in Tromsø, Norway. For further information regarding AMAP or ordering of reports, please contact the AMAP Secretariat (The Fram Centre, P.O. Box 6606 Stakkevollan, N-9296 Tromsø, Norway) or visit the AMAP website at www.amap.no.

AMAP Secretariat

The Fram Centre,
P.O. Box 6606 Stakkevollan,
N-9296 Tromsø, Norway

T +47 21 08 04 80
F +47 21 08 04 85

www.amap.no

ISBN – 978-82-7971-111-7

ARCTIC COUNCIL

AMAP
Arctic Monitoring and Assessment Programme